

*See  
for Radio 3*

BIOMASS  
ASSOCIATION  
OF THE  
ALASKA  
Commercial Shell

Volume II. Physical Oceanography and  
Meteorology

Principal Investigators' Reports  
for the Year Ending March 1976

U. S. DEPARTMENT OF COMMERCE  
National Oceanic and Atmospheric Administration



U. S. DEPARTMENT OF INTERIOR  
Bureau of Land Management

April 1976

Annual Reports from Principal Investigators

- Volume:
1. Marine Mammals
  2. Marine Birds
  3. Marine Birds
  4. Marine Birds
  5. Fish, Plankton, Benthos, Littoral
  6. Fish, Plankton, Benthos, Littoral
  7. Fish, Plankton, Benthos, Littoral
  8. Effects of Contaminants
  9. Chemistry and Microbiology
  10. Chemistry and Microbiology
  11. Physical Oceanography and Meteorology
  12. Geology
  13. Geology
  14. Ice

# Environmental Assessment of the Alaskan Continental Shelf

## Volume 11. Physical Oceanography and Meteorology

*Fourth quarter and annual reports for the reporting period ending March 1976,  
from Principal Investigators participating in a multi-year program of environmental  
assessment related to petroleum development on the Alaskan Continental Shelf.  
The program is directed by the National Oceanic and Atmospheric Administration  
under the sponsorship of the Bureau of Land Management.*

ENVIRONMENTAL RESEARCH LABORATORIES / Boulder, Colorado / 1976



## CONTENTS

| <u>Research<br/>Unit</u>   | <u>Proposer</u>   | <u>Title</u>  | <u>Page</u> |
|----------------------------|---|---|-------------|
| 48                         | Donald E. Barrick<br>WPL/NOAA   | Development and Operation of HF<br>Current-Mapping Radar Units-<br>Physical Oceanography  | 1           |
| 81                         | G. L. Hufford<br>U. S. Coast Guard  | Beaufort Shelf Surface Currents   | 9           |
| 91                         | K. Aagaard<br>Dept. of Ocean.<br>U. of Wash.<br>D. P. Haugen<br>Applied Physics Lab.<br>U. of Wash. | Current Measurements in the<br>Beaufort Sea   | 11          |
| 111                        | Robert Carlson<br>Inst. of Water Res.<br>U. of Alaska   | Effects of Seasonability and<br>Variability of Streamflow on<br>Nearshore Coastal Areas   | 23          |
| 138/<br>139/<br>147        | Stanley P. Hayes<br>James D. Schumacher<br>PMEL   | Gulf of Alaska Study of Mesoscale<br>Oceanographic Processes (GAS-MOP)  | 75          |
| 140/<br>146/<br>149/<br>31 | J. A. Galt<br>PMEL  | Numerical Studies of Alaskan Region   | 107         |
| 141/<br>145/<br>148        | J. D. Schumacher<br>PMEL<br>L. K. Coachman<br>Dept. of Ocean.<br>U. of Wash.                        | Bristol Bay Oceanographic Processes<br>(B-BOP)  | 213         |
| 151                        | Knut Aagaard<br>Dept. of Ocean.<br>U. of Wash.  | STD Mappings of the Beaufort Sea Shelf  | 249         |
| 217                        | Donald V. Hansen<br>AOML  | Outer Continental Shelf Energy<br>Program   | 267         |
| 235                        | T. Laevastu<br>Oceanography Dept.<br>Env. Prediction<br>Facility<br>Naval Postgraduate<br>School    | Preparation of Hydrodynamical-Numer-<br>ical and Three-Parameter Small-Mesh<br>Atmospheric Models for Coastal Waters<br>in the Gulf of Alaska | 275         |
| 289                        | Thomas C. Royer<br>IMS/U. of Alaska   | Mesoscale Currents and Water Masses<br>in the Gulf of Alaska  | 293         |

## CONTENTS

| <u>Research<br/>Unit</u> | <u>Proposer</u>                                       | <u>Title</u>   | <u>Page</u> |
|--------------------------|---|--|-------------|
| 307                      | Robin D. Muench<br>IMS/U. of Alaska                   | Historical and Statistical Oceanographic Data Analysis and Ship of Opportunity Program | 359         |
| 335                      | R. J. Callaway<br>EPA                                 | Transport of Pollutants in the Vicinity of Prudhoe Bay                                 | 427         |
| 347                      | Harold W. Searby<br>AEIDC<br>William A. Brower<br>NCC | Marine Climatology of the Gulf of Alaska and the Bering and Beaufort Seas              | 757         |
| 357                      | F. Favorite<br>NMFS/NWFC<br>J. H. Johnson<br>NMFS/PEG | Physical Oceanography of the Gulf of Alaska  | 787         |
| 367                      | Bernard Walter<br>Robert Reynolds<br>PMEL             | Near-Shore Atmospheric Modification  | 923         |

## ANNUAL REPORT

### RU48 - Development and Operation of HF Current-Mapping Radar Units -- Physical Oceanography

#### I. Task Objectives

The primary objectives of the proposed program are twofold: (i) to implement a proven radar concept into a transportable, easily assembled and operated pair of units capable of producing a map of near-surface currents on location in real time, and to calibrate the system as to its accuracy; (ii) to operate the radars at coastal areas of interest along the Gulf of Alaska seacoast in support of the OCSEAP objectives in physical oceanography. We plan to request a series of recommendations on where specifically we will operate; possibilities for this calendar year include the lease areas around Cook Inlet and Kodiak Island. Additional areas could include regions in which other relevant experiments are planned, such as any controlled oil-spill tests or deployments of near-shore Lagrangian drifter buoys.

#### II. Field and Laboratory Activities

1. Laboratory Activities. Nearly all activities since the beginning of the program have been of a laboratory nature, viz., the analysis, design, simulation, and construction of a pair of current-sensing radar units. Mr. Michael Evans was designated Project Leader of the overall program, under Dr. Donald Barrick, Chief of the Sea State Studies Program Area of the Wave Propagation Laboratory. Karl Sutterfield has been with the program since its inception, in charge of the effective utilization of the computer systems for the operation, support, and control of the radars. Mr. Jack Riley joined the team February 1975, and is in charge of developing the graphic and display software for the system. Dr. Bob Weber is implementing all of the software for the reduction and mathematical processing of the received radar signal data. Mr. Don Lund joined the group in August 1975, and at present is primarily responsible for the construction of several of the RF elements of the system. In March 1976, LT Craig Blasingame was assigned to this project; he is currently in charge of all logistics arrangements in support of our upcoming field operations. Messrs. Dan Law, Jack Hawkins, William Everard, and Scott Spettel have been assisting on a part-time basis in the design and assembly of the various digital and RF hardware components of the system. Finally, several of the hardware construction and assembly tasks have been contracted out to engineers of Astro Engineering Corporation and ERBTEC Associates, who are located close by.

2. Field Activities. The decision was made in August 1975 that the first unit pair would be field tested near Miami, Florida during the Spring of 1976. The primary reasons for this decision were: (i) The relatively well-known current patterns of the Gulf Stream should facilitate in assessing the accuracy of the system. (ii) Logistic and technical support has been offered for these tests by NOAA/AOML, the University of Miami, and Nova University. Mr. Evans conducted site surveys in Florida during November, in preparation for these field tests. He discussed logistic support with representatives of the above three organizations, as well as with personnel from other government installations in the area (such as Coast Guard and Department of Defense facilities). He obtained photographs as well as topographic and aerial maps of the area and potential sites. As a result, it is planned that one site will be located at the south end of the Miami Beach peninsula and the other near Fort Lauderdale (at Nova University) about 40 km away.

### III. Results

1. Designs. All system-level designs have been completed. All of the hardware components being constructed in-house have been designed.

2. Procurements. All items to be procured externally have been ordered. Major hardware items purchased commercially include: (i) the electronic laboratory test gear; (ii) computer support facilities; (iii) the radar receivers; (iv) the minicomputers for the field units. All of these major hardware items have been delivered. In fact, the only hardware items which have not as yet been delivered are several minor (but necessary) digital interfaces. This dilemma resulted from an error in our Purchasing department; by attempting to circumvent normal-priority channels, it appears we can have these final components by the first week in May.

3. In-House Fabrication. Several hardware items have been designed and are being constructed in-house. These include: (i) transmitter-drivers; (ii) transmitter power amplifiers; (iii) receiving antennas; (iv) transmitting antennas; (v) radio telemetry gear (between sites); (vi) fast Fourier-Transform digital hardware; (vii) array-processing digital hardware; (viii) data-acquisition board, consisting of the sample and hold circuits, the analog-to-digital converters, and the digital pre-averaging circuits; (ix) semi-conductor buffer memory; (x) graphic display hardware; (xi) systems-integration hardware, including special high-efficiency power supplies, power sequencing circuitry, and fault-analysis circuitry. Prototype designs and models of all of the above components have been completed and are operating. The team is presently in the process of completing the construction of the final operational versions of these components.



4. System Integration. As the individual hardware items are delivered or constructed, they are being integrated into the overall system which will go into the field. Each radar unit consists of two weather-proof fiberglass cases containing shock-mounted racks; all of the digital and RF gear necessary for operation in the field at one site is to be contained in two such cases. About 80% of this system integration is now completed. Each case will weigh less than 175 pounds in the field, capable of being handled by two persons. A considerable amount of attention is being given to system reliability and interference shielding.

5. System Performance Analyses. Based upon the system design specifications, an analysis of system performance has been completed. This study shows that the maximum range from each radar unit should be of the order of 70 km. An analysis of azimuthal angle-of-arrival accuracy shows that insignificant position errors will result when signal-to-noise ratio exceeds 10 decibels. An optimization study indicates that the ideal separation between the two units is approximately 40 km.

6. System Software. Integration of operating-system software for control of the various hardware components is essentially completed. Graphics and display software (for making on-site current maps) has been completed. The radar-signal data-processing software has also been completed and checked out.

7. System Simulation. Using the graphics/display software and the signal data-processing software, simulations have been run in the laboratory. These simulations -- instead of using actual radar signals -- employ simulated signals consisting of the (random) sea-echo signal and a (random) noise signal, as would be received by the actual radar at each of the three antenna terminals. The sea-echo signal includes the effect of the current pattern on the Doppler shift. Any desired current pattern can be inserted on the signal. These simulated signals are then processed by the same software to be used in the field. Hence, such simulations permit one to: (i) debug and check out the system software before actually going into the fields; (ii) obtain a feel for the accuracy of the output product (i.e., the current maps); (iii) modify and improve the system software where certain inaccuracies and weaknesses are detected from the simulations.

8. Antennas. The transmitting antenna system was conceived to be moderately directive, so that (i) higher signals could be obtained from desired ocean regions, and (ii) signals from unwanted areas (for example, behind the radar) could be eliminated. A design study contract was given to Lawrence Livermore Laboratories, which has an international reputation in the area of numerical antenna analysis. Based on their study (now completed), we selected and constructed Yagi monopole antennas consisting of both three vertical elements (for a wider pattern) and four vertical

elements (for a narrower pattern). A photo of the three element version is shown attached. (The vertical elements are about 9 feet high, and the entire device can be erected on the beach in about 1/2 hour.) The antenna has been checked out electrically, and the measured parameters agree very closely with those predicted by Livermore. (The agreement was far better than expected.) Azimuthal patterns (looking down from above) for the three and four element antennas are appended here.

The receiving antenna system consists of three short elements. While one version has been built and checked out, we are re-designing (in-house) this antenna system to be much smaller and more lightweight. The receiving antenna dimensions are much less critical than those of the transmitting antenna. The new design should be ready by the Miami field tests. (If not, the older version will be used.)

9. Operating Frequencies. We have recently received frequency allocations from IRAC for all of our upcoming operations. We are permitted to select any frequencies in the band between 25.330 and 28.000 MHz; these allocations we presently consider satisfactory for all of our operations.

10. Theoretical Analyses. Several non-system, oceanographic factors will limit the accuracy of the system for measuring near-surface currents. One of these is the nonlinear interactions of surface waves, which generate Doppler-shift errors that are not associated with the currents. Examination of this mechanism theoretically shows that such errors -- expressed in terms of radial current velocity -- can always be expected to be less than 10 cm/s, with typical errors of the order of 5 cm/s.

11. Reporting Activities. A major technical report has been prepared and is presently in the final stages of review. This report describes the theory behind the concept, the system design as presently configured, analyses predicting system performance, and system simulations showing current-field maps produced by the actual radar field software using realistic input signals. This report should be cleared for distribution by about May 1976.

#### IV. Preliminary Interpretation of Results

None.

#### V. Problems Encountered/Recommended Changes

There have thus far been no major technical difficulties on the project which have set us back in any substantial way. However, minor bureaucratic slip-ups and shortcomings affecting the normal flow of the project have been numerous, and cumulatively have caused some overall delay in the schedule we originally anticipated. The bureaucratic shortcomings are a result of beginning a new project (as this was) but being faced with the requirement that we operate in a "normal-priority" ERL mode. These

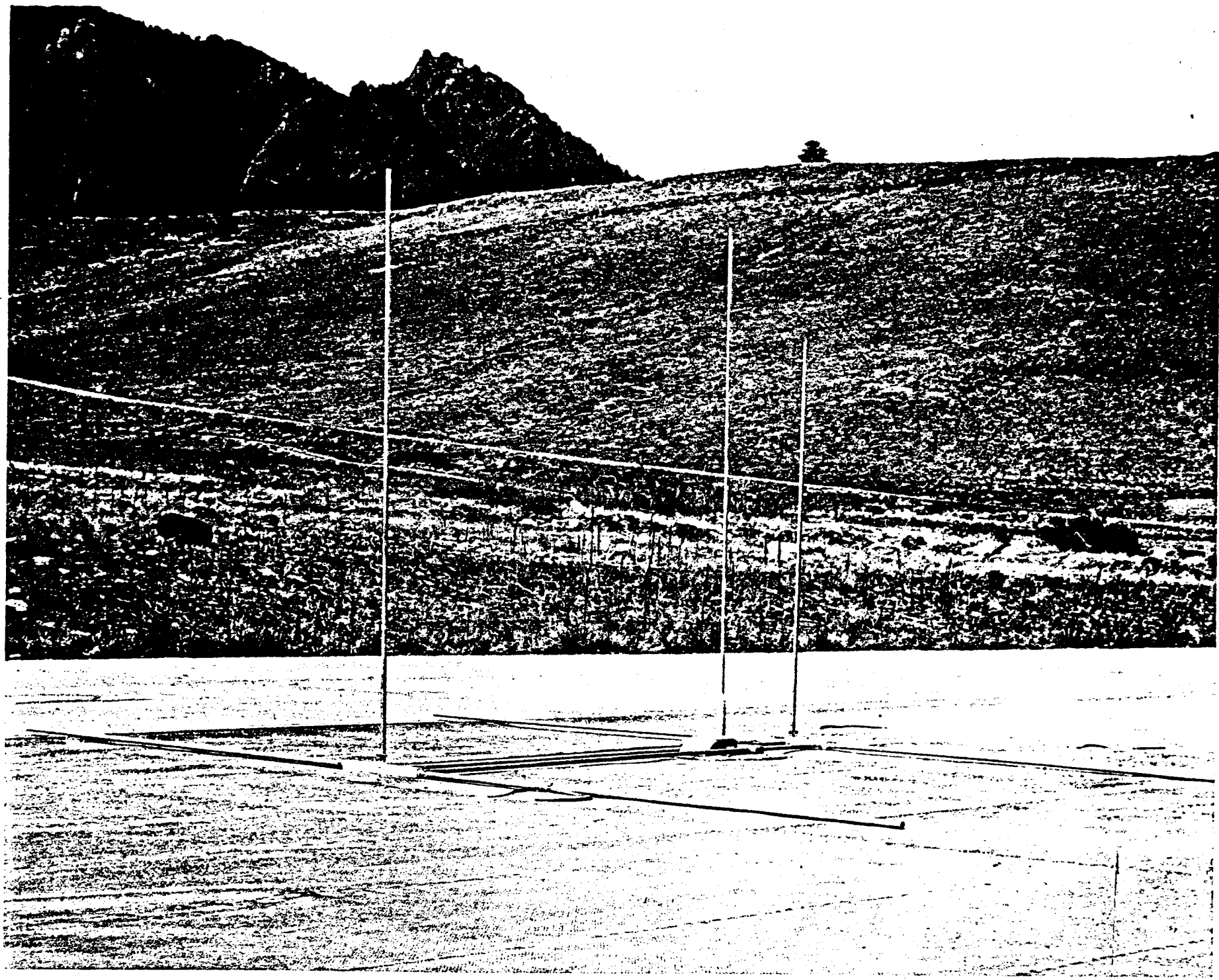
bureaucratic shortcomings have fallen into three major categories: (i) inadequate staffing, and slip-ups by our Personnel department in processing forms on our project personnel; (ii) errors by our Purchasing department which have resulted in procurement delays; (iii) numerous (sub-professional) flaws in components prepared by our ERL machine shops, which involved additional costs and re-doing these items. In addition, funding from the other sponsoring agencies has never been forthcoming in either a timely or adequate fashion; this has cost us in terms of attempting to meet our OCSEAP schedule with inadequate total resources.

We detailed these difficulties in a memorandum to John Robinson (dated April 8, 1976). After meetings with Dr. Hess and OCSEAP staff, we began to receive the support from ERL management that we need to avoid further bureaucratic delays during the final, crucial assembly and field testing phase. In addition, our project staff is working numerous unpaid hours. As a result, we are noticing a marked improvement in the required flow of events in this final phase, and can again anticipate beginning operations in Alaska in midsummer, as originally scheduled (barring any unforeseen catastrophes).

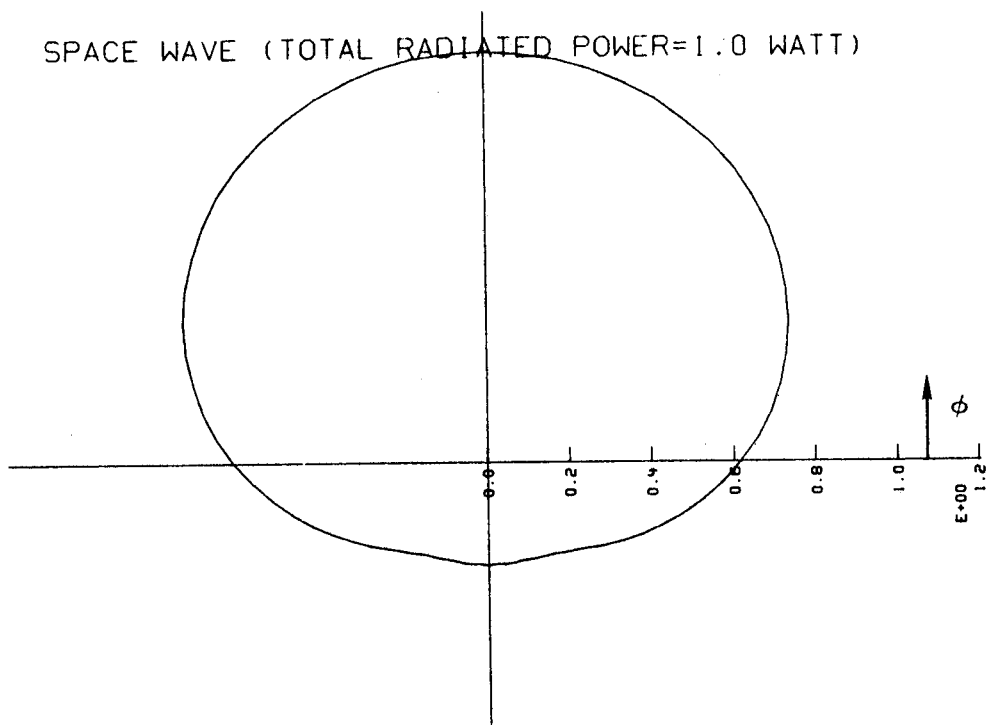
#### VI. Estimate of Funds Expended

(1 March 1975 - 31 March 1976)

1. Funds Expended (Salaries and Other Objects)    \$520,000
2. Funding Obtained to Date
  - a) NOAA/ERL  
    FY75        \$40K
  - b) OCSEAP  
    FY75        \$240K  
    FY76        \$ 40K
  - c) Coast Guard  
    FY75        \$50K
  - d) ERDA  
    FY75        \$ 0K  
    FY76        \$50K

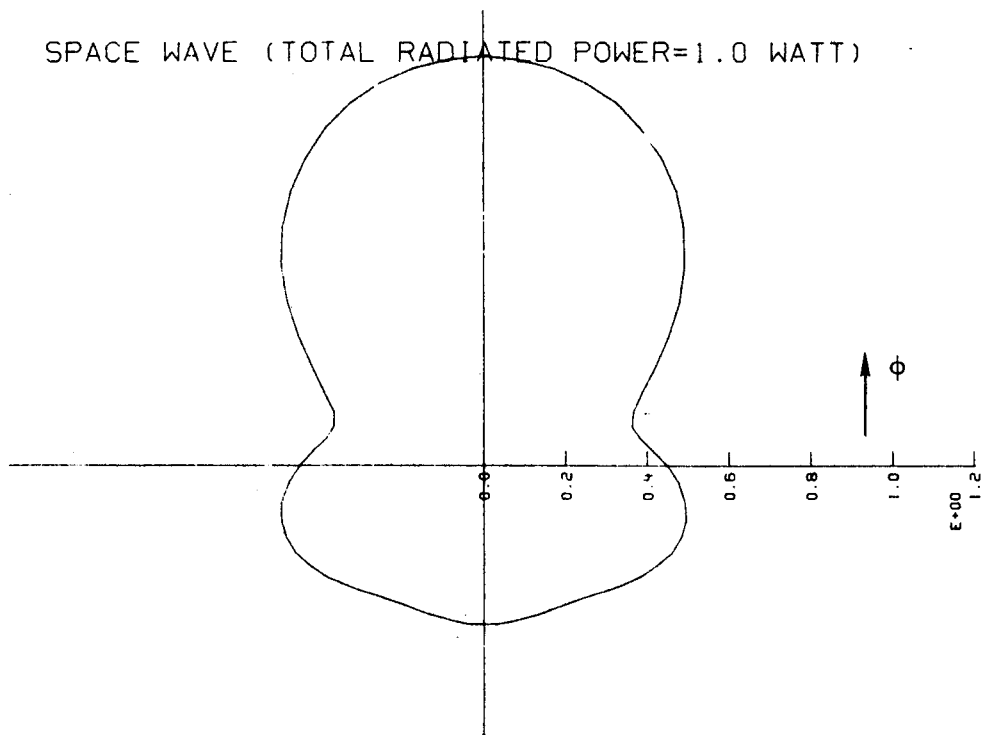


SPACE WAVE (TOTAL RADIATED POWER=1.0 WATT)



Azimuthal pattern of 3-element current-sensing-radar transmitting antenna.

SPACE WAVE (TOTAL RADIATED POWER=1.0 WATT)



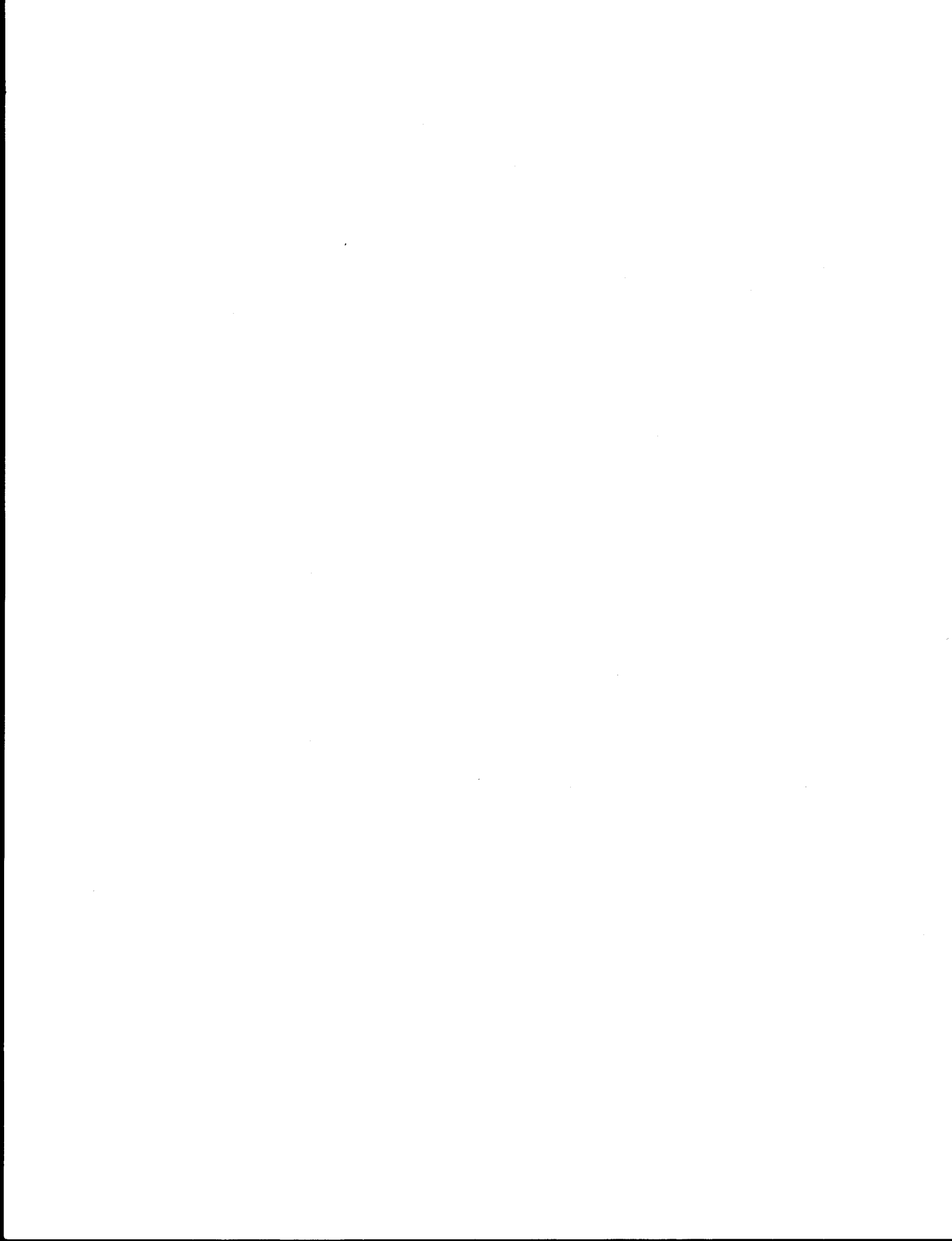
Azimuthal pattern of 4-element current-sensing-radar transmitting antenna.



RU 81

NO REPORT SUBMITTED

Icebreaker was unavailable for studies during 1975 field season.





ANNUAL REPORT

Contract No.:

03-5-022-67 TO 3

Research Unit No.:

91

Reporting Period:

1 April 1975 -- 31 March 1976

Number of Pages:

10

Current Measurements in the Beaufort Sea

Knut Aagaard

Department of Oceanography

Dean Haugen

Applied Physics Laboratory

University of Washington  
Seattle, Washington 98195

26 March 1976

## I. Summary

There is a considerable need for direct long-term current measurements at selected sites on the Beaufort Sea shelf and slope, in areas which generally can be expected to be permanently ice covered. The need is dictated by the importance of advective mechanisms in transporting and dispersing pollutants and substances of biological and geological importance. Because of the ice cover, data recovery becomes a formidable experimental problem. We will shortly deploy six current meters on these moorings. The systems are designed to both acoustically telemeter current and temperature data to the surface, as well as be recoverable (together with the internally recorded data) through the ice.

## II. Introduction

A. The general objective of this research unit is to provide long-term Eulerian time series of currents at selected locations on the outer shelf and slope of the Beaufort Sea, so as to describe and understand the circulation and dynamics of the outer shelf and slope. The time series must be long enough to define the important temporal scales of motion.

B. The area of interest is in general ice-covered throughout the year, so that the specific objective must be to recover the current measurements from anchored arrays despite the presence of ice.

C. Long-term direct current measurements are necessary to describe and understand the circulation on the shelf and the exchange between the shelf and the deep Arctic Ocean. This circulation and exchange are physical mechanisms which transport and disperse pollutants and substances of biological and geological importance. The water motion also influences the ice distribution.

## III. Current state of knowledge

The only time series of current measurements on the Beaufort shelf that is of significant length is from a single current meter moored in water 54 m deep about 70 km ENE of Barrow during 15 days of August 1972. Other current meter measurements are also from summer and have been made in water shallower than 20 m and were of very short duration. By piecing together these observations, along with the indirect evidence provided by summer hydrographic measurements and two four-month long current records from Barrow Canyon during spring and summer, one can arrive at only some general ideas about the Beaufort shelf circulation, and then only during summer.

Water originating in the Bering Sea and modified by its passage through the Chukchi flows ENE north through Barrow Canyon at speeds as high as  $100 \text{ cm sec}^{-1}$ . Subsequently, the majority of this flow probably turns eastward and enters the Beaufort Sea. On the shelf some 70 km ENE, the eastward motion has been observed to average  $60 \text{ cm sec}^{-1}$  during a six-day interval. The eastward flow, concentrated on the outer shelf, can be traced through hydrographic evidence at least as far as Barter Island at  $143^\circ\text{W}$ . Measurements have shown that atmospheric conditions can temporarily reverse the flow both in Barrow Canyon and on the western Beaufort shelf.

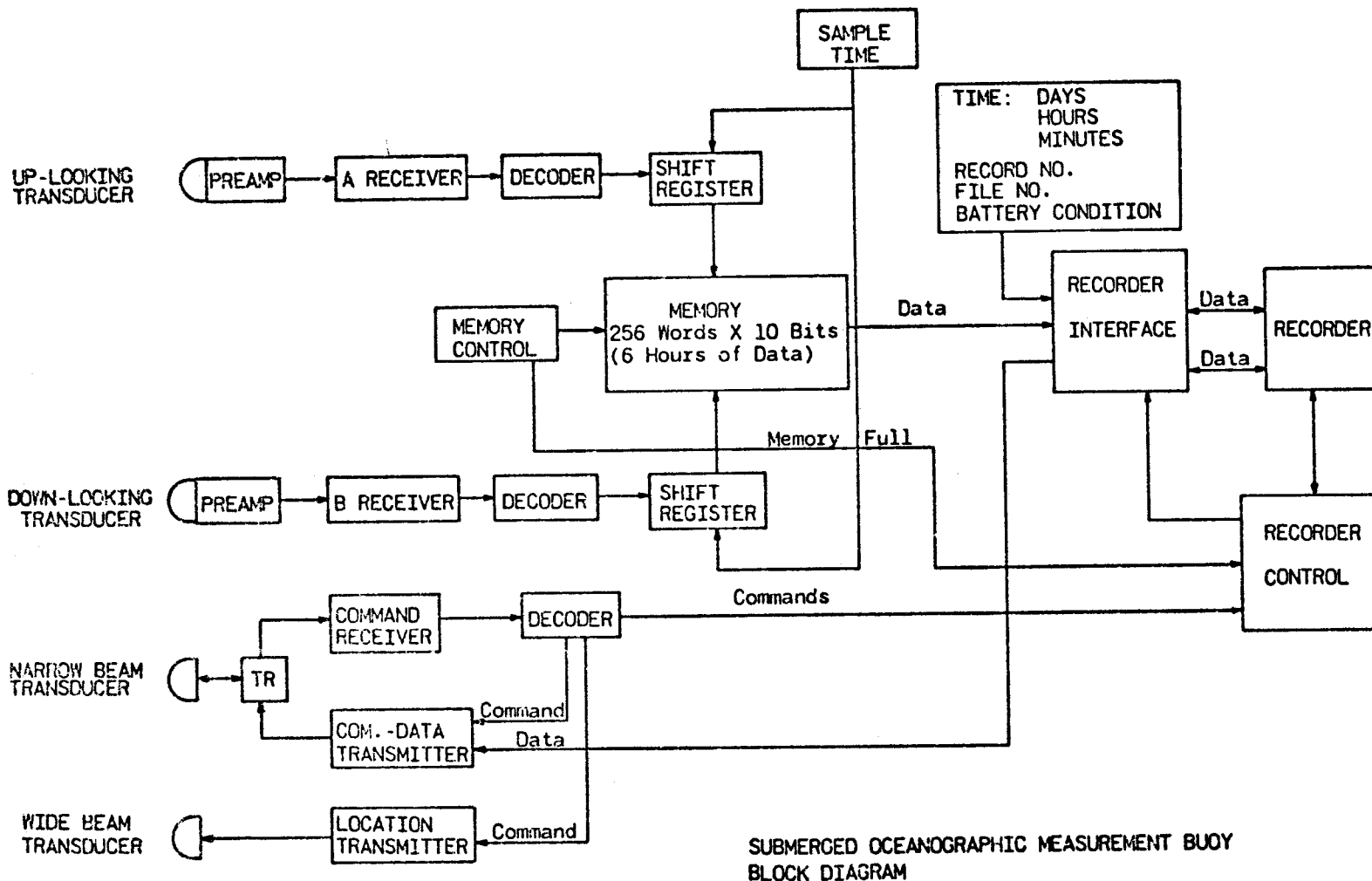
Summer observations have also indicated the likelihood of an intermittent upwelling regime on the eastern part of the shelf. It appears that the upwelling is a response to locally strong easterly winds, and that the water upwelled onto the shelf moves westward.

While tidal effects are thought to be small, storm surges and related effects may be important in effecting changes of short time scale.

Essentially nothing is known of the advective exchange between the shelf and the deep basin.

#### IV. Study area

The area of interest extends eastward from Pt. Barrow along the entire northern Alaska coast, i.e., from about  $156^\circ 30'\text{W}$  to  $141^\circ\text{W}$ , a lateral distance of 600 km. The shelf is narrow, with the shelf break typically 80-90 km offshore. The total runoff is relatively small, highly seasonal, and concentrated in a very few rivers of any consequence, the largest of which is the Colville. The area is covered by sea ice, both first- and multi-year, through all but 2-3 months. Even during the height of summer, ice is usually found well onto the shelf.



SUBMERGED OCEANOGRAPHIC MEASUREMENT BUOY  
BLOCK DIAGRAM

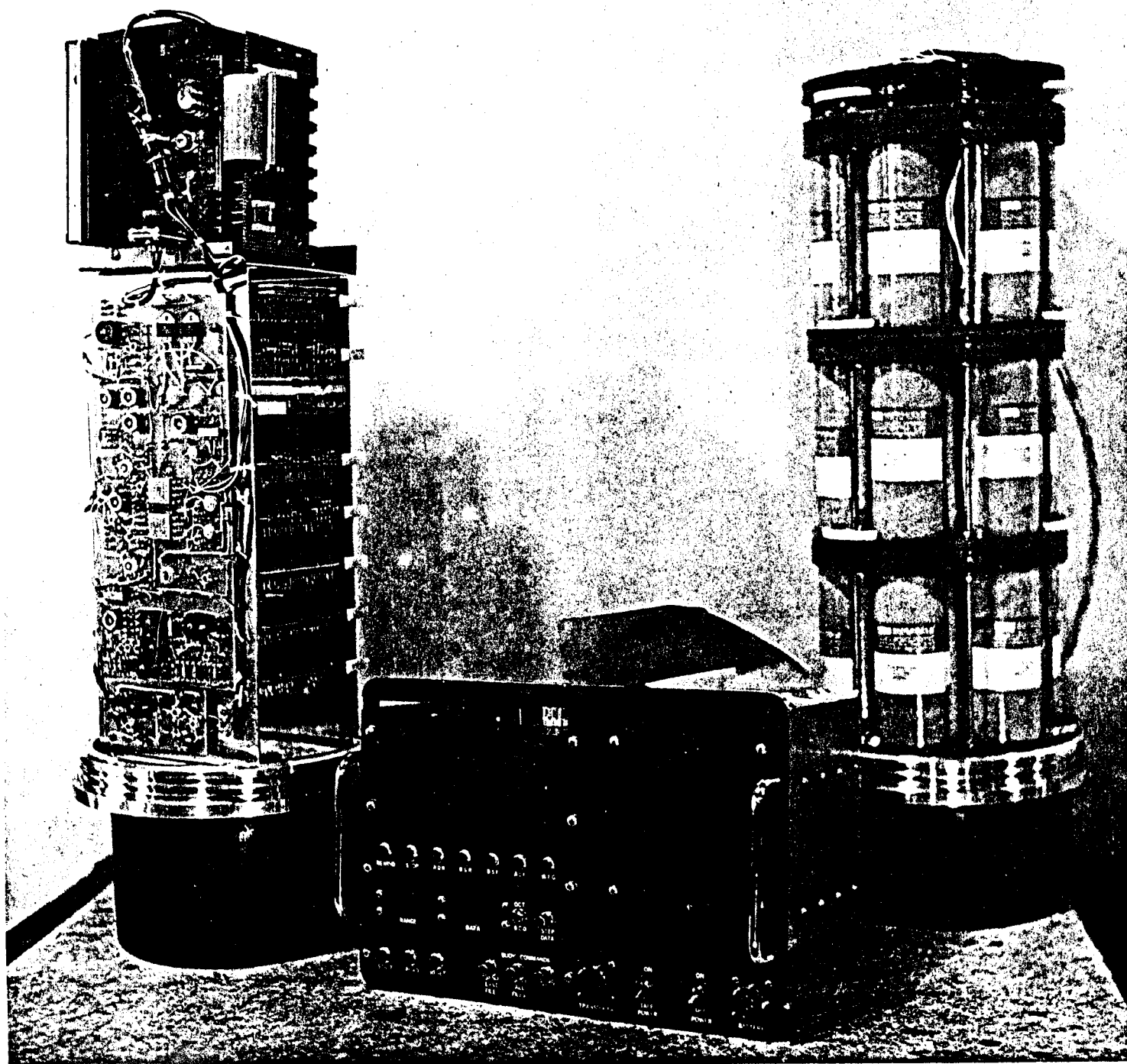


Figure 2. 16

## V. Data collection

It is obviously impossible to attempt intensive time series coverage of the entire region. One is in practice limited to measurements at a few points, hopefully key ones. We selected to measure in Barrow Canyon, at a point down-canyon from the earlier measurements, where the Bering Sea source waters for the Beaufort shelf presumably have begun turning eastward. We also selected two sites more nearly midway along the shelf, at about 150°W. One of these is on the outer shelf and one part-way down the slope, the idea being to get not only a representation of the shelf and adjacent slope flow regimes, but also to examine the possible exchanges between these regimes.

All of these sites can in general be expected to be covered by ice. Since anchored current meters record internally, so that data retrieval is dependent upon instrument recovery (something which has not been done in ice-covered waters), we decided on an alternative set of approaches that provide redundancy in data recovery. The first approach was to transmit the data acoustically. This involves storing the data in such a way that they can be recalled at very high rates upon command, the recall being done from the ice on an opportunity basis. This method has two side benefits, viz. that the current meters can be left in place as long as they continue to function, and that data recovery can be made as often as desired. The second approach to data recovery was to have the instruments record internally as usual, equip them with acoustic releases, and provide the arrays with an acoustic ranging and bearing system to enable pinpointing their position under the ice after having been released and risen to the under-ice surface. A hole can then be cut in the ice and a diver used to attach recovery lines and to aid in bringing the mooring up through the hole.

Each instrumentation system thus is comprised of an anchor, an acoustic anchor release, a lower current meter, a data buoy, an upper current meter, and flotation. The current meters provide current speed, direction, and temperature in binary code. The data buoy is linked acoustically to the current meters, and it houses power supply, digital tape recorder, timing and control electronics, and acoustic telecommunication subsystems. The data buoy and associated systems have been developed and built at the University of Washington. The instrumentation is designed to operate for up to two years. Figure 1 shows a block diagram of the data buoy, and Figure 2 a photo of the electronics, power supply and surface control unit.



## VI. Results

In situ tests of the instrumentation began in Puget Sound on 11 March. Deployment of all three mooring systems in the Beaufort Sea is scheduled for April.

## VII. Discussion

The original plan called for deployment of the first mooring in Barrow Canyon in March, with the other two moorings following in April. We now anticipate all three to be deployed at the same time in April. The major reason for this change is that specifications and delivery schedules for several of the buoy components were not met by the respective manufacturers. For example, when the tape recorder arrived, it proved to be substantially different from specifications. This then in turn required extensive redesign of the recorder control and interface electronics. The redesign has now been completed, implemented, and bench tested.

## VIII. Conclusion

The need for direct long-term current measurements on the shelf and slope, in areas which are generally permanently ice covered, is considerable. We feel we have a very good start on this formidable experimental problem, and we look forward to deployment of three current measuring systems this spring. Our present feeling is that the systems should be left in place as long as feasible, beyond the present contract year if possible.

## IX. Needs for further study

The early data return from the moorings presently scheduled for deployment will no doubt provide shape to future experiments. However, the results

of the temperature-salinity mappings (see annual report, research unit no. 151) already indicate that there is a real need to look carefully at the possible sinking and spreading into the Canadian Basin pycnocline waters modified on the Beaufort shelf. At present we visualize that a series of CTD sections between  $154^{\circ}$ - $148^{\circ}$ W will have to be made in conjunction with several current meter installations near the shelf break.

## X. Summary of fourth quarter operations

## A. Field activities

Field testing is presently in progress in Puget Sound. Three systems with a total of six current meters are to be deployed in the Beaufort Sea in April.

## B. Estimate of funds expended

## Department of Oceanography, as of 5 March 1976

|                               |         |
|-------------------------------|---------|
| 1. Salaries - faculty & staff | \$1,309 |
| 2. Benefits                   | 196     |
| 3. Indirect costs             | 573     |
| 4. Equipment                  | 33,846  |
| 5. Supplies                   | 15,790  |
| 6. Travel                     | 504     |
|                               | <hr/>   |
| total                         | 52,218  |

## Applied Physics Laboratory, through 29 February 1976

|   |        |
|---|--------|
| 1. Salaries   | 31,976 |
| 2. Benefits, administrative expenses,<br>indirect costs | 31,915 |
| 3. Purchases and materials                              | 17,970 |
|   | <hr/>  |
| total   | 79,861 |

Total estimated expenditures \$132,079



ANNUAL REPORT

Contract # 03-5-022-56

Research Unit # 111

Reporting Period 4/1/75 - 3/31/76

Number of Pages 38

EFFECTS OF SEASONABILITY AND VARIABILITY OF STREAMFLOW ON  
NEARSHORE COASTAL AREAS

Dr. Robert F. Carlson

Institute of Water Resources

University of Alaska

March 31, 1976

## OCS ANNUAL REPORT

### Effects of Seasonability and Variability of Streamflow on Nearshore Coastal Areas

R. F. Carlson, Principal Investigator

#### I. Summary of Objectives with Respect to Oil and Gas Development:

An understanding of the seasonability and variability of streamflow is of considerable engineering importance to the imminent oil and gas development. Streamflow variability, the effects of seasonal ice, as well as sediment characteristics and ice jam flooding have considerable impact on nearshore and estuarine areas. This is especially so in areas where sea ice remains intact after the initiation of river break-up. This occurs in nearly all rivers and streams in the North Bering, Chukchi, and Beaufort Seas, because the extensive areas of shorefast ice formed annually in these areas. The estuarine and shorefast areas are presently being developed and leased and this development is likely to continue throughout the O.C.S. program. An analysis of the annual seasonability of streamflow, expected break-up data, expected freeze-up data, and sediment characteristics are all necessary information to insure safe and efficient offshore development.

On the Gulf of Alaska coast, where precipitation is higher and the effects of offshore ice are more limited, streamflow variation, the spring flood, and the sparse data that is available make it necessary to establish indices of seasonability and variability to allow for extrapolation to ungaged streams. More on the scope of the study will be found in the next section.

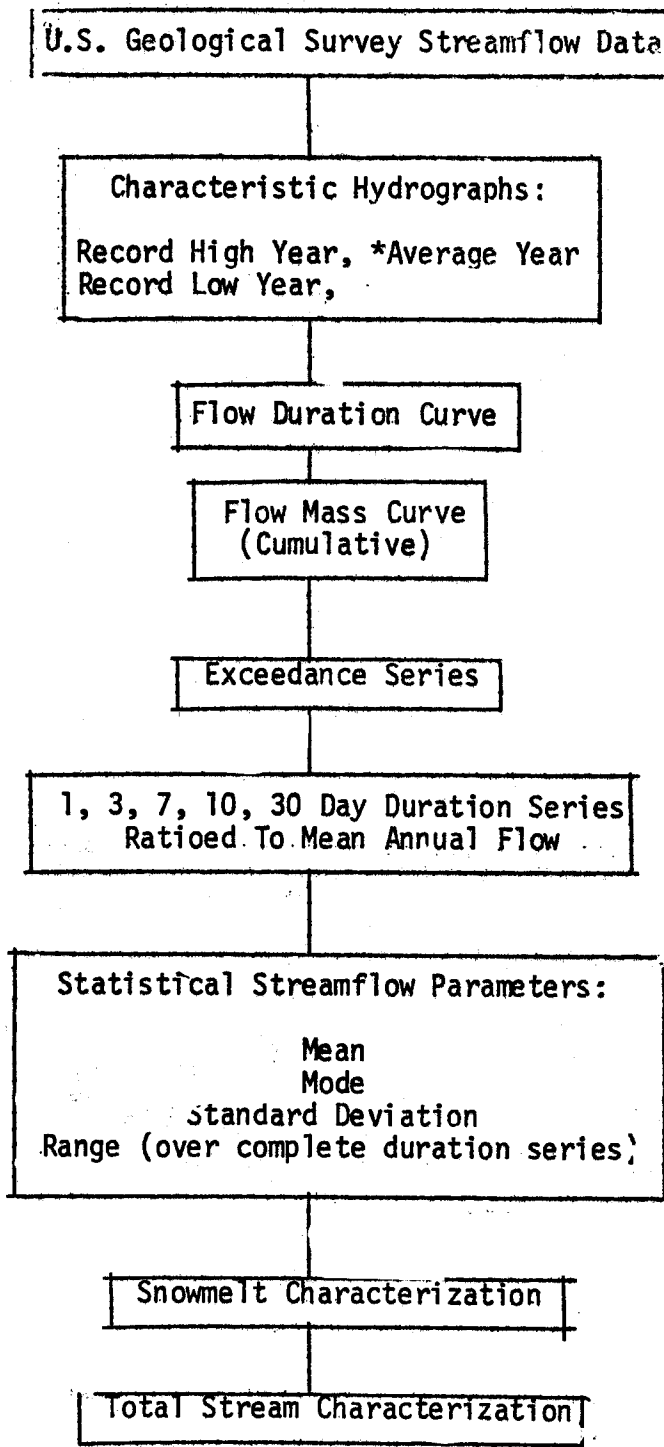
## II. Introduction:

### A. General nature and scope of the study:

This study is attempting to examine the variability of streamflow in all gaged Alaskan rivers and streams which terminate in the ocean. There are 41 such streams which have been gaged for varying periods of time by the U.S. Geological Survey, Water Resources Division. Attempts have been made to characterize streamflow statistically using standard hydrological methods. The analysis scheme which is followed in the flow chart which follows. In addition to the statistical characterization, the following parameters will be described for each stream when possible:

1. average period of break-up initiation (10 day period)
2. average period of freeze-up (10 day period)
3. miscellaneous break-up and freeze-up data
4. relative hypsometric curve for each basin.
5. observations on past ice jam flooding
6. verbal description of annual flow variation
7. use of original indices developed in this study (described in section B) to relate streamflow variability to basin characteristics and regional climate.

FLOW CHART - O.C.S. STREAM CHARACTERIZATION



\*Average Year is that year during which the mean annual flow was closest to the mean annual flow for the length of record.



B. Specific Objectives:

1. The primary objective of this study is to develop a characterization of coastal streams in Alaska which is relevant for engineering applications, useful to the imminent OCS petroleum development, and also generally useful to as many other agencies, individuals, and commercial interests who have needs for such information.
2. Realizing that characterization of streams in other regions of the United States may not be adequate to describe Alaskan streams, an original approach was used to develop an index for stream characterization in this study. After trying several indices, it was decided that a graphic plot of the ratio of the 1, 3, 7, 10, and 30 day maximum cumulative daily flows to the mean annual flow was an adequate characterization index. This index is a strong indication of short term variability, and is also probably a function of basin size. Several examples of this index are included in the results.
3. A grouping of most ungaged streams was accomplished using regional and physical similarities to gaged streams as criteria. This grouping is intended to be a guide for extrapolation of the characterization of gaged streams to streams which have similar basin areas, climate, and elevation distributions, but are not gaged by the U.S. Geological Survey.
4. An attempt was made to establish a relationship between precipitation and elevation in order to better characterize snowmelt patterns.

5. NOAA and LANDSAT satellite imagery are being used as major sources of information to characterize snowmelt in both gaged and ungaged basins.
6. Sediment relationships are being investigated whenever possible using all available sources of information.

C. Relevance to problems of petroleum development:

1. Ice and spring break-up are critical engineering problems which need to be considered for nearshore oil development and exploration. Logistics and scheduling may be severely disrupted by unforeseen or unknown problems related to rivers, spring run-off, and ice. A problem unique to the Arctic is that of flooding of the shorefast ice at the mouths of rivers during spring break-up. Satellite observations of several ungaged streams in the Arctic indicate that this event is endemic but the timing of the initial flooding is variable. Ice jams are a problem, especially on the Yukon River. A major danger from ice jams is the possibility of a rapid break of the jam which could release dammed water and cause flooding downstream. Floating ice is also an engineering hazard. Ice jams will be discussed further in the results section.

Snow cover and snowmelt characteristics which will be investigated in this study should lead to a better understanding of snow melt rate. The relationships which exist between melt rate and runoff may also become more evident. A knowledge of these influences on nearshore development will be important to petroleum development as well as the planning and public works agencies of government.

### III. Current State of Knowledge:

As stated in our original proposal, we know of no directly related research being carried out by others. A bibliographic search was made using the OASIS system. A report entitled "Environmental Studies of an Arctic Estuarine System" (EPA, 1975) contains baseline information on the effects of river flow in an Arctic estuary, which is relevant to this work. Many papers address the problem of coastal breakup in Arctic areas (Newburg, 1974, Antonov, *et al.*, 1972, Reimnitz, *et al.*, 1974, Barnes, *et al.*, 1973, Walker, 1973, McCloy, 1970, Reimnitz, *et al.*, 1972, Walker, 1970). A discussion of the land hydrology of Southcentral coastal zone is found in Carlson (1972). A regional discussion of sediment yield in Alaskan streams is given by Guymon (1974).

Some correlative studies of snow measurements made on the ground with remote sensing observations have been done by Bilello (1974). Poulin (1974) used infrared satellite imagery to determine the hydrologic characteristics of snow-covered terrain.

Carlson (1974), and Newburg (1974) both addressed the effects of permafrost on river hydrology. Permafrost or glacial influences effect nearly all major hydrologic systems in Alaska.

The general state of knowledge for characterizing streams in lieu of coastal development is inadequate. More hydrologic research has been done in the Beaufort Sea drainage than elsewhere. No areas of Alaska are as well studied, and no direct research is being carried out.

#### IV. Study Areas:

We are characterizing all gaged streams in all the O.C.S. areas of interest:

1. Gulf of Alaska
2. Southern Bering Sea
3. Northern Bering - Chukchi Seas
4. Beaufort Sea

#### V. Sources, Methods:

Our major source of data is the U.S. Geological Survey streamflow records and water quality data. Using a tape which contains all the stream records of interest, we have written programs to extract the statistical parameters and hydrograph records from the tape. This data enables us to characterize the seasonability and variability of streamflow.

To obtain break-up and freeze-up information, the standard U.S. Geological Survey annual water resources data catalogs were examined for evidence of those events in the record. Some data on break-up and freeze-up is also available from the U.S. Weather Service, and from the Environmental Atlas of Alaska (Johnson and Hartman, 1969).

The snowmelt characterization will be accomplished using both NOAA - Very High Resolution Radiometer (VHRR) and LANDSAT satellite imagery, as well as any aerial photography which may become available as a result of the OCS remote sensing program.

Much of our data has been updated to include the 1974 data which recently has become available.

Our computer processing work has been additionally aided by existing programs supplied by the Alaska district of the U.S. Army Corps of Engineers in Anchorage. The selection of the 1, 3, 7, 10, and 30 day maximum period flows have been accomplished through one of the Corps' programs. By determining the ratio of these flow durations to the mean annual flow, a quantitative indicator of streamflow variability has been established.

Sedimentation characterizations have not yet been accomplished. U.S. Geological Survey data will also be the main source of this information.

## VI. Results

Four exemplary river characterizations are presented. Each river is from a different area of interest of the OCS leasing program. They are as follows:

| TABLE 1                        |                        |  |               |
|--------------------------------|------------------------|--|---------------|
| River                          | Region                 | Basin Area                                     | Record Length |
| Kenai River @ Soldotna         | Gulf of Alaska         | 5,210 km <sup>2</sup> (2010 mi <sup>2</sup> )  | 9 years       |
| Kulchak River @ Igiugig        | South Bering           | 16,800 km <sup>2</sup> (6500 mi <sup>2</sup> ) | 7 years       |
| Kobuk River @ Ambler           | North Bering - Chukchi | 17,020 km <sup>2</sup> (650 mi <sup>2</sup> )  | 9 years       |
| Kupurak River @ near Deadhorse | Beaufort               | 8,107 km <sup>2</sup> (3130 mi <sup>2</sup> )  | 3 years       |

Following the scheme of the characterization flow chart for each river, some of the characterizations are shown along with a relative hypsometric curve, breakup and freeze-up data and snowmelt information when available. The variability is shown via plots of the ratios of the 1, 3, 7, 10, and 30 day maximum flows to the mean annual flow for the period of record. Major plot routines for

stream characterizations will be computer produced and will be submitted as they become available. These include the maximum, minimum, and average hydrographs, and the flow mass curve.

Kenai River at Soldotna:

Mean Annual Flow: 5371 CFS

Mode: 1000 CFS

Standard Deviation: 18888 CFS

Range: Maximum recorded flow: 30000 CFS

Minimum recorded flow: 770 CFS

Breakup Period: \*Mean 10-day

Initiation period - April 22 - May 1

Average Date (U.S.W.S. Record - 15 years) - April 16

Freeze-up Period: \*Mean 10-day

Initiation Period - November 5-14

Ice is never very thick and usually unsafe for a man to cross the river all winter.

Records of freeze-up and break-up from the U.S. Coast Pilot for the period 1937-1952 give an average freeze-up date of December 10, and an average break-up of April 2. The earliest break-up occurred March 18, 1952 and the latest April 14, 1951. Freeze-up was earliest on November 23, 1951 and latest on December 26, 1937. These figures differ somewhat from the estimates from the streamflow records given above.

The Kenai River has a very subtle seasonal change, and consequently it is extremely difficult to determine the freeze-up date from only streamflow records. Any such estimates should be used with this qualification in mind, especially if a river shows a low level of seasonal variability, as the Kenai does.

---

\*Estimates from annual streamflow records.

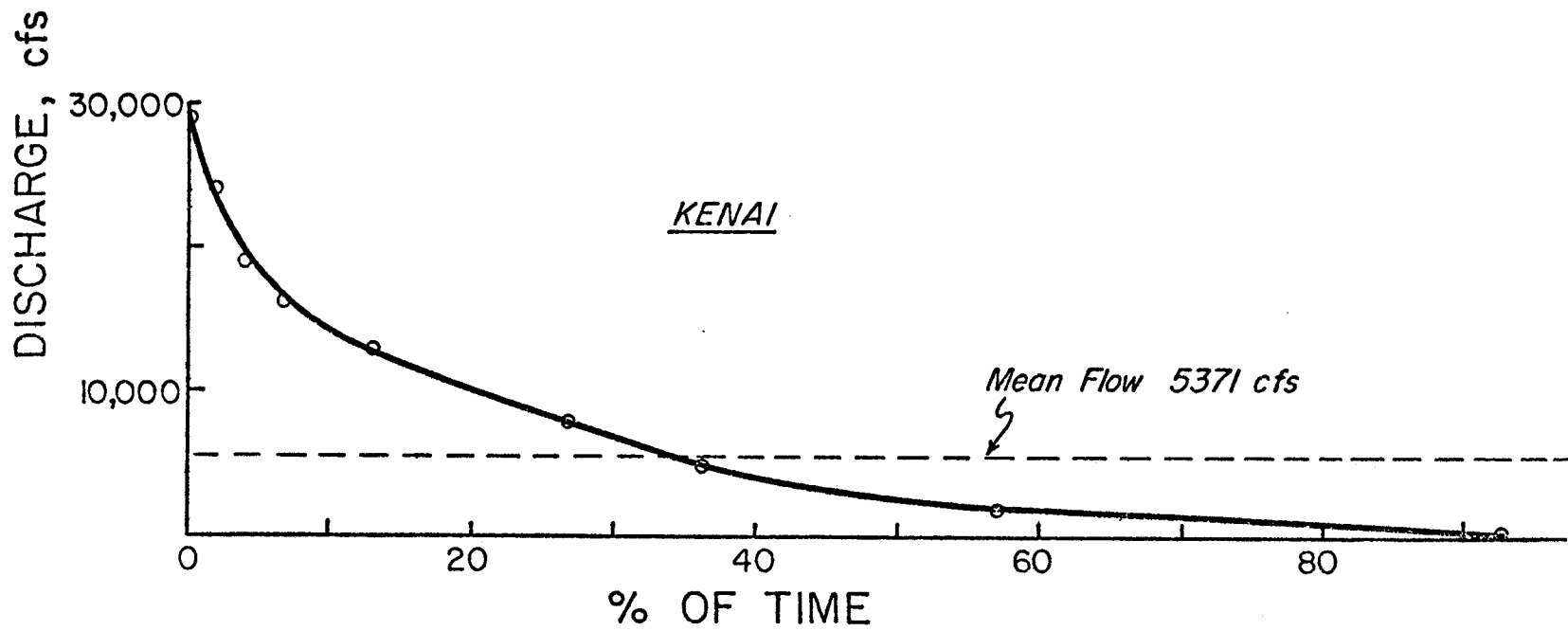


Figure 1: Flow Duration Curve - Kenai River at Soldotna.  
(Record Length - 9 years)



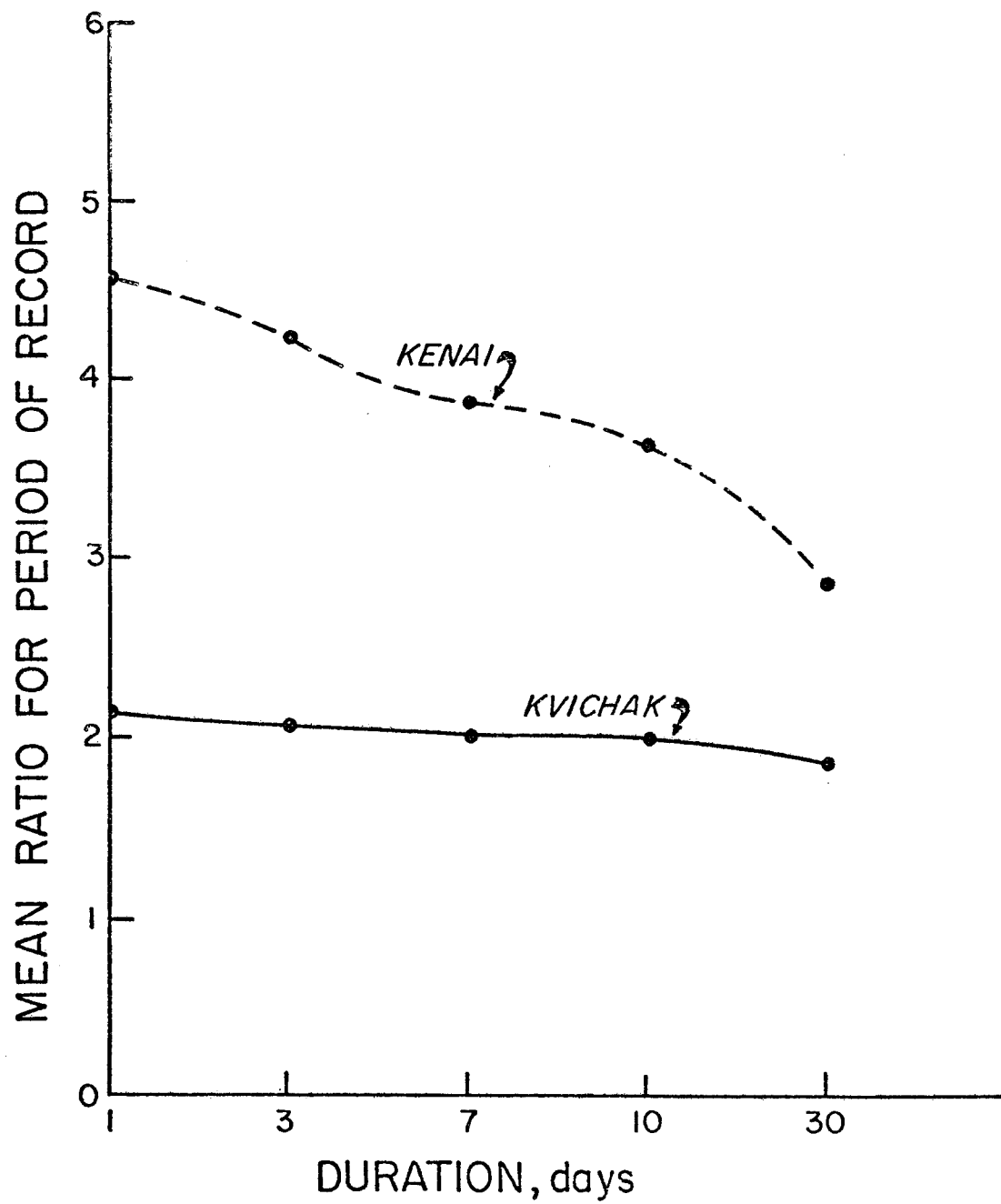


Figure 2: Ratios of the Average 1, 3, 7, 10, and 30 day Maximum Annual Flows to the Mean Annual Flow for the Kenai and Kvichak Rivers. Note the Distinct Lack of Variability Indicated by the Kvichak Curve.

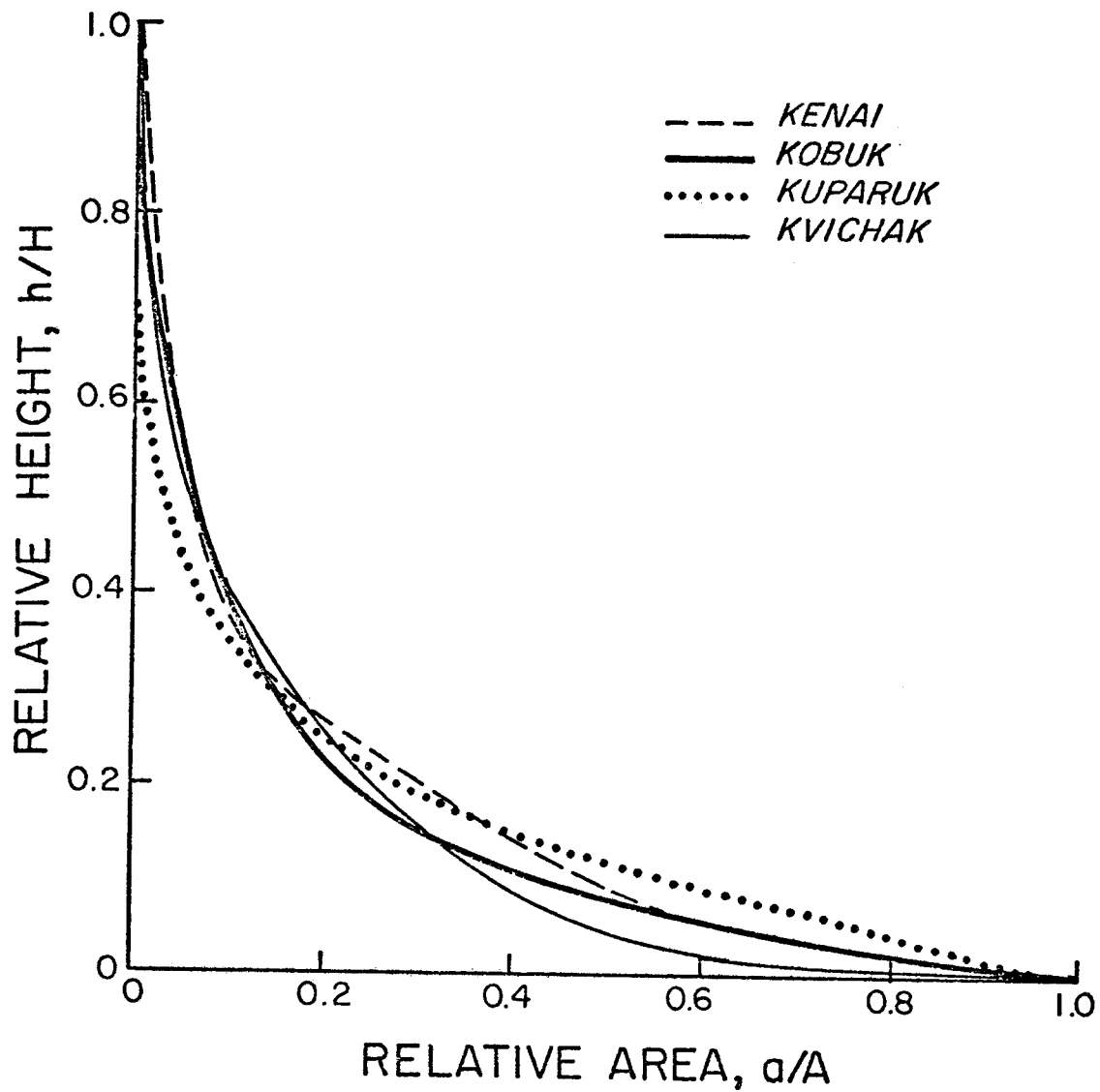


Figure 3: Relative Hypsometric Curves for the Kenai, Kobuk, Kuparuk, and Kvichak Rivers.  $H$  = Maximum Elevation,  $A$  = Total Drainage Area, and  $a$  = Drainage Area Above a Given Elevation  $h$ .

Kvichak River at Igiugig:

Mean Annual Flow: 16980 CFS

Mode: 13000 CFS

Standard Deviation: 3782 CFS

Range: Maximum recorded flow - 43000 CFS

Minimum recorded flow - 6400 CFS

Break-up Period: \*Mean 10-day

Initiation period - May 10-19

Freeze-up Period: \*Mean 10-day

Initiation period - November 27 - December 6

Little could be determined about the thickness of ice, however, data from the U.S. Coast Pilot gives the average freeze-up and break-up of the Kvichak River for the period 1937-1940. Average break-up was May 4, and the earliest break-up was April 26. Average freeze-up was December 22, the latest having occurred on January 30, and the earliest on November 23. Obviously, since there are only three years of record, and ice conditions are so variable, it is difficult to predict freeze-up with any assurance.

---

\*Estimated from annual streamflow records.

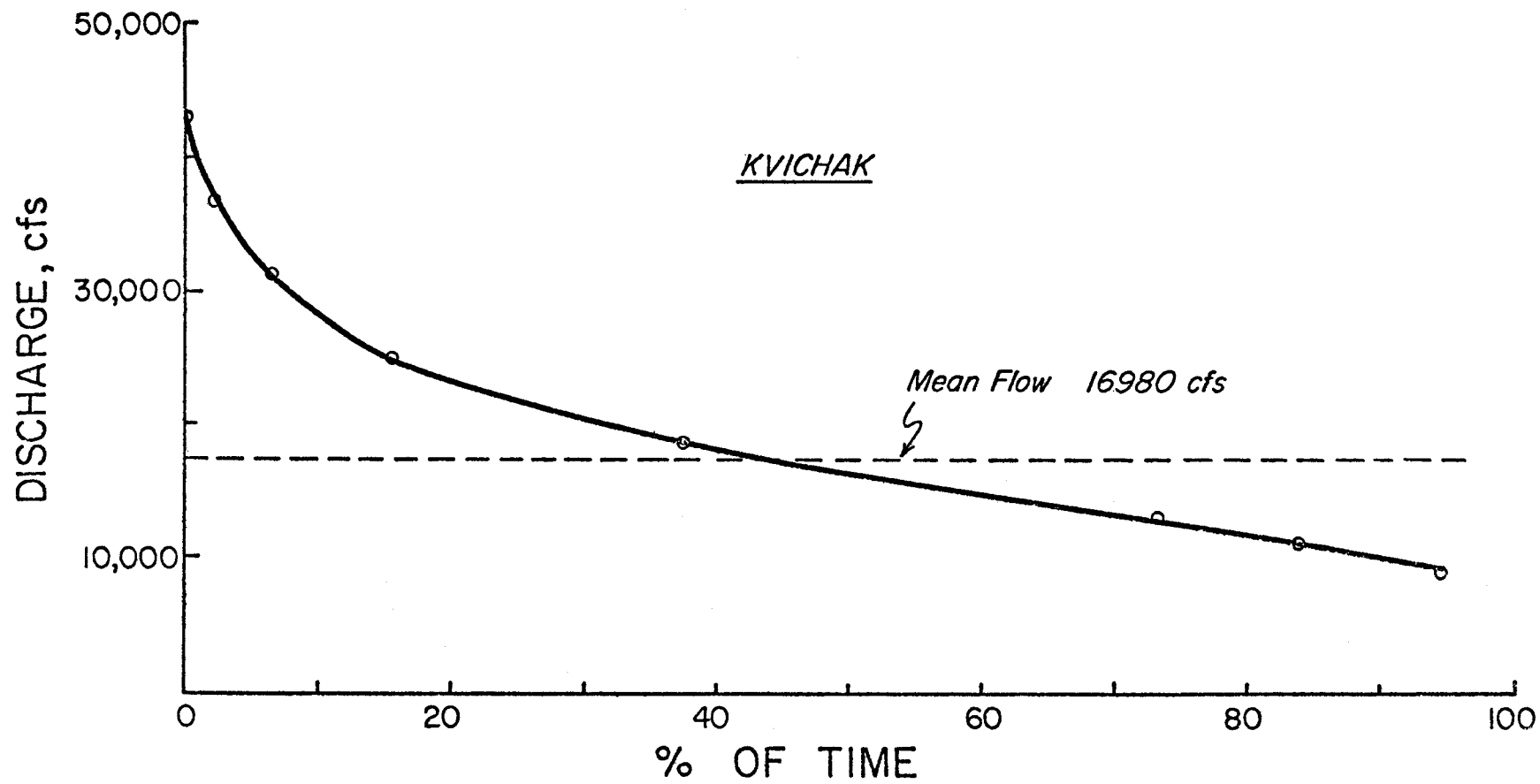


Figure 4: Flow Duration Curve - Kvichak River at Iglugig.  
(Record Length - 7 years)

Kobuk River at Ambler:

Mean Annual Flow: 9481 CFS  
Mode: 1300 CFS (winter flow - not gaged)  
Standard Deviation: 24549 CFS  
Range: Maximum recorded flow - 95000 CFS  
Minimum recorded flow - undetermined  
Break-up Period: \*Mean 10-day  
Initiation period - May 12-21  
Freeze-up Period: \*Mean 10-day  
Initiation Period - October 9-18

Additional ice information is available on ice conditions at four different villages on the Kobuk River which pre-dates 1952. The information is shown below:

DATES OF ICE BREAKUP AND FREEZE-UP

|              |             | <u>Ice breakup</u> |         |         | <u>Ice freeze-up</u> |          |          |
|--------------|-------------|--------------------|---------|---------|----------------------|----------|----------|
| <u>Place</u> |             |                    |         |         |                      |          |          |
| Noorvik      | Kobuk River | May 29             | 5/18/25 | 6/11/22 | Oct. 11              | 9/26/48  | 10/25/22 |
| Kiana        | "           | May 18             | 5/ 7/40 | 5/29/39 | Oct. 18              | 10/10/39 | 11/ 4/38 |
| Kobuk        | "           | May 19             | 5/11/43 | 5/29/45 | Oct. 21              | 10/ 9/39 | 11/ 2/38 |
| Shungnak     | "           | May 21             | 5/12/41 | 5/29/45 | Oct. 16              | 10/ 7/19 | 10/25/40 |

\*Estimated from U.S.G.S. streamflow data.

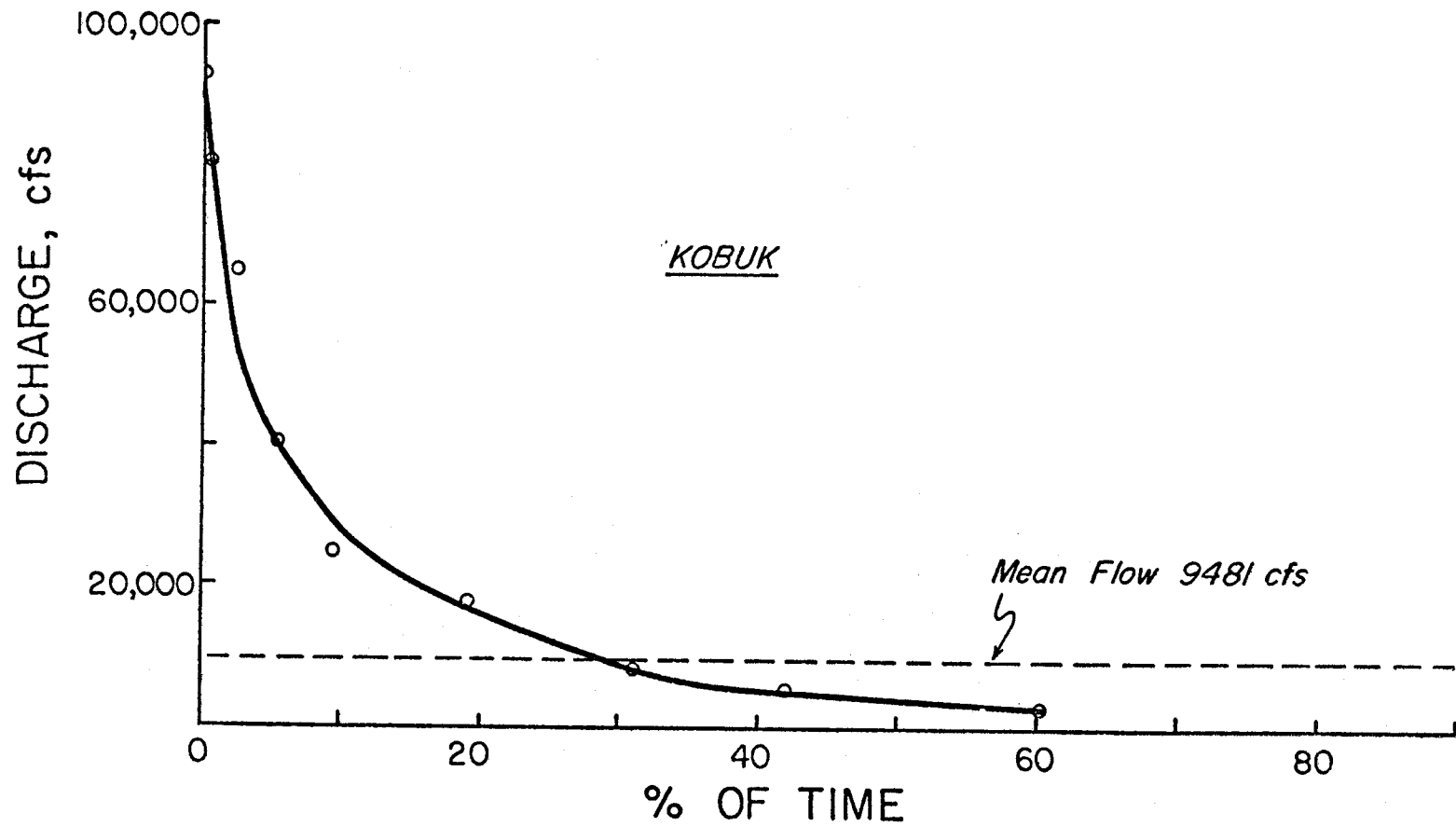


Figure 5: Flow Duration Curve - Kobuk River at Ambler.  
(Record Length - 9 years)

Kuparuk River near Deadhorse:

Mean Annual Flow: 1600 CFS (winter flow estimated)

Mode: 10 CFS (winter flow estimated)

Standard Deviation: 31809 CFS

Range: Maximum recorded flow - 82000 CFS

Minimum recorded flow - 10 CFS

Breakup Period: \*Mean 10-day

Initiation period - May 20 - June 8

Freezeup Period: \*Mean 10-day

Initiation period - September 20-29

Additional breakup information is available from NOAA satellite imagery and LANDSAT satellite imagery.

---

\*Estimated from the U.S.G.S. streamflow data.

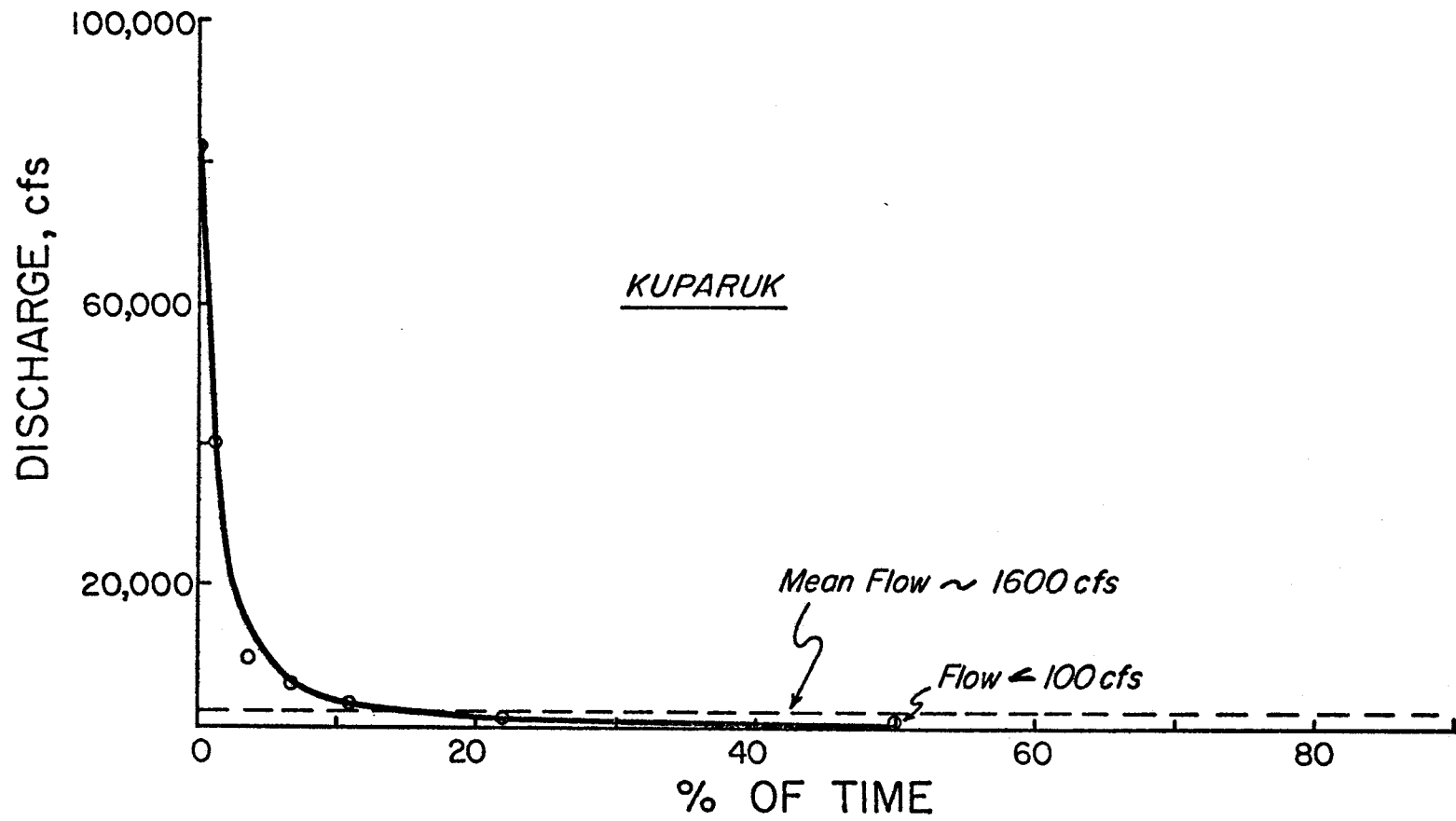


Figure 6: Flow Duration Curve - Kuparuk River Near Deadhorse.  
(Record Length - 3 years)



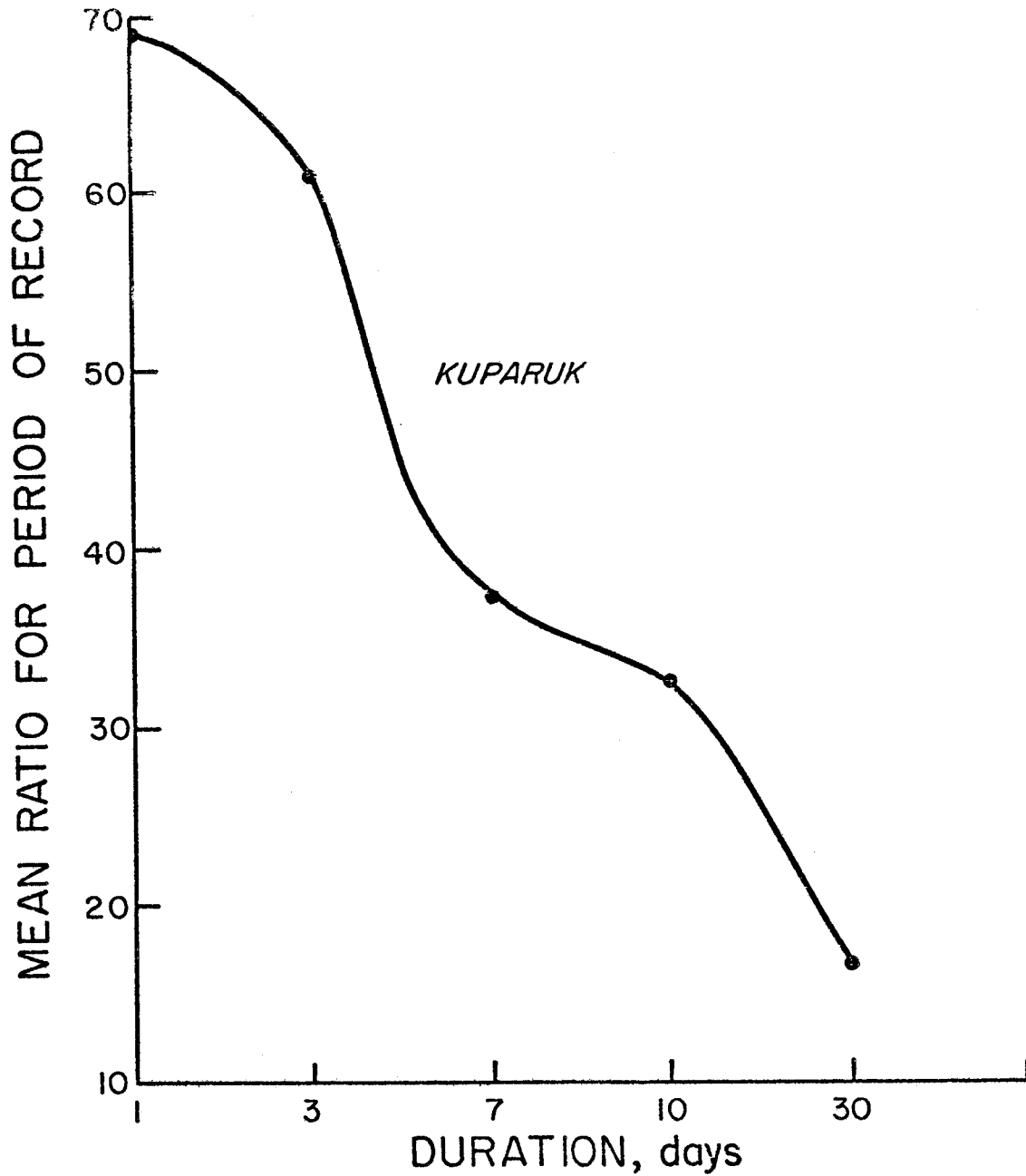


Figure 7: Average of the Annual 1, 3, 7, 10, 30 Day Maximum Flows to the Mean Annual Flow for the Kuparuk River. Note that the Maximum 1 Day Flow is 68 Times Larger than the Annual Mean Flow.

### Snowmelt Characterizations:

#### 1. General observations - NOAA VHRR satellite imagery:

Snowmelt begins in the lowlands of the southern half of Alaska (south of the Yukon River) during the month of April and in the extreme southern part of the state in March. Melt in interior Alaska often begins at about the same time as in the coastal areas and proceeds rapidly because of the drier conditions and the more continental climate.

First areas to become snowfree are the low-lying regions of the Tanana Valley, the Copper River valley north of Chitina, the Matanuska Valley, and low areas of the Yukon Valley above Rampart, and downstream from Tanana to Ruby. The valleys of the upper Sagavanirktok, Itkillik, Killik, and Anaktuvuk Rivers and some of their tributary valleys are also snowfree early in the season. However, these river valleys are more often subject to wind erosion of the snowpack and consequently less runoff results from these snowfree areas than from areas further south.

Snowmelt then spreads to the lower Koyukuk, and throughout the interior lowlands of the Tanana and Yukon Valley. Slowly, the areal extent of snowmelt increases through the lowlands of the state, including the lower Kuskokwim River valley. As the days become warmer by mid-May, most of the elevations less than 900 meters are snowfree and coastal areas in the southern half of Alaska are melting or snowfree. Enhanced thermal IR imagery from the NOAA-3 satellite indicates that on May 12, 1975, melting was occurring or complete at most elevations everywhere in Alaska except the coastal plain and lower foothills of the Arctic Slope region.

Generally, shorefast ice and snow near the western Alaskan coast lags other areas of melt. Probably this is a result of the "heat sink" effect

of the shorefast ice, sea ice, ice-covered lakes, and the overall influence of the cooler, marine climate. These combined effects also dominate the snowmelt on Alaska's Arctic Slope. The snowcover in this region is the last area of seasonal snow cover to disappear, often persisting until early June. This results in an anomalous pattern of snowmelt in the North Slope region. The mid-elevations (600-900 meters) are the areas of snowmelt initiation on the Arctic Slope, and snowmelt proceeds in both directions from these mid-elevations, with the lowest elevations often the last to become snowfree.

INDIVIDUAL BASIN OBSERVATIONS  
(LANDSAT AND NOAA-VHRR SATELLITE IMAGERY)

Kenai River Basin:

This basin consists of two geological provinces, the Kenai mountains, and a relatively flat coastal plain, which have different geomorphological characteristics. In addition to its complicated geology, the basin has several (six) glaciers of varying sizes which contribute to the runoff as well as three major lakes, Skilak, Kenai, and Upper Russian Lake. Snowmelt and accumulation are accordingly variable, and the lakes appear to regulate streamflow which masks rapid changes in runoff.

The Kenai and Snow Rivers (a tributary) are also subject to glacier dammed lake outburst floods. These floods are caused by the release, either sudden or gradual, of glacier dammed lakes at the headwaters of the Snow River (Post and Mayo, 1971). A history of glacier dammed lake outburst floods on the Kenai River is also given by Post and Mayo (1971).

Snowmelt observations are difficult in the Kenai Peninsula using remote sensing techniques, and only a very few days during April and May are clear enough for adequate satellite views. Snow was still evident on April 22, 1975, but had melted over much of the basin below an altitude of 150 meters by May 18. Generally snowmelt is altitude related in the Kenai Peninsula following the expected scheme of melt from the lowest to higher elevations. Melt of glaciers and high mountain snow continues intermittently all summer depending upon weather. Average snow depth for the Kenai River basin is measured at the following sites by the U.S.D.A. Soil Conservation Service:

TABLE 2

| Site         | Elevation<br>(m feet) | Average<br>Water Content of<br>Snow Pack (cm) | Years of Record |
|--------------|-----------------------|---|-----------------|
| Jean Lake    | 187 m<br>(620 ft)     | 2.28 cm (0.9 in)                              | 5               |
| Kenai Summit | 421 m<br>(1390 ft)    | 25.4 cm (10.0 in)                             | 5               |

### Kvichak River Snowmelt Characterization

The Kvichak River basin although larger, is similar in complexity to the Kenai River basin. The Kvichak River drains both Lake Clark and Lake Iliamna, and therefore changes in runoff are not rapid due to the attenuation and storage of these lakes. Glaciation is minimally present. More than 53% of the basin lies below 150 meters elevation. No snowcourse measurements are made in the Kvichak drainage. Consequently the only snowmelt observations available are those from satellite imagery.

Although at a lower latitude than most of the Kenai Peninsula, the initiation and progress of snowmelt is generally delayed in time compared to the Kenai Peninsula. On May 6, 1975, only small snowfree areas are present at the southwestern end of Lake Iliamna. By May 9, however, most of the area below 150 meters elevation has melted, probably the result of very warm weather. On May 17, the situation has not changed considerably, and ice still completely covers Lake Iliamna and Lake Clark.

By June 3, 1975 melt had substantially reduced the snowpack and snow was present only above  $\sim 1500$  m. Snowmelt runoff probably enhances melt on the lakes in the basin as meltwater floods the surface, increasing the melt rate.

### Kobuk River - Snowmelt Characterization:

In most of western and northern Alaska, there are no snowcourse measurements and it is only possible to describe the snowmelt sequence using satellite imagery.

Very small patches of melting snow were apparent on the NOAA imagery of May 8, 1974. A week later on 15 May a major portion of the lower elevations

have experienced melting with some snowfree areas. Ablation rate appears to be generally correlated with elevation as in most of southern and interior Alaskan basins. Melt is 95% complete by June 10 and probably is 100% complete by June 20. No glaciation is present, even though altitudes reach 2050 m.

Although Hotham Inlet remains frozen until at least June 10, 1975, never were there any signs of the sea ice being flooded by fresh water from the Kobuk.

#### Kuparuk River - Snowmelt Characterization:

The Kuparuk River basin is one of the several river basins on Alaska's North Slope which exhibits a peculiarly different snowmelt pattern from the usual scheme in which snow melts in the lowlands first and melt progresses toward the higher elevations.

In the Kuparuk basin, snowmelt is initiated at the higher elevations during the last week in May, and progresses toward the lower, farther north coastal plain, which is the last area to become snowfree. Because of this, meltwater flows down the stream channel overtop the ice and floods large areas of shorefast sea ice. Melt occurs rapidly and is usually completed by the third week in June, but can be later. In the three years of record, from 60 to 80% of all runoff for the entire year constituted snowmelt runoff in the month of June.

A NOAA image, dated June 4, 1975 is on the following page. It shows flooding of the shorefast ice at the mouths of the Colville, Kuparuk, Sagavanirktok and Canning Rivers, and in Kasegaluk Lagoon on the northwest coast of Alaska. The anomalous snowmelt pattern is also very evident in this image.

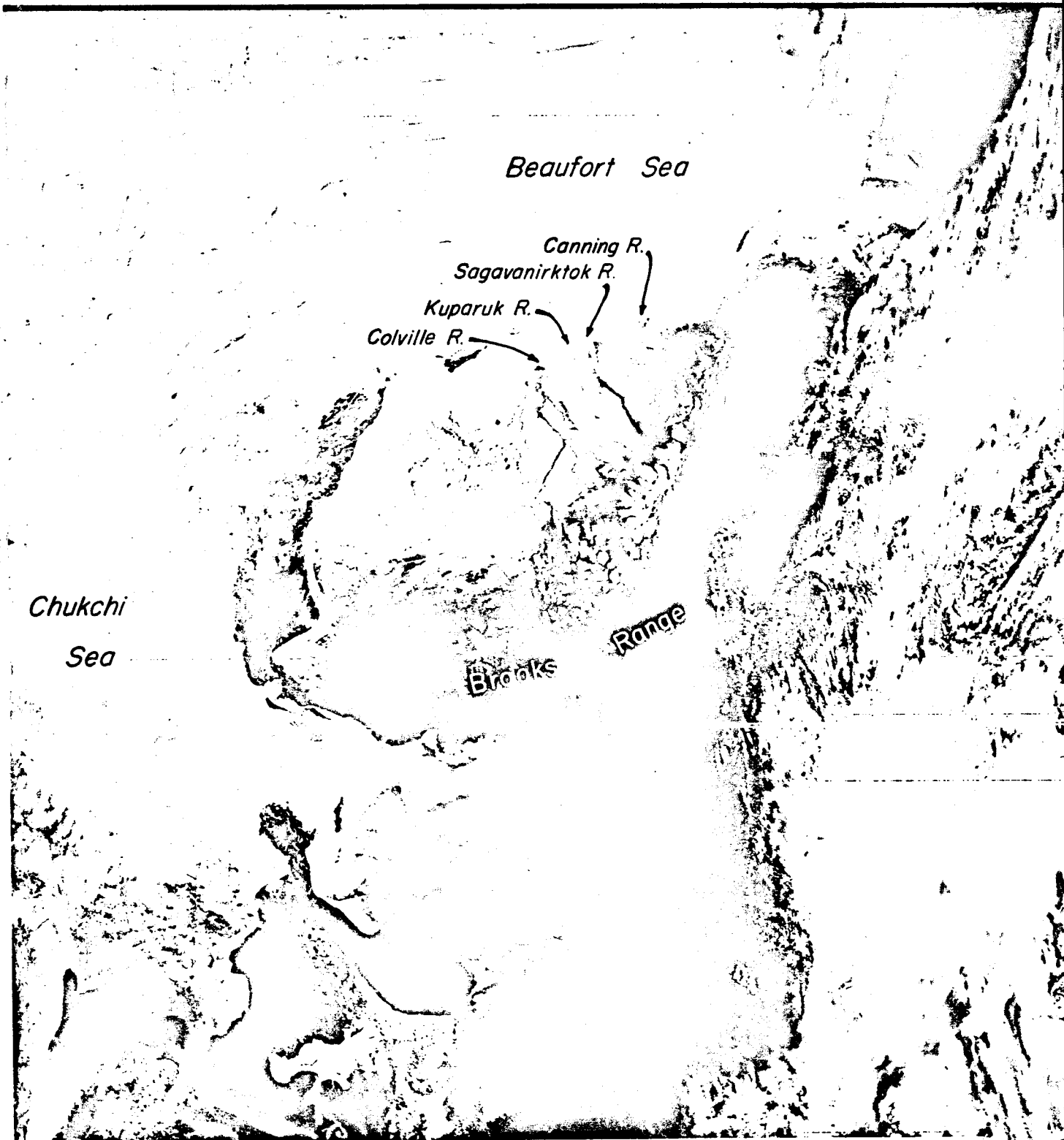


Figure 8: NOAA-VHRR Satellite Image, Visible Band, June 4, 1975. Meltwater is Flooding the Shorefast Sea Ice at the Mouths of the Sagavanirktok, Canning, Kuparuk, Colville and Utukok River (Kasegaluk Lagoon). The North Slope Snowmelt Pattern is also Clearly Illustrated.

5:21:02:48 2519

V2F2276 04JUN75 N4 13S



## VII. Discussion:

Only part of the total characterization for each of the four representative rivers is given here. The graphic elements mentioned earlier were not presented since they will be produced using computer plot routines which are still being developed. This includes the flow mass curve, maximum, minimum, and average hydrograph and the exceedence series.

We have tried to be as encyclopedic as possible and yet concise and give a condensed characterization. This is the reason for the use of the 1, 3, 7, 10, and 30 day average annual maximum flow ratios. This plot yields an understandable graphic characterization of the average variability of streamflow. The snowmelt description is a qualitative description of the seasonal effects on runoff.

As can be seen from the snowmelt characterization, and from the 1, 3, 7, 10, and 30 average maximum flow plots, there does appear to be a regional character of streams in each of the four areas of O.C.S. interest. It is more evident in the larger streams. Gulf Coast and Cook Inlet area rivers, with the influence of glaciers and lakes, have a stable hydrograph which does not fluctuate rapidly in response to precipitation. Flood dangers are present on the Kenai, Copper, Rude, and Knik Rivers due to the presence of glacier dammed lakes in the basins. On the west side of Cook Inlet, similar dangers exist on the Beluga, Chakachatna, McArthur and Big Rivers, although less is known about the frequency of outburst flood events on these streams.

Most of the gaged rivers in the Southern Bering Sea are strongly influenced by large lakes in the drainage basins (Kvichak, Nuyakuk, Wood Rivers). Variability in flow is attenuated by the lakes and seasonal variations also are not dramatic or rapid. The Kuskokwim River Basin is large and has seasonal variations similar to most interior Alaskan streams.

Two rivers are gaged in the North Bering - Chukchi region : the Kuzitrin, on the Seward Peninsula, and the Kobuk River which drains a large area of the southwestern Brooks Range. This region has a hybrid climate which is influenced by both interior and arctic Alaskan conditions. Precipitation is relatively light and spring snowmelt runoff is the major factor in seasonal variability of streamflow.

These two rivers are representative of the major river types in the region. The Kuzitrin drains a piedmont-type area and its basin is not large (4450 km<sup>2</sup>). The Kobuk River basin is 17,020 km<sup>2</sup> in area, equally large percentages of the drainage basin in the Brooks Range as well as lowlands. Since these rivers were the only gaged streams in the region, a reference list was developed in order to facilitate comparison of the many un-gaged streams with gaged streams in the four OCS regions. Streams were listed according to similarity to gaged streams on the general basis of region, basin size, and elevation distribution (Table 3).

Only three streams are gaged on Alaska's North Slope, the Kuparuk, Sagavanirktok, and the Putuligayuk Rivers. The Kuparuk is characterized by a low gradient, long stream length, and low elevation distribution. The Putuligayuk basin is confined to the Arctic coastal plain and reflects huge extremes of seasonability and variability in streamflow. The Sagavanirktok has a steep gradient and is highly braided. All these rivers have high variability in seasonal flow and the spring snowmelt runoff is the major contribution to flow. Although surface water is frozen in the Arctic for up to 8 months of the year, both the Sagavanirktok and the Kuparuk are suspected to sustain low levels of flow throughout the winter.

TABLE 3  
 CLASSIFICATION OF UNGAGED RIVERS  
 BY SIMILARITY TO GAGED RIVERS

| Gaged River                  | Ungaged River   | Region  |
|------------------------------|---|---|
| Chakachatna River            | Drift River<br>MacArthur River<br>Katnu River<br>Grecian River<br>Johnson River<br>Beluga River   | Gulf Coast - Cook Inlet   |
| Nellie Juan River            | Rude River<br>Lowe River  |   |
| Little Susitna River         | Chuit River<br>Theodore River   |   |
| Eagle River<br>Kuichak River | Peter's Creek<br>Naknek River<br>Egegik River<br>Ugashik River  | South Bering - Bristol Bay  |
| Kuzitrin River               | Utukok River<br>Kokolik River<br>Avalik River<br>Kukpowruk River<br>Pitmegea River<br>Kukpuk River<br>Kivalina River<br>Wulik River<br>Hot Springs Creek<br>Aglapuk River<br>Mudyutok River<br>Buckland River<br>Koyuk River<br>Tagagawik River | North Bering - Chukchi<br><br>Coastal Streams<br>Draining N.W. Alaska       |
| Kobuk River                  | Noatak River  | Seward Peninsula Drainages  |
| Kuparuk River                | Ikpikuk River<br>Shaviovik River  | Selawik Basin   |
| Putuligayuk River            | Meade River<br>Ivisaruk River<br>Kaoluk River<br>Avalik River<br>Okpiksak River<br>Kadleroshilik River<br>Fish Creek  | Beaufort Sea-Arctic Alaska<br>Low Elevation dist.<br>and long stream length |
|                              |   | Coastal Plain drainages   |

Table 3 Continued

| Gaged River         | Ungaged River  | Region  |
|---------------------|--|---|
| Sagavanirktok River | Tamavariak River<br>Katakturuk River<br>Sadlerochit River<br>Hulahula River<br>Jago River<br>Okpilak River<br>Aichilik River<br>Egaissrak River<br>Kongakut River<br>Marsh Creek | Beaufort Sea<br><br>Steep gradient,<br>Immature River,<br>Some Braiding |

Another area of stream characterization which is important but not represented in any of the four rivers presented is that of ice jam susceptibility. As an example of the magnitude of this problem, two satellite images are included which show large flooded areas on the Yukon River during 1975. Both were caused by ice jams and both covered areas larger than 2500 km<sup>2</sup> squared. The first was located near Holy Cross and the second in the delta of the Yukon River. The images are included as Figures 9 and 10. Ice jams, in addition to causing huge floods, may also release suddenly causing increases in stage and current.

#### Concluding Remarks:

An attempt has been made here to present a partial example of the streamflow characterizations which we are developing. Much remains to be completed.

These characterizations should prove valuable to engineering evaluations of offshore sites, as they might be affected by various hydrologic hazards and seasonal variation.

Work is proceeding on the remaining computer plot routines which will be used to plot hydrographs and the flow mass curves.

#### IX. Needs for Further Study:

Characterization of the coastal streams of Alaska would be greatly aided by additional gaging of streams. In particular, rivers which are unique and should be gaged include the Colville, Utukok, Wulik, Koyuk, and Canning Rivers. These rivers would fill gaps in the understanding of some of the more unique river systems in Alaska, as well as give perspective to the study of those rivers already gaged.

It was determined while doing background research for this study that very little research, if any, has addressed the question of biological responses to seasonal streamflow variations. This area of work deserves more attention.

Local studies of orographic precipitation effects are necessary to better understand this effect in Alaska. This is presently too little data available to adequately assess snow depth increases with elevation on either a local or regional basis.



Figure 9: Standard Thermal Infrared NOAA Satellite Image (Enlargement) Showing the Area Flooded by an Ice Jam Near Holy Cross on the Yukon River, May 24, 1975. Flooded Area is  $\sim 2,700 \text{ km}^2$  ( $1,050 \text{ mi}^2$ ).

58

YUKON DELTA  
FLOOD  
May 29, 1975

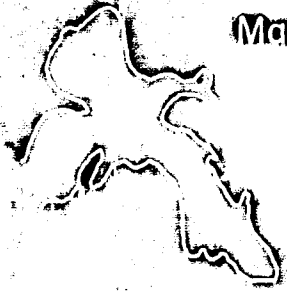
A thermal infrared satellite image of the Yukon River Delta. The image is mostly white with some dark, irregular shapes. A large, irregularly shaped area in the center is outlined in black, representing the flooded area. The text 'YUKON DELTA FLOOD' and 'May 29, 1975' is printed in the upper right quadrant of the image.

Figure 10: Thermal Infrared NOAA Satellite Image (Enlargement) Showing an Ice Jam Flood in the Yukon River Delta, May 29, 1975. Flooded Area is Approximately 2,750 km<sup>2</sup> (1,100 sq. mi.).



## REFERENCES

- Anderson, D. M.; Gatto, L. W.; McKim, H. L., and Petrone, A. (1973). Sediment distribution and coastal processes in Cook Inlet, Alaska. IN: Symposium on Significant Results obtained from the Earth Resources Satellite-1: Vol. 1, Tech. presentations: Section B, GSFC, March 5-9, 1973, NASA SP-327, p. 1323-1339.
- Bilello, M. (1974). Measurements of snow and ice for correlation with data collected by remote systems. IN: Advanced Concepts and Techniques in the Study of Snow and Ice Resources, held at Monterey, California, December 2-6, 1973, Nat. Acad. Sci., Wash., D.C., pp. 283-293.
- Campbell, W. J. and Martin, S. (1973). Oil and ice in the arctic ocean: possible large scale interactions. *Science* 181(4094):56-58, July 6, 1973.
- Carlson, R. F. (1972). The land hydrology of the south-central coastal zone, IN: A Review of the oceanography and renewable resources of the Northern Gulf of Alaska: Univ. of Alaska, Inst. of Marine Science Report S72-23, Sea Grant Report 73-3, Sec. 7, pp. 149-152.
- Carlson, R. F. (1974). Permafrost hydrology: an Alaskan experience, IN: Permafrost hydrology: Proceedings of a Workshop Seminar, 1974, Calgary, Alberta, February 26-28, 1974, Environment Canada, pp. 45-49, Ottawa.
- Guymon, G. L. (1974). Regional sediment yield analysis of Alaska streams. *Jour. of the Hydraulics Div., ASCE*, 100(HY1), paper 10255, pp. 41-41, Jan.
- Johnson, P., and Hartman, C. W. (1969). Environmental Atlas of Alaska. Inst. of Water Resources, Univ. of Alaska, College.
- Kane, D. L., and Carlson, R. F. (1973). Hydrology of central arctic river basins of Alaska, Report No. IWR-41, 51 pp.

- McCloy, J. M. (1970). Hydrometeorological relationships and their effects on the levels of a small Arctic delta, *Geografiska Annaler* 52A(3-4), pp. 223-241.
- Newbury, R. W. (1974). River hydrology in permafrost areas. IN: *Permafrost Hydrology: Proceedings of a Workshop Seminar, 1974, Calgary, Alberta, February 26-28, 1974, Environment Canada*, pp. 31-37.
- Post, A. and Mayo, L. (1971). Glacier dammed lakes and outburst floods in Alaska, U.S. Geological Survey, *Hydrological Investigations* HA-455.
- Poulin, A. O. (1974). Hydrologic characteristics of snow-covered terrain from thermal infrared imagery. IN: *Advanced Concepts and Techniques in the Study of Snow and Ice Resources, held at Monterey, California, December 2-6, 1973, Nat. Acad. Sci., Wash., D.C.*, pp. 494-503.
- Reimnitz, E., and Marshall, N. F. (1965). Effects of the Alaska Earthquake and Tsunami on recent deltaic sediments. *J. Geoph. Res.* 70(10) pp. 2363-2576, May 15.
- Reimnitz, E., and Bruder, K. F. (1972). River discharge into an ice covered ocean and related sediment dispersal. *Geol. Soc. of Amer. Bull.*, 83(3), pp. 861-866.
- Walker, H. J. (1973). Spring discharge of an Arctic river determined from salinity measurements beneath sea ice, *Water Resources Research* 9(2), pp. 474-480.

OCS COORDINATION OFFICE

University of Alaska

ENVIRONMENTAL DATA SUBMISSION SCHEDULE

DATE: March 31, 1976

CONTRACT NUMBER: 03-5-022-56      T/O NUMBER: 4      R.U. NUMBER: 111

PRINCIPAL INVESTIGATOR: Dr. Robert F. Carlson

No environmental data are to be taken by this task order as indicated in the Data Management Plan. A schedule of submission is therefore not applicable<sup>1</sup>.

NOTE: <sup>1</sup> Data Management Plan has been approved and made contractual.

OCS COORDINATION OFFICE

University of Alaska

ESTIMATE OF FUNDS EXPENDED

DATE: March 31, 1976  
 CONTRACT NUMBER: 03-5-022-56  
 TASK ORDER NUMBER: 4  
 PRINCIPAL INVESTIGATOR: Dr. Robert Carlson

Period April 1, 1975 - March 31, 1976\* (12 mos)

|                  | <u>Total Budget</u>     | <u>Expended</u>         | <u>Remaining</u>        |
|------------------|-------------------------|-------------------------|-------------------------|
| Salaries & Wages | 26,200.00               | 14,293.84               | 11,906.16               |
| Staff Benefits   | 4,430.00                | 2,464.94                | 1,965.06                |
| Equipment        | -0-                     | -0-                     | -0-                     |
| Travel           | 855.00                  | 575.90                  | 279.10                  |
| Other            | <u>3,900.00</u>         | <u>508.42</u>           | <u>3,391.58</u>         |
| Total Direct     | <u>35,385.00</u>        | <u>17,843.10</u>        | <u>17,541.90</u>        |
| Indirect         | <u>14,987.00</u>        | <u>8,176.08</u>         | <u>6,810.92</u>         |
| Task Order Total | <u><u>50,372.00</u></u> | <u><u>26,019.18</u></u> | <u><u>24,352.82</u></u> |

\* Preliminary cost data, not yet fully processed.

Following is part 2 of the quarterly report R.U.# 111 for the period ending December 31, 1975. This was received after the printing of the Quarterly Reports, July - September 1975, therefore is included here.

RECEIVED  
JAN 19 1976  
NEGOA

OCS COORDINATION OFFICE

University of Alaska

Quarterly Report for Quarter Ending December 31, 1975

Project Title: Effects of Seasonability and Variability  
of Streamflow on Nearshore Coastal Areas

Contract Number: 03-5-022-56

Task Order Number: 4

Principal Investigator: Dr. Robert F. Carlson

ph. oc.  
R. F. III

I. Task Objectives

The initial task has been to outline the basic analysis plan for the project. This has been accomplished. A data gathering effort is proceeding at present and the data will be prepared for computer analysis.

II. Activities

A tape record of all the streams and streamflow which directly affect the coast of Alaska has been obtained from the U. S. Army Corps of Engineers. The records include only those streams gaged by the U. S. Geological Survey. Streams which are not gaged have been categorized according to similarities with gaged streams in order that ungaged streams may be described and their parameters and extrapolations from the gaged streams. This is especially necessary for Alaskan streams since less than 40% of the coastal rivers and streams are presently gaged. The streamflow characterization involving use of the computer for analysis of the streamflow record is presently being delayed pending the debugging and online operation of the new Honeywell system. A flow chart of the analysis is appended, as is a listing of the rivers.

A. Bibliography

Extensive background studies and data are available for the coastal environment and dynamics in Alaska. A bibliography is assembled, and a bibliographic search was requested from OASIS in Washington, D.C. This search has resulted in a bibliography of nearly 550 entries.

B. Computer Run Request

The U. S. Army Corps of Engineers in Anchorage, in addition to having the U.S.G.S. streamflow records, also has several "operational" programs for hydro-

logic applications. One of these programs selects the 1, 3, 7, 10 and 30 day maximum flows for each stream. This information is very useful in stream-flow characterization. Therefore, rather than wait for the startup of the Honeywell system, we decided to contract that program work to the Corps of Engineers.

C. NOAA Imagery Observations: 1975

A list of observations from the NOAA-VHRR satellite imagery for the 1975 season is appended to this report. NOAA imagery provides the best available daily synoptic view of Alaska and gives a nearly continuous chronology of the spring snowmelt and other breakup features.

D. In order that a "check" is available for the computer runs, hand calculations of an entire statistical characterization of one river from each of the four O.C.S. investigation regions is being carried out. The rivers are:

1. Gulf Coast - Kenai R. @ Soldotna.
2. S. Bering - Kvichak R. @ Iguigig.
3. N. Bering - Chukchi - Kobuk R. @ Ambler.
4. Beaufort Sea - Kuparuk R. near Deadhorse.

These calculations follow the analysis flow chart and are about 60% complete at this writing.

In conjunction with streamflow characterization, hypsometric curves for 12 rivers have been calculated.

E. An attempt was made to correlate orographic precipitation effects with basin location and the precipitation measurements made at the nearest U. S. Weather Station. Snow survey measurements were used as well as cumulative snowfall records at the U.S.D.A. snowcourse sites. Only 14 data points were available because of the sparseness of snowcourses at higher elevations on the coast and the general lack of data. Local effects are very influential and variability between sites on the coast and inland is enormous. A rough estimate of 2.97 cm/1000m (0.35 in/1000 ft) of water equivalent was calculated, however, little confidence can be placed in this result without further data.

### III. Results

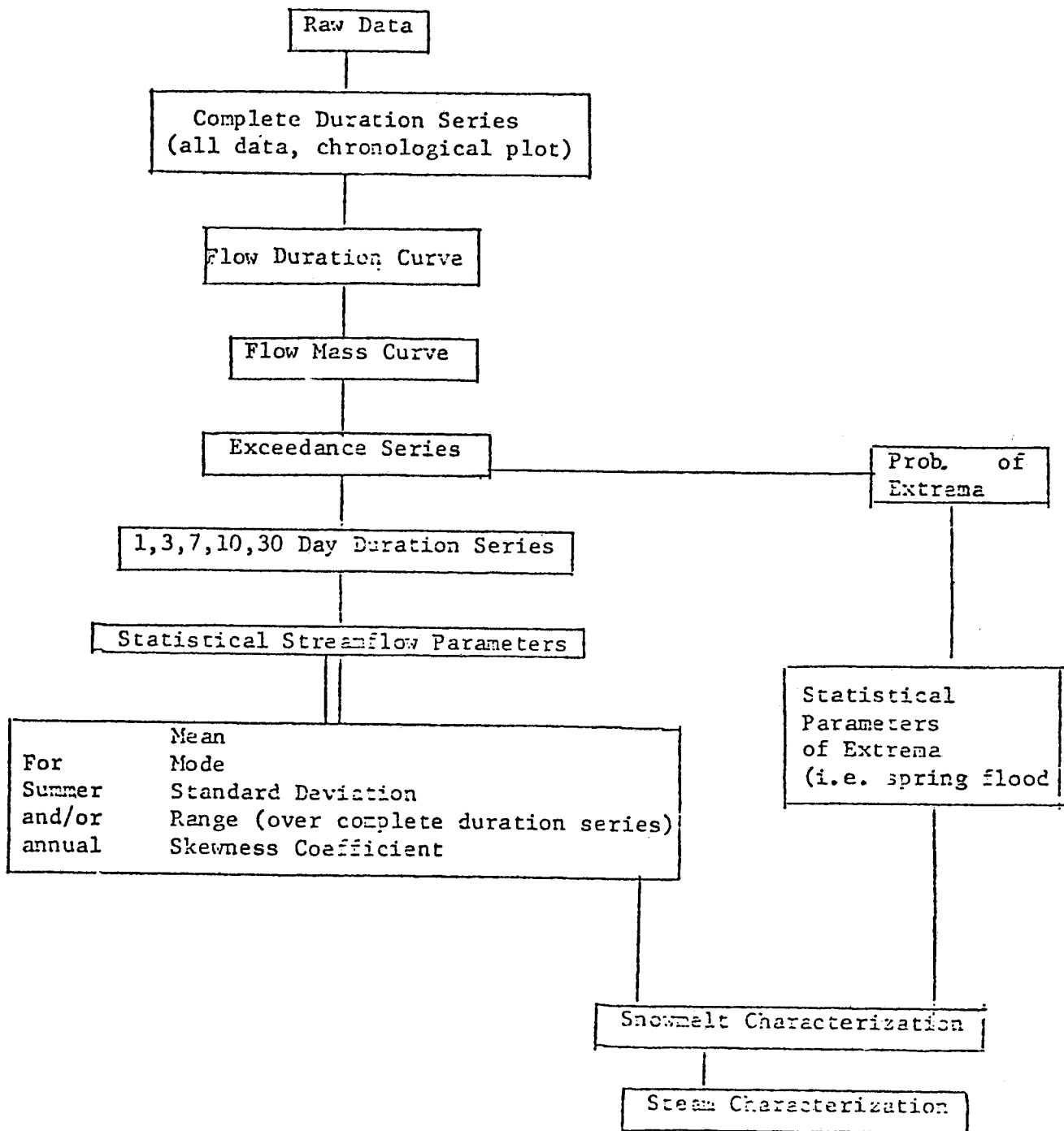
No conclusive results have been obtained.

IV. Problems Encountered

None.



FLOW CHART - O.C.S. STREAM CHARACTERIZATION



|            |    |      |    |      |   |     |  |
|------------|----|------|----|------|---|-----|--|
| 15.2120.00 | 10 | 1955 | 10 | 1970 | 9 | 180 | COPPER RIVER NR CHITINA ALASKA                     |
| 15.2160.00 | 10 | 1947 | 10 | 1970 | 9 | 276 | POWER CREEK NEAR CORDOVA, ALASKA                   |
| 15.2190.00 | 10 | 1964 | 9  | 1970 | 9 | 73  | WF OLSEN BAY C NR CORDOVA AK                       |
| 15.2370.00 | 10 | 1960 | 12 | 1965 | 6 | 55  | NELLIE JUAN RIVER NR HUNTER ALASKA                 |
| 15.2377.00 | 10 | 1964 | 10 | 1968 | 6 | 45  | RESURRECTION R NR SEWARD AK                        |
| 15.2385.00 | 10 | 1965 | 5  | 1968 | 9 | 41  | LOWELL C AT SEWARD AK                              |
| 15.2386.00 | 10 | 1966 | 9  | 1966 | 9 | 1   | SPRUCE C NR SEWARD AK                              |
| 15.2390.00 | 10 | 1957 | 10 | 1970 | 9 | 156 | BRADLEY RIVER NEAR HOMER, ALASKA                   |
| 15.2400.00 | 10 | 1953 | 10 | 1966 | 9 | 156 | ANCHOR RIVER AT ANCHOR POINT ALASKA                |
| 15.2416.00 | 10 | 1963 | 5  | 1970 | 9 | 89  | NINILCHIK RIVER AT NINILCHIK ALASKA                |
| 15.2420.00 | 10 | 1949 | 10 | 1970 | 9 | 252 | KASILOF RIVER NR KASILOF ALASKA                    |
| 15.2580.00 | 10 | 1947 | 10 | 1970 | 9 | 276 | KENAI RIVER AT COOPER LANDING ALASKA               |
| 15.2663.00 | 10 | 1965 | 5  | 1970 | 9 | 65  | KENAI R AT SOLDOTNA AK                             |
| 15.2679.00 | 10 | 1967 | 10 | 1970 | 9 | 36  | RESURRECTION CREEK NEAR HOPE, ALASKA               |
| 15.2725.50 | 10 | 1965 | 10 | 1970 | 9 | 60  | GLACIER CREEK AT GIRWOOD, ALASKA                   |
| 15.2746.00 | 10 | 1966 | 10 | 1970 | 9 | 48  | CAMPBELL CREEK NEAR SPENARD, ALASKA                |
| 15.2751.00 | 10 | 1966 | 6  | 1970 | 9 | 52  | CHESTER CREEK AT ARCTIC BLVD. AT ANCHORAGE, ALASKA |
| 15.2765.00 | 10 | 1963 | 5  | 1970 | 9 | 89  | SHIP CREEK AT ELMENDORF AIR FORCE BASE, ALASKA     |
| 15.2771.00 | 10 | 1965 | 10 | 1970 | 9 | 60  | EAGLE RIVER AT EAGLE RIVER, ALASKA                 |
| 15.2810.00 | 10 | 1959 | 10 | 1970 | 9 | 132 | KNIK RIVER NEAR PALMER, ALASKA                     |
| 15.2840.00 | 10 | 1949 | 10 | 1970 | 9 | 252 | MATANUSKA RIVER AT PALMER, ALASKA                  |
| 15.2920.00 | 10 | 1947 | 0  | 1970 | 9 | 252 | SUSITNA RIVER AT GOLD CREEK ALASKA                 |
| 15.2924.00 | 10 | 1958 | 10 | 1970 | 9 | 144 | CHIULITNA RIVER NR TALKEETNA ALASKA                |
| 15.2927.00 | 10 | 1964 | 6  | 1970 | 9 | 76  | TALKEETNA RIVER NEAR TALKEETNA, ALASKA             |
| 15.2943.00 | 10 | 1959 | 10 | 1970 | 9 | 132 | SKWENTNA RIVER NEAR SKWENTNA, ALASKA               |
| 15.2945.00 | 10 | 1959 | 10 | 1970 | 9 | 132 | CHAKACHATNA RIVER NR TYONEK ALASKA                 |
| 15.2957.00 | 10 | 1964 | 3  | 1968 | 9 | 55  | TERROR R AT MOUTH NR KODIAK AK                     |
| 15.2960.00 | 10 | 1951 | 10 | 1970 | 9 | 228 | UGANIK RIVER NEAR KODIAK, ALASKA                   |
| 15.2972.00 | 10 | 1963 | 6  | 1970 | 9 | 88  | MYRTLE CREEK NR KODIAK ALASKA                      |
| 15.3005.00 | 10 | 1967 | 8  | 1970 | 9 | 38  | KVICHAK R AT IGUIGIG AD                            |
| 15.3020.00 | 10 | 1953 | 10 | 1970 | 9 | 204 | NUYAKUK RIVER NEAR DILLINGHAM, ALASKA              |
| 15.3040.00 | 10 | 1951 | 10 | 1970 | 9 | 228 | KUSKOKWIM RIVER AT CROCKED CREEK ALASKA            |
| 15.5648.00 | 10 | 1956 | 10 | 1970 | 9 | 168 | YUKON RIVER AT RUBY ALASKA                         |
| 15.5652.00 | 10 | 1922 | 3  | 1966 | 9 | 535 | YUKON RIVER NEAR KALTAG ALASKA                     |
| 15.7120.00 | 10 | 1962 | 8  | 1970 | 9 | 98  | KUZITRIN RIVER NEAR NOME ALASKA                    |
|            |    |      |    |      |   |     | KOBUK RIVER AT AMBLER                              |
|            |    |      |    |      |   |     | KUPARUK RIVER NEAR DEADHORSE                       |
|            |    |      |    |      |   |     | PUT R. NEAR DEADHORSE                              |
|            |    |      |    |      |   |     | SAG R. NEAR SAGWON                                 |

NOAA IMAGERY OF USE IN OCS CHARACTERIZATION - 1975

| AA IMAGERY<br>BIT NO. & DATE | SNOWMELT<br>OBSERVATION   | PLUME<br>OF SEDIMENT<br>OR OVERFLOW  | LOCATION OF<br>OBSERVATION | FLOODING<br>CAUSE   | CIRCULATION<br>FEATURE                 | NOTES  |
|------------------------------|---|--|----------------------------|---|--|--|
| 306 18 May 75                | Melt Completed<br>on Most Cook<br>Inlet Lowlands  |  | Entire State               |   |  | Strong Wave<br>Cloud/Wind<br>Effect  |
| thru 22 May Cloudy           |   |  |                            |   |  |  |
| 354 23 May 75                | Melt Proceeding<br>Coastal Lowlands<br>Kusk-Yuk Delta   |  |                            |   | Coastal Area<br>Much Cloudier<br>Again |  |
| 331 24 May 75                | Ice Persists Along<br>Coastal Areas (North<br>of Toziak)<br>Probably Shorefast                                  |  | Yukon River<br>Innoko R.   | Aniak/Holy-<br>cross Flood<br>Ice Jam<br>~1000 mi. <sup>2</sup>             |  | *Breakup of River<br>Dominate  |
| 444 29 May 75                | Melt Complete<br>Throughout<br>Most of Brooks<br>Range, Interior<br>S. Central<br>Seward Peninsula<br>of Alaska | Ice Flooded<br>Off Sag R.<br>on N. Slope<br>also off<br>Canning R.                                   | Entire State               | Yukon Delta<br>Flooded - Ice<br>Jam, Tidal Effects<br>1050 mi. <sup>2</sup> |  | Sag R. Not Visible<br>for 4 previous<br>Days Flow Initia-<br>tion Indetermina- |
| 494 02 Jun 75                | Melt Complete<br>Except for N.<br>Slope   |  |                            |   |  | N. Slope Nearly<br>Continuously<br>Cloudy Since<br>29 May                      |
| 506 03 Jun 75                |   | Sea Ice Flooded<br>Off:<br>Sag<br>Colville<br>Canning<br>Sadlerochit<br>Hulahula<br>Jago<br>Okililak |                            |   |  | Sea Ice Still<br>Intact Along<br>Shore N. of<br>Hazen Bay                      |

Good Demonstrative Example

NOAA IMAGERY OF USE IN GCS CHARACTERIZATION - 1975

| <u>NOAA IMAGERY<br/>ORBIT NO. &amp; DATE</u> | <u>SNOWMELT<br/>OBSERVATION</u>  | <u>PLUME<br/>OF SEDIMENT<br/>OR OVERFLOW</u> | <u>LOCATION OF<br/>OBSERVATION</u>                             | <u>FLOODING/<br/>CAUSE</u> | <u>CIRCULATION<br/>FEATURE</u>                 | <u>NOTES</u>   |
|--|--|--|--|----------------------------|--|--|
| #2081 30 Apr 75                              | Melting Temp.<br>Present   |  | Throughout Interior<br>and Lower Yukon and<br>Kuskokwim Valley |                            |  | Some evidence<br>of Snowfree<br>Area                     |
| #2093 01 May 75                              | Melting and<br>Snowfree Areas<br>Present   |  | Interior (Tan. Valley)<br>Yukon, Lower Kuskokwim               |                            | Coastal Weather<br>Effects Dominate            | *  |
| #2105 02 May 75                              | Matakuska Valley<br>& Copper R. Valley<br>Clear Observation<br>Lowlands Snowfree |  | Cook Inlet, Copper<br>River Valley & Interior                  |                            |  | First Clear<br>Weather Obs<br>of Cook Inl<br>& Copper R. |
| #2143 05 May 75                              | Generally Snowfree<br>in Cen. Yukon &<br>Porcupine R. Valleys                    |  | Interior & Cook Inlet  |                            | Ice in Cook<br>Inlet W. Side<br>of Inlet       |  |
| #2156 06 May 75                              | Snowfree Area of<br>North Slope Clearly<br>Visible                               |  | N. Slope of Brooks<br>Range                                    |                            | Clearing of<br>Ice in Norton<br>Sound          | Sag R. Visi<br>Effects of<br>or Haul Roa                 |
| #2168 07 May 75                              | Further Melting<br>Throughout Int.<br>& Copper Valley                            |  | Entire State   |                            | Coastal Ice<br>Degrading So.<br>of Bering Str. | " "  |
| #2193 09 May 75                              | Extensive Melt in<br>Interior Alaska   |  | S. Coast Cloudy - Rest<br>of State Clear or P. Cldy.           |                            |  | Yukon R. Ice<br>Still Intac                              |
| #2218 11 May 75                              | Extensive Further<br>Melting Occurred  |  | Entire State   |                            |  | Record High<br>Temps. Inte                               |
| #2231 12 May 75                              | 75% Complete<br>in Interior  |  | North of Alaska Range  |                            |  | Brooks Range<br>Melting                                  |
| #2221 16 May 75                              | 80% Complete So.<br>of Brooks and No.<br>of Alaska Range                         |  | Alaska, N. of Alaska<br>Range                                  |                            | Coastal Weather<br>Variance<br>Indicated       | *Cloudy S.<br>Alaska Range                               |

\*Good Demonstrative Example

NOAA IMAGERY OF USE IN OCS CHARACTERIZATION - 1975

| NOAA IMAGERY<br>ORBIT NO. & DATE | SNOWMELT<br>OBSERVATION   | PLUME<br>OF SEDIMENT<br>OR OVERFLOW                                 | LOCATION OF<br>OBSERVATION    | FLOODING<br>CAUSE   | CIRCULATION<br>FEATURE                             | NOTES   |
|----------------------------------|---|---|-------------------------------|---|--|---|
| 51 05 Jun 75                     | Snow Definitely<br>Melting on No.<br>Slope  | Major Overflow<br>Water at Mouths<br>of Most Rivers<br>on No. Slope |                               | Overflow Flooding<br>No. Slope Rivers                       |  |   |
| 544 06 Jun. 75                   |   |   | Northern Alaska               | Kasegaluk Lagoon<br>Completely Flooded<br>by Overflow Water |  |   |
| 594 10 Jun 75                    | Coastal Shore-<br>fast Ice Generally<br>Absent So. of Cape<br>Rodney, Seward<br>Peninsula<br>No. Slope Snowmelt<br>50% Complete |   | Western Alaska &<br>No. Slope |   |  |   |
| 71                               |   |   |                               |   |  |   |
| 607 11 Jun 75                    | Snowmelt on No.<br>Slope 70%<br>Complete  |   | Entire State                  |   | Coastal Fog and<br>Weather Again<br>Evident        |   |
| 619 12 Jun 75                    | No. Slope Snowmelt<br>80% Complete  |   | Entire State                  |   | Coastal Weather *<br>Again Evident-Fog-<br>Stratus |   |
| 920 06 Jul 75                    | Teschepuk L.<br>Still Frozen<br>Ice Still<br>Intact No. of<br>Icy Cape  | Huge Sediment<br>Plume off<br>McKenzie R.                           | No. Slope                     |   |  | Ice Normally<br>Still Present<br>Along Beaufort<br>Sea Coast in<br>Early July |
| 132 23 Jul 75                    | Ice Lead Open<br>to Barrow  |   |                               |   |  | Ice Close but.<br>Only Obstructs<br>Passage Between<br>Barrow & Smith<br>Bay  |

Good Demonstrative Example

OCS COORDINATION OFFICE

University of Alaska

ENVIRONMENTAL DATA SUBMISSION SCHEDULE

DATE: December 31, 1975

CONTRACT NUMBER: 03-5-022-56      T/O NUMBER: 4      R.U. NUMBER: 111

PRINCIPAL INVESTIGATOR: Dr. Robert F. Carlson

No environmental data are to be taken by this task order as indicated in the Data Management Plan. A schedule of submission is therefore not applicable<sup>(1)</sup>.

NOTE: (1) Data management plan was submitted to NOAA in draft form on October 9, 1975 and University of Alaska approval given on November 20, 1975. We await formal approval from NOAA.

IS COORDINATION OFFICE

University of Alaska

ESTIMATE OF FUNDS EXPENDED

DATE: December 31, 1975  
CONTRACT NUMBER: 03-5-022-56  
TASK ORDER NUMBER: 4  
PRINCIPAL INVESTIGATOR: Dr. Robert Carlson

Period April 1 - December 31, 1975\* (9 mos)

|                  | <u>Total Budget</u> | <u>Expended</u>  | <u>Remaining</u> |
|------------------|---------------------|------------------|------------------|
| Salaries & Wages | 26,200.00           | 6,309.80         | 19,890.20        |
| Staff Benefits   | 4,430.00            | 1,072.66         | 3,357.34         |
| Equipment        | -0-                 | -0-              | -0-              |
| Travel           | 855.00              | 575.90           | 279.10           |
| Other            | <u>3,900.00</u>     | <u>265.25</u>    | <u>3,634.75</u>  |
| Total Direct     | 35,385.00           | 8,223.61         | 27,161.39        |
| Indirect         | <u>14,987.00</u>    | <u>3,609.21</u>  | <u>11,377.79</u> |
| Task Order Total | <u>50,372.00</u>    | <u>11,832.82</u> | <u>38,539.18</u> |

\* Preliminary cost data, not yet fully processed.





ANNUAL REPORT

Contract #R7120846  
#R7120847

Research Unit #138, 139, 147

Reporting Period: 1 July 1975 -  
31 March 1976

Number of Pages:

GULF OF ALASKA STUDY OF MESOSCALE  
OCEANOGRAPHIC PROCESSES (GAS-MOP)

Dr. S. P. Hayes

Dr. J. D. Schumacher

Pacific Marine Environmental Laboratory  
National Oceanic and Atmospheric Administration  
3711 15th Avenue N.E.  
Seattle, Washington 98105

April 1, 1976

## I. SUMMARY

The objective of this research is to describe the mesoscale oceanic circulation on the continental shelf in the Gulf of Alaska in order to characterize the intermediate scale advective and diffusive processes. These processes are inherently important to the assessment of potential pollution problems due to OCS petroleum development. The study discussed here when combined with the meteorological research, additional physical oceanographic research, and the theoretical modelling research of other investigators forms a coherent program to describe the physical milieu within the proposed OCS lease areas.

From the data collected and analyzed to date several tentative conclusions may be drawn: (a) The mean flow is high (on the order of 25 cm/sec) and directed to the west generally following the local isobaths. (b) The regional variations in the flow indicate a weak mean flow with large variability behind Kayak Island, larger mean flow in Kodiak Island region, and possible interaction of flow near Unimak Pass with flow in the Bering Sea. (c) During winter the storm-induced velocity changes are large (on the order of 30 cm/sec) and mainly barotropic; these velocity changes are well-correlated with the wind. (d) During spring the velocity field appears more complex and nonlocal forcing is suggested. (e) The summertime density stratification produces baroclinic flow and smaller coherence of the currents in the vertical.

The conclusions are tentative. There have been relatively few opportunities for seasonal intercomparisons. Nevertheless the data series are beginning to form the basis for a statistically meaningful description of the circulation on the continental shelf.

## II. INTRODUCTION

### A. General Nature and Scope of Study

The objective of this research is to describe the mesoscale oceanic circulation on the continental shelf in the Gulf of Alaska. Together with additional observational and theoretical programs, these studies will attempt to characterize the intermediate and large-scale advective and diffusive processes within proposed OCS lease areas.

The average circulation in the Gulf of Alaska has been attributed to the westward flowing Alaskan Current. This large-scale phenomenon is produced by the response to the global wind forcing. On intermediate scales the circulation will be modified by bathymetry and in addition it will respond to a variety of local and nonlocal forcing functions. Locally, the wind-generated response will be important. These lead to near-surface Ekman flows, sea surface slopes (and hence barotropic velocity components) and modification of the density stratification (and hence baroclinic velocity fields). The nonlocal effects include tidal currents and shelf waves. These can significantly modulate the mean flow and hence the response to the local wind field.

In an ideal world, we could recreate the ocean in a computer model and generate the oceanic velocity fields from first principals. However, the real ocean is so rich in variability that a priori modelling is impractical. Rather, observational results must be accumulated and events documented in order that the models may be guided into the correct approximations. In this manner the models may be used to extend the observational results, so that we may predict what will probably happen in a given situation.

The experimental program discussed here was designed with this philosophy in mind. The immenseness of the continental shelf in the Gulf of Alaska defies saturation of measurements. Instead the program provided regional coverage to establish the statistics of the velocity field at a few points. This was supplemented by a process-oriented study in one selected area. This study related the velocity field to the wind forcing, the bathymetry, the sea surface slope, and the density field. The process-oriented experiments are required in order to interpret the statistical observations.

The report presented here discusses work in progress. Only preliminary inferences on causal relationships will be presented. Many of these are based on pilot studies involving a small subset of the total data.

## B. Specific Objectives

The observational program is discussed conveniently in terms of the regional and process experiments defined above.

### 1. Regional experiment

Three moorings, 62, WGC-1, WGC-2, comprise the region experiment. These were each separated by roughly 600 km and they spanned the Gulf of Alaska Shelf from Yakutat to Unimak Pass. Their intent was to gather statistical data on the nature of the temporal and large-scale spatial velocity variability. Near mooring 62 (which was also part of the process experiment) bottom pressure measurements were made. In addition, there was a pressure gauge on WGC-2. These provided the data for coupling the velocity field to the sea surface slope and hence the barotropic velocity component. Similarly, a large-scale CTD grid was occupied by a separate research group (Royer, University of Alaska). This provided the data for comparison of measured and inferred baroclinic velocities and a test for geostrophic and nongeostrophic components.

### 2. Process-oriented experiment

This moderately intense study of a specific area involves seven moorings within a square of roughly 50 km to a side. Four of these moorings have only a bottom-mounted pressure gauge. The others have pressure gauges and current meters or only current meters. Station 62 is part of this array as well as the regional array. The array is composed of two lines perpendicular to the coastline extending from the 50 m contour to the shelf break (250 m). Station 62 is in the center of the lines. The objectives of this bottom pressure gauge and current meter array are:

## a. Line 1

- (1) Region of relatively flat/smooth topography
- (2) Offshore/onshore sea surface slope
  - (a) Spatial scale of the sea surface slope
  - (b) Calculate alongshore geostrophic currents from sea surface slope and compare with measured currents
  - (c) Time scale of setup of slope
  - (d) Tidal analysis
  - (e) Shelf waves, quasi-geostrophic waves, eddies

## b. Line 2

- (1) Alongshore sea surface slope
  - (a) Investigate as a function of offshore distance
  - (b) Effects of bottom topography between lines 1 and 2
  - (c) Calculate onshore/offshore geostrophic flow
- (2) Offshore-onshore sea surface slope
  - (a) Offshore scale (see b.(1)(a) above)
  - (b) Dependence on slope on water depth compared to distance offshore

In addition to the velocity and pressure measurements, a small number of closely-spaced CTD stations were made along lines 1 and 2 to define baroclinic effects.

## C. Application to Petroleum Development Hazard Assessment

Once oil is loosed on the sea, it undergoes a series of physical and chemical changes. Volatile components are released to the atmosphere and soluble components dissolved into the waters. The ubiquitous oil-consuming bacteria begin to multiply, metabolizing the floating and dissolved oil. The small solubility of hydrocarbons in seawater becomes appreciable as the oil spreads over vast areas. The net effect of these processes is to produce tarry masses surrounded by thin slicks of the lighter, more volatile components. These thin slicks appear to be consumed quickly, perhaps

within a few hours (Zachariassen, 1968). The tarry masses are attached more slowly. Wave action may produce oily emulsions.

During the time oil is floating on the surface, it moves under the influence of the winds. If the currents in a region of an oil slick are not a direct result of the winds, e.g., tidal current prevalent in the near-shore environment, the oil will move in some direction between that of the wind and that of the current. However, no satisfactory theory exists today to predict the exact velocity of an oil patch under these conditions.

Oil patches tend to disperse and dissipate with time, especially during high seas. Four hundred tons of oil released in the Gulf of Mexico as a result of a broken undersea well head dissipated completely in high seas within 7 miles of the drilling site (Air and Water News, 1969). However, the large slicks from the Torrey Canyon drifted hundreds of miles (Smith, 1968), as contiguous masses. The exact distance an oil slick travels without dissipating is a function of its size and the sea state. This distance cannot adequately be predicted at this time.

Oil properties alter markedly with time as the spill spreads, evaporates, dissolves, or is consumed. Crude oil will fractionate rapidly by evaporation of its lighter components and more slowly by the loss of successive higher boiling fractions. The fractions boiling at less than 700°F tend to volatilize from the sea surface. Data on the evaporation of Kuwait Crude, bubbled with nitrogen, indicate a 25% evaporation loss after 25 hrs (Berridge, et al., 1968a).

Without this lighter fraction the pour points of most oils are above the temperature of the water in which they are spilled. The residue then forms a gelatinous mass which will not spread. Evaporation may proceed to where the specific gravity of the residue is greater than that of seawater (Berridge, et al., 1968b). Evaporation and eventual sinking may have been the fate of the oil from the Anne Mildred Brovig, which was wrecked in the North Sea. Residue from Iranian Heavy Crude has a specific gravity of 1.027, higher than most surface seawater.

From this brief description of the behavior of oil in the sea, it is apparent that two distinct environmental problems accompany petroleum development. Type I, or catastrophic oil spills, and Type II, chronic or long-term oil seepage and accumulation. This research unit addresses both of these in the following manner: The eventual effect of Type I problems depends on where the spilled oil goes, the time scale of its motion, and diffusion of the oil along the trajectory. This study provides information on the mean transport of oil and an indication of rates of dispersion. Type II problems require a better understanding of behavior of oil in the water column itself rather than on the surface. After evaporation of short-chain hydrocarbons, the residue is likely to be mixed into the water column and thereby scavenged by suspended particulate matter. The problem now becomes one of understanding net transport of suspended material. This process is directly related to advective and diffusive

fields within the water column. An understanding of these processes again requires the description and understanding of the velocity field and its driving mechanisms.

### III. CURRENT STATE OF KNOWLEDGE

The historical data base and the results of the first year OCSEP studies were summarized in the Annual Report, April 1975 (Galt, 1975), and in a subsequent manuscript (Galt and Royer, 1975). Briefly, the mean circulation in the Gulf of Alaska is dominated by the Alaskan gyre (Dodimead, *et al.*, 1963). The northern boundary of this gyre is the Alaskan Current. This westward flow generally parallels the coastline. There are indications that the flow intensifies as it proceeds westward along the Alaskan Peninsula (Favorite, 1967). This may be related to a change from an eastern boundary to a western boundary current (Thompson, 1972).

Seasonally, the Gulf of Alaska is dominated by the Aleutian Low in winter and the North Pacific High in summer. During winter this low pressure system leads to winds from the southeast and severe storms. The onshore Ekman transport produces a downwelling situation on the continental shelf. In summer, lighter winds prevail and a relaxation of the wintertime setup ensues (Royer, 1975).

Prior to the OCSEP studies, little information was available on the sea surface slope in the Gulf of Alaska. Some analyses of coastal sea level included Alaskan stations. Of note is the study of Pattullo, *et al.* (1954), which concluded that the seasonal excursion of sea level (uncorrected for atmospheric pressure) was about 25 cm. Recently, Reid and Mantyla (1975) observed that the atmospheric pressure variations accounted for 50% of the sea level change. They tried to relate the seasonal variations to changes in the baroclinic structure of the Alaskan Current. However, their wintertime data set is sparse and the results are only suggestive.

The daily variations in sea level which could be storm-induced were briefly studied by Groves (1956). He included Alaskan stations in his discussion. However, his intent was to provide a general statistical comparison of stations throughout the world. There is little direct application of his work to the present study.

### IV. STUDY AREA

The study area is the Gulf of Alaska continental shelf (fig. 1). The regional experiment (moorings 62, WGC-1, WGC-2) extends from Icy Bay to Unimak Pass. The process-oriented experiment is located offshore of Icy Bay and involves the two lines of pressure gauges SLS-A to SLS-F, as well as station 62. Also shown are stations 60 and 61 which were not deployed during the period considered in this report; however, their analysis is discussed.

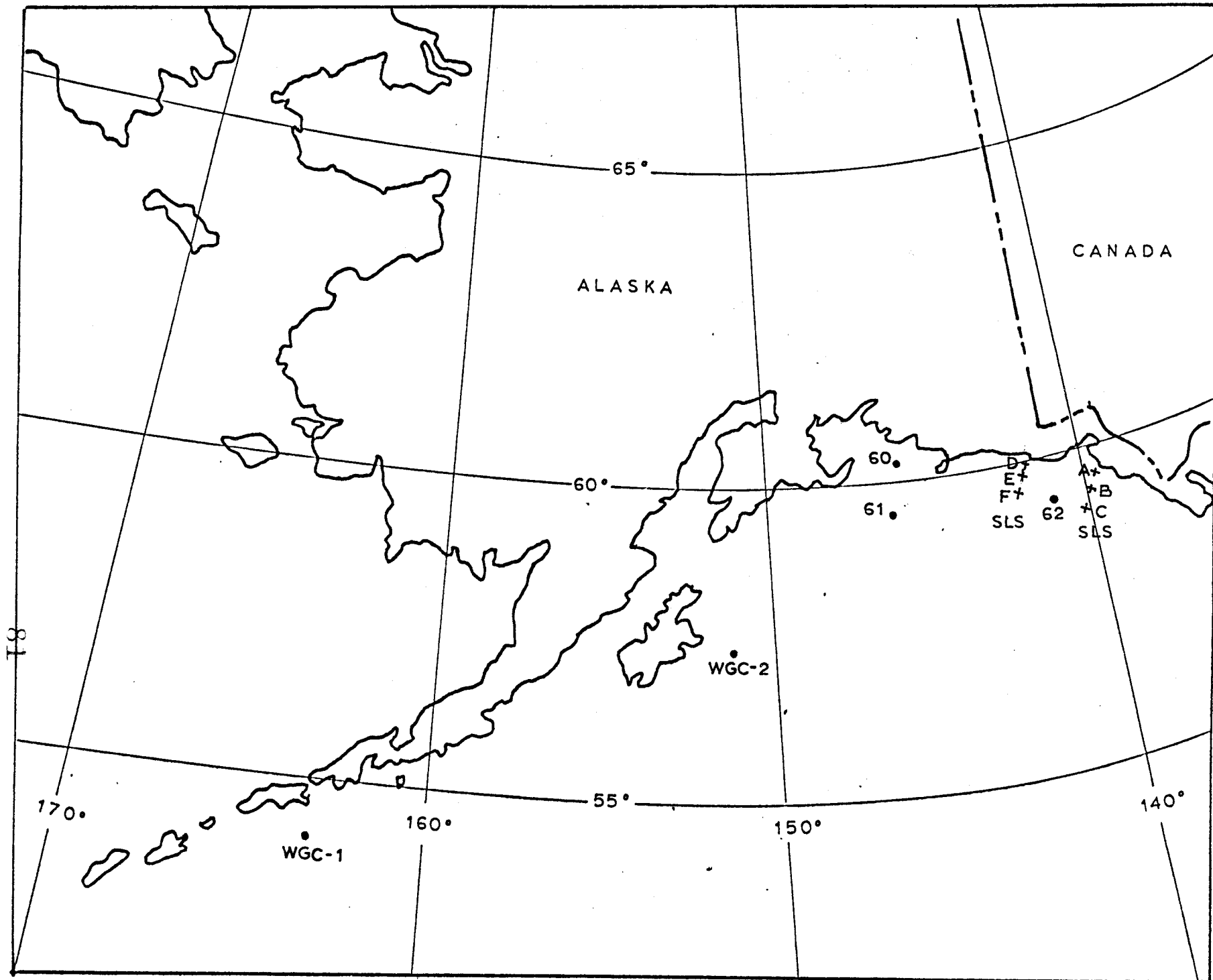


Figure 1. Station positions in the Gulf of Alaska.

## V. PROGRAM RATIONALE AND METHODS OF DATA COLLECTION

The following work has been initiated or completed during the period 1 July 1975 - 31 March 1976:

- A. Long-term moorings 62, WGC-1, WGC-2 have been deployed and maintained. The data from these arrays have been used to examine advective processes by characterizing spatial distribution of mean flow in the study area.
- B. Short-term records from 60 and 61 were examined to look at special processes west of Kayak Island.
- C. Analysis was completed for the FY-75 pilot study (February to May 1975) off Icy Bay. This involved wind, surface currents, midwater and bottom currents, and bottom pressure.
- D. Spectral energy from several levels at 62 has been calculated to examine the balance between the advective and dispersive processes.

To date, five cruises have been completed from September 1975 to mid-March 1976. Hydrographical data was collected using the following equipment:

Plessey 9040 CTD inputed to the PODAS system aboard the Discoverer  
Plessey 9040 CTD and Plessey 8400 data logger aboard the Miller Freeman.

Water samples were taken using a Rosette sampler equipped with Niskin bottles. Salinity samples were drawn and salinity determinations were made using the ship's inductive salinometer. Reversing thermometers (calibrated by NOIC) were employed to develop field correction factors for the CTD system.

Aanderaa RCM-4 current meters were used on the moored arrays. The tapes were processed by PMEL/UW's Aanderaa tape system.

The bottom pressure measurements are made with an internally recording pressure-temperature gauge (PTG) designed by A. M. Zwilling of the OARS Project at PMEL. The gauge records on digital tape cassette the integral value of pressure and temperature once every 15 min. A technical report describing the gauge is in preparation. The first deployment of this type of gauge in the Gulf of Alaska was in November 1975. The gauges were recovered in March and data analysis is proceeding. A prototype gauge was tested off Oregon in June 1975 and it worked properly.

Before and after deployments the gauges are calibrated at the Northwest Regional Calibration Center in Bellevue, Washington. They are calibrated at three temperatures (8°C, 5°C, 3°C) in order to check for temperature dependency. In some gauges temperature effects equivalent to a water level change of 1 cm/°C have been observed. Recently NWRCC has improved their pressure testing capabilities and we anticipate that better control on long-term drift should be obtainable.



## VI. RESULTS

- A. The following tables summarize current meter and pressure gauge records collected to date. CTD data collected thus far are listed in Section X, Summary of 4th Quarter Operations, which summarizes field operations for the entire reporting period.

Current Meter Station 62-D, 59°32.95'N, 142°5.28'W

Observation Period: 4 June 1975 - 18 September 1975

| Instrument<br>Depth (m)         | 20                                      | 50                                      | 100                                     | 178                                     |
|---------------------------------|---|---|---|---|
| Meter No.                       | 601                                     | 603                                     | 1452                                    | 602                                     |
| Observation<br>Period<br>(days) | 2316 June 4<br>2148 Sept. 18<br>(105.9) | 2318 June 4<br>2142 Sept. 18<br>(105.9) | 2319 June 4<br>2140 Sept. 18<br>(105.9) | 2317 June 4<br>2141 Sept. 18<br>(105.9) |
| Speed                           | ✓ *                                     | ✓                                       | ✓                                       | ✓                                       |
| Direction                       | ✓ *                                     | ✓                                       | ✓                                       | ✓                                       |
| Conductivity                    | ✓ *                                     | ✓                                       | ✓                                       | ✓                                       |
| Temperature                     | ✓ *                                     | ✓                                       | ✓                                       | ✓                                       |
| Pressure                        | ✓ *                                     | ✓                                       | ✓                                       | ✓                                       |

\* At various times each channel in meter 601 gives data values = zero, indicating possible temporary malfunction.

✓ Means meter equipped with sensor.

. . . . .

Current Meter Station 62-E, 59°34.31'N, 142°10.0'W

Observation Period: 19 September 1975 - 20 November 1975

| Instrument<br>Depth (m)         | 24.5                                    | 54.5                                    | 104.5                                   | 177.5                                   |
|---------------------------------|---|---|---|---|
| Meter No.                       | 1682                                    | 1681                                    | 1680                                    | 1679                                    |
| Observation<br>Period<br>(days) | 1918 Sept. 19<br>2319 Nov. 20<br>(62.2) | 1917 Sept. 19<br>2317 Nov. 20<br>(62.2) | 1916 Sept. 19<br>2318 Nov. 20<br>(62.2) | 1915 Sept. 19<br>2316 Nov. 20<br>(62.2) |
| Speed                           | ✓                                       | ✓                                       | ✓                                       | ✓                                       |
| Direction                       | ✓                                       | ✓                                       | ✓                                       | ✓                                       |

|              |   |   |   |     |
|--------------|---|---|---|-----|
| Conductivity | ✓ | ✓ | ✓ | ✓   |
| Temperature  | ✓ | ✓ | ✓ | ✓   |
| Pressure     | ✓ | ✓ | ✓ | ✓ * |

\* Pressure gauge on 1679 was "capped off" and gave no data.

✓ Means meter equipped with sensor.

.....

Current Meter Station WGC-1B, 54°01.4'N, 163°01.8'W

Observation Period: 1 November 1975 - lost

| Instrument<br>Depth (m)         |             |             |
|---------------------------------|-------------|-------------|
| Meter No.                       | 1455        | 645         |
| Observation<br>Period<br>(days) | 2305 Nov. 1 | 2305 Nov. 1 |
| Speed                           | ✓           | ✓           |
| Direction                       | ✓           | ✓           |
| Conductivity                    | ✓           | ✓           |
| Temperature                     | ✓           | ✓           |
| Pressure                        | ✓           | ✓           |

✓ Means meter equipped with sensor.

.....

Current Meter Station WGC-2B, 57°26.7'N, 150°29.4'W

Observation Period: 29 November 1975 - to be recovered  
in March 1976

| Instrument<br>Depth (m)         |              |              |
|---------------------------------|--------------|--------------|
| Meter No.                       | 1674         | 1456         |
| Observation<br>Period<br>(days) | 0153 Nov. 29 | 0153 Nov. 29 |
| Speed                           | ✓            | ✓            |

|              |   |   |
|--------------|---|---|
| Direction    | ✓ | ✓ |
| Conductivity | ✓ | ✓ |
| Temperature  | ✓ | ✓ |
| Pressure     | ✓ | * |

TG 2A Pressure  
Gauge #54                      0153

\* Means meter not equipped with sensor.

✓ Means meter equipped with sensor.

. . . . .

Current Meter Station WGC-1A, 54°1.7'N, 162°59.8'W

Observation Period: 4 September 1975 - 1 November 1975

|                                 |                                       |                                       |
|---------------------------------|---------------------------------------|---------------------------------------|
| Instrument                      |                                       |                                       |
| Depth (m)                       | 20                                    | 100                                   |
| Meter No.                       | 1678                                  | 1677                                  |
| Observation<br>Period<br>(days) | 1915 Sept. 4<br>0815 Nov. 1<br>(57.5) | 1916 Sept. 4<br>0817 Nov. 1<br>(57.5) |
| Speed                           | ✓                                     | ✓                                     |
| Direction                       | ✓                                     | ✓                                     |
| Conductivity                    | ✓                                     | ✓                                     |
| Temperature                     | ✓                                     | ✓                                     |
| Pressure                        | ✓                                     | ✓                                     |

✓ Means meter equipped with sensor.

. . . . .

Current Meter Station WGC-2A, 57°27.1'N, 150°29.6'W

Observation Period: 21 September 1975 - 28 November 1975

|                                 |   |   |
|---------------------------------|---|---|
| Instrument                      |   |   |
| Depth (m)                       | 20                                      | 100                                     |
| Meter No.                       | 1684                                    | 1683                                    |
| Observation<br>Period<br>(days) | 1905 Sept. 21<br>2321 Nov. 28<br>(68.2) | 1904 Sept. 21<br>2320 Nov. 28<br>(68.2) |
| Speed                           | ✓                                       | ✓                                       |
| Direction                       | ✓                                       | ✓                                       |
| Conductivity                    | ✓                                       | ✓                                       |
| Temperature                     | ✓                                       | ✓                                       |
| Pressure                        | ✓                                       | ✓                                       |

✓ Means meter equipped with sensor.

.....

Current Meter Station WGC-3A

Observation Period - To be deployed in March 1976

.....

Current Meter Station G2-F

Observation Period - 18 September 1975 - March 1976

.....

Bottom Pressure Station SCS-4, 59°46.2'N, 141°28.6'W

Observation Period: 18 Nov. 1975 - to be recovered in March

.....

Bottom Pressure and Current Meter Station SLS-5, 59°40.2'N, 141°39.7'W

Observation Period 18 Nov. 1975 - to be recovered in March

.....

Bottom Pressure Station SLS-6, 59°15.5'N, 141°59.2'W

Observation Period: 18 Nov. 1975 - to be recovered in March

B. The following articles have appeared or have been submitted for publication during FY-76.

Hayes, S. P. and J. R. Holbrook (1975). Response of the bottom pressure to winter storms in the N.E. Gulf of Alaska. EOS 12: 1010, 1975.

Hayes, S. P. and J. D. Schumacher (1976). Preliminary description of circulation on the continental shelf in the N.E. Gulf of Alaska: February-May 1975. Submitted to Journal of Geophysical Research.

Holbrook, J. R., D. Halpern, and S. P. Hayes (1975). Response of surface and near-bottom shelf currents to a winter storm in the Gulf of Alaska. EOS 12: 1006.

## VII. DISCUSSION

To date (not including work presented in last year's Annual Report) this project has conducted five cruises, deploying 21 current meter and/or bottom pressure gauge arrays, recovering seven arrays, conducting a 25-hr CTD time series at WGC-2 and CTD measurements along lines 1 and 2 in the Icy Bay region. Moored arrays WGC-2B and SLS-4 to be recovered this March have not been found, and WGC-1B has been recovered (March 12) but both current meters have lost their vanes and rotors. Reprogramming thus far includes the addition of five current meters to the process-oriented experiment in support of the bottom pressure gauge measurements, the addition of STA WGC-3A, located west of Shelikof Strait and, to address the question of gyral circulation west of Kayak Island (indicated both in satellite photographs and diagnostic model), STA 60 and STA 61 have been reoccupied and a new moored array, STA 69, has been added. This station is on a line running due south from STA 60 to STA 61 at a position which lies south of Tar Bank. If eddies exist here, then an examination of coherency among the three arrays should yield a first estimate of their spatial and temporal scales.

The analysis conveniently divides into a discussion of the spatial and temporal variability exhibited by the large-scale array and a discussion of the results of the Icy Bay pilot study which lead to the process-oriented experiment in that region. Current meter records from STA 62, STA 61, WGC-2, and WGC-1 were processed and analyzed. The observed mean flow along the Gulf of Alaska shelf-break is shown in figure 2, which was constructed from the following values:

| <u>STA</u> | <u>Observation<br/>Period</u>    | <u>Mean Flow (cm/sec)</u> |                    | <u>Direction</u> |
|------------|----------------------------------|---------------------------|--------------------|------------------|
|            |                                  | <u>at 20 m depth</u>      | <u>100 m depth</u> |                  |
| 62E        | 20 Sept. 1975<br>to 21 Nov. 1975 | 21.9                      |                    | 308              |
|            |                                  | 13.7                      |                    | 311              |

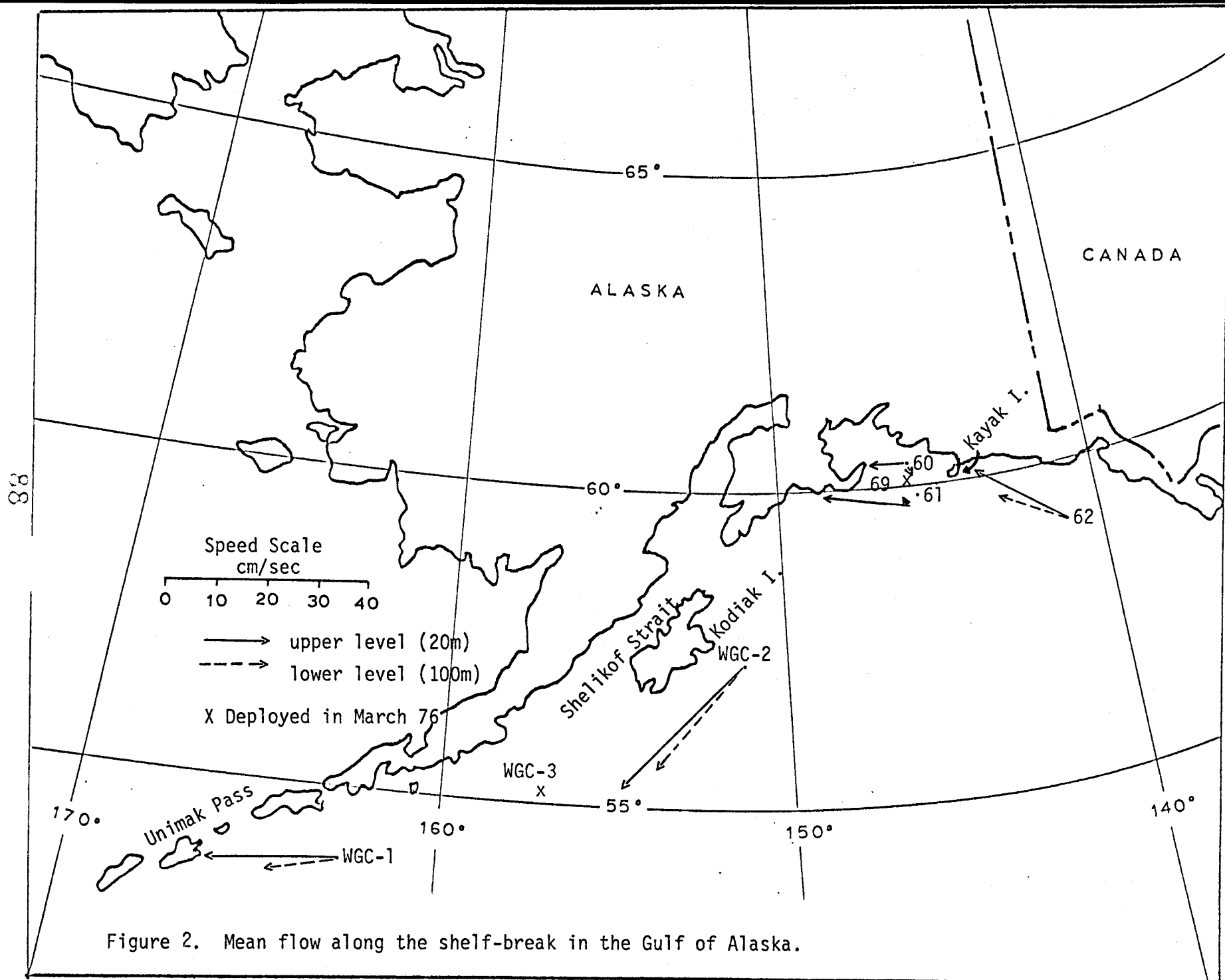


Figure 2. Mean flow along the shelf-break in the Gulf of Alaska.

|       |                                  |              |            |
|-------|----------------------------------|--------------|------------|
| 61    | 16 Aug. 1974<br>to 15 Nov. 1974  | 18.9<br>1.8  | 283<br>303 |
| WGC-1 | 5 Sept. 1975<br>to 2 Nov. 1975   | 27.0<br>15.0 | 263<br>257 |
| WGC-2 | 22 Sept. 1975<br>to 28 Nov. 1975 | 32.9<br>25.6 | 229<br>226 |
| 60    | 2 July 1974<br>to 26 Aug. 1974   | 7.3<br>1.2   | 277<br>156 |

The Alaskan Shelf Stream flows westward from STA 62, generally along the shelf break. Off Kodiak Island, this flow is intensified and attains the maximum mean flow observed. The stream maintains a high mean flow as it exits the study area south of Unimak Pass (WGC-1).

An examination of the 35-hr filtered record from 20 m depth at WGC-1 reveals that with the exception of a 1½-day period during early September (9-11) and a 1-day period beginning on October 23, the mean flow has westward components and that the direction of the mean flow fluctuates about the true west axis by + 45°. A presentation of the current meter record, low-pass filtered (2.86-hr) and constructed as a progressive vector diagram (PVD) is shown in figure 3. In contrast, the mean flow, at WGC-2 is directed, within + 25° of the record mean flow direction of 229° (TN). The PVD for this record is shown in figure 4.

The total variance in the record from WGC-1 (20 m depth) is 982.2 (cm/sec)<sup>2</sup> of which nearly 72% is contained in the tidal frequency bands. A tidal-response analysis yields tidal constituent speeds up to 20 cm/sec directed along a north-south axis. Although the tidal speeds are large and tidal frequency bands constitute the majority of the total variance, the Alaskan Shelf Stream is the major influence on the flow regime at WGC-2. This is more evident in the current record from 100 m depth. In this record, the variation in direction of the mean flow is + 10° from the direction of the net drift (226°TN). The effects of local current driving mechanisms at WGC-2 are small and the mean flow is exceptionally consistent in direction.

At STA 61, the 35-hr filtered current record indicates a higher degree of variability in both speed and direction than was observed at either of the western Gulf of Alaska moored arrays. However, the net drift (fig. 5) still indicates that the influence of the Alaskan Shelf Stream dominates the low frequency flow. A similar picture evolves from the records collected at STA 62 (fig. 6).

The change of total variance with depth at STA 62 was examined. In particular, the records for September through November 1975 (fig. 7) indicate that low-frequency processes dominate the energy spectra at the upper

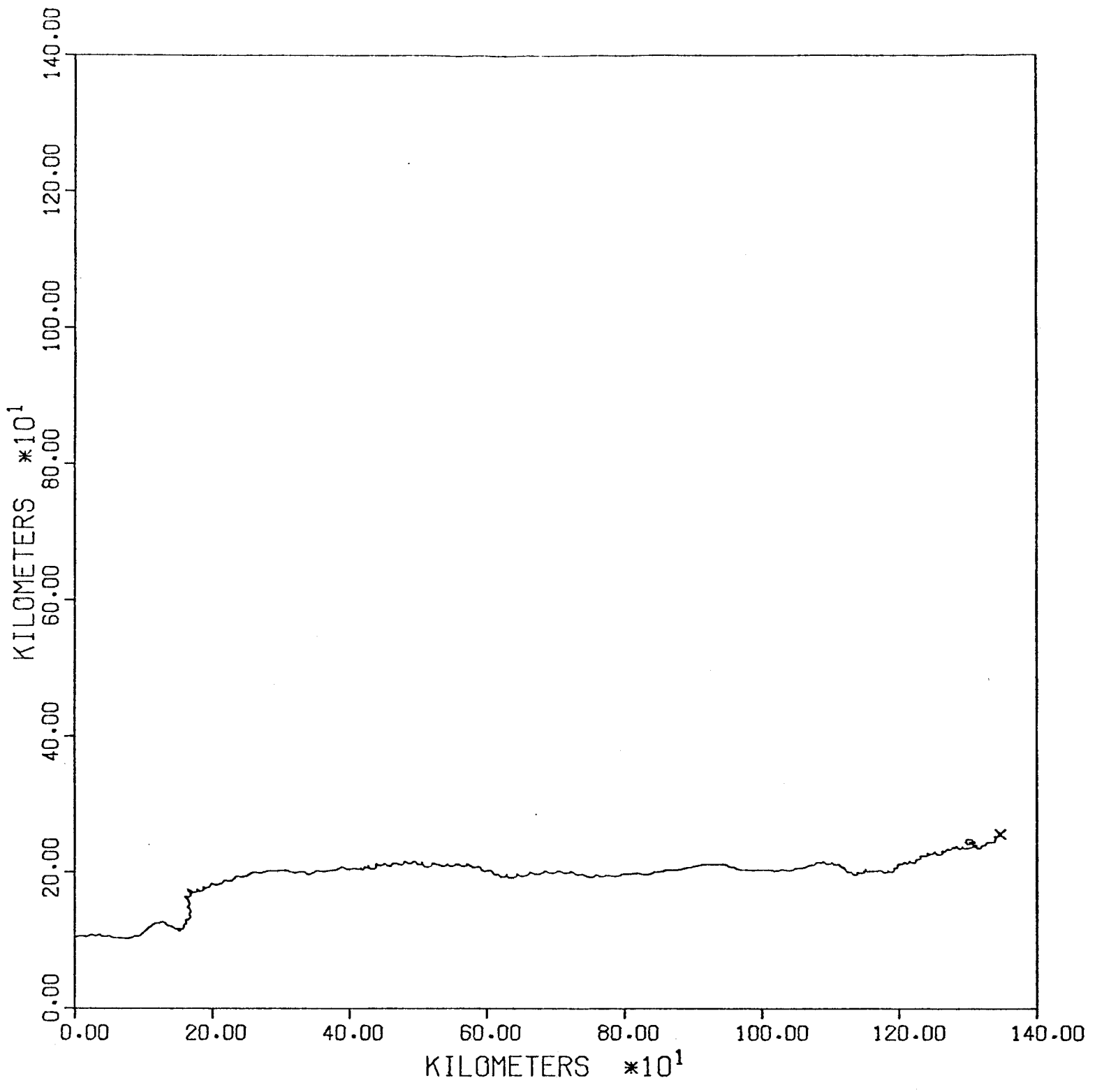


Figure 3. PVD constructed from measurements at WGC-1 during September to November 1975.



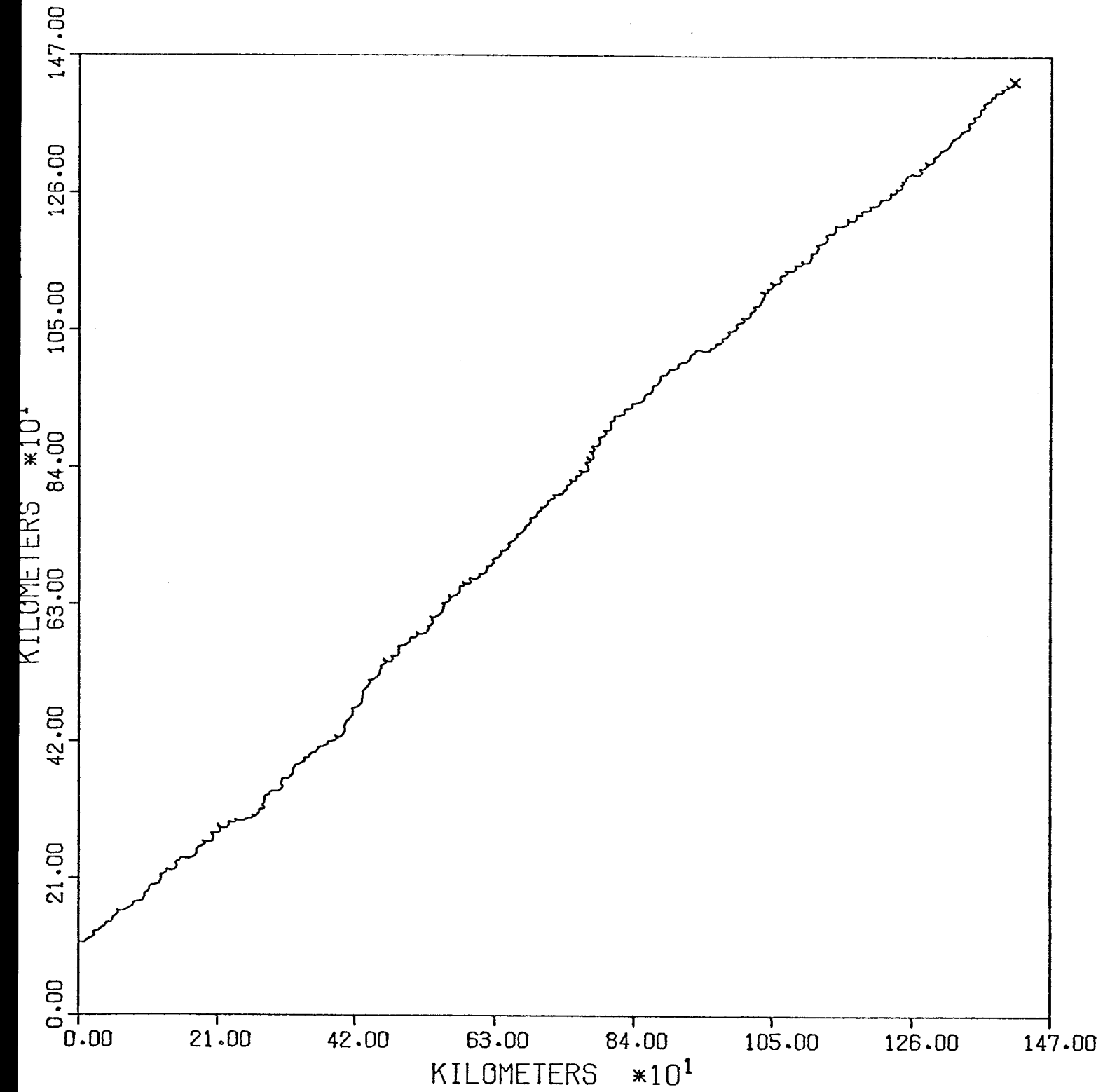


Figure 4. PVD constructed from measurements at WGC-2.

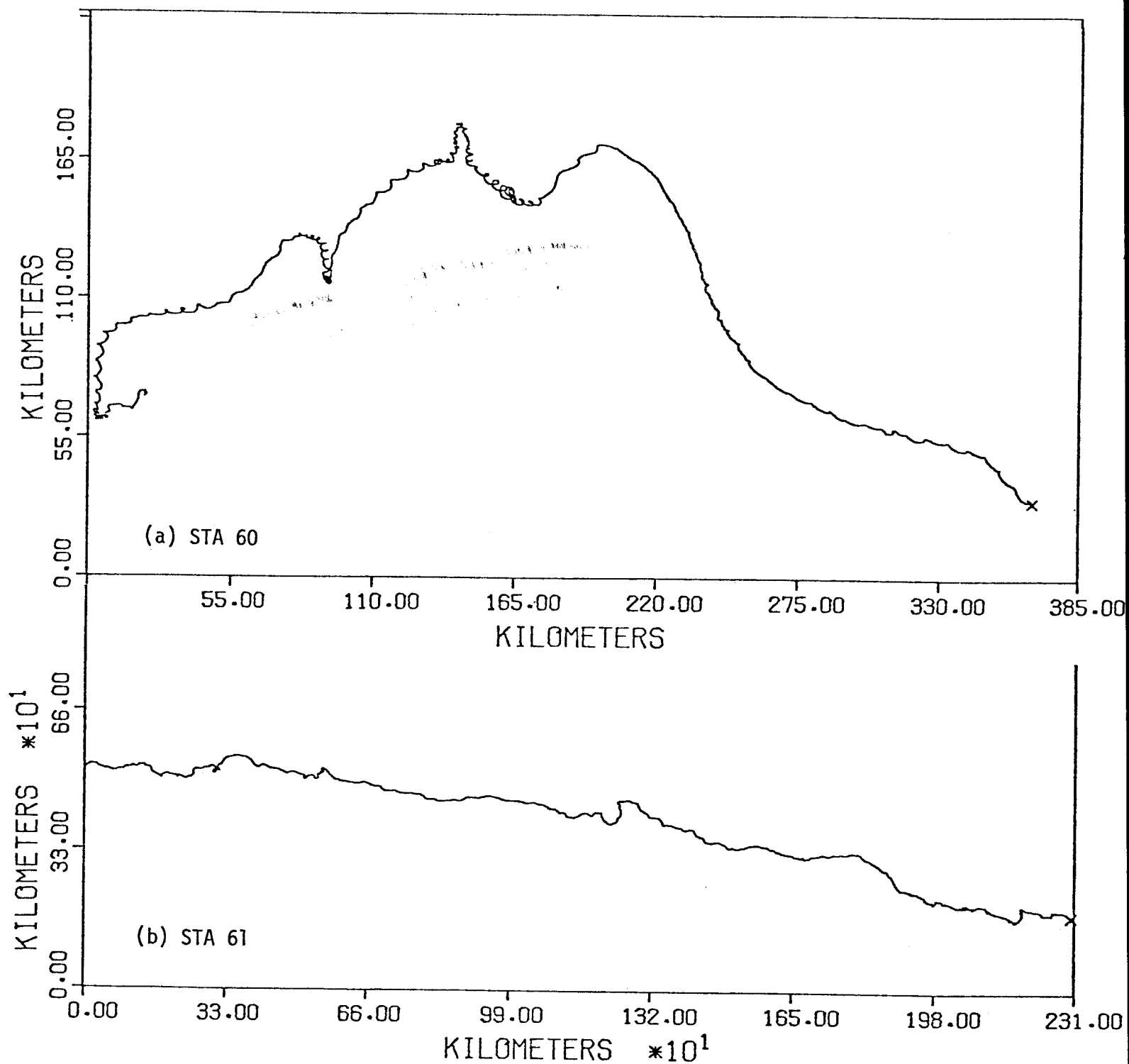


Figure 5. PVD constructed from measurements at (a) STA 60 and (b) STA 61 during summer regime 1974.

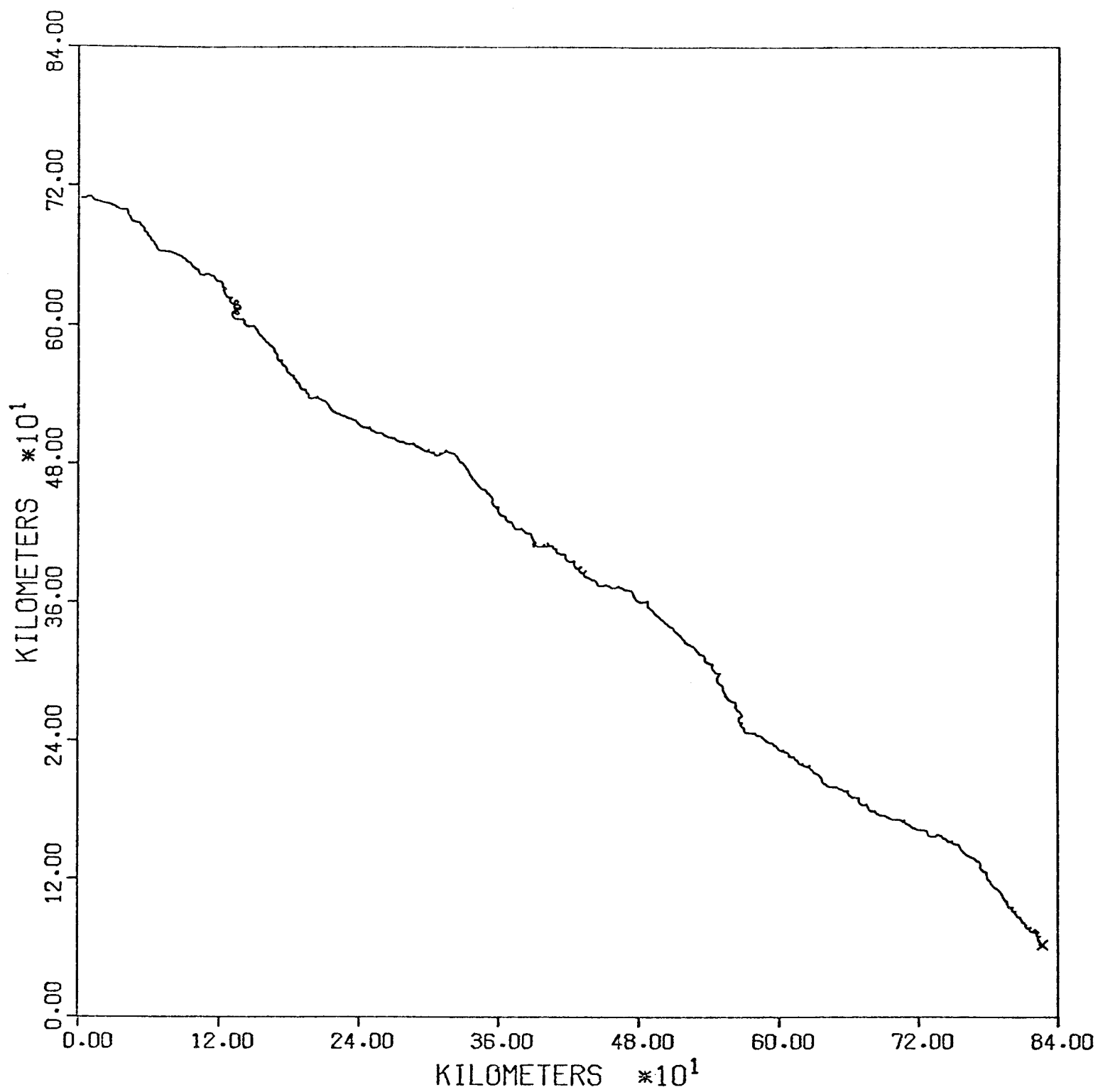


Figure 6. PVD constructed from measurements at STA 62.

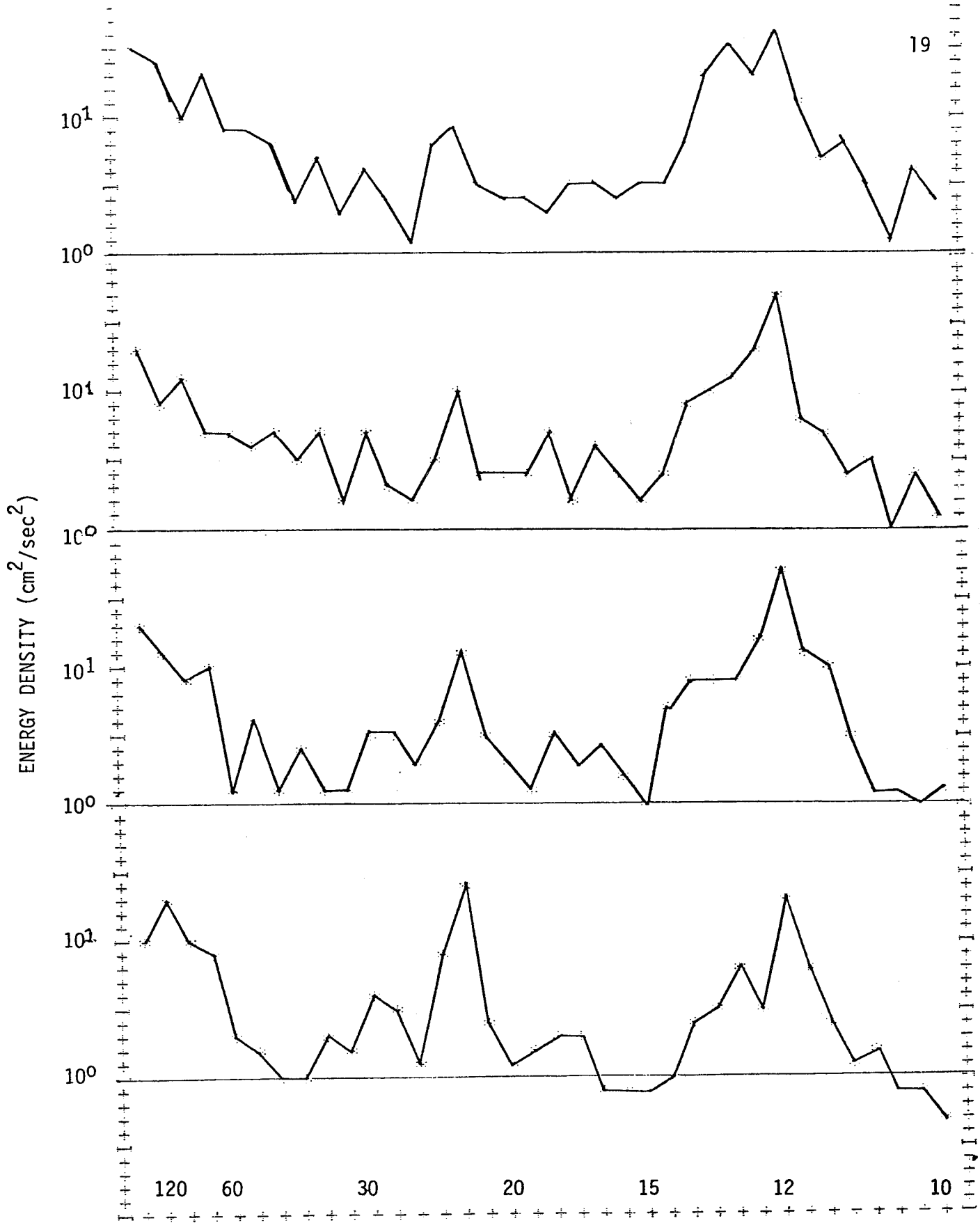


Figure 7. Energy density variation with depth recorded at STA 62, September 19 to November 21, 1975.

level, whereas tidal frequency band processes become more important with increasing depth. Rotary coherence between the 25 m depth and 105 m depth records yields significant values (at the 95% level) for low-frequency (90 hrs or greater) bands. This is in contrast to the results from 62B (winter regime) where significant coherence was found over a broad frequency range. The change in coherency indicates a seasonal variation, the records from 62B were collected during the winter (slight density stratification) whereas the records from 62F indicate a higher degree of density stratification. Therefore, during summertime, baroclinic flow is greater and coherence between currents is decreased in the vertical.

The Alaskan Shelf Stream dominates the mean flow along the shelf break over the entire extent of the study area. The range in net drift speeds used at 20 m depth was found to be 19 to 33 cm/sec, with the direction being westward along the local bathymetry. A result of this phenomenon is that local driving mechanisms have less influence on the flow regime. This can be contrasted with the results from Bristol Bay which indicate that higher frequency processes dominate and net flow is low.

A comparison of data from STA 61 and STA 60 which is located west of Kayak Island (see fig. 2) and STA 60 can be made, although the time periods when these stations were occupied does not overlap and statistical techniques cannot be applied. As indicated in figure 6, the flow measure at 20 m depth at STA 60 lacks consistency in direction and there are reversals in the flow. The mean flow at the lower current meter (90 m) was more than an order of magnitude less than that observed at any of the shelf-break stations and has a net offshore drift. This is the only station in the Gulf of Alaska study region which has a net offshore drift. Perhaps it is in this locality that suspended particulate matter is transported from glacial and river sources off the shelf to form a mid-depth (400 m - 500 m) maximum which has been found in the suspended particulate matter program. To resolve the flow regime in this shelf region a process-oriented experiment is required.

We now consider the data collected in the pilot study off Icy Bay during FY-75. In this experiment a single pressure gauge was deployed along with a current meter on mooring SLS-1. The instruments were deployed from February to May 1975. These records have been analyzed in conjunction with the current data from mooring 62B, the coastal sea level, atmospheric pressure, and wind data from Yakutat, and the 6-hourly winds calculated from the Fleet Numerical Weather Central synoptic pressure fields (Bakun, 1975).

The time series have all been filtered with a 40-hr cutoff low pass filter to reduce the tidal signal. The alongshore components of the resultant series are shown in figure 8.

First, consider the bottom pressure series at Yakutat and at SLS-1. The Yakutat series was constructed from the measured sea level and atmospheric pressure assuming 1 mb equals 1 cm. The two series are remarkably similar. The linear regression between them is 0.96 with a regression coefficient

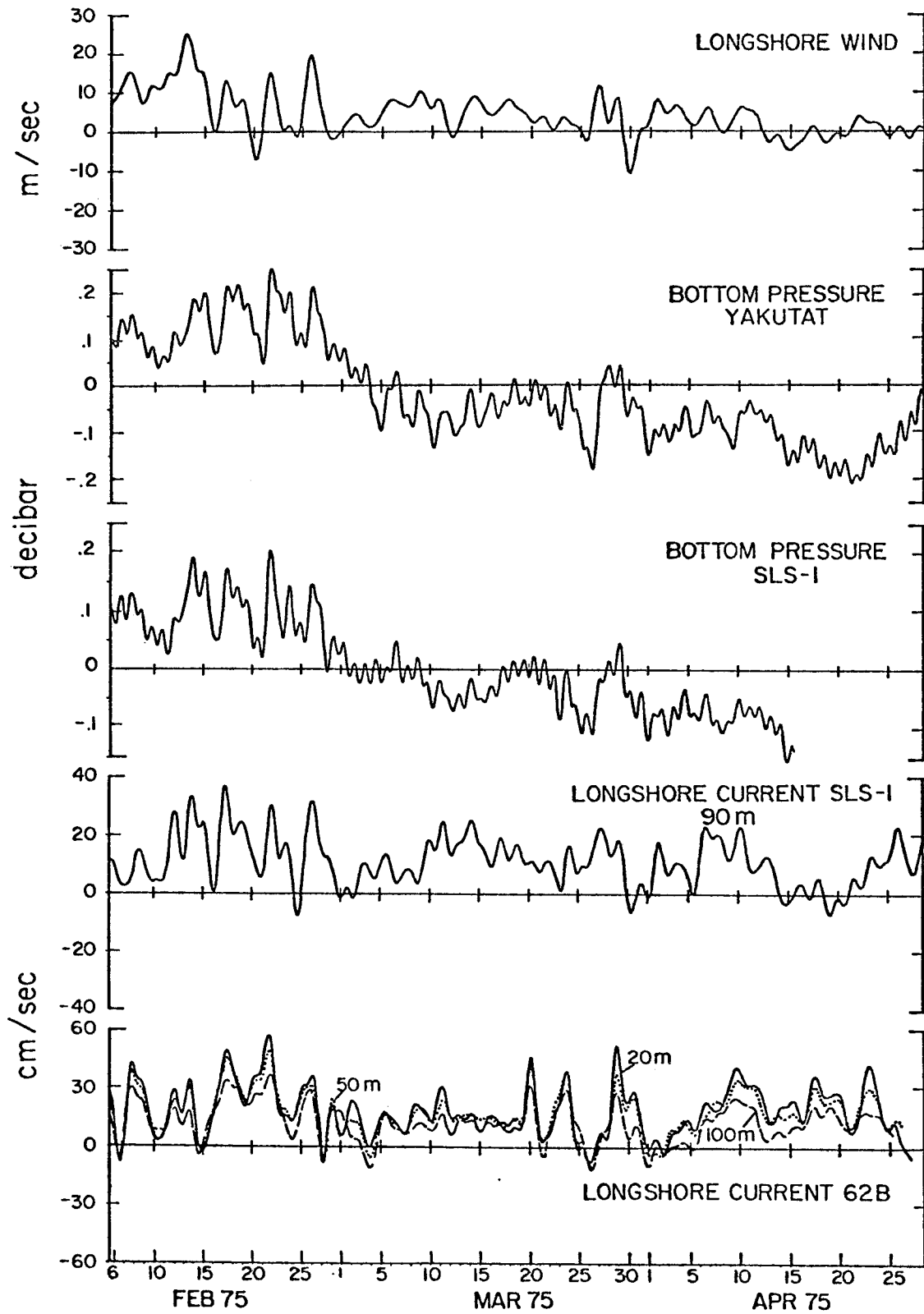


Figure 8. Time series of measurements from Icy Bay pilot experiment February-May 1975.

of 1.25 indicating that the Yakutat values are 25% greater than the SLS-1 measurements. The similarity of the two series is to be expected considering that the 100 m contour (i.e., the depth of the pressure gauge at SLS-1) is less than 5 km offshore of Yakutat. Nevertheless it is heartening to know that local effects due to Yakutat Bay do not seriously distort the Yakutat record. It remains representative of open ocean conditions. As an example of a coastal tidal station which does show marked local effects, Cordova is compared with Yakutat in figure 9. Both records show the storm-induced bottom pressure changes during February (17, 22, 26 Feb.), however, the excursions at Cordova are larger and more sharply peaked. This is presumably caused by the influence of Prince William Sound.

Returning to figure 8, all records show the occurrence of storm-induced response during February. The calculated longshore winds must be considered as only approximate indicators of the true velocity. However, comparison of these winds with shipboard and moored buoy measurements does show qualitative agreement (Holbrook, *et al.*, 1975). Also, as we shall show later, these winds appear more indicative of the true wind field than the Yakutat winds. In any case, there are at least four periods of high winds during February. The ocean responds quickly to these storms. Increases in the daily mean alongshore velocity of about 40 cm/sec (35 km/day) were observed at the 20 and 50 m levels. These velocity changes were accompanied by 15 cm increases in the bottom pressure.

After March 1, the frequency and the intensity of the storms decreased. The mean wind stress dropped by over a factor of 6 from February to March-April. Between the two periods the mean bottom pressure dropped 12 cm. However, the alongshore velocity did not mirror the bottom pressure change; at 90 m depth only 2 cm/sec change was observed from February to March-April. The relationship between the fluctuations in current and bottom pressure are also complex during the March-April period. For example, on March 20 and 23 the current meter records at all levels on 62B show large increases. Neither the bottom pressure nor the currents on SLS-1 show similar variations. On March 30 the 62B currents and the SLS-1 bottom pressure appear correlated; however, the 90 m currents show little change. Thus qualitatively the relationships among the measurements seems simpler in February than in the subsequent period.

This qualitative statement is borne out by subsequent analysis. Barotropic response of the currents on the shelf is suggested by the similarity of the currents at 20 m and at 100 m on 62B. For barotropic flows the velocity and pressure time series should be linearly related:

$$v = \left(\frac{f}{gL}\right) p + b \quad (1)$$

where  $f$  is the Coriolis term,  $g$  is the gravitational acceleration,  $L$  is the length scale of the pressure slope. If the linear correlation coefficient is high, then equation 1 can be used to find  $L$ . In table 1 the results are shown for the correlation of the 90 m currents and the

Table 1. Linear correlation of velocity and pressure time series on SLS-1. CC is the linear correlation coefficient. RC is the regression coefficient, and L is the inferred length scale. The 95% confidence interval is shown.

| LINEAR CORRELATION (P, V) |     |     |                         |        |
|---------------------------|-----|-----|-------------------------|--------|
| Interval                  | CC  | 95% | RC (sec <sup>-1</sup> ) | L (km) |
| 5 Feb - 18 April          | .35 | .26 | 0.31                    | 250    |
| 5 Feb - 1 March           | .74 | .41 | 1.51                    | 52     |
| 8 March - 15 April        | .14 | .31 | 0.26                    |        |

$$\Delta V = \frac{g}{fL} \Delta P = (RC)\Delta P$$



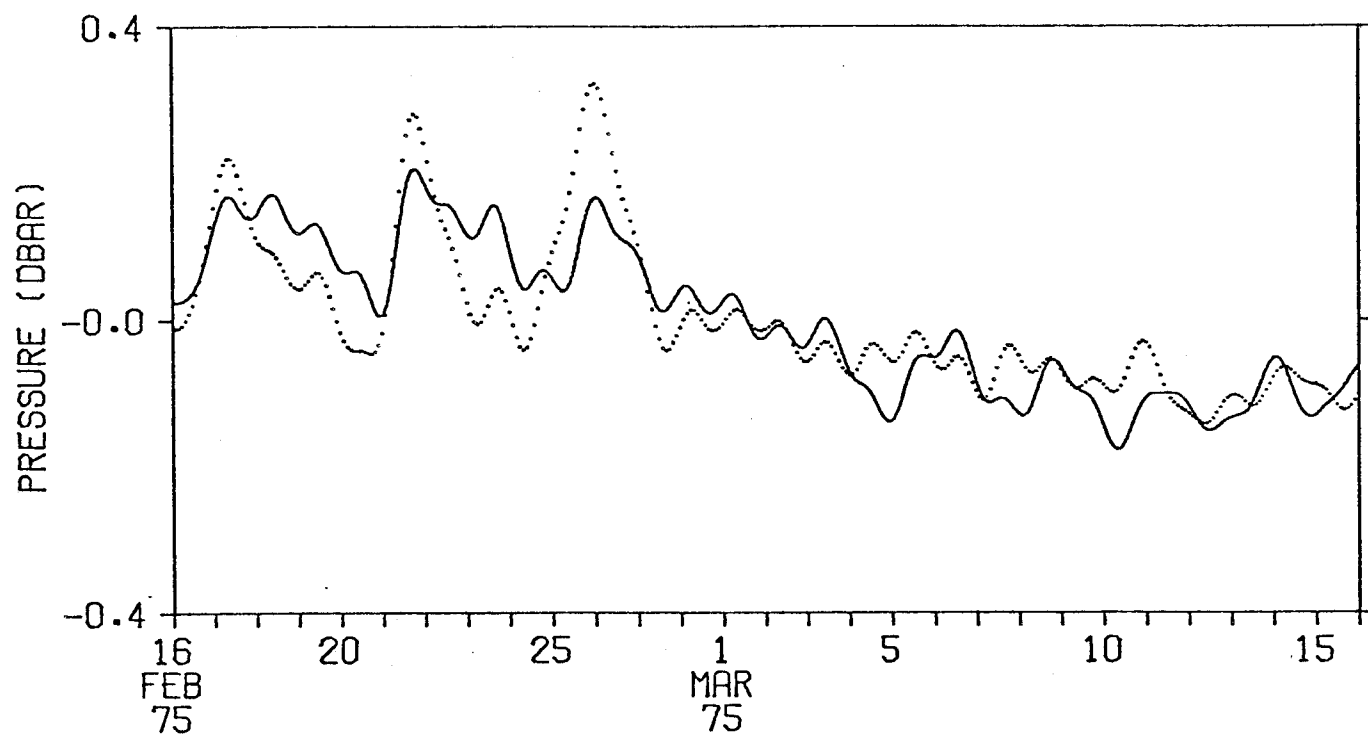


Figure 9. Bottom pressure (adjusted sea level) at Yakutat (solid) and Cordova (dotted).

bottom pressure for the entire experiment and for the winter and spring periods. During winter the correlation coefficient is high, the length scale  $L$  is comparable to the shelf width. However, during spring the correlation is insignificant. Thus, the simple barotropic response model fails. Either baroclinic effects or a variety of length scales must become increasingly important during spring.

The complexity of the spring oceanic response is further suggested by figure 10. The coherence between the Yakutat bottom pressure and the calculated alongshore wind field is shown for January-February and April-May. During winter the coherence is large over a broad spectral range. However, in the spring record this coherence never rises above the 95% confidence limit for no coherence. Thus, the data imply that nonlocal forcing becomes increasingly important during spring. This may merely reflect the absence of dominant storms during this period.

The final analysis compares the response of the bottom pressure to alongshore and onshore winds. In figure 11 the Yakutat measured winds and the calculated winds are compared with SLS-1 bottom pressure. Clearly, the alongshore winds are more effective than the onshore winds in producing setup. Also, the calculated winds show a larger coherence than the measured Yakutat winds. This is due to the contamination of the coastal winds by local topography. Whether better wind-ocean correlations would result from direct wind measurements over the open ocean remains unknown.

### VIII. CONCLUSIONS

To date, data collected, processed and analyzed from the Gulf of Alaska indicate the following preliminary conclusions:

- A. The mean flow is high (of order 25 cm/sec) and directed to the west generally following the local isobaths.
- B. There are considerable variations in the mean flow and in the fluctuations. The flow near Kodiak Island is larger than that measured at other shelf break locations. West of Kayak Island the mean flow is weak but the fluctuations are large.
- C. During winter storm-induced velocity changes are of the same order as the mean flow. These appear to be mainly barotropic and hence linearly related to the sea surface slope.
- D. During spring the velocity field is more complex. The fluctuations in the velocity do not correlate simply with the bottom pressure. It appears that nonlocal forcing may be important.
- E. The seasonal change in the density stratification is reflected in the coherence of the currents. During winter high coherence from 20 m to 100 m is observed. In the summer the coherence is lower.

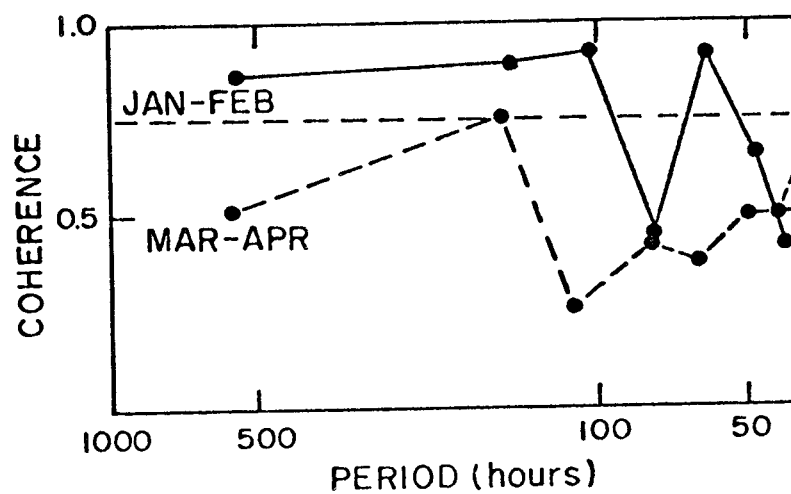


Figure 10. Coherence between calculated winds and Yakutat bottom pressure for two seasons.

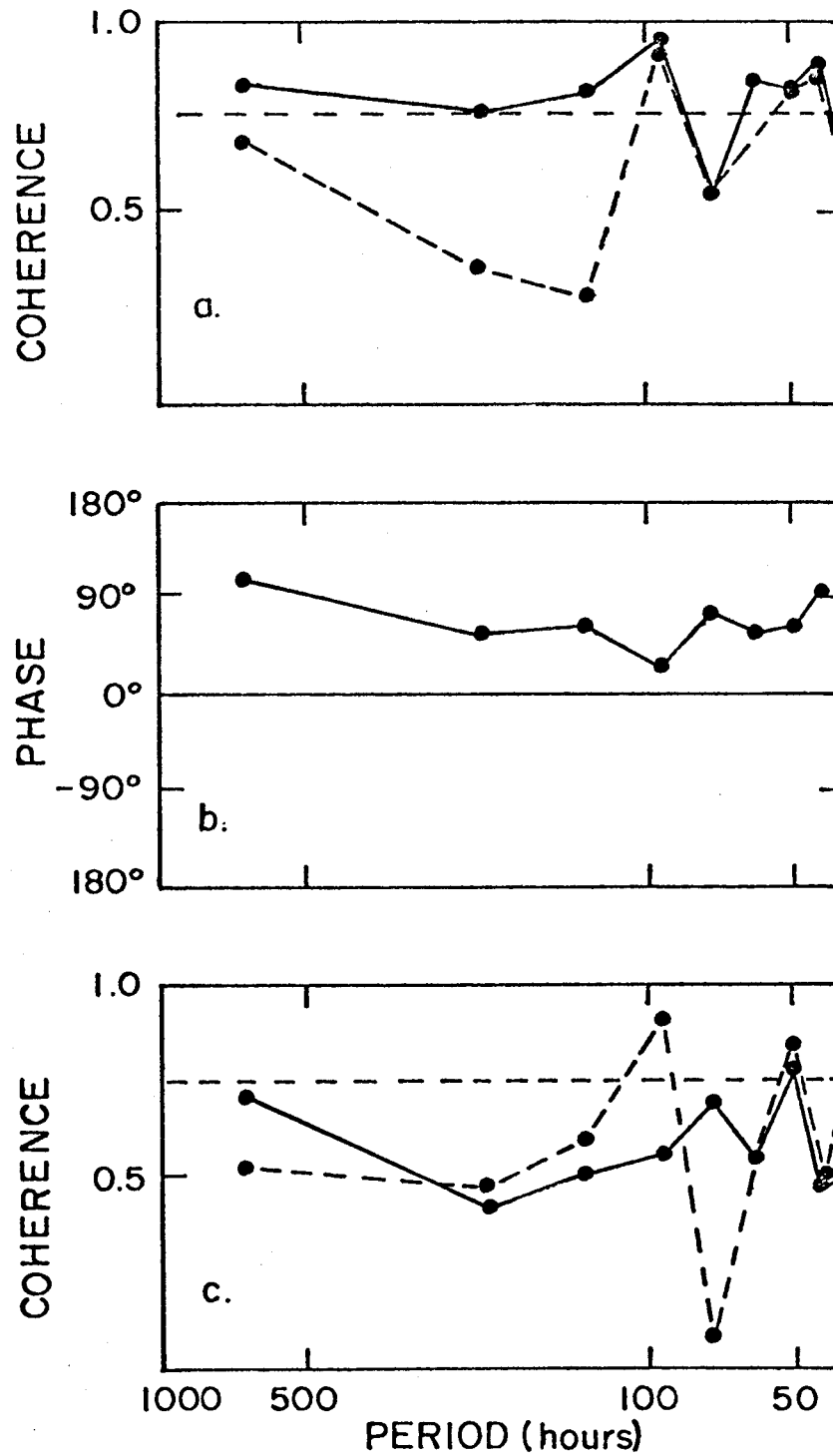


Figure 11. Coherence between calculated winds (solid) or measured Yakutat winds (dashed) and SLS-1 bottom pressure a) alongshore winds, b) phase for alongshore winds, c) onshore winds.

## IX. NEEDS FOR FURTHER STUDY

The regional large-scale experiment has delineated variations in the statistical structure of the flow at a few locations throughout the Gulf of Alaska. Although all areas indicate a mean flow which can be identified as an on-shelf manifestation of the Alaskan Current, there are considerable differences in the magnitude of the mean flow and in the relative contributions of the fluctuations. These are probably due to both temporal and spatial variability. That is, the time series are not sufficiently long to resolve the true flow characteristics and (in all likelihood) there are indeed true differences in the flow at different locations.

Therefore, the continued studies in the Gulf of Alaska must contain long-term measurements on the large-scale regional grid as well as on the smaller-scale process experiments which will define the dynamics responsible for the observed flow. The regional stations which have been initiated should be continued. In addition, the process-oriented experiment off Icy Bay should be completed. A full year record is required in order to resolve the seasonal changes. In addition, new process-oriented experiments should be developed. These include: (1) a study west of Kayak Island to resolve the question of eddy generation (This experiment should be coordinated with meteorological and suspended particulate matter programs.); (2) a study of Cook Inlet/Sheikof Strait to examine flow regime in the transition zone from shelf to estuarine dynamics; and (3) a study on the western Gulf of Alaska shelf to examine sea level changes, wind field, and velocity field dynamics. Also, a study near Kodiak Island should be initiated to investigate the anomalous sea level changes observed there. Additional large-scale stations are required to reduce the 600 km scale between stations.

The new experimental areas will build on the present arrays. In all cases the large-scale regional array will provide the long-term monitor stations which describe the climate in which the finer-scale process experiments operate. These latter should extend across the shelf from the shallow water to the shelf break. They should be supported by detailed STD surveys in the experiment area.

Finally, the importance of wind measurements should be stressed. We have noted that calculated winds are more coherent with oceanic variables than are shore-measured winds. What improvements wind stress measured over the water would provide are not known. This should be investigated. In addition, surface current measurements are not being made at present from moored buoys. These currents can be derived from the wind and interior current field under some conditions. Measurements to establish this should be made.

## X. SUMMARY OF 4th QUARTER OPERATIONS

| <u>Activity</u>  | <u>Personnel</u>                |
|--|---------------------------------|
| A. <u>Discoverer</u> , Cruise RP-4-DI-75B, Leg II, 2-11 Sept. 1975 |                                 |
| Station WGC-1  | Dr. J. Schumacher, PMEL/NOAA,   |
| Lat. 54°01.72'N  | Chief Scientist                 |
| Long. 162°59.84'W  | Dr. L. Coachman, U. of W.       |
| Depth: 188 m   | Mr. R. Tripp, U. of W.          |
| Two Aanderaa RCM   | Mr. R. Newman, PMEL/NOAA        |
|  | Mr. D. Stith, PMEL/NOAA         |
|  | Mr. S. Harding, U. of W.        |
|  | Mr. J. Ruehle, USF & WS         |
| B. <u>Surveyor</u> , RP-4-SU-75C, Leg II, 16-22 Sept. 1975         |                                 |
| Station WGC-2A depl.   | Mr. N. P. Laird, PMEL/NOAA,     |
| Lat. 57°27.1'N   | Chief Scientist                 |
| Long. 150°29.6'W   | Mr. S. Raam, PMEL/NOAA          |
| Depth: 186 m   | Mr. R. Carlone, PMEL/NOAA       |
| Two Aanderaa RCM   | Mr. D. Stith, PMEL/NOAA         |
| 25-hr CTD time series at WGC-2A                                    | Mr. W. Hoffman, O.S.U.          |
|  | Ms. C. Handel, USF & WS         |
| Station 62D recov.   |                                 |
| Station 62E depl.  |                                 |
| Lat. 59°31'N   |                                 |
| Long. 142°10'W   |                                 |
| Depth: 188 m   |                                 |
| Four Aanderaa RCM  |                                 |
| C. <u>Discoverer</u> , RP-4-DI-75B, Leg II, 18-24 Nov. 1975        |                                 |
| Station 62E recov.   | Dr. S. Hayes, PMEL/NOAA,        |
| Station 62F depl.  | Chief Scientist                 |
| Lat. 59°34.67'N  | Lt. Cmdr. H. Milburn, PMEL/NOAA |
| Long. 142°11.44'W  | Mr. J. Glenn, PMEL/NOAA         |
| Depth: 188 m   | Mr. C. Pearson, PMEL/NOAA       |
| Four Aanderaa RCM  | Mr. J. Haslett, PMEL/NOAA       |
| Station SLS-4 depl.  |                                 |
| Lat. 59°46.2'N   |                                 |
| Long. 141°28.6'W   |                                 |
| Depth: 52 m  |                                 |
| Pressure-temperature   |                                 |

## C. (Continued)

Station SLS-5 depl.  
Lat. 59°40.2'N  
Long. 141°39.7'W  
Depth: 99 m  
Two Aanderaa RCM  
One geodyne cm  
Pressure-temperature

Station SLS-6 depl.  
Lat. 59°15.5'N  
Long. 141°59.2'W  
Depth: 258 m  
Pressure-temperature

Five CTD stations  
on line 1

D. Miller Freeman, RP-4-MF-75B, Leg IIB, 28-29 Nov. 1975

Station WGC-2A recov.  
Station WGC-2B depl.  
Lat. 57°26.7'N  
Long. 150°29.4'W  
Two Aanderaa CM + 1 PG

Mr. C. Pearson, PMEL/NOAA  
Chief Scientist  
Mr. J. Haslett, PMEL/NOAA  
Mr. M. Rauzon, USF & WS  
Mr. M. Kirchoff, USF & WS

## REFERENCES

- Air and Water News, March 24, 1969, p. 3.
- Bakun, A. (1975). Wind-driven convergence-divergence of surface waters in the Gulf of Alaska. (Abstract) Trans. Amer. Geophys. Un. 56: 1008.
- Berridge, S. A., M. T. Thew, and A. G. Loriston-Clark (1968a). The formation and stability of emulsions of water in crude petroleum and similar stocks, J. Institute Petroleum 54(539): 333-357.
- Berridge, S. A., R. A. Dean, F. G. Fallows, and A. Fish (1968b). Properties of persistent oils at sea. J. Institute Petroleum 54(539): 300-307.
- Dodimead, A. J., F. Favorite, and T. Hirano (1963). Salmon of the North Pacific Ocean, Part II, Review of Oceanography of the subarctic Pacific Ocean region. Inst. N. Pacific Fish. Comm. Bull., No. 13, 195 pp.
- Favorite, F. (1967). The Alaskan Stream. Inst. N. Pacific Fish. Comm. Bull., No. 21, 53 pp.
- Galt, J. A. (1975). Annual Report on Physical Oceanography in the N.E. Gulf of Alaska.
- Galt, J. A. and T. C. Roger (1975). Physical Oceanography and Dynamics of the N.E. Gulf of Alaska.
- Groves, G. W. (1956). Day-to-day variations of sea level. In Interaction of Sea and Atmosphere Meteorological Monographs, 2(10).
- Hebard, J. F. (1961). Currents in the southeastern Bering Sea. I.N.P.F.C. Bulletin 5:9-16.
- Pattullo, J. W. Munk, R. Revelle, and E. Strong (1955). The seasonal oscillation in sea level. J. Marine Res. 14: 88-155.
- Reid, J. C. and A. W. Mantyla (1975). On the seasonal variation of sea elevations along the coast of the northern North Pacific Ocean. (Abstract) Trans. Amer. Geophys. Un. 56: 1008.
- Royer, T. C. (1975). Seasonal variations of waters in the northern Gulf of Alaska. Deep-Sea Res. 22(6): 403-416.
- Thompson, R. E. (1972). On the Alaskan Stream. J. Phys. Ocean. 2: 363-371
- Zachariasen, F. (1968). Oil pollution in the Sea: Problems for future work. Research paper P-432, Institute for Defense Analysis, June.



Annual Report

Numerical Studies of Alaskan Region

RU 140, 146, 149, 31

Principal Investigator: J. A. Galt, PMEL/ERL  
3711 15th Avenue N.E.  
Seattle, Washington 98105  
(206) 442-4598; FTS 399-4598

I. Summary of objectives, conclusions and implications with respect to  
OCS oil and gas development

These studies have been directed at the numerical modeling and simulation of oceanographic processes. Primary emphasis has been concentrated on phenomena that affect the transport and dispersion of pollutants. Each potential OCS lease area has its own unique physical environment and available data base. As a consequence of this, the approach taken during these studies has varied somewhat from area to area. Even considering the variations from one area to the next, it is easy to summarize the objectives in generic terms. The first question that must be answered is related to the advection. Where is the water going? or, more to the point, where would we expect to find a pollutant (usually floating oil) moving if it were accidentally released into the marine environment? The second question that must be answered is related to dispersion. Basically, here we need to know the uncertainty, or scatter that the simple advective pathways are likely to show. On a smaller scale, it is also necessary to know the spreading and ultimately the dilution that a single patch of released pollutant would undergo as it moved along its trajectory.

The circulation and mixing processes that typically occur in the waters over the continental shelf are extremely complex. The basic governing equations are rich in solutions, which are themselves immensely complicated by such factors as irregular geometry and stratification. Faced with these compound difficulties and the demands of an applied research program, we must seek ways of optimizing the research output in a timely fashion. To do this, the basic equations must be simplified. The phenomena that are excluded from these reduced formulations must be investigated separately, or entered in a parameterization. There are clearly some hazards in this approach, but they can be minimized by the careful integration of the theoretical modeling efforts and the observation program. In this sense, we may think of these efforts as empirical models. From another point of view, the models will be useful to extend and interpolate the observational data in a dynamically consistent way. Whatever the point of view, the key point is that the modeling and observational programs should not be considered as separate entities. The optimum returns for OCS environmental assessment will depend on mutually supportive observational and modeling component studies.

To date, the modeling studies in cooperation with the rest of the physical oceanography program elements have been able to describe circulation patterns for some of the OCS region in considerable detail. In other areas, dominant physical processes have been identified and simulations have been initiated. From the results so far, it seems clear that these studies can

integrate certain facets of the OCS program and present results that are a useful part of the assessment evaluation. The implications of this work for OCS development are best considered in a larger context of the whole program. As an example of the type of input these studies can provide, the reader is referred to Appendix I of this report, "Circulation Studies on the Alaska Continental Shelf Off the Copper River Delta" by J. A. Galt.

## II. Introduction

### A. General nature and scope of study

The numerical modeling and simulation studies are designed to provide information on advection and diffusion processes, aid in the interpretation of observational data, and present the results in an easy to interpret integrated form. In its simplest statement, we may consider the fate of some pollutant that is introduced into the marine environment. Three distinct generic processes may act on the pollutant. First, it may be advected, or be carried along by the water currents that it happens to be in. The fact that these currents may be caused by tidal forces, thermohaline distributions, or wind stress mixed in an undetermined way may complicate the specification of the actual current, but as far as the pollutant problem is concerned it is just floating with the flow. The second process acting on a pollutant is dispersion, or mixing. This spreading is primarily due to the non-linear interaction of high frequency components to the current. This basically turbulent process is not well understood theoretically, but a number of approximate models, or simulations, have been developed that yield useful results. The major observable ramification of this process is the diffusion

and subsequent dilution of pollutants. The third process of interest is the in-place supply or utilization of the pollutant. The supply is determined by a source distribution, i.e., spills, chronic release, etc. The utilization will be determined by evaporation and bio-chemical processes which can loosely be referred to as weathering. These three processes and their effect on a pollutant can be summarized in what oceanographers refer to as the distribution of variables equation (chemical engineers call the same equation the mass balance equation). It can be written as follows:

$$\frac{\partial C}{\partial t} = -\nabla((V_w + V_c)C) + \nabla(K\nabla C) + R_c$$

|                    |   |                         |   |                     |   |                         |
|--------------------|---|-------------------------|---|---------------------|---|-------------------------|
| observed<br>change | = | $-\nabla((V_w + V_c)C)$ | + | $\nabla(K\nabla C)$ | + | $R_c$                   |
|                    |   | advection               |   | diffusion           |   | in-place<br>source/sink |

The research components presented in this report all attempt to describe some portion of the advective or diffusive input required for this equation. A typical element will concentrate on some tractable segment of the advection. For example, a diagnostic model has been developed. This looks at the steady or quasi-steady components of the mean flow. It specifically excludes tides, but accounts for stratification, and complex bathymetry. Clearly this model cannot be the whole answer. In fact, for areas dominated by tides (for example, Cook Inlet) this might not even make a credible first approximation. Out of context, each of these models is an attempt to isolate and describe some segment of the flow or mixing. They should be applied to regions where they represent the dominant, or at least a significant fraction of the governing dynamics. In some areas the regional dynamics will be complex enough so that several of the basic component models will have to be combined to give an adequate description of the flow fields.

To get an over-view of how these isolated components would be incorporated into the more general assessment process, it is useful to consider a conceptual model of a pollutant trajectory study. Such a conceptual model is schematically represented in figure 1. In the center is the basic trajectory model (represented by the distribution of variables equation). Feeding into it are the three basic processes: advection, diffusion and in-place pollutant reaction, plus the appropriate software development to present the integrated output in an intelligible form. In the next level out from the center are the specific model components, developed to supply information to the central model for synthesis and integration. Up stream even more (farther out from the center) are additional support models and observational programs that supply the basic empirical data for regional definition and model verification.

The work that is discussed in this report is intended to fill in some of the lower and left-hand sections of this diagram. Proposed work for the coming year will concentrate on gaps and the upper and right-hand side of the conceptual design.

#### B. Specific objectives

The specific objective of this research is to describe advective and diffusive processes and synthesize the results into a form that can be easily incorporated into the overall assessment process. This is to be done for as many of the OCS areas as time and data allow. Tools are being developed that can be applied in any region where the dynamics is appropriately represented and data for verification and boundary condition specification are available.

BIOLOGICAL RECONNAISSANCE

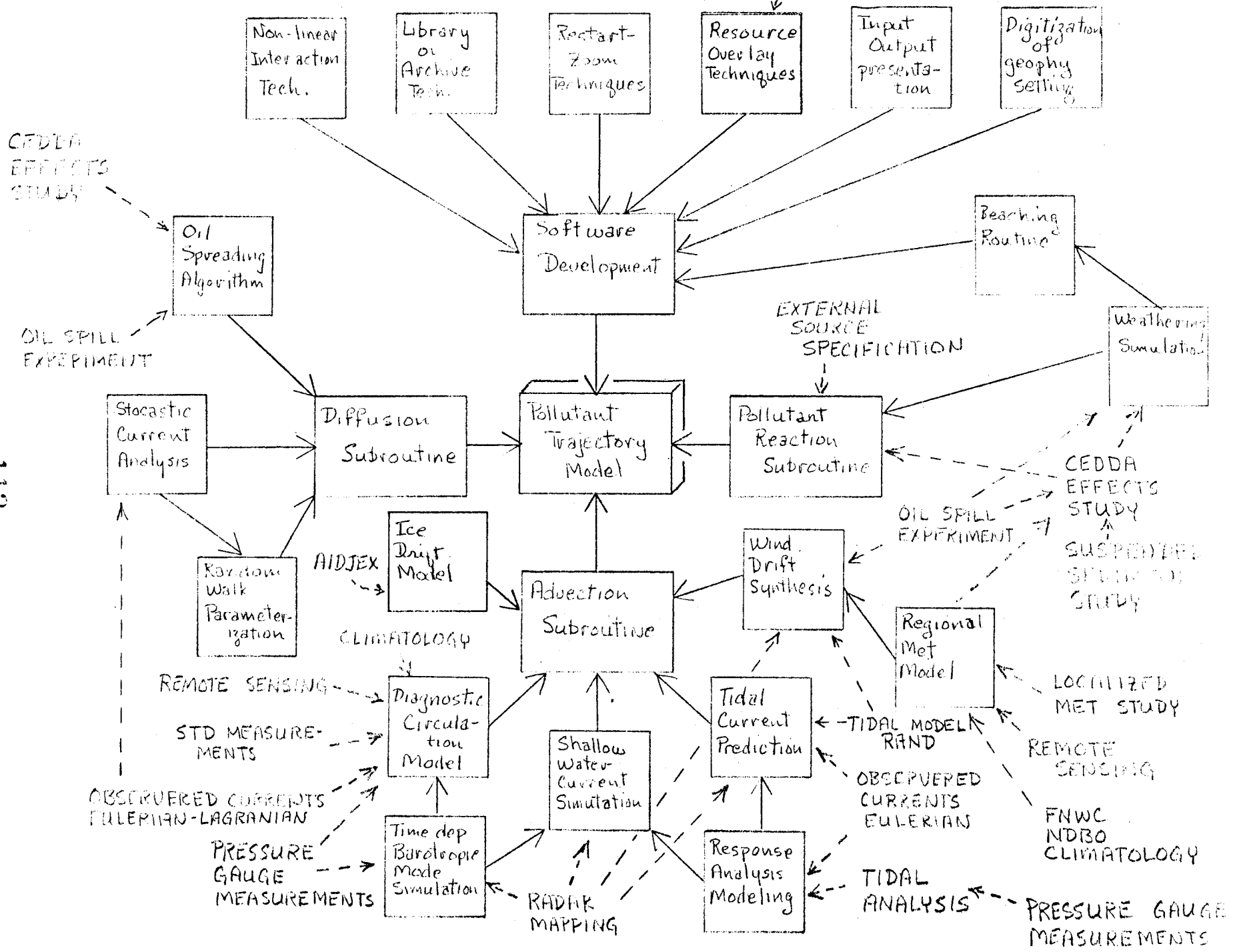


Figure 1.

112

### C. Relevance to problems of petroleum development

To assess the potential impact of oil and gas development on the marine environment, there are two fundamental questions that must be answered. First: if petroleum is released into the environment, where will it go and how much will it be diluted? Second: what are the environmental components that will be damaged by petroleum, or what is at risk? These studies directly address the first question.

The general method in which these studies were carried out makes it impractical to follow the suggested format for the remainder of the report. The following section will both describe and discuss the elements of the work that has been carried out. The conclusions that can be derived from the work will be either presented along with the description or in extended documentation attached as appendices.

## III. Discussion of work carried out

### A. Gulf of Alaska

#### 1) Diagnostic model -

A diagnostic circulation model was developed during the previous contract year and an initial run carried out on geophysical data from the Gulf of Alaska (First year physical oceanography annual report for NEGQA). The theoretical development of the model has been documented in a IIOAA technical report (Galt, 1975). These early studies were forwarded to the Department of the Interior for input into their initial resource assessment.

During the present contract year the results of the model have been carefully checked against observational data and the numerical techniques used have been significantly refined. The model has been used to explore

the sensitivity of the represented currents in the Gulf of Alaska to variations in boundary condition, triangulation schemes, stratification, and numerical interpolation techniques. In addition, the model has been run for a number of contrived data sets and geometries for which an analytic solution is available. The results of this testing and a complete documentation of the numerical techniques and computer algorithms are presented in a second NOAA technical report (Watabayashi, 1976).

2) Localized circulation analysis using the diagnostic model -

The general features of the circulation predicted by the diagnostic model in the Gulf of Alaska have been compared to the earlier analysis of the currents for the region (Galt and Royer, 1975). The results indicate that the model can reproduce the mean circulation patterns in some detail. In addition, by examining alternate settings of the boundary conditions, it was possible to adjust the magnitudes of the predicted currents so that they accurately reproduced the measured currents available from moored current meter installations within the model domain. Used in this manner, the model could be keyed on observations of the currents at one location and in turn predict the flow for the entire region. A complete study using summer data for the Gulf was carried out and fully documented in report form (Galt, 1976). This report is included as appendix I and was available to the Department of the Interior for consideration in the later stages of their pre-lease assessment studies.

3) Stochastic analysis of current meter and wind data -

To estimate the potential scatter, or variance expected in pollutant trajectories, it was necessary to examine the non-steady or time-dependent part of the currents. By doing this, empirical estimates of the



dispersion can be obtained. These estimates are based on a stochastic analysis of time series data, assume a first order Markov process, and can be used in conjunction with the mean flow prediction from the diagnostic model, or any other source. This analysis was carried out for the near surface current meter records available from the Gulf of Alaska.

A number of oil spill trajectory models exist which include the wind drift effects in a stochastic form. In particular, the Department of the Interior's assessment models require this type of input. Because of this, an additional stochastic analysis of wind field data (available through FNWC) was carried out so that the results could be included in their study.

A brief description of this analysis and a representative selection of the results are presented here. A more complete coverage is available and will be incorporated into the development of the trajectory model proposed for next year and outlined in the introduction of this report.

#### Stochastic Model Description

Markov Chain Theory, as it was applied in this model, is based on a class of finite states of action for a given phenomenon. For a stochastic model of currents, a relevant class of states needed to be chosen. This model was based on eight direction classes and three speed classes, allowing twenty-four finite states. The direction classes were designated the eight major compass directions in degrees, plus all points within  $22.5^\circ$  of the compass direction, excluding the lower boundary point ( $X_0 - 22.5^\circ < X \leq X_0 + 22.5^\circ$ ). The direction classes spanned the field completely.

The speed classes were based on arbitrary cut-offs in velocity magnitude. These cut-off values were chosen so that the field of speeds would be roughly divided into thirds. In all cases, the mean velocity was removed from the data before processing.

The first thirty days of six different current meter records from the Gulf of Alaska were analyzed by the Markov process in separate runs. The model calculated, if the current was in a certain state of time  $t_1$ , the probability of its state at time  $t_2$ . The time increment ( $t_1 - t_2$ ) was one hour. The regular sampling interval of each current record was some integer fraction of an hour, so records were skipped accordingly. The intermediate result of the model for each current meter was an array, dimensioned twenty-four by twenty-four, which listed the probability of each state being stepped to any state.

The second part of the model used the probability tables to look at the scatter produced in the current, excluding the mean flow. One thousand points were iterated independently through time using mean speeds and directions for each given state. Each point was given the same initial state and position. The probability table gave a weighting to each possible new state as a fraction of one (1.0). A random number generator with evenly distributed values from zero (0.0) to one (1.0) selected the new state, and a new speed and direction were given the particle from information about that state. Each iteration represented one time step. Scatter diagrams of the thousand points were made once every six hours for the first forty-eight hours for each current meter record.

The model was also applied to wind data from Fleet Numerical Weather Central for a station at 60°N and 145°W. The regular sampling interval of these data was six hours, so the probability analysis was stepped every six hours instead of one hour as for the current meter records. Two separate runs were made,

one for summer 1974 velocities and another for winter 1975 velocities. Each analysis was conducted over ninety days of records instead of thirty as for the current meter records. Otherwise the analysis proceeded similarly. The scatter diagrams were of the same character, but necessarily of a larger scale than for those of the current meter records.

#### Random Walk Model Description

The random walk model was essentially a simplified version of the second part of the stochastic model. Instead of using a probability table to give a weighting to the various possible next states, the random walk model used a random number generator from zero (0.0) to one (1.0) in cosine and sine relationships to directly choose the u and v components of velocity for each iteration of every point. Scatter diagrams were made once every six hours for the first forty-eight hours.

#### Stochastic Model and Random Walk Model Discussion

The probability arrays for the stochastic model were highly diagonalized, that is, the currents tended to change only slowly and stayed in the same state or in adjacent states for long periods of time. This is reasonable considering the time step was only an hour for the ocean currents and also considering the coarseness of the direction and speed classes defined for each state. The probability array for the current meter deployed at station 62C 59° 33'N and 142° 16'W, beginning June 4, 1975, is an example (figure 2).

The scatter produced by the stochastic model for each of the current meters varies only slightly in either scope or skewedness. The scatter diagram for station 62C after 48 hours is included as an example (figure 3).

The random walk model seems to copy the stochastic model closely in the degree of scatter as shown by the scatter diagram for the random walk model after 48 hours (figure 4). Since the random walk model is a much smaller and cheaper program to run than the full Markov process stochastic model and gives similar results, it would seem prudent to use the random walk model for future calculations requiring information about scatter with time. In cases where the Markov model indicates a strong anisotropy, it may still be possible to simulate the net scatter with a simpler random walk model introducing an appropriate anisotropic variation in step size. Techniques for parameterizing these anisotropies are being studied.

#### 4) Regional meteorological model research -

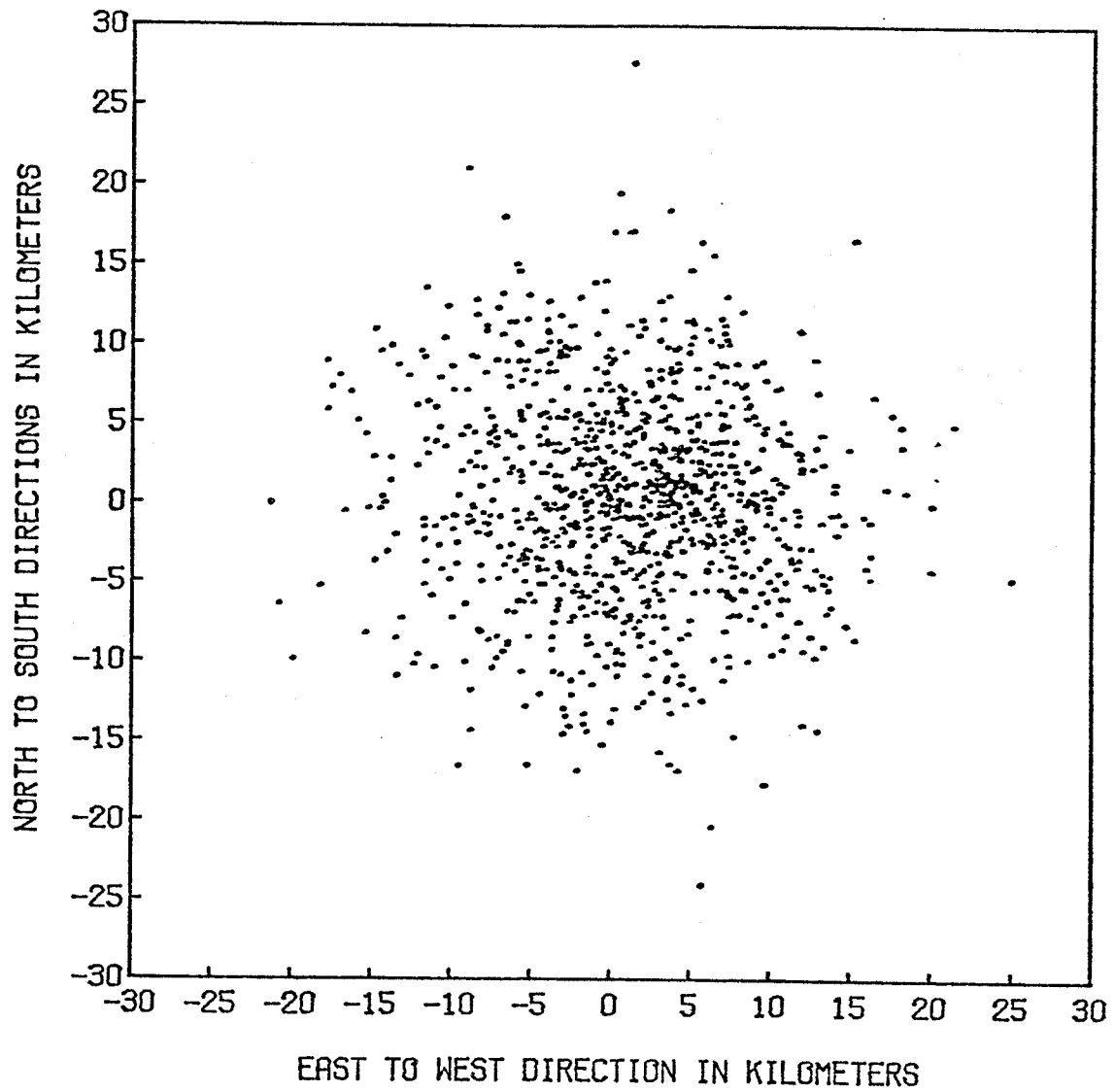
Local winds may have a pronounced effect on pollutant trajectories, and initial studies of the Gulf of Alaska OCS region have indicated that near the coastline the surface winds may differ significantly from what the large scale synoptic patterns might indicate. In order to get a better quantitative understanding of these phenomena, a small scale meteorological study was started. During the present contract year, a literature search was carried out and various potentially useful models were identified. The basic criteria that any model would have to satisfy were: 1) it must include at least parameterization of appropriate physical processes so that the near coastal winds could be simulated; 2) it must be able to run off available input data and be closely integrated with the process-oriented, observational, meteorological studies being carried out by OCSEAP; and 3) the program must be inexpensive enough to be run on numerous regional and synoptic settings so that statistical representations of near shore winds can be generated for a number of OCS areas.

PROBABILITY ARRAY FOR STATION 62C

| LOW<br>N<br>1 | MED<br>N<br>2 | HIGH<br>N<br>3 | LOW<br>NE<br>4 | MED<br>NE<br>5 | HIGH<br>NE<br>6 | LOW<br>E<br>7 | MED<br>E<br>8 | HIGH<br>E<br>9 | LOW<br>SE<br>10 | MED<br>SE<br>11 | HIGH<br>SE<br>12 | LOW<br>S<br>13 | MED<br>S<br>14 | HIGH<br>S<br>15 | LOW<br>SW<br>16 | MED<br>SW<br>17 | HIGH<br>SW<br>18 | LOW<br>W<br>19 | MED<br>W<br>20 | HIGH<br>W<br>21 | LOW<br>NW<br>22 | MED<br>NW<br>23 | HIGH<br>NW<br>24 |
|---------------|---------------|----------------|----------------|----------------|-----------------|---------------|---------------|----------------|-----------------|-----------------|------------------|----------------|----------------|-----------------|-----------------|-----------------|------------------|----------------|----------------|-----------------|-----------------|-----------------|------------------|
| .139          | .098          | .000           | .167           | .014           | .034            | .000          | .000          | .000           | .050            | .000            | .000             | .000           | .000           | .000            | .000            | .025            | .000             | .125           | .000           | .000            | .250            | .000            | .000             |
| .111          | .410          | .200           | .021           | .014           | .034            | .000          | .000          | .000           | .000            | .000            | .000             | .000           | .000           | .000            | .000            | .000            | .000             | .125           | .103           | .000            | .094            | .387            | .000             |
| .000          | .033          | .533           | .000           | .014           | .034            | .000          | .000          | .000           | .000            | .000            | .000             | .000           | .000           | .000            | .000            | .000            | .000             | .000           | .000           | .037            | .000            | .097            | .188             |
| .306          | .016          | .000           | .229           | .143           | .034            | .171          | .000          | .000           | .075            | .000            | .000             | .028           | .026           | .000            | .000            | .000            | .000             | .063           | .000           | .000            | .000            | .032            | .000             |
| .111          | .262          | .033           | .208           | .443           | .103            | .000          | .029          | .027           | .000            | .000            | .000             | .000           | .026           | .000            | .000            | .000            | .000             | .000           | .000           | .000            | .094            | .000            | .000             |
| .000          | .066          | .133           | .000           | .100           | .448            | .000          | .000          | .000           | .000            | .000            | .000             | .000           | .000           | .000            | .000            | .000            | .000             | .000           | .000           | .000            | .000            | .032            | .000             |
| .000          | .016          | .000           | .125           | .043           | .000            | .400          | .118          | .027           | .150            | .000            | .000             | .000           | .000           | .000            | .000            | .000            | .000             | .000           | .000           | .000            | .000            | .000            | .000             |
| .028          | .000          | .000           | .000           | .129           | .034            | .114          | .324          | .054           | .050            | .061            | .033             | .000           | .000           | .000            | .077            | .000            | .000             | .000           | .000           | .000            | .000            | .000            | .000             |
| .000          | .000          | .000           | .000           | .014           | .241            | .029          | .118          | .568           | .000            | .000            | .100             | .000           | .000           | .000            | .000            | .000            | .000             | .000           | .000           | .000            | .000            | .000            | .000             |
| .000          | .000          | .000           | .042           | .057           | .034            | .114          | .147          | .027           | .300            | .061            | .000             | .194           | .053           | .000            | .000            | .000            | .000             | .000           | .000           | .000            | .000            | .000            | .000             |
| .000          | .000          | .000           | .042           | .000           | .000            | .057          | .176          | .000           | .025            | .636            | .033             | .000           | .000           | .000            | .000            | .000            | .000             | .000           | .000           | .000            | .000            | .000            | .000             |
| .000          | .000          | .000           | .000           | .000           | .000            | .029          | .029          | .270           | .000            | .091            | .467             | .000           | .000           | .000            | .000            | .000            | .000             | .000           | .000           | .000            | .000            | .000            | .000             |
| .028          | .000          | .000           | .083           | .000           | .000            | .000          | .029          | .000           | .175            | .061            | .000             | .444           | .079           | .000            | .077            | .025            | .000             | .000           | .000           | .000            | .000            | .000            | .000             |
| .000          | .000          | .000           | .042           | .000           | .000            | .029          | .029          | .027           | .075            | .061            | .133             | .139           | .368           | .073            | .000            | .025            | .000             | .000           | .026           | .000            | .000            | .000            | .000             |
| .000          | .000          | .000           | .000           | .000           | .000            | .000          | .000          | .000           | .050            | .030            | .233             | .000           | .105           | .585            | .000            | .025            | .043             | .000           | .000           | .000            | .000            | .000            | .000             |
| .028          | .000          | .000           | .021           | .000           | .000            | .029          | .000          | .000           | .000            | .000            | .000             | .028           | .053           | .000            | .000            | .100            | .022             | .000           | .000           | .000            | .063            | .000            | .000             |
| .000          | .000          | .000           | .000           | .000           | .000            | .000          | .000          | .000           | .025            | .000            | .000             | .056           | .184           | .098            | .231            | .425            | .065             | .000           | .000           | .000            | .063            | .032            | .000             |
| .000          | .000          | .000           | .000           | .000           | .000            | .000          | .000          | .000           | .000            | .000            | .000             | .000           | .053           | .244            | .077            | .050            | .565             | .031           | .051           | .037            | .031            | .000            | .000             |
| .000          | .016          | .000           | .000           | .000           | .000            | .029          | .000          | .000           | .025            | .000            | .000             | .083           | .053           | .000            | .308            | .050            | .000             | .250           | .154           | .000            | .094            | .032            | .000             |
| .000          | .000          | .000           | .000           | .014           | .000            | .000          | .000          | .000           | .000            | .000            | .000             | .000           | .000           | .000            | .154            | .200            | .109             | .094           | .333           | .111            | .031            | .097            | .000             |
| .000          | .000          | .000           | .000           | .000           | .000            | .000          | .000          | .000           | .000            | .000            | .000             | .000           | .000           | .000            | .000            | .174            | .000             | .103           | .481           | .000            | .000            | .063            | .063             |
| .250          | .000          | .000           | .021           | .014           | .000            | .000          | .000          | .000           | .000            | .000            | .000             | .028           | .000           | .000            | .077            | .025            | .000             | .219           | .026           | .000            | .219            | .065            | .031             |
| .000          | .082          | .067           | .000           | .000           | .000            | .000          | .000          | .000           | .000            | .000            | .000             | .000           | .000           | .000            | .000            | .050            | .000             | .094           | .179           | .111            | .063            | .194            | .031             |
| .000          | .000          | .033           | .000           | .000           | .000            | .000          | .000          | .000           | .000            | .000            | .000             | .000           | .000           | .000            | .000            | .022            | .000             | .026           | .222           | .000            | .032            | .688            | .688             |

Figure 2.

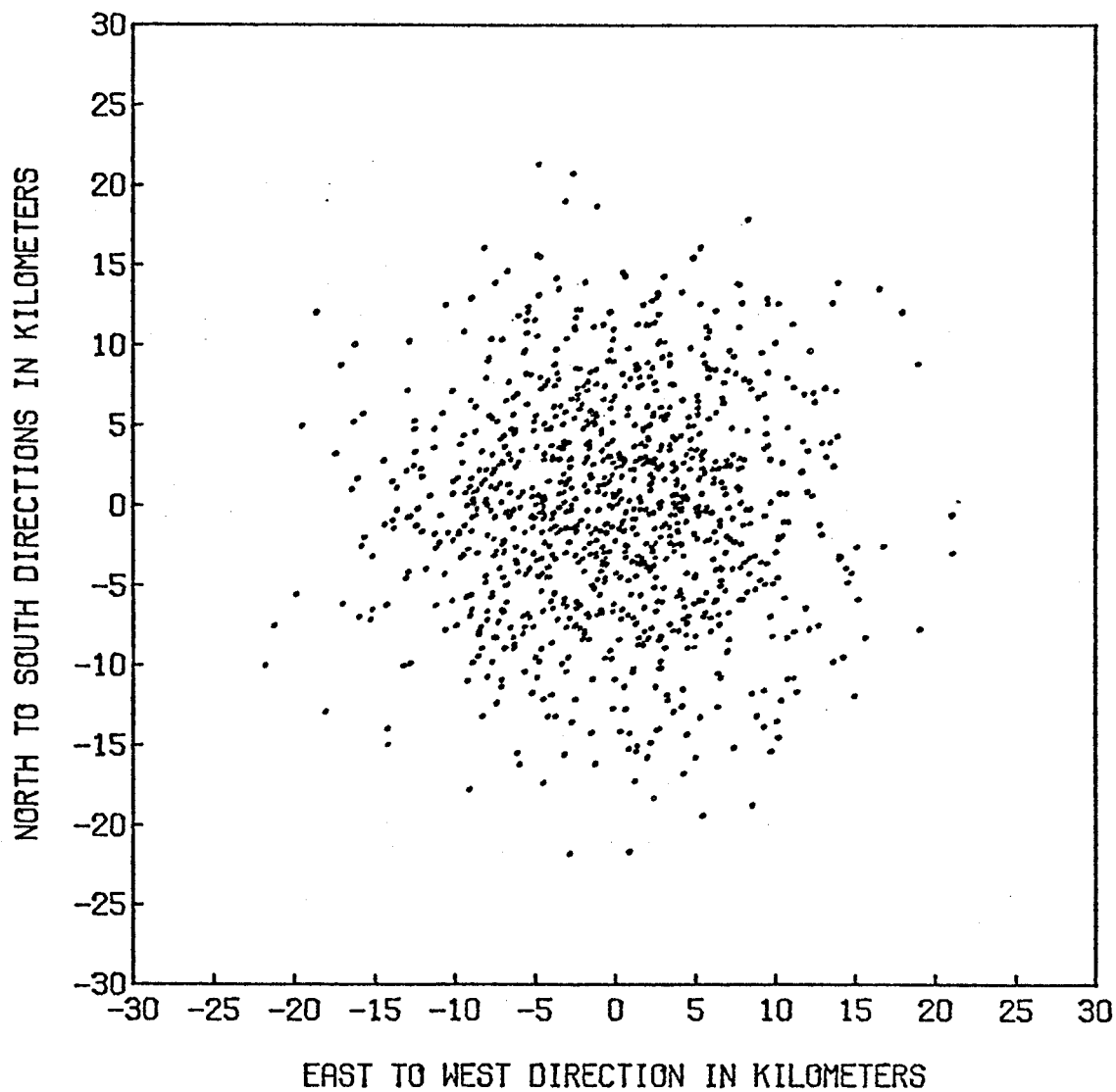
STOCHASTIC MODEL FOR STATION 62C  
SCATTER AFTER HOURS



X2 (.9623,6.941) VERSUS Y2 (.3459,6.517) 1000 VALUES

Figure 3.

RANDOM WALK MODEL  
SCATTER AFTER 48 HOURS



X2 (-.2009,6.805) VERSUS Y2 (-.1425,6.929) 1000 VALUES

Figure 4.

After a literature search was completed, two models were selected for additional study (Danard, 1976, and Lavoie, 1972, 1974). The computer codes for these models were obtained and adapted to run on computers available to PMEL researchers. The initial tests have concentrated on running these models with the same set of input data to compare their relative merits and develop useful graphics displays. The continued use of these models in close coordination with the observational meteorology program and surface wind drift model development is proposed for the coming year.

## B. The Bering Sea

### 1) Diagnostic modeling -

The diagnostic model was not used for the analysis of Bering Sea data this contract year because the necessary STD data were not available. This segment of the modeling effort was reprogrammed to concentrate study on the Gulf of Alaska to supply input for the lease sale scheduled in April 1976.

### 2) General circulation study of the Bering Sea -

A general circulation model for the Bering Sea has been formulated and programmed to run on the University of Washington CDC 6400. Initially, two different models were considered and both were tested for efficiency and their ability to realistically represent the Bering Sea. The test runs indicate that the formulation chosen is dynamically consistent and feasible. A major difficulty remains, however, in that the initialization and spin-up of the model is a lengthy and expensive procedure. A more detailed description of this facet of the model development is presented in Appendix II of this report.



Work on the GCM of the Bering Sea is continuing in two phases: 1) a coarse grid version of the model is being tested and spun-up using the CDC 6400 at the University of Washington, and 2) we are investigating the possibility of using faster NOAA computers for finer resolution runs that will interpolate off the spin-up results from the coarse grid study.

3) Theoretical study of long wave characteristics for Bristol Bay -

A study of the long wave characteristics of the Bristol Bay Region is being carried out using techniques developed by Dr. R. Preisendorfer at JTRE/ERL and documented in a series of NOAA reports (Preisendorfer, 1976). The numerical techniques for computer solution of the governing equations, derived from classical canal theory (Preisendorfer and Gonzalez, 1973) are being developed. When completed, these studies should be able to identify long wave characteristics that can be compared to analysis of observational records from the moored current meters and may lead to useful techniques for interpolating and extrapolating these data. The major work associated with this facet of the modeling program should be completed within a few months.

C. Beaufort Sea

The proposed work in the Beaufort Sea was to do a study of sea ice, identify research that is presently underway, and consider how this research might best be applied to OCS related problems.

When one first views the Beaufort Sea, the most conspicuous feature is the ice. For most of the year, this part of the ocean has a lid on it.

The lid is itself not a simple cover, but a complex jumble of flows, holes, and ridges. It is impossible to consider the biology, geology, or physics of the area without first taking account of the ice. In this report, I will confine my attention to the physical properties of the ice and its effect on the physical oceanography of the region.

Studies of sea ice have been going on for some time. Significant research efforts have been directed at understanding the dynamic and thermodynamic properties of ice, stimulated primarily by interest in global climate. A number of studies have also focused on the problem of ice forecasting inspired by the pragmatic demands associated with attempting ship operations in high latitudes. The distinction between these two classes of studies is obviously not exact and many studies yielded useful insights for both problems. When considering the importance of sea ice influences on questions related to OCS development, we can also expect to draw heavily on this previous research, but it should be kept in mind that attempting an environmental assessment will introduce a somewhat broader class of problems than has been considered in the past. Much remains to be done.

A number of characteristics of sea ice are of direct interest when compiling information for an OCS assessment. The ways that oil might be entrained or incorporated into the pack ice; advection, or trajectory specification; and hazards to mechanical structures are a few obvious examples. In addition to these, the ice pack indirectly affects a number of physical processes that are themselves important factors in an assessment analysis. The ice cover significantly modifies the thermodynamic exchange at the sea surface, which in turn will affect the mixing processes throughout the water column. The ice cover

also acts to modify the wind stress patterns that drive the ocean currents. In a sense, the ice cover can be thought of as a filter that the wind stress must operate through to drive the ocean. From available data, it is clear that the details of how this filter works are very complex and essentially unknown. The wind driven effects enter the oceanographic considerations in three distinct places, and it is likely that an ice cover would modify each differently. First of all, storm surges are of interest for the Beaufort Sea coast and profoundly affected by an ice cover, with a different response for positive and negative surges. It is also likely that the compactness of the ice will be important. A second problem is the local surface wind drift. Obviously the ice will make a difference here, but it is far from obvious what the quantitative difference might be. The third class of wind driven effects relates to how the wind stress sets up the sea surface slope and the subsequent barotropic mode. In many coastal regions this is a major factor in determining currents. For ice covered areas, the regional extent and compactness will certainly be important, but at present there are not even any suggested parameterizations that could be tested for possible use in coastal areas. From these considerations we can get some idea of the scope of the ice problems (within the context of an assessment program), at least insofar as the physically related processes are concerned. The next step will be to narrow down on a more careful description of the ice itself, and finally a few brief recommendations and what research areas may provide useful results.

As a preamble, it is safe to say that Arctic sea ice is an extremely complex medium, where many different scales and classes of phenomena occur.

The mechanical, the dynamic, and the thermodynamic properties all contribute to the distribution and movement of sea ice, and each facet represents a sizable research area in its own right.

The mechanical properties of sea ice are immensely complicated by the heterogeneity of the material itself. On the smallest scale, platelets are only loosely ordered with interstitial saltwater in brine tubes. The details of this small scale structure are continually undergoing changes even within individual pieces of ice with temperature, temperature history, and salinity representing the dominant variables. It is of note that this time history has a multi-year influence and that large amounts of historical information are actually integrated into the ice fabric. In addition, quite large changes in the mechanical properties are accounted for in this way. On a larger scale, sea ice shows inhomogeneity due to both dynamic and thermodynamic processes. Flows are cracked and broken, then forced together, forming rafts and ridges. In this jumble the actual mechanical properties of individual pieces of ice are masked by the extremely complex character of the aggregate. Typically, it is the mechanical properties on this scale that ships or platforms will have to deal with in Arctic operations. On an even larger scale (on the order of 100 km), the statistical properties of the aggregate pack ice appear to stabilize and certain of the gross mechanical properties may be parameterized in an admittedly complex but tractable form. A number of large scale ice studies have been made using various gross parameterizations, and many have given useful insights.

The Arctic Ice Dynamics Joint Experiment (AIDJEX), which is currently under way, represents the most advanced version of this type study to date. One perhaps obvious point is that any forecasting scheme will have to address this regional scale and parameterizations of this type will play a very important role in model design and planning of observational support efforts.

The dynamics of sea ice motion are complicated and obviously not independent of mechanical characteristics. All of the multi-scale mechanical properties have corresponding ramifications for the dynamics. Major forcing for ice motion appears to come from the wind, with ocean currents playing a secondary role. Once in motion, Coriolis forces and ice flow interactions come into play. Wind stress measurements will be a key input to any ice program, and at the present time there is not adequate attention given to obtaining the required coverage. The ocean circulation problem is somewhat more global in the sense that currents, particularly along the northern coast of Alaska, are forced by a system that covers the entire Canadian Basin of the Arctic. This would tend to make matters more complicated if a complete dynamic description of the currents were required, but for the assessment problem the currents could be simply described from an observational program and the difficulties should not be insurmountable. The dynamics associated with ice flow interactions is of major importance and quite complex. Heuristic arguments can be advanced to show that the divergence, convergence, and shearing of the motion, as well as the mechanical characteristics of the aggregate flows, are all significant controlling parameters. In many instances,

stress can be effectively transmitted over hundreds of kilometers. This sets a limit on the smallest region that can be addressed in a forecast, i.e., single point schemes will always give limited results. This scale over which stress is transmitted will also determine the scale of the observational net and regional algorithms that incorporate this as well as complex coastal geometries will be essential for acceptable results.

The thermodynamics of sea ice ultimately control the growth and decay of the pack and is the third major factor that must be addressed by any proposed forecasting plan. Central factors controlling the thermodynamic properties of ice are temperature, temperature history, snowfall, salinity, surface albedo, and ocean heat flux. In some respects, this aspect of sea ice behavior is fairly well understood. A number of excellent one-dimensional models have explored the functional dependence of ice growth and decay on ice formation and accumulations can be correlated with such parameters as freezing degree days. On a multi-season basis, the temperature history controls brine drainage and salinity distributions within the ice, and this has a strong input into the mechanical properties. Snow fall acts to insulate the upper surface of the ice and inhibit continued freezing. Seasonal patterns in snowfall interacting with open water distribution can then introduce multi-year cycles in regional ice thickness. The albedo of the snow/ice surface controls the amount of solar insolation available for summer melting. Finally, the relatively warm underlying ocean offers a continual trend for melting. The actual freezing temperature is controlled by surface salinity, but turbulent fluxes will depend on distributions throughout the surface layers. The details of the heat flux process are

very poorly understood and may depend on internal waves, quasi-geostrophic eddies or baroclinic instabilities. The thermodynamic processes will be particularly important in attempting to make intermediate and long range ice forecasts and major attention should go to documenting appropriate input data.

Thus far, we have included a brief overview of how ice may affect processes that are of interest in an OCS assessment and the relevant characteristics of the ice itself. A careful bibliographic search of related literature was carried out. The major source of current ice research papers is found in the AIDJEX bulletins which are exclusively devoted to ice-related studies. A number of additional listings are presented in appendix III. These are listed first as a master list and then stratified under the general heading of ocean circulation, ice mechanics, numerical modeling, air-sea interaction, and oil with ice.

Based on the review carried out so far, there are a number of relevant OCS-related questions that should be addressed. These form the basis for the following recommendations: 1) State-of-the-art ice models should be applied to the near shore areas of the Beaufort Sea. 2) Observational programs should concentrate on local meteorological conditions and actual ice movement using remote sensing techniques wherever possible. And 3) A study should be undertaken to determine how wind stress couples to the ocean through a sea ice cover. If this could be done and successfully parameterized, numerous coastal circulation models developed and extensively tested elsewhere would become available for the study of Arctic areas.

## References

- Galt, J. A. (1975) Development of a simplified diagnostic model for the interpretation of oceanographic data. NOAA Tech. Report ERL 339-PMEL 25
- Galt, J. A. and Thomas C. Royer (1975) Physical oceanography and dynamics of Northeast Gulf of Alaska (preprint). Proceedings of the Symposium of Science and Technology in the Gulf of Alaska Oct 16-17, 1975. Sponsored by AINA and U. of Alaska.
- Preisendorfer, Rudolph W. (1976) Marching Long Surface Waves Through Two-Port Basins. NOAA Tech. Report NOAA-JTRE-132
- Preisendorfer, Rudolph W. and Frank J. Gonzalez, Jr. (1975) Classical Canal Theory Vol I and II. NOAA Tech. Report NOAA-JTRE-83.
- Watabayashi, Glen (1976) A finite element solution technique for a diagnostic shelf circulation model. NOAA Tech. Report ERL-PMEL (in press)



Appendix I

Use of Diagnostic Model  
with Time-Dependent Barotropic Mode Simulation  
to Estimate Trajectories

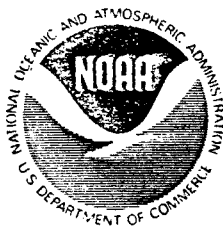
Observational Data Input from STD, Moored Current Meter,  
Lagrangian Drifter, FNWC Weather, and Remote Sensing Programs

# Circulation Studies on the Alaskan Continental Shelf Off the Copper River Delta

J.A. Galt

*Report of studies in the Northeast Gulf of Alaska, part of a multi-year program of environmental assessment related to petroleum development on the Alaskan Continental Shelf. The program is directed by the National Oceanic and Atmospheric Administration under the sponsorship of the Bureau of Land Management.*

March 1976



## CONTENTS

|                                   | Page |
|-----------------------------------|------|
| Acknowledgements. . . . .         | v    |
| Abstract. . . . .                 | .vii |
| Introduction. . . . .             | 1    |
| Numerical Modeling Study. . . . . | 3    |
| Current Observations. . . . .     | 9    |
| Satellite Imagery . . . . .       | 13   |
| Trajectory Analysis . . . . .     | 23   |
| Conclusions . . . . .             | 35   |
| References. . . . .               | 36   |

## ACKNOWLEDGEMENTS

The results presented in this study are based on research carried out by a number of principal investigators working under contract to the Bureau of Land Management-funded OCSEAP office. Their timely contribution of both data and ideas was essential. I am particularly grateful to Dr.'s Muench, Royer, and Belon from the University of Alaska. Dr. Hansen, Messrs. Charnell and Bakun from NOAA also made significant contributions.

In addition to the data collection and analysis, many extra hours of computer programming support were required for the numerical simulations. Particular thanks go to Ms. Pease (PMEL-NOAA) and Mr. Watabayashi (Department of Oceanography, University of Washington) for their efforts.

## ABSTRACT

Circulation patterns on the Alaskan Continental Shelf adjacent to the Copper River Delta were analyzed by numerical modeling techniques, direct current observations, and satellite imagery, which are combined to describe regional flow characteristics. A system of complex gyres or extreme meanders in the region are described as typical summer phenomena associated with fresh water runoff from the Copper River.

The implications of these features with respect to potential petroleum-related contaminants were explored through trajectory analyses. The results of these studies indicate that in summer rather lengthy contract periods may be anticipated in the region and that high probabilities exist for eventual shoreline impact.

During low runoff periods in winter, it is assumed that the gyre formations would be less well developed, suggesting a more predominately westward motion of the currents. Superimposed on this flow, however, are winter wind effects that in this area would tend to provide a strong onshore component to pollutants associated with petroleum development.

# CIRCULATION STUDIES ON THE ALASKAN CONTINENTAL SHELF OFF THE COPPER RIVER DELTA

J. A. GALT

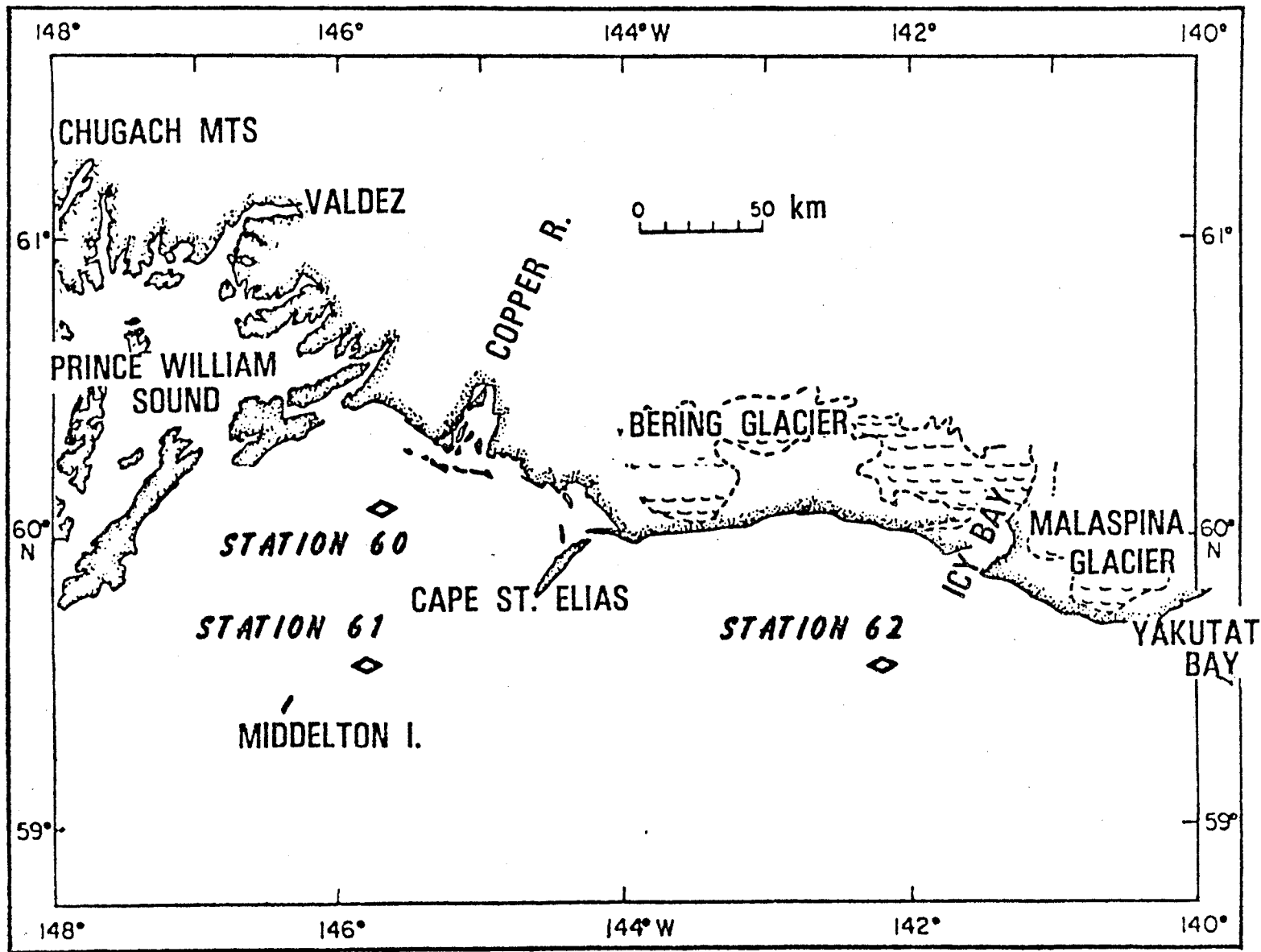
## INTRODUCTION

A large-scale oceanographic and environmental study is underway in the Northeast Gulf of Alaska sponsored by the Bureau of Land Management and administered by the Outer Continental Shelf Environmental Assessment Program (OCSEAP) Office, National Oceanic and Atmospheric Administration. The study has been underway since mid-1974 and has focussed primarily on gathering sufficient environmental information to provide a basis with which to predict and assess the impacts that may be associated with petroleum development in the region.

One facet of the study is directed toward gaining a more complete understanding of the advective effects of currents, or more specifically the trajectories that could be expected from pollutants that might be released into the environment. A variety of investigative techniques have been incorporated into this study including numerical modeling or computer simulations, analysis of satellite imagery, observation of seawater properties, direct Eulerian measurements of currents from moored arrays of current meters, Lagrangian current measurements from satellite-tracked drogues, and the analysis of meteorological data.

It is the object of this manuscript to up-date and integrate the analysis of the several circulation related components of the study which have, for the most part been carried out by various scientists under contract to OCSEAP. This paper is not intended to represent a complete scientific analysis of this remarkable set of data but rather provides a timely synthesis of current thinking, offered as possible input for decisions regarding the leasing of several tracks in the region for petroleum development.

Currents on the Continental Shelf region between Seward and Yakutat (fig. 1) have recently been described in a paper by Galt and Royer (1975). The mean or long-term average flow in this region appears to be dominated by the westward



137  
I.2

Figure 1. Region of study. Station numbers indicate locations of moored current meter arrays.

flowing Alaskan Stream whose core follows nearly along the shelf break (200 m bathymetric contour). This is particularly true for the region east of Cape St. Elias. However, to the west, on the relatively wide shelf between Middleton Island and the Copper River Delta, smaller scale features become more important and the mean flow is much more difficult to describe. It is this complex region that is the target of studies presented in this work. Superimposed on the mean flow are annual cycles related to changes in regional wind patterns and local river run-off. In the summer, surface flows tend to be slightly offshore and the westward drift weakens, but this is in no way uniform throughout the Copper River region, and in a number of instances gyres appear which imply trajectories that lead onshore with in some cases relatively lengthy residence in the region. During the winter, the situation is less clear with regard to the presence of gyres, but the intensity of the westward flow increases and strong winds give a decided onshore component to the surface flow.

In the remainder of this paper, the various investigative techniques that have contributed to the understanding of flow conditions off the Copper River region are briefly described. Following these studies, the preliminary results of a simple trajectory model analysis will be presented. The final section will synthesize the results of the various components and summarize the present state of trajectory estimates for the Shelf region bounded by the Copper River Delta, Cape St. Elias, and Middleton Island.

#### NUMERICAL MODELING STUDIES

A numerical model or computer simulation of the steady or quasi-steady circulation expected in a Continental Shelf region has been developed as part of the OCSEAP studies. The theoretical descriptions of the model are presented by Galt (1975). The model includes the first-order effects of density variations within the ocean waters, complex bathymetry, and irregular coastal configurations as well as wind driven surface flows and frictional currents along the bottom. The model is diagnostic in that certain segments of the flow are determined from observational data. In particular the temperature and salinity data collected on a routine oceanographic cruise are used to specify the variations of the currents with depth, but not the actual magnitude of surface flow. The observed or hypothesized winds are used to specify the surface wind drift layer. Once these data are incorporated into the model, the remaining components of the flow are determined subject to the geostrophic and Ekman dynamics and the kinematic constraints associated with continuity of the flow.

The mathematical form of the model equations requires boundary conditions around the edge of the region to effect a solution. In this particular model, the crucial boundary values are sea surface elevations, which are unknown and essentially unmeasurable in any absolute sense. This difficulty is a common characteristic of so called "open boundary" models. To use the model with confidence and overcome the uncertainties associated with the boundary conditions, two approaches are used. First a series of computer runs is carried out to explore the implications of various boundary condition settings. These runs



indicate the sensitivity of the model to variations in the boundaries and establish plausible ranges. The second approach is to collect an independent set of current data for a location within the model domain. This can then be used to check against the currents predicted by the model and thus delineate the appropriate boundary conditions.

The initial case study was originated with a data set obtained for the Northeast Gulf of Alaska region in July 1974 (*R/V ACONA*-Royer-chief scientist), taken to be representative of summer conditions that year. Wind data were obtained in digitized form derived from forecasts made by the Fleet Numerical Weather Central, Monterey, California. In addition, three moored current meter arrays (60, 61, 62; see fig. 1) were available for the summer to provide an independent verification of model results.

The first model run considered only homogenous water, i.e., density variations caused by temperature and salinity variations were ignored. The results of this case are shown in figure 2, where the dominant flow of the Alaskan Stream is clearly evident. On the shelf region between Middleton Island and the Copper River, the flow is much weaker but uniformly to the west. The next model run used identical boundary conditions and wind data but included the details of the temperature and salinity observations. The results of this case are seen in figure 3. The predominately westward flow is still evident on the Shelf east of Cape St. Elias, but two gyres are evident in the region just to the west of Cape St. Elias. The one nearest to shore is the weaker; it moves counter-clockwise and carries water from offshore in toward the coastline immediately south of the Copper River. The second gyre, just offshore from the first, is the stronger and clockwise, carrying water in an offshore direction past Cape St. Elias. These gyres are obviously related to the density distribution; close examination of the data reveals that run off from the Copper River introduces less saline water that contributes to this region of lower density.

To check the sensitivity of the model to boundary variations, a series of cases were run. For four of these cases the velocities predicted by the model at current meter moorings 60, 61, 62 (fig. 1) are presented in figures 4, 5, and 6. These figures indicate the  $u$  component (east-west, positive to the east),  $v$  component (north-south, positive to the north), and total magnitude of the velocity  $|v|$ .

At station 60 (fig. 4), which was located just southwest of the Copper River delta, the model predicts relatively weak flow to the west (negative  $u$  and small  $v$ ). As the boundary conditions are varied, the flow is seen to increase. This current meter was located just west of the inshore (counter-clockwise) gyre predicted by the model.

The currents predicted at station 61 (fig. 5) are significantly stronger than those of 60. In this case, the flow is predominately to the west-northwest (negative  $u$  and small  $v$ ), with the magnitude of the flow monotonically increasing. A look at the predicted currents at station 62 (fig. 6) reveals the same sort of behavior, with the exception that the flow is directed toward the northwest.

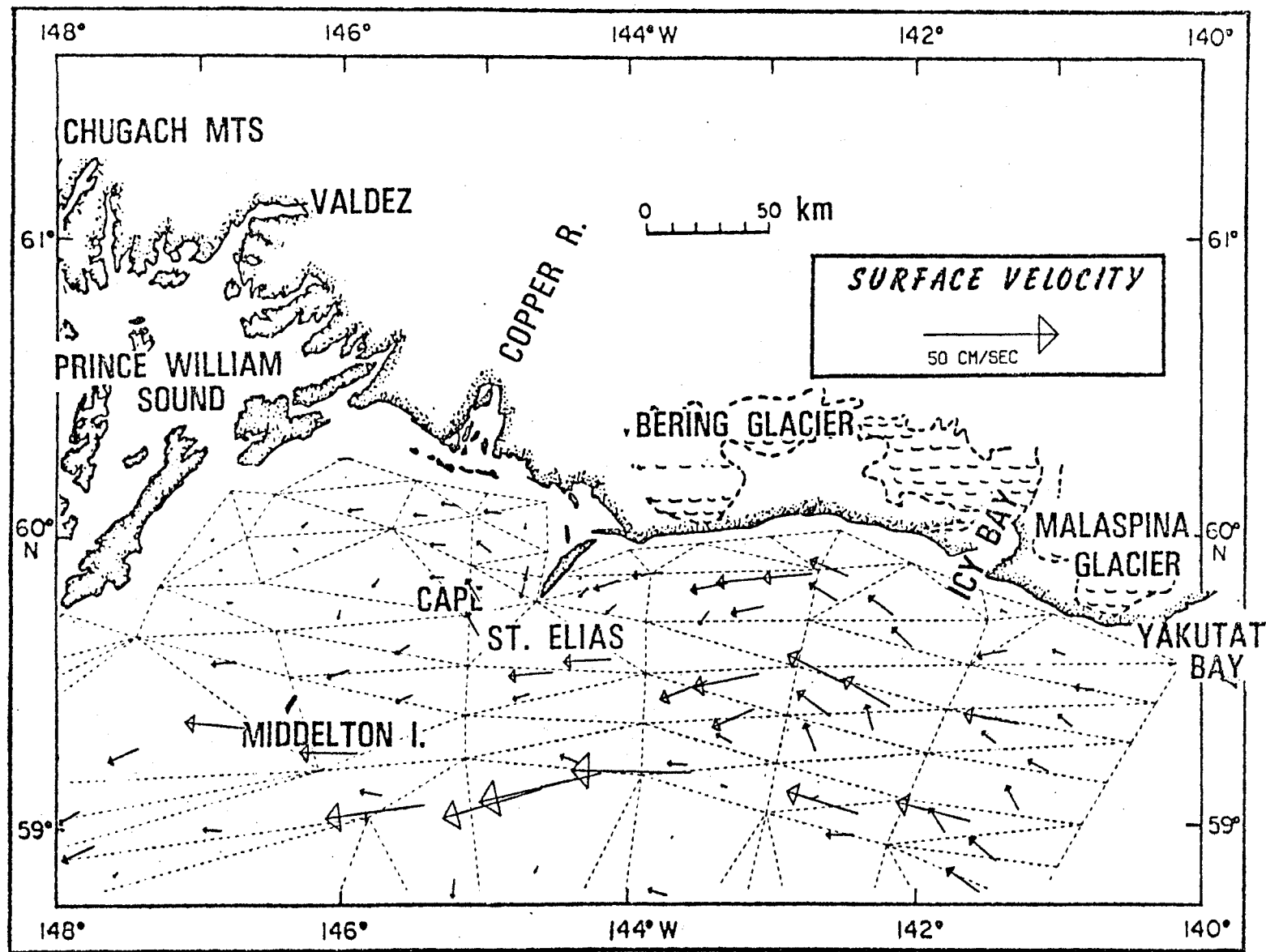


Figure 2. Numerical modeling results for test case assuming homogeneous water. Vertices of triangles indicate oceanographic station locations used for input data.

I-6  
141

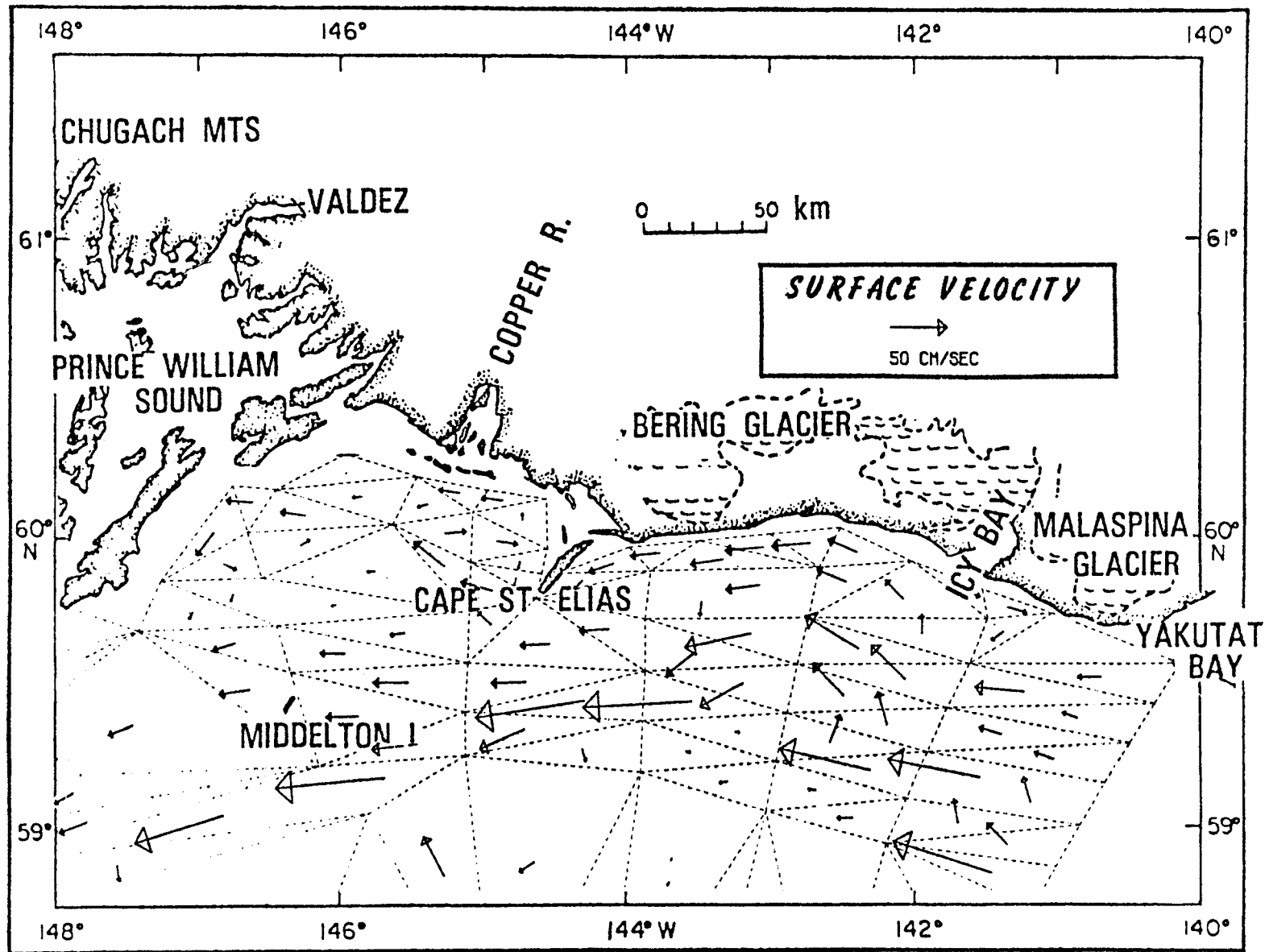


Figure 3. Numerical model results for test case using density data collected July, 1974. Vertices of triangles indicate oceanographic station locations used for input data.

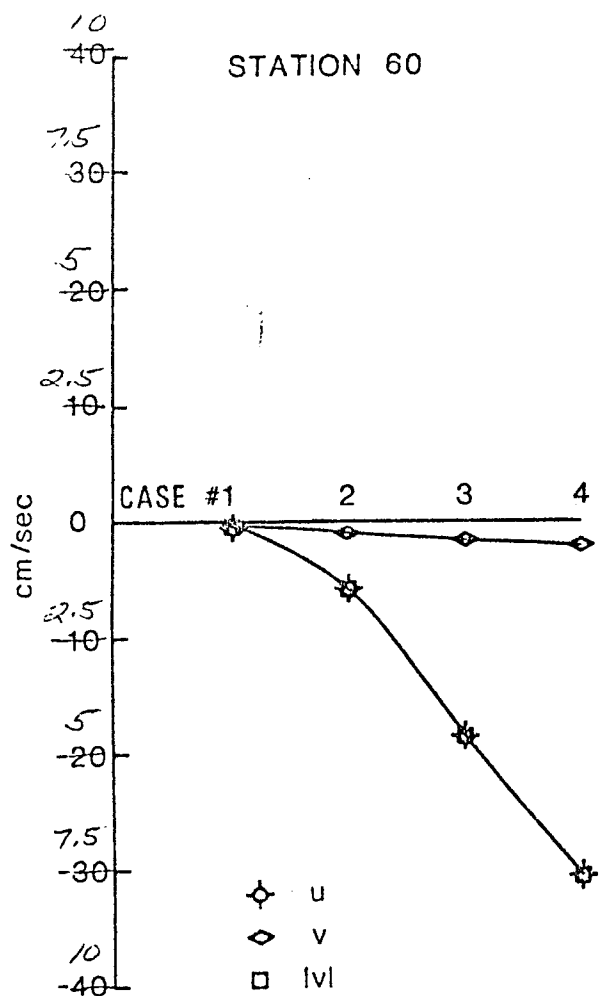


Figure 4. Currents predicted by the numerical model for the location of current meter station 60. Cases one through four represent various setting on the boundary conditions.  $u$  is the east-west component of the current (east positive).  $v$  is the north-south component of the current (north positive).  $|v|$  is the magnitude of the current.

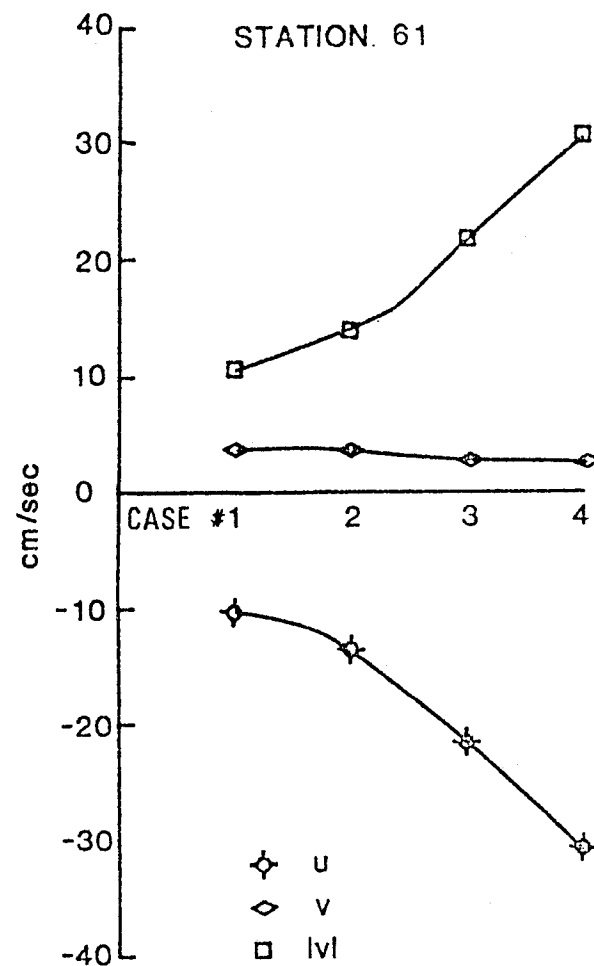


Figure 5. Currents predicted by the numerical model for the location of current meter station 61. Cases one through four represent various setting on the boundary conditions.  $u$  is the east-west component of the current (east positive).  $v$  is the north-south component of the current (north positive).  $|v|$  is the magnitude of the current.

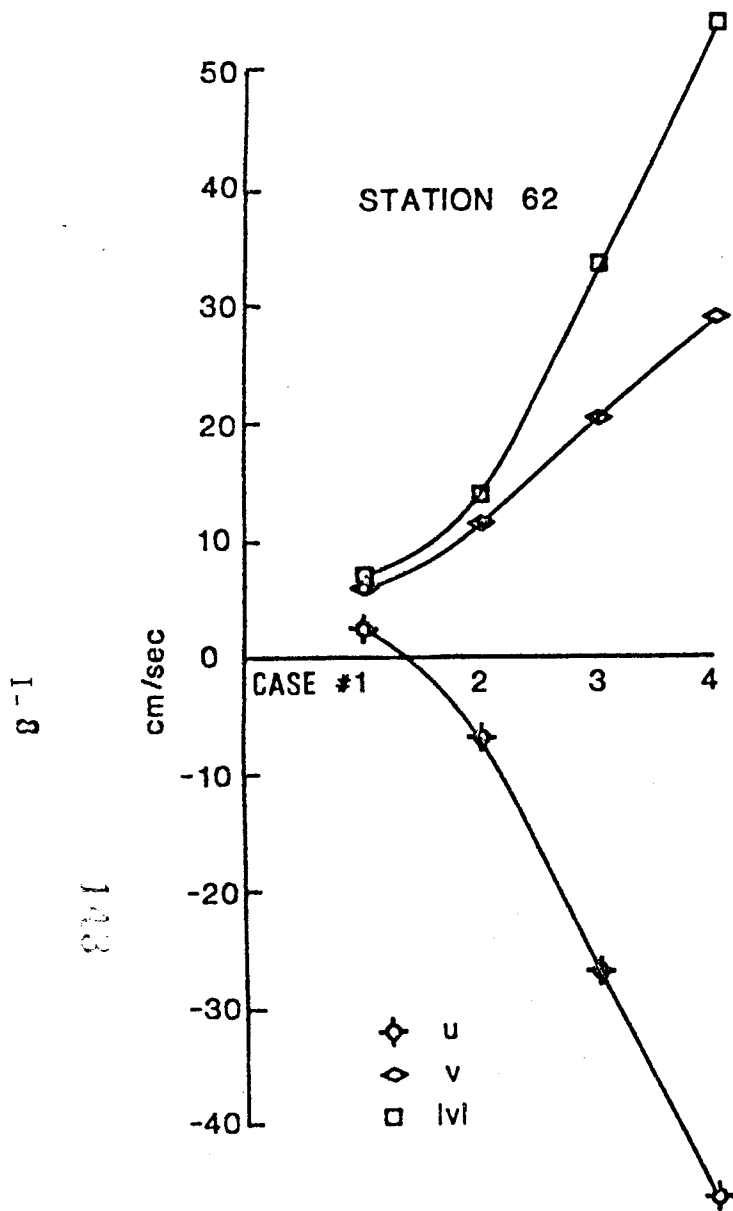


Figure 6. Currents predicted by the numerical model for the location of current meter station 62. Cases one through four represent various setting on the boundary conditions.  $u$  is the east-west component of the current (east positive).  $v$  is the north-south component of the current (north positive).  $|v|$  is the magnitude of the current.

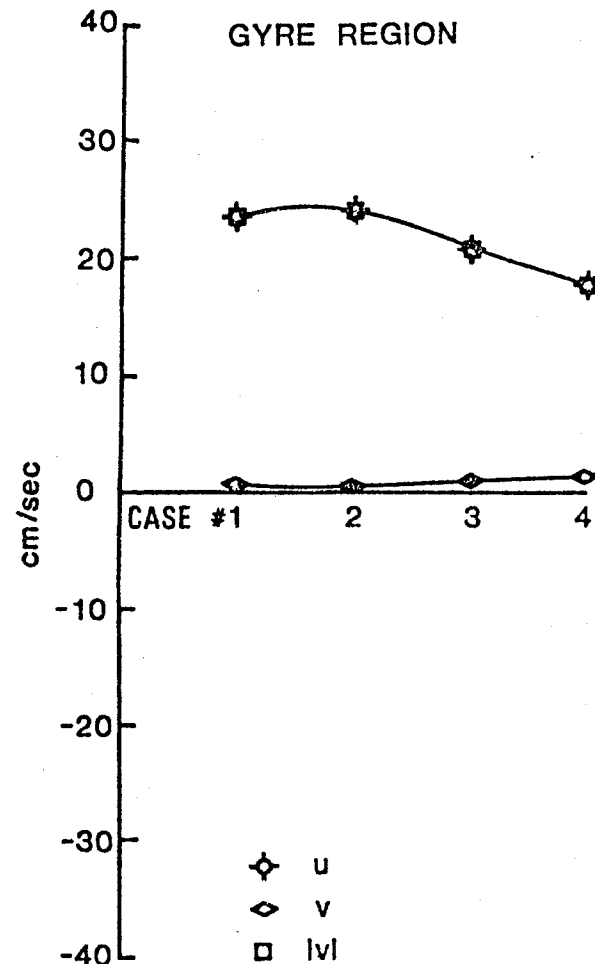


Figure 7. Currents predicted by the numerical model for the location of the gyre region. Cases one through four represent various setting on the boundary conditions.  $u$  is the east-west component of the current (east positive).  $v$  is the north-south component of the current (north positive).  $|v|$  is the magnitude of the current.

## CURRENT OBSERVATIONS

For a few selected locations direct observations of currents in the Northeast Gulf of Alaska are available in two forms. The first data were obtained from the tracking of free drifting drogues. This was accomplished via a satellite system that telemetered drogue positions on each orbit within range. By plotting successive positions, use obtained a Lagrangian trajectory of the motion. The second source of data was obtained moored arrays of current meters. These simply record the currents at a single point giving Eulerian speed and direction readings every few minutes.

The drogue tracking studies obtained data from one set of buoys released southeast of Yakutat in September 1975. Two trajectories are shown in figure 8. The drogues moved slightly onshore and then westward. The one closest to shore traveled significantly faster than the one that was released farther offshore. The offshore drogue spent nearly a week looping back and forth before it got into the dominant westward stream. These drogues did not enter the region west of Cape St. Elias, but they do give valuable data that can be compared with the results of the numerical modeling experiments. Once they were in the westward stream, typical speed for the drogues was 28cm/sec. If we compare the currents indicated in figure 3, we find the direction predicted by the model generally agrees well with the direction indicated by the drogue track. In addition, by looking at figure 6 we see that the boundary conditions selected during the numerical exploration clearly bracket this typical speed. This then tends to strengthen the projections of the model and suggests that it is faithfully reproducing at least the major flow features.

Next we consider the current meter data collected at station 62 (fig. 1). Data from this location are available for the summers of both 1974 and 1975.

Figure 9 shows the 1975 data. The daily mean currents are in the form of a row of stick diagrams and a vector sum of the total observed currents (progressive vector diagram), which indicates the net motion over the length of the record. The average direction of the observed flow is northwest with some shifts in direction occurring at a periodicity of approximately five days to a week. The speed of the flow varies considerably from time to time, but the range is nominally within the limits of the results spanned by the numerical experiments (fig. 6). The mean direction and typical speeds observed at station 62 are consistently reproduced by the model studies. The oscillations in directions seen in the observed currents are most likely caused by shelf wave phenomena and individual weather events. The dynamics responsible for these responses are not included in the model, and thus this level of detail cannot be expected in the numerical simulations.

Another set of current meter data — collected during the summer of 1974, — was available from station 61. They are presented in figure 10. This current meter location, like station 62, was along the outer edge of the Continental Shelf, and except for the direction (slightly north of west in this case) it looks very similar to what was observed at station 62. The model results at this point are also reproducing the salient features of the flow (fig. 5).

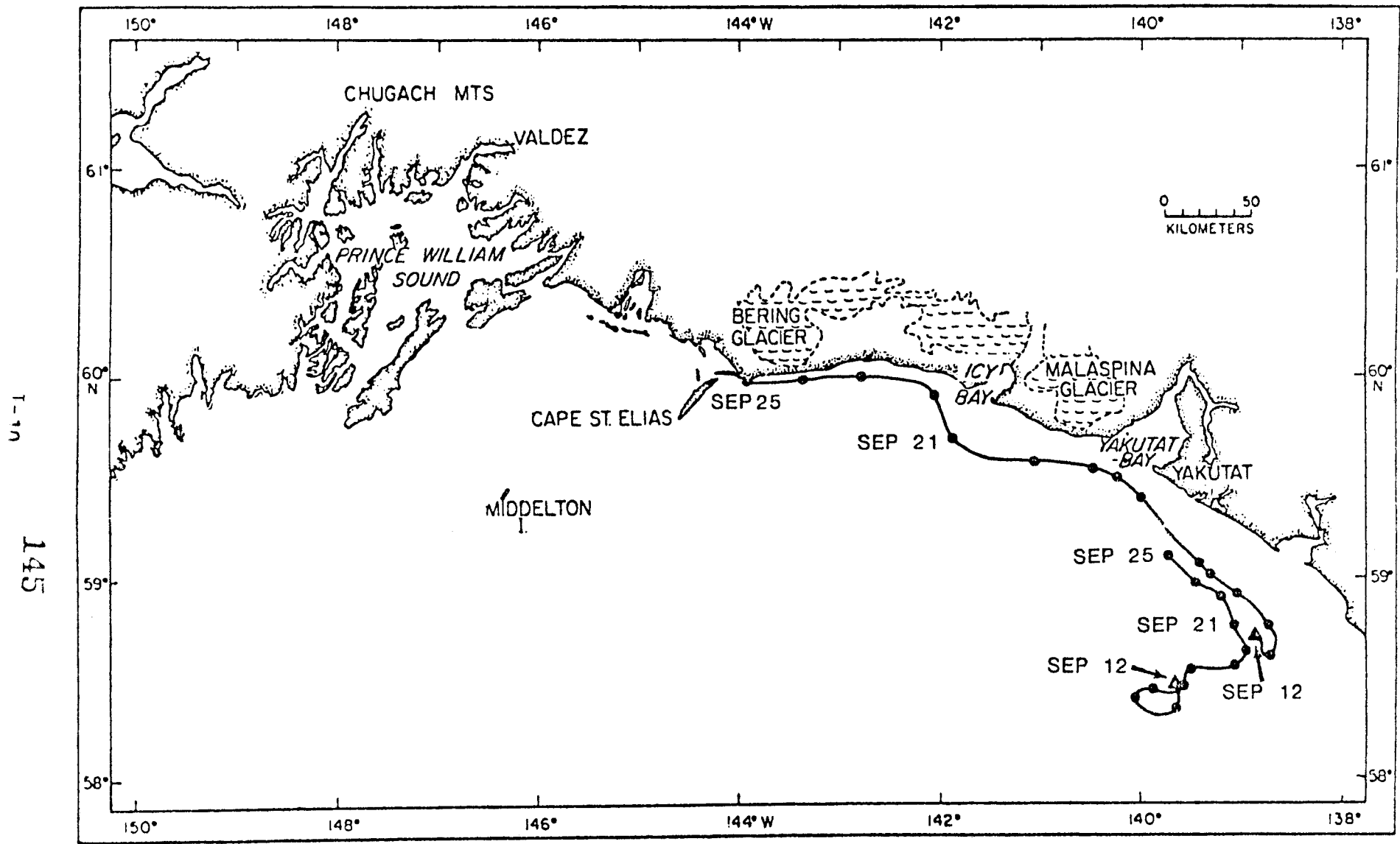


Figure 8. Lagrangian drogue trajectories for set released south of Yakutat September, 1975 and tracked via satellite.

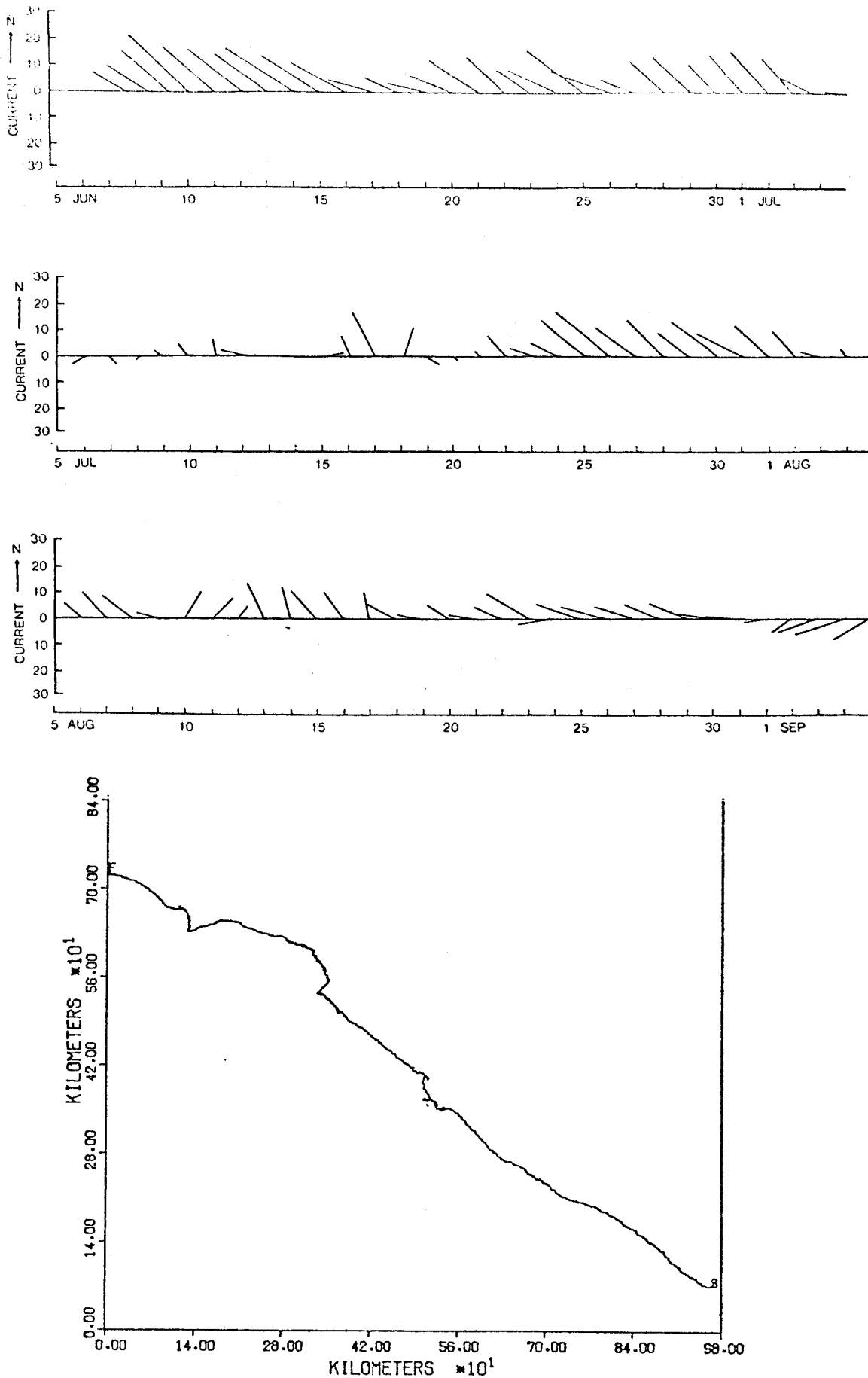


Figure 9. Observed currents from station 62. Stick diagrams indicate speed and direction of daily mean currents. Lower figure indicates progressive vector diagram or net motion of water past the current meter.



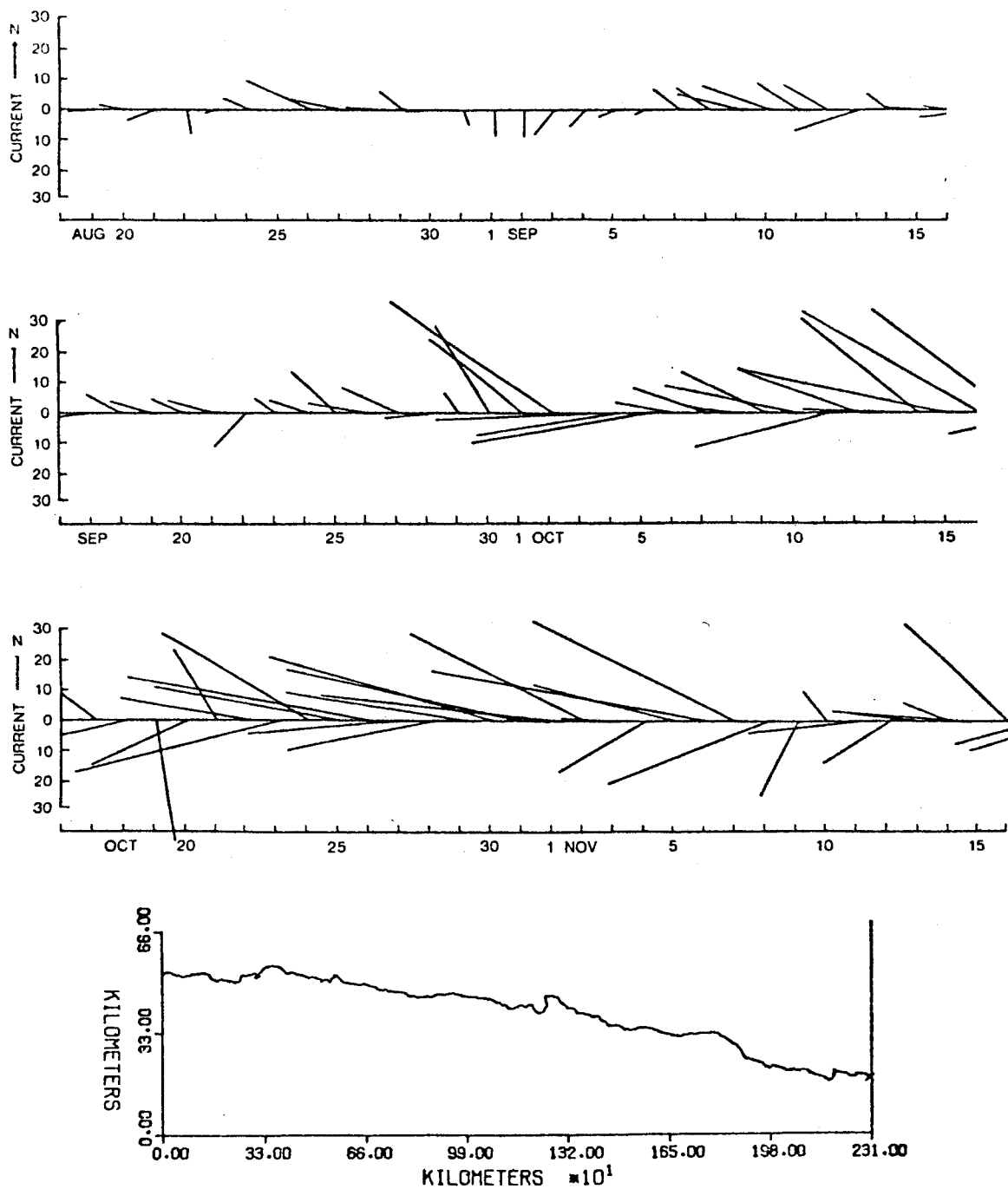


Figure 10. Observed currents from station 61. Stick diagrams indicate speed and direction of daily mean currents. Lower figure indicates progressive vector diagram or net motion of water past the current meter.

The final set of current meter data (fig. 11) available were from station 60, which was located southwest of the Copper River Delta. Here again the flow is generally westward with oscillations to the north and south. When we compare this with the model results shown in figure 4, the westward flow is clearly predicted. Both the predicted and observed currents are significantly smaller than those seen along the outer edge of the Shelf; the model provides slightly lower values than the field observations. For this location, the north-south variations are relatively large compared with the mean flow. These oscillations in the current's direction are perhaps a reflection of the nearby gyre system, since these eddies will tend to shift their position slightly from time to time.

In conclusion, observed currents tend to confirm model results. The model includes appropriate physics to represent the major features of the flow and the general circulation of the region. The range of boundary values used in the numerical experimentation gives predicted flows that span the observed data. In the details of the observed flow are certain characteristics that the model will not be able to represent. In particular, shelf wave phenomena cause oscillations in the speed and direction of the flow which are not reproduced by the model. In addition, the spatial resolution of the model is limited and the exact position of current features cannot be predicted to any greater accuracy than the available input data. This means that although the model clearly recognizes the local dynamics that lead to gyres, its resolution with respect to position is no better than that enabled by station spacing.

The model does indicate a complex circulation pattern to the west of Cape St. Elias in the vicinity of the Copper River. This flow appears as gyres or extreme meanders and is dynamically associated with the low salinity water formed by the Copper River effluent. The flow in this region is relatively insensitive to flow conditions along the outer edge of the Continental Shelf, or to the east of Cape St. Elias.

#### SATELLITE IMAGERY

Satellite images of ocean regions have proved useful in a number of areas by providing detailed, although qualitative, information on the scale and position of various circulation features. Studies of sediment transport in coastal regions around Alaska have made extensive use of these data (Burbank, 1974). For the present study, satellite imagery from the ERTS-1 satellite and the NOAA-3 satellite have been examined for the region bounded by Cape St. Elias, Middleton Island, and the Copper River. In the ERTS photographs multi-spectral bands 4 and 5 indicate the presence of suspended sediment in the surface water. When sources for this sediment are clearly identified (the Copper River, Bering Glacier, or shallow nearshore regions northwest of Kayak Island), the advective or downstream plume of sediment indicates the direction of flow and often gives quite detailed information on spatial scales and mixing processes. For the NOAA 3 satellite imagery, the IR bands give useful delineation of current structures for cases where a thermal contrast exists. All non-cloudy ERTS-1 imagery for the region was examined. These nine figures are reproduced in chronological order.

Following is a brief discussion on each photograph giving an interpretation of the implied circulation.

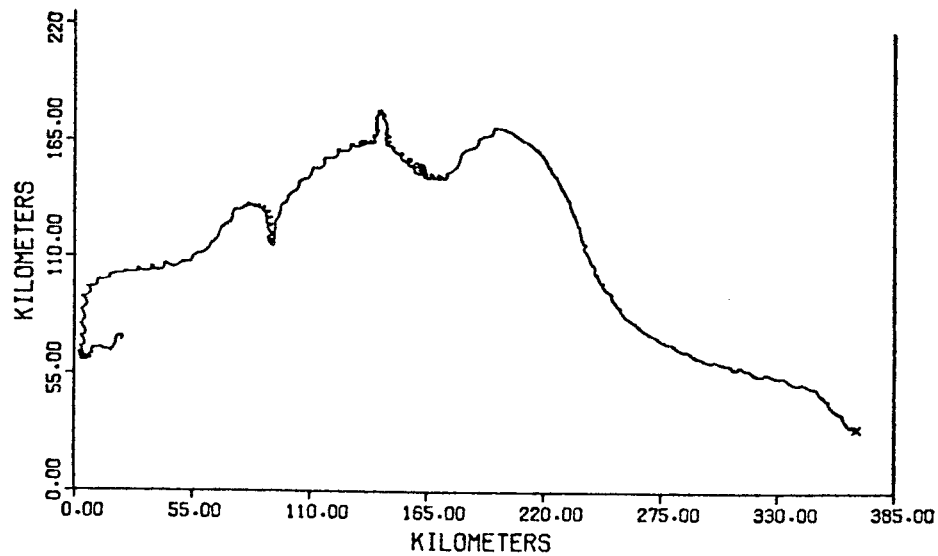
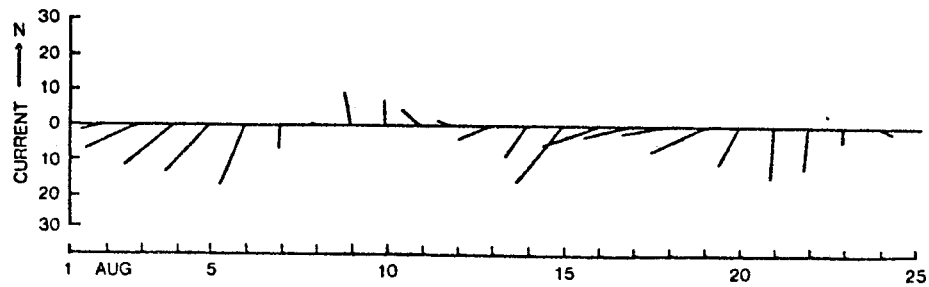
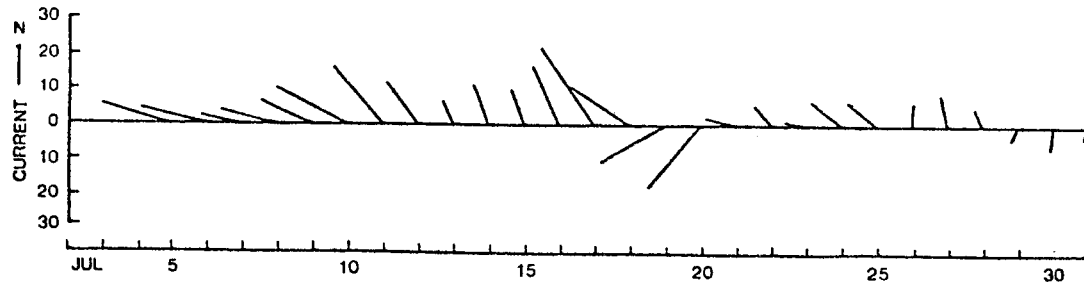


Figure 11. Observed currents from station 60. Stick diagrams indicate speed and direction of daily mean currents. Lower figure indicates progressive vector diagram or net motion of water past the current meter.



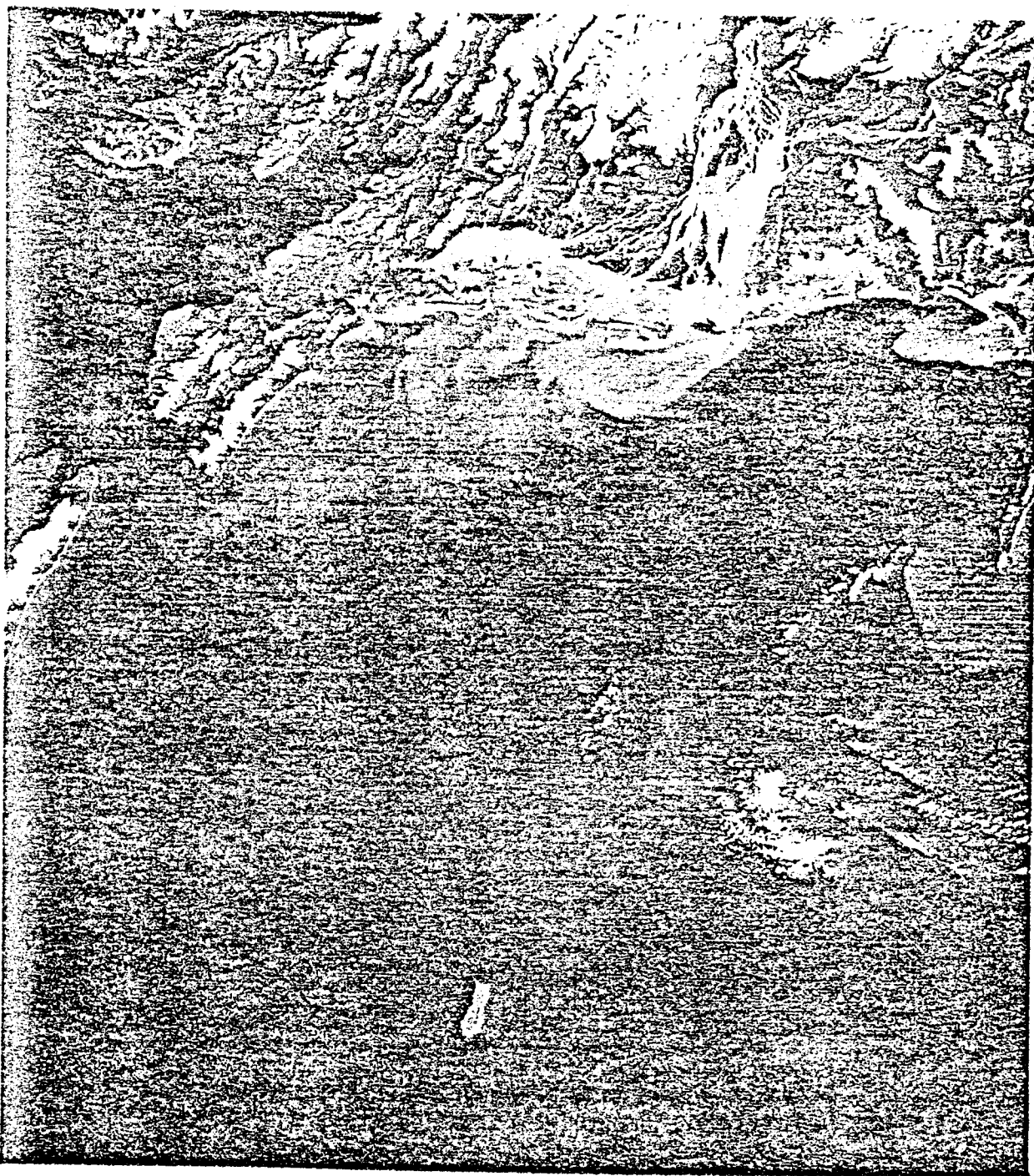
A-1 (September 24, 1972). Here flow is seen to move west along the shoreline. In the area just west of the Copper River, the plume moves offshore and back to the east. A gyre with counter-clockwise rotation is indicated between Cape St. Elias and the mouth of the Copper River.



A-2 (October 12, 1972). Here heavy sediment loads are seen in MSB 4. South of Cape St. Elias a clockwise intrusion of less sediment laden water is seen as an indication of a general intermediate scale clockwise circulation.



A-3 (June 21, 1973). This image has a significant amount of cloud cover, but within the area of interest sediment near the coast is moving west and a plume from the Copper River appears to be moving partially offshore and back to the east.



A-4 (August 14, 1973). Here is excellent evidence of a double gyre system. Between Cape St. Elise and the Copper River Delta the indicated flow is counter-clockwise. Flow along the west side of Kayak Island is north, flow along the coast is west, and in the vicinity of the river mouth a component of the flow is offshore and back to the east closing the gyre. Farther offshore between Cape St. Elias and Middleton Island, a large clockwise gyre is evident.

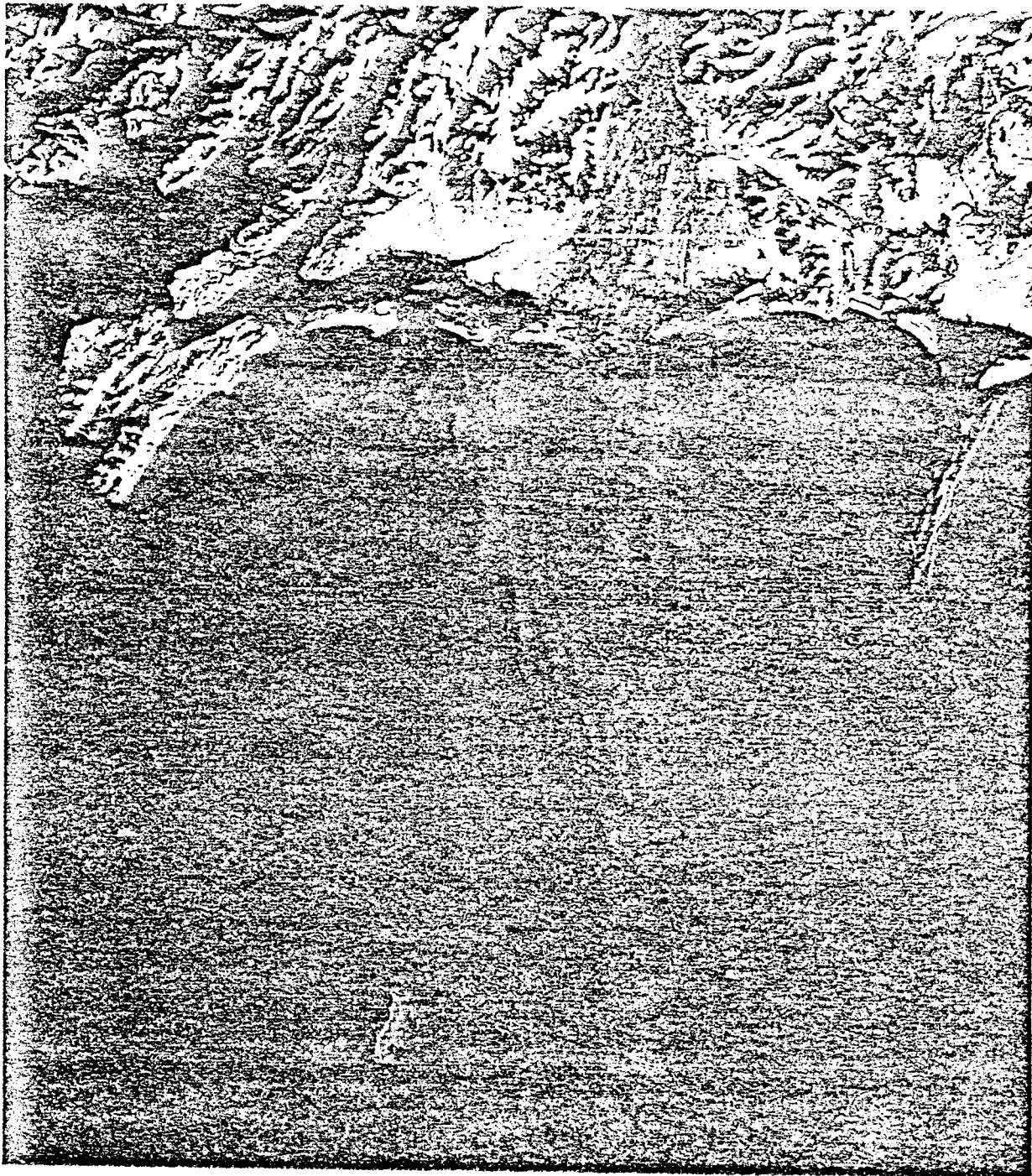


A-5 (September 18, 1973). Here clouds cover most of the area of interest, but southwest of Cape St. Elias there is evidence of a gyre. The sense of rotation is not clear. Near the coast the flow is once again to the west with some evidence of offshore movement just west of the river mouth.





A-6 (October 7, 1973). This image shows evidence of a large gyre located between Cape St. Elias and Middleton Island which is similar to what was seen in A-4 but slightly farther offshore. Inshore between Cape St. Elias there appears to be counter-clockwise circulation, but the details are less clear.



A-7 (November 12, 1973). This is the one clear image (less than 30 percent cloud cover) obtained for this area during a period other than summer (June to October). Here there is no evidence of a gyre, but there appears to be an interesting drainage wind phenomena coming down the Copper River Valley.



A-8 (July 17, 1974). One NOAA 3 - IR image was also carefully examined. Although this has less resolution than the ERTS imagery, it is particularly useful in that it was obtained just after the July 1974 oceanographic cruise data were collected and thus should represent the conditions used in the model study in some detail. In this image the water associated with the Alaskan stream indicates the pattern of the flow in the region between Cape St. Elias and Middleton Island. Here a clockwise gyre is evident. The water coming out of the Copper River is also thermally recognizable and is seen to move offshore and back to the east, indicating a counter-clockwise gyre in the region between Cape St. Elias and the Copper River. A comparison of these patterns with the results of the model study for the same period (fig. 3) indicates excellent agreement, certainly to within the limited spatial resolution afforded by the model.

In summary, the available satellite imagery supports a number of conclusions concerning the circulation in the region. First, during the summer, the presence of gyres in this region appears ubiquitous. Their position varies from time to time and the area may shift from a double gyre to single gyre system. In all cases, the nearshore circulation supports the evidence for a counter-clockwise gyre. As a second point, the non-summer data (limited though they are) do not indicate the presence of gyres. This is consistent with the model results that show the gyre system is at least partially dependent on Copper River run off. As a final point, the one satellite image that is available for that period when the model exploration was carried out strongly supports the model results in terms of the placement and orientation of the gyres.

### TRAJECTORY ANALYSIS

The numerical modeling or simulation results presented so far appear to yield a quite reasonable representation of major flow characteristics. Where current meter measurements are available, the model can accurately reproduce the mean speed and direction of the flow by the appropriate choice of boundary condition settings. Where simultaneous measurements from several locations are available, the model shows reasonable internal consistency and the trajectory data from Lagrangian drogue studies appear to support the larger scale current patterns predicted by the numerical experiments. Finally, the relatively complex circulation pattern indicated by the model east of Cape St. Elias is strongly supported by satellite observations.

At this point it seems reasonable to consider the model results as an acceptable, first-order representation or integration of the available observational data. The model's results can be used to interpolate in a dynamically consistent and quantitative manner where data are not available. This can be done with some confidence so long as the model limitations are kept in mind. In particular: (1) Shelf wave phenomena are not properly represented; thus certain transient features cannot be reproduced. (2) The spatial resolution will be no better than the station data spacing. (3) The very nearshore region is not really represented, dynamically or geometrically. The extent to which the first of these limitations may be a problem is indicated in the current meter records (figures 2, 10, and 11); and the restrictions imposed by limitations No. 2 and No. 3 can be estimated from figure 12, which shows an overlay of the model grid on a detailed outline of the coast.

The model results were used to simulate trajectories or water particle parthways using the following procedure. The observed current meter record was low pass filtered to obtain a running daily mean. This was then sampled every six hours. The magnitude of this flow was then used with either figure 5 or 6 to determine which boundary condition settings were appropriate. For values between particular cases, a linear interpolation was used on predicted velocities. In this manner, the model could be keyed to the current meter record and a time stepping of the entire velocity field obtained. Once this velocity field was obtained, trajectories were calculated by advecting marked particles in six hour increments. In the following figures, the results are presented in two series. The first series (figs. 13 to 17) initiates trajectories to the east of

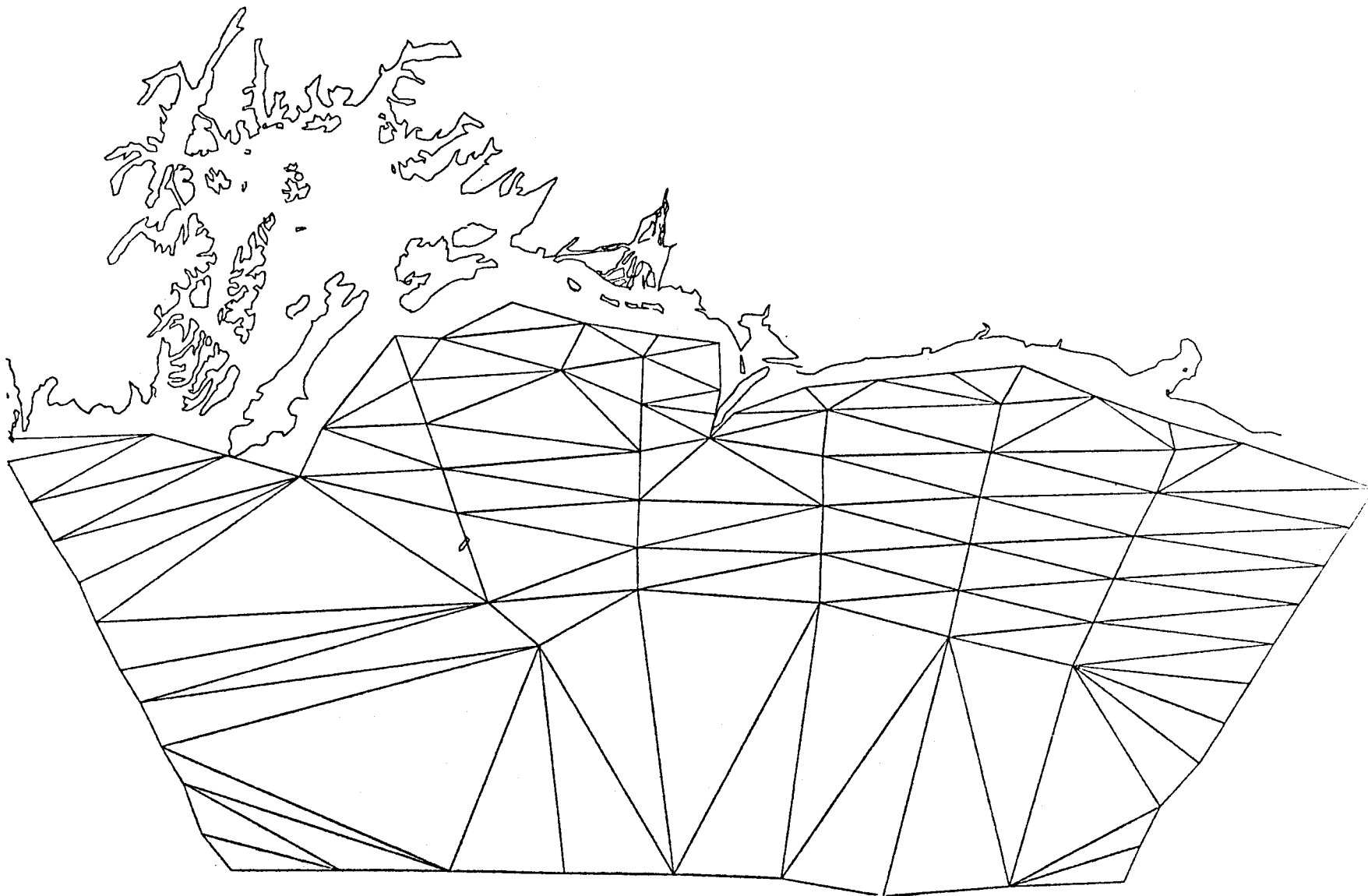


Figure 12. Grid used in numerical modeling studies superimposed on detailed outline of the coast.

Cape St. Elias and is keyed on current meter station 62. The second series (figs 18 to 21) initiates trajectories west of Cape St. Elias and is keyed on current meter station 61. In both cases the starting point of the trajectory is marked with a circle, and after each week the pathway is marked with a (\*). Trajectories that did not exit the model were continued for 30 days. Note that this trajectory analysis does not include any mixing effects, and thus from purely kinematic grounds it is unlikely for particles to leave the model or go ashore. In actual fact, mixing and exchange processes are extremely active nearshore (note mixing scales evident in satellite images), and many of the trajectories that simply run along the edge of the model would be expected to impact the coastline.

We may describe the trajectory studies briefly as follows. Figures 13 and 14 present trajectories initiated from a variety of locations, all starting on August 17, 1974. Figures 15, 16, and 17 present six trajectories each that are initiated from a single location at one week intervals starting on August 17, 1974.

Figure 18 presents four trajectories initiated on August 16, 1974, along a north-south line extending out from the Copper River. This clearly indicates the double gyre system. The northern release travels around the counter-clockwise gyre and moves across the Copper River Delta. The second release travels around the clockwise gyre  $1\frac{1}{2}$  times and impacts on Kayak Island. The next release is south of the gyres and moves generally westward and toward Prince William Sound. The release farthest south moves generally westward and then back across Middleton Island.

Figure 19 presents four trajectories initiated on August 16, 1974, along an east-west line offshore from the Copper River Delta. Only the western most release escapes the counter-clockwise gyre; the remainder are carried first east and then inshore past the Copper River Delta.

Figure 20 presents trajectories released from two locations (three for each) starting on August 16, 1974, with successive releases a week apart. All of the releases from the northern site are carried around the counter-clockwise gyre and past the Copper River Delta. The releases from the southern site indicate variability of the gyre. One path leads west, a second goes around the gyre once and then west and the third circles the gyre  $1\frac{1}{2}$  times to end up on Kayak Island.

Figure 21 presents six trajectories all released from a point farther offshore and to the west. Here the influence of the gyres is totally lacking and the general westward drift of the region is evident. As before, the first release was on August 16, 1974, with a week between succeeding releases.

This trajectory analysis has delineated the extent and influence of the gyre circulation patterns predicted west of Koyak Island from the summer 1974 data available. Once again these trajectories only indicate the advective patterns of the flow and thus do not include any mixing or dispersive effects that could be expected to add downstream scatter and uncertainty to the pathways presented in these figures.

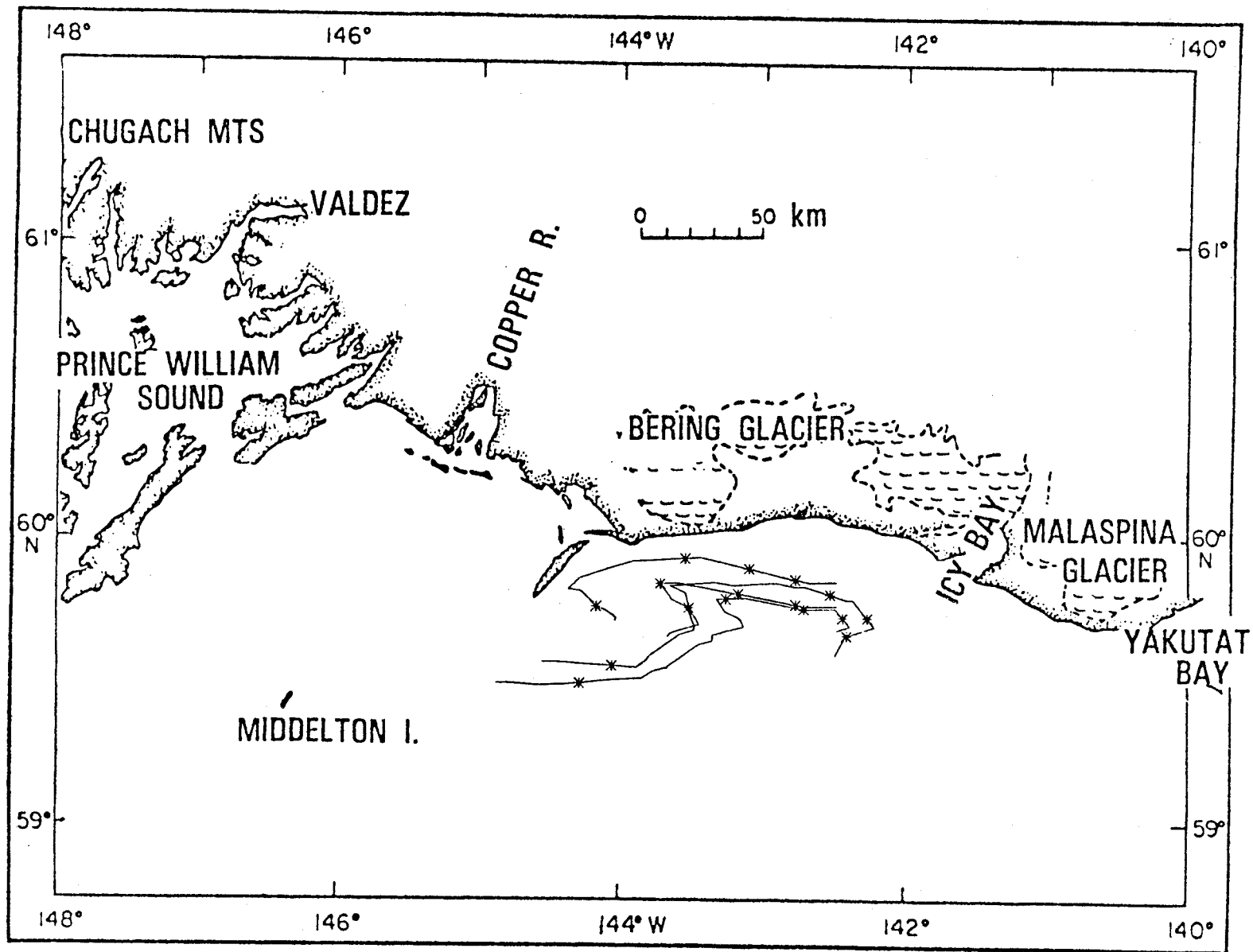


Figure 13. Four trajectories initiated on a north-south line released on August 17, 1974, and keyed on current meter station 62.

162

I-27

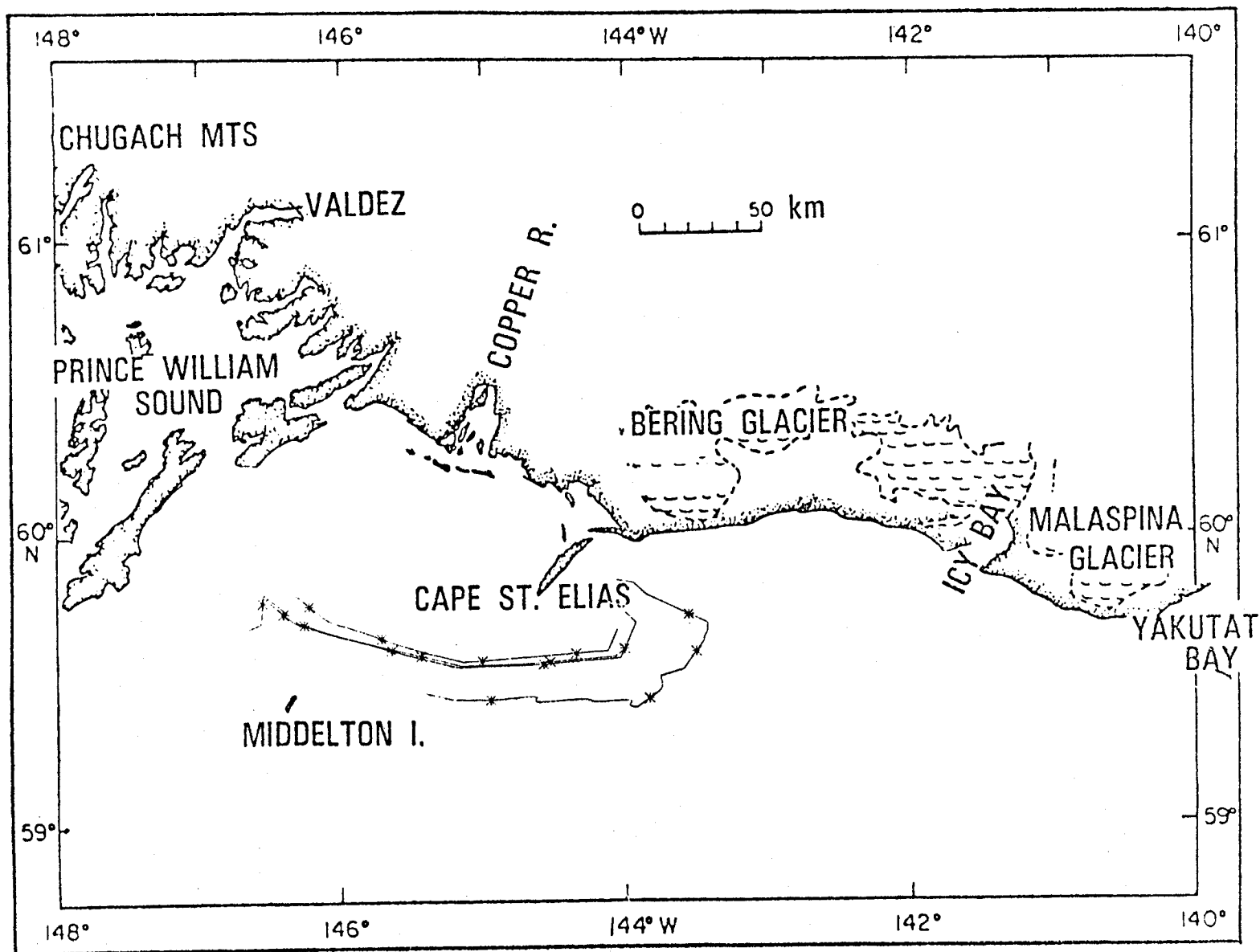


Figure 14. Three trajectories initiated on a north-south line released on August 17, 1974, and keyed on current meter station 62.



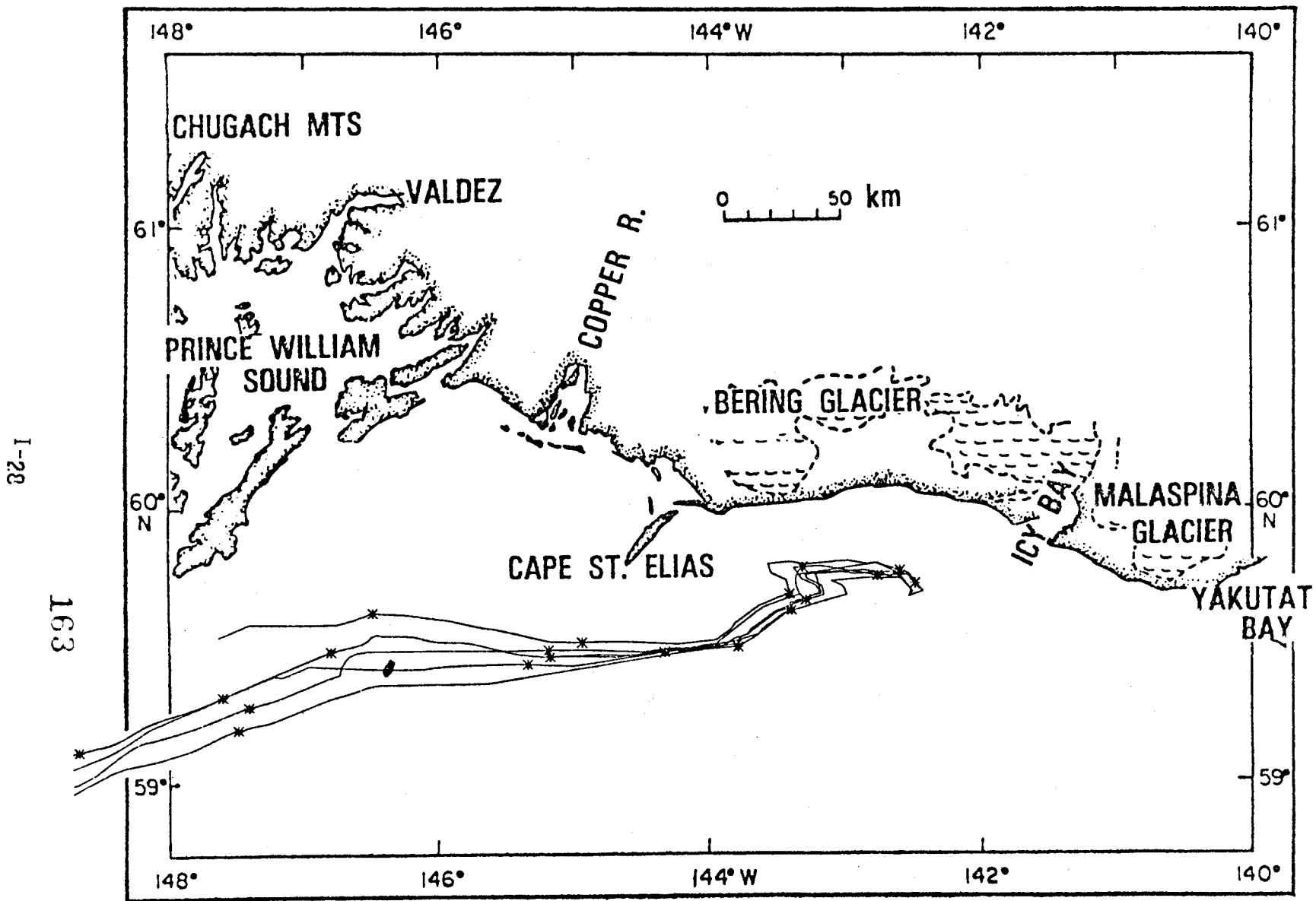


Figure 15. Six trajectories released from a single location at one week intervals starting on August 17, 1974, and keyed on current meter station 62.

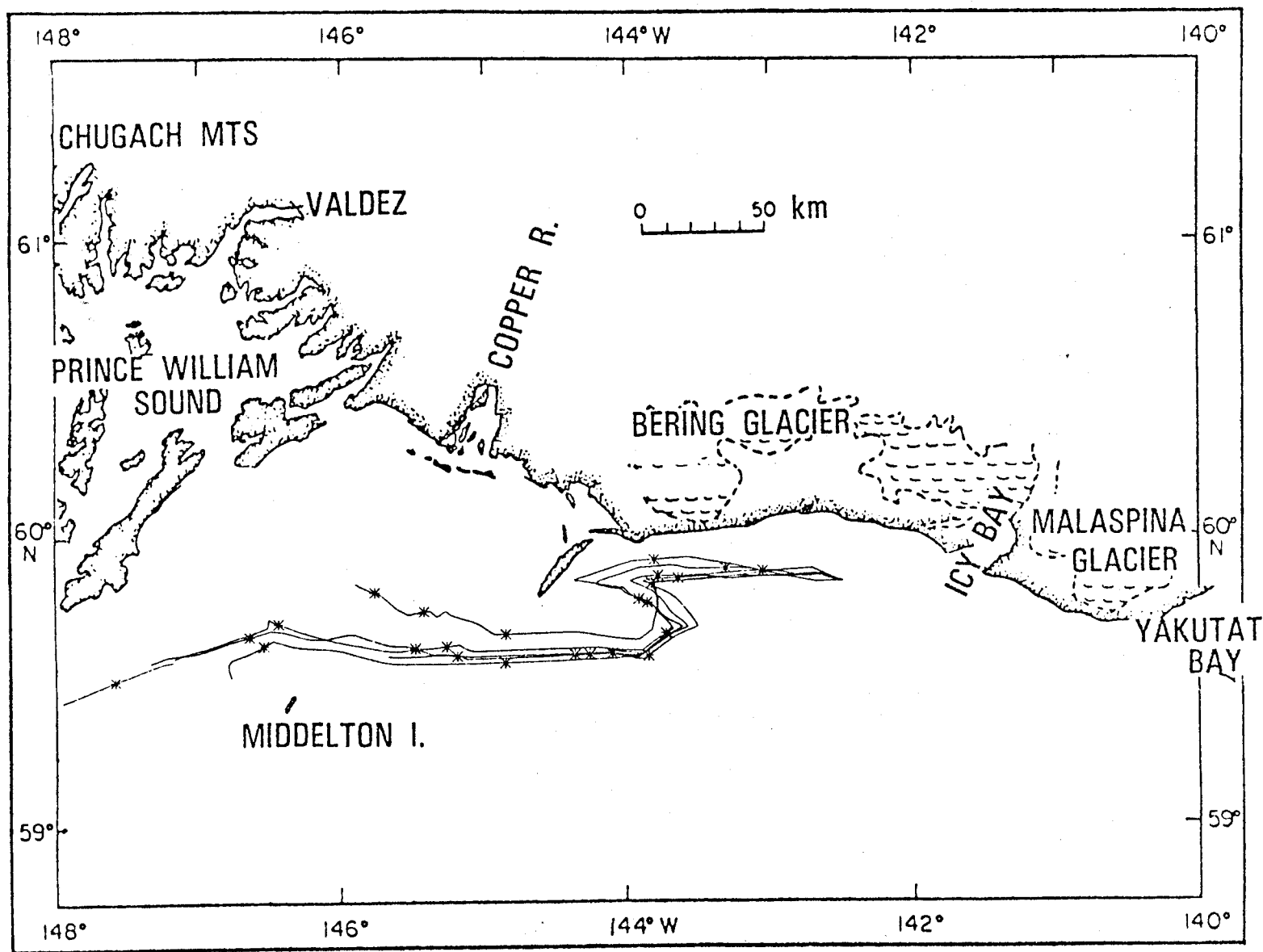


Figure 16. Six trajectories released from a single location at one week intervals starting on August 17, 1974, and keyed on current meter station 62.

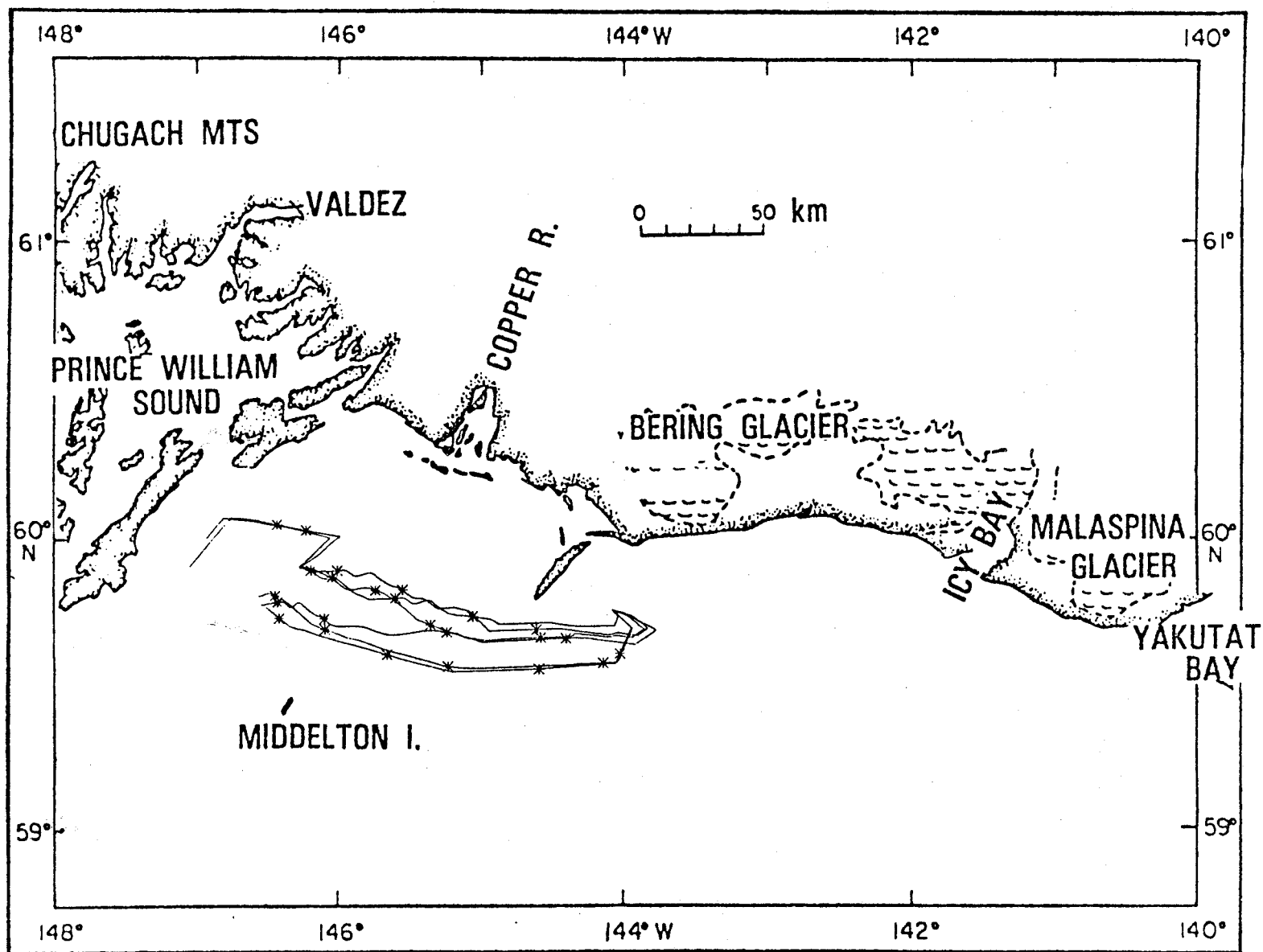


Figure 17. Six trajectories released from a single location at one week intervals starting on August 17, 1974, and keyed on current meter station 62.

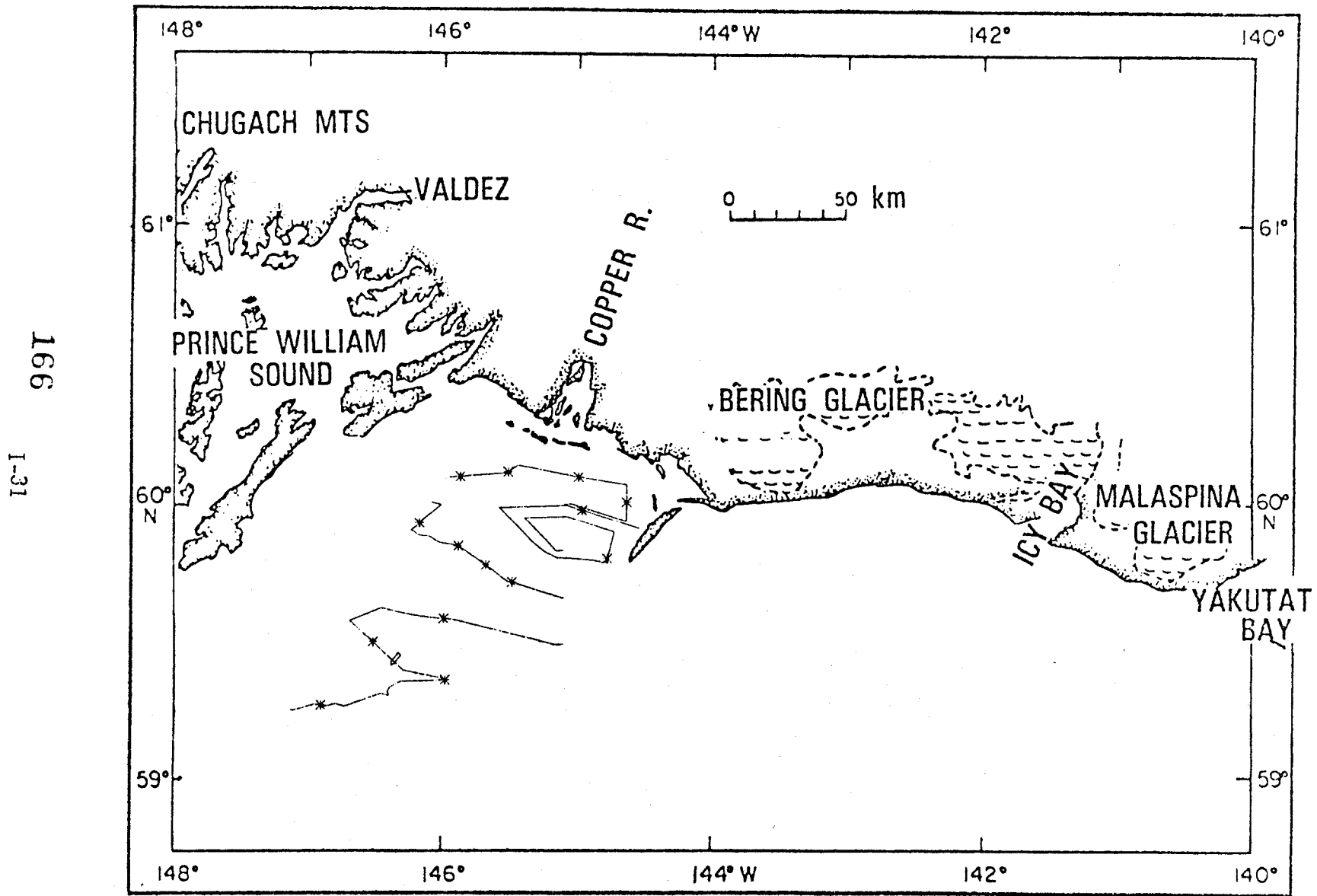


Figure 18. Four trajectories initiated on a north-south line released on August 16, 1974, and keyed on current meter station 61.

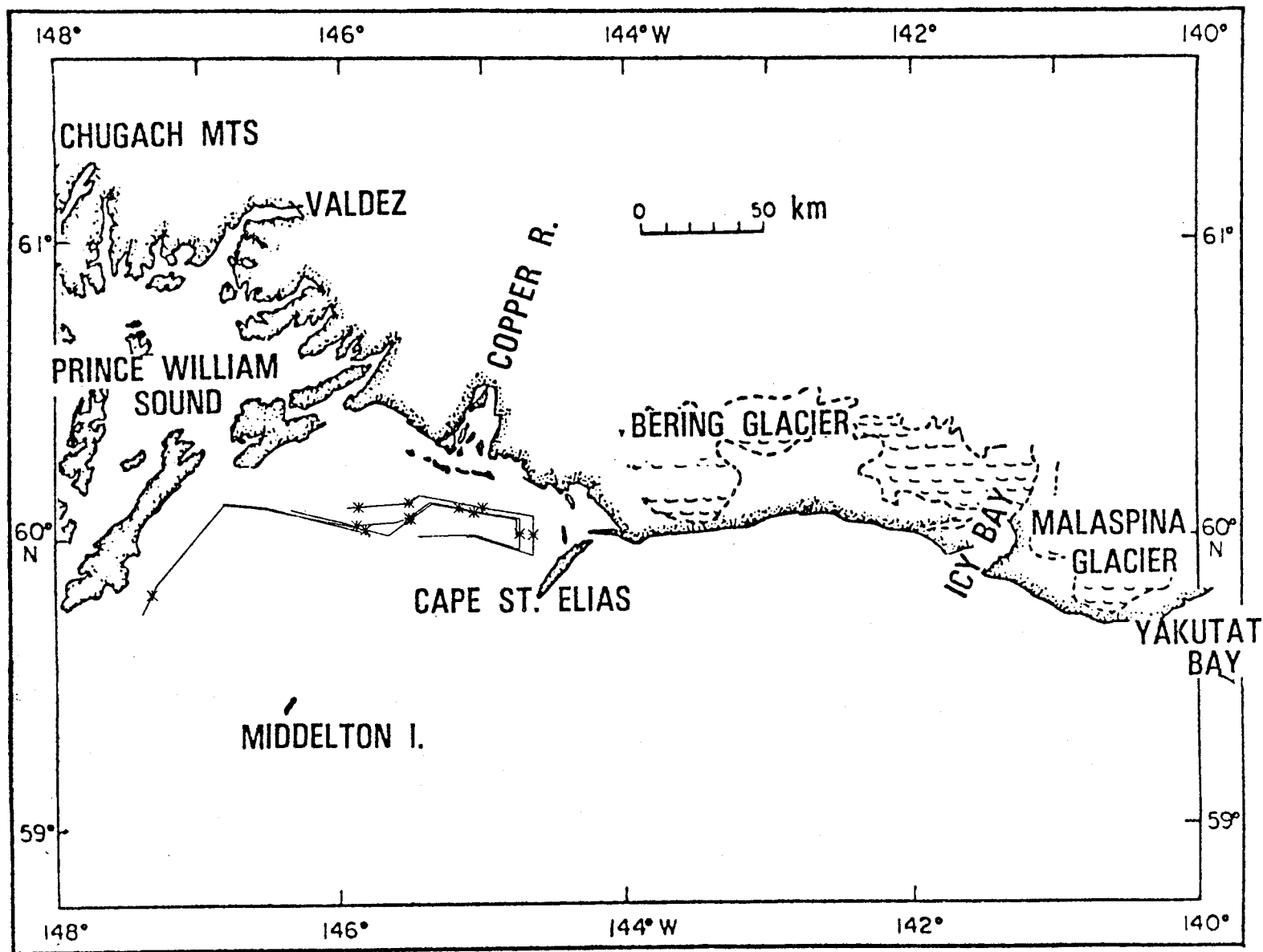


Figure 19. Four trajectories initiated on a east-west line released on August 16, 1974, and keyed on current meter station 61.

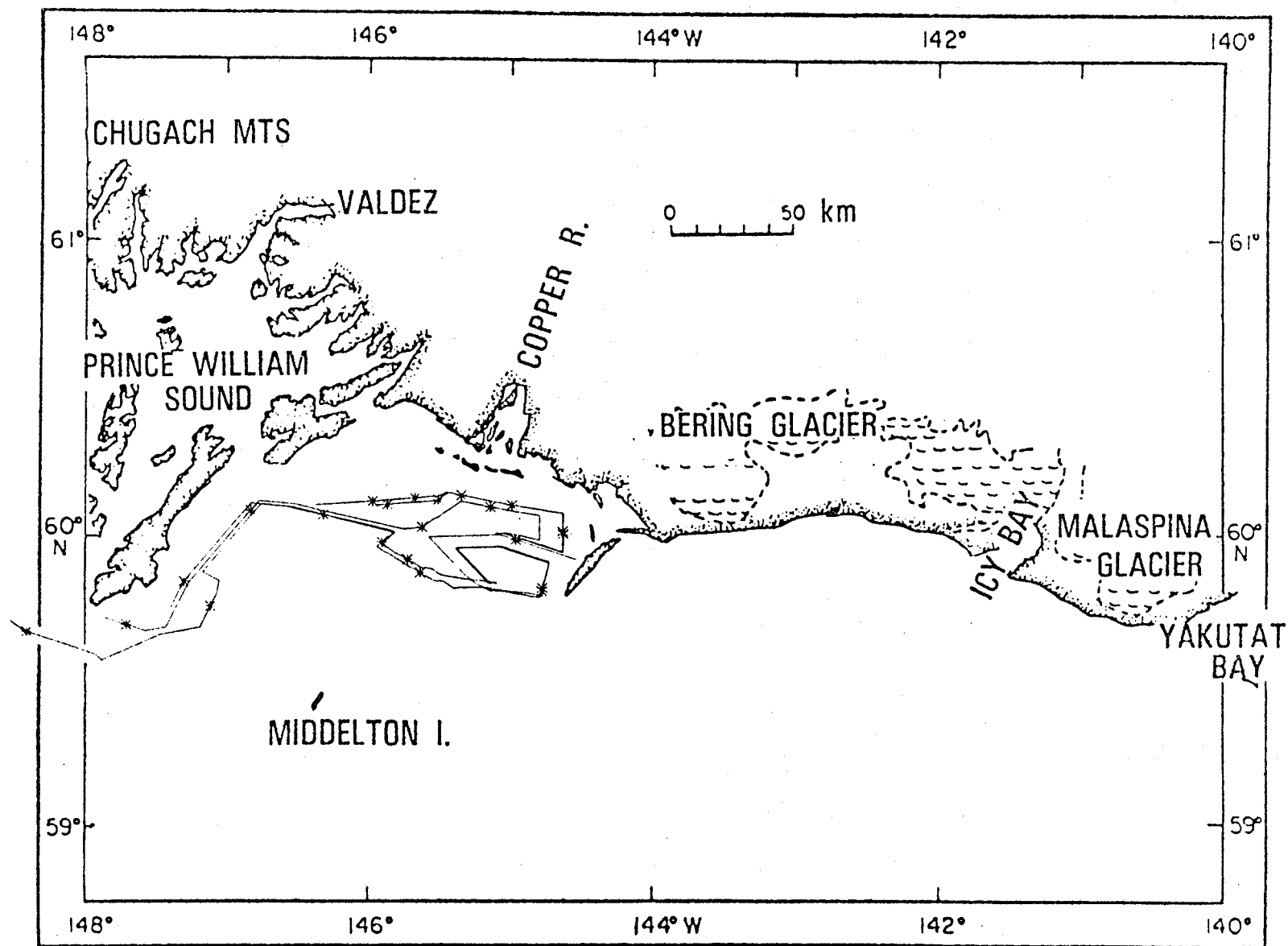


Figure 20. Three trajectories each initiated from two different locations. Released at one week intervals starting on August 16, 1974, and keyed on current meter station 61.

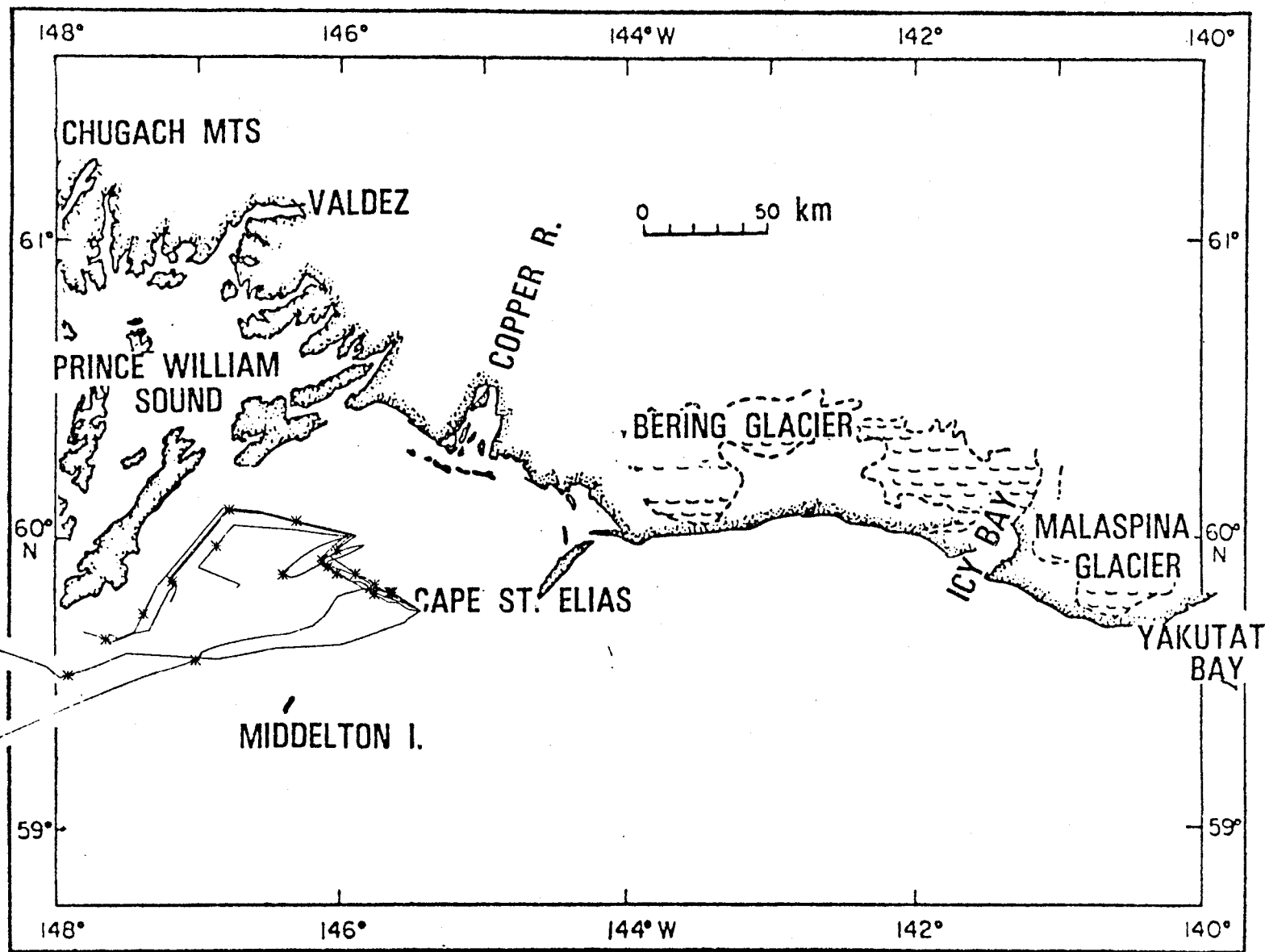


Figure 21. Six trajectories released from a single location at one week intervals starting August 16, 1974, and keyed on current meter station 61.

I-34

169

## CONCLUSIONS

Circulation in the Northeast Gulf of Alaska has been under active study since July 1974. In this particular facet of the study, a special focus is directed toward the region bounded by Cape St. Elias, Middleton Island, and the Copper River Delta. In this investigation, numerical modeling techniques, moored current meter data, Lagrangian drifters, and the analysis of satellite imagery all give a mutually supporting picture of the flow characteristics.

Although the typical flow across the Continental Shelf in the Northeast Gulf of Alaska is uniformly from east to the west, the region off of the Copper River Delta is dominated during the summer by gyres and extreme meander patterns indicating many smaller scale features. The numerical model studies indicate that these gyres are associated with both the local geometry/bathymetry and the presence of fresh water runoff from the Copper River. The direct current measurements offer a means of determining the appropriate boundary conditions for the numerical experimentation, and the general character of the gyres was found not particularly sensitive to the offshore choice of boundary conditions. An analysis of the available satellite imagery shows that gyre or eddy like structures are present virtually all of the time during the summer, although the position and details of the patterns may vary from case to case.

Trajectory analyses based on model results and observed currents indicate the nature of expected pathways from a number of release sites. These show that, for the region bounded by Cape St. Elias on the south and the western extreme of the Copper River Delta on the west, trajectories have a high probability of moving east and north. This carries them into areas where impact along the west coast of Kayak Island or the Copper River Delta are a distinct possibility. The studies indicate that releases farther offshore or displaced to the west are less likely to move into the Copper River Delta/Kayak Island vicinity. Satellite imagery shows mixing in the nearshore region is typically quite active. Pollutants whose trajectories reach this area can be expected to show significant variance from the pathways presented in the model in view of the fact that the model does not include dispersive or stochastic elements.

No winter data or cases have been studied yet, but some conjectures are possible. During low run off periods, it is assumed that the gyre formations would be less well developed. This would tend to suggest a more predominately westward motion to the currents. Superimposed on this however are strong wind effects that in this area tend to drive surface water against the coast. This process is evident in the observed density fields and has been discussed by Royer (1975).

Our present level of understanding indicates the region south of the Copper River Delta is dominated by gyre like currents in the summer that tend to carry trajectories toward shore. During the winter, wind drift would dominate trajectory paths and would similarly tend to result in the onshore movement of pollutants associated with petroleum development.



## REFERENCES

- Burbank, David C. (1974). Suspended Sediment Transport and Deposition in Alaskan Coastal Waters. M.S. Thesis, Inst. of Marine Science, Univ. of Alaska, Fairbanks. ✓
- Galt, J. A. (1975). Development of a Simplified Diagnostic Model for the Interpretation of Oceanographic Data. NOAA Tech. Report ERL 339-PMEL 25 (U.S. Government Printing Office, Washington, D.C.).
- Galt, J. A., and Thomas C. Royer (1975). Physical oceanography and dynamics of the Northeast Gulf of Alaska (preprint). Proceedings of the Symposium on Science and Technology in the Gulf of Alaska. Oct. 16-17, 1975. Sponsored by Arctic Institute of North America and the University of Alaska. ✓
- Royer, Thomas C. (1975). Seasonal variations of waters in the northern Gulf of Alaska. *Deep Sea Res.*, 22(6):403-416. ✓

Appendix II

Numerical Simulation of the Bering Sea  
General Circulation -- A Status Report

by

Y. J. Han

## Introduction

Despite the general recognition of the importance of the Bering Sea in fisheries, ecology, and potential offshore mining industries, the present knowledge of the Bering Sea general circulation is very fragmentary. Largely due to technical difficulties in oceanographic observations, the presently available observational data reveal only uncertain knowledge of surface current velocities, and very little about the deep basin circulation.

Although the Bering Sea is a very well defined oceanic region, and thus it presents a unique mathematical initial-boundary problem, the complicated geometry of the Basin and the inherent difficulties of the non-linear nature of the flow processes usually make it impossible for theoretical oceanographers to do any quantitative flow analysis. Fortunately, however, recent development of numerical modeling techniques offers a great potential in solving general oceanic problems. A number of oceanic general circulation models have already been developed by several climate study groups and have successfully simulated many of the observed large scale features of the ocean currents and temperature distribution.

During the past year, we have adopted two ocean general circulation models: one developed by Dr. Semtner at UCLA (1974) and the other developed by Dr. Haney (1974) at the Naval Postgraduate School. The model codes have been successfully tested on the University of Washington CDC 6400 computer. A careful evaluation of the two programs in terms of efficiency and flexibility suggests

that Dr. Semtner's program is adequate for the Bering Sea study. This program is found flexible enough to allow any geometrical configuration and bottom topography of the model ocean. Furthermore, the FORTRAN code is written so that it allows for high speed computation and low memory requirement. An initial version of the Bering Sea model with a realistic configuration and bathymetry has already been tested and the modified code has been verified to be energetically consistent to within a small truncation error.

We propose to carry out a full scale Bering Sea study with the model mentioned above. We intend to make numerical experiments in two phases. In the spin-up phase, a coarse grid resolution ( $\sim 100$  km x 100 km) will be used. In the second phase, the grid resolution will be doubled, and the model will be reinitialized with the data obtained by interpolations from the instantaneous fields at the end of the spin-up phase. The circulation will be driven both mechanically and thermally by prescribing the observed wind stress (computed from the observed pressure map) and the sea surface temperature.

We expect to see significant seasonal variation of the flow characteristics which might be due to strong annual wind stress variations of an order of magnitude. Although the grid resolution of the model may be inadequate to resolve all the details of the bottom topography, the model will depict the basic topographical features (deep basin, shelf break, ridges, etc.) in the sea. Also, a careful analysis of the model results would reveal the basic mechanisms which are responsible for the coupling between the deep basin circulation and the shelf circulation.

## Model Description

### 1. The governing equations

The model ocean is based on the primitive equations, which assume the hydrostatic approximation and the corresponding consistent formulations for the Coriolis force and the metric terms in the equation of motion (Phillips, 1966). The Boussinesq approximation is also made, so that the variation of density is recognized only in the calculation of the buoyancy force. The subgrid transports of momentum, heat and salt (the transport not resolved by the grid) are taken into account by a "down gradient mixing" hypothesis. The model Equations are presented by Semtner (1974) and will not be duplicated here.

### 2. Method of solution

Following Bryan (1969), the total motion is decomposed into two parts: namely, the vertically integrated motion (barotropic component) and the deviation of the total motion from the vertical mean motion (baroclinic component). The rigid-lid condition imposed at the model ocean surface results in the vertically integrated flow being non-divergent and, hence, a volume transport stream function can be defined. A prediction equation for the stream function is then obtained by taking the curl of the vertically averaged equations of motion. The resulting vorticity equation requires inversion of second order differential operator to obtain the stream function. The detail of the method of inversion is described in Semtner (1974).

The vertical shear current is predicted from the primitive equations after subtracting the vertical mean equations.

In summary, five prognostic variables (stream function, two components of the shear current, temperature, and salinity) are predicted, and three diagnostic variables (vertical velocity, density, and pressure) are determined from the diagnostic relations. The total velocity is obtained by adding the vertical shear component of the velocity to the vertical mean velocity.

The finite difference analogue that replaces the differential equations in the actual calculation is the scheme of Bryan (1969), which is designed to maintain certain integral constraints satisfied by the differential equations: the conservation of total mass, the conservation of total kinetic energy under pure inertial processes, and the conservation of total energy under adiabatic-frictionless processes. The details of the finite difference formulations are described in Semtner (1974).

### 3. Physical model of the Bering Sea and boundary conditions

Figures 1 and 2 show the configuration of the Bering Sea resolved by two grid mesh systems. The continuous bottom topography is approximated by 7 discrete values, and the depth of the Bering Strait, the depths of the major Aleutian passes and the basin depth are modified in the processes (figure 3).

At the sea bottom, fluxes of momentum, heat, and salt are taken to be zero. At the sea surface, wind stress, sea surface temperature and salinity distribution will be prescribed from observations.

At lateral walls, a no-slip condition  $(u, v) = 0$  is imposed, and no flux of heat or salt is allowed. For the open boundaries of the grid, components  $\bar{u}$  and  $\bar{v}$  of the vertical mean flow will be specified from various sources.

The internal mode velocities  $u'$  and  $v'$  are assumed to have zero normal derivatives at open boundaries. The surface of the sea is assumed to be a horizontal rigid lid.

By means of this assumption, high frequency external gravity waves are filtered out, without seriously affecting the lower frequency motions in which most of the energy is concentrated. At the ocean bottom, flow is required to parallel the slope.

#### Wind Stress

Wind stress can be estimated by a conventional drag law if surface wind is known. Unfortunately, wind measurements over the Bering Sea are very sparse in space and time, since they generally come from a handful of ship stations. For the numerical model, therefore, wind stress will be computed indirectly from surface pressure data. The wind velocity at anemometer height is obtained by multiplying geostrophic wind speed by a factor  $\gamma$  changing geostrophic wind direction by an angle  $\alpha$ . The constant  $\gamma$  here is 0.7, while  $\alpha$  is  $19^\circ$ . The surface pressure data provided by U.S. National Climatic Center will be used for the present experiment.

#### Heat and Salt Fluxes

The surface boundary condition on the thermodynamic energy equation is  $(\frac{\partial T}{\partial Z})_0 = \frac{Q_0}{\kappa \rho_0 C}$ , where  $Q_0$  is the surface heat flux and  $C$  is the specific heat of water. For the calculation of the surface heat flux,  $Q_0$ , Haney's empirical formulation is used (1974), in which  $Q_0 = D(T_A(\lambda, \phi, t) - T_1(\lambda, \phi, t))$ , where  $T_1$  is an apparent atmospheric equilibrium temperature which is almost identical to the surface air temperature at high latitude;  $T_1$  is the calculated temperature of the top layer of the sea; and  $D = 60 \text{ } 1\text{y/day } ^\circ\text{C}$  is the constant

determined by Haney from observational data. The surface air temperature based on National Climatic Center will be used for the present experiment.

Since data (rates of precipitation, evaporation, runoff) are not available for an explicit calculation of salt flux at the sea surface, the surface salinity distribution (figures 4-5) taken from Favorite (1974) will be prescribed as upper boundary conditions for salt equation.

#### Conditions at Open Boundaries

At open boundaries of the grid, cross-sections of temperature and salinity are required, along with estimates of vertically integrated transports. The model has four open boundaries along the Aleutian-Commander island arc: Kamtchatka Strait, Commander-Near strait, Central Aleutian pass, and Western Aleutian pass. Also, the Bering Strait is modeled as an open boundary. The widths and depths of the open boundaries are adjusted to match the observed bathymetry within the limits imposed by grid resolutions. Cross-sections of temperature and salinity are obtained from various sources, and visually averaged values in the area of each grid box are chosen for the grid point at the center of the box. Integrated volume transport values on the open sections are chosen from various estimates presently available. It should be mentioned, however, that at the present stage, there are many uncertainties in transport estimates at the various passages.

The chosen values of temperature, salinity and mass transports (annual mean) are given in Tables 1-5. The first line of each table gives values of the transport stream function in Sverdrup's ( $1\text{sv} = 10^6 \text{ m}^3/\text{sec}$ ). Then temperature in degrees centigrade and salinity in parts per thousand are shown for each grid box. All tables are to be viewed from the south.



The temperature and salinity cross-sections in Tables 1-4 are based on hydrographic data by Favorite (1974) and Arsenev (1967). A net transport of 18 sv outward through the Kamtchatka Strait is in close agreement with an estimate of 18.4 sv by Arsenev and summer values (20 sv) by Hughes and Coachman (1974). A net transport of 14 xv inward across the Commander-Near Strait was taken from Arsenev, and it is greater than an estimate (10 sv) by Favorite (1974) but less than Hughes and Coachman's (25 sv). The total inflows through Western and Central Aleutian are based on the estimates made by Arsenev (1967).

For the Bering Strait, temperature and salinity values in Table 5 are taken from cross-sections in Coachman and Aagaard (1966). The total transport (1 sv) outward was chosen from the estimates (1.1 sv) by Arsenev (1967).

#### 4. Test Run

We have tested the Bering Sea model in a closed basin with idealized forcing functions. The purpose of the test was to insure an internal consistency of the model. Correct balances of volume integrated terms in the energy, heat, and salt equations were obtained. The truncation errors (non-linear exchange error and energy conversion error) are extremely small and, in fact, they are smaller than any major energy transformation terms by many orders of magnitude.

II-10

180

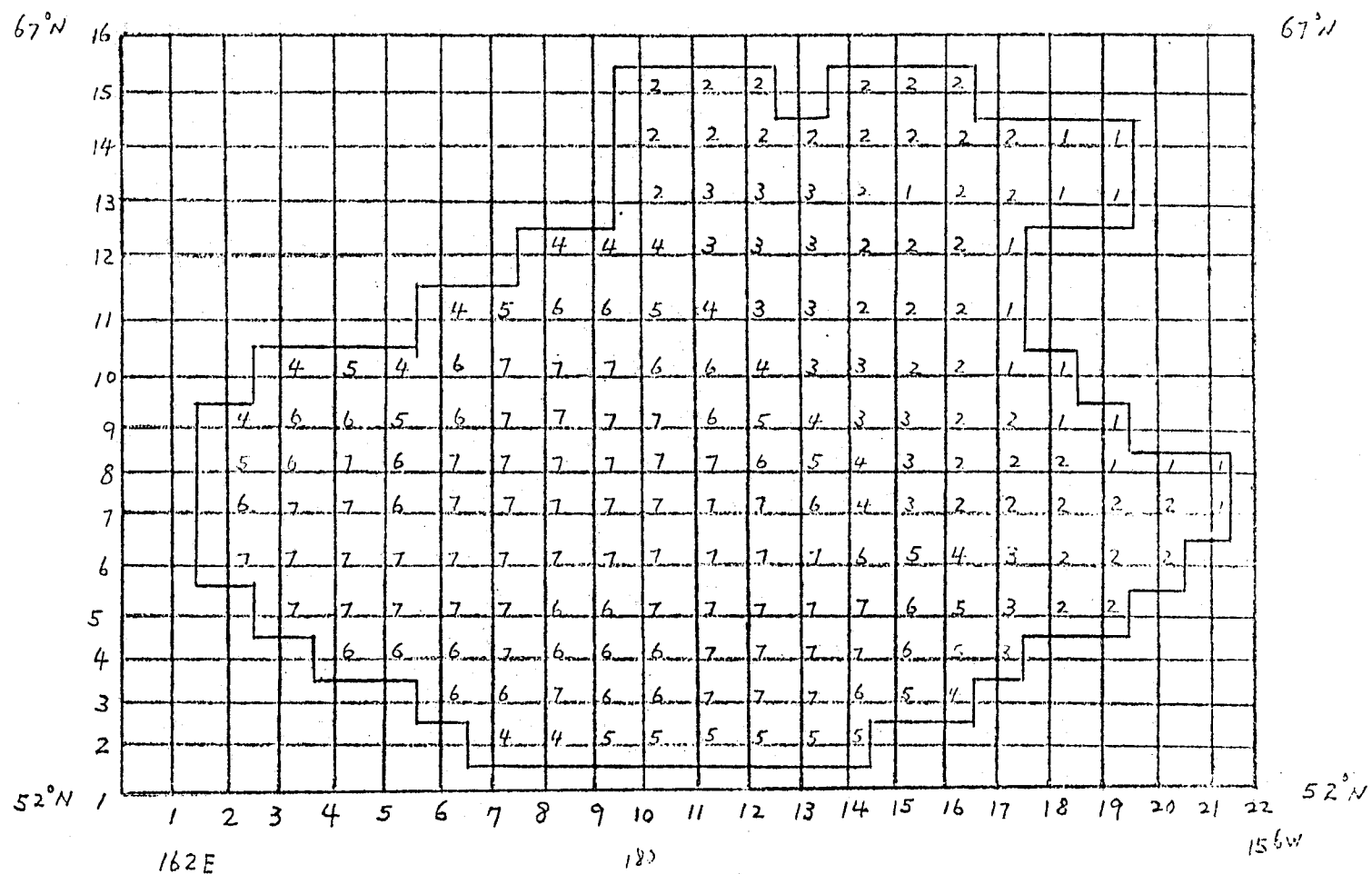


Figure 1. Bering Sea Basin resolved by (2° long. x 1° lat.) mesh. Integers indicate the number of layers at grid points.

181

11-11

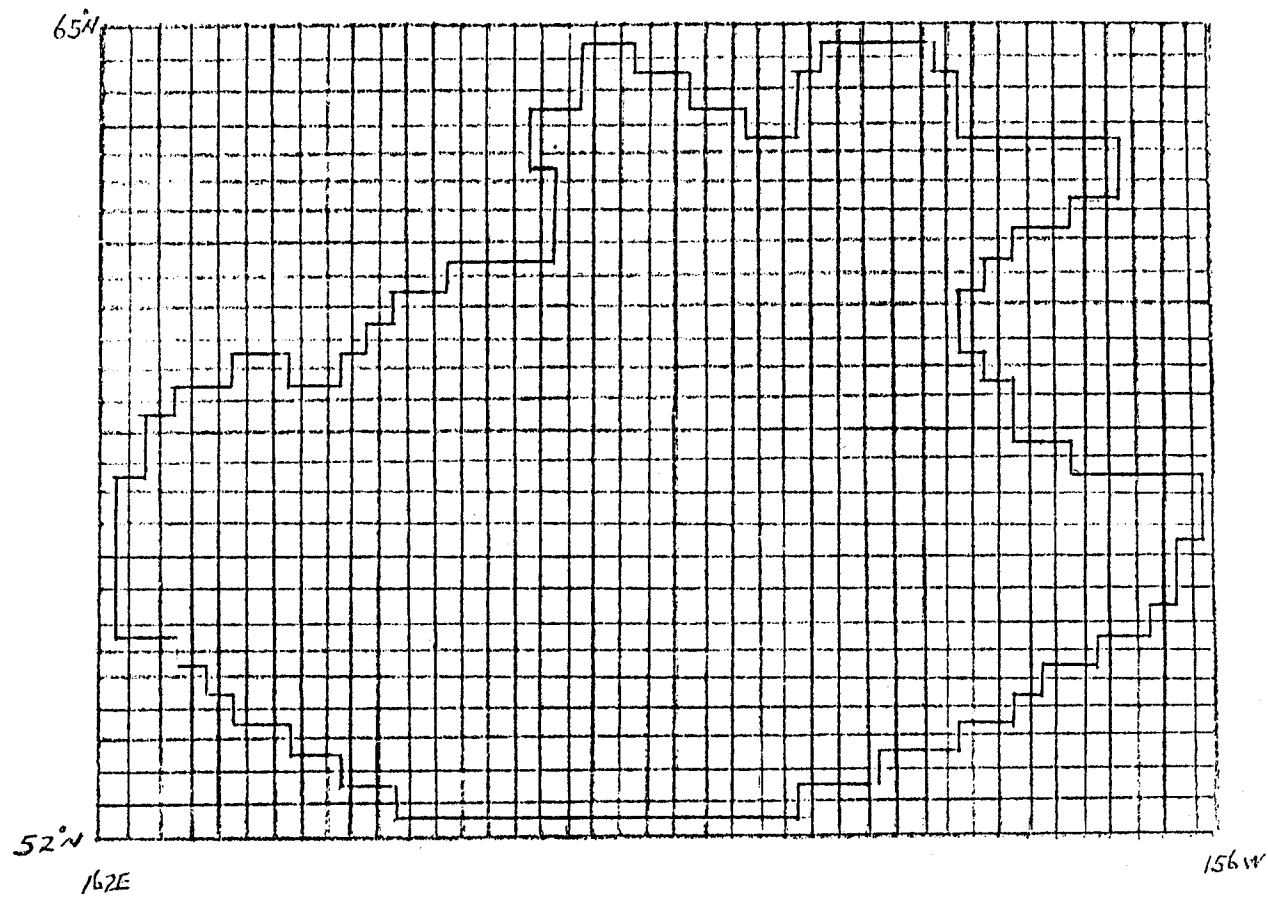


Figure 2. Bering Sea Basin resolved by ( $1^{\circ}$  long. x  $0.5^{\circ}$  lat.) mesh.

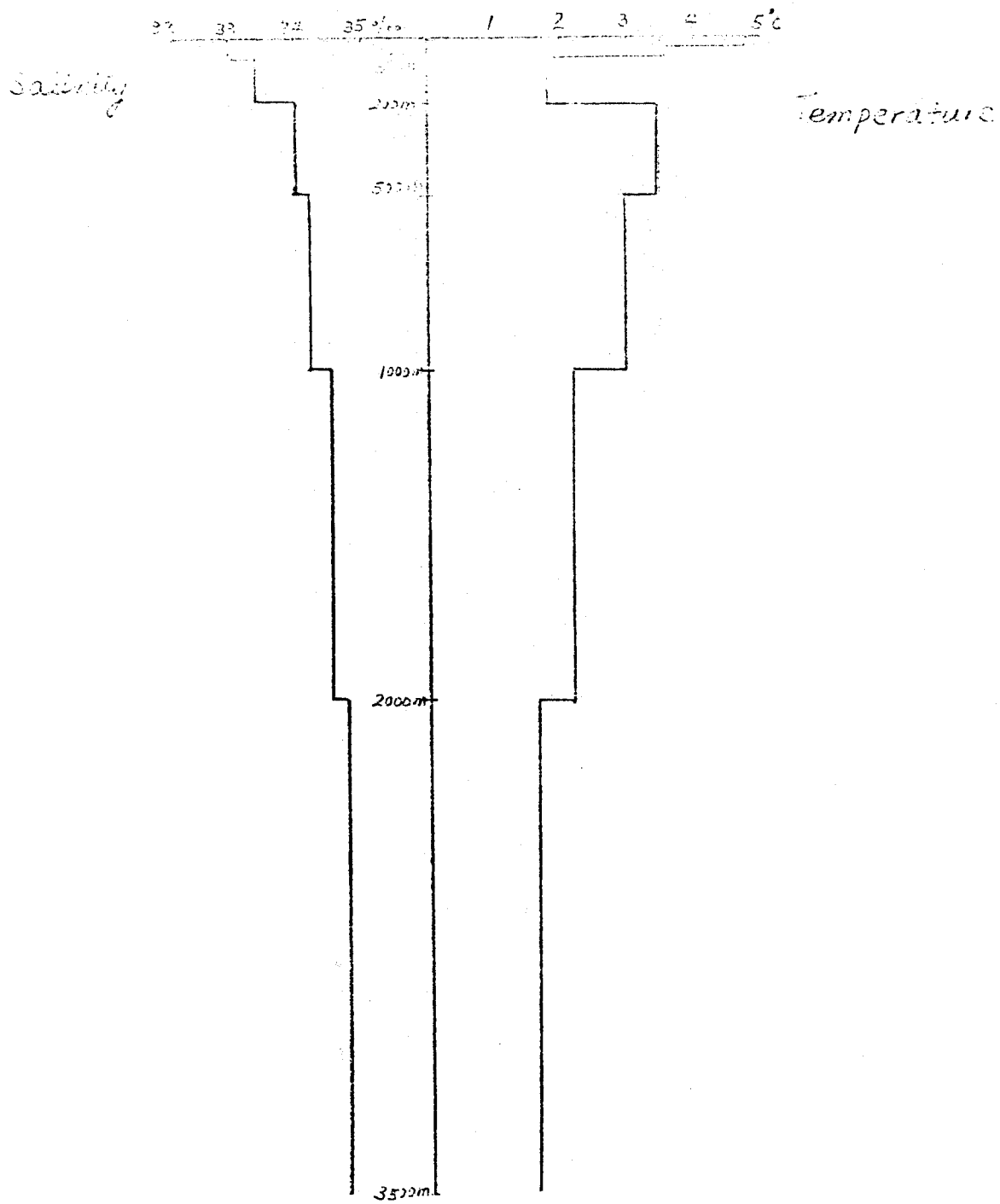


Figure 3. Depth of vertical layers and initial distribution of temperature and salinity.

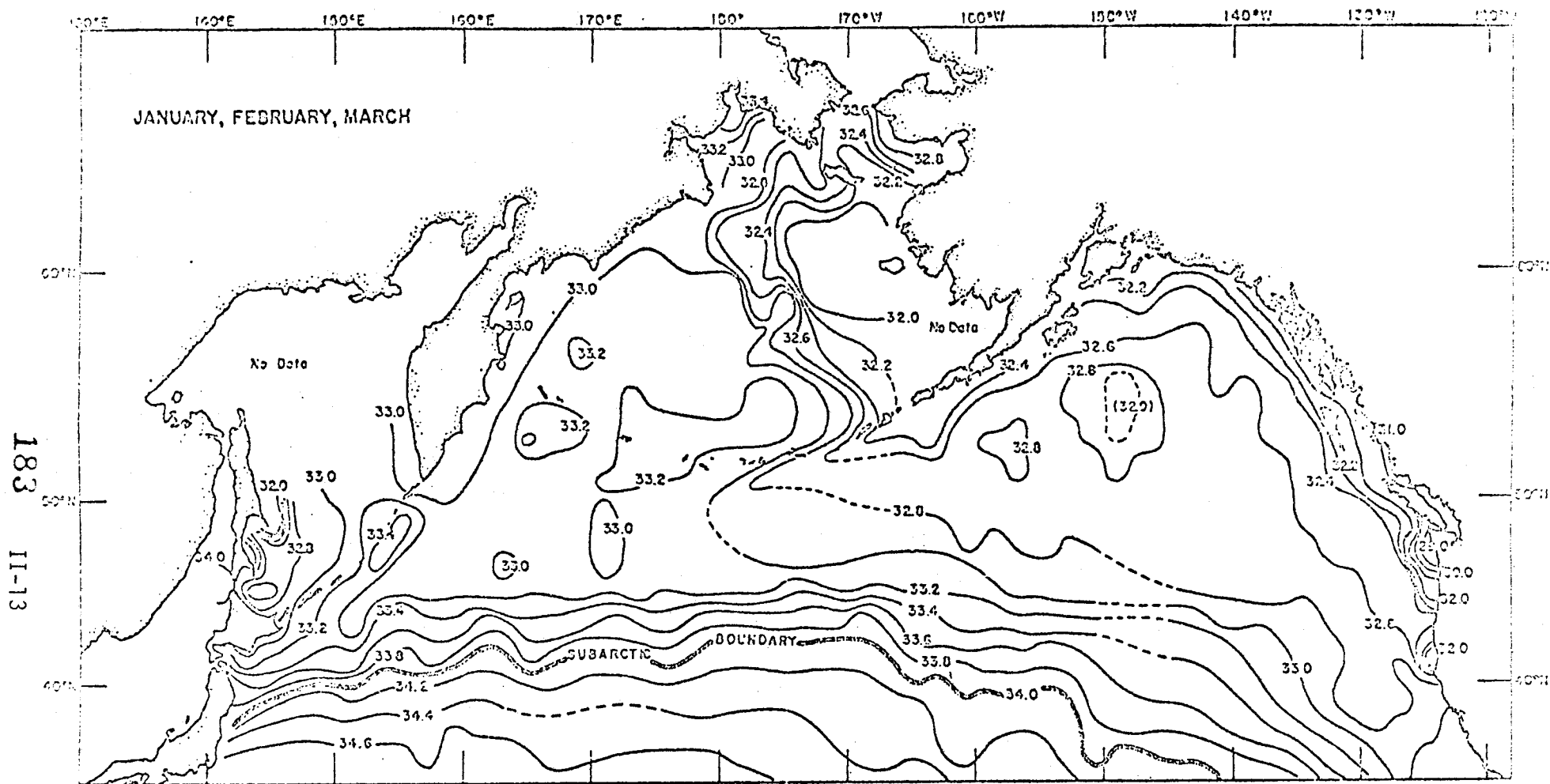


Figure 4.

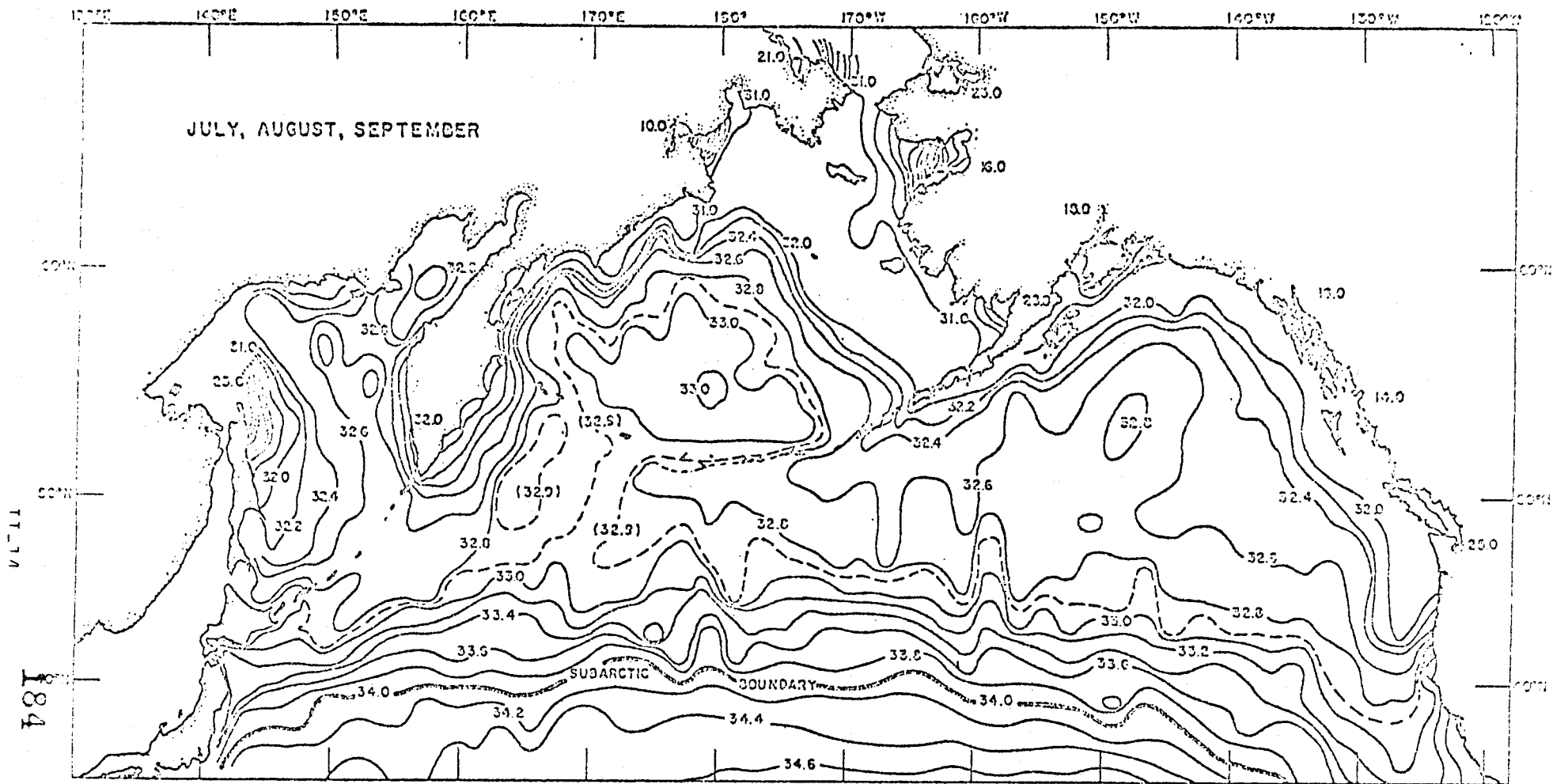


Figure 5.

| 18           | 0            |
|--------------|--------------|
| 5.0<br>32.0  | 5.0<br>32.6  |
| 4.0<br>32.1  | 4.0<br>32.7  |
| 2.0<br>32.7  | 2.0<br>33.2  |
| 3.2<br>33.6  | 3.2<br>33.8  |
| 3.2<br>34.2  | 3.2<br>34.3  |
| 2.0<br>34.6  | 2.0<br>34.6  |
| 1.6<br>34.65 | 1.6<br>34.65 |

Table 1. T, S, and  $\Psi$  for Kamtchaka Strait

Stream function  $\Psi$  in Sverdrups is shown on the top line. Temperature ( $^{\circ}\text{C}$ ) and salinity ( $^{\circ}/_{\text{oo}}$ ) are given for each grid box. Section is viewed from the south.

| 0            | 7           | 14           |
|--------------|-------------|--------------|
| 4.5<br>33.02 | 4.8<br>33.0 | 5.2<br>33.07 |
| 4.0<br>33.05 | 4.0<br>33.1 | 4.7<br>33.1  |
| 2.2<br>33.3  | 2.6<br>33.4 | 3.2<br>33.3  |
| 3.5<br>33.9  | 3.7<br>33.9 | 3.6<br>33.8  |
| 3.1<br>34.3  | 3.1<br>34.3 | 2.7<br>34.3  |
| 2.2<br>34.5  | 2.2<br>34.5 | 2.2<br>34.5  |

Table 2. T, S, and  $\Psi$  for Commander-Near Strait

| 14           | 15           |
|--------------|--------------|
| 5.6<br>33.1  | 5.6<br>33.1  |
| 7.2<br>33.15 | 7.2<br>33.15 |
| 3.7<br>33.15 | 3.7<br>33.15 |
| 3.9<br>33.7  | 3.9<br>33.7  |

Table 3. T, S, and  $\Psi$  for Western Aleutian Pass



| 15            | 19            |
|---------------|---------------|
| 4.9<br>33.15  | 4.9<br>33.15  |
| 4.5<br>33.2   | 4.5<br>33.2   |
| 3.75<br>33.27 | 3.75<br>33.27 |
| 3.77<br>33.65 | 3.77<br>33.65 |
| 3.37<br>34.15 | 3.37<br>34.15 |

Table 4. T, S, and  $\Psi$  for Central Aleutian Pass

| 18          | 19          |
|-------------|-------------|
| 3.0<br>32.8 | 5.0<br>31.0 |
| 2.0<br>32.9 | 2.4<br>32.0 |

Table 5. T, S, and  $\Psi$  for Bering Strait

## References

- Aagaard, K. (1970). Wind-driven transports in the Greenland and Norwegian Seas. Deep-Sea Res. 17, 281-291.
- Arsenev, V.S. (1967). Currents and water masses of the Bering Sea. (Trans., 1968, Na. Mar. Fish. Serv., Northwest Fish. Center, Seattle, Wash.) 135 pp.
- Bacon, J.C. (1973). "Numerical Investigation of Bering Sea Dynamics". NPGS M.S. Thesis, 60 pp.
- Bryan, K. (1969). A numerical method for the study of the circulation of the World Ocean. J. Comput. Phys., 4, 347-376.
- Coachman, L.M., and K. Aagaard (1966). On the water exchange through Bering Strait. Limnol. Oceanogr., 11, 47-59.
- Dodimead, A.J., F. Favorite, and T. Hirano (1963). Salmon of the North Pacific Ocean - Part II - Review of oceanography of the Subarctic Pacific Region. Bull. Int. N. Pacif. Fish. Commn., 13, 195 pp.
- Favorite, F (1974) Flow into the Bering Sea through Aleutian island passes. Oceanography of the Bering Sea. Proc. An international symposium. 3-37.
- Favorite, F., A.J. Dodimead, K. Nasu (1974) Oceanography of the subarctic Pacific Ocean (in preparation)
- Haney, R.L. (1971) "A numerical study of the large scale response of an ocean circulation to surface heat and momentum flux". UCLA Ph.D. Thesis. 191 pp.
- Haney, R.L. (1974) A numerical study of the response of an idealized ocean to large-scale surface heat and momentum flux. Journal of Physical Oceanography, 4, 2 145-167.
- Ohtani, K. (1973) Oceanographic structure in the Bering Sea. Mem. Fac. Fish. Hokkaido Univ. XXI, 1, 65-106.
- Phillips, N.A. (1966b) The equations of motion for a shallow rotating atmosphere and the "traditional approximation". Journal of the Atmospheric Sciences, 23. 626-628.
- Semtner, A.J. (1973) "A numerical investigation of arctic ocean circulation. Princeton Univ. Ph.D. Thesis, 251 pp.
- Semtner, A.J. (1974) An oceanic general circulation model with bottom topography. Technical Report No. 9, Numerical Simulation of Weather and Climate. Dept. Meteorology, University of California, Los Angeles, 37 pp.
- Takenouti, A.Y., and K. Ohtani (1974) Currents and water masses in the Bering Sea. Proc. An international symposium, 39-57.

Appendix III

Bibliography of Ice Related Papers

MASTER LIST

- Atlas, R. M. (1973). "Fate and Effects of Oil Pollutants in Extremely Cold Marine Environments," Office of Naval Research, Final Report, Oct. 1973.
- Ayers, R. C., H. O. Johns, and J. L. Glaeser (1974). "Oil Spills in the Arctic Ocean: Extent of Spreading and Possibility of Large-Scale Thermal Effects," Science, Nov. 1974, pp. 843-844.
- Badgley, F. I. (1966). In Proceedings of the Symposium on the Arctic Heat Budget and Atmospheric Circulation, Rand Corp. Mem. No. RM-5233-NSF (The Rand Corp., Santa Monica, CA), pp. 267-277.
- Banke, E. and S. Smith (1973). "Wind Stress on Arctic Sea Ice," J.G.R. 78(33), 7871-7883.
- Barber, F. G. (1971). "Report of the Task Force - Operation Oil" (Cleanup of the Arrow oil spill in Chedabucto Bay), Minister of Transport, Canada.
- Barber, F. G. (1973). "Oil Spilled with Ice: Some Qualitative Aspects," Conference on Prevention and Control of Oil Spills, pp. 563-567.
- Brown, A. L. (1954). An Analytical Method of Ice Potential Calculation, U. S. Navy Hydrographic Office, Washington, D.C. (Tech. Report TR-5).
- Brown, R. A. (1972). "The Candidates for the AIDJEX Planetary Boundary Model," Symposium on Sea-Air Interaction in Polar Regions, IV. - Arctic Ocean Dynamical Studies, b. Numerical Modelling Experiments. Reported in Trans. A.G.U. 53(11):1015 (Nov. 1972). (Abstract only.)
- Bryan, K. (1969). "Climate and the Ocean Circulation, III. The Ocean Model," Monthly Weather Review 97(11): 806-827.
- Businger, J. A. (1972). "The Transfer of Momentum from the Atmosphere to the Sea-Ice Surface," Symposium on Sea-Air Interaction in Polar Regions, IV. - Arctic Ocean Dynamical Studies, a. Processes of Momentum Transfer. Reported in Trans. A.G.U. 53(11): 1014 (Nov. 1972). (Abstract only.)
- Callaway, E. B. (1954). An Analysis of Environmental Factors Affecting Ice Growth, U. S. Naval Hydrographic Office, Washington, D.C. (Tech. Report TR-7).
- Campbell, W. J. (1965). "The Wind Driven Circulation of Ice and Water in a Polar Ocean," J.G.R. 70(14): 3279-3301.
- Campbell, W. J., S. Martin (1973). "Oil and Ice in the Arctic Ocean: Possible Large-Scale Interactions," Science, July 1973, pp. 56-58.
- Canadian Arctic Resource Committee. "Offshore Drilling in the Beaufort Sea, Northern Perspectives 2(2).
- Chen, E. G., J. C. K. Overall, and C. R. Phillips (1974). "Spreading of Crude Oil on an Ice Surface," Canadian Journal of Chemical Engineering, 52, Feb. 1974.
- Coachman, L. K. (1969). "Physical Oceanography in the Arctic Ocean: 1968," Arctic 22(3): 214-224.
- Coachman, L. K., and C. A. Barnes (1963). "The Movement of Atlantic Water in the Arctic Ocean," Arctic 16(1): 9-16.

- Coachman, L. K., and C. A. Barnes (1961). "The Contribution of the Bering Sea Water to the Arctic Ocean," Arctic 14(3): 147-161.
- Colony, R. (1975). "The Boundary Determination Problem for the AIDJEX Ocean," AIDJEX Bulletin 28 (March): 87-97.
- Coon, M. D. (1972). "Mechanical Behavior of Compacted Arctic Ice Floes," Preprints, Offshore Technology Conference, Houston, Texas, 1-3 May, 1972. OTC 1684. American Institute of Mining, Metallurgical, and Petroleum Engineers.
- Coon, M. D. (1972). "Constitutive Laws for Pack Ice," Symposium on Sea-Air Interaction in Polar Regions, Dec. 5, 1972. Reported in Trans. A.G.U., 53(11): 1007, Nov. 1972. (Abstract only.)
- Coon, M. D., G. A. Maykut, R. S. Pritchard, D. A. Rothrock, and A. S. Thorndike (1974). "Modelling the Pack Ice as an Elastic-Plastic Material," AIDJEX Bulletin 24 (May): 1-105.
- Coon, M. D. and R. S. Pritchard (1974). "Application of an Elastic-Plastic Model of Arctic Pack Ice," The Coast and Shelf of the Beaufort Sea, Ed. J. C. Reed and J. E. Slater, Arlington, VA: Arctic Institute of N. Amer.
- Corton, E. L. (1954). The Ice Budget of the Arctic Pack and Its Application to Ice Forecasting, U. S. Navy Hydrographic Office, Washington, D. C. (Tech. Report TR-6).
- Cox, G. F. N. and W. F. Weeks (1972). "Variation of Salinity in Multiyear Sea Ice," Symposium on Sea-Air Interaction in Polar Regions, Dec. 5, 1972. Reported in Trans A.G.U., 53(11): 1008, Nov. 1972. (Abstract only.)
- Deslauriers, P.C. (1975). "Oil Pollution in Ice Infested Waters (A Survey of Recent Development)," Unpublished Report, Aug. 1, 1975.
- Doronin, Yu. P. (1970). "On a Method of Calculating the Compactness and Drift of Ice Floes (K Metodike Rascheta Splochnosti I Dreifa L'Dov)." Proceedings of the Arctic and Antarctic Research Institute (Trudy Arkt. I Antarkt. In-Ta), 291: 5-17 (English transl., AIDJEX Bulletin No. 3 (Nov. 1970), pp. 22-39).
- Eide, L. I., and S. Martin (1972). "Brine Channels in Sea-Ice: A Laboratory Study." Symposium on Sea-Air Interaction in Polar Regions, Dec. 5, 1972., reported in Trans. A.G.U., 53(11): 1008, Nov. 1972. (Abstract only.)
- Evans, R. J. and D. A. Rothrock (1975). "Stress Fields in Pack Ice," Third International Symposium on Ice Problems, Hanover, New Hampshire.
- Felzenbaum, A. I. (1958). "The Theory of the Steady Drift of Ice and the Calculation of the Long Period Mean Drift in the Central Part of the Arctic Basin," Problems of the North 2: 5-15, 13-44.
- Fletcher, J. O. (1965). The Heat Budget of the Arctic Basin and Its Relation to the Climate, Rand Corp. Rep. No. R-444-PR (The Rand Corp., Santa Monica, CA).
- Foster, T. D. (1968). "Haline Convection Induced by the Freezing of Sea Water," J. Geophys. Res. 73(6): 1933-1938.
- Foster, T. D. (1972). "Haline Convection in Polynyas and Leads," J. Physical Ocean. 2: 462-469.

- Foster, T. D. (1975). "Heat Exchange in the Upper Arctic Ocean," AIDJEX Bulletin 28: 151-166.
- Gade, H. G., R. A. Lake, E. L. Lewis, and E. R. Walker (1974). "Oceanography of an Arctic Bay," Deep-Sea Res., 21(7): 547-571.
- Galt, J. A. (1973). "A Numerical Investigation of Arctic Ocean Dynamics," J. Phys. Ocean. 3(4): 379-396.
- Galt, J. A. (1972). "A Barotropic Numerical Model of the Arctic Ocean," Symposium on Sea-Air Interaction in Polar Regions - IV. - Arctic Ocean Dynamical Studies, b. Numerical Modelling Experiments. Reported in Trans. A.G.U. 53(11): 1015. (Nov. 1972). (Abstract only.)
- Galt, J. A. (1972). "The Development of a Homogeneous Numerical Ocean Model for the Arctic Ocean," NPS-58G172071A, Naval Postgraduate School, Monterey, CA. (AD #744925 NTIS)
- Galt, J. A. (1967). "Current Measurements in the Canadian Basin of the Arctic Ocean, Summer 1965." U. of Wa., Dept. of Ocean., Tech. Report No. 184.
- Getman, Lt. J. H. (1975). "United States Coast Guard Arctic Oil Pollution Program," Conference on Prevention and Control of Oil Pollution.
- Glaeser, LTJG J. L., USCGR, LCDR G. P. Vance, USCG (1971). "A Study of the Behavior of Oil Spills in the Arctic," Final Report, U. S. Coast Guard, Washington, D. C., Feb. 1971. (Ref. No. AD717142, F.S.T.I., Springfield, VA, 1971)
- Glaeser, LTJG J. L., USCGR, LCDR G. P. Vance, USCG (1972). "A Study of the Behavior of Oil Spills in the Arctic," Offshore Technology Conference, May 1972.
- Gloersen, P., T. C. Chang, T. T. Wilheit, and W. J. Campbell (1973). Polar Sea Ice Observations by Means of Microwave Radiometry, X-652-73-341, Goddard Space Flight Center, Greenbelt, MD.
- Golden, P. C. (1974). "Oil Removal Techniques in an Arctic Environment," Marine Technology Society Journal 8(1): 38-43, Jan. 1974.
- Hibler, W. D., S. F. Ackley, W. K. Crowder, H. L. McKim, and D. M. Anderson (1974). "Analysis of Shear Zone Ice Deformation in the Beaufort Sea Using Satellite Imagery," The Coast and Shelf of the Beaufort Sea, Ed. J. C. Reed and J. E. Slater, 285-296, Arlington, VA: Arctic Institute of N. Amer.
- Hibler, W. D. III, S. J. Mock, and W. B. Tucker III (1974). "Classification and Variation of Sea Ice Ridging in the Western Arctic Basin," J.G.R. 79(18): 2735-2743 (June 20, 1974).
- Hibler, W. D. III, W. F. Weeks, A. Kovacs, and S. F. Ackley (1973). "Differential Sea Ice Drift I: Spatial and Temporal Variations in Sea Ice Deformation," AIDJEX Bulletin 21 (July): 79-113.
- Holland, W. R. (1967). "On the Wind-Driven Circulation in an Ocean with Bottom Topography," Tellus 19(4): 582-599.
- Holmgren, B. (1972). "Some Results of Radiation Measurements During the 1972 AIDJEX Pilot Study," Symposium on Sea-Air Interaction in Polar Regions, IIa - Convective and Radiative Processes in Arctic Ocean Boundary Layer, reported in Trans. A.G.U. 53(11): 1010 (Nov. 1972). (Abstract only.)

- Hoult, D. P., S. Wolfe, O'Dea, and J. P. Patureau (1974). "Oil in the Arctic," Final Report, U. S. Coast Guard, Washington, D.C., Feb. 1974.
- Hoult, D. P. (1971). "The Aging of Oil Spilled in the Arctic," U. S. Coast Guard, Washington, D.C., Aug. 1971, Contract DOT-CG-12438-A.
- Hunkins, K. S. (1974). "Subsurface Eddies in the Arctic Ocean," Deep-Sea Research 21(12): 1017-1034.
- Hunkins, K. L. (1975). "The Oceanic Boundary Layer and Stress Beneath a Drifting Ice Flow," J.G.R. 80(24): 3425-3433, Aug. 20, 1975.
- Hunkins, K. L. (1972). "Momentum Exchange Between the Ocean and Drifting Ice," Symposium on Sea-Air Interaction in Polar Regions, IV. - Arctic Ocean Dynamical Studies, a. Processes of Momentum Transfer, Reported in Trans. A.G.U. 53(11): 1014 (Nov. 1972). (Abstract only.)
- Jerbo, A. (1973). "Two Types of Oil Spills in Swedish Inland Waters, Tests of New Materials, Ideas and Methods," Prevention and Control of Oil Spills, pp. 563-567.
- Keevil, B. E., R. O. Ramseier (1975). "Behavior of Oil Spilled Under Floating Ice," Conference on Prevention and Control of Oil Pollution, San Francisco, March 1975.
- Koburger, Capt. C. W., and Lt. J. H. Getman (1974). "Oil Spill Problems in Cold Climates: The Coast Guard Attacks the Alaskan Oil Spill Problem," Naval Engineers Journal, Dec. 1974, pp. 59-64.
- Kowalik, Z. (1972). "Wind Driven Circulation in a Shallow Stratified Sea," Deutsche Hydrographische Zeitschrift, 25(6): 265-278.
- Lamp, H. J. (1973). "Lake Champlain: A Case History on the Cleanup of #6 Fuel Through Five Feet of Solid Ice at Near-Zero Temperatures," Prevention and Control of Oil Spills, pp. 271-276.
- Langleben, M. P. and E. R. Pounder (1975). "On the Air Drag of an Arctic Ice Floe," Geophys. Res. Letters, 2(1): 15-18.
- Langleben, M. P. and E. R. Pounder (1972). "On the Air Drag of an Arctic Ice Floe," Symposium on Sea-Air Interaction in Polar Regions, IV. Arctic Ocean Dynamical Studies, a. Processes of Momentum Transfer, Reported in Trans. A.G.U. 53(11): 1015 (Nov. 1972). (Abstract only.)
- Lee, O. S. and L. S. Simpson (1959). A Practical Method of Predicting Sea Ice Formation and Growth, U. S. Navy Hydrographic Office, Washington, D.C. (Tech. Report TR-4).
- Masaomi, Akagawa (1973). "The Characters of Atmospheric Circulation in the Years with Abnormal Sea Ice Conditions Along the Okhotsk Coast of Hokkaido, Japan," Oceanogr. Mag. 24(2): 81-100.
- Maykut, G. A. (1972). "Thermodynamic Considerations in the Formulation of Dynamic Models of Arctic Sea Ice," Symposium on Sea-Air Interaction in Polar Regions: IV - Arctic Ocean Dynamical Studies, b. Numerical Modelling Experiments, Reported in Trans. A.G.U. 53(11): 1016 (Nov. 1972). (Abstract only.)

- Maykut, G. A. and A. S. Thorndike (1973). "An Approach to Coupling the Dynamics and Thermodynamics of Arctic Sea Ice," AIDJEX Bulletin, 21 (July): 23-29.
- Maykut, G. A. and N. Untersteiner (1971). "Some Results from a Time Dependent, Thermodynamic Model of Sea Ice," J.G.R. 76(6): 1550-1575.
- Maykut, G. A. and N. Untersteiner (1969). Numerical Prediction of the Thermodynamic Response of Arctic Sea Ice to Environmental Changes, RM-6093-PR, Rand Corp., Santa Monica, CA.
- McLean, A. Y. (1972). "The Behavior of Oil Spilled in a Cold Water Environment," Offshore Technology Conference, May 1972, pp. 129-140.
- McLeod, W. R. and D. L. McLeod (1974). "Measures to Combat Arctic and Subarctic Oil Spills," Journal of Petroleum Technology, March 1974.
- McMinn, LTJG T. J., USCGR (1972). "Crude Oil Behavior on Arctic Winter Ice," Final Report, U. S. Coast Guard, Washington, D.C., Sept. 1972.
- McMinn, LTJG T. J., USCGR, and LTJG P. Golden (1973). "Behavior Characteristics and Cleanup Techniques of North Slope Crude Oil in an Arctic Winter Environment," Conference on Prevention and Control of Oil Pollution.
- McPhee, M. G. and J. D. Smith (1975). "Measurements of the Turbulent Boundary Layer Under Pack Ice," AIDJEX Bulletin, 29 (July): 49-92.
- McPhee, M., and J. D. Smith (1972). "Flow in the Vicinity of a Small Pressure Ridge Keel," Symposium on Sea-Air Interaction in Polar Regions, Iib. Lower Ice Surface and Top Ocean Structure, Reported in Trans. A.G.U., 53(11): 1012 (Nov. 1972). (Abstract only.)
- Miles, M. K. (1974). "An Index of Pack-Ice Severity off Newfoundland and Its Secular Variation," Met. Mag., 103(1222): 121-125.
- Milne, A. R. (1970). "The Transition from Moving to Fast Ice in Western Viscount Melville Sound," Arctic, 23(1): 45-46, March 1970.
- Mock, S. J., W. D. Hibler III (1972). "Ridging Intensity Variations in the Arctic Basin," Symposium on Sea-Air Interaction in Polar Regions, Dec. 5, 1972, Reported in Trans. A.G.U., 53(11): 1008, Nov. 1972. (Abstract only.)
- Mohaghegh, M. M. (1972). "Strength of Sea Ice Sheets," Symposium on Sea-Air Interaction in Polar Regions: I. The Arctic Ocean Ice, December 5, 1975, Reported in Trans. A.G.U., 53(11): 1009 (Nov. 1972). (Abstract only.)
- Moir, J. R., Lau, Y. L. (1975). "Some Observations of Oil Slick Containment by Simulated Ice Ridge Keels," Frozen Sea Research Group, Victoria, B.C., March 1975.
- Moore, D. W. and P. P. Niiler (1974). "A Two-Layer Model for the Separation of Inertial Boundary Currents," J. Mar. Res., 32(3): 457-484.
- Muench, R. D. (1971). "The Physical Oceanography of the Northern Baffin Bay Region," Arctic Institute N. Amer., Baffin Bay - North Water Project, Sc. Report No. 1.



- Mukherji, B. (1972). "Crack Propagation in Sea Ice - 'A Finite Element Approach'," Symposium on Sea-Air Interaction in Polar Regions: I. The Arctic Ocean Ice, Dec. 5, 1975, Reported in Trans. A.G.U., 53(11): 1009 (Nov. 1972). (Abstract only.)
- Munk, W. H. (1950). "On the Wind-Driven Ocean Circulation," J. Met., 7(2): 79-93.
- Nazintsev, Yu. L. (1971). "Estimating the Lateral Melting of Drift Ice, in Investigations of the Ice Conditions in the Arctic Seas and Methods of Forecasting and Computation," Ed. by N. A. Volkova, Hydrometeorological Press, Leningrad, Trudy (Proceedings), Vol. 303 (Translated by I.P.S.T. for N.S.F. and appearing in AIDJEX Bulletin No. 17).
- Newton, J. L., K. Aagard, and L. K. Coachman (1974). "Baroclinic Eddies in the Arctic Ocean," Deep-Sea Res., 21(9): 707-719.
- Nikiforov, Ye. B., A. M. Gudkovich, Yu. I. Yefimov, and M. A. Romanov (1967). "Principles of a Method for Computing Ice Redistribution Under the Influence of Wind During the Navigation Period in Arctic Seas," Proceedings of the Arctic and Antarctic Research Institute (Trudy Arkt. i Antarkt. In-Ta.) 275: 5-25 (English Trans., AIDJEX Bulletin, 3 (Nov. 1970): 22-39.
- Nye, J. F. (1973). "The Physical Meaning of Two-Dimensional Stresses in a Floating Ice Cover," AIDJEX Bulletin, 21 (July 1973): 1-8.
- Parmerter, R. R. (1972). "Pressure Ridges: A Basic Deformation Mechanism in Arctic Sea Ice," Symposium on Sea-Air Interaction in Polar Regions, I. The Arctic Ocean Ice, Dec. 5, 1975, Reported in Trans. A.G.U., 53(11): 1009 (Nov. 1972). (Abstract only.)
- Parmerter, R. R. (1974). "A Mechanical Model of Rafting," AIDJEX Bulletin 23 (Jan. 1974): 97-115.
- Parmerter, R. R. and M. D. Coon (1973). "Mechanical Models of Ridging in the Arctic Sea Ice Cover," AIDJEX Bulletin 19 (March 1973): 59-112.
- Paquette, R. G. and R. H. Bourke (1973). Oceanographic Measurements near the the Arctic Ice Margins, Naval Postgrad. School, NPS-58PA73121A: 91 pp. (Unpublished).
- Paulson, C. A. and N. Untersteiner (1974). Comment on "Wind Profiles over Sea Ice" by M. P. Langleben, Geophys. Res. Letters, 1(7): 313-314.
- Pritchard, R. S. and R. Colony (1974). "One-Dimensional Difference Scheme for an Elastic-Plastic Sea Ice Model," AIDJEX Bulletin 26 (Sept.): 48-58.
- Ramseier, R. O. (1971). "Oil Pollution in Ice-Infested Waters," Proceedings International Symposium on Identification and Measurement of Environmental Pollutants, Ottawa, June 1971, pp. 271-276.
- Ramseier, R. O. (1973). "Possible Fate of Oil in the Arctic Basin," First World Congress on Water Resources, Chicago, Sept. 1973.
- Ramseier, R. O., G. S. Gantcheff, and L. Colby (1973). "Oil Spill at Deception Bay, Hudson Strait," Environment Canada, Scientific Series No. 29, 1973, 61 pp.

- Rothrock, D. A. (1973). "The Steady Drift of an Incompressible Ice Cover," AIDJEX Bulletin 21 (July): 49-78.
- Rothrock, D. A. (1974). "The Energetics of Plastic Deformation in Pack Ice," AIDJEX Bulletin 27 (Nov.): 68-83.
- Rothrock, D. A. (1975). "The Mechanical Behavior of Pack Ice," Annual Review of Earth and Planetary Sciences, 3: 317-342, Palo Alto, CA.
- Rothrock, D. A. (1975). "The Steady Drift of an Incompressible Arctic Ice Cover," J.G.R., 80(3): 387-397.
- Schaus, R. H. (1971). A Thermodynamic Model of a Central Arctic Open Lead, Thesis, Naval Postgraduate School, Monterey, CA.
- Schultz, L. A., P. C. Deslauriers, R. P. Voelker, O. M. Hasted, and D. E. Abrams (1975). "Tests of Oil Recovery Devices in Broken Ice Fields," U. S. Coast Guard, Washington, D.C., July 1975.
- Semtner, A. J. (1972). "A Numerical Investigation of Arctic Ocean Circulation," Symposium on Sea-Air Interaction in Polar Regions, IV. - Arctic Ocean Dynamical Studies, b. Numerical Modelling Experiments, Reported in Trans. A.G.U., 53(11): 1015 (Nov. 1972). (Abstract only.)
- Shapiro, L. H. and J. J. Burns (1975). "Satellite Observations of Sea Ice Movement in the Bering Strait Region," The Coast and Shelf of the Beaufort Sea, Ed. J. C. Reed and J. E. Slater, Arlington, VA: Arctic Institute of N. Amer.
- Short, A. D., W. J. Wiseman, Jr. (1975). "Coastal Breakup in the Alaskan Arctic," Geol. Soc. of Amer. Bull., 86(2): 199-202 (Feb. 1975).
- Smith, S. D., and E. G. Banke (1972). "Wind Stress on Arctic Sea Ice," Symposium on Sea-Air Interaction in Polar Regions, IV. Arctic Ocean Dynamical Studies a. Processes of Momentum Transfer, Reported in Trans. A.G.U., 53(11): 1015 (Nov. 1972). (Abstract only.)
- Stull, R. B. (1973). Inversion Rise Model Based on Penetrative Convection, Thesis, Dept. of Atmos. Sciences, Univ. of Wash., Seattle, WA.
- Thorpe, M. R., S. D. Smith, and E. G. Banke (1972). "Eddy Correlation Measurements of Evaporation and Sensible Heat Flux over Arctic Sea Ice," Symposium on Sea-Air Interaction in Polar Regions, IIa. Convective and Radiative Processes in the Arctic Ocean Boundary Layer, Reported in Trans. A.G.U., 53(11): 1009 (Nov. 1973). (Abstract only.)
- Veronis, G. (1973). "Model of World Ocean Circulation: 1. Wind-Driven, Two-Layer," J. Mar. Res., 31(3): 228-288.
- Vorwinkel, E. and S. Orvig (1966). "Inversion over the Polar Ocean," Polar Meteorology, Technical Note 87: 39-59.
- Weeks, W. F. (1972). "Properties and Morphology of Sea Ice," Symposium on Sea-Air Interaction in Polar Regions Dec. 5, 1972, Reported in Trans. A.G.U., 53(11): 1007, Nov. 1972. (Abstract only.)

- Witting, J. (1972). "Arctic Ice Circulation Model," Symposium on Sea-Air Interaction in Polar Regions, IV - Arctic Ocean Dynamic Studies, b. Numerical Modelling Experiments Dec. 7, 1972, Reported in Trans. A.G.U., 53(11): 1016 (Nov. 1972). (Abstract only.)
- Wittman, W. I., and G. P. MacDowell (1964). Manual of Short-Term Sea Ice Forecasting, U. S. Naval Oceanographic Office, Washington, D. C. (Spec. Pub. SP-82).
- Wittman, W., and J. Schule (1966). In: Proceedings of the Symposium in the Arctic Heat Budget and Atmospheric Circulation, Rand Corp. Mem. No. RM-5233-NSF, pp. 215-246.
- Wolfe, S. L., and D. P. Hault (1972). Effects of Oil Under Sea Ice, U. S. Coast Guard, Washington, D. C., Aug. 1972.
- Zubov, N. N. (1943). Arctic Ice, Moscow, Translated for AFCRC by U. S. Naval Oceanographic Office and The American Meteorological Society.

- Bryan, K. (1969). "Climate and the Ocean Circulation, III. The Ocean Model," Monthly Weather Review 97(11): 806-827.
- Campbell, W. J. (1965). "The Wind Driven Circulation of Ice and Water in a Polar Ocean," J.G.R. 70(14): 3279-3301.
- Coachman, L. K. (1969). "Physical Oceanography in the Arctic Ocean: 1968," Arctic 22(3): 214-224.
- Coachman, L. K., and C. A. Barnes (1963). "The Movement of Atlantic Water in the Arctic Ocean," Arctic 16(1): 9-16.
- Coachman, L. K., and C. A. Barnes (1961). "The Contribution of the Bering Sea Water to the Arctic Ocean," Arctic 14(3): 147-161.
- Evans, R. J. and D. A. Rothrock (1975). "Stress Fields in Pack Ice," Third International Symposium on Ice Problems, Hanover, New Hampshire.
- Felzenbaum, A. I. (1958). "The Theory of the Steady Drift of Ice and the Calculation of the Long Period Mean Drift in the Central Part of the Arctic Basin," Problems of the North 2: 5-15, 13-44.
- Fletcher, J. O. (1965). The Heat Budget of the Arctic Basin and Its Relation to the Climate, Rand Corp. Rep. No. R-444-PR (The Rand Corp., Santa Monica, CA).
- Gade, H. G., R. A. Lake, E. L. Lewis, and E. R. Walker (1974). "Oceanography of an Arctic Bay," Deep-Sea Res., 21(7): 547-571.
- Galt, J. A. (1973). "A Numerical Investigation of Arctic Ocean Dynamics," J. Phys. Ocean. 3(4): 379-396.
- Galt, J. A. (1972). "A Barotropic Numerical Model of the Arctic Ocean," Symposium on Sea-Air Interaction in Polar Regions - IV. - Arctic Ocean Dynamical Studies, b. Numerical Modelling Experiments. Reported in Trans. A.G.U. 53(11): 1015. (Nov. 1972). (Abstract only.)
- Galt, J. A. (1972). "The Development of a Homogeneous Numerical Ocean Model for the Arctic Ocean," NPS-58G172071A, Naval Postgraduate School, Monterey, CA. (AD #744925 NTIS)
- Galt, J. A. (1967). "Current Measurements in the Canadian Basin of the Arctic Ocean, Summer 1965." U. of Wa., Dept. of Ocean., Tech. Report No. 184.
- Holland, W. R. (1967). "On the Wind-Driven Circulation in an Ocean with Bottom Topography," Tellus 19(4): 582-599.
- Hunkins, K. S. (1974). "Subsurface Eddies in the Arctic Ocean," Deep-Sea Research 21(12): 1017-1034.
- Hunkins, K. L. (1975). "The Oceanic Boundary Layer and Stress Beneath a Drifting Ice Flow," J.G.R. 80(24): 3425-3433, Aug. 20, 1975.
- Kowalik, Z. (1972). "Wind Driven Circulation in a Shallow Stratified Sea," Deutsche Hydrographische Zeitschrift, 25(6): 265-278.

- McPhee, M. G. and J. D. Smith (1975). "Measurements of the Turbulent Boundary Layer Under Pack Ice," AIDJEX Bulletin, 29 (July): 49-92.
- Mock, S. J., W. D. Hibler III (1972). "Ridging Intensity Variations in the Arctic Basin," Symposium on Sea-Air Interaction in Polar Regions, Dec. 5, 1972; Reported in Trans. A.G.U., 53(11): 1008, Nov. 1972. (Abstract only.)
- Moore, D. W. and P. P. Niiler (1974). "A Two-Layer Model for the Separation of Inertial Boundary Currents," J. Mar. Res., 32(3): 457-484.
- Muench, R. D. (1971). "The Physical Oceanography of the Northern Baffin Bay Region," Arctic Institute N. Amer., Baffin Bay - North Water Project, Sc. Report No. 1.
- Munk, W. H. (1950). "On the Wind-Driven Ocean Circulation," J. Met., 7(2): 79-93.
- Newton, J. L., K. Aagard, and L. K. Coachman (1974). "Baroclinic Eddies in the Arctic Ocean," Deep-Sea Res., 21(9): 707-719.
- Paquette, R. G. and R. H. Bourke (1973). Oceanographic Measurements near the the Arctic Ice Margins, Naval Postgrad. School, NPS-58PA73121A: 91 pp. (Unpublished).
- Rothrock, D. A. (1973). "The Steady Drift of an Incompressible Ice Cover," AIDJEX Bulletin 21 (July): 49-78.
- Rothrock, D. A. (1975). "The Steady Drift of an Incompressible Arctic Ice Cover," J.G.R., 80(3): 387-397.
- Semtner, A. J. (1972). "A Numerical Investigation of Arctic Ocean Circulation," Symposium on Sea-Air Interaction in Polar Regions, IV. - Arctic Ocean Dynamical Studies, b. Numerical Modelling Experiments, Reported in Trans. A.G.U., 53(11): 1015 (Nov. 1972). (Abstract only.)
- Shapiro, L. H. and J. J. Burns (1975). "Satellite Observations of Sea Ice Movement in the Bering Strait Region," The Coast and Shelf of the Beaufort Sea, Ed. J. C. Reed and J. E. Slater, Arlington, VA: Arctic Institute of N. Amer.
- Short, A. D., W. J. Wiseman, Jr. (1975). "Coastal Breakup in the Alaskan Arctic," Geol. Soc. of Amer. Bull., 86(2): 199-202 (Feb. 1975).
- Veronis, G. (1973). "Model of World Ocean Circulation: 1. Wind-Driven, Two-Layer," J. Mar. Res., 31(3): 228-288.

- Banke, E. and S. Smith (1973). "Wind Stress on Arctic Sea Ice," J.G.R. 78(33), 7871-7883.
- Brown, A. L. (1954). An Analytical Method of Ice Potential Calculation, U. S. Navy Hydrographic Office, Washington, D.C. (Tech. Report TR-5).
- Callaway, E. B. (1954). An Analysis of Environmental Factors Affecting Ice Growth, U. S. Naval Hydrographic Office, Washington, D.C. (Tech. Report TR-7).
- Campbell, W. J. (1965). "The Wind Driven Circulation of Ice and Water in a Polar Ocean," J.G.R. 70(14): 3279-3301.
- Colony, R. (1975). "The Boundary Determination Problem for the AIDJEX Ocean," AIDJEX Bulletin 28 (March): 87-97.
- Coon, M. D. (1972). "Mechanical Behavior of Compacted Arctic Ice Floes," Preprints, Offshore Technology Conference, Houston, Texas, 1-3 May, 1972. OTC 1684. American Institute of Mining, Metallurgical, and Petroleum Engineers.
- Coon, M. D. (1972). "Constitutive Laws for Pack Ice," Symposium on Sea-Air Interaction in Polar Regions, Dec. 5, 1972. Reported in Trans. A.G.U., 53(11): 1007, Nov. 1972. (Abstract only.)
- Coon, M. D., G. A. Maykut, R. S. Pritchard, D. A. Rothrock, and A. S. Thorndike (1974). "Modelling the Pack Ice as an Elastic-Plastic Material," AIDJEX Bulletin 24 (May): 1-105.
- Coon, M. D. and R. S. Pritchard (1974). "Application of an Elastic-Plastic Model of Arctic Pack Ice," The Coast and Shelf of the Beaufort Sea, Ed. J. C. Reed and J. E. Slater, Arlington, VA: Arctic Institute of N. Amer.
- Corton, E. L. (1954). The Ice Budget of the Arctic Pack and Its Application to Ice Forecasting, U. S. Navy Hydrographic Office, Washington, D. C. (Tech. Report TR-6).
- Cox, G. F. N. and W. F. Weeks (1972). "Variation of Salinity in Multiyear Sea Ice," Symposium on Sea-Air Interaction in Polar Regions, Dec. 5, 1972. Reported in Trans A.G.U., 53(11): 1008, Nov. 1972. (Abstract only.)
- Doronin, Yu. P. (1970). "On a Method of Calculating the Compactness and Drift of Ice Floes (K Metodike Rascheta Splochnosti I Dreifa L'Dov)." Proceedings of the Arctic and Antarctic Research Institute (Trudy Arkt. i Antarkt. In-Ta), 291: 5-17 (English Transl., AIDJEX Bulletin No. 3 (Nov. 1970), pp. 22-39).
- Eide, L. I., and S. Martin (1972). "Brine Channels in Sea-Ice: A Laboratory Study." Symposium on Sea-Air Interaction in Polar Regions, Dec. 5, 1972., reported in Trans. A.G.U., 53(11): 1008, Nov. 1972. (Abstract only.)
- Evans, R. J. and D. A. Rothrock (1975). "Stress Fields in Pack Ice," Third International Symposium on Ice Problems, Hanover, New Hampshire.
- Foster, T. D. (1968). "Haline Convection Induced by the Freezing of Sea Water," J. Geophys. Res. 73(6): 1933-1938.
- Foster, T. D. (1972). "Haline Convection in Polynyas and Leads," J. Physical Ocean. 2: 462-469.

- Gloersen, P., T. C. Chang, T. T. Wilheit, and W. J. Campbell (1973). Polar Sea Ice Observations by Means of Microwave Radiometry, X-652-73-341, Goddard Space Flight Center, Greenbelt, MD.
- Hibler, W. D., S. F. Ackley, W. K. Crowder, H. L. McKim, and D. M. Anderson (1974). "Analysis of Shear Zone Ice Deformation in the Beaufort Sea Using Satellite Imagery," The Coast and Shelf of the Beaufort Sea, Ed. J. C. Reed and J. E. Slater, 285-296, Arlington, VA: Arctic Institute of N. Amer.
- Hibler, W. D. III, S. J. Mock, and W. B. Tucker III (1974). "Classification and Variation of Sea Ice Ridging in the Western Arctic Basin," J.G.R. 79(18): 2735-2743 (June 20, 1974).
- Hibler, W. D. III, W. F. Weeks, A. Kovacs, and S. F. Ackley (1973). "Differential Sea Ice Drift I: Spatial and Temporal Variations in Sea Ice Deformation," AIDJEX Bulletin 21 (July): 79-113.
- Hunkins, K. L. (1975). "The Oceanic Boundary Layer and Stress Beneath a Drifting Ice Flow," J.G.R. 80(24): 3425-3433, Aug. 20, 1975.
- Langleben, M. P. and E. R. Pounder (1975). "On the Air Drag of an Arctic Ice Floe," Geophys. Res. Letters, 2(1): 15-18.
- Lee, O. S. and L. S. Simpson (1959). A Practical Method of Predicting Sea Ice Formation and Growth, U. S. Navy Hydrographic Office, Washington, D.C. (Tech. Report TR-4).
- Maykut, G. A. and A. S. Thorndike (1973). "An Approach to Coupling the Dynamics and Thermodynamics of Arctic Sea Ice," AIDJEX Bulletin, 21 (July): 23-29.
- McPhee, M. G. and J. D. Smith (1975). "Measurements of the Turbulent Boundary Layer Under Pack Ice," AIDJEX Bulletin, 29 (July): 49-92.
- Miles, M. K. (1974). "An Index of Pack-Ice Severity off Newfoundland and Its Secular Variation," Met. Mag., 103(1222): 121-125.
- Milne, A. R. (1970). "The Transition from Moving to Fast Ice in Western Viscount Melville Sound," Arctic, 23(1): 45-46, March 1970.
- Mock, S. J., W. D. Hibler III (1972). "Ridging Intensity Variations in the Arctic Basin," Symposium on Sea-Air Interaction in Polar Regions, Dec. 5, 1972, Reported in Trans. A.G.U., 53(11): 1008, Nov. 1972. (Abstract only.)
- Mohaghegh, M. M. (1972). "Strength of Sea Ice Sheets," Symposium on Sea-Air Interaction in Polar Regions: I. The Arctic Ocean Ice, December 5, 1975, Reported in Trans. A.G.U., 53(11): 1009 (Nov. 1972). (Abstract only.)
- Moir, J. R., Lau, Y. L. (1975). "Some Observations of Oil Slick Containment by Simulated Ice Ridge Keels," Frozen Sea Research Group, Victoria, B.C., March 1975.
- Mukherji, B. (1972). "Crack Propagation in Sea Ice - 'A Finite Element Approach'," Symposium on Sea-Air Interaction in Polar Regions: I. The Arctic Ocean Ice, Dec. 5, 1975, Reported in Trans. A.G.U., 53(11): 1009 (Nov. 1972). (Abstract only.)

- Nikiforov, Ye. B., A. M. Gudkovich; Yu. I. Yefimov, and M. A. Romanov (1967). "Principles of a Method for Computing Ice Redistribution Under the Influence of Wind During the Navigation Period in Arctic Seas," Proceedings of the Arctic and Antarctic Research Institute (Trudy Arkt. i Antarkt. In-Ta.) 275: 5-25 (English Trans., AIDJEX Bulletin, 3 (Nov. 1970): 22-39.
- Nye, J. F. (1973). "The Physical Meaning of Two-Dimensional Stresses in a Floating Ice Cover," AIDJEX Bulletin, 21 (July 1973): 1-8.
- Parmarter, R. R. (1972). "Pressure Ridges: A Basic Deformation Mechanism in Arctic Sea Ice," Symposium on Sea-Air Interaction in Polar Regions, I. The Arctic Ocean Ice, Dec. 5, 1975, Reported in Trans. A.G.U., 53(11): 1009 (Nov. 1972). (Abstract only.)
- Parmarter, R. R. (1974). "A Mechanical Model of Rafting," AIDJEX Bulletin 23 (Jan. 1974): 97-115.
- Parmarter, R. R. and M. D. Coon (1973). "Mechanical Models of Ridging in the Arctic Sea Ice Cover," AIDJEX Bulletin 19 (March 1973): 59-112.
- Pritchard, R. S. and R. Colony (1974). "One-Dimensional Difference Scheme for an Elastic-Plastic Sea Ice Model," AIDJEX Bulletin 26 (Sept.): 48-58.
- Rothrock, D. A. (1973). "The Steady Drift of an Incompressible Ice Cover," AIDJEX Bulletin 21 (July): 49-78.
- Rothrock, D. A. (1974). "The Energetics of Plastic Deformation in Pack Ice," AIDJEX Bulletin 27 (Nov.): 68-83.
- Rothrock, D. A. (1975). "The Mechanical Behavior of Pack Ice," Annual Review of Earth and Planetary Sciences, 3: 317-342, Palo Alto, CA.
- Rothrock, D. A. (1975). "The Steady Drift of an Incompressible Arctic Ice Cover," J.G.R., 80(3): 387-397.
- Short, A. D., W. J. Wiseman, Jr. (1975). "Coastal Breakup in the Alaskan Arctic," Geol. Soc. of Amer. Bull., 86(2): 199-202 (Feb. 1975)
- Weeks, W. F. (1972). "Properties and Morphology of Sea Ice," Symposium on Sea-Air Interaction in Polar Regions Dec. 5, 1972, Reported in Trans. A.G.U., 53(11): 1007, Nov. 1972. (Abstract only.)
- Witting, J. (1972). "Arctic Ice Circulation Model," Symposium on Sea-Air Interaction in Polar Regions, IV - Arctic Ocean Dynamic Studies, b. Numerical Modelling Experiments Dec. 7, 1972, Reported in Trans. A.G.U., 53(11): 1016 (Nov. 1972). (Abstract only.)
- Wittman, W. I., and G. P. MacDowell (1964). Manual of Short-Term Sea Ice Forecasting, U. S. Naval Oceanographic Office, Washington, D. C. (Spec. Pub. SP-82).
- Zubov, N. N. (1943). Arctic Ice, Moscow, Translated for AFCRC by U. S. Naval Oceanographic Office and The American Meteorological Society.



- Brown, A. L. (1964). An Analytical Method of Ice Potential Calculation, U. S. Navy Hydrographic Office, Washington, D.C. (Tech. Report TR-5).
- Brown, R. A. (1972). "The Candidates for the AIDJEX Planetary Boundary Model," Symposium on Sea-Air Interaction in Polar Regions, IV. - Arctic Ocean Dynamical Studies, b. Numerical Modelling Experiments. Reported in Trans. A.G.U. 53(11):1015 (Nov. 1972). (Abstract only.)
- Bryan, K. (1969). "Climate and the Ocean Circulation, III. The Ocean Model," Monthly Weather Review 97(11): 806-827.
- Callaway, E. B. (1954). An Analysis of Environmental Factors Affecting Ice Growth, U. S. Naval Hydrographic Office, Washington, D.C. (Tech. Report TR-7).
- Campbell, W. J. (1965). "The Wind Driven Circulation of Ice and Water in a Polar Ocean," J.G.R. 70(14): 3279-3301.
- Colony, R. (1975). "The Boundary Determination Problem for the AIDJEX Ocean," AIDJEX Bulletin 28 (March): 87-97.
- Coon, M. D. (1972). "Mechanical Behavior of Compacted Arctic Ice Floes," Preprints, Offshore Technology Conference, Houston, Texas, 1-3 May, 1972. OTC 1684. American Institute of Mining, Metallurgical, and Petroleum Engineers.
- Coon, M. D. (1972). "Constitutive Laws for Pack Ice," Symposium on Sea-Air Interaction in Polar Regions, Dec. 5, 1972. Reported in Trans. A.G.U., 53(11): 1007, Nov. 1972. (Abstract only.)
- Coon, M. D., G. A. Maykut, R. S. Pritchard, D. A. Rothrock, and A. S. Thorndike (1974). "Modelling the Pack Ice as an Elastic-Plastic Material," AIDJEX Bulletin 24 (May): 1-105.
- Coon, M. D. and R. S. Pritchard (1974). "Application of an Elastic-Plastic Model of Arctic Pack Ice," The Coast and Shelf of the Beaufort Sea, Ed. J. C. Reed and J. E. Slater, Arlington, VA: Arctic Institute of N. Amer.
- Corton, E. L. (1954). The Ice Budget of the Arctic Pack and Its Application to Ice Forecasting, U. S. Navy Hydrographic Office, Washington, D. C. (Tech. Report TR-6).
- Doronin, Yu. P. (1970). "On a Method of Calculating the Compactness and Drift of Ice Floes (K Metodike Rascheta Splochnosti I Dreifa L'Dov)." Proceedings of the Arctic and Antarctic Research Institute (Trudy Arkt. i Antarkt. In-Ta), 291: 5-17 (English transl., AIDJEX Bulletin No. 3 (Nov. 1970), pp. 22-39).
- Evans, R. J. and D. A. Rothrock (1975). "Stress Fields in Pack Ice," Third International Symposium on Ice Problems, Hanover, New Hampshire.
- Felzenbaum, A. I. (1958). "The Theory of the Steady Drift of Ice and the Calculation of the Long Period Mean Drift in the Central Part of the Arctic Basin," Problems of the North 2: 5-15, 13-44.
- Galt, J. A. (1973). "A Numerical Investigation of Arctic Ocean Dynamics," J. Phys. Ocean. 3(4): 379-396.
- Galt, J. A. (1972). "A Barotropic Numerical Model of the Arctic Ocean," Symposium on Sea-Air Interaction in Polar Regions - IV. - Arctic Ocean Dynamical Studies b. Numerical Modelling Experiments. Reported in Trans. A.G.U. 53(11): 1015. (Nov. 1972). (Abstract only.)

- Kowalik, Z. (1972). "Wind Driven Circulation in a Shallow Stratified Sea," Deutsche Hydrographische Zeitschrift, 25(6): 265-278.
- Langleben, M. P. and E. R. Pounder (1975). "On the Air Drag of an Arctic Ice Floe," Geophys. Res. Letters, 2(1): 15-18.
- Lee, O. S. and L. S. Simpson (1959). A Practical Method of Predicting Sea Ice Formation and Growth, U. S. Navy Hydrographic Office, Washington, D.C. (Tech. Report TR-4).
- Maykut, G. A. (1972). "Thermodynamic Considerations in the Formulation of Dynamic Models of Arctic Sea Ice," Symposium on Sea-Air Interaction in Polar Regions: IV - Arctic Ocean Dynamical Studies, b. Numerical Modelling Experiments, Reported in Trans. A.G.U. 53(11): 1016 (Nov. 1972). (Abstract only.)
- Maykut, G. A. and A. S. Thorndike (1973). "An Approach to Coupling the Dynamics and Thermodynamics of Arctic Sea Ice," AIDJEX Bulletin, 21 (July): 23-29.
- Maykut, G. A. and N. Untersteiner (1971). "Some Results from a Time Dependent, Thermodynamic Model of Sea Ice," J.G.R. 76(6): 1550-1575.
- Maykut, G. A. and N. Untersteiner (1969). Numerical Prediction of the Thermodynamic Response of Arctic Sea Ice to Environmental Changes, RM-6093-PR, Rand Corp., Santa Monica, CA.
- McPhee, M. G. and J. D. Smith (1975). "Measurements of the Turbulent Boundary Layer Under Pack Ice," AIDJEX Bulletin, 29 (July): 49-92.
- Miles, M. K. (1974). "An Index of Pack-Ice Severity off Newfoundland and Its Secular Variation," Met. Mag., 103(1222): 121-125.
- Mohaghegh, M. M. (1972). "Strength of Sea Ice Sheets," Symposium on Sea-Air Interaction in Polar Regions: I. The Arctic Ocean Ice, December 5, 1975, Reported in Trans. A.G.U., 53(11): 1009 (Nov. 1972). (Abstract only.)
- Moore, D. W. and P. P. Niiler (1974). "A Two-Layer Model for the Separation of Inertial Boundary Currents," J. Mar. Res., 32(3): 457-484.
- Mukherji, B. (1972). "Crack Propagation in Sea Ice - 'A Finite Element Approach'," Symposium on Sea-Air Interaction in Polar Regions: I. The Arctic Ocean Ice, Dec. 5, 1975, Reported in Trans. A.G.U., 53(11): 1009 (Nov. 1972). (Abstract only.)
- Nazintsev, Yu. L. (1971). "Estimating the Lateral Melting of Drift Ice, in Investigations of the Ice Conditions in the Arctic Seas and Methods of Forecasting and Computation," Ed. by N. A. Volkova, Hydrometeorological Press, Leningrad, Trudy (Proceedings), Vol. 303 (Translated by I.P.S.T. for N.S.F. and appearing in AIDJEX Bulletin No. 17).
- Nikiforov, Ye. B., A. M. Gudkovich, Yu. I. Yefimov, and M. A. Romanov (1967). "Principles of a Method for Computing Ice Redistribution Under the Influence of Wind During the Navigation Period in Arctic Seas," Proceedings of the Arctic and Antarctic Research Institute (Trudy Arkt. i Antarkt. In-Ta.) 275: 5-25 (English Trans., AIDJEX Bulletin, 3 (Nov. 1970): 22-39.
- Nye, J. F. (1973). "The Physical Meaning of Two-Dimensional Stresses in a Floating Ice Cover," AIDJEX Bulletin, 21 (July 1973): 1-8.

- Parmeter, R. R. (1972). "Pressure Ridges: A Basic Deformation Mechanism in Arctic Sea Ice," Symposium on Sea-Air Interaction in Polar Regions, I. The Arctic Ocean Ice, Dec. 5, 1975, Reported in Trans. A.G.U., 53(11): 1009 (Nov. 1972). (Abstract only.)
- Parmeter, R. R. (1974). "A Mechanical Model of Rafting," AIDJEX Bulletin 23 (Jan. 1974): 97-115.
- Parmeter, R. R. and M. D. Coon (1973). "Mechanical Models of Ridging in the Arctic Sea Ice Cover," AIDJEX Bulletin 19 (March 1973): 59-112.
- Pritchard, R. S. and R. Colony (1974). "One-Dimensional Difference Scheme for an Elastic-Plastic Sea Ice Model," AIDJEX Bulletin 26 (Sept.): 48-58.
- Rothrock, D. A. (1973). "The Steady Drift of an Incompressible Ice Cover," AIDJEX Bulletin 21 (July): 49-78.
- Rothrock, D. A. (1974). "The Energetics of Plastic Deformation in Pack Ice," AIDJEX Bulletin 27 (Nov.): 68-83.
- Rothrock, D. A. (1975). "The Mechanical Behavior of Pack Ice," Annual Review of Earth and Planetary Sciences, 3: 317-342, Palo Alto, CA.
- Rothrock, D. A. (1975). "The Steady Drift of an Incompressible Arctic Ice Cover," J.G.R., 80(3): 387-397.
- Schaus, R. H. (1971). A Thermodynamic Model of a Central Arctic Open Lead, Thesis, Naval Postgraduate School, Monterey, CA.
- Semtner, A. J. (1972). "A Numerical Investigation of Arctic Ocean Circulation," Symposium on Sea-Air Interaction in Polar Regions, IV. - Arctic Ocean Dynamical Studies, b. Numerical Modelling Experiments, Reported in Trans. A.G.U., 53(11): 1015 (Nov. 1972). (Abstract only.)
- Stull, R. B. (1973). Inversion Rise Model Based on Penetrative Convection, Thesis, Dept. of Atmos. Sciences, Univ. of Wash., Seattle, WA.
- Veronis, G. (1973). "Model of World Ocean Circulation: 1. Wind-Driven, Two-Layer," J. Mar. Res., 31(3): 228-288.
- Witting, J. (1972). "Arctic Ice Circulation Model," Symposium on Sea-Air Interaction in Polar Regions, IV - Arctic Ocean Dynamic Studies, b. Numerical Modelling Experiments Dec. 7, 1972, Reported in Trans. A.G.U., 53(11): 1016 (Nov. 1972). (Abstract only.)
- Wittman, W. I., and G. P. MacDowell (1964). Manual of Short-Term Sea Ice Forecasting, U. S. Naval Oceanographic Office, Washington, D. C. (Spec. Pub. SP-82).

- Badgley, F. I. (1966). In Proceedings of the Symposium on the Arctic Heat Budget and Atmospheric Circulation, Rand Corp. Mem. No. RM-5233-NSF (The Rand Corp., Santa Monica, CA), pp. 267-277.
- Banke, E. and S. Smith (1973). "Wind Stress on Arctic Sea Ice," J.G.R. 78(33), 7871-7883.
- Bryan, K. (1969). "Climate and the Ocean Circulation, III. The Ocean Model," Monthly Weather Review 97(11): 806-827.
- Businger, J. A. (1972). "The Transfer of Momentum from the Atmosphere to the Sea-Ice Surface," Symposium on Sea-Air Interaction in Polar Regions, IV. - Arctic Ocean Dynamical Studies, a. Processes of Momentum Transfer. Reported in Trans. A.G.U. 53(11): 1014 (Nov. 1972). (Abstract only.)
- Campbell, W. J. (1965). "The Wind Driven Circulation of Ice and Water in a Polar Ocean," J.G.R. 70(14): 3279-3301.
- Colony, R. (1975). "The Boundary Determination Problem for the AIDJEX Ocean," AIDJEX Bulletin 28 (March): 87-97.
- Coon, M. D. (1972). "Mechanical Behavior of Compacted Arctic Ice Floes," Preprints, Offshore Technology Conference, Houston, Texas, 1-3 May, 1972. OTC 1684. American Institute of Mining, Metallurgical, and Petroleum Engineers.
- Cox, G. F. N. and W. F. Weeks (1972). "Variation of Salinity in Multiyear Sea Ice," Symposium on Sea-Air Interaction in Polar Regions, Dec. 5, 1972. Reported in Trans A.G.U., 53(11): 1008, Nov. 1972. (Abstract only.)
- Eide, L. I., and S. Martin (1972). "Brine Channels in Sea-Ice: A Laboratory Study." Symposium on Sea-Air Interaction in Polar Regions, Dec. 5, 1972., reported in Trans. A.G.U., 53(11): 1008, Nov. 1972. (Abstract only.)
- Evans, R. J. and D. A. Rothrock (1975). "Stress Fields in Pack Ice," Third International Symposium on Ice Problems, Hanover, New Hampshire.
- Fletcher, J. O. (1965). The Heat Budget of the Arctic Basin and Its Relation to the Climate, Rand Corp. Rep. No. R-444-PR (The Rand Corp., Santa Monica, CA).
- Foster, T. D. (1968). "Haline Convection Induced by the Freezing of Sea Water," J. Geophys. Res. 73(6): 1933-1938.
- Foster, T. D. (1972). "Haline Convection in Polynyas and Leads," J. Physical Ocean. 2: 462-469.
- Foster, T. D. (1975). "Heat Exchange in the Upper Arctic Ocean," AIDJEX Bulletin 28: 151-166.
- Gade, H. G., R. A. Lake, E. L. Lewis, and E. R. Walker (1974). "Oceanography of an Arctic Bay," Deep-Sea Res., 21(7): 547-571.
- Galt, J. A. (1973). "A Numerical Investigation of Arctic Ocean Dynamics," J. Phys. Ocean. 3(4): 379-396.
- Galt, J. A. (1972). "The Development of a Homogeneous Numerical Ocean Model for the Arctic Ocean," NPS-58G172071A, Naval Postgraduate School, Monterey, CA. (AD #744925 NTIS)

- Gloersen, P., T. C. Chang, T. T. Wilheit, and W. J. Campbell (1973). Polar Sea Ice Observations by Means of Microwave Radiometry, X-652-73-341, Goddard Space Flight Center, Greenbelt, MD.
- Hibler, W. D., S. F. Ackley, W. K. Crowder, H. L. McKim, and D. M. Anderson (1974). "Analysis of Shear Zone Ice Deformation in the Beaufort Sea Using Satellite Imagery," The Coast and Shelf of the Beaufort Sea, Ed. J. C. Reed and J. E. Slater, 285-296, Arlington, VA: Arctic Institute of N. Amer.
- Hibler, W. D. III, W. F. Weeks, A. Kovacs, and S. F. Ackley (1973). "Differential Sea Ice Drift I: Spatial and Temporal Variations in Sea Ice Deformation," AIDJEX Bulletin 21 (July): 79-113.
- Holmgren, B. (1972). "Some Results of Radiation Measurements During the 1972 AIDJEX Pilot Study," Symposium on Sea-Air Interaction in Polar Regions, IIA - Convective and Radiative Processes in Arctic Ocean Boundary Layer, reported in Trans. A.G.U. 53(11): 1010 (Nov. 1972). (Abstract only.)
- Hunkins, K. L. (1975). "The Oceanic Boundary Layer and Stress Beneath a Drifting Ice Flow," J.G.R. 80(24): 3425-3433, Aug. 20, 1975.
- Hunkins, K. L. (1972). "Momentum Exchange Between the Ocean and Drifting Ice," Symposium on Sea-Air Interaction in Polar Regions, IV. - Arctic Ocean Dynamical Studies, a. Processes of Momentum Transfer, Reported in Trans. A.G.U. 53(11): 1014 (Nov. 1972). (Abstract only.)
- Langleben, M. P. and E. R. Pounder (1975). "On the Air Drag of an Arctic Ice Floe," Geophys. Res. Letters, 2(1): 15-18.
- Langleben, M. P. and E. R. Pounder (1972). "On the Air Drag of an Arctic Ice Floe," Symposium on Sea-Air Interaction in Polar Regions, IV. Arctic Ocean Dynamical Studies, a. Processes of Momentum Transfer, Reported in Trans. A.G.U. 53(11): 1015 (Nov. 1972). (Abstract only.)
- Masaomi, Akagawa (1973). "The Characters of Atmospheric Circulation in the Years with Abnormal Sea Ice Conditions Along the Okhotsk Coast of Hokkaido, Japan," Oceanogr. Mag. 24(2): 81-100.
- Maykut, G. A. (1972). "Thermodynamic Considerations in the Formulation of Dynamic Models of Arctic Sea Ice," Symposium on Sea-Air Interaction in Polar Regions: IV - Arctic Ocean Dynamical Studies, b. Numerical Modelling Experiments, Reported in Trans. A.G.U. 53(11): 1016 (Nov. 1972). (Abstract only.)
- Maykut, G. A. and A. S. Thorndike (1973). "An Approach to Coupling the Dynamics and Thermodynamics of Arctic Sea Ice," AIDJEX Bulletin, 21 (July: 23-29.
- Maykut, G. A. and N. Untersteiner (1971). "Some Results from a Time Dependent, Thermodynamic Model of Sea Ice," J.G.R. 76(6): 1550-1575.
- Maykut, G. A. and N. Untersteiner (1969). Numerical Prediction of the Thermodynamic Response of Arctic Sea Ice to Environmental Changes, RM-6093-PR, Rand Corp., Santa Monica, CA.
- McPhee, M. G. and J. D. Smith (1975). "Measurements of the Turbulent Boundary Layer Under Pack Ice," AIDJEX Bulletin, 29 (July): 49-92. 207

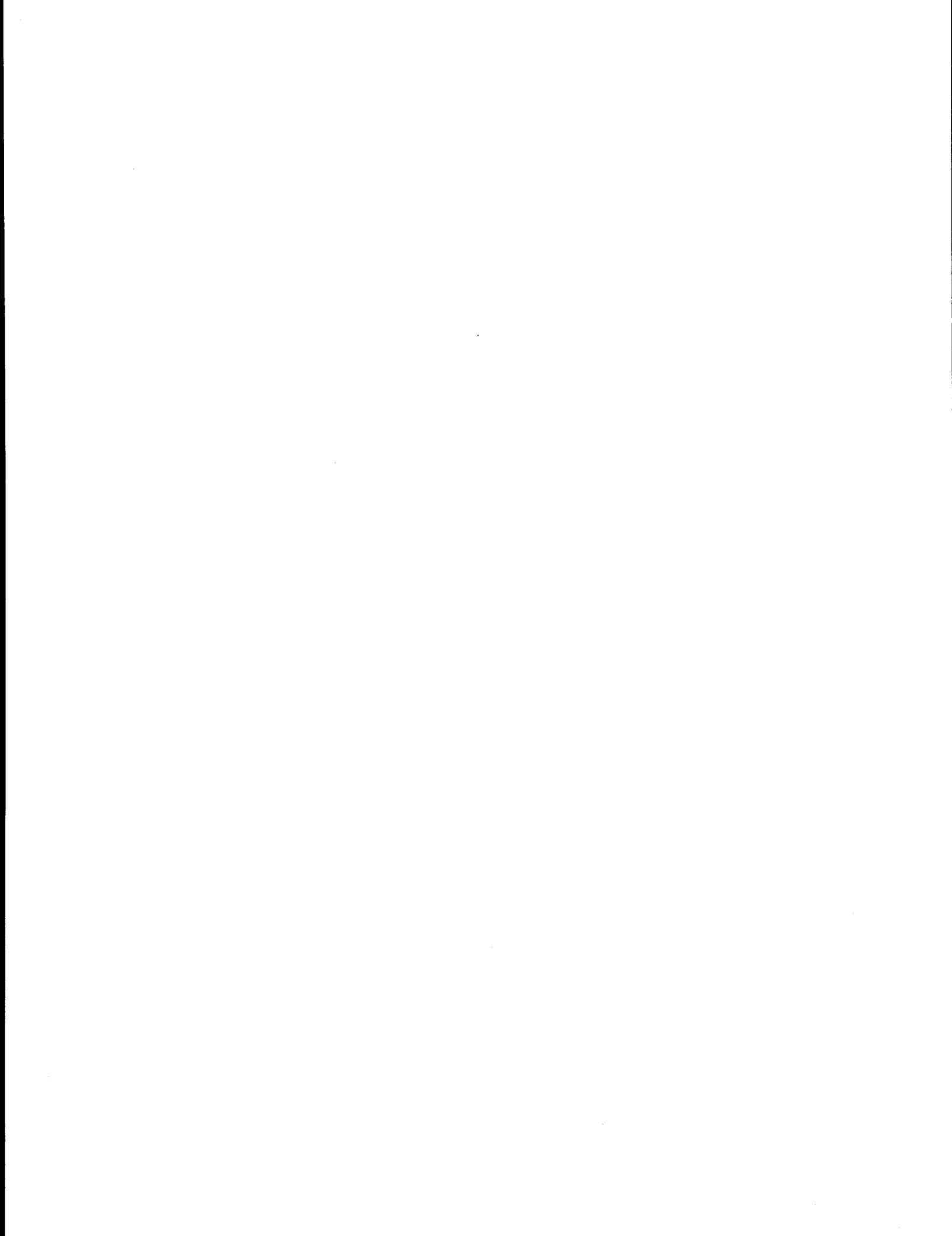
- McPhee, M., and J. D. Smith (1972). "Flow in the Vicinity of a Small Pressure Ridge Keel," Symposium on Sea-Air Interaction in Polar Regions, IIB. Lower Ice Surface and Top Ocean Structure, Reported in Trans. A.G.U., 53(11): 1012 (Nov. 1972). (Abstract only.)
- Milne, A. R. (1970). "The Transition from Moving to Fast Ice in Western Viscount Melville Sound," Arctic, 23(1): 45-46, March 1970.
- Mock, S. J., W. D. Hibler III (1972). "Ridging Intensity Variations in the Arctic Basin," Symposium on Sea-Air Interaction in Polar Regions, Dec. 5, 1972, Reported in Trans. A.G.U., 53(11): 1008, Nov. 1972. (Abstract only.)
- Moore, D. W. and P. P. Niiler (1974). "A Two-Layer Model for the Separation of Inertial Boundary Currents," J. Mar. Res., 32(3): 457-484.
- Munk, W. H. (1950). "On the Wind-Driven Ocean Circulation," J. Met., 7(2): 79-93.
- Nazintsev, Yu. L. (1971). "Estimating the Lateral Melting of Drift Ice, in Investigations of the Ice Conditions in the Arctic Seas and Methods of Forecasting and Computation," Ed. by N. A. Volkova, Hydrometeorological Press, Leningrad, Trudy (Proceedings), Vol. 303 (Translated by I.P.S.T. for N.S.F. and appearing in AIDJEX Bulletin No. 17).
- Nikiforov, Ye. B., A. M. Gudkovich, Yu. I. Yefimov, and M. A. Romanov (1967). "Principles of a Method for Computing Ice Redistribution Under the Influence of Wind During the Navigation Period in Arctic Seas," Proceedings of the Arctic and Antarctic Research Institute (Trudy Arkt. i Antarkt. In-Ta.) 275: 5-25 (English Trans., AIDJEX Bulletin, 3 (Nov. 1970): 22-39.
- Parmeter, R. R. (1972). "Pressure Ridges: A Basic Deformation Mechanism in Arctic Sea Ice," Symposium on Sea-Air Interaction in Polar Regions, I. The Arctic Ocean Ice, Dec. 5, 1975, Reported in Trans. A.G.U., 53(11): 1009 (Nov. 1972). (Abstract only.)
- Paquette, R. G. and R. H. Bourke (1973). Oceanographic Measurements near the the Arctic Ice Margins, Naval Postgrad. School, NPS-58PA73121A: 91 pp. (Unpublished).
- Paulson, C. A. and N. Untersteiner (1974). Comment on "Wind Profiles over Sea Ice" by M. P. Langleben, Geophys. Res. Letters, 1(7): 313-314.
- Rothrock, D. A. (1973). "The Steady Drift of an Incompressible Ice Cover," AIDJEX Bulletin 21 (July): 49-78.
- Rothrock, D. A. (1975). "The Steady Drift of an Incompressible Arctic Ice Cover," J.G.R., 80(3): 387-397.
- Schaus, R. H. (1971). A Thermodynamic Model of a Central Arctic Open Lead, Thesis, Naval Postgraduate School, Monterey, CA.
- Shapiro, L. H. and J. J. Burns (1975). "Satellite Observations of Sea Ice Movement in the Bering Strait Region," The Coast and Shelf of the Beaufort Sea, Ed. J. C. Reed and J. E. Slater, Arlington, VA: Arctic Institute of N. Amer.
- Short, A. D., W. J. Wiseman, Jr. (1975). "Coastal Breakup in the Alaskan Arctic," Geol. Soc. of Amer. Bull., 86(2): 199-202 (Feb. 1975).

- Smith, S. D., and E. G. Banke (1972). "Wind Stress on Arctic Sea Ice," Symposium on Sea-Air Interaction in Polar Regions, IV. Arctic Ocean Dynamical Studies a. Processes of Momentum Transfer, Reported in Trans. A.G.U., 53(11): 1015 (Nov. 1972). (Abstract only.)
- Stull, R. B. (1973). Inversion Rise Model Based on Penetrative Convection, Thesis, Dept. of Atmos. Sciences, Univ. of Wash., Seattle, WA.
- Thorpe, M. R., S. D. Smith, and E. G. Banke (1972). "Eddy Correlation Measurements of Evaporation and Sensible Heat Flux over Arctic Sea Ice," Symposium on Sea-Air Interaction in Polar Regions, IIA. Convective and Radiative Processes in the Arctic Ocean Boundary Layer, Reported in Trans. A.G.U., 53(11): 1009 (Nov. 1973). (Abstract only.)
- Vorwinkel, E. and S. Orvig (1966). "Inversion over the Polar Ocean," Polar Meteorology, Technical Note 87: 39-59.
- Witting, J. (1972). "Arctic Ice Circulation Model," Symposium on Sea-Air Interaction in Polar Regions, IV - Arctic Ocean Dynamic Studies, b. Numerical Modelling Experiments Dec. 7, 1972, Reported in Trans. A.G.U., 53(11): 1016 (Nov. 1972). (Abstract only.)
- Wittman, W., and J. Schule (1966). In: Proceedings of the Symposium in the Arctic Heat Budget and Atmospheric Circulation, Rand Corp. Mem. No. RM-5233-NSF, pp. 215-246.
- Zubov, N. N. (1943). Arctic Ice, Moscow, Translated for AFCRC by U. S. Naval Oceanographic Office and The American Meteorological Society.

- Atlas, R. M. (1973). "Fate and Effects of Oil Pollutants in Extremely Cold Marine Environments," Office of Naval Research, Final Report, Oct. 1973.
- Ayers, R. C., H. O. Johns, J. L. Glaeser (1974). "Oil Spills in the Arctic Ocean: Extent of Spreading and Possibility of Large-Scale Thermal Effects," Science, Nov. 1974, pp. 843-844.
- Barber, F. G. (1971). "Report of the Task Force - Operation Oil"(Cleanup of the Arrow oil spill in Chedabucto Bay), Minister of Transport, Canada.
- Barber, F. G. (1973). "Oil Spilled with Ice: Some Qualitative Aspects," Conference on Prevention and Control of Oil Spills, pp. 563-567.
- Campbell, W. J., S. Martin (1973). "Oil and Ice in the Arctic Ocean: Possible Large-Scale Interactions," Science, July 1973, pp. 56-58.
- Canadian Arctic Resource Committee. "Offshore Drilling in the Beaufort Sea," Northern Perspectives 2(2).
- Chen, E. C., J. C. K. Overall, C. R. Phillips (1974). "Spreading of Crude Oil on an Ice Surface," Canadian Journal of Chemical Engineering, 52, Feb. 1974.
- Deslauriers, P. C. (1975). "Oil Pollution in Ice Infested Waters (A Survey of Recent Development)," Unpublished Report, Aug. 1, 1975.
- Getman, Lt. J. H. (1975). "United States Coast Guard Arctic Oil Pollution Program," Conference on Prevention and Control of Oil Pollution.
- Glaeser, LTJG J. L., USCGR, LCDR G. P. Vance, USCG (1971). "A Study of the Behavior of Oil Spills in the Arctic," Final Report, U. S. Coast Guard, Washington, D. C., Feb. 1971. (Ref. No. AD717142, F.S.T.I., Springfield, VA, 1971)
- Glaeser, LTJG J. L., USCGR, LCDR G. P. Vance, USCG (1972). "A Study of the Behavior of Oil Spills in the Arctic," Offshore Technology Conference, May 1972.
- Golden, P. C. (1974). "Oil Removal Techniques in an Arctic Environment," Marine Technology Society Journal 8(1): 38-43, Jan. 1974.
- Hoult, D. P., S. Wolfe, O'Dea, and J. P. Patureau (1974). "Oil in the Arctic," Final Report, U. S. Coast Guard, Washington, D.C., Feb. 1974.
- Hoult, D. P. (1971). "The Aging of Oil Spilled in the Arctic," U. S. Coast Guard, Washington, D.C., Aug. 1971, Contract DOT-CG-12438-A.
- Jerbo, A. (1973). "Two Types of Oil Spills in Swedish Inland Waters, Tests of New Materials, Ideas and Methods," Prevention and Control of Oil Spills, pp. 563-567.
- Keevil, B. E., R. O. Ramseier (1975). "Behavior of Oil Spilled Under Floating Ice," Conference on Prevention and Control of Oil Pollution, San Francisco, March 1975.
- Koburger, Capt. C. W., and Lt. J. H. Getman (1974). "Oil Spill Problems in Cold Climates: The Coast Guard Attacks the Alaskan Oil Spill Problem," Naval Engineers Journal, Dec. 1974, pp. 59-64.



- Lamp, H. J. (1973). "Lake Champlain: A Case History on the Cleanup of #6 Fuel Through Five Feet of Solid Ice at Near-Zero Temperatures," Prevention and Control of Oil Spills, pp. 271-276.
- McLean, A. Y. (1972). "The Behavior of Oil Spilled in a Cold Water Environment," Offshore Technology Conference, May 1972, pp. 129-140.
- McLeod, W. R. and D. L. McLeod (1974). "Measures to Combat Arctic and Subarctic Oil Spills," Journal of Petroleum Technology, March 1974.
- McMinn, LTJG T. J., USCGR (1972). "Crude Oil Behavior on Arctic Winter Ice," Final Report, U. S. Coast Guard, Washington, D.C., Sept. 1972.
- McMinn, LTJG T. J., USCGR, and LTJG P. Golden (1973). "Behavior Characteristics and Cleanup Techniques of North Slope Crude Oil in an Arctic Winter Environment," Conference on Prevention and Control of Oil Pollution.
- Moir, J. R., Lau, Y. L. (1975). "Some Observations of Oil Slick Containment by Simulated Ice Ridge Keels," Frozen Sea Research Group, Victoria, B.C., March 1975.
- Ramseier, R. O. (1971). "Oil Pollution in Ice-Infested Waters," Proceedings International Symposium on Identification and Measurement of Environmental Pollutants, Ottawa, June 1971, pp. 271-276.
- Ramseier, R. O. (1973). "Possible Fate of Oil in the Arctic Basin," First World Congress on Water Resources, Chicago, Sept. 1973.
- Ramseier, R. O., G. S. Gantcheff, and L. Colby (1973). "Oil Spill at Deception Bay, Hudson Strait," Environment Canada, Scientific Series No. 29, 1973, 61 pp.
- Schultz, L. A., P. C. Deslauriers, R. P. Voelker, O. M. Hasted, and D. E. Abrams (1975). "Tests of Oil Recovery Devices in Broken Ice Fields," U. S. Coast Guard, Washington, D.C., July 1975.
- Wolfe, S. L., and D. P. Hoult (1972). Effects of Oil Under Sea Ice, U. S. Coast Guard, Washington, D. C., Aug. 1972.



Annual Report

Contract # R7120849

Research Unit # 141, 145, 148

Reporting Period: 1 April 1975 -  
31 March 1976

Number of Pages: 34

Bristol Bay Oceanographic Processes (B-BOP)

Dr. J.D. Schumacher,  
Pacific Marine Environmental Laboratory  
and  
Dr. L.K. Coachman,  
Dept. of Oceanography-University of Washington

## I SUMMARY

The objective of this work unit is to relate oceanic advective and diffusive processes to potential pollution problems due to OCS petroleum development. From data collected, processed, and analyzed to date, the following conclusions have been made. The mean flow during fall 1975 in Bristol Bay was small (on the order of 1 cm/sec) and was directed toward the northwest flowing along the 50m depth contour; most of the variance energy was in tidal frequency bands; and major events in the flow regime occurred as pulses in the mean flow. This study has provided initial information on mean transport and an indication of the relative importance of dispersion in the Bristol Bay region.

## II INTRODUCTION

### A. Objective

The objective of this work unit is to relate oceanic advective and diffusive processes to potential pollution problems due to OCS petroleum development. The two specific goals are to:

1. Describe the general water circulation in the study area for both summer and winter regimes.
2. Determine spatial and temporal variability in the velocity-field and obtain indications of spatial coherence.

### B. Tasks

The specific tasks of this program are as follows:

1. Hydrographic data acquisition. This task enables density fields to be computed and the baroclinic component of the velocity-field to be calculated. Section plots of the CTD data will be examined and estimates obtained for stability as well as temporal variability in the density field. If water masses can be characterized, the magnitude of advective effects can be estimated.
2. Current meter data. This task is required to describe the spatial and temporal variability of the circulation at specific sites. Direct velocity measurements will be used to establish correlations between sea-surface slope variations and velocity-field variations. Additionally, direct measurements, combined with inferred velocities from CTD data are used to establish the geostrophic and non-geostrophic components in the baroclinic flow.
3. Pressure gauge data. These data will be used to determine the relative sea-level changes and to examine set-up associated with storm surges.

Data from these collection activities will yield a description of the velocity field and lead to a better understanding of the relative importance of various driving mechanisms which cause water movement.

### C. Application to Petroleum Development Hazard Assessment

Once oil is loosed on the sea, it undergoes a series of physical and chemical changes. Volatile components are released to the atmosphere and soluble components dissolved into the waters. The ubiquitous oil-consuming bacteria begin to multiply, metabolizing the floating and dissolved oil. The small solubility of hydrocarbons in sea water becomes appreciable as the oil spreads over vast areas. The net effect of these processes is to produce tarry masses surrounded by thin slicks of the lighter, more volatile components. These thin slicks appear to be consumed quickly, perhaps within a few hours<sup>1/2</sup>. The tarry masses are attacked more slowly. Wave action may produce oily emulsions.

During the time oil is floating on the surface, it moves under the influence of the winds and currents. If the currents in a region of an

oil slick are not a direct result of the winds, e.g., tidal current prevalent in the near shore environment, the oil will move in some direction between that of the wind and that of the current. However, no satisfactory theory exists today to predict the exact velocity of an oil patch under these conditions.

Oil patches tend to disperse and dissipate with time, especially during high seas. Four hundred tons of oil released in the Gulf of Mexico as a result of a broken undersea well head dissipated completely in high seas within seven miles of the drilling site<sup>2/</sup>. However, the large slicks from the Torrey Canyon drifted hundreds of miles<sup>3/</sup>, as contiguous masses. The exact distance an oil slick travels without dissipating is a function of its size and the sea state. This distance cannot adequately be predicted at this time.

Oil properties alter markedly with time as the spill spreads, evaporates, dissolves, or is consumed. Crude oil will fractionate rapidly by evaporation of its lighter components and more slowly by the loss of successive higher boiling fractions. The fractions boiling at less than 700°F tends to volatilize from the sea surface. Data on the evaporation of Kuwait Crude, bubbled with nitrogen, indicate a 25% evaporation loss after 25 hours<sup>4/</sup>.

Without this lighter fraction the pour points of most oils are above the temperature of the water in which they are spilled. The residue then forms a gelatinous mass which will not spread. Evaporation may proceed to where the specific gravity of the residue is greater than that of sea water<sup>5/</sup>. Evaporation and eventual sinking may have been the fate of the oil from the 'Anne Mildred Brovig,' which was wrecked in the North Sea. Residue from Iranian Heavy Crude has a specific gravity of 1.027, higher than most surface sea water.

From this brief description of the behavior of oil in the sea, it is apparent that two distinct environmental problems accompany petroleum development. Type I, or catastrophic oil spills, and Type II, chronic or long-term oil seepage and accumulation. This research unit addresses both of these in the following manner: The eventual effect of Type I problems depends on where the spilled oil goes, the time-scale of its motion, and diffusion of the oil along the trajectory. This study provides information on the mean transport of oil and an indication of rates of dispersion. Type II problems require a better understanding of behavior of oil in the water column itself rather than on the surface. After evaporation of short-chain hydrocarbons, the residue is likely to be mixed into the water column and thereby scavenged by suspended particulate matter. The problem now becomes one of understanding net transport of suspended material. This process is directly related to advective and diffusive fields within the water column. An understanding of these processes again requires the description and understanding of the velocity-field and its driving mechanism.

### III CURRENT STATE OF KNOWLEDGE

Studies in Bristol Bay involving direct measurements of the flow field prior to the B-BOP program number four:

1. four 38-hour anchored stations (not simultaneous in central Bristol Bay<sup>6/</sup>). From the data it was interpreted the bay contained a general cyclonic circulation, with eastward inflow north of the Alaska peninsula and westward flow in the central bay;
2. three 14-day current records from 100m depth in Pribilof Canyon<sup>7/</sup>. The mean flows ( $4-9 \text{ cm sec}^{-1}$ ) were in-canyon and parallel to the canyon axis at the particular location;
3. numerous spot measurements from a Japanese crabber which showed large tidal signals (so that mean flow could not be determined); and
4. a 24-hr current station close to the western tip of Nunivak Island in August 1934, which gave a mean flow north at  $17 \text{ cm sec}^{-1}$  <sup>8/</sup>.

A few isolated drift bottle returns support the concept of a net inflow into southern Bristol Bay parallel to the Alaska peninsula, and also a net flow northwest across Kusokwim Bay and north past Nunivak Island.

Many hydrographic data have been taken over the years, but mostly in summer and not systematically. The most comprehensive survey was that of Redwing<sup>9/</sup>. From these data it was concluded that inner Bristol Bay contained a cyclonic circulation. The Oshoro Maru has occupied stations in Bristol Bay during June and July each year since 1963<sup>10/</sup>. These data allow basic definition of the water masses, and when we achieve some understanding of the circulation and mixing in the system will prove most valuable in assessing annual variability. Takenouti and Ohtani<sup>11/</sup> reported on the distribution of water masses and an interpretation of the circulation based on these data (Fig. 1). We have also been conducting preliminary analyses based primarily on Oshoro Maru data.

The three water masses are:

1. Bering Sea Water (AS). The highest salinities in the system, normally  $32.5 > S > 33.2$  o/oo but with some annual variability. Temperatures show a narrow range ( $3-4^{\circ}\text{C}$ ). The water may come direct from the Alaskan Stream via Unimak Pass, but the same characteristics hold for the upper 200m of Bering Sea basin water distributed all along the shelf break.
2. Coastal Water (CW). This is the low salinity water ( $S < 31.5$  o/oo) and is distributed around the perimeter of the bay adjacent to the land. In June the temperatures of these water columns are warm to the bottom ( $> 4^{\circ}\text{C}$ ).
3. Shelf water (CA). Intermediate salinities ( $31.5 > S > 32.5$  o/oo) but also cold deeper in the water columns (in June never  $> 2^{\circ}\text{C}$ ). The degree of cold (minimum temperature) encountered in June varies between  $-10^{\circ}\text{C}$  and  $2^{\circ}\text{C}$  and is highly correlated ( $r=0.95$ ) with the degree-days of frost of the previous winter. This water is always found on the central shelf in a tongue-shaped extension

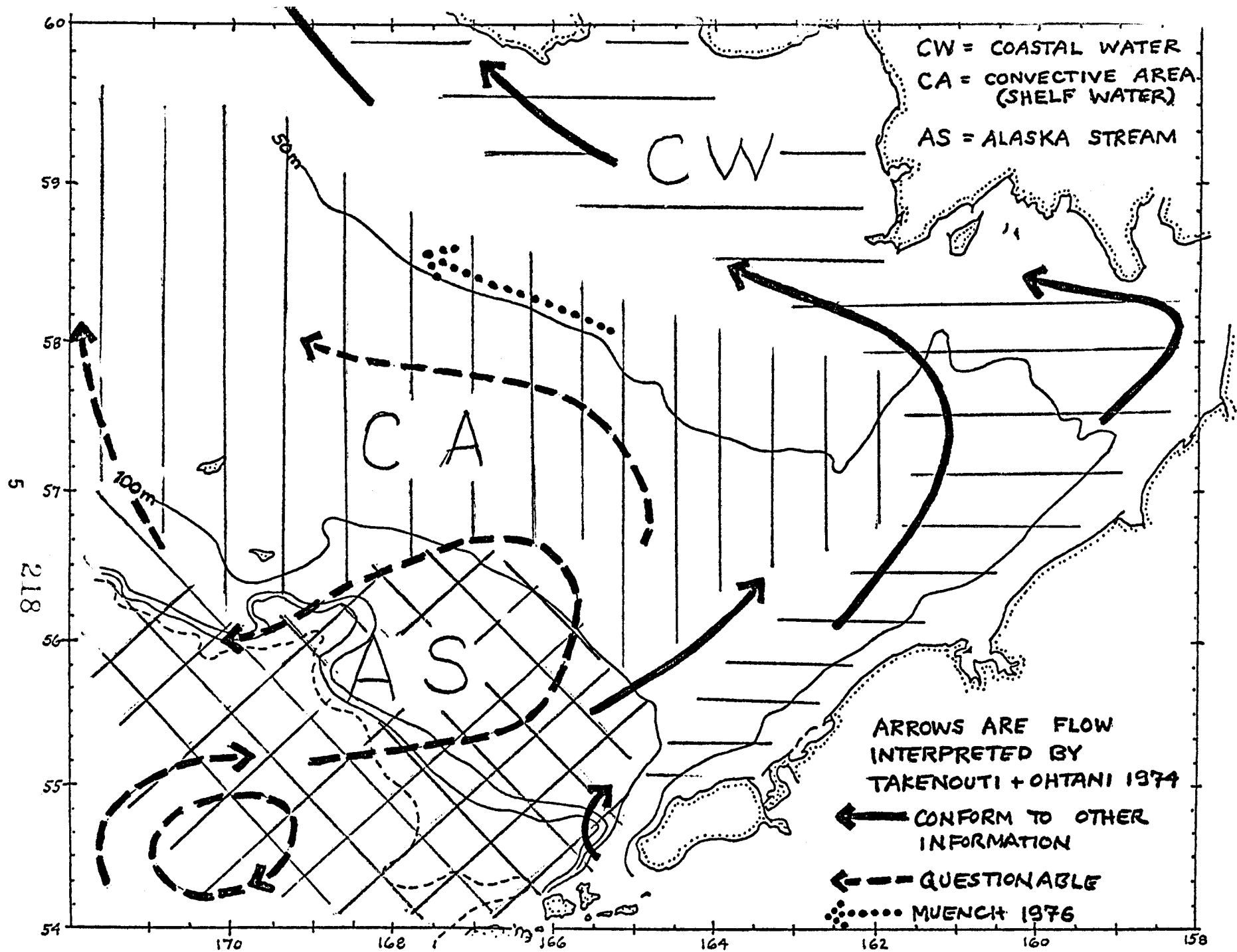


Figure 1. Inferred general circulation from historical data.



from the northwest.

The distributions of the water masses given by Takenouti and Ohtani (Fig. 1) are in a general way correct, but their extent (and hence the boundaries between them) vary greatly. For example, Alaskan Stream water has in some years been found much farther in the bay and farther up on the shelf east of the Pribilofs than shown. The boundary between CA and CW waters is in general sharper than between AS and CA or AS and CW, and usually located close to the 50m depth contour (not in Kuskokwim Bay as suggested in Fig. 1). Muench<sup>12/</sup> reported a section across this boundary and found it to be a significant front -- landward (in CW water) there was relatively strong northwest flow (cf. arrow in Fig. 1) while seaward, in CA water, there was little flow.

Part of the circulation pattern inferred by Takenouti and Ohtani (the solid arrows of Fig. 1) conforms to the other evidence namely: (i) the general inflow parallel to the Alaskan peninsula which brings in the high salinity water (but quite variable in extent) (ii) the cyclonic circulation around inner Bristol Bay, and (iii) northwest flow landward of the 50m isobath, primarily of CW water. Their flow pattern for the central and western parts of the bay does not conform to other evidence (dashed arrows). The ubiquitous tongue-like extension of CA water from the northwest into the central bay can only be (a) maintained by a flow along the axis of the tongue, i.e. toward the southeast, or (b) a residue water in a low flow area, shaped by flow around it. The evidence of high correlation of cold temperatures of central bay water with degree-days of frost of the previous winter argues strongly for the latter -- thus CA water would be primarily shelf water relict from the previous winter. Mean flow in this region would be small.

No speculation is possible on flow patterns in the central and western portions of the area, other than that it is probably quite variable and associated with as yet undetermined causes. High salinity water (AS) has been found in significant quantities on the shelf east of the Pribilofs sometimes, and there are cases of two separate centers of cold in the CA water mass.

#### IV STUDY AREA

This research unit addresses the physical oceanography of Bristol Bay (Fig. 2). This Bay is defined as the area south of a line drawn between Nunivak Island and the Pribilof Islands, with the shelf-break (200m contour) as the western boundary and the Alaska Peninsula/Aleutian Islands as the southern boundary. This region encompasses approximately 400,000 km<sup>2</sup> of shelf waters, most of which lies between the 50m and the 100m depth contours.

Fresh water input is primarily from the Kuskokwim River drainage area, which enters the study region at the northeast corner. To the southeast a number of small rivers (Nushagak, Kvichak, Naknek) also provide freshwater. The major connection with western Gulf of Alaska waters is through Unimak Pass which lies near the southwest corner of the study area.

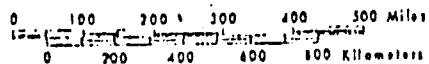
During about 5 months of the year on the order of 60% of the study region is ice-covered. The ice is one-year winter ice, generally less than a meter thick, with many open areas of water and a hummocky surface due to variable effects of winds, currents and tides. Ice formation begins in sheltered lagoons in mid-October and builds to the most severe conditions in February and March. General northward retreat of the ice begins in April.

128° 132° 136° 140° 144° 148° 152° 156° 160° 164° 168° 172° 176° 180° 176° 172° 168° 164° 160° 156° 152° 148° 144° 140° 136° 132° 128° 124° 120° 116° 112°

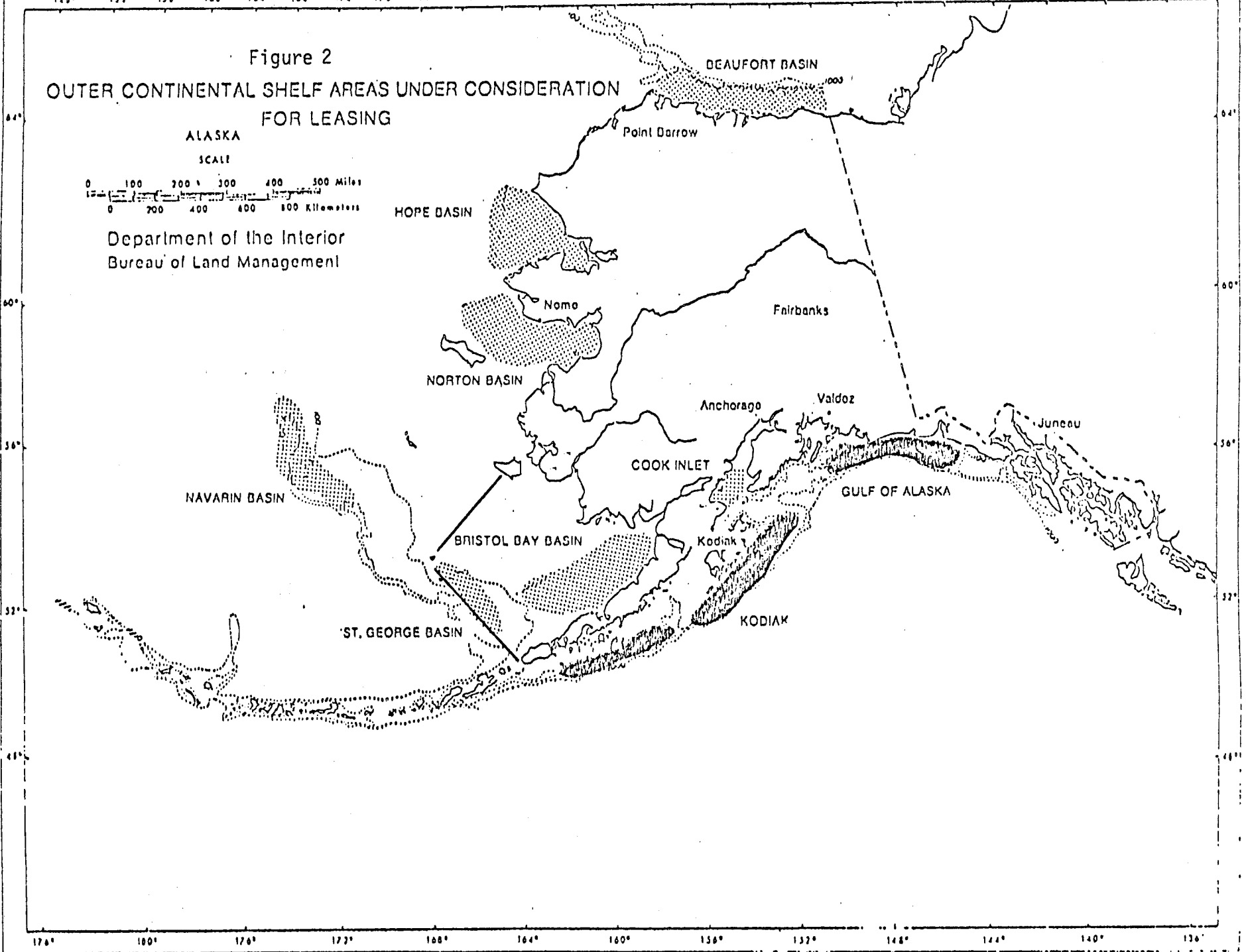
Figure 2  
OUTER CONTINENTAL SHELF AREAS UNDER CONSIDERATION  
FOR LEASING

ALASKA

SCALE



Department of the Interior  
Bureau of Land Management



8

221

176° 180° 176° 172° 168° 164° 160° 156° 152° 148° 144° 140° 136°

## V PROGRAM RATIONALE AND METHODS OF DATA COLLECTION

In order to address the goals of this work unit, the following program was completed during the period 1 April 75 - 31 March 76:

1. Long-term moored arrays (BC-1, BC-2, BC-3 and BC-4) were deployed and maintained. The data from these arrays were used to examine advective processes by characterizing spatial distribution of mean flow in the study area.
2. Data from BC-2 were used to examine the scope of dispersive processes through analysis of high frequency variability in both the upper and lower levels of the water column.
3. Spectral energy from both levels at BC-2 has been calculated to examine the balance between the advective and dispersive processes.
4. Data from continuously sampling temperature sensors on BC-2 and BC-4 were used to examine changes in the vertical structure of the water column.
5. Pressure gauge data from BC-2 and BC-4 were used to examine the magnitude and frequency of major long period changes in sea-level.

To date, two cruises have been completed during September and November 1975. Hydrographical data was collected using the following equipment:

Plessey 9040 CTD inputed to the PODAS system aboard the DISCOVERER.

Plessey 9040 CTD and Plessey 8400 data logger aboard the MILLER FREEMAN.

Water samples were taken using a rosette Sampler equipped with Niskin Bottles. Salinity samples were drawn and salinity determinations were made using the ships inductive salinometer. Reversing thermometers (calibrated by NOIC) were employed to develop field correction factors for the CTD system.

Aanderaa RCM-4 current meters and Aanderaa TG-2A pressure gauges were used on the moored arrays. The ensuing magnetic tapes were processed by PMEL/UW's Aanderaa tape system.

## VI RESULTS

The following tables summarized current meter and pressure gauge records collected to date. CTD data collected thus far are listed in Section X, Summary of Fourth Quarter Operations, which summarizes field operations for the entire reporting period.

CURRENT METER STATION BC-1A                    55°24.63'N  
    167°57.57'W

Observation Period     6 Sept 75 → 21.7 Sept 75

|                                 |  |  |
|---------------------------------|--|--|
| Instrument                      |  |  |
| Depth (m)                       | 20                                     | 100                                    |
| Meter No.                       | 1687                                   | 1686                                   |
| <hr/>                           |  |  |
| Observation<br>Period<br>(Days) | 0212 Sept 6<br>~1800 Sept 21<br>(15.7) | 0212 Sept 6<br>~1800 Sept 21<br>(15.7) |
| Speed                           | ✓ fails after 3 days                   | ✓                                      |
| Direction                       | ✓                                      | ✓                                      |
| Conductivity                    | ✓                                      | ✓                                      |
| Temperature                     | ✓                                      | ✓                                      |
| Pressure                        | ✓                                      | ✓                                      |
| <hr/>                           |  |  |
| TG-2A<br>Pressure Gauge<br>#87  | Not recovered                          |  |

Recovered by Japanese ~9/21/75; possibility #1687 "snagged" after 3 days in water.

✓ means meter equipped with sensor

CURRENT METER STATION BC-2A

57°4.29'N  
163°19.47'W

Observation Period 8 Sept 75 → 5 Nov 75

|                |             |             |
|----------------|-------------|-------------|
| Instrument     |             |             |
| Depth (m)      | 20          | 50          |
| Meter No.      | 1676        | 1675        |
| <hr/>          |             |             |
| Observation    | 1831 Sept 8 | 1830 Sept 8 |
| Period         | 1832 Nov 5  | 1831 Nov 5  |
| (Days)         | (58.0)      | (58.0)      |
| Speed          | ✓           | ✓           |
| Direction      | ✓           | ✓           |
| Conductivity   | ✓           | ✓           |
| Temperature    | ✓           | ✓           |
| Pressure       | ✓           | ✓           |
| <hr/>          |             |             |
| TG-2A          | 58.0 Days   |             |
| Pressure Gauge |             |             |
| #85            |             |             |

✓ means meter equipped with sensor

CURRENT METER STATION BC-4A      58°37.0'N  
168°14.0'W

Observation Period      7 Sept 75 → 4 Nov 75

Instrument  
Depth (m)                      30                                      47  
Meter No.

---

| Observation<br>Period<br>(Days) | 1905 Sept 7<br>2145 Nov 4<br>(58.1) | 1905 Sept 7<br>2145 Nov 4<br>(58.1) |
|---------------------------------|-------------------------------------|-------------------------------------|
| Speed                           | ✓                                   | ✓                                   |
| Direction                       | ✓                                   | ✓                                   |
| Conductivity                    | x                                   | x                                   |
| Temperature                     | ✓                                   | ✓                                   |
| Pressure                        | ✓                                   | ✓                                   |

---

✓ means meter equipped with sensor

x means meter not equipped with sensor

CURRENT METER STATION BC-3A      55<sup>0</sup>01.5'N  
165<sup>0</sup>10.3'W

Observation Period    6 Nov 75 → to be recovered in March

CURRENT METER STATION BC-4B      58<sup>0</sup>37.0'N  
168<sup>0</sup>14.1'W

Observation Period    5 Nov 75 → to be recovered in March

CURRENT METER STATION BC-1B      55<sup>0</sup>24.0'N  
167<sup>0</sup>58.4'W

Observation Period    4 Nov 75 → to be recovered in March

CURRENT METER STATION BC-2B      57<sup>0</sup>03.7'N  
163<sup>0</sup>21.8'W

Observation Period    5 Nov 75 → to be recovered in March



## VII DISCUSSION

To date this project has conducted two cruises, deploying seven current meter and pressure gauge arrays, recovering two arrays, and conducting twenty-nine CTD casts at stations from the master CTD grid and a 12-hr time series at BC-2A (see figure 3). Moored array BC-1A was trawled by a Japanese fishing vessel on 22 September and fortunately they returned the array's two current meters; however, the acoustic release and pressure gauge were lost. In order to reduce further equipment lost at this station, the location was moved approximately 10km due east from its original position on the 100 fathom contour. The 100km contour apparently is a guideline for trawling. Moored array BC-3A, originally designed as a shelf-break station, was reprogrammed to investigate flow in the region northeast of Unimak Pass in the Bristol Bay Basin. This is intended to provide data critical to understanding circulation within the basin and more closely supports intensive field operations this summer.

Hydrographic data acquired by the NOAA Ship DISCOVERER, using the PODAS system, is not yet available for interpretation. On the November MILLER FREEMAN cruise, the Plessey 8400 digital data logger failed to operate properly; however, digitized analog trace data were used to investigate some general water column features.

Since the data acquisition phase of this project was designed to be in an intensive mode during May to September 1976, and there were problems with CTD data retrieval, the ensuing discussion and conclusions are preliminary.

Moored arrays BC-2A and BC-4A (two current meters and a pressure gauge each) have been recovered and their records processed. The following discussion is based on these records which span the time period from early September to November 1975.

The current meter records presented in this report have been filtered to remove noise using both 2.86-hr low-pass and 35-hr low-pass filters. The 2.86-hr filter has an energy response such that over 99% of the energy is passed at a period of 5 hours, and less than 0.1% at 2 hours. The 35 hour filter passes over 99% of the energy at 60 hours, and less than 0.1% at 26 hours. The 2.86-hr filter is 8 hours long (thus 4 hours of data are lost at the beginning and end of the series), and the 35-hr filter is 120 hours long (losing 60 hours off each end). The second filter essentially removes tidal and inertial effects and yields mean flow. Each of the filters is convolved with the original series. The output of the 2.86-hr filter is resampled on an hourly basis, while the output of the 35-hr filter is resampled on a six-hourly basis.

The data presented in the current meter figures (i.e., Fig. 3,4,7) are by row:

- row a - north-south 2.86-hr filtered current components
- row b - east-west 2.86-hr filtered current components
- row c - 35-hr filtered current velocities presented every 6 hours
- row d - temperature sensor record from the current meter
- row e - salinity (when available) calculated from the conductivity sensor in the current meter

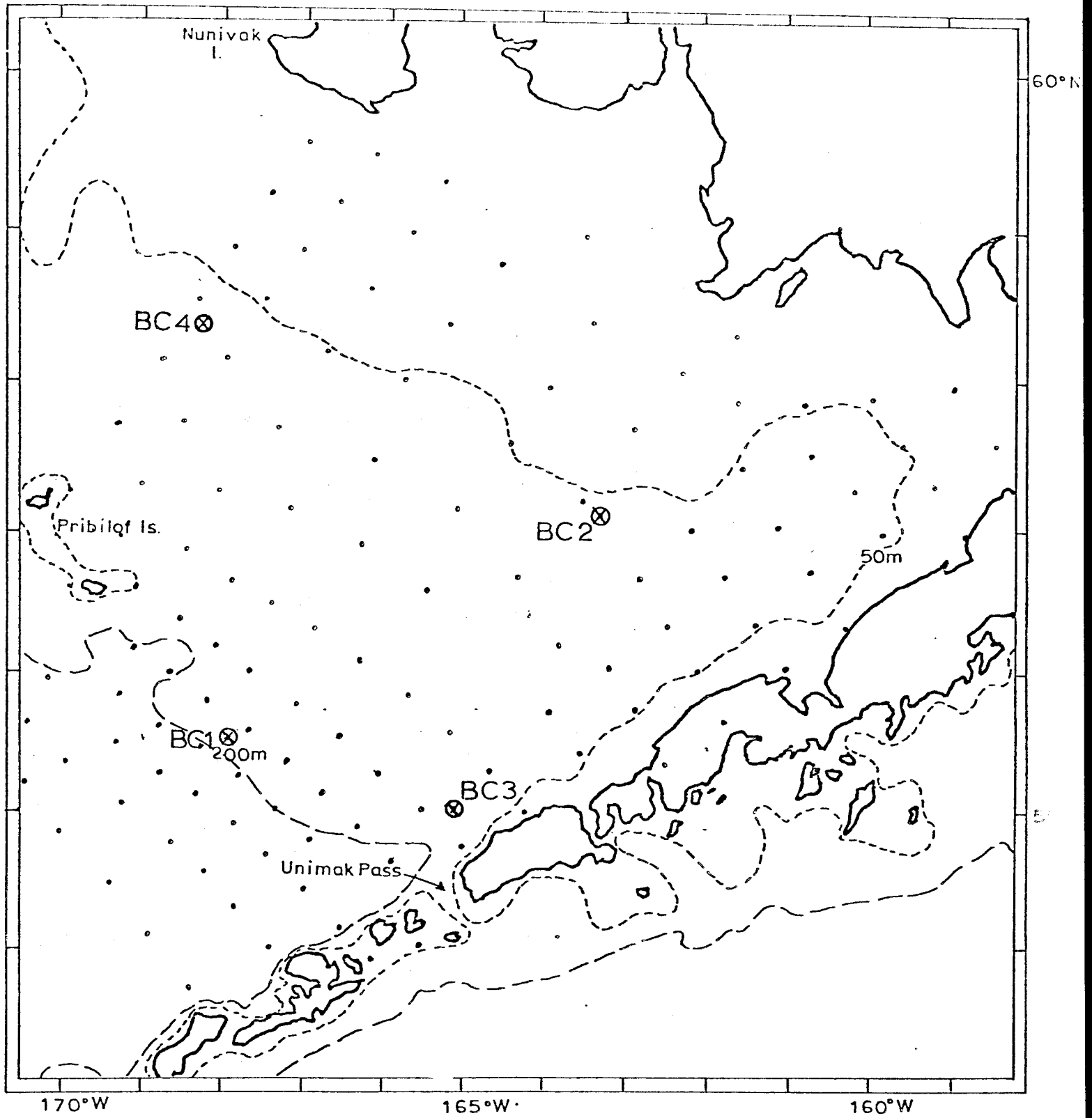


Figure 3. Master CTD grid (•) and present moored array locations in Bristol Bay.

In addition, the 2.86-hr filtered data are used to construct the progressive vector diagram (PVD) in figure 10.

Current meter data from the two stations indicate that in general flow is dominated by tidal activity and that there is a very little residual mean flow. Instantaneous speeds for BC-2 range up to 50 cm/sec and over 60 cm/sec at BC-4. While this activity in a typical Gulf of Alaska Shelf region would suggest a long period component of up to 10 cm/sec, these Bristol Bay data show inconsequential mean flows. For the 58 day records from Sept - Nov 1975, mean flows were:

|        |           |                                    |
|--------|-----------|------------------------------------|
| BC-2A: | 20m depth | 0.60 cm/sec at 304 <sup>0</sup> TN |
|        | 50m depth | 0.95 cm/sec at 300 <sup>0</sup> TN |
| BC-4A: | 30m depth | 2.56 cm/sec at 297 <sup>0</sup> TN |
|        | 47m depth | 0.53 cm/sec at 206 <sup>0</sup> TN |

Although the mean is weak and quite variable, the long records show that mean flow was parallel to the 50m isobath in a general northwest direction.

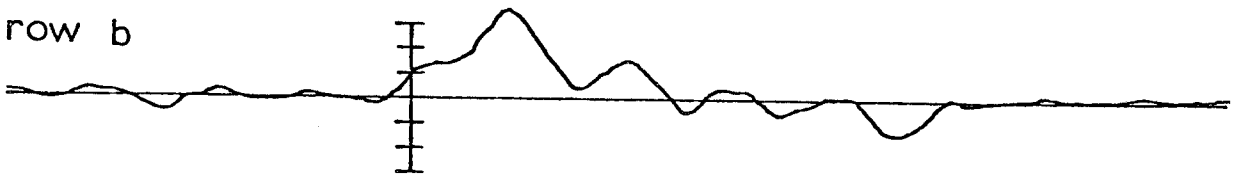
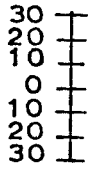
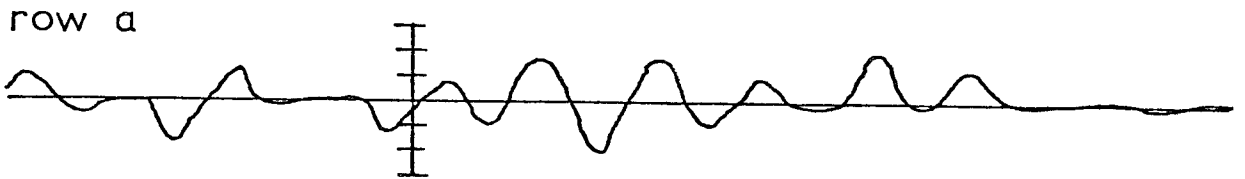
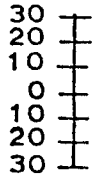
These low mean flows are not surprising if both mooring locations were in CA water. Water mass distribution arguments (see III) favor the concept of low net flow in this water mass and probably significantly greater net flows closer to shore (in CW water). Records from BC-3 when available as well as from the additional records from the summer 1976 intensive phase should shed light on this aspect of the circulation.

At the two central locations isolated events played the significant role in shelf circulation. For a three day period around 18 September mean net flow increased dramatically without a concomitant increase in instantaneous speeds. The event arrived precipitously, and then gradually decreased in magnitude to the originally quiescent flow. This same sort of event occurred 35 days later near the end of the records. Storm activity has in this region a period of occurrence of 7 to 10 days, suggesting that local storm activity is in general not the controlling mechanism for this event. Because of the evident importance of these pulses subsequent discussion concentrates on the changes occurring and evaluation of reasons for this behavior.

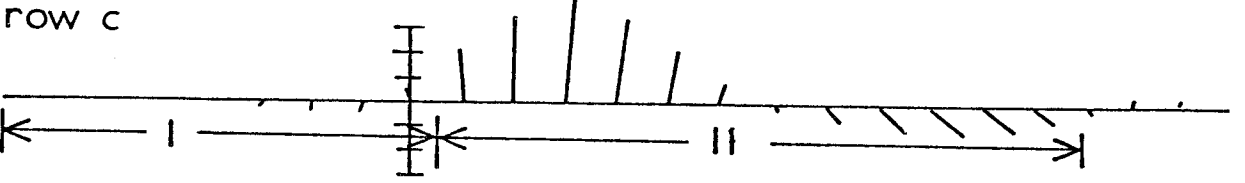
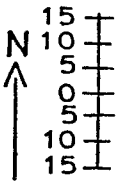
The record segment in figure 4 is typical of the event structure in BC-2 and BC-4; it shows transition from low mean flow to short duration pulse and return. In the first portion (I) the mean flow was less than 2 cm/sec and often close to zero; in the second portion (II) there was a pulse of activity with net flow up to 20 cm/sec, and then after 3 days mean flow returned to near zero. During this entire segment the velocity field associated with higher frequency bands (rows a and b) had speeds on the order of 30 to 40 cm/sec. The event occurring in September coincided both with a change in temperature (September 18) and a reduction of speeds in high frequency bands to nearly zero (Sept 21-23). The former change is shown more clearly on the BC-2 record from 20m below the surface (figure 5). There is a sudden drop in temperature from approximately 8°C to 6°C. This section of the record also indicates that the high frequency speeds approached zero after the passage of the event.

An estimate of the change of sea level associated with this structural change can be obtained from the pressure gauge data from BC-2. Figure 6 shows the bottom pressure data filtered to remove frequencies higher than 1 cy/day. These data are accompanied by estimates of atmospheric pressure and wind speed derived from the synoptic charts of the area.

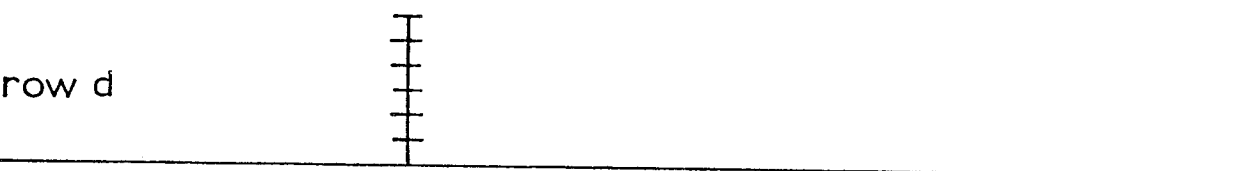
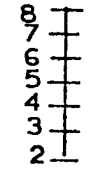
SOUTH-NORTH WEST-EAST



CURRENT



TEMP



SALINITY

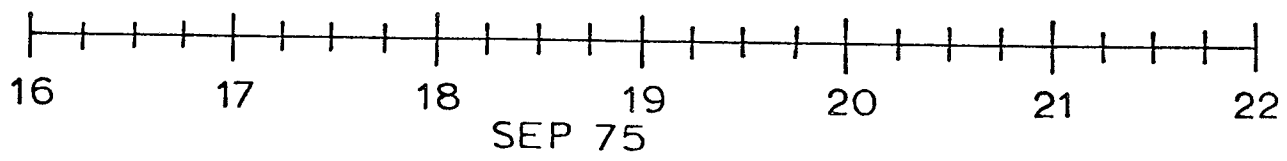
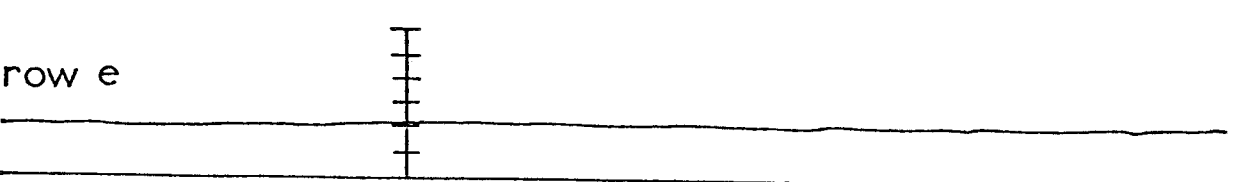
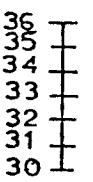


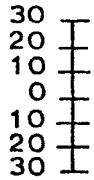
Figure 4. Segment of the processed current meter record from 50m depth at BC-2.

SOUTH-NORTH WEST-EAST

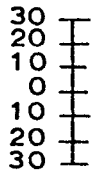
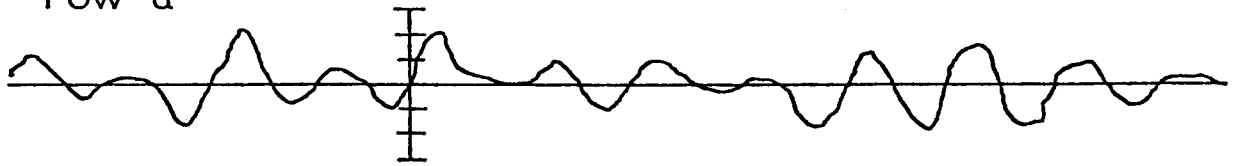
CURRENT

TEMP

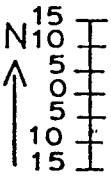
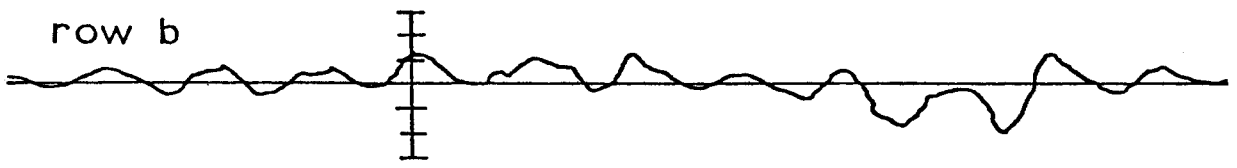
SALINITY



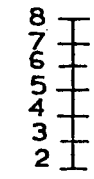
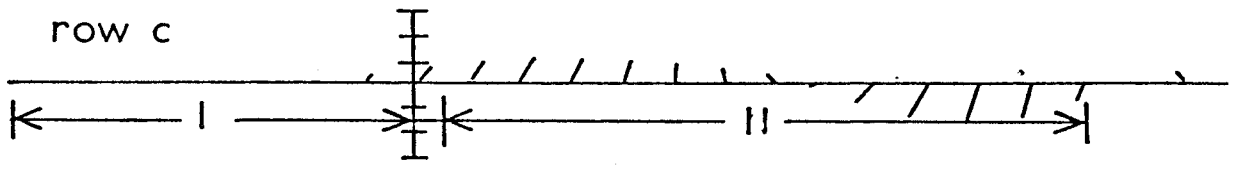
row a



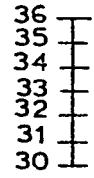
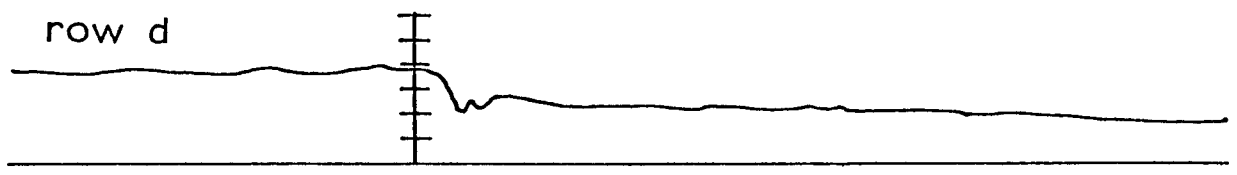
row b



row c



row d



row e

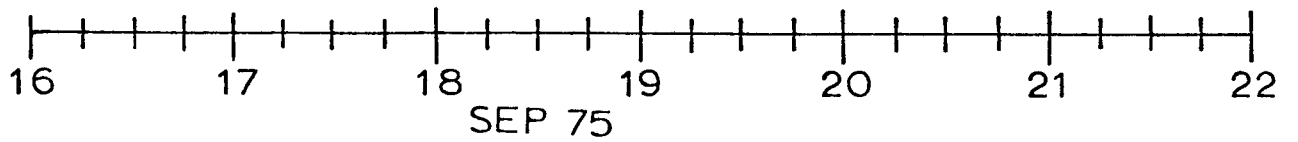
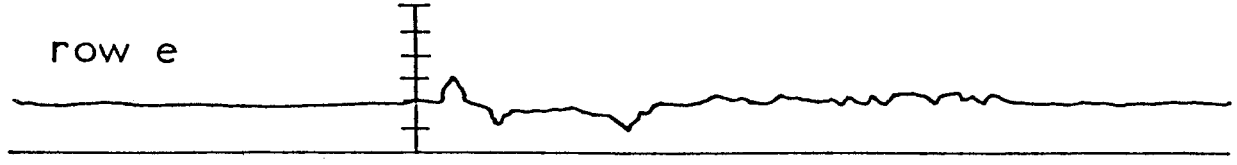


Figure 5. Segment of the processed current meter record from 20m depth at BC-2.

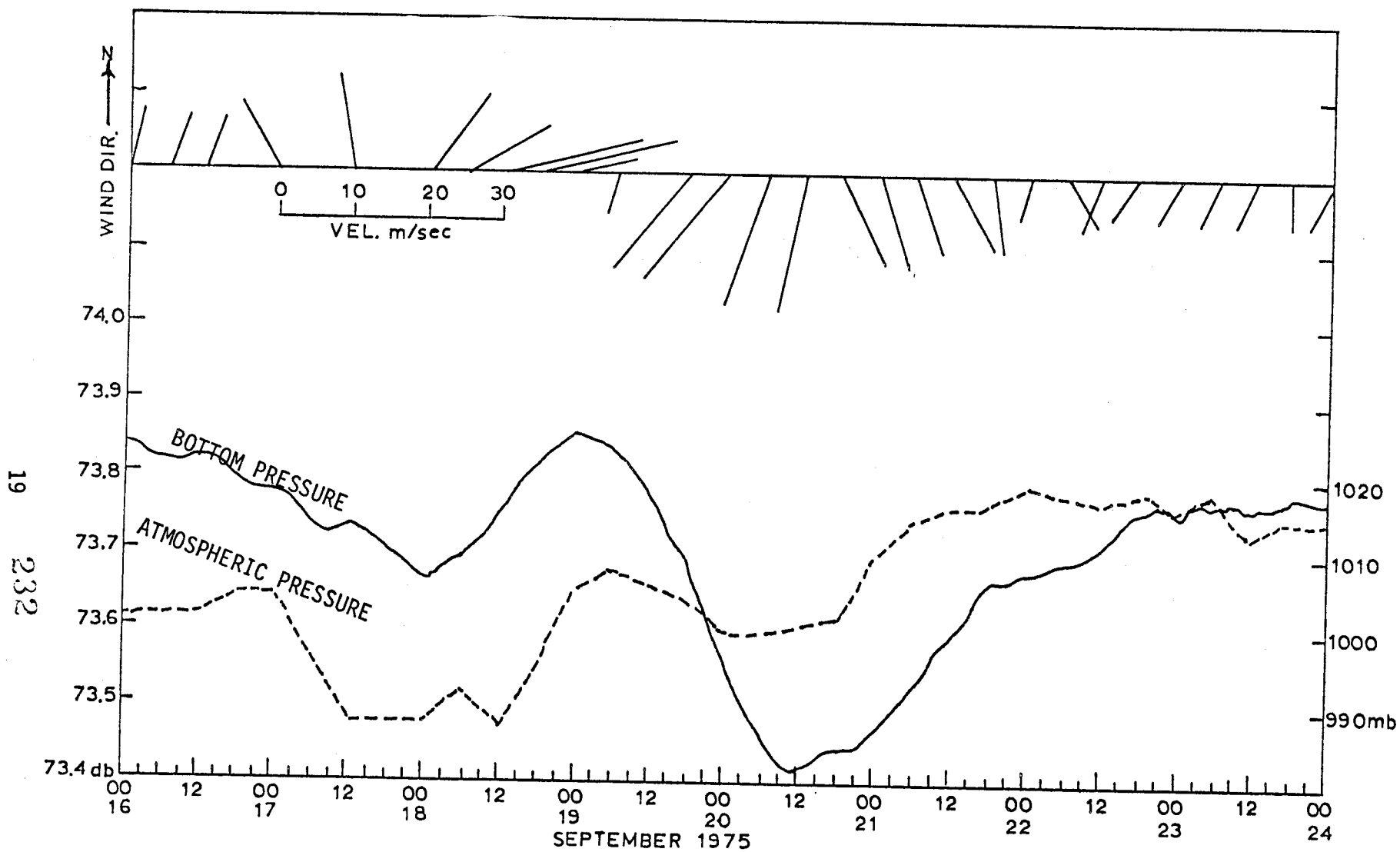


Figure 6. Winds, bottom pressure and atmospheric pressure at BC-2 during first observed mean flow pulse.

From September 15th to 18th changes in bottom pressure are proportional to changes in the atmospheric pressure with gradual decrease in both. The increase in pressures noted on the 18th and 19th indicate that atmospheric response lags the bottom pressure by about 10 hours and has not as great a range. Similarly the decrease in pressures exhibited on the 19th and 20th are not proportional or in phase. Winds from mid-September 19 until September 21 are stronger than previously (up to 40kt), and oriented in such a direction to induce water flow at the surface to the southwest, parallel to the Aleutian coastline. The data indicate a return to proportionality of response beyond September 22. Density data obtained from the current meters show only a small increase in density which suggests that the pressure gauge data reflect a drop in sea level of about 35cm. Synoptic chart data indicate a high pressure cell located in the Arc of the Aleutians and that isobars parallel the land mass. Regional wind blew westward along the Aleutian Peninsula. The records from both the upper and lower current meters indicate that a more normal tidal speed signal reappeared after about 1½ days at 20m depth and 3 days at 50m depth.

The pressure record indicates that there are no long-term changes in relative sea-level after 21 September until about 22 October (figure 7). On October the drop in atmospheric pressure was accompanied by an increase in bottom pressure. The event persisted until the 25th when the system apparently returned to normal. Again winds were observed to increase (over 40kt) and be in a direction which would induce surface flow to the northeast, parallel to the Aleutian coastline. Accounting for density change and atmospheric pressure variations, the bottom pressure indicates a sea level increase of the order of some 50cm of water. On the 22nd of October an atmospheric pressure low was centered in the lower Bering Sea with the isobars parallel to the Aleutian coastline. This should cause wind induced flow into Bristol Bay resulting in the observed sea level change. While the September event represents a sea level drop induced by wind driving water offshore, the October event shows the reverse. The situation is similar to conditions in the mid-Atlantic Bight where Beardsley and Butman<sup>13/</sup> report conditional response of shelf water to storm center location.

The record from the upper meter (30m depth) at BC-4 also had a pulse in the flow regime during September (figure 8). The temperature record has a periodic passage of warm (6°C) and then cold (4°C) water masses. An analog trace from a CTD cast taken when this array was deployed shows that the thermocline was located at approximately the same depth as this meter. Thus, most of the higher frequency fluctuations are related to vertical changes in water column height; however, after the events passed, temperatures remained constant. The temperature record from the lower current meter (47m depth) is generally the same as above. At station BC-4, current meter separation was insufficient to detect two layer structure. There are two possibilities for the changes in temperature at BC-2 and BC-4: (i) advection of a front past the sensors, and this phenomena occurred in pulses; or (ii) permanent raising of the thermocline (thinning of the upper layer). We note that BC-4 location is close to where Muench<sup>12/</sup> reported his description of the sharp front between CW and CA water masses.

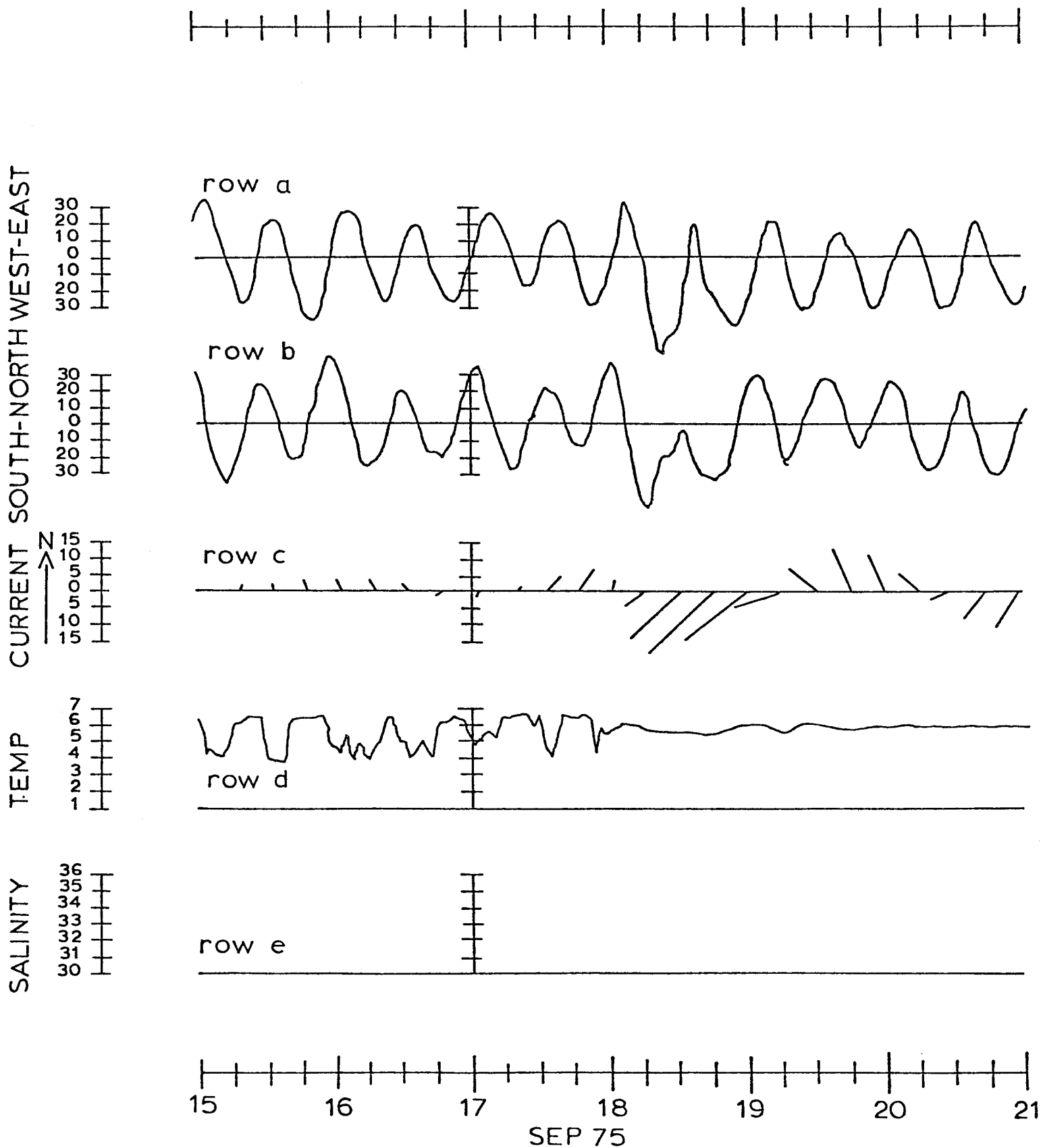


Figure 8. Segment of the processed current meter record from 30m depth at BC-4.



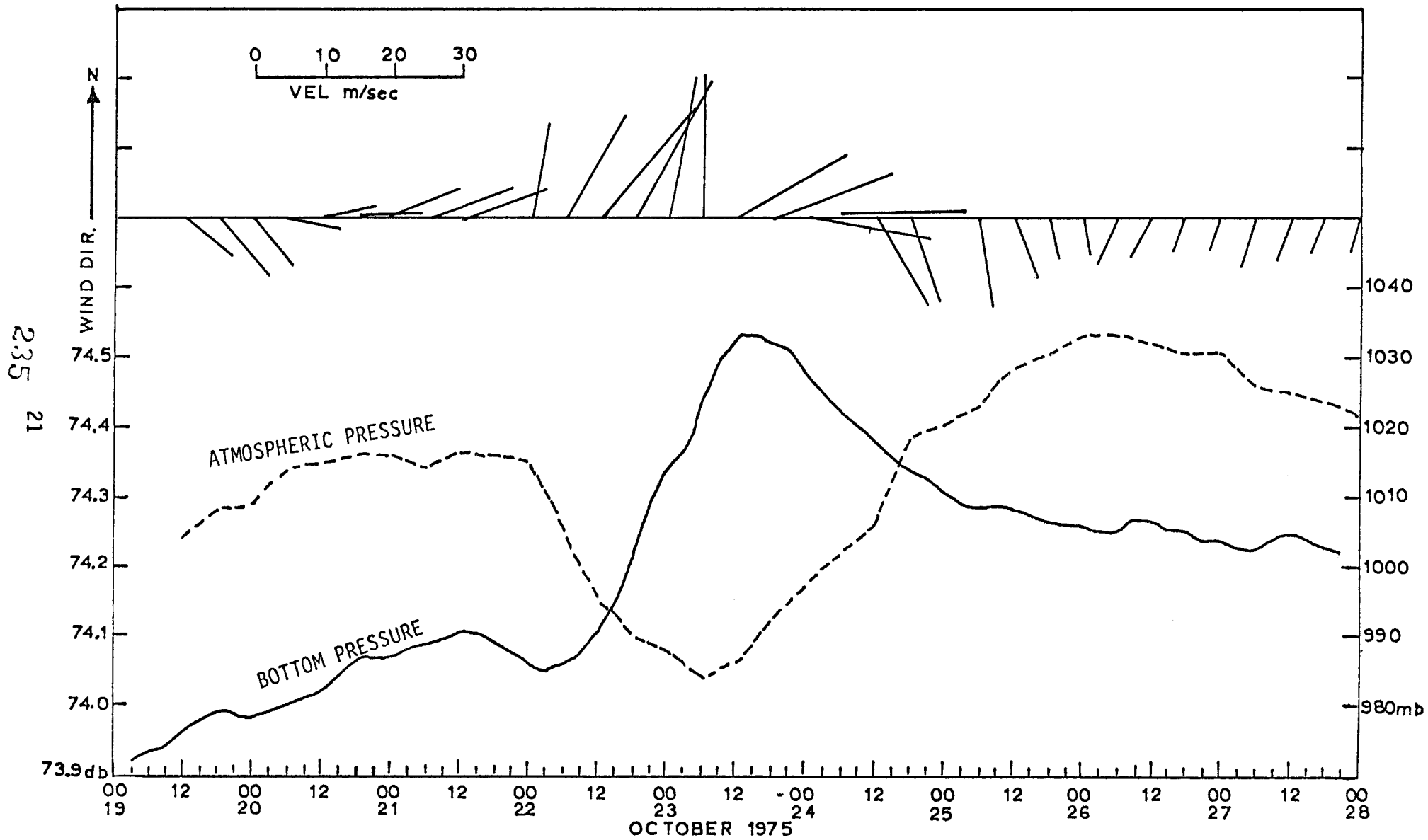


Figure 7. Winds, bottom pressure and atmospheric pressure from BC-2 during second observed mean flow pulse.

During the October sea-level change event, there again is a drastic increase in the mean flow as is shown in figure 9. Prior to 23 October, at BC-2, mean speed was less than 10 cm/sec, whereas on the 23rd there were mean speeds 40 to 50 cm/sec. At the same time, the temperature record indicates an increase of about 1.5°C (at 50m depth) to 4°C which is the same temperature recorded at 20m depth. The salinity values calculated for this depth indicate a mean decrease of 0.150/oo, and remained relatively constant thereafter. This indicates that the front of less saline waters had moved pass BC-2 and low salinity water stayed there for the remainder of the record. After the advective and sea-level events, the temperature structure at both depths is the same and shows a slow decrease as would be expected from convective cooling during winter. Thus, the vertical structure at BC-2 changed from two layers to a well-mixed homogeneous single layer below 20m in about 4 to 6 hours on October 23. As can be seen from CTD data taken on 5 November (figure 10), the water column had remained well mixed to this time. This sudden change in vertical structure of the water column may be an indication that a lateral frontal system has passed through the region of moored array BC-2.

The advective pulse event on 23 October is also clear in the record from BC-4 (figure 11). At this site the temperature structure showed a decrease from 5°C to ~3°C as the water was advected northward and then a return to higher temperature values when the advection had a southward flowing component. These temperature changes also suggest the passage of a frontal system at moored array BC-4.

Further evidence for the existence of a lateral front is shown in Figure 12. The mapping of surface isohalines during September showed the nearshore or coastal waters (CW) extended seaward to the area near the 50m depth contour. Seaward of this contour lay CA water. When remaining CTD data become available, the distinction between these two water masses and a more specific characterization of them will be possible.

The PVD (figure 13) from BC-2 at 50m depth clearly indicates the existence of two advective pulses, the first in a nearly due northward direction, which is in agreement with the mean flow (figure 4) and the second in a northwestward direction, again in agreement with the current meter record (figure 9). The majority of motion is in fluctuating paths with only a few clear pulses of activity. In particular at BC-2A, the total recorded variance at 20 meters (after 2.86-hr filtering) is 436.3 cm<sup>2</sup>/sec<sup>2</sup>. To ascertain which frequencies dominate the record, spectral analyses were conducted (figure 14). As expected, a large fraction of the total variance lies in the tidal frequency bands. A tidal analysis program, based on harmonic constants measured at Dutch Harbor, generated a predicted tidal-series containing a total variance of 308.5 cm<sup>2</sup>/sec<sup>2</sup>. Approximately 71% of the variance in this record can be accounted for by tidal activity. The dominant species in the harmonic analysis, which is also evident in the spectral diagram, were found to be the semi-diurnal component which contains the N<sub>2</sub>, M<sub>2</sub> and S<sub>2</sub> constituents. These constituents contained approximately 75% of the tidal variance and had a clockwise rotation. This clockwise sense of rotation is also indicated in the PVD's.

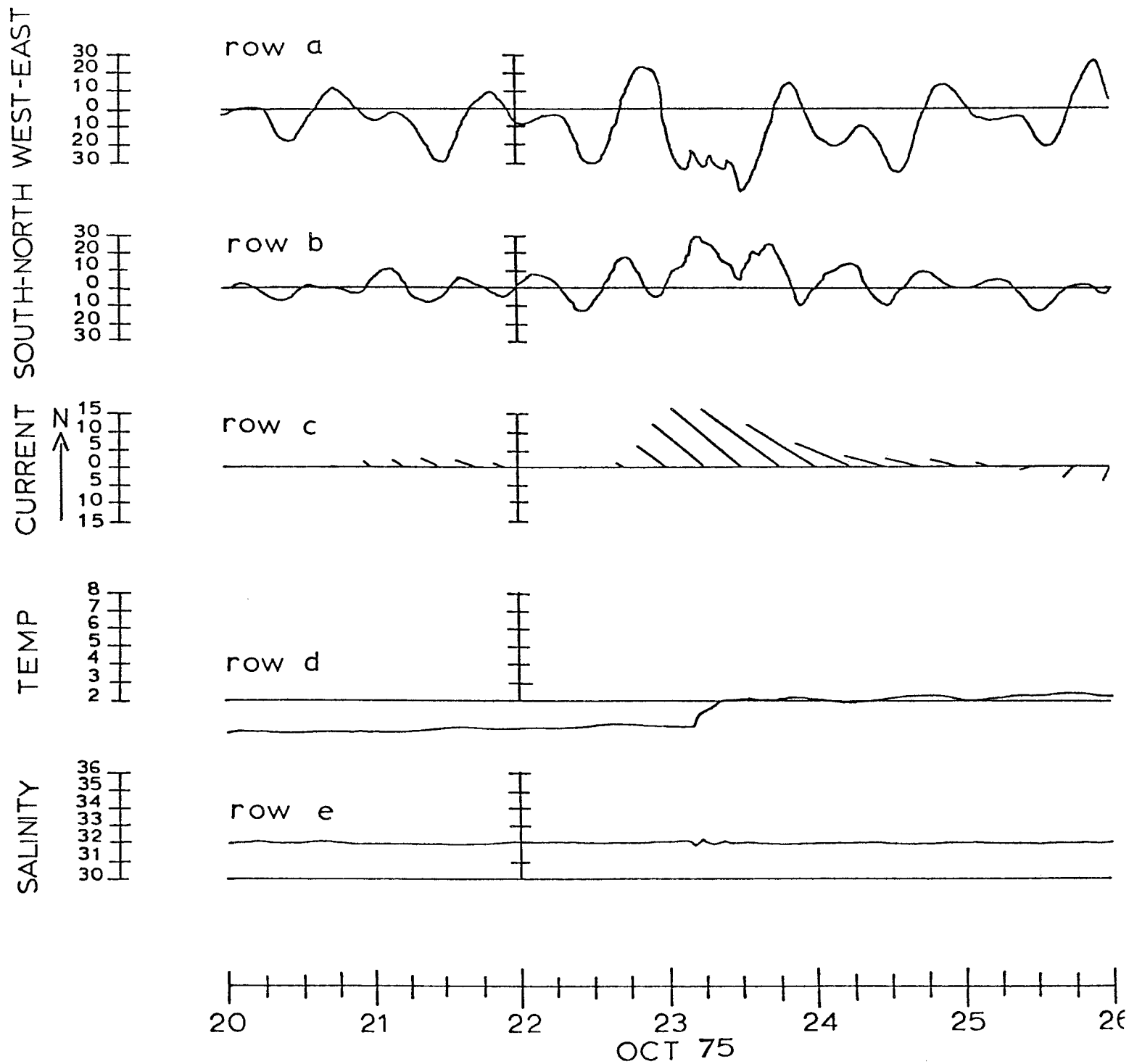


Figure 9. Segment of the processed current meter record from 50m depth at BC-2.

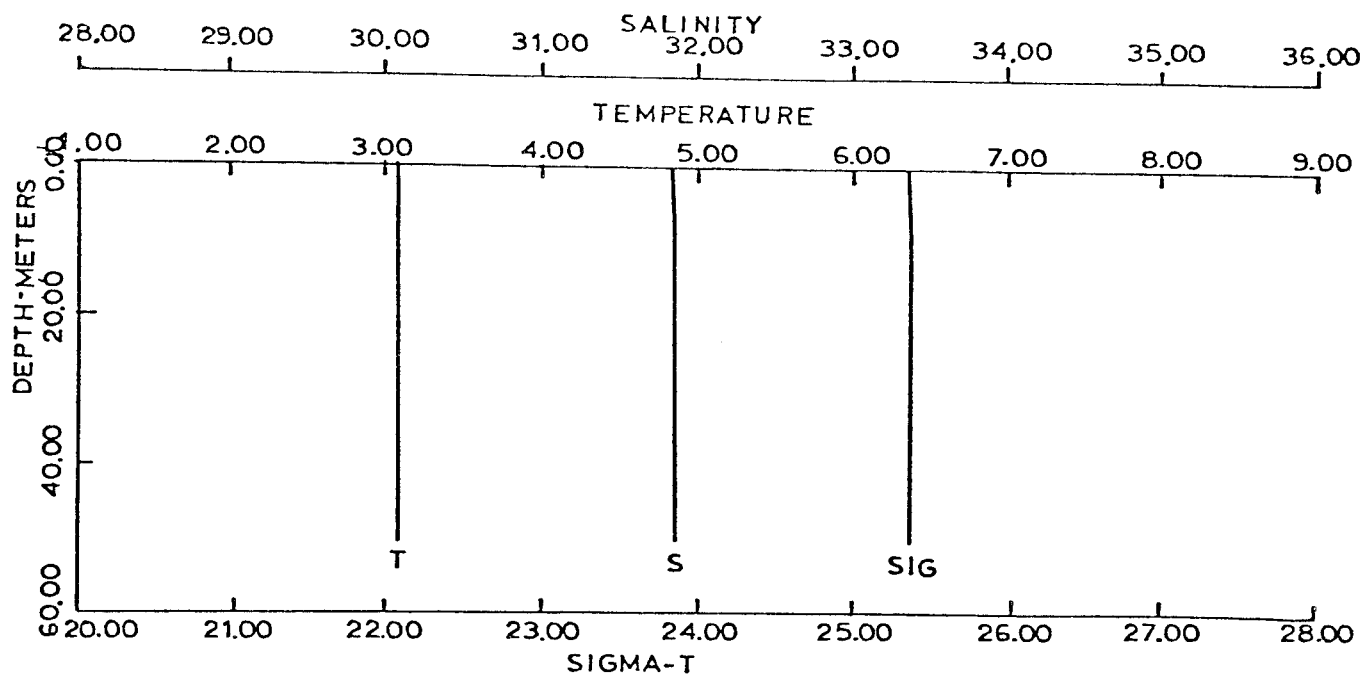


Figure 10. Vertical profiles of temperature, salinity and sigma-t taken at BC-2 on 5 November 1975.

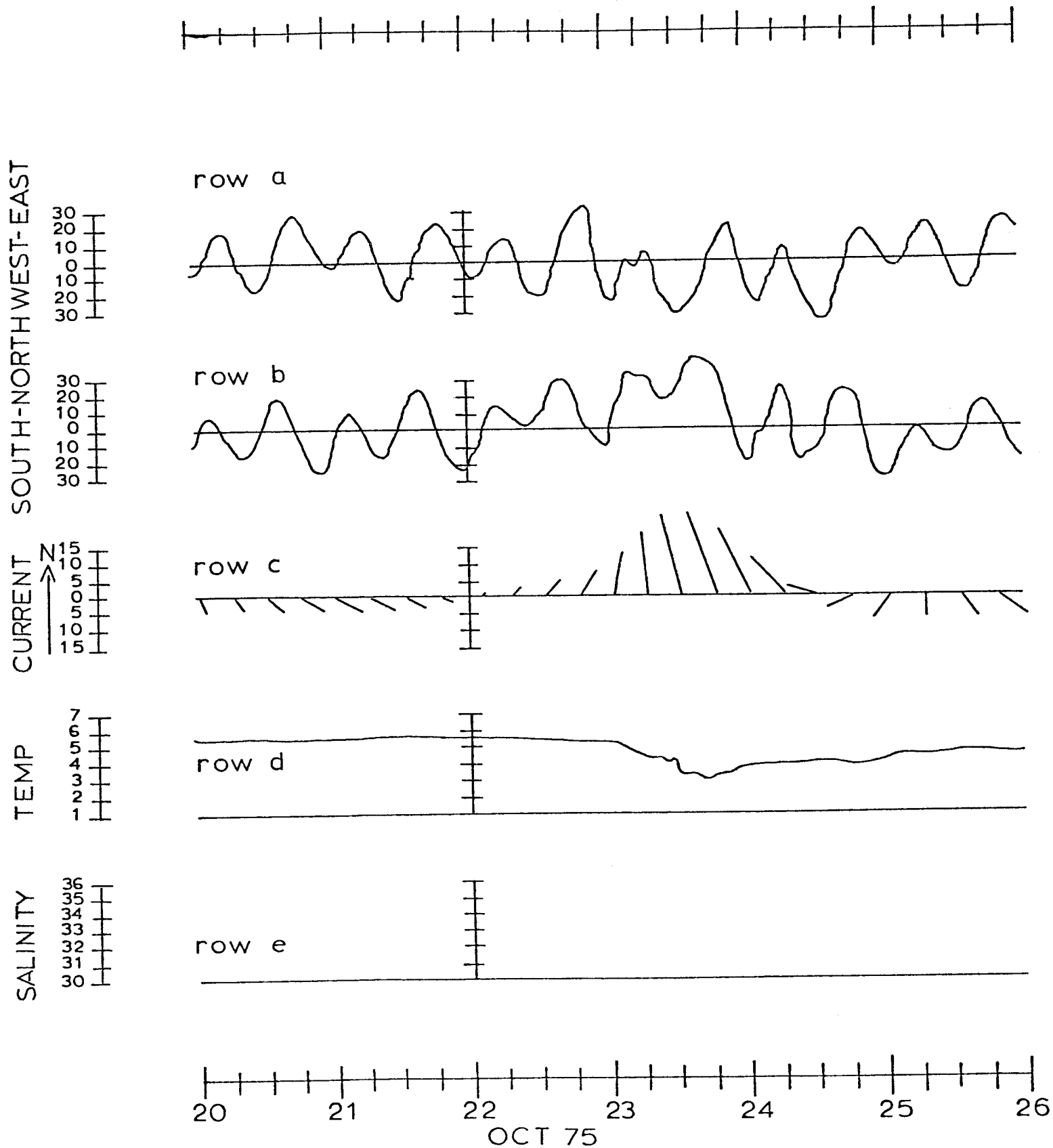


Figure 11. Segment of the processed current meter record from 47m depth at BC-4 during second mean flow pulse.

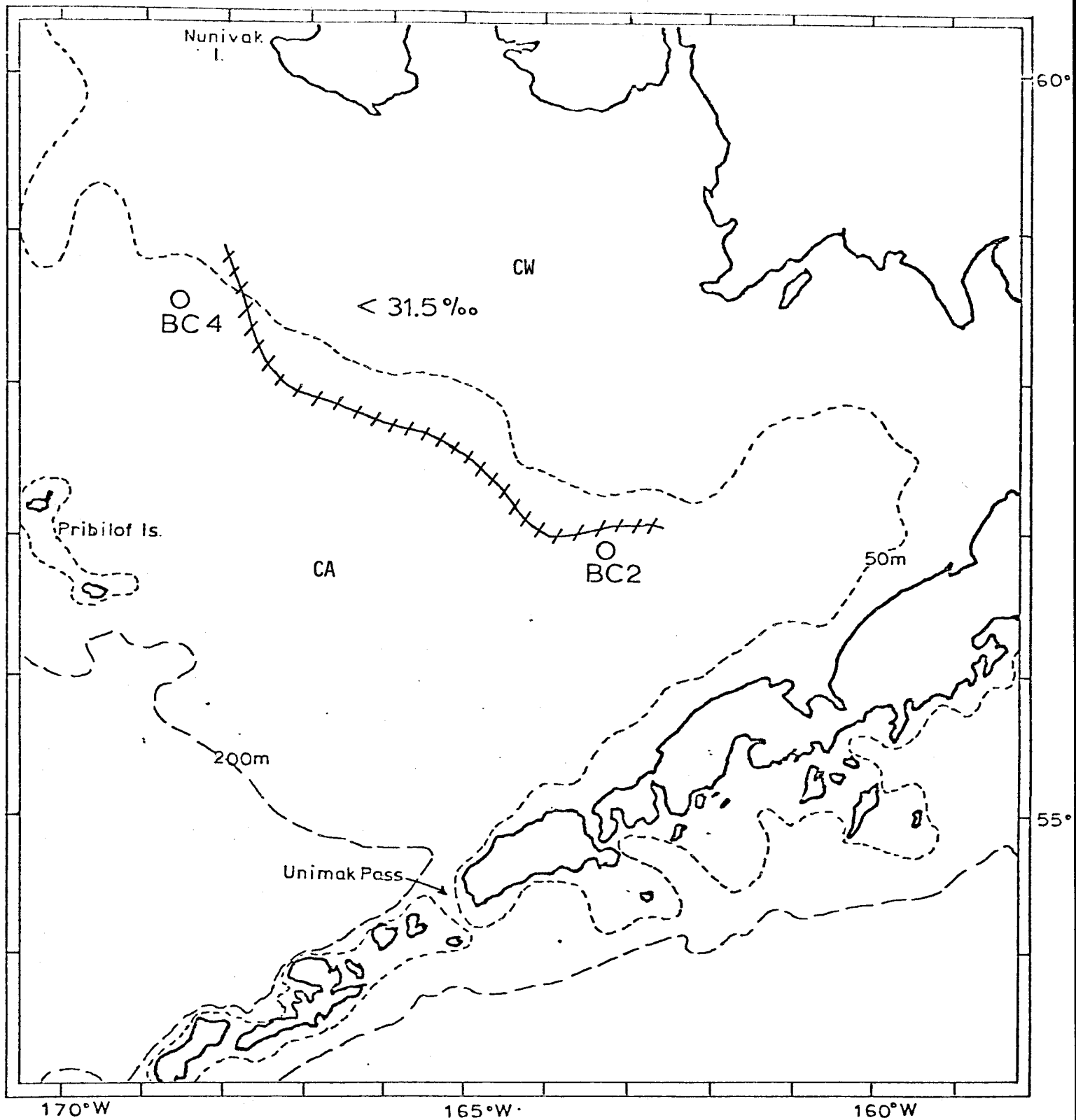


Figure 12. Boundary between coastal water (CW) and convective area (shelf water, CA) as indicated from surface salinities during September 1975.

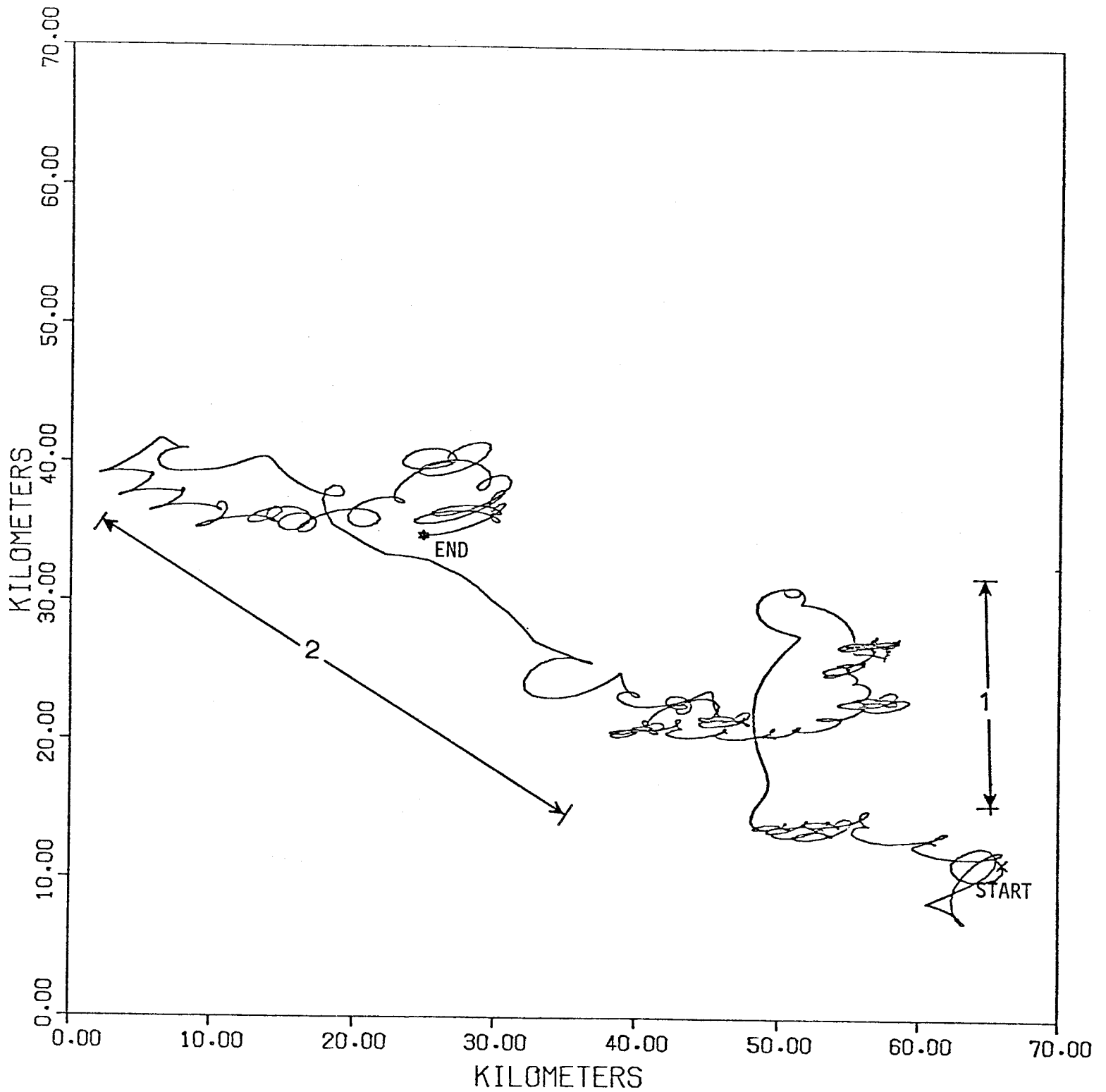


Figure 13. Progressive Vector Diagram (PVD) constructed from current meter record from 50m depth at BC-2 indicating the two observed mean flow pulses (1 in September and 2 in October 1975).

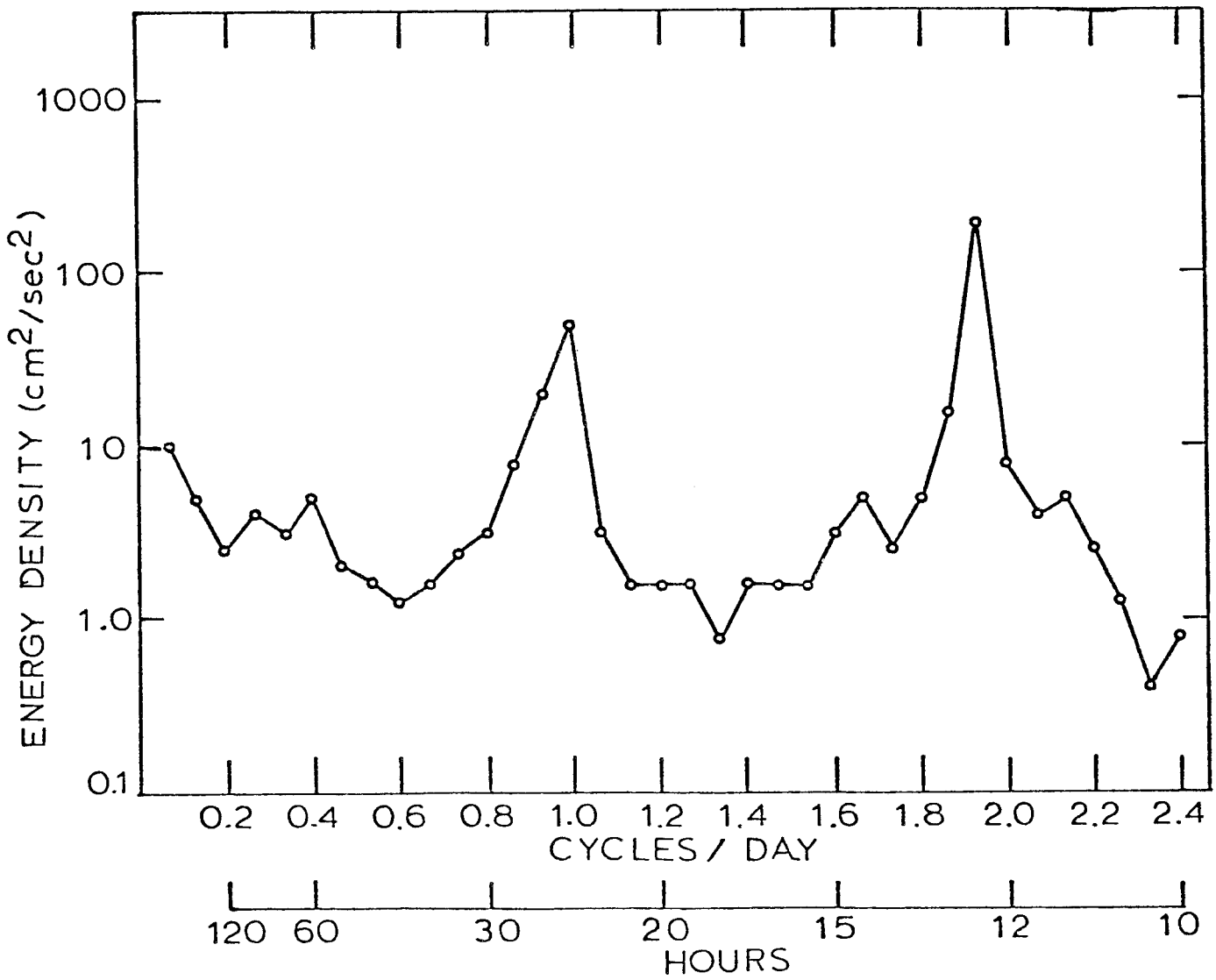


Figure 14. Spectral energy density for the current meter record from 20m depth at BC-2.



## VIII CONCLUSIONS

To date, data collected, processed and analyzed from Bristol Bay indicate the following preliminary conclusions:

- (1) The mean flow was small in the central bay with most (>70%) of the variance energy in the tidal frequencies.
- (2) Major events occurred as pulses in the mean flow in those locations raising it over a three day period from near zero to over 30 cm/sec and back to near zero.
- (3) Major changes in the relative sea-level are associated with flow pulses. Two of these events were recorded between September and November 1975. The events seem unrelated to local storms, but are probably related with substantial movement of water onto or off of the shelf.
- (4) The passage of pulses resulted in large temperature changes (about 2°C) at BC-2 and BC-4. On 23 October, 1975 the passage of an event changed the vertical structure at BC-2 from 2 layers to a homogeneous structure (>20m) in less than  $\frac{1}{2}$  day.
- (5) There appears to be a frontal system between warmer and less saline coastal waters and colder more saline shelf waters which has its seaward boundary near the 50m depth contour. Perturbations in this lateral front could account for observed water mass changes at BC-2 and BC-4. Changes in frontal position were correlated with the pulses.

## IX NEEDS FOR FURTHER STUDY

The implication that pulses are critical in understanding the advective regime suggest that an effective program element be the collection of long-term (at least 2 years) pressure gauge and current meter data in the central bay and near-shore waters. The ensuing records could be examined for periodicity of pulses and possibly yield a clearer understanding of the driving mechanisms. In addition, long-term records would allow statistically significant determinations of extreme flow conditions to be calculated.

Spatial and temporal scales of the frontal system need further investigation. This suggests a re-emphasis on CTD surveys and time-series CTD stations to further examine both temporal and spatial variability. Such re-emphasis would result in higher density CTD grid and small length scale current meter and pressure gauge experiments in the near shore zone. In particular, data acquisition should be focussed in the region of the 50m depth contour.

These needs will begin to be addressed by the intensive field program which will be undertaken this summer. Moored arrays will be deployed at sites selected from analysis of data collected to date, and hopefully from records to be recovered during March 1976.

X SUMMARY OF 4<sup>th</sup> QUARTER OPERATIONS: BERING SEA

| SHIP       | CRUISE ID             | DATE          | ACTIVITY  | PERSONNEL  |
|------------|-----------------------|---------------|---|--|
| DISCOVERER | RP-4-DI-75B<br>LEG II | 2-11 Sept. 75 | <p>Station BC-1A depl.<br/>                     Lat. 55°24.63'N<br/>                     Long. 167°57.46N<br/>                     Depth-201meters<br/>                     Two Aanderaas RCM+1PG</p> <p>Station BC-2A Depl.<br/>                     Lat. 57°04.29'N<br/>                     Long. 163°19.47'<br/>                     Depth-65meters<br/>                     Two Aanderaa RCM+1PG</p> <p>Station BC-4A Depl.<br/>                     Lat. 58°36.96'W<br/>                     Long. 168°13.96'W<br/>                     Depth-55meters<br/>                     Two Aanderaa RCM+1PG</p> <p>CTD casts at master grid<br/>                     stations 15,37,48,61,39,19,4<br/>                     22,44,64,76,68,88,122,&amp;96.<br/>                     CTD casts after each array<br/>                     was deployed. One twelve hr.<br/>                     time series at station BC-2A.<br/>                     Total of 224 surface salinity<br/>                     and temp. stations were col-<br/>                     lected.</p> <p>There were 45 15-min. transect<br/>                     bird counts taken and 10 sta-<br/>                     tionary bird counts made.</p> | <p>Dr. J. Schumacher, PMEL/NOAA,<br/>                     Chief Scientist<br/>                     Dr. L. Coachman, U.of W.<br/>                     Mr. R. Tripp, U. of W.<br/>                     Mr. R. Newman, PMEL/NOAA<br/>                     Mr. D. Stith, PMEL/NOAA<br/>                     Mr. S. Harding, U.of W.<br/>                     Mr. J. Ruehle, USF &amp; WS</p> |

## BERING SEA

| SHIP           | CRUISE ID            | DATE            | ACTIVITY   | PERSONNEL  |
|----------------|----------------------|-----------------|--|--|
| MILLER FREEMAN | RP-4-MF-75B<br>LEG I | 30 Oct-8 Nov 75 | Searched vicinity of BC-1A to recover the release and pressure gauge. The mooring had been damaged by Japan. trawler. No success.  | Mr. R. Reed, PMEL/NOAA<br>Chief Scientist<br>Mr. D. Stith, PMEL/NOAA<br>Mr. R. Carlone, PMEL/NOAA<br>Mr. D. Tripp, U.of W.<br>Mr. R. Taylor, U.of W. |
|                |                      |                 | Station BC-1B deployed<br>Lat. 55°24.0'<br>Long. 167°58.4'<br>Depth<br>Two Aanderaa RCM+1PG  |  |
|                |                      |                 | Station BC-2A recovered<br>Station BC-2B deployed<br>Lat. 57°03.7'<br>Long. 163°21.8'<br>Depth-66meters<br>Two Aanderaa RCM+1PG    |  |
|                |                      |                 | Station BC-3A recovered<br>Station BC-3B deployed<br>Lat. 55°01.5'N<br>Long. 165°10.3'W<br>Depth-115meters<br>Two Aanderaa RCM+1PG |  |
|                |                      |                 | Station BC-4A recovered<br>Station BC-4B deployed<br>Lat. 58°36.3'N<br>Long. 168°13.4'W<br>Depth-55meters<br>Two Aanderaa RCM+1PG  |  |
|                |                      |                 | There were 14 CTD casts taken at BC-2, BC-4, BC-3, BB-111, BB-100, BB-91, BB-71, BB-46, BB-25, BB-35, BB-36, BB-26, BB-16, BB-15.  |  |

## REFERENCES

1. Zachariasen, F. "Oil Pollution in the Sea: Problems for Future Work". Research Paper P-432, Institute for Defense Analysis, June 1968.
2. Air and Water News, March 24, 1969, page 3.
3. Smith, J.E. "'Torrey Canyon' Pollution and Marine Life," Cambridge University Press, London, 1968.
4. Berridge, S.A., M.T. Thew, and A.G. Loriston-Clark, The formation and stability of emulsions of water in crude petroleum and similar stocks, J. Institute Petroleum 54 (539), 333-357, 1968.
5. Berridge, S.A., R.A. Dean, F.G. Fallows, and A. Fish, Properties of persistent oils at sea, J. Institute Petroleum 54 (539), 300-307, 1968.
6. Hebard, J.F. 1961. Currents in the southeastern Bering Sea. I.N.P.F.C. Bulletin no.5, pp. 9-16.
7. Kinder, T.H., 1976. Circulation along the northeastern continental slope of the Bering Sea. University of Washington Ph.D. thesis.
8. Barnes, C.A. and T.G. Thompson, 1938. Physical and chemical investigations in Bering Sea and portions of the North Pacific Ocean. University of Washington Publications in Oceanography, vol. 3, no. 2, pp. 35-79.
9. Dodimead, A.J., F. Favorite and T. Hirano, 1963. Oceanography of the subarctic Pacific region. I.N.P.F.C. Bulletin no. 13, pp. 177-89.
10. Data Record of Oceanography Observations and Exploratory Fishing, Faculty of Fisheries, Hokkaido University, nos. 8-18.
11. Takenouti, A.Y. and K. Ohtani, 1974. Currents and water masses in the Bering Sea: a review of Japanese work. Chapter 2, pp. 39-57 in Oceanography of the Bering Sea. D.W. Hood and E.J. Kelley, eds. Institute of Marine Science, University of Alaska, Occasional Publication no. 2.
12. Muench, R.D., 1976. A note on eastern Bering Shelf hydrographic structure. Deep-Sea Research.
13. Beardsley, R.C. and B. Butman. Circulation of the New England continental shelf: response to strong winter storms. Geophysical Research Letters, pp. 181-184, 1974.



ANNUAL REPORT

Contract No.:

03-5-022-67, TO 1

Research Unit No.:

151

Reporting Period:

1 April 1975 -- 31 March 1976

Number of Pages: 18

STD Mappings of the Beaufort Sea Shelf

Knut Aagaard

Department of Oceanography

University of Washington

Seattle, Washington 98195

25 March 1976

## I. Summary

Through a series of CTD sections across the Beaufort Sea shelf we have traced the seasonal hydrographic sequence through the fall and winter. Oceanographically, the Beaufort shelf is much like the deep Canadian Basin itself, at least from fall on. However, there is a regard in which the shelf may have distinct and considerable oceanographic significance: it very likely provides a feed of subsurface waters into the Canadian Basin. Should this be the case, one could visualize the possibility of injecting a variety of substances from the shelf into the Arctic Ocean pycnocline, as contrasted with a spreading confined to the near-surface.



## II. Introduction

A. The general objective of this research unit is to provide seasonally distributed synoptic temperature-salinity mapping of the Beaufort Sea shelf and the dynamically related region of the slope. Such mappings are an essential prerequisite to, and component of all physical oceanographic studies of the shelf, and of modeling for both shelf circulation and ice dynamics.

B. The specific objective is to utilize in a portable configuration the resolving ability of a digitally-recording CTD profiling system. By carrying this system aboard a helicopter along with required ancillary equipment, key CTD sections across the shelf and out over the slope can be accomplished quite rapidly.

C. Determining the seasonal hydrographic structure of the region contributes essentially to studies of the diffusive and advective processes on the shelf. These in turn are the physical mechanisms which transport and disperse pollutants and substances of biological and geological importance.

## III. Current state of knowledge

Except for the brief ice-free period during summer, hydrographic stations have never been taken in this area. During summer quite large temperature and salinity ranges and gradients can be expected on the shelf. Temperatures range from near-freezing to more than 5°C, and salinities from brackish to greater than 33‰.

In summer an eastward intrusion of relatively warm water originating in the Bering and Chukchi seas appears to be a regular feature of the circulation on the outer shelf, being typically located seaward of the 40m isobath. This water has been identified at least as far east as 143°W.

Summer observations have also indicated the likelihood of an intermittent upwelling regime on the eastern part of the shelf. The upwelled water is relatively cold, low in oxygen and high in nutrients. It appears that the upwelling is a response to locally strong easterly winds and that the upwelled water on the shelf moves westward.

#### IV. Study area

The area of interest extends eastward from Pt. Barrow along the entire northern Alaska coast, i.e., from about  $156^{\circ}30'W$  to  $141^{\circ}W$ , a lateral distance of nearly 600 km. The shelf is narrow, with the shelf break typically 80-90 km offshore. The total runoff is relatively small, highly seasonal, and concentrated in a very few rivers of any consequence, the largest of which is the Colville. The area is covered by sea ice, both first and multi-year, through all but two to three months. Even during the height of summer, ice is usually found well onto the shelf.

#### V. Data collection

Three representative hydrographic sections across the shelf and slope were selected, extending normal to the coast line and with their southern terminus at approximately  $153^{\circ}W$  (Pitt Point section),  $147^{\circ}30'W$  (Narwhal Island section), and  $142^{\circ}30'W$  (Humphrey Bay section). The sections begin near the 20 m isobath and terminate in deep water well out over the slope, with a typical station separation of 11 km. To sample through the seasonal cycle, three periods were chosen, viz. October-November (fall), February (winter), and May-June (spring).

At present the only practical way of accomplishing such sections synoptically is by use of helicopter and CTD profiling equipment in a portable configuration. The present work is probably the first attempt at a synoptic oceanographic survey using these techniques.

The field procedure is as follows. After fixing the station site (using DEW line radar), the helicopter lands. It is unloaded, the winch and generators started immediately, and electronics and heating equipment hooked up. A hole about 50 cm on a side is cut through the ice using auger and ice chisel. The depth is sounded and the CTD cast proceeds, using a small gas-powered winch equipped with slip rings. The maximum permissible sensor depth is about 600 m. A Nansen bottle with reversing thermometers is hung above the sensors for purposes of calibrating each cast. The profiling system (Plessey 9400,8400) records digitally on magnetic tape via the data logger inside the helicopter. The entire operation from landing to takeoff typically takes about one hour. The calibration bottle salinity samples are frozen and analyzed with an inductive salinometer upon return to Barrow at the end of the cruise.

## VI. Results

The stations from the fall cruise are listed in Table 1 and those from winter in Table 2. The stations extend to the bottom or 600m, whichever is less. The contoured sections of temperature and salinity are shown in Figs. 1-3 (fall) and Figs. 4-6 winter). A result that should not be overlooked is the successful demonstration of the feasibility of the techniques themselves.

## VII. Discussion

*The ensuing remarks are intended only as preliminary.*

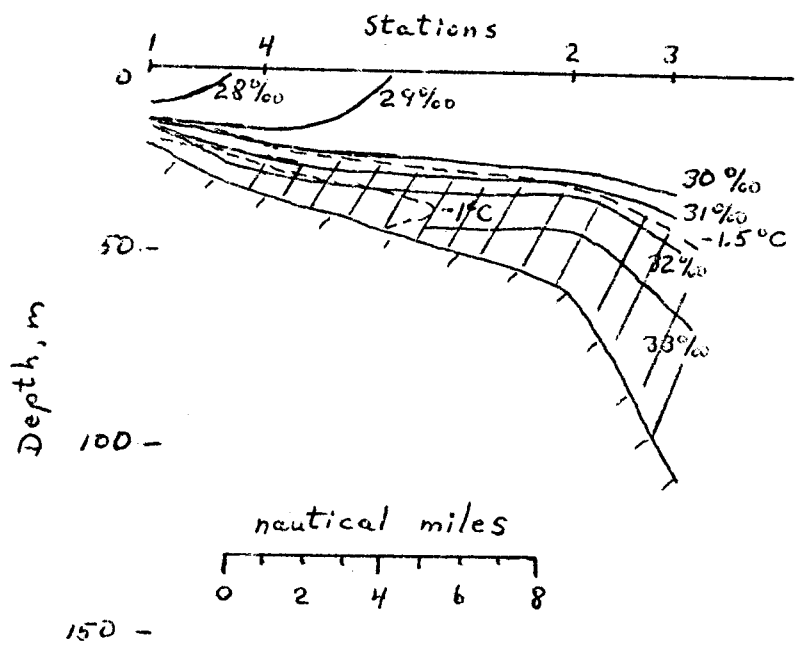
During fall there was a very marked salinity (and hence density) stratification below the upper 20 m or so. The salinity in the upper

Table 1

| <u>Station No.</u> | <u>Date (GMT)</u> | <u>Latitude (N)</u> | <u>Longitude (W)</u> | <u>Sounding (m)</u> |
|--------------------|-------------------|---------------------|----------------------|---------------------|
| 1                  | 26 October 1975   | 71°08.7'            | 152°39.9'            | 25                  |
| 2                  | 29                | 71°19.1'            | 152°34.0'            | 59                  |
| 3                  | 31                | 71°21.6'            | 152°35.0'            | 102                 |
| 4                  | 1 November        | 71°11.5'            | 152°38.0'            | 37                  |
| 5                  | 2                 | 70°37.0'            | 147°55.8'            | 22                  |
| 6                  | 2                 | 70°45.0'            | 147°45.6'            | 37                  |
| 7                  | 3                 | 70°50.8'            | 147°37.0'            | 40                  |
| 8                  | 3                 | 71°08.5'            | 146°29.0'            | >1460               |
| 9                  | 3                 | 71°03.0'            | 146°36.5'            | >1460               |
| 10                 | 4                 | 70°30.0'            | 147°24.0'            | 21                  |
| 11                 | 4                 | 70°35.5'            | 147°11.0'            | 35                  |
| 12                 | 4                 | 70°57.5'            | 146°43.0'            | 67                  |
| 13                 | 4                 | 70°52.7'            | 146°47.0'            | 57                  |
| 14                 | 5                 | 70°46.5'            | 147°00.0'            | 44                  |
| 15                 | 5                 | 70°41.0'            | 147°08.0'            | 35                  |
| 16                 | 6                 | 70°41.0'            | 141°39.0'            | 598                 |
| 17                 | 7                 | 70°34.4'            | 141°47.0'            | 304                 |
| 18                 | 9                 | 70°02.0'            | 142°28.0'            | 20                  |
| 19                 | 9                 | 70°07.6'            | 142°20.8'            | 44                  |
| 20                 | 9                 | 70°13.1'            | 142°15.0'            | 47                  |
| 21                 | 10                | 70°18.6'            | 142°07.1'            | 49                  |
| 22                 | 10                | 70°29.7'            | 141°53.0'            | 66                  |
| 23                 | 10                | 70°23.8'            | 142°00.0'            | 55                  |

Table 2

| <u>Station/<br/>Cast No.</u> | <u>Date (GMT)<br/>Feb. 1976</u> | <u>Latitude<br/>(°N)</u> | <u>Longitude<br/>(°W)</u> | <u>Sounding<br/>(m)</u> |
|------------------------------|---------------------------------|--------------------------|---------------------------|-------------------------|
| 1,2                          | 20                              | 71°06.5'                 | 152°52.5'                 | 22                      |
| 3                            | 20                              | 71°12.0'                 | 152°43.5'                 | 31                      |
| 4,5                          | 21                              | 71°17.5'                 | 152°36.0'                 | 48                      |
| 6                            | 21                              | 71°23.1'                 | 152°27.0'                 | 124                     |
| 7                            | 21                              | 71°28.5'                 | 152°21.0'                 | 124                     |
| 8                            | 22                              | 71°34.0'                 | 152°11.8'                 | 241                     |
| 9                            | 23                              | 71°39.3'                 | 152°03.9'                 | >1200                   |
| 10                           | 24                              | 71°45.2'                 | 151°54.8'                 | >1200                   |
| 11                           | 25                              | 70°29.5'                 | 147°24.0'                 | 17                      |
| 12                           | 25                              | 70°35.0'                 | 147°16.5'                 | 32                      |
| 13                           | 25                              | 70°40.5'                 | 147°09.0'                 | 37                      |
| 14                           | 26                              | 70°47.0'                 | 146°59.0'                 | 46                      |
| 15                           | 26                              | 71°02.9'                 | 146°37.0'                 | 1138                    |
| 16,17                        | 27                              | 70°57.6'                 | 146°44.0'                 | 179                     |
| 18                           | 28                              | 70°07.5'                 | 142.23.0'                 | 31                      |
| 19                           | 29                              | 70°13.0'                 | 142°15.0'                 | 44                      |
| 20                           | 29                              | 70°18.4'                 | 142°07.5'                 | 47                      |
| 21                           | 29                              | 70°24.1'                 | 141°57.5'                 | 55                      |
| 22                           | 29                              | 70°29.5'                 | 141°54.0'                 | 71                      |
| 23                           | 29                              | 70°34.3'                 | 141°45.0'                 | 395                     |
| 24                           | 29                              | 70°40.3'                 | 141°37.0'                 | 578                     |



Scale is identical on Figs. 1-6

256

Fig. 1 Pitt Point section,  
October - November 1975

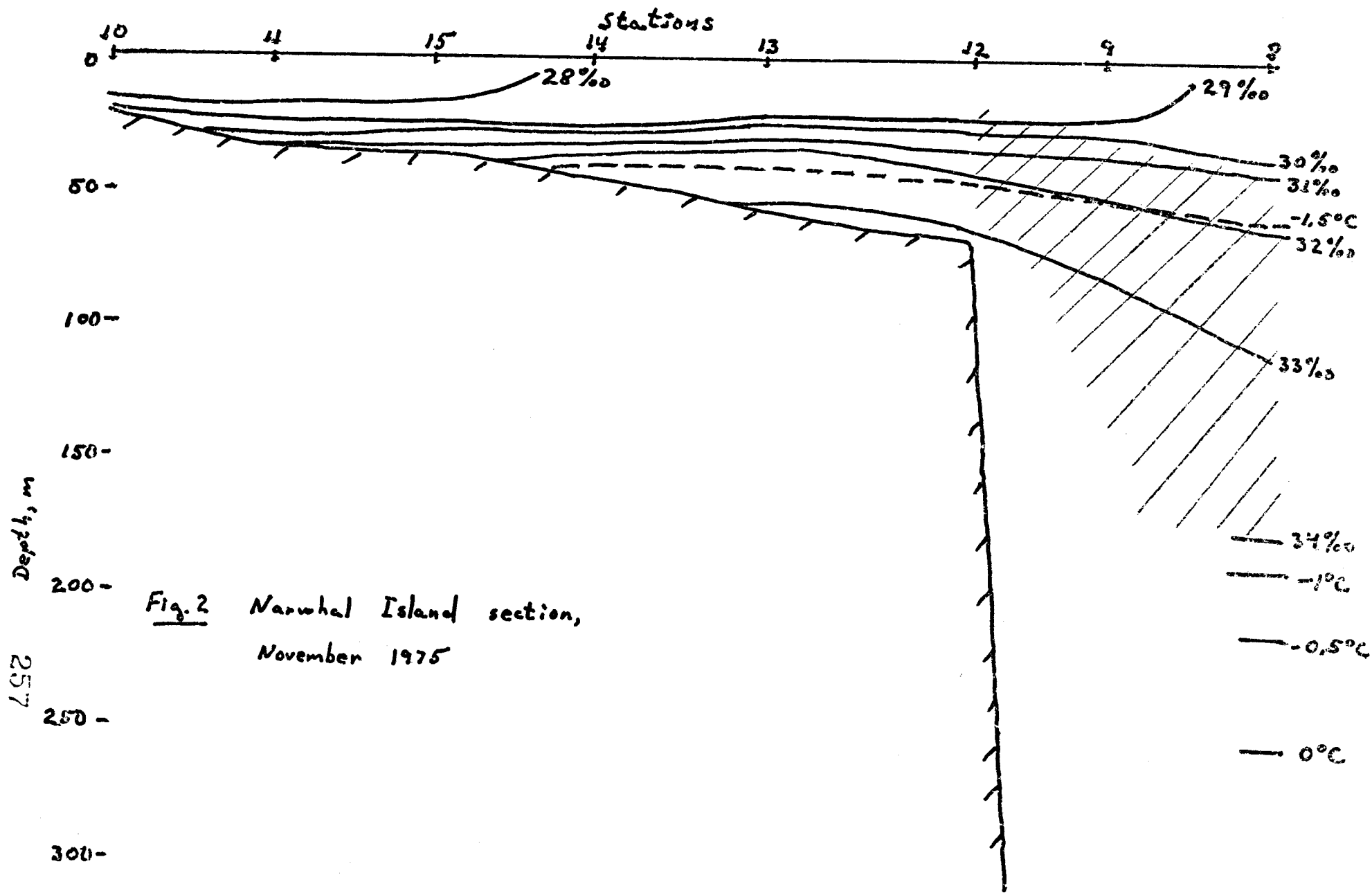


Fig. 2 Narwhal Island section,  
November 1975

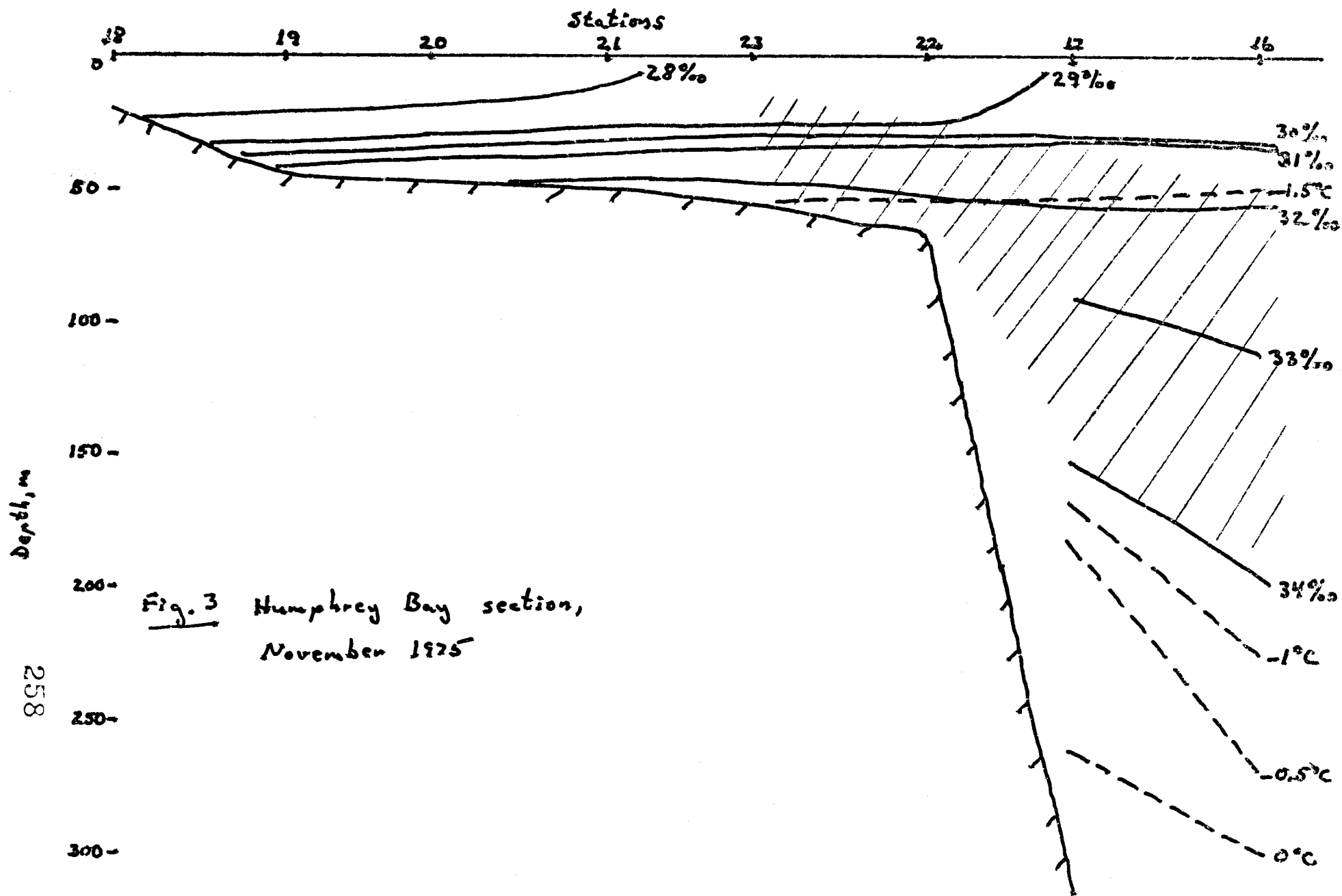


Fig. 3 Humphrey Bay section,  
November 1975



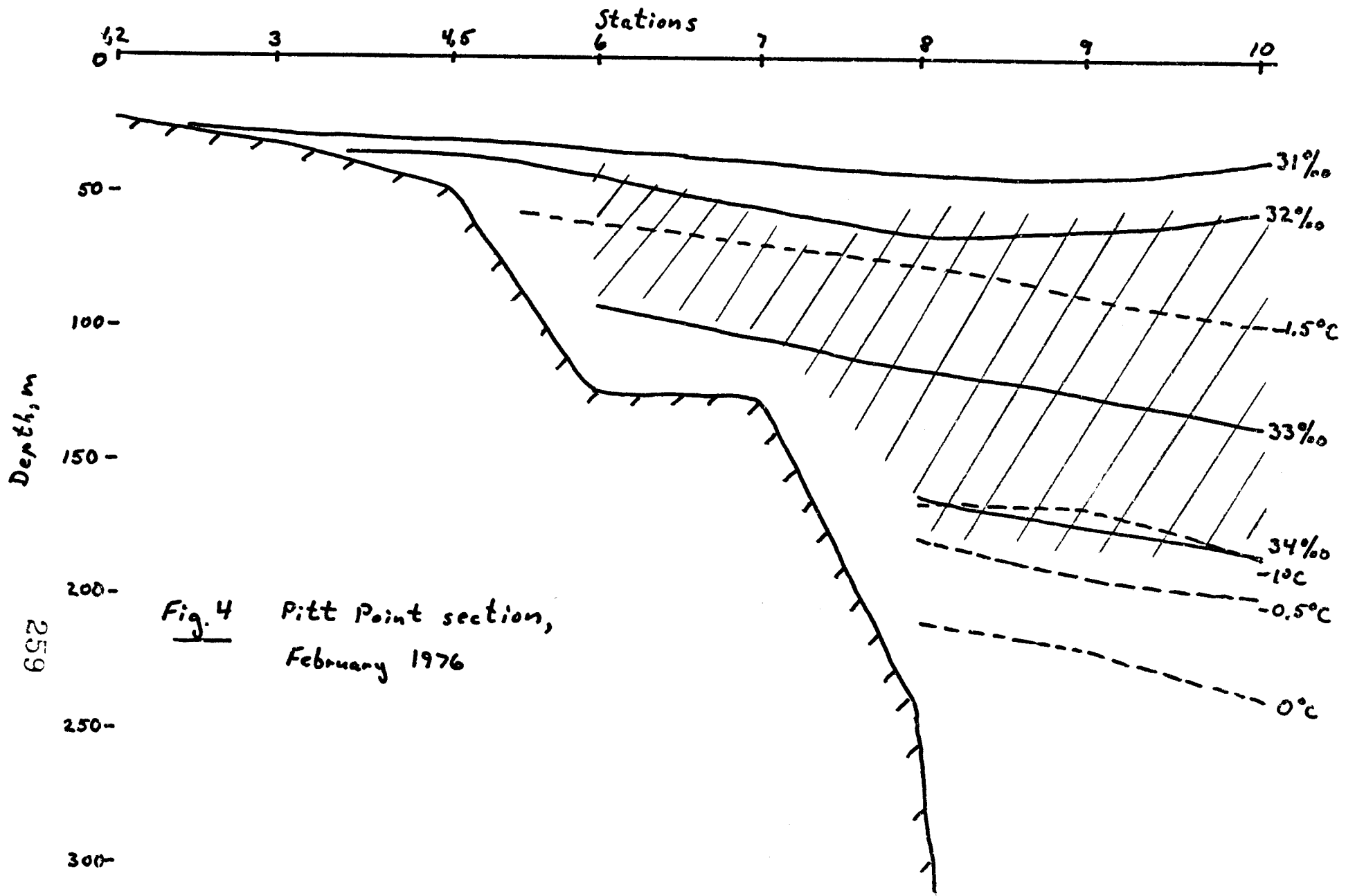


Fig. 4 Pitt Point section,  
February 1976

259

300-

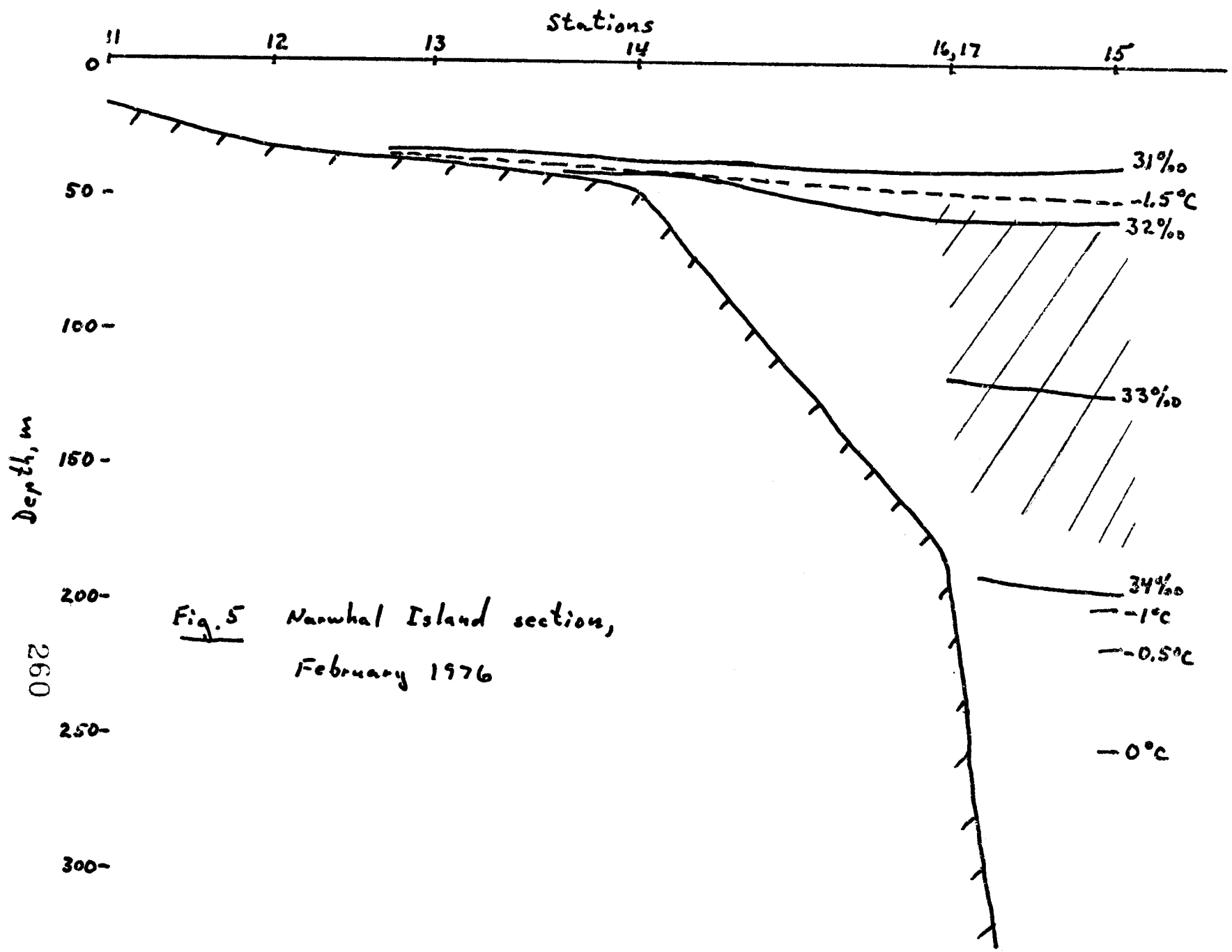


Fig. 5 Narwhal Island section,  
February 1976

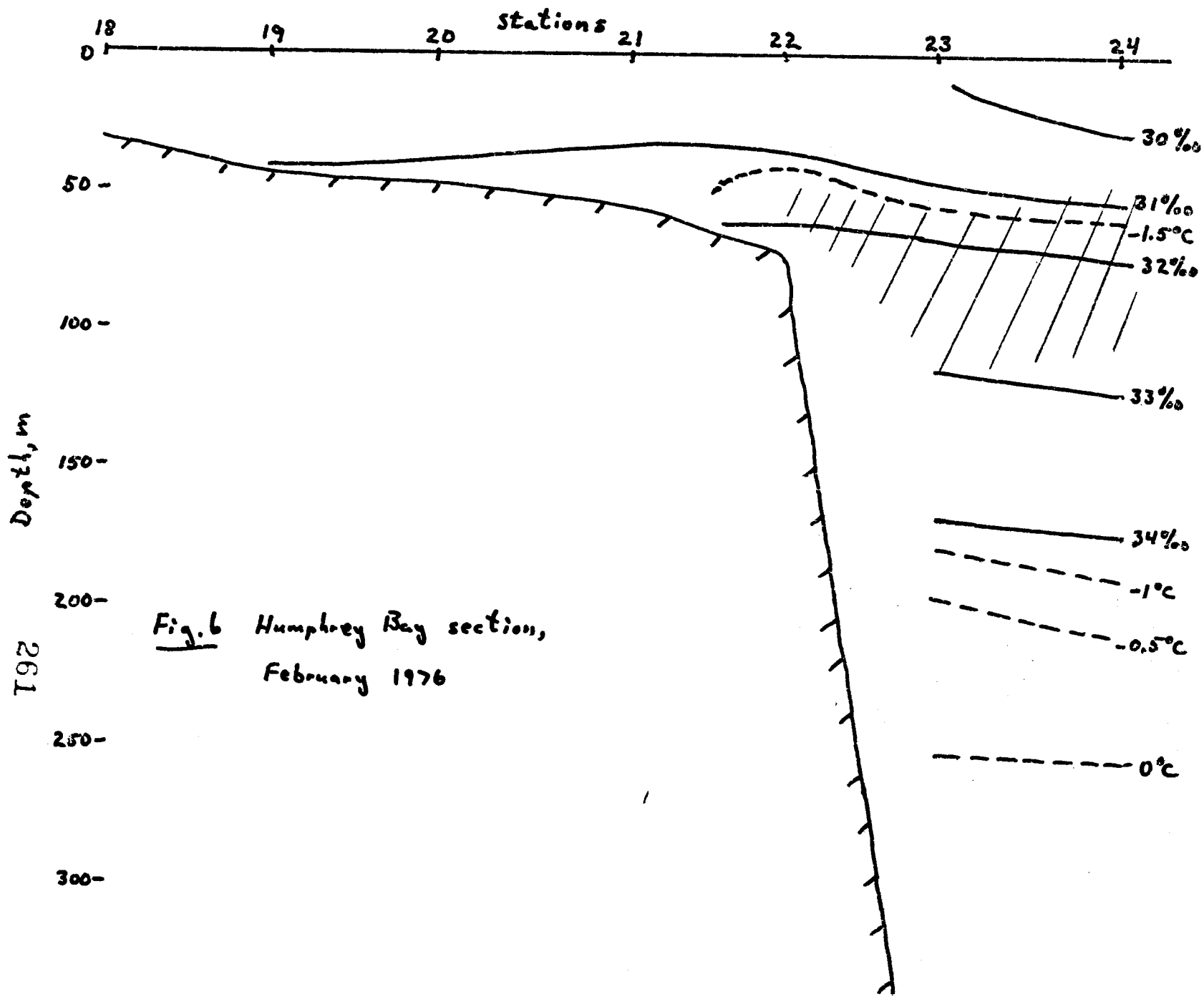


Fig. 6 Humphrey Bay section,  
 February 1976

261

layer was relatively low, being always less than 30%, and on the inner shelf considerably less than 28%. The salinity gradually increased seaward. These conditions are remnants of the summer hydrography. The near-bottom salinities were quite high, so that on the outer shelf the water was above 33% in the two sections farthest west. The temperatures in the upper layer were generally near the freezing point, but with some tendency towards a slight supercooling (relative to atmospheric pressure). With the exception of the Pitt Point section, the shelf waters were in their entirety within less than  $0.3^{\circ}\text{C}$  of being isothermal.

In winter the overall stratification on the shelf was markedly less. The upper more nearly homogeneous layer extended deeper than in the fall, typically below 30m. The salinity in the upper layer was higher, being above 31% everywhere on the shelf. In the two eastern sections the upper layer salinity decreased somewhat seaward. The near-bottom salinities on the shelf were in each section lower than during fall, except for the areas closest to shore. The water temperatures were typically lower by about  $0.1^{\circ}\text{C}$  than during fall, and in the upper layer the water showed a slight (on the average about  $0.03^{\circ}\text{C}$ ) but definite supercooling. The shelf waters were again within about  $0.3^{\circ}\text{C}$  of being isothermal, and this time at the Pitt Point section also.

The mean winter salinities over the shelf in the three sections are almost identical, being very close to 31%. In the two eastern sections the mean fall salinities are also similar, being in the range 29.5-29.7%, with the Humphrey Bay section the lower of the two. Over three and one-half months separate the fall and winter cruises, during which time one might expect in excess of 1 m of new ice to be formed. This amount is about right to account for the observed salinity increase at the two eastern sections.

However, in the Pitt Point section the mean salinity increased scarcely at all, with the mean value in fall having been 31‰, far above that of the eastern sections. An advective salt flux out of the region must therefore be invoked.

The dynamic topography is on the whole quite flat, as seen from the rather small isohaline slopes. The only very clear trend is a general seaward dip of the isopleths over the outer shelf and the slope. This appears in all the sections. Geostrophic calculations show an associated typical velocity on the order of  $10 \text{ cm sec}^{-1}$  westward at 50 m relative to 200 m. This probably represents the southwestern part of the Beaufort gyre which is intensified along the Alaskan coast. To the extent that dynamic calculations in the upper 20 m are meaningful, one can hypothesize an eastward movement in that layer over the shelf, but only during the fall cruise. This is based on the general increase in upper layer salinities (and hence densities) proceeding out across the shelf.

A very important feature of all the sections is the presence on the slope and near the outer shelf of a series of subsurface temperature inversions. An example is shown in Fig. 7, depicting the temperature between 68 and 156 m at station 8 from the winter cruise. This station was at about the shelf break on the Pitt Point section. There is a great deal of apparent interleaving, with typical temperature changes of  $0.06^\circ\text{C}$  over about 3 m. The fluctuations are centered around a value close to  $-1.5^\circ\text{C}$ . Particularly noticeable is the large absolute maximum at 125 m, underlain by a broad minimum near 140 m. These features are strongly reminiscent of the temperature extremes found throughout the Canadian Basin of the Arctic Ocean. In Figs. 1-6 the stations and depth ranges

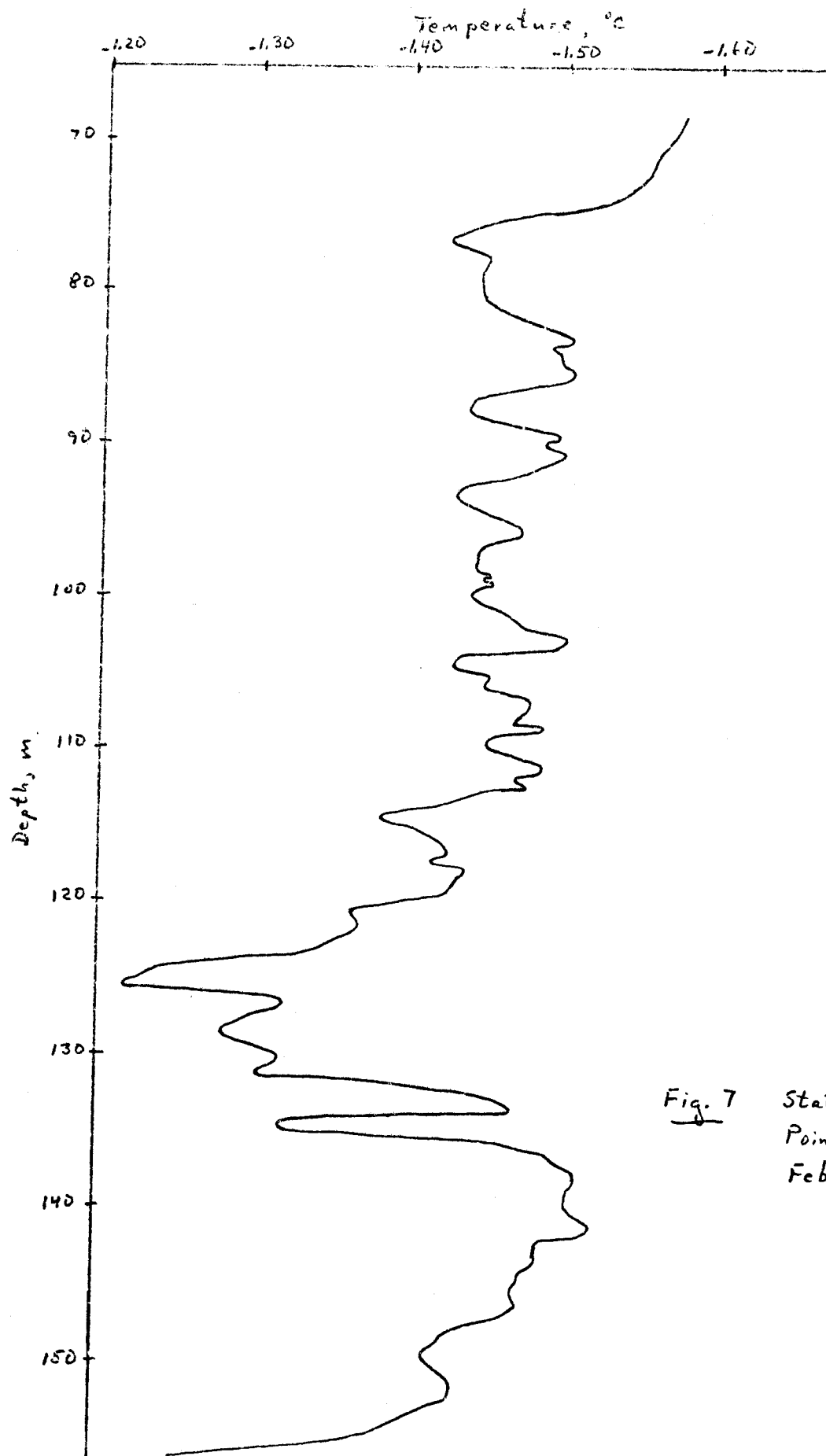


Fig. 7 Station 8, Pitt  
Point section,  
February 1976

for which a series of temperature inversions were observed are indicated by the hatching. Notice that in each case the area of temperature inversions sinks from the outer shelf down into the slope waters. In the fall Pitt Point section, the inversions were in fact present well onto the inner shelf which was occupied by relatively warm and high-salinity water, presumably of Bering Sea origin. These features all combine to strongly suggest that beginning in the fall, the north Alaskan shelf is in fact feeding water into the pycnocline region of the Arctic Ocean and contributing to the temperature structure which is characteristic of the lower Arctic Water of the entire Canadian Basin.

#### VIII. Conclusions

The general impression from the preliminary results discussed so far is of a region which oceanographically is much like the deep Canadian Basin itself. Undoubtedly this is associated at least in part with the very low runoff, which makes the Beaufort an atypical Arctic shelf sea.

It appears, however, that there is a regard in which the Beaufort shelf is of distinct and considerable oceanographic significance, viz. that it very likely constitutes a source of subsurface waters for the Canadian Basin. Should this indeed be the case, one could visualize the possibility of spreading a variety of substances from the shelf into the Arctic Ocean pycnocline. In other words, spreading from the shelf is not necessarily confined to the surface layers. The implications may be considerable.

#### IX. Needs for further study

The possible sinking and spreading of waters modified on the Beaufort

shelf into the Canadian Basin needs to be examined more carefully. At present I visualize a series of CTD sections between 154°-148°W, probably in conjunction with several current meter installations. These would begin in the fall.

X. Summary of fourth quarter operation

A. Field activities

The stations occupied on the winter cruise are shown in Table 2. The aircraft used was a Bell 205 chartered from ERA helicopters. The field party consisted of two persons, Knut Aagaard and Clark Darnall, both from the University of Washington.

B. Estimate of funds expended as of 5 March 1976.

|                                 |          |         |
|---------------------------------|----------|---------|
| 1. Salaries - faculty and staff |          | \$2,079 |
| 2. Benefits                     |          | 226     |
| 3. Indirect costs               |          | 911     |
| 4. Supplies and equipment       |          |         |
| 29 October report               | \$22,664 |         |
| CTD calibration                 | 500      |         |
| generator                       | 555      |         |
| miscellaneous supplies          | 3,710    |         |
| total supplies & equipment      |          | 27,429  |
| 5. Travel                       |          | 3,024   |
|                                 |          | <hr/>   |
| Total Expenditures              |          | 33,669  |



RU ~~217~~ #217

RECEIVED  
MAR 30 1976

NEGOA

ANNUAL REPORT

OUTER CONTINENTAL SHELF ENERGY PROGRAM

Dr. Donald V. Hansen  
NOAA/AOML  
Miami, Florida

26 March 1976

## ANNUAL REPORT - OCSEP

### I. Summary

This endeavor addresses Task B-2, Determination of Evaluation Patterns and Development of Knowledge Needed for Prediction of Transport of Petroleum Related Pollutants. The Lagrangian current data resulting from this effort will provide data for oil spill simulation scenarios and parameter adjustment criteria for numerical diagnostic models of surface flow in the OCS Gulf of Alaska region. The development of improved diagnostic models will allow prediction of pollutant trajectories based on the distribution of basic parameters. Also characteristic flow patterns will be discernable allowing for evaluation of petroleum development criteria based on projected pollutant impact zones. Due to hardware problems, the bulk of data expected of this project remain to be collected subsequent to 1 April 1976. Such data as have been collected prior to this time show that:

(a) Near surface currents in the area are to the west as expected, and sustained speeds on the order of one knot are not unusual.

(b) There is indication of very strong topographic influence upon the flow in that current trajectories tend to parallel isobaths, and shoal areas appear to have a lee eddy structure, as might also be expected of islands, that may tend to retain pollutants.

(c) Surface pollutants released in the area off Yakutat Bay are likely to go ashore on or east of Kayak Island within two weeks.

### II. Introduction

The general outline of this study is the acquisition of near surface flow trajectories throughout the entire N.E. Gulf of Alaska OCS region with particular emphasis on the lease area from Yakutat Bay to Prince William Sound. The device for acquiring this information is the NIMBUS-6 satellite and associated TWERLE/RAMS system. Satellite tracked buoys with projected one year operating capability are drogued to the

30 meter level of the water column. Concurrently the systems will be monitoring environmental parameters (wind speed, surface water temperature).

The resulting data products will consist of time series of geographic position, wind speed, sea surface temperature and drogue status. Derived data products will consist of Lagrangian velocity time correlation functions for the region on a seasonal basis for application to dispersion modelling. Lagrangian space correlations will be attempted, but are not likely to be well determined by the modest number of buoys. Correlations between environmental parameters and trajectory events will be compiled.

Two features of immediate relevance to petroleum development are contained in the data; input to numerical models and visually expressive current trajectories. Of these two features the input to numerical models is of the highest significance in that it will allow for better predictive modelling of current transports in areas of potential petroleum development. The characteristic flow trajectories, however, have high visual impact and are easily understood by lay and professional alike and therefore, are of substantial value in debate on the subject of potential petroleum spill impacts.

### III. Current State of Knowledge

Some small amount of circulation data is presently available for the Gulf of Alaska OCS. Prior to initiation of this project however no detailed Lagrangian data suitable for construction of pollutant projections based on Lagrangian statistics is available.

### IV. Study Area

The area of study is the Gulf of Alaska OCS, primarily in the region of the westward flowing coastal currents. The area of interest is loosely bounded by Yakutat Bay to the east and Kodiak Island to the west in the coastal portion of the Gulf of Alaska gyre.

#### V. Sources, Methods, and Rationale of Data Collection

A buoy is in view of the NIMBUS-6 satellite for about three orbits twice a day. This usually results in two to four valid positions per day. The parameter measurement is derived from count information between successive orbits. The counters increment at a rate proportional to the parameter sensed, therefore, the resultant information represents an integrated or averaged value of the parameter history between passes.

The buoy identification, time, doppler information, and count totals are relayed from the satellite reviewing stations, to Goddard Spaceflight Center where the position and count data for the system user are determined. The user then converts the data into time series of position and parameters for further analysis.

As a general statement, the currents along the OCS Gulf of Alaska region are to the west, therefore, the buoy deployment area is at the eastern limits of the area. The first buoy deployments were at the extreme eastern limits of the area in the lee of Fairweather Ground. Future deployments will be somewhat further west to avoid lee effects and provide information more typical to the OCS region. Deployments are made in groups of three buoys on a quarterly scale. This procedure will allow seasonal development of seasonal Lagrangian statistics.

#### VI. Results

To date five buoy systems have been deployed with successful data reception on two. This is not an impressive record. However, the failure modes identified and redesign affected for the OCS deployment have affected system designs not only for this Gulf of Alaska effort, but the world wide deployment as well. The program to date has resulted in two revised versions of packaging systems for improved transport survival, has revealed a generic problem in the early systems, and has exposed design weaknesses in the second generation system. The third

generation systems and corrected second generation systems will be available for the remainder of the operation. The final result will be a system capable of surviving both severe transit and environmental conditions.

The two successful buoy deployments resulted in 24 buoy days of position and environmental data. These buoys were deployed ten miles to the lee of Fairweather Ground on September 12th. The innermost buoy resided in the lee of the eastern portion of Fairweather Ground for about a day with little net motion, yet exhibiting a tight eddy motion with speeds of about one knot around the eddy perimeter. During the second day the buoy became entrained in a coastal jet-like current issuing between the coast and Fairweather Ground. The coastal jet seems to be physically constrained to a 10-mile width where it passes between the coast and the Ground. For the next nine days the buoy appeared to reside in the coastal jet and paralleled the fifty fathom curve in its course. Buoy speeds during this period were of the order 0.3 knots for the first five days and one knot until September 22nd. Then the trajectory departed radically from its previous history and moved directly inshore until it was running westward within five miles of the beach. Even with the proximity to the beach the buoy was moving with speeds of 0.7 knots.

During this same period the buoy deployed at the western edge of the bank seemed to be trapped in an eddy-like feature in the lee of the bank. This eddy motion consisted of two complete circuits of 15 miles in length and 10 miles in breadth with daily average speeds in excess of one knot at times. Upon completion of the second circuit the buoy moved eastward to the opposite edge of Fairweather Ground at which point it was trapped in a small eddy for a brief period before being entrained in the coastal jet current like the other buoy. Buoy speeds while in the coastal jet were generally less than 0.5 knots.

Parameter returns were approximately 70% complete. Two full histories of load cell tension, two partial histories of wind speed, and one temperature record were obtained. Wind records were obtained for the first ten days of drogue history, then both units failed. There was sufficient information returned, however, to indicate the passage of two significant weather events. Temperature data were obtained only for the eastern buoy. Sea surface temperatures were essentially constant at 11.5°C with slight variation throughout the drift. Significant cooling was noted near the end of the record reflecting the presence of somewhat cooler water very close inshore.

#### VII. Discussion

The trajectories indicate a definite lee effect to circulation behind Fairweather Ground. This can lead to entrapment of surface born contaminants for some period of time behind the shoals before entrainment in the coastal flow. Flow between the Ground and the coast appears to be intermittent with substantial variation in speed, 0.5 to 1.0 knots. Flow issuing from the region tends to reflect bathymetric control quite strongly. Around day 262 (Sept 19) events in drogue tension histories indicate substantial reduction in drogue effectiveness, the effect of which indicates that true surface flow is carried to shore. The flow in the immediate vicinity of the coast appears to be longshore to the west; and any surface contaminants would be distributed along the coast from Icy Bay to Cape Suckling or Kayak Island. Nothing can be said from these data of the currents west of Kayak Island.

The period of observation was characterized by short duration storms, three days duration, with brief periods of moderate winds, one to two days, between the storm events. This type of weather pattern is characteristic for the time of year of the observations.

VIII. With only two relatively short trajectories at hand it is premature to draw sweeping conclusions, but the observations described

above suggest that surface pollutants on the continental shelf off or west of Yakutat Bay are likely to go ashore to the west within two weeks.

IX. A continued observational program is required to obtain enough information to characterize the Lagrangian flow in the region. The observational program is only 25% complete at this point due to re-engineering required for equipment survival in the harsh environment. Revisions in production schedules should allow all deployments to be complete by September 1976 and most of the relevant information should be in hand by December 1976. It is expected that improved buoy design will improve the system lifetimes to the point that interchange between the Gulf of Alaska and the North Pacific circulation will be viewed. Future deployment sites will provide improved opportunity to utilize the improved lifetimes and concurrently provide more data characteristic to the region of immediate OCSEAP interest. The sites are such that the systems should track through the highly instrumented region of Icy Bay and flow westward along the coast, eventually joining the Pacific regime. A region of intense interest should be sampled as the buoys pass by Kayak Island. If there is exchange between eddy flow behind Kayak Island and the general Gulf of Alaska circulation, this exchange may be reflected in the trajectories as the buoys pass by Kayak Island.

During discussions with the scientific steering committee, it was determined that deployment in the southeast Bering Sea of whatever small number of buoys could be arranged would be of great benefit to the project in that area. It has now been established that these additional buoys can be obtained, and Dr. Butler has given verbal assurance that the required additional funding will be provided, so this additional activity is underway.

It was recommended also that in future deployments, some buoys should be dropped further offshore in order that they may pass more

closely to certain current meter moorings, and so that they will be able to sample currents farther to the west.

The deployment schedule presently planned for the remainder of the project is as follows:

| <u>Time</u> | <u>Area</u> | <u>Ship</u>    |
|-------------|-------------|----------------|
| 5/05-14     | GOA         | DISCOVERER     |
| 3/25-6/18   | Bering      | MAUNA WAVE     |
| 7/12-24     | GOA         | DISCOVERER (?) |
| Sept/Oct    | GOA         | ?              |

X. Fourth Quarter Operations Summary

1. NOAA Ship DISCOVERER, November 1975.
2. D. Pashinski, NOAA/AOML, Program Representative
3. NIMBUS-6 Satellite tracked drifting buoy systems.
4. OCSEAP-Gulf of Alaska, off Yakutat Bay.
5. Two of three systems were deployed. No data were collected due to premature failure of the system resulting from a design defect. The third system was returned to the manufacturer for failure analysis.

March 25, 1976



RECEIVED  
MAR 12 1976

Progress Report

NEGOA

Research Unit #235

Reporting Period

1 July 1975 to 1 April 1976

17 pp.

PREPARATION OF HYDRODYNAMICAL-NUMERICAL  
AND 3-PARAMETER SMALL-MESH ATMOSPHERIC MODELS  
FOR COASTAL WATERS IN GULF OF ALASKA

Principal Investigator  
T. Laevastu  
Naval Environmental Prediction Research Facility  
Monterey, California 93940

15 March 1976

# HYDRODYNAMICAL-NUMERICAL OCEANIC AND SMALL-MESH ATMOSPHERIC MODELS FOR THE GULF OF ALASKA

## I Summary

The objectives of this research unit are (1) to program numerical models for analysis/prediction of currents, sea level change (e.g. tides), surface winds and advection and (2) diffusion of pollutants in real time for use in various oil exploration problems, drilling operations, and shipping.

Three two-layer Hydrodynamical-Numerical (HN) models with overlapping boundaries have been programmed, covering the Alaskan coast of the Gulf of Alaska. The principal inputs of these models are tides (at the open boundaries), wind, "permanent" (thermohaline) current and any release of pollutants. The principal outputs (either as time series at given locations, or as instantaneous area outputs at any given time) are currents, sea level and distribution of pollutants.

The small-mesh meteorological model has been programmed to obtain detailed surface wind analyses/forecasts. It takes the boundary conditions from a "standard" hemispheric analysis/forecast. Also available are spectroangular wave and surf forecasting models, though these were not part of this work unit.

The above models are ready and preliminary outputs have been obtained. Some additional tuning of the open boundary treatment is necessary. Furthermore program documentation and running instructions must be written.

## II Introduction

This research unit is for numerical modeling of the coastal ocean and the near-surface layer of the atmosphere. The applied aim of this research is to produce numerical models for operational purposes such as for prediction of wind currents, movement of oil spill and related environmental parameters. Additional requirements are that the models must be capable of not only the reproduction of "normal" conditions and processes, but also of more rare and violent events. The models must be ready for specific applications with minor specific inputs which are available in routine synoptic observations.

## III Current State

At present, the HN models (of which there are three slightly different types available) are the only numerical models which have reproduced the relatively complex condi-

tions and processes in coastal areas with satisfactorily verifiable results. Therefore a multilayer HN model was adapted to achieve the objectives of this research unit. Among the more difficult problems in this work were the treatment (prescription) of open boundaries and of open, overlapping boundaries, and the prescription of the "permanent" (thermohaline) current. These problems have been solved satisfactorily, though further tuning with real data is needed.

Excluding the tides, the other major driving forces of the ocean are of atmospheric origin (e.g., surface winds). It is necessary to introduce these driving forces into the HN models in detail, especially during rare violent events (storms). The conventional numerical hemispheric atmospheric models (grid size 380 km at 60° N) do not satisfactorily reproduce the mesoscale conditions and processes near the coasts and at atmospheric fronts. Therefore, a small-mesh baroclinic atmospheric model was adapted for the Gulf of Alaska. The boundary and initial conditions for this model are extracted from hemispheric analysis/forecasts and the small-mesh model is used for up to 48-hour forecasts. Surface winds for input into HN model are extracted from this small-mesh atmospheric model.

#### IV Results

The numerical models have been programmed, debugged and preliminarily tuned. Example outputs have been provided to Mr. M. Pelto NOAA/OCSEAP-Juneau Project Office. Furthermore, small-mesh atmospheric model deck and preliminary documentation have been provided upon request to Environment Canada, Western Regional Office, Vancouver.

Figures (1 to 15) of the computational grids and some examples of outputs from the models are appended to this report. Outputs can be taken at any number of selected points in the form of a time series, or as instantaneous area outputs at any specified time interval. It should be noted that outputs for research or operational purposes should be taken as numerical computer printout rather than Varian (or Calcomp) plots. The latter are especially unsatisfactory in respect of pollution (e.g., oil spill) distribution, as some of the enclosed figures indicate.

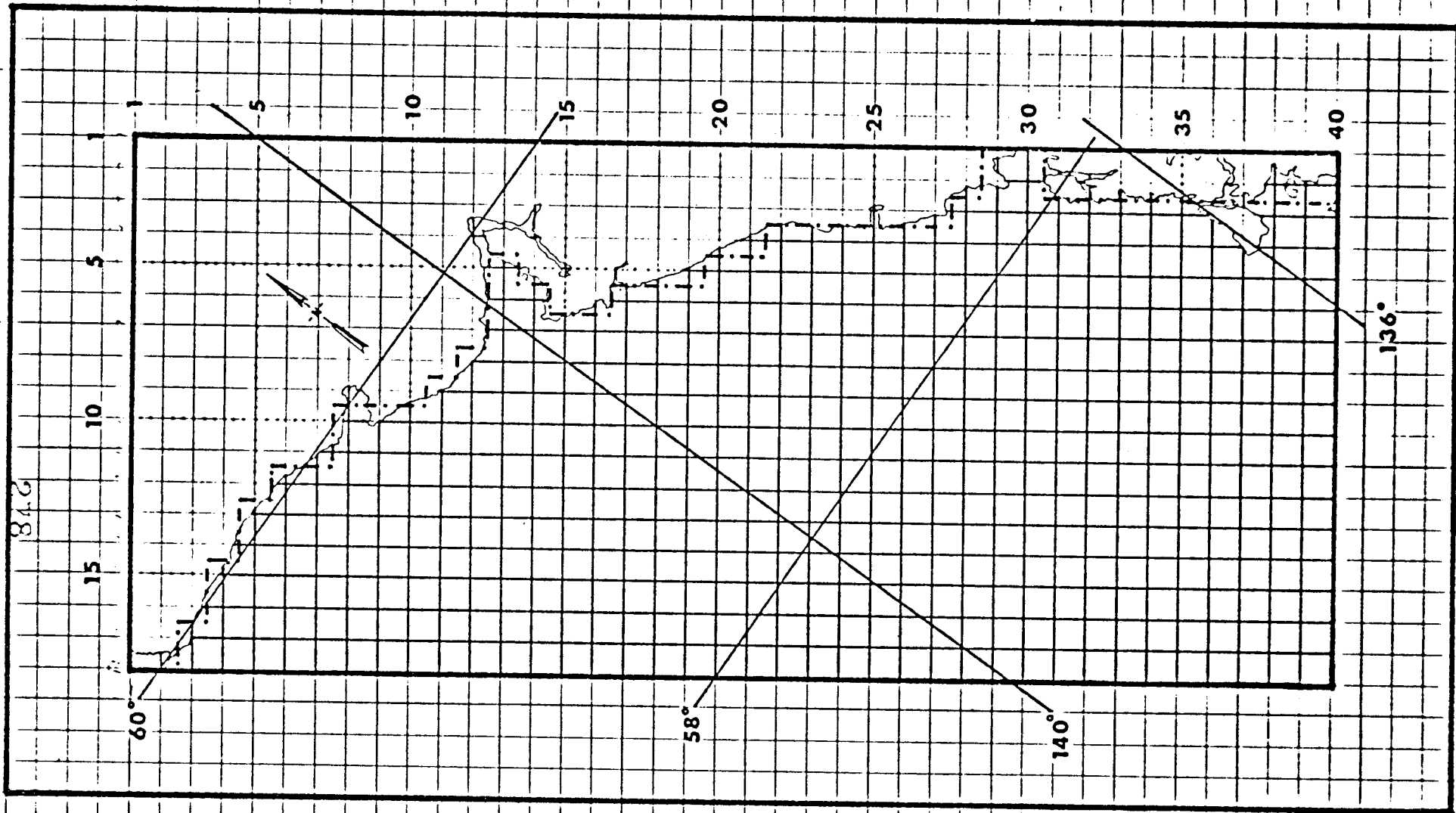
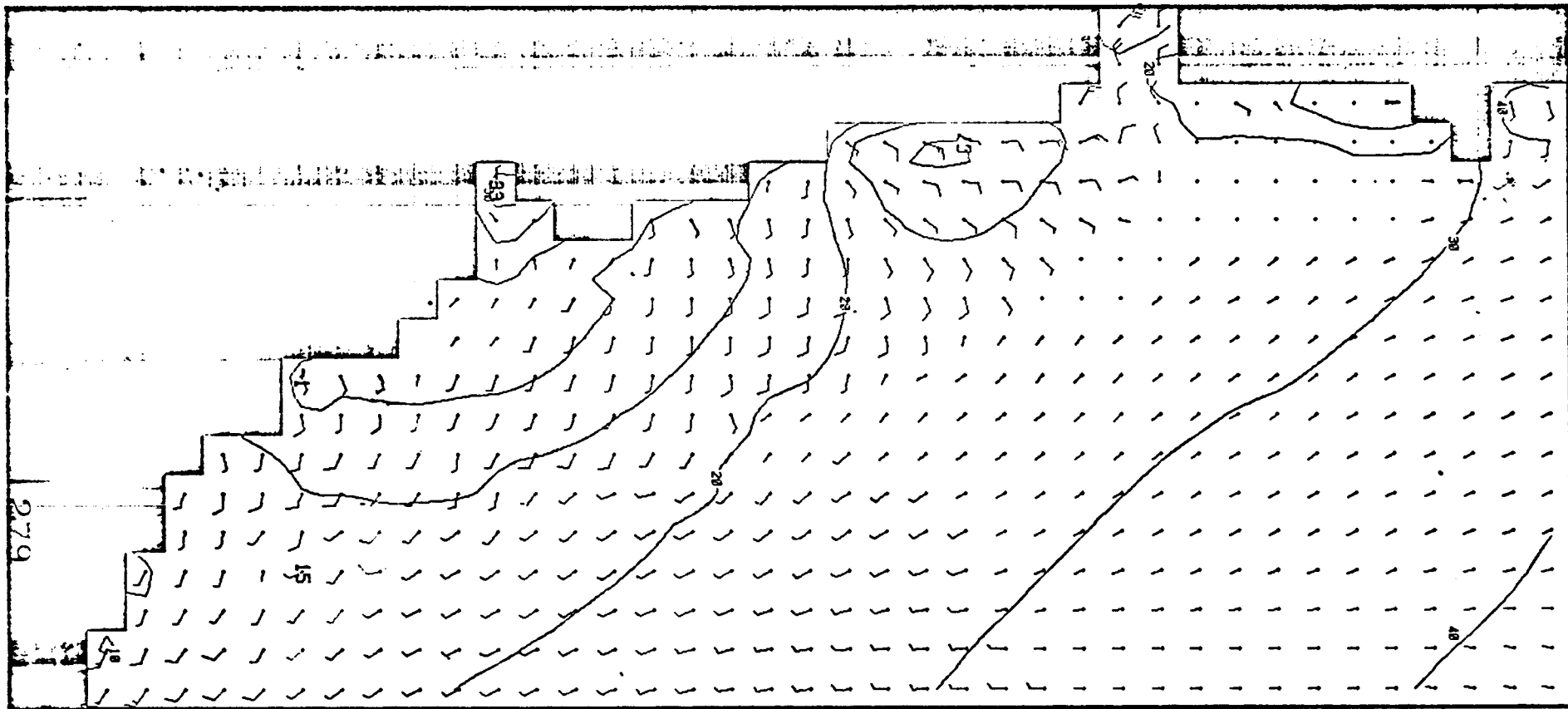
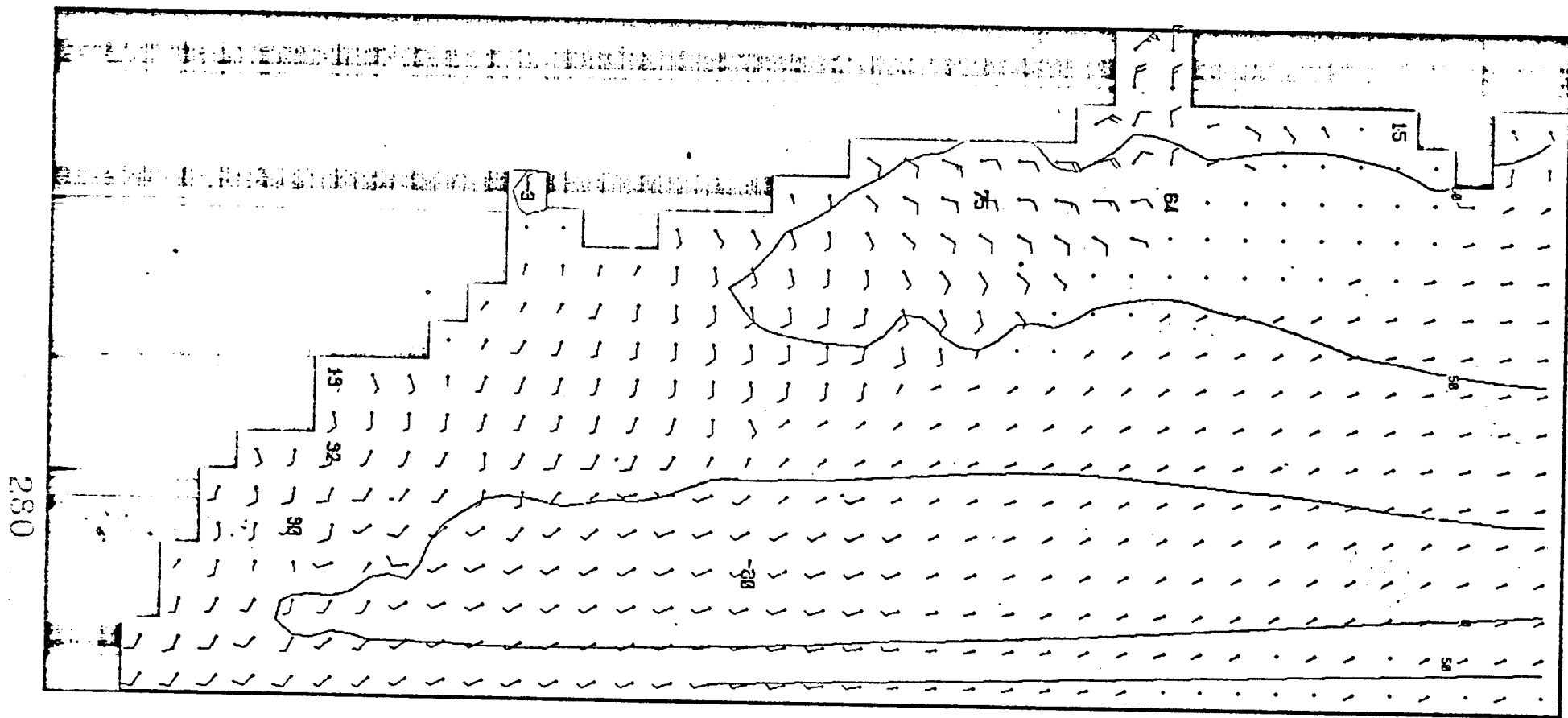


Fig. 1 Computation grid for BLM-1



LAYER 1. TIME(S.) 54000.

Fig. 2 Example of instantaneous surface currents and sea level (tides) output; BLM-1



LAYER 2. TIME(S.) 54000.

HR 15

Fig. 3 Example of instantaneous "second layer" currents and thermo-  
cline depth change output; BLM-1

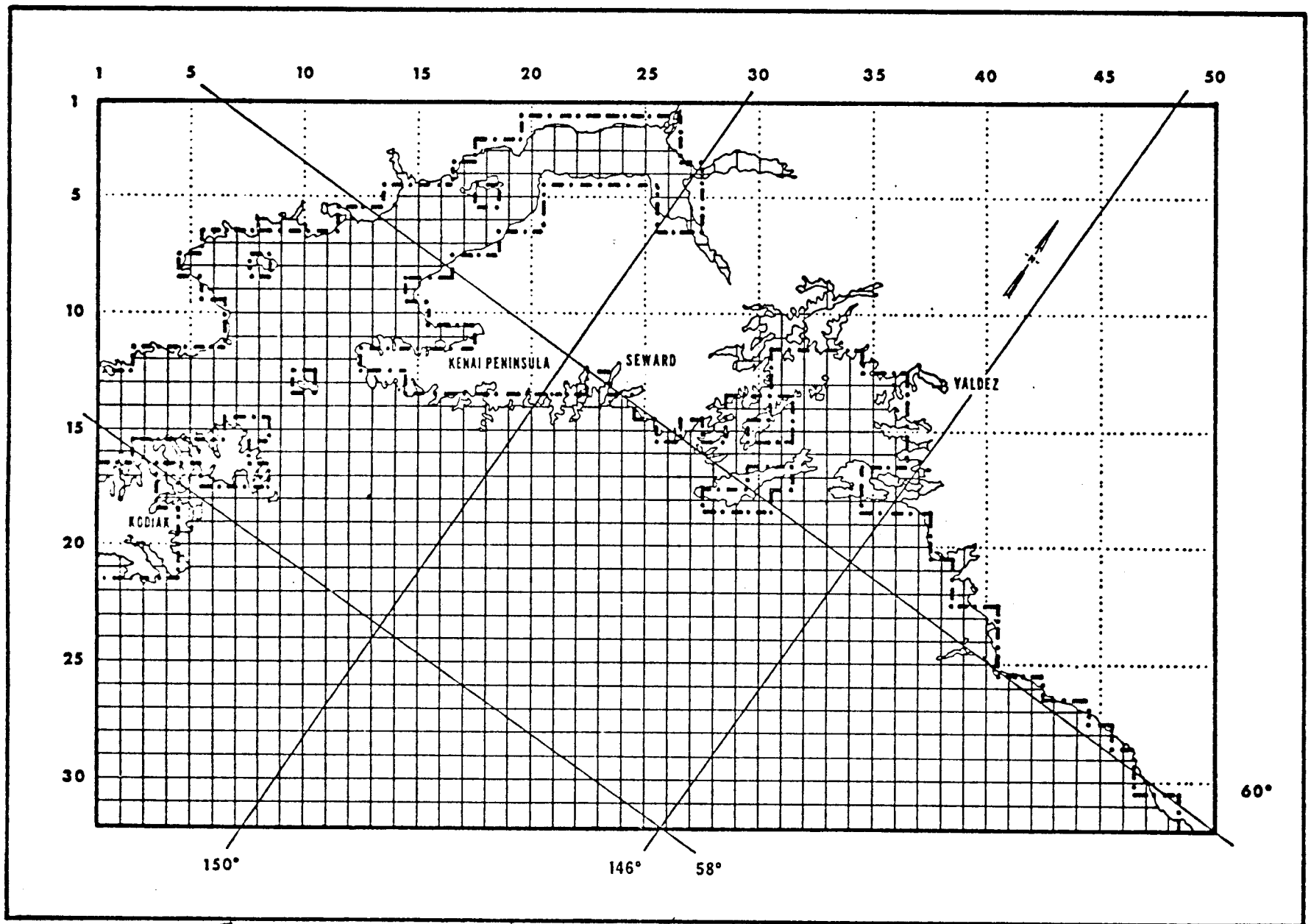
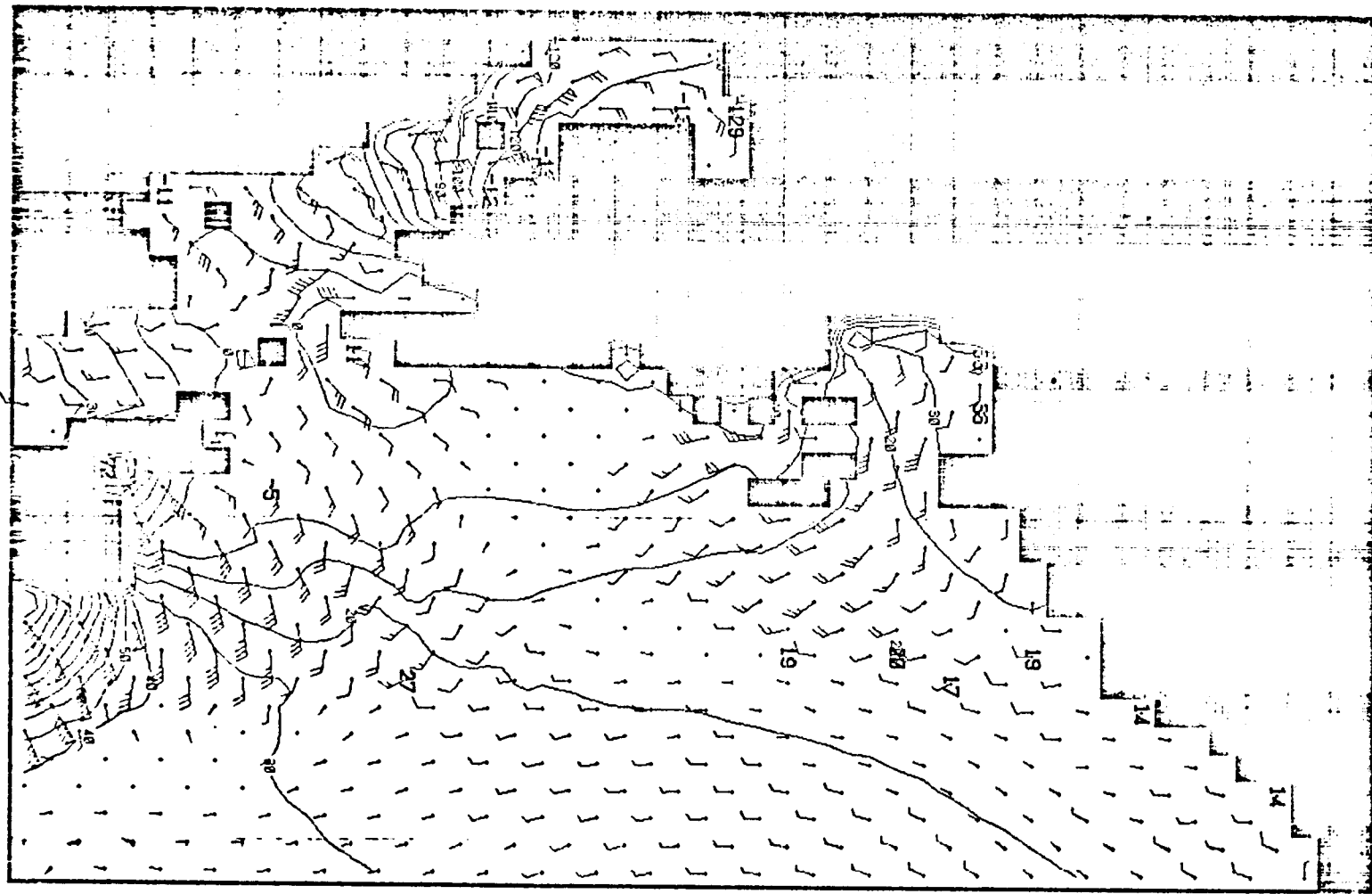


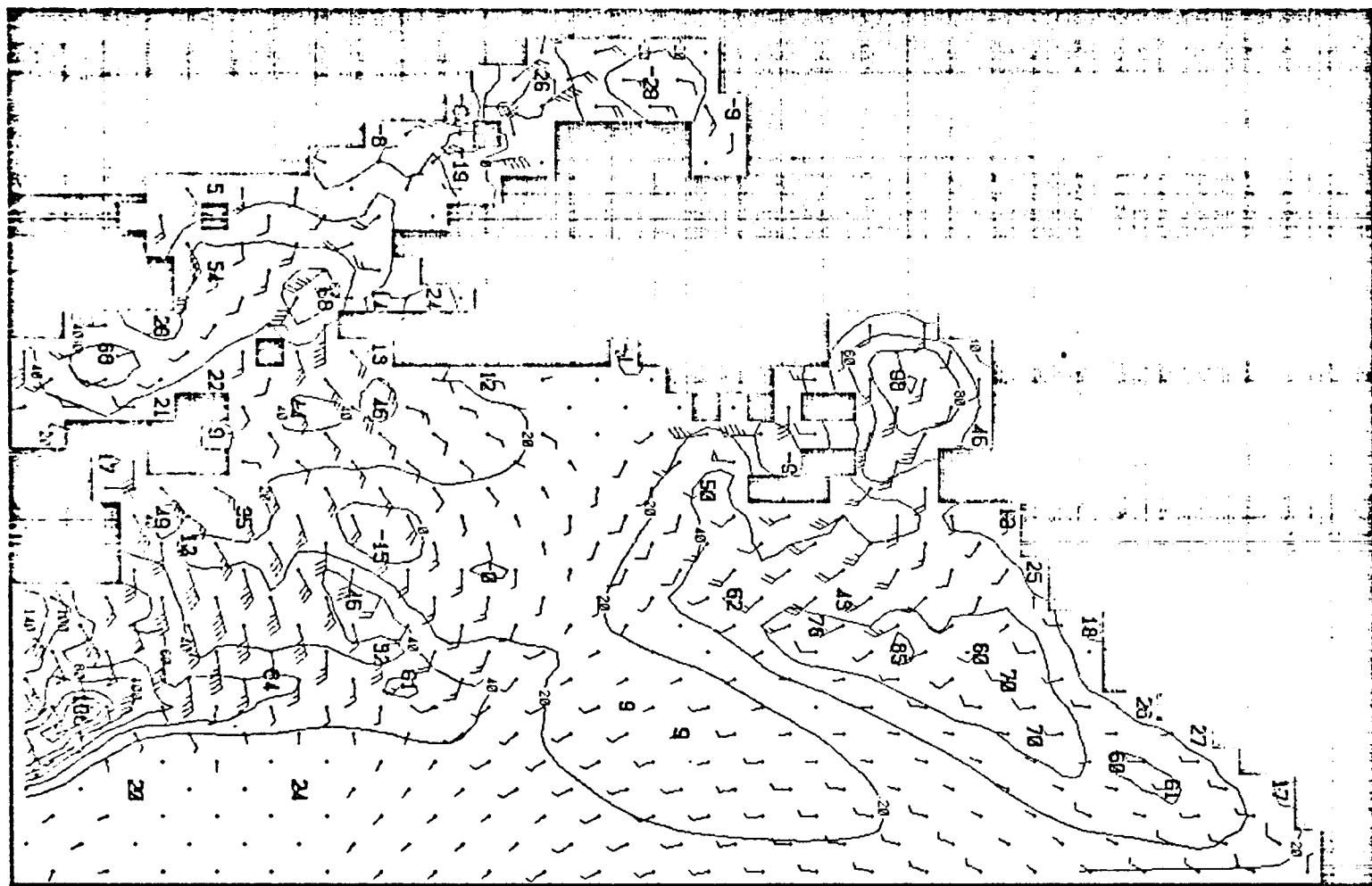
Fig. 4 Computation grid for BLM-2



LAYER 1. TIME(S.) 144000.

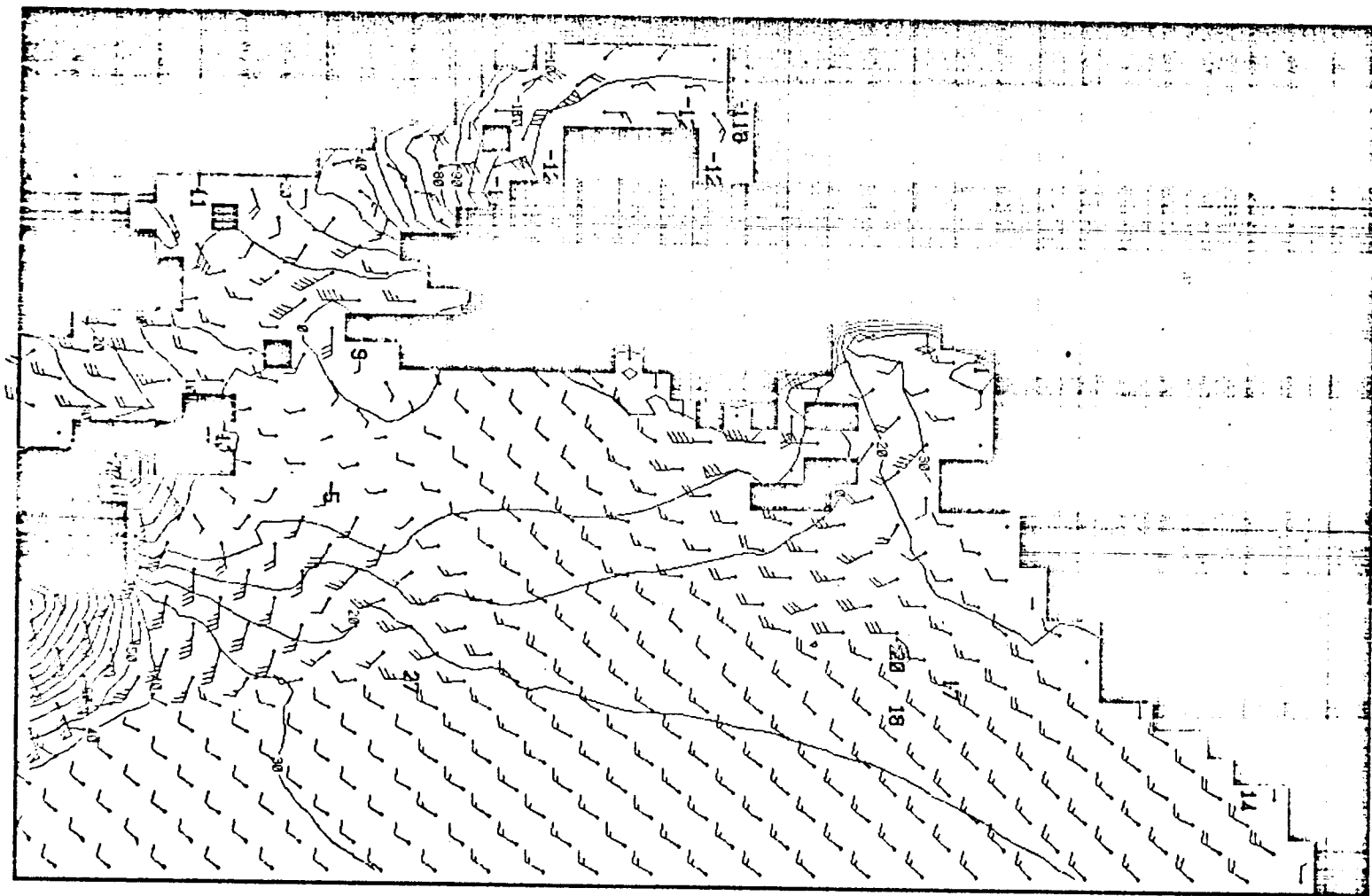
*Fig. 5 Example of sfc currents and tides; BLM-2 (no wind)*





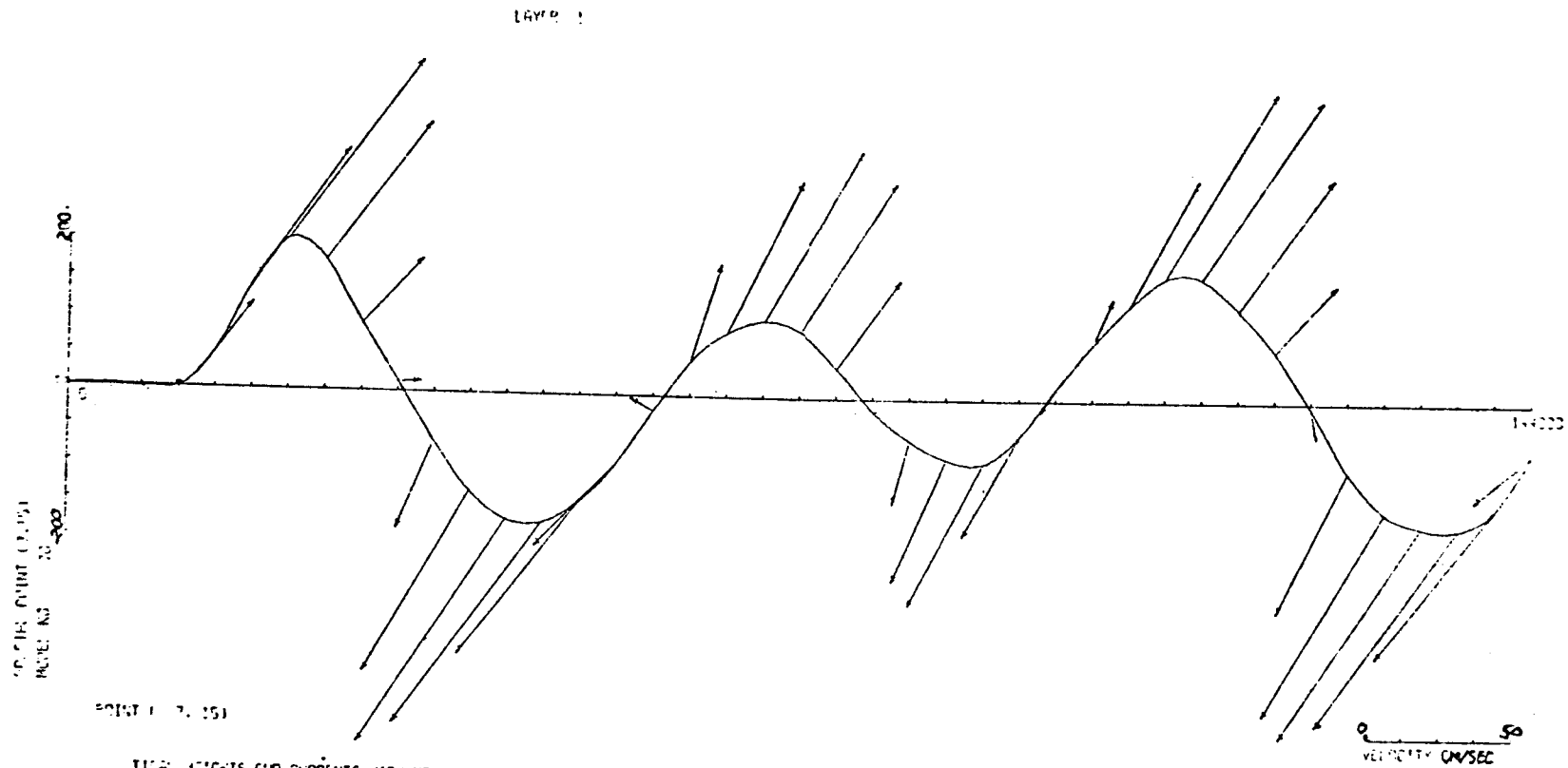
LAYER 2. TIME(S.) 144000.

Fig. 6 Example of "second layer" currents and MLD change,  
BLM-2 (no wind)



LAYER 1. TIME(S.) 144000.

Fig. 7 Example of sfc currents and tides; BLM-2  
(wind 10 m/sec from S)



TIDAL HEIGHTS AND CURRENTS WITH NO WIND  
 GULF OF ALASKA - BLAKE SPAD COOK INLET, SEWARD, AND VALDEZ

ANAHEIM, CALIFORNIA CHART NO. 99

NOV 1966

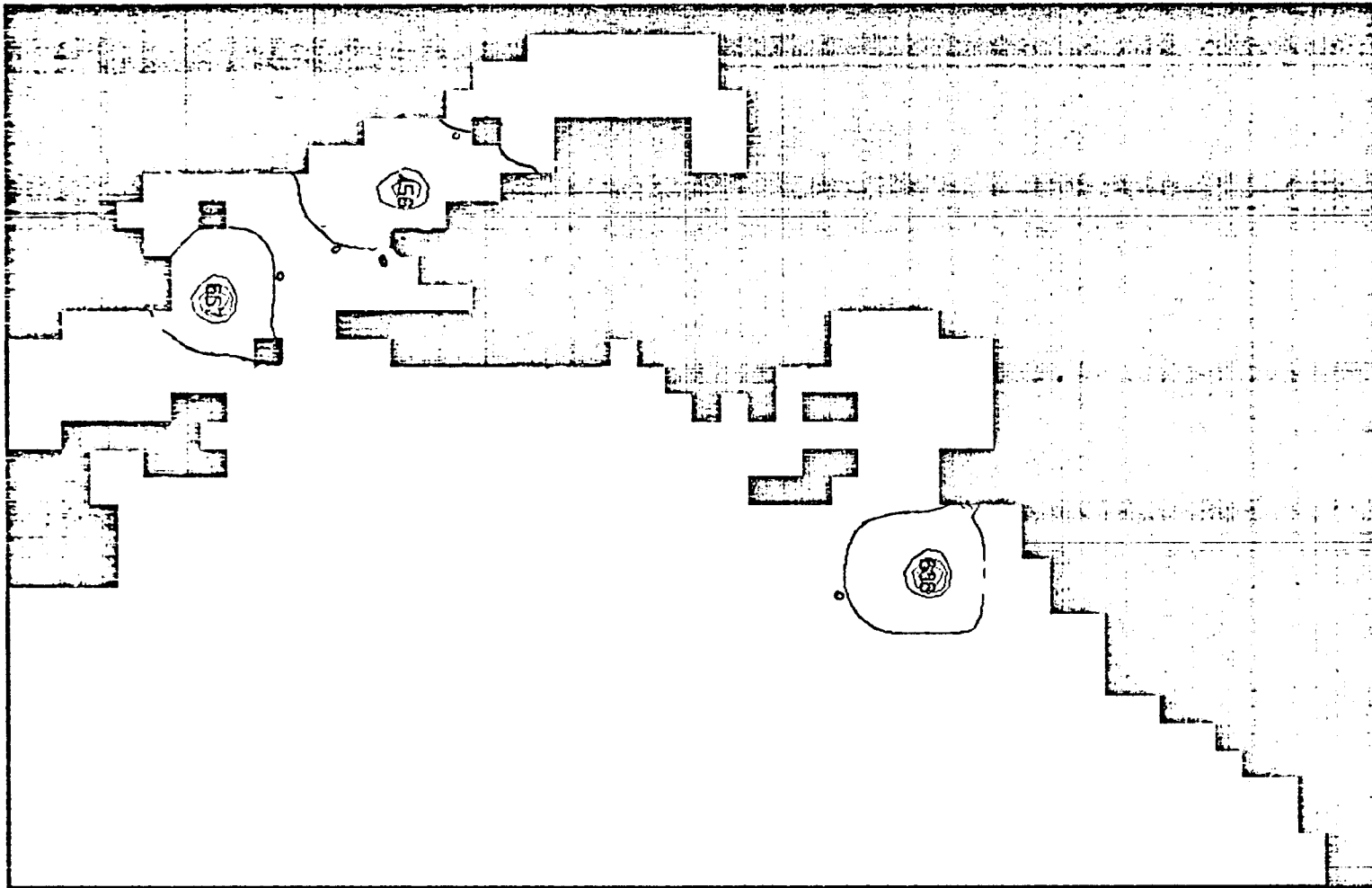
CALIFORNIA COMPUTER PRODUCTS, INC., ANAHEIM, CALIFORNIA CHART NO. 99

PLOT NO. 114

007

CALIFORNIA COMPUTER PRODUCTS

Fig. 8 Example of tides and currents at a point  
 in Cook Inlet



LAYER 1. TIME(S.) 144000.

*Fig. 9 Distribution of "pollutants" from three continuous release points after a full tidal cycle.*

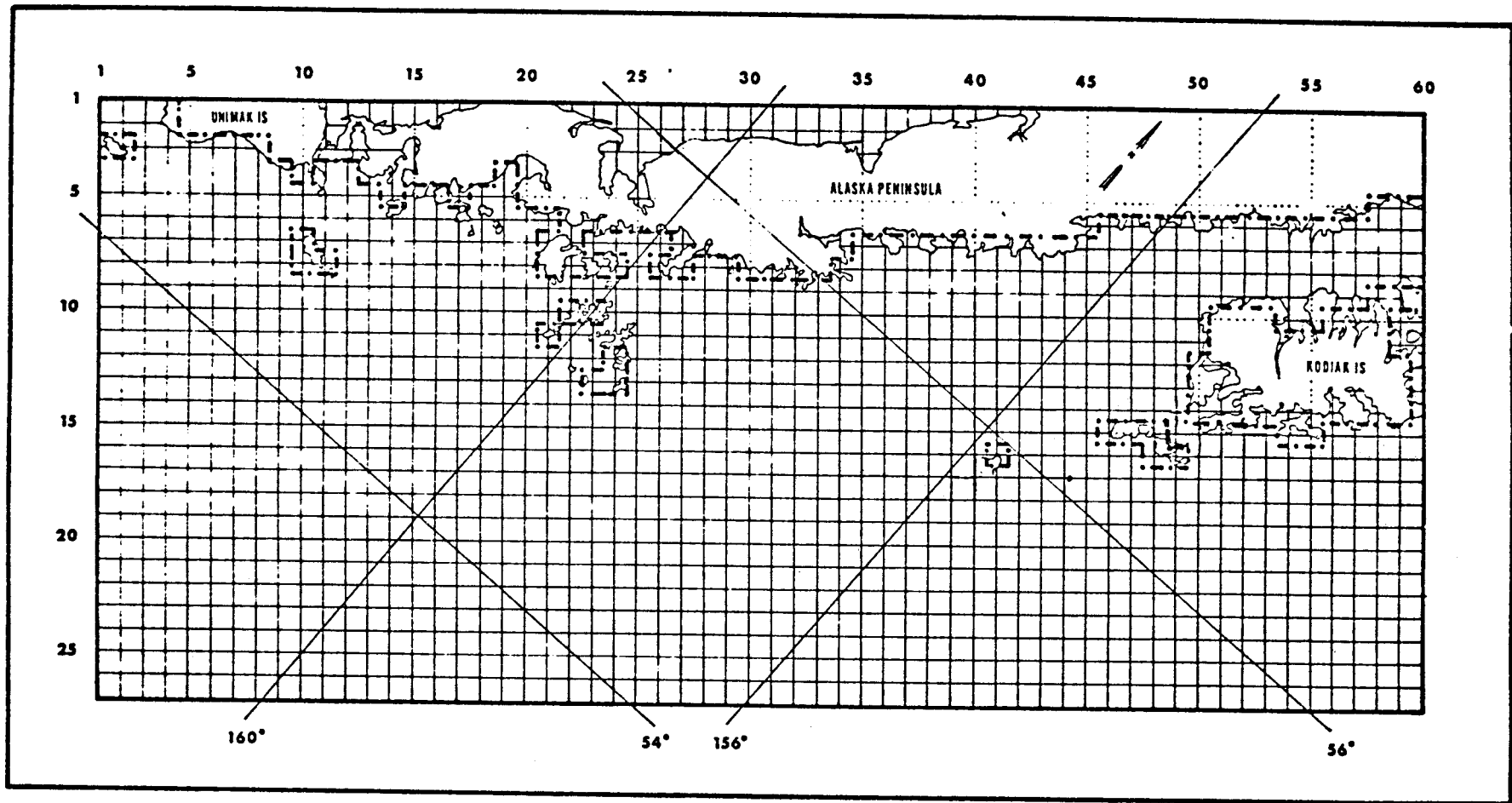


Fig. 10 Computation grid for BLM-3

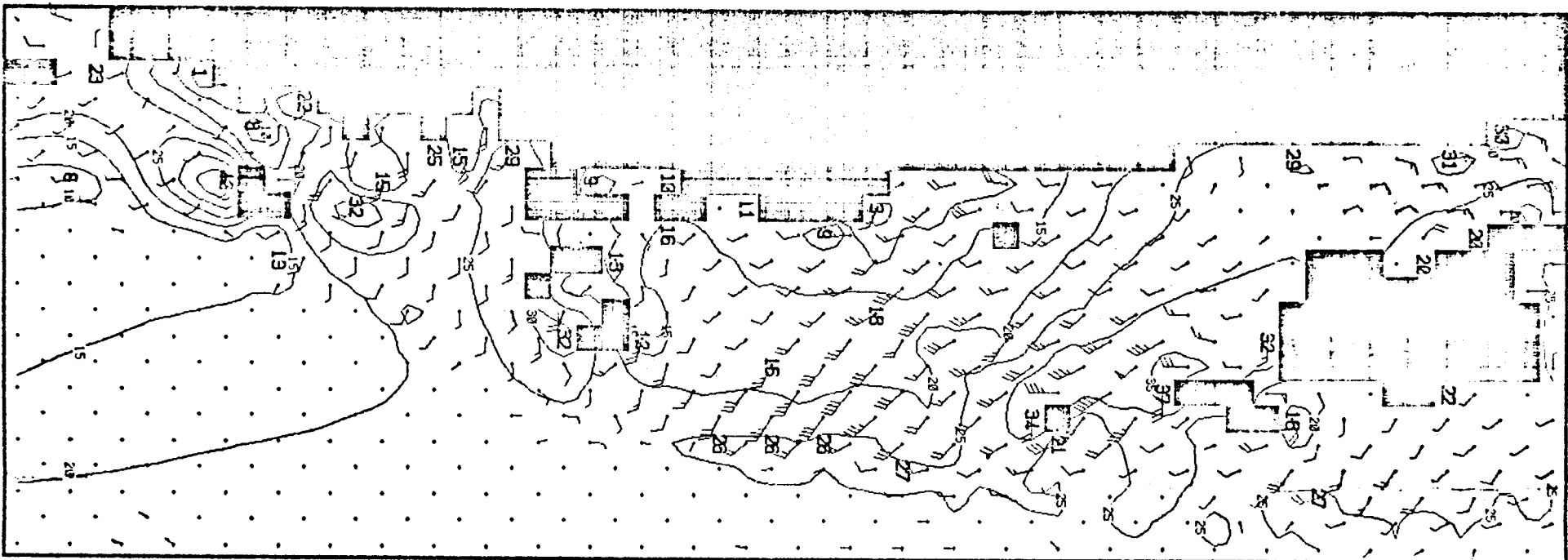
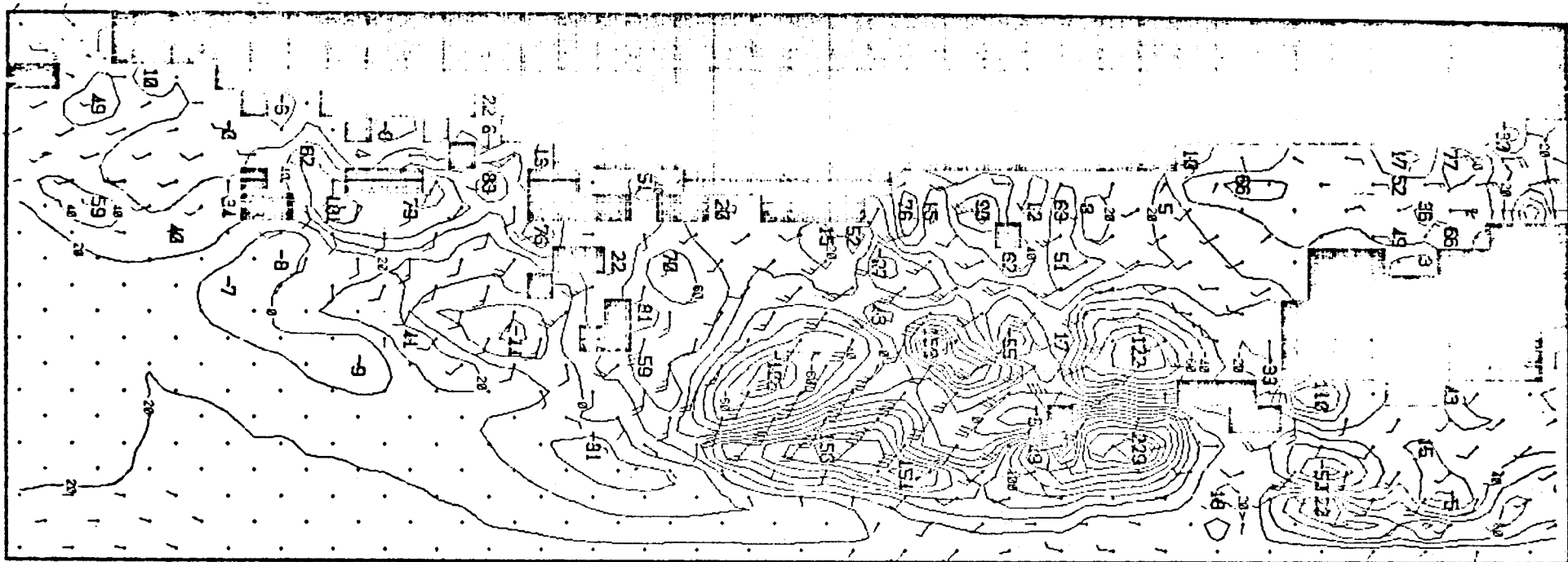
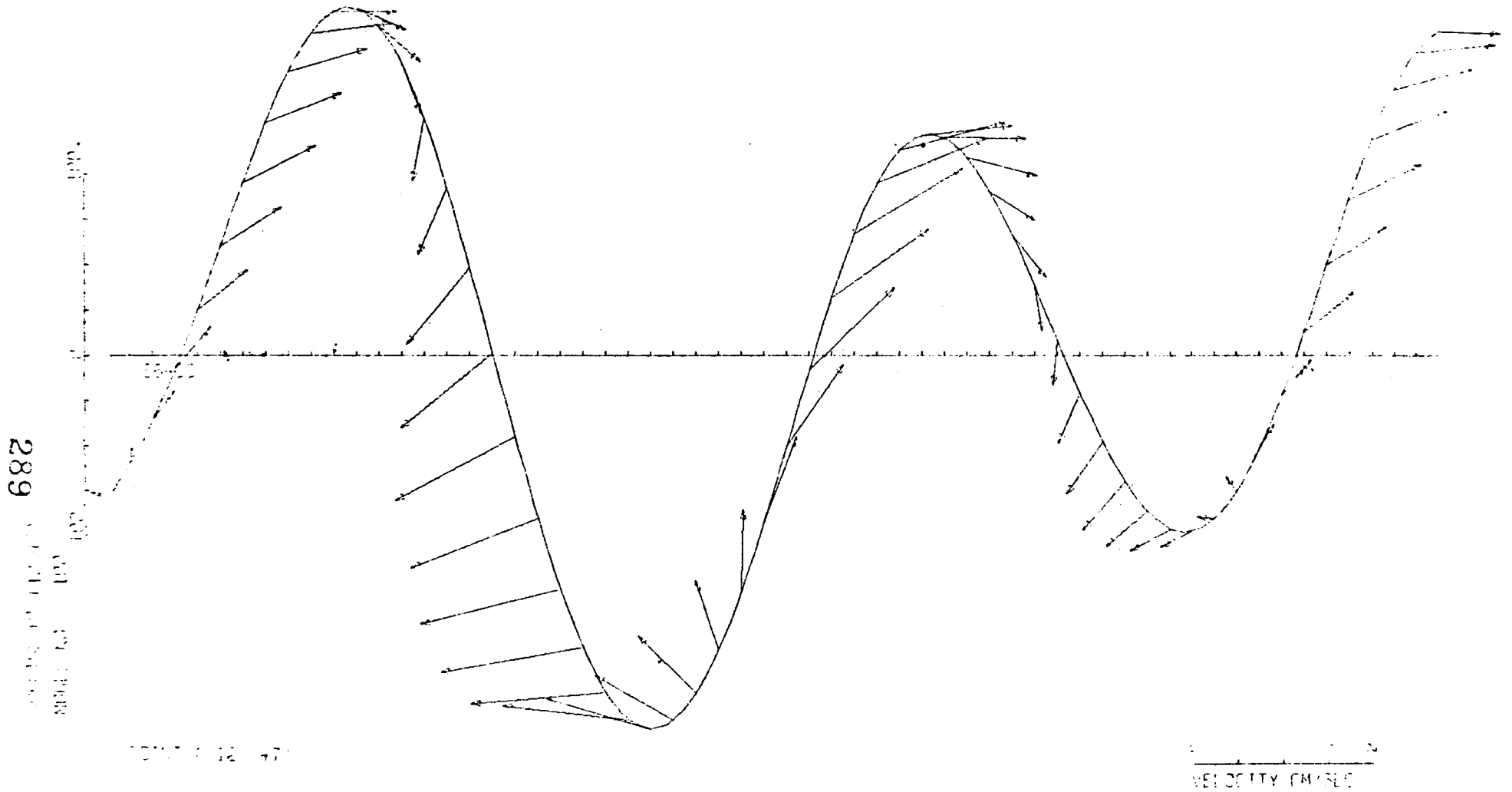


Fig. 11 Examples of instantaneous surface currents and tides (above), and "second layer" currents and change of thermocline depth (below) at a specific time (tidal phase); BLM-3 (no winds)



LAYER 1



TIDAL HEIGHTS AND CURRENTS  
LAYER 3, OPTIMIZED B-N MODEL FOR S.L.M. GULF OF ALASKA, WESTERN GRID.

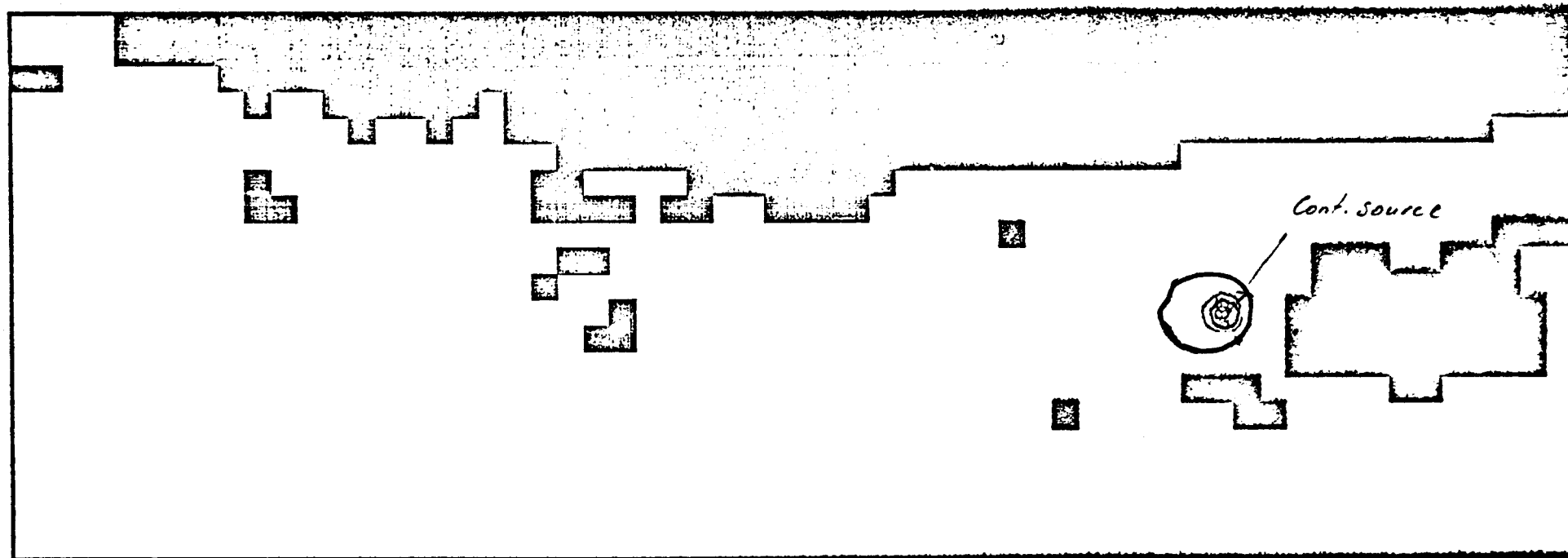
CALIFORNIA COMPUTER PRODUCTS, INC. ANAHEIM, CALIFORNIA CHART NO. 00

MADE IN U.S.A.

007

CALIFORNIA COMPUTER PRODUCTS, INC.

Fig. 12 Example of time series of currents and tides at a specific point in BLM-3



LAYER 1. TIME(S.) 144000.

Fig 13 Example of distribution of "pollutants" from one continuous source after a full tidal cycle; BLM-3 (no wind)



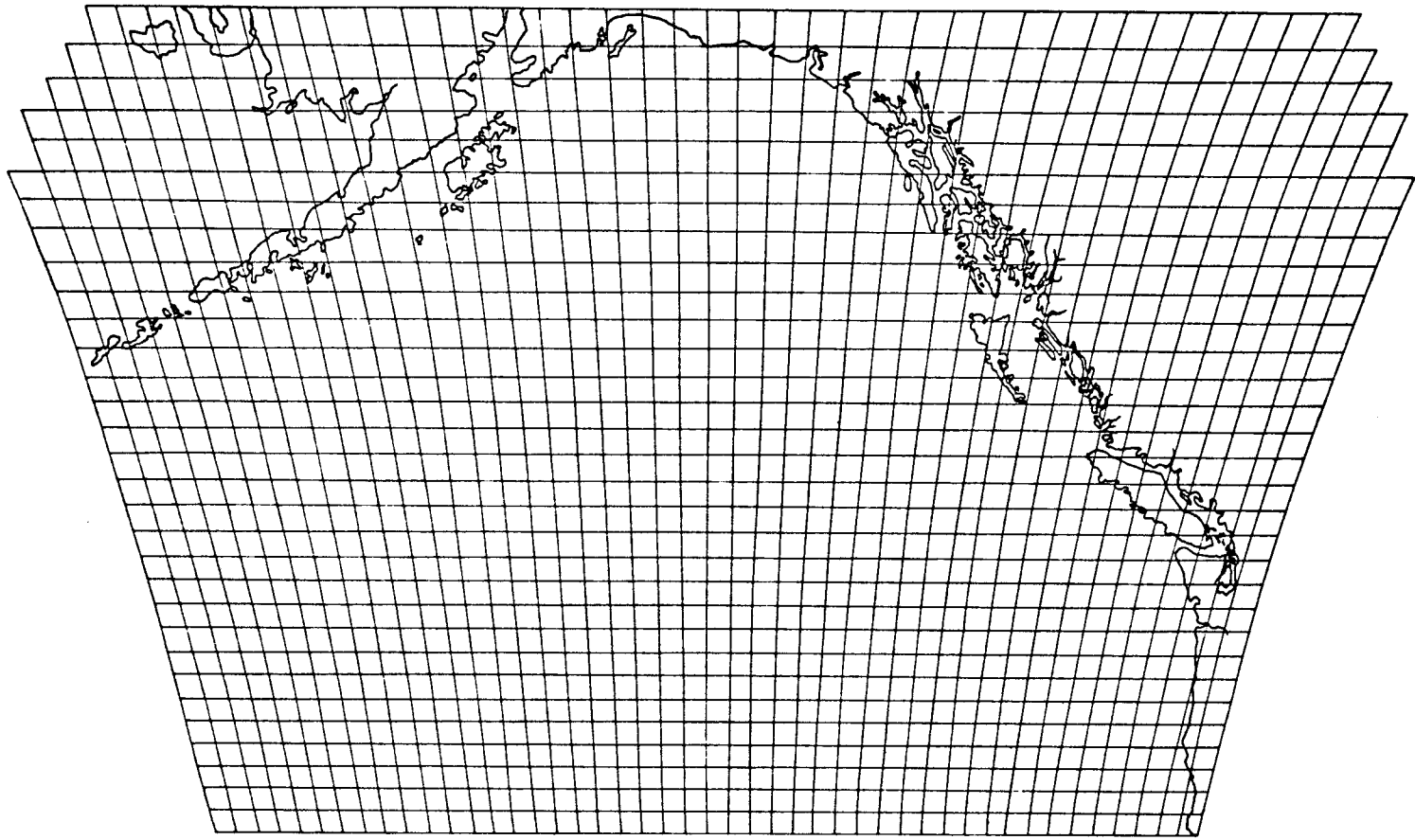


Fig. 14. Computation grid for small-mesh meteorological model

DATE 1 JUL 36 GMT 0000 + 36 H  
 REF LINE .100001+03 SPACING .250000+00

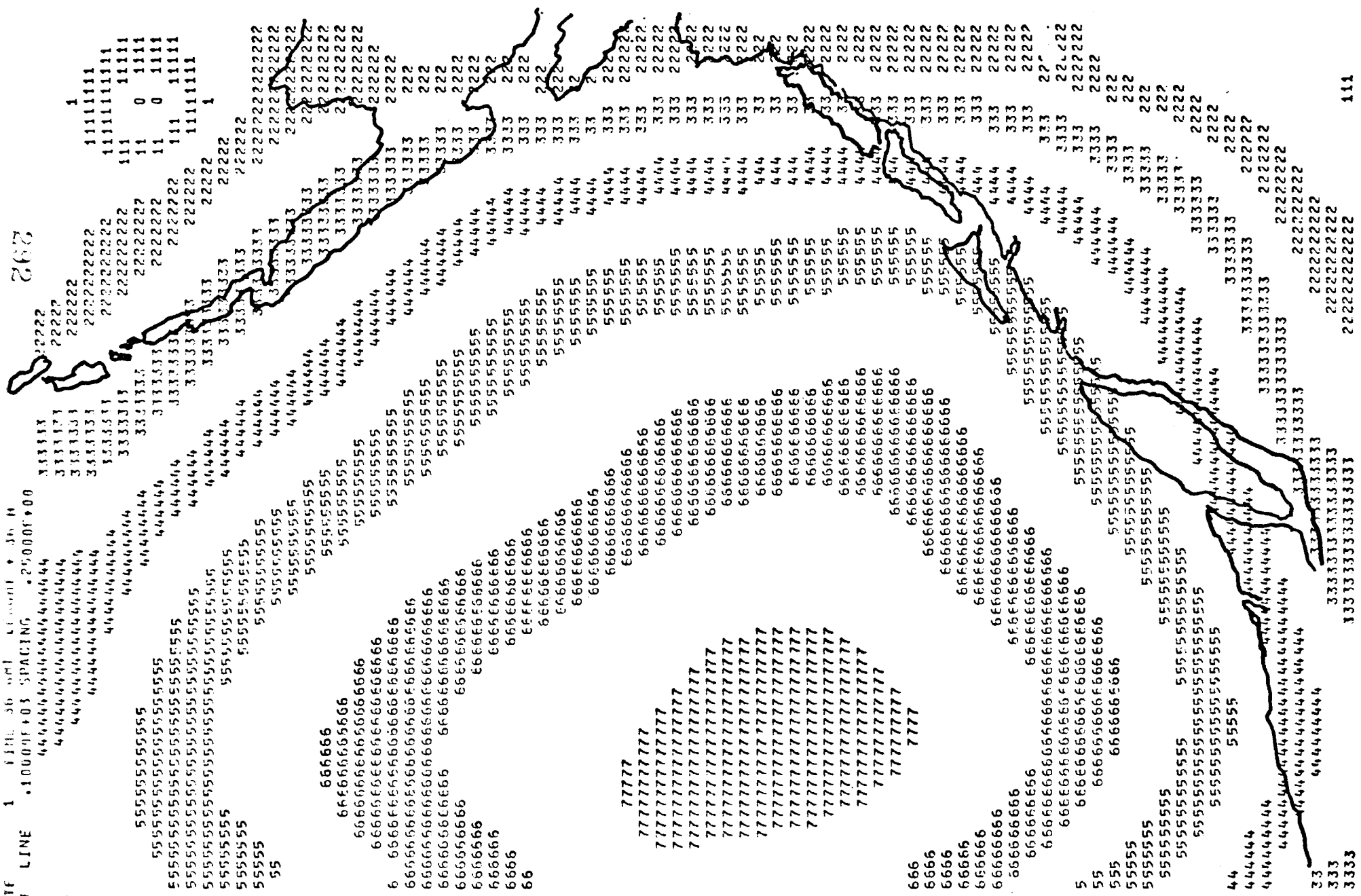


Fig. 15 36 hours surface pressure forecast for 00Z 1 June 1973

ANNUAL REPORT

MESOSCALE CURRENTS AND WATER MASSES IN THE GULF OF ALASKA

Contract #03-5-022-56

Research Unit #289

Reporting Period 7/1/75-3/31/76

Number of Pages 65

Dr. Thomas C. Royer  
Institute of Marine Science

UNIVERSITY OF ALASKA

March 31, 1976

I. Summary of objectives, conclusions and implications with respect to OCS oil and gas development.

The objectives of this study are to define the physical-chemical environment, transports of pollutants and the long-term monitoring of the physical-chemical environment in the Gulf of Alaska. Conclusions from this year's work include that there are variations in the scale lengths (and probably time scales) of the physical processes in the Gulf of Alaska. The shortest scale lengths were found northeast of Kodiak Island where very complex flows were seen. Another important conclusion is that nearshore surface water can be advected well offshore, as is apparently the case near Kayak Island. While the general flow is as expected, the perturbations on this flow have an important implication in the transport of pollutants.

II. Introduction

This study is devoted to determining the ocean transports in the Gulf of Alaska and the distribution of water masses within the region. It is concerned with both the steady state currents and their shorter term variations such as the seasonal variations. Specific objectives include the direct measurement of the currents at selected sites and the acquisition of hydrographic data both on the shelf and in nearby deep water to determine the water mass distribution and density field from which flow can be determined. The study is relevant to both the short term and the chronic pollution problems posed by development of the natural resources of the region. It provides input to numerical models which produce trajectories of surface water in the

region. These theoretical trajectories can be verified through the use of the water mass analysis.

### III. Current State of Knowledge

The current status of knowledge of the physical environment in the Gulf of Alaska is best reflected in the paper by Galt and Royer (1975) which is included as an appendix to this report. Conditions for the subarctic Pacific are reviewed by Dodimead, Favorite, and Hirano (1963) and for the Gulf of Alaska by Royer (1975). The past knowledge yields general information on direction of flow and gross distribution of coastal water masses. There is very little knowledge on the year to year or season to season variations in either the currents or the water masses. Prior to this study by OCS, there were no data available from moored current meter arrays in the region and only a single multiyear study on the water masses in the Gulf of Alaska. Some generalizations can be made for all coastal areas, however, and specific theories can be applied. However, since the control of the density is via salinity, the region differs from most other coastal regions. Finally, the large amplitude of the seasonal wind stress brings about dramatic seasonal variations possibly not seen elsewhere.

### IV. Study Area

See Figures 1 and 2

### V. Data Collection

To determine the seasonal variation of the transports, currents and water masses, a sampling program must be carried out on a seasonal basis. The temperature and salinity versus depth are measured quar-

terly at each of the station positions indicated in Figures 1 and 2. From these data, the spatial distribution of the directly measured parameters plus derived quantities such as density and dynamic height are mapped as both vertical and horizontal cross-sections. From these data, the baroclinic current structure can be calculated. The hydrographic data are also used as input for the numerical model of the coastal circulation being developed by PMEL personnel. In addition to the computation of baroclinic currents the hydrographic data are used to trace water masses throughout the region. For example, a warm subsurface parcel of water can be observed in the transects across the shelf and its relative position tracked. The methods used to gather the salinity, temperature data are either an STD or CTD system which measures either salinity or conductivity electronically and records on magnetic tape. The data are calibrated using water samples gathered from sample bottles hung on the wire which lowers the STD or CTD probe through the water column.

In order to understand why various types of current observations are necessary, it is helpful to visualize the total current as a sum of several types of separate currents. Fofonoff (1962) presents the total current as a sum of baroclinic and barotropic geostrophic components and the Ekman wind drift component. The baroclinic current field can be determined from the density field which is a reason for the hydrographic data. The barotropic current field can be determined from the sea level slope. A satisfactory method of measuring the sea level slope over a large region is not yet developed. Instead, the barotropic current must be measured at a point (current meter array) or the slope measured between

several points (tide gauges on mooring and shore). The Ekman component is generally determined from available surface wind data.

The above methods are utilized to determine the barotropic current component. A current meter array has been deployed for the direct measurement of currents at 5 locations in the water column. The array was installed at station 9 (see Figure 1) with meters at 20, 30, 50, 100 and 260 meters beneath the sea surface. From these data the the barotropic (or depth independent) portion of the current can be determined along with the baroclinic (or depth dependent) portion. The array yields direct current measurements at a single point. This information is combined with the hydrographic data to produce estimates of flow over the entire continental shelf. The second method of measuring the barotropic current involves the determination of the sea level slope across the shelf. The bottom pressure at the station 9 mooring is compared with the sea level measured at Seward. The difference in the sea levels is a measure of the barotropic geostrophic current on the shelf. Without direct current measurements at some point between the shore and station 9, the actual amplitude of the barotropic current cannot be determined; but information on its long-term and seasonal fluctuations can be gained from these two sea level measurements.

The STD/CTD data obtained by this project since July 1974 through March 1976 include occupying the northeastern station grid (GASSE) nine times and the western station grid (GASSO) twice. The data for fiscal year 1975 cruises for which the Institute of Marine Science, University of Alaska were primarily responsible, have been

compiled into a report (Royer, 1976) available from the OCS Juneau office or the University of Alaska. The report consists of track plots, vertical profiles, vertical cross-sections and abbreviated data listings. The CTD data for GASSE and GASSO obtained in September 1975 aboard the SILAS BENT has been organized in a similar format to the previous CTD (portions of these data are included in this report). The CTD data from a cruise conducted aboard the SURVEYOR are not yet available as a result of problems in processing the original tapes. The data logger used in that cruise is of a different type than previously used in the project. The CTD data for GASSE from the MOANA WAVE (March 1976) is currently being processed.

Historical oceanographic data from NODC are being used to establish normal conditions. As mentioned in last year's report, these data are limited in both number and coverage. Other concurrent hydrographic data such as the U.S. Coast Guard sections P2, P7, P8 and P9 (Figure 3) are being used to determine the normalcy of the deep ocean geostrophic baroclinic currents.

Meteorological data for the region has been obtained on a routine basis from several sources. Local weather is received from the U.S. Weather Service with the exception of the Middleton Island data which comes through NCC via Kansas City. We are also "on line" to receive the NOAA-2 and 3 satellite data which provides information on both the atmospheric clouds and sea surface temperature. The satellite data are received locally at the Gilmore Creek tracking station and are enhanced locally. The meteorological data from the environmental buoys EB-03 and EB-33 are obtained on an irregular



basis. In addition to these primary data, a derived quantity, the upwelling index, and with other transport computations are received on a continuing basis from the Fleet Numerical Weather Center in Monterey, California. These derived data are being used to evaluate the effect of the wind stress fields on the ocean circulation in the Gulf of Alaska. Coastal sea levels are being obtained from the observatory in Palmer, Alaska. Pertinent sea level data are digitized and keypunched. Wave data from a station near Middleton Island obtained by University of Alaska personnel prior to 1974 is available and is being analyzed.

## VI. Results

During this year's support, three successful hydrographic cruises have been carried out. The cruises are:

| <u>Ship</u> | <u>Date</u>         | <u>Region</u>            |
|-------------|---------------------|--------------------------|
| Silas Bent  | 1 Sept-26 Sept 1975 | N.E. & W. Gulf of Alaska |
| Surveyor    | 28 Oct-17 Nov 1975  | N.E. & W. Gulf of Alaska |
| Moana Wave  | 21 Feb-5 March 1976 | N.E. Gulf of Alaska      |

The MOANA WAVE did not cover the western section of the Gulf of Alaska due to time constraints. However, in addition to the usual coverage of the northeastern grid, during the MOANA WAVE cruise, the shelf transect out of Seward was covered three times in two weeks. This will allow the evaluation of changes in the water properties due to short term effects.

### A. Temperature-Salinity Relationships and Baroclinic Transports

Temperature and salinity characteristics of surface water can be used to map flows over limited times and regions. The strong

fresh water input near Yakutat and Tey Bay serves as an excellent water mass indicator. It has been found by this technique that as the longshore circulation passes westward around Kayak Island, the surface flow continues in a southwesterly direction. It does not turn northwestward from this point as has been suggested by previous studies. This low density water retains its features as it travels nearly parallel to the shelf break until it moves beyond the Cook Inlet area. Past this point, mixing destroys these water properties. NOAA-2 and 3 IR and visible imagery has revealed the spatial extent of this surface feature (Figure 4). It can be seen that the flow off Kodiak is parallel to the shelf break and therefore well offshore.

Preliminary impressions from the temperature-salinity data gathered in the western Gulf of Alaska (GASSO), are that the circulation has evidence of westward intensification with surface baroclinic currents in excess of 40 cm/s adjacent to the shelf break. The baroclinic transports across these transects are approximately  $6-11 \times 10^6 \text{ m}^3/\text{sec}$  with the majority of the transport occurring immediately offshore of the shelf break in the upper 700 meters of water. For comparison, the transports for the transects in the northeastern Gulf of Alaska (GASSE) range from .03 to  $4 \times 10^6 \text{ m}^3/\text{sec}$  for the same time of year (September).

While the transports differ for the two regions subsurface temperature features are continuous in the deep gulf. Salinity is the primary controller of density in this region of the world's oceans and therefore a stable water column can contain temperature inversions.

In general, there exists a cold layer representing the winter mixing. This layer extends from approximately 100-110 m upward. Its upper limit depends on the season. In winter, of course, it extends to the surface, whereas in summer its height is 20-30 m. This cold water mass is most generally found over the deeper waters of the Gulf of Alaska. Shoreward and beneath this cold water lens is a core of warmer, more saline water. It is found from generally 130-170 meters in very close proximity to the continental slope. Its origin is not as obvious as the adjacent cold water lens, but T-S relationships indicate that it is formed at the surface near the subarctic convergence ( $38^{\circ}$ - $42^{\circ}$ N). From the region of formation it is transported northward and overlaid by fresher, less dense water. It is expected that this water has a seasonal fluctuation in its properties which are dependent upon conditions at its time of formation and the mixing characteristics of the water column. In September 1975, this subsurface warm core disappears between the Mitrofanina and Paulof transects (Figures 5 & 6) probably due to mixing.

Beneath these two subsurface features, the water properties appear to be consistent from season to season (or cruise to cruise). Above these features the water properties vary on a seasonal basis from heat and fresh water input and convergence due to the wind stress. Seasonal variations are present throughout the water column over the continental shelf.

#### B. Current Meter Data

The current meter array at NEGOA 60 (2 July-26 August 1974) was located in the lee of Kayak Island broken down in the following manner.

A low pass Butterworth digital filter with half power point at 1/3 c.p.h. (cycles per hour) was applied to all the data. Then a sixth order decimation of the record resulted in an hourly time series.

Following mean removal and detrending by a linear least squares method (u,v) pairs were plotted to yield scatter diagrams, Figures 7, 8, 9 and 10. On the time scale of one hour there is decreasing randomness and magnitude of motion with depth. Surface boundary layer and baroclinic motions are of greatest influence at 20 and 30 meters depth, whereas, organized rotary motions (barotropic tides) showing topographical influence are most significant at 90 meters depth.

Raw and smoothed autospectra of U (E-W velocity), V (N-S velocity), and speed hourly time series have four major peaks. The first mode diurnal, first mode semi-diurnal, and second mode semi-diurnal tidal oscillations at .0410, .0807, .1614 c.p.h. respectively are dominant in nearly all autospectra. Maximum energy invariably occurs at the first semi-diurnal frequency and has a value of order  $1 \times 10^3$  (cm/sec) <sup>2</sup>/c.p.h. A peak at frequency .0046 c.p.h. ( $\approx$ 218 hours period) or greater is evident in the V autospectra. This peak is characterized by decreasing energy with depth. It is believed that this feature is a result of periodic variations of wind stress, unfortunately, definite quantitative description is not possible because only tenuous resolution can be obtained with the existing record length.

The current meter data from NEGOA 64 (April-June 1975) has not been analyzed. The data tape was received from PMEL in February 1976. The current meter array at station 9 (September 1975-???) is still in the field.

### C. Upwelling Index

The effect of wind stress on the coastal water structure circulation is being evaluated through the coastal upwelling index and its anomaly (Bakun, 1973). A comparison of the parameters at 60°N, 149°W (Figure 11) for the nearly two years of this study indicate that during both summers, the region had an index of approximately zero (no tendency to upwell or downwell due to wind stress). That is, no convergence or divergence at surface waters. The index shows dissimilar conditions during the two winters. The 1974-75 winter had a positive anomaly in the November, December and January switching to negative in February whereas the 1975-76 winter had a negative anomaly in November and a positive anomaly in December and January and about zero in February. These conditions caused a maximum downwelling for the first winter in February with a very sharp peak. The second winter's downwelling was a maximum in November with a very broad peak extending into February. In other words, the wind field on a month to month basis was very different for the two winters. These conditions will be compared with the hydrographic data when they become available.

### D. Wave Studies

Analysis of surface wave data gathered off Middleton Island in 1973 has been carried out with partial support by this project. The results are best summarized in the abstract of a paper presented at the American Geophysical Union meeting in December (Roberts and Royer, 1975):

A bottom mounted surface wave gauge was operated at 70m near Middleton Island in the Gulf of Alaska for 10 days in October and

November 1973. Hourly spectra from the first of the record reveal a peak around 0.065 Hz which moves toward higher frequencies for about 18 hours. The frequency of the peak then remains constant for about 24 hours, after which it again increases. The changes are well correlated with a large storm which remained stationary in the North Pacific, then moved rapidly into the Gulf of Alaska and subsided. Wave group velocities are used to estimate possible distances of the wave source from the gauge. The actual distances of the storm from the gauge show a close correlation with wave-derived distance. There is also some evidence in the spectra of amplification of waves whose group velocity equals the velocity of the storm.

Comparison with changes in wave spectra for a storm in the North Atlantic in March 1968 indicates the same time rate of change in the spectral peak as was found in the North Pacific for time periods when the storms are subsiding.

#### E. Sea Level Studies

The sea level data are being digitized and prepared for analysis. It is expected that the data might be developed into a method of determining the circulation on the adjacent continental shelf from the coastal sea level. The feasibility of such a method has been explained by Reid and Mantyla (1976) on a seasonal basis. The question as to whether it can be used as a reliable monitoring technique for coastal circulation has yet to be fully tested.

## VII. Conclusions

Within the second year of this study, the majority of the effort of the project personnel has been devoted to the gathering and processing of the hydrographic data. The types and number of data will permit a quantum jump in knowledge of the circulation of the Gulf of Alaska. Prior to the synthesis of these data into a set of concise conclusions, comments must be restricted to some limited details.

The temperature-salinity measurements show that the waters overlying the continental shelf in the northern Gulf of Alaska change on a seasonal basis. The causes of these changes are the input of heat and freshwater and variations in wind stress. Features in the vicinity of the shelf break and further offshore are semi-continuous around the gulf. The data indicate that the surface water inshore and eastward of Kayak Island moves southwestward and is located along the continental shelf break as it passes Kodiak Island. Apparently, there is a different surface water mass regime west of Kayak Island and inshore from Middleton Island.

The changes in complexity of the horizontal structure of the water masses are evident from both the satellite and hydrographic data. Northeast of Cook Inlet the offshelf water column reveals mesoscale changes in density and therefore current structure. However, as one progresses westward along the Alaska Stream these complexities disappear. The hypothesis is that these features are caused by perturbations around Middleton Island and the change in the flow from purely zonal to a meridional one.

The baroclinic currents determined from the T-S data are greater in the western Gulf of Alaska (GASSO) than in the northeastern portion

(GASSE). Surface currents reach 45 cm/s in the western section and 30 cm/s in the other. The baroclinic transports relative to the deepest common sampling depth for each station pair range from  $0.03 \times 10^6$  cm/sec for the Hinchinbrook line to  $11.4 \times 10^6$  m<sup>3</sup>/s for the Paulof Bay line in September 1975. Assuming a barotropic current speed of 20 cm/s, surface currents in excess of one knot are expected near the shelf break off Kodiak Island.

#### VIII. Needs for Further Study

With the hydrographic data available to this time, we are only capable of making crude estimates of the seasonal variations in circulation on the shelf in the northern Gulf of Alaska and the data for the western section is another year behind. The STD/CTD work should continue for several more years, until insight into the physical processes is gained at which time a more modest monitoring program could be established. The frequency of observations remains fixed at 4-5 times per year.

The current meter installation at station 9 should continue to provide long term current flow estimates along with shorter term variations near the shelf break. These data in conjunction with the sea level measurements can also provide input for both baroclinic and barotropic geostrophic circulation models. A major facet of the future research will be to determine the seasonal variations in flow. With seasonal wind stress variations being large, it is probable that the seasonal current variations are also large. The current meter data should also provide information on the time scale of the forcing functions in the Gulf of Alaska.



The use of satellite IR and visible data should continue in the future. While these data do not stand by themselves, when used in conjunction with the hydrographic data they are useful in achieving a broad general impression of the spatial distribution of sea surface temperature. Other satellite data that would be useful are the sea level that the SEASTAT satellite was to measure and imagery from the GOES satellite.

Work should be initiated on the measurement of surface wind waves in the Gulf of Alaska on a continuing basis. Very few such measurements have been carried out previously, but the status of the technology today should allow such a study at a relatively modest cost. These data could be used for general estimates of wind wave spectra, but more important the data would serve as a "ground truth" for the Fleet Numerical Weather Center wave forecasting program. Personnel at the University of Alaska are interested in beginning such a program in the next fiscal year.

IX. Summary of last quarter operations

1. Ship Schedule

R/V MOANA WAVE, 21 February - 5 March 1976

2. Scientific Party

T. Royer, Chief Scientist, IMS, University of Alaska  
L. Morgan, IMS, University of Alaska  
B. Kopplin, " " " "  
F. Waite, " " " "  
M. Kirchoff, U.S. Fish and Wildlife Service, Anchorage

3. Methods

CTD sampling  
Current meter recovery and deployment  
Surface hydrocarbon analysis  
Bird and Mammal observations

4. Sample locations - CASSE grid (see Figure 1)

5. Data collected

88 CTD stations

12 Suroto Tows

27 Surface Hydrocarbon samples

Approximately 1400 miles of trackline

## References

- Bakun, A. 1973. Coastal upwelling indices, west coast of North America, 1946-71. NOAA Technical Report NMFS SSRF-671, 103 pp.
- Dodimead, A. J., F. Favorite and T. Hirano. 1963. Review of oceanography of the Subarctic Pacific Ocean. *In: Salmon of the North Pacific Ocean*, International North Pacific Fisheries Commission, Bulletin Number 13, 195 pp.
- Fofonoff, N. P. 1962. Dynamics of ocean currents. *In: The Sea, Volume I*, M. N. Hill, Editor, Interscience, New York, pp. 323-395.
- Galt, J. A. and T. C. Royer. 1975. Physical oceanography and dynamics of the N.E. Gulf of Alaska (Paper presented at Arctic Institute Symposium on the Gulf of Alaska, Anchorage, October 1975) 14 pp.
- Reid, J. L. and A. W. Mantyla. 1976. The effect of Geostrophic Flow Upon Coastal Sea Elevations in the northern North Pacific Ocean, Unpublished manuscript, 24 pp.
- Roberts, J. and T. C. Royer. 1975. Time dependent surface ocean wave spectra in the Gulf of Alaska, Transactions of the American Geophysical Union.
- Royer, T. C. 1975. Seasonal variations of waters in the northern Gulf of Alaska, *Deep-Sea Research* 22(6):403-416.
- Royer, T. C. 1976. Hydrographic Data Report, Northeast Gulf of Alaska, July 1974-June 1975, Unpublished Technical Report.

FIGURE CAPTIONS

- Figure 1. STD/CTD station grid for northeastern Gulf of Alaska, GASSE
- Figure 2. STD/CTD station grid for western Gulf of Alaska, GASSO
- Figure 3. Locations of U.S. Coast Guard sections for the N.E. Pacific which are occupied quarterly.
- Figure 4. Sea surface temperature in Gulf of Alaska for July 1974 from NOAA satellite.
- Figure 5. Upper layer temperature cross-section for Mitrofanina Island transect (see Figure 2) for September 1975.
- Figure 6. Upper layer temperature cross-section for Paulof Bay transect (see Figure 2) for September 1975.
- Figure 7. Scatter diagram for NEGOA 60, 20 meters after mean and linear trend are removed.
- Figure 8. Scatter diagram for NEGOA 60, 30 meters after mean and linear trend are removed.
- Figure 9. Scatter diagram for NEGOA 60, 50 meters after mean and linear trend are removed.
- Figure 10. Scatter diagram for NEGOA 60, 90 meters after mean and linear trend are removed.
- Figure 11. Coastal Upwelling Index for  $60^{\circ}149^{\circ}$  with anomaly, 1971-1976 (after Bakun, 1973).

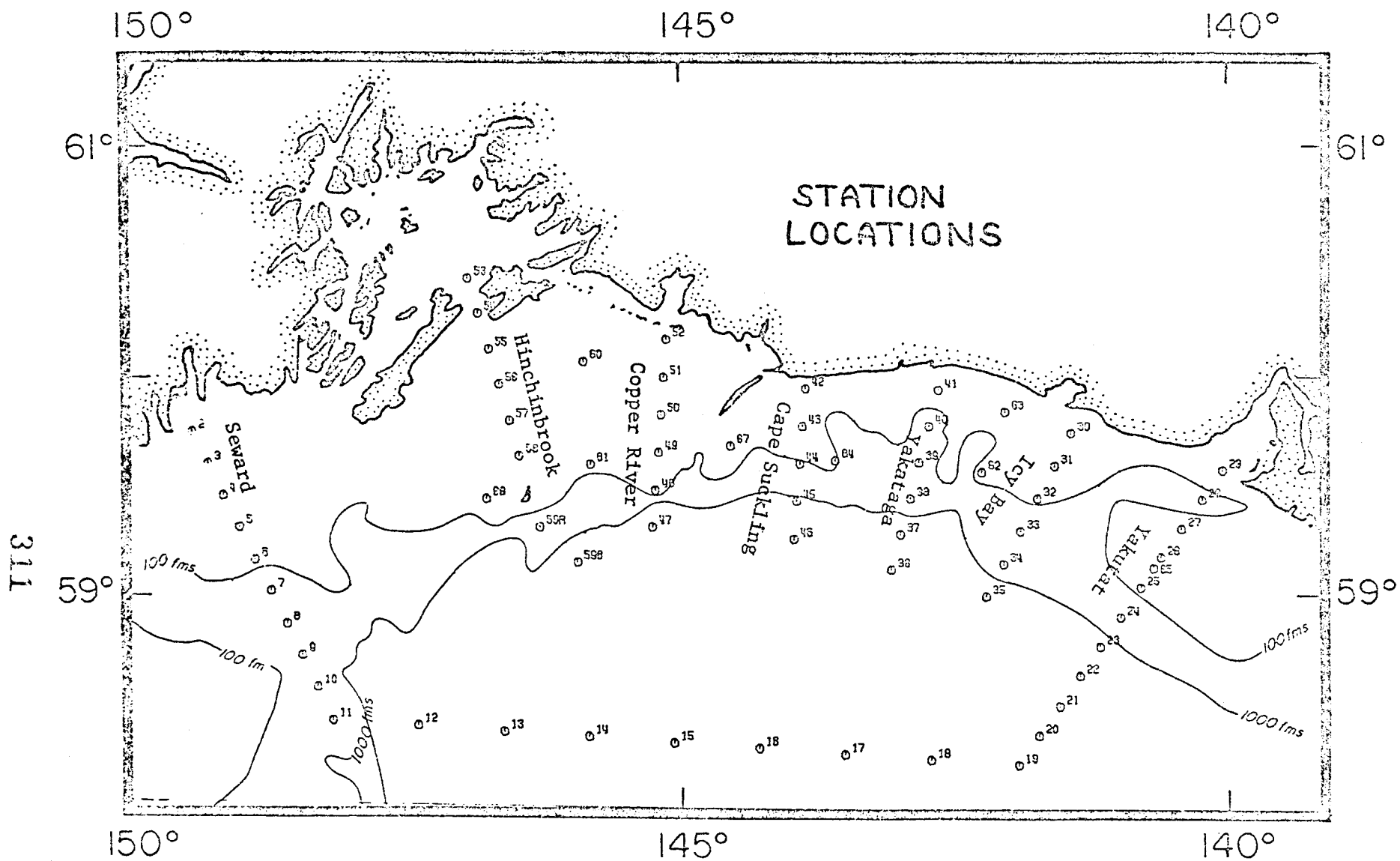


Figure 1. STD/CTD station grid for northeastern Gulf of Alaska, GASSE

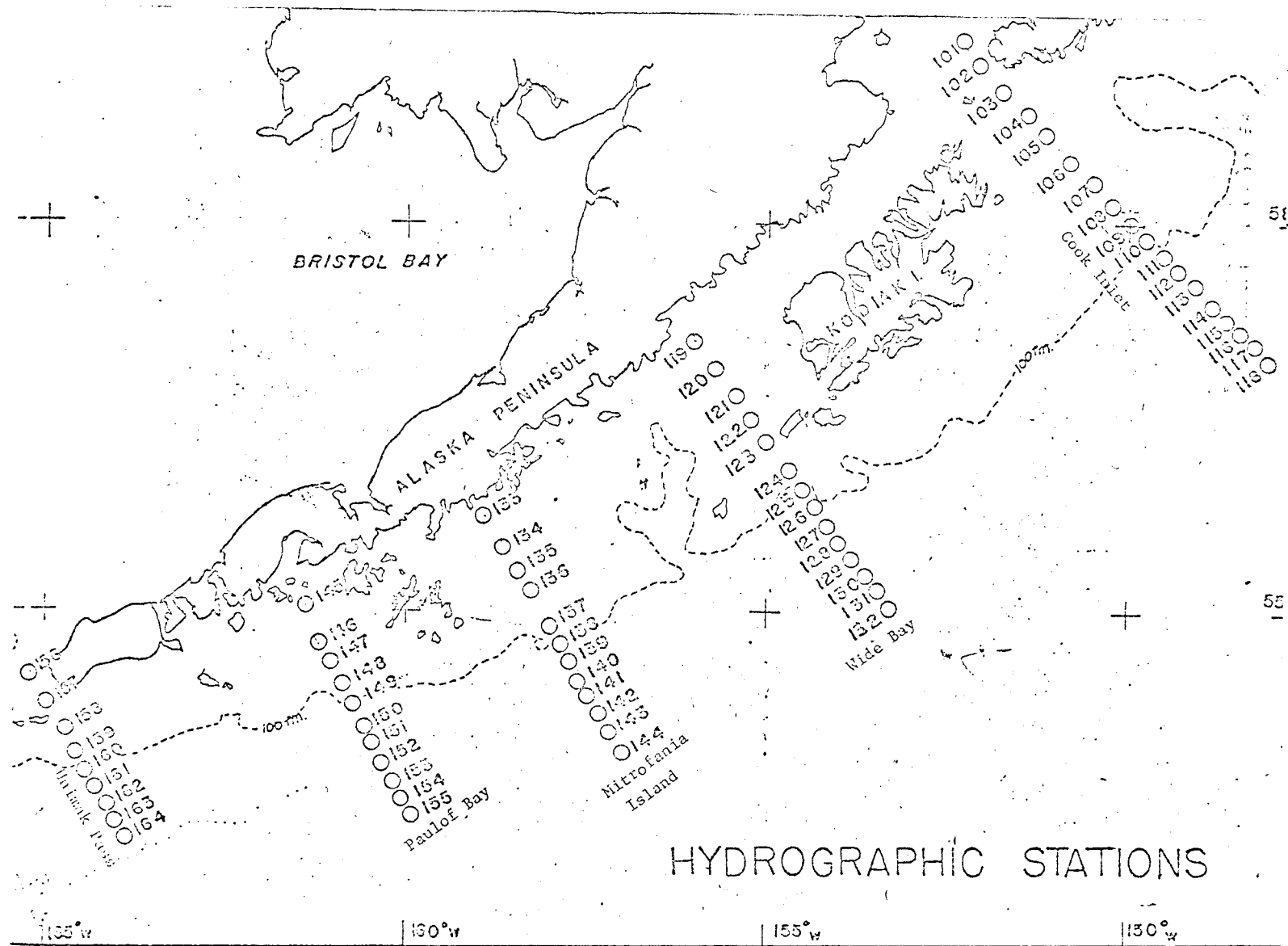


Figure 2. STD/CTD station grid for western Gulf of Alaska, GASSO

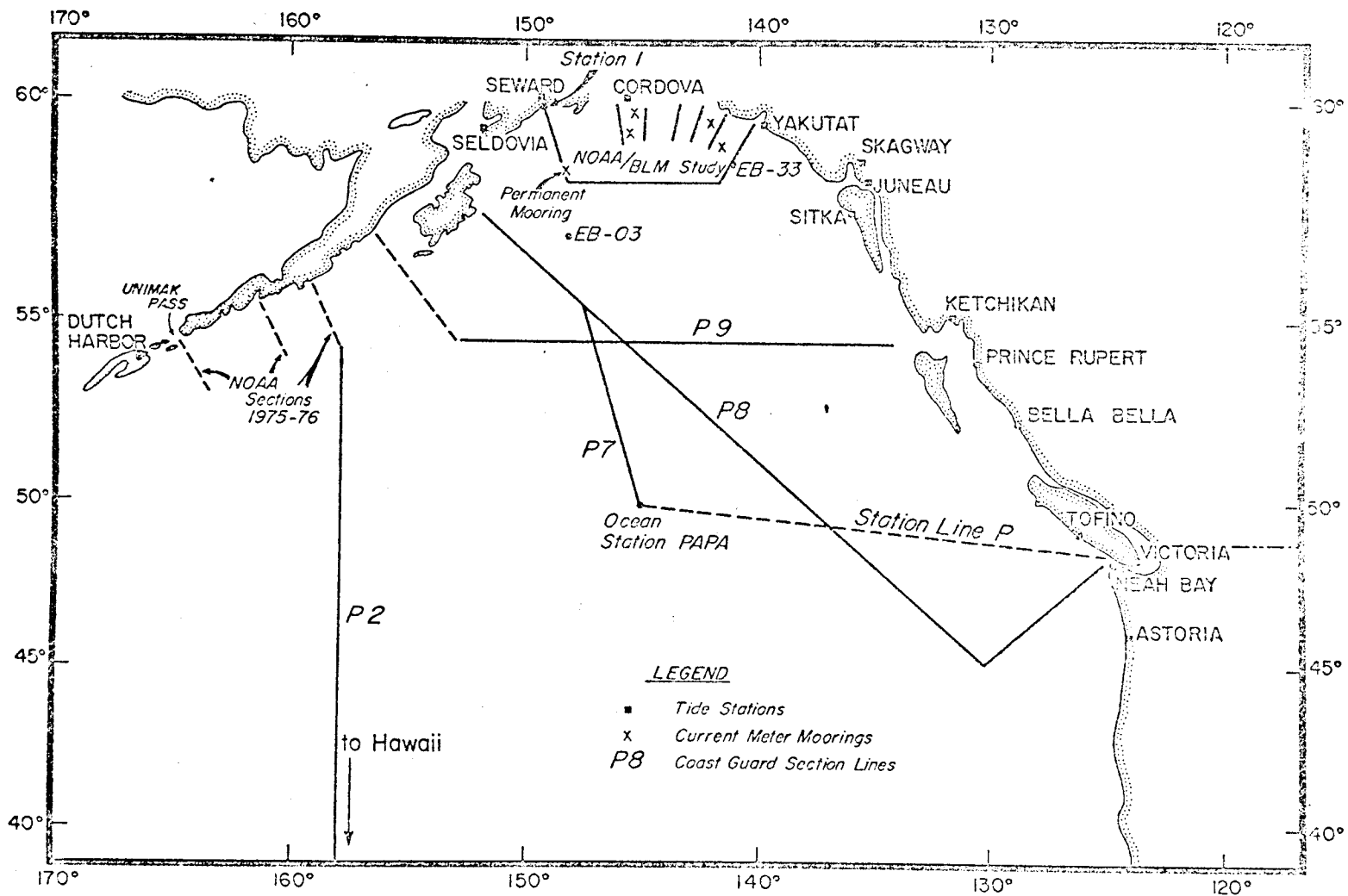


Figure 3. Locations of U.S. Coast Guard sections for the N.E. Pacific which are occupied quarterly.

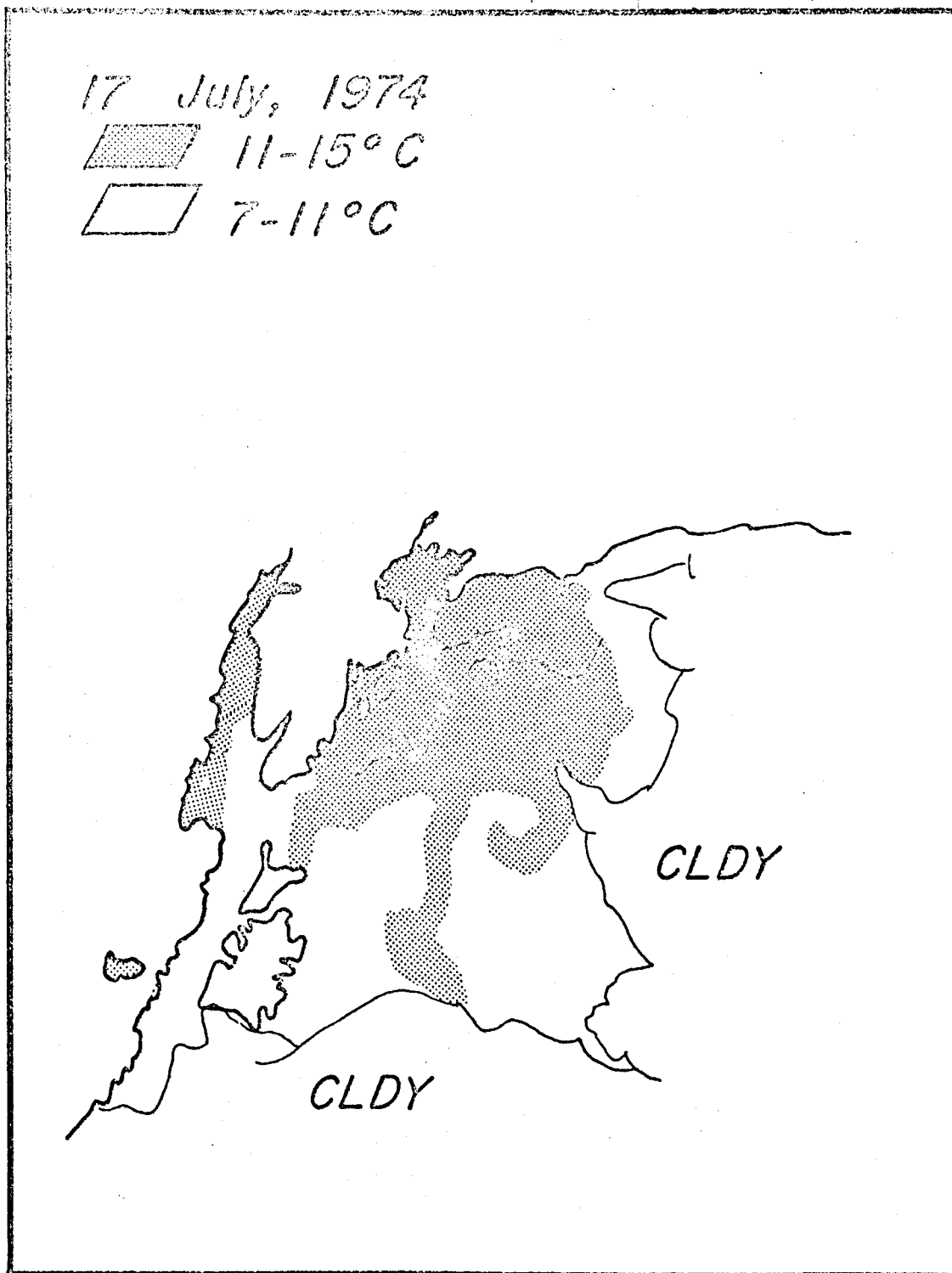


Figure 4. Sea surface temperature in Gulf of Alaska for July 1974 from NOAA satellite.



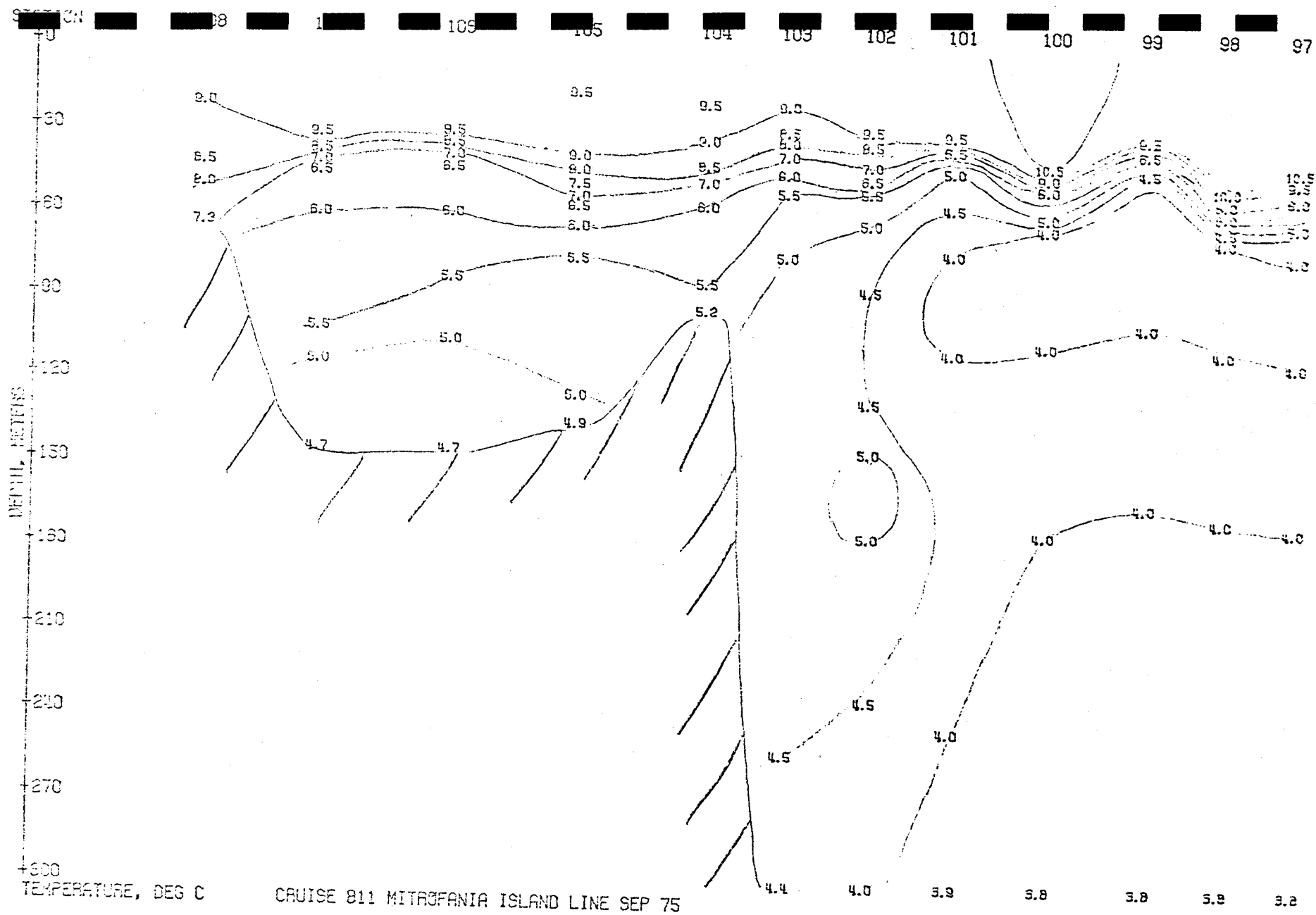


Figure 5. Upper layer temperature cross-section for Mitrofanía Island transect (see Figure 2) for September 1975.

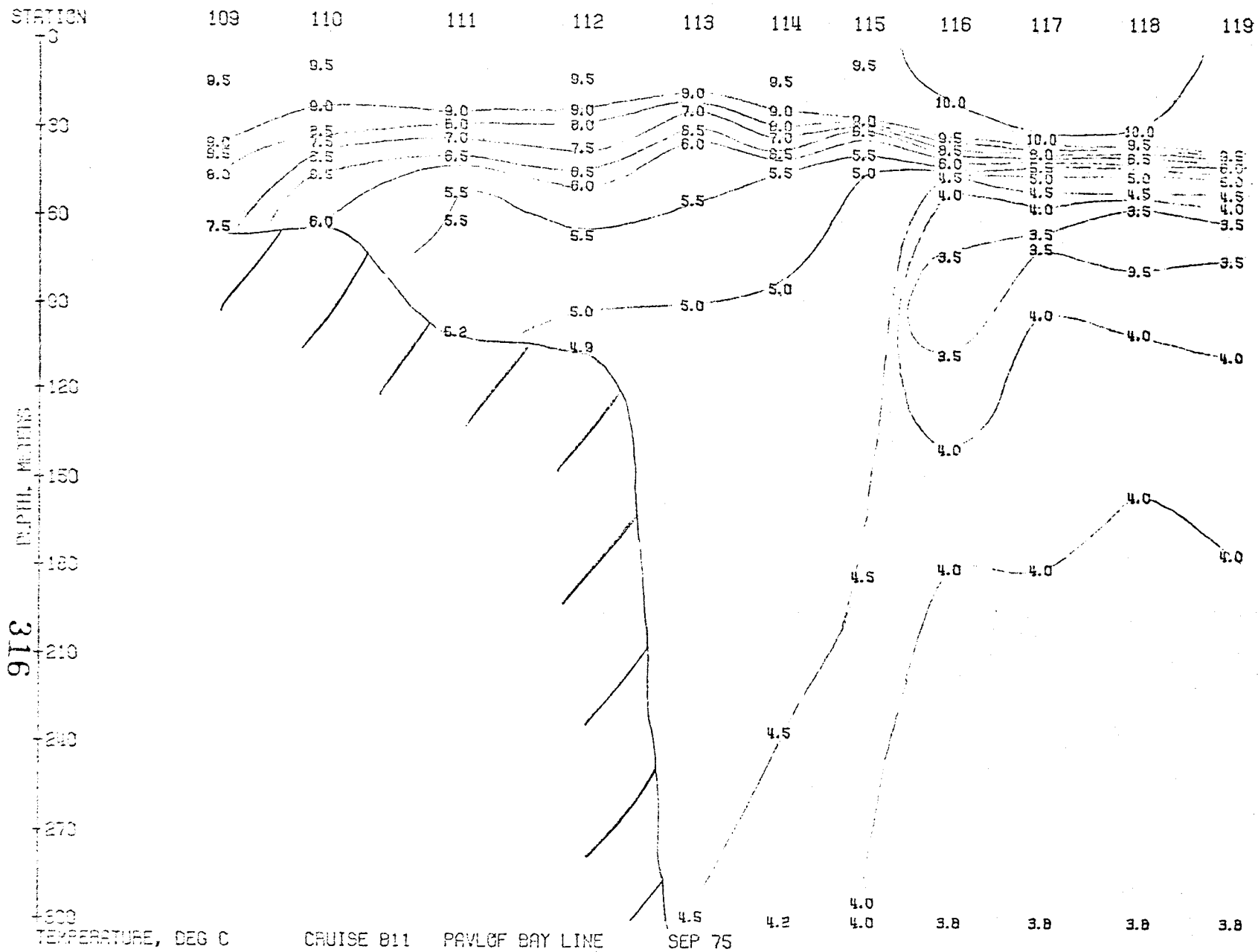


Figure 6. Upper layer temperature cross-section for Paulof Bay transect (see Figure 2) for September 1975.

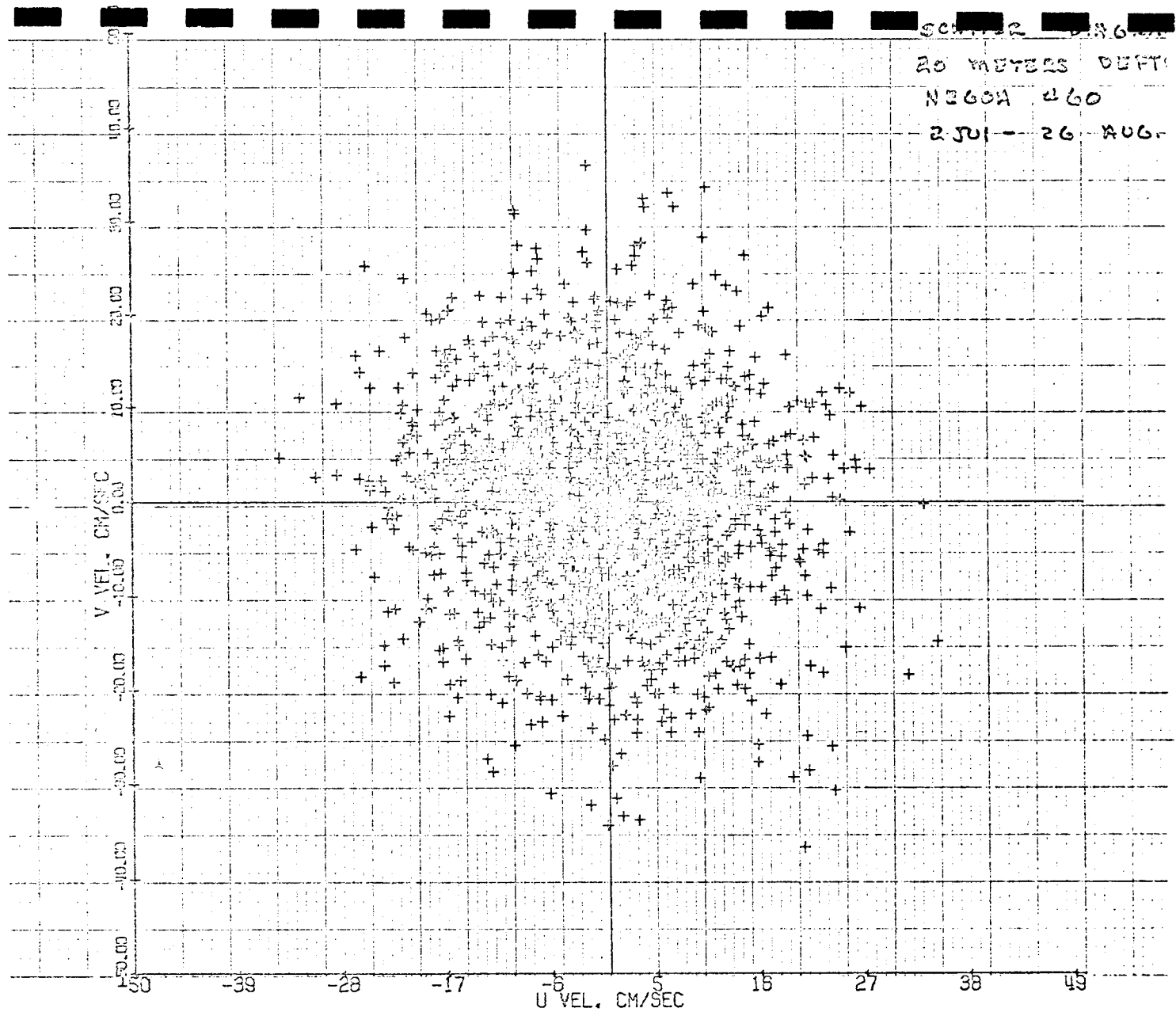


Figure 7. Scatter diagram for NEGOA 60, 20 meters after mean and linear trend are removed.

318

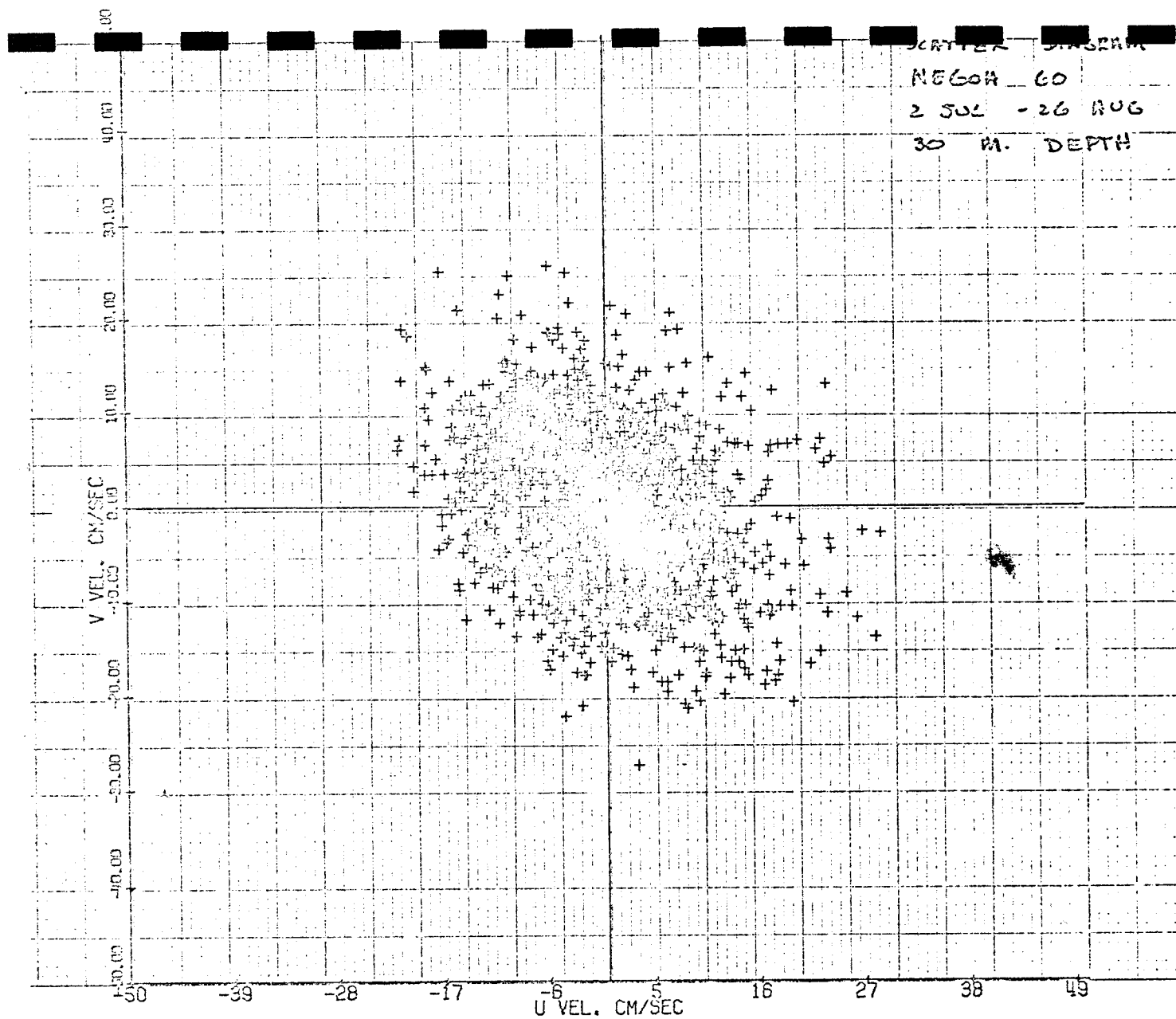


Figure 8. Scatter diagram for NEGOA 60, 30 meters after mean and linear trend are removed.

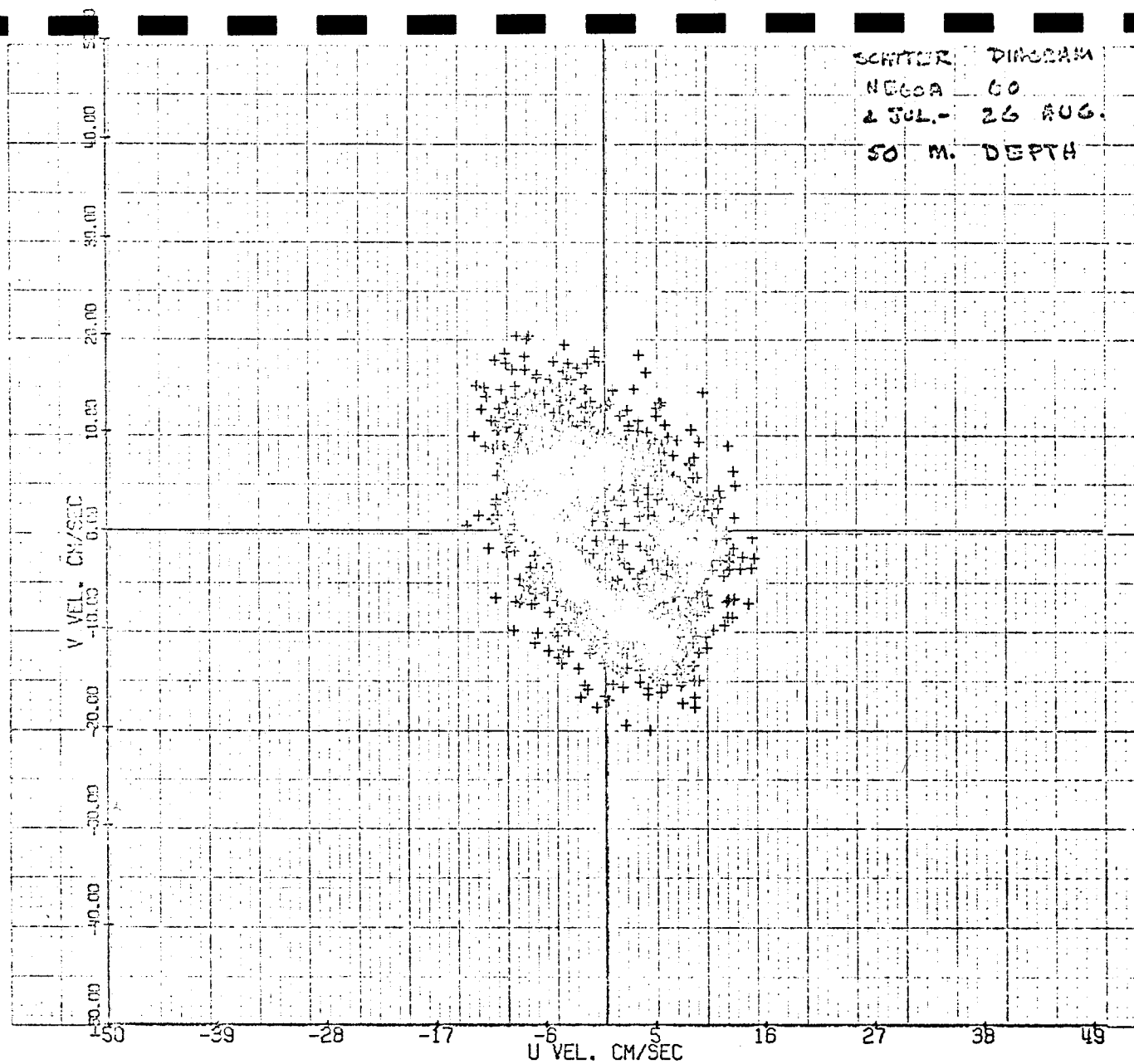


Figure 9. Scatter diagram for NEGOA 60, 50 meters after mean and linear trend are removed.

022

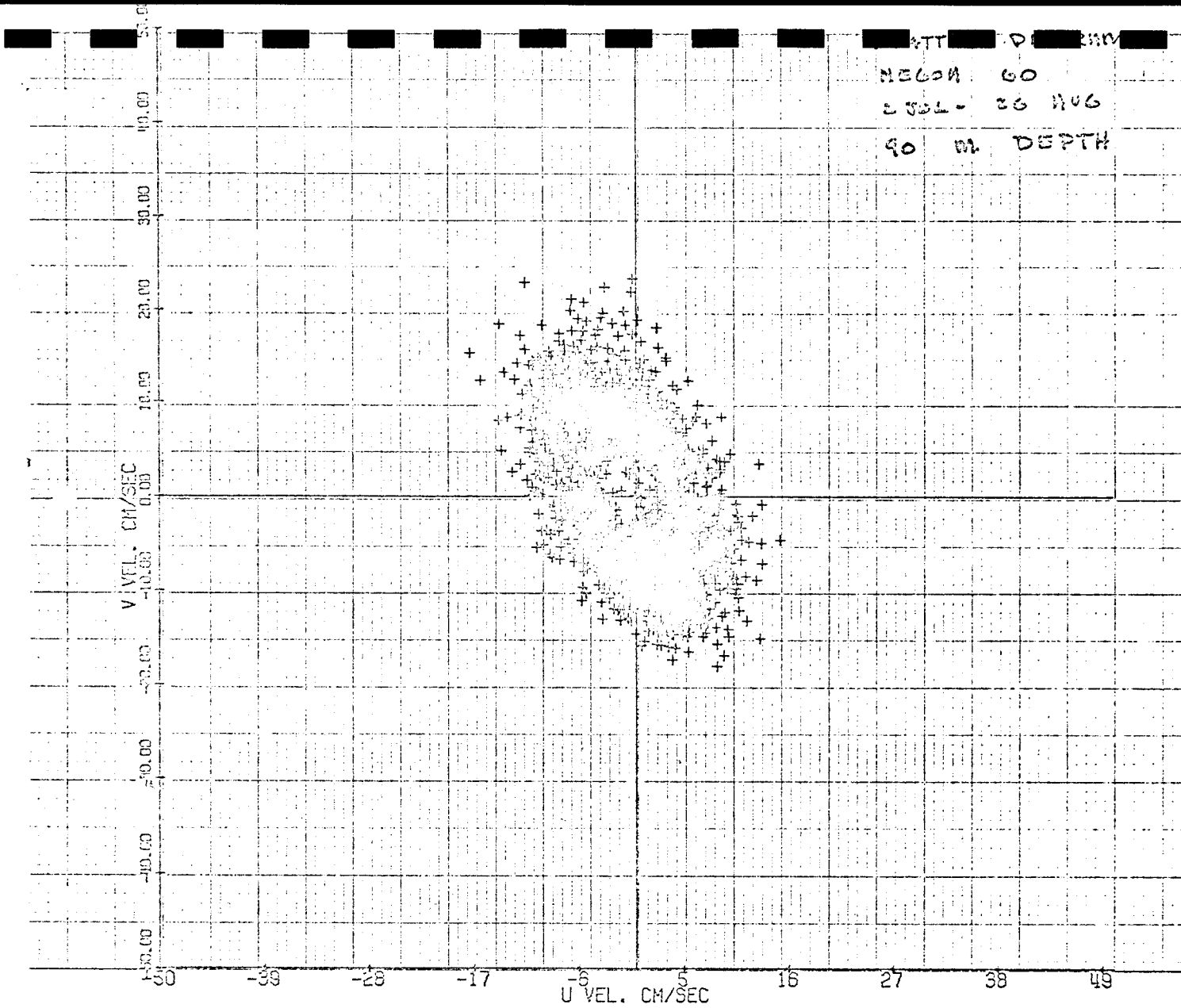
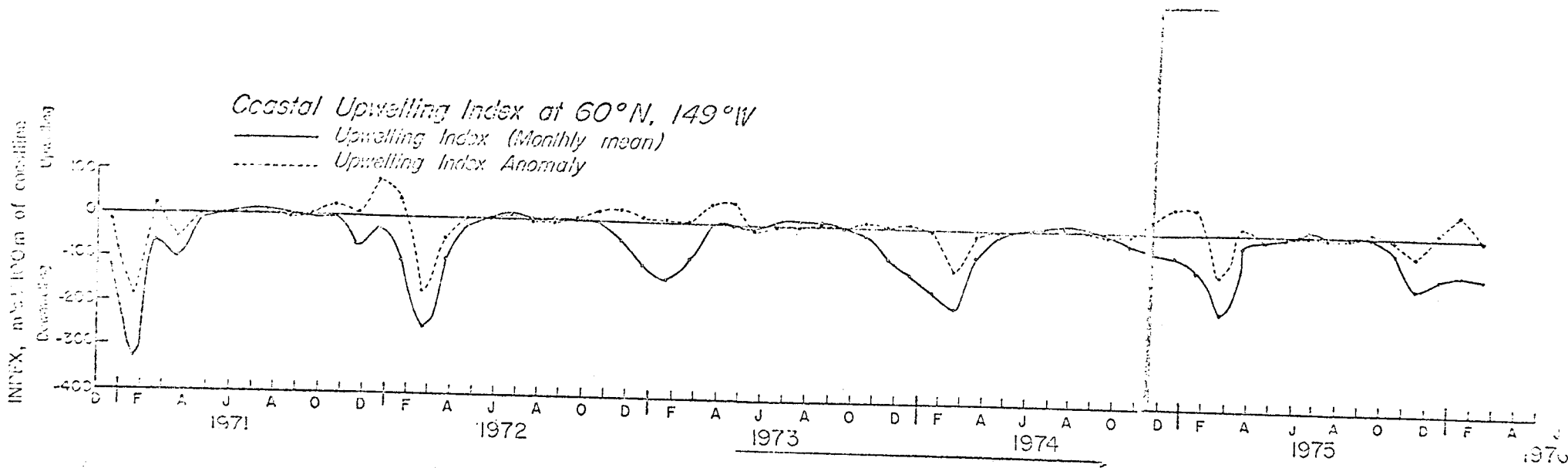


Figure 10. Scatter diagram for NEGOA 60, 90 meters after mean and linear trend are removed.



321

Figure 11. Coastal Upwelling Index for 60°149° with anomaly, 1971-1976 (after Bakun, 1973)

APPENDIX

(This Paper was presented at the Arctic Institute of  
North America's Symposium on the Gulf of Alaska,  
October 1975, in Anchorage, Alaska)



## Physical Oceanography and Dynamics

of the

Beaufort Sea

by

J. A. Goff and Thomas C. Royer

The continental shelf area between Seward and Yakutat has recently come under intense study because of interest in off-shore oil development. Bathymetric surveys, direct current measurements, meteorological studies and numerical modeling have been included in these studies.

The mean or steady flow appears to be dominated by the large-scale features of the Alaskan Stream. This is particularly true east of Cape St. Elias, but to the west on the relatively wide shelf behind Middleton Island smaller scale features tend to become more important.

Superimposed on the mean flow are annual cycles related to seasonal changes in the regional wind patterns. Summer surface flow tends to be offshore and the westward flowing currents weaken. In winter the surface flow has an onshore component that causes an accumulation of water and downwelling along the coast. There is a transition and acceleration of the regional currents in fall.

On a local short period scale a number of transient phenomena have been observed. These in turn modify the mean and seasonal patterns described above. Examples of internal tides, local response to intense storms and coastal atmospheric boundary layers are presented and discussed briefly.

PHYSICAL OCEANOGRAPHY AND DYNAMICS  
OF THE NORTHEAST GULF OF ALASKA

J. A. Galt and Thomas C. Royer

INTRODUCTION

Recent studies in the Gulf of Alaska have concentrated on the nearshore region in the northernmost sector between Seward and Yakutat (fig. 1). An intensive program has combined the results of hydrographic surveys, direct current observations, meteorological studies, and numerical modeling. This study is continuing, so the results that will be presented here are those of the initial phase of analysis and should be considered as somewhat speculative.

The data have made it possible to extend the results of earlier large-scale studies (Dodimead, et al., 1963) and localized variability investigations (Royer, 1975). We will begin with a general description of the region and a brief discussion of the factors controlling the mean circulation. Secondly, the seasonal variability and associated dynamic processes will be considered. Finally, short period effects and localized dynamic processes can be identified or documented in a few cases and some of the major unresolved questions in the circulation will be pointed out.

The present study has been motivated largely by the increasing interest in oil potential in the Gulf of Alaska and has been sponsored primarily by the Outer Continental Shelf Office of the Bureau of Land Management. The authors have had a major role in the study but there have been significant contributions from other investigators both in terms of actual field studies and helpful discussions. In particular, we are indebted to Drs. Favorite, Halpern, and Tabata.

## MEAN CIRCULATION

As a point of departure, we may consider the analog trace that would be obtained from a typical hydrographic station in deep water off Yakutat. Figure 2 is the record from station 41 taken during the July 1974 cruise on the *Acona*. The salinity generally increases with depth, but there are several distinctive features that can be identified in the temperature trace. Most apparent is the subsurface temperature minimum at 80 meters and the maximum at 130 meters. These both represent water that is not formed locally. This water takes on its characteristics elsewhere and is carried into this region by the currents that are part of the larger Gulf of Alaska circulation. Concentrating first on the deeper temperature maximum one can identify this as water that was formed near the surface, well south in the vicinity of the North Pacific drift (probably at the subarctic convergence) (Sverdrup, et al., 1942). As the current turned north and formed the large-scale counterclockwise gyre that is found in the Gulf of Alaska, the water was swept along and encountered surface water that was more dilute and consequently less dense. This forced the warmer and more saline water below the surface where it continues on at approximately the level of the  $\sigma_t = 26.5$  surface. The distribution of this warm layer will then indicate the path along which this water is being carried. The water found in the minimum layer is also formed at the surface south of the region of interest. In this case, the water is formed in the winter somewhere in the central part of the gyre. The northward spreading of this layer helps to delineate between the presumably sluggish circulation within the center of the gyre and the faster, narrow current moving around its edge. Confining our attention to these two features for the moment, it is possible to trace some of the implications suggested by the data.

Figure 3 gives the temperature distribution around the outside of the region of interest. (For reference, the viewer would be looking north at a vertical section with Seward off the page to the left and Yakutat off the page to the right.) These data were collected in July 1974. The warm water is clearly not a uniform layer, but a relatively narrow filament. Thus the flow from the south enters the region in a narrow stream at station 41 (temp  $> 5.5^{\circ}\text{C}$  at 130 m). The same water seems to exit the region, at least in part, between stations 44-46. And then it enters again at station 49 and exits finally at station 52. To confirm that this is in fact the same water, we can plot the depth of the  $\sigma_t = 26.4$  surface on figure 3. This has been done with a dotted line and clearly links the isolated filaments of warm water together. It is also clear that between regions where the warm water goes into the region and comes out again the cold water layer becomes more apparent (i.e., at stations 42-43 and 50). The relatively complex distribution of the  $\sigma_t = 26.4$  surface suggests a clockwise intermediate scale gyre along the boundary of the region. From what little historical data are available, apparently this is an anomalous situation (personal communication, Dr. F. Favorite, National Marine Fisheries Service).

To obtain a somewhat different perspective of how this warm layer moves through the region we may look at the temperature distribution along section lines extending perpendicular to the coast. Figure 4 shows the temperature vs. depth along a line which is just to the east of Icy Bay collected from the ship *Surveyor* in June 1975. Here the current has narrowed and contacts the shelf at about 150 m depth. The current appears to be about 40 kilometers wide here and has moved inshore relative to its position farther to the east, as presented in the prior discussion.

As the current moves inshore, the low temperature layer can also be seen to spread inward at a slightly higher level. Slightly west of Icy Bay is a region where the shelf break angles sharply toward the coast. The current moves inshore here and appears to be following the 150 m isobath. However, it does not turn as sharply as the bathymetry and once again forms a wider current. The colder layer also appears to have a shoreward intrusion along this line of stations. Farther to the west the shelf becomes wider again. The warm layer once again narrows and appears to move off the shelf into slightly deeper water.

West of Cape St. Elias the shelf is much wider ( $\approx 100$  km) and the distribution becomes more complex. There is little evidence of a well-defined warm core except for a possible residual offshore. In addition, there are many small-scale features in the pattern. These details appear at only one station and are subsequently very difficult to contour.

Now we may shift our attention to the horizontal distribution of this warmer layer which we take to represent the relatively strong, large-scale currents associated with the Alaskan Stream and the general circulation of the entire Gulf of Alaska.

A relatively complete set of STD data was collected off the ship *Oceanographer* in February 1975. These data were examined to determine the position of the warm subsurface layer, or filament. A plot of the temperature on the  $\sigma_t = 26.5$  surface is shown in figure 5. Here, a belt of temperature  $> 5.5^\circ\text{C}$  is found flowing east to west over the continental slope region. The actual temperatures in this layer were well above those found during the summer with the maximum actually over  $6.2^\circ\text{C}$ . This is due to this water requiring roughly half a year to be transported from the surface and around the gyre to this region of the Gulf of Alaska. Once again, these data suggest splitting of the current in the eastern part of the region off Yakutat.

In April 1974 the *Rainier* collected CTD data for the area. Although the data set was not complete, the axis of the warm layer current could be identified and is shown in figure 6. The temperature range along the axis is indicated and, as can be seen, the values are somewhat lower than those observed in January.

The *Surveyor* data collected in June 1975 also shows the distribution of the warm core. Figure 7 shows the distribution of temperature on  $\sigma_t = 26.5$  surface. Once again, the warm layer current is seen to flow along the continental slope. The temperature in this layer is slightly cooler than in April and there is some indication that it is closer inshore.

In addition to the temperature and salinity data, direct current measurements were made. Current meter measurements are particularly valuable in circulation studies since they measure directly a quantity that is of interest. Also, modern current meters are capable of obtaining high time resolution so that short period variations in the current can be resolved. In the present study the direct current measurement program has been largely successful and a great quantity of data is being analyzed.

First, we can consider the longer period or quasi-steady components to the flow. To obtain an estimate of these, we average the currents for a week and present them as a mean progressive vector diagram for the week. This effectively removes most of the tidal signal.

The first data to be considered comes from station 60 (see fig. 1) which was located in the western portion nearshore between the mouth of the Copper River and Middleton Island. The observations cover an 8-week period from July 1974 to August 1974. Over this summer period, the upper flow is predominately towards the west at up to 100 km/week but the direction is variable. In the lower layer the flow is quite small (on the order of 3 cm/sec), indicating a substantial baroclinic shear.

The current data from station 61 have been similarly examined. Figure 8 presents the data for an upper and lower meter for 14 weeks, extending from August 1974 to November 1974. This station was located near the edge of the shelf midway between Middleton Island and Cape St. Elias (see fig. 1). In this case, the flow is again generally to the west and consistent in its direction, particularly for the upper meter. The seasonal buildup throughout October and November is pronounced, although the lower layer does not exhibit the same response. The general direction of the flow corresponds closely to the local bathymetric contours and apparently the steepness of the bottom slope dominates the flow direction along this segment of the shelf break independent of season.

The results from station 62 are presented in figure 9. These data cover a 23-week period from August 1974 to February 1975. Once again, data from an upper and a lower meter are presented. The station is located near the shelf break offshore from Icy Bay (see fig. 1). As before, the direction of the flow is consistent except for a short period late in December when the flow is weak and has a pronounced easterly drift. Most of the time the flow is NNW at both levels, with weaker flow at depth. As in the results from station 61, the flow shows a marked increase through the fall and tends to align itself along the local isobath. Both of these features are consistent with the probable barotropic pressure gradient that would be created with the buildup of seasonal downwelling in response to the winter wind regime.

From the temperature, salinity, and direct current meter data, it is possible to make several conjectures about the first-order large-scale currents of the region. The currents in the eastern segment of the region (Yakutat to Cape St. Elias) are contaminated year-round by a flow that is part of the large-scale Gulf of Alaska circulation. The current flows near the shelf break following the 150 m isobath. In this region, where the continental shelf is

narrow, the current will dominate close to shore (a few tenths of kilometers). The tendency of the currents to follow the bathymetry indicates that the flow direction is approximately the same from top to bottom although vertical shear is likely. It is important to note that the first-order currents in this area are not locally driven. This means that large-scale perturbations in this flow, like the anticyclonic gyre, cannot be discussed without input data from the larger-scale systems. In particular, the current is generated over the entire Gulf of Alaska, or NE Pacific, and the entire region would have to be examined to understand the complete dynamics of the flow.

In the western segment of the region (Cape St. Elias to Seward) the warm layer current associated with the Alaska Stream moves offshore and the relatively wide shelf region behind Middleton Island is largely free from the influence of this flow. It appears that the currents in this area are generally weaker than those found in the eastern segment. The typical horizontal scale of the distributions is less and the local influence of winds and shelf topography, along with discharges from the Copper River and Prince William Sound, will be much more pronounced.

The preliminary analysis of the current meter data presents a picture that is basically consistent with what has been developed from the hydrographic data. The large-scale quasi-steady flow in the eastern region reflects a stronger flow dominated by components that follow bathymetric contours. The flow on the shelf in the western region is weaker and more variable, at least in the summer.

A diagnostic circulation model has been developed to use with hydrographic and wind stress data. This can be used with various combinations of boundary conditions and compared to the results from current meter measurements. Preliminary results indicate that the mean flow can be well-represented with a



geostrophic plus Ekman balance. The bathymetry clearly plays a dominant role in the flow dynamics and the initial model tests indicate a good qualitative agreement with the baroclinic or density-induced effects.

Locally the flow follows the isobaths even in regions where the topography may be quite complex. Modifying this tendency slightly is the effect induced by the baroclinicity and bathymetry interacting together which moves the flow gradually into deeper water.

#### SEASONAL VARIATIONS IN THE CIRCULATION

The description thus far has concentrated on the largest scale feature that appears to represent somewhat mean or average conditions over the entire year. Superimposed on this flow are a complex series of shorter period variations.

The seasonal variations in atmospheric forcing are discussed in some detail by Royer (1975). They can be briefly summarized by figure 10. During the winter the winds in the northern Gulf of Alaska are from the southeast giving surface currents onshore. During the summer winds are much weaker and from the southwest, resulting in slight offshore surface currents. The implications of this variability can be seen in the oceanographic data fields and the hydrographic data can be examined to provide some initial estimates of how the transients may behave.

Station 1 (the innermost station on the Seward line) has been occupied on an irregular basis since 1970. It provides an opportunity to ascertain the seasonal changes at a point on the shelf in the Gulf of Alaska. The salinity changes (figure 11a) demonstrate a strong annual input of freshwater at the surface from late spring through late fall. Coincident with the decrease in surface salinity is an increase in near-bottom salinity. The source for this

near-bottom water is in the vicinity of the shelf break. Its intrusion onto the shelf is probably the result of large-scale wind stress changes over the region since the monthly mean upwelling index (figure 11b) is well correlated with these changes in the near-bottom water. The index represents the onshore-offshore component of the Ekman wind drift transport. Upwelling indicates surface water moving offshore with near-bottom water moving onshore to replace it. The reverse occurs under downwelling conditions. The strong downwelling during the winter appears to act as a flushing mechanism that cycles the shelf waters onshore-offshore annually.

This presumably will take place to some extent all along the shelf and act as a first-order perturbation on the warm water current associated with the Alaska Stream. To get a better insight into the possible spatial dependence of this wind-driven effect, we can consider seasonal changes in the density structure.

The vertical temperature and salinity structures were measured along a line normal to the coastline near Icy Bay in February and in May. These distributions confirm the results suggested in the previous paragraph. During February the isopycnals appear to be displaced offshore and the water nearly mixed over the shelf. This results in very little baroclinic shear with the geostrophic velocities essentially independent of depth. By May the shelf waters are more stratified with what appears as a relaxation of the downwelling condition. The isopycnal are inclined indicating something like 10 cm/sec shear in the geostrophic flow in the upper 100 m. During the summer when this current shear is a maximum there is still no evidence that it is likely to set up a counter-current. Thus the flow in the lower layer may be somewhat reduced or sluggish compared to the winter, but the direction appears to be uniformly westward along the coast. As was mentioned in the previous section the current meter records

clearly indicate the seasonal buildup of the currents (figs. 8 and 9). These can also be correlated with the wind stress buildup and the onshore pile-up of surface water.

#### SMALL-SCALE VARIATIONS IN THE CIRCULATION

Thus far we have considered the larger general circulation and its seasonal variations. On a smaller scale, the flow will exhibit changes in time and space related to tides, individual storms and a variety of different waves. These kinds of variations are inherently difficult to examine in the density data. However, some time series CTD measurements were collected at several locations and they provide some interesting examples. Figure 12 gives the vertical profile of  $\sigma_t$  at hourly intervals at station 62 in June. The dotted line indicates the mixed layer depth and appears to be dominated by an oscillation at approximately semidiurnal tidal frequency. This suggests an internal tide with an amplitude of something on the order of 10 meters. A similar series collected at station 63 in February indicated an intrusion of water along the bottom on the order of 10 meters thick and appearing over just a few hours.

Near-surface current meter and wind measurements were made at 3 m below the surface and 4 m above the surface during February 1975 at station 63, a site located in about 100 m of water approximately 25 km from the coast off Icy Bay (see fig. 1) (Holbrook, et al., 1975). The results indicated that the coastal wind measurements at Yakutat were not representative of near-surface wind observations made 25 km from the coast, probably because of the influence of coastal terrain. Prior to the arrival of a storm on February 11 the vector-averaged mean value of the near-surface currents between February 3-10 was about  $12 \text{ cm sec}^{-1}$  towards the northeast. After the onset of the storm the currents increased in magnitude; e.g., the vector-averaged current speed from February 11-15 was about  $44 \text{ cm sec}^{-1}$ .

Currents recorded at 10 m above the bottom at station 63 showed a similar response to the passage of the February 11 storm. Prior to the arrival of the storm the vector-averaged mean current speed was  $3 \text{ cm sec}^{-1}$ . During the occurrence of the storm, the vector-mean current speed increased to  $21 \text{ cm sec}^{-1}$ . The direction of the storm-generated current near the bottom was almost the same as the direction of the current near the surface and approximately along the local isobaths.

When dealing with the small-scale or locally controlled events in the circulation it is clear that the regional winds are of primary significance. To get some idea of how the local winds might be correlated with oceanographic events, a meteorological study was carried out to obtain estimates of regional wind stress.

The National Weather Service produces pressure maps of the Alaska area at their regional office in Anchorage. These maps are based on hand analysis by the local Meteorologist-In-Charge and reflect all available input on the standard world weather net. The pressure fields were digitized and calculations were carried out for geostrophic winds, surface winds, wind stress and curl of the wind stress.

Fleet Numerical Weather Central at Monterey runs a numerical forecast of weather for the northern hemisphere and from this computer-generated pressure fields are available for the Alaska region. The same type of analysis was carried out on this data to obtain geostrophic winds, surface winds, wind stress and curl of the wind.

A third source of regular wind data was available from EB-33 stations south of Yakutat off the continental shelf. It is interesting to compare these three independent sources of data. Figures 13 and 14 give the east-west and north-south components of the surface wind. It is immediately clear that the

three sources give substantially better agreement on the north-south component than they do for the east-west. This is not surprising since the east-west winds depend on the north-south pressure gradients which are not well resolved with any of the available data. Contrasted to this, the north-south winds depend primarily on pressure data along the coast, which is well sampled in the inputs to the National Weather Service.

Carrying this one step further, we may note that the wind stress is proportional to the wind speed squared, and thus any differences in calculated speed will be accentuated in the stress calculation.

The problem of along-shore wind stress turns out to be fairly sensitive to the onshore-offshore pressure gradients. This component of the stress is in turn of fundamental importance in understanding the upwelling or downwelling cycles as well as the potential for the onshore transport of spilled pollutants. The appropriate length scale for the pressure field normal to the Alaskan coastline must be delineated to properly address these questions. In an attempt to look at these variables, some lower atmosphere measurements were made in February in conjunction with the *Oceanographer* cruise.

Figure 15 indicates the water and air temperature at EB-33. Early in February there is an extreme outflow of cold continental air that results in a very unstable air-sea temperature difference of approximately 8 degrees. This could be expected to result in intense air/sea exchange with the subsequent modification of the atmospheric boundary layer. To investigate this possibility a series of radiosondes was taken on a station line normal to the coast. The results are presented in figure 16. The boundary layer grows quickly in the first 30-50 km off the coast and this may well be the appropriate scale for the wind shear along the coast.

Based on these data, a simplified model of this cold air breakout can be developed (fig. 17). The questions of how much influence these breakouts have on the coastal weather patterns, or even how often they occur, is of considerable interest to the applied problems addressed by this study.

#### CONCLUSIONS

In summary, the hydrographic data support the idea of a fairly stable mean circulation dominated by the Alaska Stream and modified by an onshelf-offshelf perturbation correlated with the regional winds. Superimposed on this are significant smaller scale (in both time and space) variations related to storms or tides and possibly other influences. There appears to be a difference in the dominance of the Alaska Stream with regard to the regions east and west of Cape St. Elias. On the east, global forcing seems more important and the Stream's influence is seen close inshore. On the west, the Stream is well offshore and local forcing appears to be more significant.

The current meter data have added several new insights. The buildup of the currents during the fall gives a quantitative measure of the response of the system to the seasonal change in the wind forcing (downwelling). In addition, the relatively rapid response of the currents to wind events has been noted and is of considerable interest. During the winter, outflows of cold continental air result in major perturbations on the local wind fields and these may dominate the nearshore circulation dynamics.

## REFERENCES

- Dodimead, A. J., F. Favorite and T. Hirano (1963). Review of oceanography of the subarctic Pacific region. In: Salmon of the North Pacific Ocean, Bulletin International North Pacific Fisheries Commission, 13, 195 pp.
- Holbrook, J. R., D. Halpern and S. P. Hayes (1975). Response of surface and near-bottom shelf currents to a winter storm in the Gulf of Alaska, Trans. of Am. Geophy. Union.
- Royer, Thomas C. (1975). Seasonal variations of waters in the northern Gulf of Alaska, Deep-Sea Res. 22 (6): 403-416.
- Sverdrup, H. U., Martin W. Johnson and Richard H. Fleming (1942). The Oceans, Prentice Hall, 1087 pp.

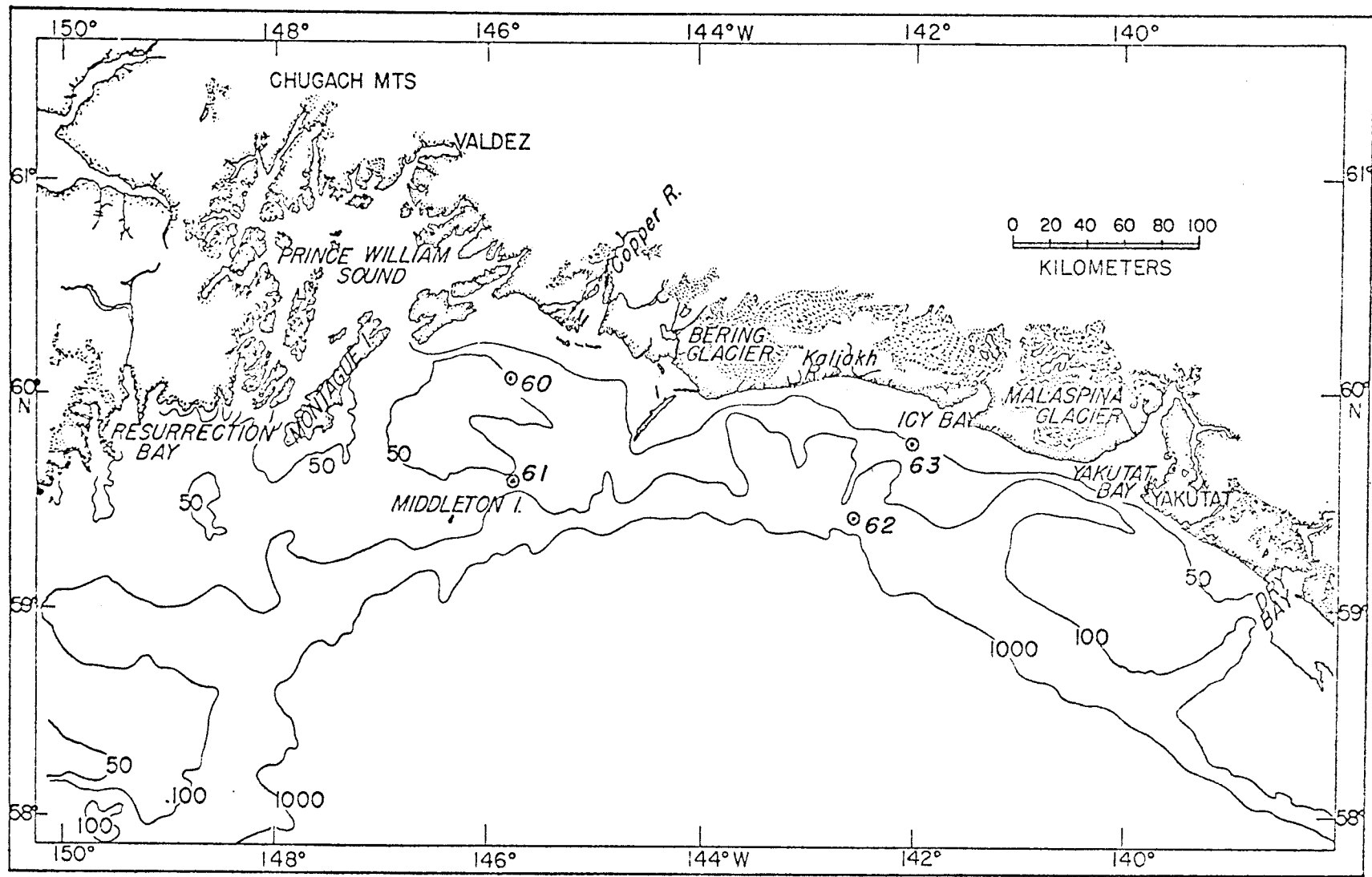
## LIST OF FIGURES

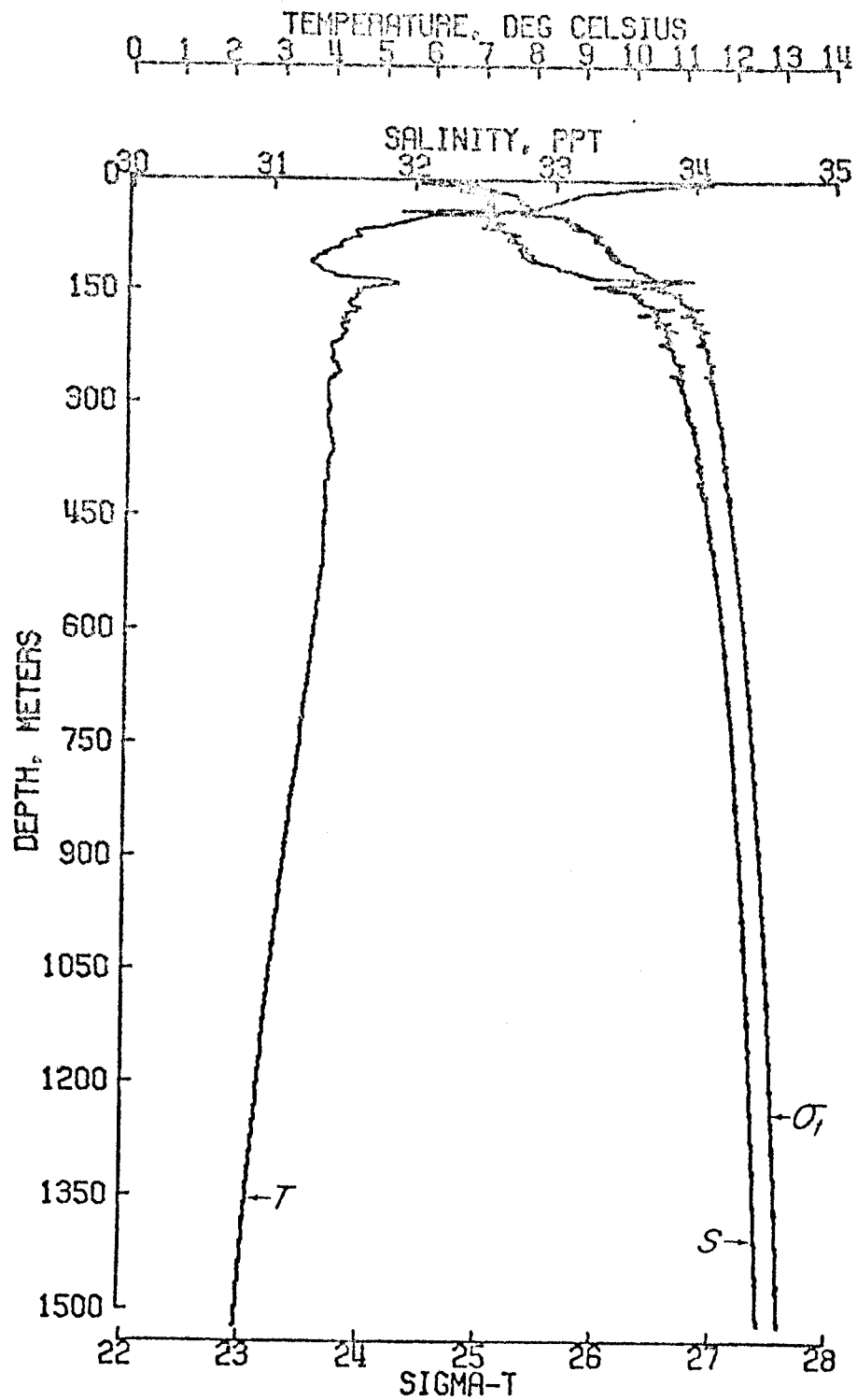
- Fig. 1. Region of study in the Gulf of Alaska. Depth contours given in fathoms and station locations for moored current meter arrays are indicated by station number.
- Fig. 2. Vertical profile of salinity, temperature and  $\sigma_t$  at Acona station 41, cruise 193 (58°29.3'N, 141°38.9'W).
- Fig. 3. Vertical section of temperature versus depth extending, offshore from Yakutat (STA 37-STA 43), west across the deeper offshore section of the Gulf of Alaska (STA 43-STA 51), and onshore to the continental shelf off Seward (STA 51-STA 53). The depth of the  $\sigma_t = 26.4$  surface is given by the dotted line.
- Fig. 4. Vertical section of temperature (°C) versus depth (meters) on a line of stations extending across the continental shelf off of Icy Bay.
- Fig. 5. Distribution of temperature on the  $\sigma_t = 26.5$  surface measured during February '75. Region  $> 5.5^\circ\text{C}$  indicates current region.
- Fig. 6. Distribution of the axis of the subsurface temperature maximum observed during April '74. Values along the track indicate temperature range (°C).
- Fig. 7. Distribution of temperature on the  $\sigma_t = 26.5$  surface measured during June '75. Region  $> 5.0^\circ\text{C}$  indicates current region.
- Fig. 8. Average weekly displacement for station 61 covering the period from August '74 to November '74. Values given for an upper meter (20 m depth) and a lower meter (162 m depth).
- Fig. 9. Average weekly displacements for station 62 covering the period from August '74 to February '75. Values given for an upper meter (24 m depth) and a lower meter (178 m depth).
- Fig. 10. Mean atmospheric pressure distribution over the North Pacific for winter and summer (after Dodimead, Favorite and Hirano, 1963).
- Fig. 11. (a) Time series cross-section of salinity for station 1 in Gulf of Alaska with (b) monthly mean upwelling index and its anomaly.
- Fig. 12. Vertical profiles of  $\sigma_t$  at hourly intervals at station 62 (see fig. 1) June '75. (Dotted line indicates mixed layer depth.)
- Fig. 13. North-south component of the wind stress in the coastal region of the Gulf of Alaska for January '75--PMEL indicates analysis of NWS data--MONTEREY indicates analysis FNWC data and EB-33 is from weather buoy data.
- Fig. 14. East-west component of the wind stress in the coastal region of the Gulf of Alaska for January '75--PMEL indicates the analysis of NWS data--MONTEREY indicates analysis of FNWC data and EB-33 is from weather buoy data.



- Fig. 15. Air temperature and water temperature recorded at data buoy EB-33 during periods of January and February '75.
- Fig. 16. Humidity profiles from a series of radiosonde ascents on a line of stations extending across the continental shelf off of Icy Bay. Distances from coastline are shown.
- Fig. 17. Conceptual representation of cold air outbreak normal to the Alaskan Coast during winter.

340

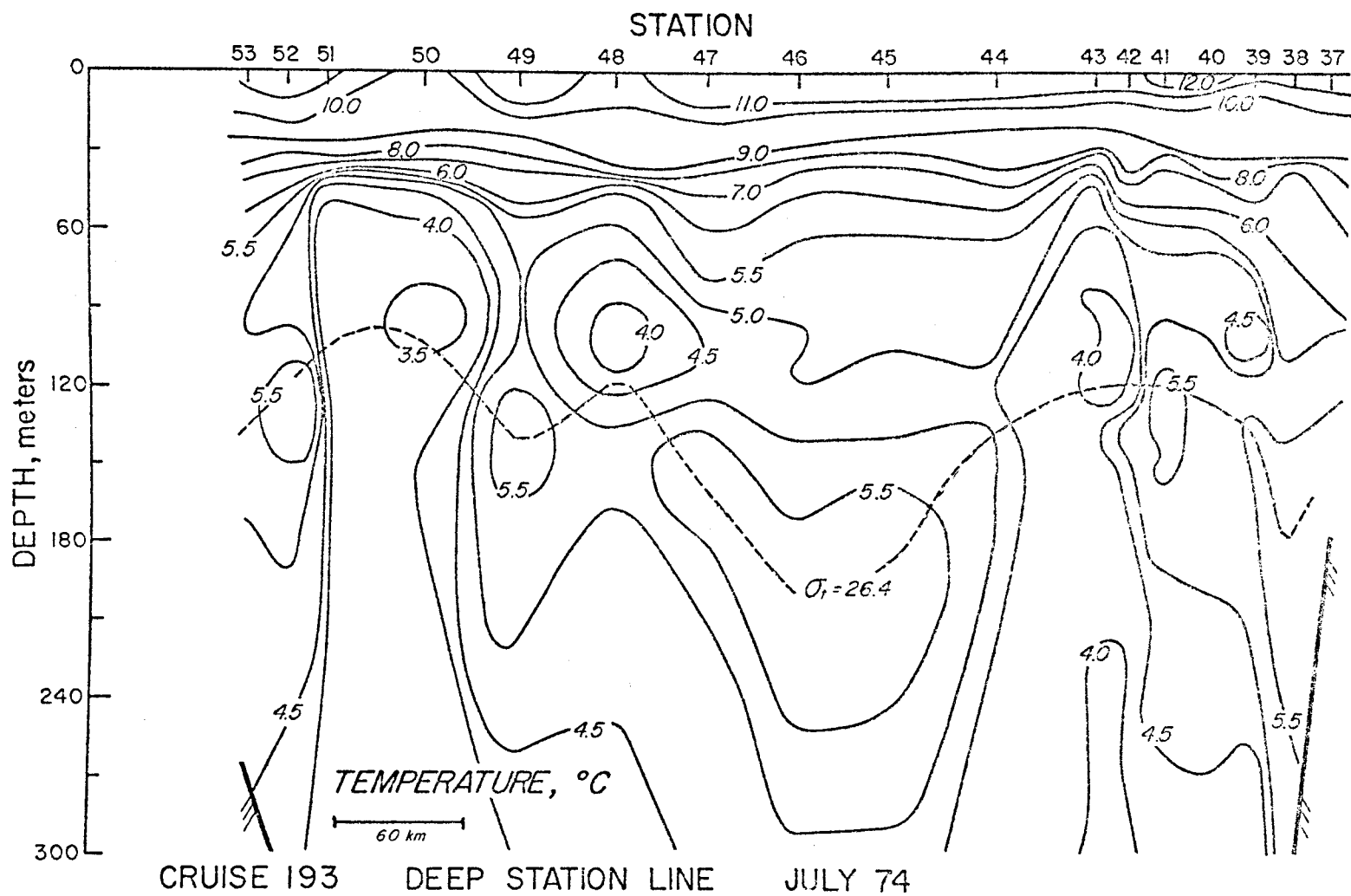




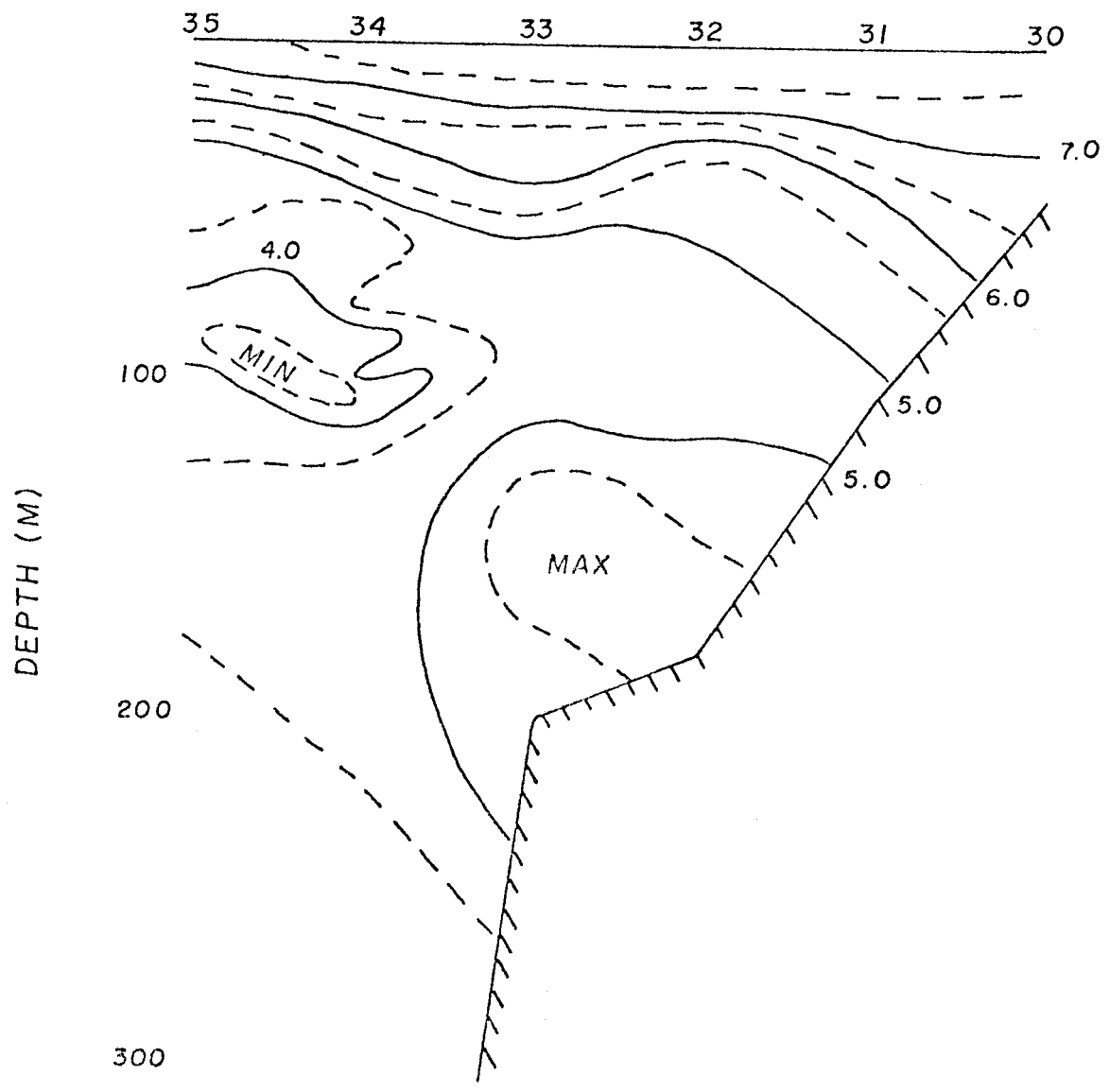
CRUISE 193

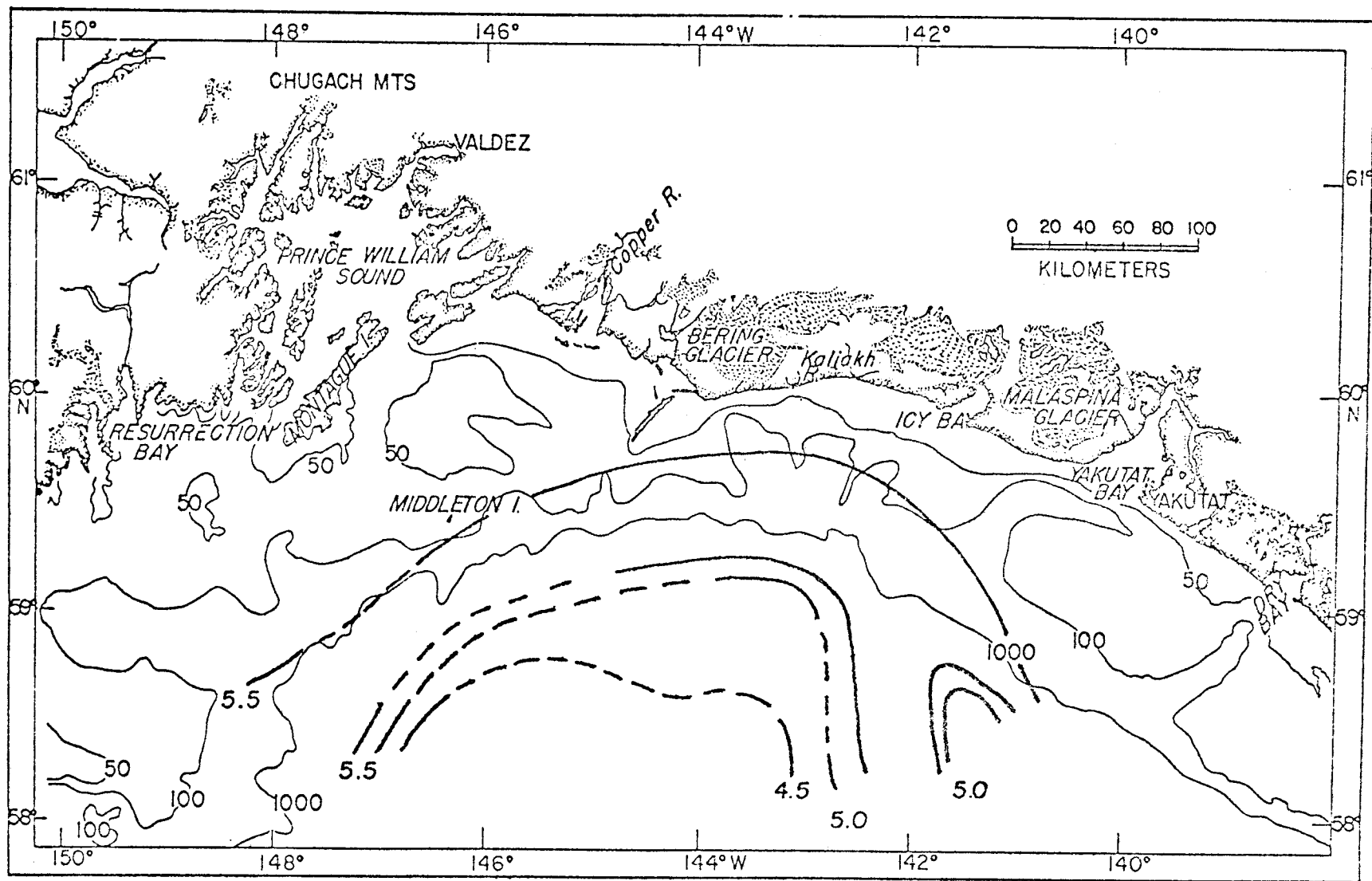
STATION 42

342

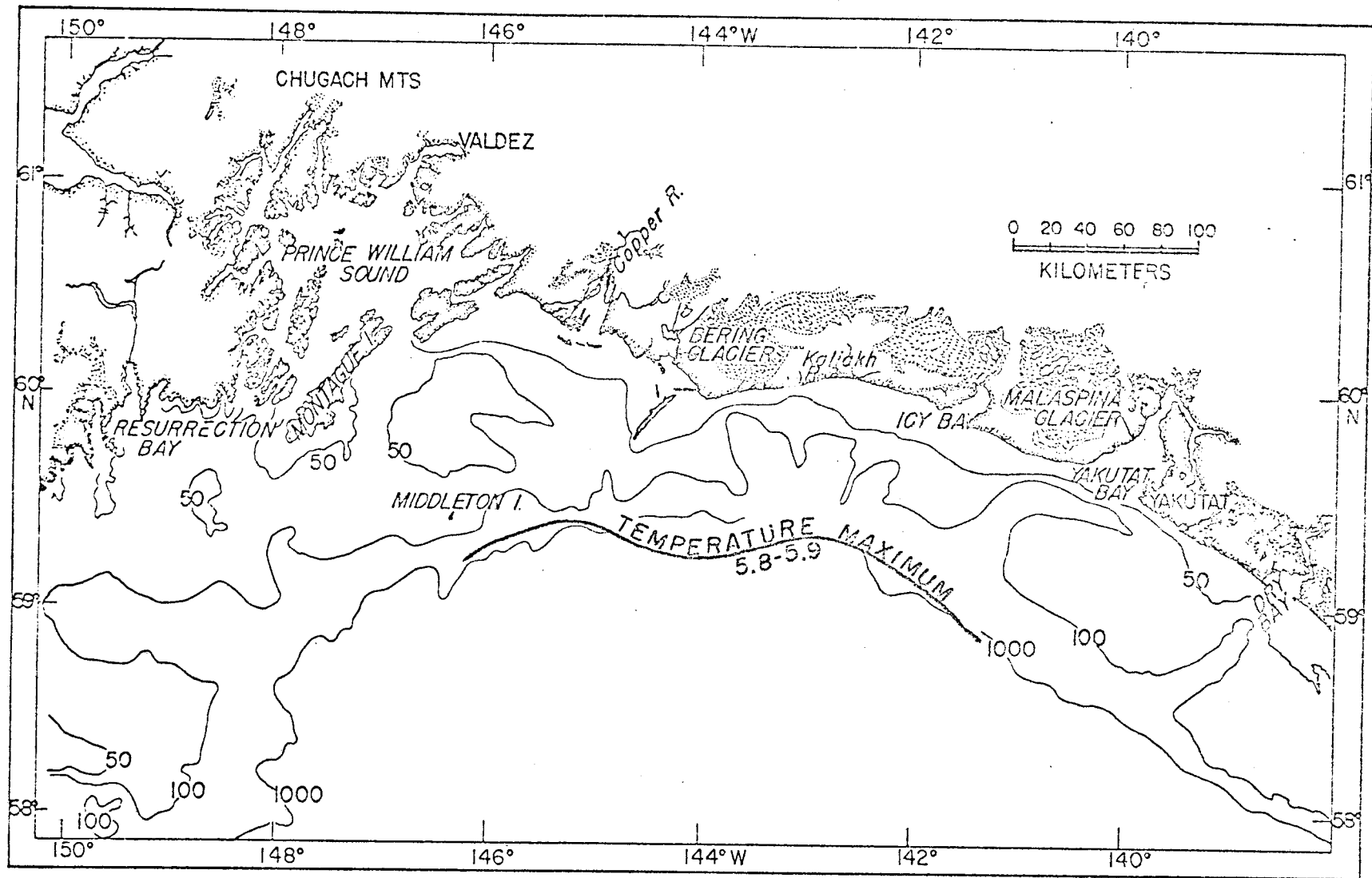


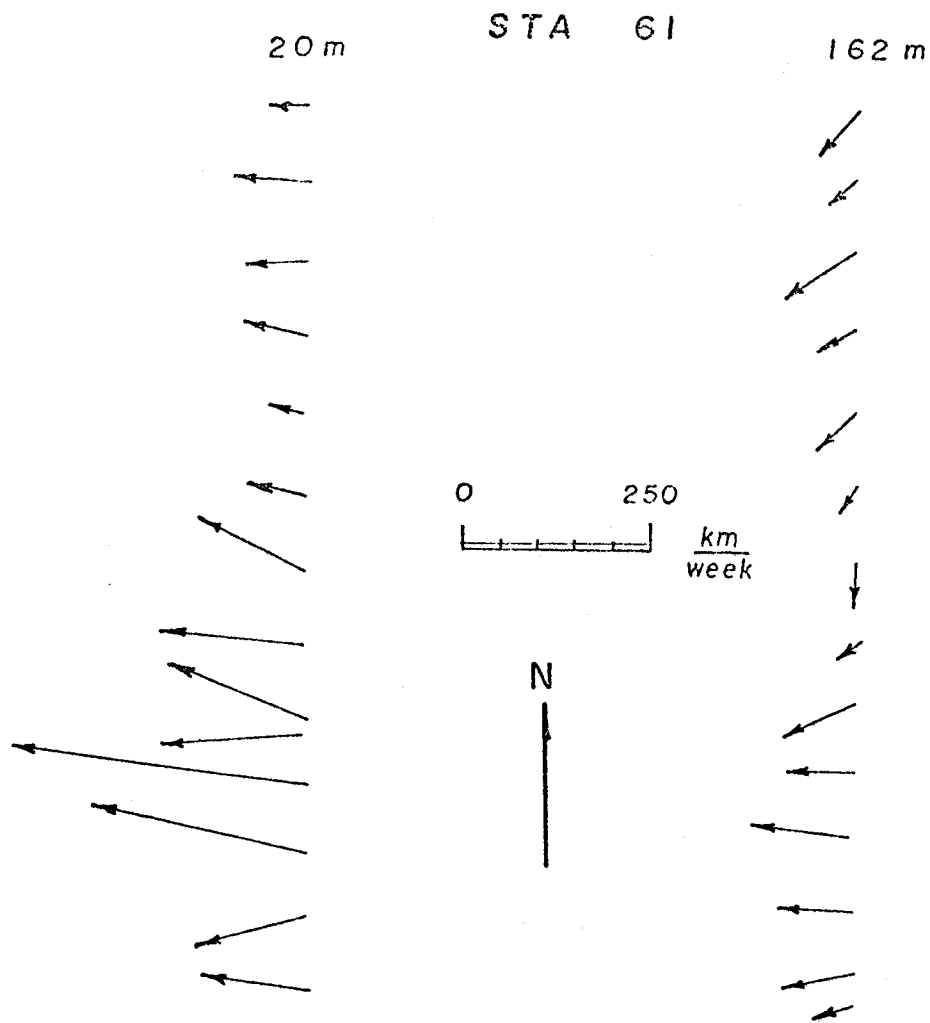
RAINIER JUNE 75  
STA NUMBER





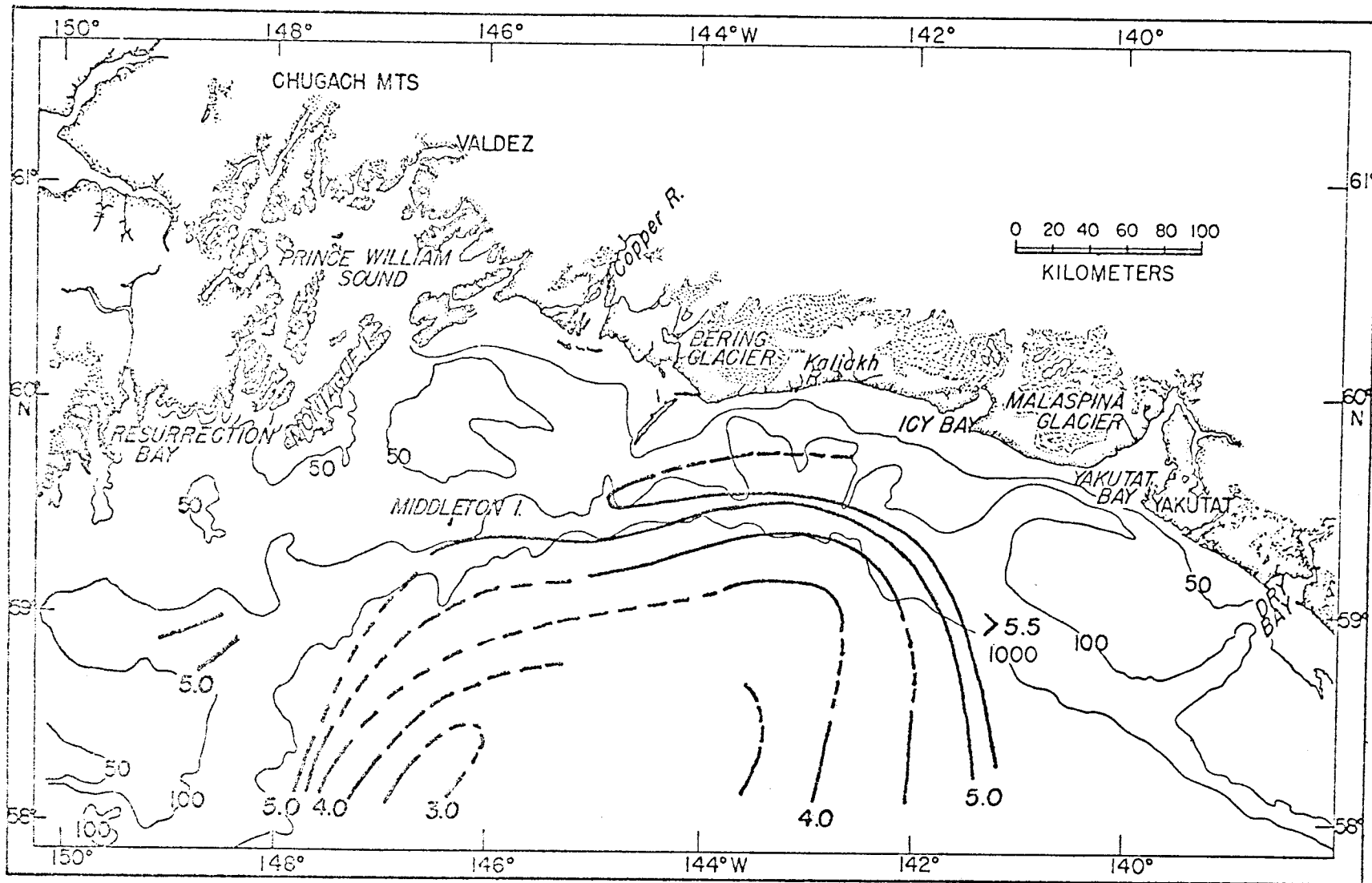
345



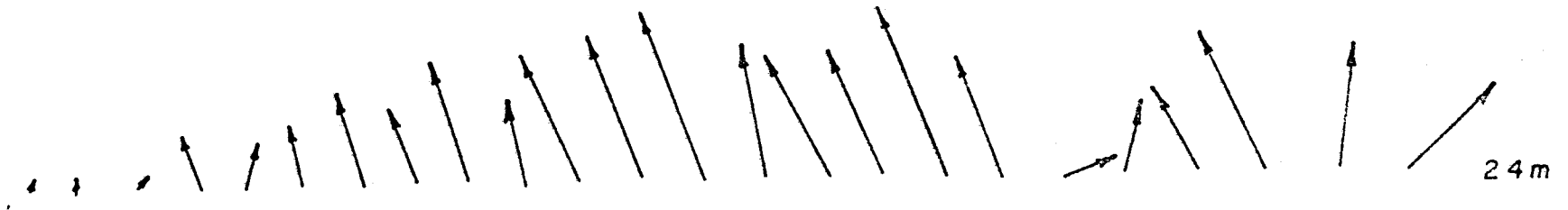




347

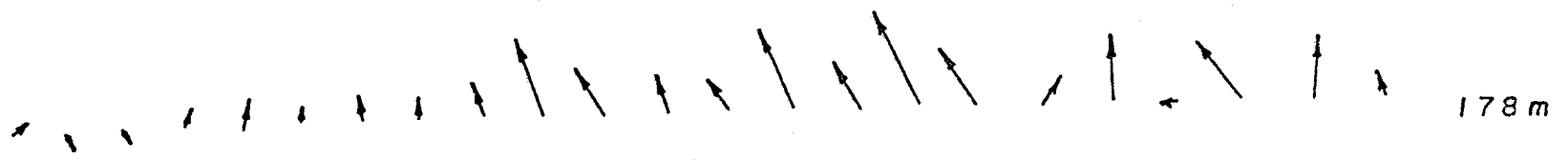
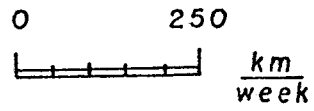


348

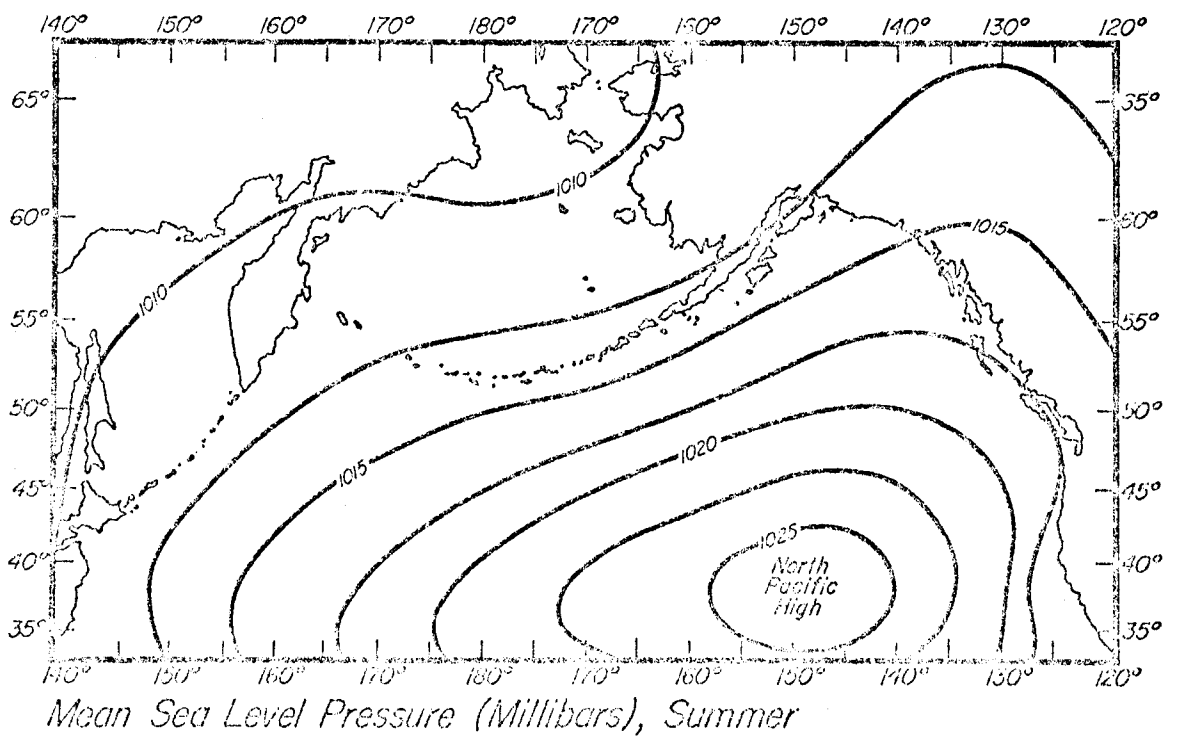
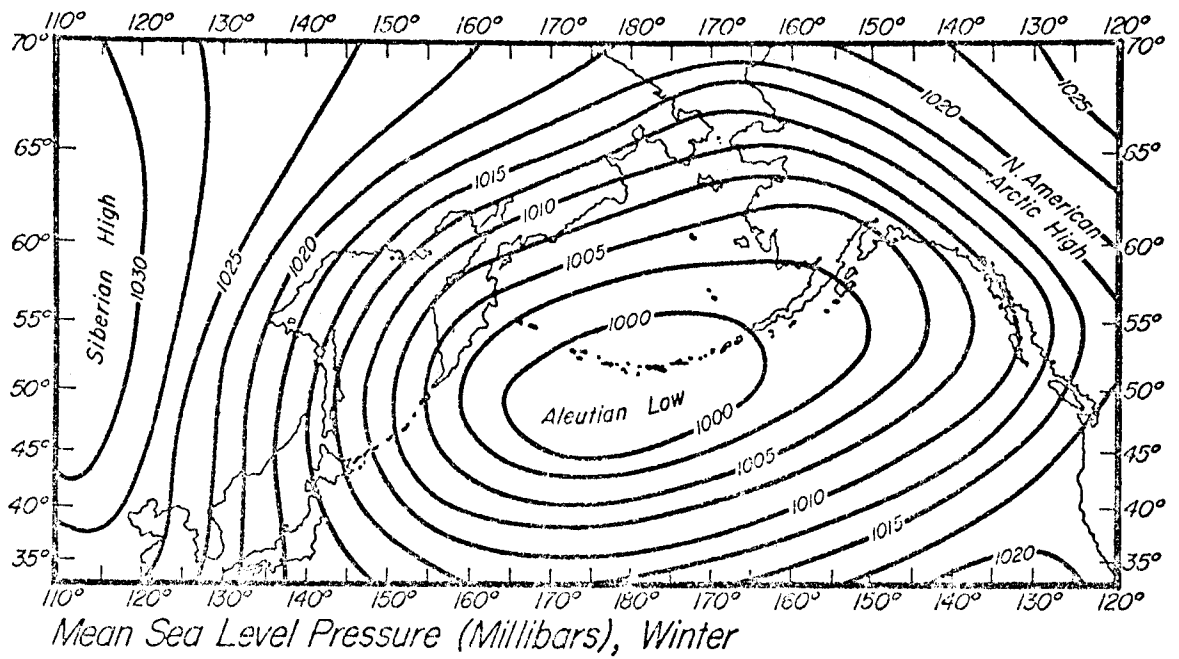


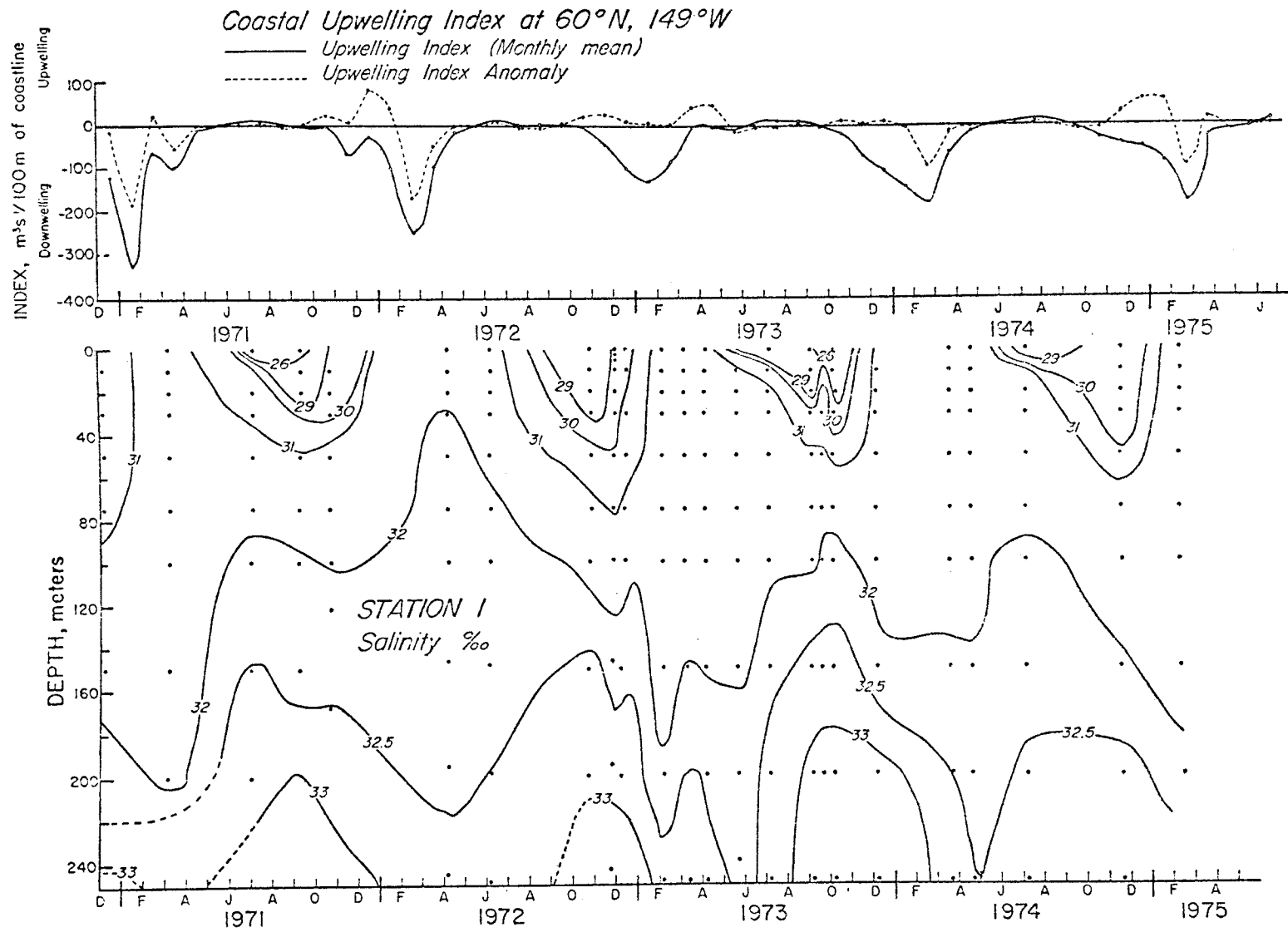
24 m

STA 62-A



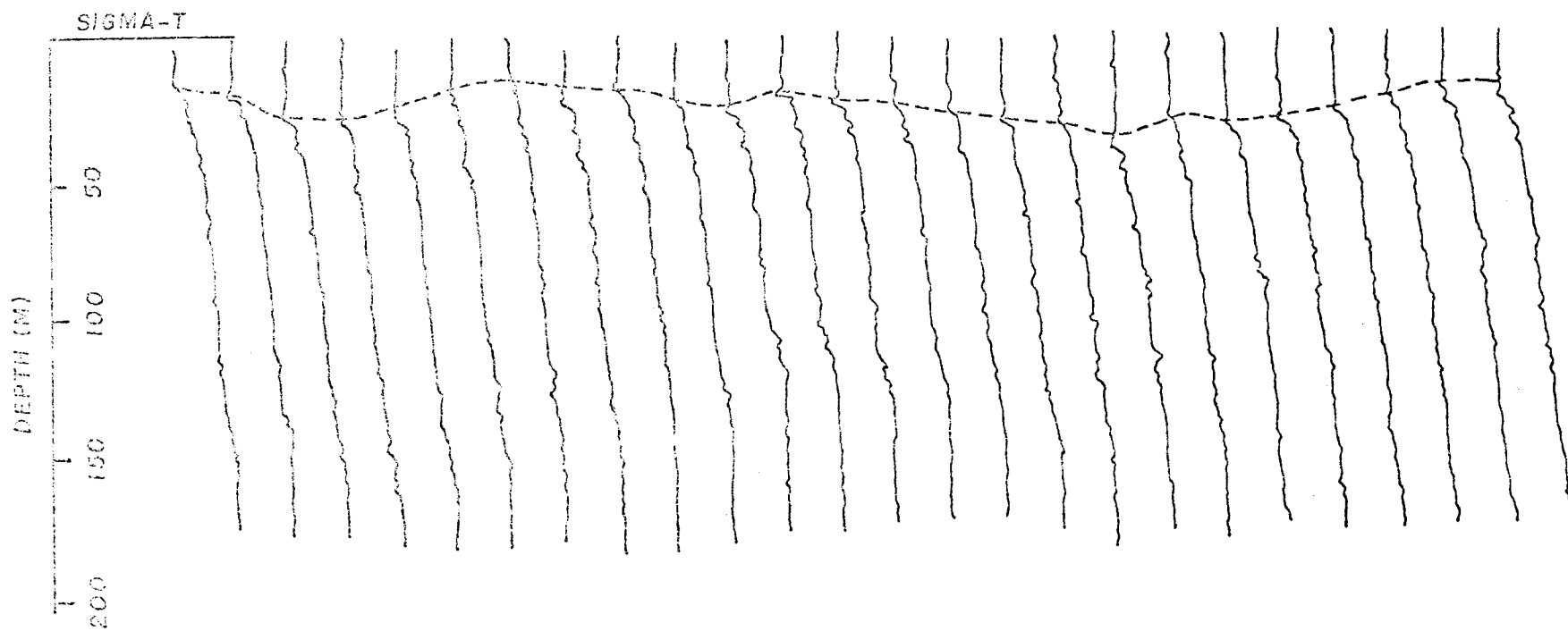
178 m



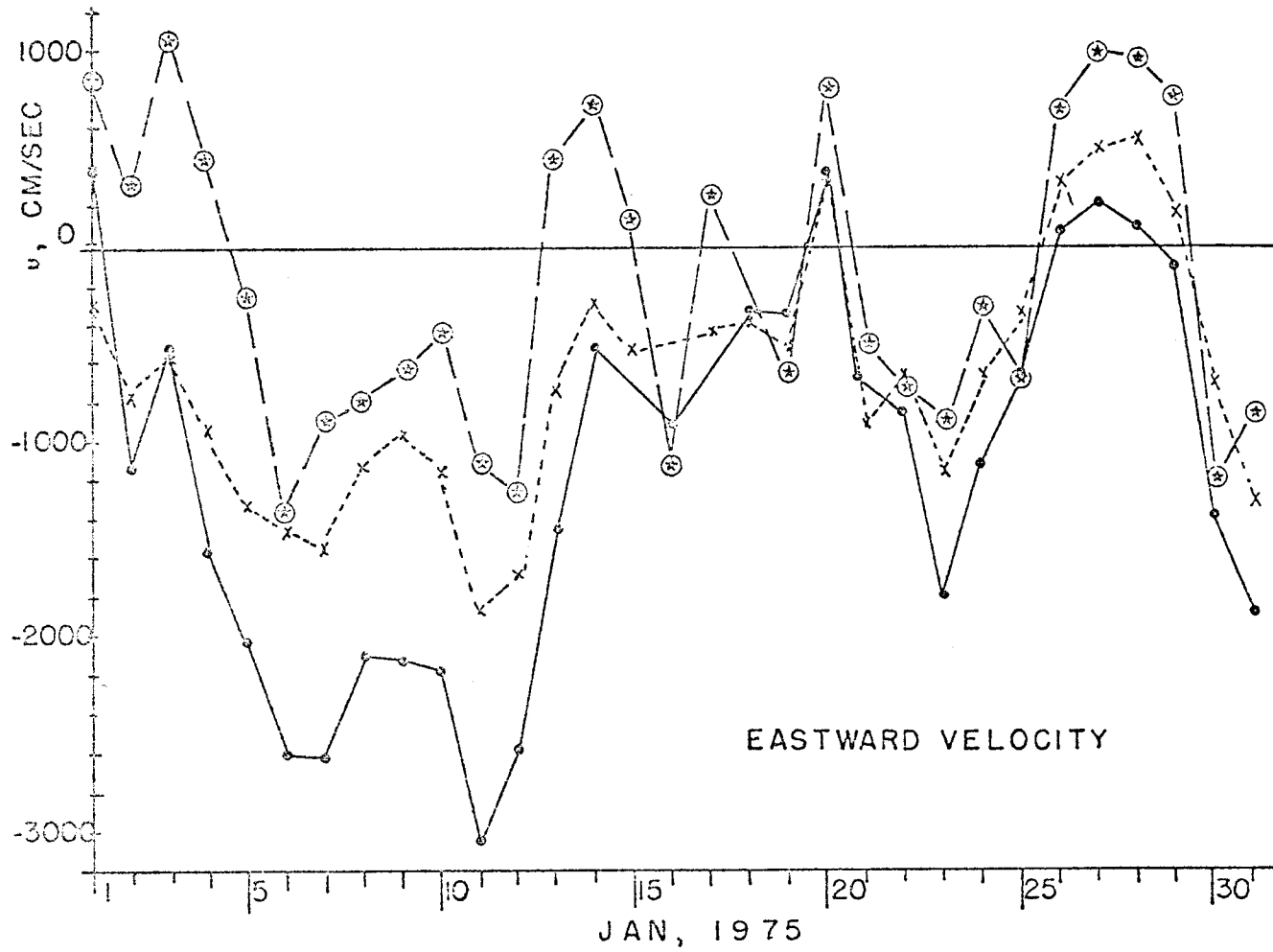


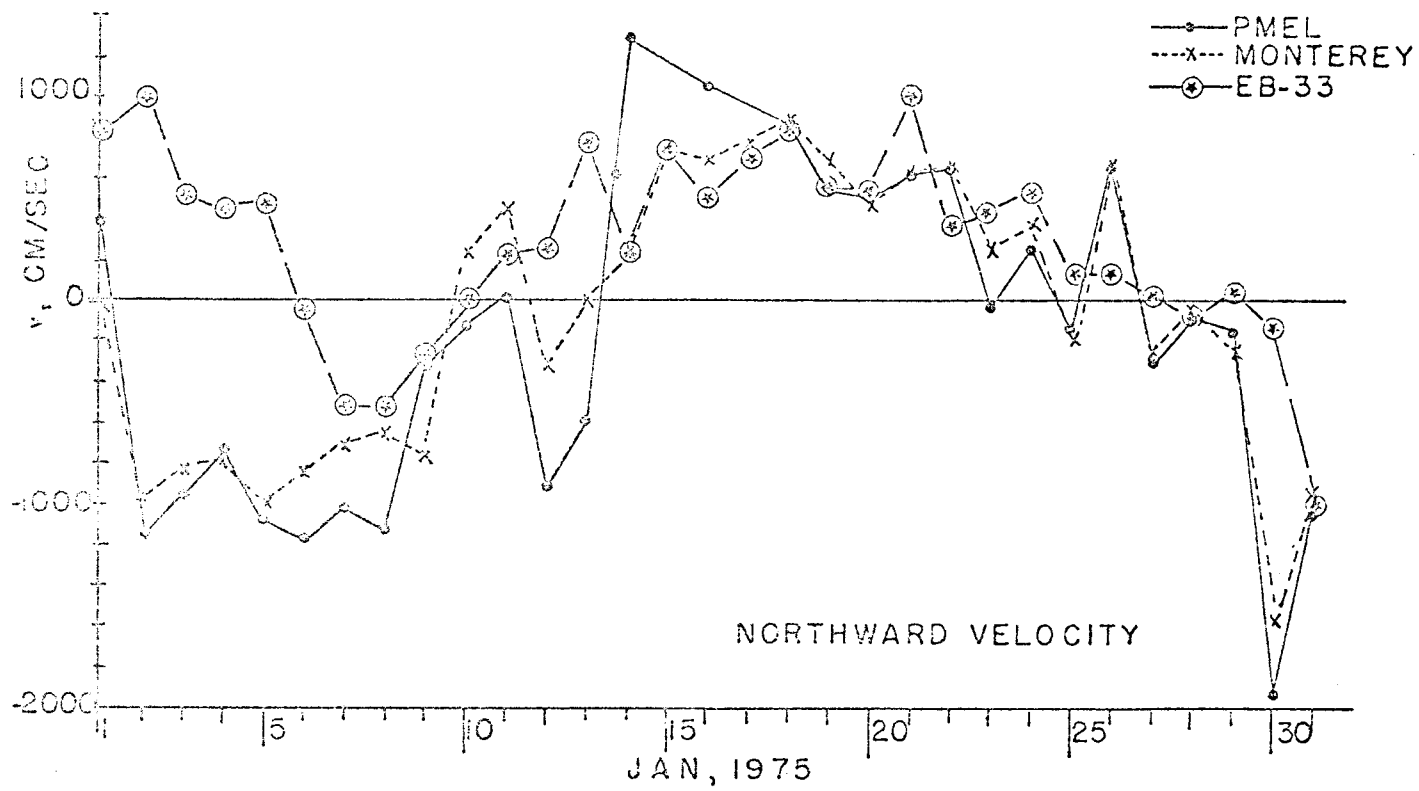
758

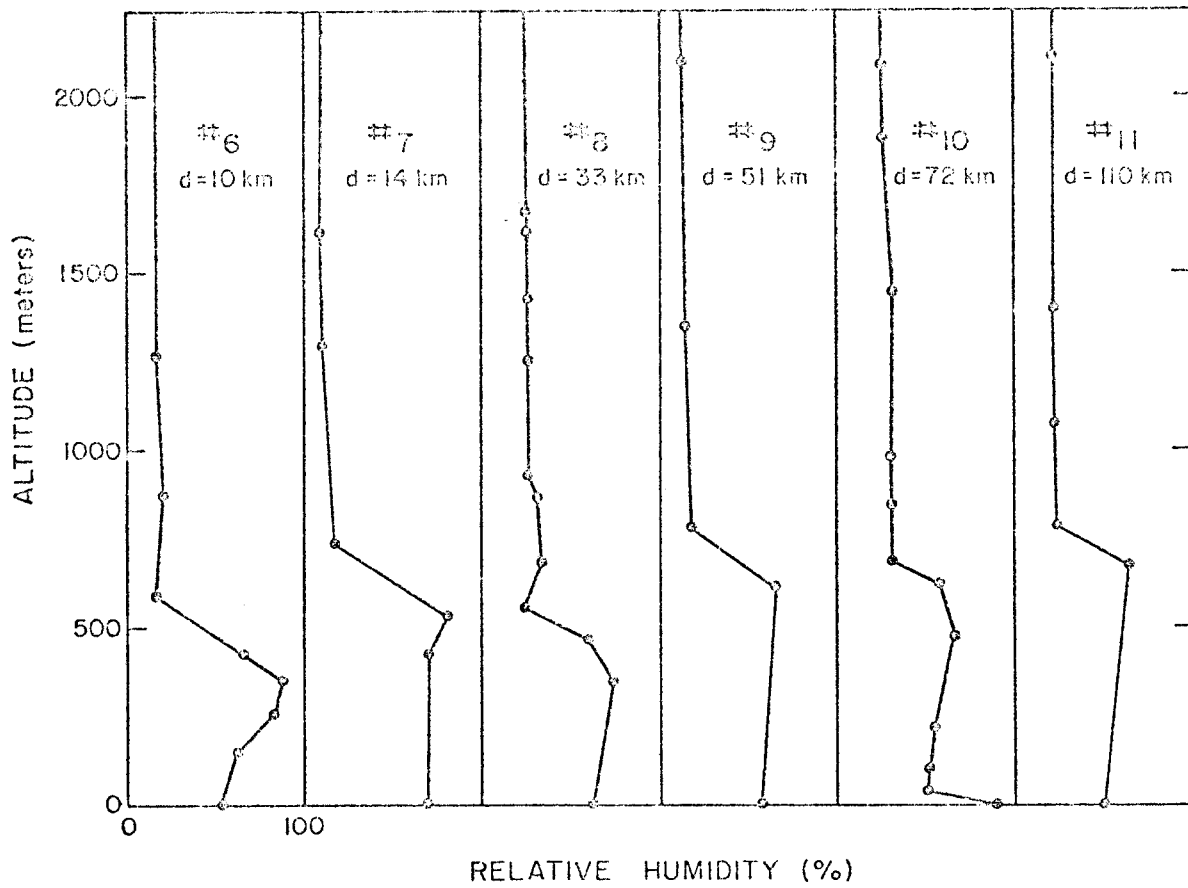
SIGMA-T VALUES OFF SET SCALE (—: ONE SIGMA-T UNIT)



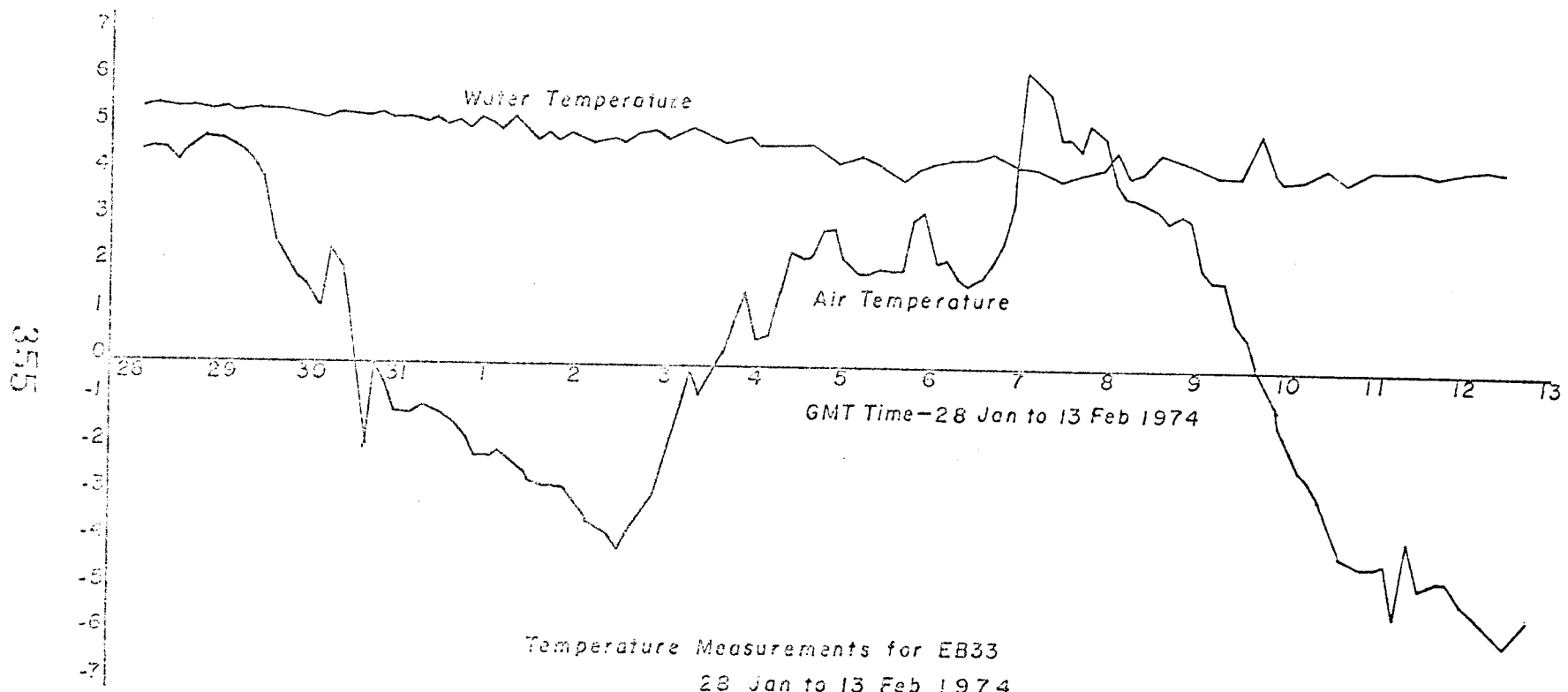
352



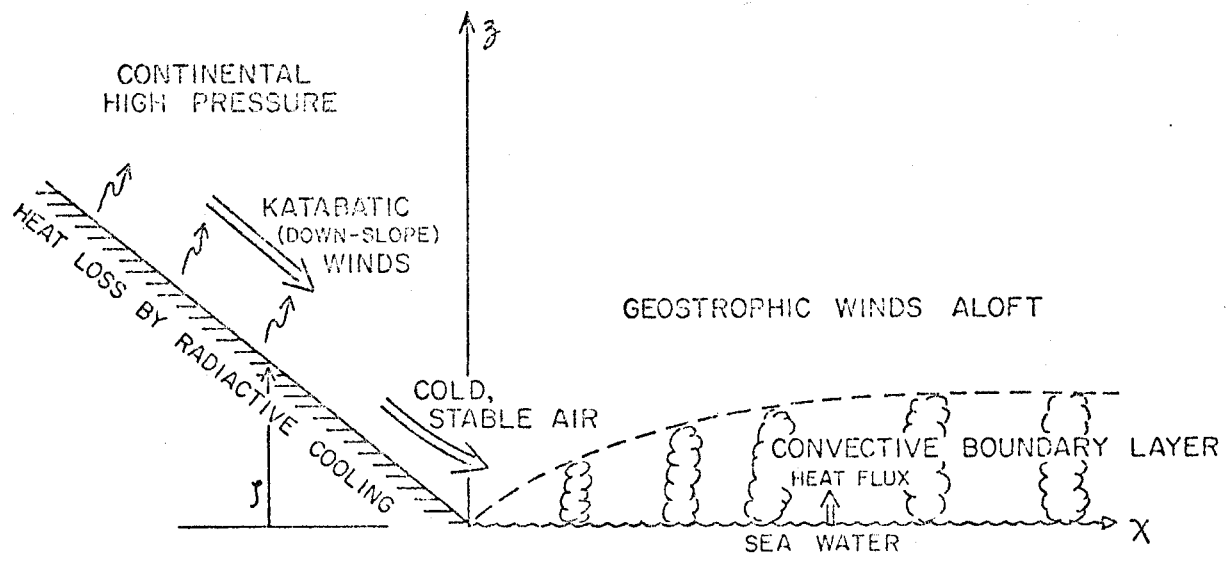








Temperature Measurements for EB33  
28 Jan to 13 Feb 1974



OCS COORDINATION OFFICE

University of Alaska

ENVIRONMENTAL DATA SUBMISSION SCHEDULE

DATE: March 31, 1976

CONTRACT NUMBER: 03-5-022-56

T/O NUMBER: 19

R.U. NUMBER: 289

PRINCIPAL INVESTIGATOR: Dr. T. C. Royer

Submission dates are estimated only and will be updated, if necessary, each quarter. Data batches refer to date as identified in the data management plan.

| <u>Cruise/Field Operation</u> | <u>Collection Dates</u>                 |           | <u>Estimated Submission Dates<sup>1</sup></u> |          |          |
|-------------------------------|---|-----------|---|----------|----------|
|                               | <u>From</u>                             | <u>To</u> | <u>Batch 1</u>                                | <u>2</u> | <u>3</u> |
| Acona #193                    | 7/1/74                                  | 7/9/74    | 4/9/76  | None     | None     |
| Acona #200                    | 10/8/74                                 | 10/14/74  | 4/9/76  | None     | None     |
| Acona #202                    | 11/18/74                                | 11/20/74  | 4/9/76  | None     | None     |
| Acona #205                    | 2/12/75                                 | 2/14/75   | 4/9/76  | None     | None     |
| Acona #207                    | 3/21/75                                 | 3/27/75   | 4/9/76  | None     | None     |
| Acona #212                    | 6/3/75                                  | 6/13/75   | 4/9/76  |          |          |
| Oceangrapher #805             | 2/1/75                                  | 2/13/75   | 4/9/76  | None     | None     |
| Silas Bent #811               | 8/31/75                                 | 9/28/75   | Submitted 2/26/76                             |          |          |
| Discoverer #812               | 10/3/75                                 | 10/16/75  | Formatting problems - Date unknown            |          |          |
| Surveyor #814                 | 10/28/75                                | 11/17/75  | 5/15/76                                       |          |          |
| Discoverer #816               | 11/23/75                                | 12/2/75   | 5/15/76                                       | None     | None     |
| Station 60                    | 6/2/74                                  | 9/10/74   | None  | 4/15/76  | None     |
| Station 64                    | 4/28/75                                 | 5/20/75   | None  | 4/15/76  | None     |
| Station 9                     | Current meter, not available in field.  |           |   |          |          |
| Station 9                     | Pressure gauge, not available in field. |           |   |          |          |
| Moana Wave MW 001             | 2/21/76                                 | 3/5/76    |   |          |          |

Note: <sup>1</sup> Data Management Plan and Data Formats have been approved and are considered contractual.

OCS COORDINATION OFFICE

University of Alaska

ESTIMATE OF FUNDS EXPENDED

DATE: March 31, 1976  
 CONTRACT NUMBER: 03-5--022-56  
 TASK ORDER NUMBER: 19  
 PRINCIPAL INVESTIGATOR: Dr. Thomas Royer

Period July 1, 1975 - March 31, 1976\* (9 mos)

|                  | <u>Total Budget</u> | <u>Expended</u>   | <u>Remaining</u>  |
|------------------|---------------------|-------------------|-------------------|
| Salaries & Wages | 132,358.00          | 48,170.26         | 84,187.74         |
| Staff Benefits   | 22,501.00           | 8,189.03          | 14,311.97         |
| Equipment        | 31,000.00           | 33,008.00         | (2,008.00)        |
| Travel           | 8,719.00            | 4,606.41          | 4,112.59          |
| Other            | <u>22,100.00</u>    | <u>14,780.47</u>  | <u>7,319.53</u>   |
| Total Direct     | <u>216,678.00</u>   | <u>108,754.17</u> | <u>107,923.83</u> |
| Indirect         | <u>75,708.00</u>    | <u>27,553.39</u>  | <u>48,154.61</u>  |
| Task Order Total | <u>292,386.00</u>   | <u>136,307.56</u> | <u>156,078.44</u> |

\* Preliminary cost data, not yet fully processed.

Contract #03-5-022-56  
Research Unit #307  
Report for 1/4/75 to 1/4/76  
58 pp.

HISTORICAL AND STATISTICAL OCEANOGRAPHIC  
DATA ANALYSIS AND SHIP OF OPPORTUNITY PROGRAM

Robin D. Muench  
Institute of Marine Science  
University of Alaska  
Fairbanks, Alaska 99701

ANNUAL REPORT  
1 APRIL, 1976

TABLE OF CONTENTS

SUMMARY . . . . . 1

    Objectives . . . . . 1

    Conclusions . . . . . 1

    Implications with regard to OCS development . . . . . 1

INTRODUCTION . . . . . 2

    General nature and scope of study . . . . . 2

    Specific objectives . . . . . 2

    Relevance to problems of petroleum development . . . . . 2

CURRENT STATE OF KNOWLEDGE . . . . . 4

STUDY AREA . . . . . 12

SOURCES, METHODS AND RATIONALE OF DATA COLLECTION . . . . . 14

RESULTS . . . . . 14

DISCUSSION AND CONCLUSIONS . . . . . 20

NEEDS FOR FURTHER STUDY . . . . . 20

SUMMARY OF FOURTH QUARTER OPERATIONS . . . . . 24

REFERENCES . . . . . 25

APPENDIX 1 . . . . . 27

    [Location of NODC oceanographic stations east of 165°W,  
    including Bristol Bay] . . . . . 27

APPENDIX 2 . . . . . 50

    [Location of NODC oceanographic stations west of 165°W,  
    extending out to the continental shelf]. . . . . 50

## I. SUMMARY

### A. Objectives

The objectives of this project are to utilize both historical and currently incoming ship-of-opportunity oceanographic data to examine large-scale circulation and mixing features on the southeastern Bering Sea shelf. Data used include temperature, salinity, dissolved oxygen and inorganic nutrients, and water mass analysis is the primary method for data analysis. Specific information sought is:

- Large scale spatial variations in water properties (heat and salt content, etc.)
- Seasonal variations in water properties.
- Long-term fluctuations in water properties, on the order of years or decades.
- Such circulation and mixing information as can be derived from the above.

These will be tied in, whenever possible, with more detailed ongoing OCS physical oceanographic studies.

### B. Conclusions

Conclusions are not yet available for the large-scale distributions of variables, because final processing of the NODC data tapes has only recently been completed and these data are still undergoing analysis. Ship-of-opportunity data have so far proven inadequate to draw conclusions concerning large-scale features. Data obtained in the Unimak Pass-Bristol Bay region by the Institute of Marine Science, University of Alaska during summer 1968 were however adequate to support existing hypotheses that a cyclonic circulation was occurring in that region. The data suggested in addition that upwelling of deeper water was occurring in central Bristol Bay. A preliminary look at the NODC data has further supported these conclusions. At present it is impossible to accurately assign rates to these processes.

### C. Implications with regard to OCS development

The hypothetical (as yet) cyclonic circulation and attendant upwelling in central Bristol Bay could have significant implications. A contaminant released near or at the bottom could be carried upwards to the surface and incorporated into the food chain there at the primary productivity level. (Vertical mixing might also act to mix bottom contaminants to the surface.) Such biological contamination could result in concentration of undesirable substances at the higher food levels, for example, fish. This is particularly significant because Bristol Bay contains one of the world's major fisheries.

## II. INTRODUCTION

### A. General nature and scope of study

This study addresses itself to the large-scale circulation and mixing processes on the southeastern Bering Sea shelf, with particular emphasis on Bristol Bay. The region of interest is indicated in Figure 1. The study is being carried out using both historical and ship of opportunity data which includes temperature, salinity, dissolved oxygen and inorganic nutrient values from throughout the water column. Information on circulation and mixing is being derived from these data using water mass analysis.

### B. Specific objectives

The objectives of this study are:

- To map the large scale horizontal and vertical fields of temperature, salinity and (where possible) dissolved oxygen and inorganic nutrients.
- To determine seasonal fluctuations in these same quantities throughout the water column.
- To determine long-term variations in heat and salt content throughout the water column and where possible to relate these to known climatological variations.
- To deduce vertical mixing parameters from the above distribution.
- To deduce horizontal and vertical advective fields, at appropriate scales in time and space, from the above distributions.

A general objective of this study will be to make all of the above points, particularly the last two items, freely available to the biological and chemical study portions of the overall OCS program, because water circulation and mixing parameters are especially important to distributions of chemical and biological matter.

### C. Relevance to problems of petroleum development

Distribution of any contaminants introduced into the marine environment is controlled by a set of several factors, one of the most important of which is water motion including mixing rates. (Others might include, for example, biodegradation) Water motions and mixing also control furthermore the distributions of organisms which are likely to be affected by such contaminants. A knowledge of these factors, as addressed in this study, is therefore requisite to predicting the probable impact of any released contaminants upon the environment. Specifically, such knowledge is necessary for:

- Predicting the locations of impacted areas, given a contaminant release at a specified locale.



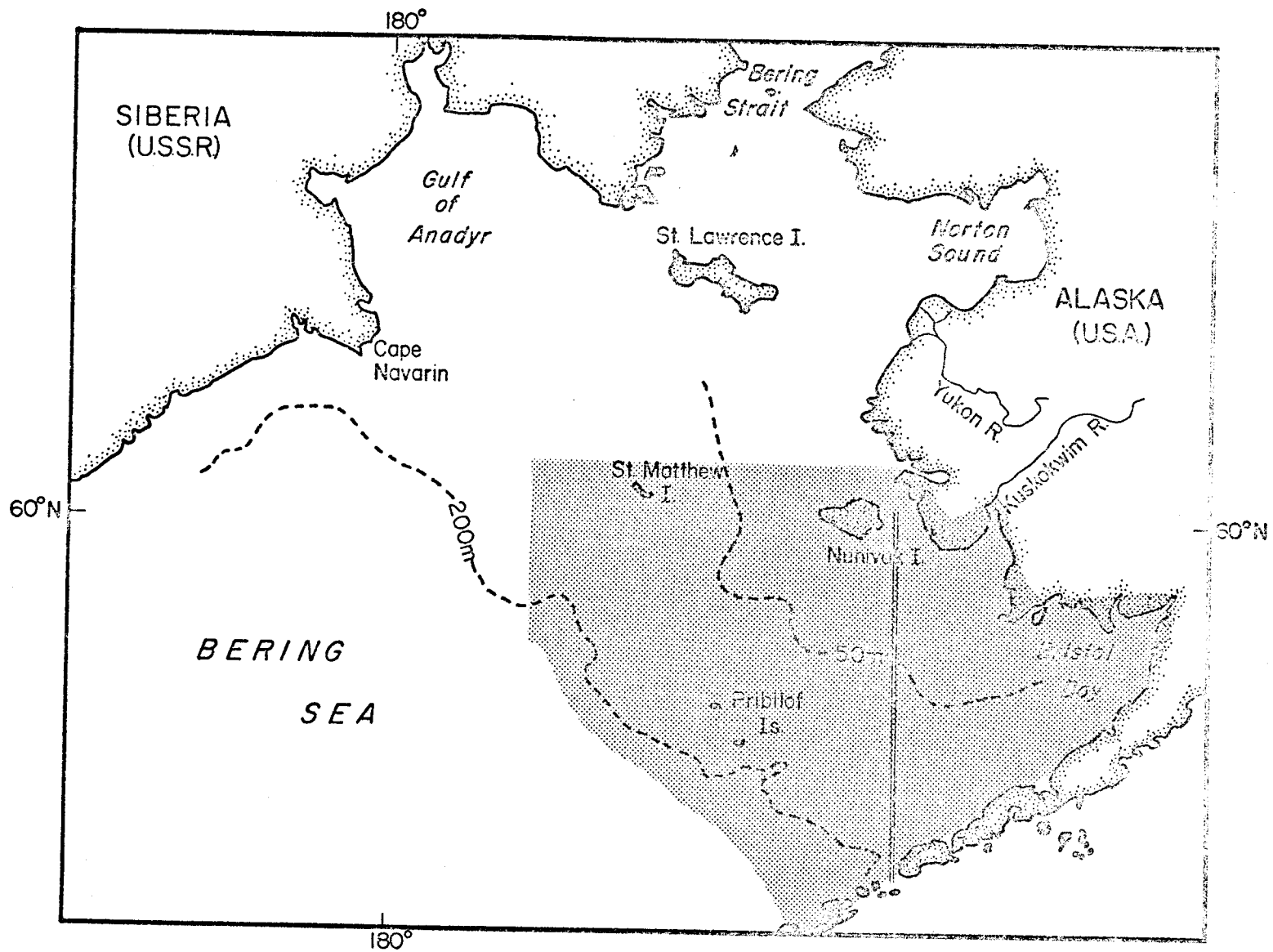


Figure 1. Geographical locations in the Bering Sea region, showing study area (shaded). Double line is division into eastern and western study areas (see text).

- Predicting the decrease with time and space of a given concentration of contaminant.
- Foreseeing interactions between biota and contaminant which may be brought about by water motion (e.g. a given group of planktonic organisms may be advected by water movement into a contaminated area).

### III. CURRENT STATE OF KNOWLEDGE

Little is currently known about circulation, mixing or distribution of water column variables in space and time for the southeastern Bering Sea. Water mass analyses can however provide an indirect means of deducing circulation, and a limited number of such studies in the southeastern Bering Sea are now available.

The first systematic surveys, those of the U.S.C.G.T. *Redwing* from 1938 to 1940, were largely confined to Bristol Bay. An analysis based primarily on these data (Dodimead *et al.*, 1963) concluded that circulation was cyclonic around the inner bay. Additional sections occupied during summer 1940 allowed definition of an oceanic water intrusion extending landwards to about Cape Seniavin and occupying the central and outer portions of the Bay. Dodimead *et al.* noted that it was impossible to ascertain from the data whether water motion was parallel to or orthogonal to the isolines. The former interpretation would imply a cyclonic circulation, while the latter interpretation would mean the water was intruding into the Bay as a tongue or wedge with attendant upward movement or upwelling.

Most of the recent studies are due to Japanese Oceanographers, including Maeda *et al.* (1968), Ohtani (1969 ) and Takenouti and Ohtani (1974). The data base for these studies, obtained from continuing cruises of the *Oshoro Maru* in June and July of every year since the 1950's, had made it possible to identify certain gross features of water mass definition and distribution.

Only one study has however attempted to apply water mass analysis to circulation (Takenouti and Ohtani, 1974). A schematic diagram showing the results of this study is given in Figure 2. The inflow along the Alaska Peninsula and cyclonic flow about inner Bristol Bay conform with the deductions of Hebard (1961) and Dodimead *et al.* (1963). In the central and northern parts of the Bay they show, however, flow out to the north and a small cyclonic gyre-like feature southeast of the Pribilofs. The lack of suitable data precludes greater resolution, and even these results must be considered speculative because they are not completely reconcilable with either current measurements or other water mass analyses.

All available temperature and salinity data from the Bering Sea up to 1973 have been computer programmed to produce maps of mean temperature and salinity (Ingraham, 1973). The lower layer as defined by its low (<2°C) temperature coincided, during June and July, with a

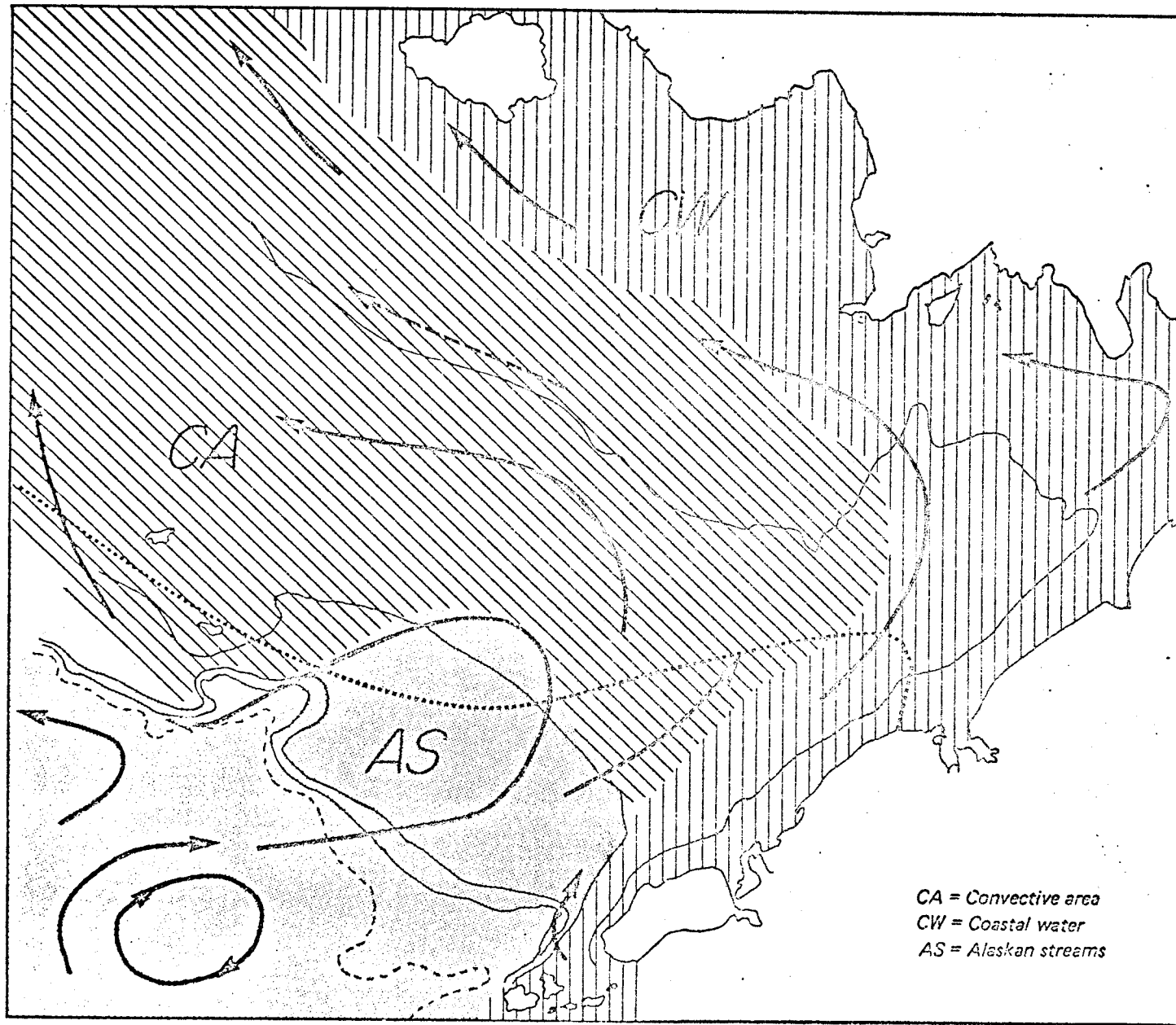


Figure 2. Distribution of water masses and deduced circulation (from Takenouti and Ohtani, 1974). Dashed arrow shows current after Muench (1974), and dotted line is approximate winter ice edge.

plot of that layer constructed by Maeda *et al.* (1968) using Japanese data collected during 1955 to 1967. Data from other months, except August, were too sparse for construction of meaningful isotherms. Mean positions of the 2°C isotherm and the 32‰ isohaline (from the Japanese data) for June and July are shown in Figure 3. Though there is considerable annual variation in the isohaline patterns, the gross features are consistent. These are the tongue-like extensions of colder water from the northwest along the central shelf into mid-Bristol Bay, and the incursion of more saline water from the southwest into the central Bay and to north of the Pribilofs.

A cyclonic circulation around inner Bristol Bay, common to the schemes of both Hebard and Takenouti and Ohtani, appears to be compatible with water mass distribution. Any suggestion that the flow continues curving to the southwest and closes a cyclonic gyre within the bay would not however be compatible with the tongue-like distribution of the cold water layer. An outstanding feature of this layer is the constancy of position of its northern boundary, defined by the 2°C isotherm and seen in data from Maeda *et al.* (1968) to coincide closely with the 50 m isobath in every year. Muench (1976) reported on an STD section which crossed this boundary at about 58°N. He observed strong horizontal temperature and salinity gradients and remarked that the solenoidal field indicated appreciable northwesterly flow landward of the front (Fig. 2). The northcentral part of Takenouti and Ohtani's (1974) circulation scheme also shows northwesterly flow in the same region in agreement (Fig. 2). Seaward of the 50 m isobath (within the cold tongue) the circulation cannot, however, be northwesterly and still maintain the southeasterly trending tongue-like distribution. As noted by Sverdrup and Fleming (1941), there are two flow possibilities: (1) around the tongue parallel to the property isolines; and (2) along the axis of the tongue towards the tip. The first case would suggest little or no mean flow in the region of the tongue; tongue water would be an artifact of winter convection associated with ice formation, to be later shaped by the circulation. The second case would call for a southeast setting flow advecting cold water, formed on the northern shelf in winter, along the central shelf into Bristol Bay. No circulation scheme has been proposed which reconciles these two.

Strong support for the first possibility is provided by the extremely high ( $r = .95$ ) correlation of the mean bottom layer temperature of the southeastern shelf in June (largely conditioned by the minimum temperature of the "cold tongue") and the degree days of frost of the previous winter (Fig. 4) (Coachman, personal communication.) The interpretation must be that the cold tongue is winterformed locally and subsequently shaped by advection.

Salinity observations may aid interpretation of the regional circulation. The highest salinity shelf water (>32‰) occupies central to outer Bristol Bay and around the Pribilofs. This water must originate either from the deep western basin or from the Alaska Stream via the easternmost passes in the Aleutian chain. Such a distribution (Fig. 3) implies a net circulation with on-shelf and

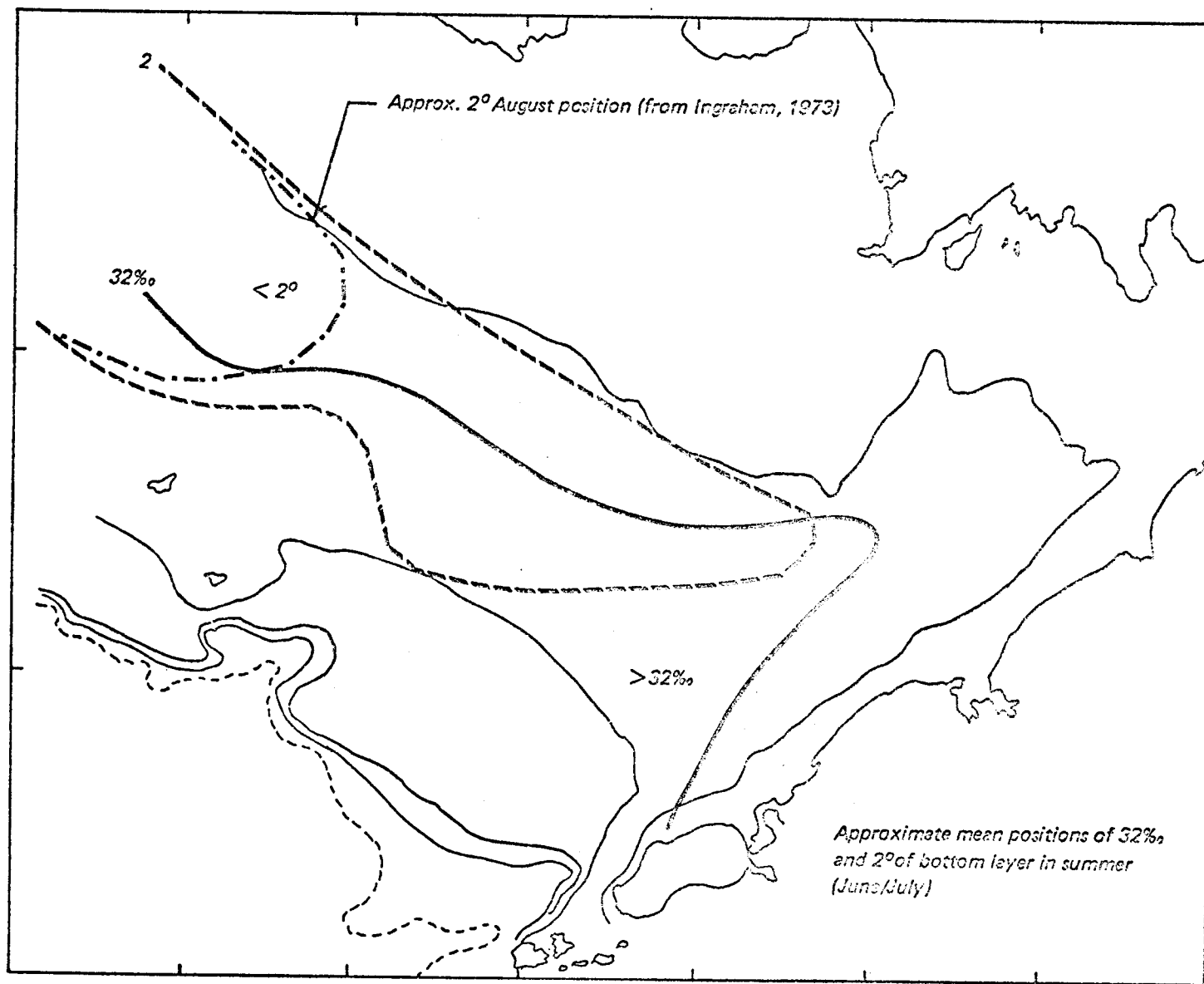


Figure 3. Lower layer temperature and salinity distribution in the southeastern Bering Sea.

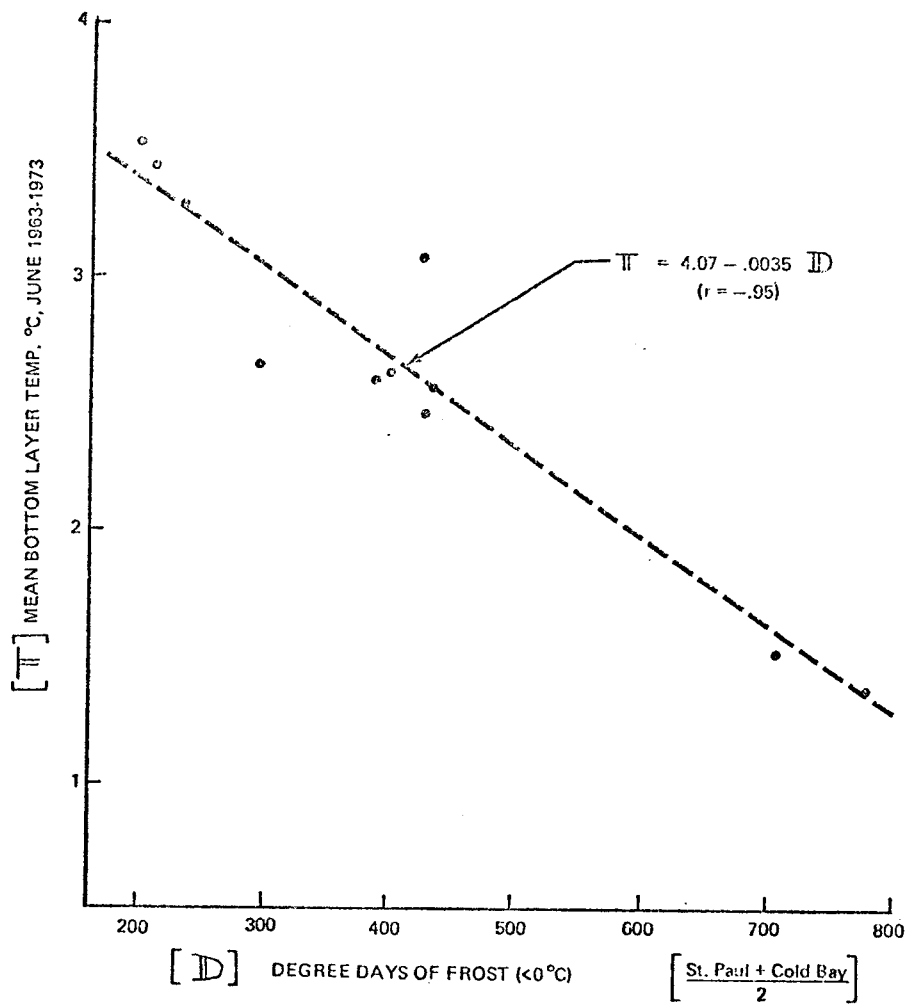


Figure 4. Correlation between mean bottom layer temperature and number of degree days of frost (L. K. Coachman, personal communication).

northerly components.

In addition to the water mass analyses, various direct measurements have been made which can aid in clarifying regional circulation patterns.

Three sets of current measurements are available from the region. Hebard (1961) reported on several 39-hour anchored measurements made during June, 1957 from each of four locations (A-D, Fig. 5). Non-tidal components in the upper (above the thermocline) and deeper layers are shown in Figure 5 (The flow at B was considered to be influenced by a strong northerly wind; a computed wind effect correction suggested that the non-tidal flow in the absence of wind may have been southwesterly as at A.) From these data, it was concluded that the bay contained a general cyclonic circulation.

Three current meter moorings were deployed for 14 days in Pribilof Canyon during July, 1974 (Kinder, unpublished). The shallower of two meters on each mooring were at 100 m depth; flow recorded by these can therefore probably be related to that of the deep water layer. Mean flows for the period were essentially up-canyon and parallel to its axis (Fig. 5).

The third set of current measurements was a set of spot measurements made in the vicinities of locations C and D (Fig. 5) from the Japanese crabber *Tokei Maru* during the summers of 1955 and 1956 (I.N.P.F.C., 1957). Because of the large tidal signals, no deductions could be made about mean flow.

Results from a 24-hour current station taken close to Nunivak Island from the *Chelan* in August, 1934 (Barnes and Thompson, 1938) are useful in interpretation of the regional circulation (location indicated on Figure 5). Mean flow was northerly, paralleling the isobaths, at about 17 cm sec<sup>-1</sup>.

Some information on circulation in the surface layer can be found in driftbottle returns, two reports of which are shown in Figure 6. This information must be regarded however as indirect, because the trajectories of the bottles between points of release and recovery are highly conjectural. Both sets of returns suggest inflow into Bristol Bay via Unimak Pass, then northeasterly flow along the north shore of the Alaska Peninsula. One bottle was returned from a location some 90 km north of Unimak Pass (Fig. 6a), and another bottle apparently drifted across or around the Bay and out to the north (Fig. 6).

Some clues concerning surface water circulation are available from late winter (January to March) sea ice observations, when the ice is at its maximum southward extent. Ice edge locations depicted in a general sense by McRoy and Goering (1974) and in greater detail for winter 1974 by Muench and Ahlén (1976) indicate a pronounced eastward indentation of the ice edge north of Unimak Pass, whereas the edge farther north roughly parallels the shelf break (Fig. 2).

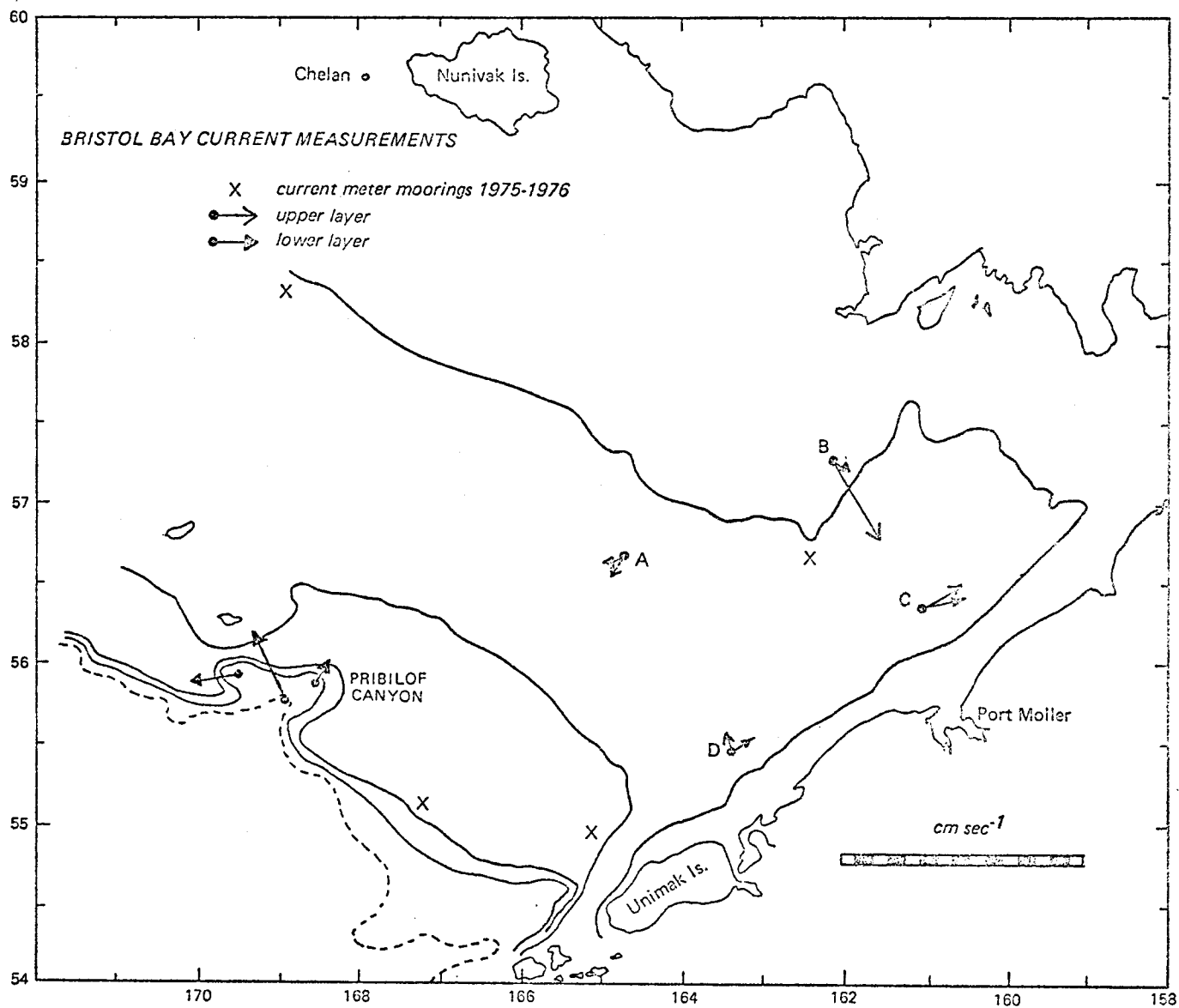


Figure 5. Current measurements in the southeastern Bering Sea (references given in text).



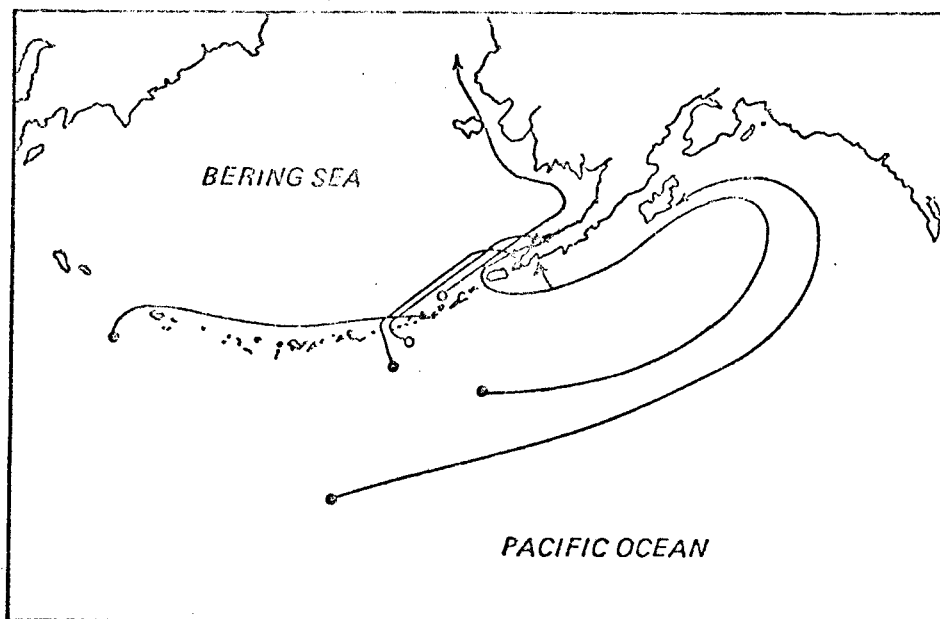
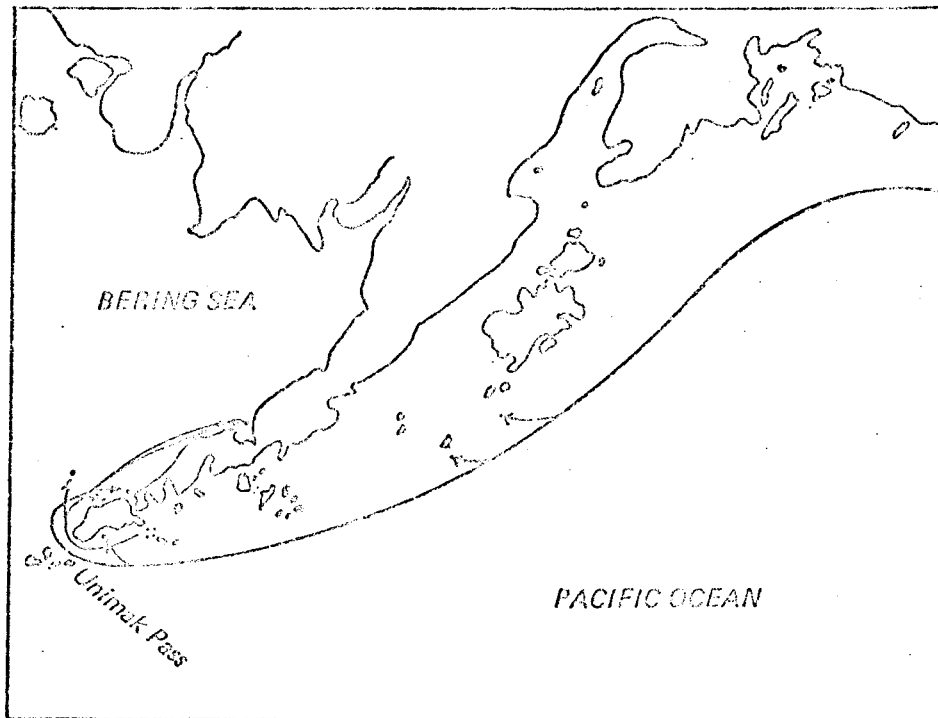


Figure 6a (upper, after Thompson and Van Cleve, 1936) and 6b (lower, after Dodimead *et al.*, 1963) summarizing drift bottle trajectories from the study area.

This indentation suggests, as did the drift bottles and current measurements, a northeasterly surface water flow along the north shore of the Alaska Peninsula.

Regional wind can provide a physical driving force for circulation in a shallow, broad shelf area such as this. Kihara (1971) attempted to correlate the halibut catch with volume of defined "Alaskan Stream Extension" water in outer Bristol Bay during 1963 to 1969, and examined the relation between these variables and wind. In his report, he published bottom distribution of the defined water mass ( $S > 32\text{‰}$  and  $1^{\circ} < T < 6^{\circ}\text{C}$ ) and computed values of "six months mean cumulative wind force (from February to July) of the northward and eastward components at Uniwak Island" (his units were not defined). Figure 7, constructed using Kihara's data, shows that the northward and eastward extent of penetration of the higher salinity water in outer Bristol Bay during any summer may be correlated with the degree of northerly wind stress that year. This suggests the important role of wind as a driving force for the circulation. More recently Muench and Ahlén (1976) have demonstrated that the sea ice moves southward in response to northerly winds during the winter, but the effect of this southward moving ice on flow in the underlying water is unknown. It is certain that the ice decreases to some extent the wind stress acting upon the water.

In summary, our knowledge of the southeastern Bering shelf flow field is incomplete. It appears probable there is net inflow along the north shore of the Alaska Peninsula, the flow continuing cyclonically around the inner bay and then turning northwest and flowing past Nunivak Island in the vicinity (probably landward) of the 50 m isobath. It seems probable that there are on-shelf water movements in the central outer bay and to the north and east of the Pribilofs. There is however insufficient information to address the problem of time variability, and the circulation during the ice-covered winter season remains essentially unknown.

#### IV. STUDY AREA

This research project addresses oceanographic processes on the southeastern Bering Sea shelf, a region extending from the coastline to the 200 m isobath, bounded on the south by the Aleutian islands and on the north by the  $60^{\circ}\text{N}$  parallel (Fig. 1). The major proportion of this region is shallow, with depths between 50 and 100 m. The Kuskokwim River provides a major source of fresh water input while smaller rivers enter around the head of Bristol Bay. The climate is severe, with winter winds generally northeasterly and consequent to a strengthening of the Aleutian Low atmospheric pressure system. During summer the winds are lighter and variable in direction. The winter ice cover extends southward nearly to the Pribilof Islands, while during the summer the region is ice-free (Figs. 1 and 2).

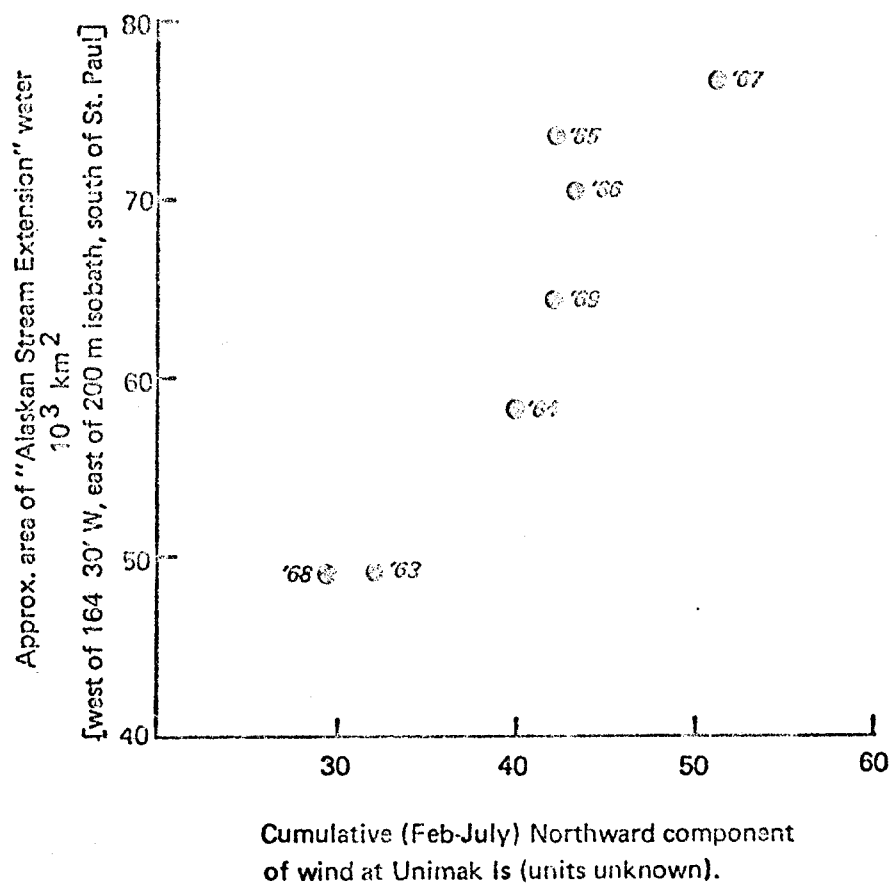


Figure 7. Correlation between northerly winds and amount of Alaska Stream water found in the southeastern Bering Sea (from Kihara, 1971).

## V. SOURCES, METHODS AND RATIONALE OF DATA COLLECTION

Data for this project have been obtained from three sources:

- Historical data contained in the NODC files.
- Historical data from sources other than the NODC files.
- Ship-of-opportunity data obtained from oceanographic vessels carrying out other than physical oceanographic projects in the Bering Sea.

The NODC data have been obtained on a magnetic tape, then converted to a hard copy printout showing temperature, salinity and (where available) dissolved oxygen and inorganic nutrient concentrations through the water column. Non - NODC historical data were obtained from such sources as the Institute of Marine Science, University of Alaska. Since it was impossible to exert any control over the collection of these data, these will not be discussed further here.

The ship-of-opportunity data have been obtained on a space and time available basis from vessels involved in carrying out other (e.g. biological oceanographic) cruises in the study region. Working under the limitations of available space and time, attempts are made on each of these cruises to obtain the best geographical coverage, in terms of station spacing and uniform density of coverage, within the study area. Of prime consideration also is the knowledge that these data may in the foreseeable future be integrated with other biological and chemical data obtained during these same cruises. Wherever possible, collection of physical oceanographic data is coordinated with collection of biological or other data. An example would be relatively closely spaced physical oceanographic stations along the pack ice edge to aid in studying the complex conditions which lead to a spring phytoplankton bloom there.

Vertical sample density at a given station can vary. Normally temperature and salinity are obtained using an STD or CTD and so are available as a virtually continuous vertical trace. Dissolved oxygen and nutrient samples are obtained at discrete depths using sample bottles. These depths are normally dependent upon sampling of other sorts (e.g. plankton tows or productivity measurements) at the same station, and spacing depends upon what is specifically being sought at a given station. This rationale allows maximum coordination between the physical oceanographic sampling and other (chemical and biological) parts of the program.

## VI. RESULTS

Results of this study may be subdivided into material from the three data sources listed above in Section V. Processing and final analysis of both the NODC and ship-of-opportunity data have been delayed by technical problems to the point where few results are as yet available from those sources. Data obtained from the R/V *ACONA* during 1968 and from the Japanese research vessel *Hakuho Maru* during 1975 were however available at the outset of this study and contri-

buted significantly to an understanding of oceanographic processes in Bristol Bay.

Temperature, salinity and inorganic nutrient concentration were measured during 17 June - 3 July 1968 in Bristol Bay by R/V *ACONA*. Locations of the 49 stations occupied are shown in Figure 8, as are the traverses along which vertical sections were constructed. Examination of these sections revealed features which provide support for an upwelling regime in eastern central Bristol Bay. The most obvious manifestation of this upwelling is an upward doming of isotherms visible along sections B-1 and B-3 (Figs. 9 and 10). This cold can have its source at depth in Bristol Bay or farther west on the shelf, where it represents a remnant of the preceding winter's cold, convective layer. The strongest argument in favor of upwelling comes however from nutrient distributions. During June-July the southeastern Bering Sea is normally nutrient depleted in its upper layers due to primary production. Central eastern Bristol Bay exhibited, however, high nutrient values ( $4\mu\text{g-at}/\text{L}$ ) which decreased to zero toward the periphery of the Bay (Figure 11). The high nutrient values, it is hypothesized, are due to an eastward and upward intrusion of deep high nutrient water from outside Bristol Bay.

A possible mechanism for such upwelling could be the bottom Ekman layer generated by the cyclonic circulation in Bristol Bay. An inward-directed flow in this bottom layer would, by volume continuity, tend to force deep water toward the surface. Calculations based on the current observations presented above (Section III) support this, as the cyclonic circulation appears to be of sufficient intensity to drive an upwelling mechanism. This has been discussed by Myers and Muench (1975).

Data obtained from the 1975 cruise of the Japanese vessel *Hakuho Maru* were not detailed enough to substantiate the patterns observed in Bristol Bay during 1968. Such data as are available are not, however, in opposition to the hypothesis presented above.

Ship-of-opportunity data were obtained during June, August and November 1975 from the NOAA vessel *Discoverer* (first two cruises) and *Miller Freeman*. Data from the first of these cruises were inadequate for physical oceanographic work due to malfunctioning of the shipboard CTD system. Data from the second are still in the final stages of processing, the considerable delay having been caused by incompatibility between the vessel's recording system and land based processing facilities. Data from the November cruise are also in processing, with a delay due to problems with the recording system on the vessel. While adequate data should in theory have been obtained to allow considerable elaboration on the above hypothesis concerning Bristol Bay circulation, hardware and processing problems have interceded to the point where no useable data have as yet become available from these cruises.

A final set of data was available on NODC tapes, which were finally obtained in satisfactory form in December 1975 after return of one earlier tape which had proven defective. These data have

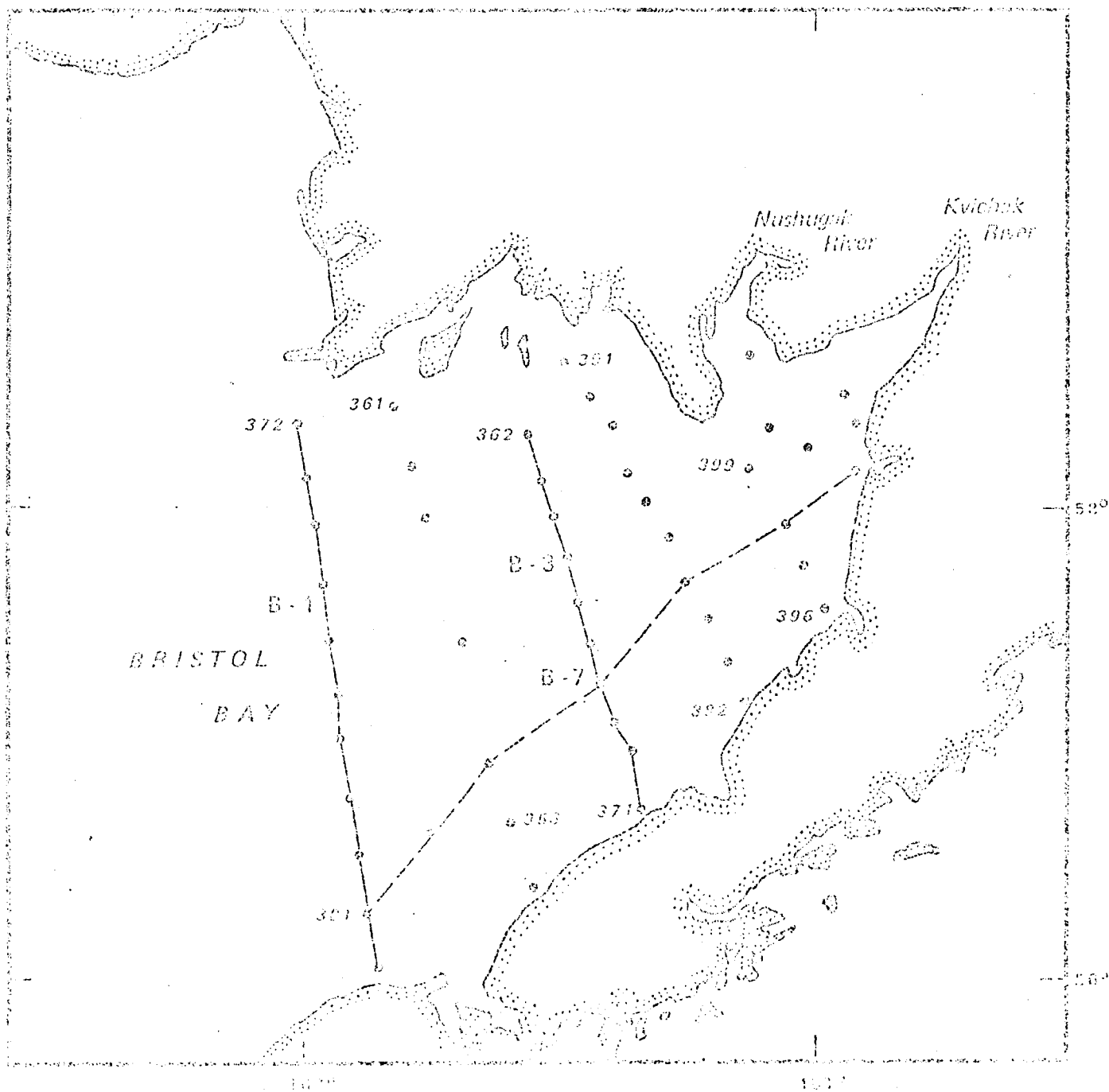


Figure 8. Locations of 1968 R/V ACONA oceanographic stations in Bristol Bay, showing station lines used to construct vertical sections.

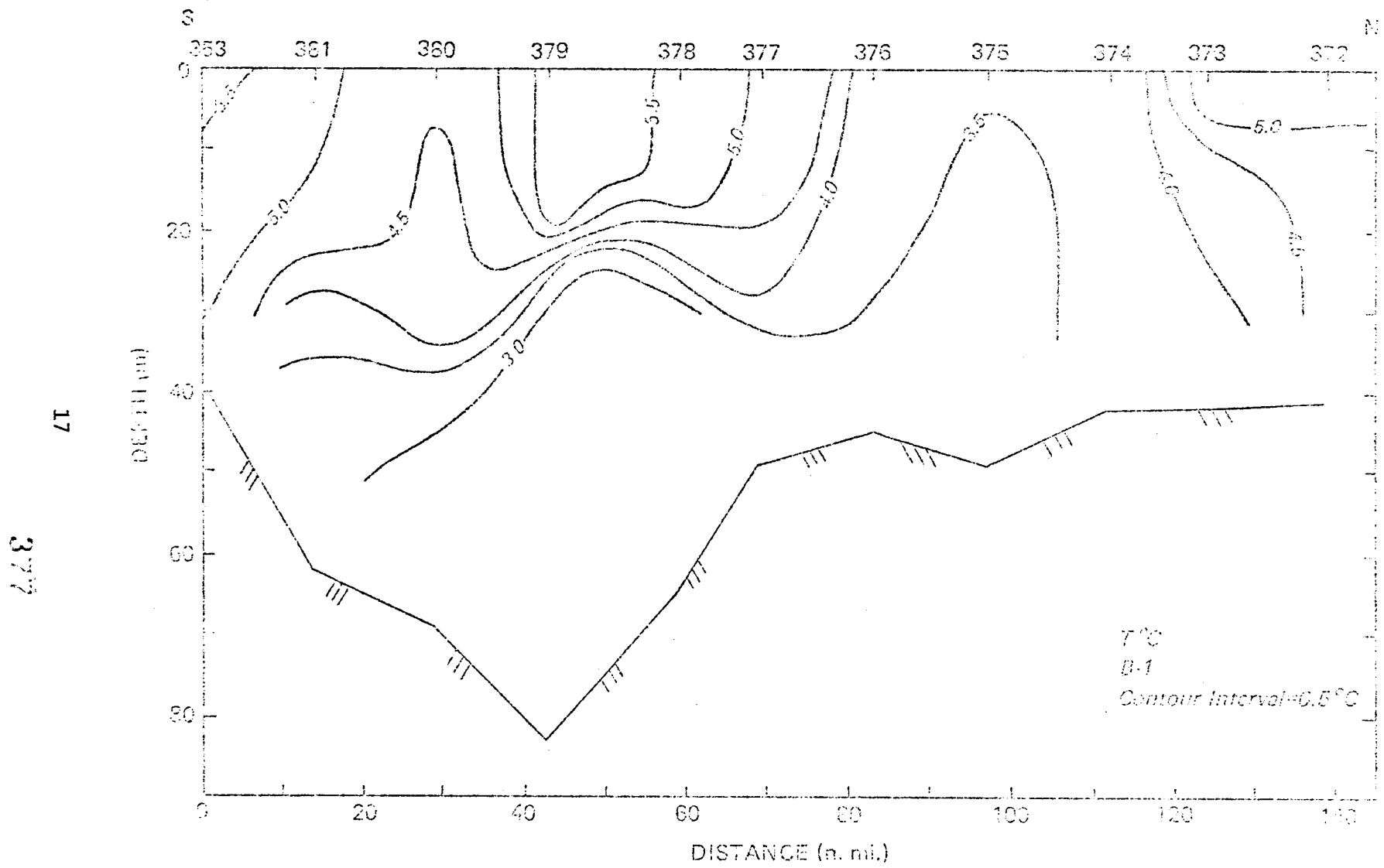


Figure 9. Temperature during June 1968 along section B-1, showing upward doming of isotherms.

18

378

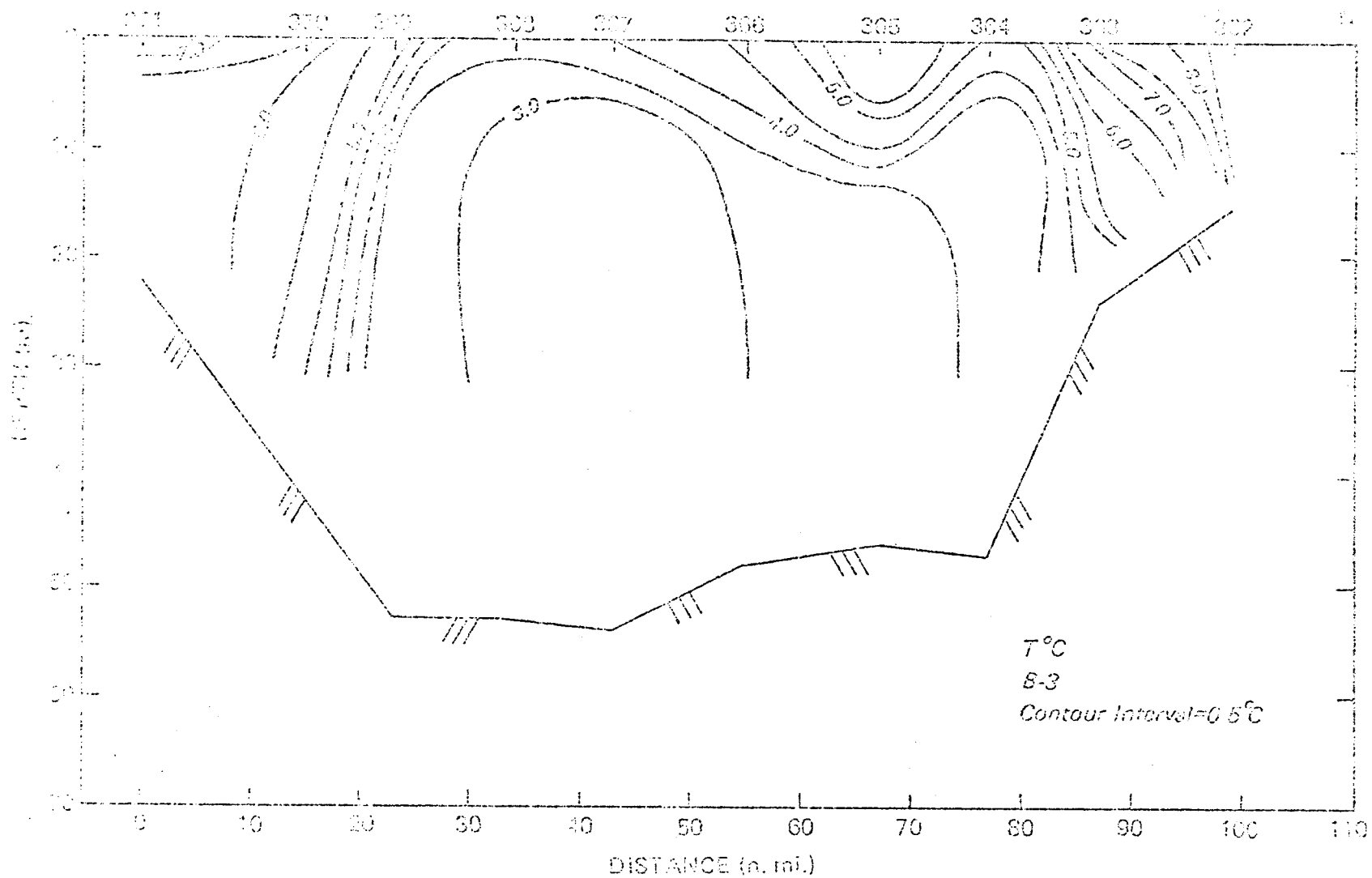


Figure 10. Temperature during June 1968 along section B-3, showing upward doming of isotherms.



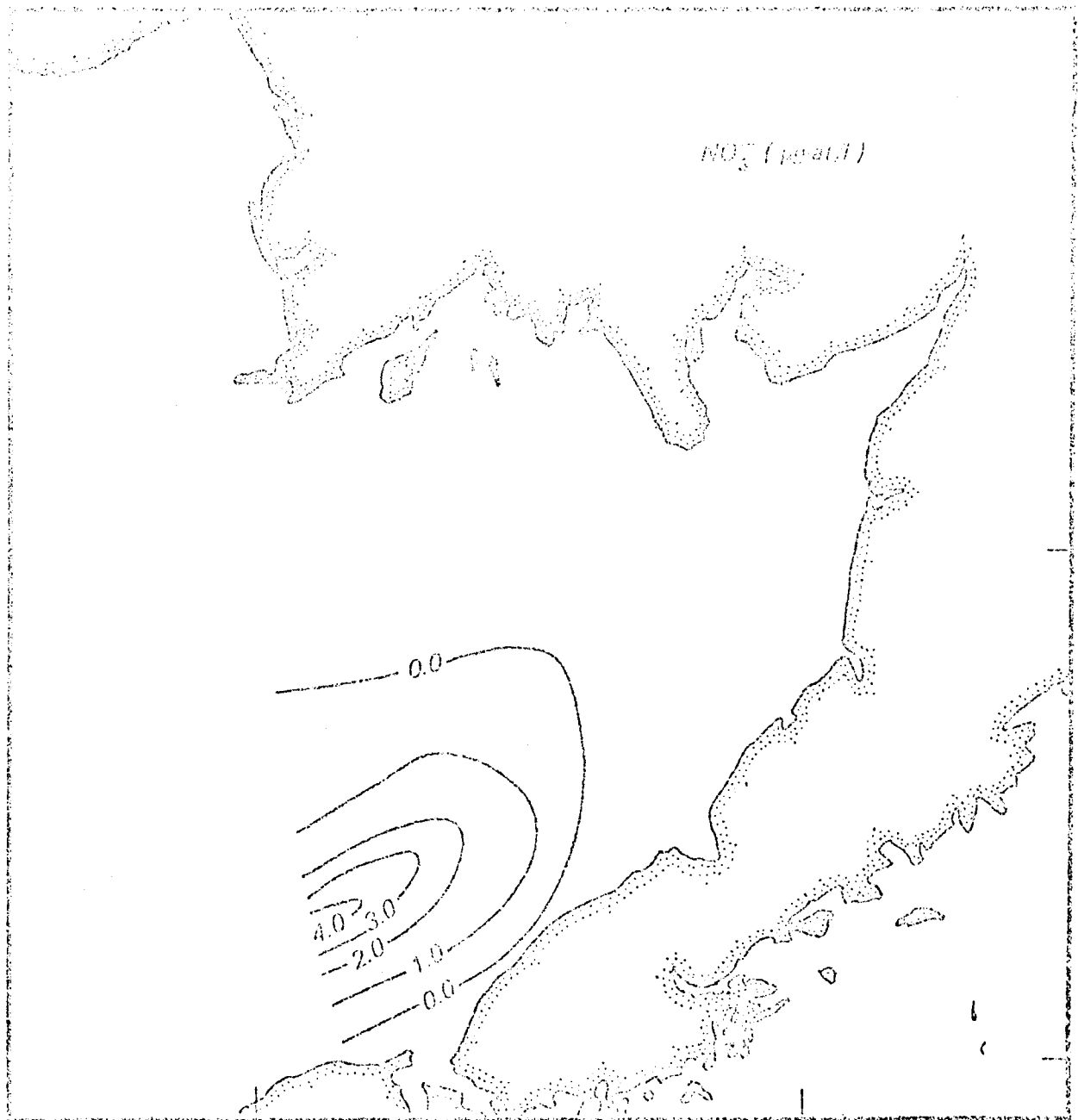


Figure 11. Surface distribution of nitrate during June 1968.

been converted to hard copy printout, tabulated according to station coverage by dates (Tables 1 and 2) and the station positions plotted (Appendix 1 and 2). For convenience sake, the region was divided in two by the 165°W meridian. The eastern region includes Bristol Bay, while the western region extends outwards to and beyond the shelf break. A glance at the Bristol Bay data indicate very good station coverage during 1938-40 and again during 1969-1972. The earlier work was that of the *Redwing*. The more recent work was due to the *Miller Freeman*. Several years worth of adequate data were obtained farther west. It is felt that these historical data will be sufficient to determine large-scale spatial variations and to estimate long-term time changes. There were virtually no winter data, however, so that delineation of seasonal variations will be impossible. The data should however be adequate to allow an estimate of winter conditions based on such features as remnants of the cold winter convective layer and known climatological parameters.

#### VII. DISCUSSION AND CONCLUSIONS

The ongoing research has so far been adequate to substantiate the presence of an upwelling region in central Bristol Bay and to suggest its causative mechanism. This in itself points out the need for continuing work, since the upwelling would tend to transport near-bottom contaminants to the near-surface zone where primary production occurs, hence introducing contaminant into the lowest levels of the regional food chain.

Due to the small quantity of data as yet analyzed for the area, it is impossible to assign quantities to these processes. We as yet know virtually nothing of the large-scale horizontal circulation in the southeastern Bering Sea, which must play a dominant role in regional transport of materials. The ongoing analysis of historical and such ship-of-opportunity data as are useable should aid in interpretation of these patterns. At this time, however, this analysis is not complete enough for such interpretation.

#### VIII. NEEDS FOR FURTHER STUDY

The final intent of this research was to investigate large-scale, long-term variations in hydrographic structure and apply water mass analyses to these to aid interpretation of the flow field. These analyses will not allow quantization of these processes, and will not delineate small-scale or short-term processes. Additional field work should therefore address the smaller scale (on the order of tens of km), shorter term (on the order of weeks)

| YEAR | JANUARY | FEBRUARY | MARCH | APRIL | MAY | JUNE | JULY | AUGUST | SEPTEMBER | OCTOBER | NOVEMBER | DECEMBER | TOTAL FOR YEAR |
|------|---------|----------|-------|-------|-----|------|------|--------|-----------|---------|----------|----------|----------------|
| 1934 |         |          |       |       |     |      | 1    |        |           |         |          |          | 1              |
| 1938 |         |          |       |       |     |      |      | 65     | 53        |         |          |          | 118            |
| 1939 |         |          |       |       | 9   | 6    | 82   | 69     |           |         |          |          | 238            |
| 1940 |         |          |       |       |     |      | 26   | 51     |           |         |          |          | 77             |
| 1941 |         |          |       |       | 11  | 4    |      |        |           |         |          |          | 15             |
| 1955 |         |          |       | 4     |     |      | 2    | 3      |           |         |          |          | 9              |
| 1956 |         |          |       |       |     | 3    | 22   | 10     | 2         |         |          |          | 37             |
| 1957 |         |          |       |       |     |      | 2    | 1      |           |         |          |          | 3              |
| 1958 |         |          |       |       |     |      | 7    |        |           |         |          |          | 7              |
| 1959 |         |          |       |       |     | 14   | 13   | 4      | 6         |         |          |          | 37             |
| 1960 |         |          |       |       |     |      | 11   |        |           |         |          |          | 15             |
| 1961 |         |          |       | 11    |     | 2    | 24   |        |           |         |          |          | 37             |
| 1963 |         |          |       |       |     |      | 3    |        |           |         |          |          | 8              |
| 1964 |         |          |       |       |     |      | 4    |        |           |         |          |          | 4              |
| 1965 |         |          |       |       |     | 3    | 12   |        |           |         |          |          | 15             |
| 1966 |         |          |       |       |     | 4    | 1    |        |           |         |          |          | 5              |
| 1967 |         |          |       |       |     | 5    | 1    |        |           |         |          |          | 6              |
| 1968 |         |          |       |       |     | 9    | 7    |        |           |         |          |          | 16             |
| 1969 |         |          |       | 57    | 50  | 71   | 101  | 79     |           |         |          |          | 358            |
| 1970 |         |          | 16    | 29    | 78  | 32   | 6    | 34     | 34        |         |          |          | 223            |
| 1971 |         |          |       |       |     | 41   |      | 32     | 30        |         |          |          | 103            |
| 1972 |         |          |       |       | 17  | 11   | 21   |        |           |         |          |          | 49             |

Table 1. Time distribution of NODC oceanographic stations east of 165°W, including Bristol Bay.

| YEAR | MONTH | JANUARY | FEBRUARY | MARCH | APRIL | MAY | JUNE | JULY | AUGUST | SEPTEMBER | OCTOBER | NOVEMBER | DECEMBER | TOTAL FOR YEAR |
|------|-------|---------|----------|-------|-------|-----|------|------|--------|-----------|---------|----------|----------|----------------|
| 1934 |       |         |          |       |       |     |      | 28   | 39     |           |         |          |          | 67             |
| 1935 |       |         |          |       |       |     |      | 5    |        |           |         |          |          | 5              |
| 1936 |       |         |          |       |       |     |      |      |        |           |         |          |          | --             |
| 1937 |       |         |          |       |       |     | 10   | 11   |        |           |         |          |          | 21             |
| 1938 |       |         |          |       |       |     |      |      |        | 5         |         |          |          | 5              |
| 1939 |       |         |          |       |       |     |      |      | 17     |           |         |          |          | 17             |
| 1940 |       |         |          |       |       |     |      | 42   | 16     |           |         |          |          | 58             |
| 1941 |       |         |          |       |       | 17  | 7    |      |        |           |         |          |          | 24             |
| 1942 |       |         |          |       |       |     |      |      |        |           |         |          |          | --             |
| 1943 |       |         |          |       |       |     |      |      |        |           |         |          |          | --             |
| 1944 |       |         |          |       |       |     |      |      |        |           |         |          |          | --             |
| 1945 |       |         |          |       |       |     |      |      |        |           |         |          |          | --             |
| 1946 |       |         |          |       |       |     |      |      |        |           |         |          |          | --             |
| 1947 |       |         |          |       |       |     |      | 4    |        |           |         |          |          | 4              |
| 1948 |       |         |          |       |       |     |      |      | 7      |           |         |          |          | 7              |
| 1949 |       |         |          |       |       |     |      | 9    | 15     |           |         |          |          | 24             |
| 1950 |       |         |          |       |       |     |      |      |        |           |         |          |          | --             |
| 1951 |       |         |          |       |       |     |      |      |        |           |         |          |          | --             |
| 1952 |       |         |          |       |       |     |      |      |        |           |         |          |          | --             |
| 1953 |       |         |          |       |       |     |      | 1    | 2      | 5         |         |          |          | 8              |
| 1954 |       |         |          |       |       |     | 8    |      |        | 2         |         |          |          | 10             |
| 1955 |       |         | 6        | 21    | 4     |     | 4    |      |        |           |         |          |          | 35             |
| 1956 |       |         |          |       |       |     | 7    | 8    | 10     | 4         |         |          |          | 29             |
| 1957 |       |         |          |       |       |     | 9    | 5    | 10     |           |         |          |          | 24             |
| 1958 |       |         |          |       |       |     | 21   | 50   | 5      |           |         |          |          | 75             |
| 1959 |       |         |          |       |       |     | 10   | 36   |        |           |         |          |          | 46             |
| 1960 |       |         | 11       |       |       |     | 22   | 10   |        | 3         | 5       |          |          | 51             |
| 1961 |       |         | 14       | 45    |       |     | 34   | 20   | 8      |           |         |          |          | 121            |

Table 2. Time distribution of NODC oceanographic stations west of 165°W extending out to the continental slope.

| YEAR | MONTH | JANUARY | FEBRUARY | MARCH | APRIL | MAY | JUNE | JULY | AUGUST | SEPTEMBER | OCTOBER | NOVEMBER | DECEMBER | TOTAL FOR YEAR |
|------|-------|---------|----------|-------|-------|-----|------|------|--------|-----------|---------|----------|----------|----------------|
| 1962 |       |         |          |       |       |     | 14   | 4    |        |           |         |          |          | 18             |
| 1963 |       |         |          |       |       |     | 20   | 13   |        |           |         |          |          | 33             |
| 1964 |       |         |          |       |       |     | 16   | 16   | 4      |           |         |          |          | 36             |
| 1965 |       |         |          |       |       |     | 15   | 24   |        |           |         |          |          | 39             |
| 1966 |       |         |          |       |       |     | 14   | 15   | 1      |           |         |          |          | 30             |
| 1967 |       |         |          |       |       |     | 17   | 5    | 4      |           |         |          |          | 26             |
| 1968 |       |         |          |       |       |     | 18   | 5    | 1      |           |         |          |          | 24             |
| 1969 |       |         |          |       | 1     | 10  | 13   | 4    | 3      |           |         |          |          | 31             |
| 1970 |       |         |          | 3     | 2     | 2   | 6    |      |        |           |         |          |          | 13             |
| 1971 |       |         |          |       |       | 42  | 81   | 11   |        | 1         |         |          |          | 135            |
| 1972 |       |         |          |       |       |     |      |      | 2      |           |         |          |          | 2              |

Table 2 (continued). Time distribution of NODC oceanographic stations west of 165°W extending out to the continental slope.

aspects of the flow field. In the event of a contaminant release, the immediate effects will be controlled by such shorter term processes. Appropriate measurements for these additional studies include direct current measurements (using drogues and current meters) and more closely spaced hydrographic stations than are now available. At least some of these additional field efforts are currently being carried out under other parts of the OCS program. Others should be addressed in future efforts.

## IX. SUMMARY OF FOURTH QUARTER OPERATIONS

### A. Ship or Laboratory Operations

No ship operations were scheduled or carried out during this period because of harsh climatic conditions in the study region. No laboratory operations were carried out because none were planned under the auspices of this project.

### B. Data analysis operations

An error-free NODC data tape was finally received just prior to this quarter and has been processed. The stations contained in this tape have been plotted as to position and tabulated with respect to time distribution (Appendices 1, 2 and Tables 1 and 2). Data tapes from the August *Discoverer* and November *Miller Freeman* cruises are still undergoing analysis.

## X. REFERENCES

- Barnes, C. A. and T. G. Thompson, 1938. Physical and chemical investigations in Bering Sea and portions of the North Pacific Ocean. U. Wash. Publ. in Oceanography, 3(2):35-79.
- Dodimead, A. J., Favorite, F. and Hirano, T., 1963. Oceanography of the subarctic Pacific region. I.N.P.F.C., Bull. 13:177-189.
- Hebard, J. F., 1961. Currents in the southeastern Bering Sea. I.N.P.F.C., Bull. 5:9-16.
- Ingraham, W. J., Jr., 1973. Maps of mean values of water temperature (C°) and salinity (‰) in the eastern Bering Sea by 1 x 1° quadrangles. NWFC MARMAP SURVEY I, Report No. 9:24 pp. Northwest Fisheries Center, NMFS-NOAA, Seattle (mimeographed).
- International North Pacific Fisheries Commission, 1957. Annual report for the year 1956. INPFC, Vancouver, Canada: 88 pp.
- Kihara, K., 1971. Studies on the formation of demersal fishing grounds 2. Analytical studies on the effect of the wind on the spreading of water masses in the eastern Bering Sea. *Bull. de la Societe Franco-Japonaise d'oceanographie*, 9(1):12-22.
- Kinder, T. H., (unpublished). The Slope Regime of the Eastern Bering Sea. U. Wash. Ph.D. Thesis (in preparation).
- McRoy, C. P. and Goering, J. J., 1974. The influence of ice on the primary productivity of the Bering Sea. In: *Oceanography of the Bering Sea with emphasis on renewable resources*. D. W. Hood and E. J. Kelley, eds., Inst. Mar. Sci., Univ. of Alaska Occasional Publ. No. 2:403-421.
- Maeda, T., Fujii, T. and Masuda, K., 1968. Studies on the trawl fishing grounds of the eastern Bering Sea - II. On the annual fluctuation of oceanographical conditions in summer season. *Bull., Japan Soc. Sci. Fish.*, 34(7):586-593 (in Japanese).
- Muench, R. D., 1976. A note on eastern Bering Sea shelf hydrographic structure; August 1974. *Deep-Sea Research* (in press).
- Muench, R. D. and Ahlnäs, K., 1976. Ice movement and distribution in the Bering Sea during March through June 1974. *Jour. Geophys. Res.* (in press).
- Myers, R. and Muench, R. D., 1975. Upwelling in central Bristol Bay. *EOS, Trans. AGU*, 56(12):1010 (abstract).
- Ohtani, K., 1969. On the oceanographic structure and the ice formation on the continental shelf in the eastern Bering Sea (in Japanese). *Bull. Fac. Fish., Hokkaido Univ.*, 20(2):94-117.

Sverdrup, H. U. and Fleming, R. H., 1941. The waters off the coast of Southern California, March to July, 1937. *Scripps Inst. of Oceanogr. Bull.* 4(10):261-378.

Takenouchi, A. Y. and Ohtani, K., 1974. Currents and water masses in the Bering Sea: a review of Japanese work. *In: Oceanography of the Bering Sea, with emphasis on renewable resources.* D. W. Hood and E. J. Kelley, eds. Inst. Mar. Sci., Univ. of Alaska Occasional Publ. No. 2:39-57.

Thompson, W. F. and R. Van Cleave, 1936. Life history of the Pacific halibut (2). Distribution and early life history. *Report Internat. Fisheries Commission* 9, 182 pp.



APPENDIX 1

Location of KONG oceanographic  
stations east of 165°W, including  
Bristol Bay

*Barrow Bay*

1934

*Bristol Bay*

*Anchorage*

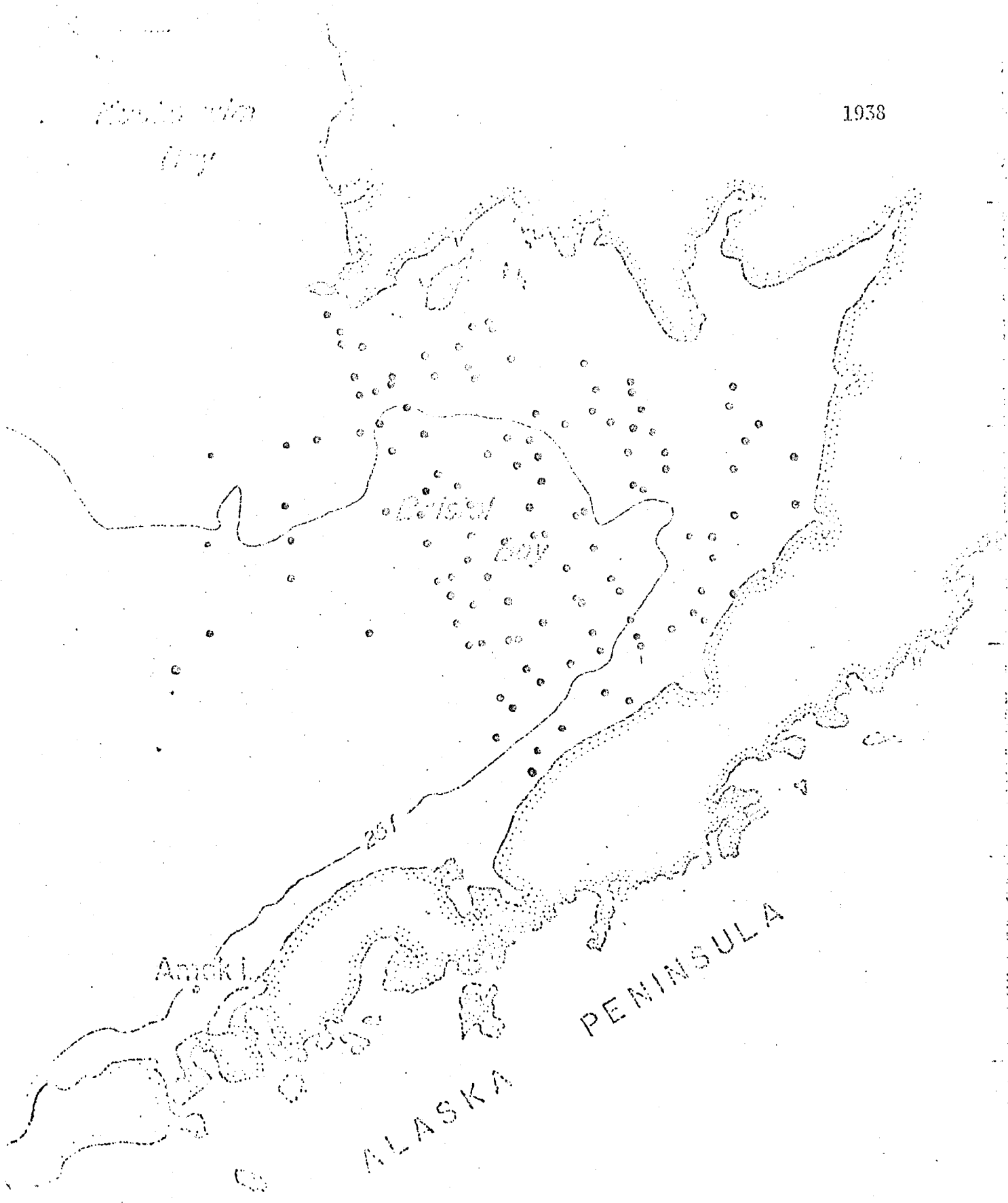
ALASKA

PENINSULA

*Denali Pass*

*Alaska*  
*1938*

1938



*Bristol Bay*

*Aniak*

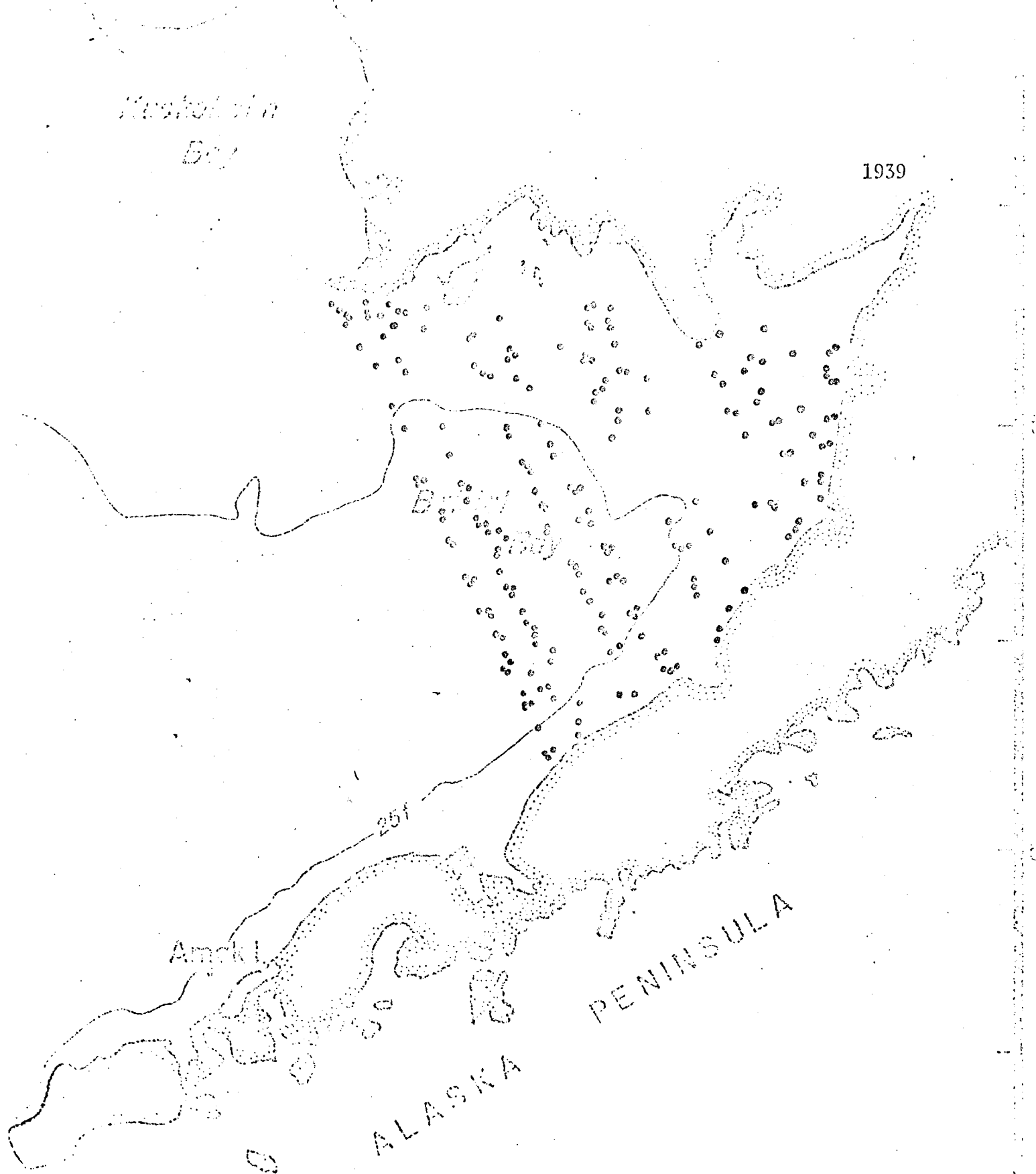
ALASKA

PENINSULA

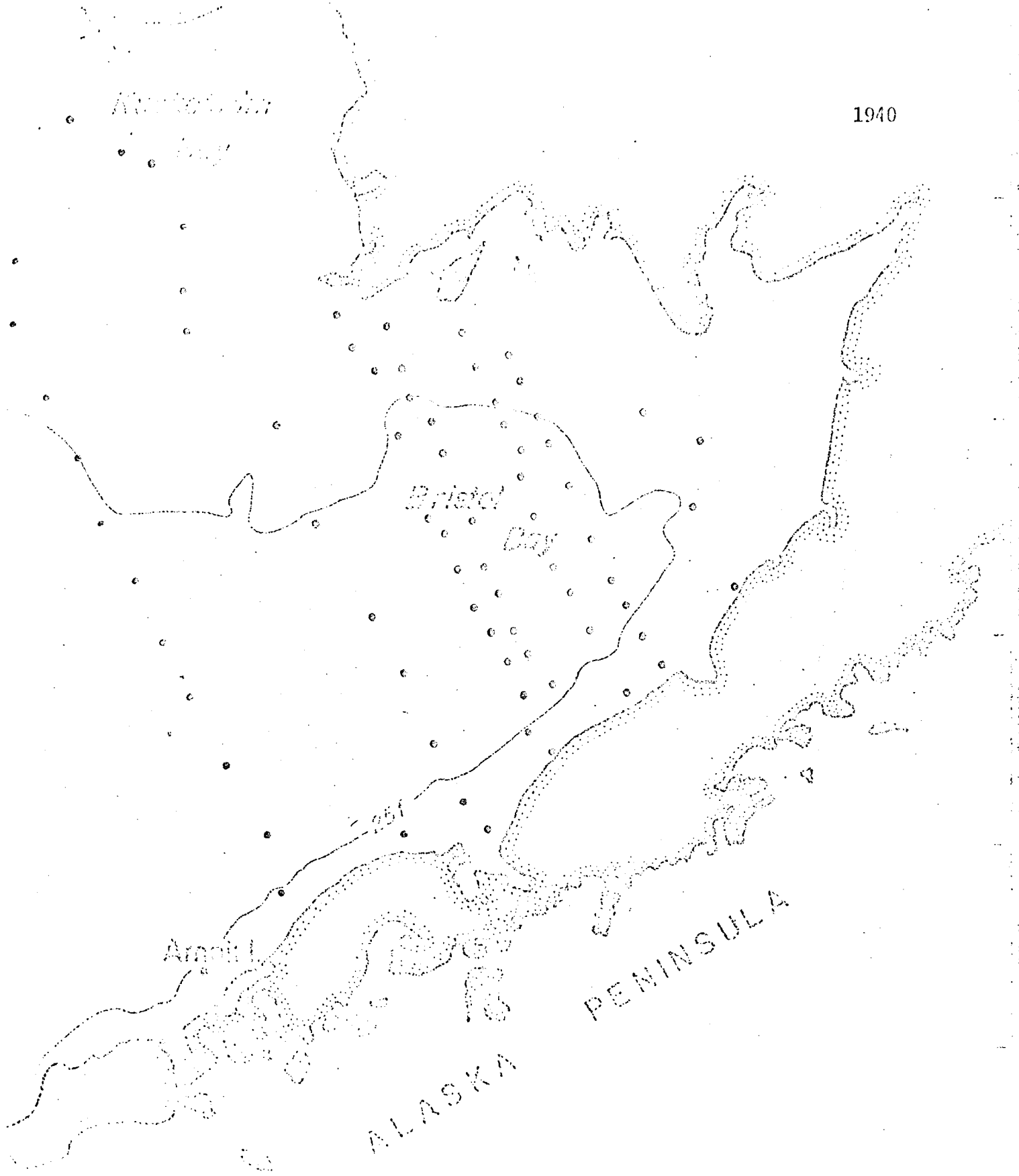
*Unalak Pass*

Westholmen  
Bay

1939



Unalak Pass



*Amakalik*

*Bristol Bay*

*Amalik*

55

ALASKA  
PENINSULA

*1940*

*Mud Lake Bay*

1941

*Bristol Bay*

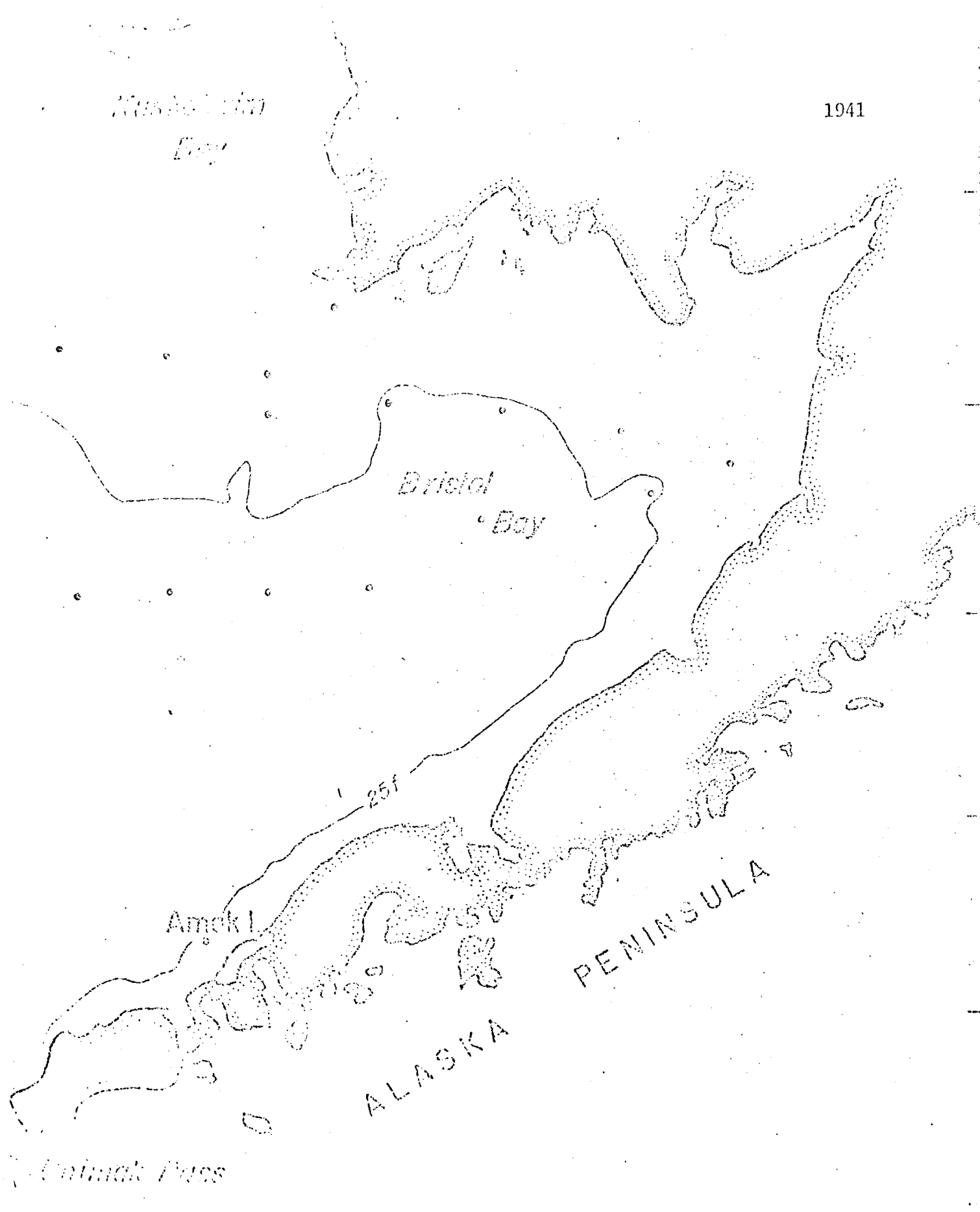
1-25f

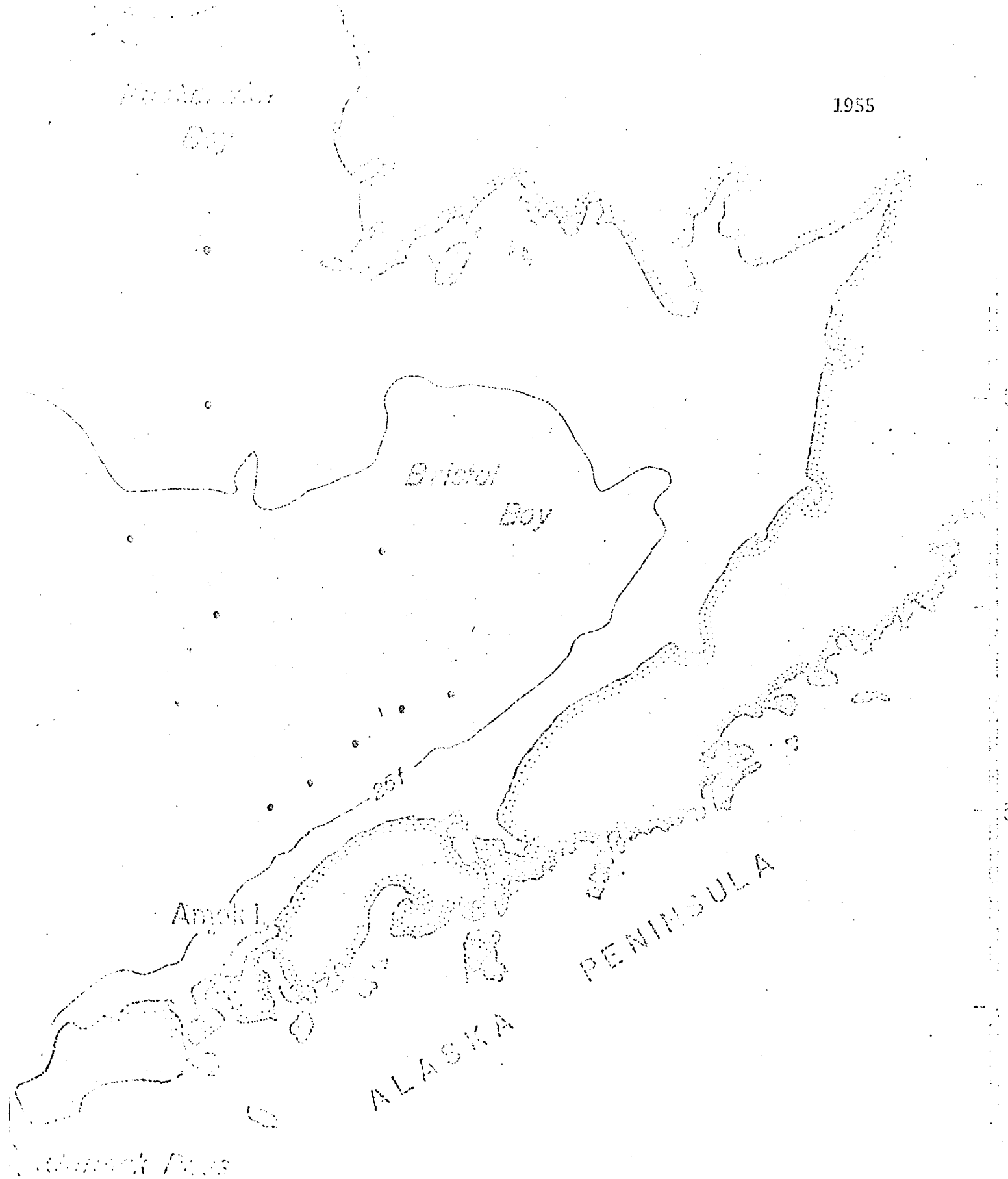
*Amak I.*

PENINSULA

ALASKA

*Unimak Pass*





*Kachemak Bay*

1956

*Bristol Bay*

231

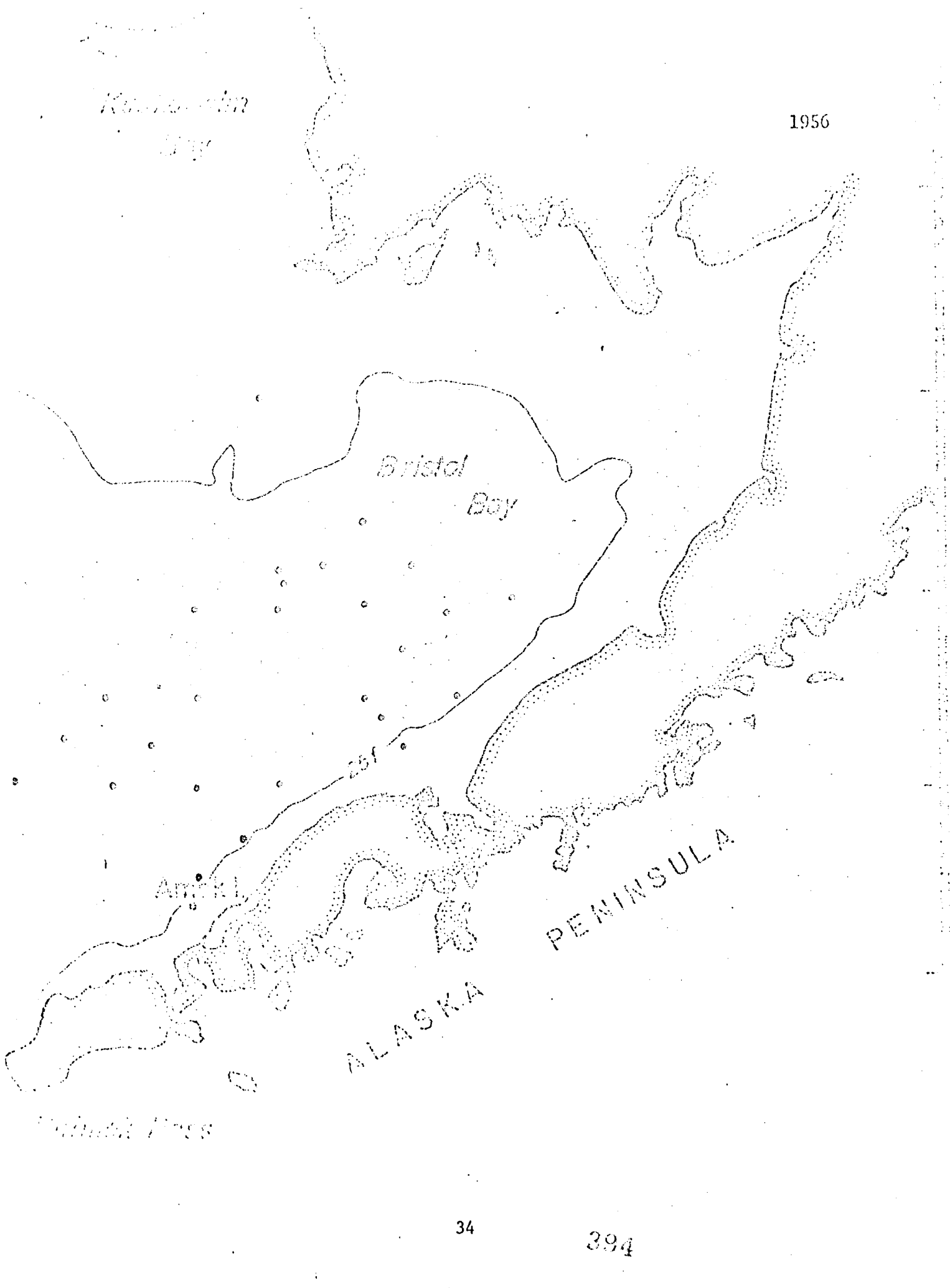
*Atkas*

*YUKON RIVER*

ALASKA

PENINSULA

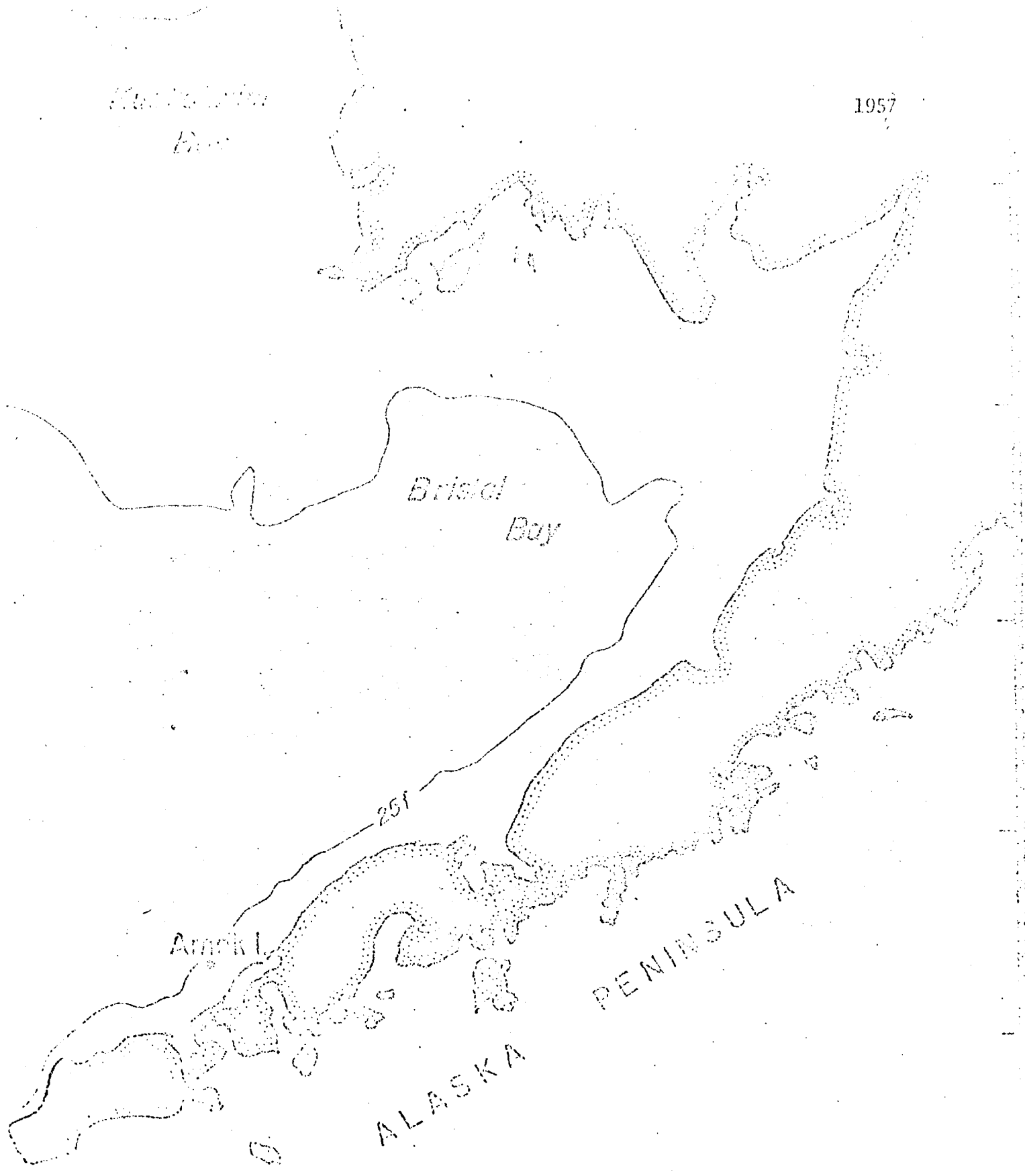
*Chitina Pass*





*Alaska*  
*Bay*

1957



*Bristol*  
*Bay*

25f

*Amukl*

ALASKA

PENINSULA

*Unalak Pass*

*Kodiak Bay*

1958

*Bristol Bay*

251

*Amak*

PENINSULA

ALASKA

*Malina Pass*

Martha's  
Bay

1959

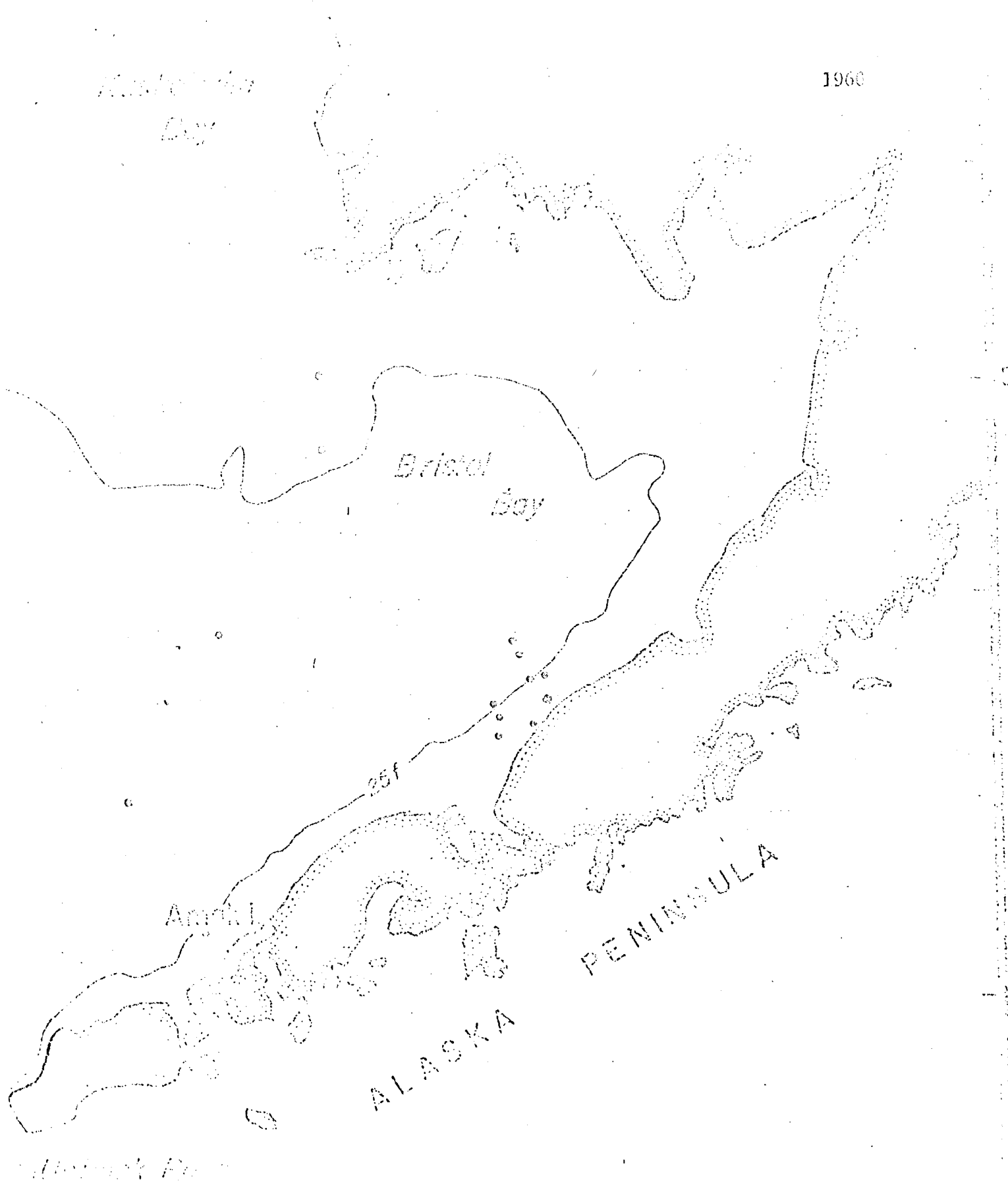
Bristol  
Bay

Amak  
Is.

PENINSULA

ALASKA

Chukchi Pass



*Resurrection Bay*

1961

*Bristol Bay*

ALASKA PENINSULA

ALASKA

*Kutchik In  
Bay*

1963

*Bristol  
Bay*

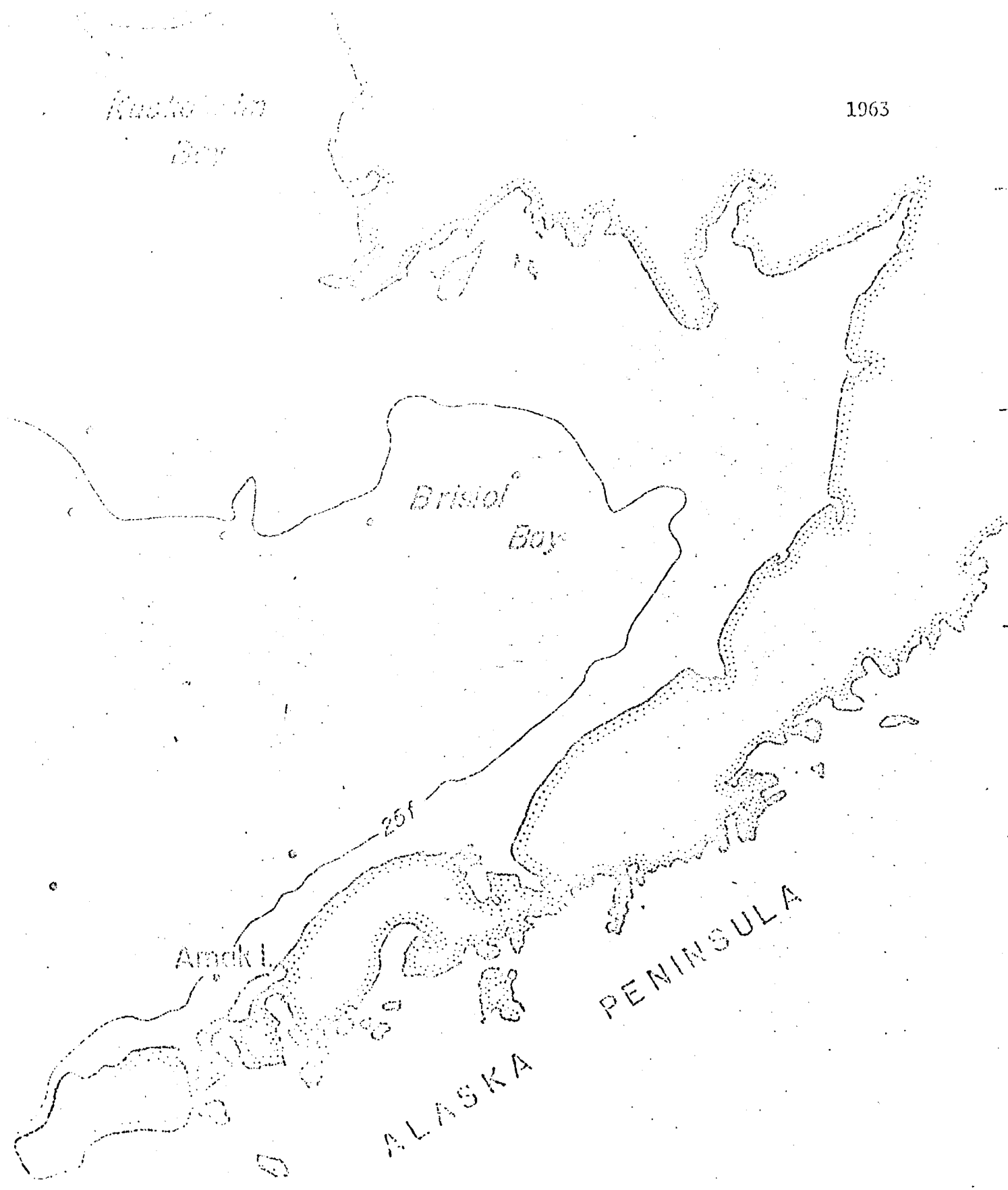
25f

*Amak I.*

PENINSULA

ALASKA

*Wahinek Pass*



*Unalakleet Bay*

1964

*Bristol Bay*

*Arctic*

ALASKA

PENINSULA

*Malina Pass*

*Historical chart*

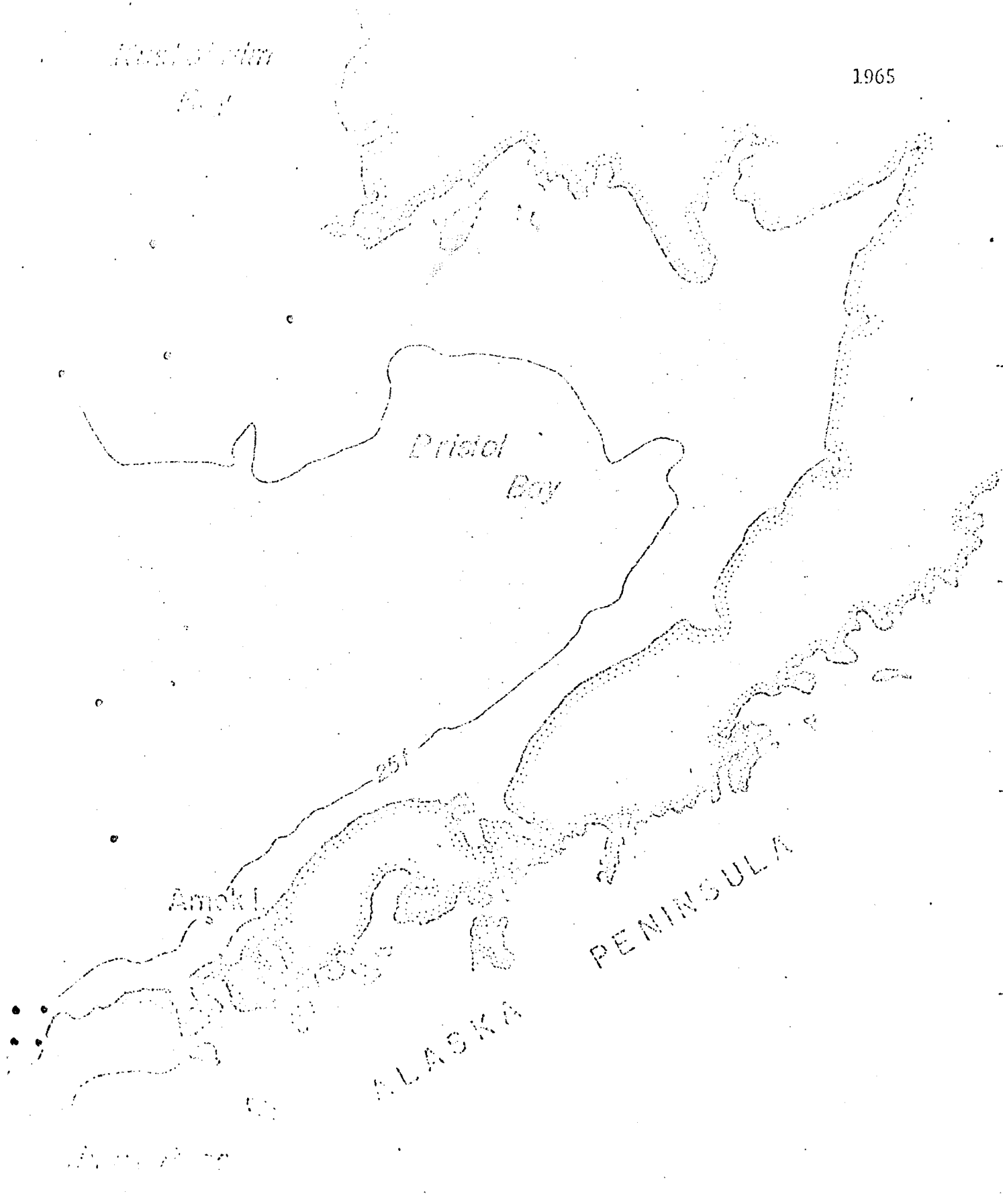
1965

*Pristol Bay*

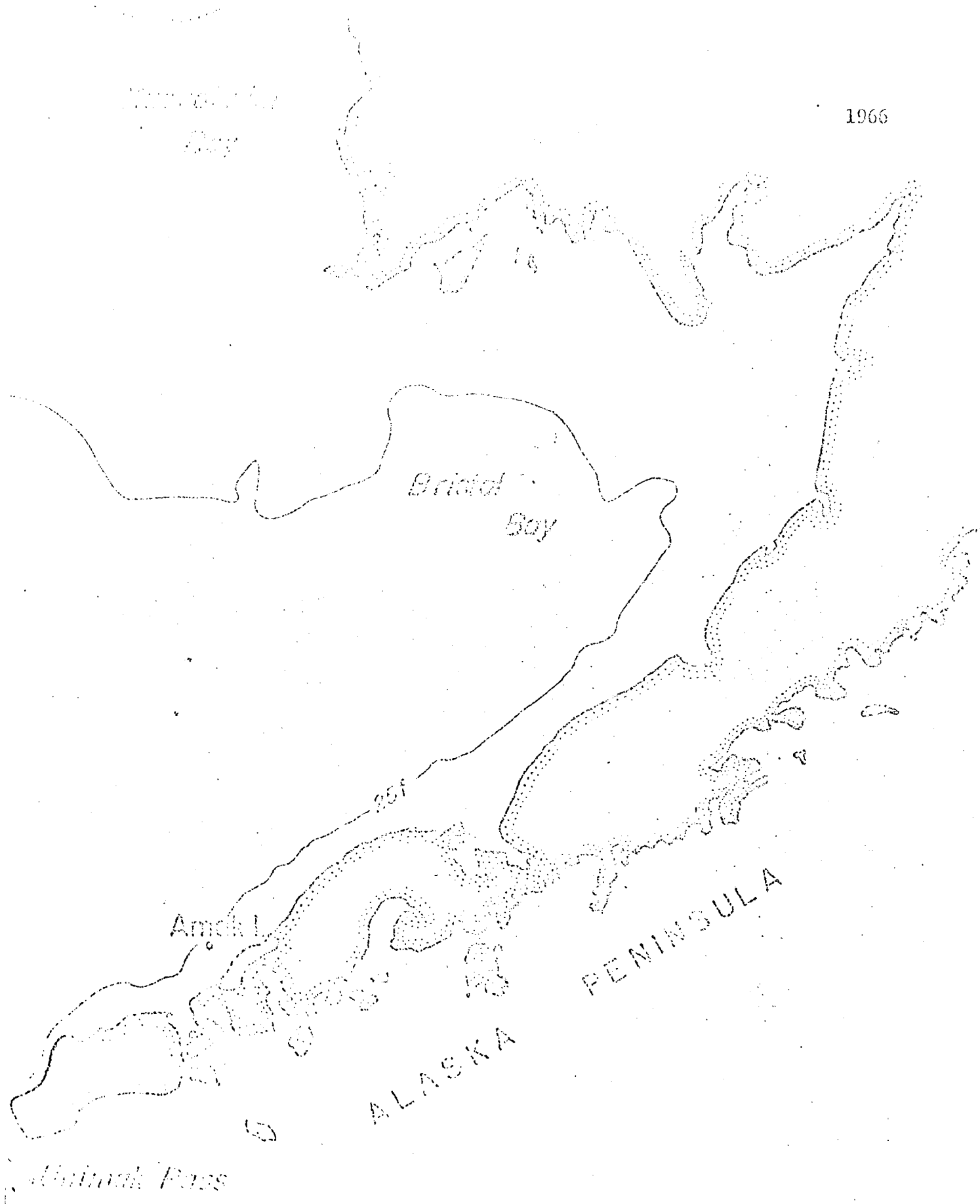
*Amok I*

ALASKA

PENINSULA







ALASKA

PENINSULA

*Alaska Peninsula*  
*Bay*

1967

*Bristol*  
*Bay*

25f

*Amak*

PENINSULA

ALASKA

*Unalaska Pass*

*Kroka Bay*

1968

*Bristol Bay*

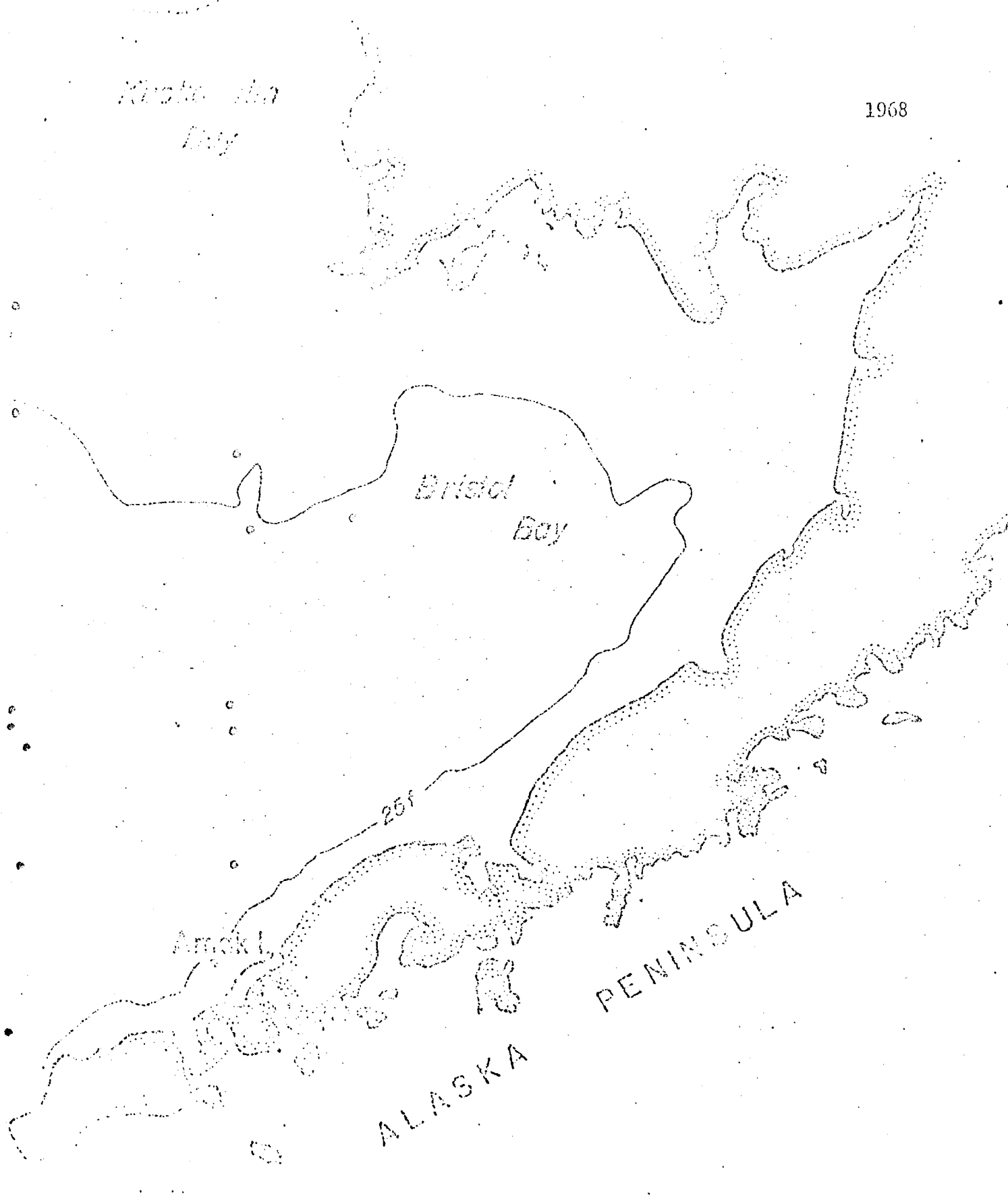
25f

*Amak L.*

PENINSULA

ALASKA

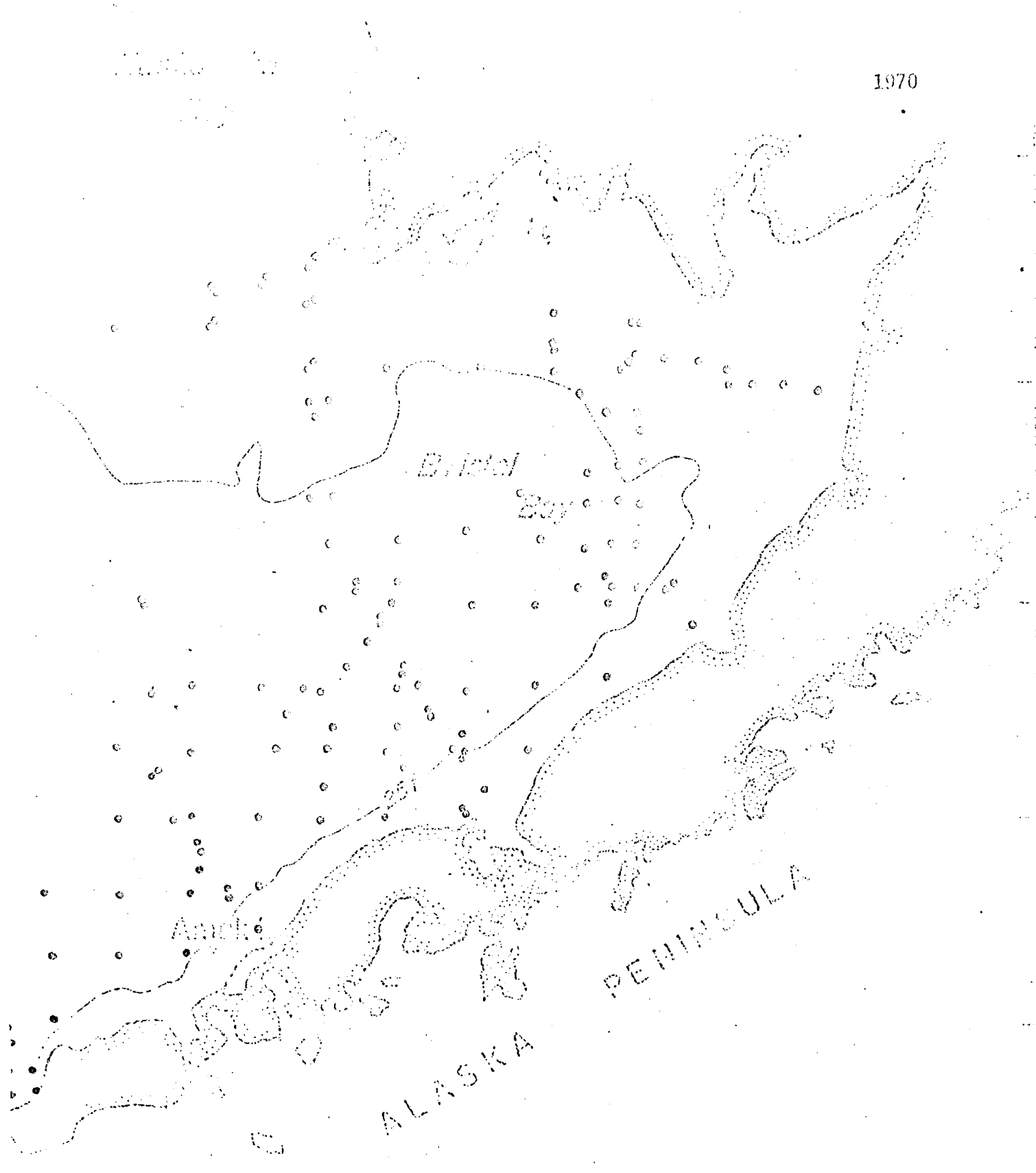
*Point Barrow*



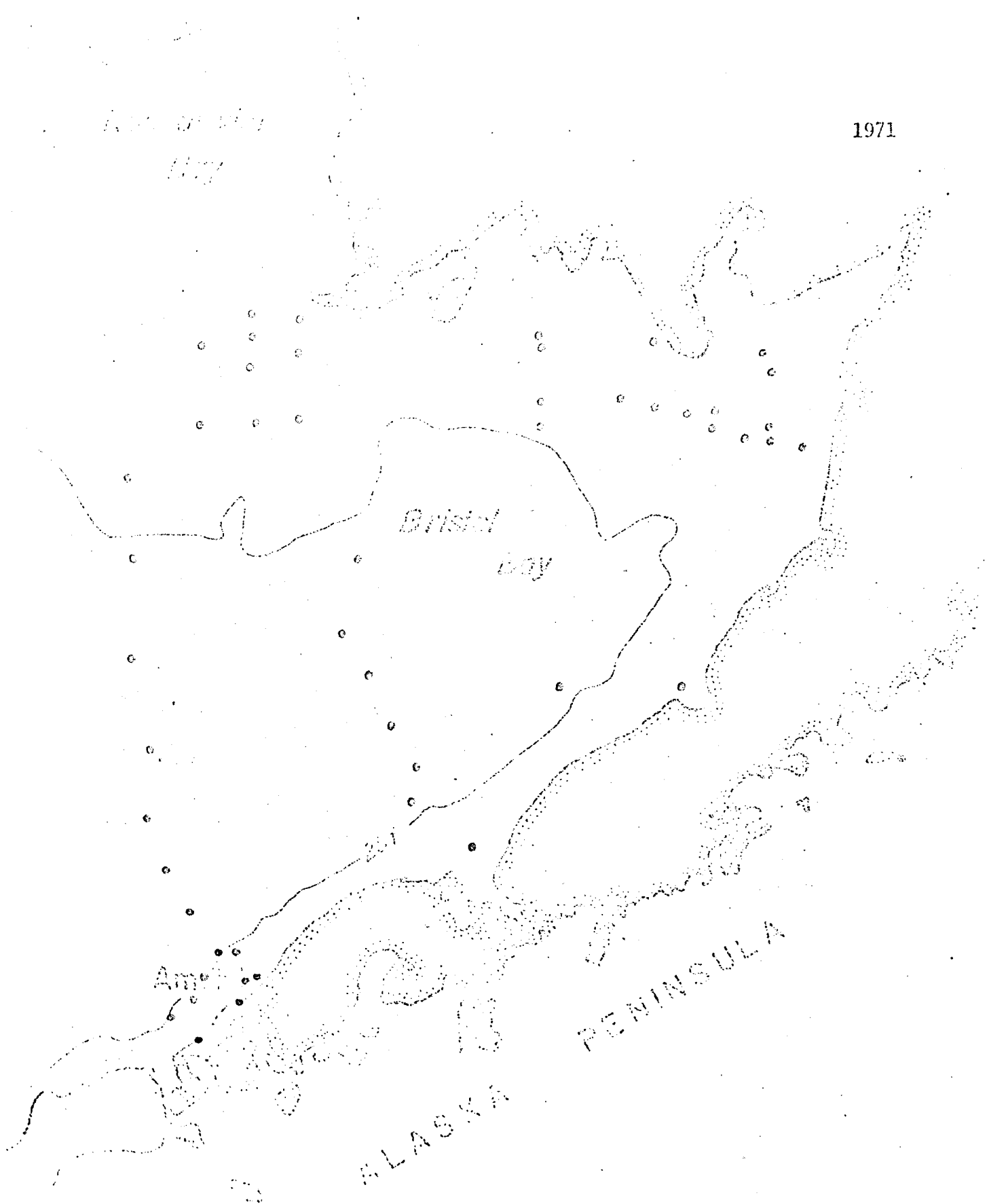


Am...

Unit 1. Pass



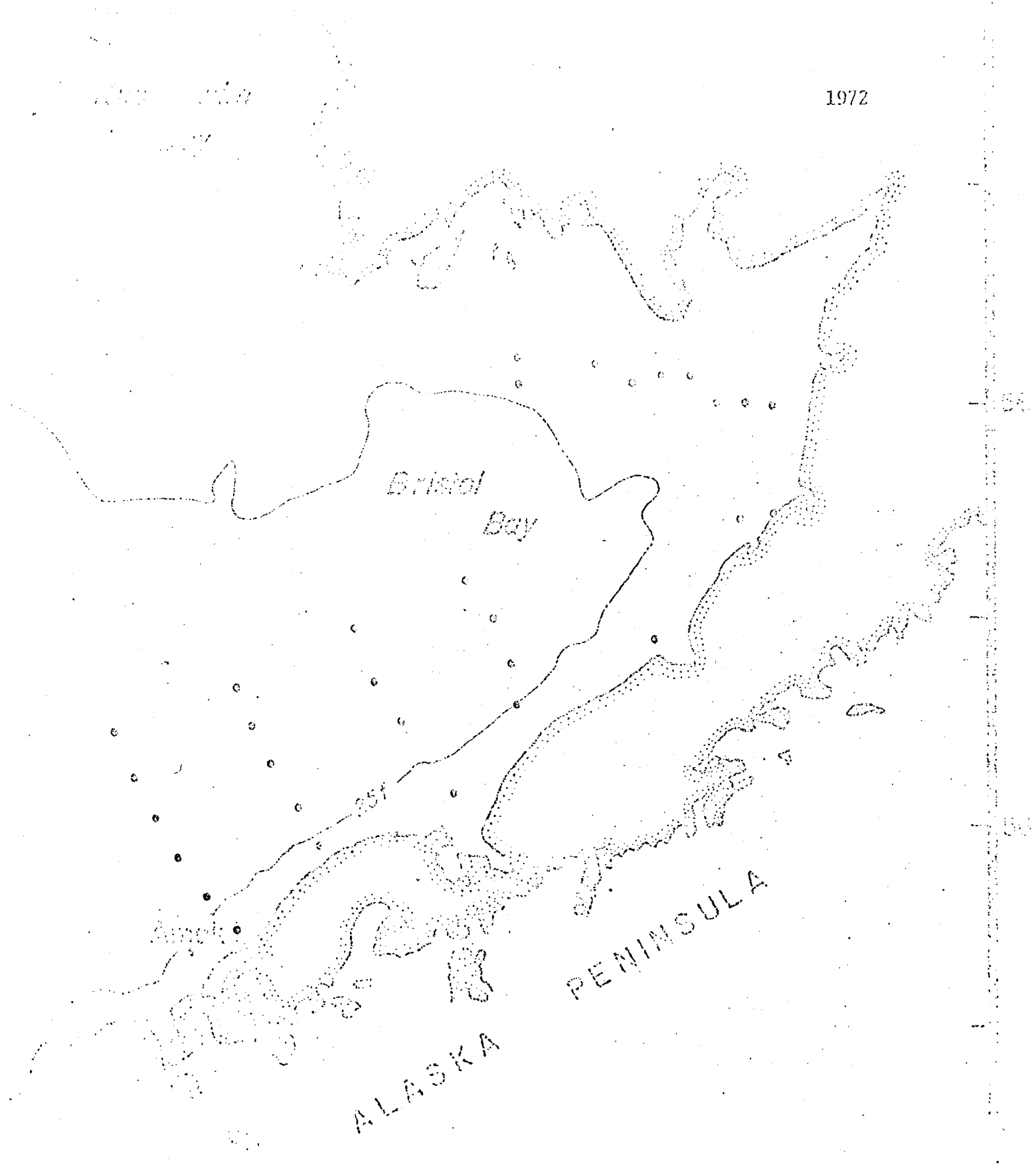
*Amtrak Pass*



1971  
1971

Am...

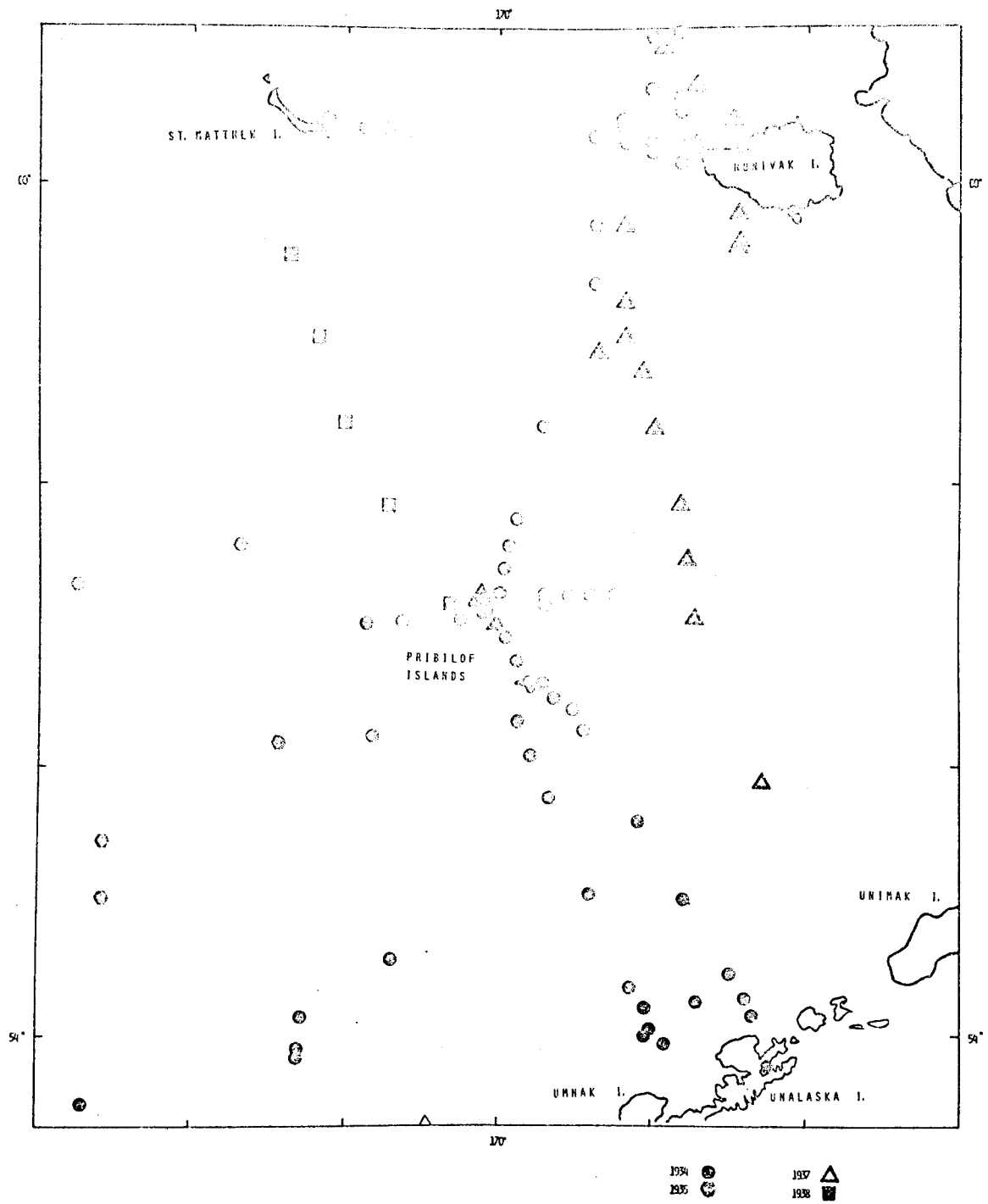
1971

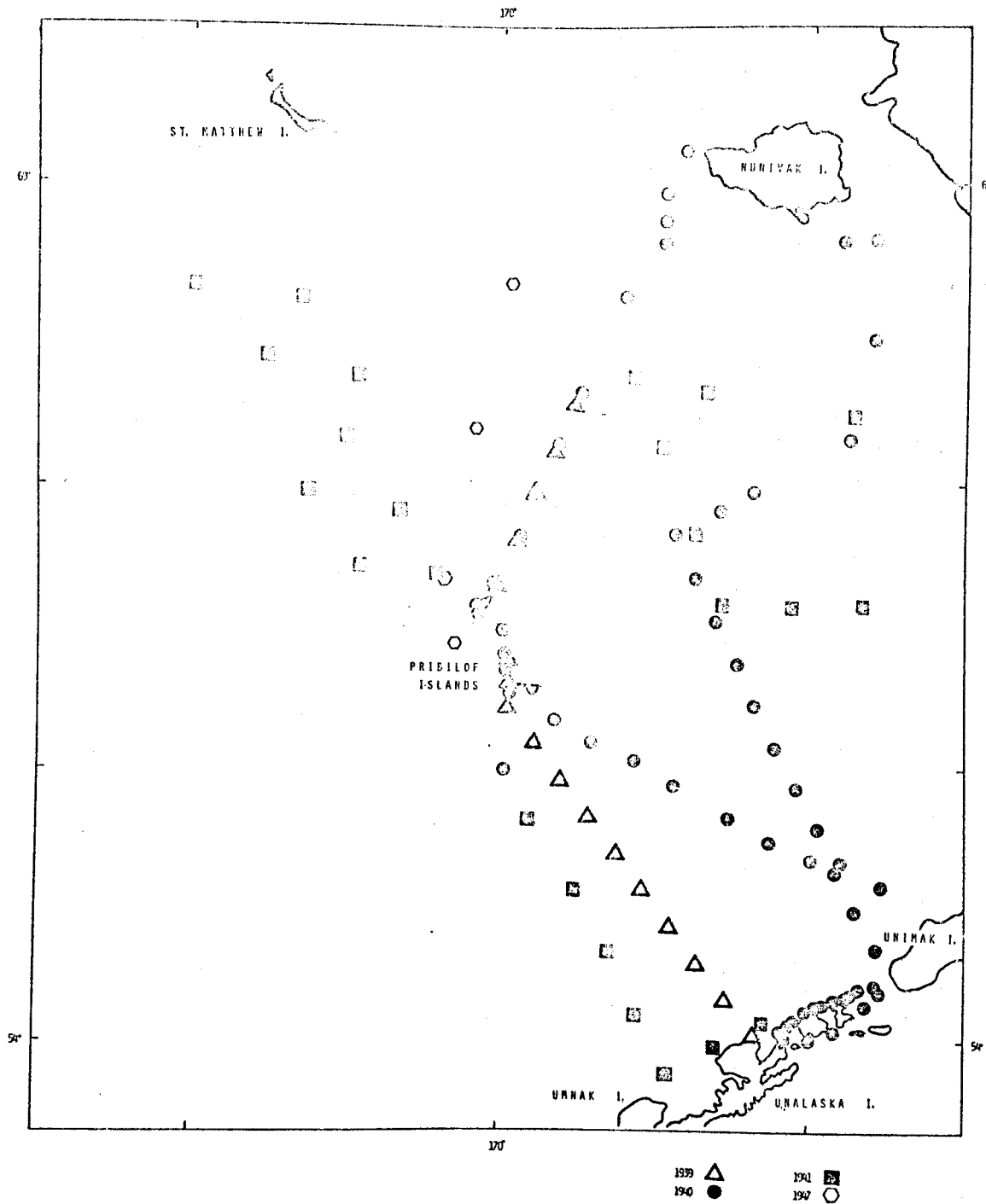


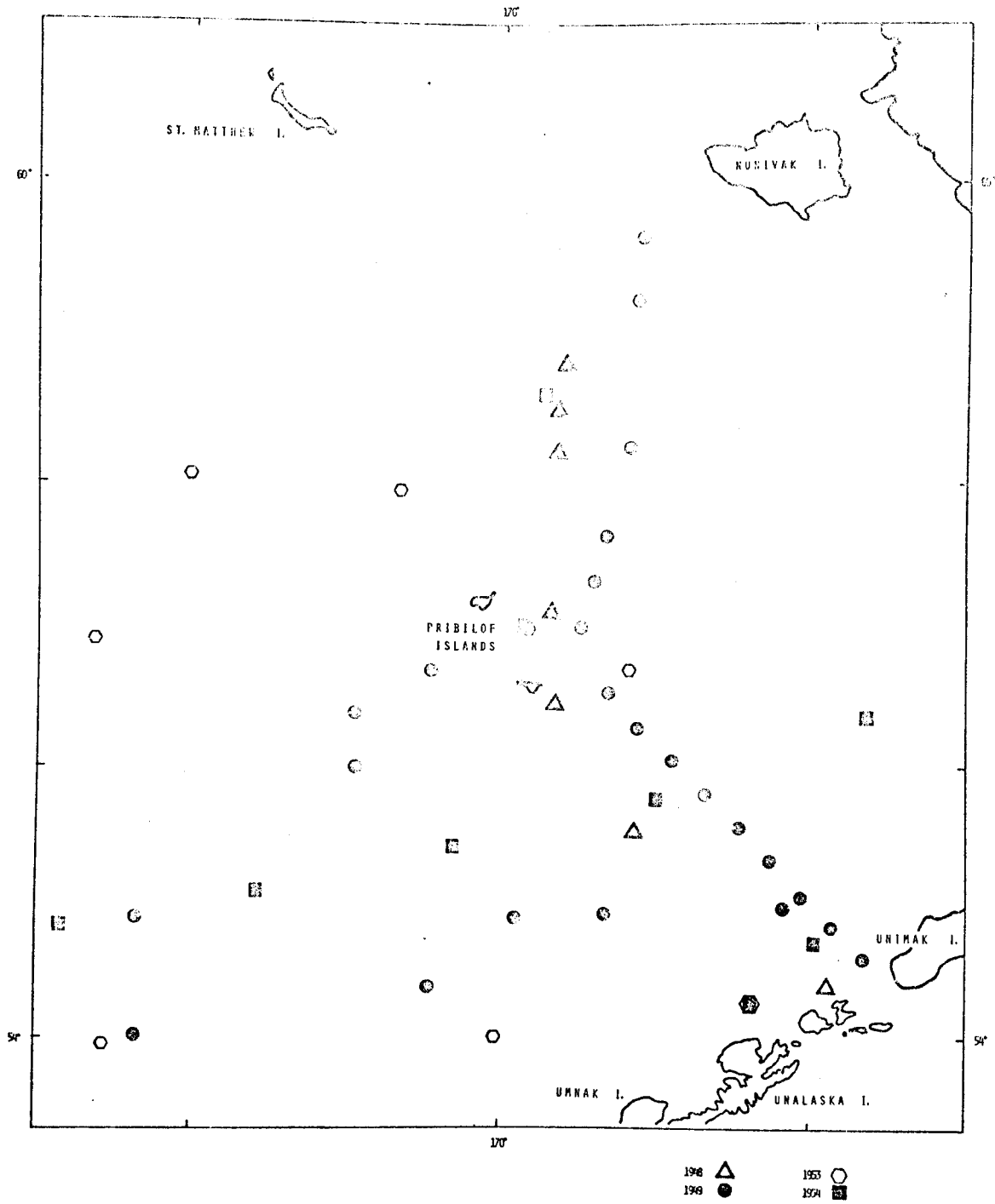
APPENDIX 2

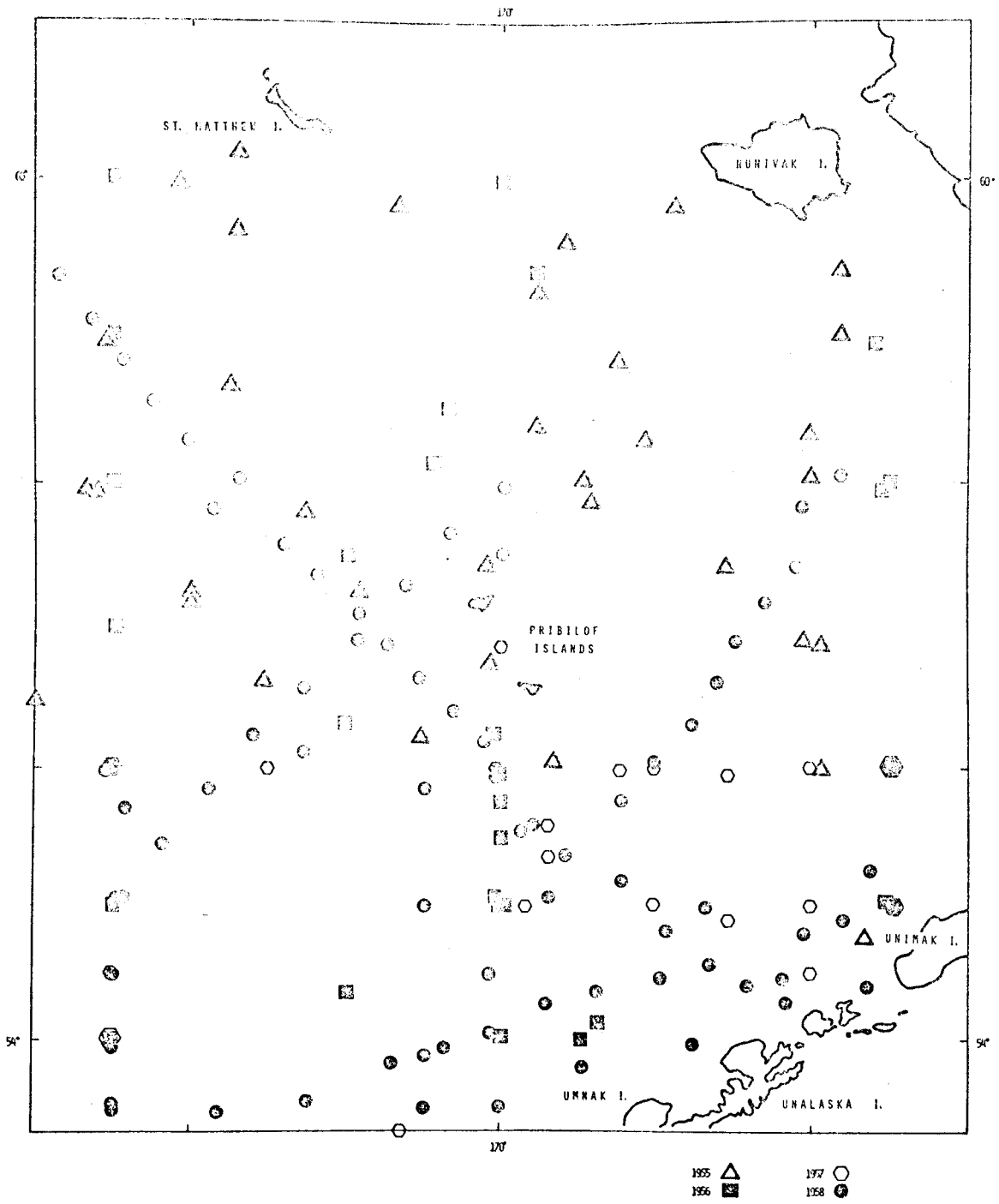
Location of HODC oceanographic  
stations west of 165°W, extending out  
to the continental shelf

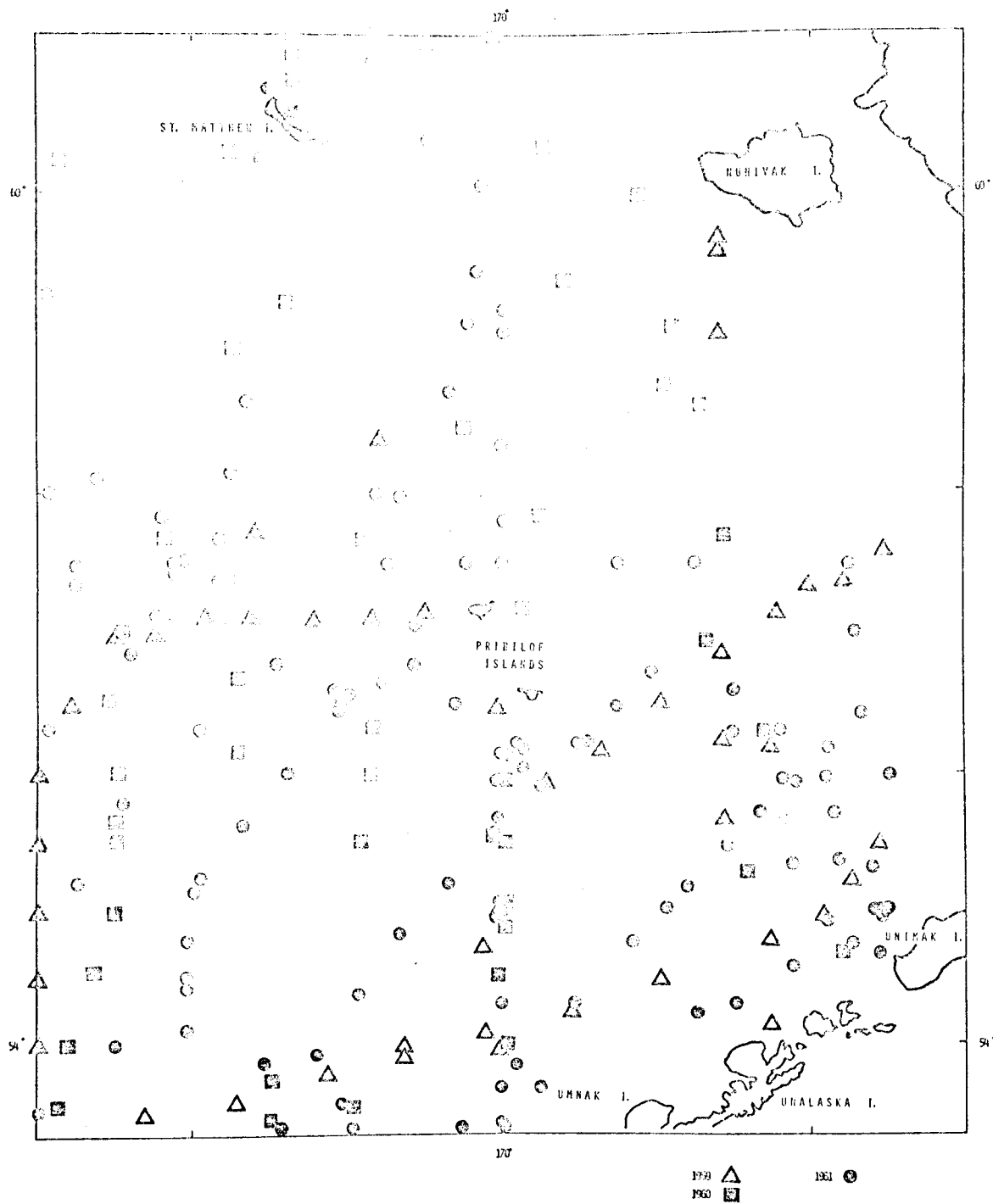


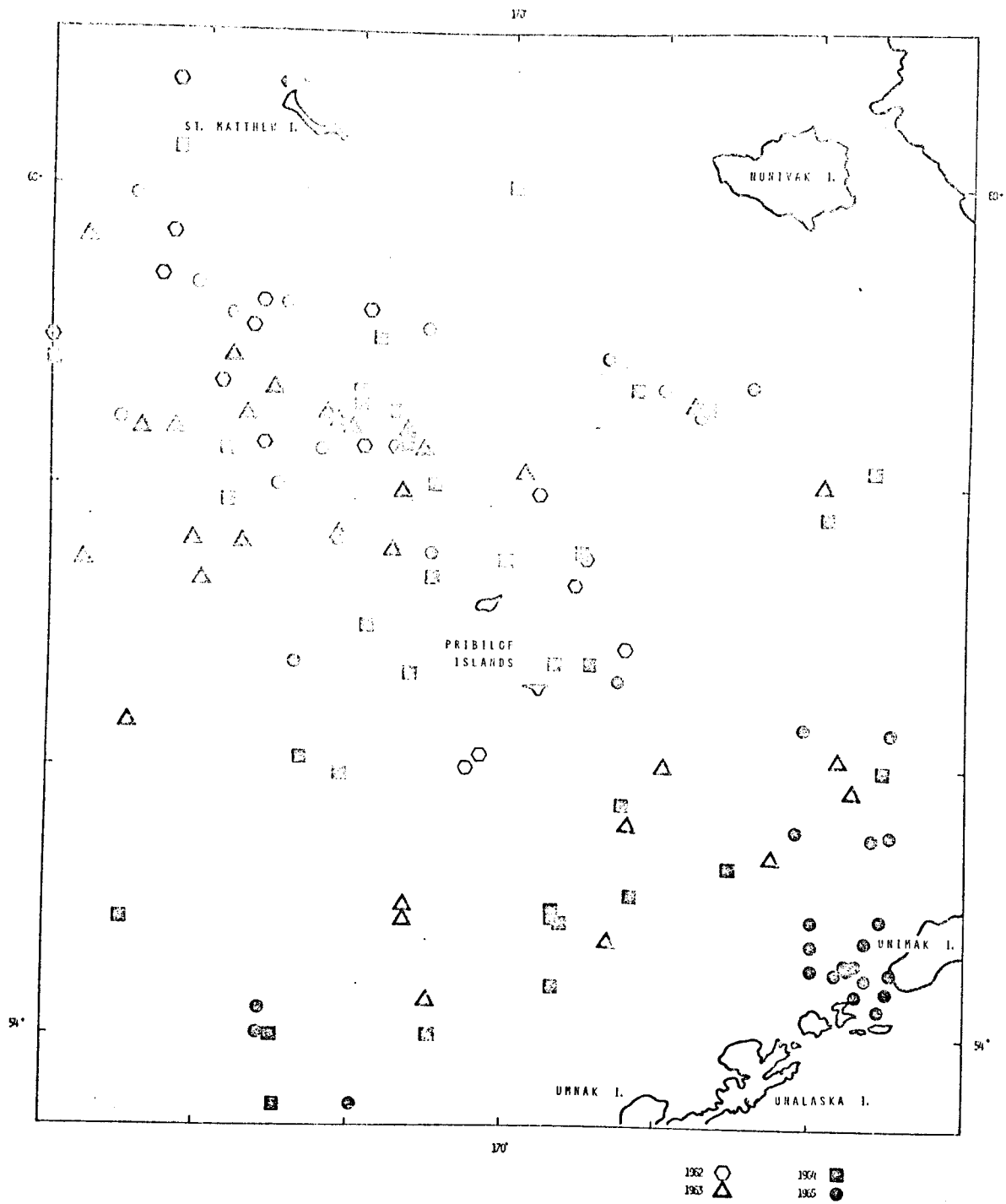


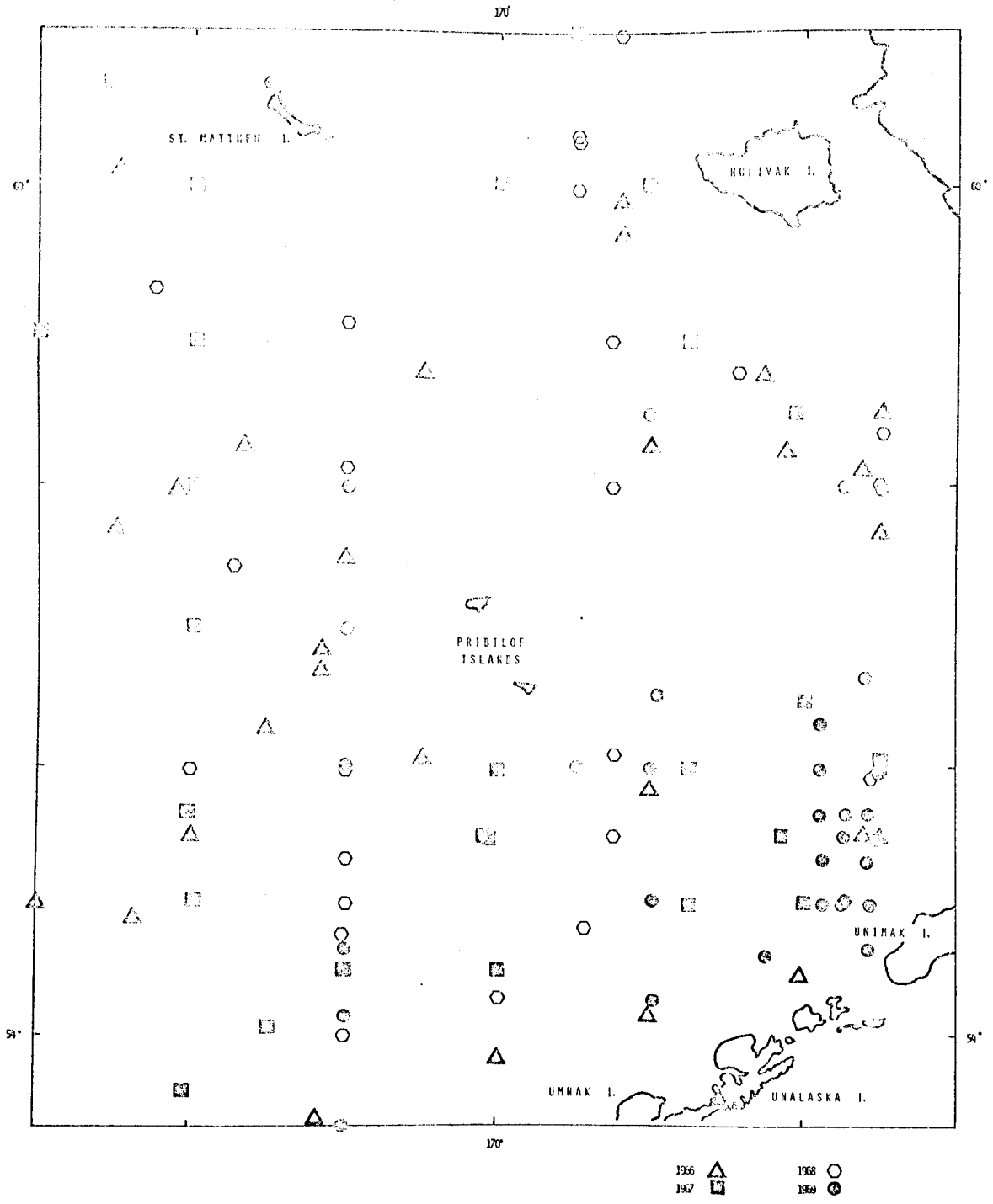


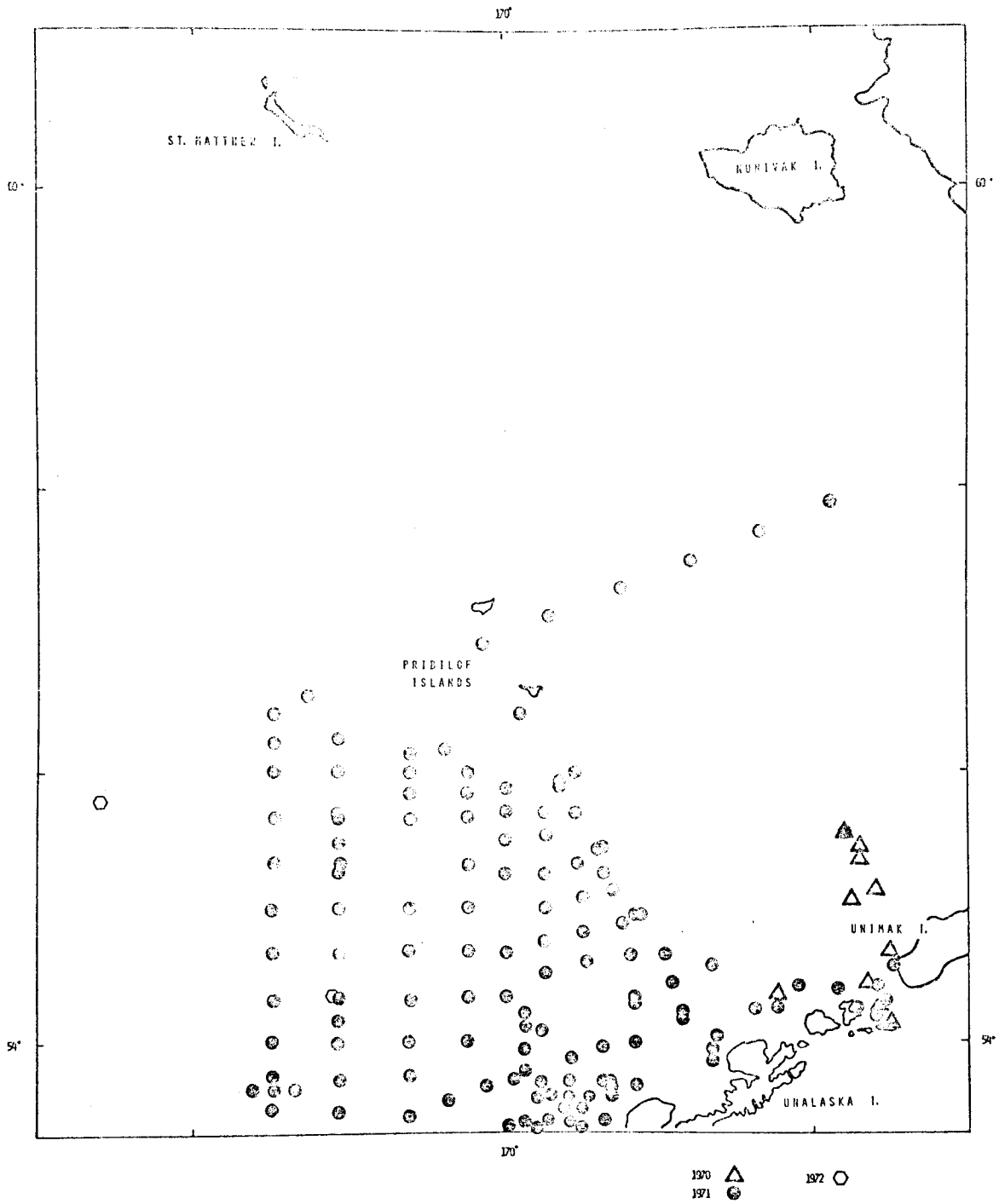














OCS COORDINATION OFFICE

University of Alaska

ENVIRONMENTAL DATA SUBMISSION SCHEDULE

DATE: March 31, 1976

CONTRACT NUMBER: 03-5-022-56 T/O NUMBER: 14 R.U. NUMBER: 307

PRINCIPAL INVESTIGATOR: Dr. R. D. Muench

Submission dates are estimated only and will be updated, if necessary, each quarter. Data batches refer to date as identified in the data management plan.

| <u>Cruise/Field Operation</u> | <u>Collection Dates</u> |           | <u>Estimated Submission Dates</u> <sup>1</sup> |
|-------------------------------|-------------------------|-----------|--|
|                               | <u>From</u>             | <u>To</u> | <u>Batch 1</u>                                 |
| Acona #197                    | 7/20/75                 | 7/30/75   | 4/9/76   |
| Discoverer Leg I & II<br>#808 | 5/15/75                 | 6/19/75   | 4/9/76   |
| Discoverer Leg I #810         | 8/9/75                  | 8/28/75   | Format problem - Date unknown                  |
| Miller Freeman #815           | 11/19/75                | 11/26/75  | 5/15/76  |

Note: <sup>1</sup> Data Management Plan and Data Format have been approved and are considered contractual.

OCS COORDINATION OFFICE

University of Alaska

ESTIMATE OF FUNDS EXPENDED

DATE: March 31, 1976  
 CONTRACT NUMBER: 03-5-022-56  
 TASK ORDER NUMBER: 14  
 PRINCIPAL INVESTIGATOR: Dr. R. D. Muench

Period April 1, 1975 - March 31, 1976\* (12 mos)

|                  | <u>Total Budget</u>     | <u>Expended</u>         | <u>Remaining</u>        |
|------------------|-------------------------|-------------------------|-------------------------|
| Salaries & Wages | 43,724.00               | 24,769.59               | 18,954.41               |
| Staff Benefits   | 7,399.00                | 4,186.67                | 3,212.33                |
| Equipment        | 2,500.00                | 2,510.00                | (10.00)                 |
| Travel           | 5,774.00                | 1,982.84                | 3,791.16                |
| Other            | <u>7,400.00</u>         | <u>3,299.79</u>         | <u>4,100.21</u>         |
| Total Direct     | <u>66,797.00</u>        | <u>36,748.89</u>        | <u>30,048.11</u>        |
| Indirect         | <u>25,009.00</u>        | <u>14,168.21</u>        | <u>10,840.79</u>        |
| Task Order Total | <u><u>91,806.00</u></u> | <u><u>50,917.10</u></u> | <u><u>40,888.90</u></u> |

\* Preliminary cost data, not yet fully processed.

Following is part 2 of the quarterly report R.U.# 307 for the period ending December 31, 1975. This was received after the printing of the Quarterly Reports, July - September 1975, therefore is included here.

RECEIVED

OCS COORDINATION OFFICE

JAN 19 1976

University of Alaska

NEGOA

Quarterly Report for Quarter Ending December 31, 1975

Project Title: Statistical and Historical Data Analysis  
and Ship-of-Opportunity Program for the  
Southeastern Bering Sea

Contract Number: 03-5-022-56

Task Order Number: 14

Principal Investigator: Dr. R. D. Muench

phys. 00.  
R.V. 3071

#### I. Task Objectives

Obtain historical data and integrate them into historical and statistical data analyses. Obtain data from ships-of-opportunity and incorporate them into the historical and statistical data analyses.

#### II. Field Activities

CTD data were obtained during a cruise on the R/V Miller Freeman in November 1975.

#### III. Results

The Bristol Bay data obtained by IMS during 1965-1970 have been analyzed and compiled into a paper for oral presentation at the Fall 1975 AGU meeting. The region of upwelling in central Bristol Bay will be discussed and documented. Some possible alternate interpretations of observed features will be presented, along with hypotheses to explain the features. Portions of the June 1975 hydrographic data obtained from the R/V Discoverer have been incorporated into the analyses, where possible.

#### IV. Problems Encountered

Revised copies of the originally defective historical data tapes from EDS (NODC) were finally obtained by mid-November. The delay of several months between return of the defective tape to EDS and their production of a new tape has prevented carrying out of meaningful historical-statistical analyses based on these data during this period. The revised tape has more over proved defective in the same way as the initial tape, although less so: several stations have been dropped from this tape.

The data tape obtained from the June 1975 R/V Discoverer cruise was not in the format request by IMS. Consequently, it has taken nearly two months to retrieve data from this tape. Upon data retrieval, it was noted that thermometric calibrations of the CTD were insufficient. (Thermometers were not rotated frequently enough and one of them was malfunctioning.) The conductivity sensor of the CTD was inoperative, so we have only discrete (bottle) salinity values. Calibration data for converting the frequency output from the CTD into temperature data, as provided us, were insufficient. Consequently, the entire data sent from the June R/V Discoverer cruise is of questionable, if not downright poor quality.

Data from the August 1975 R/V Discoverer cruise have not yet been returned to IMS from EDS. This 3-month delay is unacceptable, particularly considering that processing done by EDS should consist (by this time) of only a tape - tape conversation involving standard software.

A data tape containing unpublished Japanese oceanographic data from the study region is in the possession of the Juneau OCS Project Office. Attempts to obtain these data were initiated six months ago. The data have not yet been made available, despite several promises by the Project Office that they would, in fact, be supplied.

OCS COORDINATION OFFICE

University of Alaska

ENVIRONMENTAL DATA SUBMISSION SCHEDULE

DATE: December 31, 1975

CONTRACT NUMBER: 03-5-022-56

T/O NUMBER: 14

R.U. NUMBER: 307

PRINCIPAL INVESTIGATOR: Dr. R. D. Muench

Submission dates are estimated only and will be updated, if necessary, each quarter. Data batches refer to data as identified in the data management plan.

| <u>Cruise/Field Operation</u> | <u>Collection Dates</u> |           | <u>Estimated Submission Dates</u> <sup>(1)</sup> |
|-------------------------------|-------------------------|-----------|--|
|                               | <u>From</u>             | <u>To</u> | <u>Batch 1</u>                                   |
| Acona #197                    | 7/20/75                 | 7/30/75   | 1/15/76  |
| Discoverer Leg I & II<br>#808 | 5/15/75                 | 6/19/75   | 2/1/76   |
| Discoverer Leg I #810         | 8/9/75                  | 8/28/75   | 3/1/76   |
| Miller Freeman #815           | 11/19/75                | 11/26/75  | 5/15/76  |

Note: (1) Estimated submission dates are contingent upon final approval by NOAA of the data management plan and data format submitted NOAA in University of Alaska approved form Nov. 20, 1975.

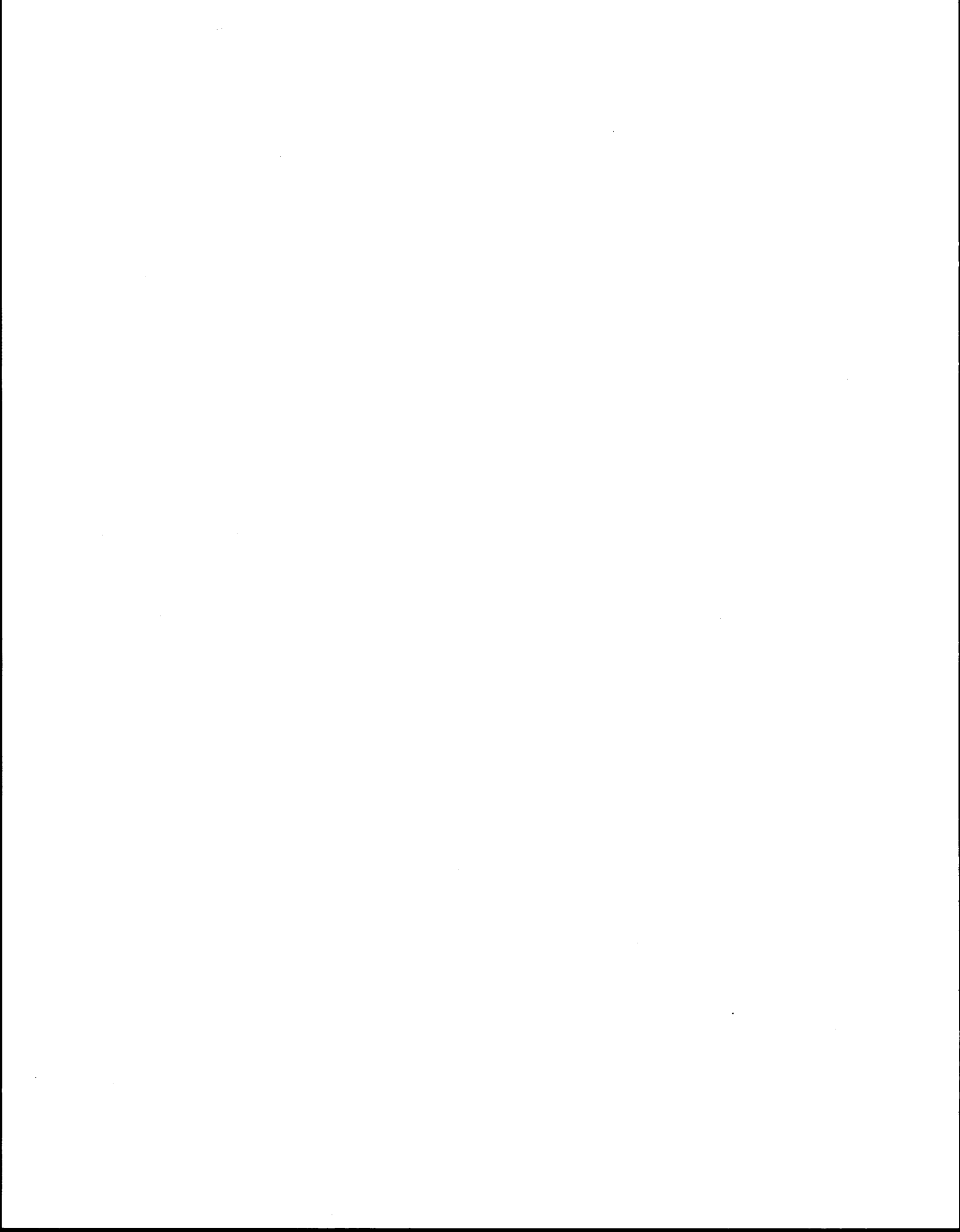
OCS COORDINATION OFFICE  
 University of Alaska  
 ESTIMATE OF FUNDS EXPENDED

DATE: December 31, 1975  
 CONTRACT NUMBER: 03-5-022-56  
 TASK ORDER NUMBER: 14  
 PRINCIPAL INVESTIGATOR: Dr. R. D. Muench

Period April 1 - December 31, 1975\* (9 mos)

|                  | <u>Total Budget</u> | <u>Expended</u>  | <u>Remaining</u> |
|------------------|---------------------|------------------|------------------|
| Salaries & Wages | 43,724.00           | 17,531.09        | 26,192.91        |
| Staff Benefits   | 7,399.00            | 2,956.75         | 4,442.25         |
| Equipment        | 2,500.00            | 2,510.00         | (10.00)          |
| Travel           | 5,774.00            | 1,164.50         | 4,609.50         |
| Other            | <u>7,400.00</u>     | <u>1,381.20</u>  | <u>6,018.80</u>  |
| Total Direct     | 66,797.00           | 25,543.54        | 41,253.46        |
| Indirect         | <u>25,009.00</u>    | <u>10,027.78</u> | <u>14,981.22</u> |
| Task Order Total | <u>91,806.00</u>    | <u>35,571.32</u> | <u>56,234.68</u> |

\* Preliminary cost data, not yet fully processed.





TRANSPORT OF POLLUTANTS IN THE VICINITY OF  
PRUDHOE BAY, ALASKA

ANNUAL REPORT TO BLM/NOAA  
OUTER CONTINENTAL SHELF PROJECT  
June 1975 - March 1976

R.U.# 335

Richard J. Callaway  
Principal Investigator

Chester Koblinsky  
Co-Investigator

MARINE & FRESHWATER ECOLOGY BRANCH  
Corvallis Environmental Research Laboratory  
Environmental Protection Agency  
200 SW 35th St.  
Corvallis, Oregon

Conducted with NOAA funding under Interagency Agreement R-50813 and  
R-60813

## FOREWORD

This annual report presents work performed from late June 1975 through March 1976. A good deal of effort was expended in the Summer of 1975 readying for a field trip scheduled to deploy instruments offshore of the Prudhoe area for the purpose of obtaining verification data for the models discussed in this report. Because the ice gods were unwilling, the field trip aborted and time was lost as a result.

The material presented in this report is based on an incomplete number of computer runs and on the authors' past experience with near-shore circulation and pollution problems. It is hoped to clarify some sections in the next few weeks. In particular, a section on the model itself and the boundary conditions imposed will be added. There are enough descriptive material and literature references for the initiated to understand the model setup, its assumption, limitations, etc. Suffice it to say that a time-varying solution of the equations of motion and continuity was employed. Terms included were local acceleration, Coriolis force, pressure gradient, and bottom stress as a quadratic term. Bottom topography was input on the grid matrix, convective acceleration was not included, although runs will be made later with it. Wind, tide, and runoff were input as boundary conditions. An explicit solution was employed requiring a rather short-time step to maintain stability.

## I. SUMMARY OF OBJECTIVES, CONCLUSIONS, AND IMPLICATIONS WITH RESPECT TO OCS OIL AND GAS DEVELOPMENT

It should be noted that the discussion which follows applies only to open water conditions. No attempt has been made here to determine the effects of shorefast or pack ice conditions on the environment studied.

A set of computer runs has been made on a section of the Arctic Coast centered about Prudhoe Bay. Large scale model simulations were reproduced in two fine-grid models interior of the larger area: Prudhoe Bay and Simpson Lagoon. Limited verification of the large-scale model was planned but not completed because of the 1975 ice year. Some verification is possible, however, based on past oceanographic studies offshore and in the vicinity of the Colville River and Simpson Lagoon. Tide records collected during 1975 inside Thetis and Stockton Islands provide the basis for tidal amplitudes used as input to the models. Additional required input data (bottom topography, winds, runoff) were obtained from USGS, NOS and other sources.

The objectives of the study are to determine flushing rates, retention times and pollutant transport in the vicinity of Prudhoe Bay. For this purpose, a single-layer model of circulation was applied in order to compute tidal elevations and surface currents. Inferences were made from the computer output as to probable transport rates and pollutant dispersion. Not all combinations of driving forces have been run as yet, i.e., variation of tidal amplitude and direction, wind velocity and runoff. Nor have the multi-layer aspects of the model been explored as much as they should be.

The objectives of the study relate to potential drilling operations in a limited section of the Arctic Coast. Additional inferences can be made as to the influence of marine operations on the environment and vice versa. Computed currents under high onshore and offshore winds in Simpson Lagoon might provide guidance to operators of

oil rigs in the lagoon. As an example, 26-knot winds in the Simpson Lagoon model result in computed currents of about 1 knot in the central channel for either onshore or offshore wind. Offshore-generated storm surge currents would result in large pressure differences and accelerated currents. A tool is available, however, to provide engineers with rather good estimates of the action of steady winds on this particular setting. Variable wind input is also possible; this would result in more rapid current fluctuations and pollutant dispersion by the increased lateral spread of material.

Simulation of tide-only, tide-plus-runoff, and tide-plus-onshore and offshore winds were made for Prudhoe Bay. Very complex circulation patterns appeared which are related to bottom topography. The inferred flushing rate in the Bay is felt to be rather inefficient for either an onshore or offshore wind. The Arco Wharf influence on circulation appears to be substantial. The Wharf has since been extended and, presumably, further modifies the circulation. A permanent counter current develops on the eastern shore of the Bay which can reintroduce material into the Bay even during an offshore wind. The features exhibited in the Prudhoe Bay model appear reasonable but should be checked by further model runs with different boundary conditions and, when possible, by field verification. The implications to oil and gas development in the Bay are that currents on the order of 1-2 knots may be present when steady winds of 20 knots exist. Higher onshore currents may exist during surge conditions; bottom topography may be exposed during offshore surge response. Substantial accumulation of continuous source pollutants is most probable in the Bay regardless of wind direction but is more likely for an onshore wind. Instantaneous releases will have retention times of varying lengths dependent on the wind set and initial position of the release. Introduction of wharves in the bay similar in extent to the present Arco wharf could modify the Bay circulation extensively. The modification may not necessarily be adverse and could accelerate flushing. The extent of such a modification can be estimated by use of the model.

Press time and plot constraints permitted only two runs of the large, offshore model (Oliktok Point to Challenger Entrance). The input tides exhibited a rotary clockwise tide current to be expected in the land of the large Coriolis force. This current was very weak, however, and masked by a weak (10-knot) onshore wind.

During no-wind conditions, the offshore islands (Midway, Cross, McClure, and Stockton) modify downstream circulation to some extent. Regular patterns, such as von Kármán vortices, were not present but it is expected that the islands could induce considerable lateral spread of pollutants. Wind, however, seemed to smooth out the irregular downstream currents. For these conditions, winds would increase vertical mixing and downwind transport, the opposite effect of the no-wind run.

Offshore current speeds were generally less than 0.1 knots for no-wind. For the 10-knot wind case, speeds were on the order of up to 0.3 knots. It is anticipated that similar current directions will prevail as the model input wind speed is increased and that offshore current speeds will be about 2-3% of the wind speed. In the deeper waters, this is a considerable current especially if exerted throughout the water column. The single layer model constrains the wind (boundary condition) to act as a body force throughout the water column. Increased speeds can be anticipated if the force acts on a shallow surface layer only.

Subsurface currents may be smaller and in opposite directions to the surface current, contributing to shearing stresses on fixed platforms. Only a few multi-layer runs have been made to date, however, and the magnitude of these possible effects is unknown.

Wind setup in the nearshore region of the large-scale model drives the circulation there. River runoff may be blocked by wind setup for periods of time resulting in large outflows when setup is relaxed.

Pollutants discharged to rivers would also accumulate during these periods; pulsed releases could penetrate rather far offshore or into the lagoons with wind reversal to an offshore direction.

Pollutants released in the nearshore region will generally remain nearshore and be transported along the coast. This region is, of course, the habitat and feeding ground of migrating birds. Arctic cod and other fish penetrate the river mouths and reside in coastal areas and would be subject to stress. Releases will also affect the resident plankton and benthic organism community with resultant effects on up the food chain.

## II. INTRODUCTION

### A. General Nature and Scope of Study

This report discusses aspects of the Prudhoe Bay Pollutant Transport project which is part of the BLM/NOAA outer continental shelf program. It summarizes progress from June 1975 through March 1976. It was preceded by a semi-annual report (Callaway and Koblinsky, 1975).

The general nature and scope of the study derives from the NOAA statement on Task B-4: "Test and evaluate potentially applicable circulation models for special areas such as those that are environmentally sensitive or of restricted circulation, such as fiords, to compare predicted oil spill trajectories and concentrations with those inferred from field experiments carried out in these areas."

We have relied on an existing numerical model of circulation and make no claims to furthering the development of theory or numerical techniques. The model is based on earlier versions developed by Professor Walter Hansen at the University of Hamburg (see, e.g., Hansen, 1962, 1966). These are usually referred to as hydrodynamical-numerical (HN) models. Subsequently, Laevastu (1974, e.g.) applied the model to many areas, further testing its applicability to pollution problems. The version used here is an optimization of Hansen's and Laevastu's efforts (Bauer, 1974). It retains most of the schematization features and uses the same difference formulations and integration techniques of the earlier works.

Other models, such as Leendertse's (1967), could have been employed but were not because of availability of the Hansen model, its compatibility with our computer facilities and our experience with it.

## B. Specific Objectives

We are interested in determining the movement of pollutants-- along a section of the Arctic Coast, especially in the Prudhoe Bay area. Under a variety of simulated environmental conditions, such as prevailing summertime winds and average river runoff, it is desired to be able to predict the most likely path of an instantaneous or continuous release of a given pollutant and flushing or retention times of the pollutants in prescribed areas. Scenarios can be accumulated which will provide managers with information as to what is likely to be encountered during and before drilling operations for a wide variety of environmental combinations. They may then be able to plan for emergency conditions or make judgments on the risks involved in a given drilling situation. Of equal importance is use of model output to interpret oceanographic field data and to plan for oceanographic expeditions.

We can use past modeling and field experience to determine whether model forecasts are "reasonable", even though verification data are lacking. Unreasonable or unanticipated results (usually associated with nonlinear model terms) may prove the most interesting to the scientist and of the most use to the manager.

## C. Relevance to Problems of Petroleum Development

A recent article in Science by Carter (1976) summarizes progress and problems associated with Canadian oil operations in the Beaufort Sea which are pertinent to U.S. efforts. Biodegradation of oil in the Arctic will be slow, as is well known. Storm surges could carry oil inshore and pollute embayments, lagoons, lakes and the beaches along the Arctic Coast. The work reported here has as its main objective the assessment of storm surge and wind-driven transport of poten-



tially oil-laden waters in the nearshore environment. Rather short term predictions are envisioned, although longer term predictions could be made, computer funds permitting.

### III. CURRENT STATE OF KNOWLEDGE

Only a brief summary of existing knowledge is presented here because of time requirements. The data discussed are incomplete but pertinent to an understanding of the results. Some of the discussion in Section V could also apply to this section. The extensive Canadian work on modeling in the Canadian Beaufort has only recently been received and is not included here.

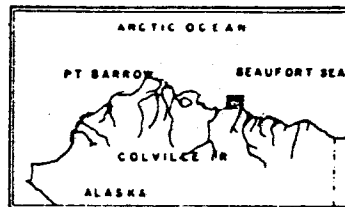
Year round oceanographic studies in the nearshore region have not been conducted for the simple fact that it is ice-covered most of the year. Some studies have been conducted during the ice-free season. Further complications arise because of the shallow shelf waters. There is an understandable reluctance to navigate oceanographic vessels in these waters. Most U.S. Coast Guard vessels are deep draft and do not ordinarily move inside the 5-fathom line. The Barrier Islands lie inside this depth so that only limited small boat activities have taken place.

An intensive nearshore study was performed in the Colville River System (Alexander et al., 1975). An investigation on Simpson lagoon currents was reported by Dygas in that report. Figure *A* shows wind and current roses for July - September 1972. The winds are taken from records at Oliktok Point; the current meter station is shown between the Point and Spy Island. Depths are in feet. Dygas found that about half the current velocity variation is due to winds, the remainder due to tidal motions and waves. Surface currents tend to flow towards the west for easterly winds and v.v. The meteorological tide wave is generally greater than the astronomical range. The barrier islands damp out Beaufort Sea swell inside the lagoons. Dygas concludes that weather patterns along the Beaufort Sea most significantly affect coastal wave and current patterns.

SIMPSON LAGOON COAST

PHYSICAL OCEANOGRAPHIC  
STUDY AREA

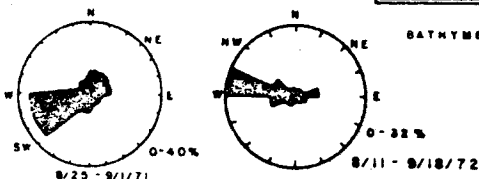
NAUTICAL MILES  
0 1 2 3 4



OLIKTOK POINT  
WIND ROSE 1972



CURRENT ROSE



BATHYMETRIC CONTOUR INTERVAL  
EQUALS TWO FEET

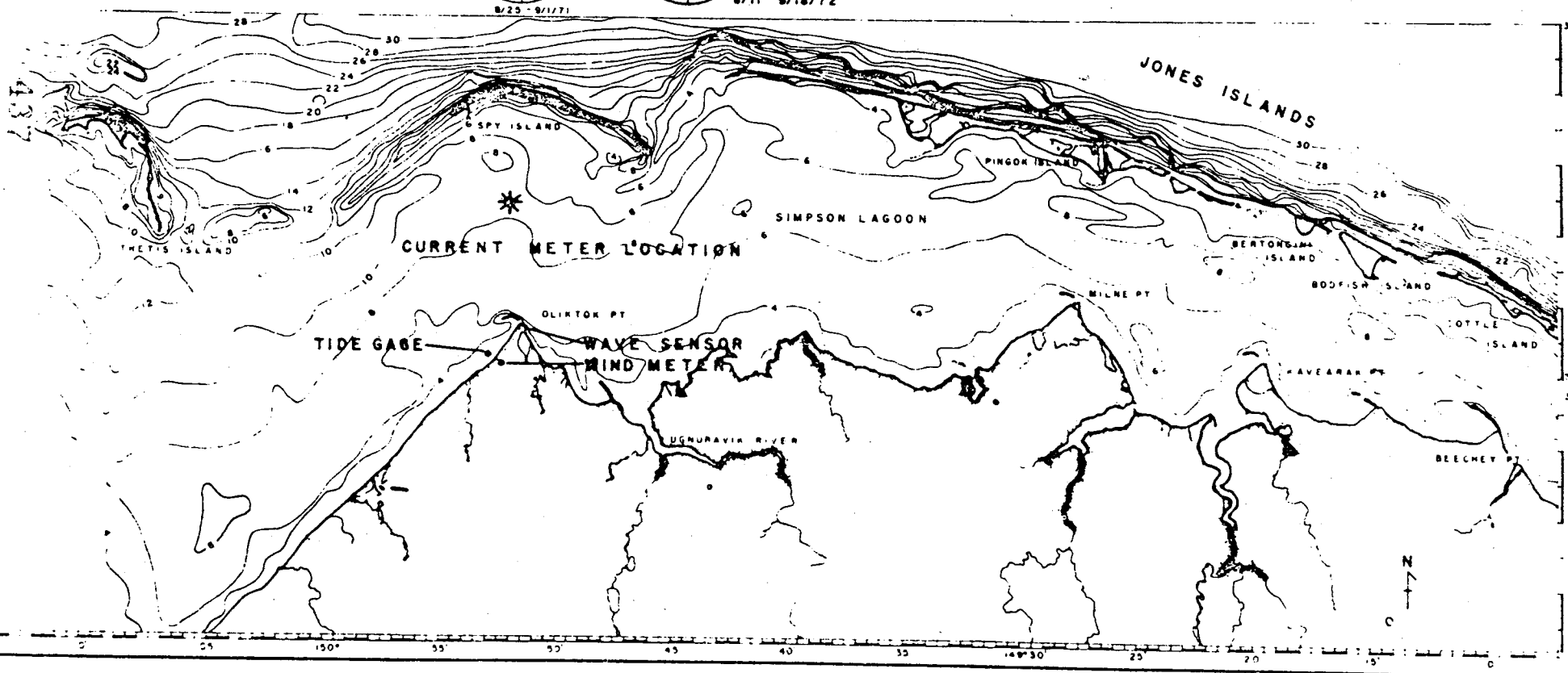


FIG. 0 - UNIVERSITY OF ALASKA STUDY  
AREA. SIMPSON LAGOON.  
From Dygas (1975)

Mountain (1974) summarized conditions on the North Alaskan Shelf. He found two primary modes of circulation: an eastward motion associated with the warm water masses from the Bering Sea and a westward motion associated with an upwelling regime. The latter scheme was based on findings by Hufford (1974). The eastward flow is sometimes far offshore, e.g. about 45n.m. at 150°W. Upwelling is observed only on the eastern portion of the shelf in response to strong easterly winds. In the regions that we have modeled, northeasterly (onshore) winds were modeled as well as offshore (southwesterly) winds. Only the single layer model was used; simulation of an upwelling velocity is not possible, although the Coriolis effect is present, driving currents to the right of the wind.

Wiseman et al. (1973) summarized nearshore currents and physical oceanography in the vicinity of Pingok Island on Simpson Lagoon. They also found that atmospheric processes were dominant. Wind-driven currents cause set up and set down at the shoreline resulting in sea level variations much greater than astronomical tidal contributions. The meteorological tides strongly affect nearshore water mass properties, at least near inlets. They emphasize the dominance of storm-induced modification of the nearshore region and suggest that short-time, fair-weather studies may be misleading.

## VI. STUDY AREA

The study area extends from east of the Colville River to Challenge entrance, which is between Stockton and Maguire Islands. Within this system, modeled by an 18X61 grid schematization with grid length of 2 km, two smaller systems are modeled: Simpson Lagoon (18X42, grid length 0.5 km) and Prudhoe Bay (17X39, grid length 0.5 km).

Offshore extent of the large-scale model is about 25 km (13.5 nm). The Simpson Lagoon model is open on the east and west. Spy Island and the Colville River delta are not included. The Prudhoe Bay model extends offshore seaward of Gull Island and westward to include the newly constructed Arco Wharf.

## V. SOURCES, METHODS, AND RATIONALE OF DATA COLLECTION

Numerical integration of the depth-averaged equations of motion and continuity over a given time step results in computation of the  $u$  and  $v$  components of velocity and the deviation of the surface elevation from a datum level. Manipulation of these data over given time periods can provide net currents, progressive vector diagrams, mass transport, etc. The input requirements to operate the model are straightforward but the data available on the Arctic coast are somewhat sparse. We have used whatever was available and believe that we can represent the systems modeled fairly well.

Required are data on bottom topography, river runoff, wind speeds and directions, and tidal amplitudes and phases along the coast. Driving forces are tides, winds, and runoff. Bottom friction and wind drag are represented by quadratic laws. Details on aspects of the above will be discussed later; here we present a discussion of the data sources available and the conversion of the data to model input. Fig. 1 shows the location of tide, river and weather stations used in the study.

### Bottom topography:

The model uses the actual bottom topography schematized so that the mean water level at a computational point is the same as it is in the real setting. Values for depths at mean low water are obtained from either the original hydrographic surveys of the area or from the latest navigation chart. Both of these items are obtained from the National Ocean Survey. We obtained the original hydrographic surveys for the region between Cape Halkett and Barter Island, and copies of the charts concerning the region from Pt. Barrow to Demarcation Point.

The mean water depths for points in the computation grid are obtained by placing a grid work of the appropriate scale on top of the relevant hydrographic survey or nautical chart and picking off the depth at the points in the grid where the velocities will be computed. These depths are then adjusted to the mean water level. In most instances

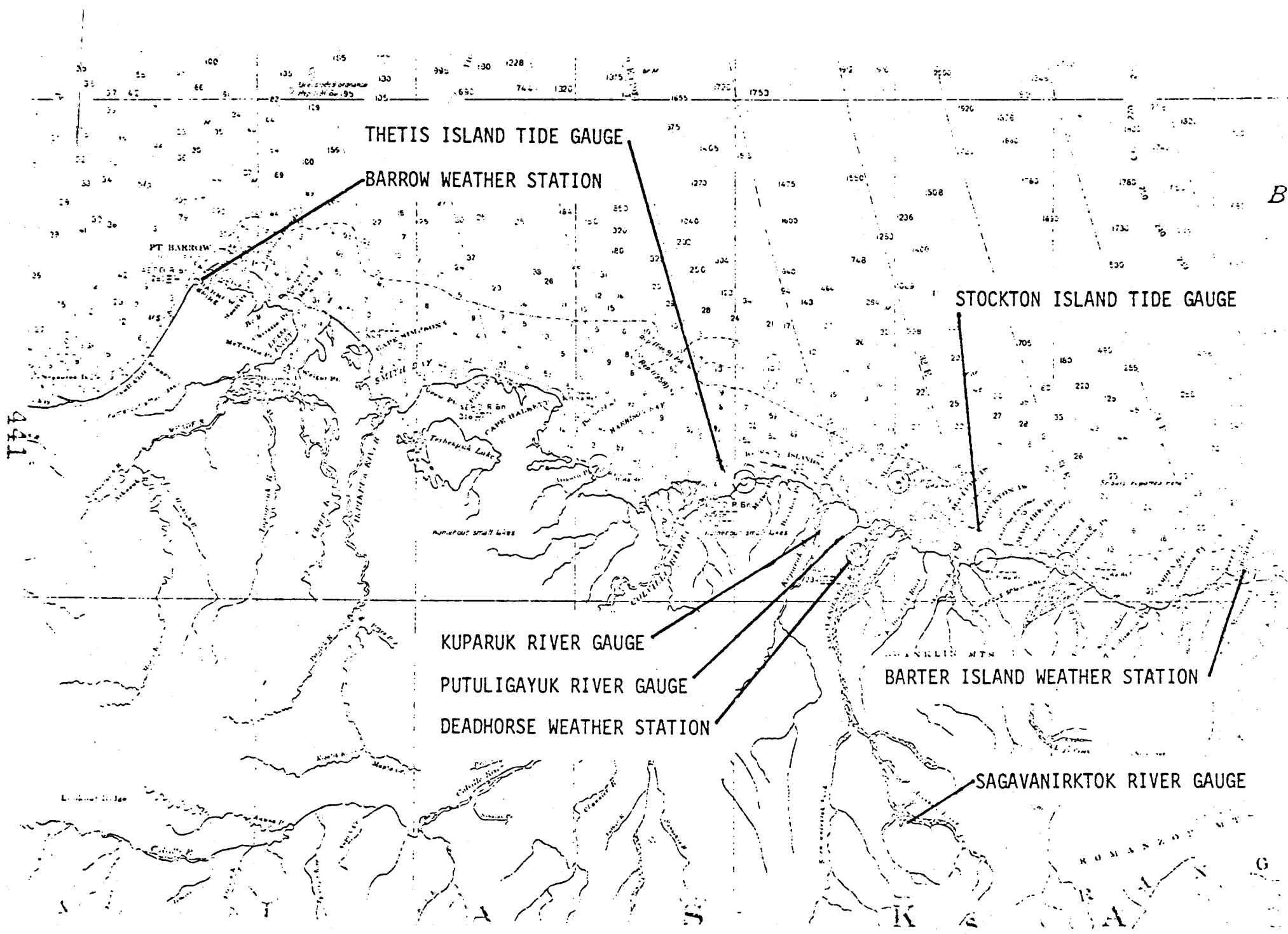


FIG. 1 - TIDE, RIVER, AND WEATHER STATIONS

RIVER FLOW DATA 1974

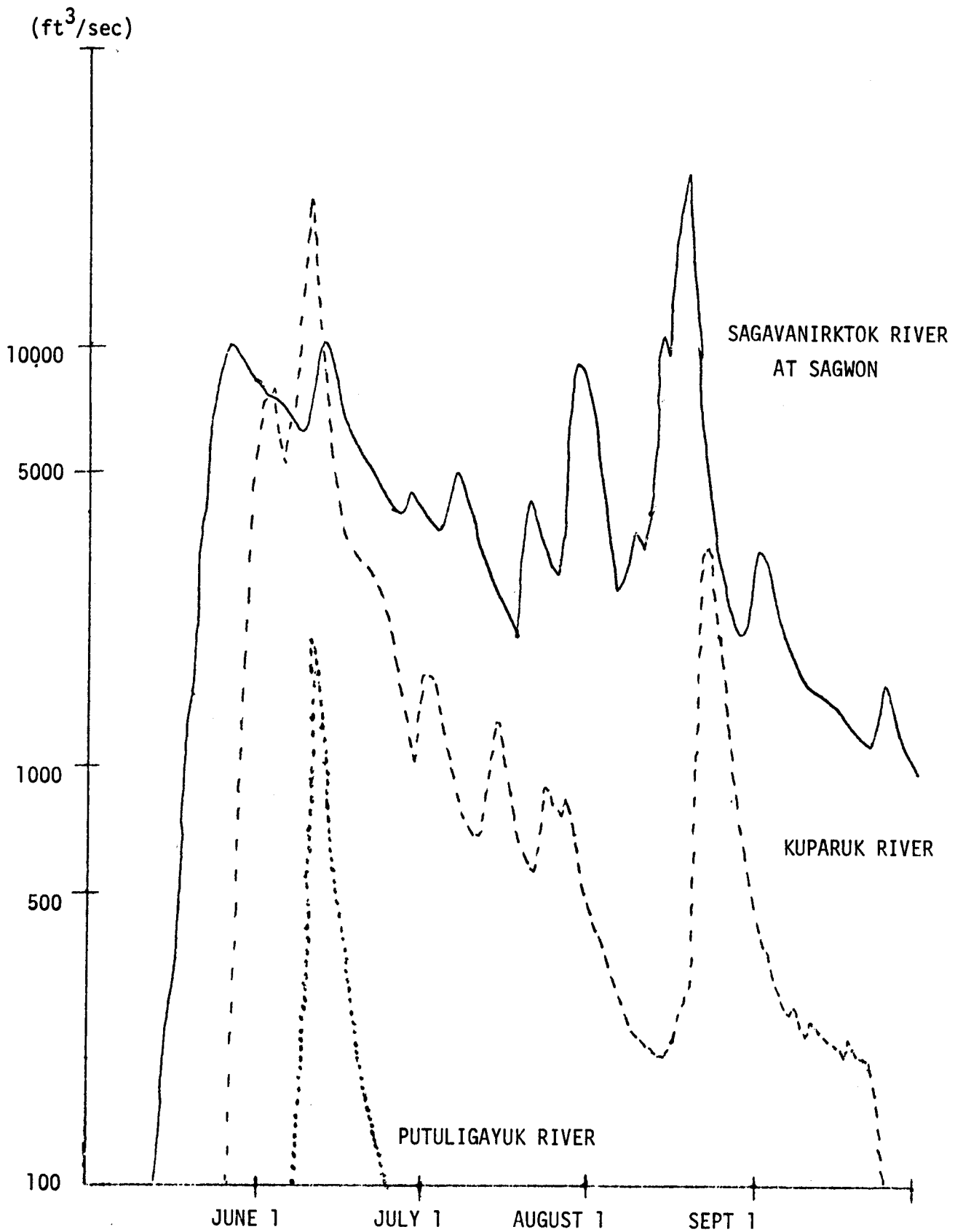


FIGURE 2. River flow data, 1974 for the Put, Kup and Sag Rivers



features with characteristic horizontal dimensions less than that of the grid are removed. Checking of the grid schematization is performed by constructing a perspective or isometric plot of the data obtained from the charts.

#### River Flow:

Only a few of the rivers in the Arctic watershed are gauged. The only streams relevant to this project which are gauged continuously by the U.S.G.S. are the Kuparuk, Sagavanirktok and Putuligayuk. Figure 2 shows the data for the 1974 summer. Some data for the discharge of the Colville River taken by Dr. H. Walker of Louisiana State University during the early 1960's has also been made available to us.

Using these given discharge rates and approximating the cross-sectional area of the rivers at their mouths from the original hydrographic surveys and nautical charts, we have found that the velocities parallel to the stream bed are all less than 5 cm/sec, after the ice breakup in June.

#### Wind Data:

We obtained meteorological data in the form of standard 3-hourly observations from the National Climatic Center for stations at Nome, Barrow, and Barter Island. Data from the Deadhorse station are hourly, and some data also exist for a station at Prudhoe Bay. A plot of the station pressure at Barrow, Deadhorse and Barter Island for August 1975 is shown in Figure 3. A significant drop in pressure is found in all three stations around August 26. This was accompanied by increases in wind speed up to 45 kt. A positive surge followed these conditions (Canadian Beaufort Sea Reports).

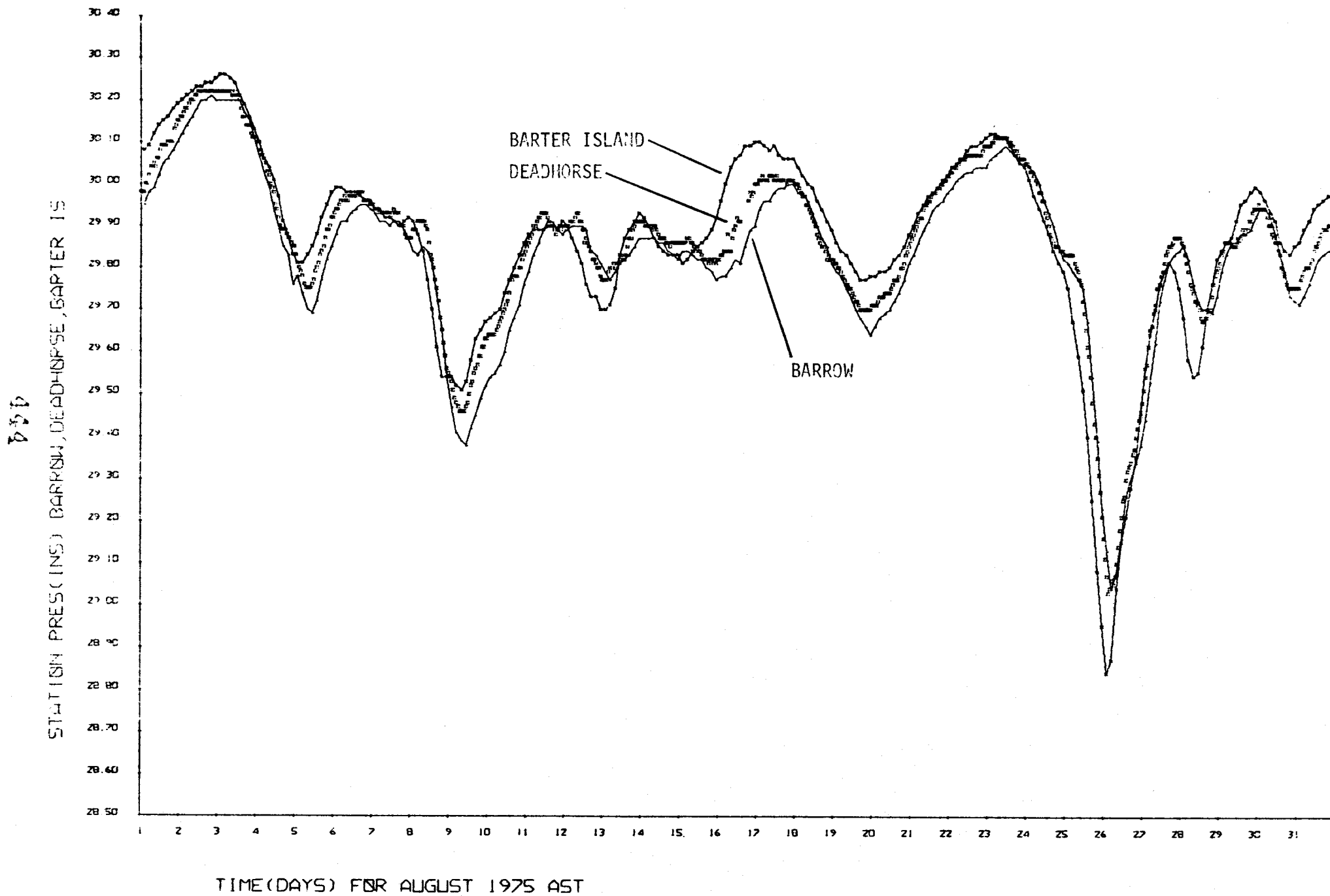


FIGURE 3. Barometric pressure at Barter Island, Deadhorse and Barrow, August, 1975

### Vertical Distribution of Properties:

The three-layer version of the model permits representation of the vertical density structure as an upper well-mixed layer, a transition zone, and a bottom layer. The upper and bottom layers can be closely approximated by single densities; the transition zone is also represented by a single density value, but is an average over the continuously increasing density in the zone. In this discussion, however, we restricted ourselves to the single-layer approximation. Two-layer models have been run but our main effort has been with the single-layer model.

Some of the past data collected in the region we are modeling has been sent to us by the National Ocean Survey. This includes all hydrographic data prior to 1972. This data is from Nansen bottle casts and does not show the continuous profile one would have from an STD. The data shows that in the deeper waters a layered structure is sometimes found with a light density water (1.015-1.020) in the upper 10 meter or less and the lower layer fairly homogeneous at around 1.025. In the shallow waters Schell (Alexander et al., op cit.) shows data for Simpson Lagoon which indicates less saline water riding on a colder and more salty layer of water. Dygas (personal communication) has indicated that with sufficient wind the layered structure disappears and becomes homogenous.

### Tides:

Although tidal amplitudes are small in comparison with other oceans, tidal forces are present and must be accounted for. Unfortunately, very little is known about the tides or their progression along the coast. Because of this, we have made some assumptions on direction and phase.

Two Bass Engineering optical lever tide recorders were installed inside Thetis and Stockton Islands. These were prepared in Barrow at the Naval Arctic Research Laboratory and installed from a float plane on August 7, 1975. They were recovered on August 29.

The recorders were mounted on tripods, fitted with a 50 pound weight, and lowered to the bottom with polypropylene rope. A 14" diameter Viny buoy was used as a marker. Table 1 gives statistics on the recorders.

The data records from the experiment and calibrations were sent to the OSU\*computer center for digitization. This project has recently been completed and the data continues to be analyzed. The data handling scheme for the tidal records is diagrammed in Figure 4.

Post experiment calibration was carried out at both room temperature water and water near the freezing point. The mean calibration constants for both showed no statistically-significant change from the pre-field experiment calibration; however, the signal to noise ratio had decreased.

Both records have several gaps of varying size as can be seen in Figure 5. One method of filling the gap is to do Fourier analysis of the records before and after the gap, if they are long enough. Using the major components of each of these records Fourier series are generated in each direction across the gap. The figure shows the comparison of patching the data using the above method and sparse real data within the gaps. The patched records and real data do not match well, indicating a strong meteorological effect upon the sea level changes.

Due to the shortness of the obtained records, intercomparison between the two gauges can be made in only a few places. These comparisons show no significant difference in phase, justifying a tide normal to the coast.

\*Oregon State University, Corvallis, Oregon.

TABLE 1  
Tide Recorder Data, Beaufort Sea, 1975

| Inst.# | Location   | Date<br>Installed | Time<br>(AST) | Date<br>Recovered | Time<br>(AST) | Lat. °N  | Long °W | Depth  | Remarks   |
|--------|------------|-------------------|---------------|-------------------|---------------|----------|---------|--------|---|
| 117    | Stockton I | Aug 7, 1975       | 1414          | Aug 29, 1975      | 1222          | 70°17.5' | 147°01' | 10 ft. |   |
| 121    | Thetis I   | Aug 7, 1975       | 1520          | Aug 29, 1975      | 1114          | 70°33'   | 150°10' | 8 ft.  | Possibly sub-merged in mud.<br>Damage to rear pedestal leg. |

447-15-

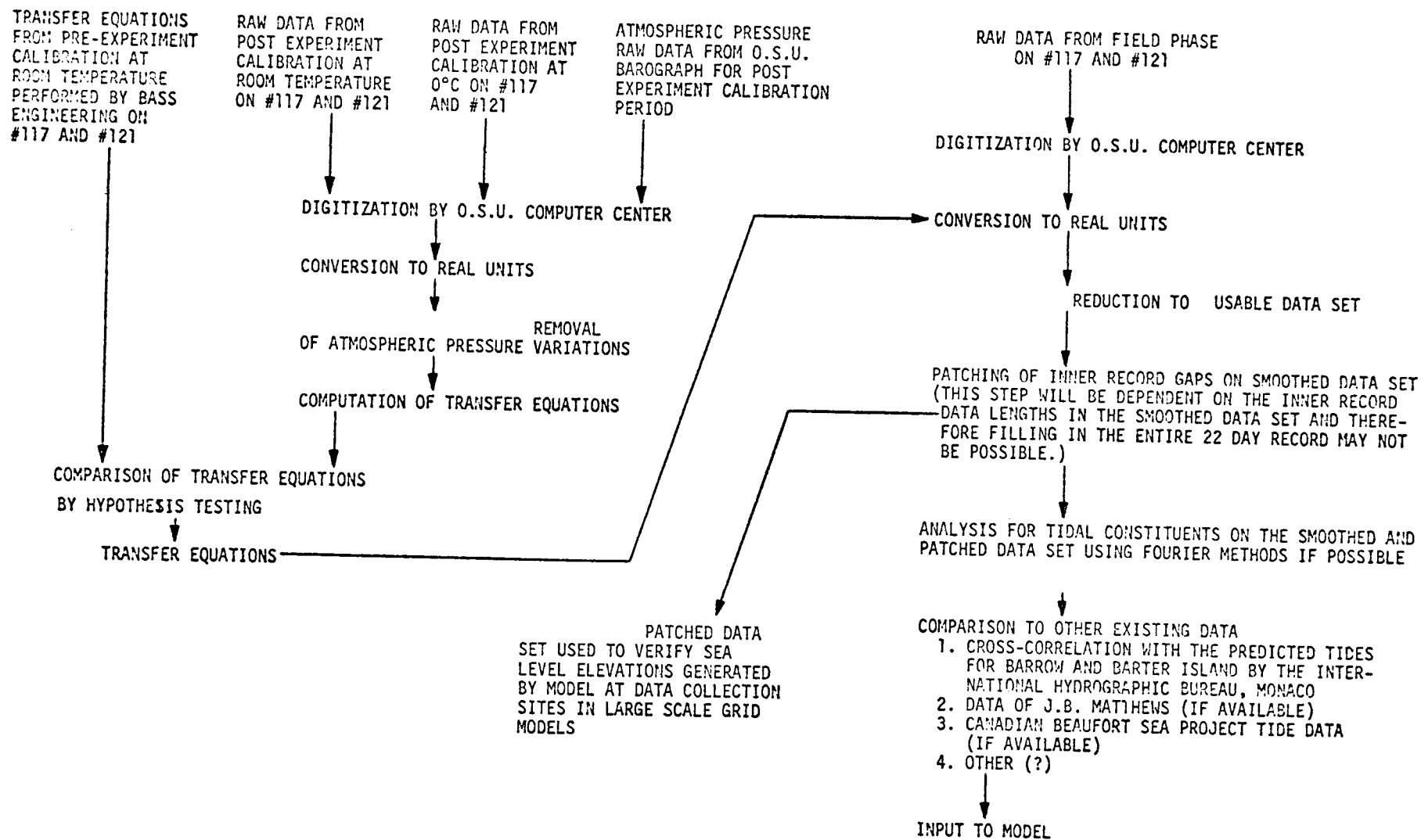
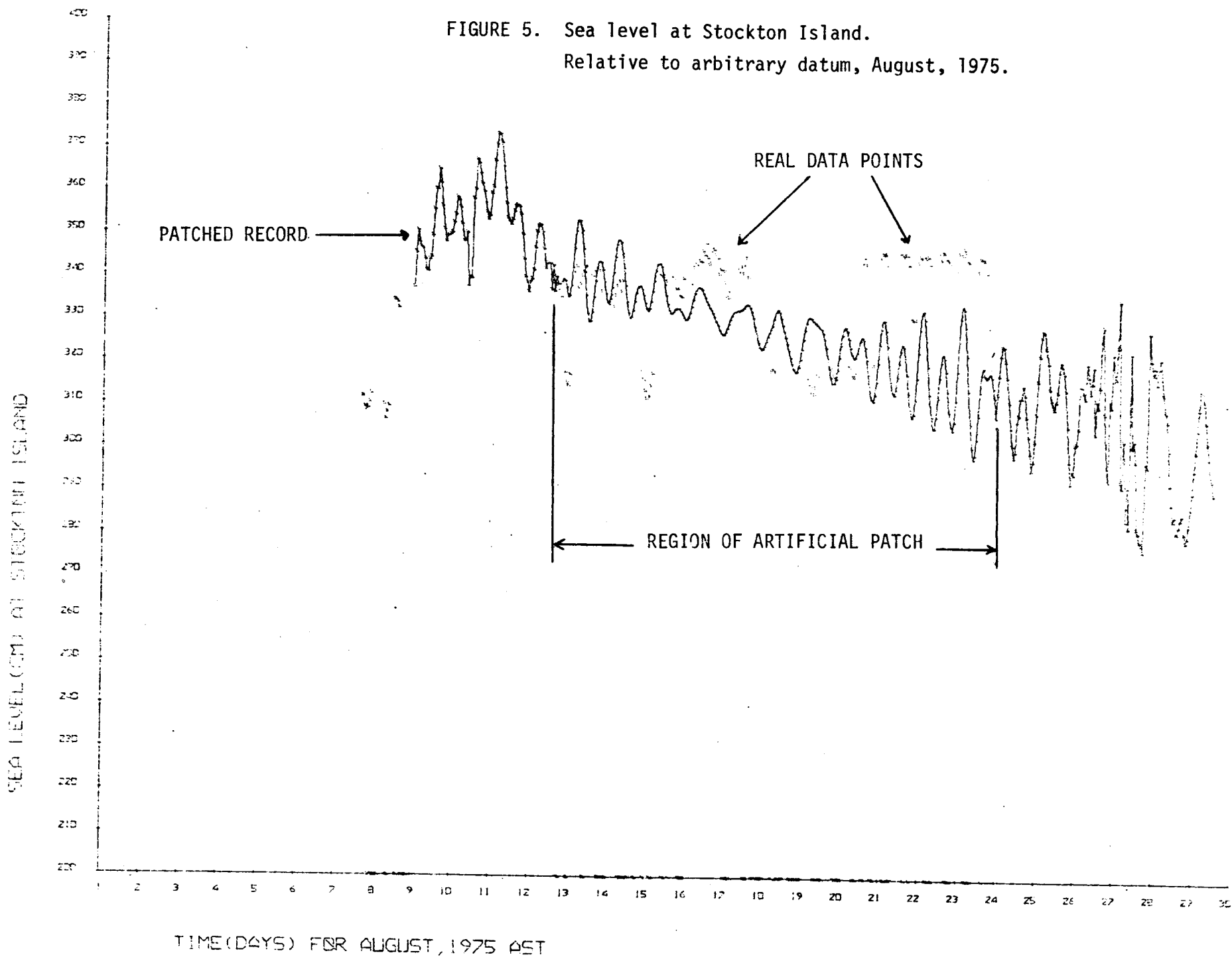


FIGURE 4 DATA PROCESSING PROCEDURES FOR SEA LEVEL DATA OBTAINED AUGUST, 1975.

FIGURE 5. Sea level at Stockton Island.  
Relative to arbitrary datum, August, 1975.



## Winds:

Wind stress on the surface probably contributes to at least half the motion in the nearshore zone. There is a fairly good body of information on wind from the DEW line station; however these data are not necessarily representative of lagoon winds. For the most part we have used as input prevailing winds as determined by Dygas (1975).

## Thermohaline Circulation:

Obviously, we cannot simulate density currents in a single layer barotropic model. Where known permanent or periodic currents exist, however, these currents can be accounted for by artificially sloping the model sea surface. For instance, if the tidal amplitudes are equal and there is no phase difference along an open boundary, the heights,  $h(t)$ , can be formulated as

$$h(t) = a_0 + \sum_{i=1}^n b_i \cos \sigma_i t$$

where  $a_0$  is the mean elevation (usually = 0) and  $b_i, \sigma_i$  are amplitudes and speeds, respectively, of the principal tidal components. If a permanent current enters that boundary with a representative speed, the slope of the sea surface can be approximated from the geostrophic equation. The  $a_0$  term in each grid can then be adjusted; the  $h(t)$  will oscillate about this sloping sea surface. These are model options; they will be utilized as the information on permanent currents becomes available or in future numerical experiments.



## VI. RESULTS

### Methods of Presentation:

One large scale and two small scale model results are presented. The large scale model (Oliktok Point to Challenge Entrance) encompasses the smaller scale models, Simpson Lagoon and Prudhoe Bay. The large scale model exhibits features that should be present in the smaller models if they are simulating their environments in a compatible manner.

Hourly output is shown in the plots in appendices A-F; sea level and currents in the Oliktok Point (OP) model are discussed first. Results for 6 hour intervals (1-6, 6-12, 12-18 hours) are summarized by pointing out time changes and permanent features. Differences between model runs, e.g., between wind and no wind cases, are also discussed. Input parameters for each run precede the output plots in the appendices. These show grid size, time step, output interval, etc.

For sea level plots, arrows pointing up are elevations above datum and down arrows are below datum.

OLIKTOK POINT TO CHALLENGE ENTRANCE WITH RIVER FLOW - NO WIND  
(See Appendix A)

Hours 1-6

Sea Level

By hour 2, tides have propagated through all grids. Smaller depressions are noted inside Simpson Lagoon and in the river entrances. At hour six larger amplitudes are present nearshore and there is a larger null zone (no arrows) east of the eastern most branch of the Sagavanirktok (Sag) River.

Currents

Currents in the outer shelf rotate in a clockwise direction from a north and east set to an onshore component with time. Seaward flow is seen in all river branches. Divergent flow is present in Simpson Lagoon, flow leaving at both entrances. Currents in Prudhoe Bay are very sluggish as indicated by the absence of arrows. At the beginning of flood (hour 6) flow enters Simpson Lagoon from both ends.

Hours 6-12

Sea Level

Elevations in Simpson Lagoon are out of phase with the specified heights on the outer boundary indicating an appropriate blocking action by the barrier islands and NS phase lag. Amplitudes in the Kup River are depressed because of the opposing river flow. East-west offshore amplitudes appear to be about the same in the upper half of the model.

Currents

Opposing currents are present in Simpson Lagoon indicating a convergence zone which migrates eastward with time. Prudhoe Bay currents zero or sluggish; some indication of counterclockwise flow. Variable current direction east of the Kup River. Southeasterly currents turn

clockwise to an offshore component. All current speeds very low, with a no current zone (no arrows) north of the Jones Island chain.

#### Hours 12-18

##### Sea Level

Depression of elevation is less in Simpson Lagoon than offshore with a lag of less than an hour indicated. Blocking action of river flow is apparent in the Kup and Sag deltas.

##### Currents

The null zone north of Jones Island persists, being replaced by eastward setting currents with time. River flow initially landward is reversed. Simpson Lagoon empties at both ends until hour 17 when westward flow predominates. Prudhoe Bay empties in a clockwise direction. Currents east of the Sag River Delta again alternate hourly. Currents rotate cyclically about the offshore islands as does the flow seaward of the islands.

OLIKTOK POINT TO CHALLENGE ENTRANCE WITH RIVER FLOW  
AND 10 KNOT WIND FROM NE

(See Appendix B)

Hours 1-6

Sea Level

Wind setup already present nearshore except in Simpson Lagoon. Persists to hour 2 in Prudhoe Bay. Amplitudes in Simpson Lagoon open water amplitudes by under one hour. Sag and Kup Rivers oppose sea level depressions.

Currents

Weak offshore tidal currents are opposed by wind and turn earlier through the tide-only runs. Currents in Simpson Lagoon directed west. Variable currents in Prudhoe Bay, eastern counter current shows; cyclonic gyre forms. Flow directed up river. Westerly set in central part of system. Currents east of Kup River more regular than no-wind case. Lagoon shore currents predominately westerly.

Hours 6-12

Sea Level

Surface elevation above datum for all grids except Simpson Lagoon, hours 6-7. Offshore amplitudes lead onshore because of speed of lagoon wave propagation. Offshore EW amplitudes about the same.

Currents

Wind and tidal flow both landward. Simpson Lagoon flow westerly except for opposing flow, hours 2-4, near the west opening. Prudhoe Bay counter current persists, cyclonic flow evident. Westerly long shore currents east of Kup River and Tigvariak Island. Uniform westerly flow offshore except in vicinity of Islands.

## Hours 12-18

### Sea Level

Delta flows result in a difference in elevation about datum in the river deltas and Prudhoe Bay, hours 12-14. Simpson Lagoon lag still apparent. Embayment east of Tigvariak Island shows effect of Stockton Island and surrounding topography.

### Current

Simpson Lagoon flow westerly. River flows reversed. Prudhoe Bay cyclonic motion and counter current prevail. Cells form in the south-west corners of embayments east of the Kup River and Tigvariak Island. Uniform westerly offshore currents except near islands.

PRUDHOE BAY. COMPARISON OF TIDE-ONLY CASE WITH TIDE PLUS RIVER FLOW  
(See Appendix C)

Hours 1-6

Sea Level

Output begins at hour 1 (3600 sec) or 1 hour after slack preceding ebb tide. Sea level falls uniformly over the Bay, there being little phase lag from the open boundary to the south shore.

Currents

Ebb currents exist east of Arco Wharf (AW); velocities attain about 1 knot out of the Putuligayuk (Put) River (no input flow, however). West of AW, the currents are slight and variable.

Hours 6-12

Sea Level

Flood tide, 6 hours duration. Tides in phase over the entire Bay except near the Put River entrance where amplitude is somewhat depressed.

Currents

East of AW, small velocity-increasing currents are present initially with some oppositely-directed flow from the Put River. Dead space (no arrows = 0 current) shown in the east lower Bay progressively fills with current to hour 8 then a large dead space is shown on the eastern border spreading across the Bay as the current shifts. West of AW, opposing currents are present until hour 10 (36000 sec). Sluggish circulation along south coast near Point McIntyre. Plots for tide and Put River flow show very little difference with tide-only case.

## Hours 12-18

### Sea Level

Ebb tide, slight depression of amplitude on the south boundary for both cases, otherwise elevations uniform over entire system.

### Currents

No real difference between both runs. Dead spot in southeast Bay fills in over hours 12-13, then opens again joining with a dead spot on the lower west bank. A null current forms east of AW enlarging from hours 13-15, then fills in. Opposing currents south of Stump Island form a large, divergent zone which gradually fills in as slack before flood approaches. Currents along the south and east coasts west of AW are usually weak and variable.

PRUDHOE BAY COMPARISON OF TIDE ONLY AND TIDE  
WITH 10 KNOT ONSHORE WIND

(See Appendix D)

Hours 1-6

Sea Level

Ebb tide. Differences are immediately apparent between the tide only (TO) run and the tide with wind (TW) run. Although the first 6 hours are considered stability-approaching computations, it is instructive to note the differences here. At hour 1 there is indicated a set-up along the south boundary for the TW case separated from the falling elevations by a zone of no change. From hours 2-6, there is a northward gradient of elevation depression, i.e., wind is opposing the falling tide. At hour 6 (slack) the lower Bay shows above datum elevations separated by a wide null zone from remnant ebb elevations.

Currents

In the main part of the Bay a cyclonic gyre can be seen to form and strengthen. Outflow along AW is indicated; outflow through the west boundary is also seen. There is a south-flowing counter current along the south coast east of the Put River.

Hours 6-12

Sea Level

Flood tide. Wind and tide in phase. Set-up can be seen from north to south, features not present in the TO run. Condition is fairly uniform in the east west direction.

Currents

The TO case showed incoming flow over most of the main Bay, with opposing currents west of AW. Large null current areas were also present. For the TW runs several gyres are present in the open Bay;



the eastern shore counter current is still present, as is the outflow along AW. Currents are weak and variable west of AW with a general westerly set.

#### Hours 12-18

#### Sea Level

Ebb cycle. Tide and wind opposed. Amplitudes were generally uniform for the T0 case. For the TW case the hours 1-6 runs are repeated somewhat except for hours 6 and 18 where the wind effect is less noticeable at hour 18.

#### Currents

In the main Bay a single large gyre dominates the circulation. Gull Island (indicated by the single grid box between AW and Heald Point) and its surrounding topography seem to position the gyre. The eastern shore counter current and opposing south boundary currents are still present. Outflow along AW persists as does the mixed flow east of AW.

PRUDHOE BAY. COMPARISON OF TIDE-ONLY WITH TIDE  
PLUS 20 KNOT OFFSHORE WIND

(See Appendix E)

Hours 1-6

Sea Level

Ebb tide, offshore wind. For the T0 case, elevations were below datum at all grid points for the whole ebb cycle. For the TW runs, above normal elevations are present on the eastern part of the Bay and, initially, near Point McIntyre. A convergent zone (no arrows) migrates east with time (hours 1-5) then moves west as flood tide begins.

Currents

Spin-up time is rather rapid as indicated by only slight differences in the current vectors with time. A general counterclockwise circulation in the bay is indicated, with most of the outflow occurring along the northeast section. The eastern shore counter current is still present, being blocked by easterly flow along the southeast boundary. Convergent flow between Stump Island and Pt. McIntyre is shown; the presence of AW interrupts the general easterly flow.

Hours 6-12

Sea Level

Flood tide. Opposing wind. At slack tide, several null zones are present. At the beginning of flood (hour 7) elevations are greater in the east and along the south boundary south of Stump Island. Amplitudes are greater than for the T0 runs, set-up being maintained higher in the east currents. The same general current structure is present over this flood cycle. No discrete gyres are present but the counterclockwise circulation predominates. The eastern boundary counter current and converging southerly current is still present. Flow is clockwise around AW. Gull Island modifies the flow in the north.

## Hours 12-18

### Sea Level

Ebb tide. Wind enforcing. At hour 12 all elevations are above datum. The following hour several null zones are present with above datum levels dominant in the southeast. A NE-SW convergent zone again migrates to the SE, separating two distinct zones.

### Currents

The same general current structure prevails. It should be noted that the northward deflection of currents north of Heald Point is due to shallow bottom topography. As with any numerical model, output shown near open or closed boundaries should be accepted cautiously because of the somewhat artificial numerical boundary conditions imposed.

SIMPSON LAGOON. WIND FROM 070°T, 26 KNOTS.

8 cm TIDE IN PHASE AT BOTH OPENINGS

(See Appendix F)

## Hours 1-6

### Sea Level

The effects of end boundary conditions are noticeable here; elevations are specified and points inward of the boundaries must adjust to them. In the interior level, depressions are on the order of 20 cm while the maximum boundary depressions are 8 cm.

### Currents

Wind set is very rapid. A localized boundary effect is noticeable in all current runs. These are shown by the vertical arrows on the north shore in the right hand corner of topographic inlets.

This results from an incorrect finite difference approximation in these corners; the overall effect is negligible. Currents at the entrance and exit are in the direction of the wind, currents in the interior follow bottom inflows and shoreline configurations. Increased velocities are noticeable north of Milne and Kavearak Points where the lagoon narrows.

#### Hours 6-12

##### Sea Level

Null elevation sections (no arrows) form on both sides of the lagoon meeting at hours 9-10 and then diverging to the open boundaries. These zones separate oppositely-directed elevations (and may again be artifacts of the specified boundary conditions).

##### Currents

Similar conditions to hours 1-6 prevail with little change from hour to hour in the overall velocity field. At the wind speed used, the astronomical tides are effectively marked by wind currents.

#### Hours 12-18

##### Sea Level

Here again the NE wind helps to depress sea level elevation in the model interior. The effect is greater on the north shore, decreasing southward.

##### Currents

The same general flow pattern is maintained. The embayment between Milne and Kavearnak Points continues to show a rather sluggish circulation. Two ungauged rivers are shown on the navigation charts in this area; these may contribute to flushing but the potential effect is not known.

SIMPSON LAGOON WIND FROM 250°T, 26 KNOTS. 8 cm TIDE  
IN PHASE AT BOTH OPENINGS

(See Appendix G)

Hours 1-6

Sea Level

Null zones (no arrows) are apparent in the beginning of the run migrating inward and nearly meeting at Milne Point at hour 5. These conditions were present in the Simpson Lagoon 070° wind run but not until hour 7-12. Elevations are reversed for the two winds, i.e., above datum elevations in the model center for 250° winds are depressions in the 070° model. End constraints are also operational in this model.

Currents

The 180° shift in wind between the two models results in a quite similar reversal of currents. Boundary effects are noticeable; there is an outward flow indicated in the NW open boundary that persists throughout the computation. The sluggish flow between Milne and Kavearnak Points is still present.

Hours 6-12

Sea Level

The null zones are still present near the open boundaries at hour 6 as is a smaller zone east of Milne Point. Hours 7-12 show a strengthening of above datum elevations in the central part of the model, end constraints controlling EW gradients.

Currents

Current structure is essentially unchanged. Bottom and solid boundary configuration constrains motion to follow bottom contours for the most part.

## Hours 12-18

### Sea Level

Similar to hours 1-6, null zones appear separating elevated from depressed areas. These migrate to the center, then towards the open boundaries.

### Currents

Remain essentially the same; bottom contour following, speeds in excess of 1 knot near Milne and Kavearnak Points.

## VII. DISCUSSION

A limited number of simulations have been conducted using the large and small scale models. Features suggested on the large scale model were present in the small models. The small models provided detail on fine scale features, such as the presence of gyres, that could not be exhibited in the larger model because of its coarse grid.

It is emphasized that verification data is practically non-existent for any of the model predictions. Some suggestive material is available for Simpson Lagoon (e.g., Dygas, op. cit.) to lend credence to the simulations where strong onshore and offshore winds were used as primary driving forces. The specification of open boundary tidal elevations at each end of the Lagoon tend to damp out ranges that might be much larger than used. Better runs may have been made if we had included the Colville River delta in the Simpson simulation. Here, however we would have been forced to presume knowledge of the Colville interaction with Harrison Bay and surrounding waters. As data becomes available, or if more computer time is set forth for numerical experimentation, the Colville system should be attempted. (We emphasize again the usefulness of numerical experimentation.)

Although the boundary constraint of an 8-cm amplitude may have limited elevations, elevations of about 20-cm did occur in the model interior. The resulting horizontal pressure gradient has the additional effect of accelerating the system.

The Simpson Lagoon system reveals a rather simple contour following circulation, at least at the rather large wind speeds we used (26 knots). At an average speed of about 1 knot, it would take a particle about 12 hours to travel the length of that part of Simpson Lagoon modeled (10 nm). The mid-channel surface vectors are about 2-3% of the wind

speed, which is in agreement with observations of the movement of oil patches subject to wind. Particles released on the north shore would tend to remain in the northern sector regardless of wind direction. Particles released on the south shore would tend to remain in the south for a NE wind but may become entrapped in the embayment west of Kavearnak Point. For a SW wind, cross-channel diffusion is more likely to occur; the embayment could also entrap particles for this wind set.

The Prudhoe Bay system is entirely different from the Simpson Lagoon both because of the more complex bottom topography and absence of barrier islands in the former. Circulation is very complex, consisting of gyres, counter currents, and areas of potential pollutant accumulations. The Stump Island-Arco Wharf system influences the western Bay circulation to a marked extent. Wind direction is very important in determining the flushing rate. Tidal currents are very weak but exhibit a general onshore - offshore component as the tide changes. Light (10 Knot) onshore winds set up definite circulation patterns. Flushing of the Bay will be slight; pollutants released in the east Bay will leave the system east of Gull Island. West of Gull Island, pollutants can enter the cyclonic gyre discussed before or migrate towards the Arco Wharf. Because of the large number of gyres in the system and the variable currents, diffusion for a release anywhere in the Bay will be rapid.

During the 20 Knot offshore wind runs, no closed gyres were present. Pollutants released west of Gull Island will circulate cyclonically about the island before exiting to the northwest. The influence of the Arco Wharf is quite evident. Extension of the Wharf could modify the Bay circulation to some degree. Before these runs were made, the wharf had been extended several hundred feet from that modeled. Future runs should consider this. The offshore limits of the model should be extended to encompass the wharf and to minimize boundary effects.



The offshore model extends from east of the Colville River to between Stockton and Maguire Islands. The grid extends about 13.5 nm offshore to about the 10 fathom curve. The grid, then, does not extend seaward enough that the advection of warm Bering Sea water (Mountain, 1974) must be modeled. As discussed by Mountain, westward flow associated with NE winds and upwelling occurs periodically. The two simulations that we have run to date are informative but do not encompass enough simulations to be conclusive. Offshore tidal currents rotate anti-cyclonically but are very weak, being less than 0.1 knot. Nearshore currents are somewhat stronger, especially in the vicinity of the Sag and Kup Rivers. The offshore islands break up the rather uniform offshore flow and could accelerate the speed of pollutants released upstream of them.

The light NE (onshore) wind over the large grid markedly affects the offshore current structure. Winds are strong enough to overcome opposing tidal currents resulting in a prevailing westerly current set. Island circulation patterns are altered somewhat from the no wind case, but the flow is still more regular. Current speeds are stronger inside the offshore islands than to seaward. Wind speed appears strong enough to block river flow indicating setup in the nearshore waters above river datum.

For this relatively-weak wind speed (10 knots) a general longshore transport is indicated. Bottom following currents are present nearshore. Advection of pollutants will be greater than for the no-wind case, but dispersion could be somewhat less due to the more uniform current structure. The general tendency for an instantaneous release in the wake of an offshore island would be for downstream transport and some lateral spread for the wind case. Vertical diffusion would depend on the depth of the mixed layer. For the no-wind case, little advection would occur but there would be significant lateral dispersion relative to the wind case.

Dispersion nearshore would be relatively great, pollutants originating offshore could reach land, enter the lagoons and embayments and the river deltas. Large extents of the coast could be affected by isolated, up-current spills or marine drilling or construction operations.

Storm surge has not been modeled as such. It is anticipated, however, that offshore drilling operations would not be affected too greatly by surges, but that nearshore, fixed facilities could be subject to considerable stress. Because of the low-lying coast considerable areas of the coast could be exposed or flooded. The model used here does not simulate surges as such because the horizontal extent of the model is too limited. Such models are, however, being used and developed by the British for their North Sea Operations and by the Canadians in their work in the Eastern Beaufort Sea. No predictions are made here on the effect on offshore structures of ice, either during the ice-growing season or of wind-blown ice fields converging in structures.

## VIII. CONCLUSIONS

- 1) Three areas judged to be of importance with regard to the OCS program were modeled with an existing HN model. Although the model is capable of handling three layers, only the one layer version is used here, both because of time and computer budget restrictions.
- 2) Sea level and current velocity were modeled for an 18 hour period in all models. Convergence was achieved rapidly and no stability problems were encountered. Prevailing winds, abstracted from weather summaries, were used in all models but not all probable cases were run.
- 3) Tidal amplitudes were taken from EPA recorders installed during the 1975 ice-free season. Amplitudes of about 8 cm (16-cm range) were observed and used as tide input. No phase difference was noticed in comparable records from the two recorders, which were separated by about 70 n.m. (130 KM). A tide wave normal to the coast was used. As better information becomes available, the direction of a wave entering the system at an angle can easily be used as input. Amplitudes greater than 8 cm can also be input, as can offshore storm surge elevations.
- 4) River runoff was found to affect the circulation in the large scale model. No river flow was used in the Simpson model; flow from the Putuligayuk River entering Prudhoe Bay did not affect sea level or the currents except near the immediate river entrance. Flows were taken from existing U.S.G.S. records and from other investigators.
- 5) Winds dominated the circulation in all models, although a no-wind model has not been run for Simpson Lagoon. At the tidal amplitude used in the models, 10-knot winds were sufficient to markedly affect circulation patterns in the large model and the Prudhoe Bay model. Rather large winds (26 Knots) were used for onshore and offshore

conditions in Simpson Lagoon. Here, bottom-following currents occurred for both directions with irregular shoreline topography modifying the rather uniform EW flow. Current velocity was about 2-3% of the wind speed. Ten knot winds in the large model were sufficient to cause enough nearshore setup to reverse river flow.

Clockwise rotary tide-only velocities offshore were marked by light (10 Knot) NE winds, direction becoming westerly throughout the tide cycle. This anticyclonic motion is to be expected in the Northern Hemisphere because of the Coriolis term. Prudhoe Bay circulation was most affected by winds, several gyres appearing with the onshore wind.

6) Several features of the small models were apparent in the large model. The east-shore counter current in Prudhoe Bay, the sluggish circulation and cyclonic flow was indicated on both models to different degrees. Simpson Lagoon circulation followed the same trends for both large - and small - scale models.

7) The general behavior of the model seems reasonable. Because of the lack of verification data, it is necessary to make judgments of this type; the models are regarded as providing insight that would not otherwise be available. Further runs should be made to encompass more conditions; verification data should be collected offshore and in Prudhoe Bay. Multiple drogue releases, in addition to anchored current meters, should be used in Prudhoe Bay. The scheduled installation of current meters offshore (encompassed by the large-scale model) should proceed in 1976. The model output from further runs should be examined to determine the optimum location of the meters.

8) Potential trajectories and the dispersion of pollutants can be estimated from the time series plots of currents presented. Offshore blowouts during low onshore wind conditions could result in widespread dispersion of pollutants along the coast. Evidence indicates transport toward the west would be most dominant during the ice-free season, although drift towards Canada could occur with westerly winds.

9) Oil spills entering rivers (of the system modeled) would be constrained to remain nearshore. Unlike freshwater from the MacKenzie system, which covers an extensive offshore area, the influence of the Kuparuk and Sagavanirktak Rivers is found to vanish within a few grid lengths from the source. Additional runs for different flows, winds and tides are needed to confirm this.

## IX. NEED FOR FURTHER STUDY

It should be borne in mind that a relatively small section of the Beaufort Sea Coast was selected here for study. Conclusions drawn only apply to these areas and cannot be extrapolated to others.

In order to predict the effects of storms, ice cover, ice scour, etc., on oil dispersion, drilling and marine operations in the entire Beaufort Sea area an extremely large and intensive study would be required. The success of such a mission would be a function of the continuity of the program, the computing facilities available, the budget, etc. Because of the large amount of basic research needed on all aspects of Arctic physical problems above, it is not obvious what the degree of success would be based upon or in what time frame it could be accomplished.

With the above in mind, we chose a smaller piece of the action and believe the results to date, although incomplete, are creditable and useful. To complete the project as it was originally proposed would mean attempting again to obtain a minimum of verification data for, at least, the offshore model.

Further computer runs are required for different wind speeds and directions, tidal amplitudes, and river runoff. The combinations are endless and only average or anticipated extreme conditions should be modeled.

As is known from other Canadian studies (Huggett et al., 1975) and our limited multi-layer simulations, bottom circulation may have little resemblance to the upper wind driven circulation. Conclusions drawn on the basis of the one-layer model should be viewed with some skepticism during conditions which are clearly stratified. The verification of such models is more difficult, of course, but should be undertaken nonetheless.

Additional runs simulating continuous and point source discharges of pollutants are required. These have not been attempted to date. Although conclusions have been drawn from the predicted current trajectories and experience with other oceanographic systems, the exhibition of pollutant transport and dispersion is quite helpful and useful in visualizing possible scenarios resulting from spills and runaway blow-outs.

To verify the dispersive prediction models, drogue and/or dye release studies are required in combination with instruments fixed in space (see, e.g., Callaway, 1975). These are not to be lightly considered endeavors, due to the rigors of the environment and the logistics involved.

## LITERATURE CITED

- Alexander, V. et al.  
1975. Environmental studies of an Arctic Estuarine system - Final Report. Institute of Marine Science, Univ. of Alaska, EPA Ecology Res. Ser. EPA - 660/3-75-026, 536 pp.
- Bauer, R. A.  
1975. Description of the optimized EPRF multi-layer hydrodynamical-numerical model. Env. Pred. Res. Fac. Tech. Paper No. 15-74, Naval Postgraduate School.
- Callaway, R. J.  
1975. Subsurface horizontal dispersion of pollutants in open coastal waters. In: Discharge of sewage from sea outfalls. Pergamon Press, pps. 297-307.
- Callaway, R. J. and C. Koblinsky.  
1975. Transport of pollutants in the vicinity of Prudhoe Bay, Alaska. Semi-annual progress report to BLM/NOAA, OCSEAP, June-November 1975. Proc. EPA, Corvallis Environmental Research Laboratory, 12 pps + 3 figures.
- Carter, L. J.  
1976. Oil drilling in the Beaufort Sea: Leaving it to luck and technology. Science 191: 929-931.
- Dygas, J. A.  
1975. A study of wind, waves and currents in Simpson Lagoon. Chapter 3 in Alexander et al. (1975). pps 15-44.
- Hansen, W.  
1962. Tides. In: The sea. Ideas and observations on progress in the study of the seas. Vol I, M. N. Hill, ed. Inter. Publ. Inc., pps. 764-801.
- Hansen, W.  
1966. The reproduction of the motion in the sea by means of hydrodynamical-numerical methods. Mitteil, des Inst. fur Meeres der Univ. Hamburg. Nr. 5. 57 pps + 28 plates.
- Hufford, G. L.  
1974. On apparent upwelling in the southern Beaufort Sea. Journal Geoph. Res. 79: 1305-1306.
- Huggett, W. S. et al.  
1975. Near bottom currents and offshore tides. Beaufort Sea Proj. Dept. Env. Tech. Report No. 16, Victoria, B. C., 38 pp.



- Laevastu, T.  
1974. A vertically integrated hydrodynamical-numerical model (W. Hansen type). Model description and operating/running instruction. Part 1 of a series of four reports. Environ. Pred. Res. Fac. Tech. Note No. 1-74. Naval Postgrad. School Monterey, CA.
- Leendertse, J. J.  
1967. Aspects of a computational model for long-period water-wave propagation. The Rand Corp., RM-5294-PR.
- Mountain, D. G.  
1974. Bering Sea water on the North Alaskan Shelf. PHD Thesis. Univ. Washington, 147 pp.
- Wiseman, W. J., jr., et al.  
1973. Alaskan Arctic Coastal processes and morphology. Tech. Report No. 149 Coastal Studies Inst. Louisiana State Univ. 171 pps.

APPENDIX A

OKILTOK POINT TO THE CHALLENGE ENTRANCE

M2 TIDE WITH 8 CM AMPLITUDE

River Flow at 5 cm/sec

No Wind

ENVIRONMENTAL PROTECTION AGENCY  
MARINE AND FRESHWATER ECOLOGY BRANCH  
OCEAN MASS TRANSPORT MODEL

M2 TIDE (AMPERCM. FROM 22.5 DEG T) RIVER FLOW 5 CM/SEC  
BEAUFORT SEA SHELF STUDY  
GRID 310 OLIKTOK POINT TO THE CHALLENGE ENTRANCE

|                       |      |                 |                |    |                 |
|-----------------------|------|-----------------|----------------|----|-----------------|
| GRID GEOMETRY         | ROWS | 18              | COLUMNS        | 61 |                 |
| GRID LENGTH           |      | 200000. CM      | ROTATION ANGLE |    | 337.5 DEG       |
| WIND DRAG COEFFICIENT |      | .0024           | MID LATITUDE   |    | 70.500 DEG. (N) |
| FRICTION COEFFICIENT  |      | .0030000 CM/SEC |                |    |                 |

|                      |           |         |         |
|----------------------|-----------|---------|---------|
|                      | LAYER 1   | LAYER 2 | LAYER 3 |
| INITIAL LAYER DEPTHS | 3000.0000 | .0000   | .0000   |
| SMOOTHING FACTORS    | .9900     | .0000   | .0000   |
| DENSITY              | 1.0250    | .0000   | .0000   |

|                                 |             |                           |          |
|---------------------------------|-------------|---------------------------|----------|
| RESULTS SAVED AT MODULUS (TIME, | 3600 SEC)=0 | RESULTS SAVED STARTING AT | 3600 SEC |
| COMPUTATIONS STARTED AT         | 0 SEC       |                           |          |
| ENDED AT                        | 64800 SEC   |                           |          |
| INCREMENTED BY                  | 60 SEC      |                           |          |
| LAYER3 PRINT OUT STARTED        |             | 3600 SEC. FREQUENCY OF    | 3600 SEC |

|                               |     |        |          |        |          |     |          |       |
|-------------------------------|-----|--------|----------|--------|----------|-----|----------|-------|
| TIDE INPUT AT                 | ROW | 1 THRU | 1        | COLUMN | 1 THRU   | 61  | TIME LAG | 0 SEC |
|                               |     |        | M2       |        | S2       | O1  | K1       |       |
| PHASE ANGLES (DEG/HR)         |     |        | 270.00   |        | .00      | .00 | .00      |       |
| AMPLITUDES (CM)               |     |        | 5.00     |        | .00      | .00 | .00      |       |
| LOWER LAYER WEIGHTING FACTORS |     |        | LAYER 2= | .00    | LAYER 3= | .00 |          |       |

|                      |  |           |         |         |         |
|----------------------|--|-----------|---------|---------|---------|
| TIDE SPEEDS (DEG/HR) |  | M2        | S2      | O1      | K1      |
|                      |  | 24.484000 | .000000 | .000000 | .000000 |

|                         |              |    |          |            |    |        |        |   |
|-------------------------|--------------|----|----------|------------|----|--------|--------|---|
| FLOW INPUT AT ROW       | 18 THRU      | 18 | COLUMN   | 19 THRU    | 19 | LAYERS | 1 THRU | 1 |
| COMPUTATIONS STARTED AT |              |    |          |            |    |        |        |   |
|                         |              |    |          |            |    |        |        |   |
| DIRECTION               | 22.5DEG TRUE |    | VELOCITY | 5.0 CM/SEC |    |        |        |   |

|                         |              |    |          |            |    |        |        |   |
|-------------------------|--------------|----|----------|------------|----|--------|--------|---|
| FLOW INPUT AT ROW       | 18 THRU      | 18 | COLUMN   | 34 THRU    | 42 | LAYERS | 1 THRU | 1 |
| COMPUTATIONS STARTED AT |              |    |          |            |    |        |        |   |
|                         |              |    |          |            |    |        |        |   |
| DIRECTION               | 22.5DEG TRUE |    | VELOCITY | 5.0 CM/SEC |    |        |        |   |

ASSIGNED MODEL NUMBER 310

SEA LEVEL

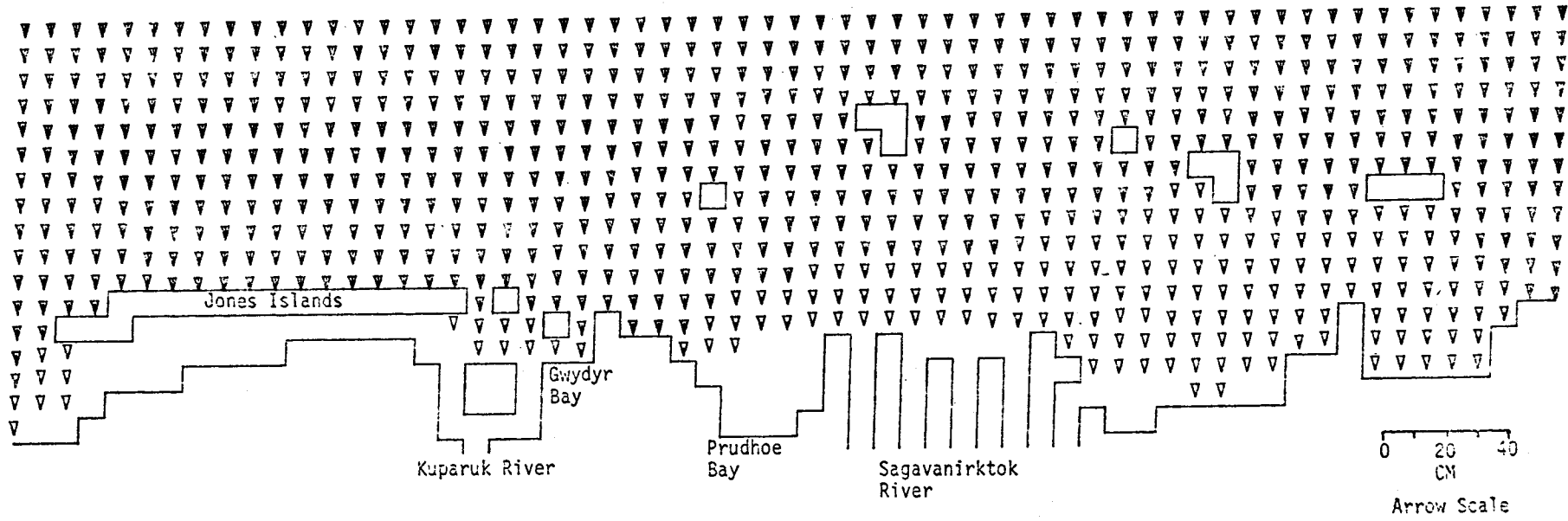
SEA LEVEL

TIME= 3600SEC

LAYER 1

MODEL NO 310

479



OLIKTOK POINT TO THE CHALLENGE ENTRANCE  
M2 TIDE (AMP=8CM, FROM 22.5 DEG T) RIVER FLOW 5 CM/SEC

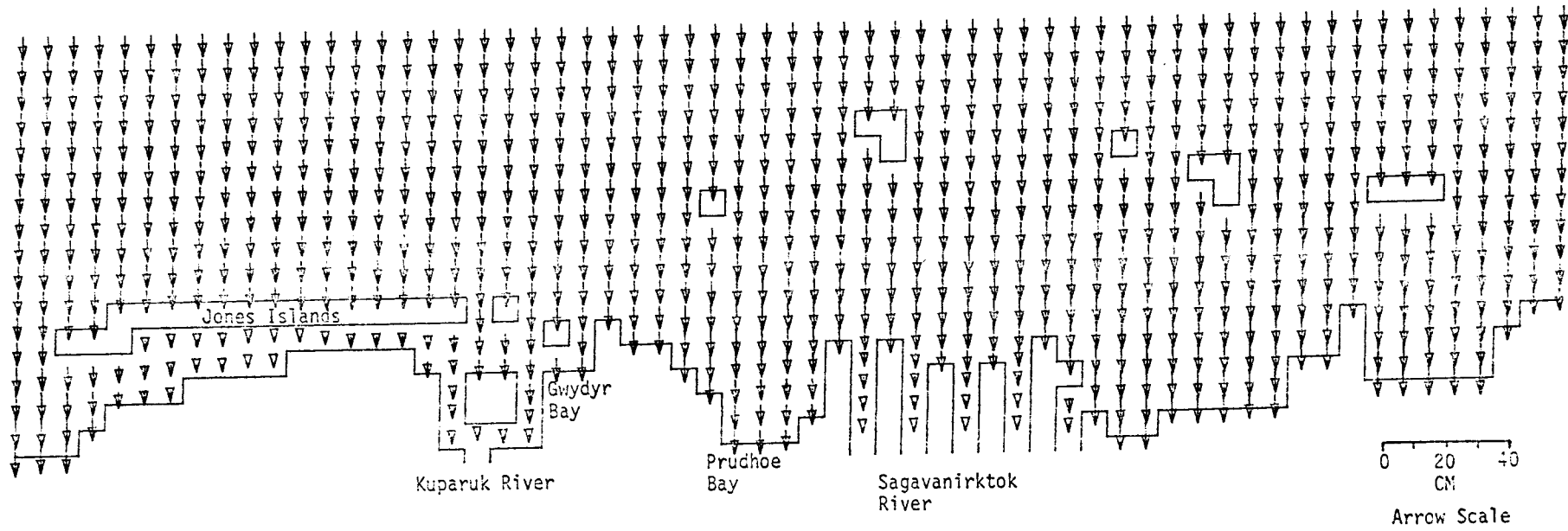
SEA LEVEL

TIME= 7200SEC

LAYER 1

MODEL NO 310

084



CLIKTOK POINT TO THE CHALLENGE ENTRANCE  
M2 TIDE (AMP=8CM, FROM 22.5 DEG T) RIVER FLOW 5 CM/SEC

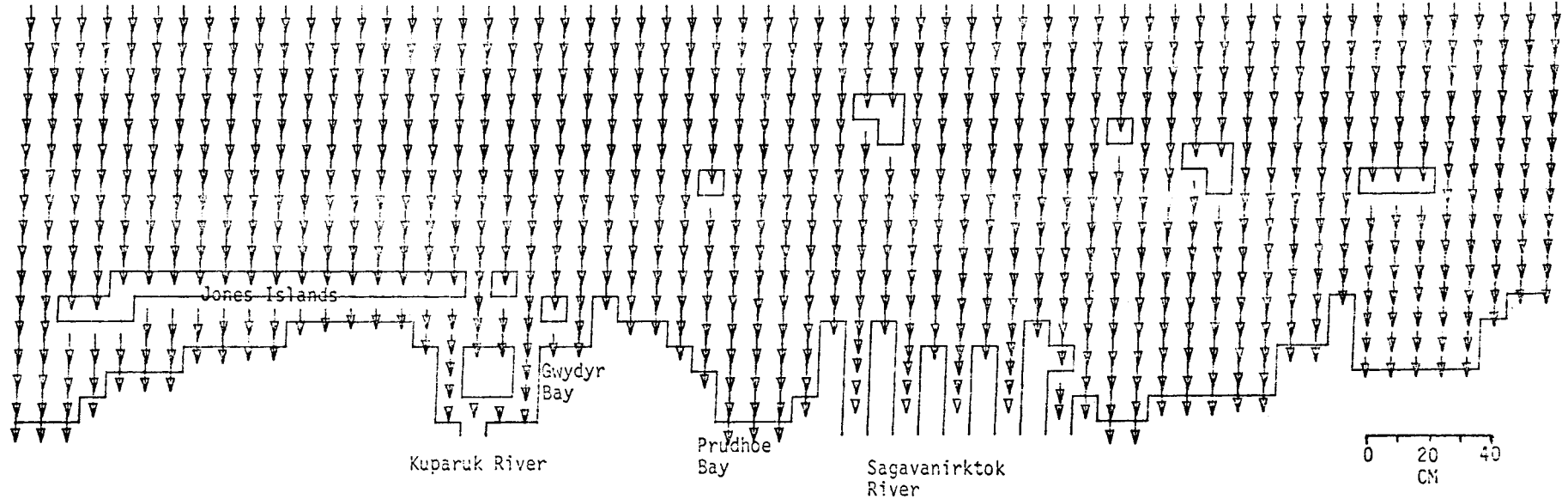
SEA LEVEL

TIME= 10800SEC

LAYER 1

MODEL NO 310

481



OLIKTOK POINT TO THE CHALLENGE ENTRANCE  
M2 TIDE (AMP=8CM, FROM 22.5 DEG T) RIVER FLOW 5 CM/SEC

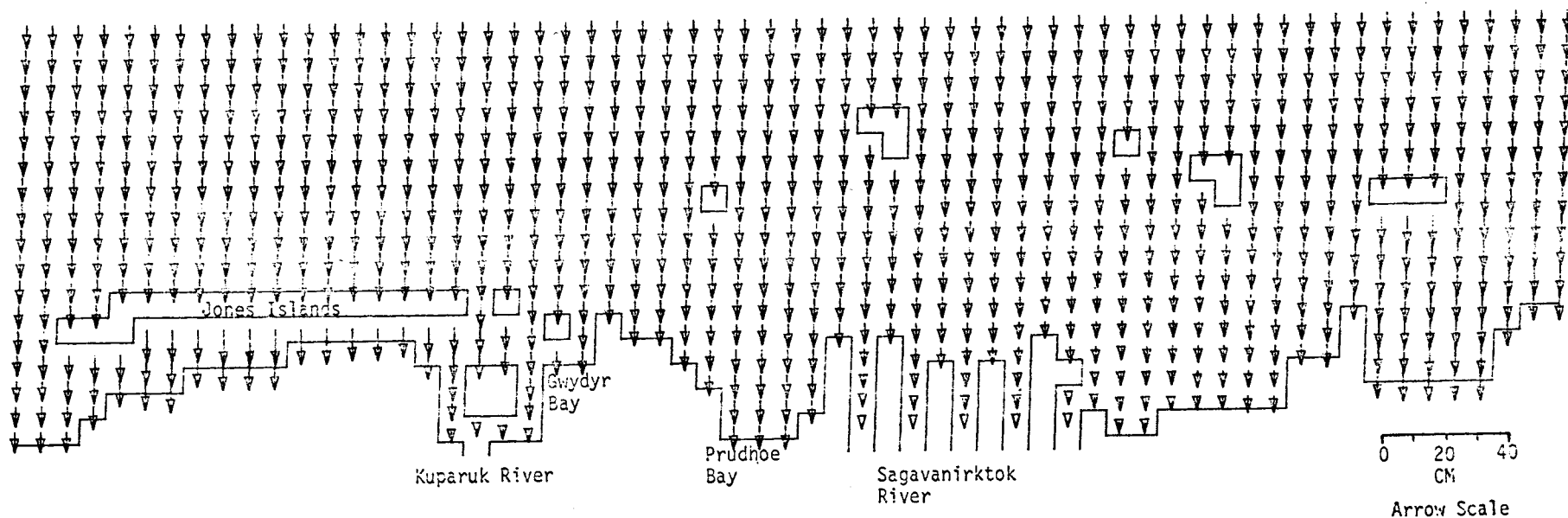
SEA LEVEL

TIME= 14400SEC

LAYER 1

MODEL NO 310

482



OLIKTOK POINT TO THE CHALLENGE ENTRANCE  
M2 TIDE (AMP=8CM, FROM 22.5 DEG T) RIVER FLOW 5 CM/SEC



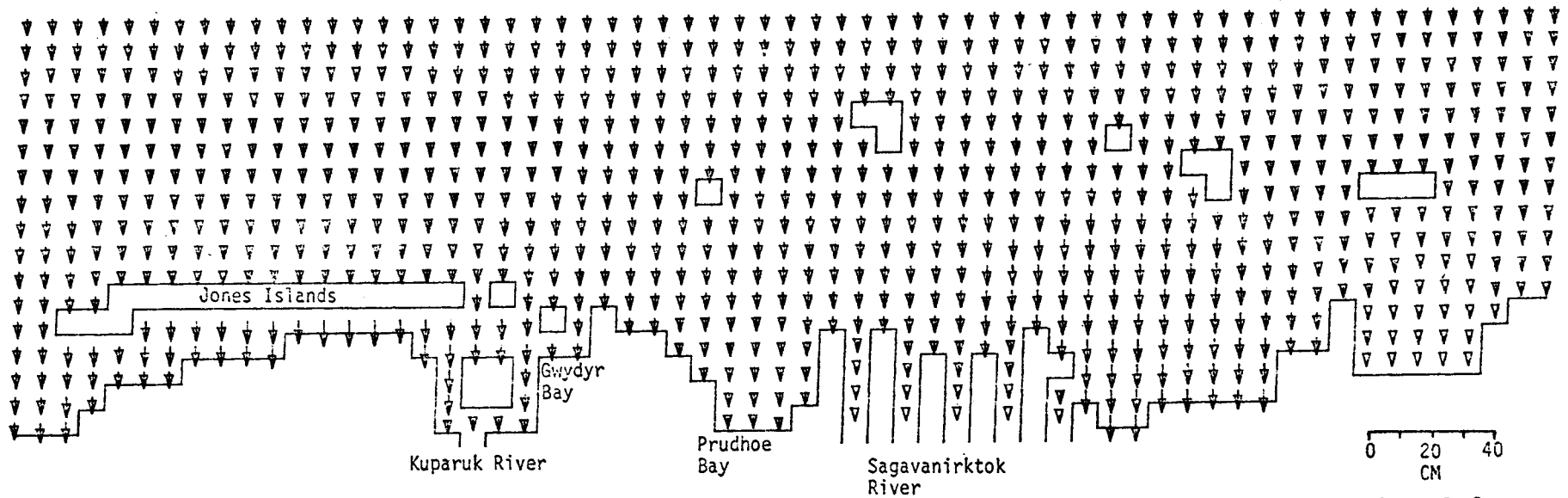
SEA LEVEL

TIME= 18000SEC

LAYER 1

MODEL NO 310

483



OLIKTOK POINT TO THE CHALLENGE ENTRANCE  
M2 TIDE (AMP=8CM, FROM 22.5 DEG T) RIVER FLOW 5 CM/SEC

0 20 40  
CM

Arrow Scale

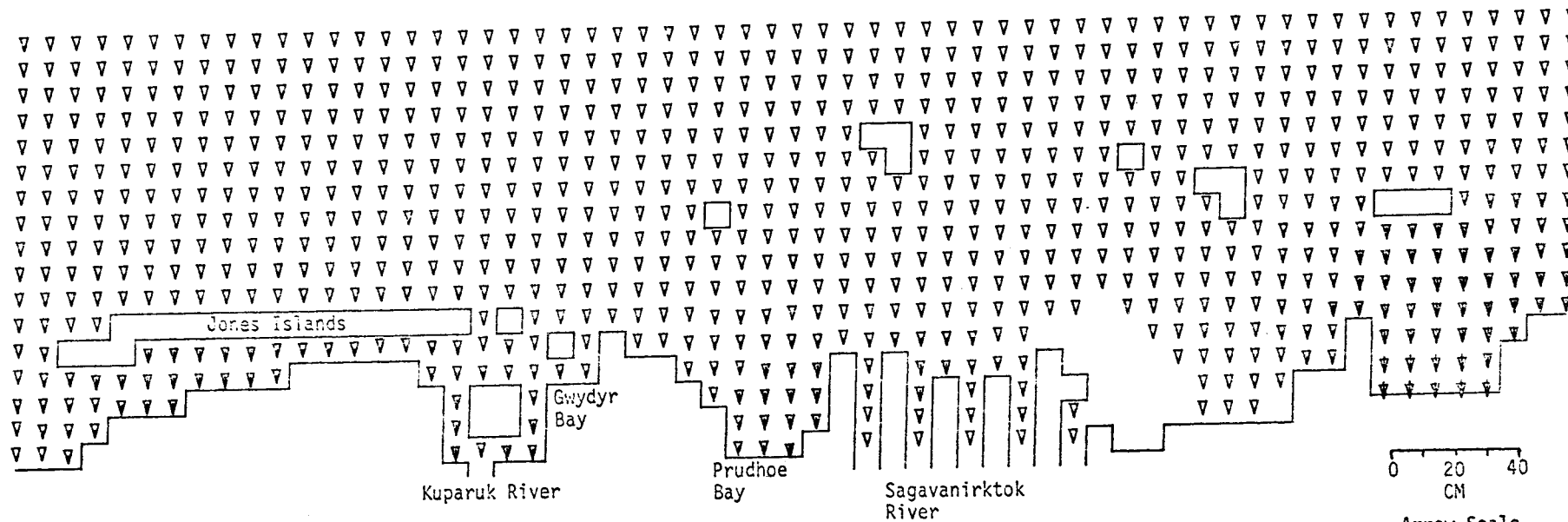
MODEL NO 310

484

SEA LEVEL

TIME= 21600SEC

LAYER 1



OLIKTOK POINT TO THE CHALLENGE ENTRANCE  
M2 TIDE (AMP=8CM, FROM 22.5 DEG T) RIVER FLOW 5 CM/SEC

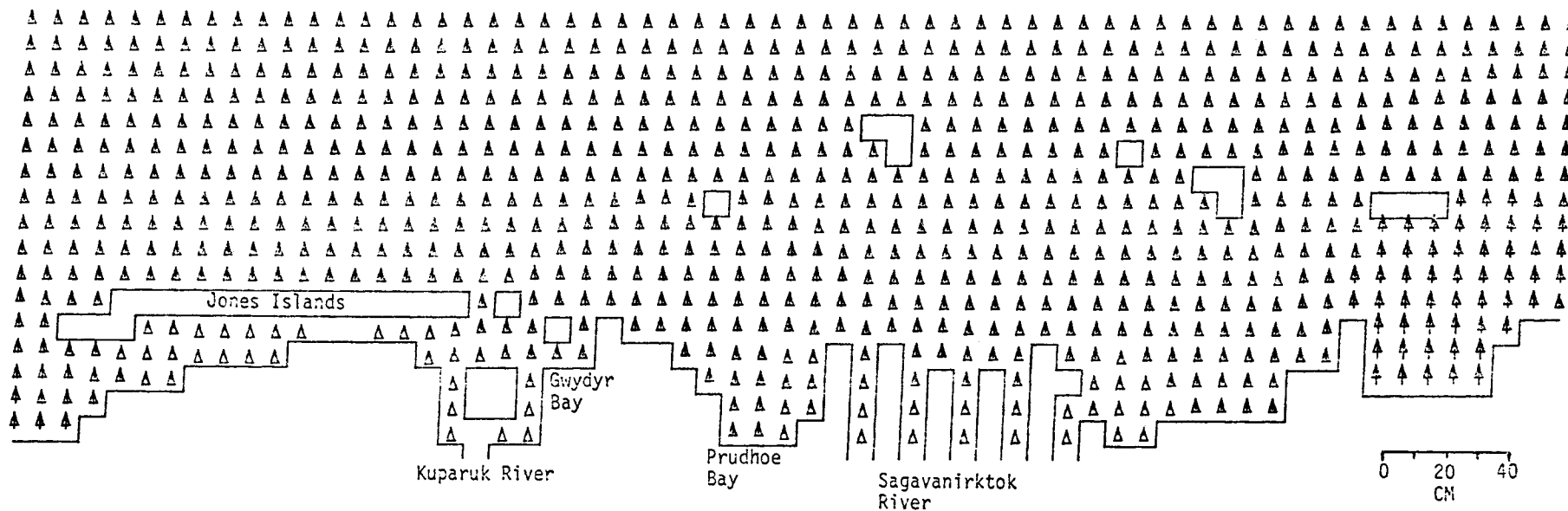
SEA LEVEL

TIME= 25200SEC

LAYER 1

MODEL NO 310

587



OLIKTOK POINT TO THE CHALLENGE ENTRANCE  
M2 TIDE (AMP=8CM, FROM 22.5 DEG T) RIVER FLOW 5 CM/SEC

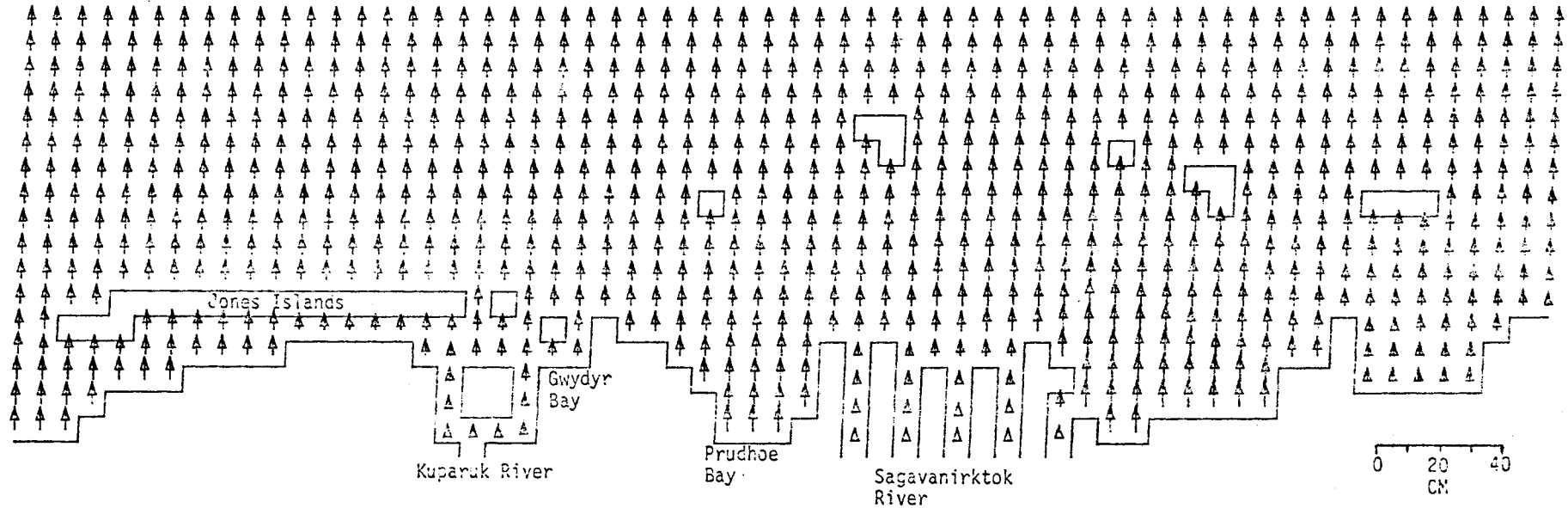
SEA LEVEL

TIME= 28800SEC

LAYER 1

MODEL NO 310

987



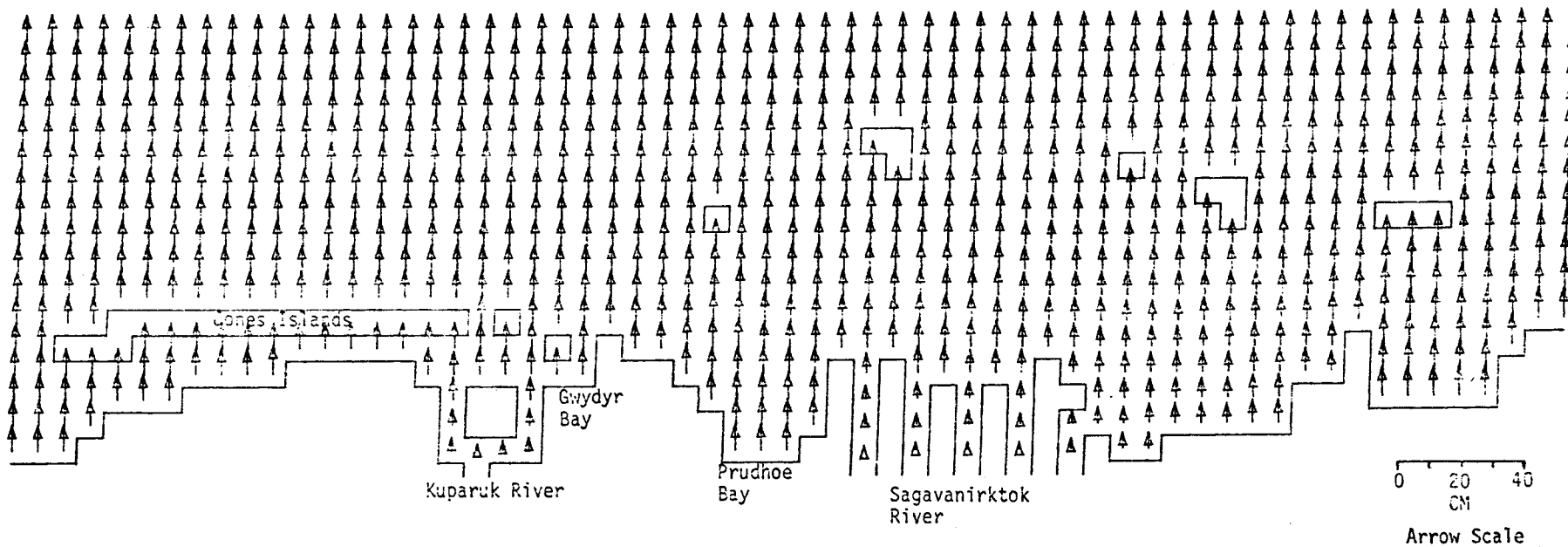
OLIKTOK POINT TO THE CHALLENGE ENTRANCE  
M2 TIDE (AMP=8CM, FROM 22.5 DEG T) RIVER FLOW 5 CM/SEC

SEA LEVEL

TIME= 32400SEC

LAYER 1

MODEL NO. 310



OLIKTOK POINT TO THE CHALLENGE ENTRANCE  
M2 TIDE (AMP=8CM, FROM 22.5 DEG T) RIVER FLOW 5 CM/SEC

487

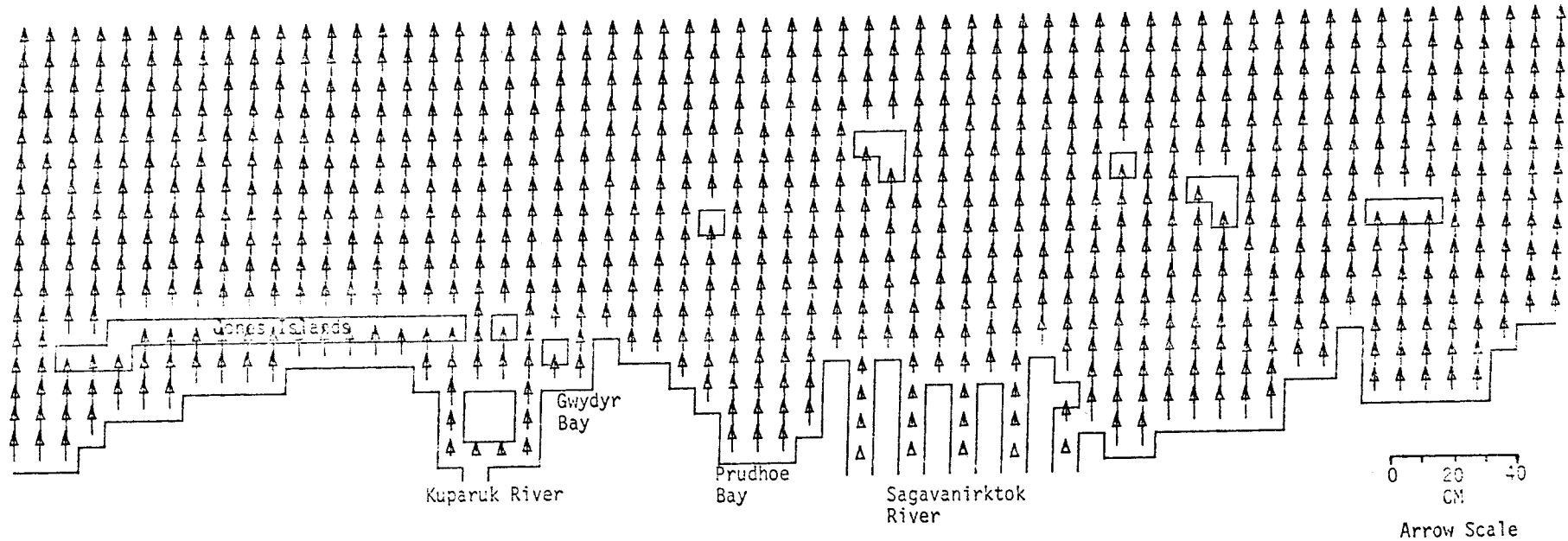
MODEL NO 310

851

SEA LEVEL

TIME= 36000SEC

LAYER 1



OLIKTOK POINT TO THE CHALLENGE ENTRANCE  
 M2 TIDE (AMP=8CM, FROM 22.5 DEG T) RIVER FLOW 5 CM/SEC

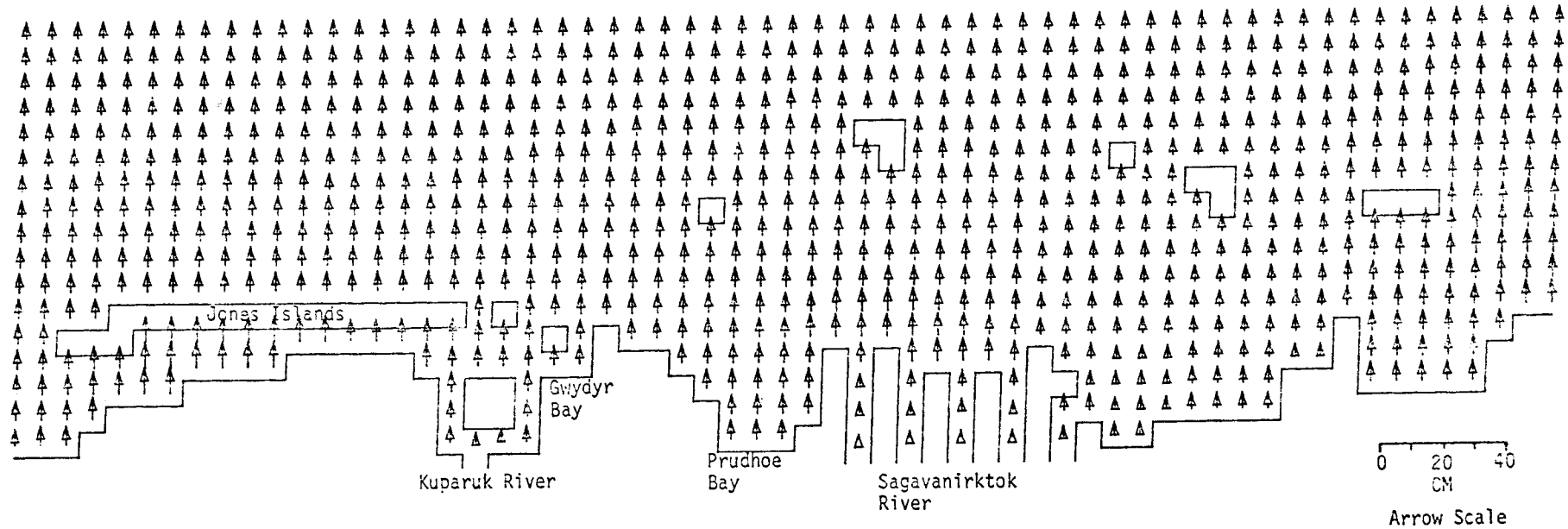
MODEL NO 310

687

SEA LEVEL

TIME= 39600SEC

LAYER 1



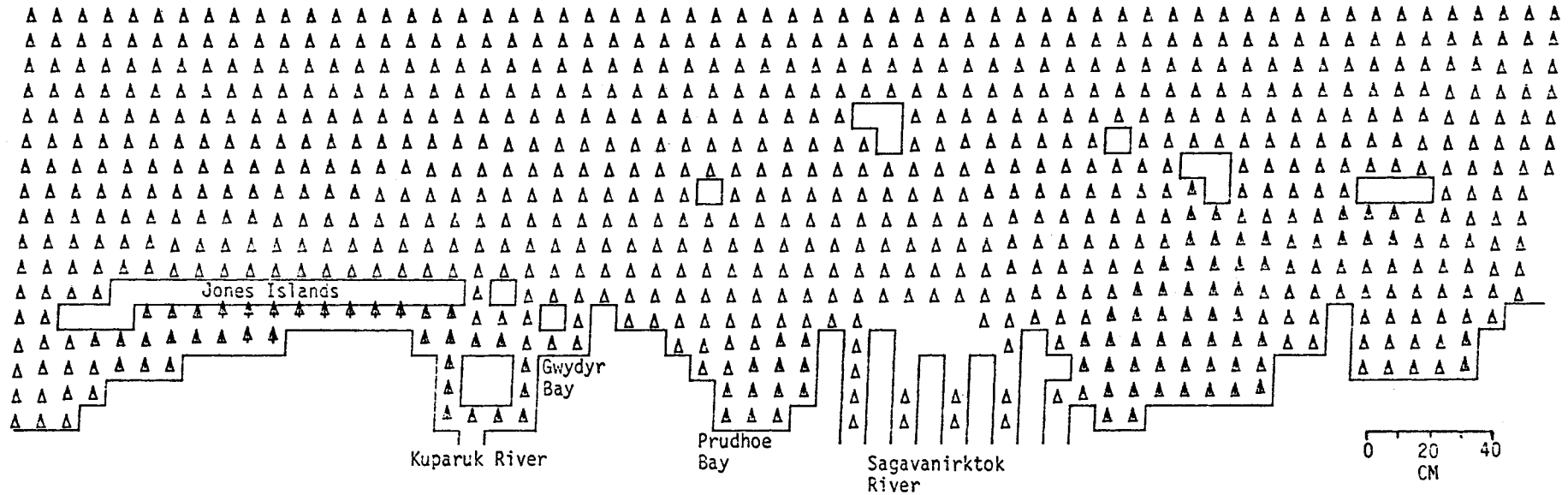
OLIKTOK POINT TO THE CHALLENGE ENTRANCE  
M2 TIDE (AMP=8CM, FROM 22.5 DEG T) RIVER FLOW 5 CM/SEC

SEA LEVEL

TIME= 43200SEC

LAYER 1

MODEL NO 310



067

OLIKTOX POINT TO THE CHALLENGE ENTRANCE  
M2 TIDE (AMP=8CM, FROM 22.5 DEG T) RIVER FLOW 5 CM/SEC

0 20 40  
CM  
Arrow Scale



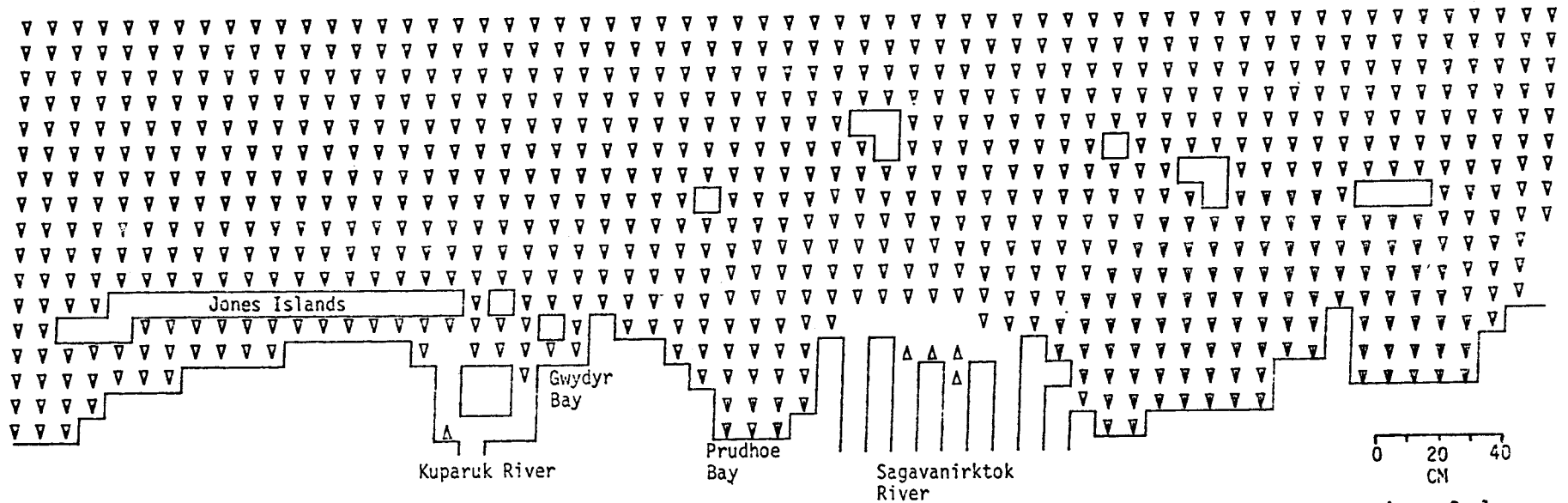
SEA LEVEL

TIME= 46800SEC

LAYER 4

MODEL NO 310

T61



OLIKTOK POINT TO THE CHALLENGE ENTRANCE  
M2 TIDE (AMP=8CM, FROM 22.5 DEG T) RIVER FLOW 5 CM/SEC

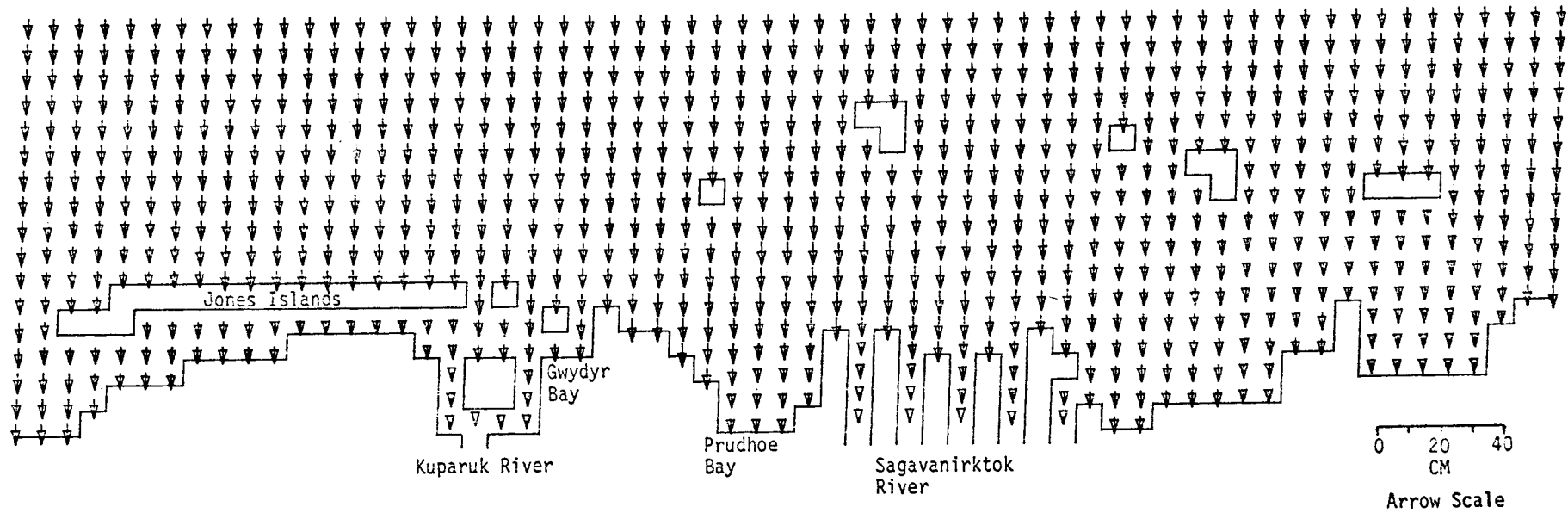
MODEL NO 310

207

SEA LEVEL

TIME= 50400SEC

LAYER 1



OLIKTOK POINT TO THE CHALLENGE ENTRANCE  
M2 TIDE (AMP=8CM, FROM 22.5 DEG T) RIVER FLOW 5 CM/SEC

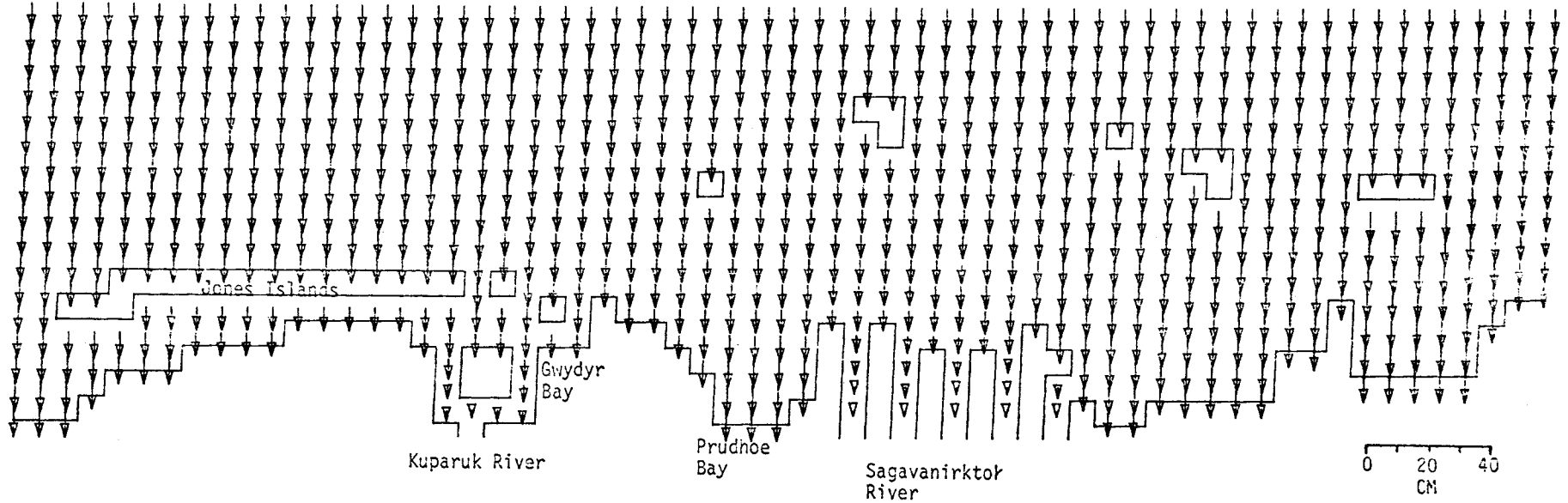
SEA LEVEL

TIME= 54000SEC

LAYER 1

MODEL NO 310

193



OLIKTOK POINT TO THE CHALLENGE ENTRANCE  
M2 TIDE (AMP=8CM, FROM 22.5 DEG T) RIVER FLOW 5 CM/SEC

0 20 40  
CM  
Arrow Scale

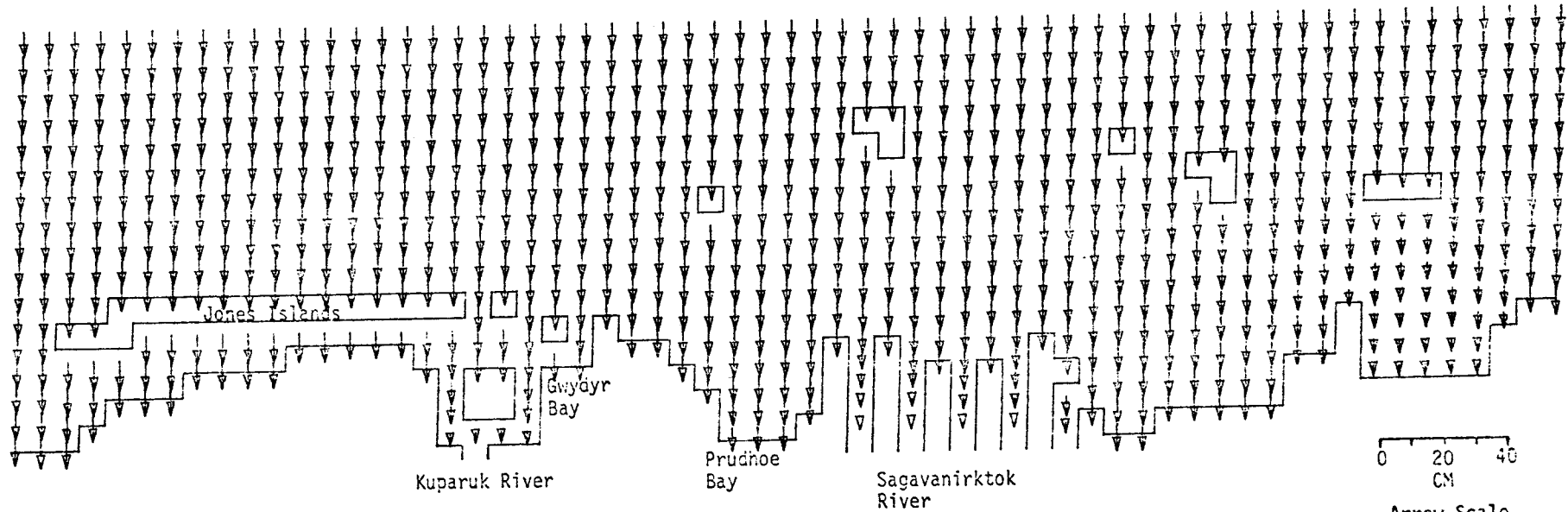
MODEL NO 310

401

SEA LEVEL

TIME= 57600SEC

LAYER 1



OLIKTOK POINT TO THE CHALLENGE ENTRANCE  
M2 TIDE (AMP=8CM, FROM 22.5 DEG T) RIVER FLOW 5 CM/SEC

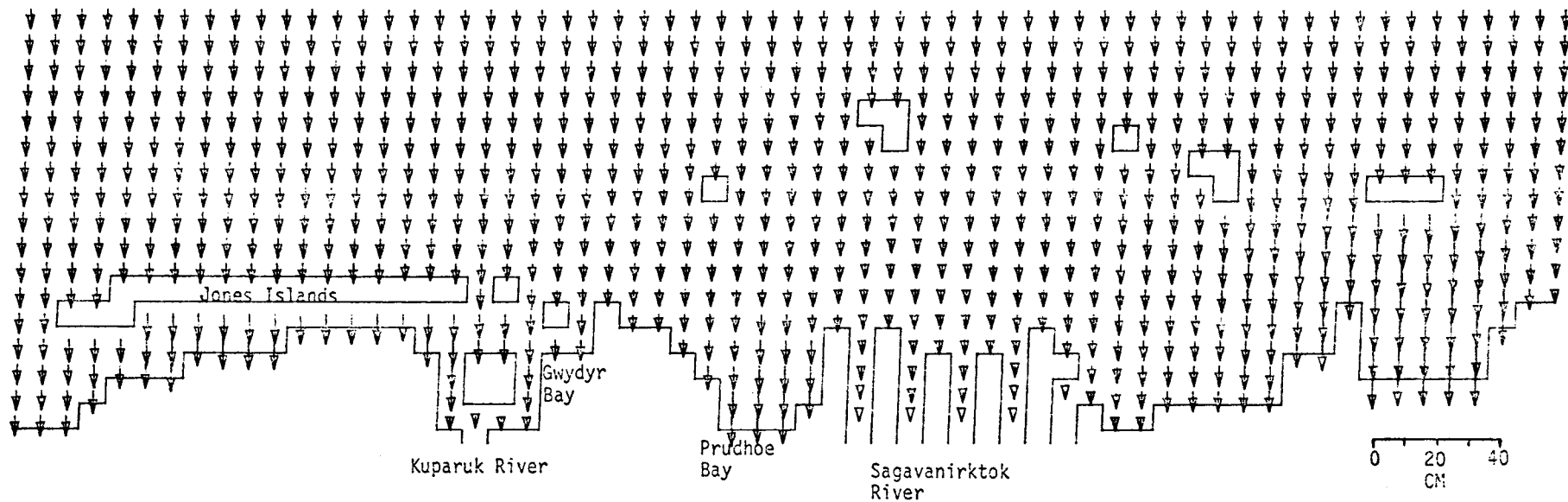
SEA LEVEL

TIME= 61200SEC

LAYER 1

MODEL NO 310

567



OLIKTOK POINT TO THE CHALLENGE ENTRANCE  
M2 TIDE (AMP=8CM, FROM 22.5 DEG T) RIVER FLOW 5 CM/SEC

0 20 40  
CM

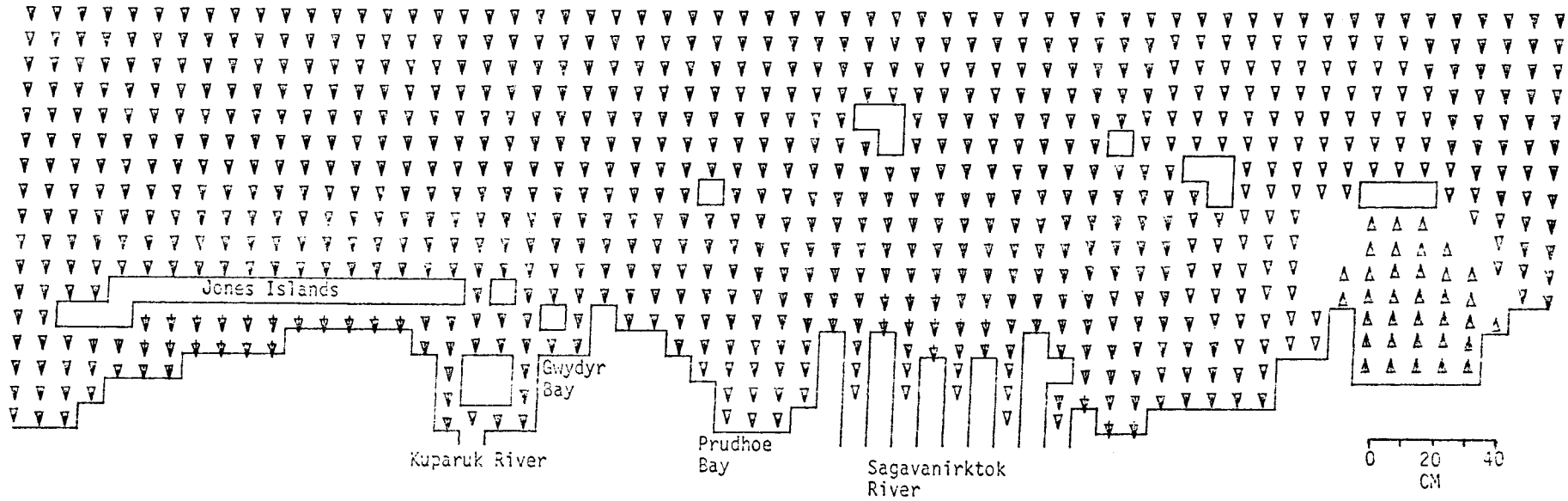
Arrow Scale

SEA LEVEL

TIME= 64800SEC

LAYER 1

MODEL NO 310



907

OLIKTOK POINT TO THE CHALLENGE ENTRANCE  
M2 TIDE (AMP=8CM, FROM 22.5 DEG T) RIVER FLOW 5 CM/SEC

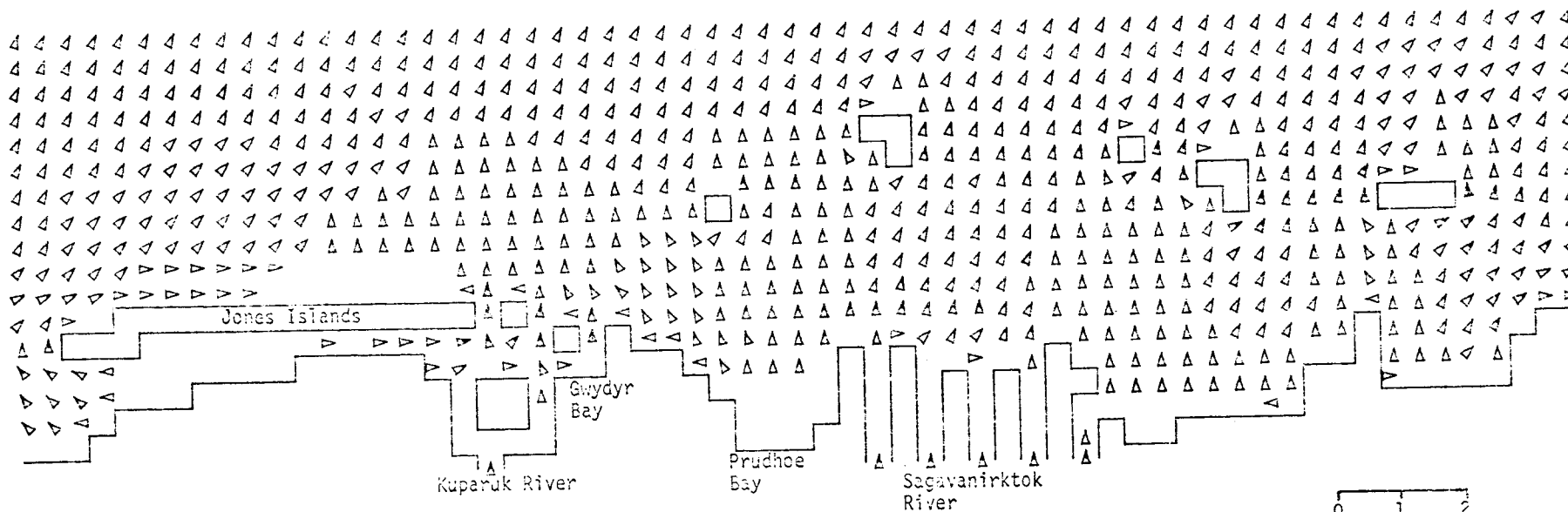
0 20 40  
CM  
Arrow Scale

CURRENTS

CURRENTS

TIME= 3600SEC

LAYER 1



OLIKTOK POINT TO THE CHALLENGE ENTRANCE  
M2 TIDE (AMP=8CM, FROM 22.5 DEG T) RIVER FLOW 5 CM/SEC

0 1 2  
Knots  
Arrow Scale

MODEL NO 31U

808

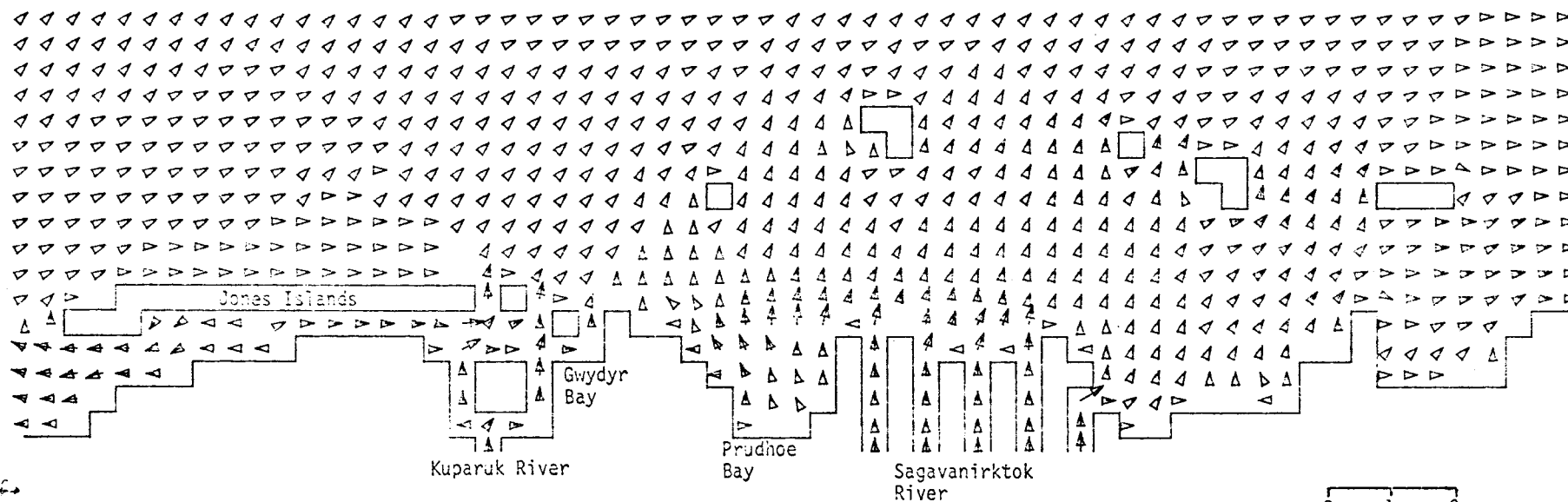


CURRENTS

TIME= 7200SEC

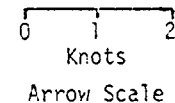
LAYER 1

MODEL NO 310



664

OLIKTOK POINT TO THE CHALLENGE ENTRANCE  
M2 TIDE (AMP=8CM, FROM 22.5 DEG T) RIVER FLOW 5 CM/SEC



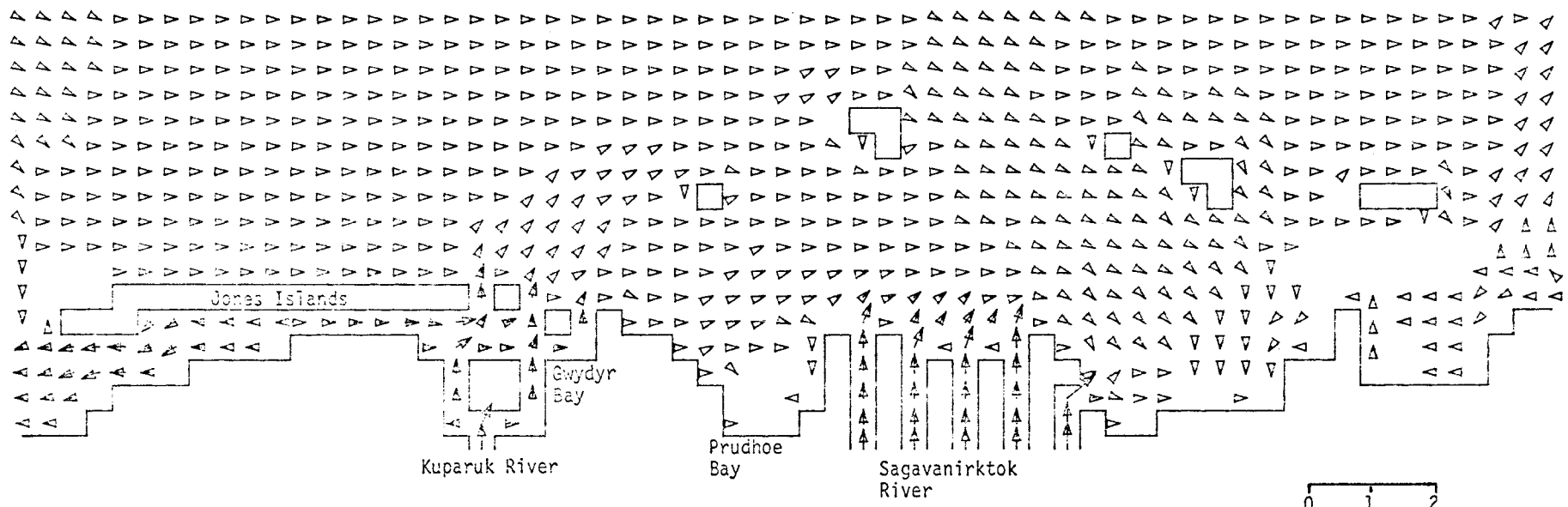
CURRENTS

TIME= 10800SEC

LAYER 1

MODEL NO 310

500



OLIKTOK POINT TO THE CHALLENGE ENTRANCE  
M2 TIDE (AMP=8CM, FROM 22.5 DEG T) RIVER FLOW 5 CM/SEC

0 1 2  
Knots  
Arrow Scale

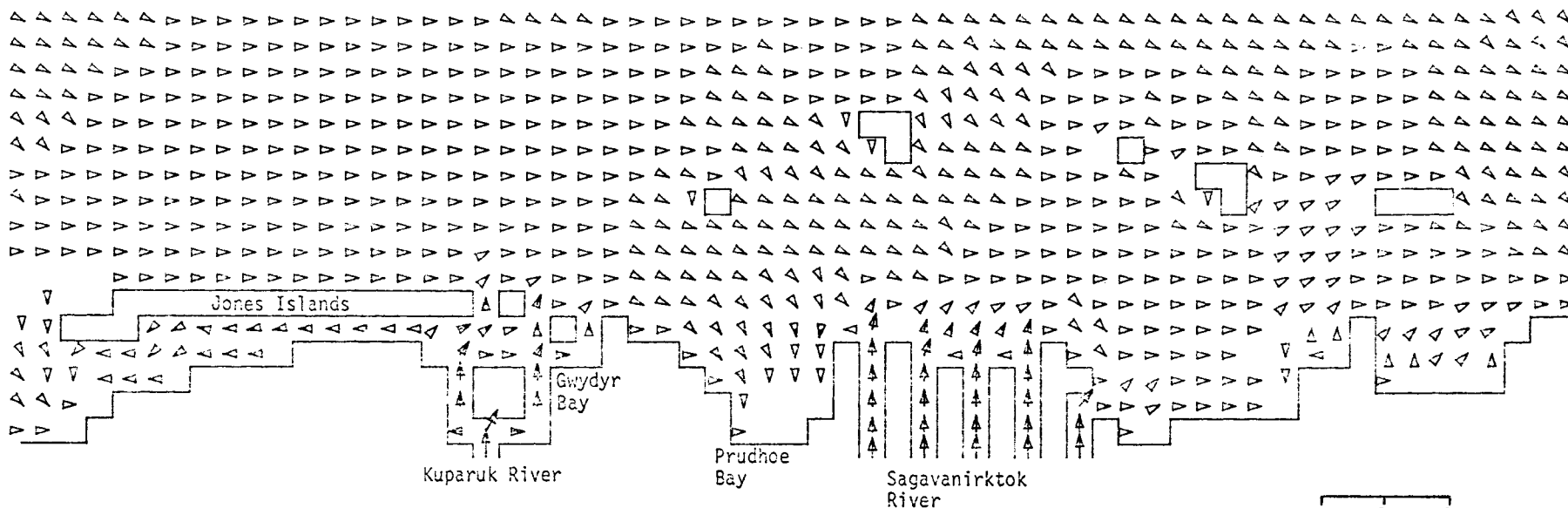
CURRENTS

TIME= 14400SEC

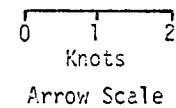
LAYER 1

MODEL NO 310

501



OLIKTOK POINT TO THE CHALLENGE ENTRANCE  
M2 TIDE (AMP=8CM, FROM 22.5 DEG T) RIVER FLOW 5 CM/SEC



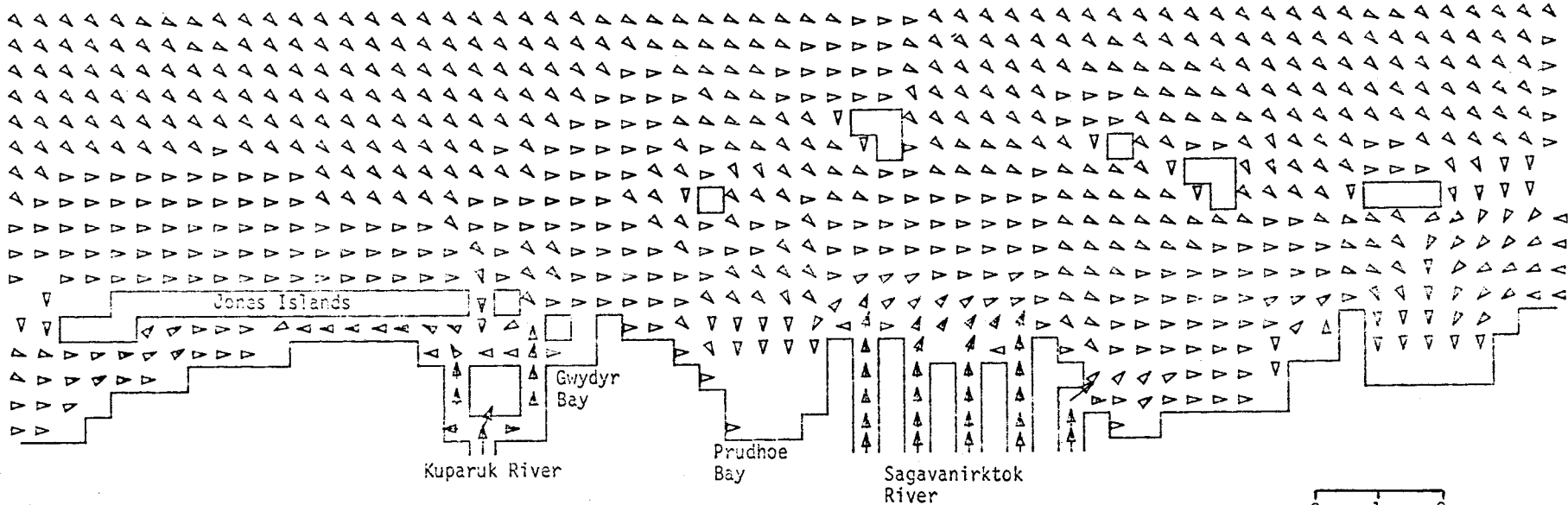
CURRENTS

TIME= 18000SEC

LAYER 1

MODEL NO 310

502



OLIKTOK POINT TO THE CHALLENGE ENTRANCE  
M2 TIDE (AMP=8CM, FROM 22.5 DEG T) RIVER FLOW 5 CM/SEC

0 1 2  
Knots  
Arrow Scale

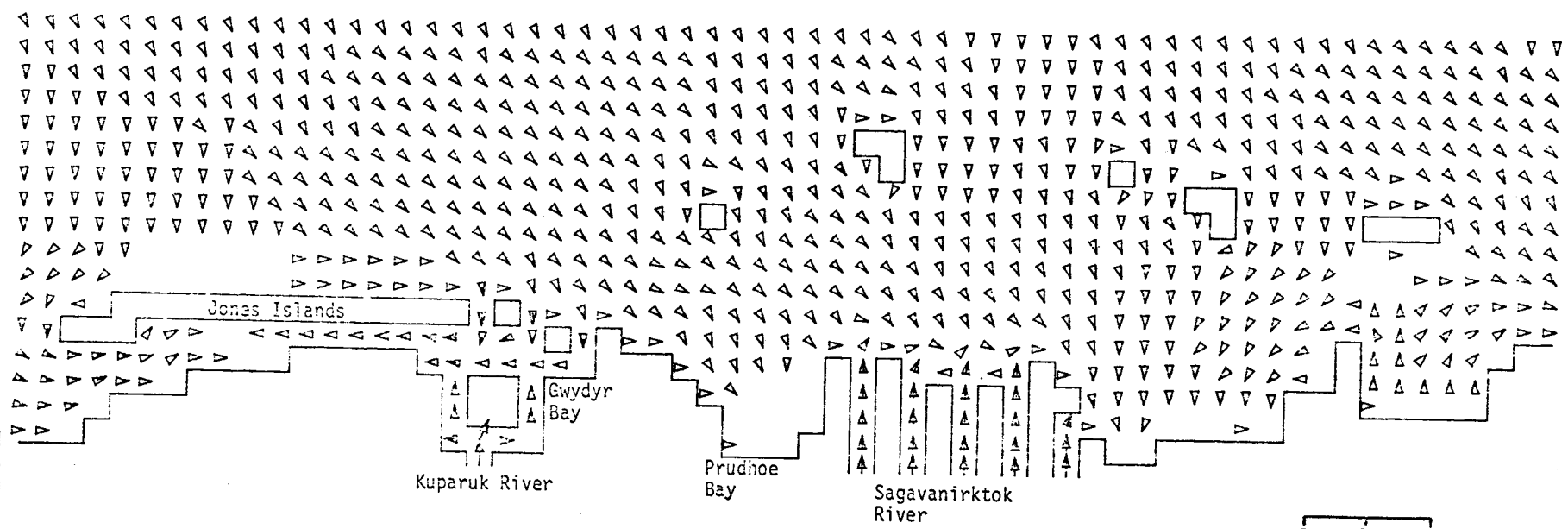
CURRENTS

TIME= 21600SEC

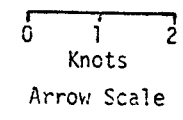
LAYER 1

MODEL NO 310

803



OLIKTOK POINT TO THE CHALLENGE ENTRANCE  
M2 TIDE (AMP=8CM, FROM 22.5 DEG T) RIVER FLOW 5 CM/SEC



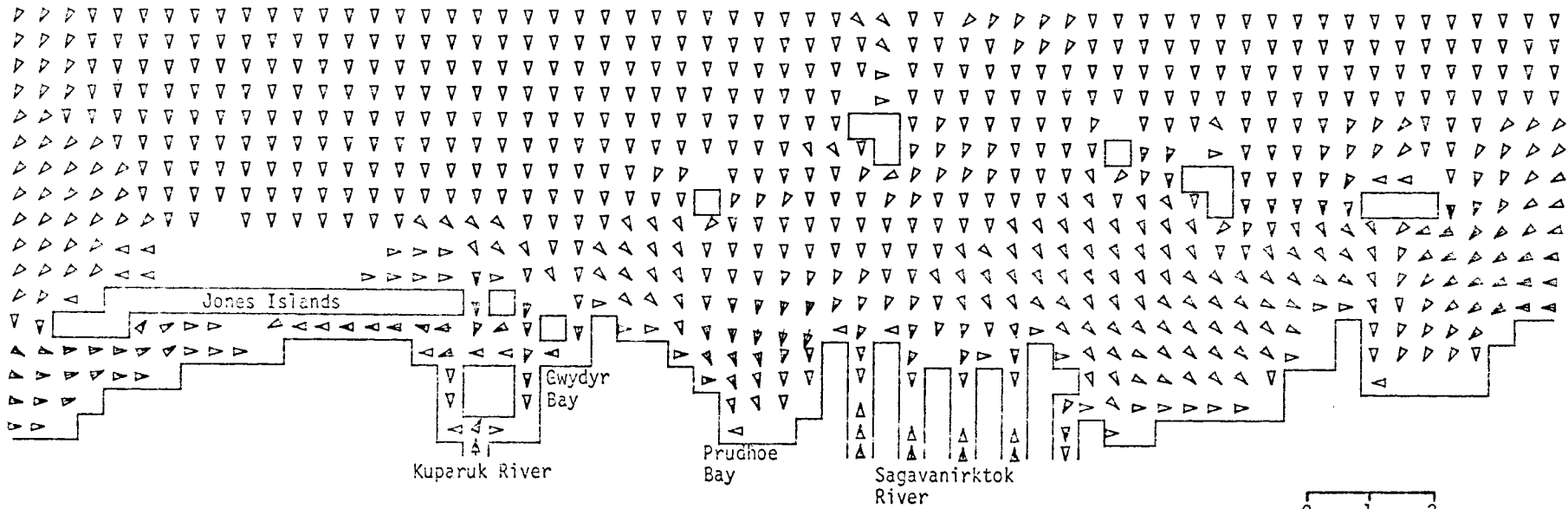
CURRENTS

TIME= 25200SEC

LAYER 1

MODEL NO 310

402



OLIKTOK POINT TO THE CHALLENGE ENTRANCE  
M2 TIDE (AMP=8CM, FROM 22.5 DEG T) RIVER FLOW 5 CM/SEC

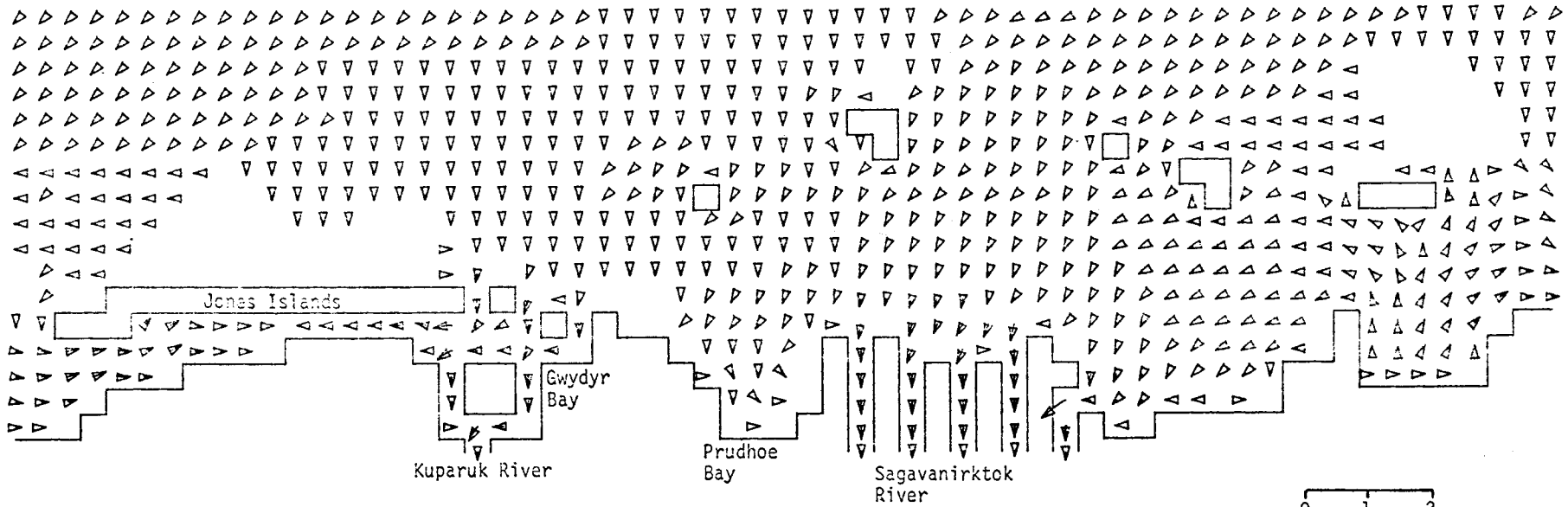
0 1 2  
Knots  
Arrow Scale

505 MODEL NO 310

CURRENTS

TIME= 28800SEC

LAYER 1



OLIKTOK POINT TO THE CHALLENGE ENTRANCE  
M2 TIDE (AMP=8CM, FROM 22.5 DEG T) RIVER FLOW 5 CM/SEC

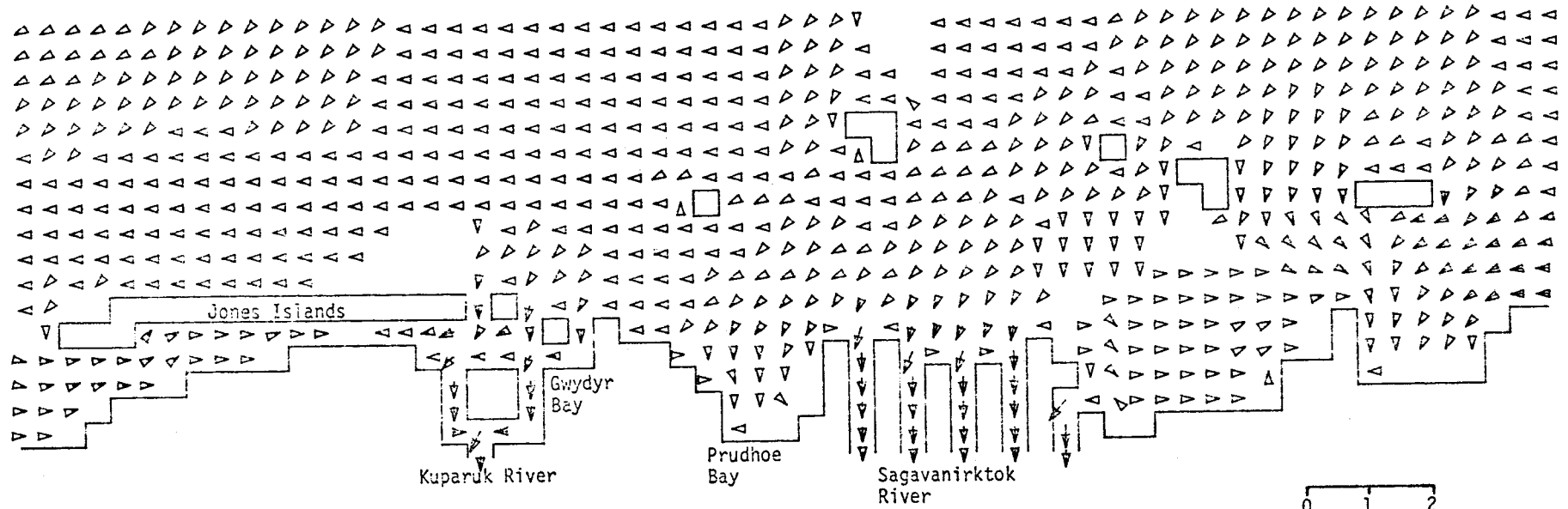
0 1 2  
Knots  
Arrow Scale

CURRENTS

TIME= 32400SEC

LAYER 1

MODEL NO 310



OLIKTOK POINT TO THE CHALLENGE ENTRANCE  
M2 TIDE (AMP=8CM, FROM 22.5 DEG T) RIVER FLOW 5 CM/SEC

0 1 2  
Knots  
Arrow Scale

505

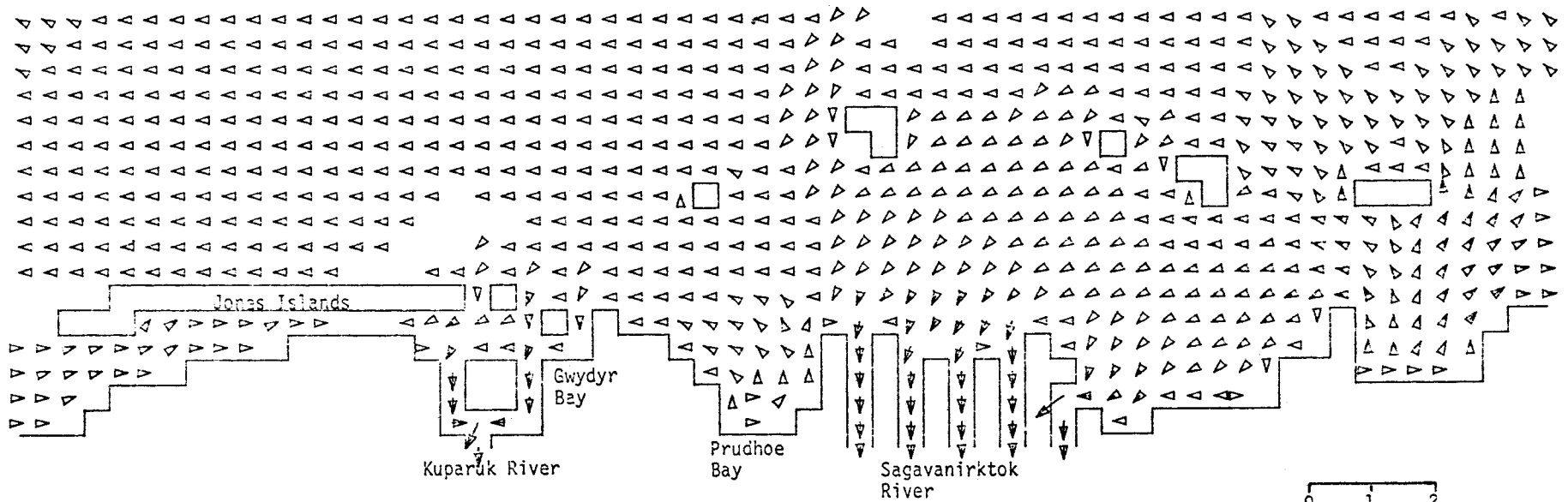


CURRENTS

TIME= 36000SEC

LAYER 1

MODEL NO 310



209

OLIKTOK POINT TO THE CHALLENGE ENTRANCE  
M2 TIDE (AMP=8CM, FROM 22.5 DEG T) RIVER FLOW 5 CM/SEC

0 1 2  
Knots  
Arrow Scale

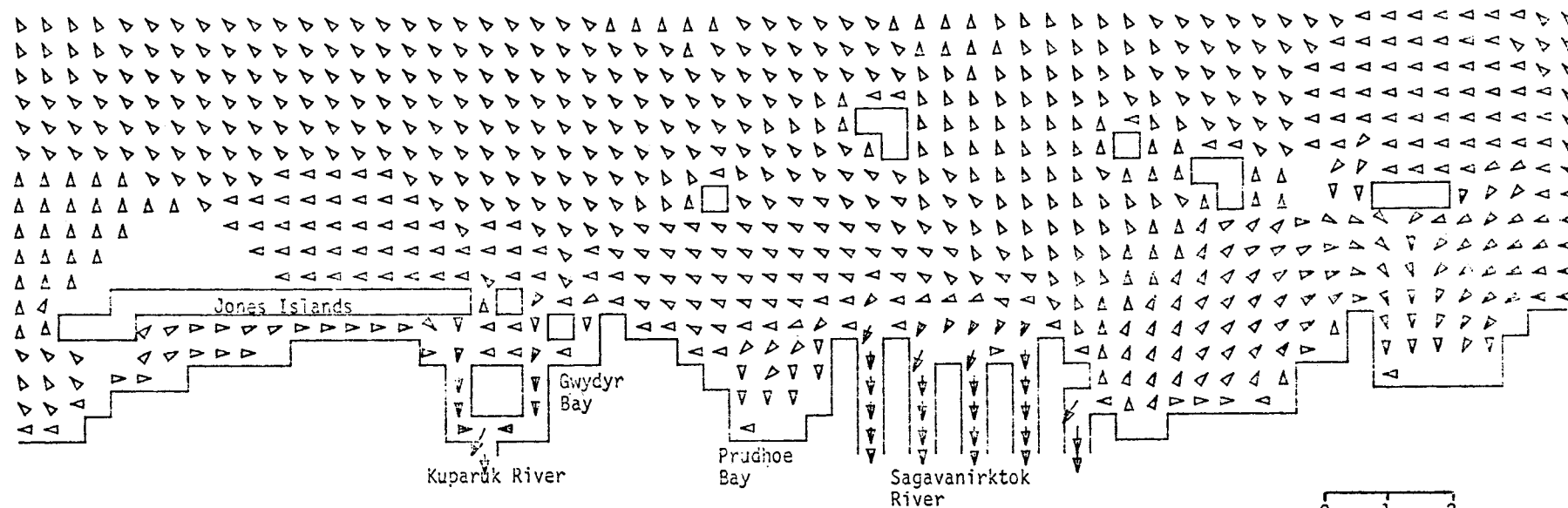
CURRENTS

TIME= 39600SEC

LAYER 1

MODEL NO 310

508



OLIKTOK POINT TO THE CHALLENGE ENTRANCE  
M2 TIDE (AMP=8CM, FROM 22.5 DEG T) RIVER FLOW 5 CM/SEC

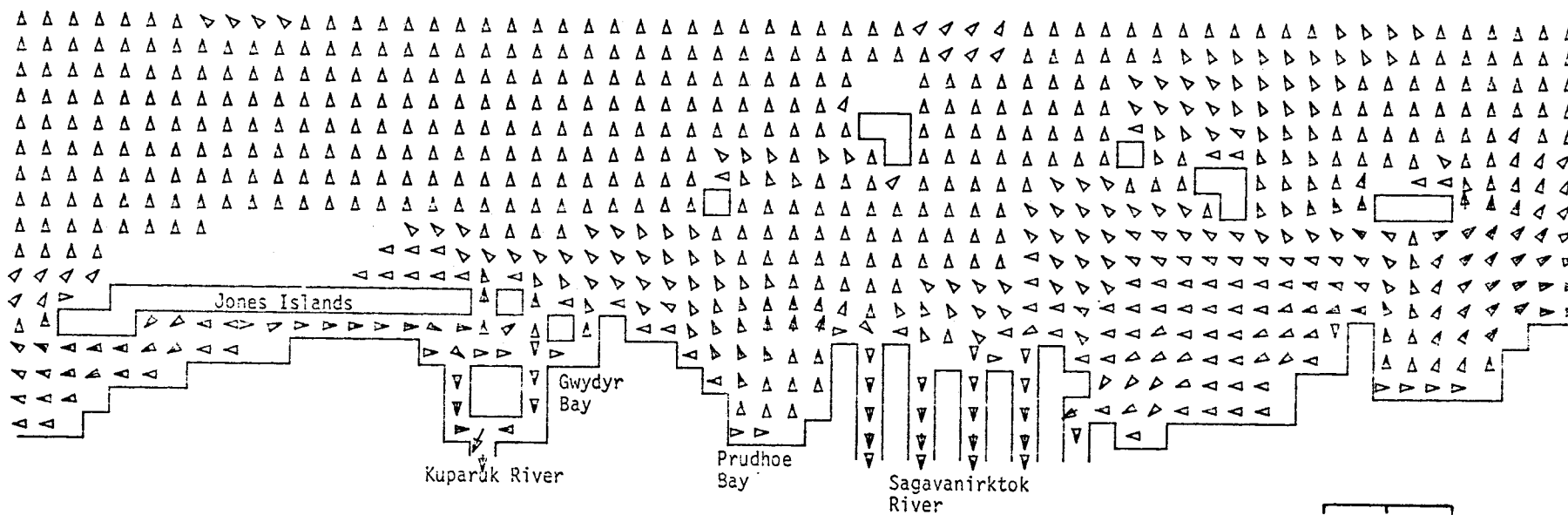
0 1 2  
Knots  
Arrow Scale

CURRENTS

TIME= 43200SEC

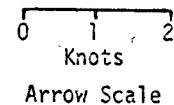
LAYER 1

MODEL NO 310



609

OLIKTOK POINT TO THE CHALLENGE ENTRANCE  
M2 TIDE (AMP=8CM, FROM 22.5 DEG T) RIVER FLOW 5 CM/SEC



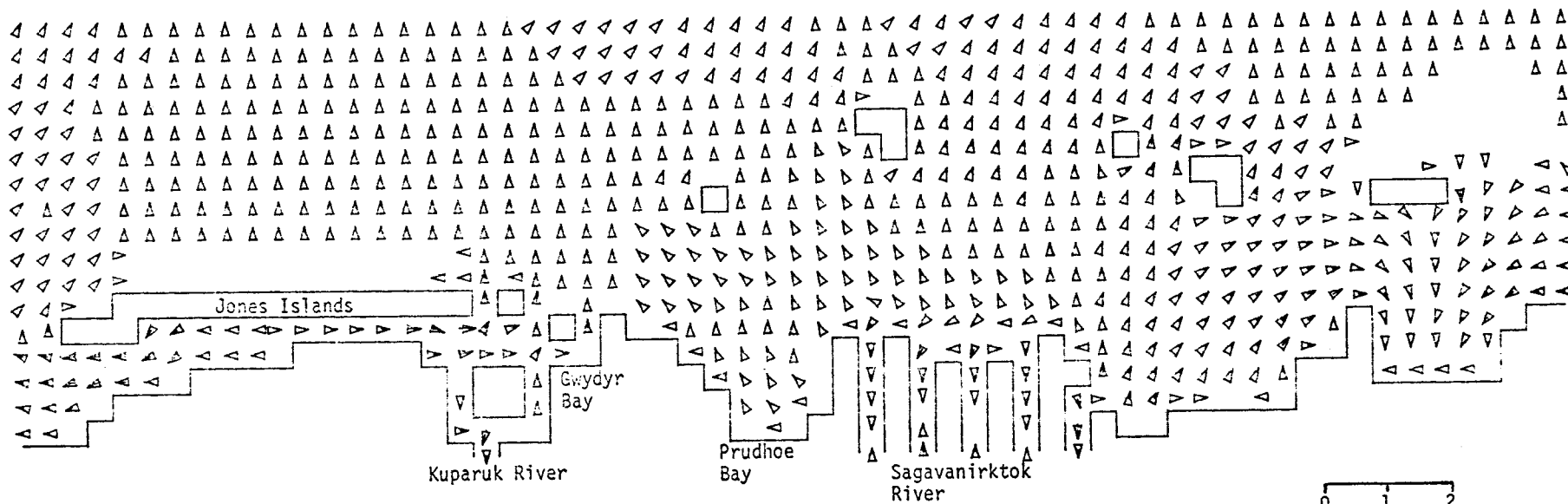
CURRENTS

TIME= 46800SEC

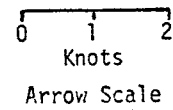
LAYER 1

MODEL NO 310

510



OLIKTOK POINT TO THE CHALLENGE ENTRANCE  
M2 TIDE (AMP=8CM, FROM 22.5 DEG T) RIVER FLOW 5 CM/SEC



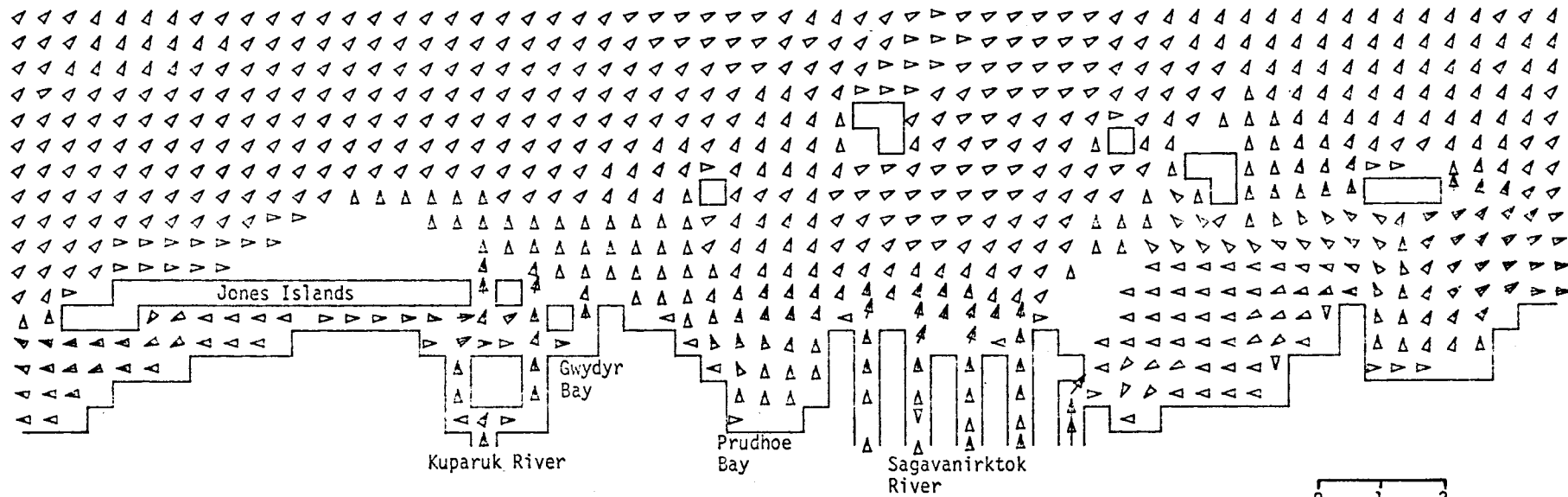
CURRENTS

TIME= 50400SEC

LAYER 1

MODEL NO 310

TTS



OLIKTOK POINT TO THE CHALLENGE ENTRANCE  
M2 TIDE (AMP=8CM, FROM 22.5 DEG T) RIVER FLOW 5 CM/SEC

0 1 2  
Knots  
Arrow Scale

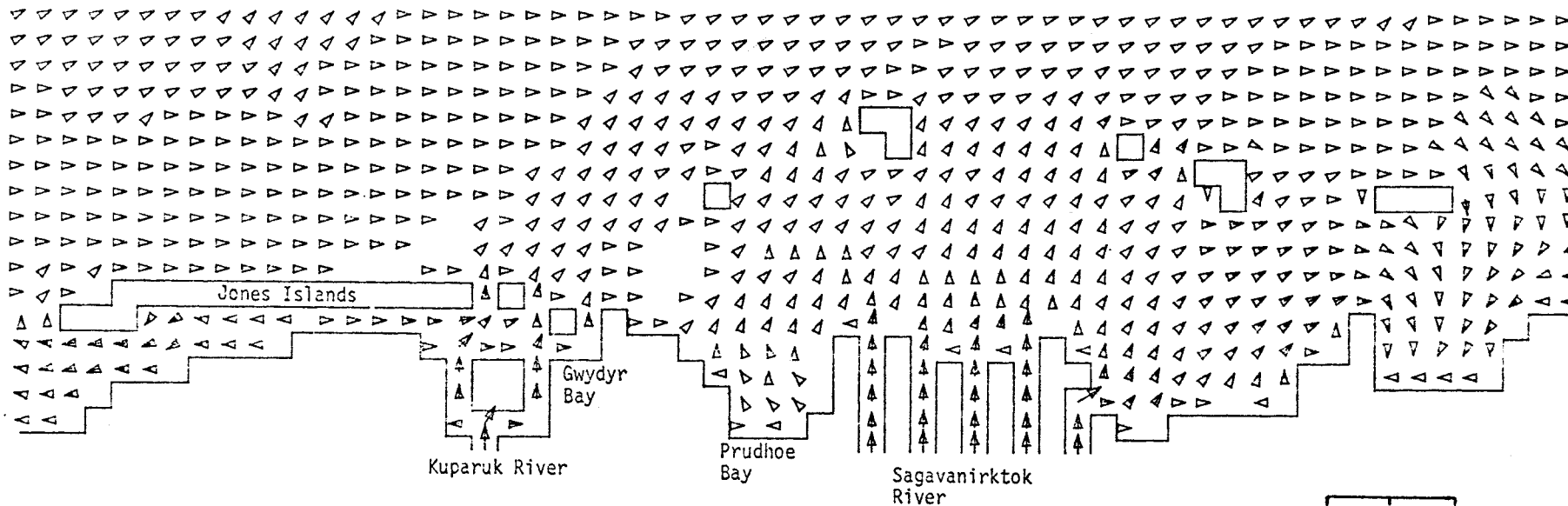
CURRENTS

TIME= 54000SEC

LAYER 1

MODEL NO 310

512



OLIKTOK POINT TO THE CHALLENGE ENTRANCE  
M2 TIDE (AMP=8CM, FROM 22.5 DEG T) RIVER FLOW 5 CM/SEC

0 1 2  
Knots  
Arrow Scale

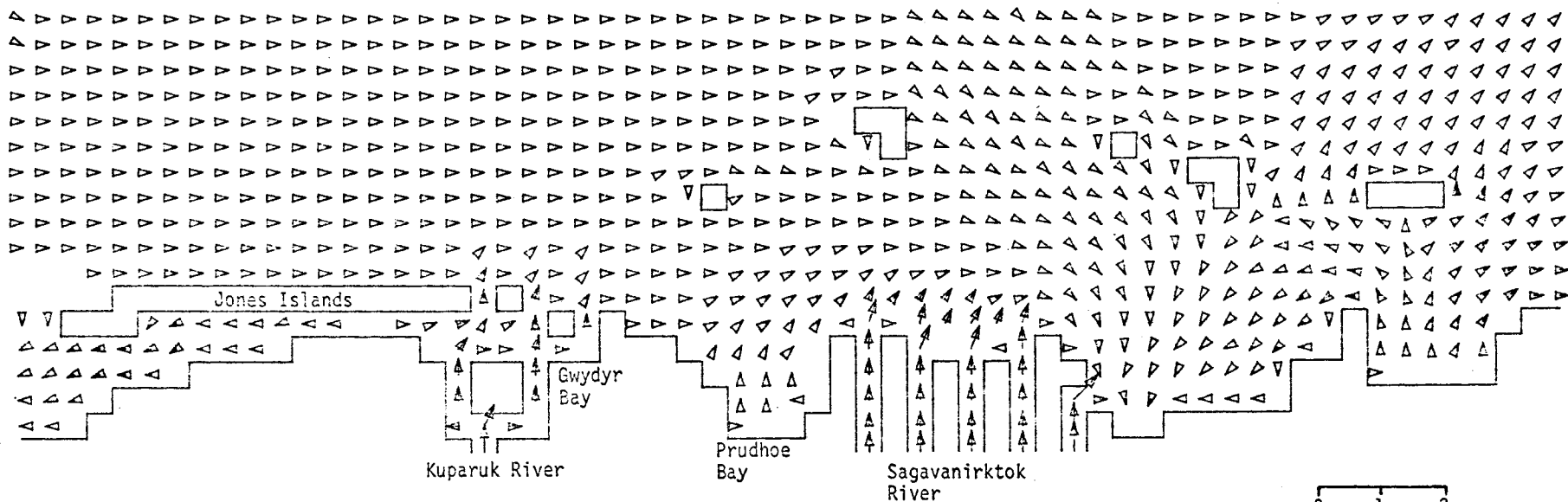
CURRENTS

TIME= 57600SEC

LAYER 1

MODEL NO. J10

513



OLIKTOK POINT TO THE CHALLENGE ENTRANCE  
M2 TIDE (AMP=8CM, FROM 22.5 DEG T) RIVER FLOW 5 CM/SEC

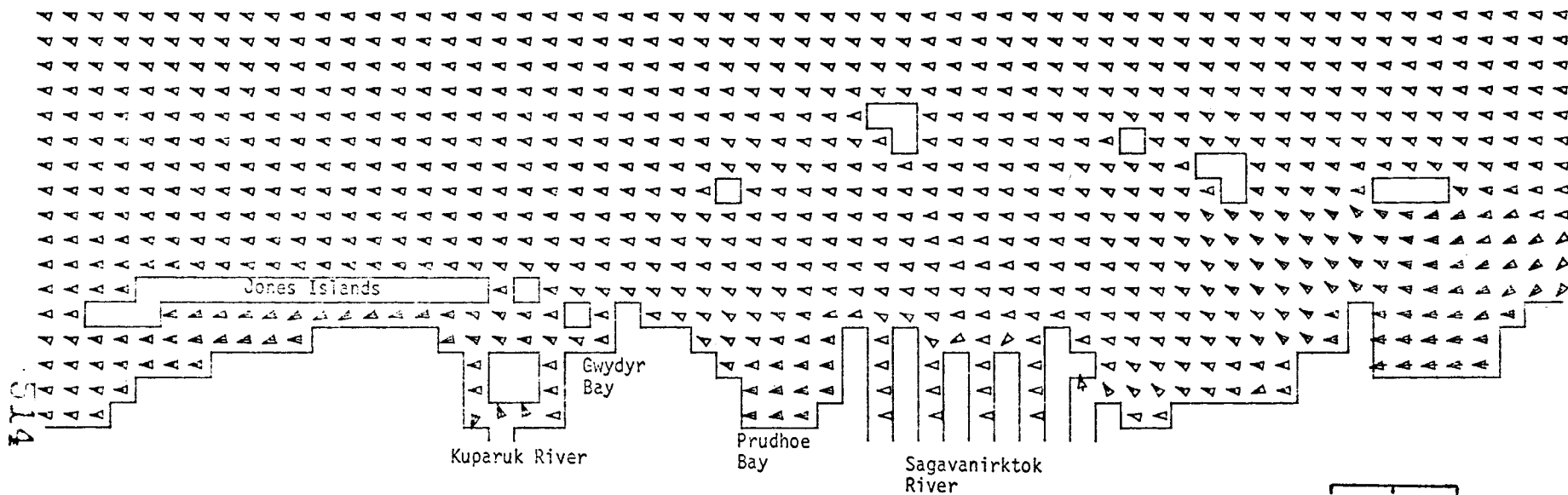
0 1 2  
Knots  
Arrow Scale

CURRENTS

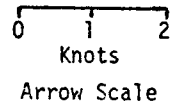
TIME= 61200SEC

LAYER 1

MODEL NO 310



OLIKTOK POINT TO THE CHALLENGE ENTRANCE  
M2 TIDE (AMP=8CM, FROM 22.5 DEG T) RIVER FLOW 5 CM/SEC





APPENDIX B

OLIKTOK POINT TO THE CHALLENGE ENTRANCE

M2 TIDE WITH 8 CM AMPLITUDE

River Flow at 5 cm/sec

10 Kt Wind From NE

SEA LEVEL

ENVIRONMENTAL PROTECTION AGENCY  
MARINE AND FRESHWATER ECOLOGY BRANCH  
OCEAN MASS TRANSPORT MODEL

M2 TIDE (AMP=8CM, FROM 22.5 DEG T) RIVER FLOW=5CM/SEC WIND FROM NE AT 10 KT  
BEAUFORT SEA SHELF STUDY  
GRID 310 GLIKTOR POINT TO THE CHALLENGE ENTRANCE

|                       |      |                 |                |    |                 |
|-----------------------|------|-----------------|----------------|----|-----------------|
| GRID GEOMETRY         | ROWS | 18              | COLUMNS        | 61 |                 |
| GRID LENGTH           |      | 200000. CM      | ROTATION ANGLE |    | 337.5 DEG       |
| WIND DRAG COEFFICIENT |      | .0024           | MID LATITUDE   |    | 70.500 DEG. (N) |
| FRICTION COEFFICIENT  |      | .0030000 CM/SEC |                |    |                 |

|                      |           |         |         |
|----------------------|-----------|---------|---------|
|                      | LAYER 1   | LAYER 2 | LAYER 3 |
| INITIAL LAYER DEPTHS | 3000.0000 | .0000   | .0000   |
| SMOOTHING FACTORS    | .9400     | .0000   | .0000   |
| DENSITY              | 1.0250    | .0000   | .0000   |

|                                 |             |                           |          |
|---------------------------------|-------------|---------------------------|----------|
| RESULTS SAVED AT MODULUS (TIME, | 3600 SEC)=0 | RESULTS SAVED STARTING AT | 3600 SEC |
| COMPUTATIONS STARTED AT         | 0 SEC       |                           |          |
| ENDED AT                        | 64800 SEC   |                           |          |
| INCREMENTED BY                  | 60 SEC      |                           |          |
| LAYER3 PRINT OUT STARTED        |             | 3600 SEC. FREQUENCY OF    | 3600 SEC |

|                               |     |        |          |        |          |     |          |       |
|-------------------------------|-----|--------|----------|--------|----------|-----|----------|-------|
| TIDAL INPUT AT                | ROW | 1 THRU | 1        | COLUMN | 1 THRU   | 61  | TIME LAG | 0 SEC |
|                               |     |        | M2       |        | S2       | U1  | K1       |       |
| PHASE ANGLES (DEG/HR)         |     |        | 270.00   |        | .00      | .00 | .00      |       |
| AMPLITUDES (CM)               |     |        | 8.00     |        | .00      | .00 | .00      |       |
| LOWER LAYER WEIGHTING FACTORS |     |        | LAYER 2= | .00    | LAYER 3= | .00 |          |       |

|                      |           |         |         |         |
|----------------------|-----------|---------|---------|---------|
| TIDAL SPEEDS (CM/HR) | M2        | S2      | U1      | K1      |
|                      | 24.984000 | .000000 | .000000 | .000000 |

|                         |     |        |           |           |        |      |       |         |
|-------------------------|-----|--------|-----------|-----------|--------|------|-------|---------|
| WIND INPUT AT           | ROW | 1 THRU | 18        | COLUMN    | 1 THRU | 61   |       |         |
| COMPUTATIONS STARTED AT |     |        | 60 SEC    |           |        |      |       |         |
| ENDED AT                |     |        | 64800 SEC | DIRECTION | 45 DEG | TRUE | SPEED | 5 M/SEC |

|                         |         |    |              |          |    |        |        |            |
|-------------------------|---------|----|--------------|----------|----|--------|--------|------------|
| FLOW INPUT AT ROW       | 18 THRU | 18 | COLUMN       | 19 THRU  | 19 | LAYERS | 1 THRU | 1          |
| COMPUTATIONS STARTED AT |         |    | 60 SEC       |          |    |        |        |            |
| ENDED AT                |         |    | 64800 SEC    |          |    |        |        |            |
| DIRECTION               |         |    | 22.5000 TRUE | VELOCITY |    |        |        | 5.0 CM/SEC |

|                         |         |    |              |          |    |        |        |            |
|-------------------------|---------|----|--------------|----------|----|--------|--------|------------|
| FLOW INPUT AT ROW       | 18 THRU | 18 | COLUMN       | 34 THRU  | 42 | LAYERS | 1 THRU | 1          |
| COMPUTATIONS STARTED AT |         |    | 60 SEC       |          |    |        |        |            |
| ENDED AT                |         |    | 64800 SEC    |          |    |        |        |            |
| DIRECTION               |         |    | 22.5000 TRUE | VELOCITY |    |        |        | 5.0 CM/SEC |

ASSIGNED MODEL NUMBER 310

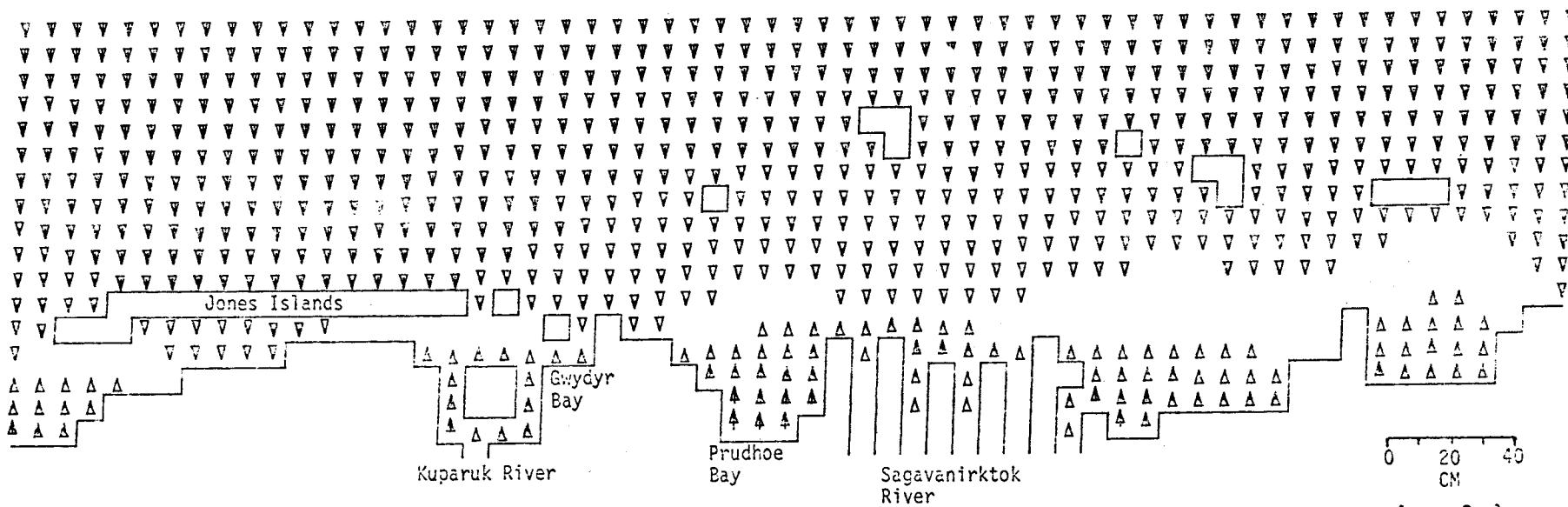
SEA LEVEL

TIME= 3600SEC

LAYER 1

MODEL NO 310

515



OLIKTOK POINT TO THE CHALLENGE ENTRANCE  
M2 TIDE (AMP=8CM, FROM 22.5 DEG T) RIVER FLOW=5CM/SEC WIND FROM NE AT 10 KT

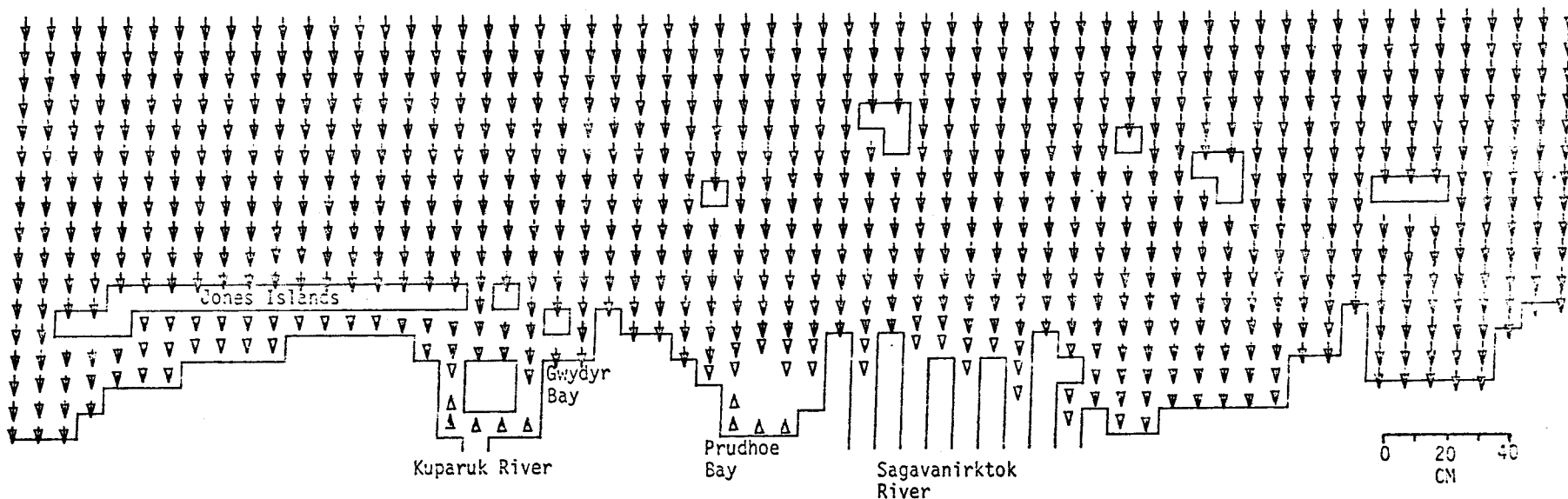
SEA LEVEL

TIME= 7200SEC

LAYER 1

MODEL NO 310

675



OLIKTOK POINT TO THE CHALLENGE ENTRANCE  
M2 TIDE (AMP=8CM, FROM 22.5 DEG T) RIVER FLOW=5CM/SEC WIND FROM NE AT 10 KT

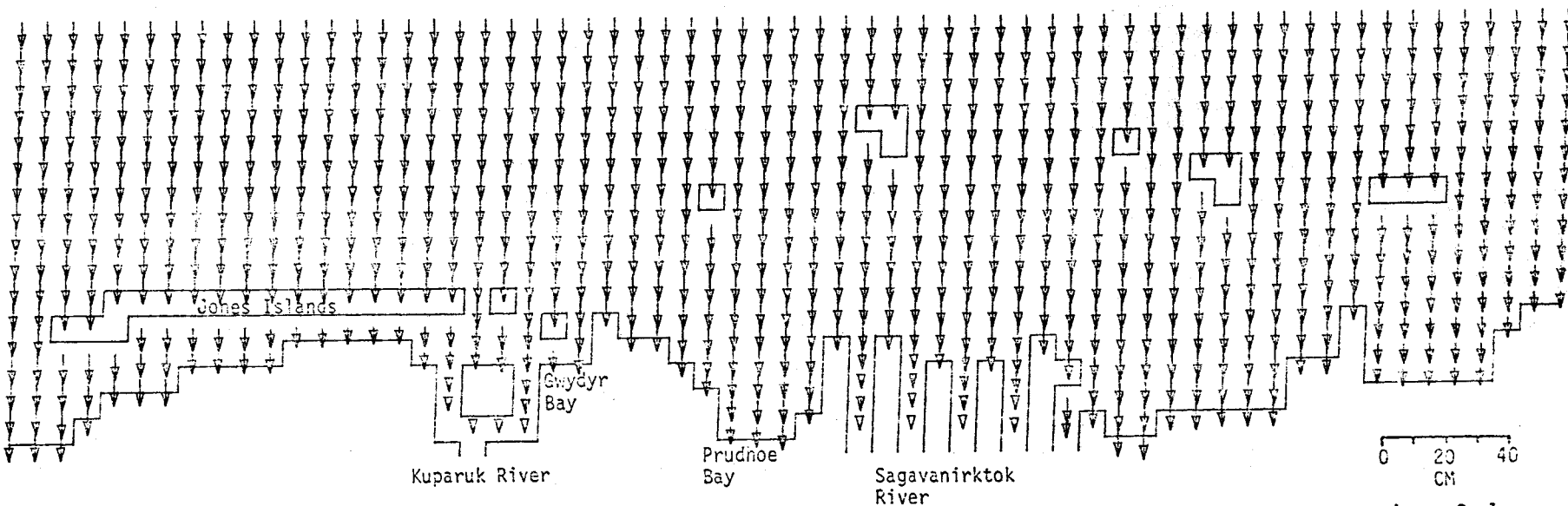
SEA LEVEL

TIME= 10800SEC

LAYER 1

MODEL NO 310

520



OLIKTOK POINT TO THE CHALLENGE ENTRANCE  
M2 TIDE (AMP=8CM, FROM 22.5 DEG T) RIVER FLOW=5CM/SEC WIND FROM NE AT 10 KT

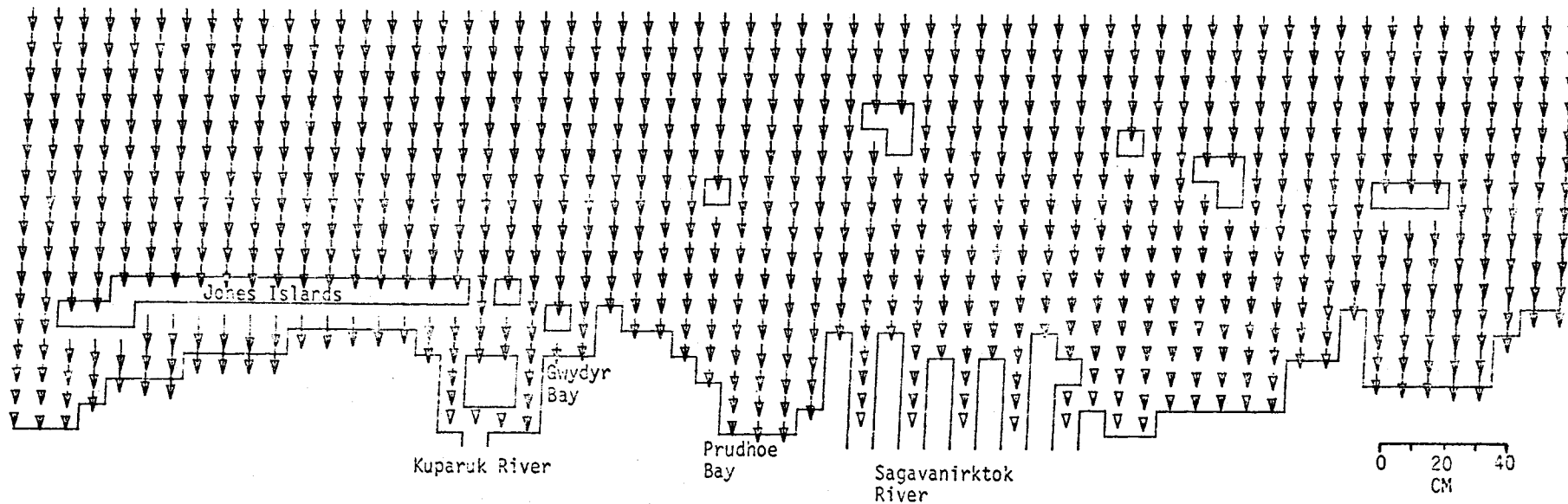
SEA LEVEL

TIME= 14400SEC

LAYER 1

MODEL NO 310

521



OLIKTOK POINT TO THE CHALLENGE ENTRANCE  
M2 TIDE (AMP=8CM, FROM 22.5 DEG T) RIVER FLOW=5CM/SEC WIND FROM NE AT 10 KT

0 20 40  
CM  
Arrow Scale

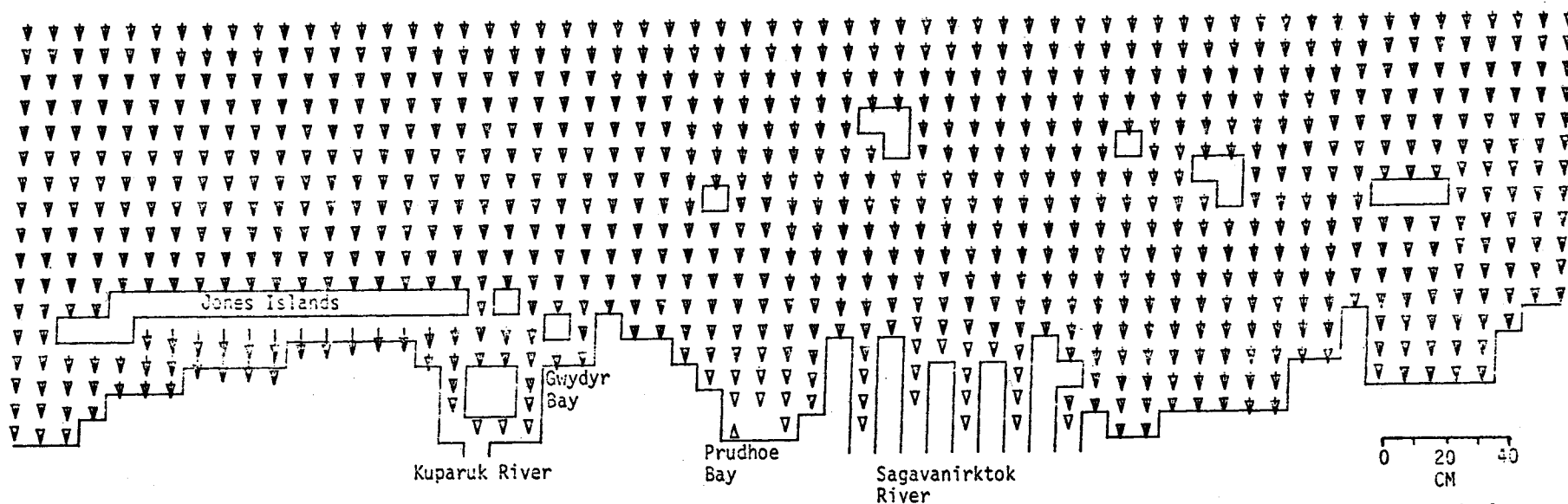
SEA LEVEL

TIME= 18000SEC

LAYER 1

MODEL NO 310

229



GLIKTOK POINT TO THE CHALLENGE ENTRANCE  
M2 TIDE (AMP=8CM, FROM 22.5 DEG T) RIVER FLOW=5CM/SEC WIND FROM NE AT 10 KT

0 20 40  
CM  
Arrow Scale

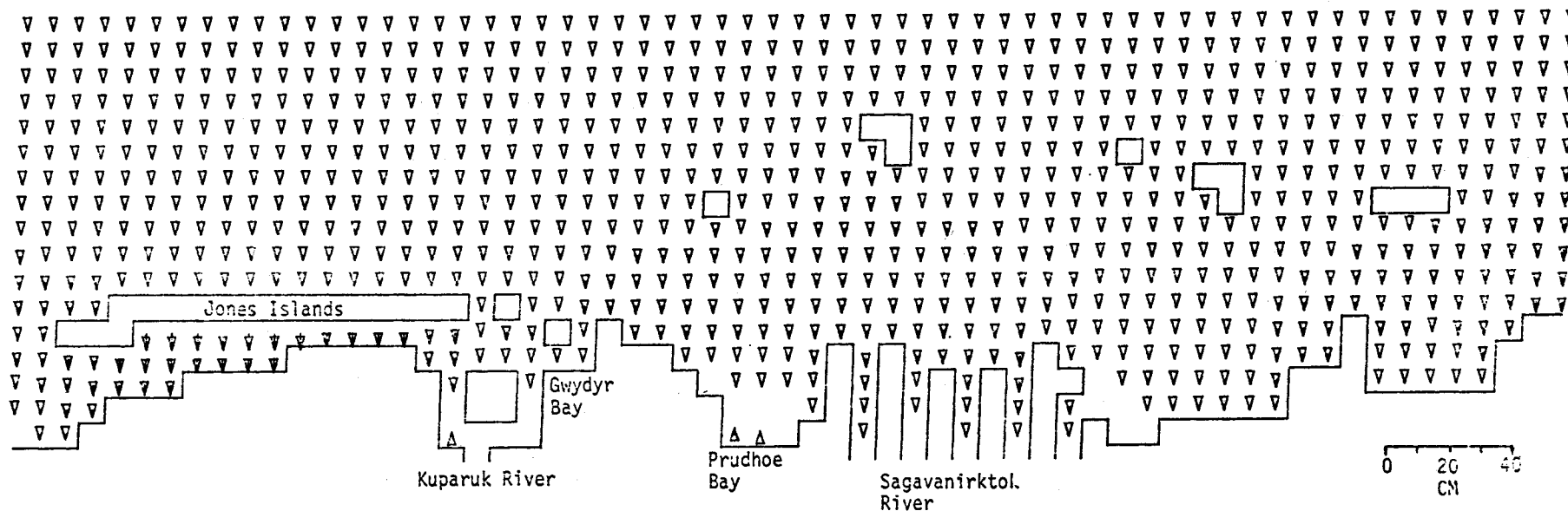


SEA LEVEL

TIME= 21600SEC

LAYER 1

MODEL NO 310  
523



OLIKTOK POINT TO THE CHALLENGE ENTRANCE  
M2 TIDE (AMP=8CL\*FROM 22.5 DEG T) RIVER FLOW=5CM/SEC WIND FROM NE AT 10 KT

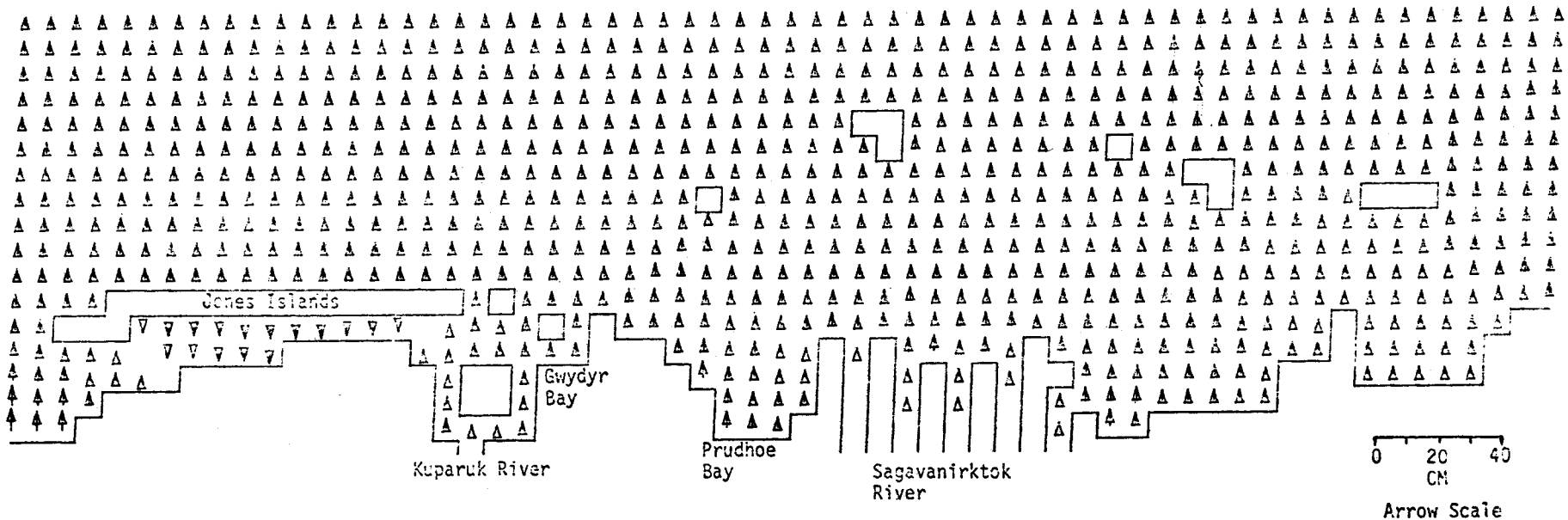
SEA LEVEL

TIME= 25200SEC

LAYER 1

MOD'L NO 310

524



OLIKTOK POINT TO THE CHALLENGE ENTRANCE  
M2 TIDE (AMP=8CM, FROM 22.5 DEG T) RIVER FLOW=5CM/SEC WIND FROM NE AT 10 KT

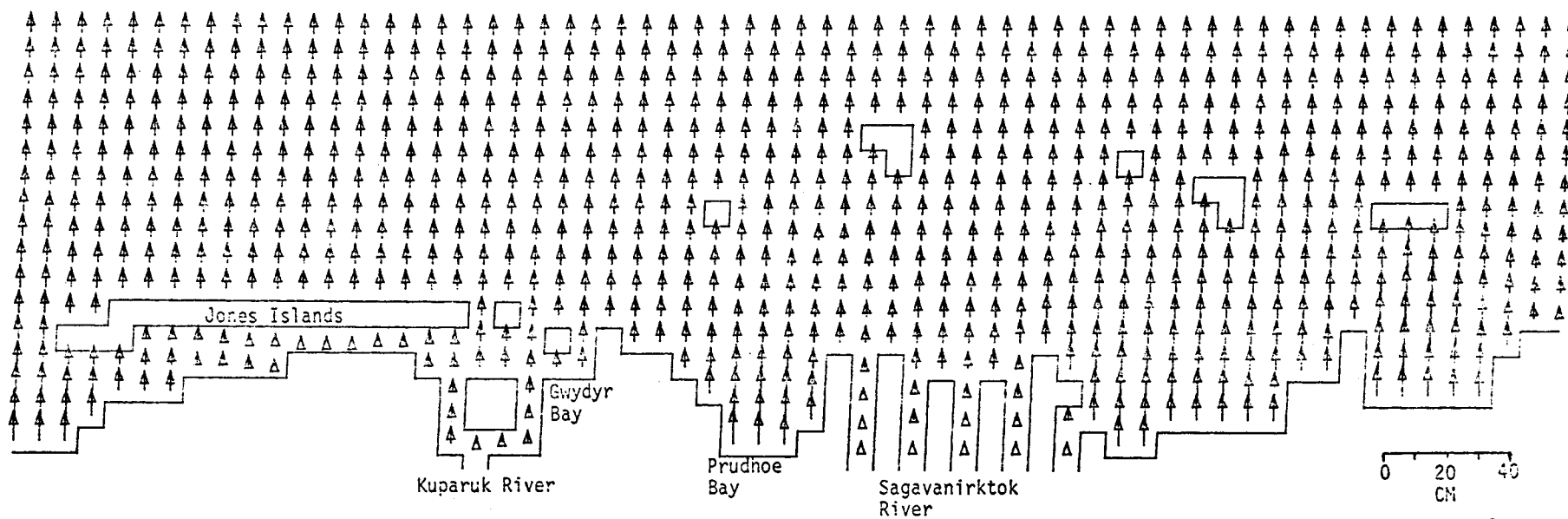
SEA LEVEL

TIME= 28800SEC

LAYER 1

MODEL NO 310

525

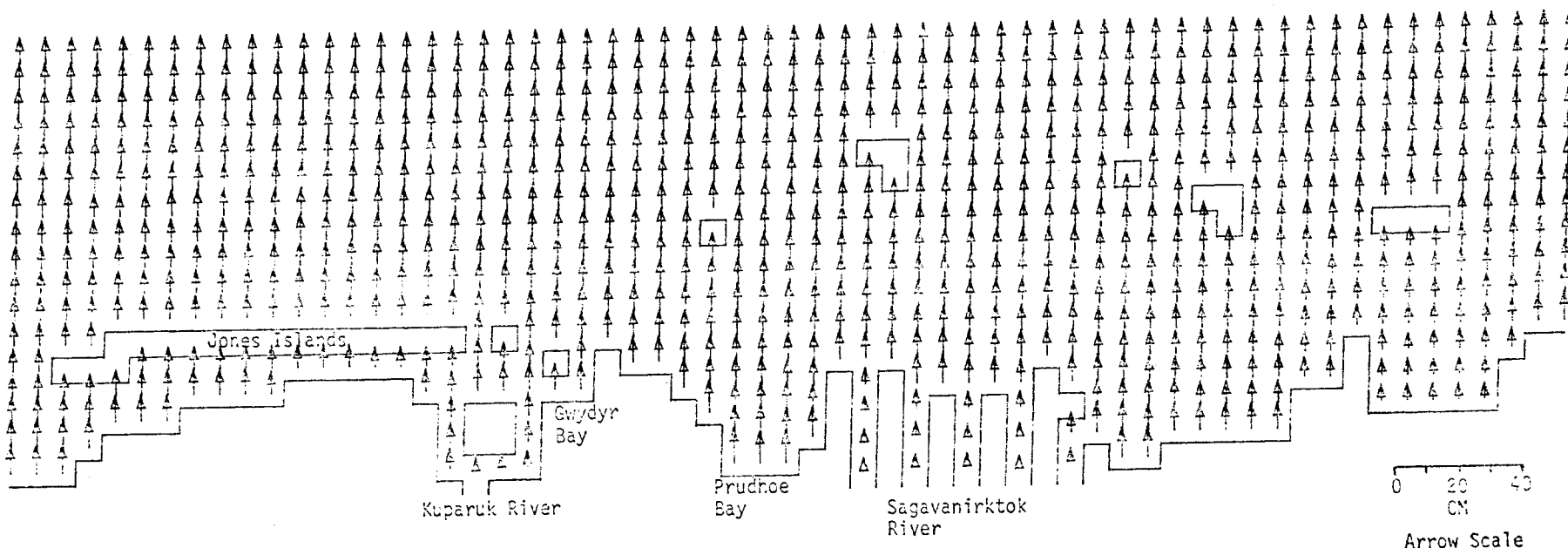


OLIKTOK POINT TO THE CHALLENGE ENTRANCE  
M2 TIDE (AMP=8CM, FROM 22.5 DEG T) RIVER FLOW=5CM/SEC WIND FROM NE AT 10 KT

SEA LEVEL

TIME= 32400SEC

LAYER 1



OLIKYOK POINT TO THE CHALLENGE ENTRANCE  
M2 TIDE (AMP=8CM, FROM 22.5 DEG T) RIVER FLOW=5CM/SEC WIND FROM NE AT 10 KT

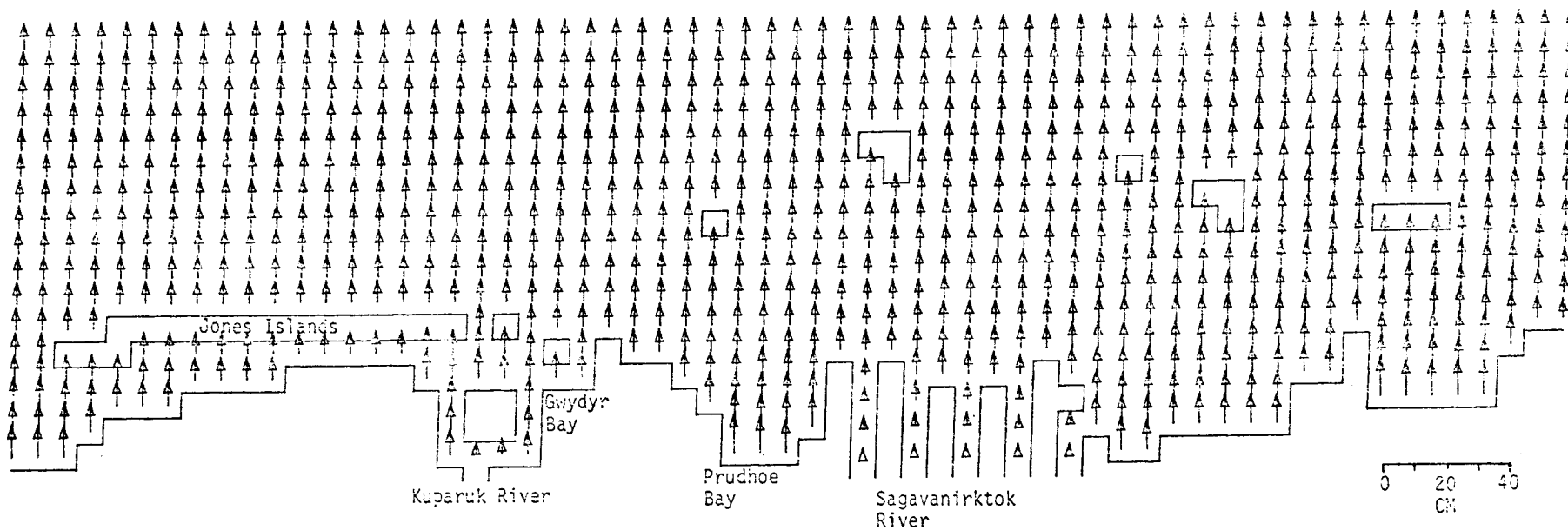
MODEL NO 310

900

SEA LEVEL

TIME= 36000SEC

LAYER 1



OLIKTOK POINT TO THE CHALLENGE ENTRANCE  
M2 TIDE (AMP=8CM, FROM 22.5 DEG T) RIVER FLOW=5CM/SEC WIND FROM NE AT 10 KT

MODEL NO 310

725

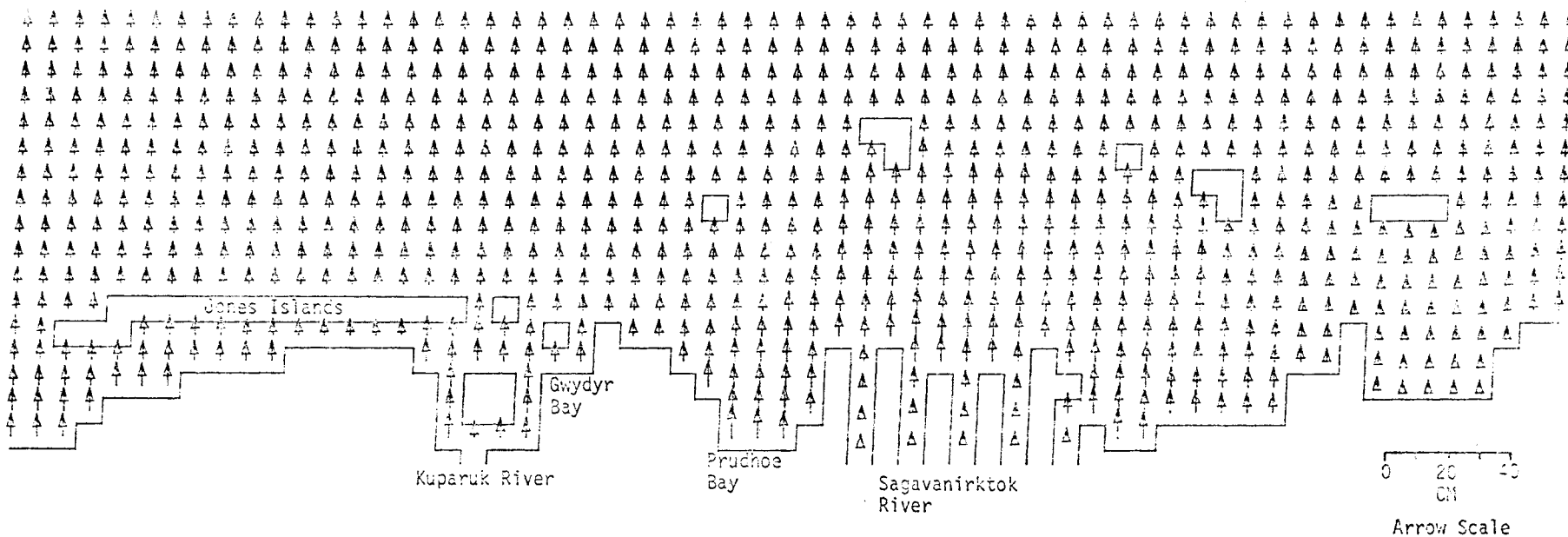
SEA LEVEL

TIME= 39600SEC

LAYER 1

MODEL NO 310

88

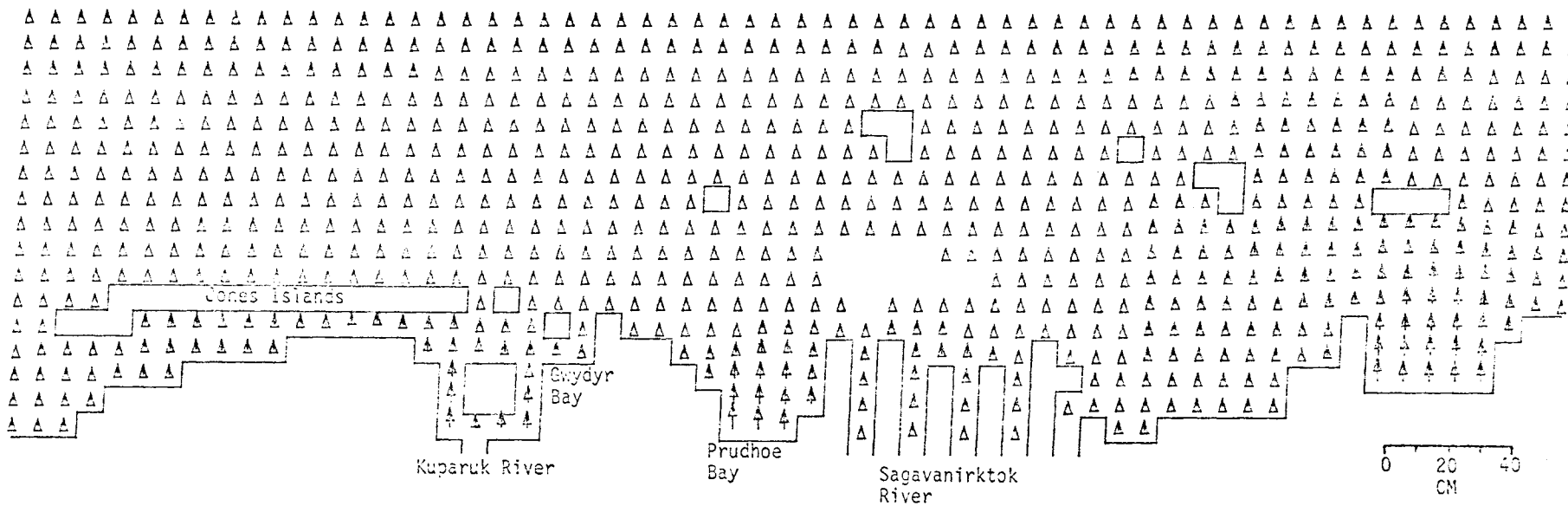


OLIKTOK POINT TO THE CHALLENGE ENTRANCE  
M2 TIDE (AMP=3CM, FROM 22.5 DEG T) RIVER FLOW=5CM/SEC WIND FROM NE AT 10 KT

SEA LEVEL

TIME= 43200SEC

LAYER 1



OLIKTOK POINT TO THE CHALLENGE ENTRANCE  
M2 TIDE (AMP=3CM, FROM 22.5 DEG T) RIVER FLOW=5CM/SEC WIND FROM NE AT 10 KT

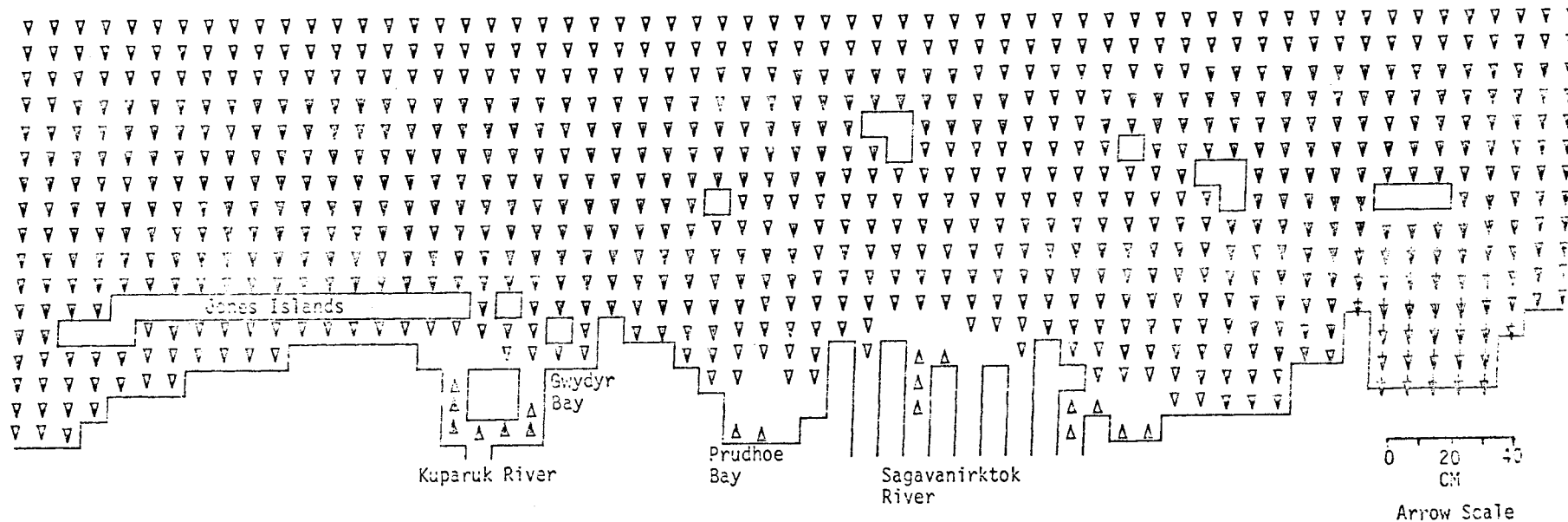
SEA LEVEL

TIME= 46800SEC

LAYER 1

MODEL NO 310

0830



OLIKTOK POINT TO THE CHALLENGE ENTRANCE  
M2 TIDE (AMP=8CM, FROM 22.5 DEG T) RIVER FLOW=5CM/SEC WIND FROM NE AT 10 KT



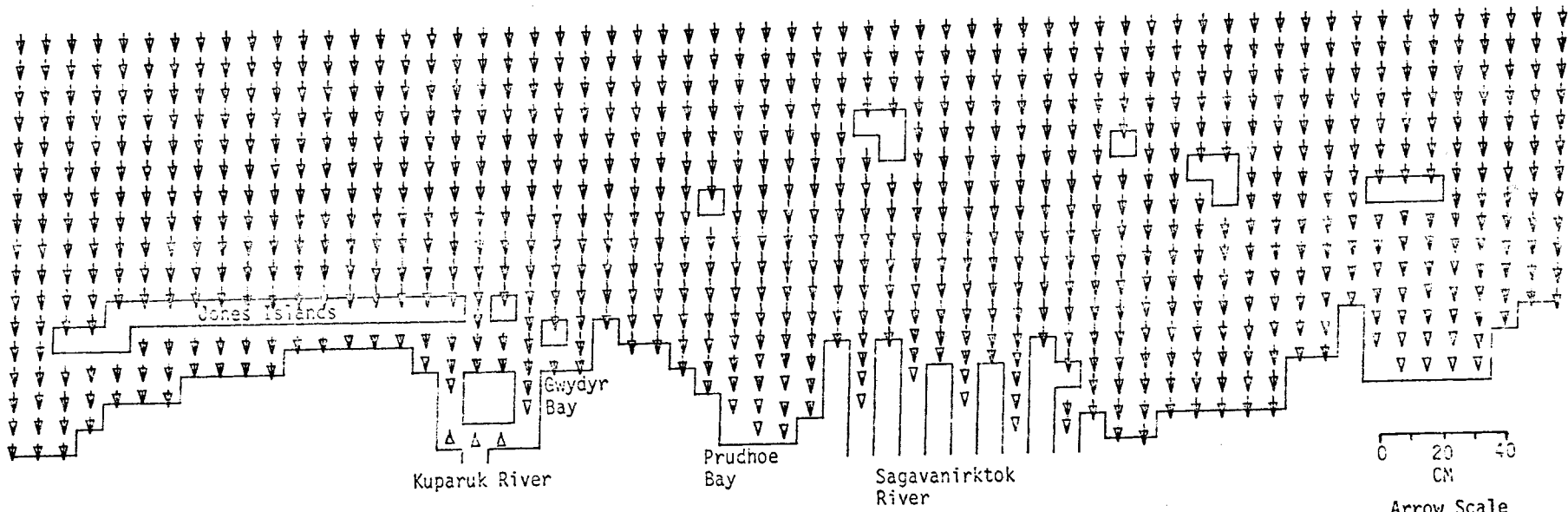
SEA LEVEL

TIME= 50400SEC

LAYER 1

MODEL No. 310

TCS



OLIKTOK POINT TO THE CHALLENGE ENTRANCE  
M2 TIDE (AMP=8CM, FROM 22.5 DEG T) RIVER FLOW=5CM/SEC WIND FROM NE AT 10 KT

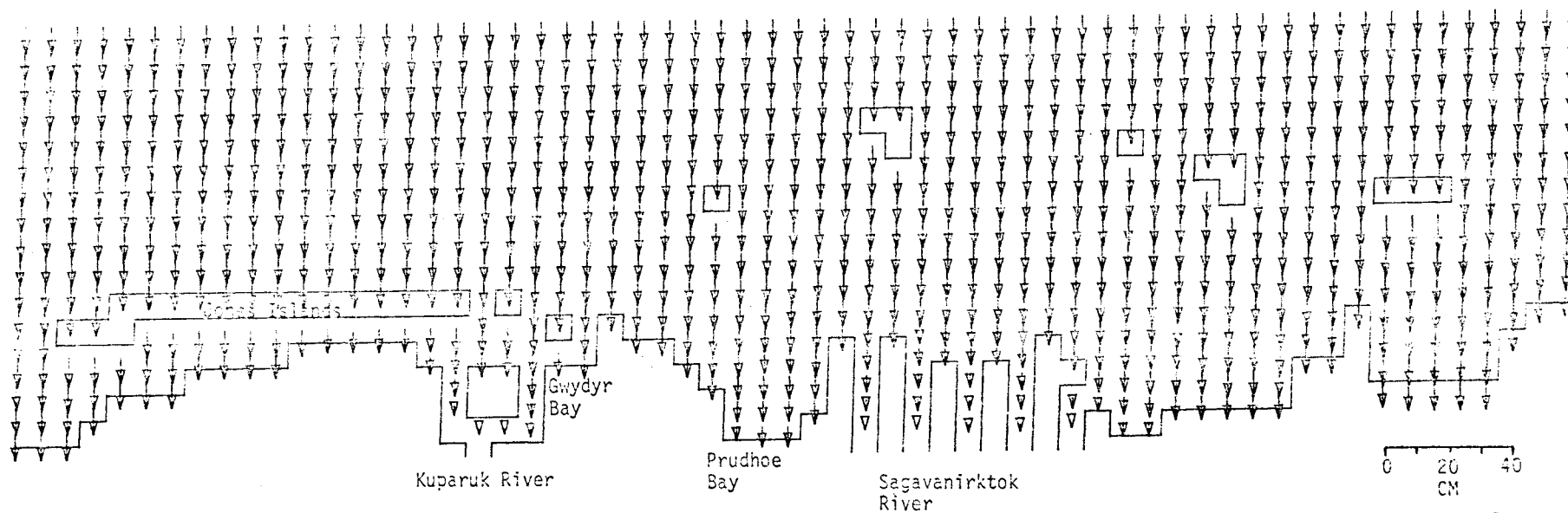
MODEL NO 310

532

SEA LEVEL

TIME= 54000SEC

LAYER 1



OLIKTOK POINT TO THE CHALLENGE ENTRANCE  
M2 TIDE (AMP=8CM, FROM 22.5 DEG T) RIVER FLOW=5CM/SEC WIND FROM NE AT 10 KT

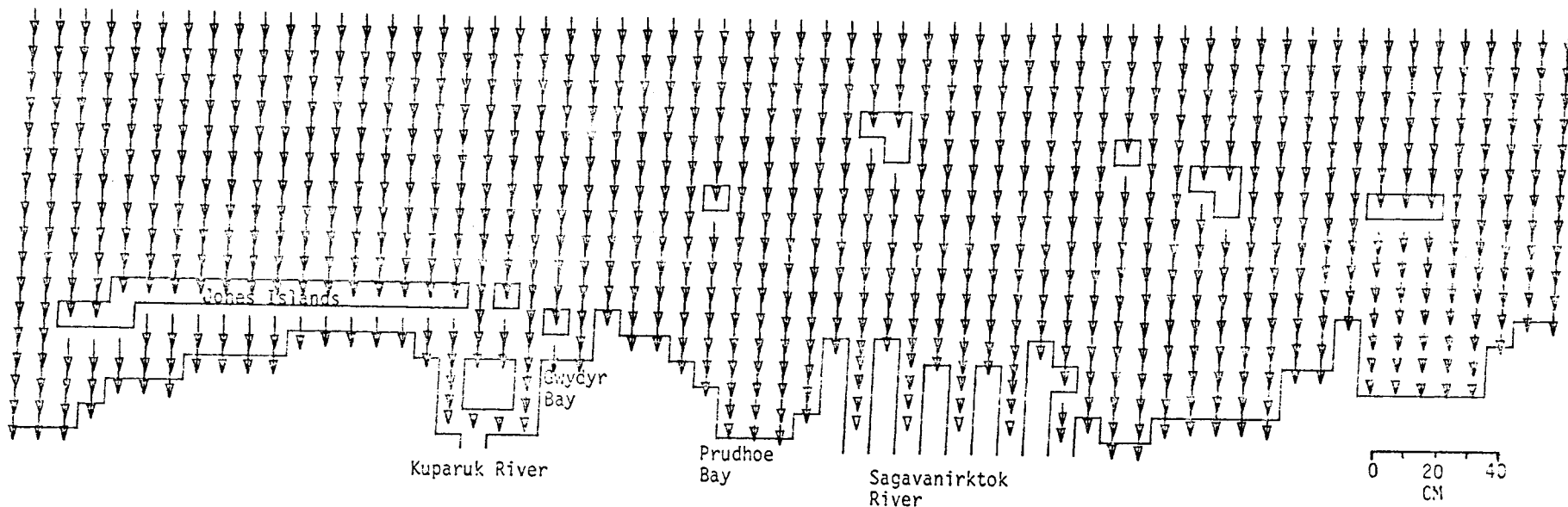
SEA LEVEL

TIME= 57600SEC

LAYER 1

MODEL NO 310

535



OLIKTOK POINT TO THE CHALLENGE ENTRANCE  
M2 TIDE (AMP=8CM, FROM 22.5 DEG T) RIVER FLOW=5CM/SEC WIND FROM NE AT 10 KT

0 20 40  
CM  
Arrow Scale

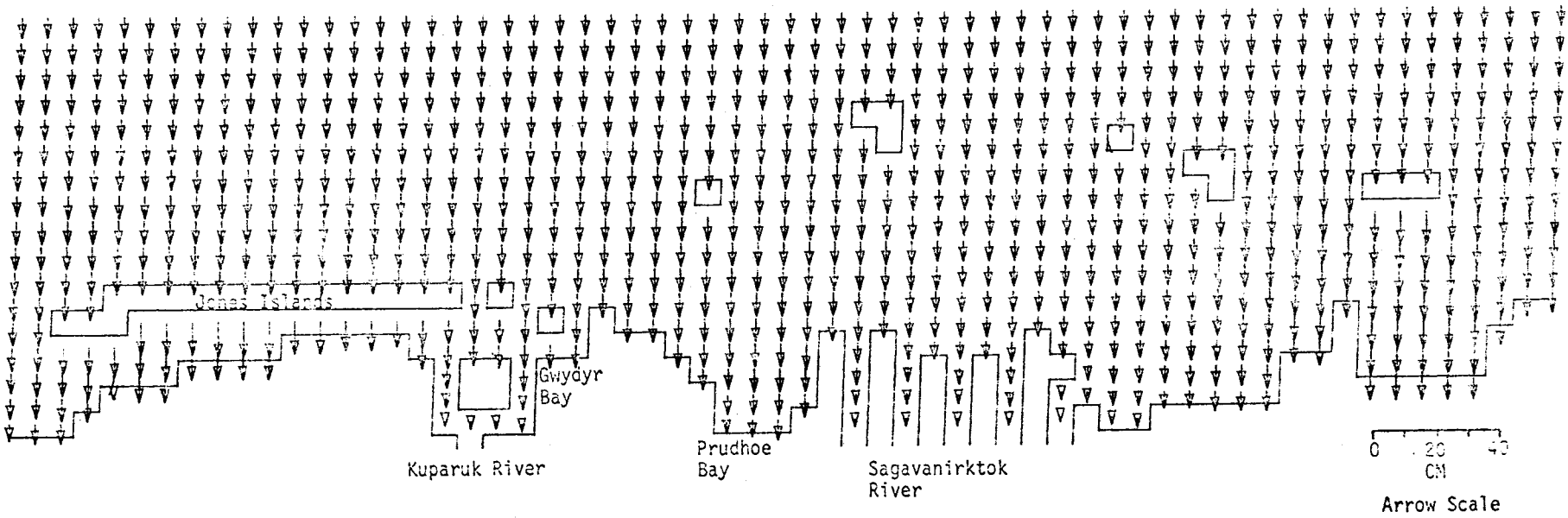
MODEL NO 310

7534

SEA LEVEL

TIME= 61200SEC

LAYER 1



OLIKTOK POINT TO THE CHALLENGE ENTRANCE  
M2 TIDE (AMP=8CM, FROM 22.5 DEG T) RIVER FLOW=5CM/SEC WIND FROM NE AT 10 KT

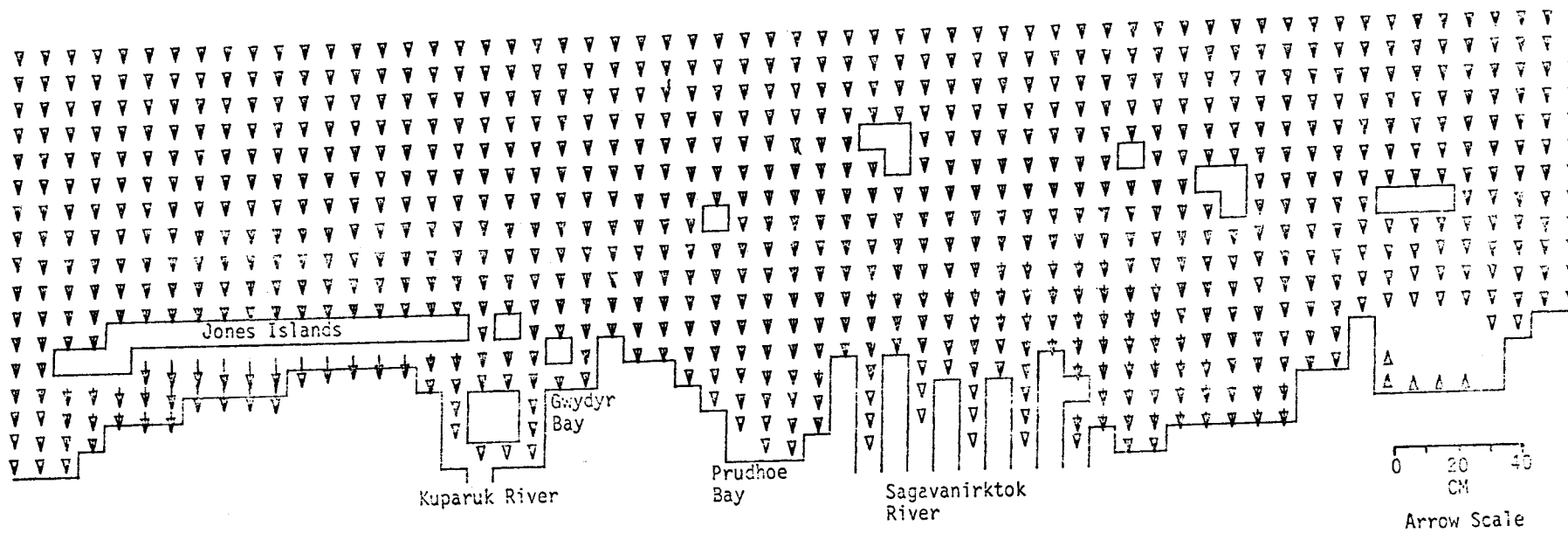
SEA LEVEL

TIME= 64800SEC

LAYER 1

MODEL NO 310

535



OLIKTOK POINT TO THE CHALLENGE ENTRANCE  
M2 TIDE (AMP=8CM, FROM 22.5 DEG T) RIVER FLOW=5CM/SEC WIND FROM NE AT 10 KT

CURRENTS

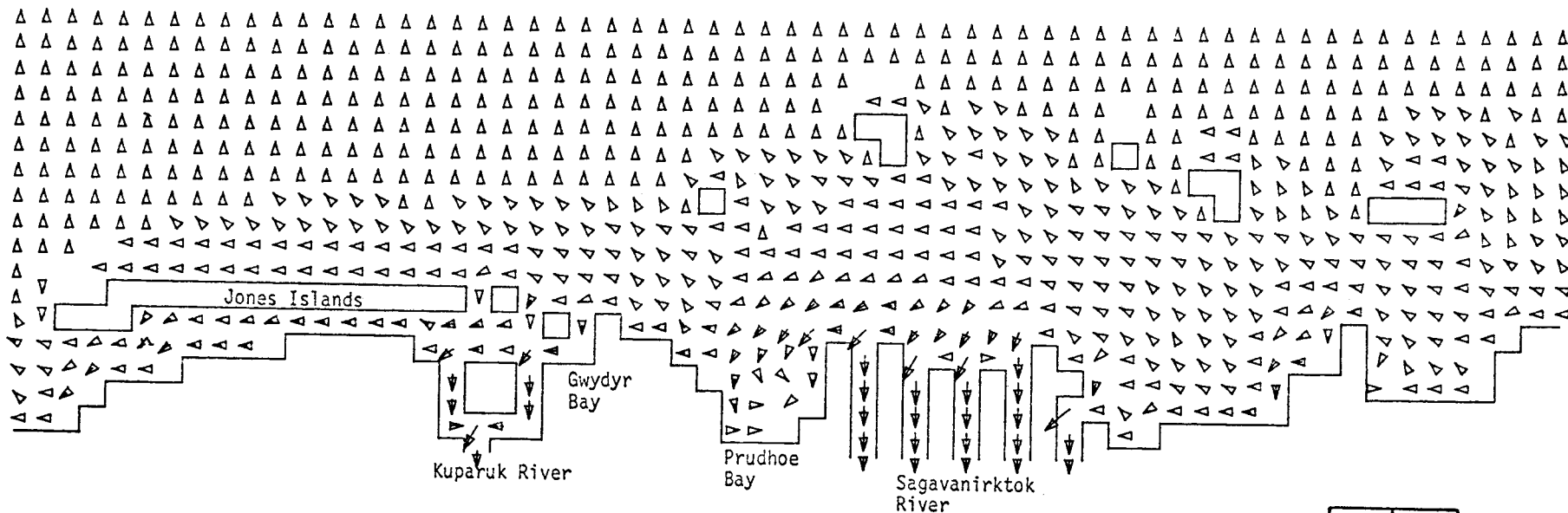
CURRENTS

TIME= 3600SEC

LAYER 1

MODEL NO 310

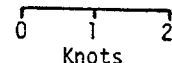
289



OLIKTOK POINT TO THE CHALLENGE ENTRANCE

M2 TIDE (AMP=8CM, FROM 22.5 DEG T) RIVER FLOW=5CM/SEC

WIND FROM NE AT 10 KT

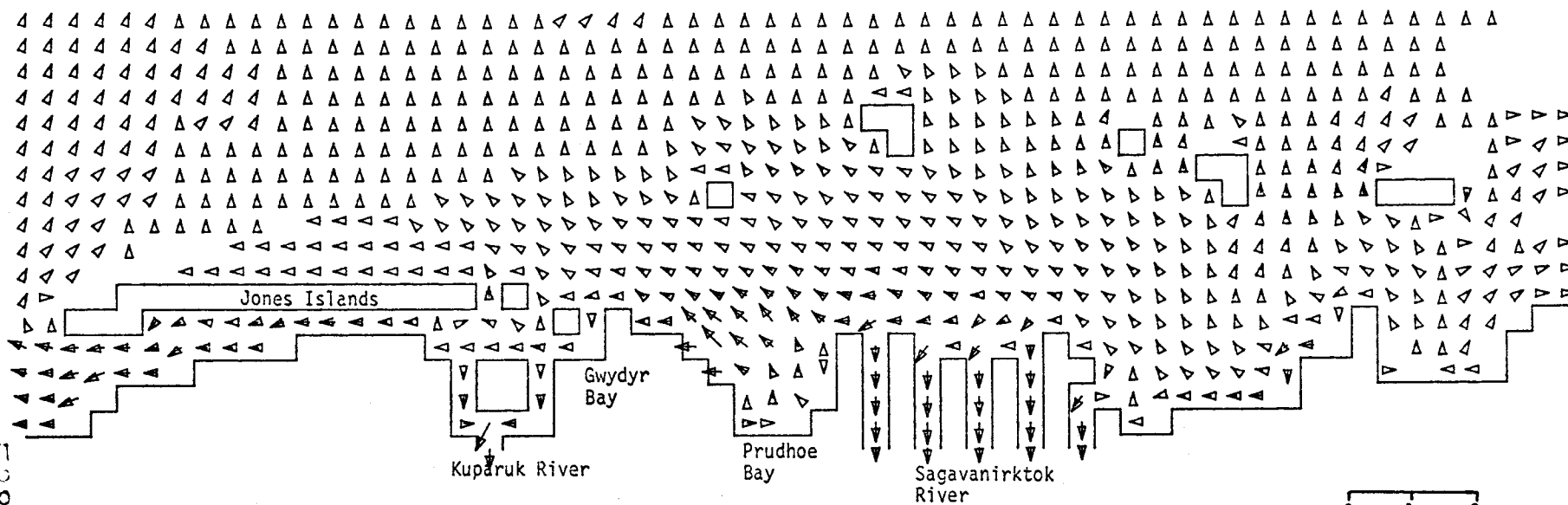


Arrow Scale

CURRENTS

TIME= 7200SEC

LAYER 1



OLIKTOK POINT TO THE CHALLENGE ENTRANCE

M2 TIDE (AMP=8CM, FROM 22.5 DEG T) RIVER FLOW=5CM/SEC WIND FROM NE AT 10 KT

0 1 2  
Knots  
Arrow Scale

MODEL NO 310

538

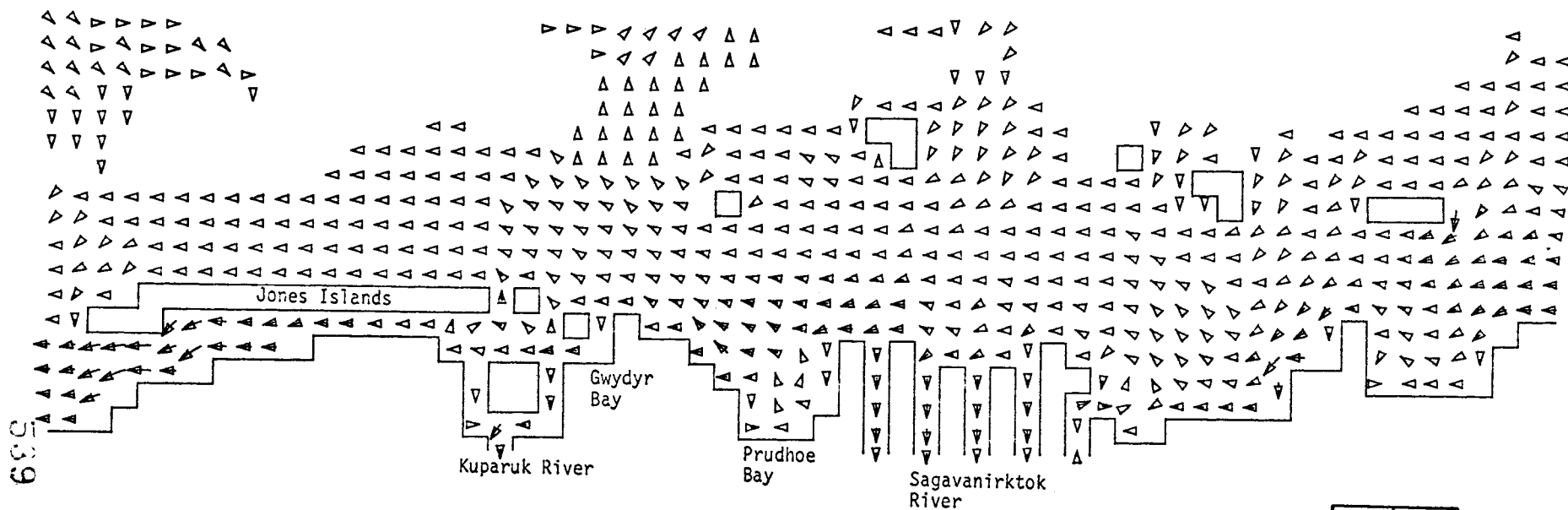


CURRENTS

TIME= 10800SEC

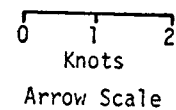
LAYER 1

MODEL NO 310



600

OLIKTOK POINT TO THE CHALLENGE ENTRANCE  
M2 TIDE (AMP=8CM, FROM 22.5 DEG T) RIVER FLOW=5CM/SEC WIND FROM NE AT 10 KT



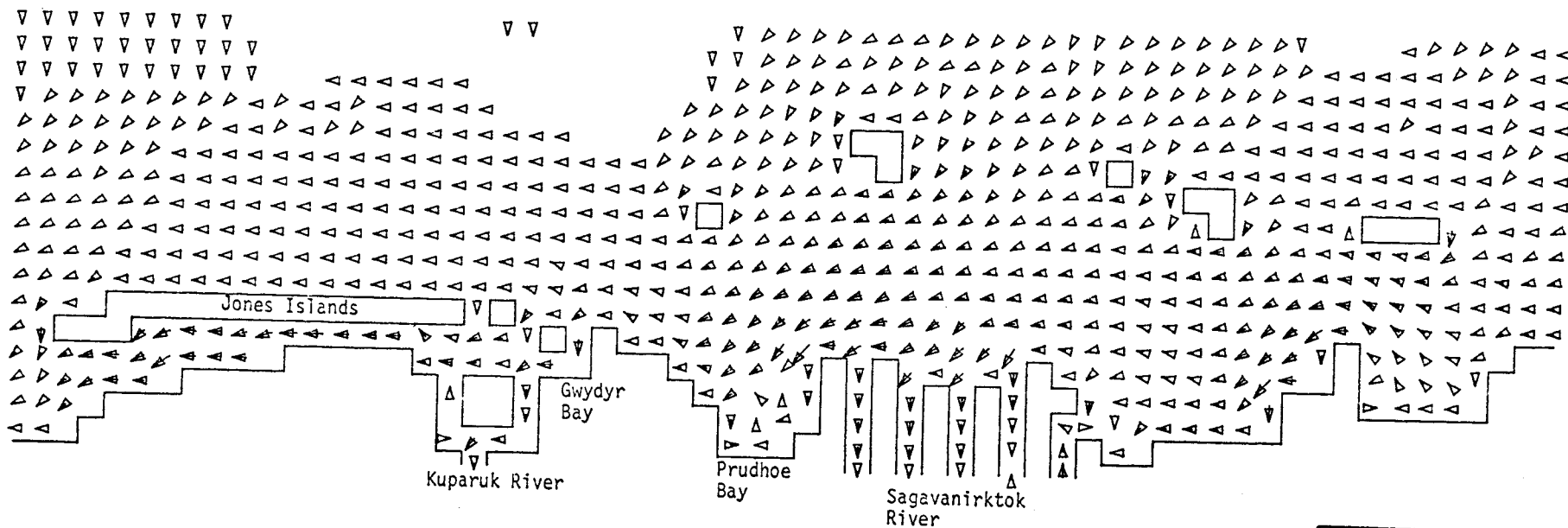
CURRENTS

TIME= 14400SEC

LAYER 1

MODEL NO 310

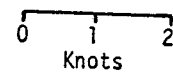
049



OLIKTOK POINT TO THE CHALLENGE ENTRANCE

M2 TIDE (AMP=8CM, FROM 22.5 DEG T) RIVER FLOW=5CM/SEC

WIND FROM NE AT 10 KT



Arrow Scale

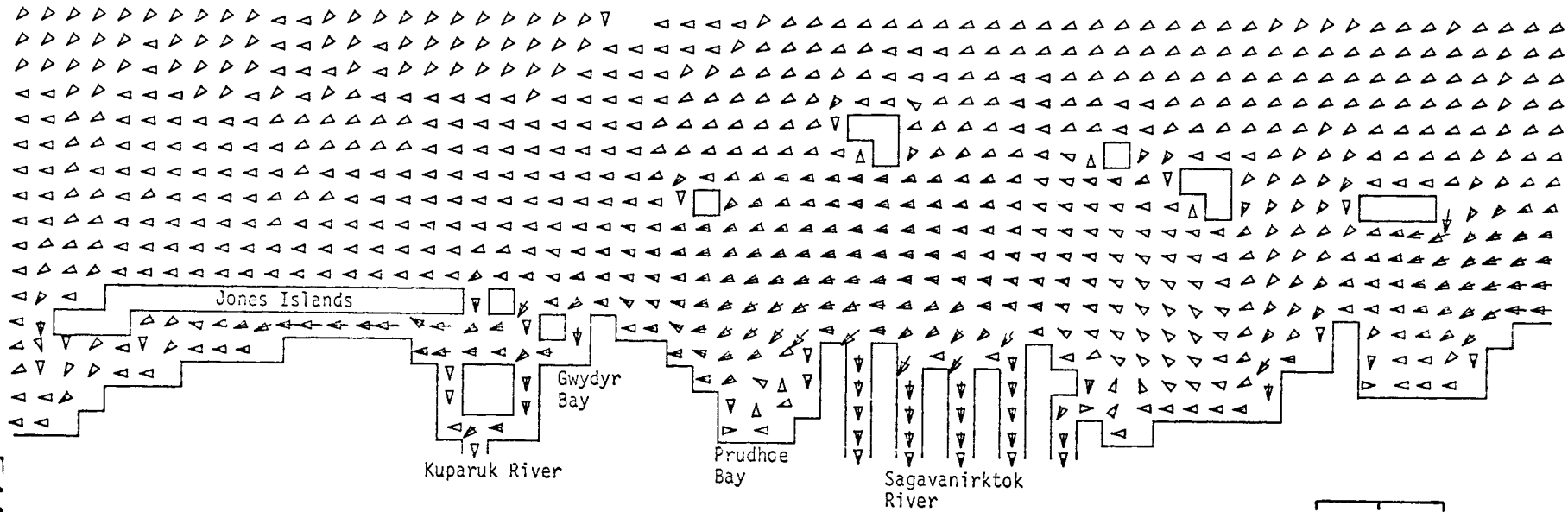
CURRENTS

TIME= 18000SEC

LAYER 1

MODEL NO 310

541



OLIKTOK POINT TO THE CHALLENGE ENTRANCE  
M2 TIDE (AMP=8CM, FROM 22.5 DEG T) RIVER FLOW=5CM/SEC WIND FROM NE AT 10 KT Arrow Scale

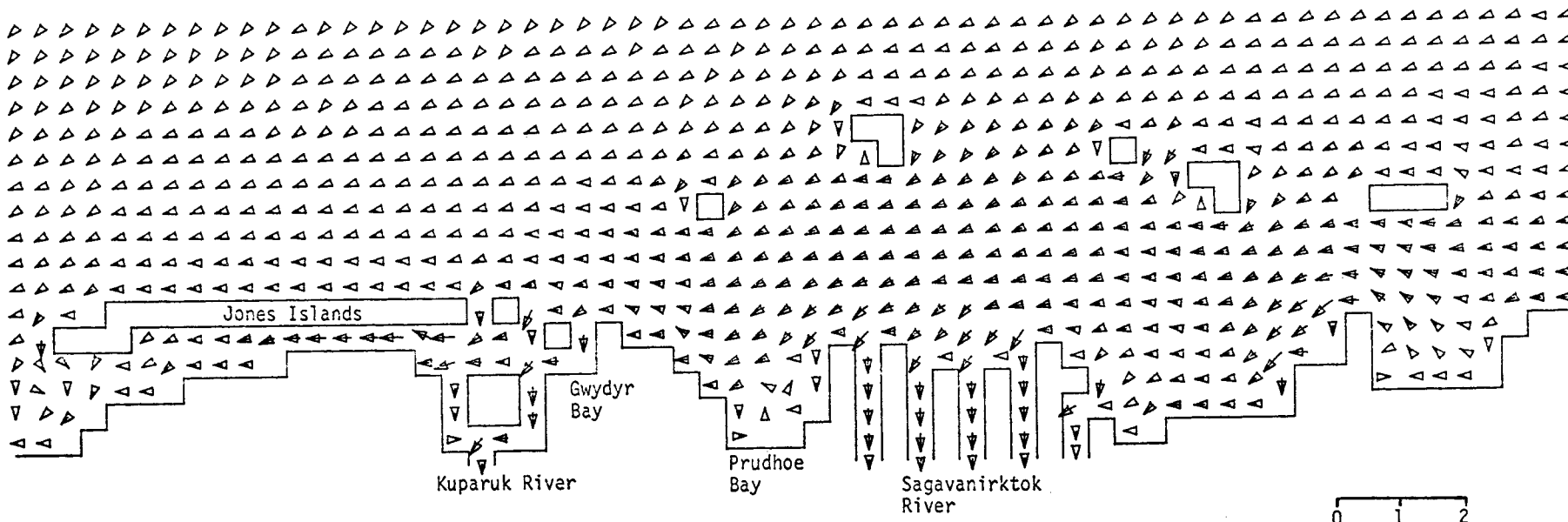
CURRENTS

TIME= 21600SEC

LAYER 1

MODEL NO 318

542



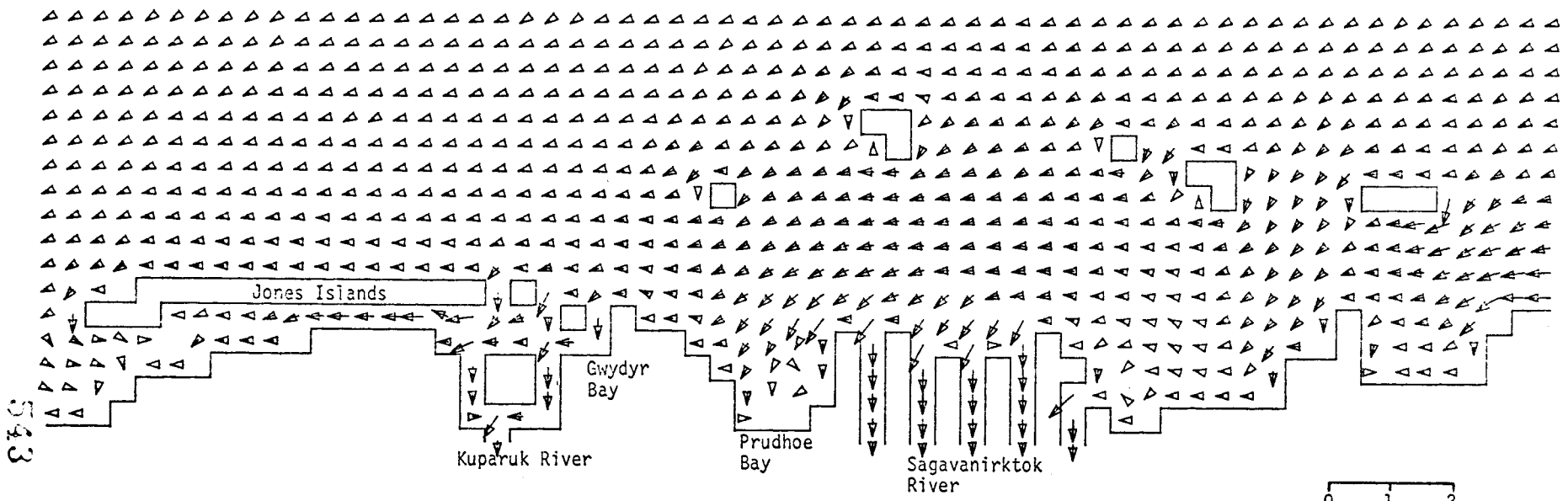
OLIKTOK POINT TO THE CHALLENGE ENTRANCE  
M2 TIDE (AMP=8CM, FROM 22.5 DEG T) RIVER FLOW=5CM/SEC WIND FROM NE AT 10 KT Arrow Scale

CURRENTS

TIME= 25200SEC

LAYER 1

MODEL NO 310



OLIKTOK POINT TO THE CHALLENGE ENTRANCE  
M2 TIDE (AMP=8CM, FROM 22.5 DEG T) RIVER FLOW=5CM/SEC WIND FROM NE AT 10 KT. Arrow Scale

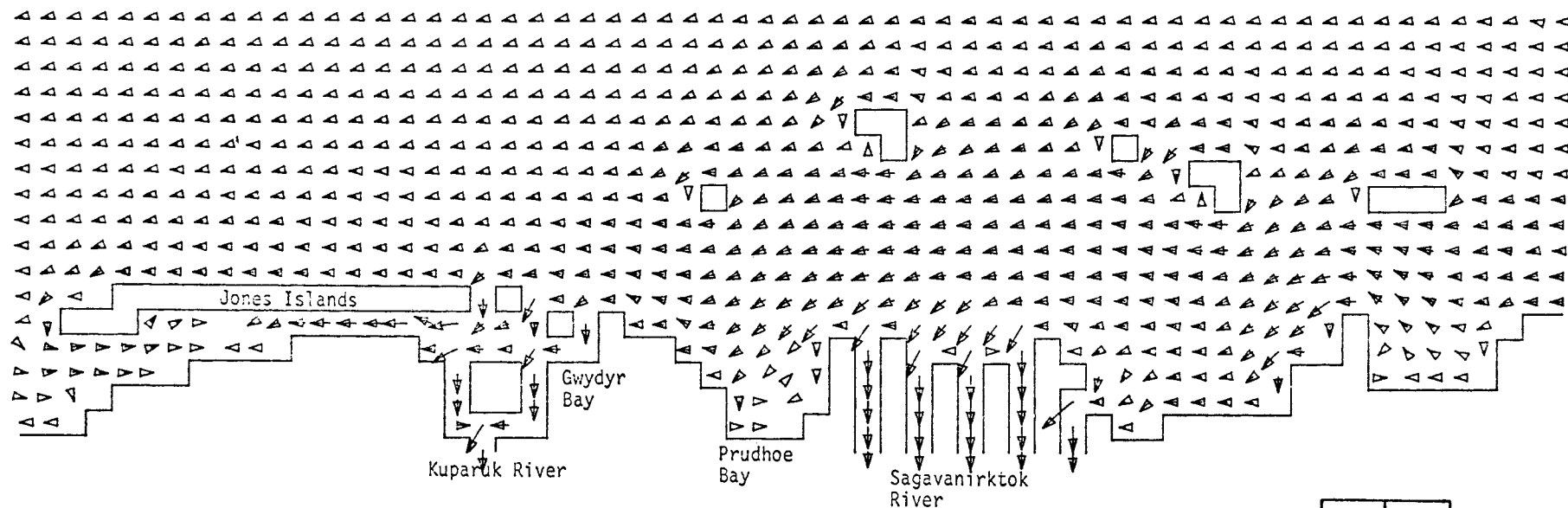
543

CURRENTS

TIME= 28800SEC

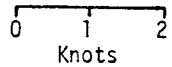
LAYER 1

MODEL NO 310



519

OLIKTOK POINT TO THE CHALLENGE ENTRANCE  
M2 TIDE (AMP=8CM, FROM 22.5 DEG T) RIVER FLOW=5CM/SEC WIND FROM NE AT 10 KT Arrow Scale



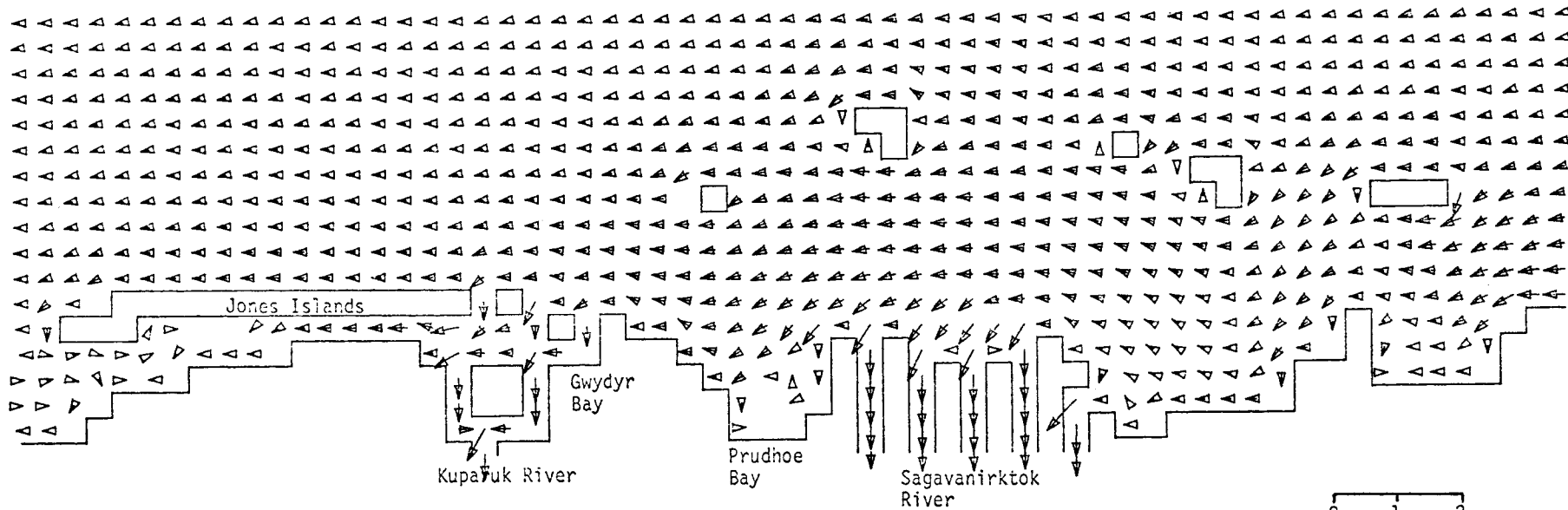
CURRENTS

TIME= 32400SEC

LAYER 1

MODEL NO 310

545



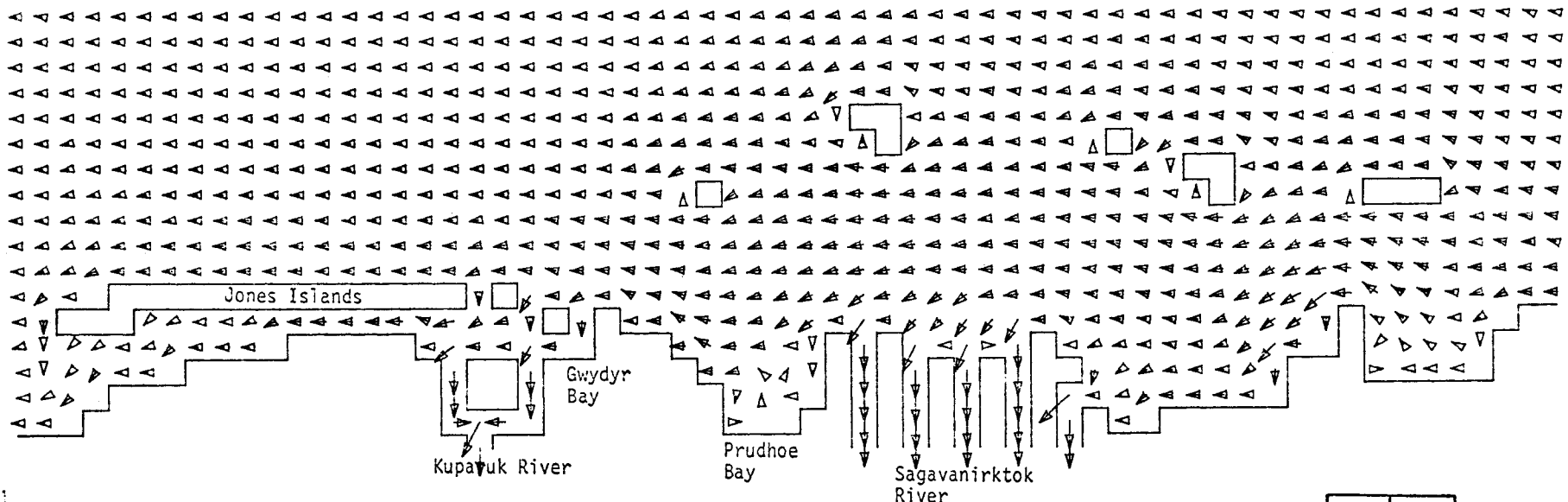
OLIKTOK POINT TO THE CHALLENGE ENTRANCE  
M2 TIDE (AMP=8CM, FROM 22.5 DEG T) RIVER FLOW=5CM/SEC WIND FROM NE AT 10 KT Arrow Scale

CURRENTS

TIME = 36000SEC

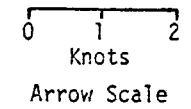
LAYER 1

MODEL NO 310



546

OLIKTOK POINT TO THE CHALLENGE ENTRANCE  
M2 TIDE (AMP=8CM, FROM 22.5 DEG T) RIVER FLOW=5CM/SEC WIND FROM NE AT 10 KT



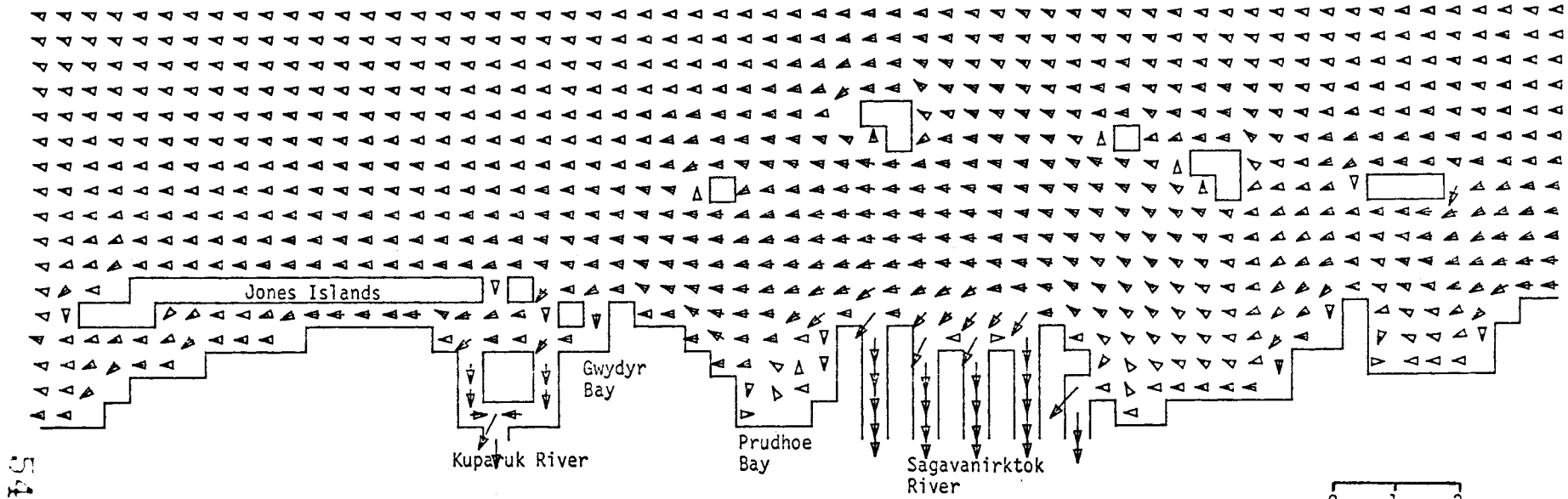


CURRENTS

TIME = 39600SEC

LAYER 1

MODEL NO 310



547

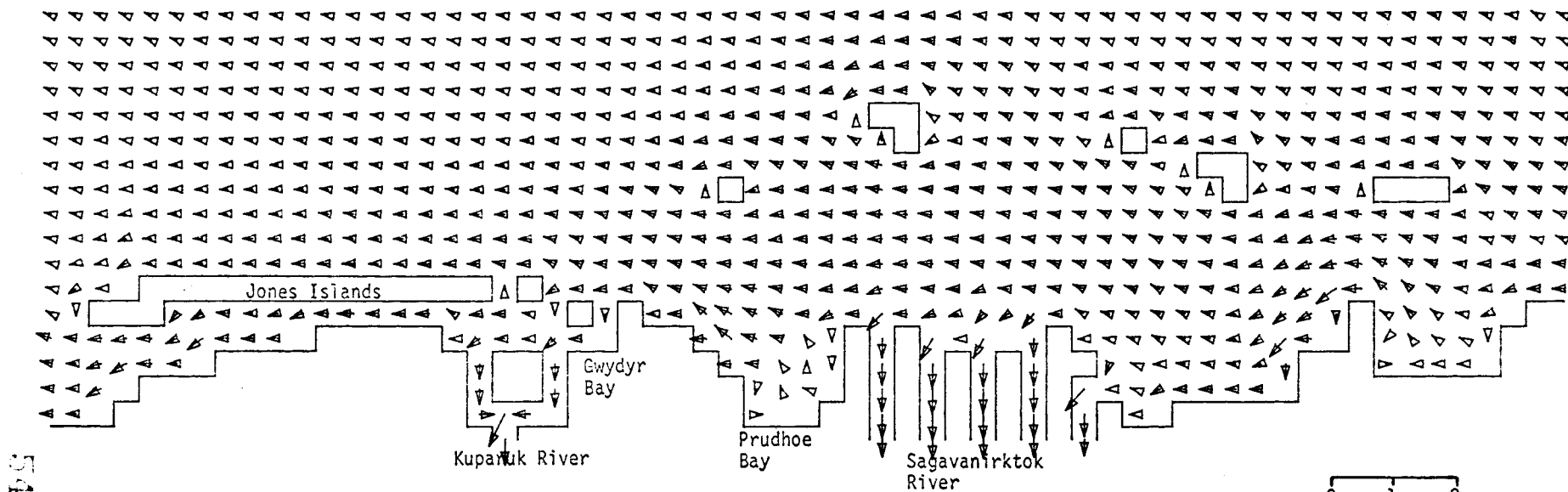
OLIKTOK POINT TO THE CHALLENGE ENTRANCE  
M2 TIDE (AMP=8CM, FROM 22.5 DEG T) RIVER FLOW=5CM/SEC WIND FROM NE AT 10 KT  
0 1 2  
Knots  
Arrow Scale

CURRENTS

TIME= 43200SEC

LAYER 1

MODEL NO 310



548

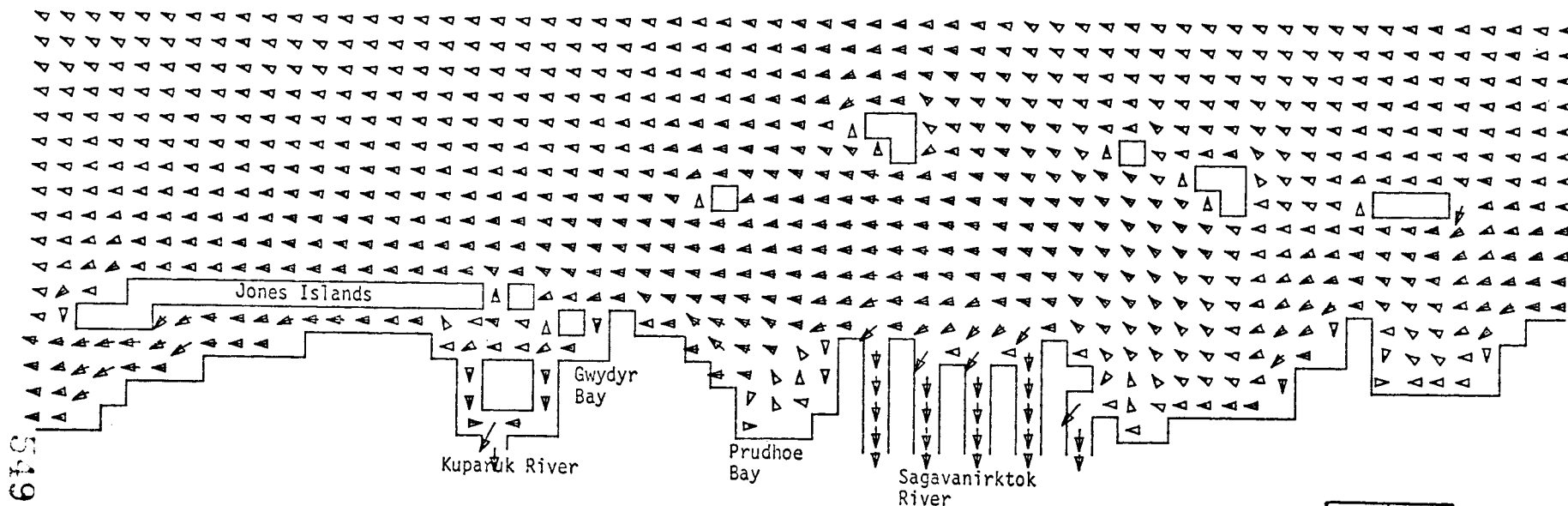
OLIKTOK POINT TO THE CHALLENGE ENTRANCE  
M2 TIDE (AMP=8CM, FROM 22.5 DEG T) RIVER FLOW=5CM/SEC WIND FROM NE AT 10 KT Arrow Scale

CURRENTS

TIME= 46800SEC

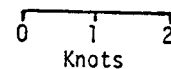
LAYER 1

MODEL NO 310



615

OLIKTOK POINT TO THE CHALLENGE ENTRANCE  
M2 TIDE (AMP=8CM, FROM 22.5 DEG T) RIVER FLOW=5CM/SEC WIND FROM NE AT 10 KT



Arrow Scale

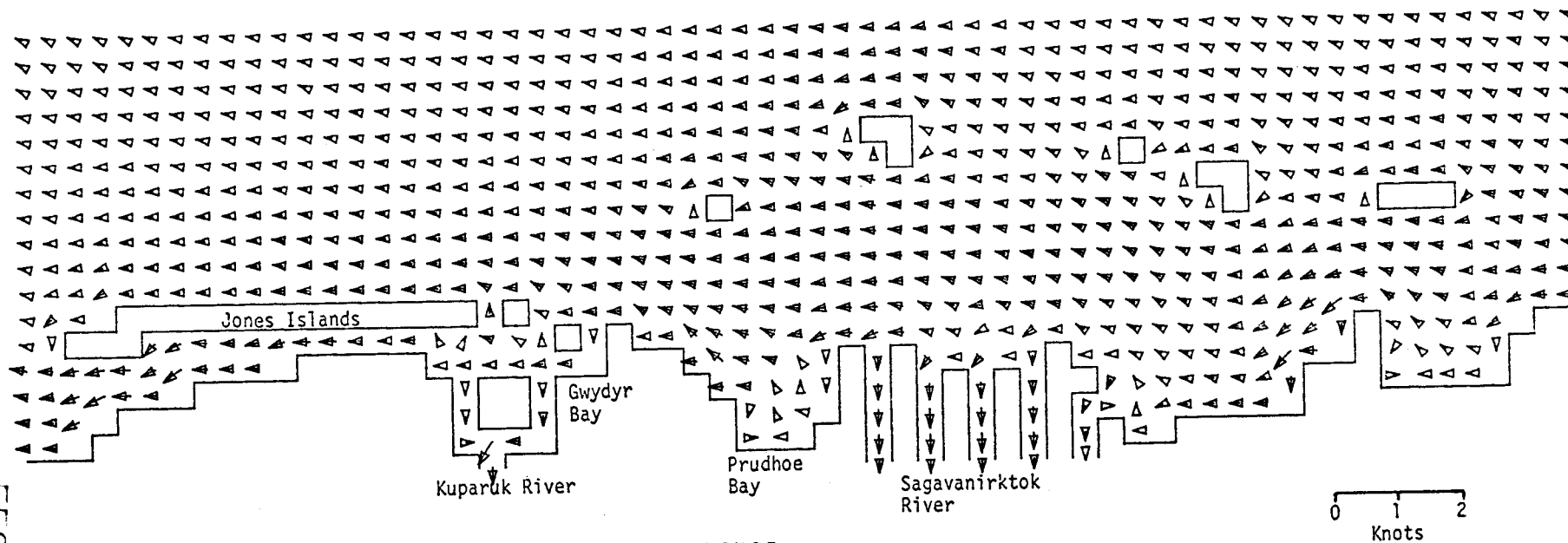
MODEL NO 310

550

CURRENTS

TIME= 50400SEC

LAYER 1



OLIKTOK POINT TO THE CHALLENGE ENTRANCE  
M2 TIDE (AMP=8CM, FROM 22.5 DEG T) RIVER FLOW=5CM/SEC WIND FROM NE AT 10 KT Arrow Scale

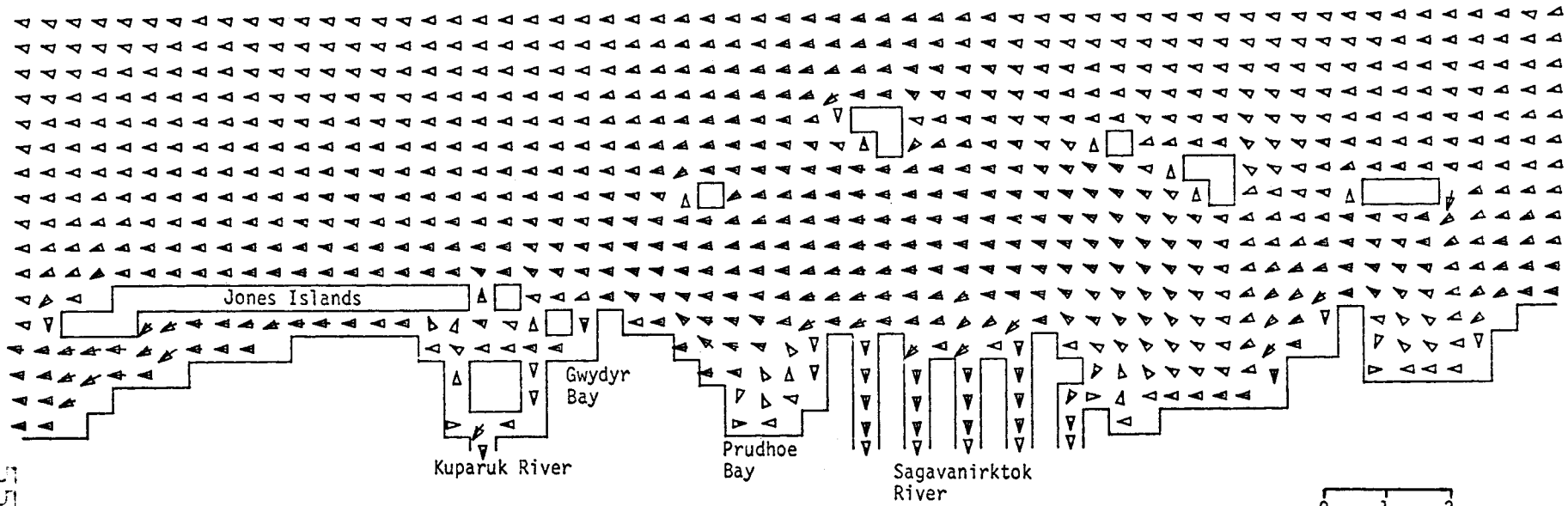
MODEL NO 310

551

CURRENTS

TIME= 54000SEC

LAYER 1



OLIKTOK POINT TO THE CHALLENGE ENTRANCE  
 M2 TIDE (AMP=8CM, FROM 22.5 DEG T) RIVER FLOW=5CM/SEC WIND FROM NE AT 10 KT Arrow Scale

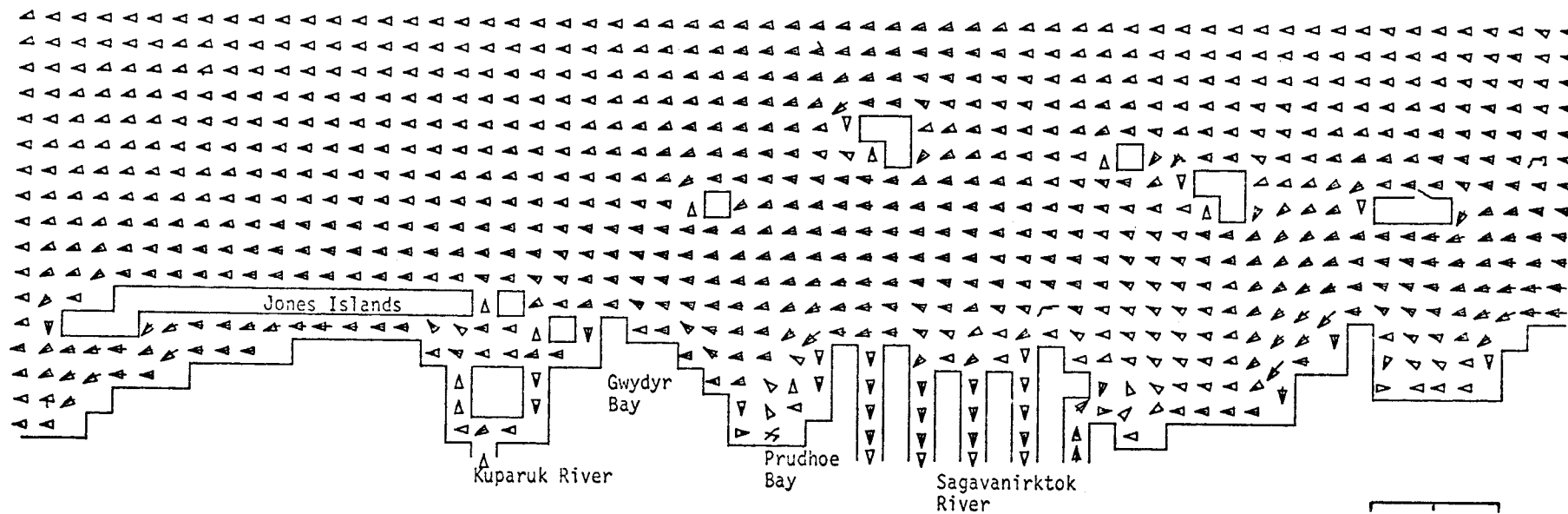
CURRENTS

TIME=

57600SEC

LAYER 1

MODEL NO 310



OLIKTOK POINT TO THE CHALLENGE ENTRANCE  
M2 TIDE (AMP=8CM, FROM 22.5 DEG T) RIVER FLOW=5CM/SEC WIND FROM NE AT 10 KT

0 1 2  
Knots  
Arrow Scale

552

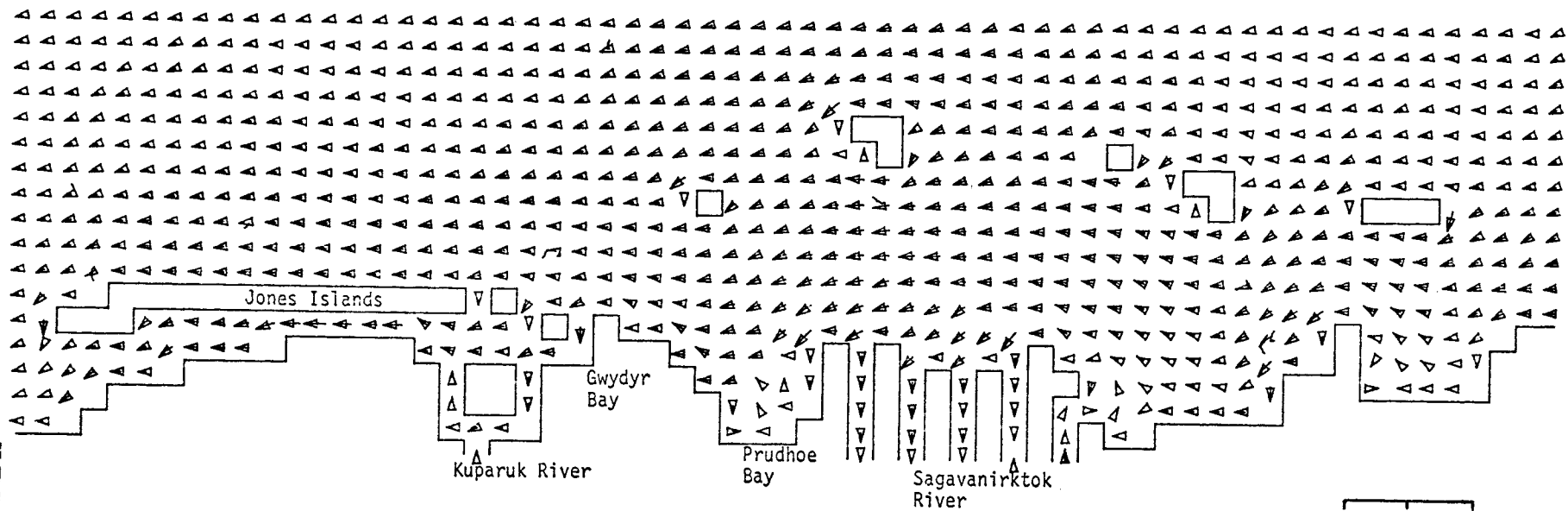
CURRENTS

TIME= 61200SEC

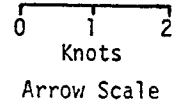
LAYER 1

MODEL NO 310

553



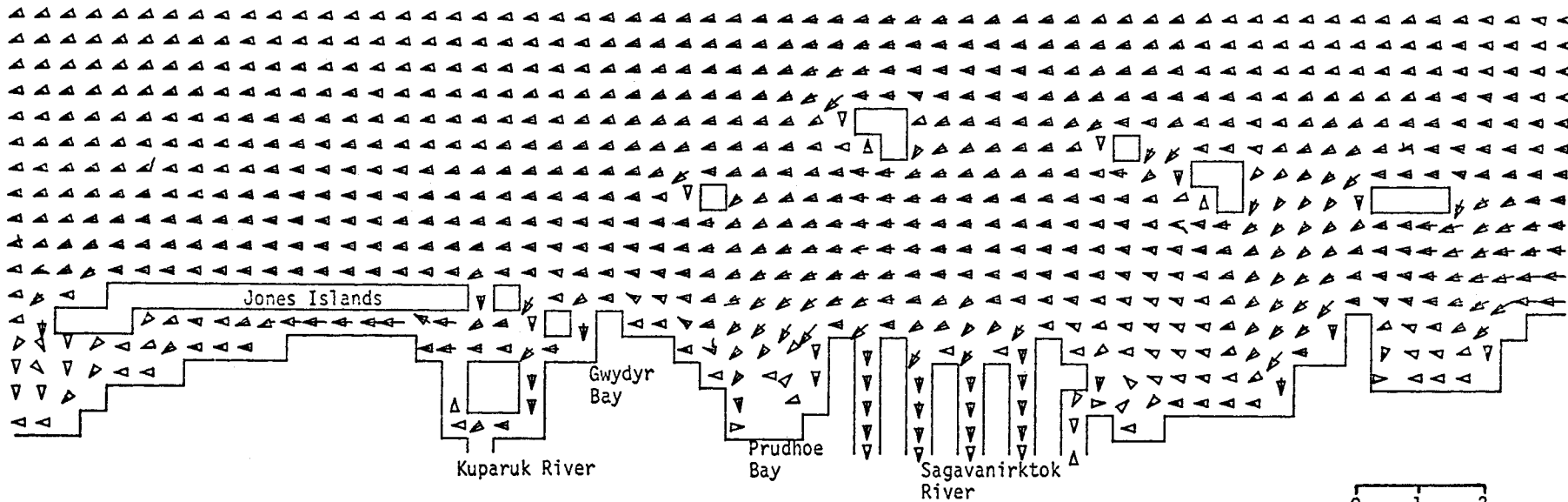
OLIKTOK POINT TO THE CHALLENGE ENTRANCE  
M2 TIDE (AMP=8CM, FROM 22.5 DEG T) RIVER FLOW=5CM/SEC WIND FROM NE AT 10 KT



CURRENTS

TIME+ 64800SEC

LAYER 1



OLIKTOK POINT TO THE CHALLENGE ENTRANCE  
M2 TIDE (AMP=8CM, FROM 22.5 DEG T) RIVER FLOW=5CM/SEC WIND FROM NE AT 10 KT

0 1 2  
Knots  
Arrow Scale

MODEL NO 310

554



APPENDIX C

PRUDHOE BAY

TIDE PLUS RIVER FLOW (5 CM/SEC). M2 TIDE WITH 8 CM  
AMPLITUDE INPUT IN PHASE ON ALL OPEN BOUNDARIES.

RUNS WITH NO RIVER INPUT ESSENTIALLY THE SAME AS THESE.

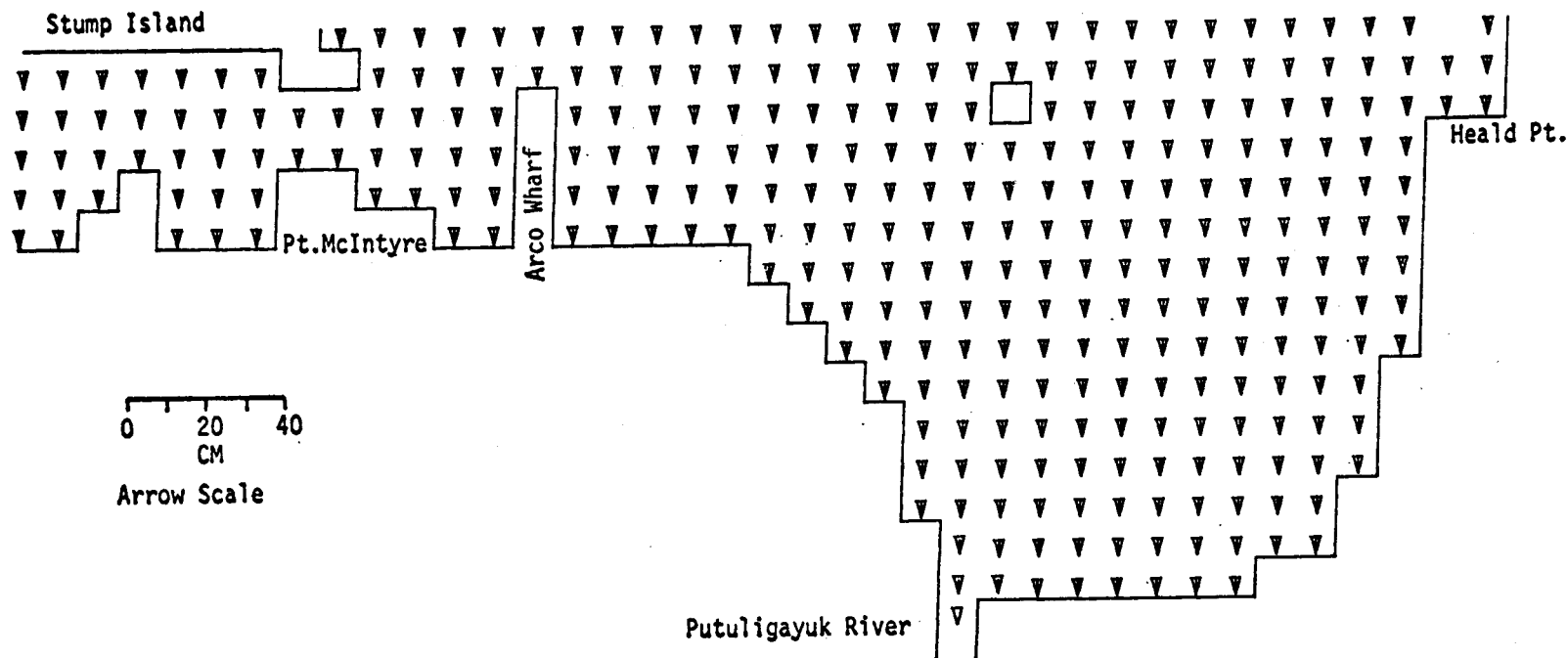
SEA LEVEL



SEA LEVEL

TIME= 3600SEC

LAYER 1



MODEL NO 10

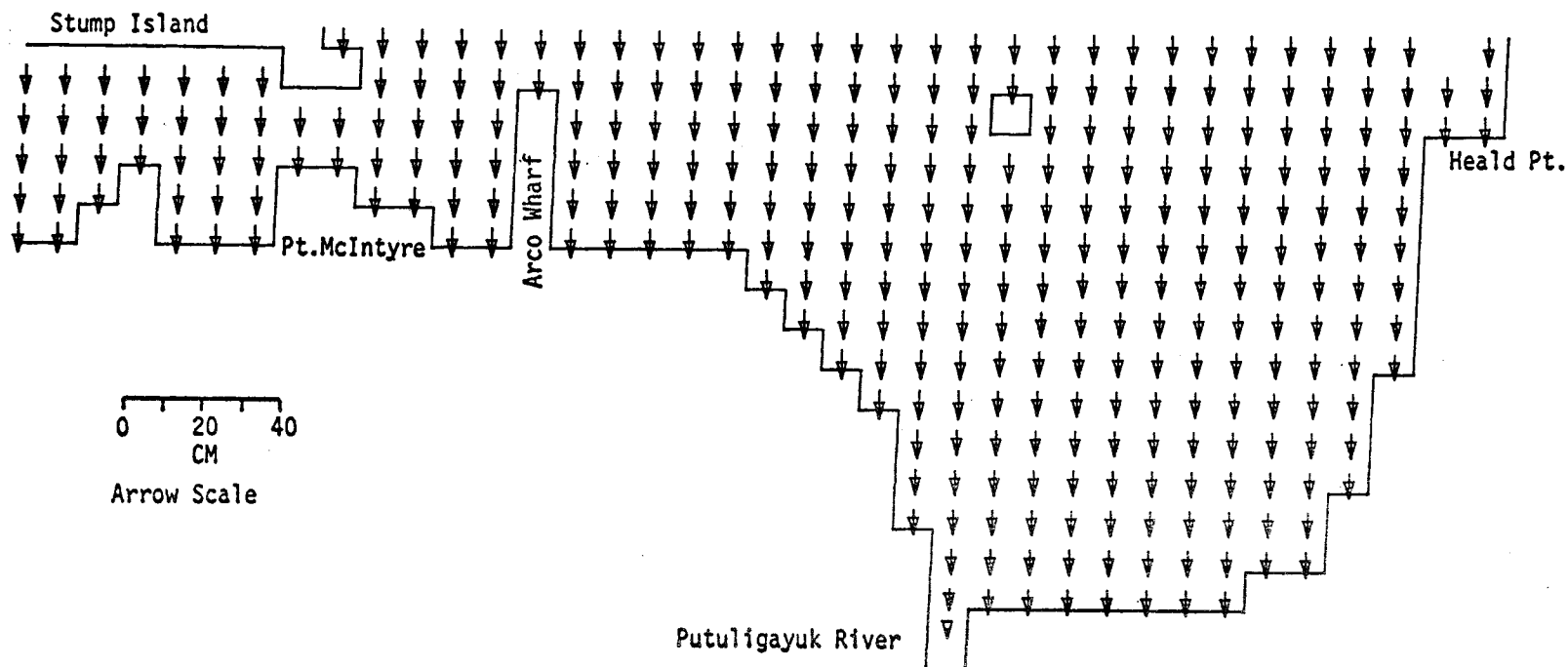
558

PRUDHOE BAY  
M2 TIDE (AMP=8 CM, IN PHASE ON OPEN BOUNDARIES) RIVER FLOW AT 5 CM/SEC

SEA LEVEL

TIME= 7200SEC

LAYER 1



MODEL NO 10

559

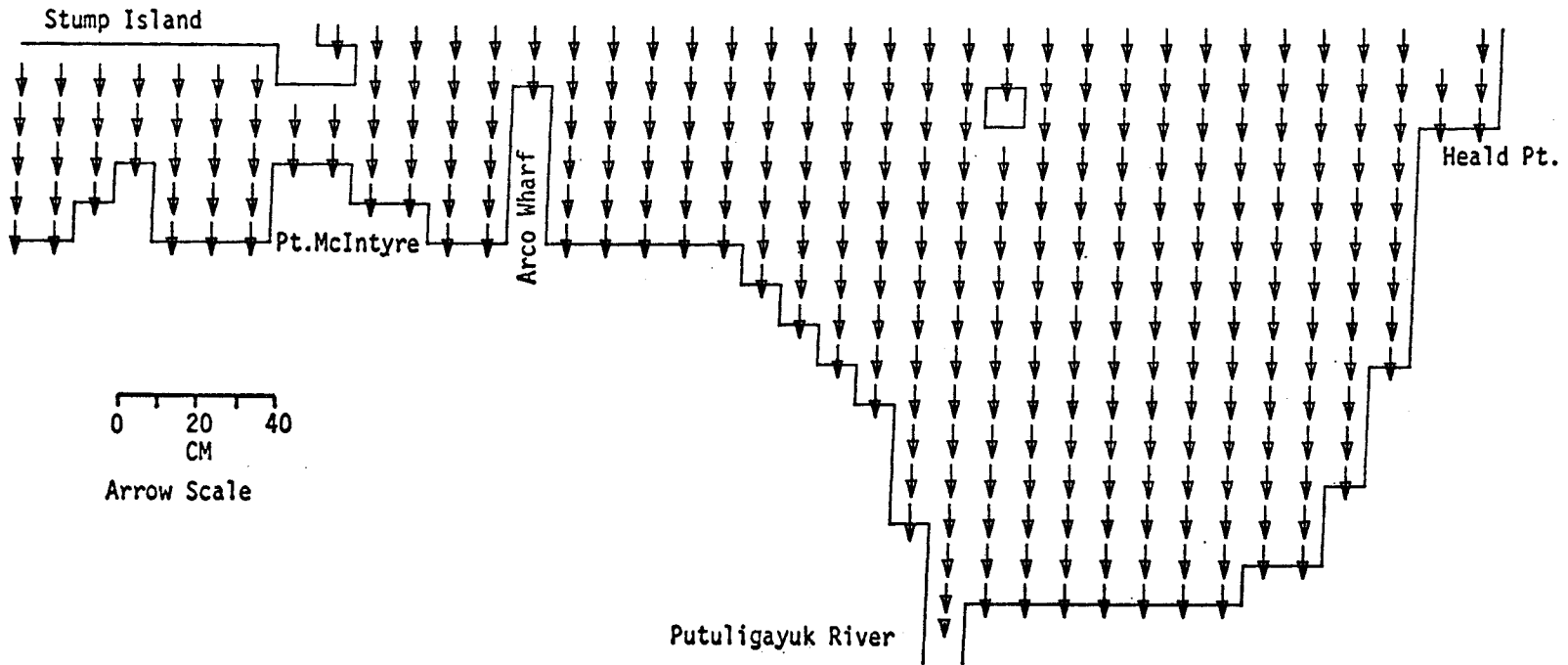
PRUDHOE BAY  
M2 TIDE (AMP=8 CM, IN PHASE ON OPEN BOUNDARIES) RIVER FLOW AT 5 CM/SEC

SEA LEVEL

TIME= 10800SEC

LAYER 1

MODEL NO 10



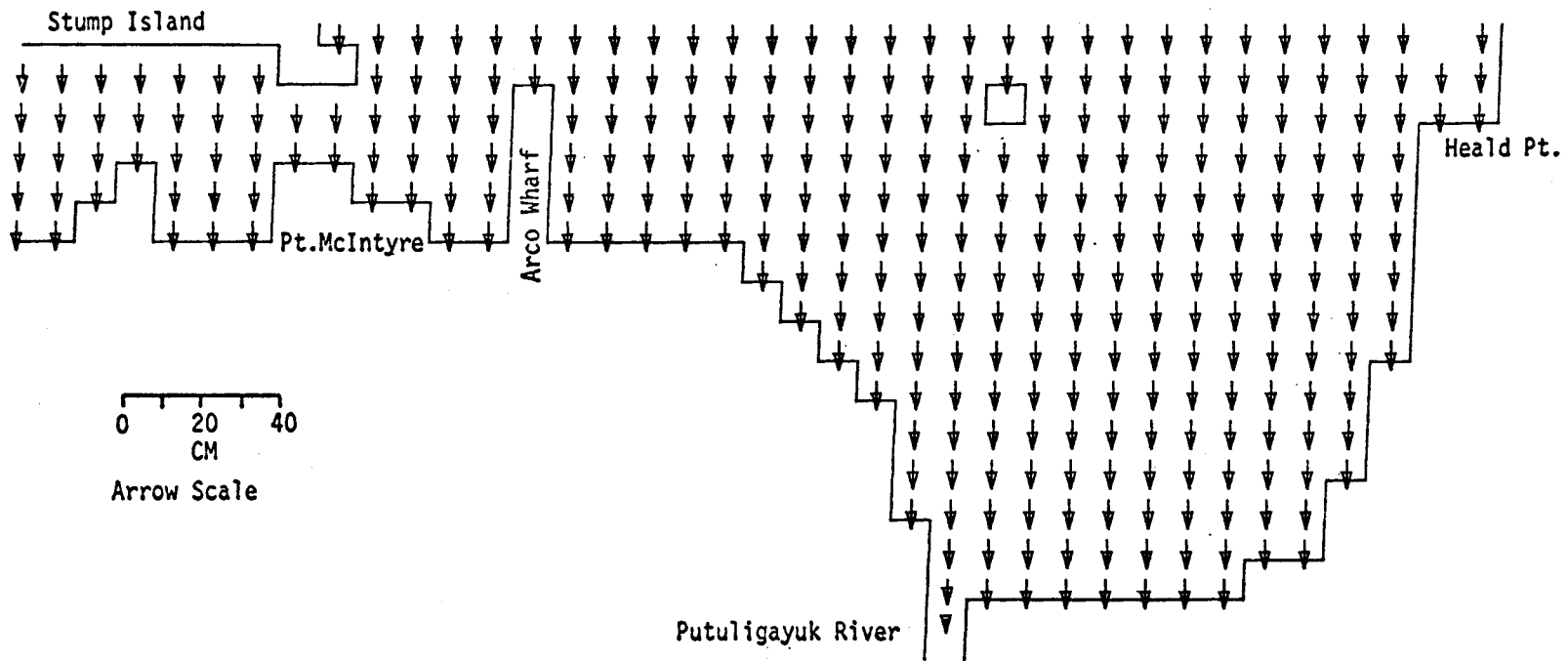
095

PRUDHOE BAY  
M2 TIDE (AMP=8 CM, IN PHASE ON OPEN BOUNDARIES) RIVER FLOW AT 5 CM/SEC

SEA LEVEL

TIME= 14400SEC

LAYER 1



MODEL NO 10

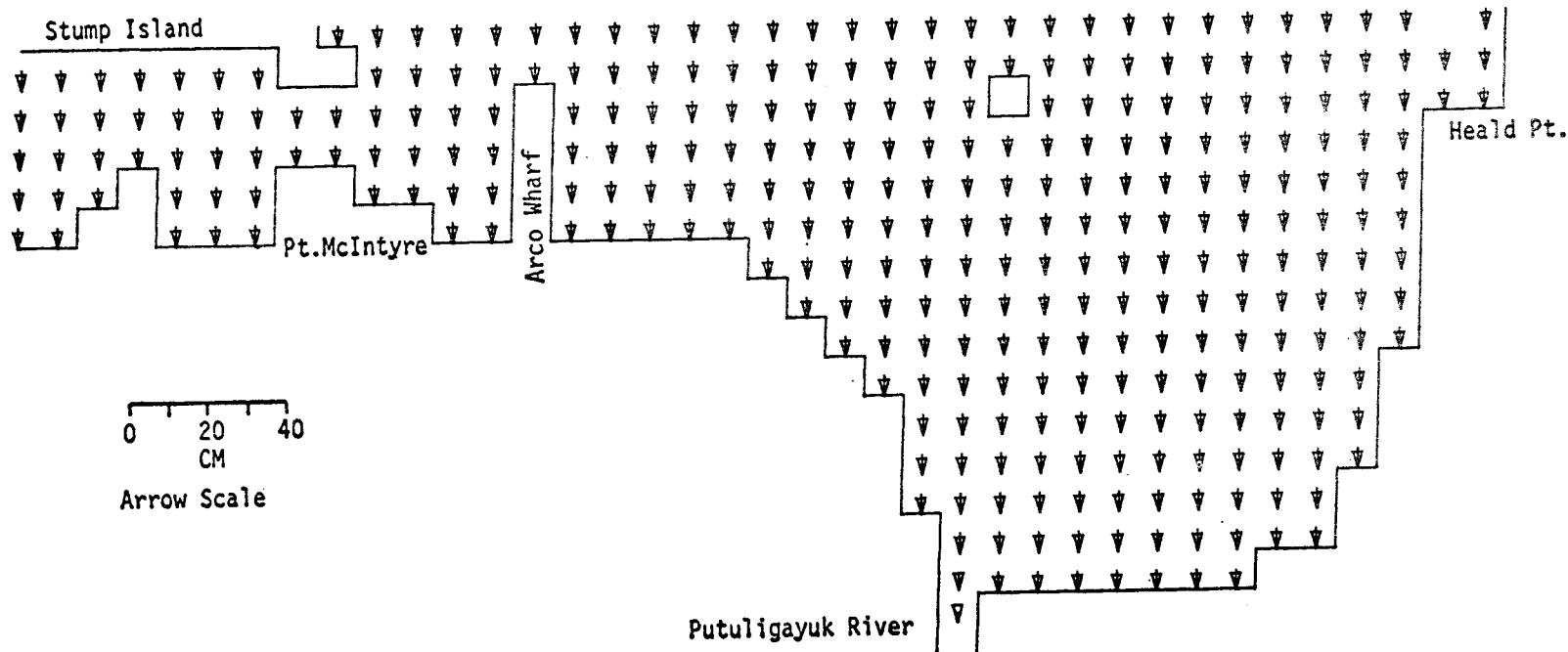
561

PRUDHOE BAY  
M2 TIDE (AMP=8 CM, IN PHASE ON OPEN BOUNDARIES) RIVER FLOW AT 5 CM/SEC

SEA LEVEL

TIME = 18000SEC

LAYER 1



MODEL NO 10

562

0 20 40  
CM  
Arrow Scale

PRUDHOE BAY

M2 TIDE (AMP=8 CM, IN PHASE ON OPEN BOUNDARIES) RIVER FLOW AT 5 CM/SEC

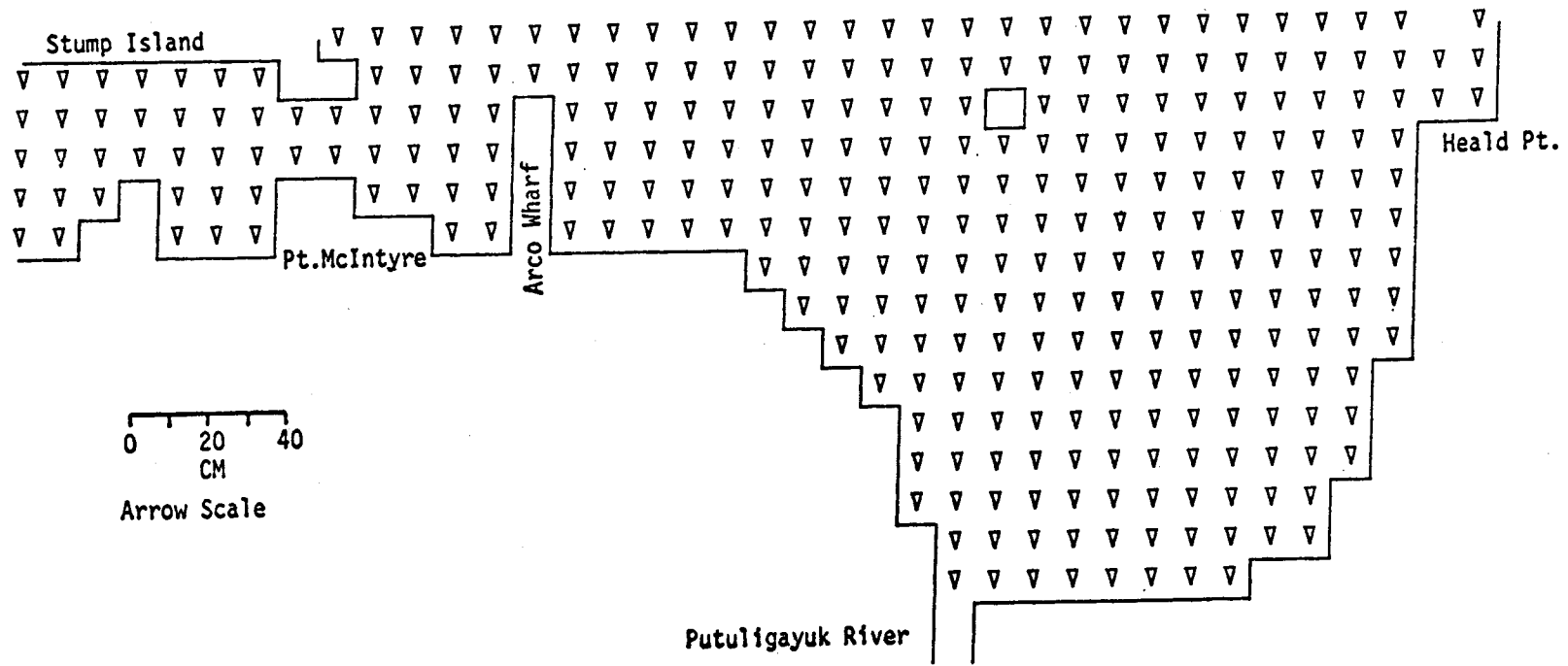


595 MODEL NO 10

SEA LEVEL

TIME= 21600SEC

LAYER 1

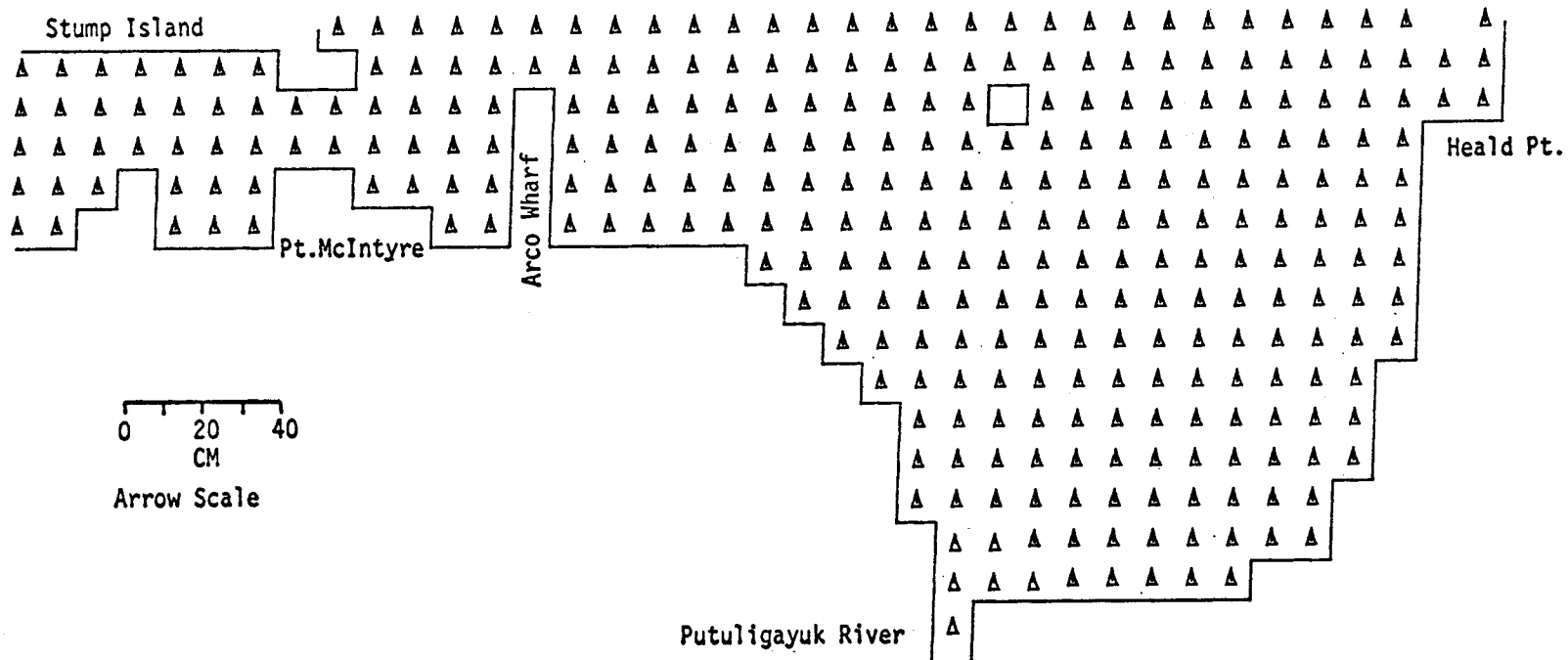


PRUDHOE BAY  
M2 TIDE (AMP=8 CM, IN PHASE ON OPEN BOUNDARIES) RIVER FLOW AT 5 CM/SEC

SEA LEVEL

TIME= 25200SEC

LAYER 1



0 20 40  
CM  
Arrow Scale

Putuligayuk River

PRUDHOE BAY

M2 TIDE (AMP=8 CM, IN PHASE ON OPEN BOUNDARIES) RIVER FLOW AT 5 CM/SEC

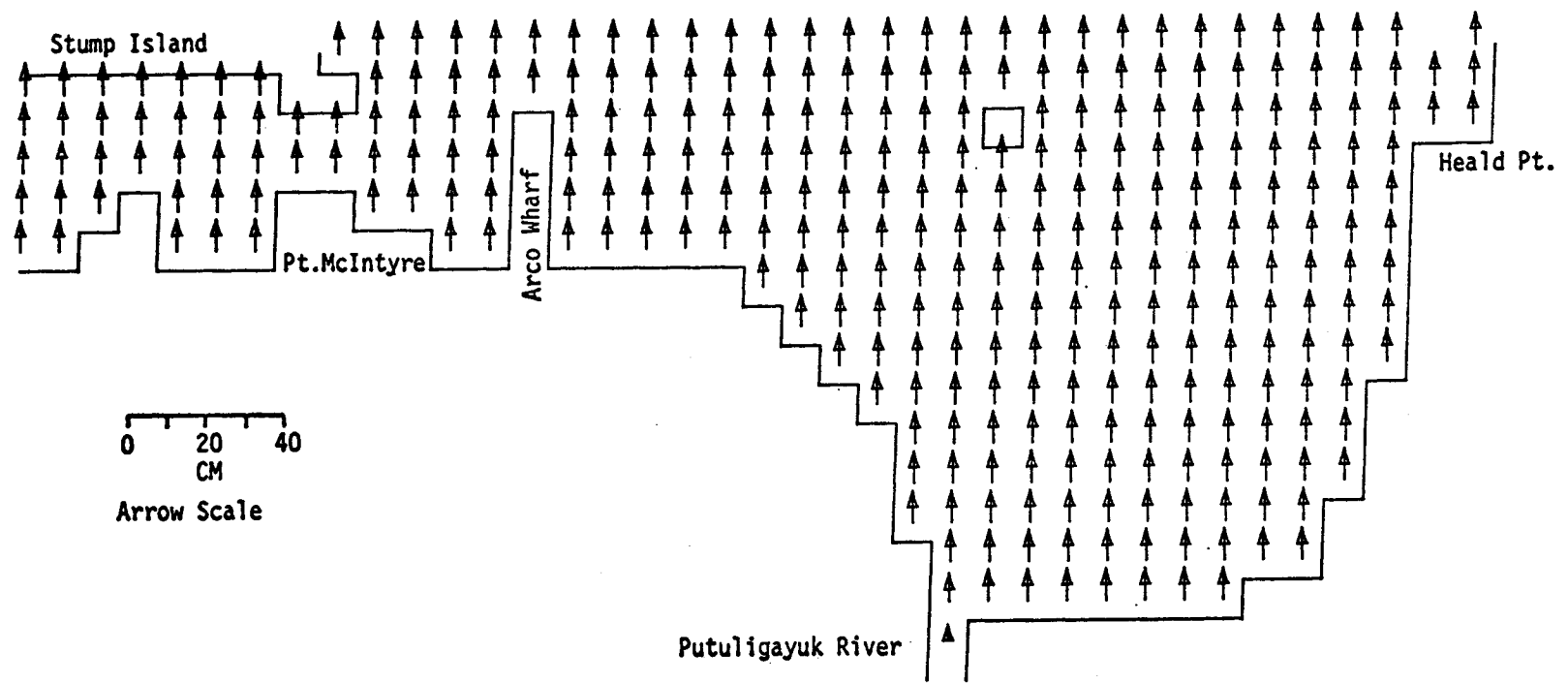
MODEL NO 10



SEA LEVEL

TIME= 32400SEC

LAYER 1



0 20 40  
CM  
Arrow Scale

Putuligayuk River

Heald Pt.

Arco Wharf

Pt. McIntyre

Stump Island

PRUDHOE BAY

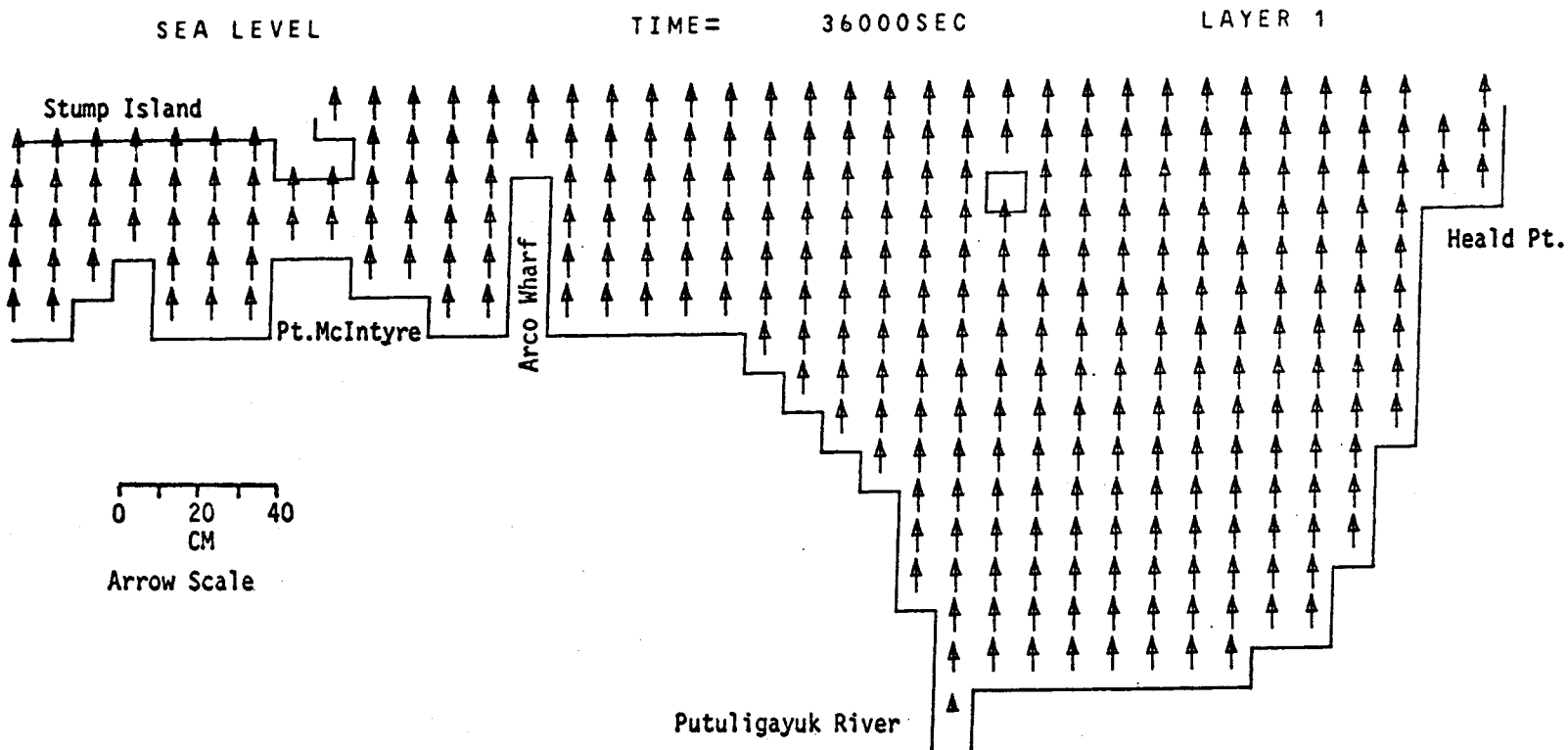
M2 TIDE (AMP=8 CM, IN PHASE ON OPEN BOUNDARIES) RIVER FLOW AT 5 CM/SEC

995

MODEL NO 10

567

MODEL NO 10



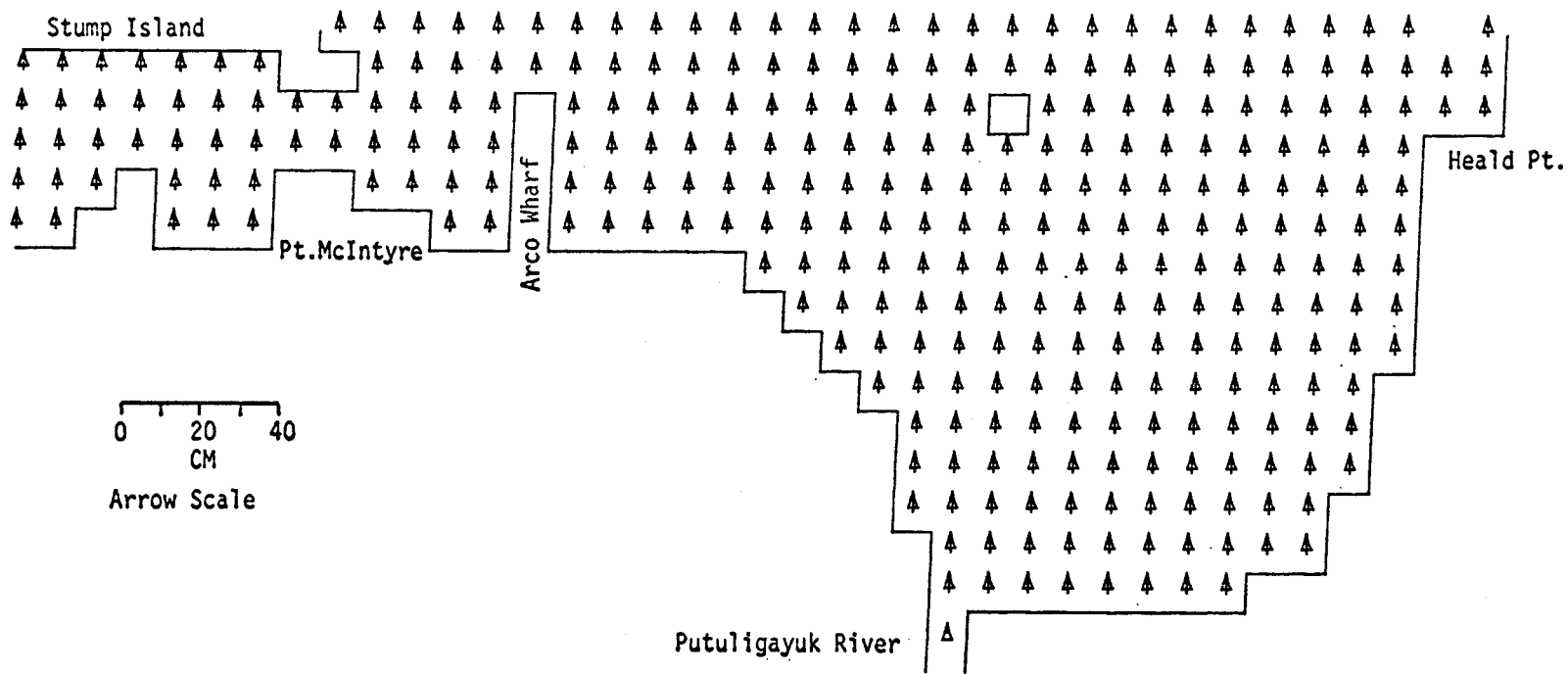
PRUDHOE BAY

M2 TIDE (AMP=8 CM, IN PHASE ON OPEN BOUNDARIES) RIVER FLOW AT 5 CM/SEC

SEA LEVEL

TIME= 39600SEC

LAYER 1



PRUDHOE BAY

M2 TIDE (AMP=8 CM, IN PHASE ON OPEN BOUNDARIES) RIVER FLOW AT 5 CM/SEC

568

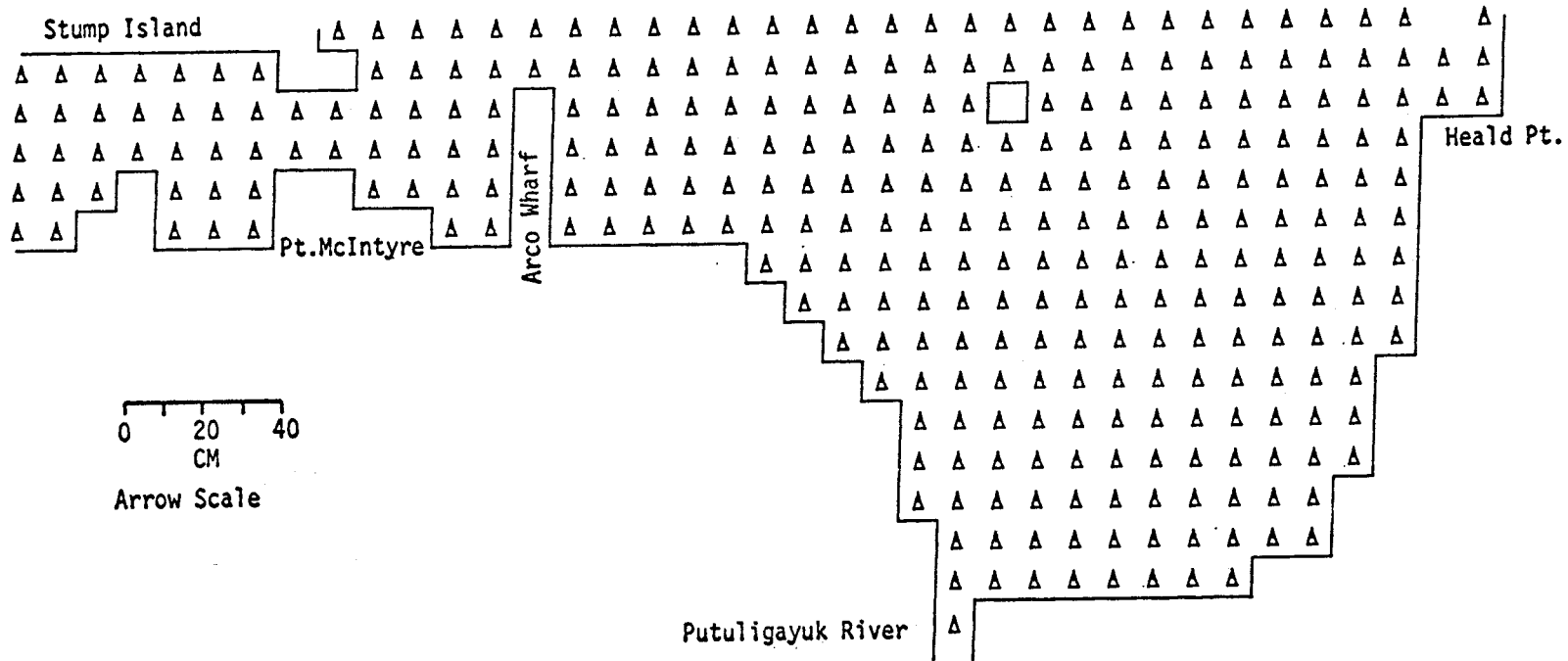
MODEL NO 10

695 MODEL NO 10

SEA LEVEL

TIME= 43200SEC

LAYER 1



0 20 40  
CM  
Arrow Scale

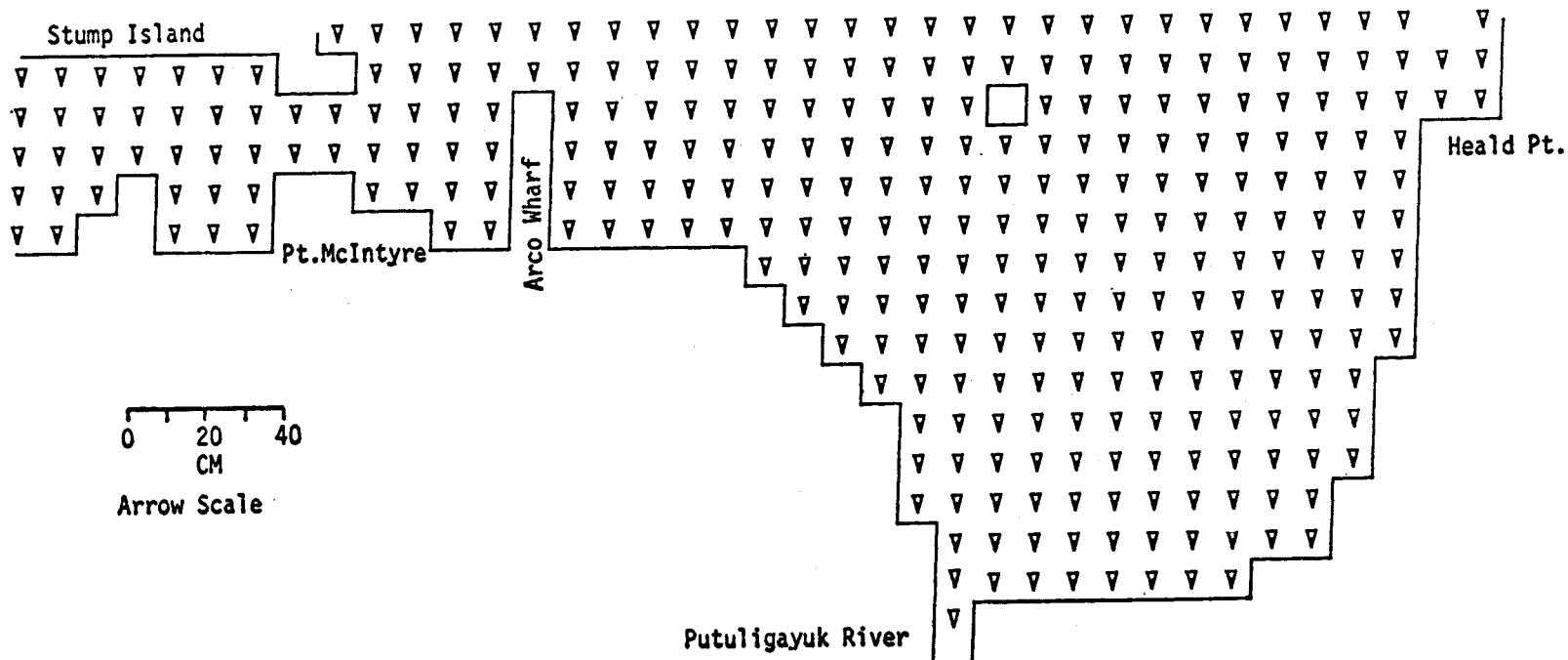
PRUDHOE BAY

M2 TIDE (AMP=8 CM, IN PHASE ON OPEN BOUNDARIES) RIVER FLOW AT 5 CM/SEC

SEA LEVEL

TIME= 46800SEC

LAYER 1



MODEL NO 10

570

0 20 40  
CM  
Arrow Scale

PRUDHOE BAY

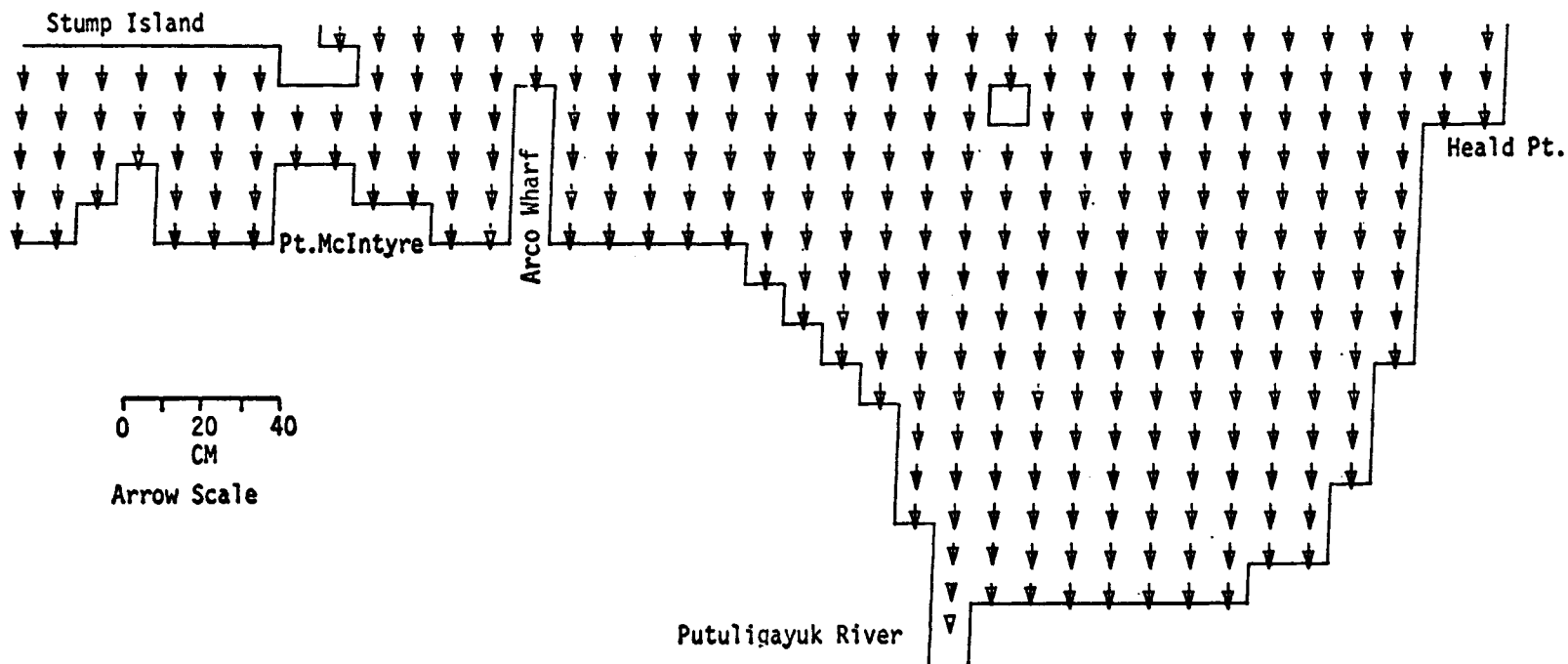
M2 TIDE (AMP=8 CM, IN PHASE ON OPEN BOUNDARIES) RIVER FLOW AT 5 CM/SEC



SEA LEVEL

TIME= 50400SEC

LAYER 1



10

MODEL NO

571

0 20 40  
CM  
Arrow Scale

PRUDHOE BAY

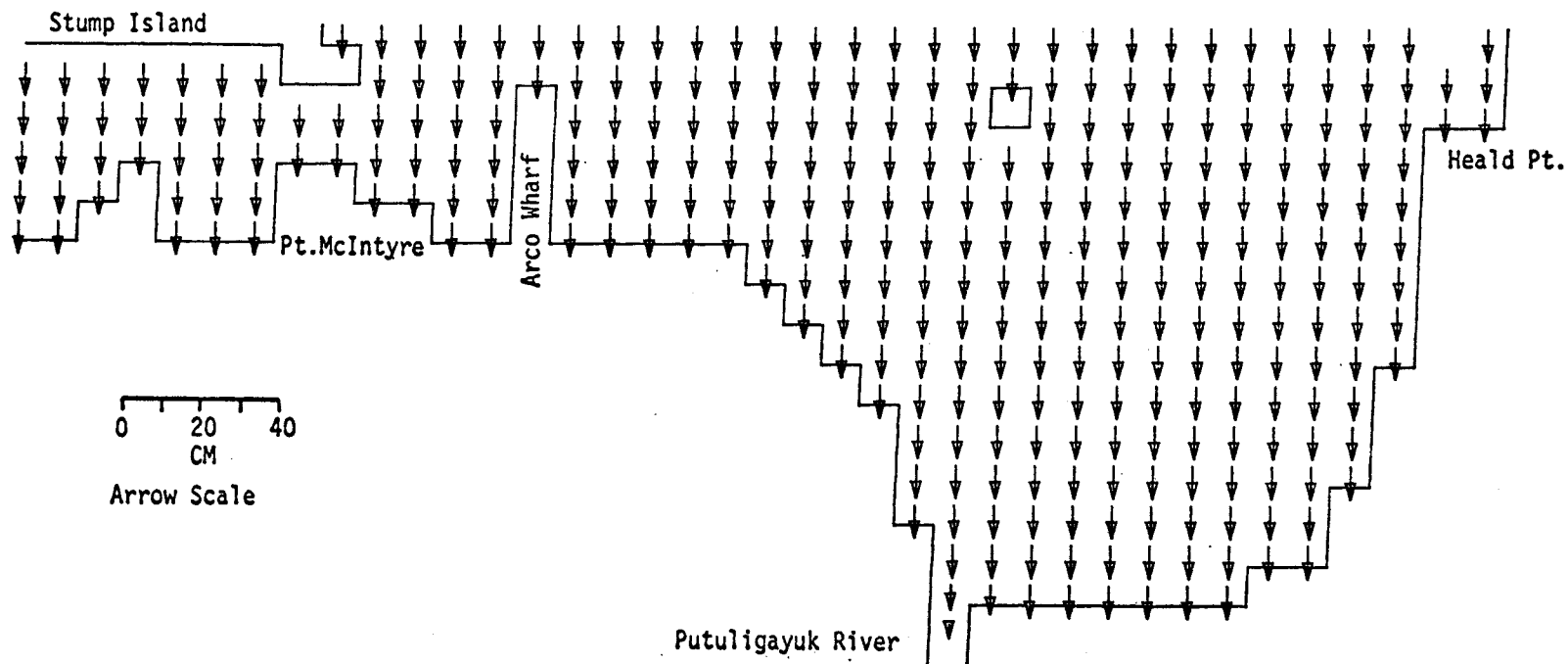
M2 TIDE (AMP=8 CM, IN PHASE ON OPEN BOUNDARIES) RIVER FLOW AT 5 CM/SEC

SEA LEVEL

TIME= 54000SEC

LAYER 1

MODEL NO 10



0 20 40  
CM  
Arrow Scale

Putuligayuk River

PRUDHOE BAY

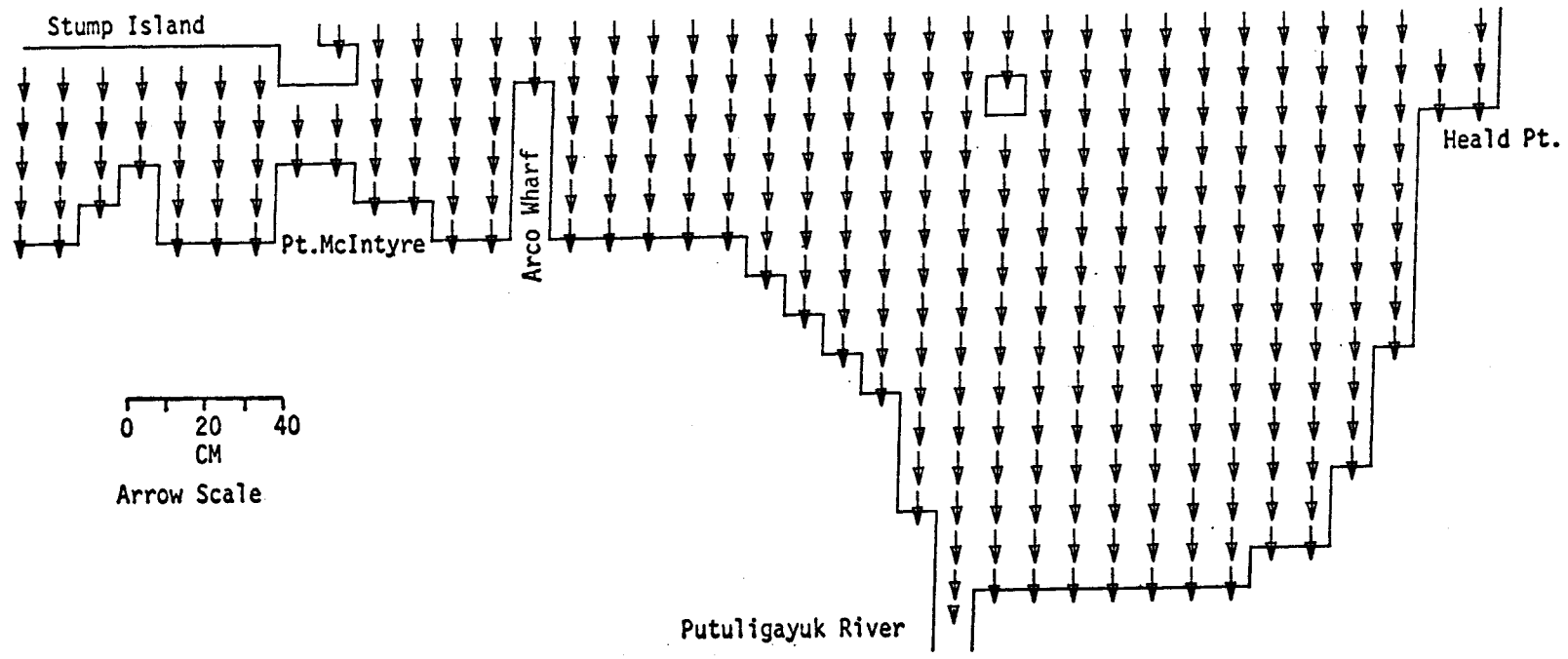
M2 TIDE (AMP=8 CM, IN PHASE ON OPEN BOUNDARIES) RIVER FLOW AT 5 CM/SEC

572

SEA LEVEL

TIME = 57600SEC

LAYER 1



MODEL NO 10

573

0 20 40  
CM  
Arrow Scale

Putuligayuk River

Heald Pt.

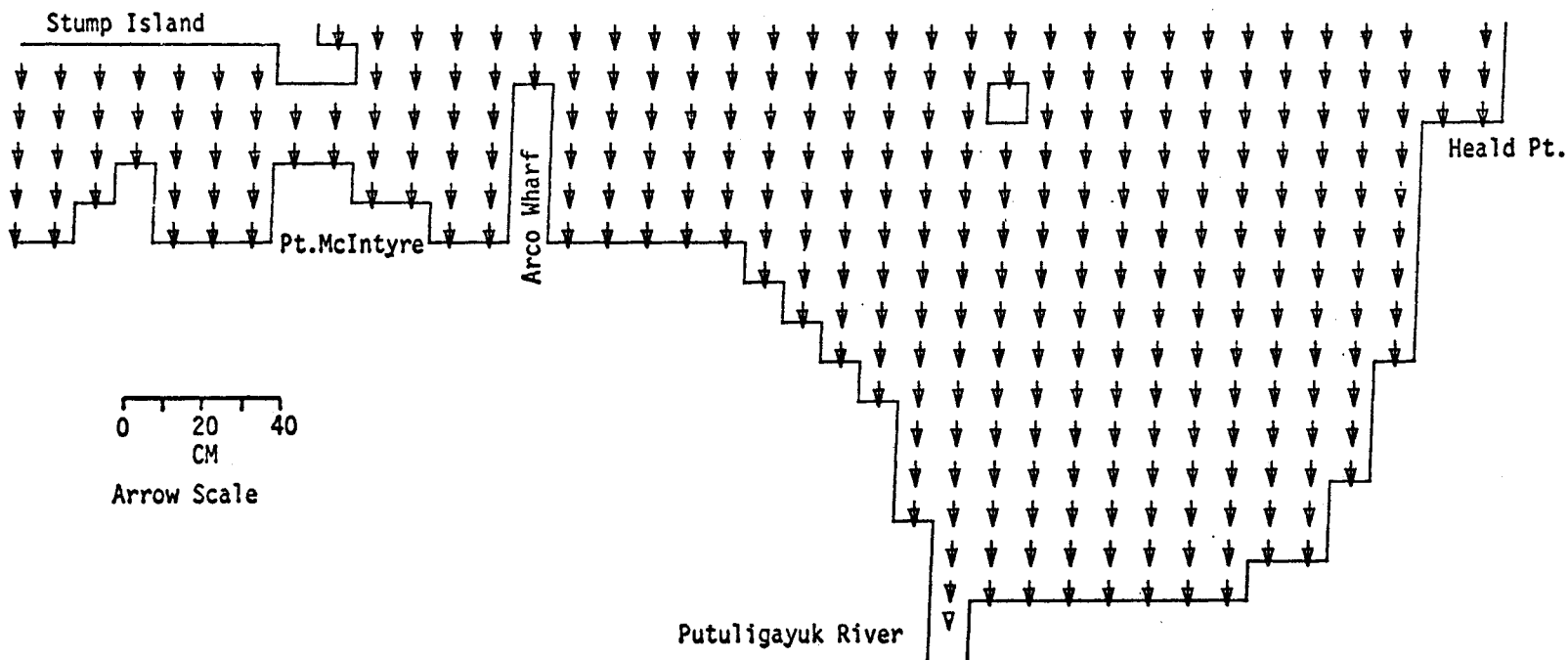
PRUDHOE BAY

M2 TIDE (AMP=8 CM, IN PHASE ON OPEN BOUNDARIES) RIVER FLOW AT 5 CM/SEC

SEA LEVEL

TIME= 61200SEC

LAYER 1



MODEL NO 10

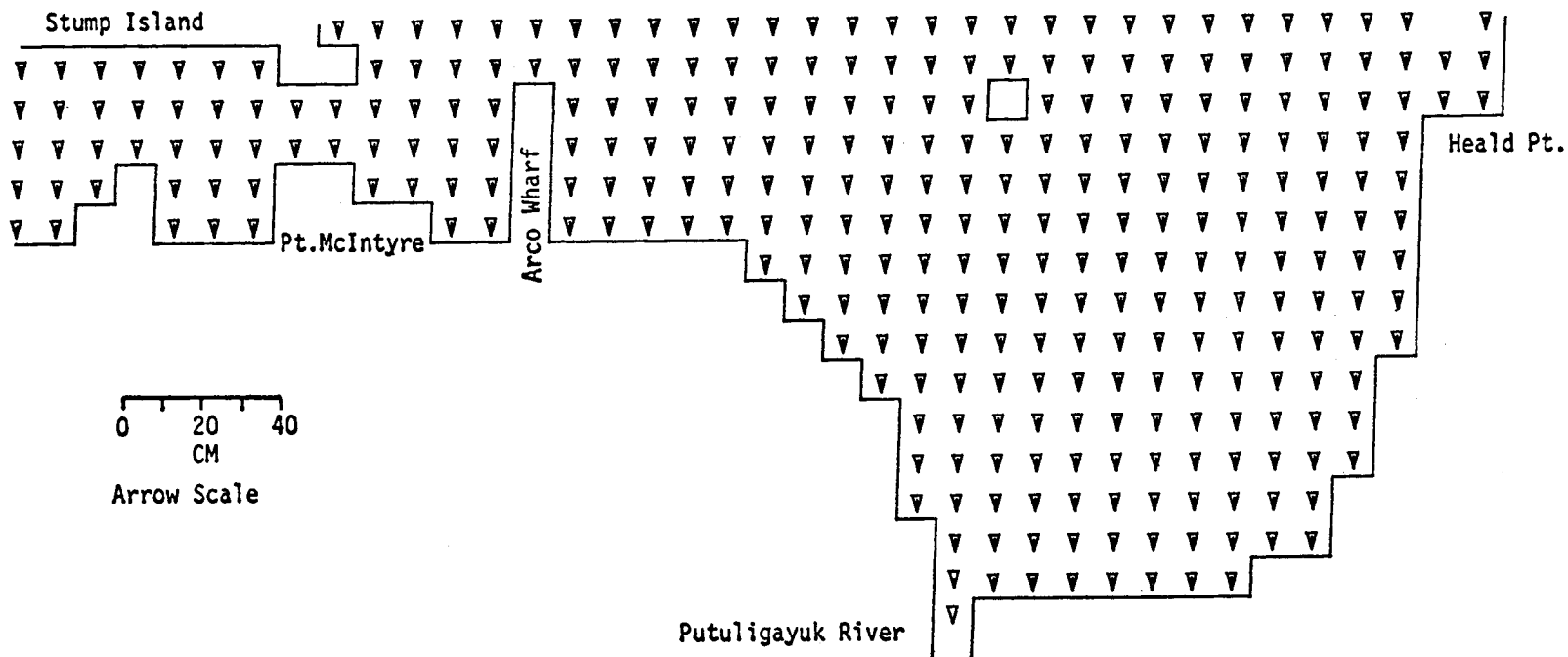
574

PRUDHOE BAY  
M2 TIDE (AMP=8 CM, IN PHASE ON OPEN BOUNDARIES) RIVER FLOW AT 5 CM/SEC

SEA LEVEL

TIME= 64800SEC

LAYER 1



MODEL NO 10

0 20 40  
CM  
Arrow Scale

PRUDHOE BAY

M2 TIDE (AMP=8 CM, IN PHASE ON OPEN BOUNDARIES) RIVER FLOW AT 5 CM/SEC

575

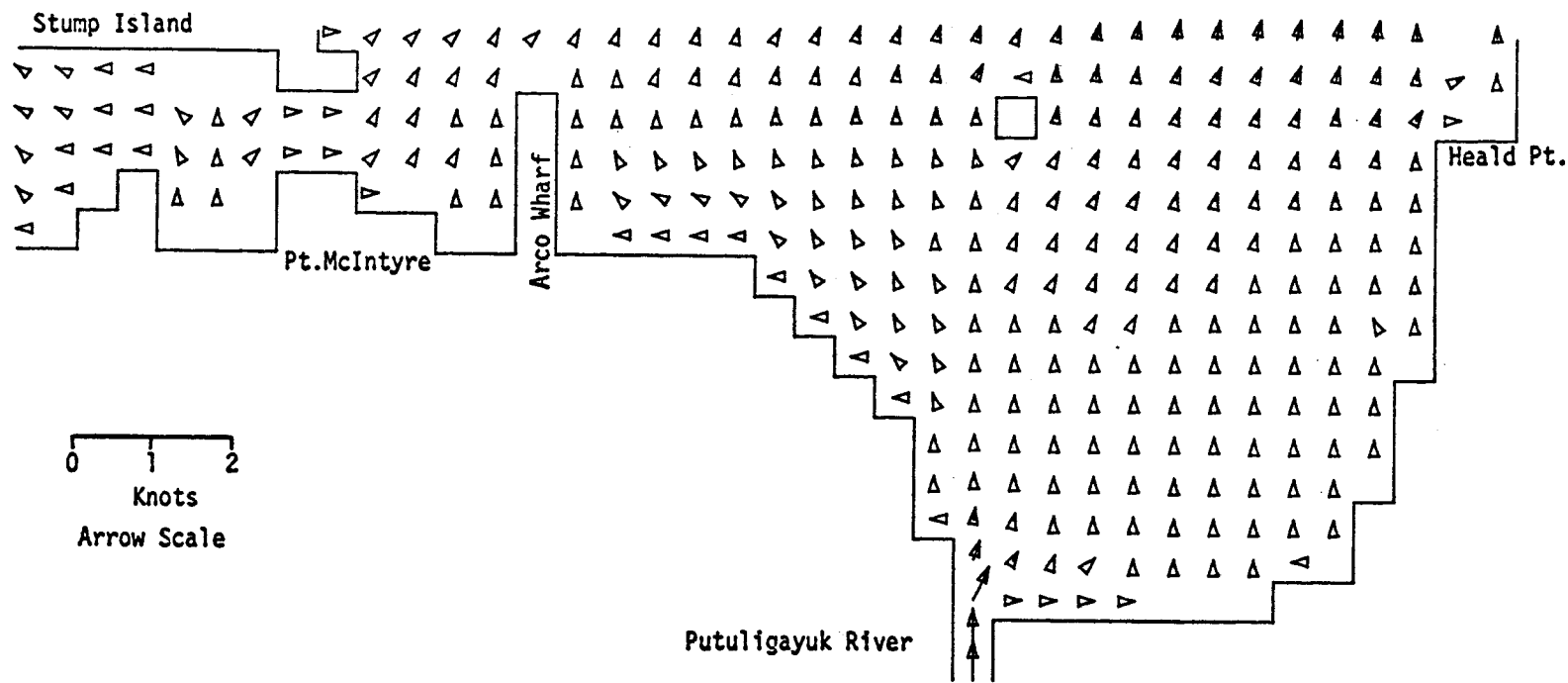
CURRENTS

CURRENTS

TIME=

3600SEC

LAYER 1



MODEL NO 10

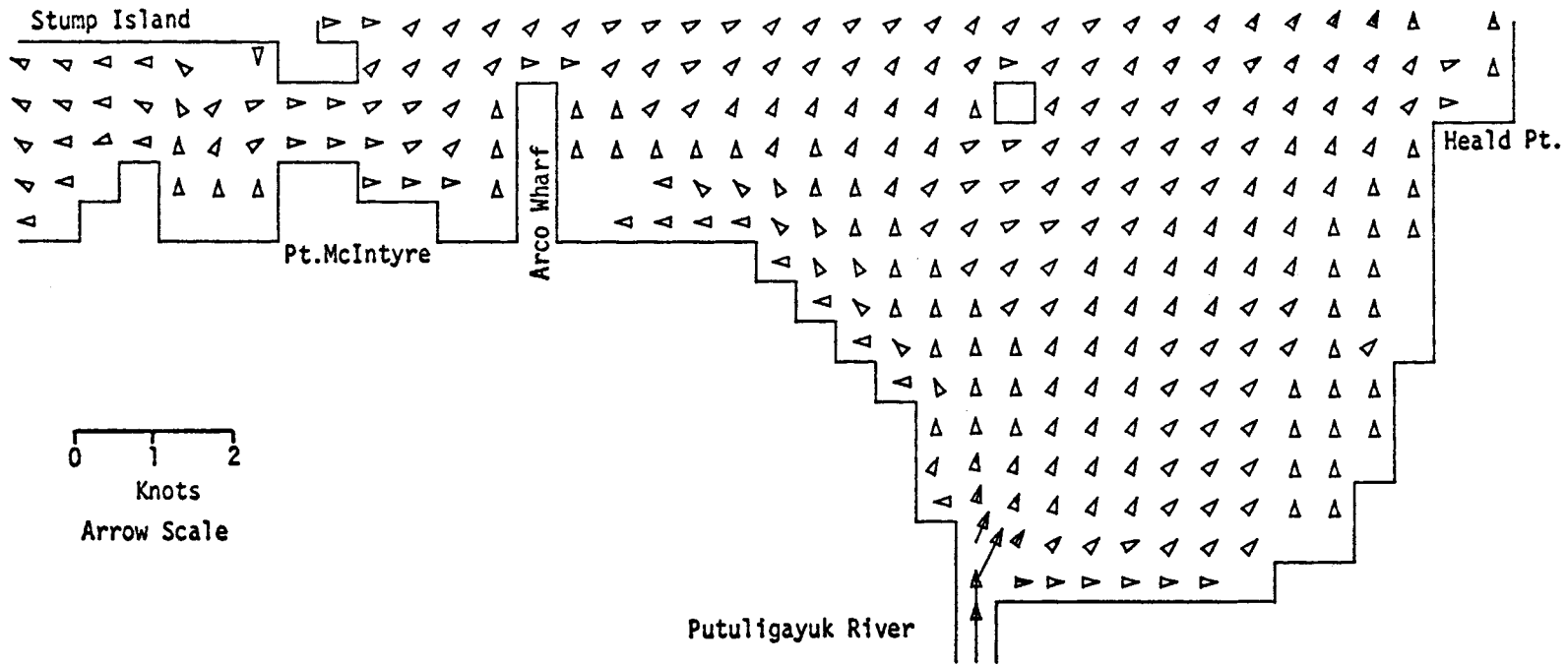
577

PRUDHOE BAY  
M2 TIDE (AMP=8 CM, IN PHASE ON OPEN BOUNDARIES) RIVER FLOW AT 5 CM/SEC

CURRENTS

TIME= 7200SEC

LAYER 1



875  
MODEL NO 10

0 1 2  
Knots  
Arrow Scale

Putuligayuk River

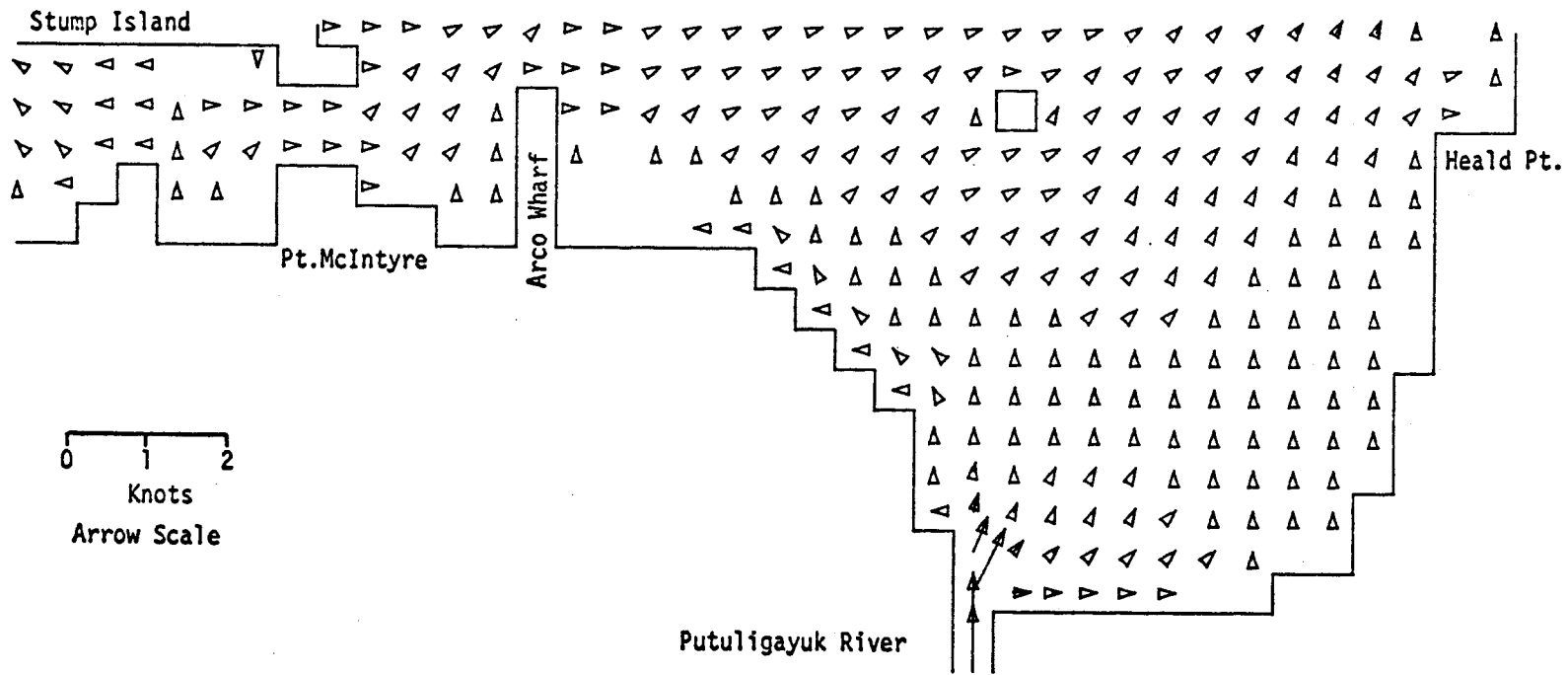
PRUDHOE BAY  
M2 TIDE (AMP=8 CM., IN PHASE ON OPEN BOUNDARIES) RIVER FLOW AT 5 CM/SEC



CURRENTS

TIME= 10800SEC

LAYER 1



10

MODEL NO

625

PRUDHOE BAY

M2 TIDE (AMP=8 CM, IN PHASE ON OPEN BOUNDARIES) RIVER FLOW AT 5 CM/SEC

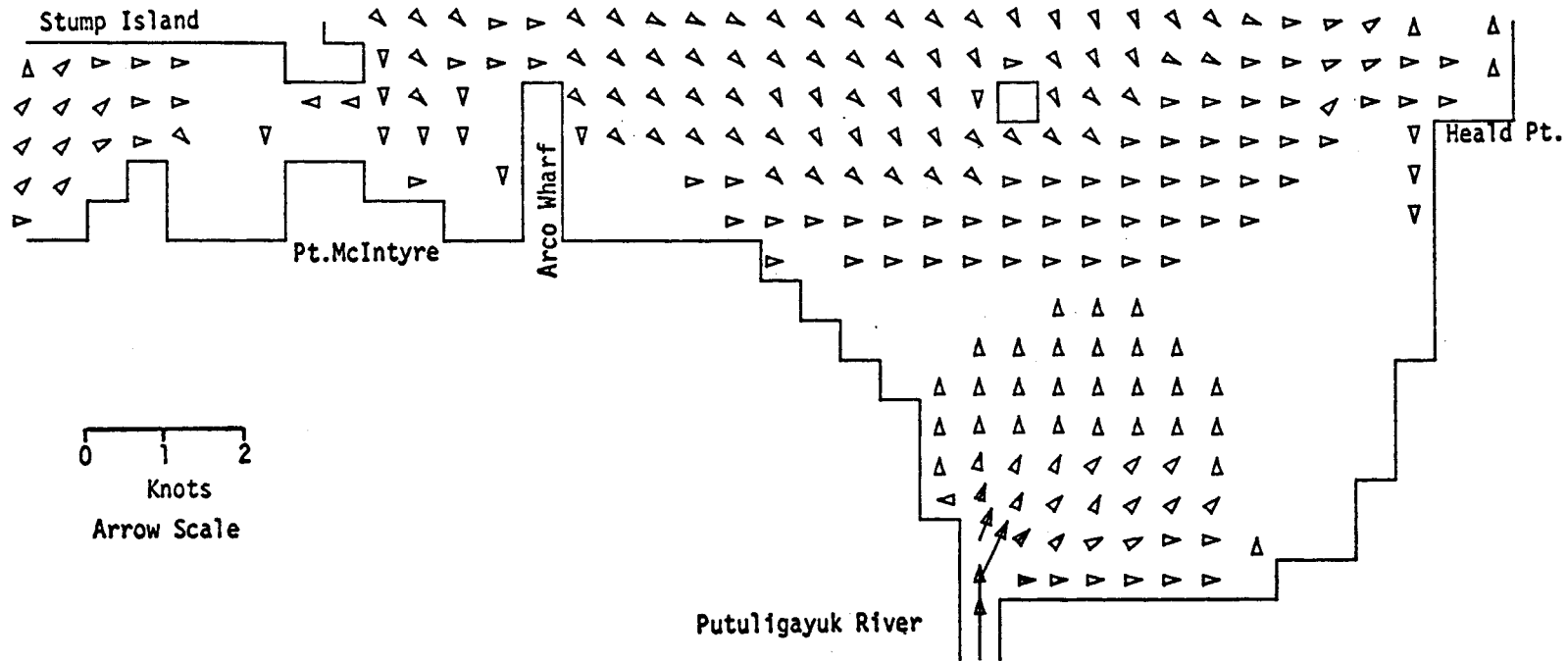
089

MODEL NO 10

CURRENTS

TIME= 14400SEC

LAYER 1



0 1 2  
Knots  
Arrow Scale

Putuligayuk River

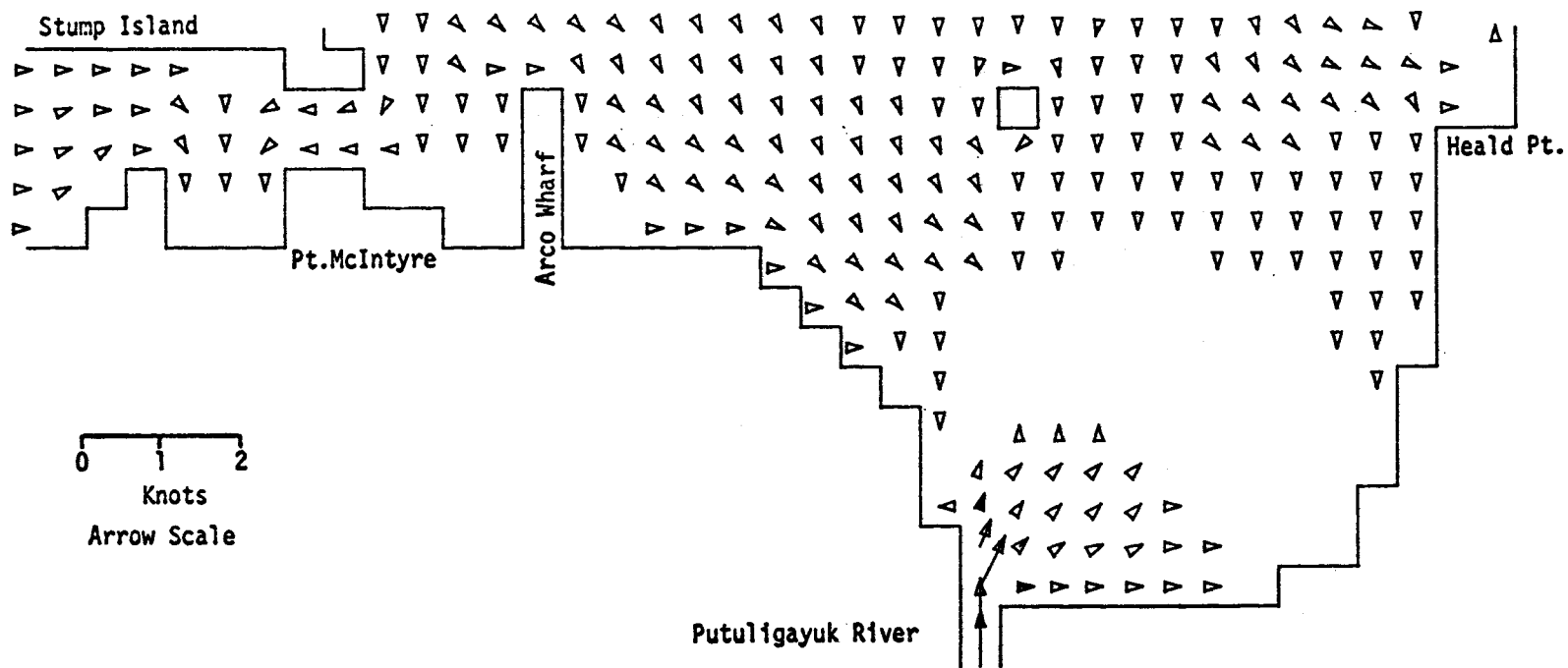
PRUDHOE BAY

M2 TIDE (AMP=8 CM, IN PHASE ON OPEN BOUNDARIES) RIVER FLOW AT 5 CM/SEC

CURRENTS

TIME= 18000SEC

LAYER 1



10

MODEL NO

TSS 581

0 1 2  
Knots  
Arrow Scale

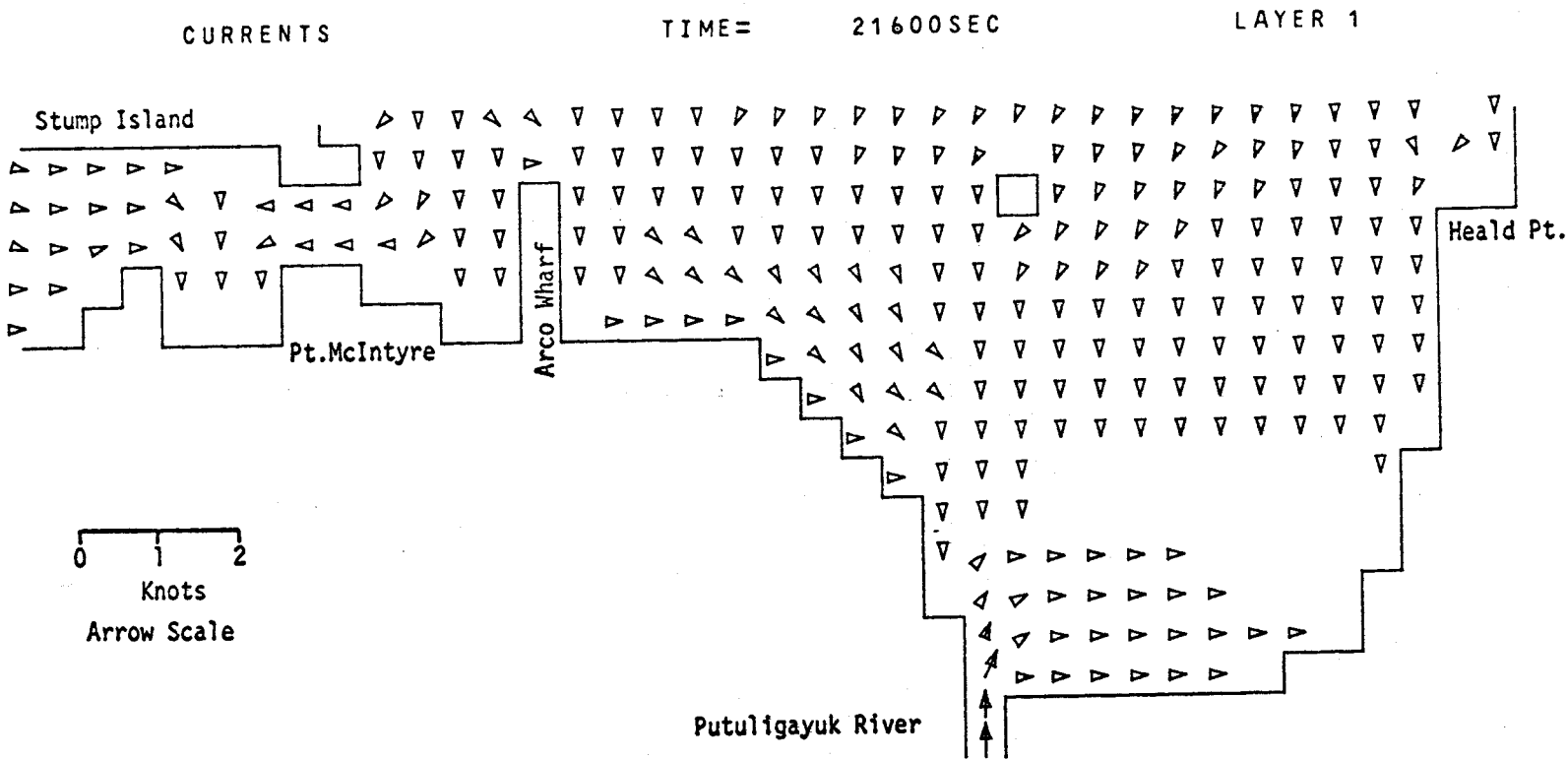
Putuligayuk River

PRUDHOE BAY

M2 TIDE (AMP=8 CM, IN PHASE ON OPEN BOUNDARIES) RIVER FLOW AT 5 CM/SEC

582

MODEL NO 10

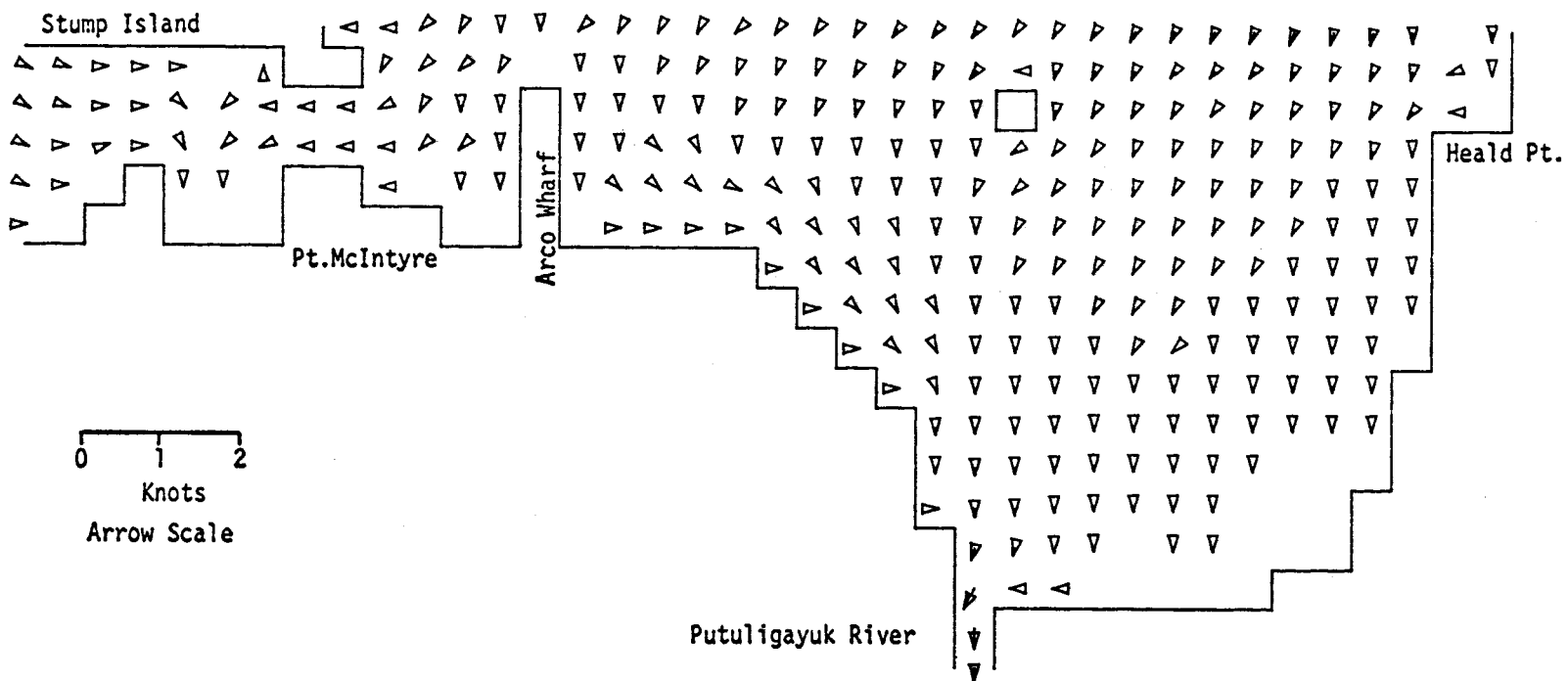


PRUDHOE BAY  
M2 TIDE (AMP=8 CM. IN PHASE ON OPEN BOUNDARIES) RIVER FLOW AT 5 CM/SEC

CURRENTS

TIME= 25200SEC

LAYER 1



MODEL NO 10

0 1 2  
Knots  
Arrow Scale

Putuligayuk River

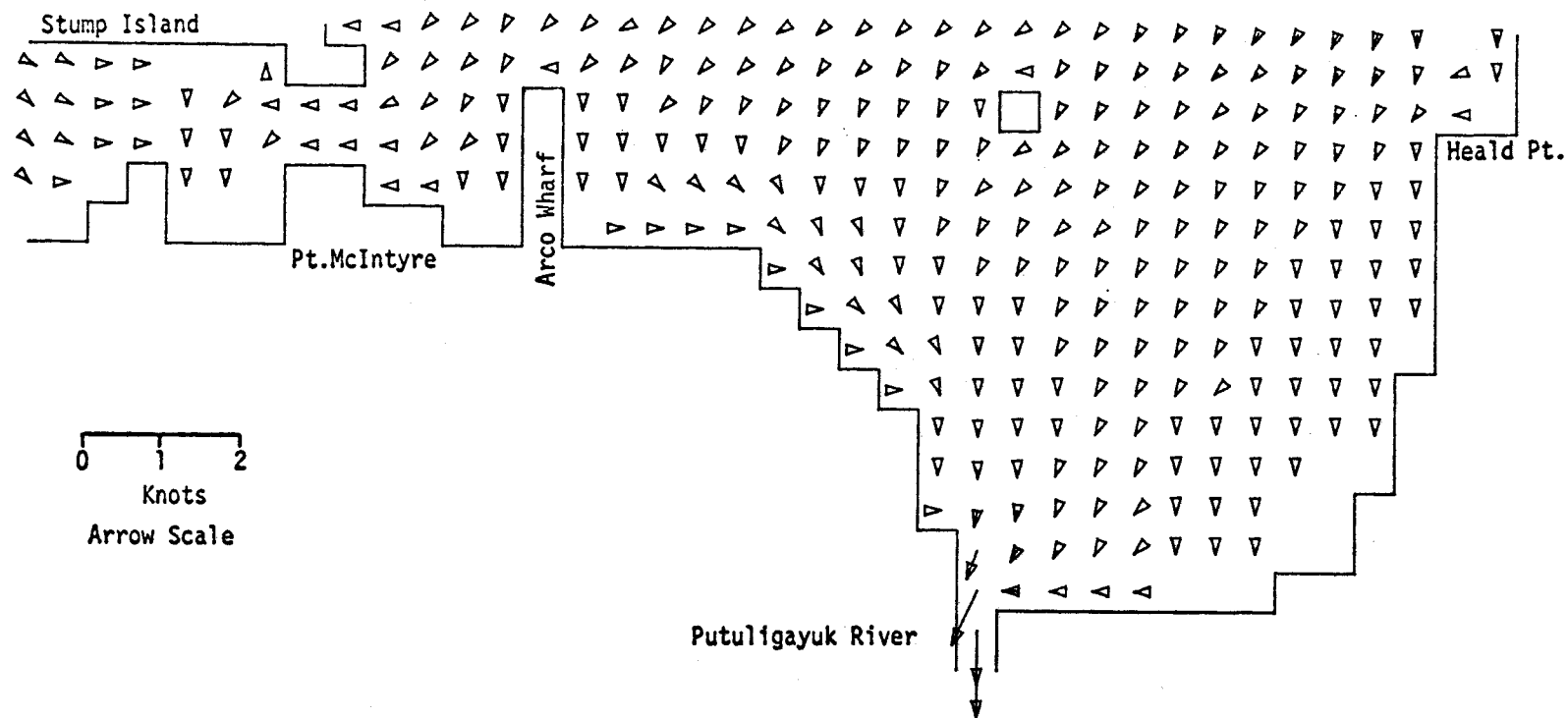
PRUDHOE BAY

M2 TIDE (AMP=8 CM, IN PHASE ON OPEN BOUNDARIES) RIVER FLOW AT 5 CM/SEC

CURRENTS

TIME= 28800SEC

LAYER 1



MODEL NO 10

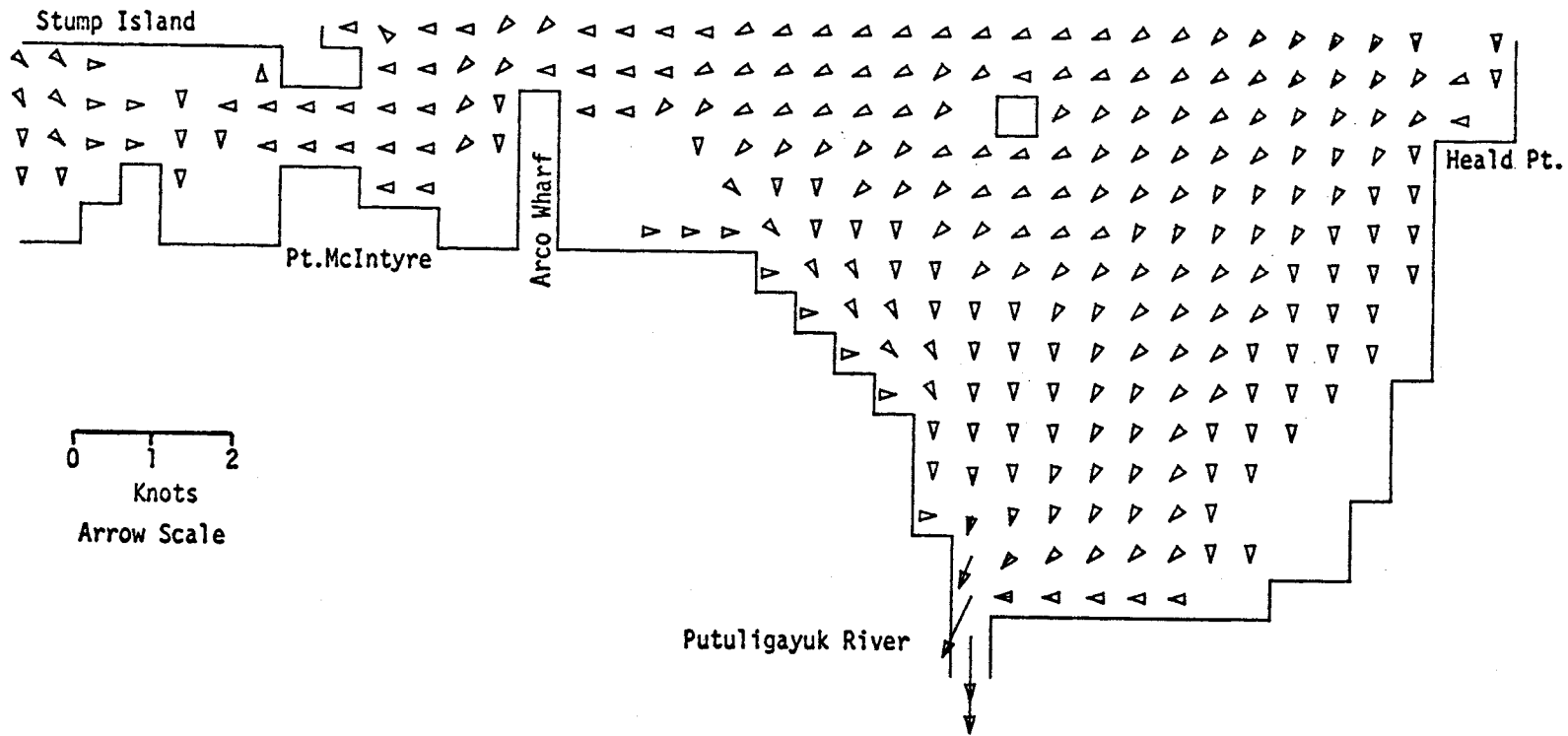
584

PRUDHOE BAY  
M2 TIDE (AMP=8 CM, IN PHASE ON OPEN BOUNDARIES) RIVER FLOW AT 5 CM/SEC

CURRENTS

TIME= 32400SEC

LAYER 1



MODEL NO 10

585

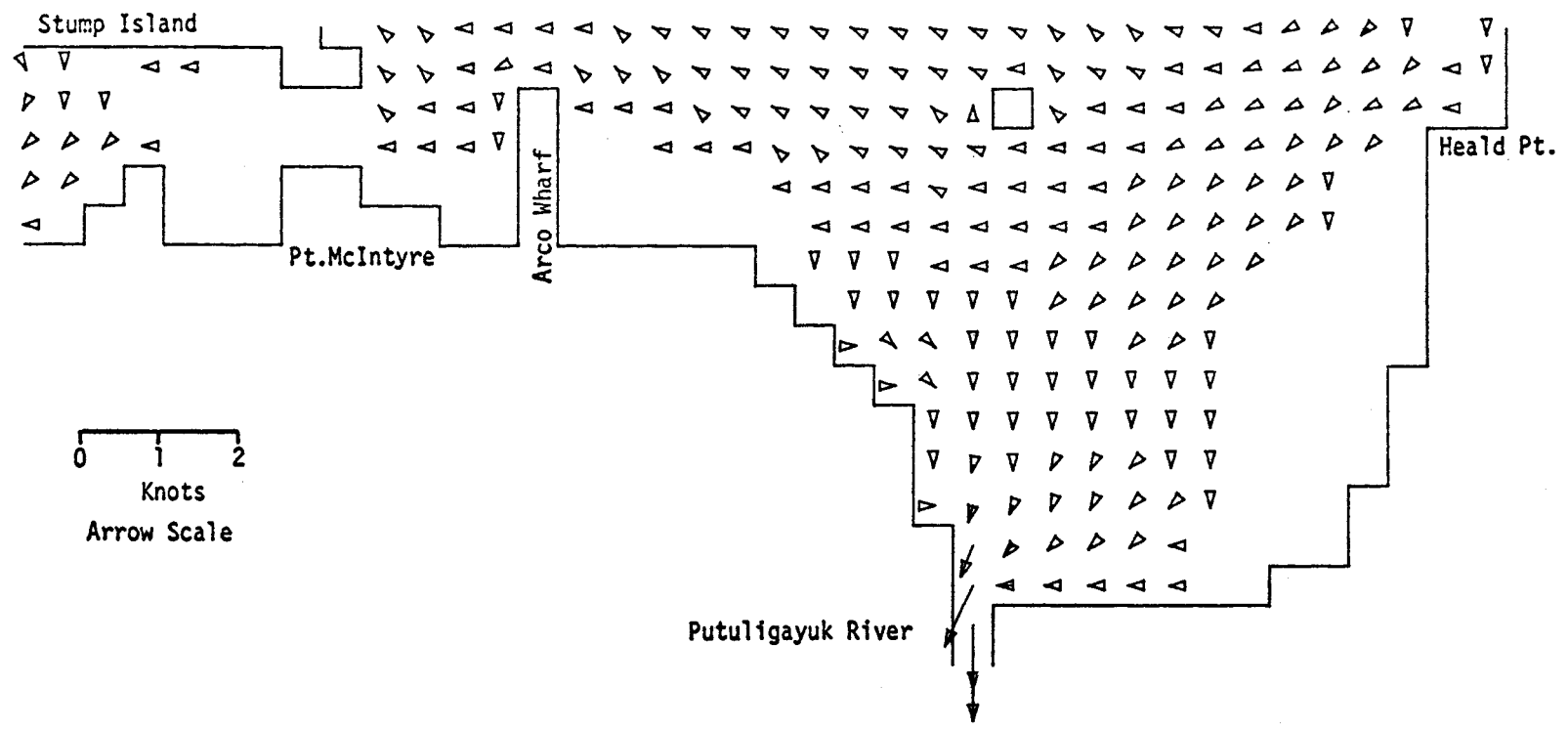
PRUDHOE BAY  
M2 TIDE (AMP=8 CM, IN PHASE ON OPEN BOUNDARIES) RIVER FLOW AT 5 CM/SEC

CURRENTS

TIME= 36000SEC

LAYER 1

10  
985 MODEL NO



0 1 2  
Knots  
Arrow Scale

Putuligayuk River

PRUDHOE BAY

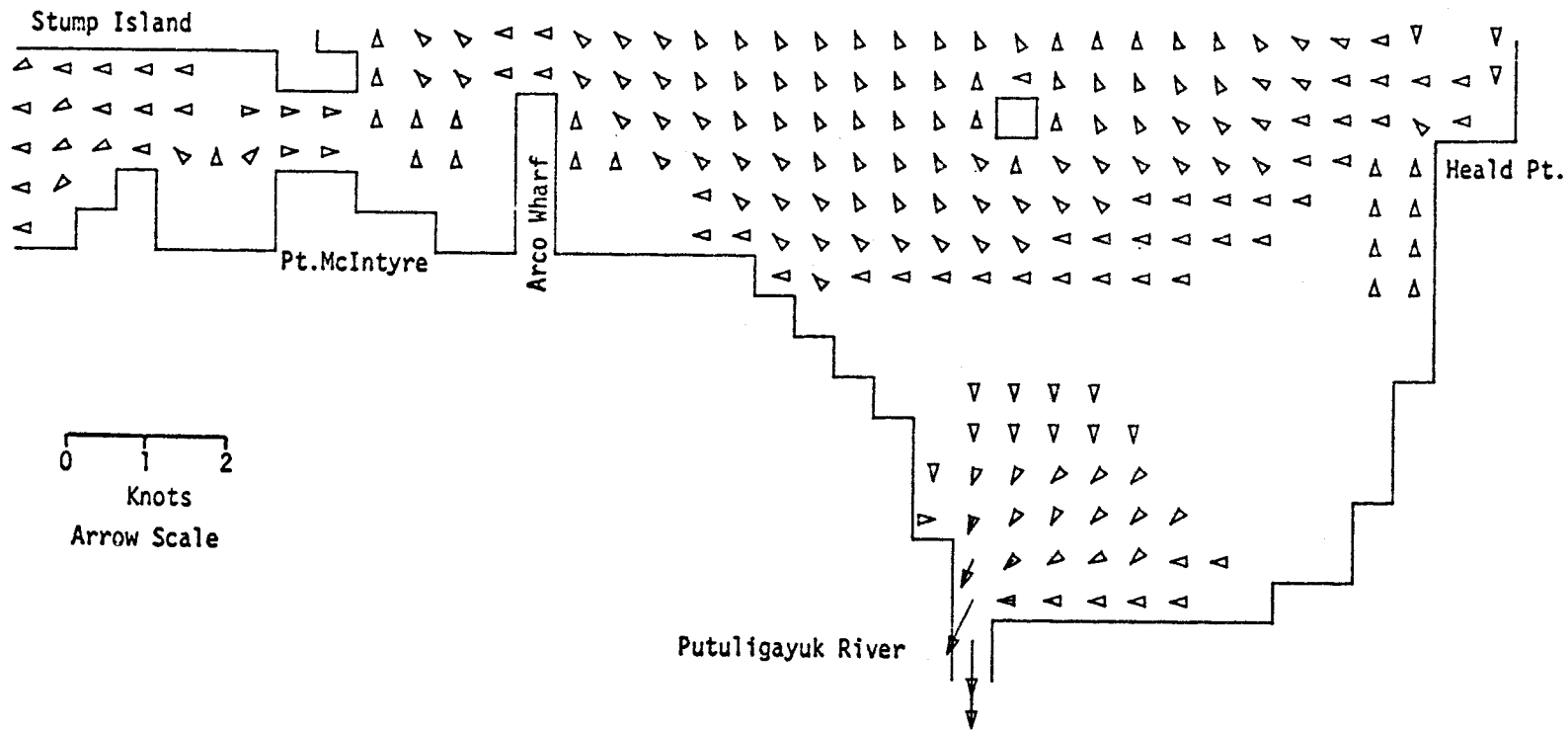
M2 TIDE (AMP=8 CM, IN PHASE ON OPEN BOUNDARIES) RIVER FLOW AT 5 CM/SEC



CURRENTS

TIME= 39600SEC

LAYER 1



MODEL NO 10

0 1 2  
Knots  
Arrow Scale

Putuligayuk River

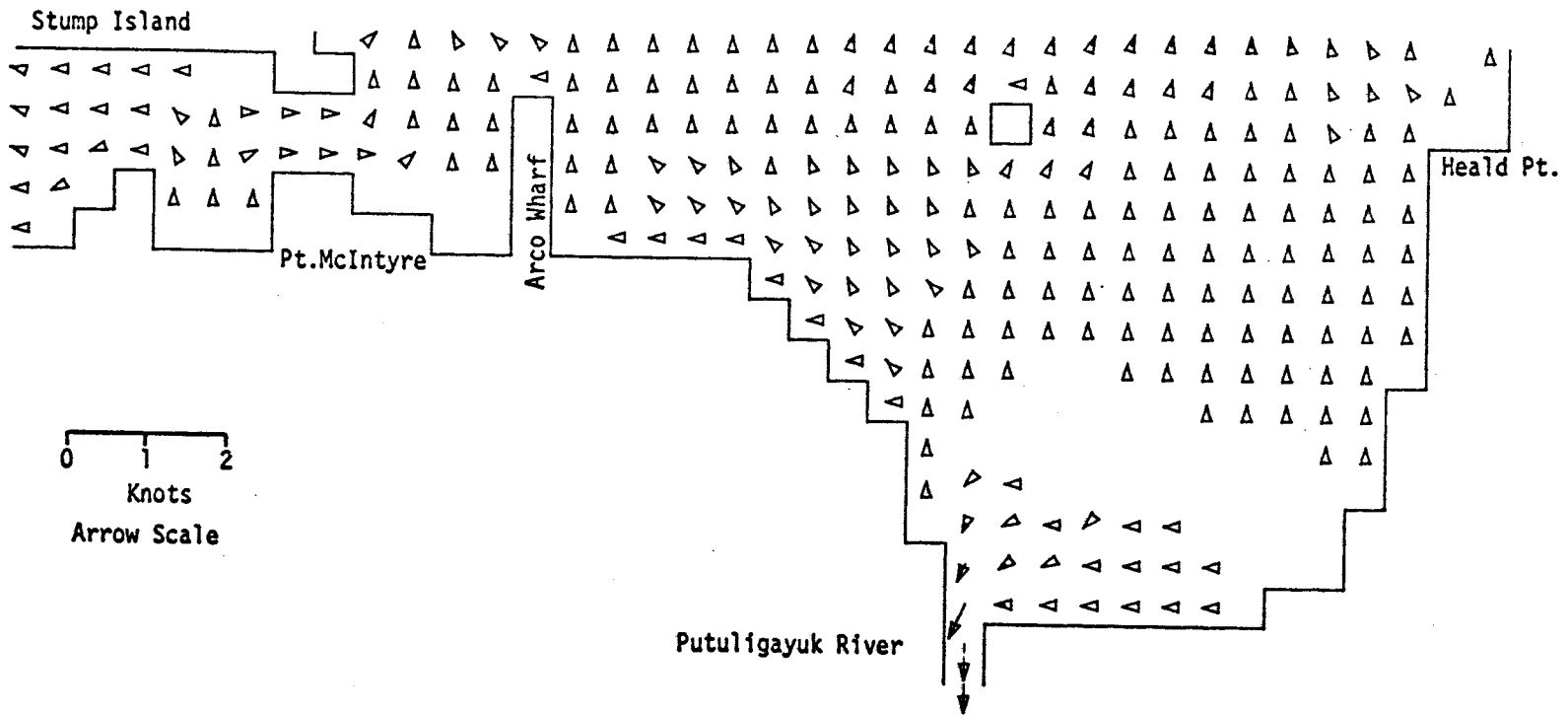
PRUDHOE BAY

M2 TIDE (AMP=8 CM. IN PHASE ON OPEN BOUNDARIES) RIVER FLOW AT 5 CM/SEC

CURRENTS

TIME= 43200SEC

LAYER 1



888

MODEL NO 10

PRUDHOE BAY  
M2 TIDE (AMP=8 CM. IN PHASE ON OPEN BOUNDARIES) RIVER FLOW AT 5 CM/SEC

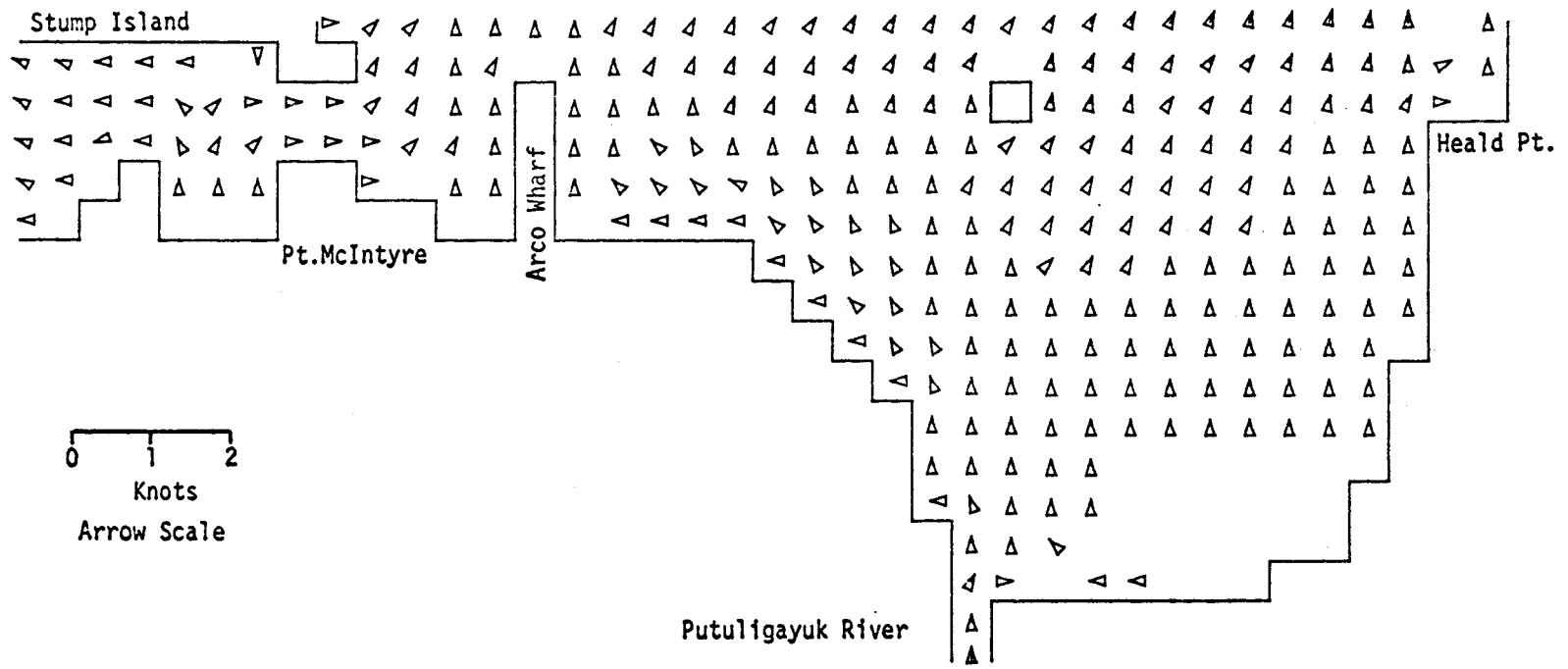
589

MODEL NO 10

CURRENTS

TIME= 46800SEC

LAYER 1

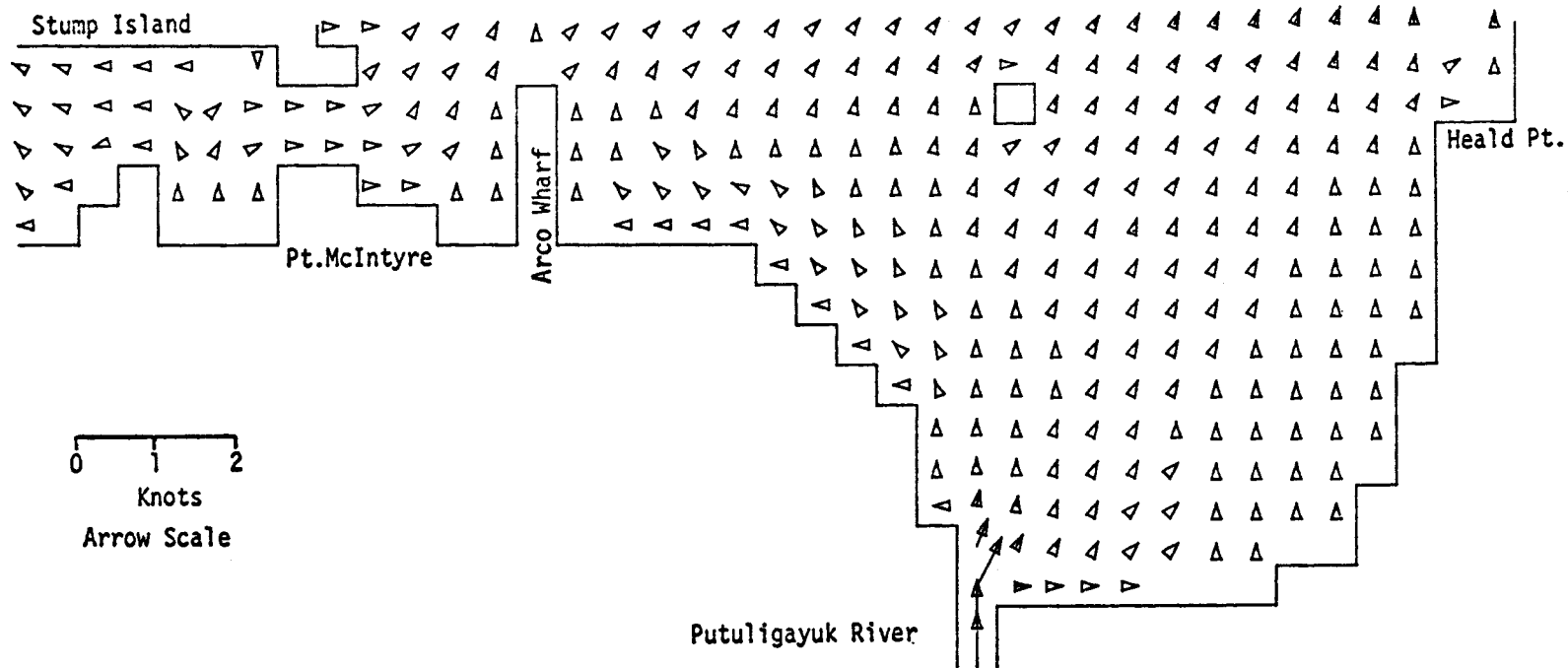


PRUDHOE BAY  
M2 TIDE (AMP=8 CM, IN PHASE ON OPEN BOUNDARIES) RTVER FLOW AT 5 CM/SEC

CURRENTS

TIME= 50400SEC

LAYER 1



10

MODEL NO

069

0 1 2  
Knots  
Arrow Scale

Putuligayuk River

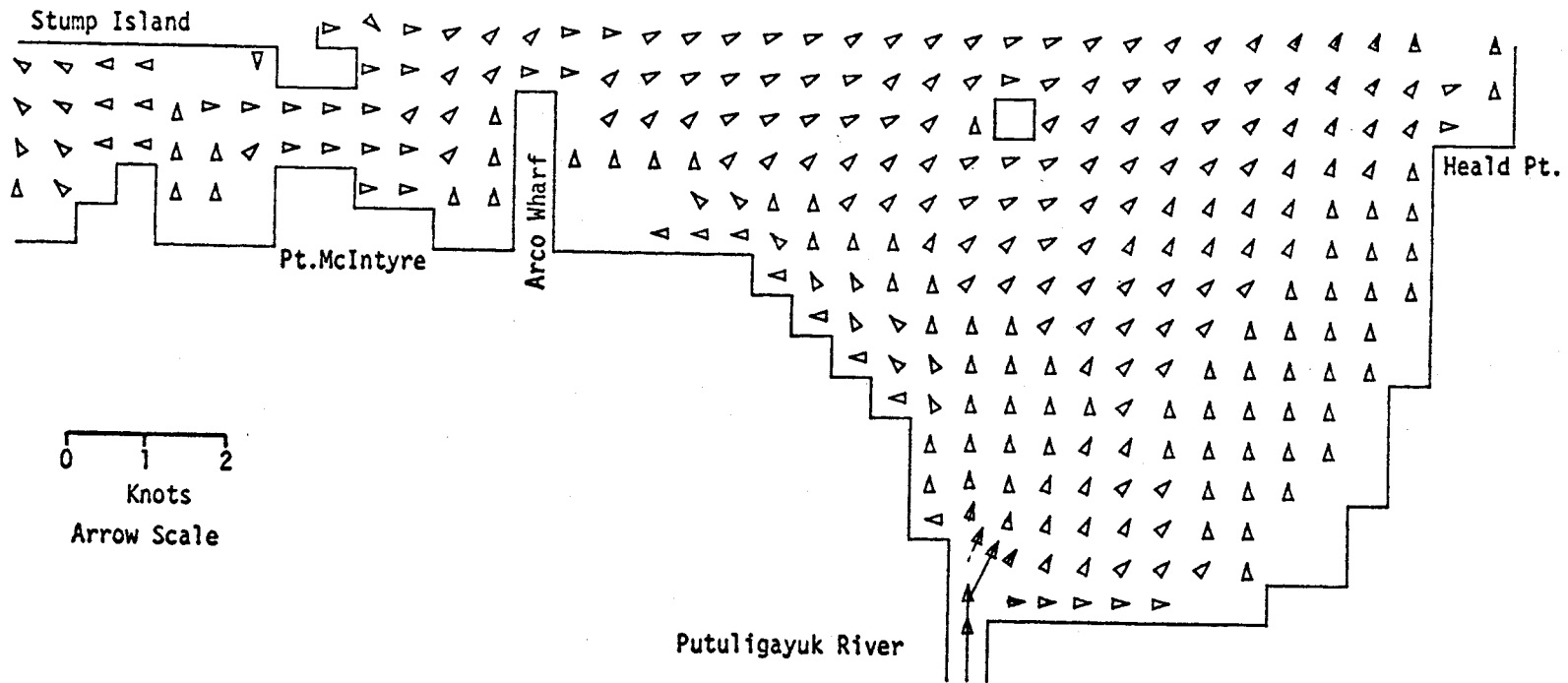
PRUDHOE BAY

M2 TIDE (AMP=8 CM, IN PHASE ON OPEN BOUNDARIES) RIVER FLOW AT 5 CM/SEC

CURRENTS

TIME= 54000SEC

LAYER 1



10

MODEL NO

591

0 1 2  
Knots  
Arrow Scale

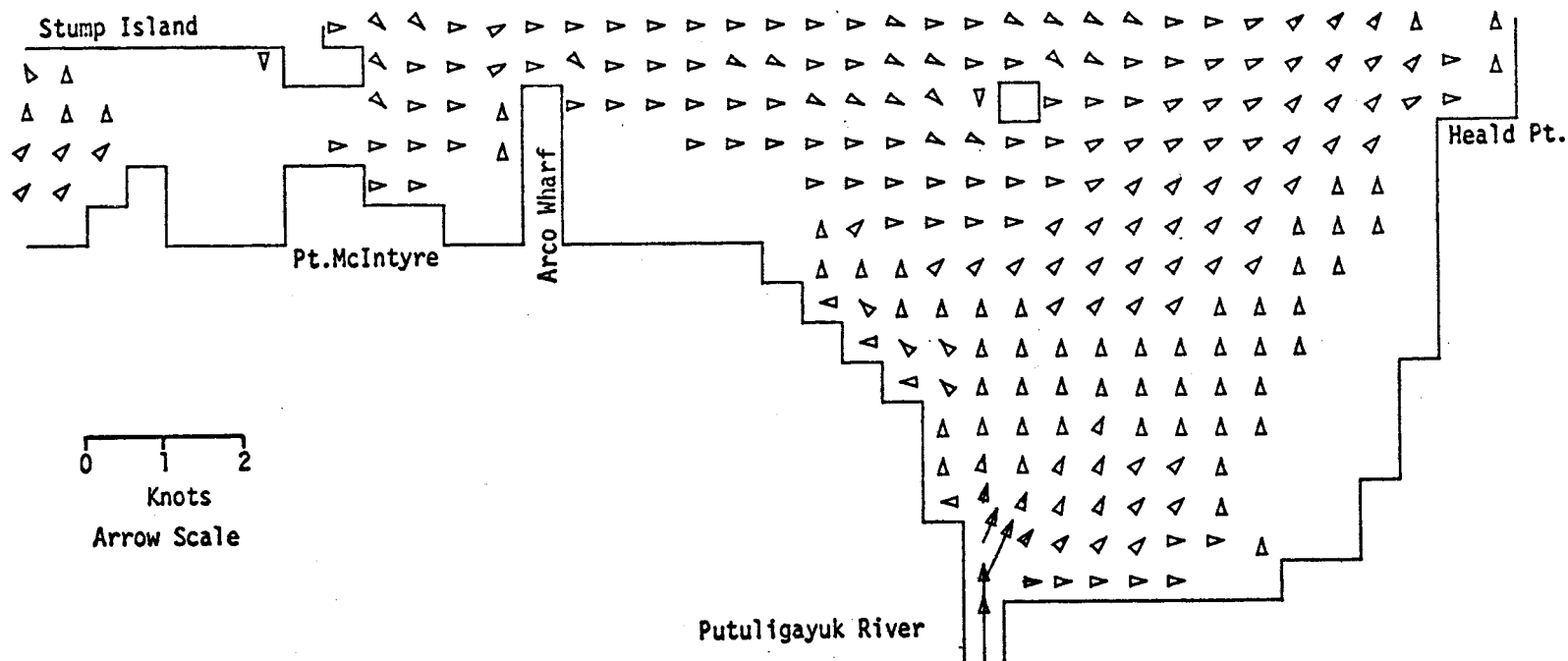
PRUDHOE BAY

M2 TIDE (AMP=8 CM, IN PHASE ON OPEN BOUNDARIES) RIVER FLOW AT 5 CM/SEC

CURRENTS

TIME= 57600SEC

LAYER 1



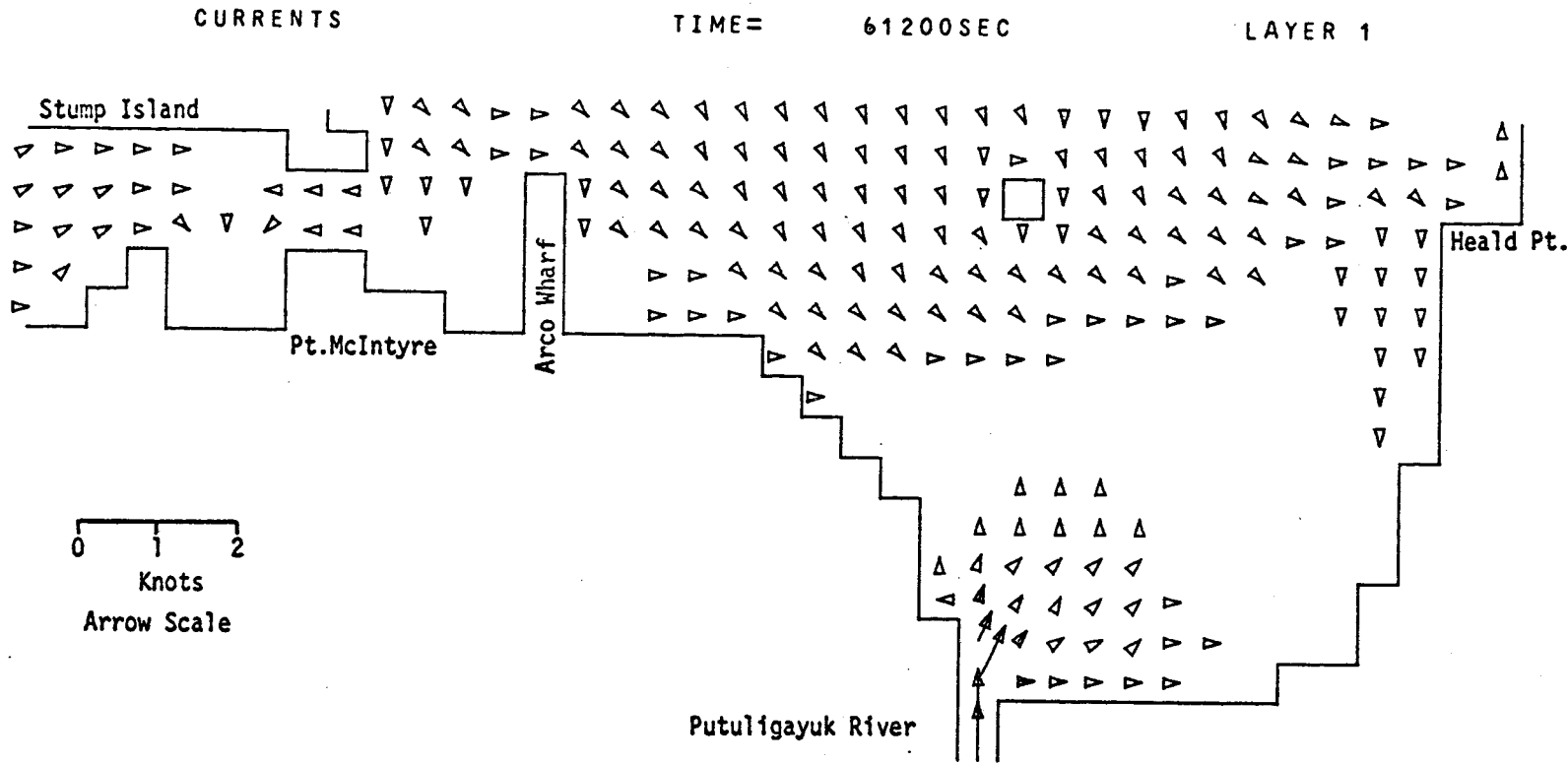
10  
MODEL NO  
592

PRUDHOE BAY

M2 TIDE (AMP=8 CM, IN PHASE ON OPEN BOUNDARIES) RIVER FLOW AT 5 CM/SEC

869

MODEL NO 10

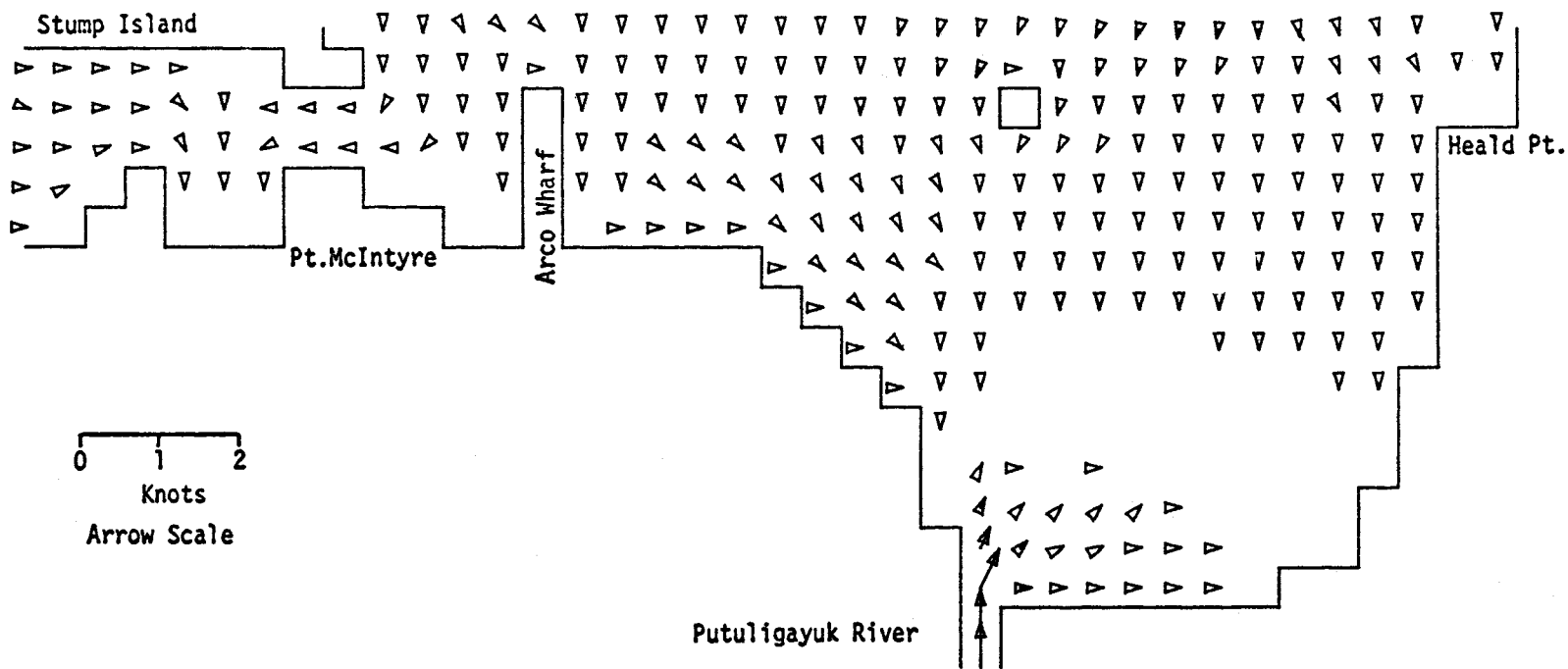


PRUDHOE BAY  
M2 TIDE (AMP=8 CM. IN PHASE ON OPEN BOUNDARIES) RIVER FLOW AT 5 CM/SEC

CURRENTS

TIME= 64800SEC

LAYER 1



10

MODEL NO

0 1 2  
Knots  
Arrow Scale

PRUDHOE BAY

M2 TIDE (AMP=8 CM, IN PHASE ON OPEN BOUNDARIES) RIVER FLOW AT 5 CM/SEC

599



APPENDIX D  
PRUDHOE BAY

M2 TIDE WITH 8 CM AMPLITUDE INPUT IN PHASE  
ON ALL OPEN BOUNDARIES  
NO RIVER FLOW  
]0 KNOT WIND ONSHORE

APPENDIX D  
PRUDHOE BAY

M2 TIDE WITH 8 CM AMPLITUDE INPUT IN PHASE

ON ALL OPEN BOUNDARIES

NO RIVER FLOW

]0 KNOT WIND ONSHORE

ENVIRONMENTAL PROTECTION AGENCY  
 MARINE AND FRESHWATER ECOLOGY BRANCH  
 OCEAN MASS TRANSPORT MODEL

M2 TIDE (AMPE=8 CM, IN PHASE ON OPEN BOUNDARIES) UNSHORE WIND AT 10 KT  
 BEAUFORT SEA SHELF STUDY  
 GRID 310 BRIDGE HAY AT 0.5 KM GRID SPACING

GRID GEOMETRY                      ROWS    17                      COLUMNS    39  
 GRID LENGTH                      50000. CM                      ROTATION ANGLE                      331.5 DEG  
 WIND DRAG COEFFICIENT                      .0024                      MID LATITUDE                      70.350 DEG. (N)  
 FRICTION COEFFICIENT                      .0030000 CM/SEC

INITIAL LAYER DEPTHS                      LAYER 1                      LAYER 2                      LAYER 3  
    300.0000                      .0000                      .0000  
 SMOOTHING FACTORS                      .9900                      .0000                      .0000  
 DENSITY                                      1.0200                      .0000                      .0000

RESULTS SAVED AT MODULUS(TIME,                      3600 SEC)=0                      RESULTS SAVED STARTING AT                      3600 SEC  
 COMPUTATIONS STARTED AT                      0 SEC  
    ENDED AT                      64800 SEC  
    INCREMENTED BY                      60 SEC  
    LAYER3 PRINT OUT STARTED                      3600 SEC. FREQUENCY OF                      3600 SEC

TIDAL INPUT AT                      ROW    1 THRU    7                      COLUMN    1 THRU    1                      TIME LAG                      0 SEC  
    M2                      S2                      01                      K1  
 PHASE ANGLES(DEG/HR)                      270.00                      .00                      .00                      .00  
 AMPLITUDES (CM)                      8.00                      .00                      .00                      .00  
 LOWER LAYER WEIGHTING FACTORS                      LAYER 2= .00                      LAYER 3= .00

TIDAL INPUT AT                      ROW    1 THRU    1                      COLUMN    8 THRU    39                      TIME LAG                      0 SEC  
    M2                      S2                      01                      K1  
 PHASE ANGLES(DEG/HR)                      270.00                      .00                      .00                      .00  
 AMPLITUDES (CM)                      8.00                      .00                      .00                      .00  
 LOWER LAYER WEIGHTING FACTORS                      LAYER 2= .00                      LAYER 3= .00

TIDAL SPEEDS (DEG/HR)                      M2                      S2                      01                      K1  
    28.984000                      .000000                      .000000                      .000000

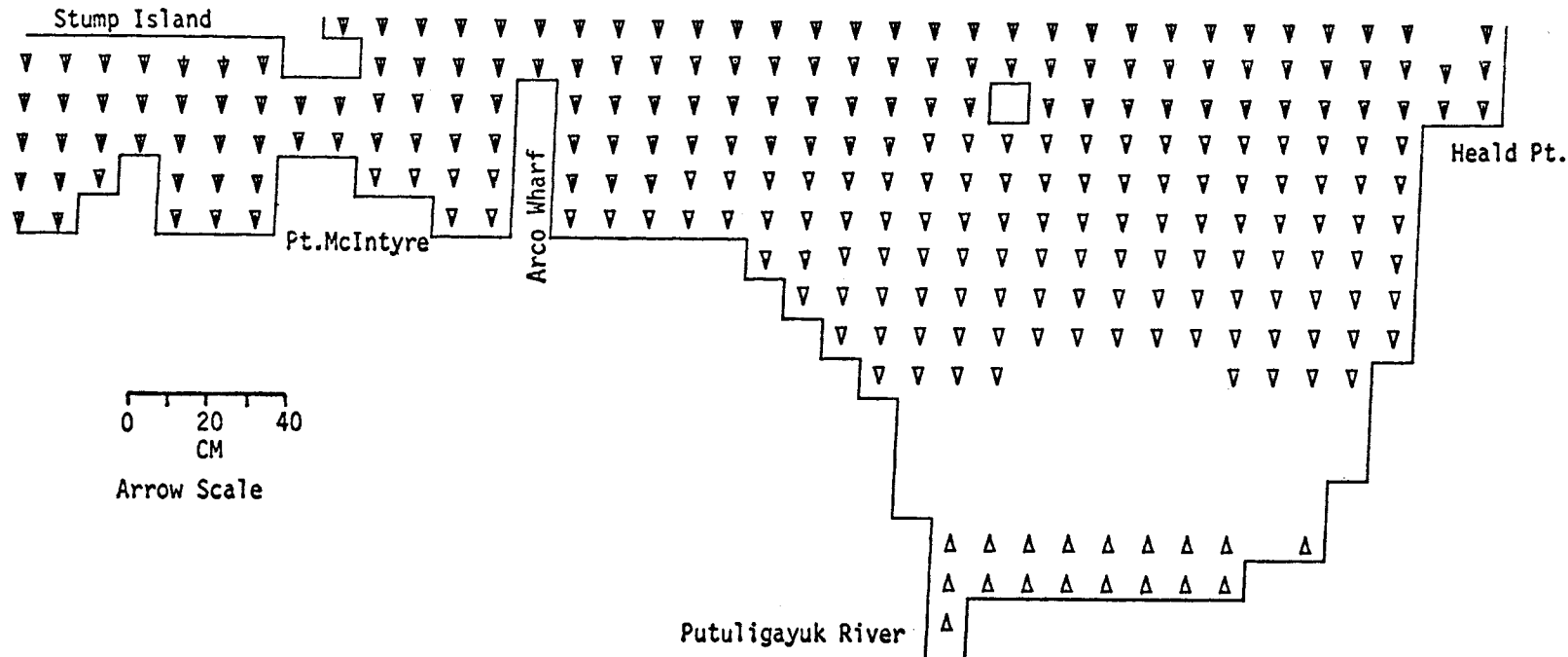
WIND INPUT AT                      ROW    1 THRU    17                      COLUMN    1 THRU    39  
 COMPUTATIONS STARTED AT                      60 SEC  
    ENDED AT                      64800 SEC DIRECTION    29 DEG TRUE SPEED                      5 M/SEC

SEA LEVEL

SEA LEVEL

TIME= 3600SEC

LAYER 1



MODEL NO 10

669

0 20 40  
CM

Arrow Scale

Putuligayuk River

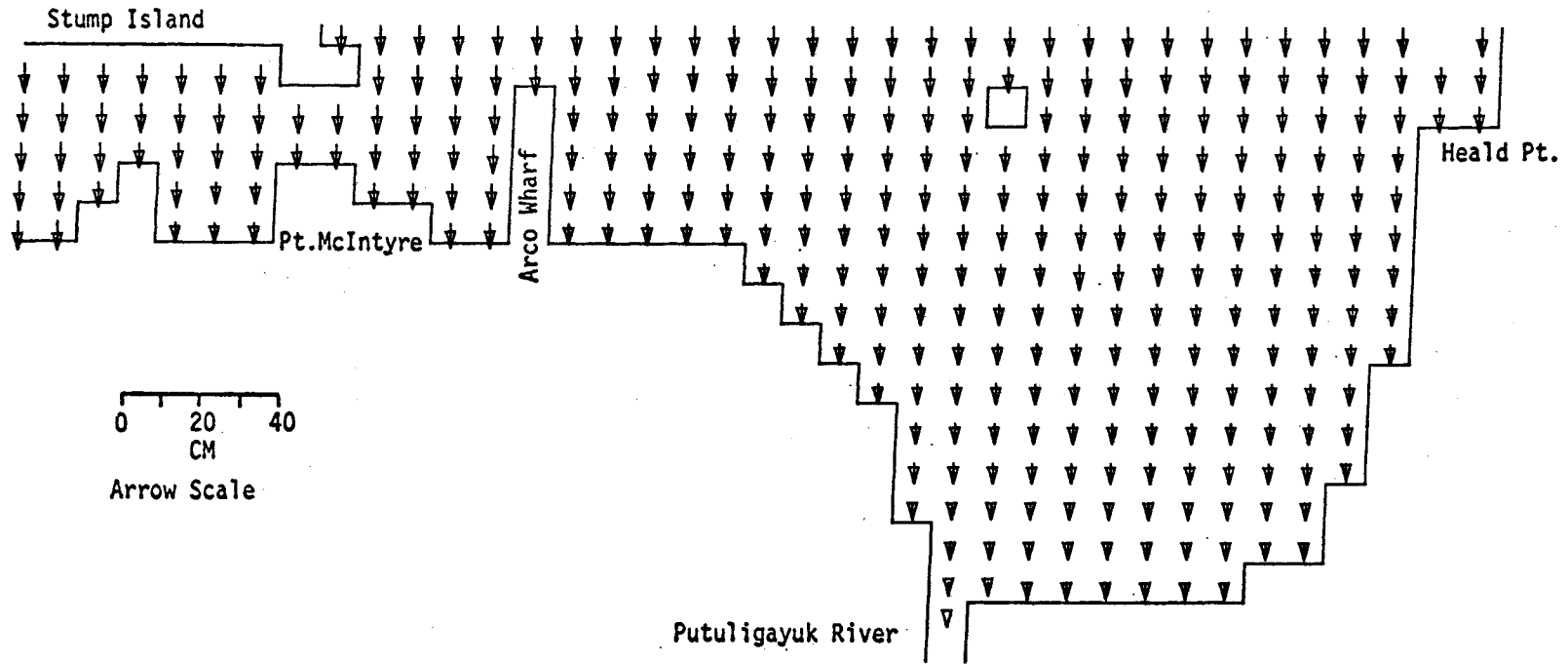
PRUDHOE BAY

M2 TIDE (AMP=8 CM, IN PHASE ON OPEN BOUNDARIES) ONSHORE WIND AT 1.0 KT

SEA LEVEL

TIME = 7200SEC

LAYER 1



009

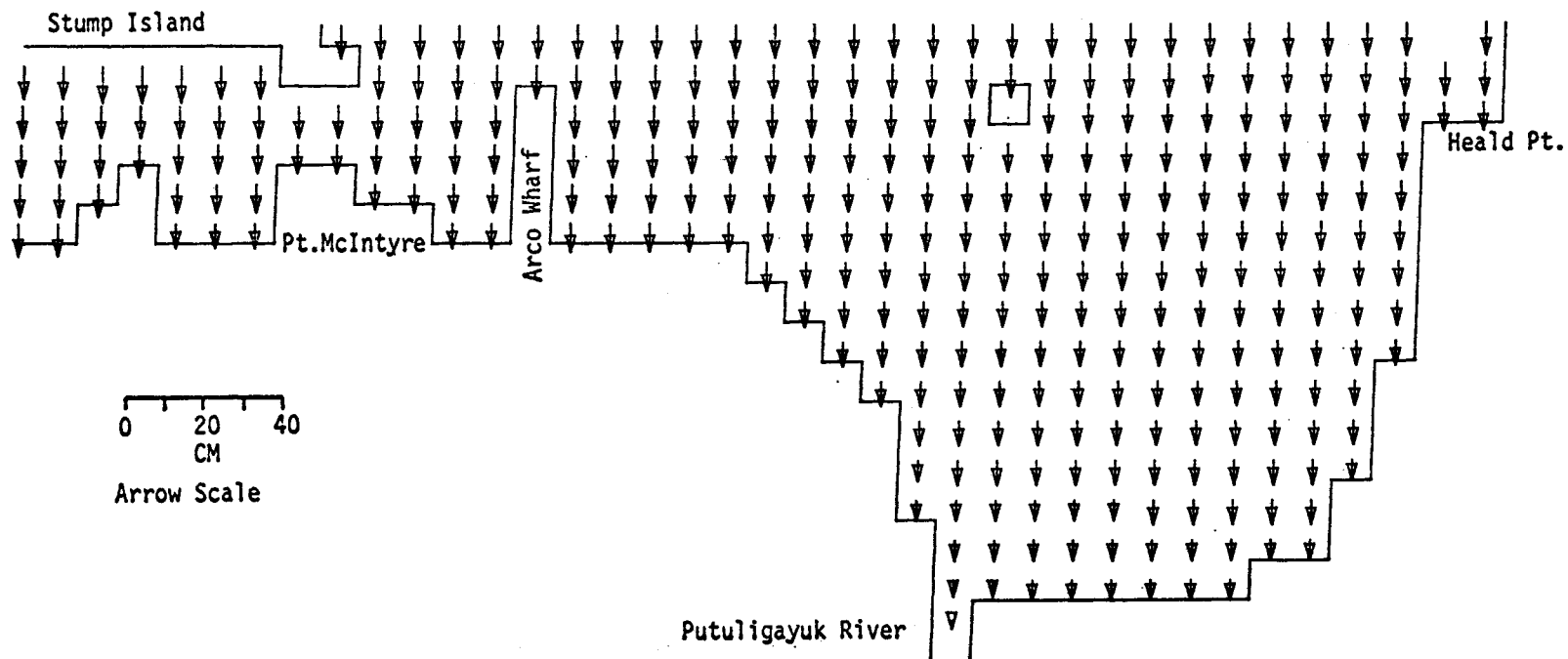
MODEL NO 10

PRUDHOE BAY  
M2 TIDE (AMP=8 CM, IN PHASE ON OPEN BOUNDARIES) ONSHORE WIND AT 10 KT

SEA LEVEL

TIME= 10800SEC

LAYER 1



T09

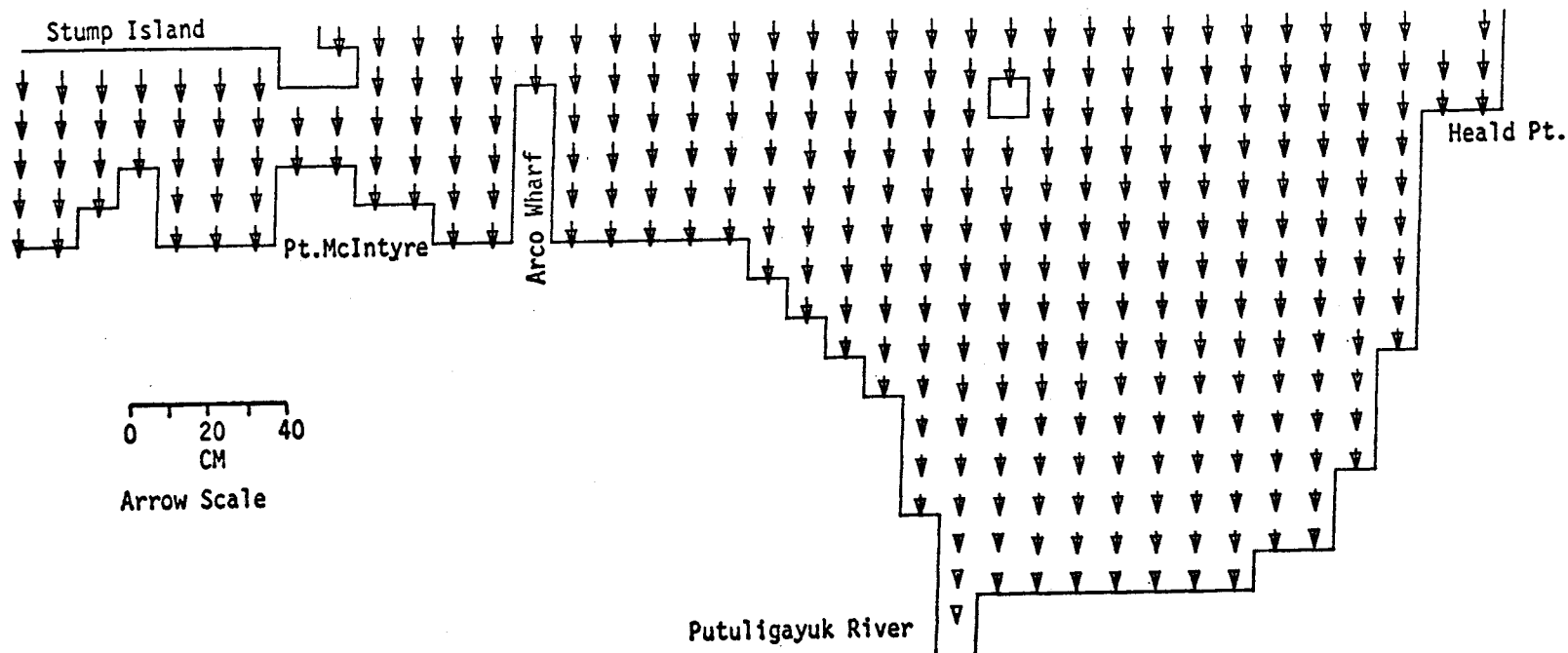
MODEL NO 10

PRUDHOE BAY  
M2 TIDE (AMP=8 CM, IN PHASE ON OPEN BOUNDARIES) ONSHORE WIND AT 10 KT

SEA LEVEL

TIME= 14400SEC

LAYER 1



MODEL NO 10

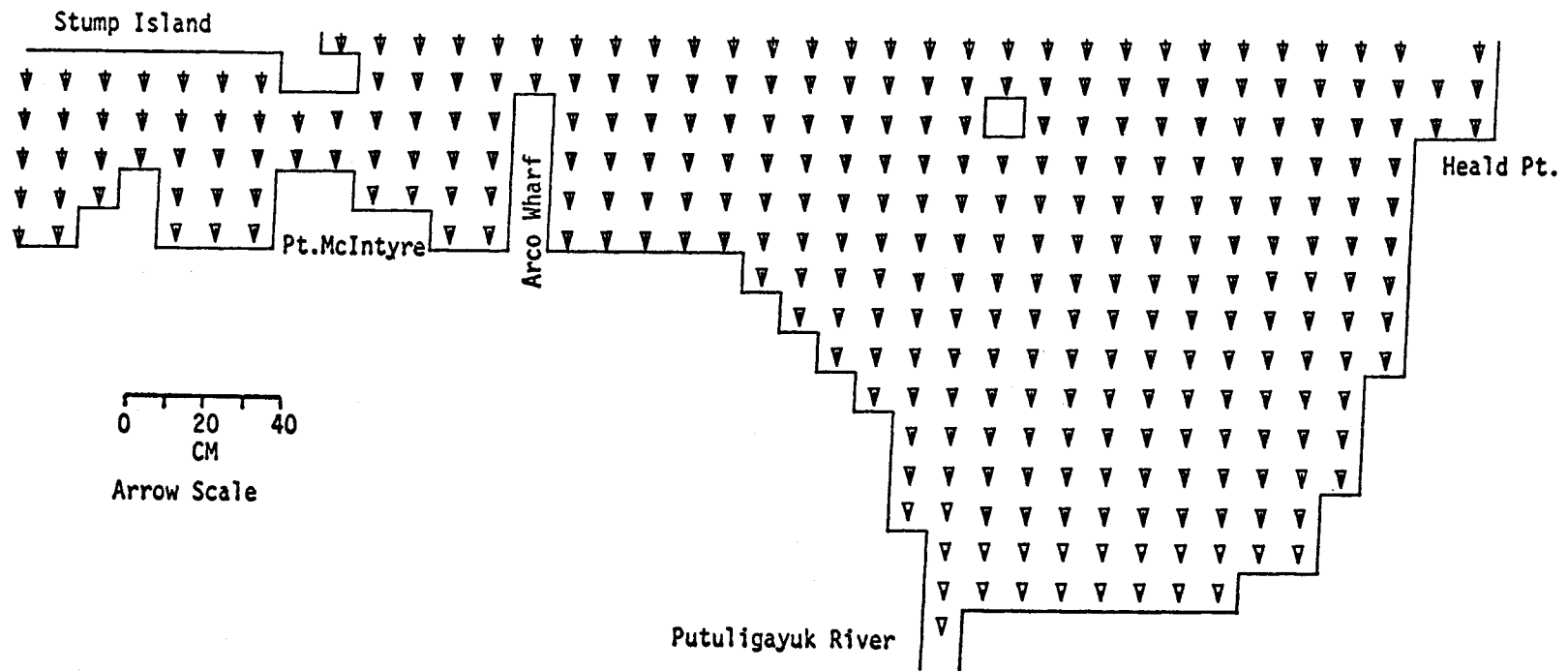
PRUDHOE BAY  
M2 TIDE (AMP=8 CM. IN PHASE ON OPEN BOUNDARIES) ONSHORE WIND AT 1.0 KT



SEA LEVEL

TIME= 18000SEC

LAYER 1



0 20 40  
CM  
Arrow Scale



Putuligayuk River

Heald Pt.

Stump Island

Pt. McIntyre

Arco Wharf

PRUDHOE BAY

M2 TIDE (AMP=8 CM, IN PHASE ON OPEN BOUNDARIES) ONSHORE WIND AT 10 KT

603

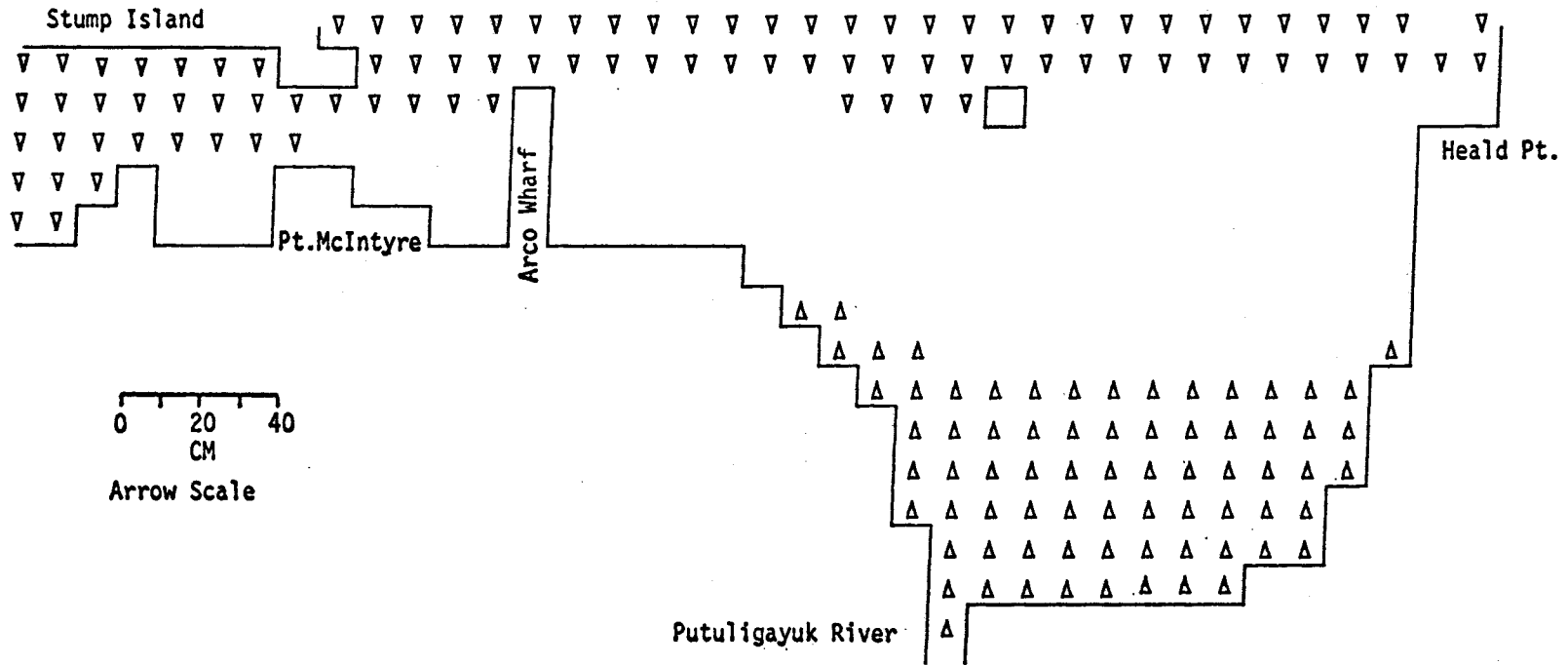
MODEL NO 10

MODEL NO 10  
504

SEA LEVEL

TIME= 21600SEC

LAYER 1



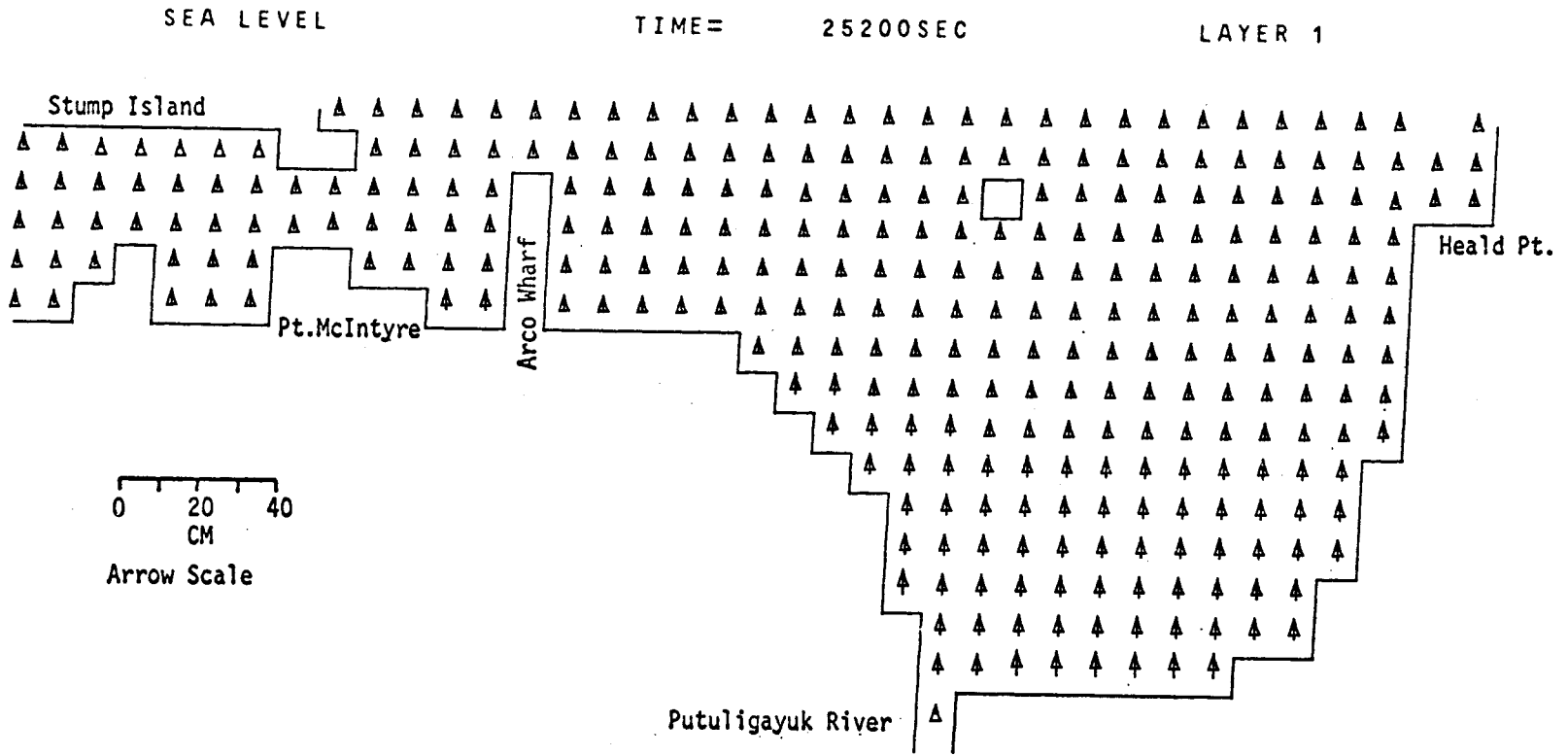
0 20 40  
CM  
Arrow Scale

PRUDHOE BAY

M2 TIDE (AMP=8 CM, IN PHASE ON OPEN BOUNDARIES) ONSHORE WIND AT 10 KT

509

MODEL NO 10

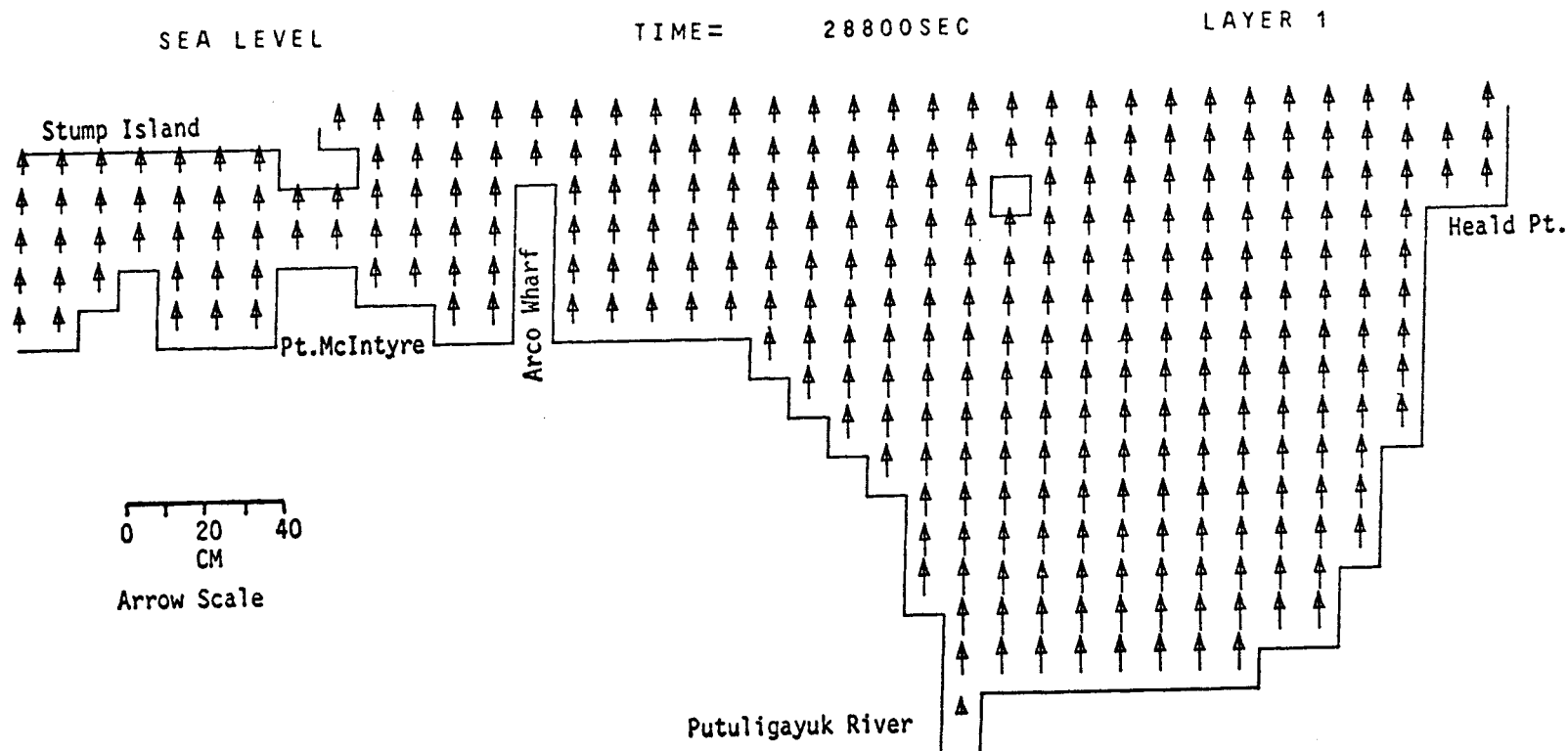


PRUDHOE BAY

M2 TIDE (AMP=8 CM, IN PHASE ON OPEN BOUNDARIES) ONSHORE WIND AT 1.0 KT

909

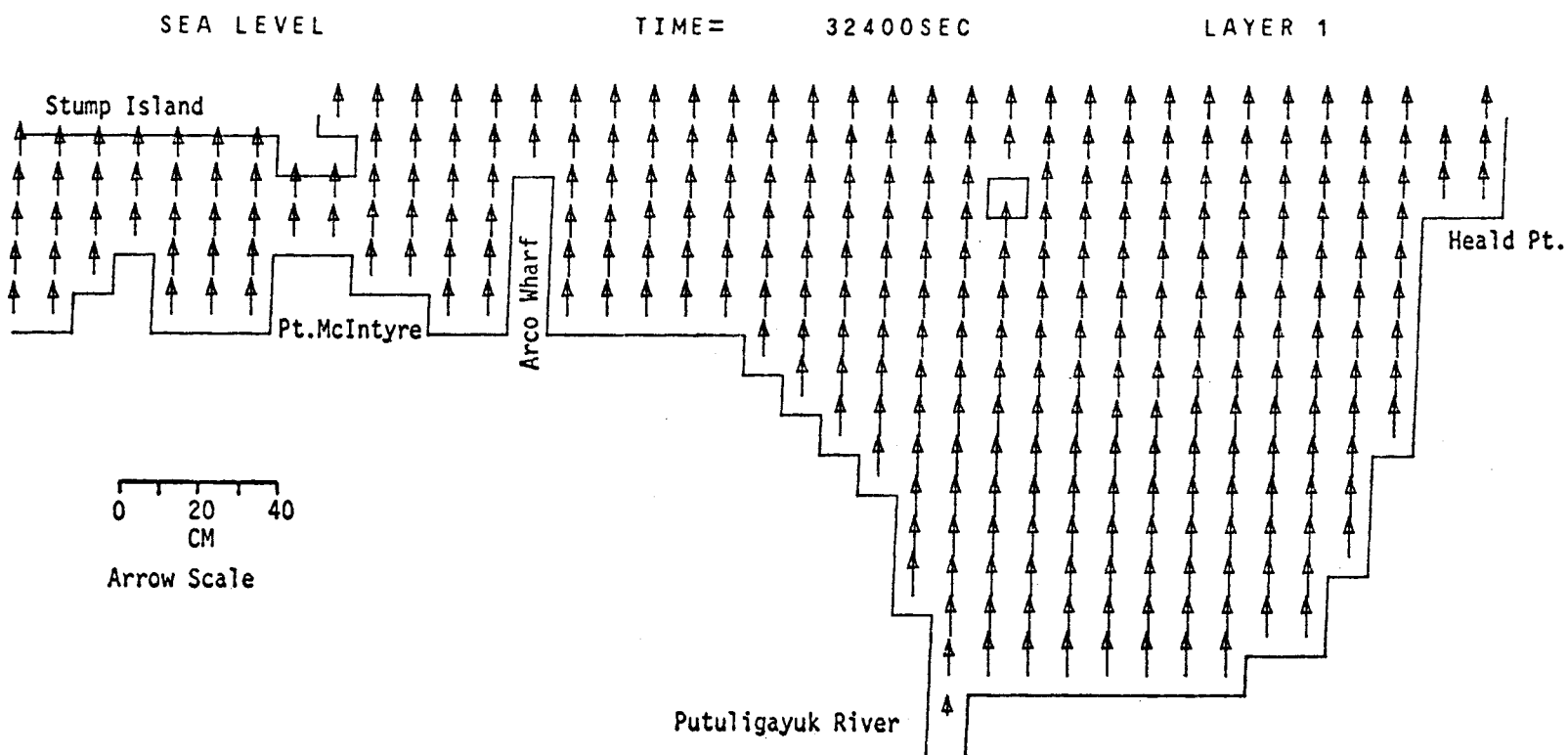
MODEL NO 10



PRUDHOE BAY  
M2 TIDE (AMP=8 CM, IN PHASE ON OPEN BOUNDARIES) ONSHORE WIND AT 10 KT

209

MODEL NO 10

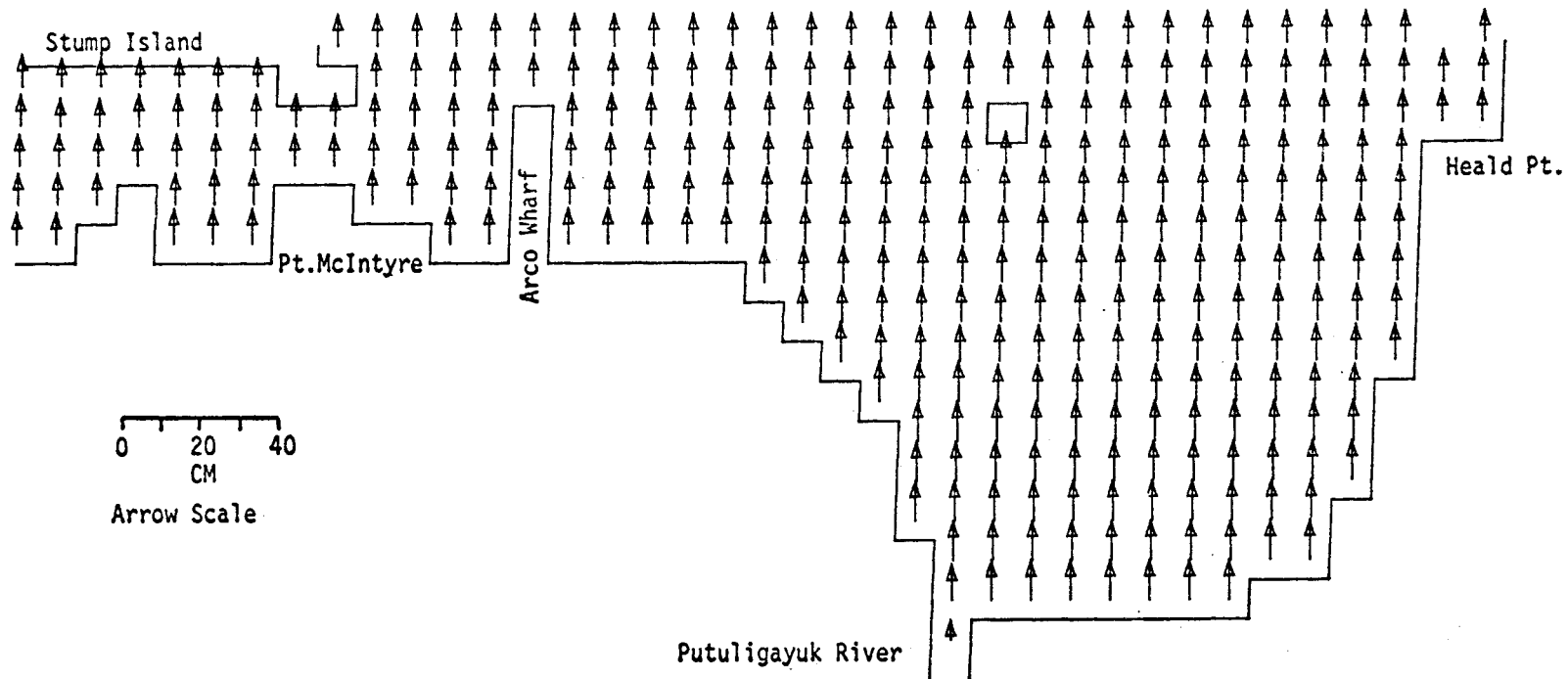


PRUDHOE BAY  
M2 TIDE (AMP=8 CM, IN PHASE ON OPEN BOUNDARIES) ONSHORE WIND AT 10 KT

SEA LEVEL

TIME = 36000SEC

LAYER 1



809  
MODEL NO 10

0 20 40  
CM  
Arrow Scale

Putuligayuk River

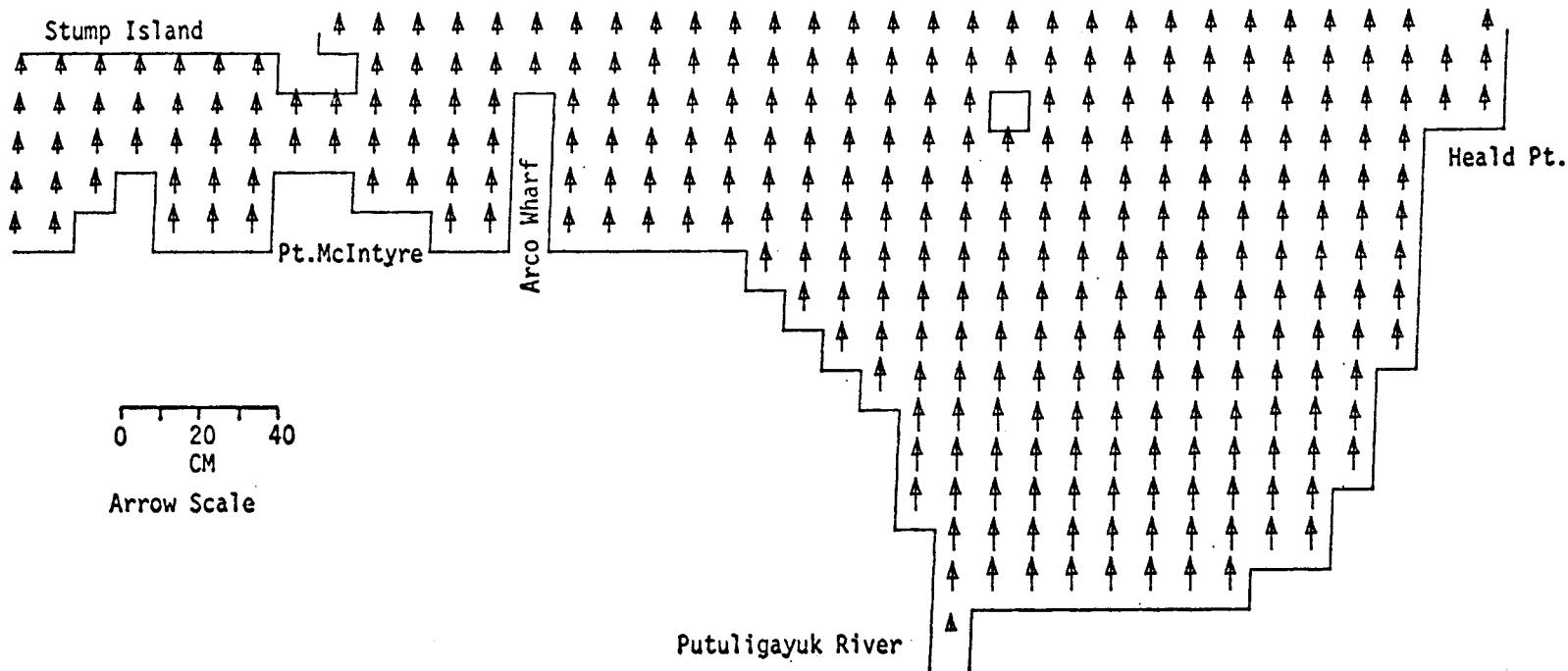
PRUDHOE BAY

M2 TIDE (AMP=8 CM, IN PHASE ON OPEN BOUNDARIES) ONSHORE WIND AT 10 KT

SEA LEVEL

TIME= 39600SEC

LAYER 1



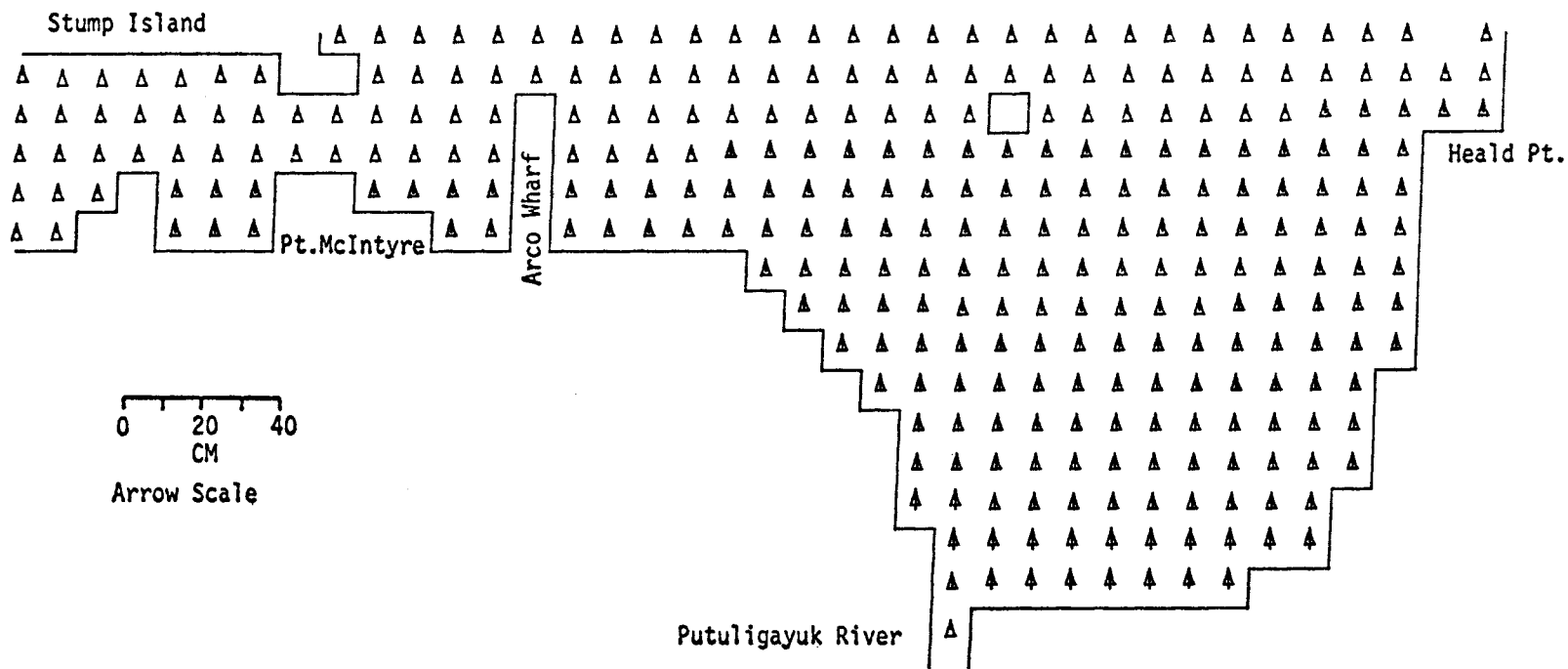
MODEL NO 10  
609

PRUDHOE BAY  
M2 TIDE (AMP=8 CM, IN PHASE ON OPEN BOUNDARIES) ONSHORE WIND AT 10 KT

SEA LEVEL

TIME= 43200SEC

LAYER 1



610

MODEL NO 10

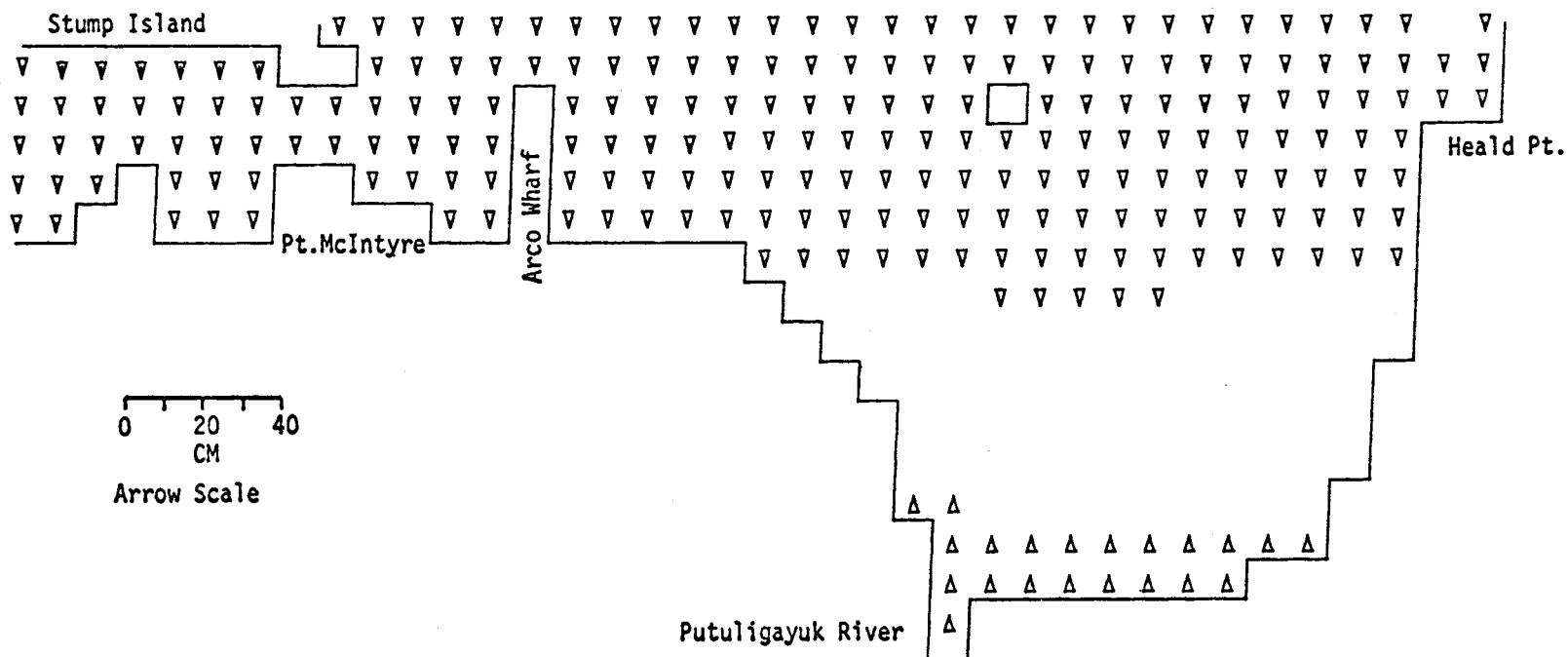
PRUDHOE BAY  
M2 TIDE (AMP=8 CM, IN PHASE ON OPEN BOUNDARIES) ONSHORE WIND AT 10 KT



SEA LEVEL

TIME= 46800SEC

LAYER 1



MODEL NO 10

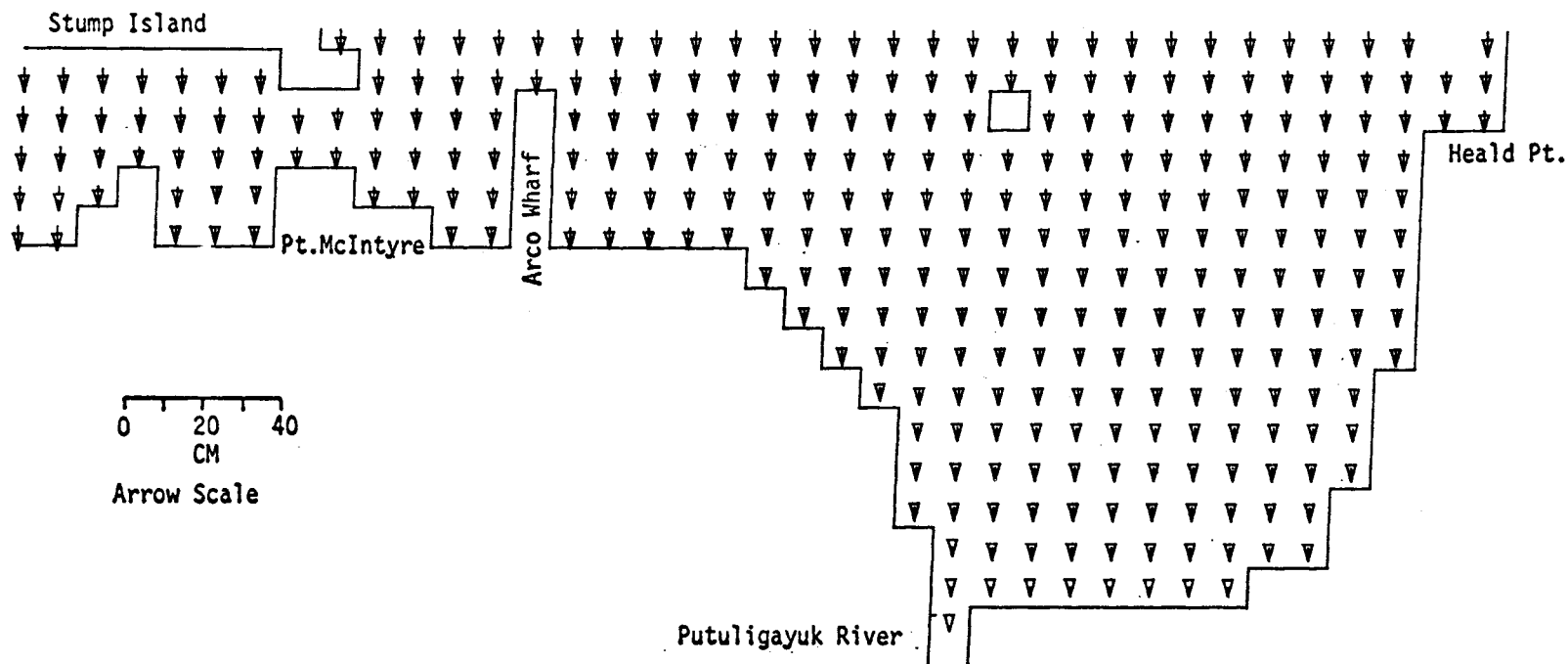
0 20 40  
CM  
Arrow Scale

PRUDHOE BAY  
M2 TIDE (AMP=8 CM, IN PHASE ON OPEN BOUNDARIES) ONSHORE WIND AT 10 KT

SEA LEVEL

TIME= 50400SEC

LAYER 1



MODE NO 10

0 20 40  
CM  
Arrow Scale

Putuligayuk River

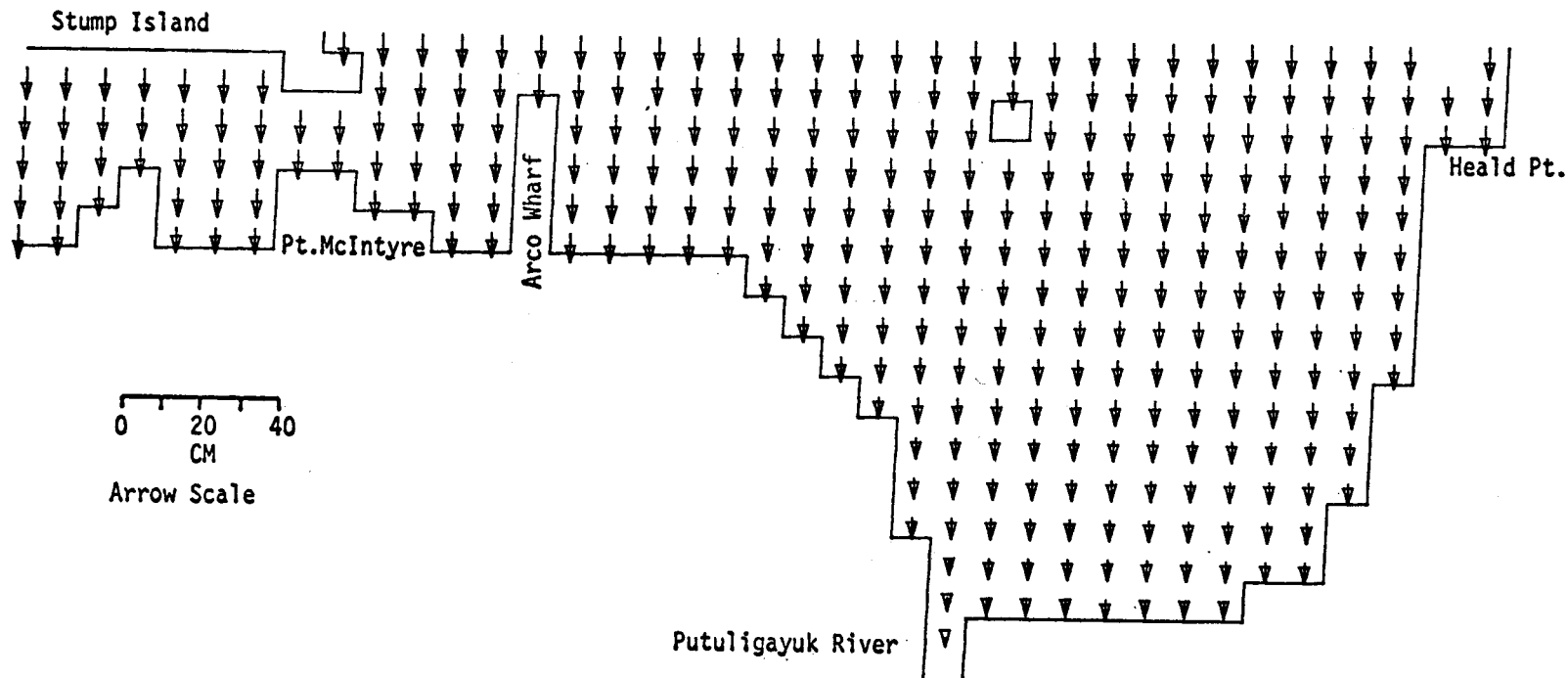
PRUDHOE BAY

M2 TIDE (AMP=8 CM, IN PHASE ON OPEN BOUNDARIES) ONSHORE WIND AT 10 KT

SEA LEVEL

TIME= 54000SEC

LAYER 1



613

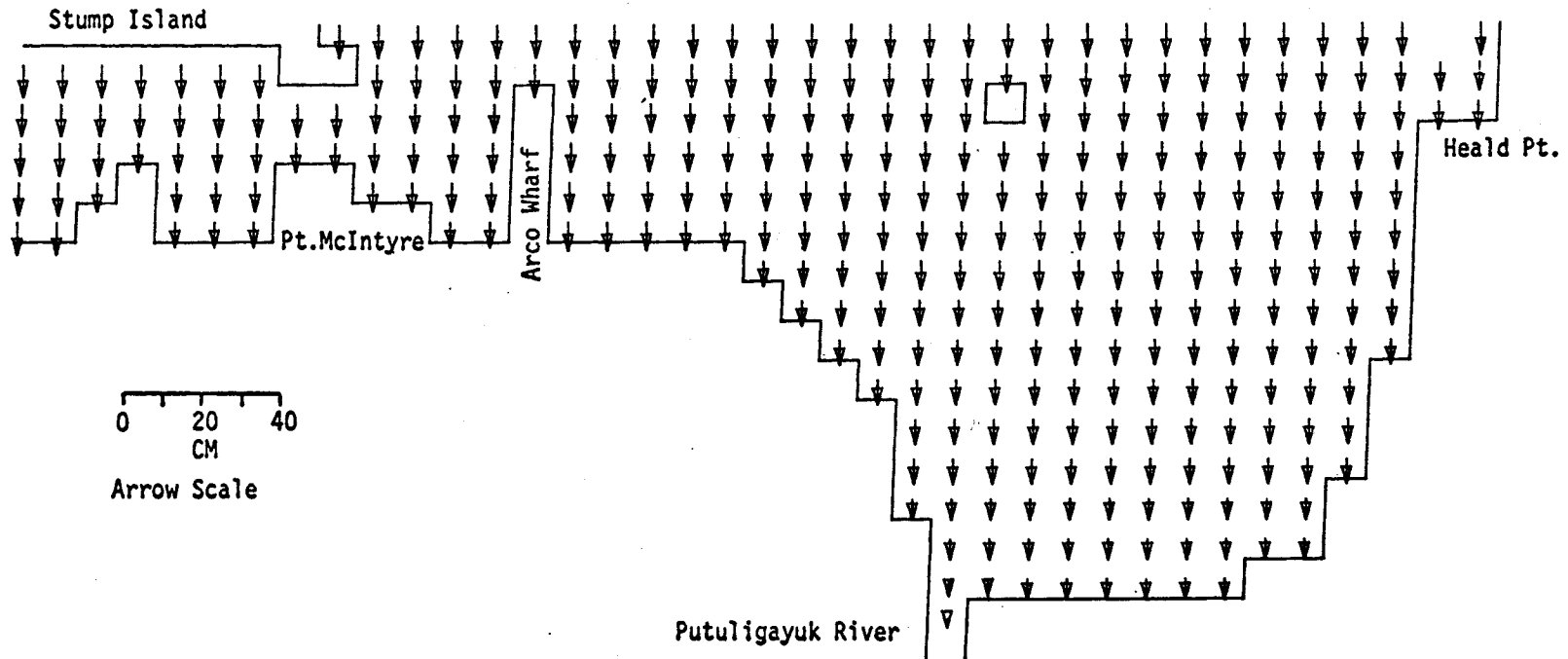
MODEL NO. 10

PRUDHOE BAY  
M2 TIDE (AMP=8 CM, IN PHASE ON OPEN BOUNDARIES) ONSHORE WIND AT 10 KT

SEA LEVEL

TIME= 57600SEC

LAYER 1



MODEL NO 10

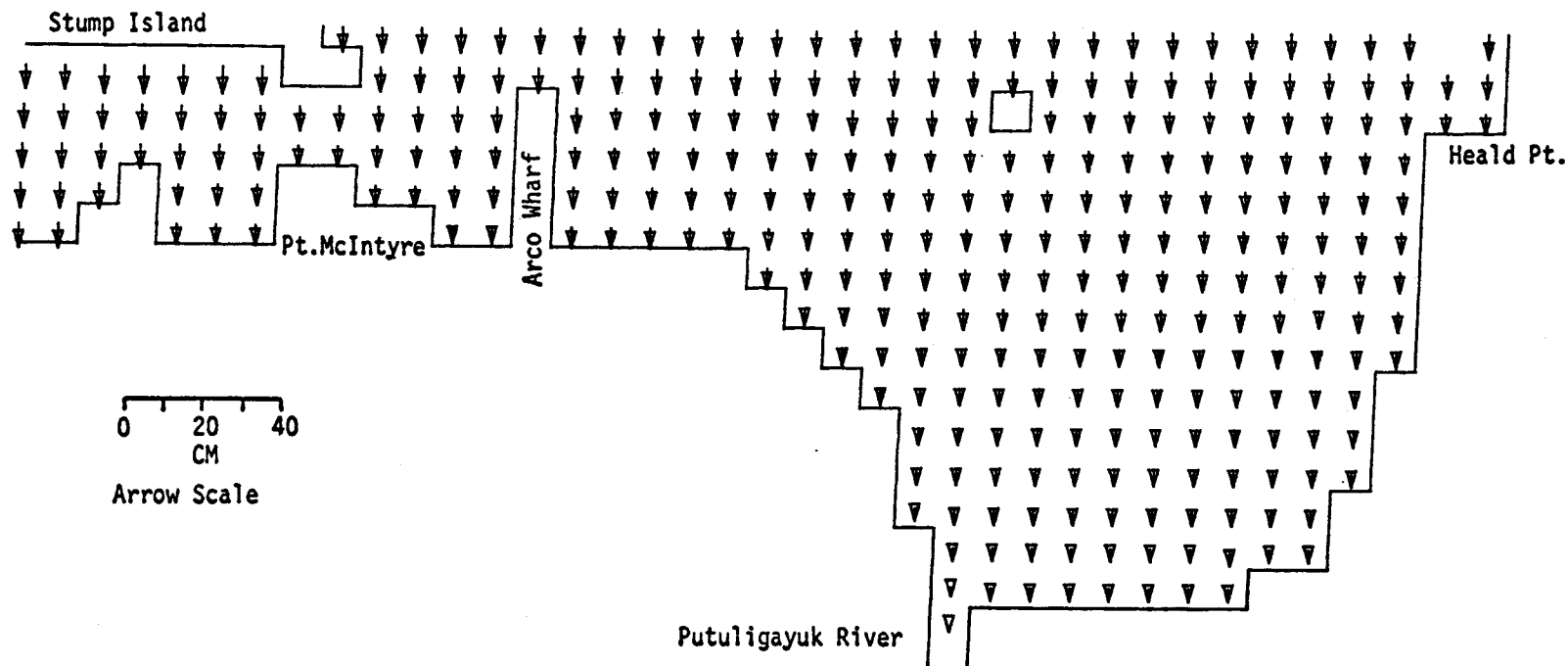
614

PRUDHOE BAY  
M2 TIDE (AMP=8 CM, IN PHASE ON OPEN BOUNDARIES) ONSHORE WIND AT 10 KT

SEA LEVEL

TIME= 61200SEC

LAYER 1



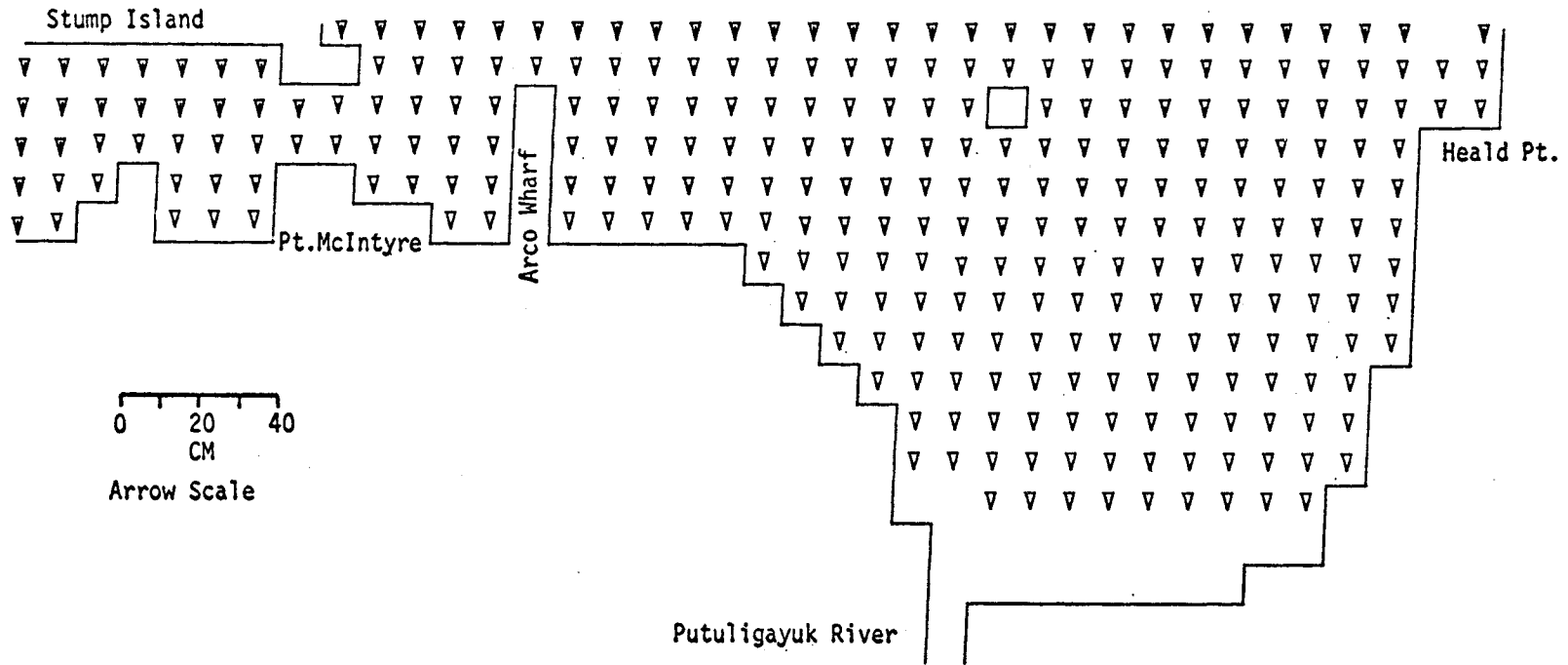
PRUDHOE BAY

M2 TIDE (AMP=8 CM, IN PHASE ON OPEN BOUNDARIES) ONSHORE WIND AT 10 KT

SEA LEVEL

TIME= 64800SEC

LAYER 1



10

MODEL NO

919

0 20 40  
CM  
Arrow Scale

Putuligayuk River

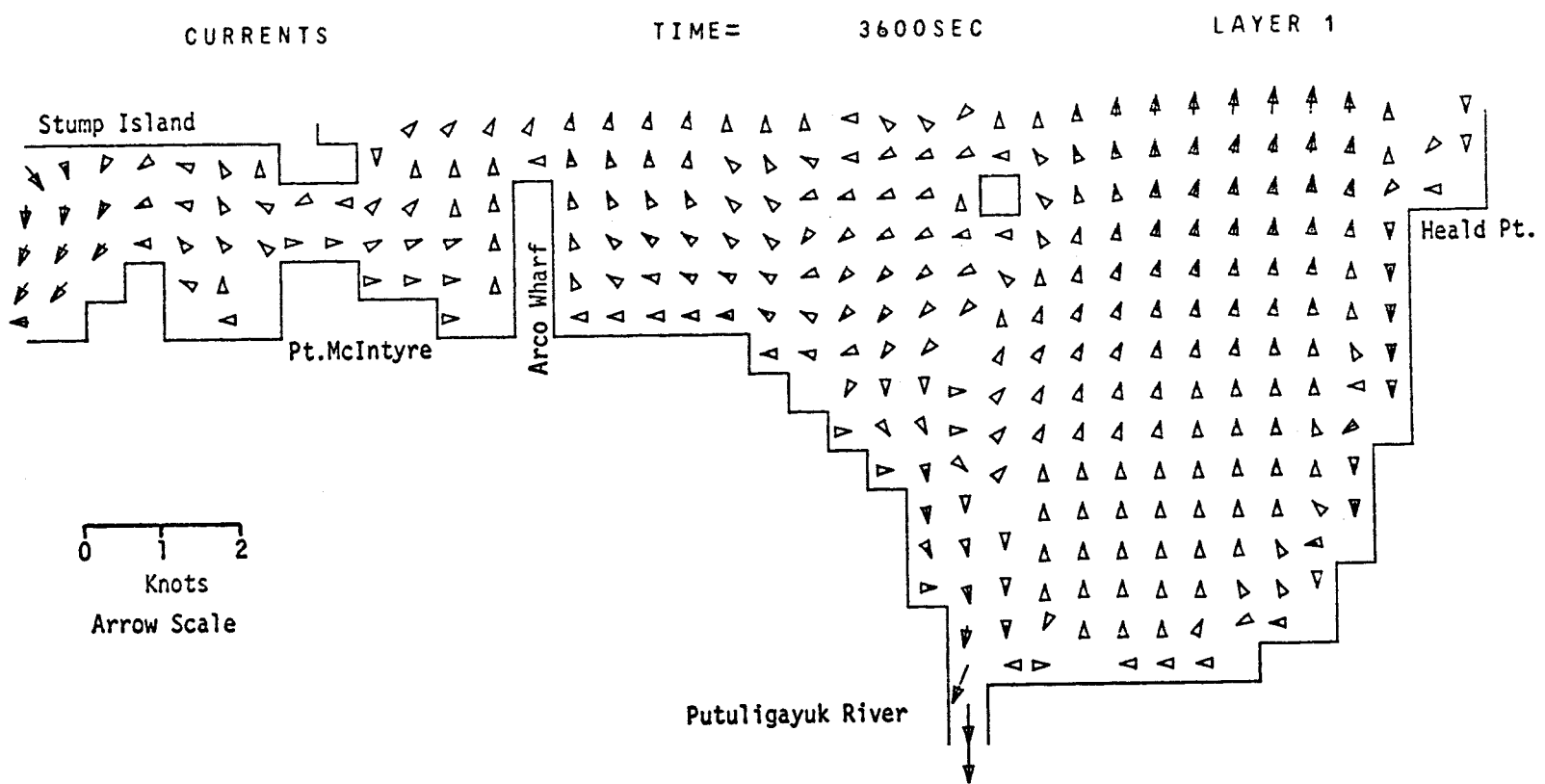
PRUDHOE BAY

M2 TIDE (AMP=8 CM, IN PHASE ON OPEN BOUNDARIES) ONSHORE WIND AT 10 KT

CURRENTS

819

MODEL NO 10



PRUDHOE BAY  
M2 TIDE (AMP=8 CM, IN PHASE ON OPEN BOUNDARIES) ONSHORE WIND AT 10 KT

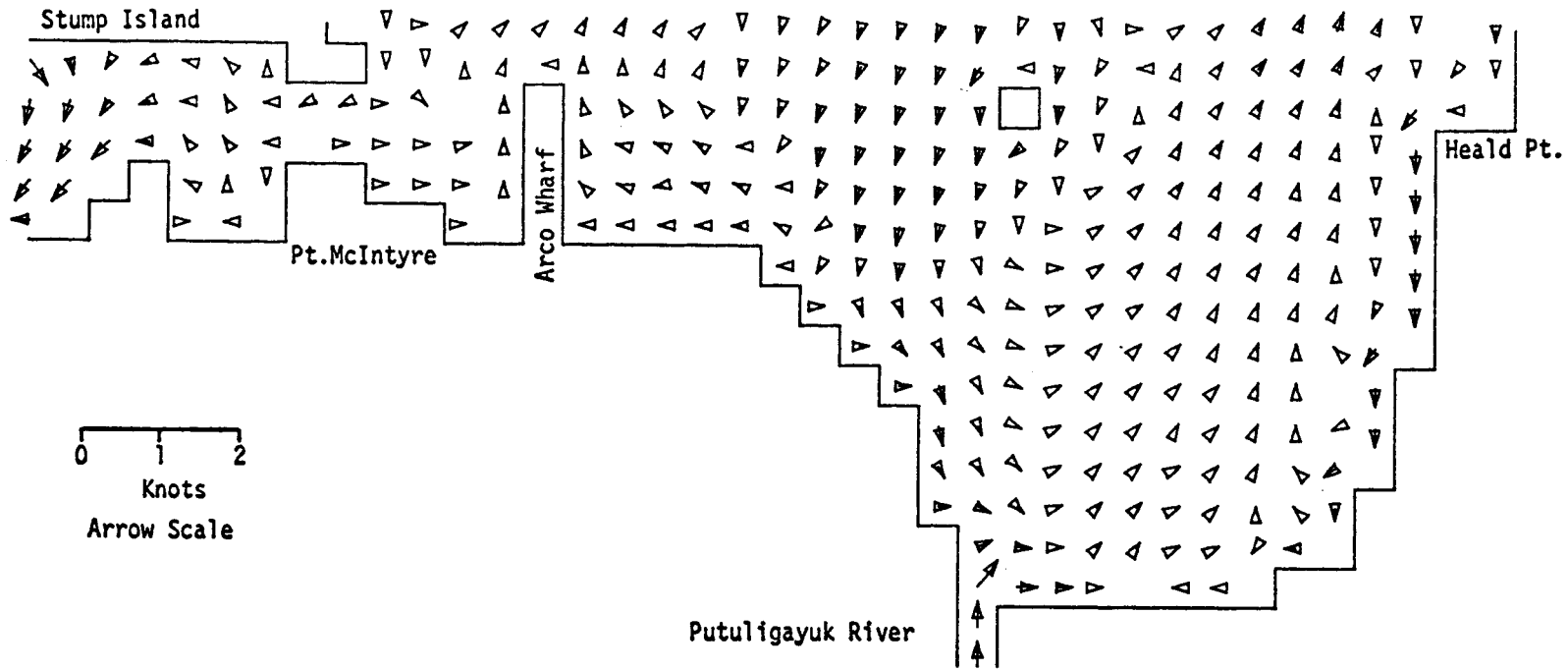


CURRENTS

TIME=

7200SEC

LAYER 1



MODEL NO 10

619

0 1 2  
Knots  
Arrow Scale

Putuligayuk River

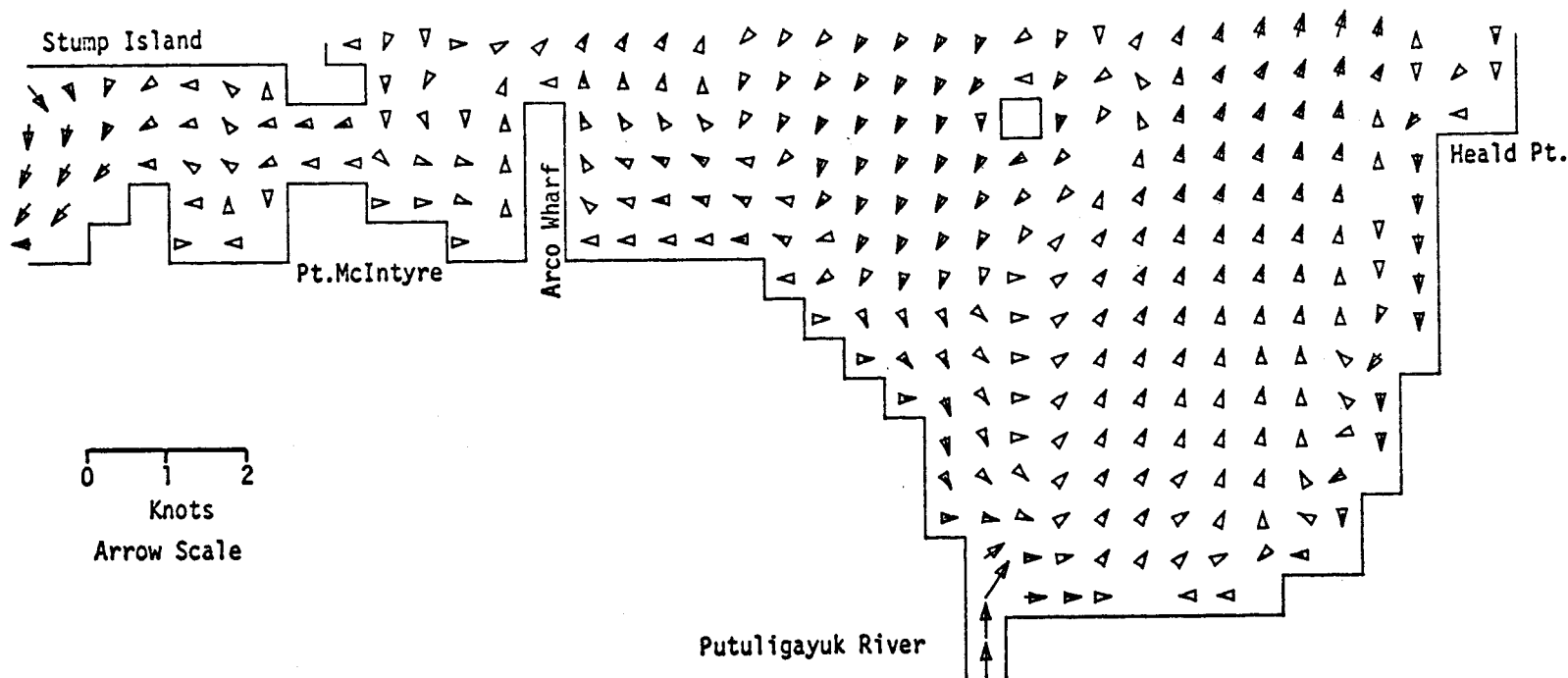
PRUDHOE BAY

M2 TIDE (AMP=8 CM, IN PHASE ON OPEN BOUNDARIES) ONSHORE WIND AT 10 KT

CURRENTS

TIME= 10800SEC

LAYER 1



10

MODEL NO

620

0 1 2  
Knots  
Arrow Scale

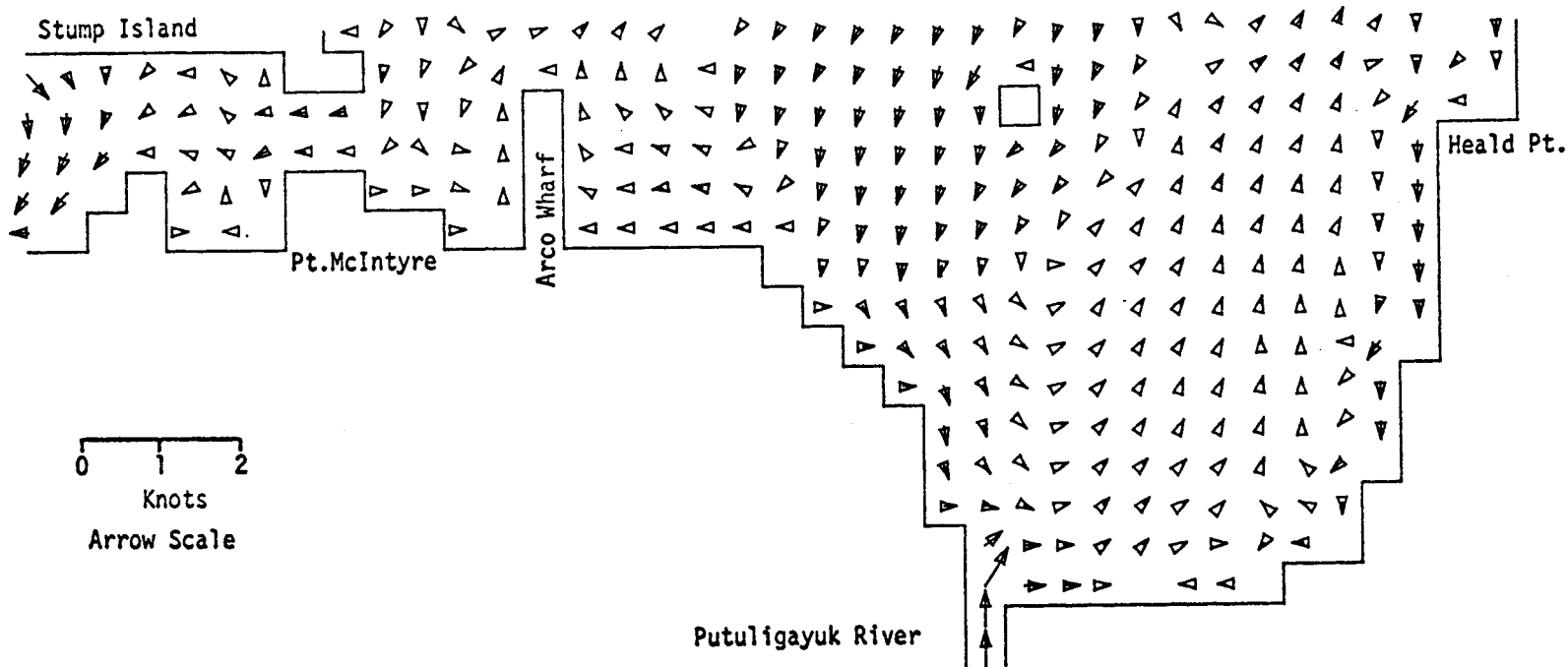
PRUDHOE BAY

M2 TIDE (AMP=8 CM, IN PHASE ON OPEN BOUNDARIES) ONSHORE WIND AT 10 KT

CURRENTS

TIME= 14400SEC

LAYER 1



PRUDHOE BAY

M2 TIDE (AMP=8 CM, IN PHASE ON OPEN BOUNDARIES) ONSHORE WIND AT 10 KT

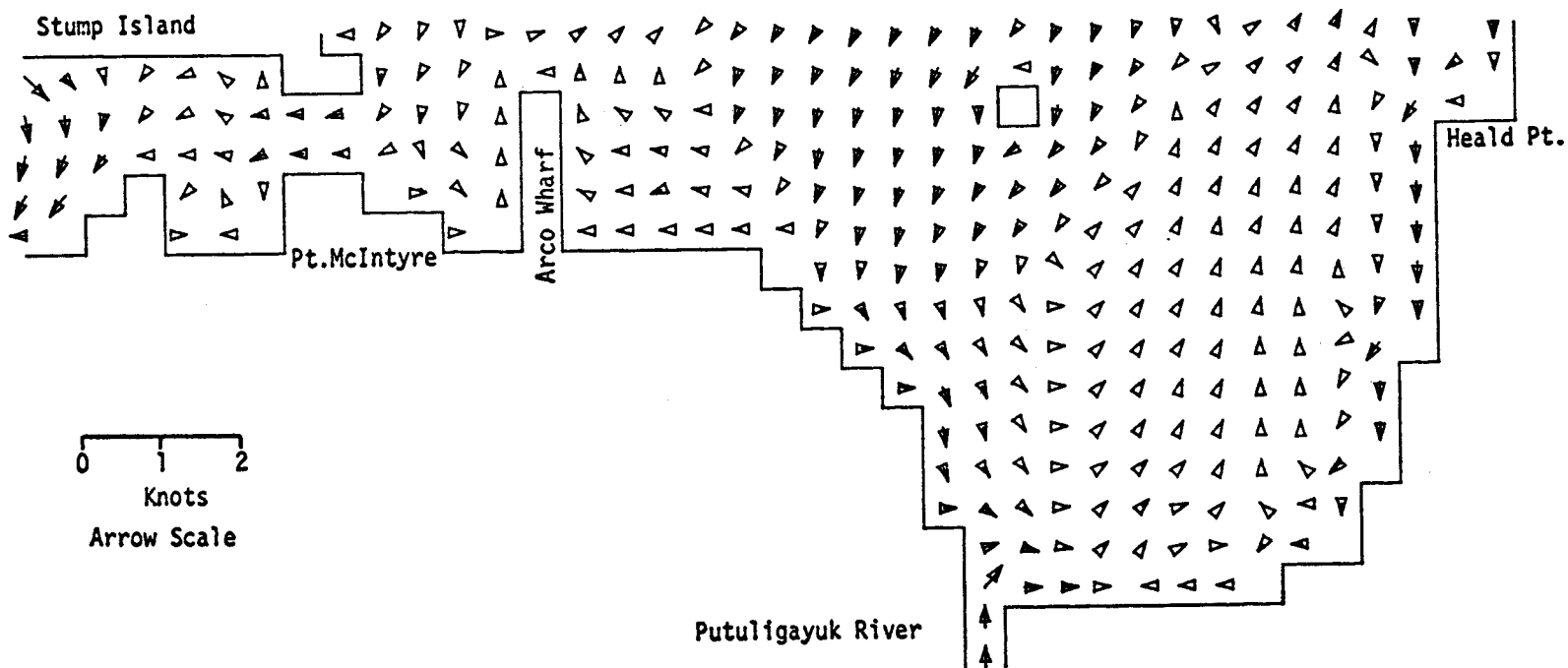
621

MODEL NO 10

CURRENTS

TIME = 18000SEC

LAYER 1



10

MODEL NO  
622

0 1 2  
Knots  
Arrow Scale

Putuligayuk River

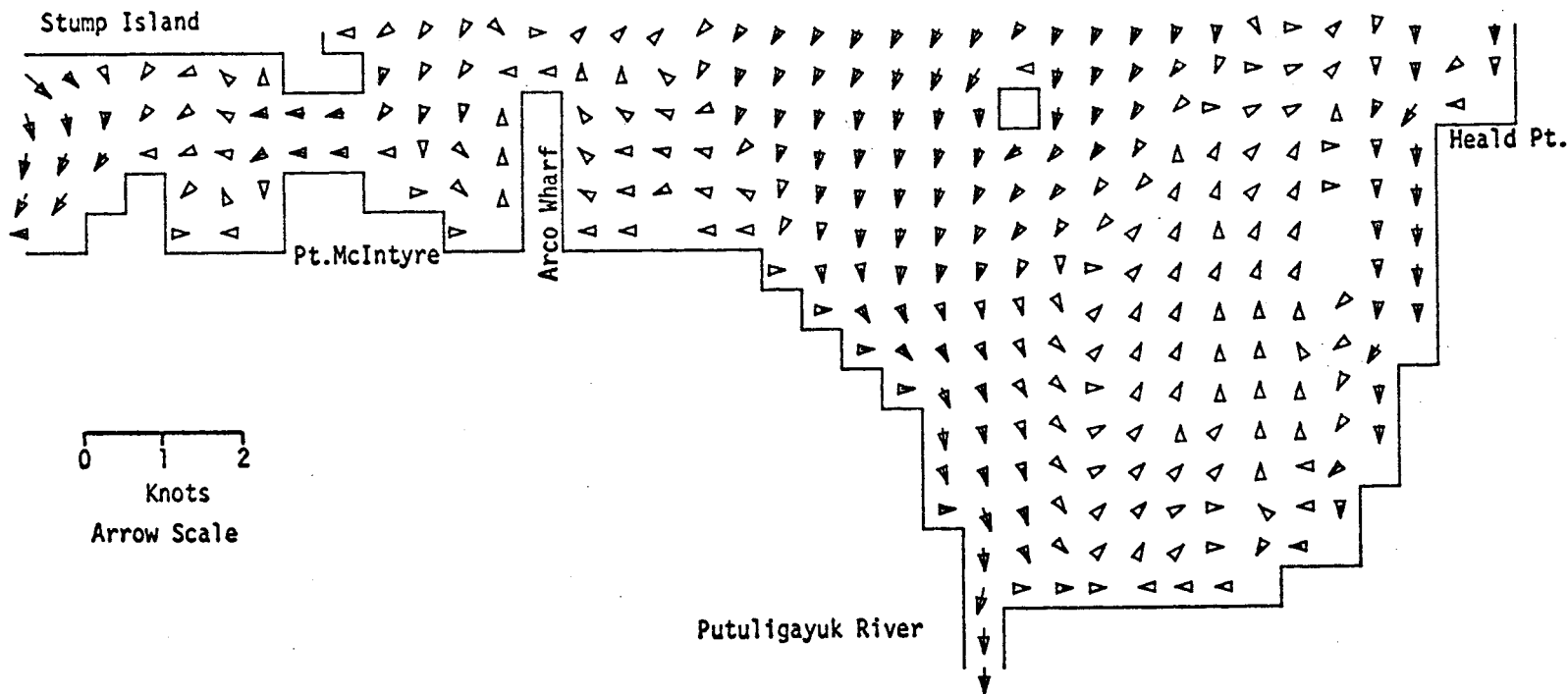
PRUDHOE BAY

M2 TIDE (AMP=8 CM, IN PHASE ON OPEN BOUNDARIES) ONSHORE WIND AT 10 KT

CURRENTS

TIME= 21600SEC

LAYER 1



MODEL NO 10

0 1 2  
Knots  
Arrow Scale

Putuligayuk River

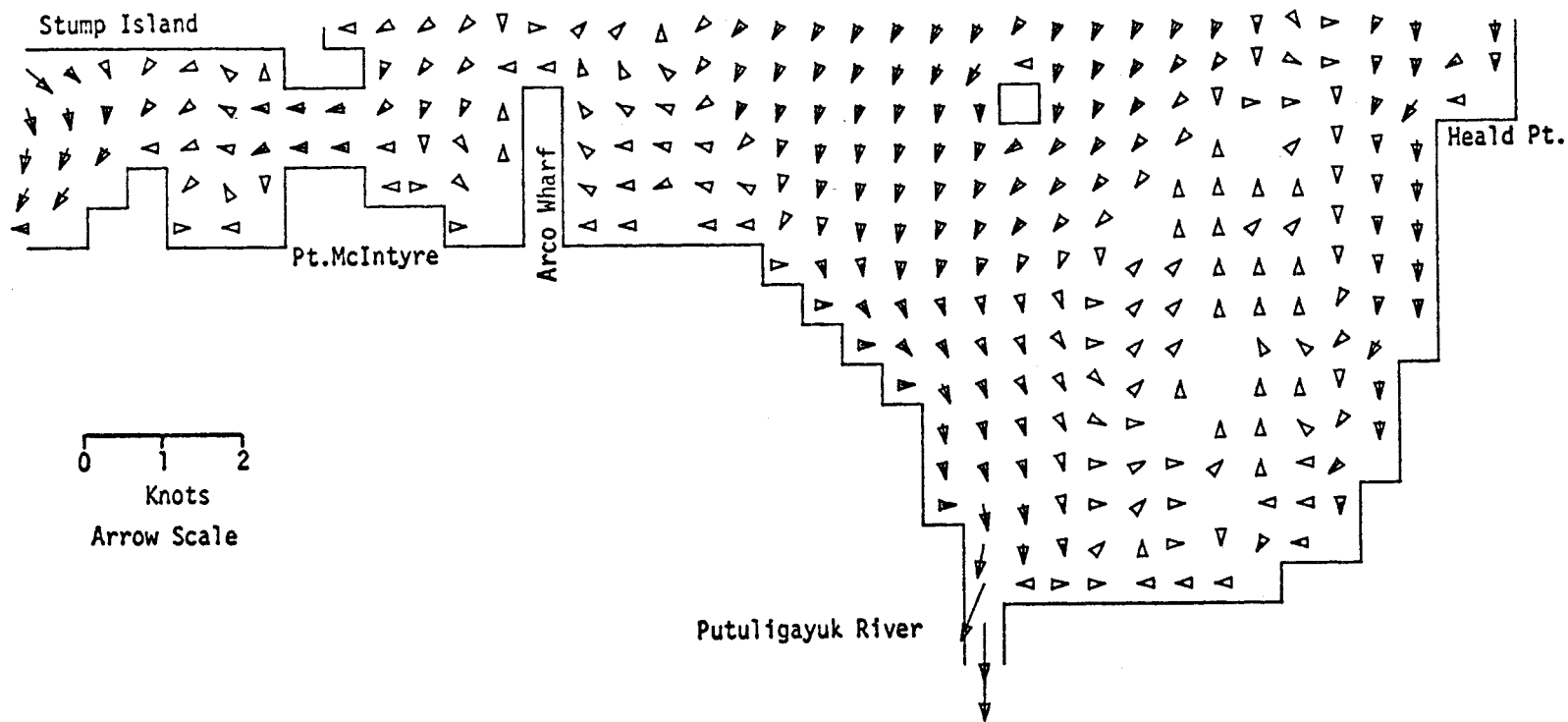
PRUDHOE BAY

M2 TIDE (AMP=8 CM, IN PHASE ON OPEN BOUNDARIES) ONSHORE WIND AT 10 KT

CURRENTS

TIME= 25200SEC

LAYER 1



MODEL NO 10  
624

0 1 2  
Knots  
Arrow Scale

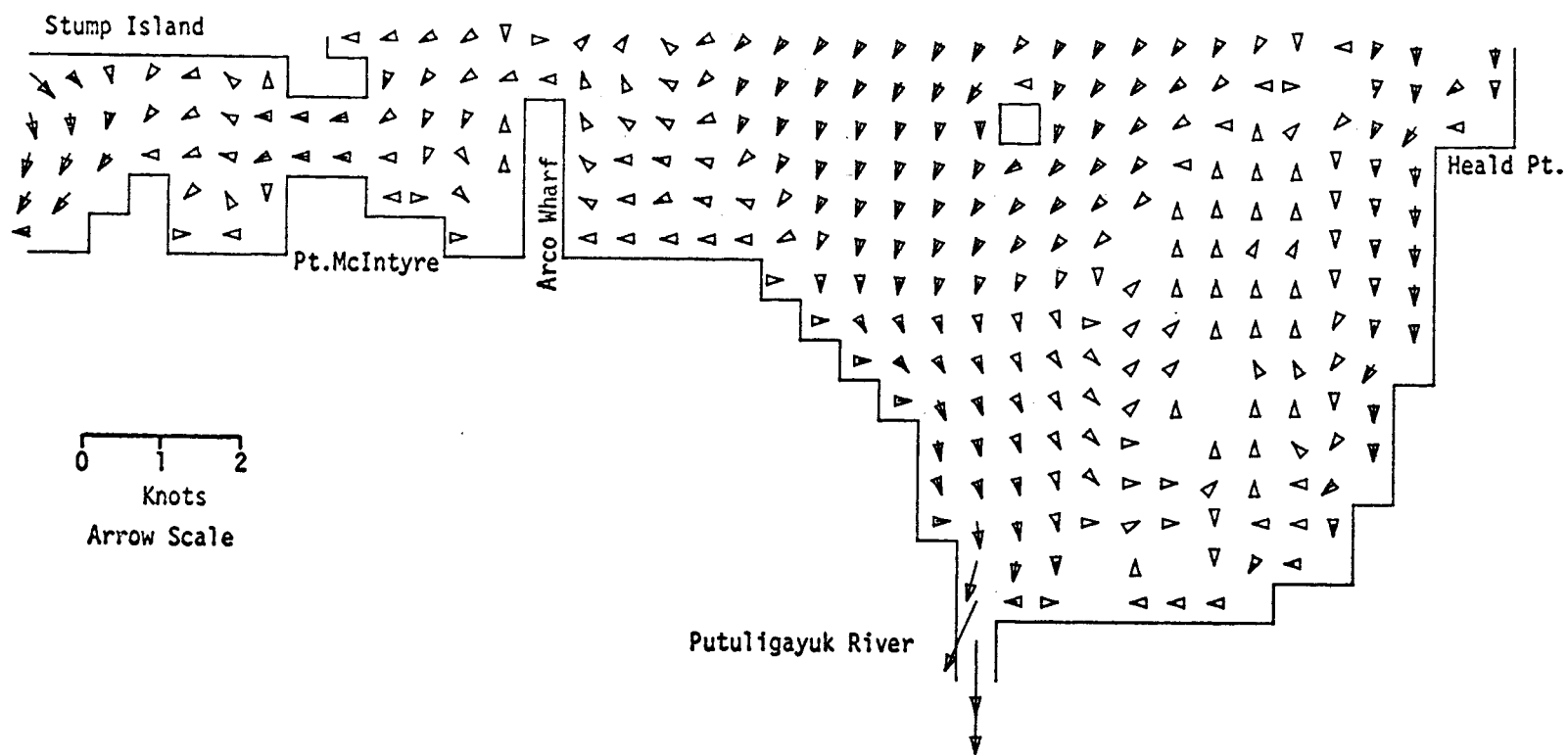
PRUDHOE BAY

M2 TIDE (AMP=8 CM, IN PHASE ON OPEN BOUNDARIES) ONSHORE WIND AT 10 KT

CURRENTS

TIME= 28800SEC

LAYER 1



0 1 2  
Knots  
Arrow Scale

Putuligayuk River

PRUDHOE BAY

M2 TIDE (AMP=8 CM, IN PHASE ON OPEN BOUNDARIES) ONSHORE WIND AT 10 KT

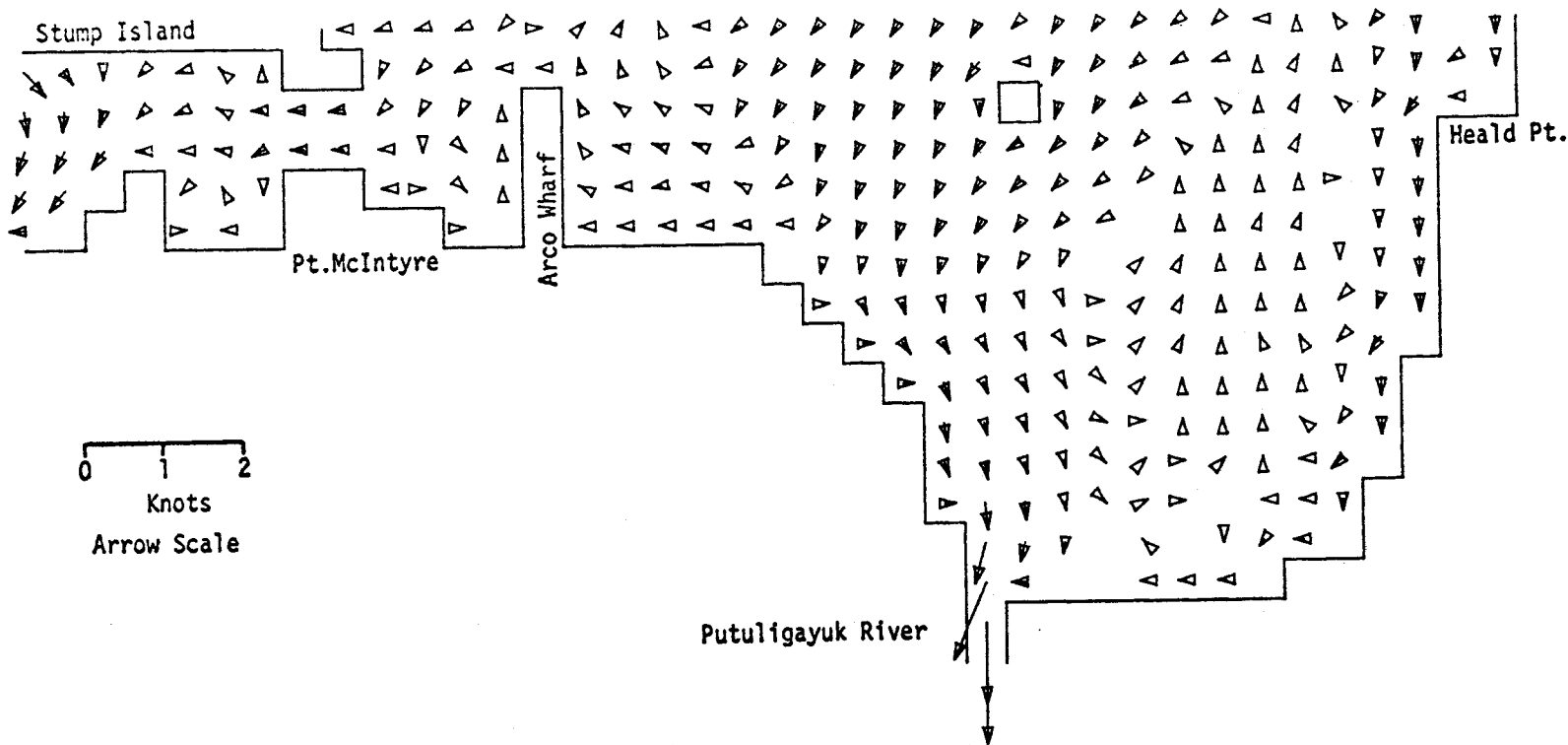
625  
MODEL NO 10

CURRENTS

TIME= 32400SEC

LAYER 1

MODEL NO 10



626

PRUDHOE BAY

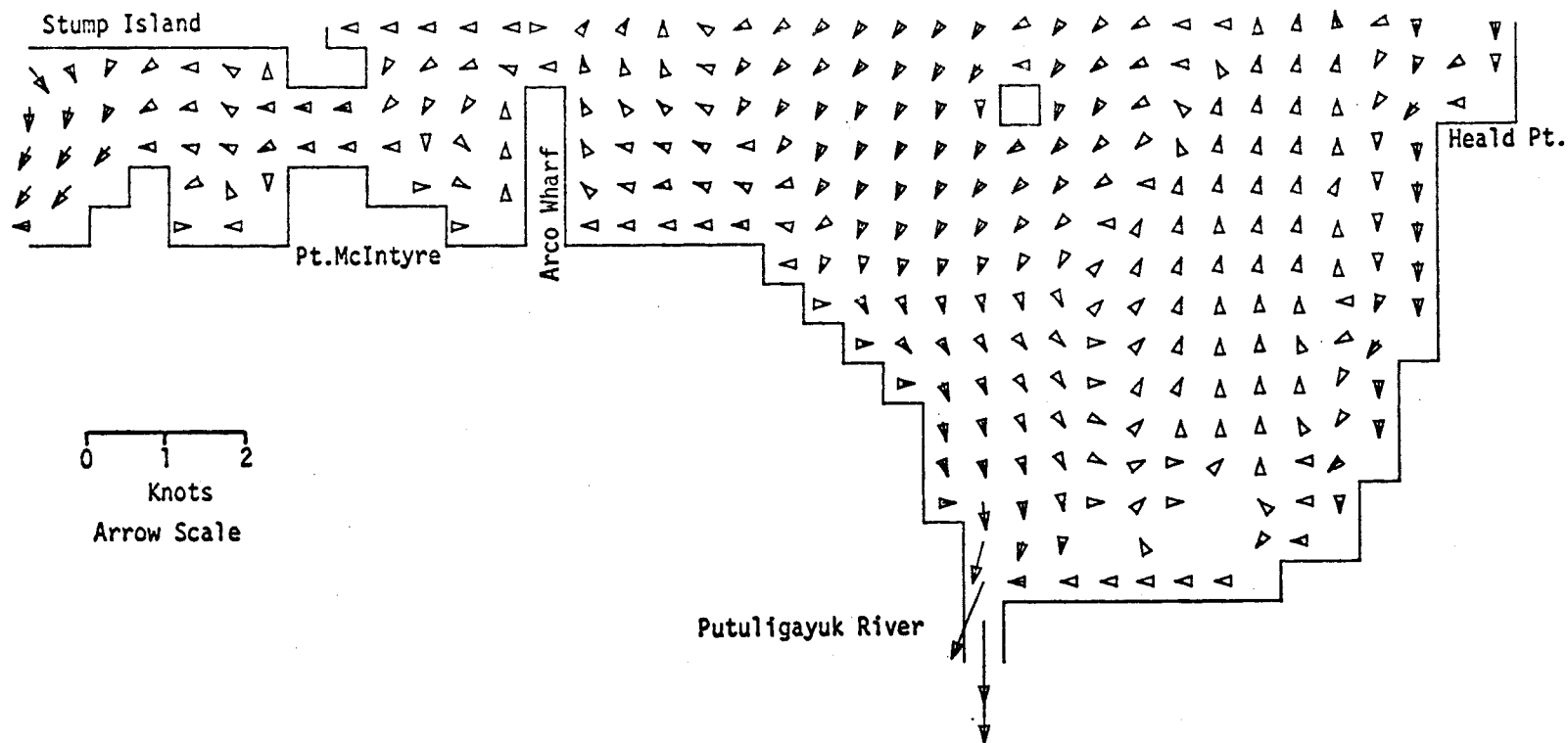
M2 TIDE (AMP=8 CM, IN PHASE ON OPEN BOUNDARIES) ONSHORE WIND AT 10 KT



CURRENTS

TIME= 36000SEC

LAYER 1



MODEL NO 10 ON TAPES 627

0 1 2  
Knots  
Arrow Scale

Putuligayuk River

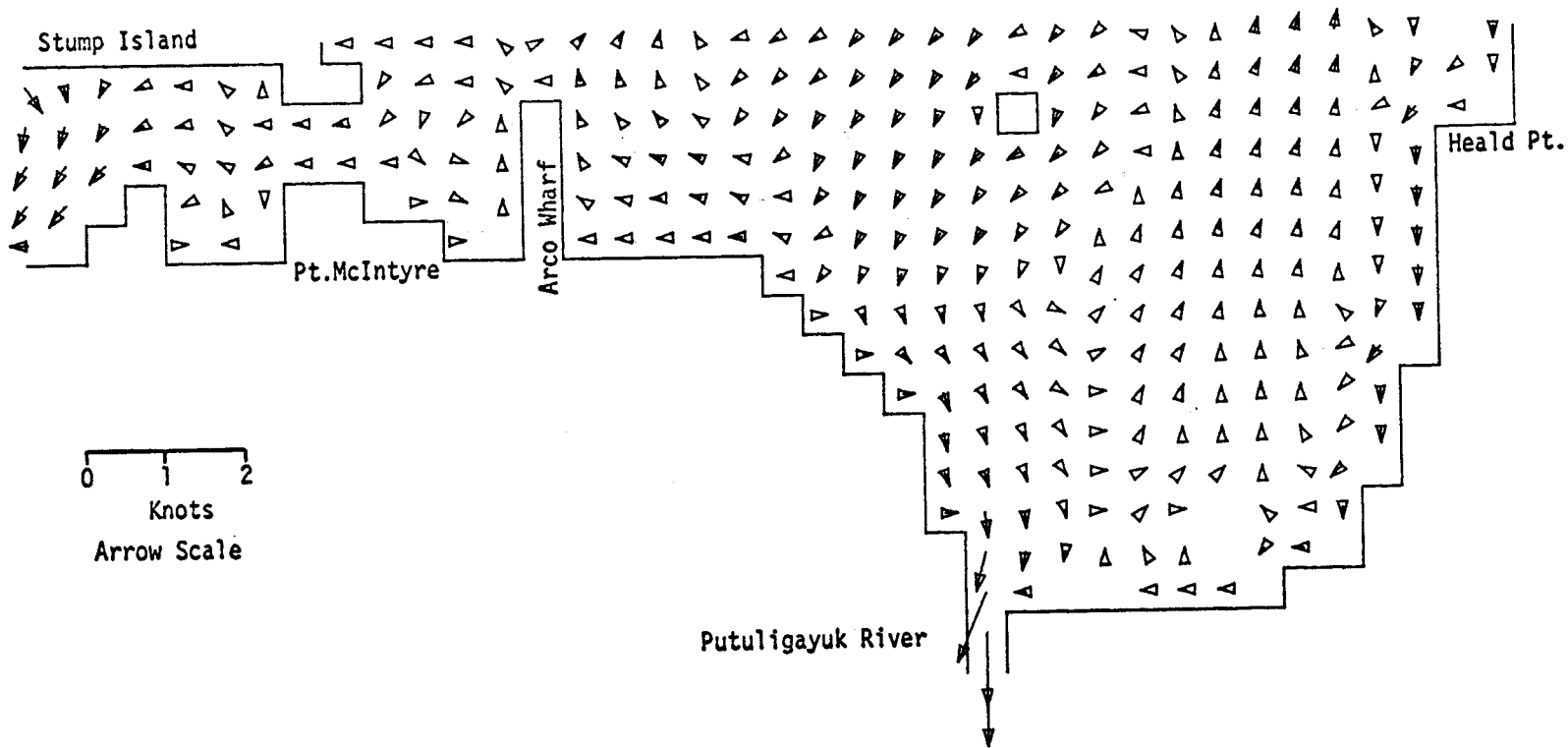
PRUDHOE BAY

M2 TIDE (AMP=8 CM, IN PHASE ON OPEN BOUNDARIES) ONSHORE WIND AT 10 KT

CURRENTS

TIME= 39600SEC

LAYER 1



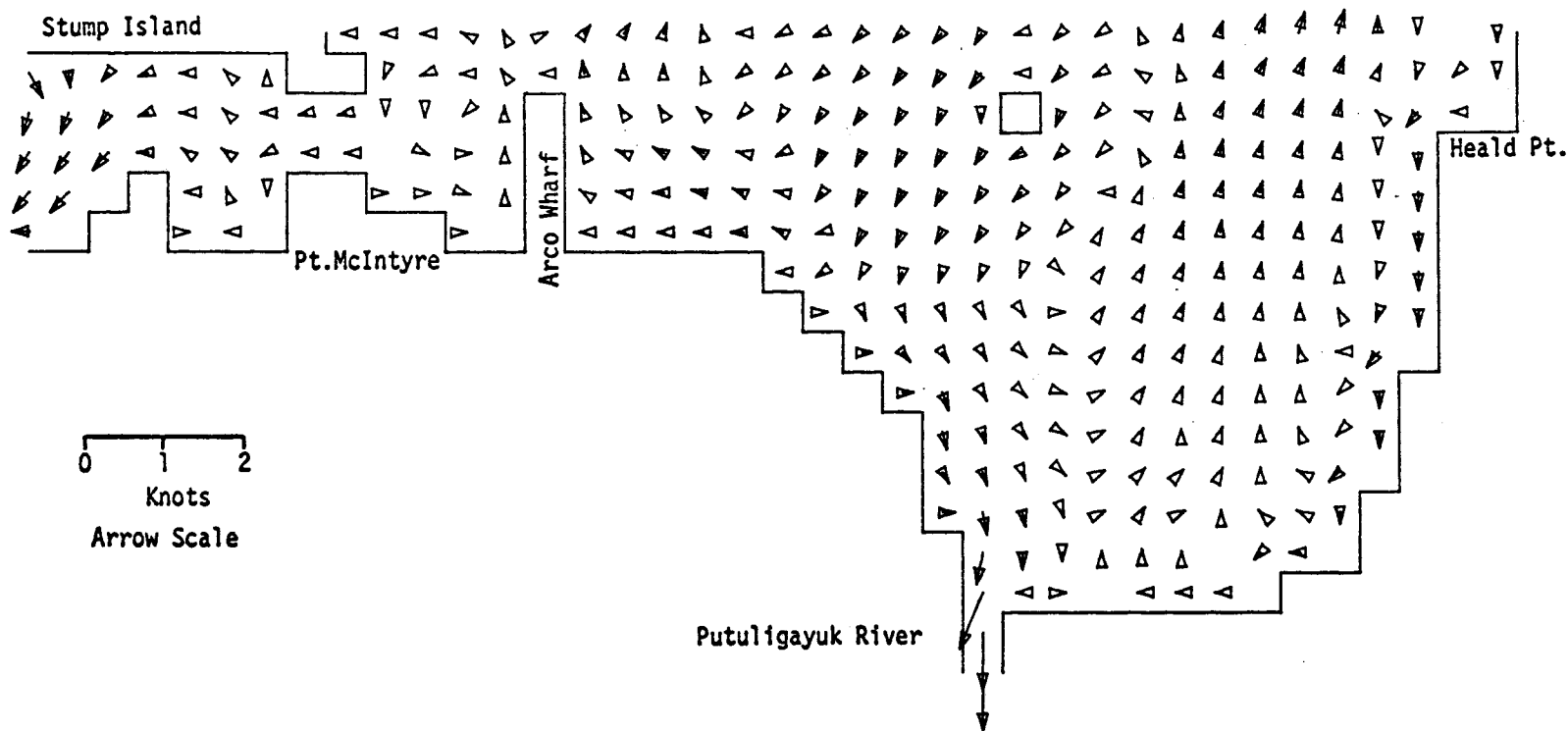
628  
MODEL NO 10

PRUDHOE BAY  
M2 TIDE (AMP=8 CM, IN PHASE ON OPEN BOUNDARIES) ONSHORE WIND AT 10 KT

CURRENTS

TIME= 43200SEC

LAYER 1



10

MODEL NO  
629

0 1 2  
Knots  
Arrow Scale

Putulgayuk River

PRUDHOE BAY

M2 TIDE (AMP=8 CM, IN PHASE ON OPEN BOUNDARIES) ONSHORE WIND AT 10 KT

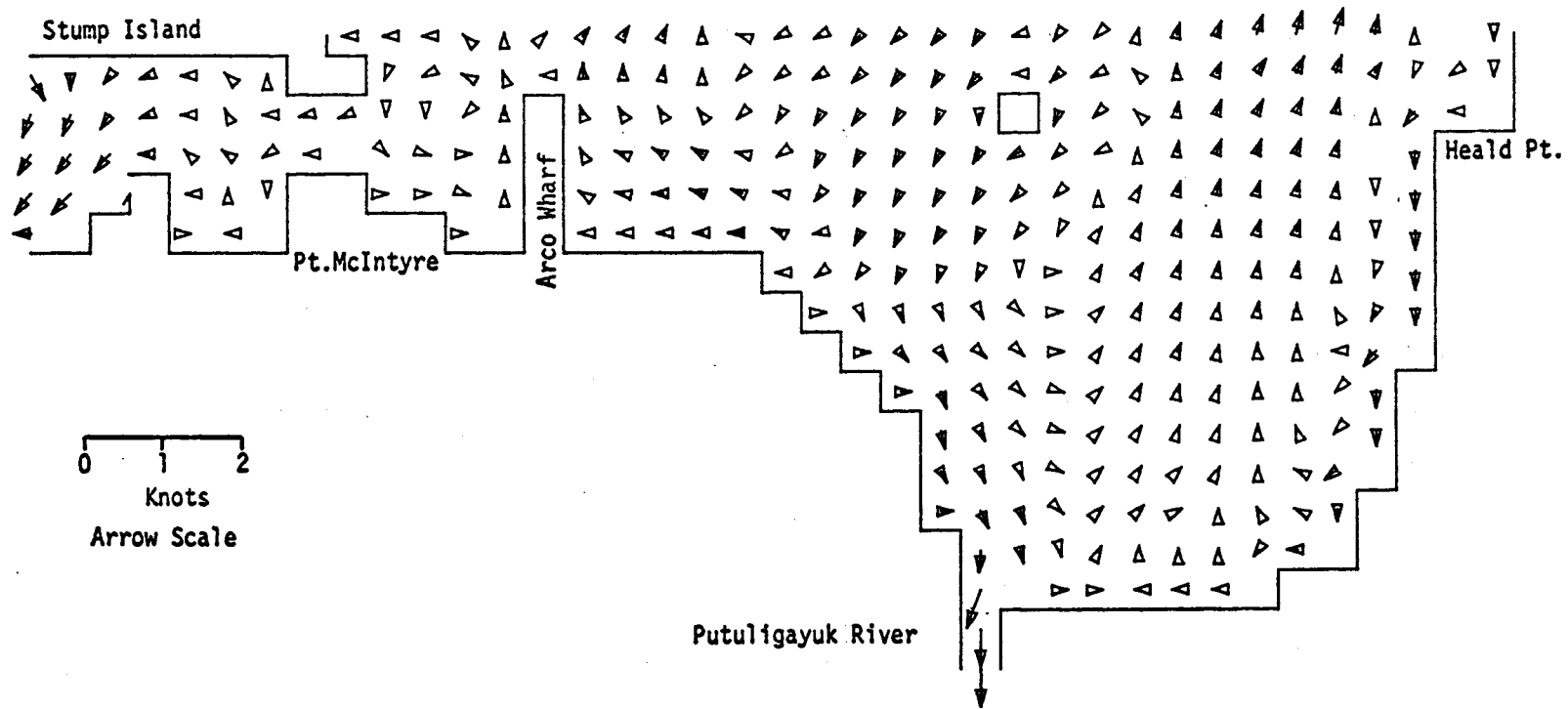
CURRENTS

TIME= 46800SEC

LAYER 1

MODEL NO 10

089



0 1 2  
Knots  
Arrow Scale

Putuligayuk River

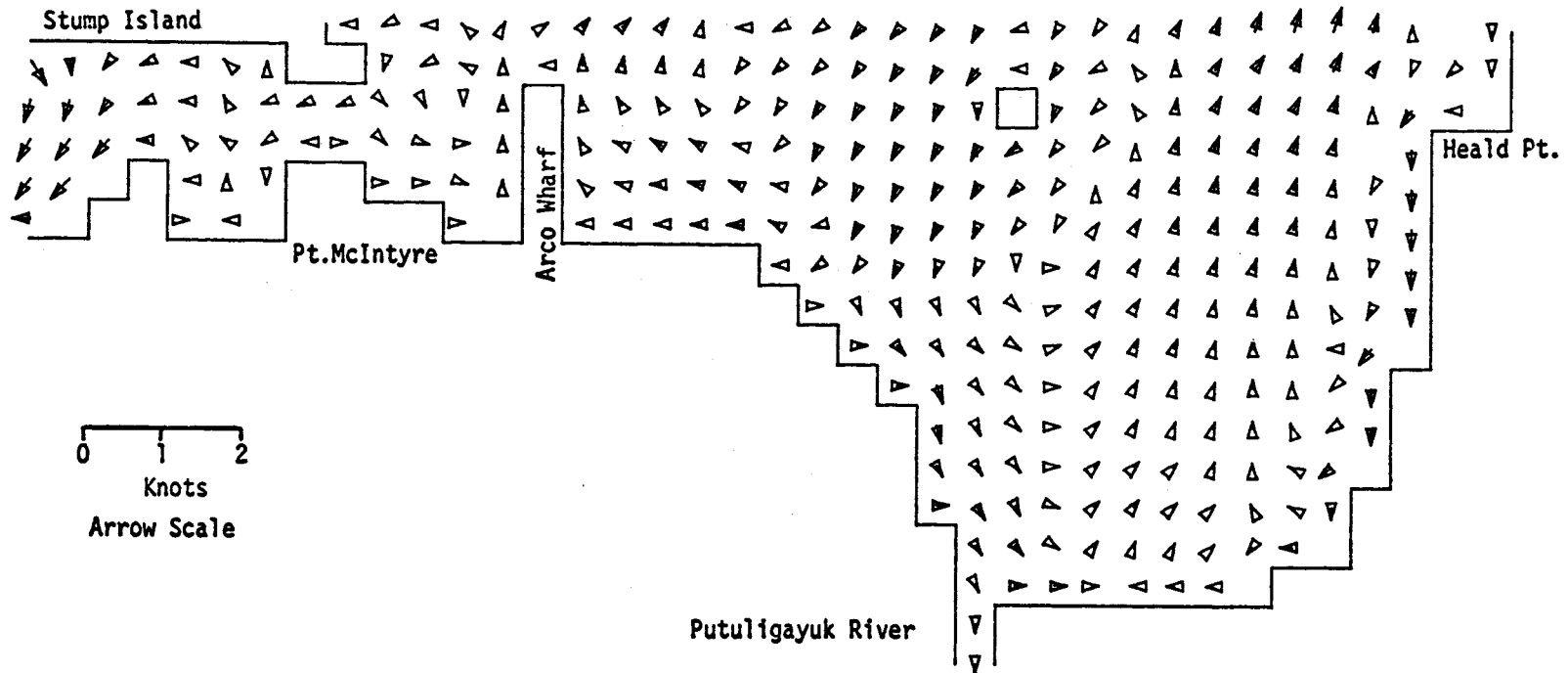
PRUDHOE BAY

M2 TIDE (AMP=8 CM, IN PHASE ON OPEN BOUNDARIES) ONSHORE WIND AT 10 KT

CURRENTS

TIME= 50400SEC

LAYER 1



MODEL NO 10

631

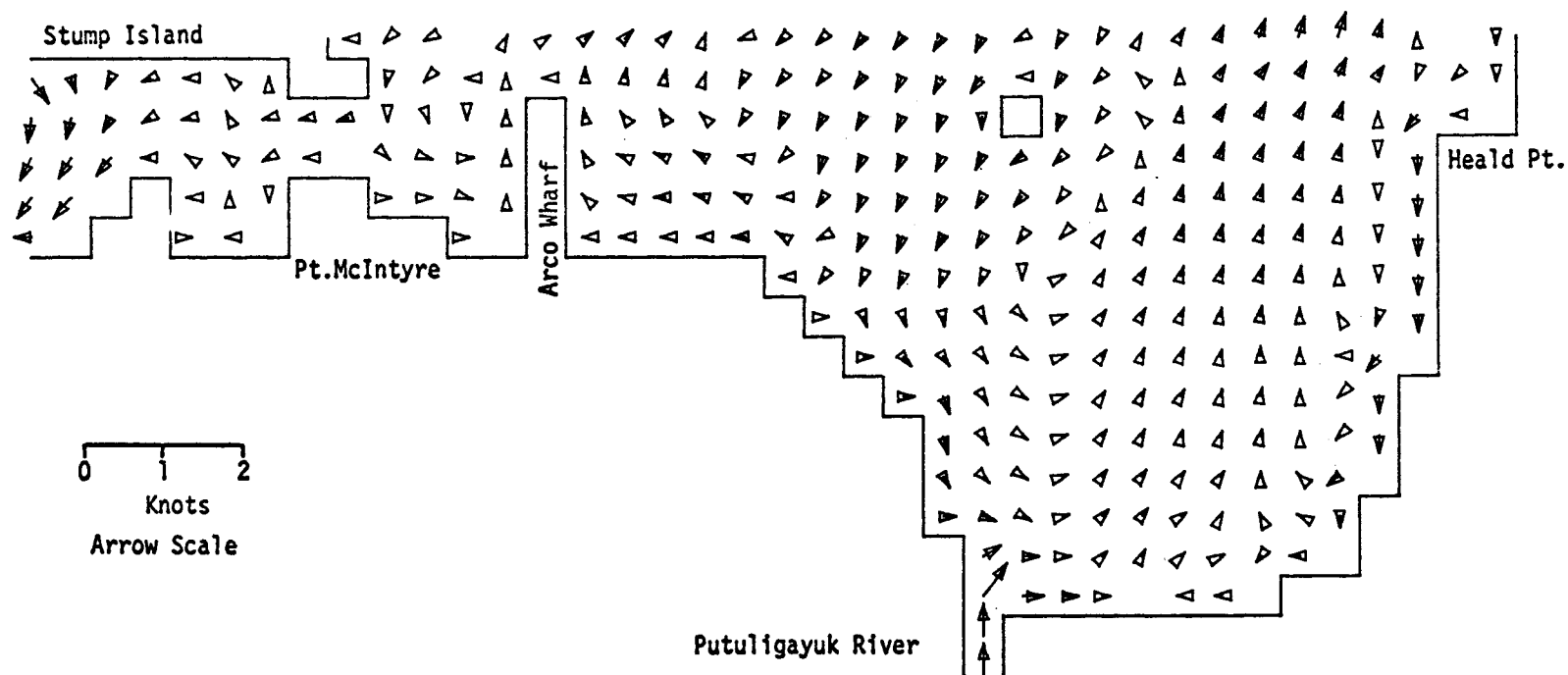
PRUDHOE BAY

M2 TIDE (AMP=8 CM, IN PHASE ON OPEN BOUNDARIES) ONSHORE WIND AT 10 KT

CURRENTS

TIME= 54000SEC

LAYER 1



MODEL NO 10

632

0 1 2  
Knots  
Arrow Scale

Putuligayuk River

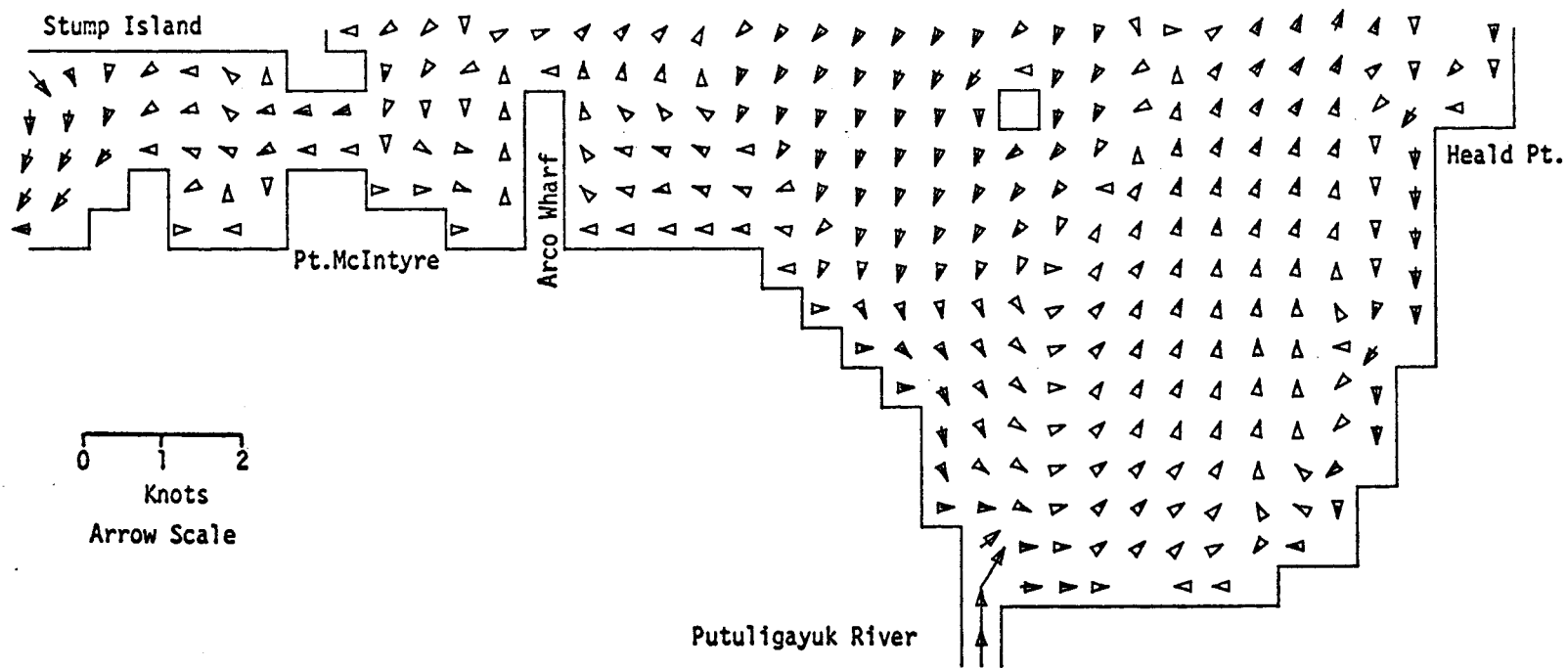
PRUDHOE BAY

M2 TIDE (AMP=8 CM, IN PHASE ON OPEN BOUNDARIES) ONSHORE WIND AT 10 KT

CURRENTS

TIME= 57600SEC

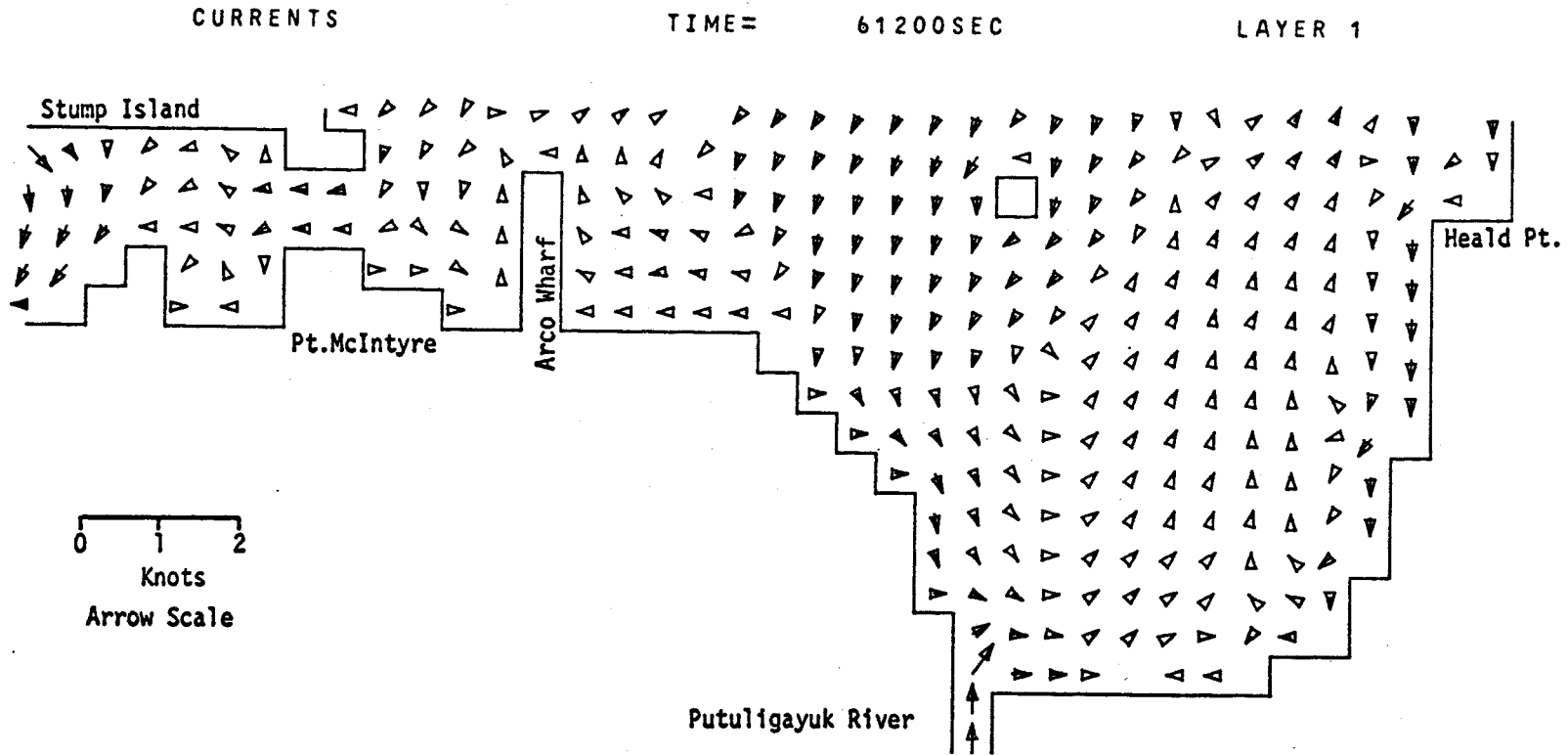
LAYER 1



PRUDHOE BAY  
M2 TIDE (AMP=8 CM. IN PHASE ON OPEN BOUNDARIES) ONSHORE WIND AT 10 KT

633  
MODEL NO 10

634  
MODEL NO 10



PRUDHOE BAY  
M2 TIDE (AMP=8 CM, IN PHASE ON OPEN BOUNDARIES) ONSHORE WIND AT 10 KT

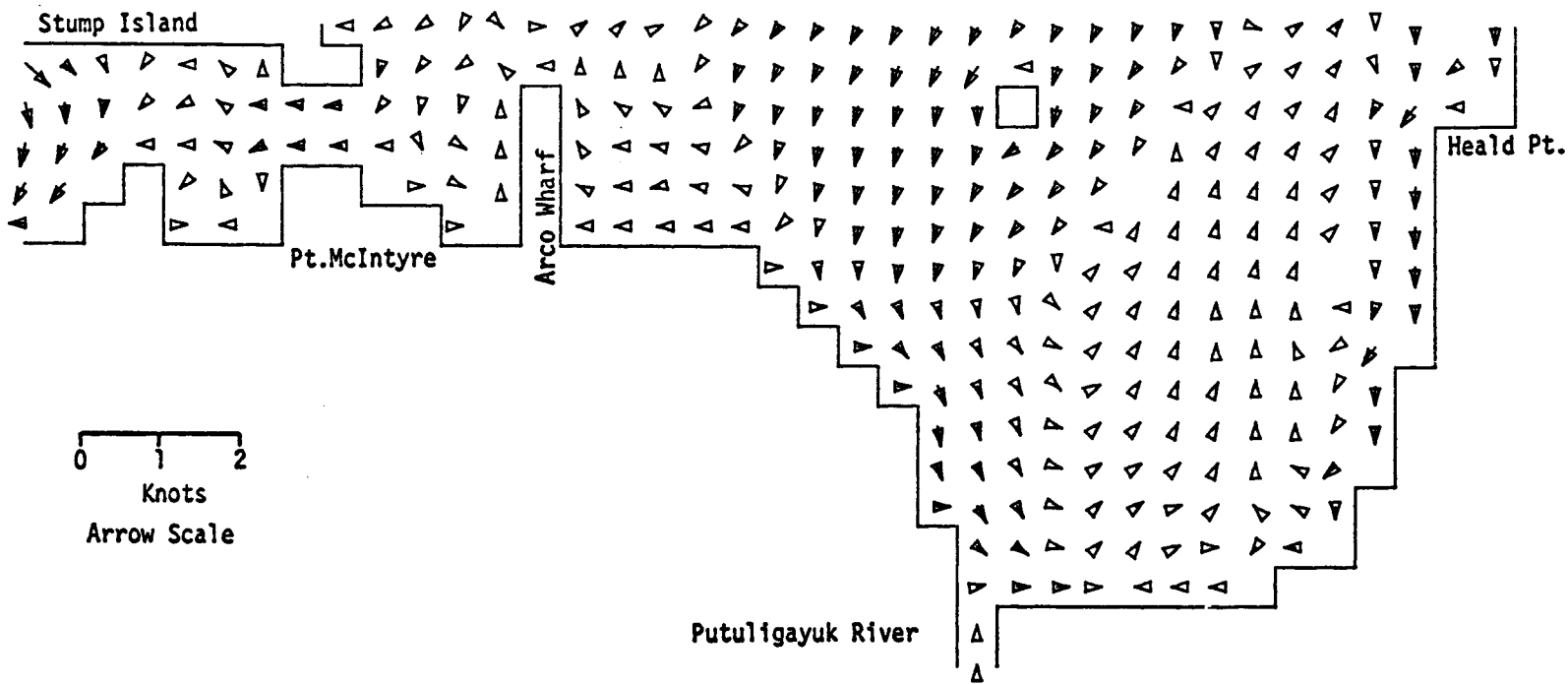


CURRENTS

TIME= 64800SEC

LAYER 1

MODEL NO 10



635

PRUDHOE BAY

M2 TIDE (AMP=8 CM, IN PHASE ON OPEN BOUNDARIES) ONSHORE WIND AT 10 KT

APPENDIX E

PRUDHOE BAY

M2 TIDE WITH 8CM AMPLITUDE INPUT IN PHASE ON ALL OPEN  
BOUNDARIES. NO RIVER INFLOW. 20 KNOT WIND OFFSHORE.

ENVIRONMENTAL PROTECTION AGENCY  
MARINE AND FRESHWATER ECOLOGY BRANCH  
OCEAN MASS TRANSPORT MODEL

M2 TIDE (AMPE=8 CM, IN PHASE ON OPEN BOUNDARIES) OFFSHORE WIND AT 20 KT  
BEAUFORT SEA SHELF STUDY  
GRID 010 PRUDHUE BAY AT 0.5 KM GRID SPACING

|                       |      |                 |                |                 |
|-----------------------|------|-----------------|----------------|-----------------|
| GRID GEOMETRY         | ROWS | 17              | COLUMNS        | 39              |
| GRID LENGTH           |      | 50000. CM       | ROTATION ANGLE | 331.5 DEG       |
| WIND DRAG COEFFICIENT |      | .0024           | MID LATITUDE   | 70.350 DEG. (N) |
| FRICTION COEFFICIENT  |      | .0030000 CM/SEC |                |                 |

|                      |          |         |         |
|----------------------|----------|---------|---------|
|                      | LAYER 1  | LAYER 2 | LAYER 3 |
| INITIAL LAYER DEPTHS | 300.0000 | .0000   | .0000   |
| SMOOTHING FACTORS    | .9900    | .0000   | .0000   |
| DENSITY              | 1.0200   | .0000   | .0000   |

|                                 |             |                           |          |
|---------------------------------|-------------|---------------------------|----------|
| RESULTS SAVED AT MODULUS (TIME, | 3600 SEC)=0 | RESULTS SAVED STARTING AT | 3600 SEC |
| COMPUTATIONS STARTED AT         | 0 SEC       |                           |          |
| ENDED AT                        | 64800 SEC   |                           |          |
| INCREMENTED BY                  | 60 SEC      |                           |          |
| LAYER3 PRINT OUT STARTED        |             | 3600 SEC. FREQUENCY OF    | 3600 SEC |

|                               |     |        |          |        |          |     |          |       |
|-------------------------------|-----|--------|----------|--------|----------|-----|----------|-------|
| TIDAL INPUT AT                | ROW | 1 THRU | 7        | COLUMN | 1 THRU   | 1   | TIME LAG | 0 SEC |
|                               |     |        | M2       |        | S2       | 01  | K1       |       |
| PHASE ANGLES (DEG/HR)         |     |        | 270.00   |        | .00      | .00 | .00      |       |
| AMPLITUDES (CM)               |     |        | 8.00     |        | .00      | .00 | .00      |       |
| LOWER LAYER WEIGHTING FACTORS |     |        | LAYER 2= | .00    | LAYER 3= | .00 |          |       |

|                               |     |        |          |        |          |     |          |       |
|-------------------------------|-----|--------|----------|--------|----------|-----|----------|-------|
| TIDAL INPUT AT                | ROW | 1 THRU | 1        | COLUMN | 8 THRU   | 39  | TIME LAG | 0 SEC |
|                               |     |        | M2       |        | S2       | 01  | K1       |       |
| PHASE ANGLES (DEG/HR)         |     |        | 270.00   |        | .00      | .00 | .00      |       |
| AMPLITUDES (CM)               |     |        | 8.00     |        | .00      | .00 | .00      |       |
| LOWER LAYER WEIGHTING FACTORS |     |        | LAYER 2= | .00    | LAYER 3= | .00 |          |       |

|                       |           |         |         |         |
|-----------------------|-----------|---------|---------|---------|
| TIDAL SPEEDS (DEG/HR) | M2        | S2      | 01      | K1      |
|                       | 24.984000 | .000000 | .000000 | .000000 |

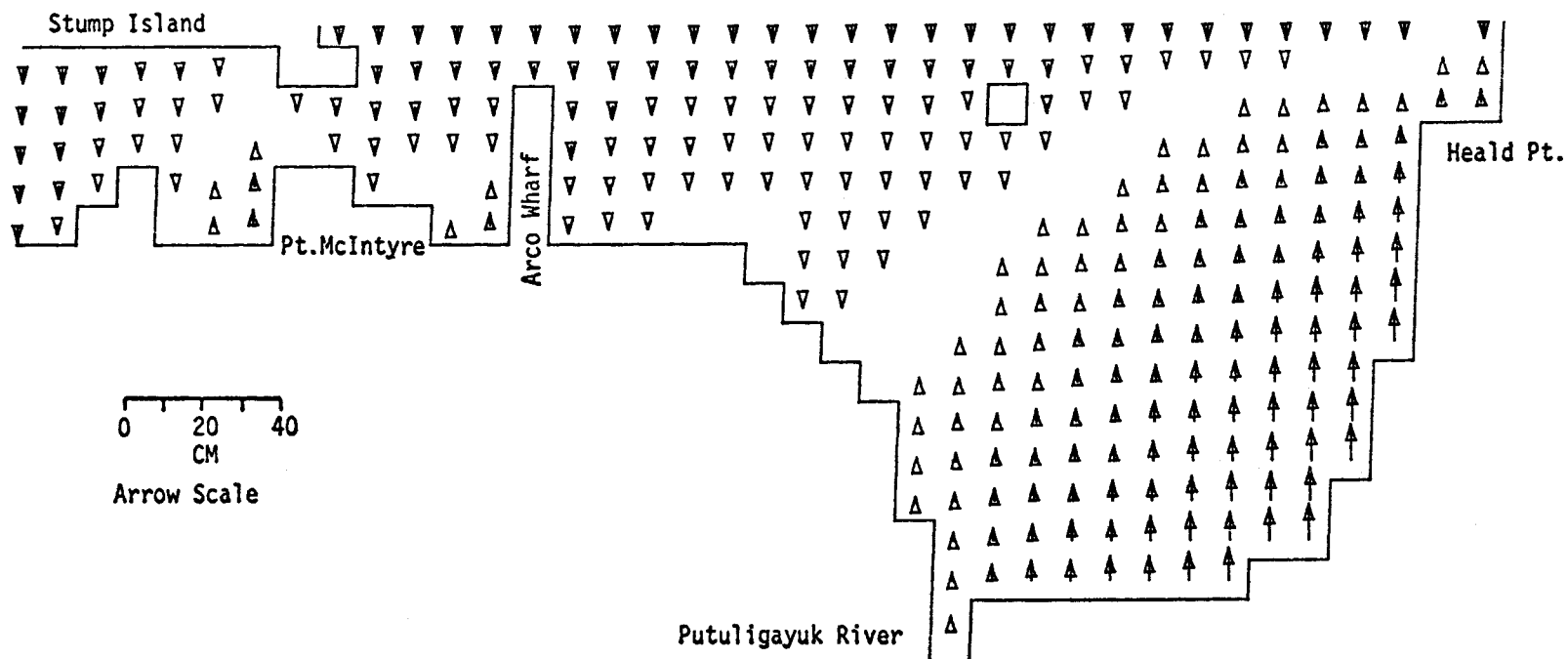
|                         |     |        |           |           |              |       |          |
|-------------------------|-----|--------|-----------|-----------|--------------|-------|----------|
| WIND INPUT AT           | ROW | 1 THRU | 17        | COLUMN    | 1 THRU       | 39    |          |
| COMPUTATIONS STARTED AT |     |        | 60 SEC    |           |              |       |          |
| ENDED AT                |     |        | 64800 SEC | DIRECTION | 331 DEG TRUE | SPEED | 10 M/SEC |

SEA LEVEL

SEA LEVEL

TIME= 3600SEC

LAYER 1



10  
MODEL NO 63

0 20 40  
CM  
Arrow Scale

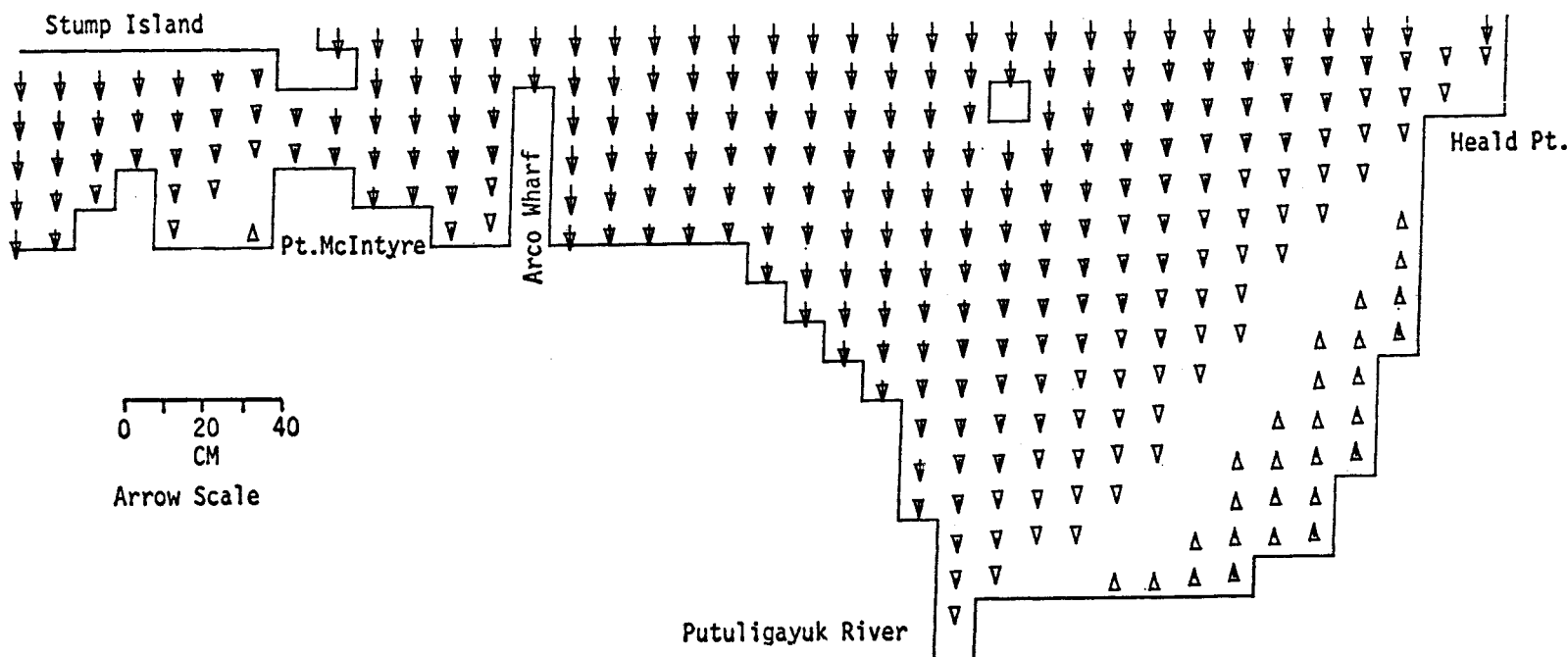
PRUDHOE BAY

M2 TIDE (AMP=8 CM, IN PHASE ON OPEN BOUNDARIES) OFFSHORE WIND AT 20 KT

SEA LEVEL

TIME= 7200SEC

LAYER 1



10

MODEL NO

640

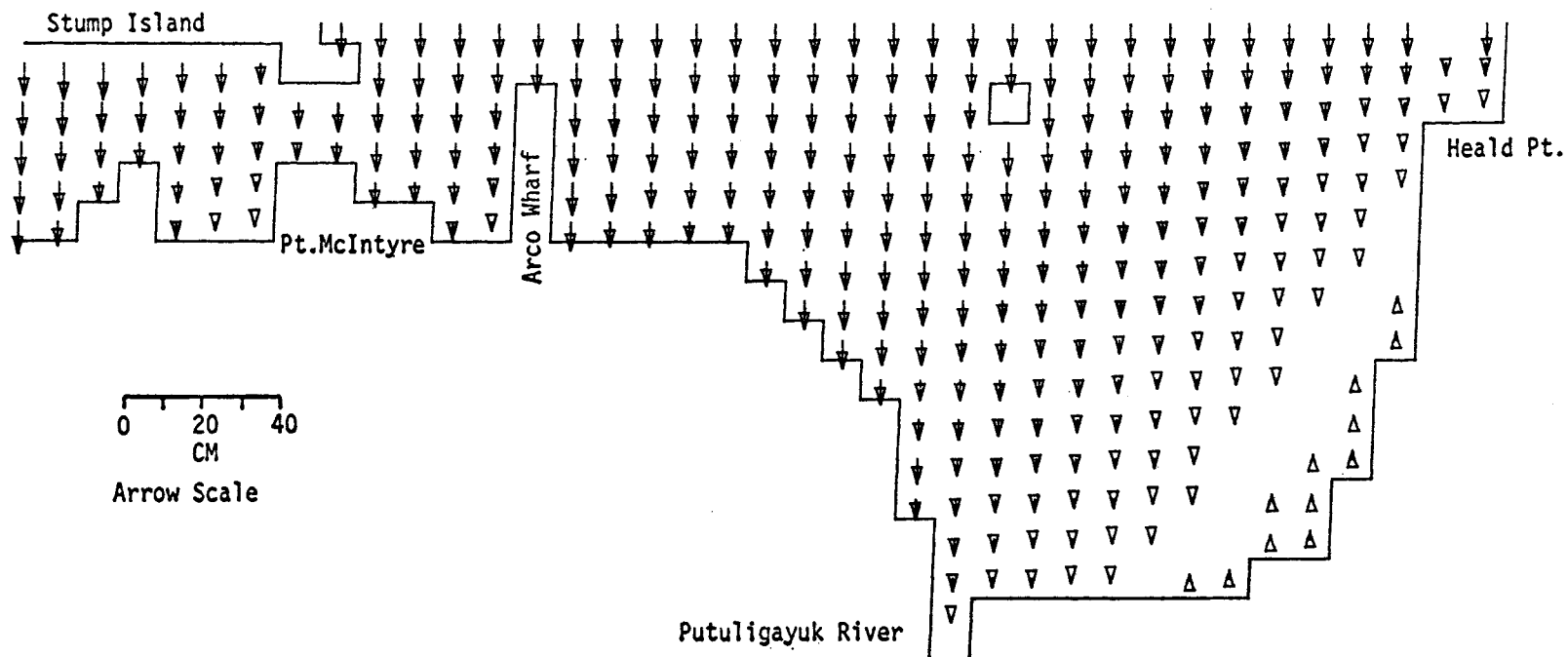
0 20 40  
CM  
Arrow Scale

PRUDHOE BAY  
M2 TIDE (AMP=8 CM, IN PHASE ON OPEN BOUNDARIES) OFFSHORE WIND AT 20 KT

SEA LEVEL

TIME= 10800SEC

LAYER 1



0 20 40  
CM

Arrow Scale

Putuligayuk River

Heald Pt.

PRUDHOE BAY

M2 TIDE (AMP=8 CM, IN PHASE ON OPEN BOUNDARIES) OFFSHORE WIND AT 20 KT

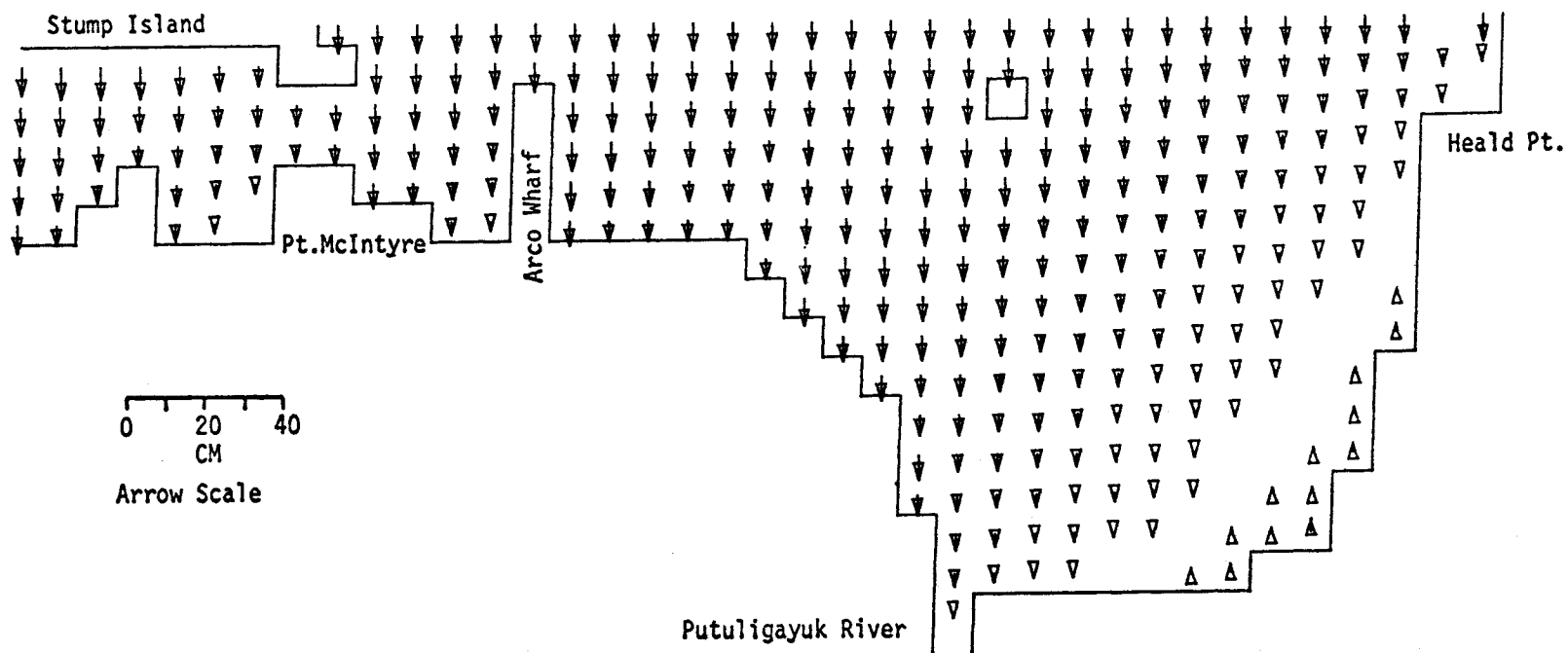
MODEL NO 10

641

SEA LEVEL

TIME= 14400SEC

LAYER 1



PRUDHOE BAY

M2 TIDE (AMP=8 CM, IN PHASE ON OPEN BOUNDARIES) OFFSHORE WIND AT 20 KT

MODEL NO 10

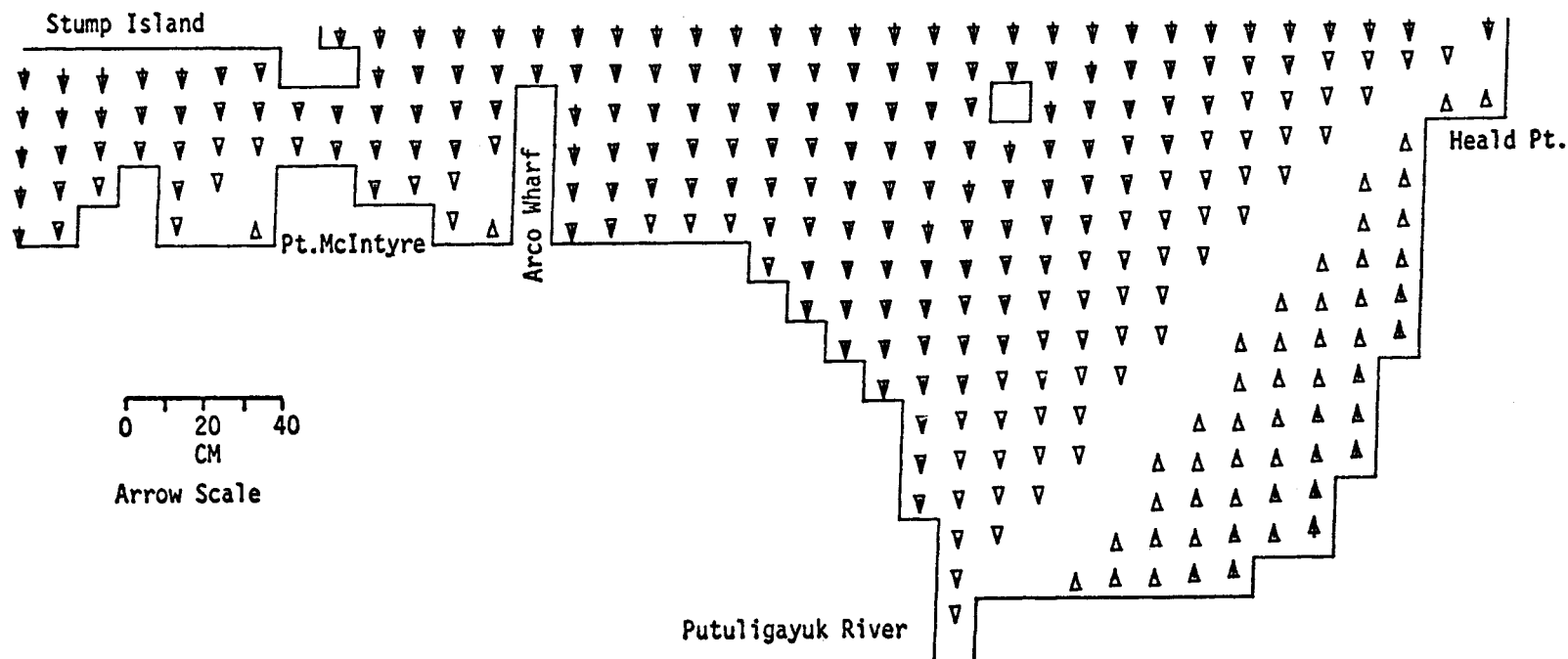
642



SEA LEVEL

TIME= 18000SEC

LAYER 1



10

MODEL NO

643

0 20 40  
CM

Arrow Scale

Putuligayuk River

Heald Pt.

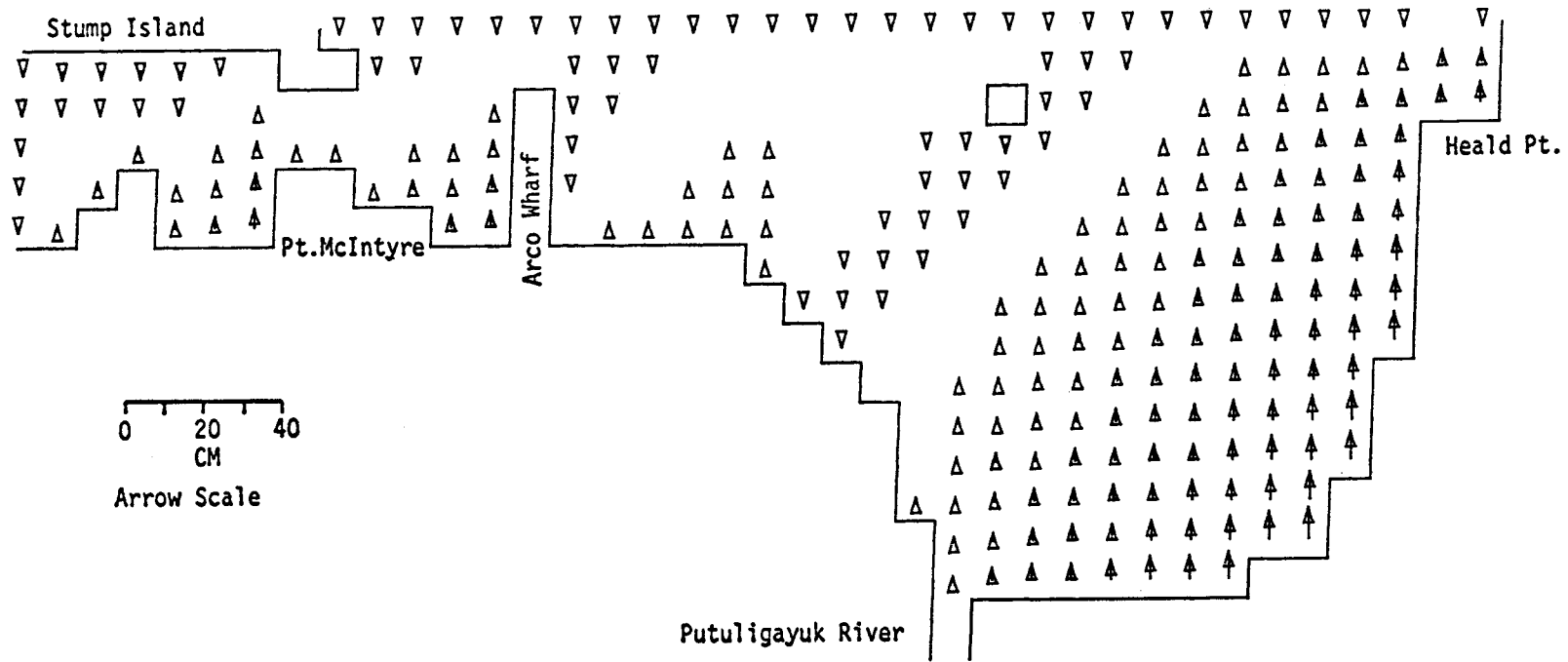
PRUDHOE BAY

M2 TIDE (AMP=8 CM, IN PHASE ON OPEN BOUNDARIES) OFFSHORE WIND AT 20 KT

SEA LEVEL

TIME= 21600SEC

LAYER 1



0 20 40  
CM  
Arrow Scale

PRUDHOE BAY

M2 TIDE (AMP=8 CM, IN PHASE ON OPEN BOUNDARIES) OFFSHORE WIND AT 20 KT

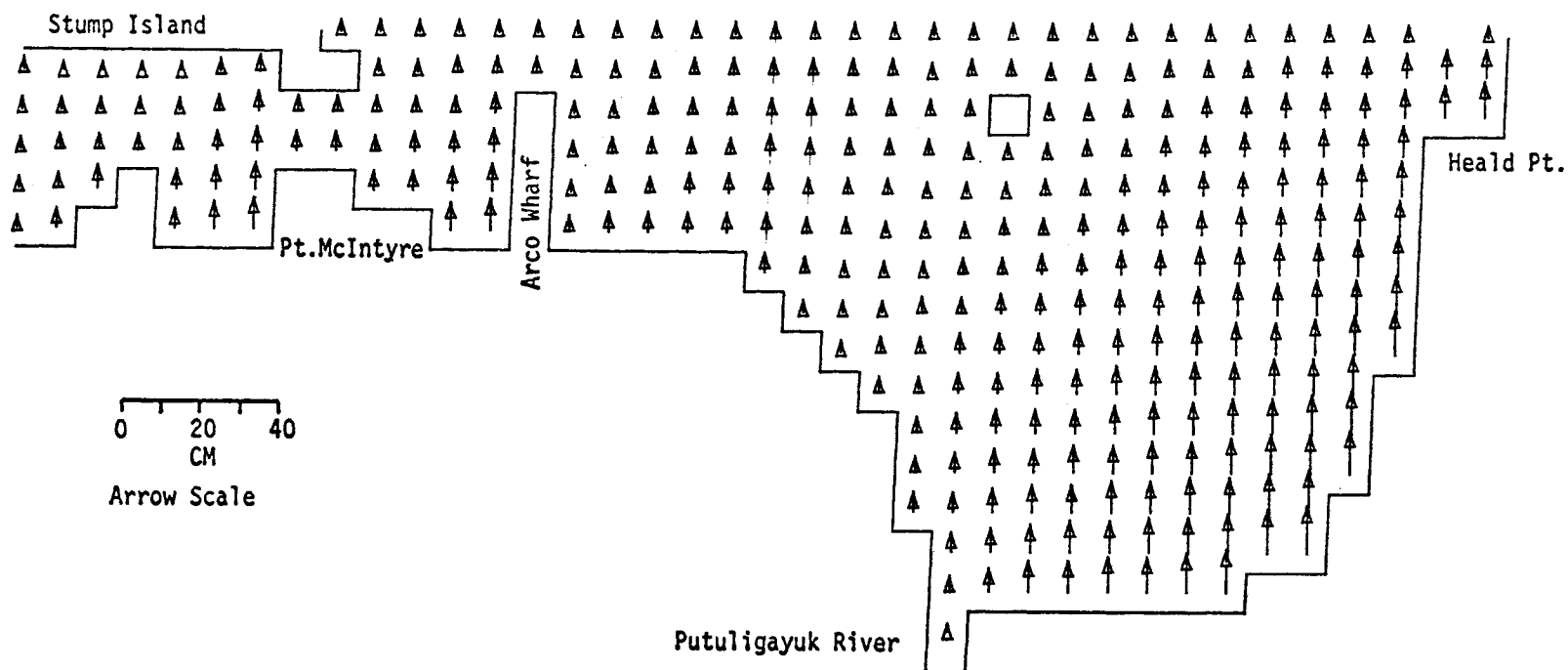
644

MODEL NO 10

SEA LEVEL

TIME= 25200SEC

LAYER 1



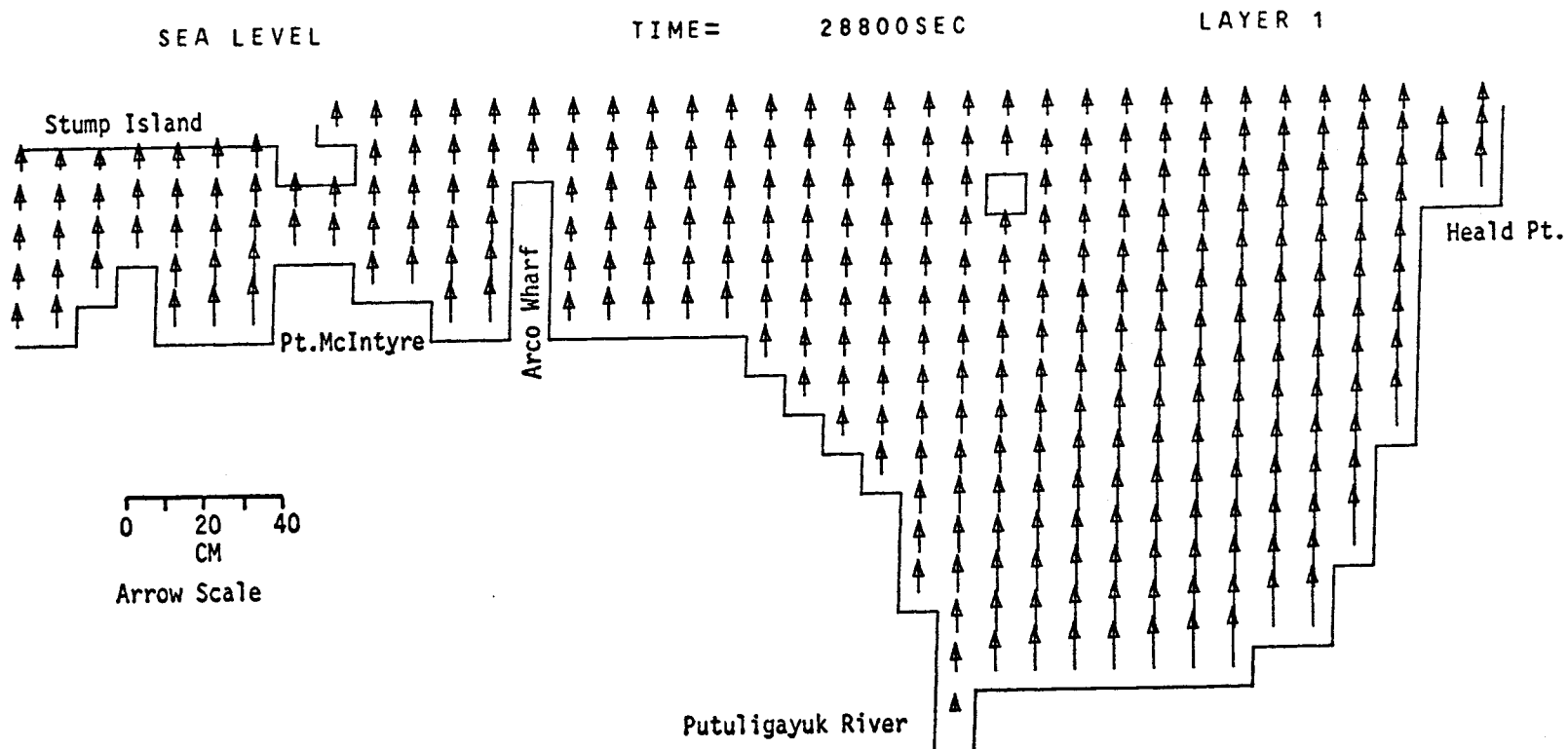
MODEL NO 10

645

0 20 40  
CM  
Arrow Scale

PRUDHOE BAY  
M2 TIDE (AMP=8 CM, IN PHASE ON OPEN BOUNDARIES) OFFSHORE WIND AT 20 KT

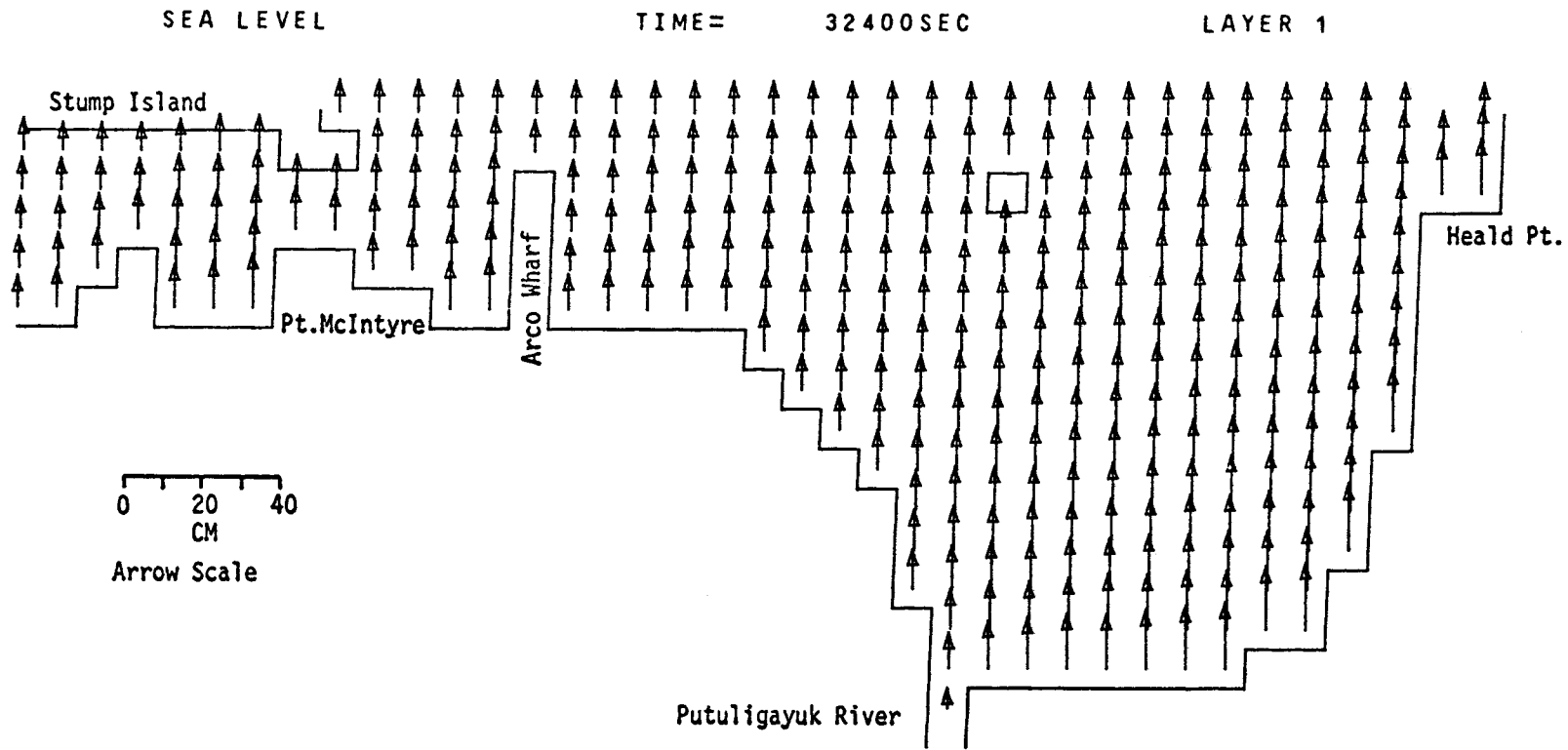
01 ON 7300W 646



PRUDHOE BAY  
M2 TIDE (AMP=8 CM, IN PHASE ON OPEN BOUNDARIES) OFFSHORE WIND AT 20 KT

647

MODEL NO 10

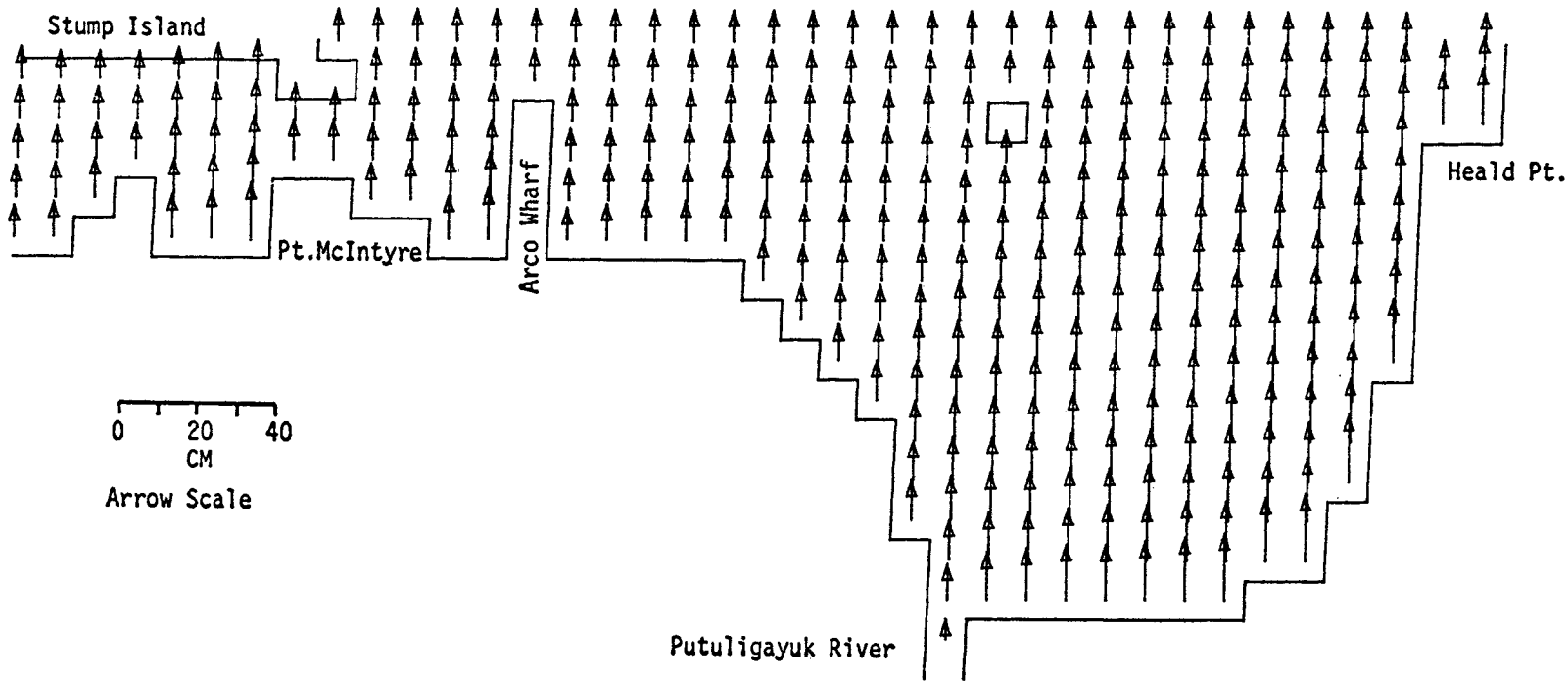


PRUDHOE BAY  
M2 TIDE (AMP=8 CM, IN PHASE ON OPEN BOUNDARIES)      OFFSHORE WIND AT 20 KT

SEA LEVEL

TIME= 36000SEC

LAYER 1



0 20 40  
CM  
Arrow Scale

Putuligayuk River

PRUDHOE BAY  
M2 TIDE (AMP=8 CM, IN PHASE ON OPEN BOUNDARIES) OFFSHORE WIND AT 20 KT

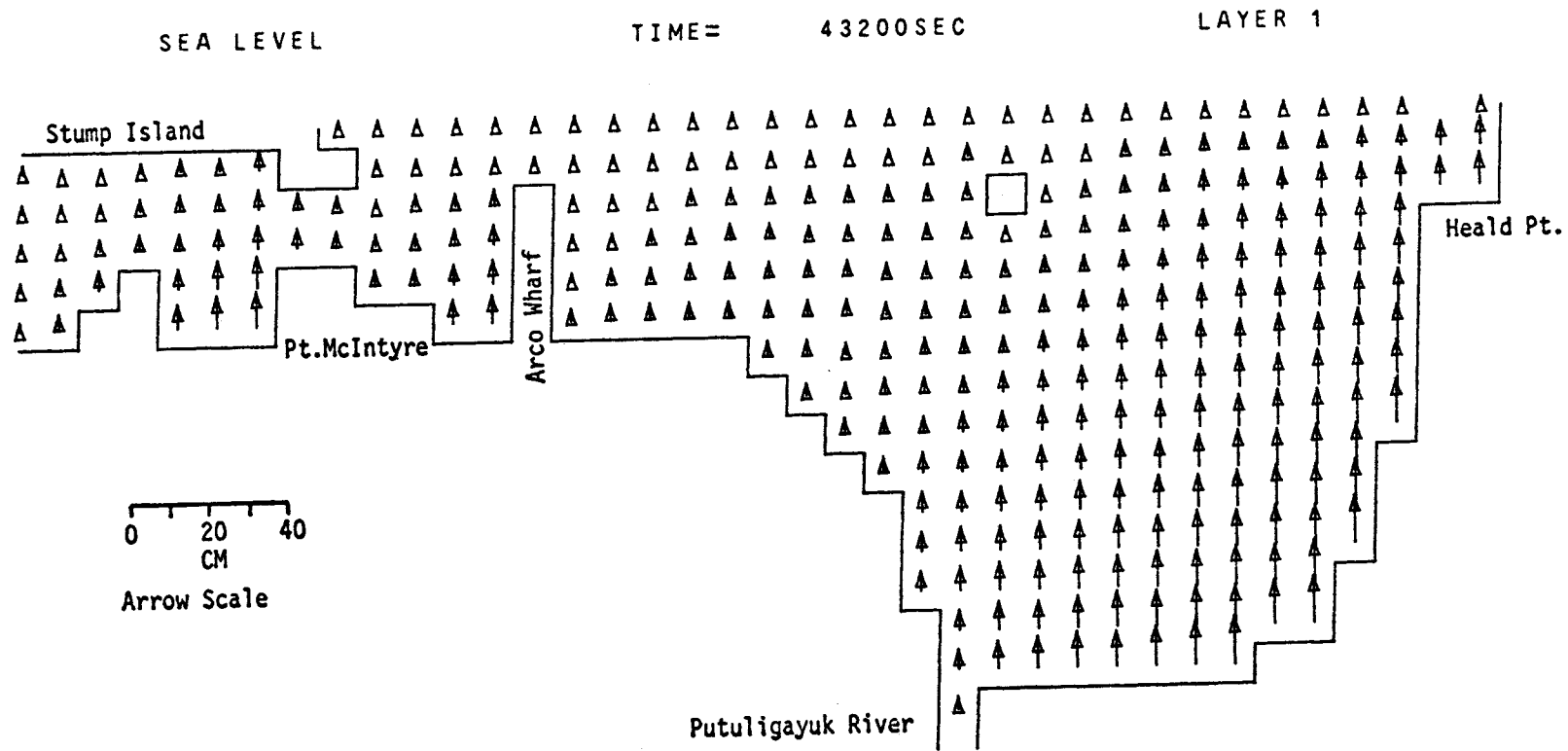
MODEL NO 10

648



059

MODEL NO 10

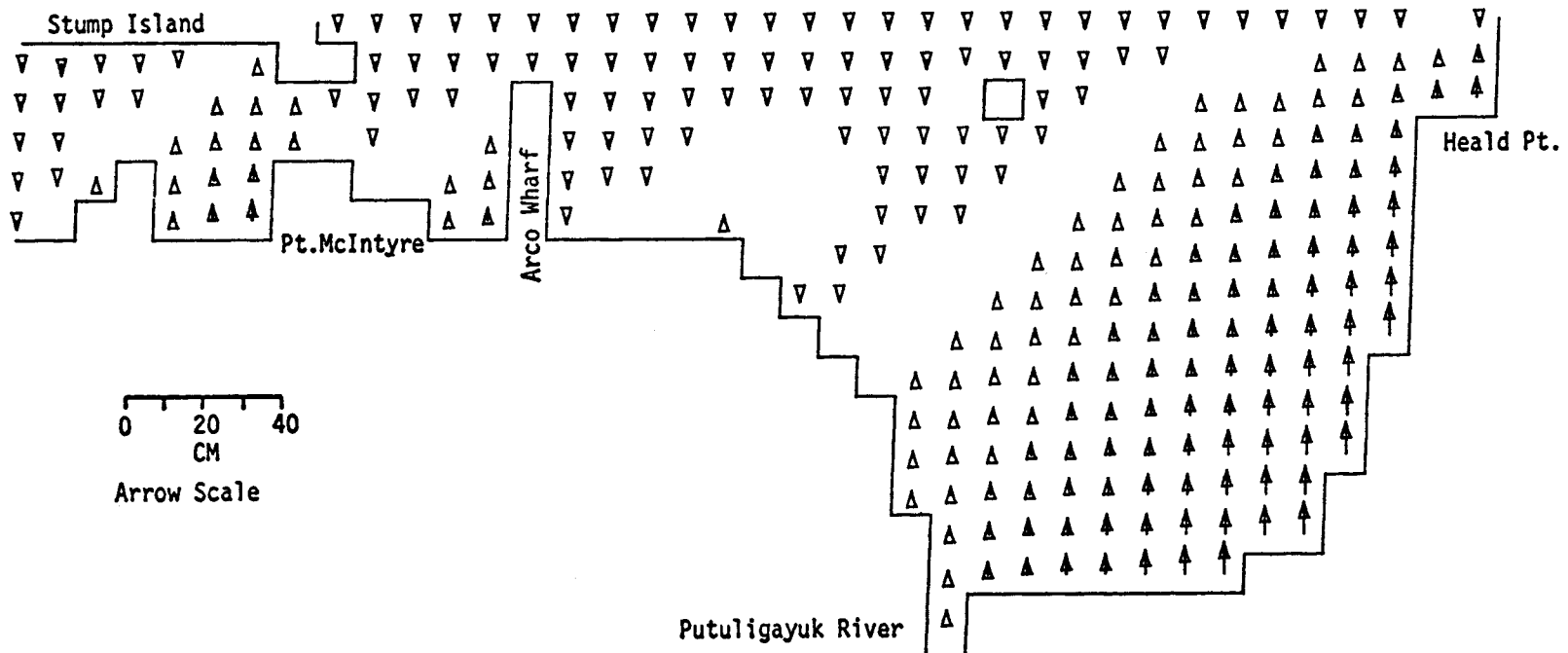




SEA LEVEL

TIME= 46800SEC

LAYER 1



10

MODEL NO

TS9

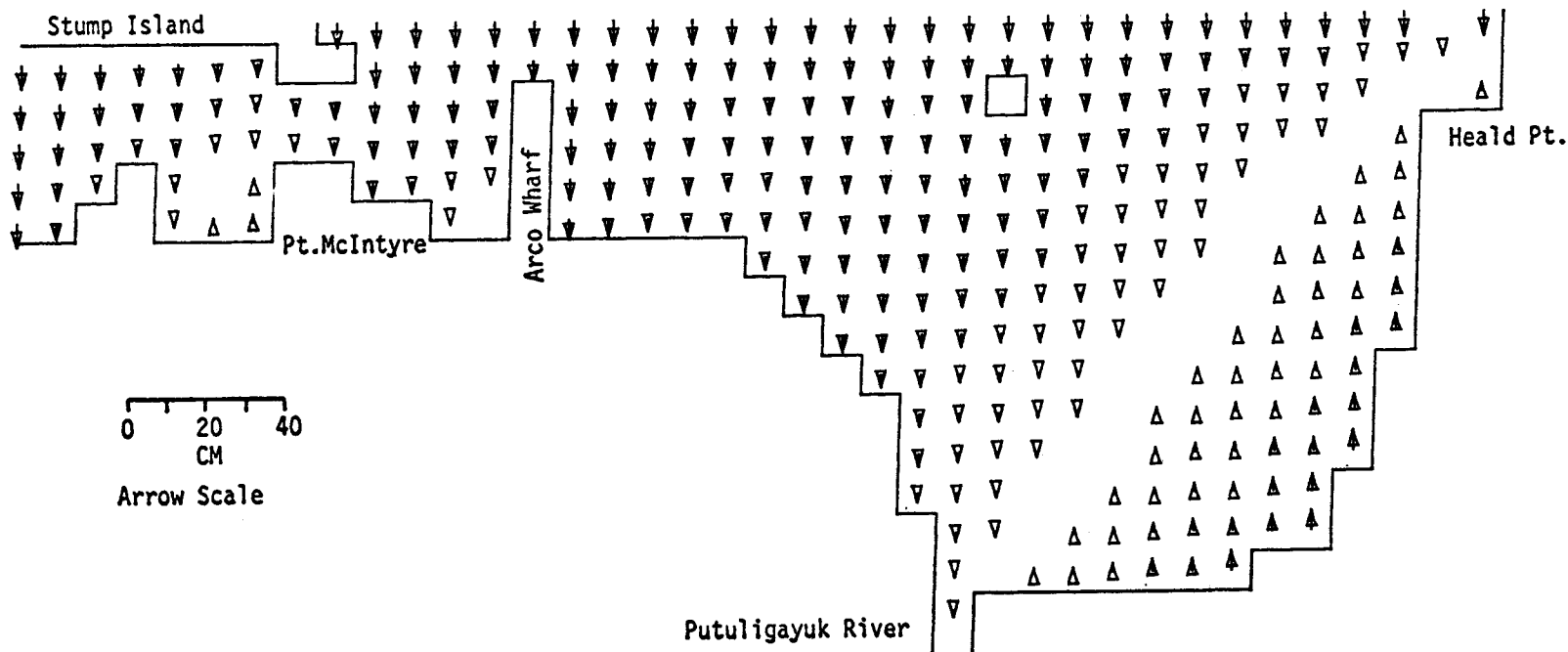
PRUDHOE BAY

M2 TIDE (AMP=8 CM, IN PHASE ON OPEN BOUNDARIES) OFFSHORE WIND AT 20 KT

SEA LEVEL

TIME= 50400SEC

LAYER 1



10

MODEL NO

652

0 20 40  
CM

Arrow Scale

PRUDHOE BAY

M2 TIDE (AMP=8 CM, IN PHASE ON OPEN BOUNDARIES) OFFSHORE WIND AT 20 KT

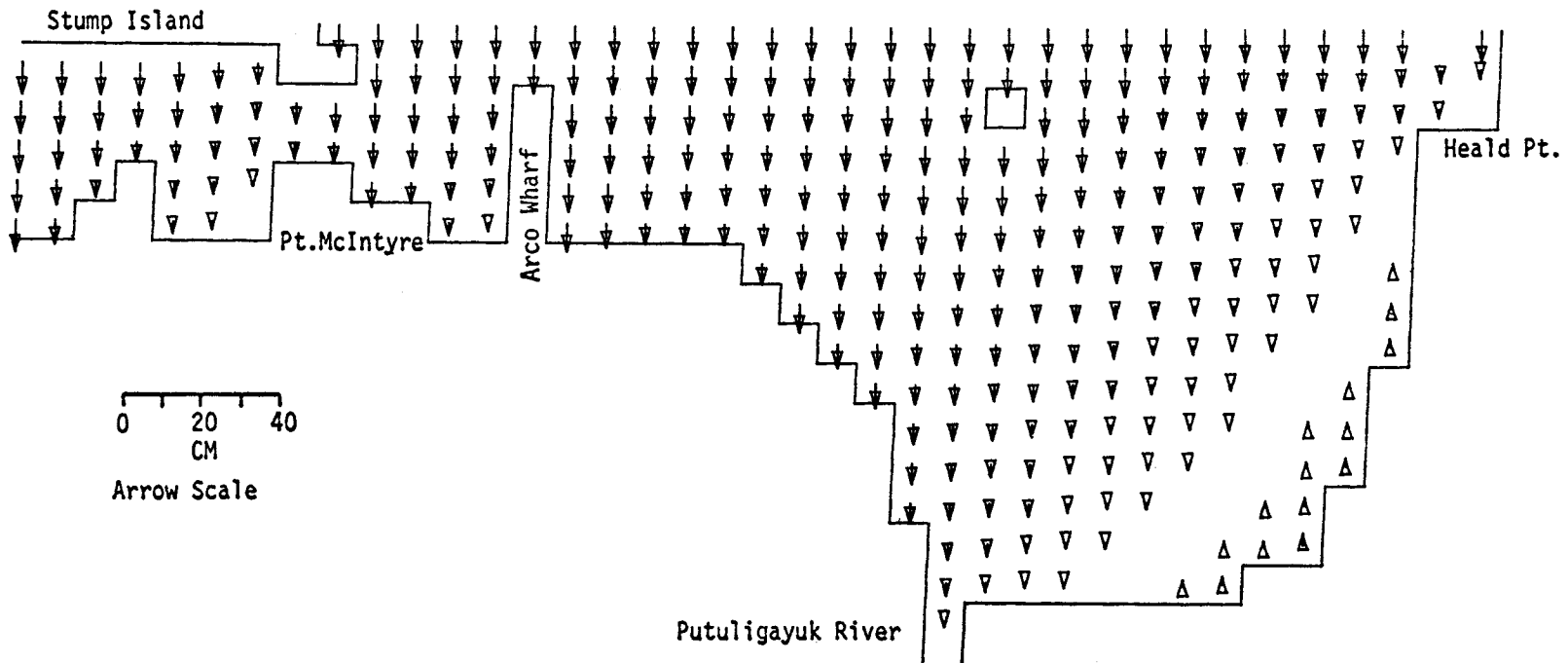
SEA LEVEL

TIME= 54000SEC

LAYER 1

10

MODEL NO  
859



0 20 40  
CM

Arrow Scale

Putuligayuk River

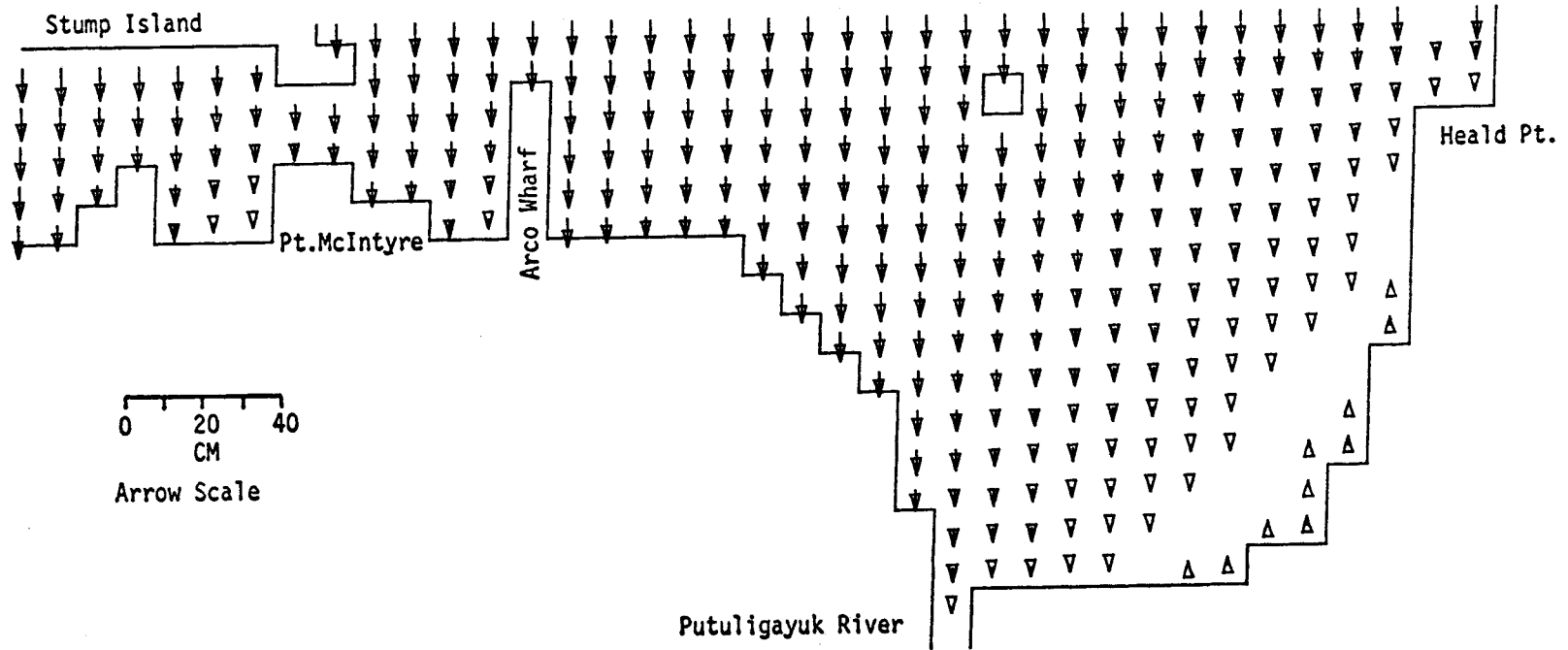
PRUDHOE BAY

M2 TIDE (AMP=8 CM, IN PHASE ON OPEN BOUNDARIES) OFFSHORE WIND AT 20 KT

SEA LEVEL

TIME= 57600SEC

LAYER 1



MODEL NO 10

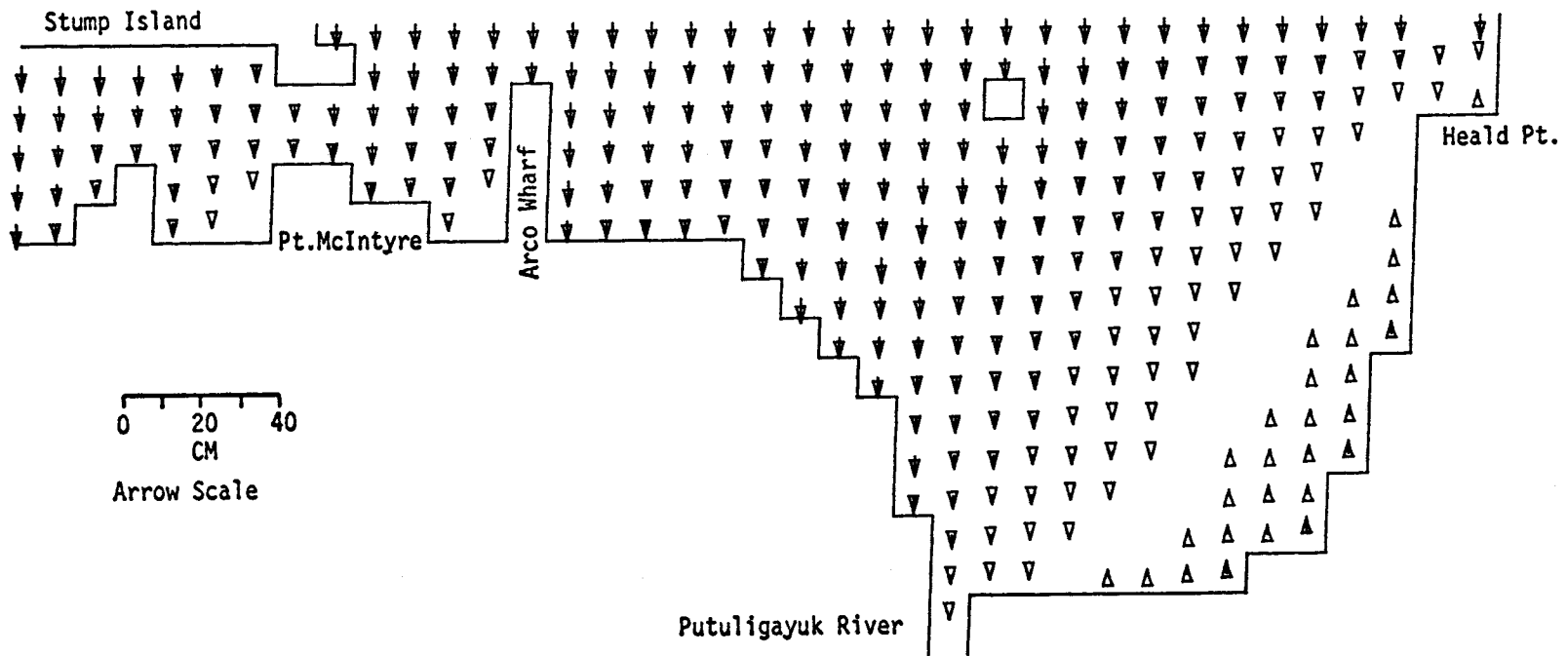
654

PRUDHOE BAY  
M2 TIDE (AMP=8 CM, IN PHASE ON OPEN BOUNDARIES) OFFSHORE WIND AT 20 KT

SEA LEVEL

TIME= 61200SEC

LAYER 1



10

MODEL NO

655

0 20 40  
CM  
Arrow Scale

Putuligayuk River

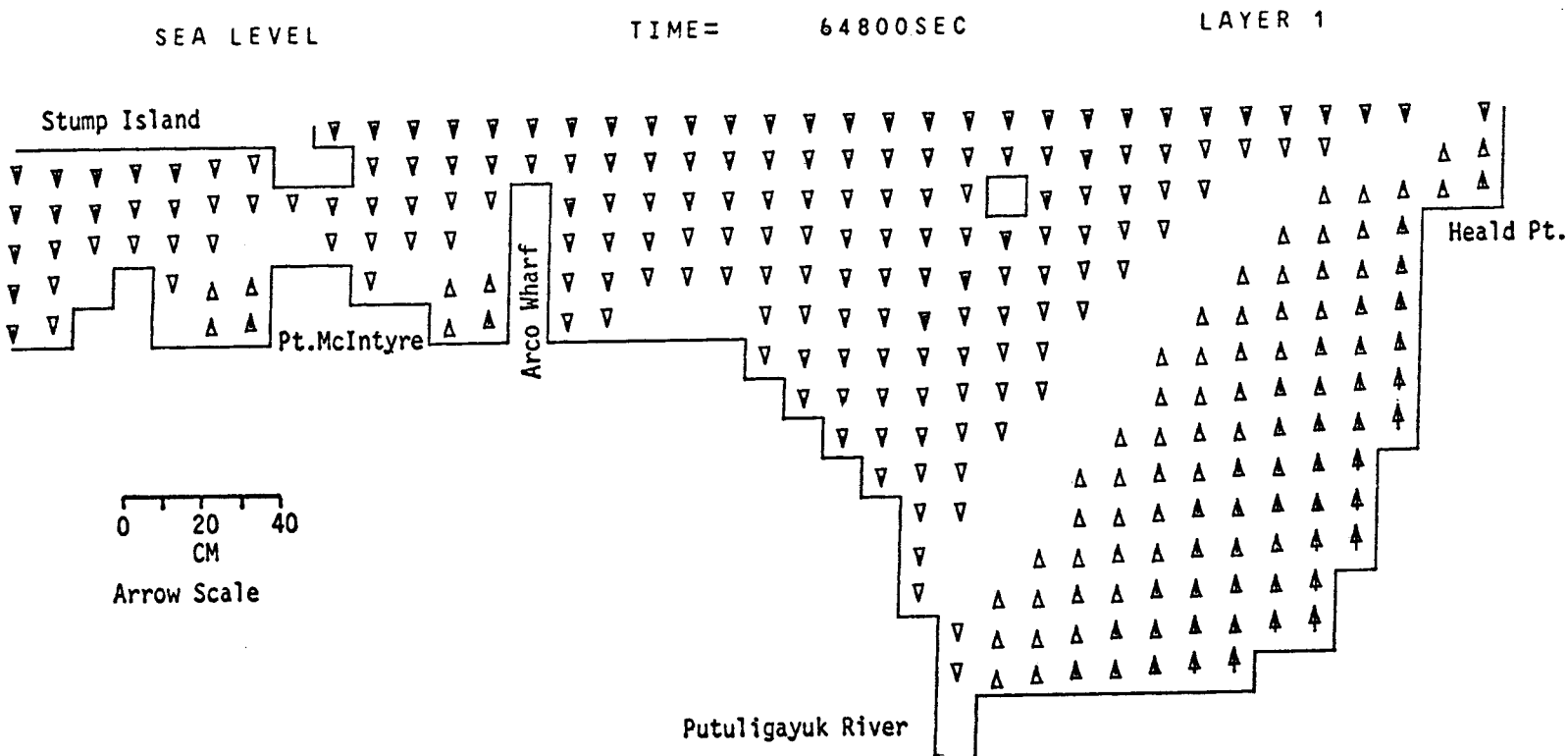
Heald Pt.

PRUDHOE BAY

M2 TIDE (AMP=8 CM, IN PHASE ON OPEN BOUNDARIES) OFFSHORE WIND AT 20 KT

656

MODEL NO 10

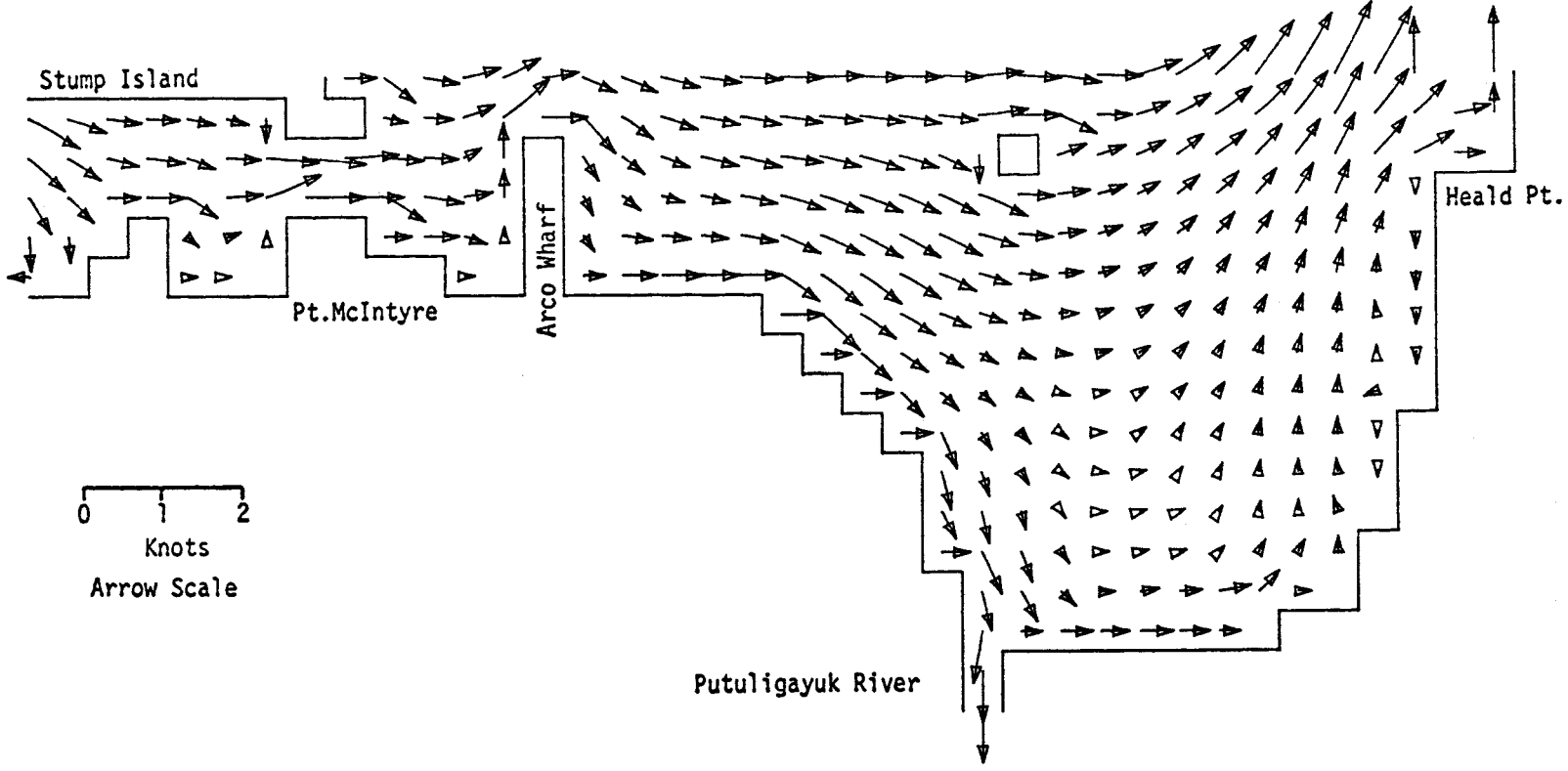


CURRENTS

CURRENTS

TIME = 3600SEC

LAYER 1



PRUDHOE BAY  
 M2 TIDE (AMP=8 CM, IN PHASE ON OPEN BOUNDARIES) OFFSHORE WIND AT 20 KT

658

MODEL NO 10

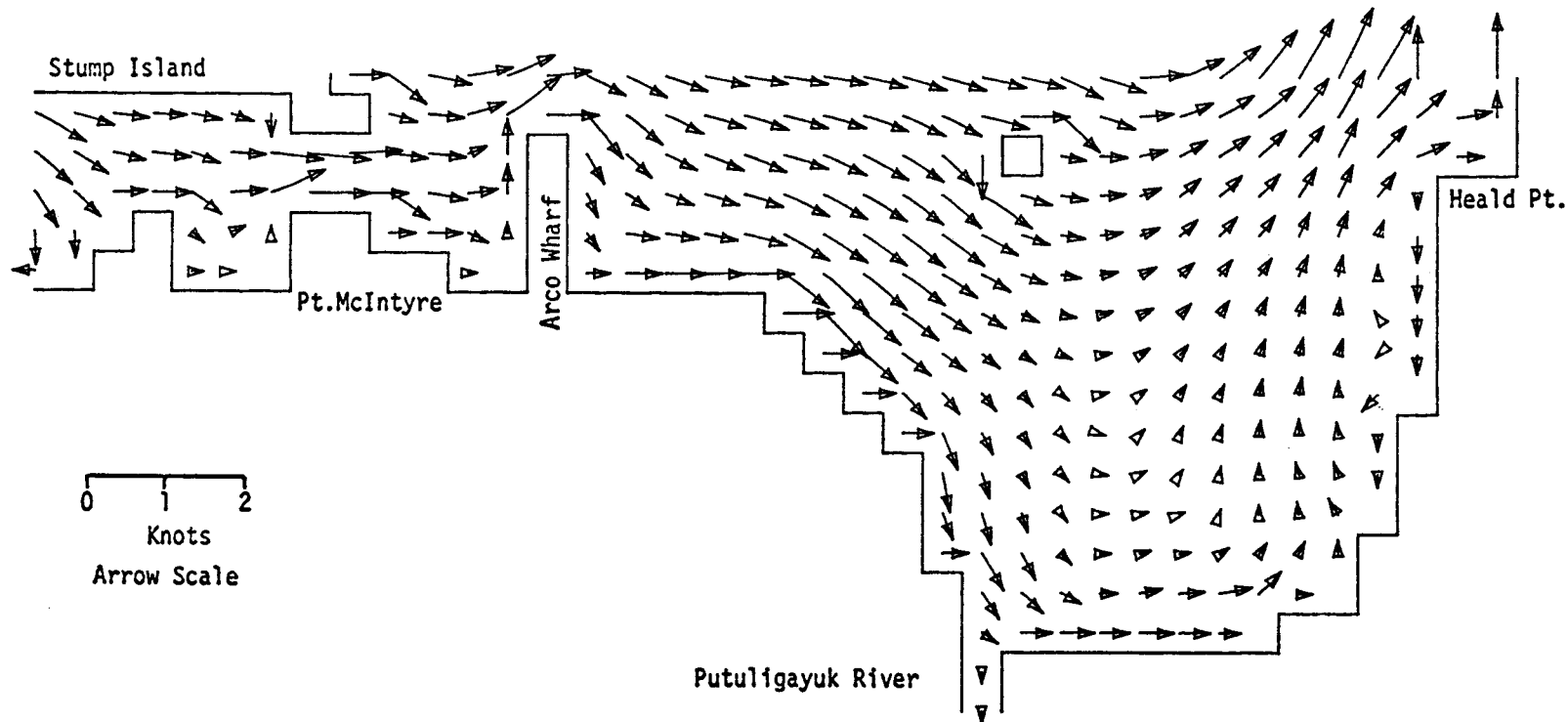


669  
MODEL NO 10

CURRENTS

TIME= 7200SEC

LAYER 1



PRUDHOE BAY  
M2 TIDE (AMP=8 CM, IN PHASE ON OPEN BOUNDARIES) OFFSHORE WIND AT 20 KT

CURRENTS

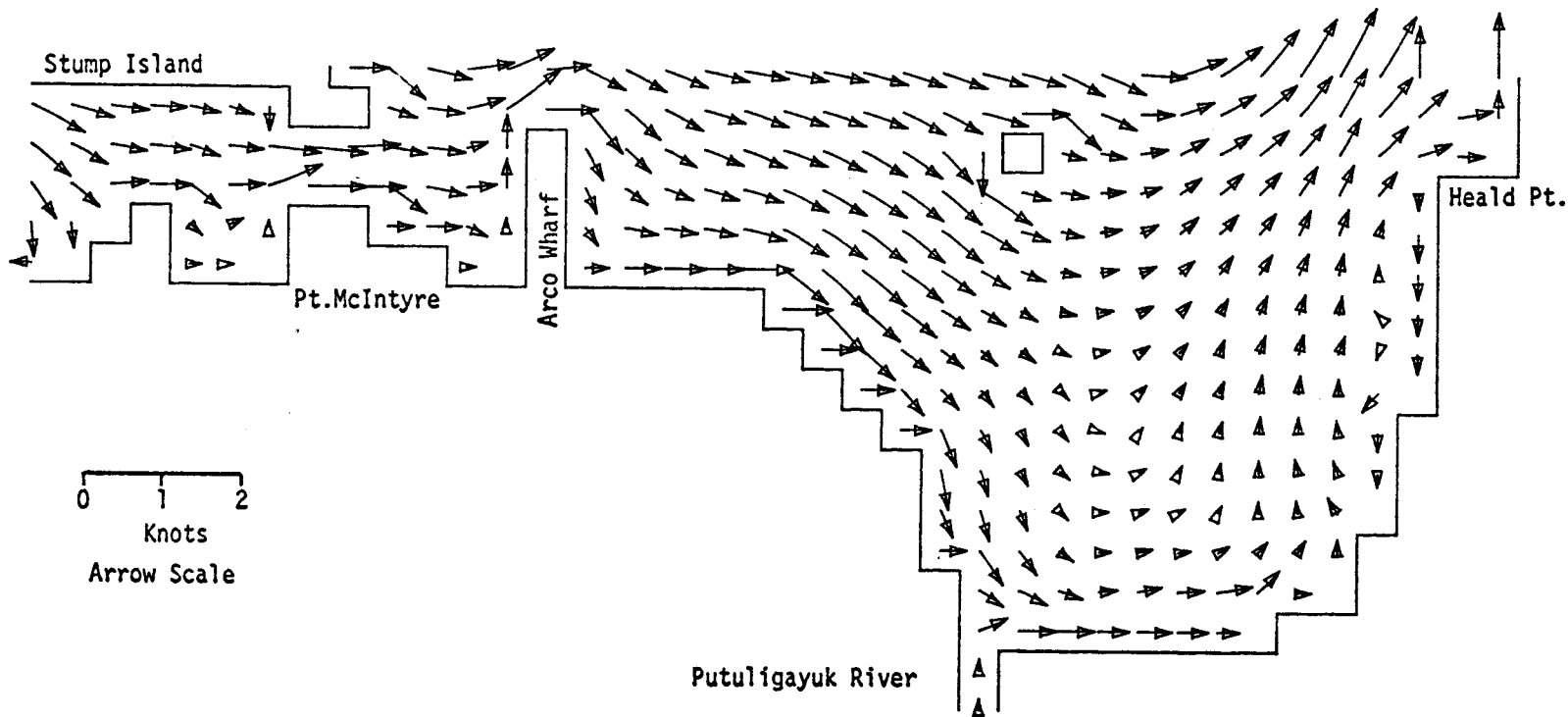
TIME= 10800SEC

LAYER 1

10

MODEL NO

099



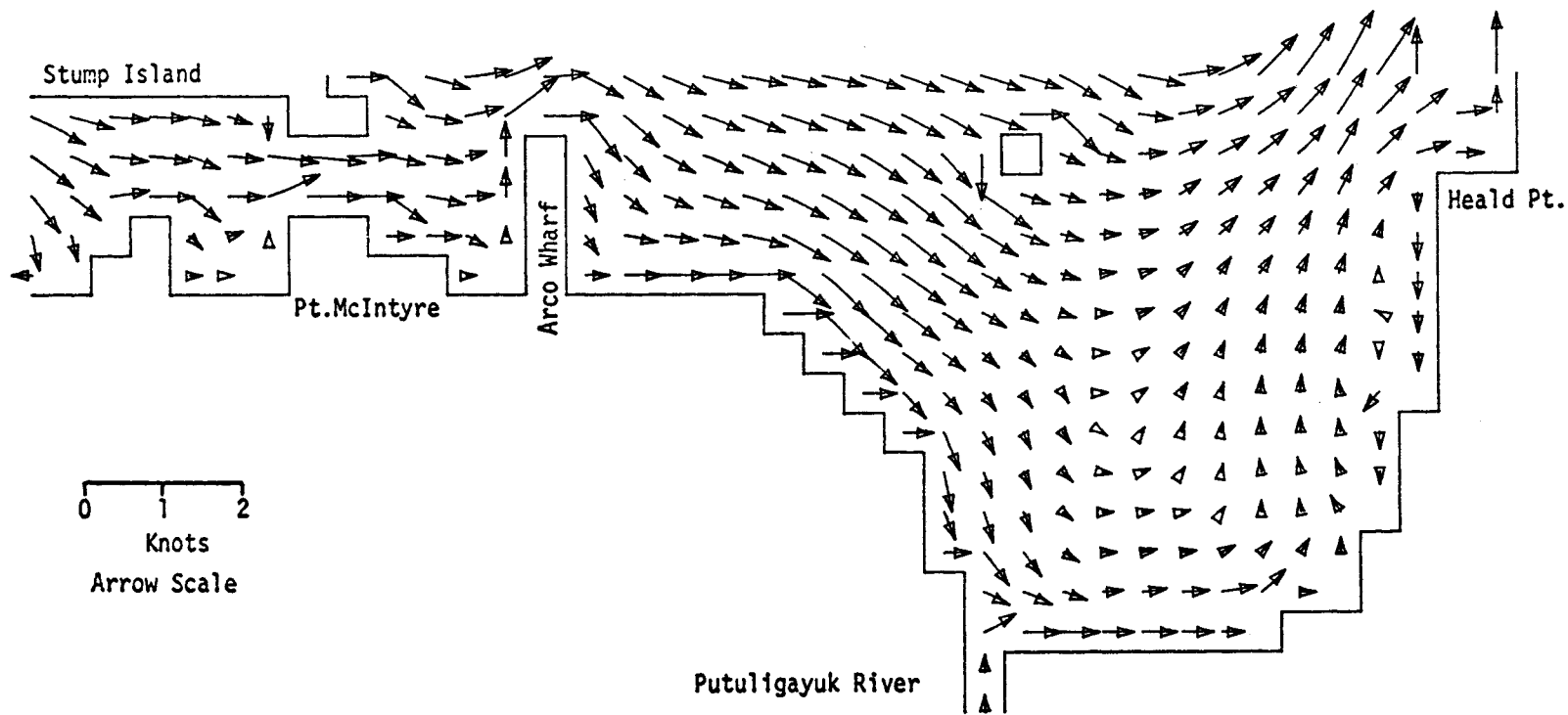
PRUDHOE BAY

M2 TIDE (AMP=8 CM, IN PHASE ON OPEN BOUNDARIES) OFFSHORE WIND AT 20 KT

CURRENTS

TIME= 14400SEC

LAYER 1



MODEL NO 10

T99  
661

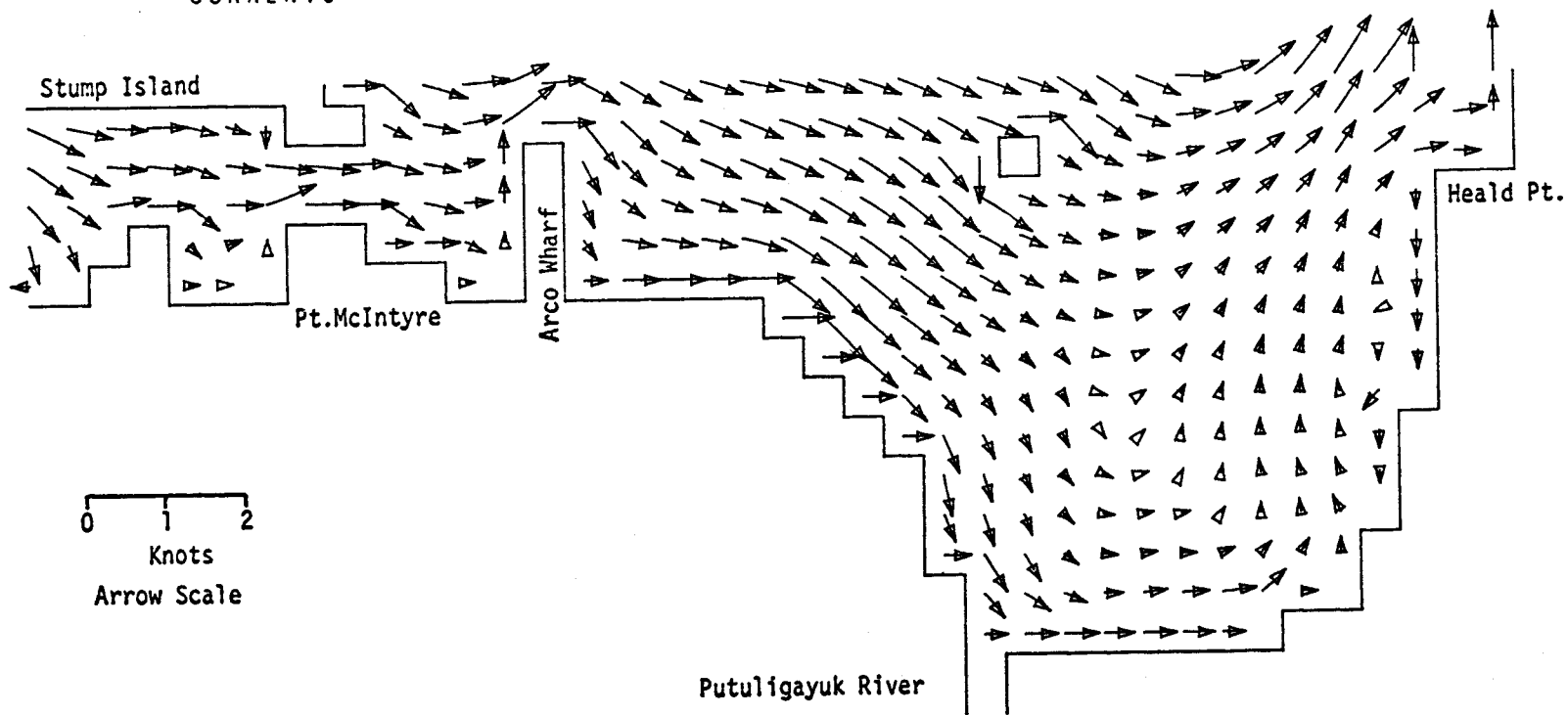
PRUDHOE BAY

M2 TIDE (AMP=8 CM. IN PHASE ON OPEN BOUNDARIES) OFFSHORE WIND AT 20 KT

CURRENTS

TIME= 18000SEC

LAYER 1



MODEL NO 10

0 1 2  
Knots  
Arrow Scale

PRUDHOE BAY

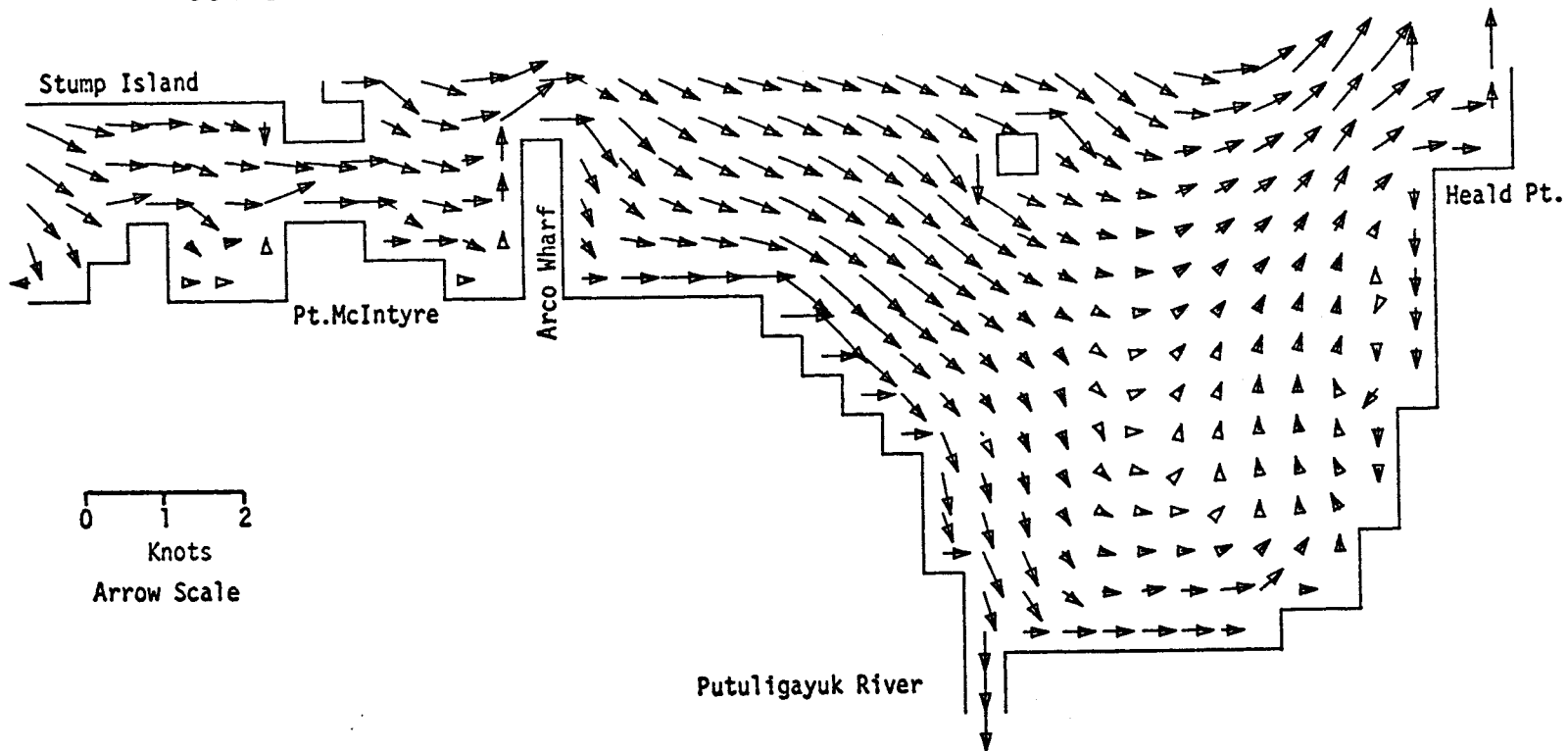
M2 TIDE (AMP=8 CM. IN PHASE ON OPEN BOUNDARIES) OFFSHORE WIND AT 20 KT

CURRENTS

TIME= 21600SEC

LAYER 1

MODEL NO  
10  
899

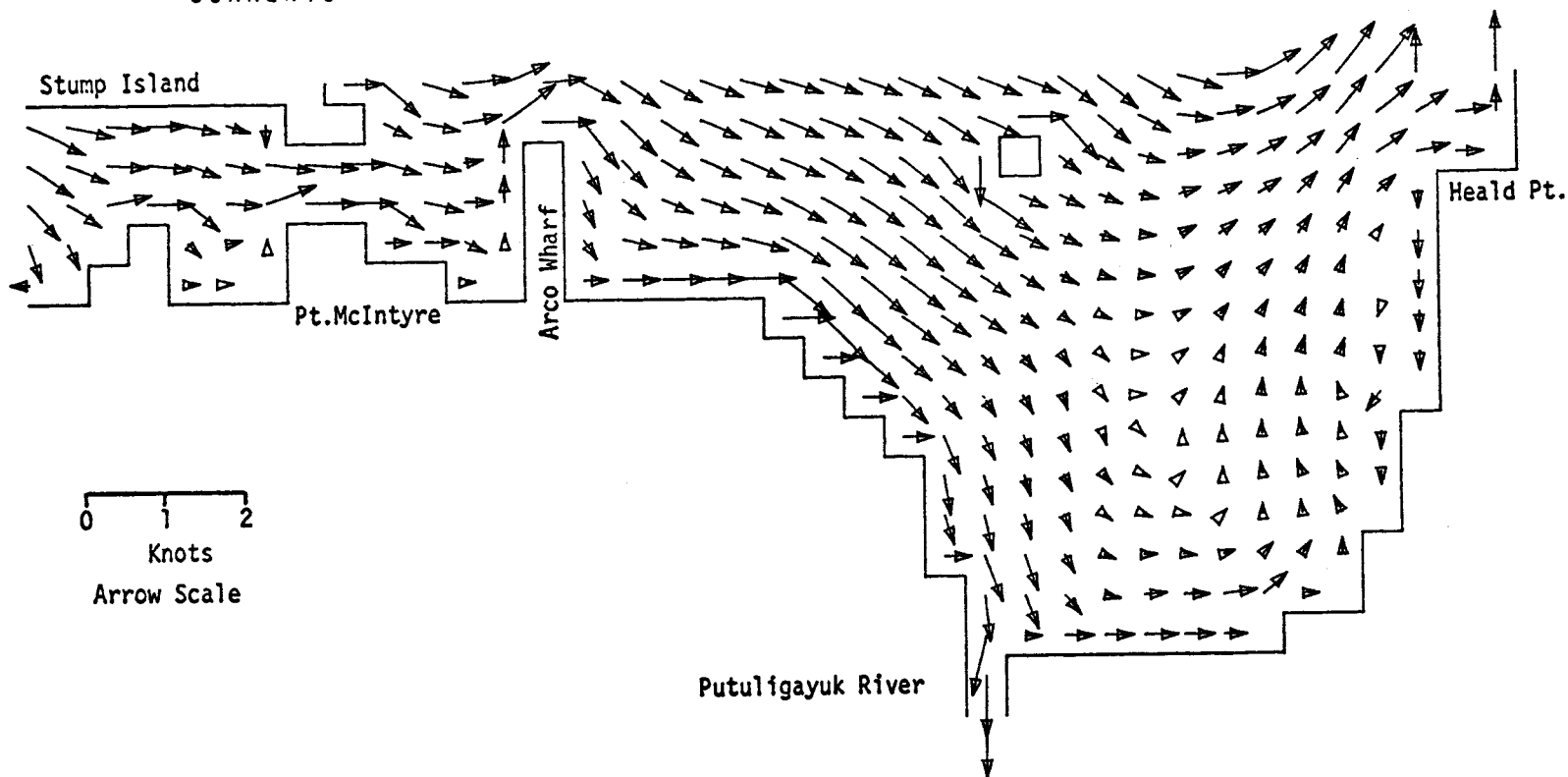


PRUDHOE BAY  
M2 TIDE (AMP=8 CM, IN PHASE ON OPEN BOUNDARIES) OFFSHORE WIND AT 20 KT

CURRENTS

TIME= 25200SEC

LAYER 1



10

MODEL NO

664

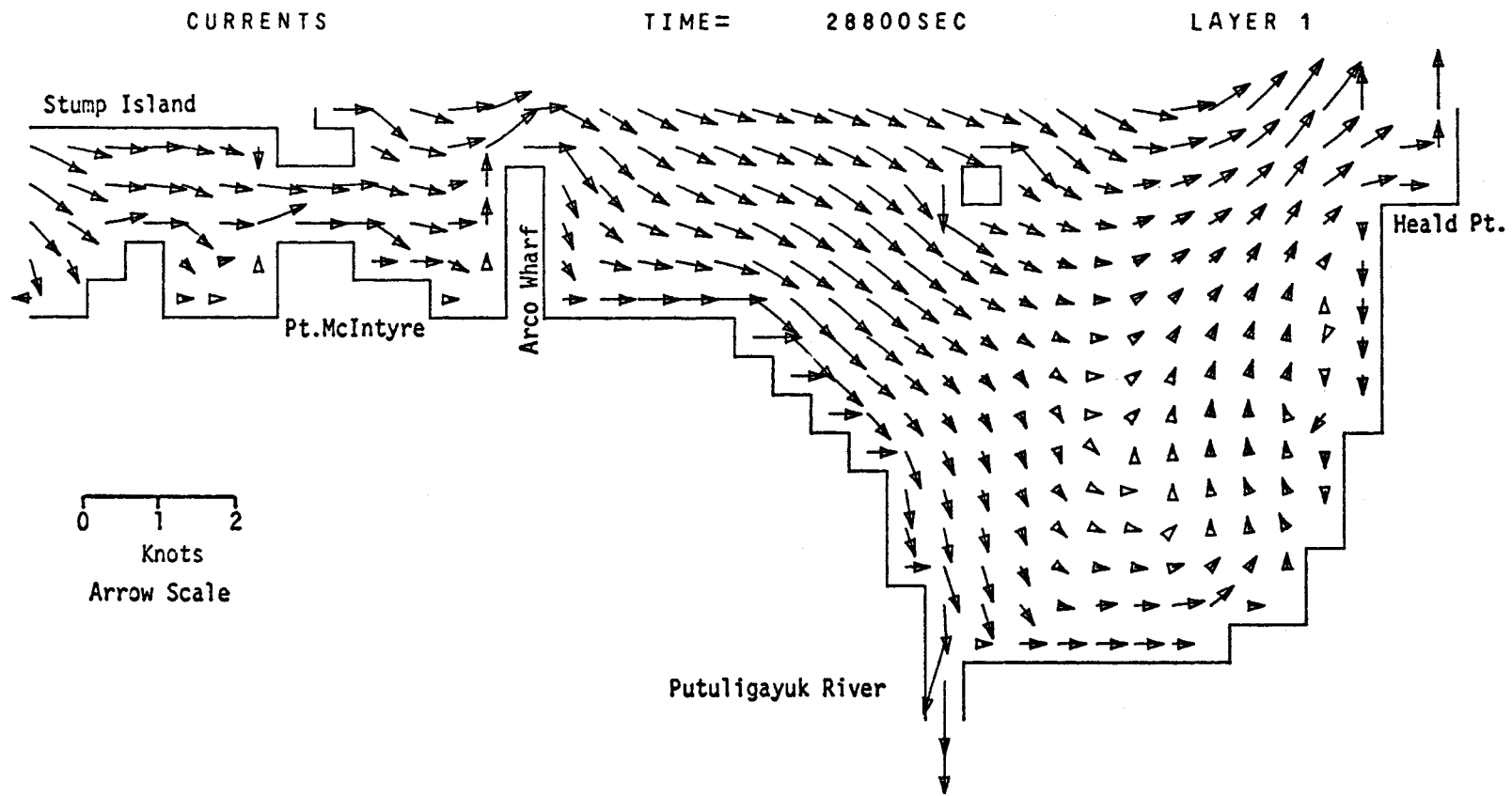
0 1 2  
Knots  
Arrow Scale

Putuligayuk River

PRUDHOE BAY

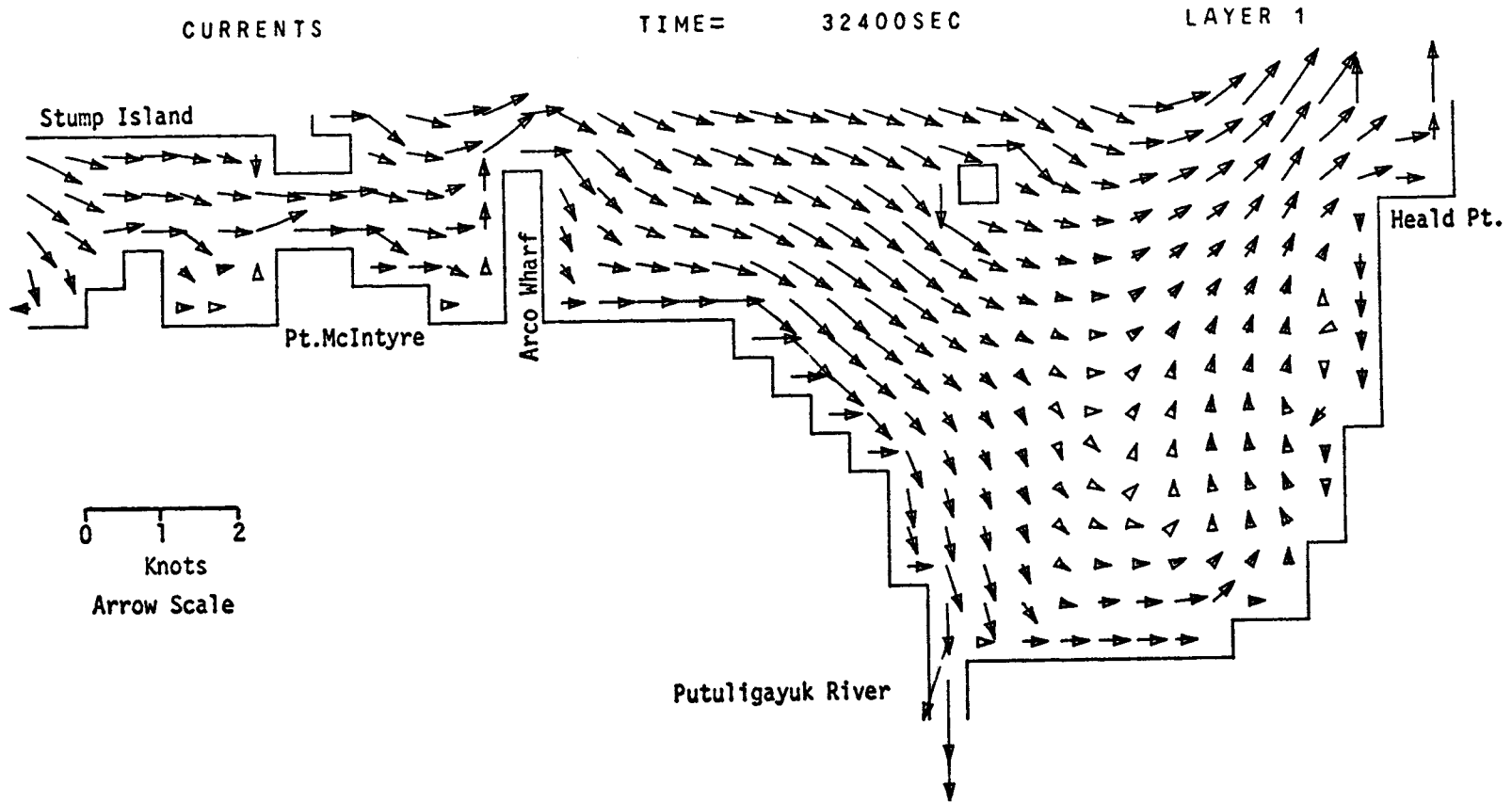
M2 TIDE (AMP=8 CM, IN PHASE ON OPEN BOUNDARIES) OFFSHORE WIND AT 20 KT

S99  
MODEL NO 10



999

MODEL NO 10

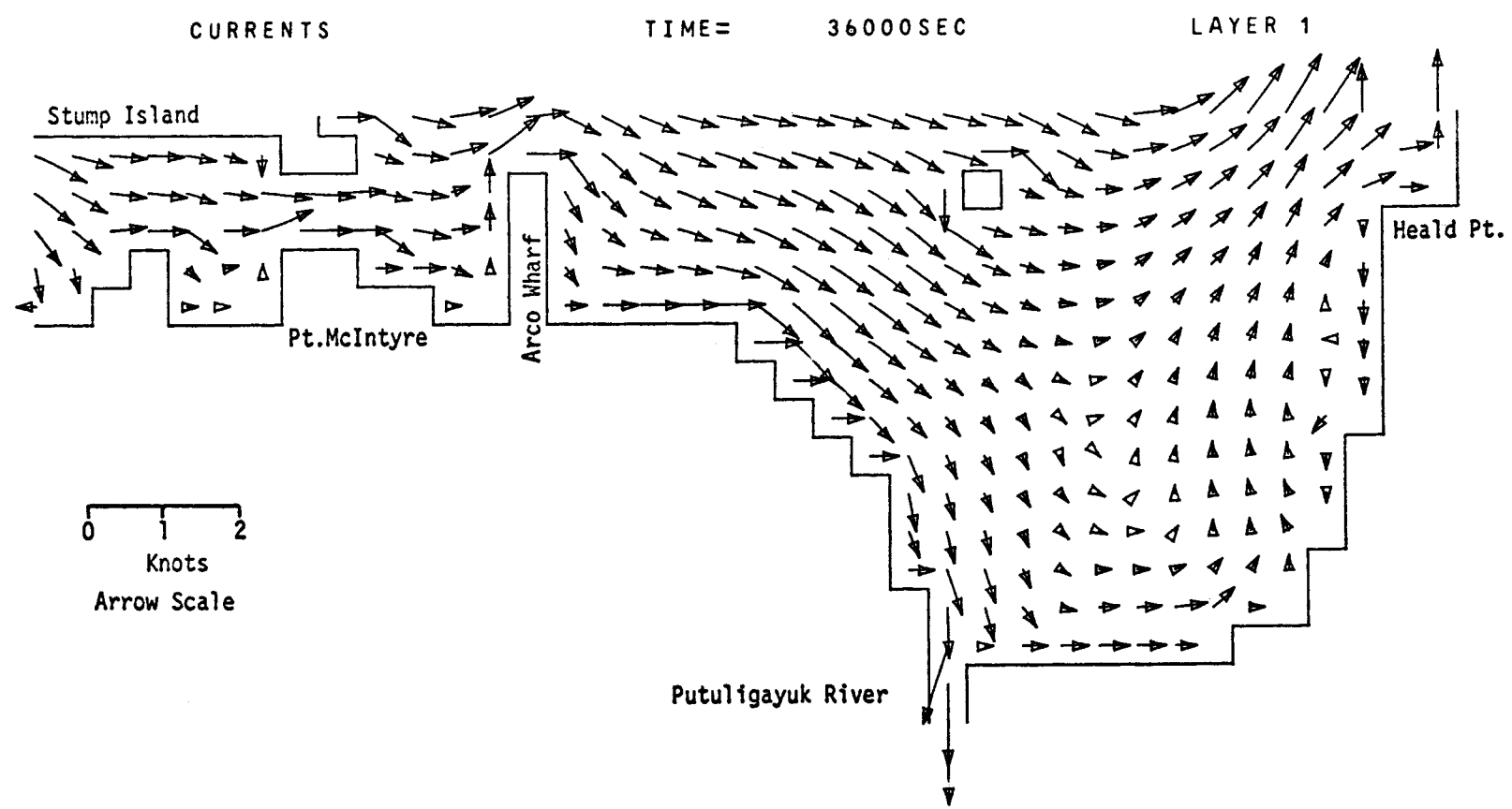


PRUDHOE BAY  
M2 TIDE (AMP=8 CM. IN PHASE ON OPEN BOUNDARIES) OFFSHORE WIND AT 20 KT



667

MODEL NO 10

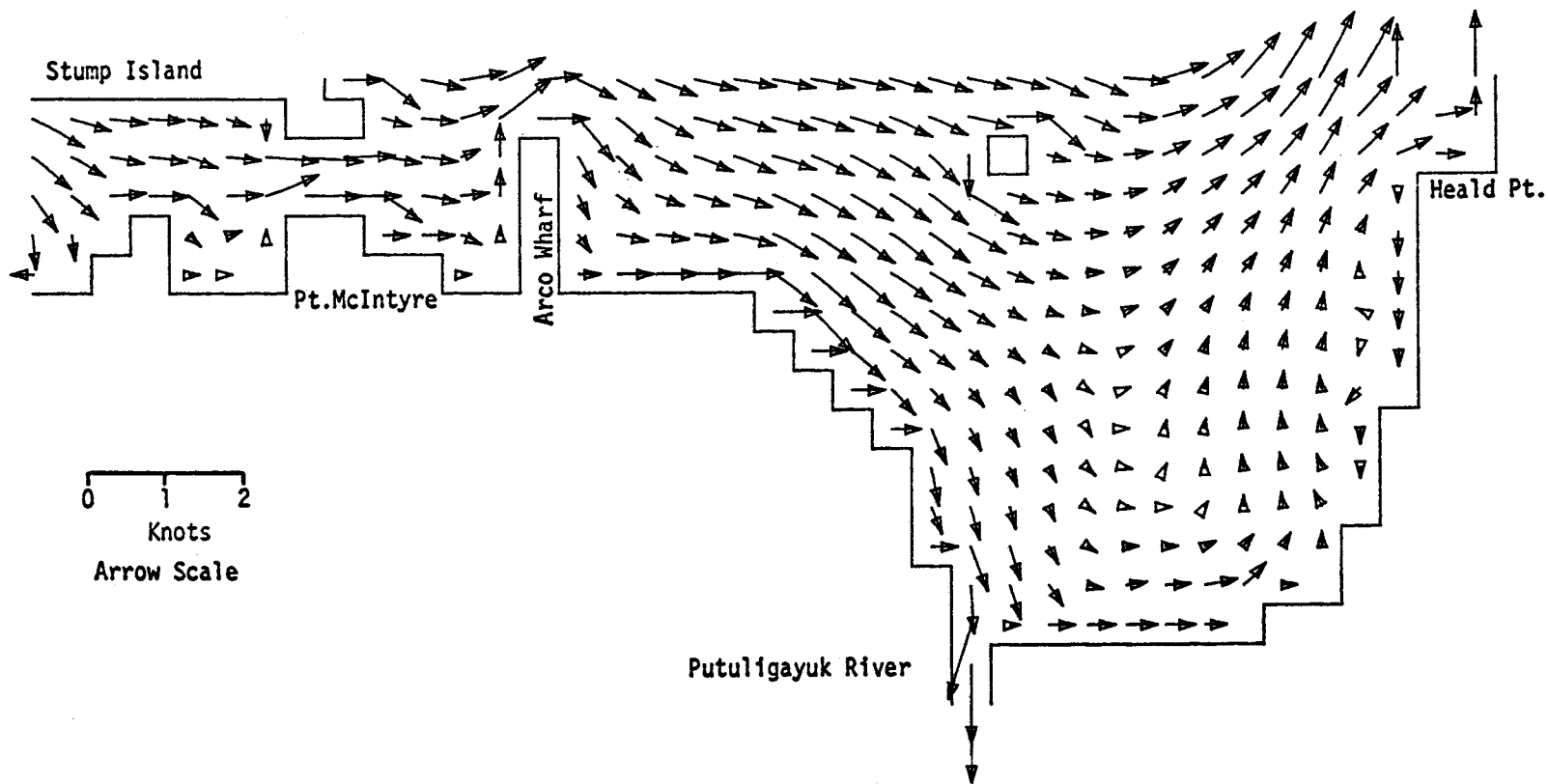


PRUDHOE BAY  
M2 TIDE (AMP=8 CM, IN PHASE ON OPEN BOUNDARIES) OFFSHORE WIND AT 20 KT

CURRENTS

TIME= 39600SEC

LAYER 1



0 1 2  
Knots  
Arrow Scale

Putuligayuk River

PRUDHOE BAY

M2 TIDE (AMP=8 CM, IN PHASE ON OPEN BOUNDARIES) OFFSHORE WIND AT 20 KT

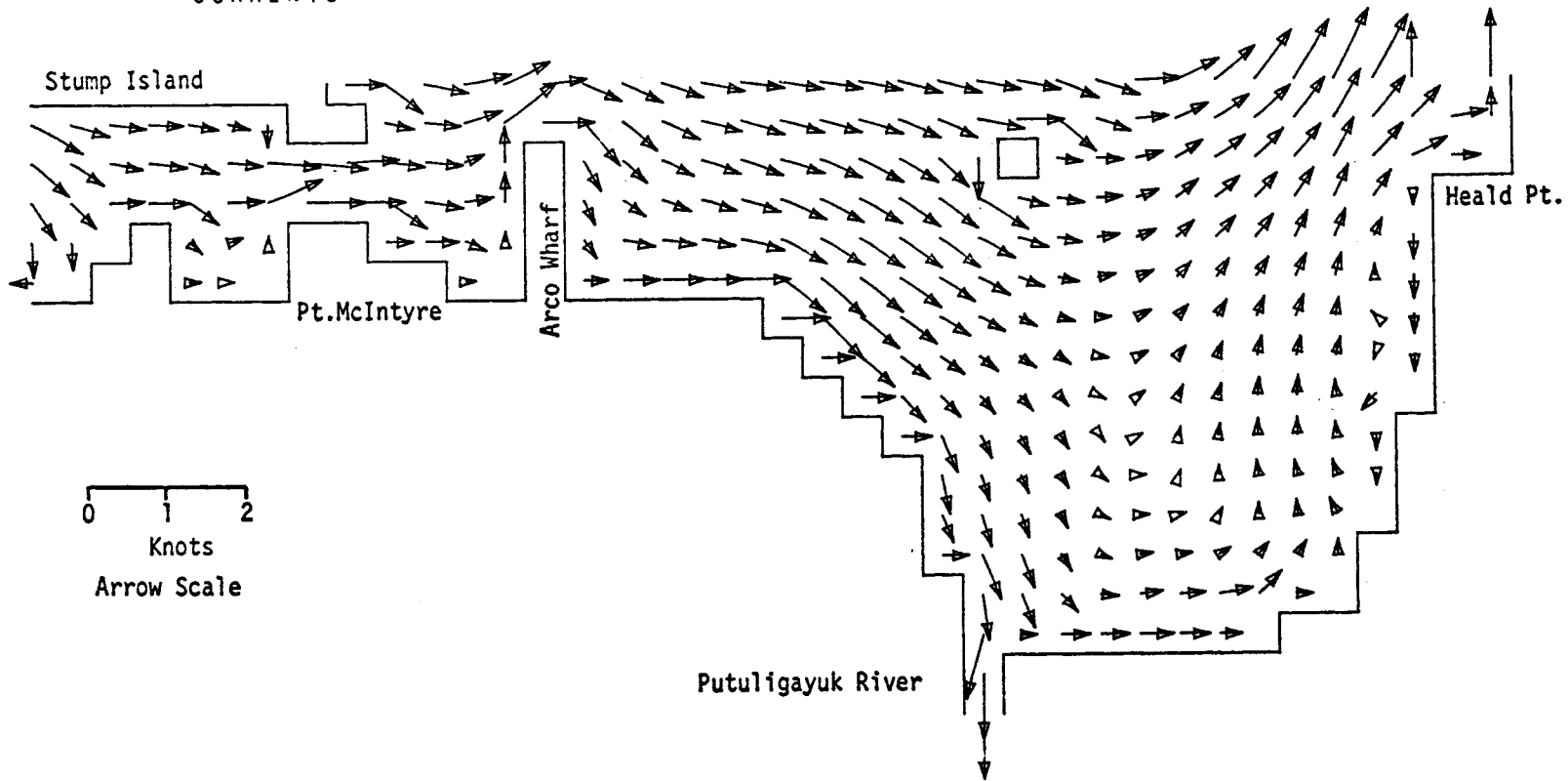
899  
MODEL NO 10

699  
MODEL NO 10

CURRENTS

TIME= 43200SEC

LAYER 1



0 1 2  
Knots  
Arrow Scale

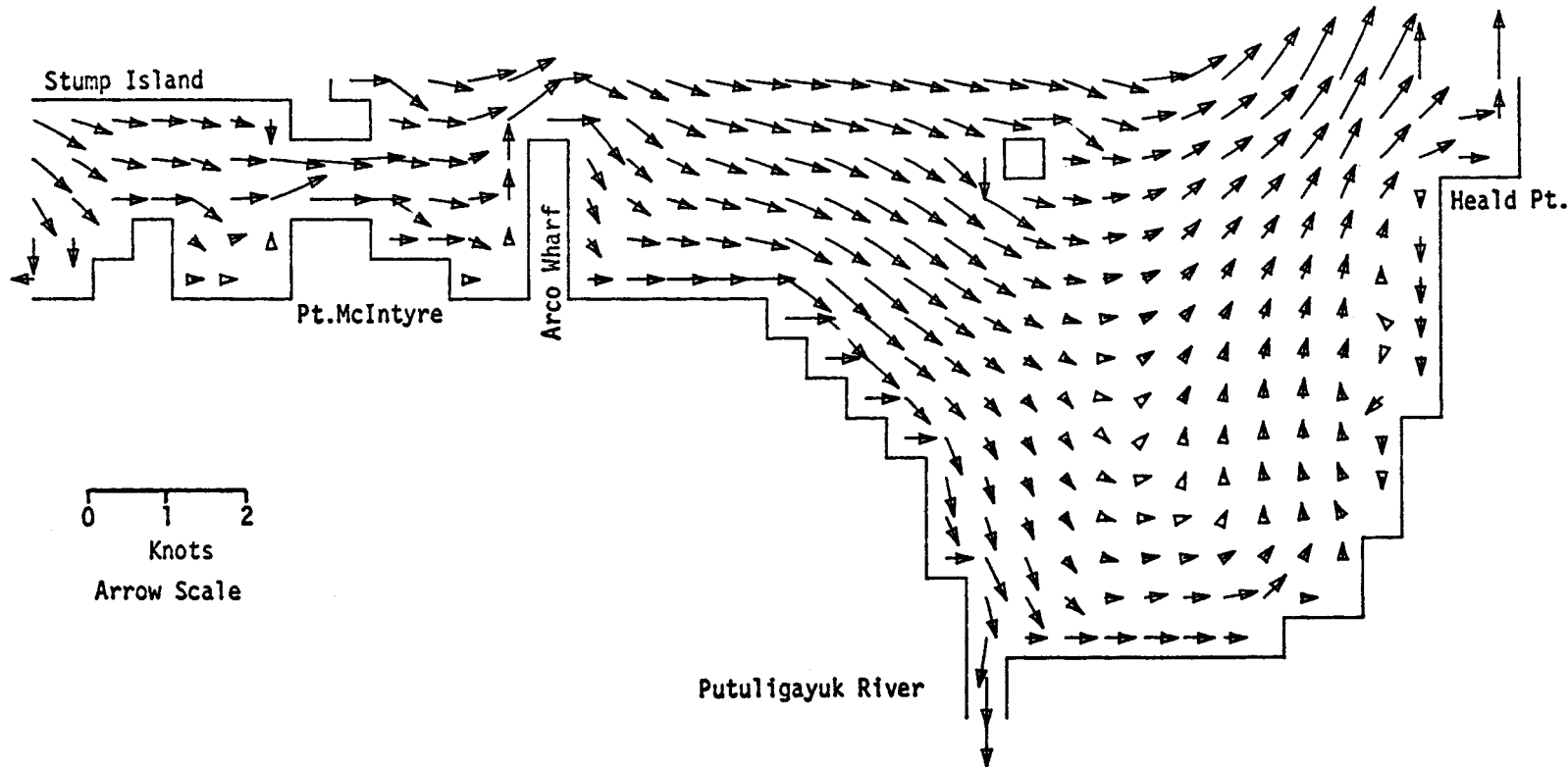
PRUDHOE BAY

M2 TIDE (AMP=8 CM, IN PHASE ON OPEN BOUNDARIES) OFFSHORE WIND AT 20 KT

CURRENTS

TIME= 46800SEC

LAYER 1



0 1 2  
Knots  
Arrow Scale

PRUDHOE BAY

M2 TIDE (AMP=8 CM, IN PHASE ON OPEN BOUNDARIES) OFFSHORE WIND AT 20 KT

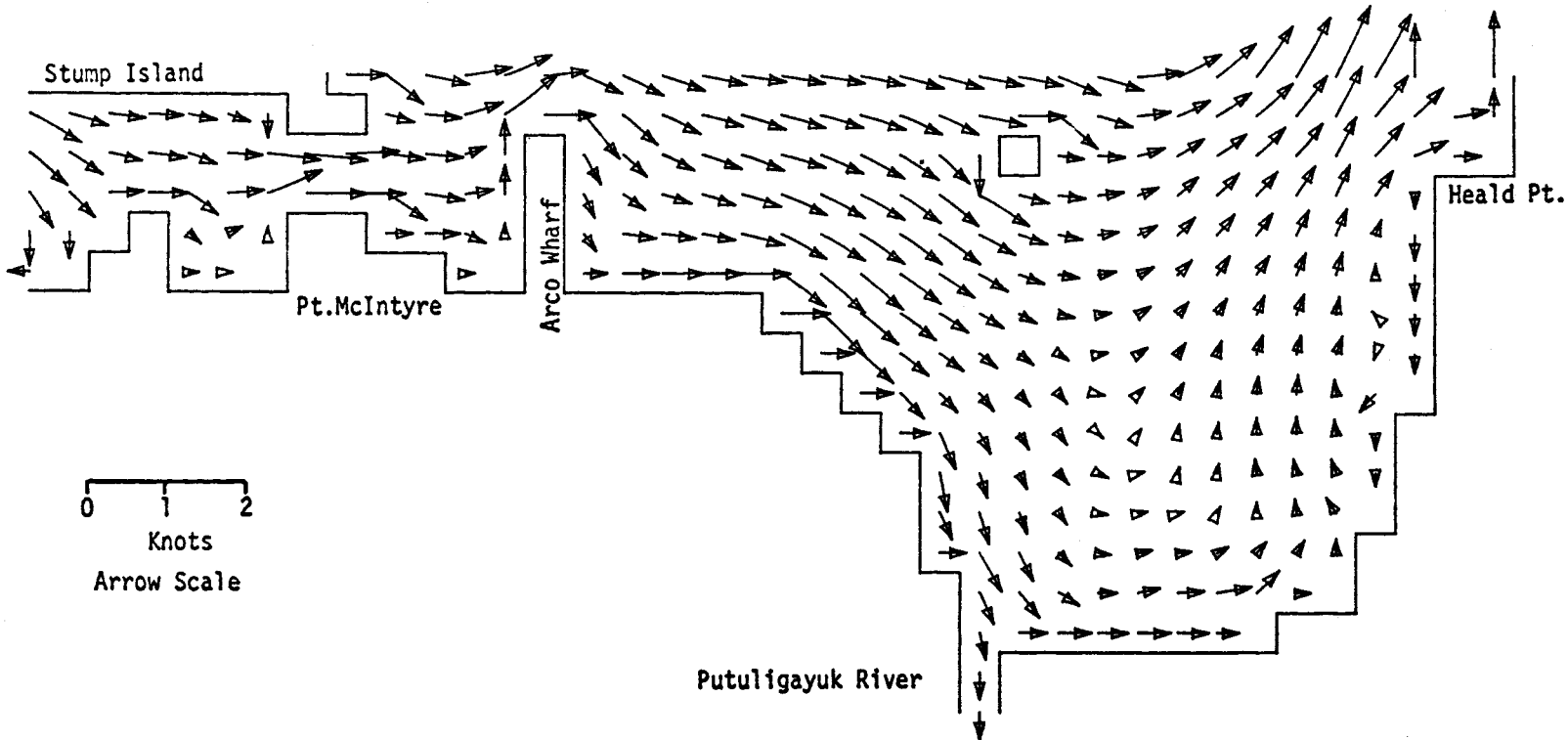
670

MODEL NO 10

CURRENTS

TIME= 50400SEC

LAYER 1



0 1 2  
Knots  
Arrow Scale

Putuligayuk River

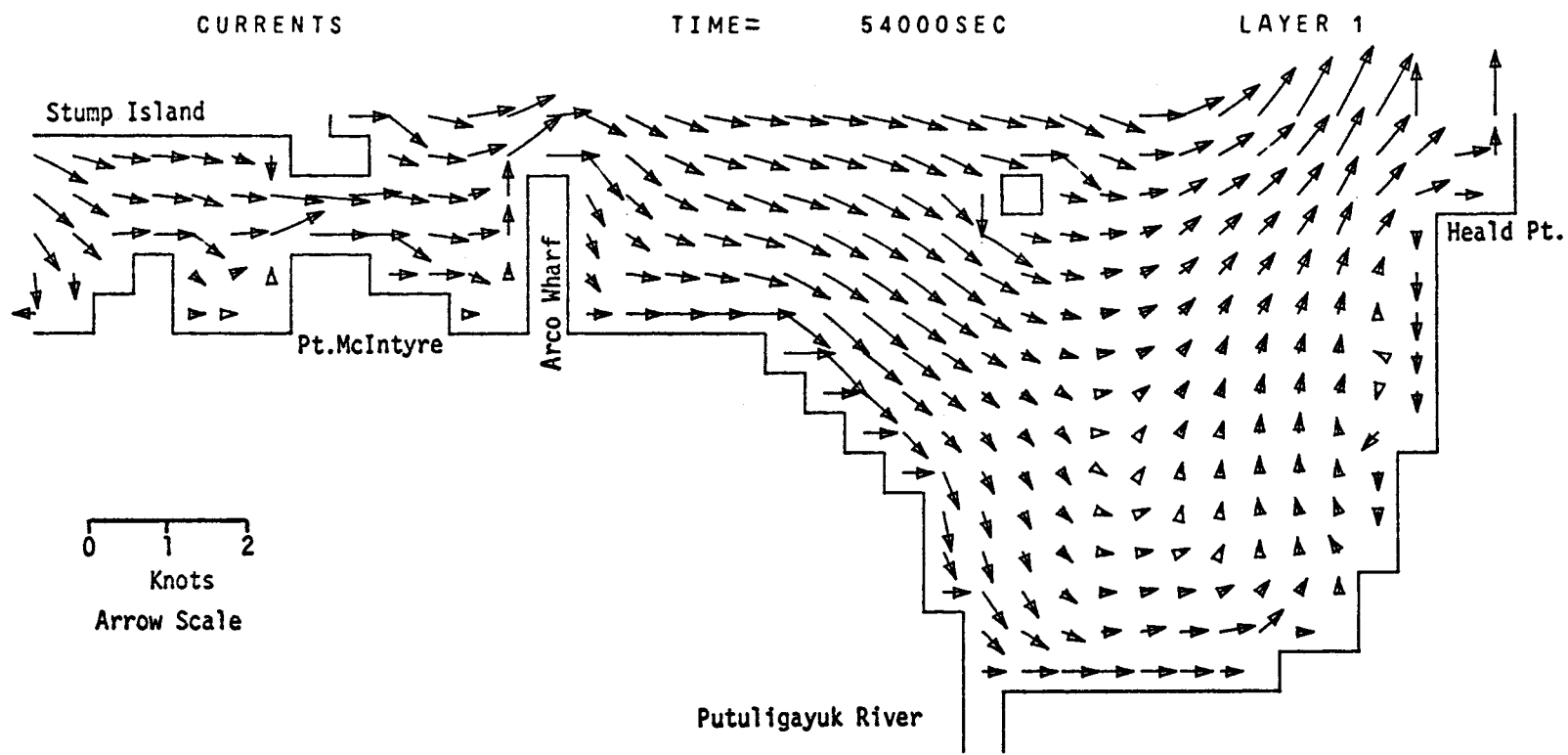
PRUDHOE BAY  
M2 TIDE (AMP=8 CM, IN PHASE ON OPEN BOUNDARIES) OFFSHORE WIND AT 20 KT

671

MODEL NO 10

672

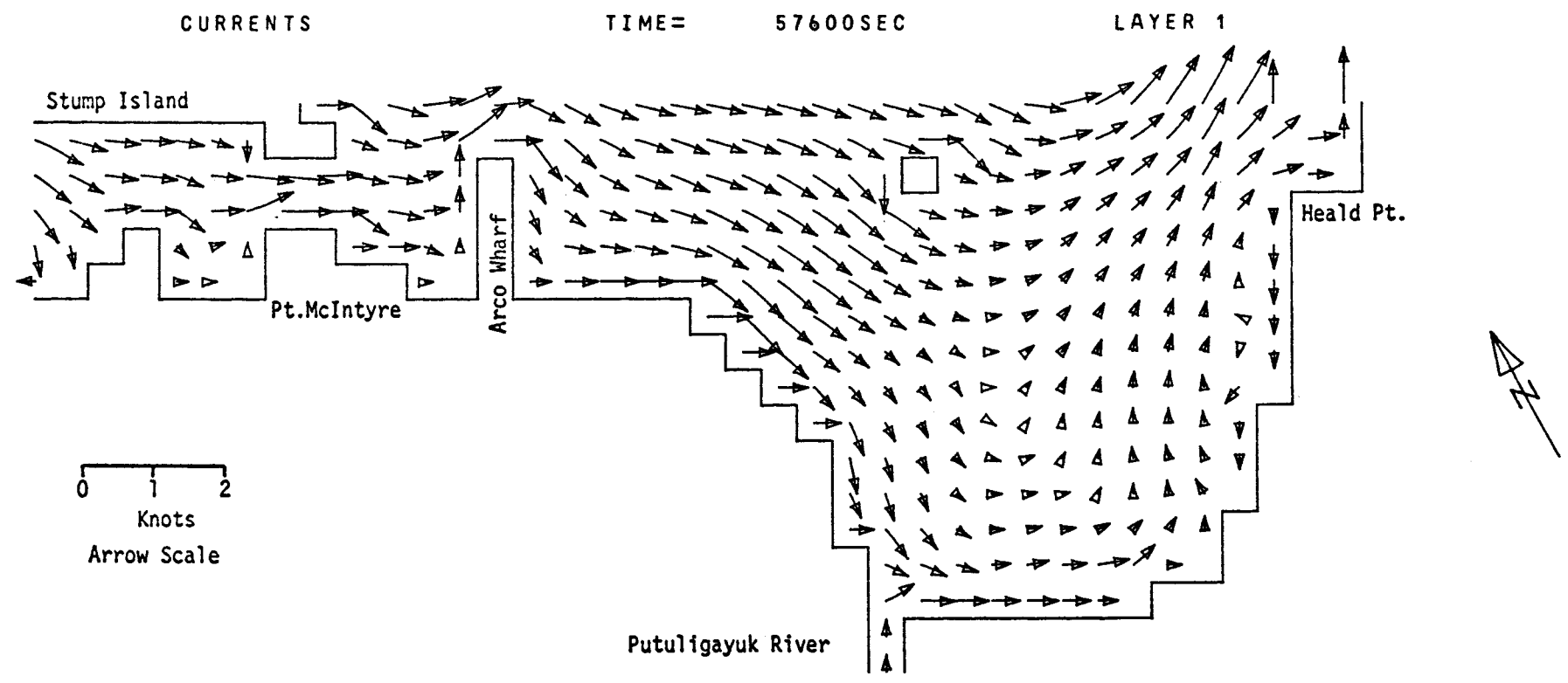
MODEL NO 10



PRUDHOE BAY  
M2 TIDE (AMP=8 CM, IN PHASE ON OPEN BOUNDARIES) OFFSHORE WIND AT 20 KT

873

MODEL NO 10

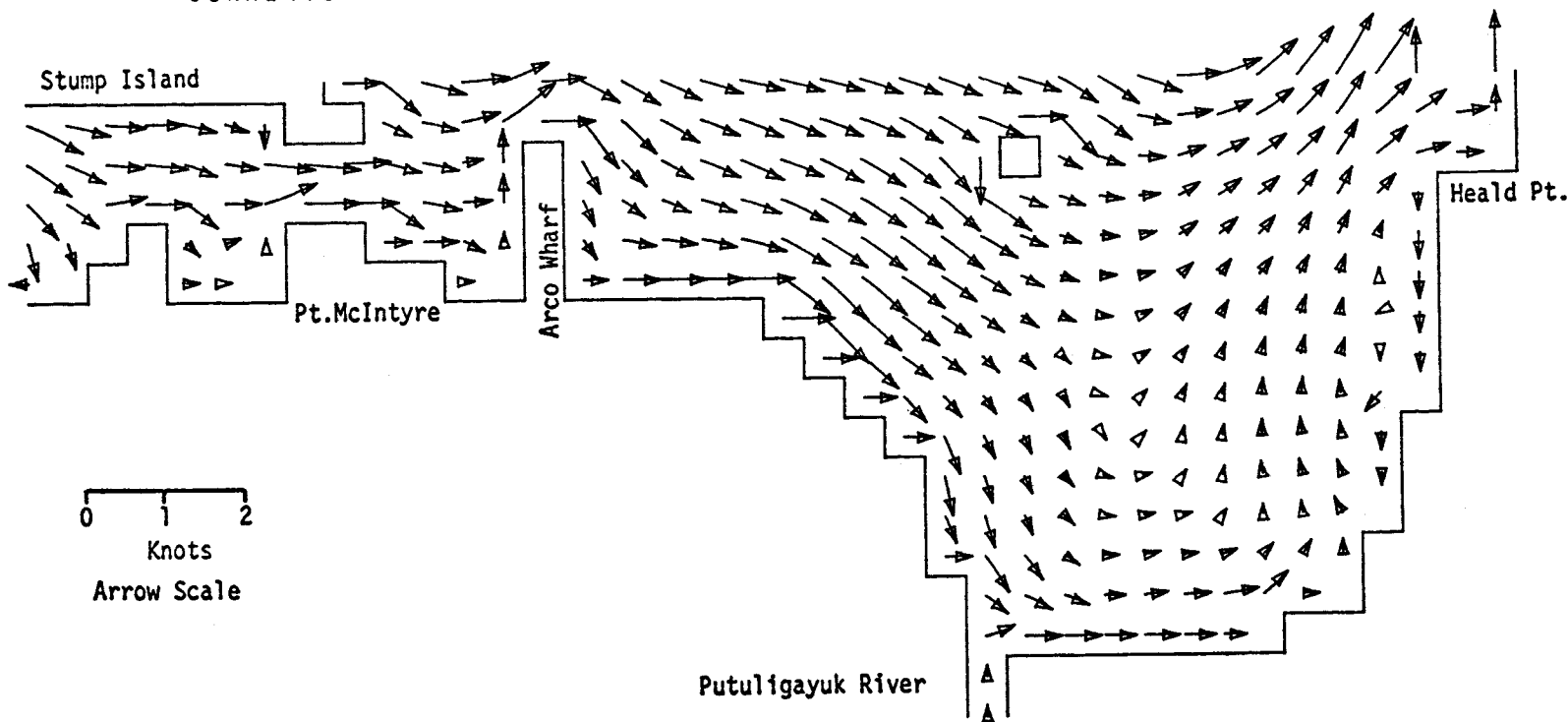


PRUDHOE BAY  
M2 TIDE (AMP=8 CM, IN PHASE ON OPEN BOUNDARIES) OFFSHORE WIND AT 20 KT

CURRENTS

TIME= 61200SEC

LAYER 1



MODEL NO 10

674

0 1 2  
Knots  
Arrow Scale

Putuligayuk River

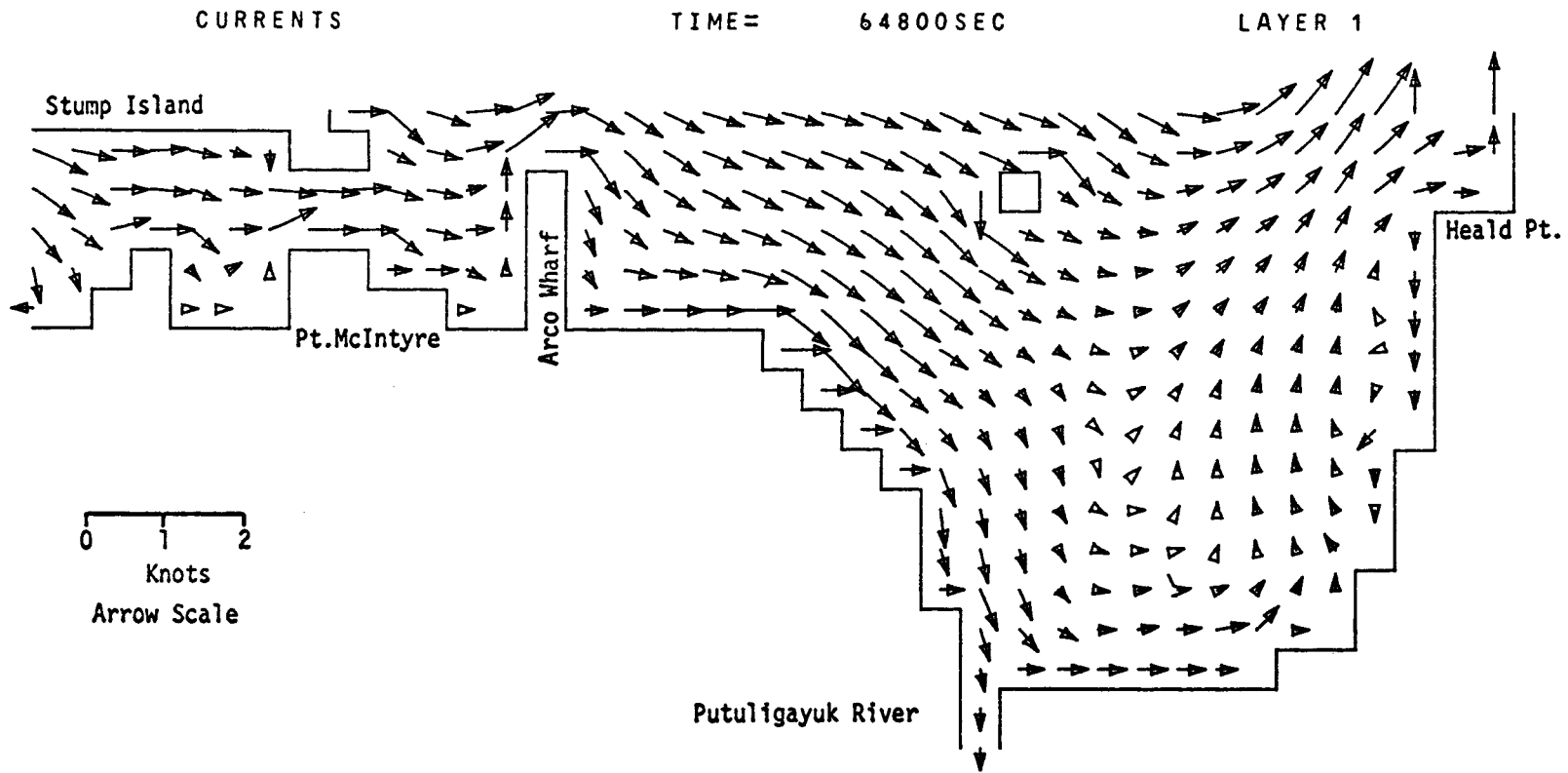
PRUDHOE BAY

M2 TIDE (AMP=8 CM, IN PHASE ON OPEN BOUNDARIES) OFFSHORE WIND AT 20 KT



075

MODEL NO 10



PRUDHOE BAY  
M2 TIDE (AMP=8 CM, IN PHASE ON OPEN BOUNDARIES) OFFSHORE WIND AT 20 KT

APPENDIX F

SIMPSON LAGOON  
M2 TIDE WITH 8 CM AMPLITUDE INPUT IN PHASE  
ON OPEN BOUNDARIES

26 knot wind from 070°T

ENVIRONMENTAL PROTECTION AGENCY  
 MARINE AND FRESHWATER ECOLOGY BRANCH  
 OCEAN MASS TRANSPORT MODEL

M2 TIDE (AMP=8 CM, IN PHASE ON OPEN BOUNDARIES) WIND FROM 70 DEG T AT 26 KT  
 BEAUFORT SEA SHELF STUDY  
 GRID 200 SIMPSON LAGOON AT 1/2 KM GRID SPACING

|                       |                 |                |                 |
|-----------------------|-----------------|----------------|-----------------|
| GRID GEOMETRY         | ROWS 18         | COLUMNS 42     |                 |
| GRID LENGTH           | 50000. CM       | ROTATION ANGLE | 345.0 DEG       |
| WIND DRAG COEFFICIENT | .0024           | MID LATITUDE   | 70.500 DEG. (N) |
| FRICTION COEFFICIENT  | .0030000 CM/SEC |                |                 |

|                      |          |         |         |
|----------------------|----------|---------|---------|
|                      | LAYER 1  | LAYER 2 | LAYER 3 |
| INITIAL LAYER DEPTHS | 300.0000 | .0000   | .0000   |
| SMOOTHING FACTORS    | .9900    | .0000   | .0000   |
| DENSITY              | 1.0200   | .0000   | .0000   |

|                                 |             |                           |          |
|---------------------------------|-------------|---------------------------|----------|
| RESULTS SAVED AT MODULUS (TIME, | 3600 SEC)=0 | RESULTS SAVED STARTING AT | 3600 SEC |
| COMPUTATIONS STARTED AT         | 0 SEC       |                           |          |
| ENDED AT                        | 64800 SEC   |                           |          |
| INCREMENTED BY                  | 60 SEC      |                           |          |
| LAYER3 PRINT OUT STARTED        |             | 3600 SEC. FREQUENCY OF    | 3600 SEC |

|                               |               |                 |          |       |
|-------------------------------|---------------|-----------------|----------|-------|
| TIDAL INPUT AT                | ROW 2 THRU 17 | COLUMN 1 THRU 1 | TIME LAG | 0 SEC |
|                               | M2            | S2              | K1       |       |
| PHASE ANGLES (DEG/HR)         | 270.00        | .00             | .00      | .00   |
| AMPLITUDES (CM)               | 8.00          | .00             | .00      | .00   |
| LOWER LAYER WEIGHTING FACTORS | LAYER 2= .00  | LAYER 3= .00    |          |       |

|                               |               |                   |          |       |
|-------------------------------|---------------|-------------------|----------|-------|
| TIDAL INPUT AT                | ROW 3 THRU 18 | COLUMN 42 THRU 42 | TIME LAG | 0 SEC |
|                               | M2            | S2                | K1       |       |
| PHASE ANGLES (DEG/HR)         | 270.00        | .00               | .00      | .00   |
| AMPLITUDES (CM)               | 8.00          | .00               | .00      | .00   |
| LOWER LAYER WEIGHTING FACTORS | LAYER 2= .00  | LAYER 3= .00      |          |       |

|                       |           |         |         |         |
|-----------------------|-----------|---------|---------|---------|
| TIDAL SPEEDS (DEG/HR) | M2        | S2      | O1      | K1      |
|                       | 29.984000 | .000000 | .000000 | .000000 |

|                         |               |                       |                |  |
|-------------------------|---------------|-----------------------|----------------|--|
| WIND INPUT AT           | ROW 1 THRU 18 | COLUMN 1 THRU 42      |                |  |
| COMPUTATIONS STARTED AT | 60 SEC        |                       |                |  |
| ENDED AT                | 64800 SEC     | DIRECTION 70 DEG TRUE | SPEED 13 M/SEC |  |

SEA LEVEL

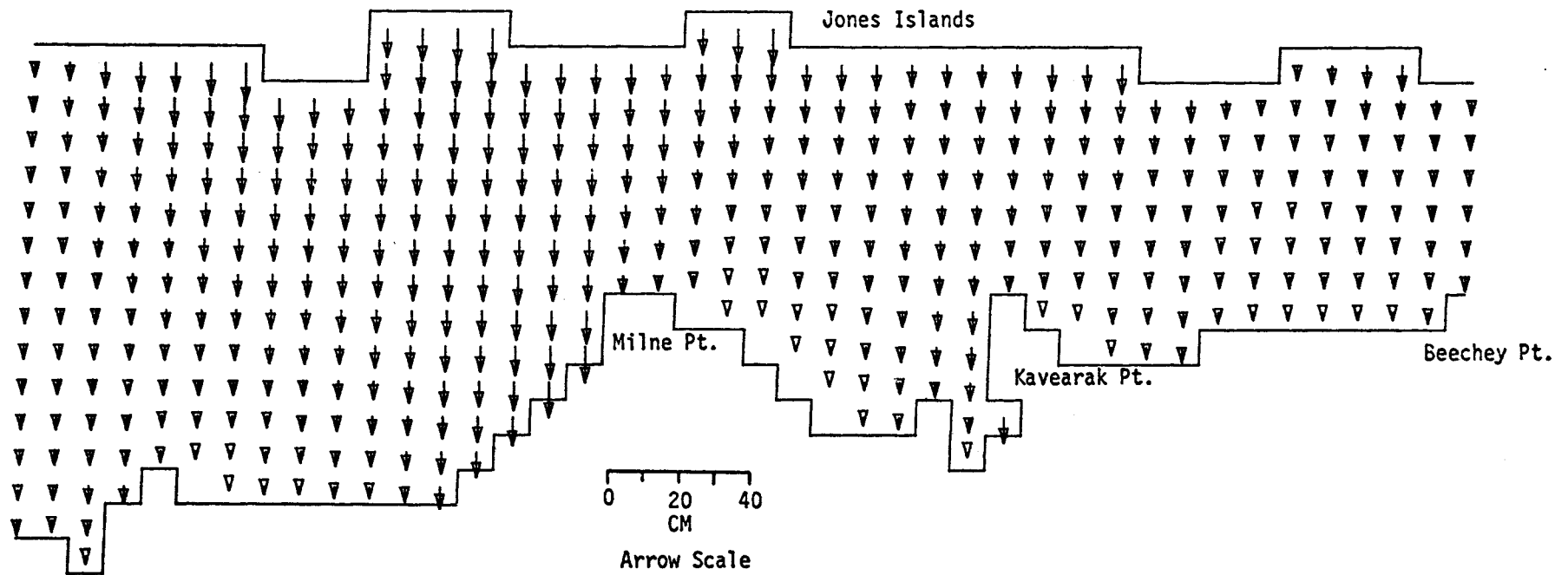
SEA LEVEL

TIME=

3600SEC

LAYER 1

MODEL NO  
200  
679



SIMPSON LAGOON

M2 TIDE (AMP=8 CM, IN PHASE ON OPEN BOUNDARIES) WIND FROM 70 DEG T AT 26 KT

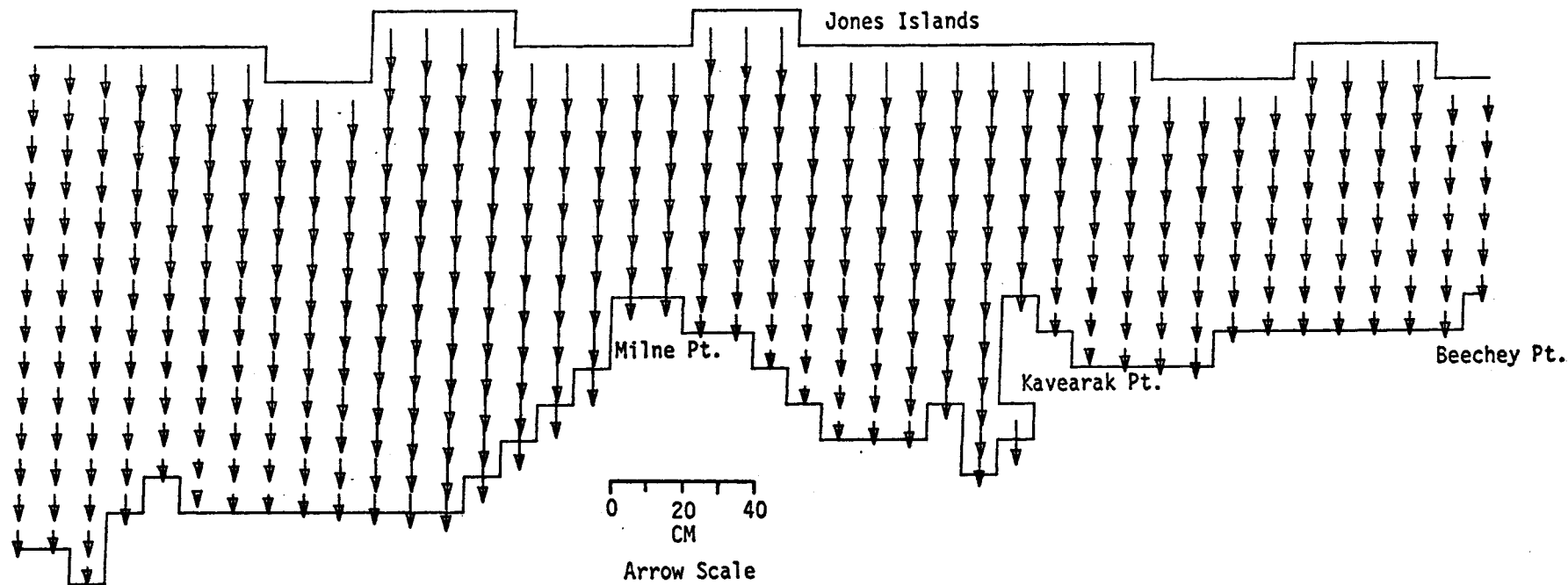
SEA LEVEL

TIME= 7200SEC

LAYER 1

MODEL NO 200

089



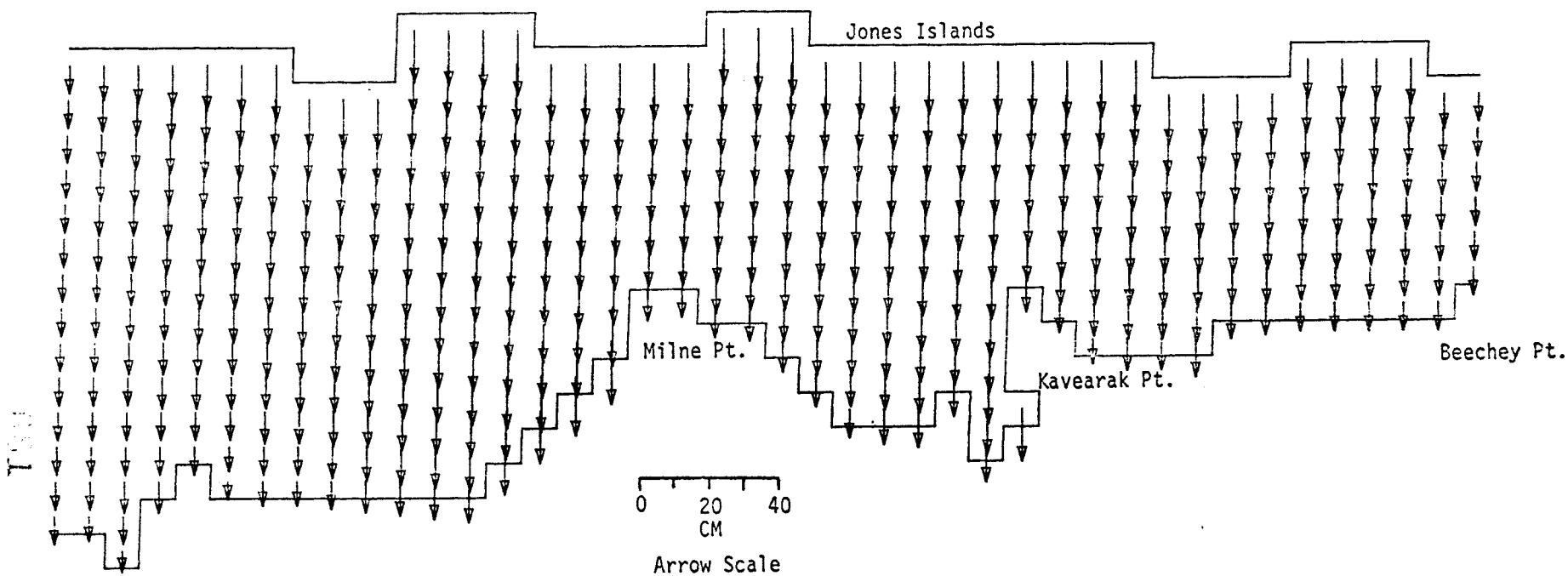
SIMPSON LAGOON

M2 TIDE (AMP=8 CM, IN PHASE ON OPEN BOUNDARIES) WIND FROM 70 DEG T AT 26 KT

SEA LEVEL

TIME= 10800SEC

LAYER 1



SIMPSON LAGOON

M2 TIDE (AMP=8 CM, IN PHASE ON OPEN BOUNDARIES) WIND FROM 70 DEG T AT 26 KT

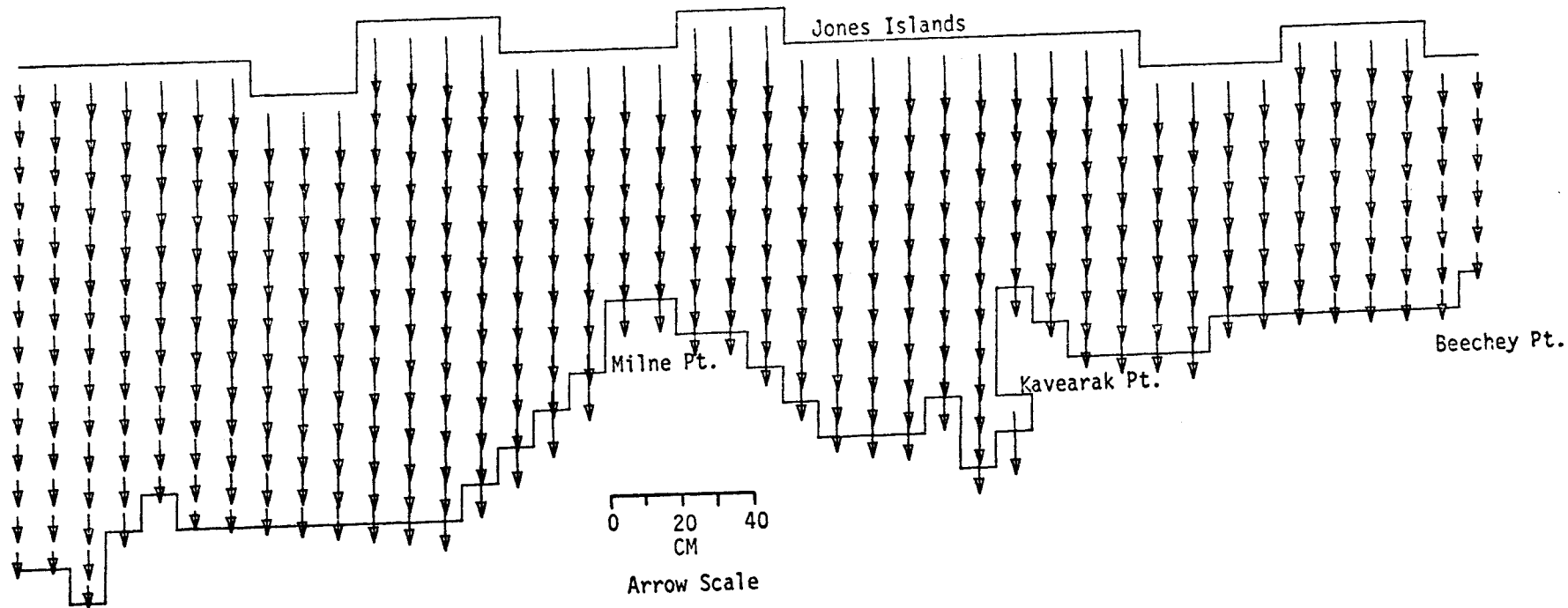
SEA LEVEL

TIME= 14400SEC

LAYER 1

MODEL NO 200

682



SIMPSON LAGOON  
M2 TIDE (AMP=8 CM, IN PHASE ON OPEN BOUNDARIES) WIND FROM 70 DEG T AT 26 KT



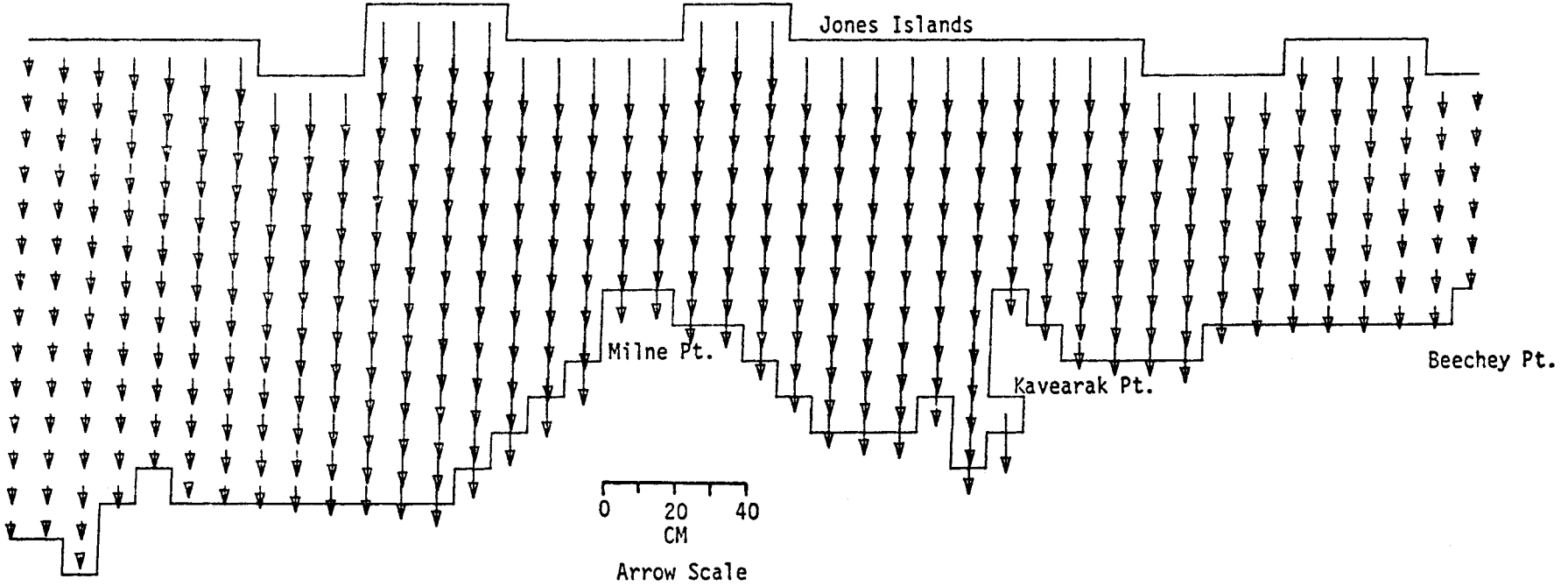
SEA LEVEL

TIME= 18000SEC

LAYER 1

MODEL NO 200

SWW

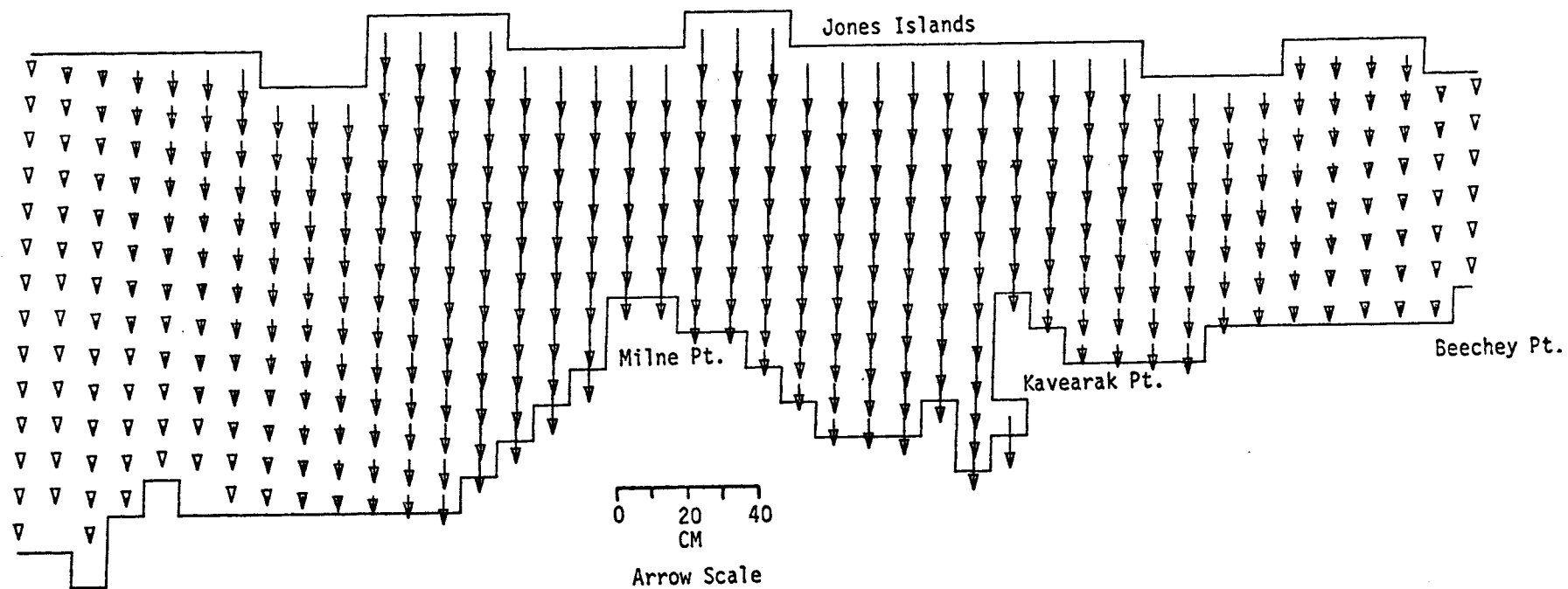


SIMPSON LAGOON  
M2 TIDE (AMP=8 CM, IN PHASE ON OPEN BOUNDARIES) WIND FROM 70 DEG T AT 26 KT

SEA LEVEL

TIME= 21600SEC

LAYER 1



SIMPSON LAGOON  
M2 TIDE (AMP=8 CM, IN PHASE ON OPEN BOUNDARIES) WIND FROM 70 DEG T AT 26 KT

MODEL NO 200

884

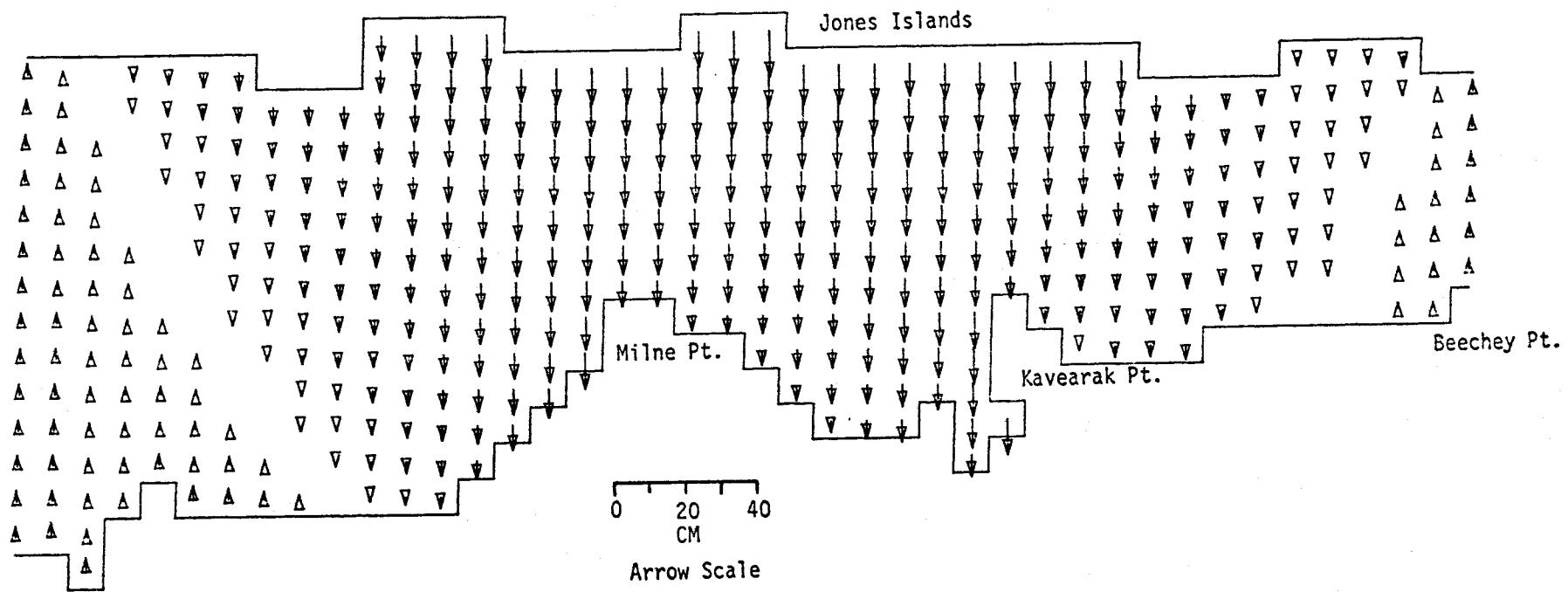
SEA LEVEL

TIME= 25200SEC

LAYER 1

MODEL NO 200

595



SIMPSON LAGOON  
M2 TIDE (AMP=8 CM, IN PHASE ON OPEN BOUNDARIES) WIND FROM 70 DEG T AT 26 KT

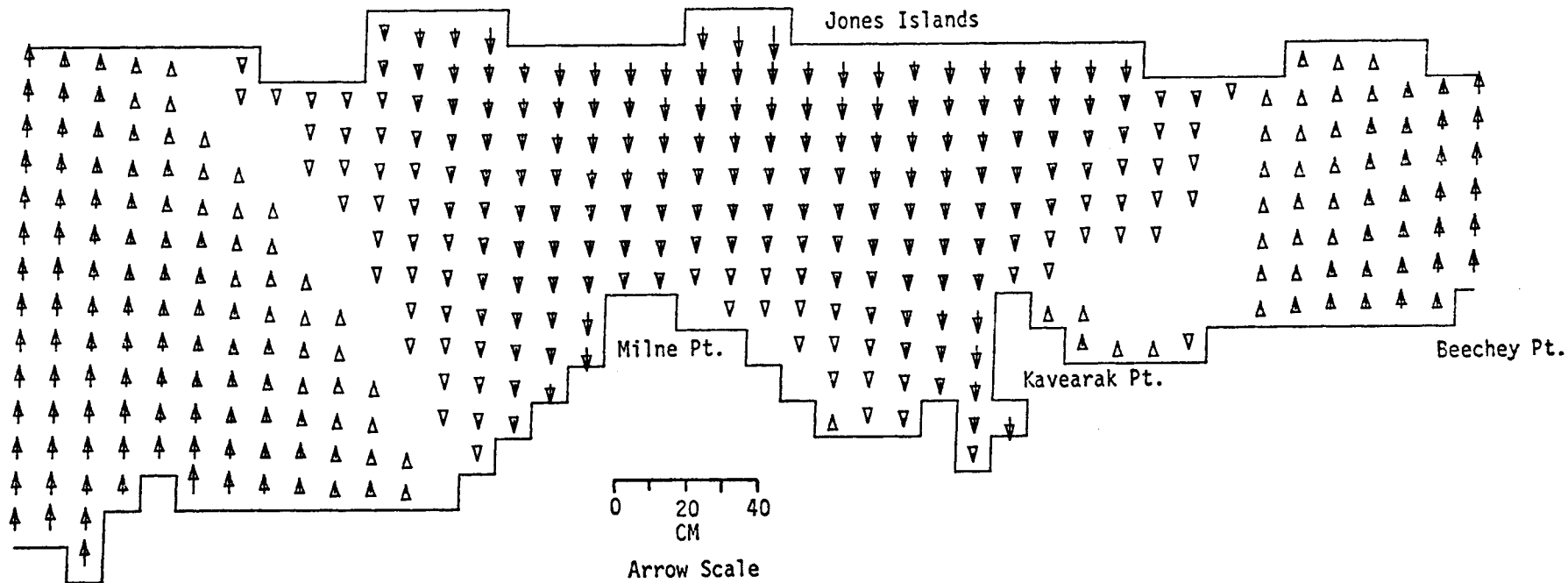
SEA LEVEL

TIME= 28800SEC

LAYER 1

MODEL NO 200

689



SIMPSON LAGOON

M2 TIDE (AMP=8 CM, IN PHASE ON OPEN BOUNDARIES) WIND FROM 70 DEG T AT 26 KT

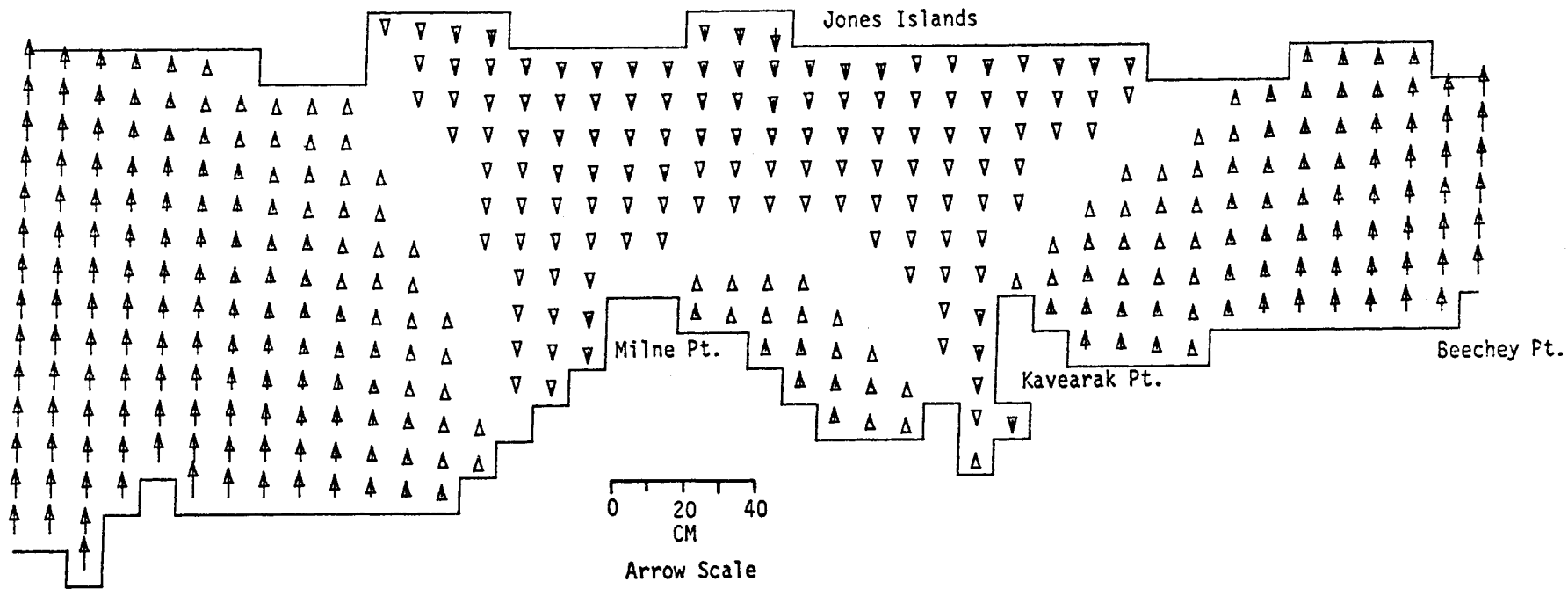
MODEL NO 200

1987

SEA LEVEL

TIME= 32400SEC

LAYER 1



SIMPSON LAGOON

M2 TIDE (AMP=8 CM, IN PHASE ON OPEN BOUNDARIES) WIND FROM 70 DEG T AT 26 KT

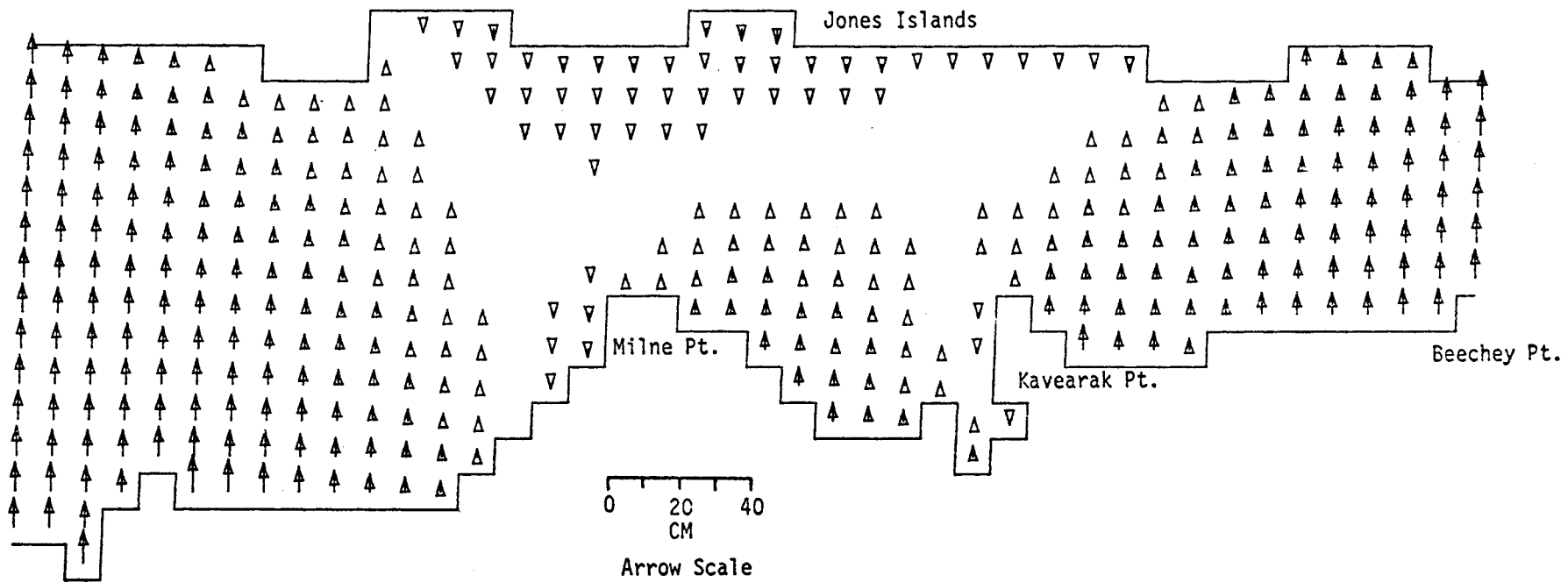
SEA LEVEL

TIME= 36000SEC

LAYER 1

MODEL NO 200

889



SIMPSON LAGOON  
M2 TIDE (AMP=8 CM, IN PHASE ON OPEN BOUNDARIES) WIND FROM 70 DEG T AT 26 KT

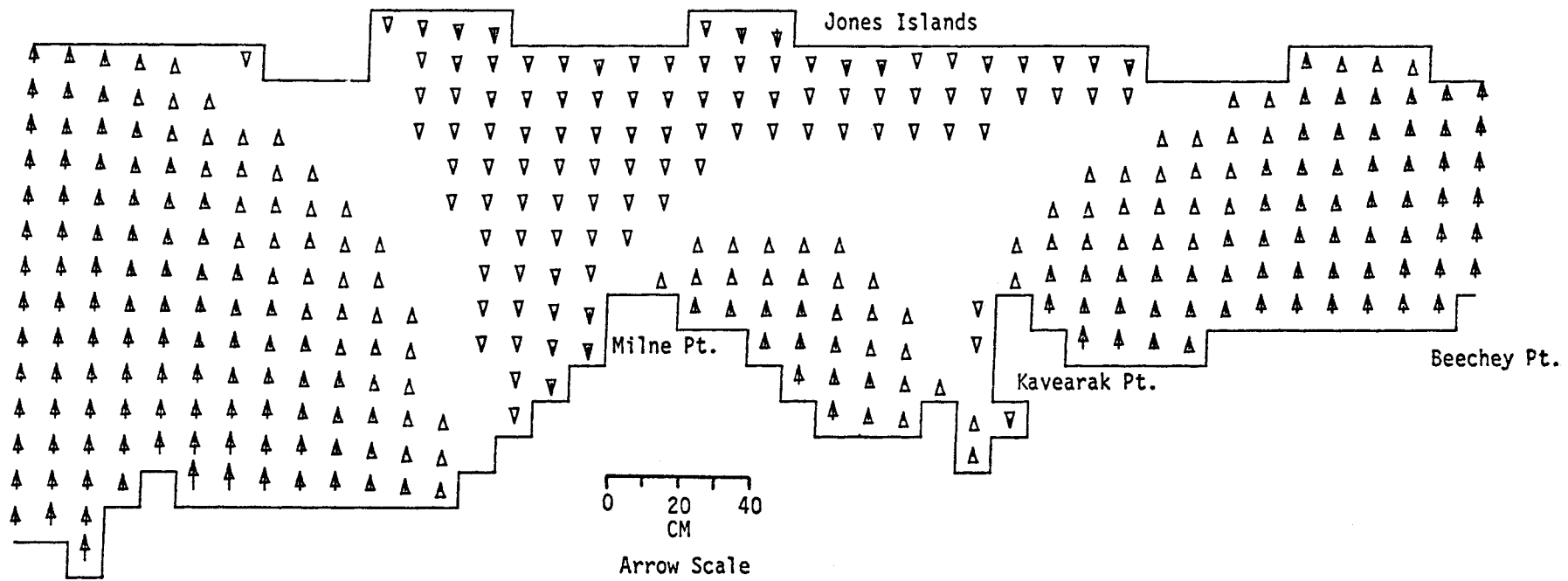
SEA LEVEL

TIME= 39600SEC

LAYER 1

MODEL NO 200

689



SIMPSON LAGOON  
M2 TIDE (AMP=8 CM, IN PHASE ON OPEN BOUNDARIES) WIND FROM 70 DEG T AT 26 KT

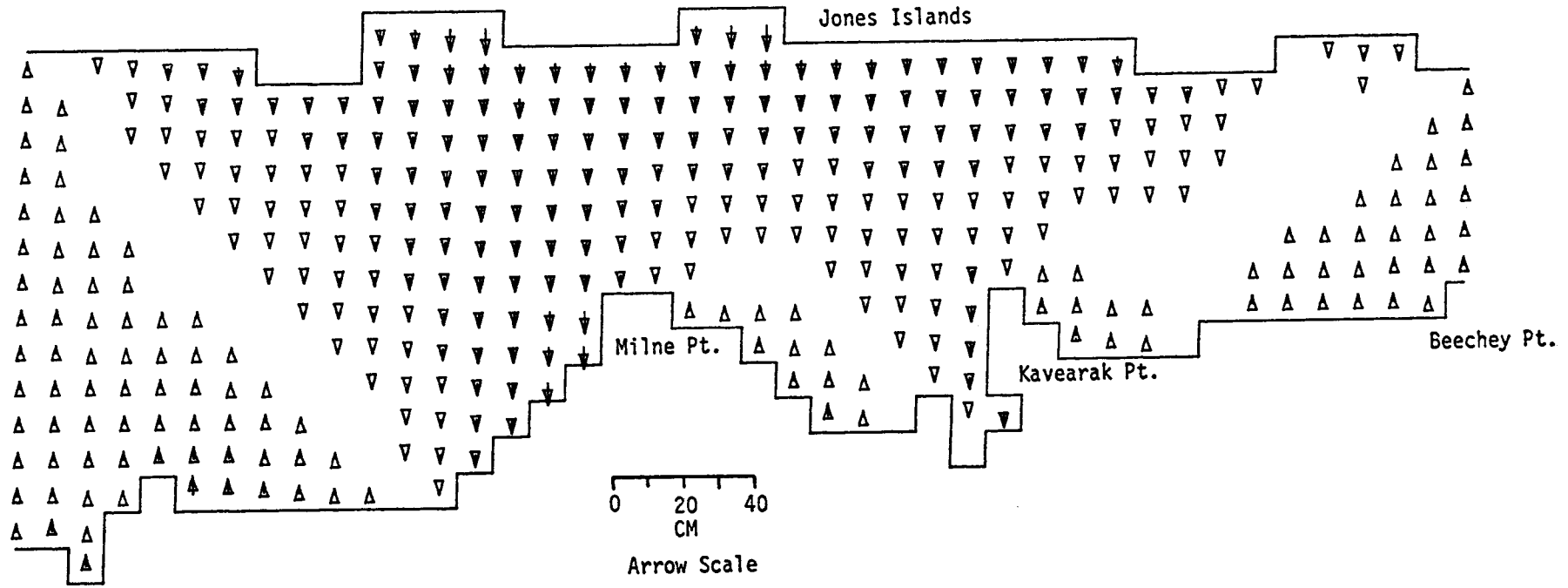
SEA LEVEL

TIME= 43200SEC

LAYER 1

MODEL NO 200

069



SIMPSON LAGOON  
M2 TIDE (AMP=8 CM, IN PHASE ON OPEN BOUNDARIES) WIND FROM 70 DEG T AT 26 KT



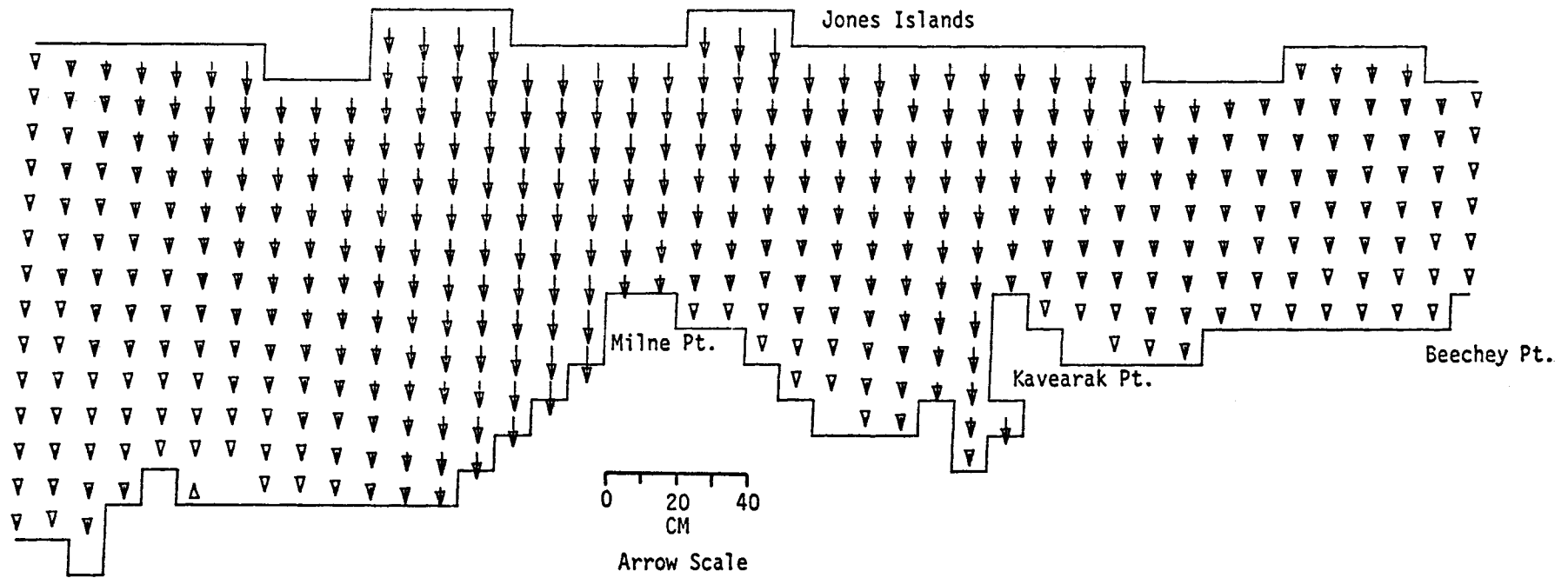
SEA LEVEL

TIME= 46800SEC

LAYER 1

MODEL NO 200

T69



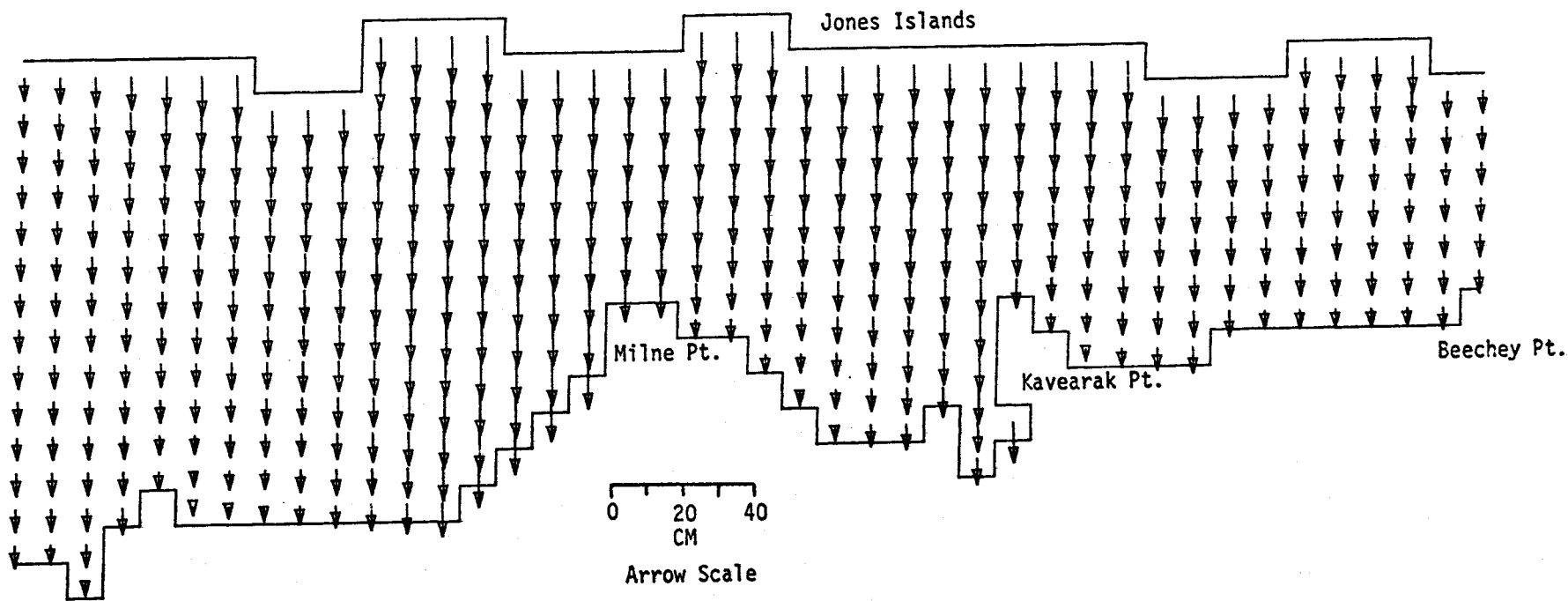
SIMPSON LAGOON  
M2 TIDE (AMP=8 CM, IN PHASE ON OPEN BOUNDARIES) WIND FROM 70 DEG T AT 26 KT

SEA LEVEL

TIME= 50400SEC

LAYER 1

MODEL NO 20  
269



SIMPSON LAGOON  
M2 TIDE (AMP=8 CM, IN PHASE ON OPEN BOUNDARIES) WIND FROM 70 DEG T AT 26 KT

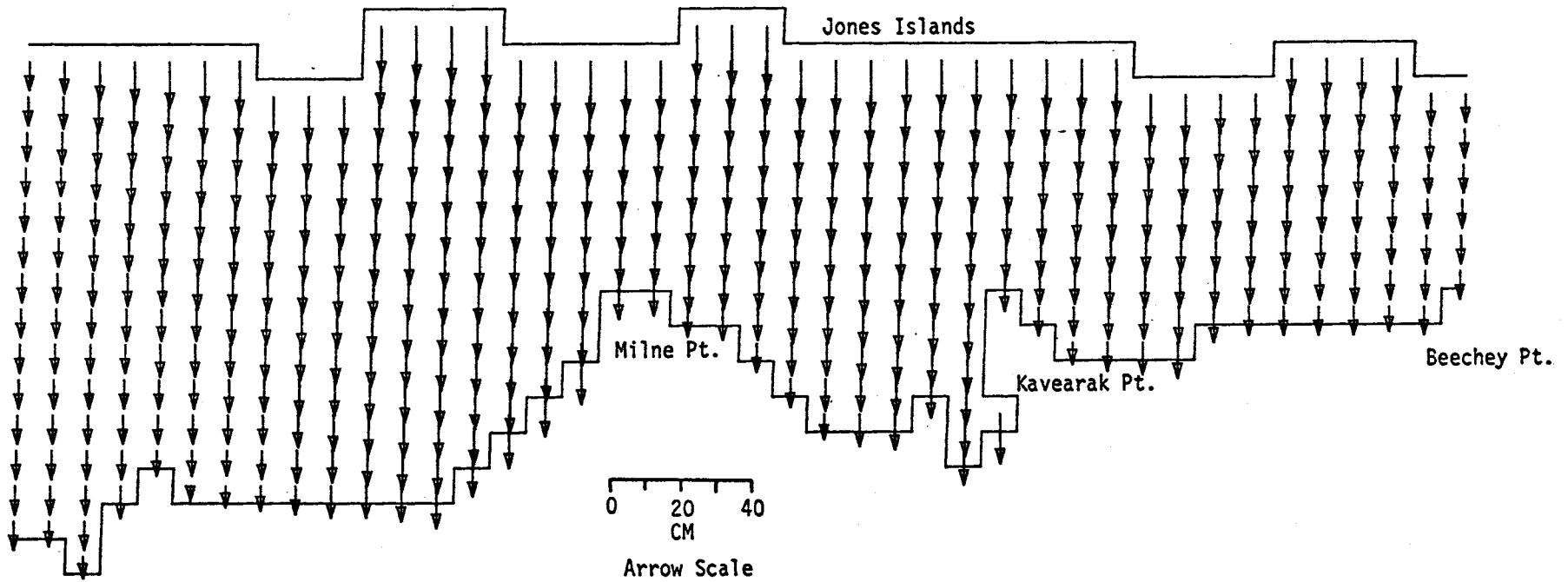
MODEL NO 200

869

SEA LEVEL

TIME= 54000SEC

LAYER 1



SIMPSON LAGOON  
M2 TIDE (AMP=8 CM, IN PHASE ON OPEN BOUNDARIES) WIND FROM 70 DEG T AT 26 KT

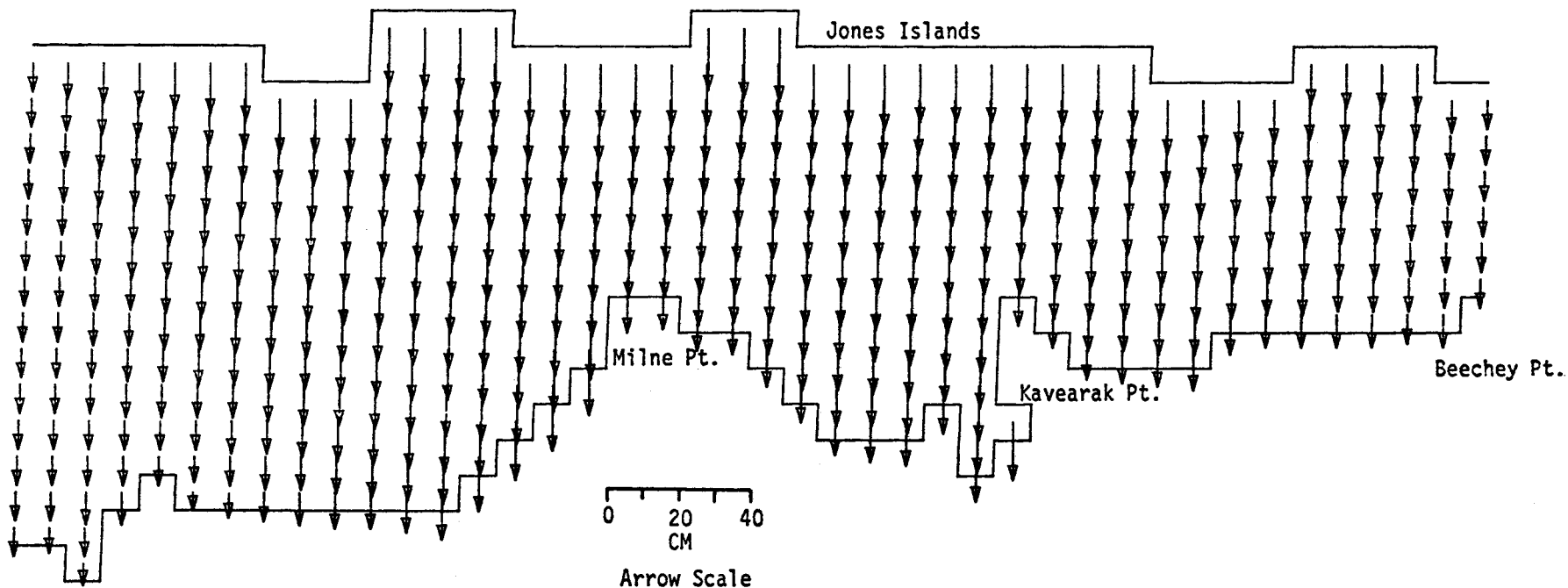
SEA LEVEL

TIME= 57600SEC

LAYER 1

MODEL NO 200

694



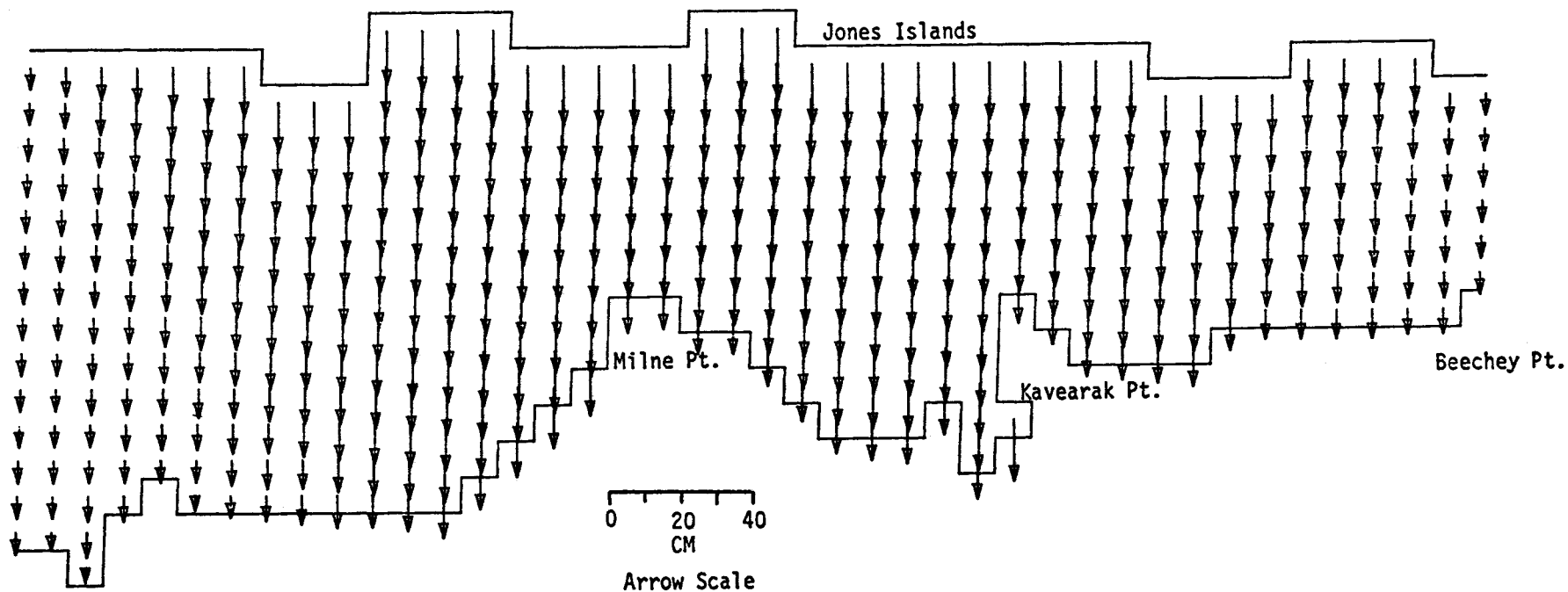
SIMPSON LAGOON  
M2 TIDE (AMP=8 CM, IN PHASE ON OPEN BOUNDARIES) WIND FROM 70 DEG T AT 26 KT

SEA LEVEL

TIME= 61200SEC

LAYER 1

MODEL NO 200  
569



SIMPSON LAGOON  
M2 TIDE (AMP=8 CM. IN PHASE ON OPEN BOUNDARIES) WIND FROM 70 DEG T AT 26 KT

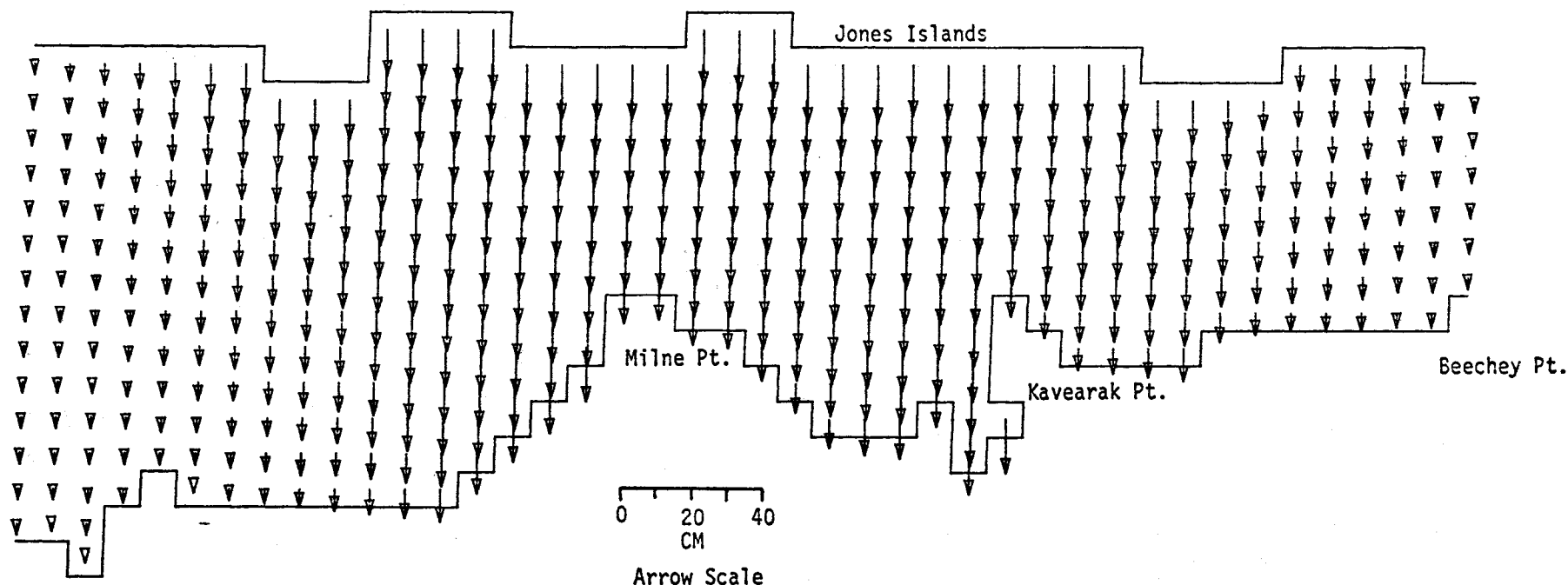
SEA LEVEL

TIME= 64800SEC

LAYER 1

MODEL NO 200

969



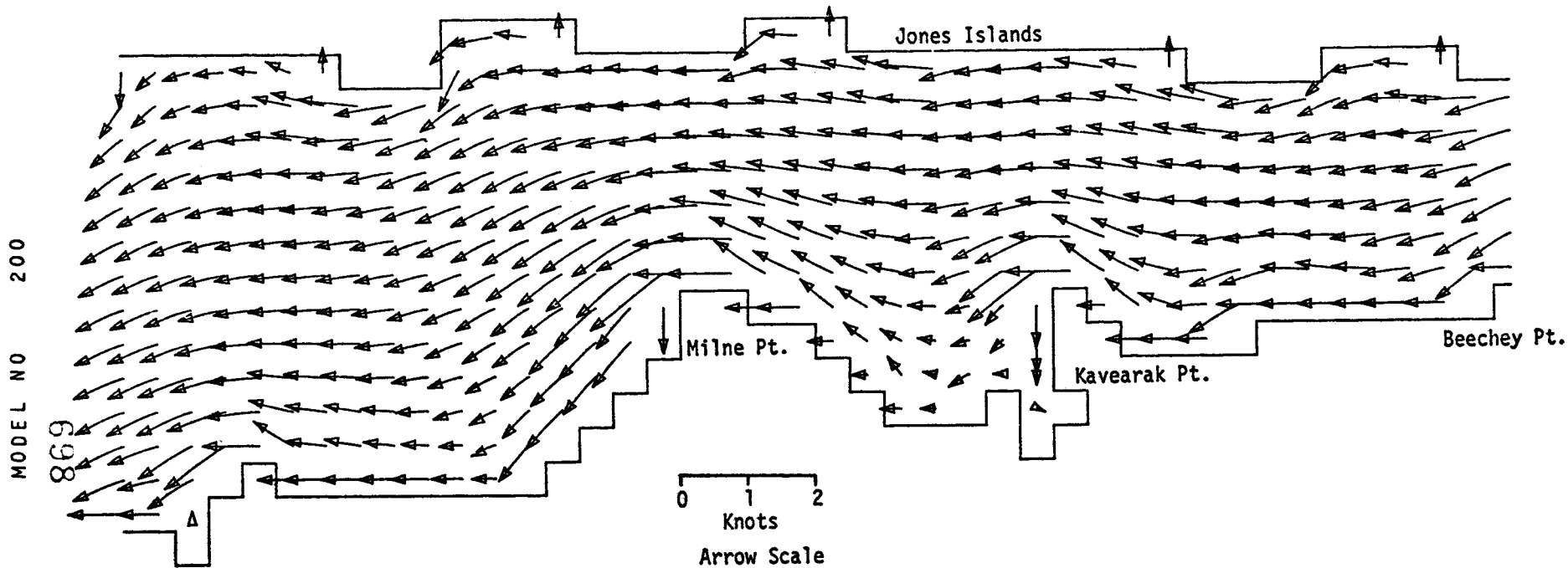
SIMPSON LAGOON  
M2 TIDE (AMP=8 CM, IN PHASE ON OPEN BOUNDARIES) WIND FROM 70 DEG T AT 26 KT

CURRENTS

CURRENTS

TIME= 3600SEC

LAYER 1



SIMPSON LAGOON

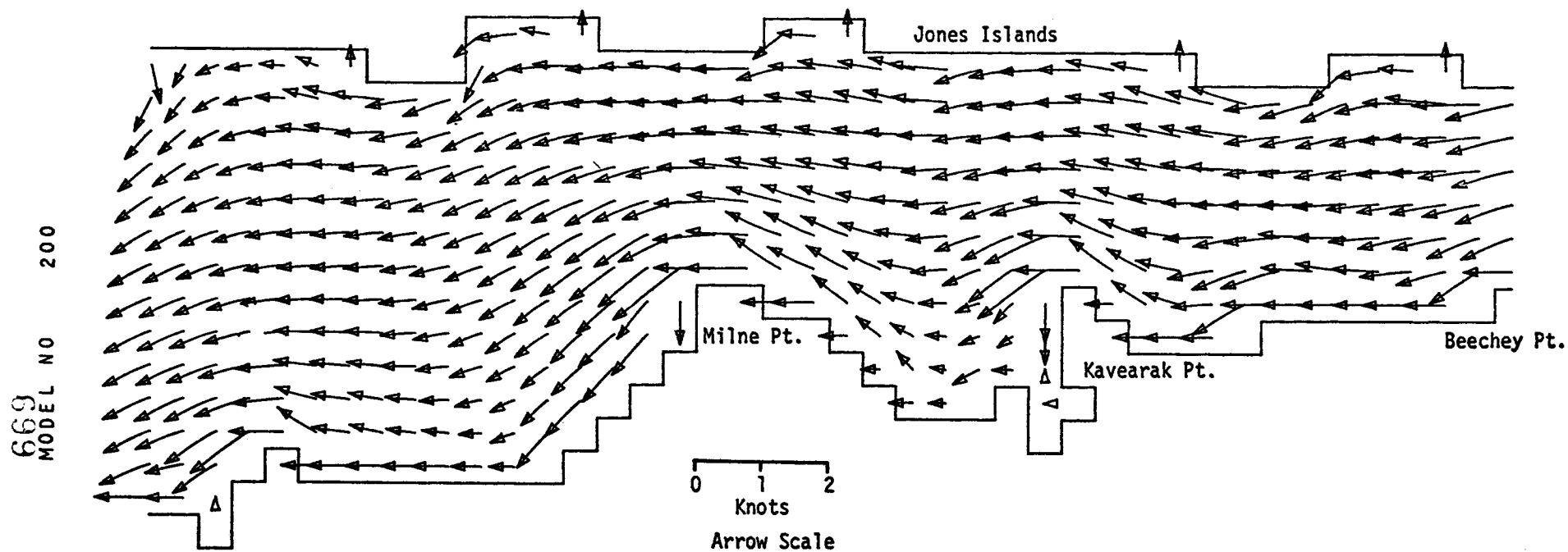
M2 TIDE (AMP=8 CM, IN PHASE ON OPEN BOUNDARIES) WIND FROM 70 DEG T AT 26 KT



CURRENTS

TIME= 7200SEC

LAYER 1

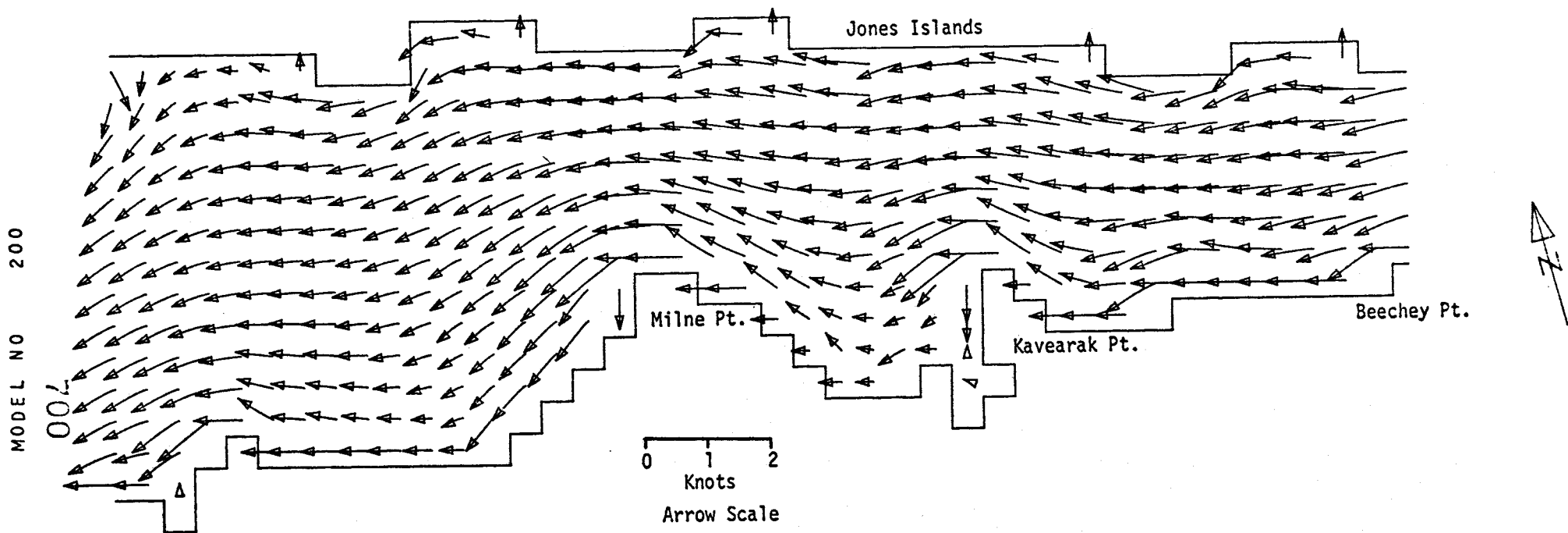


SIMPSON LAGOON  
M2 TIDE (AMP=8 CM, IN PHASE ON OPEN BOUNDARIES) WIND FROM 70 DEG T AT 26 KT

CURRENTS

TIME= 10800SEC

LAYER 1

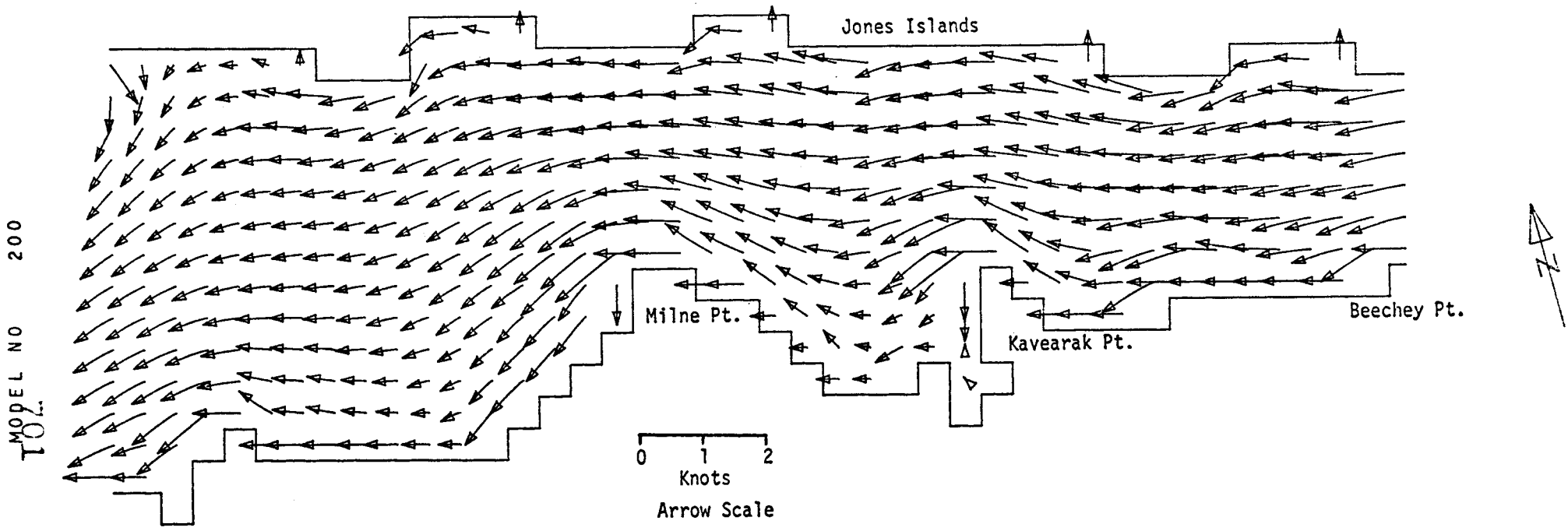


SIMPSON LAGOON  
M2 TIDE (AMP=8 CM, IN PHASE ON OPEN BOUNDARIES) WIND FROM 70 DEG T AT 26 KT

CURRENTS

TIME= 14400SEC

LAYER 1



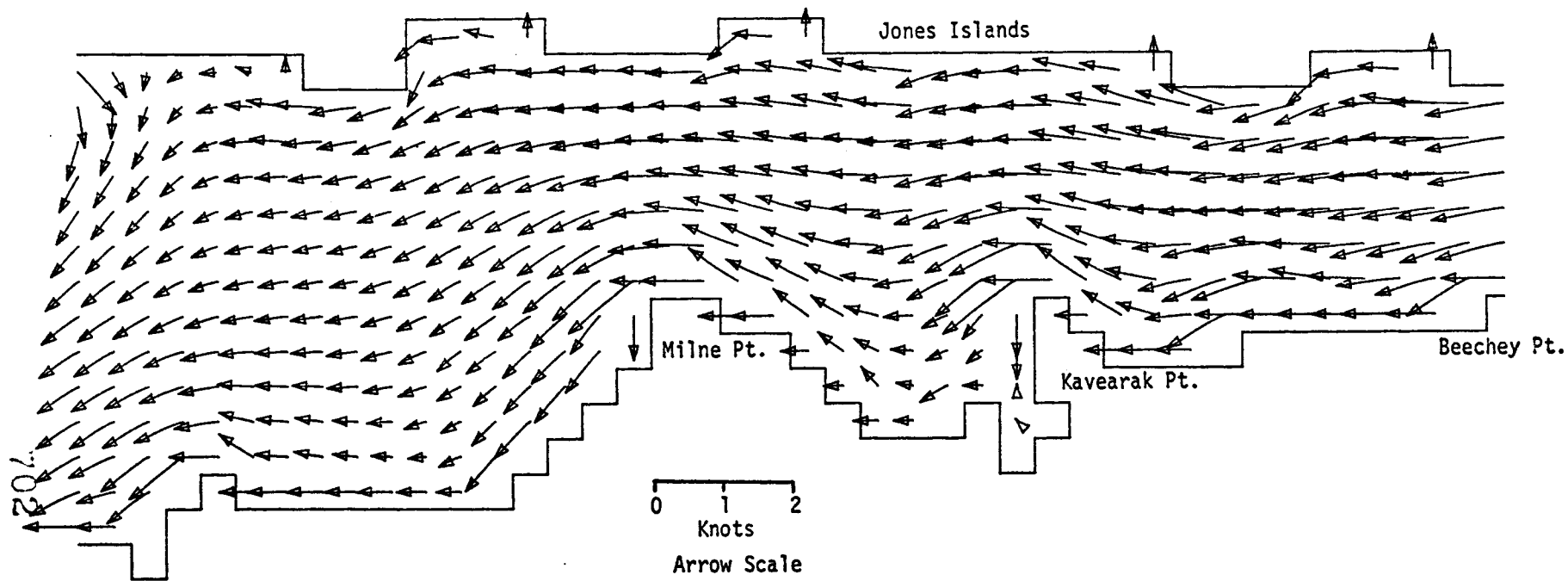
SIMPSON LAGOON

M2 TIDE (AMP=8 CM, IN PHASE ON OPEN BOUNDARIES) WIND FROM 70 DEG T AT 26 KT

CURRENTS

TIME= 18000SEC

LAYER 1



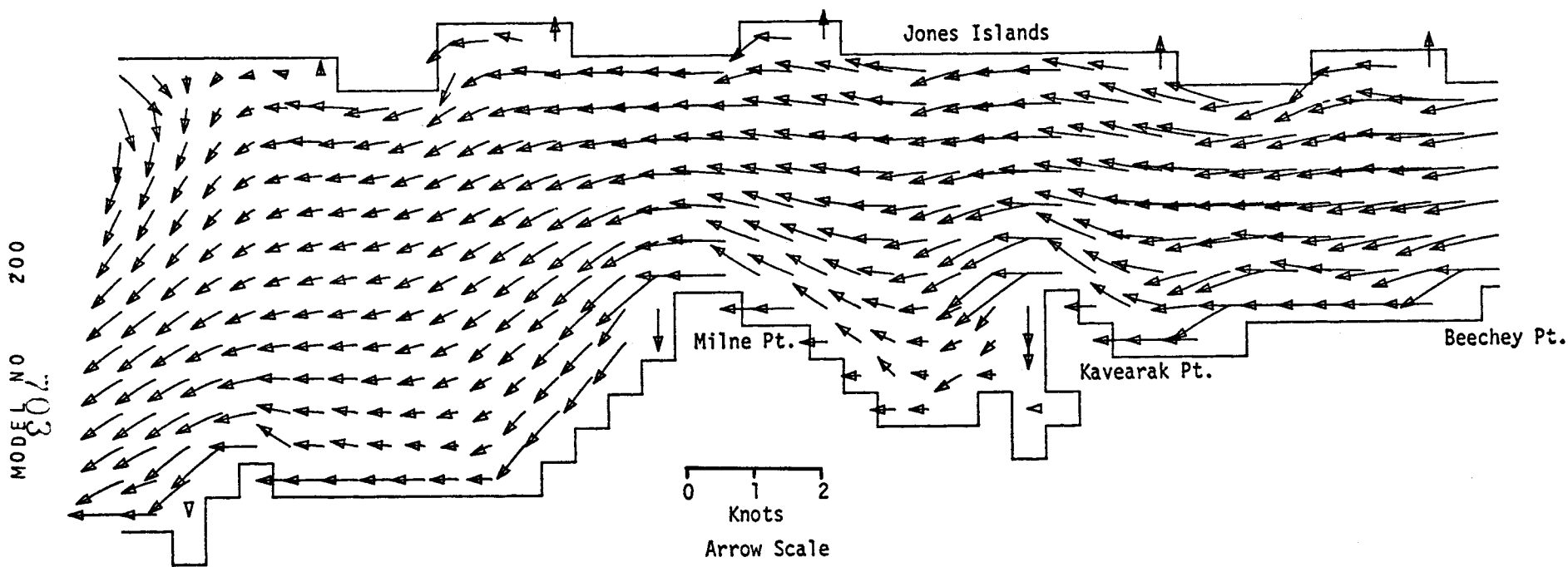
SIMPSON LAGOON

M2 TIDE (AMP=8 CM, IN PHASE ON OPEN BOUNDARIES) WIND FROM 70 DEG T AT 26 KT

CURRENTS

TIME= 21600SEC

LAYER 1

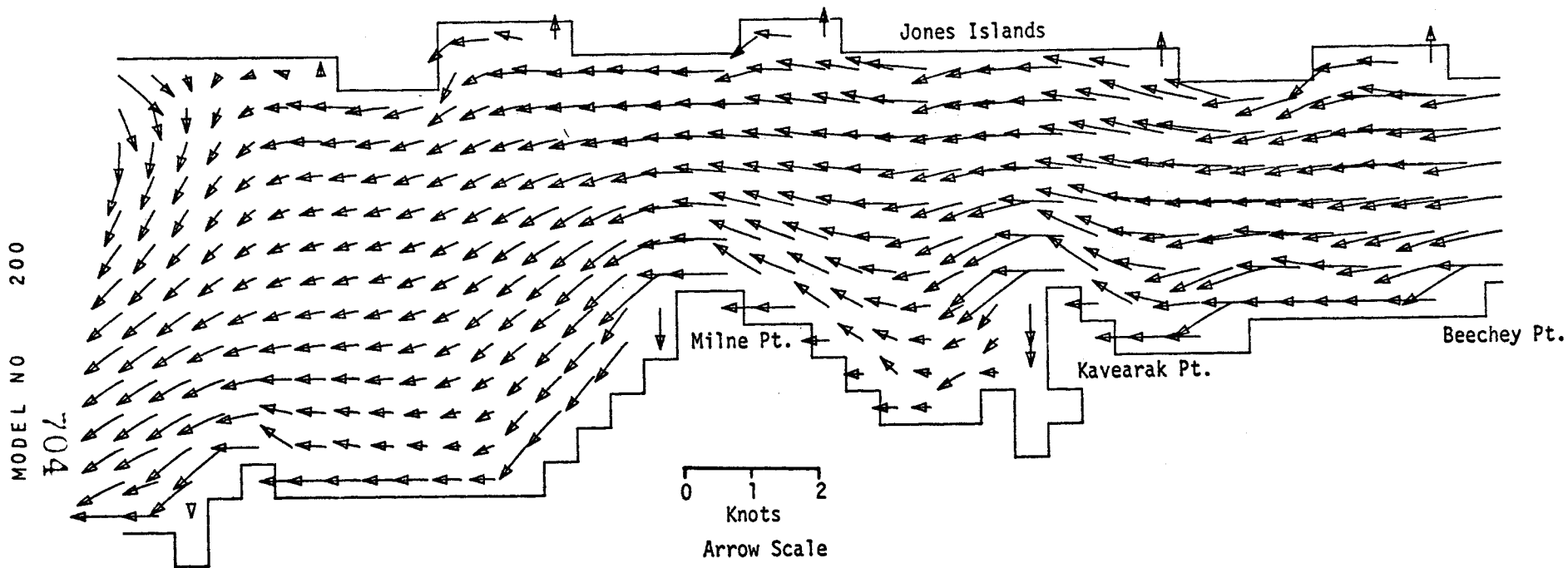


SIMPSON LAGOON  
M2 TIDE (AMP=8 CM, IN PHASE ON OPEN BOUNDARIES) WIND FROM 70 DEG T AT 26 KT

CURRENTS

TIME= 25200SEC

LAYER 1

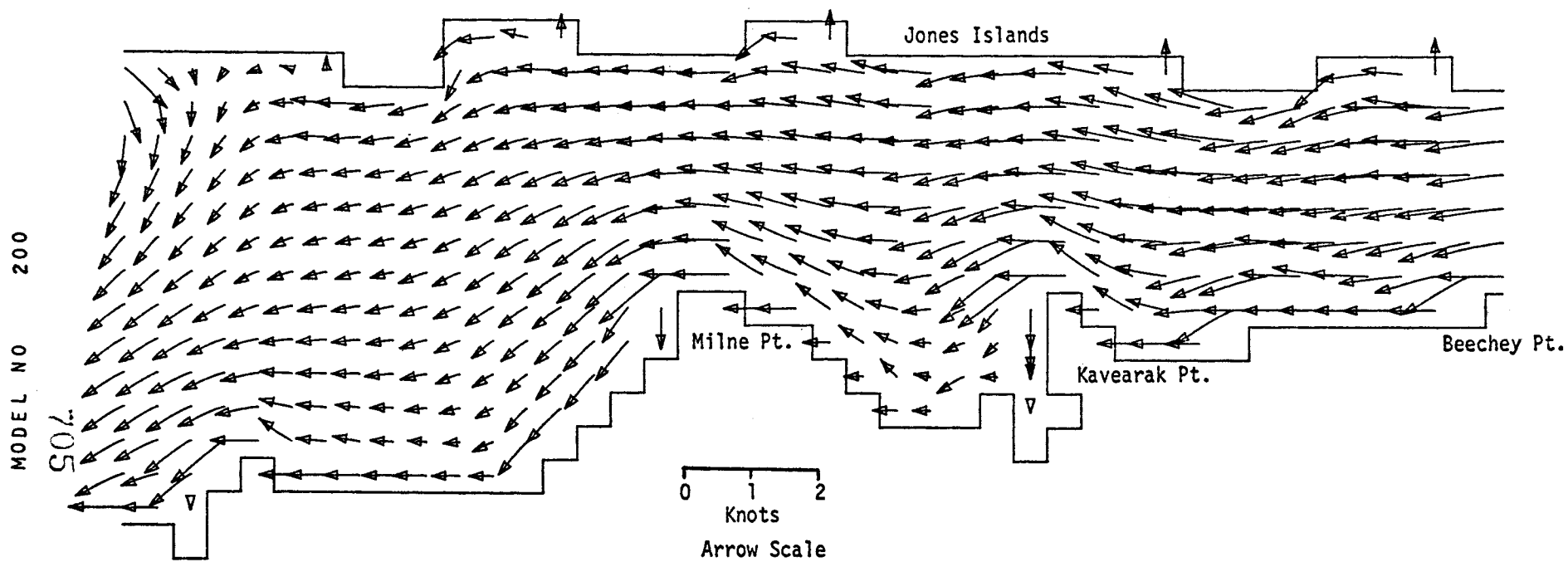


SIMPSON LAGOON  
M2 TIDE (AMP=8 CM, IN PHASE ON OPEN BOUNDARIES) WIND FROM 70 DEG T AT 26 KT

CURRENTS

TIME= 28800SEC

LAYER 1



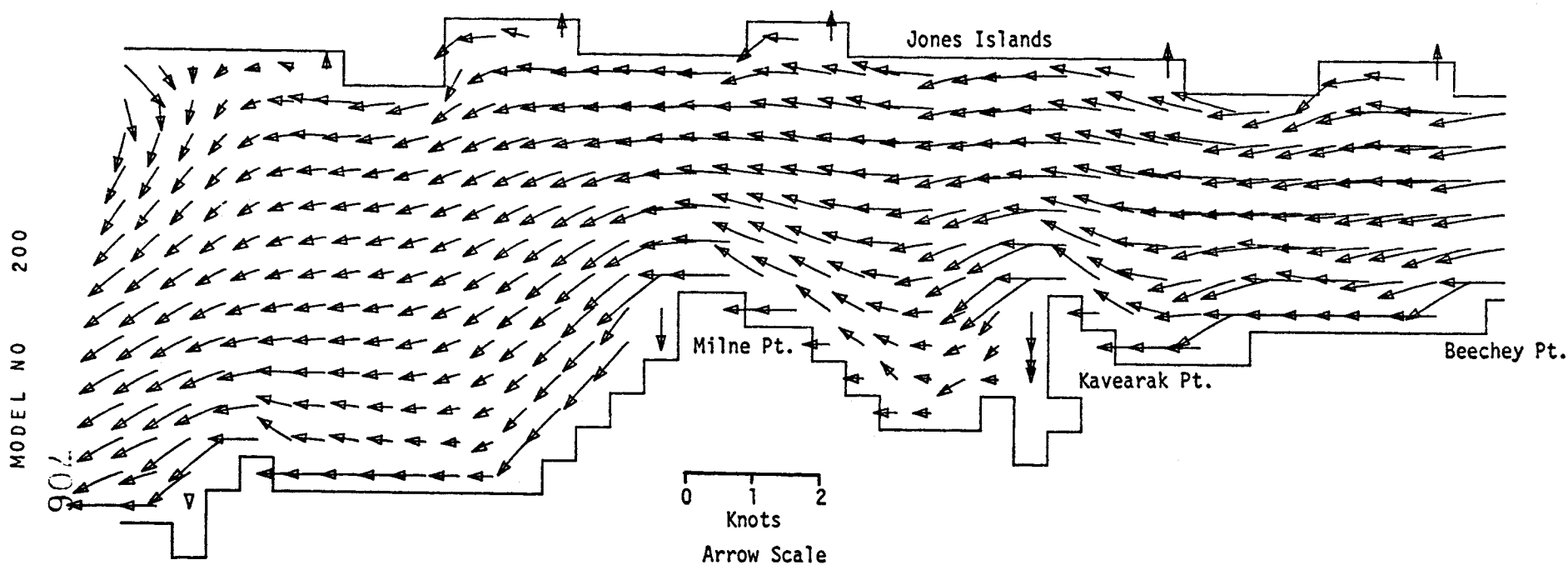
SIMPSON LAGOON

M2 TIDE (AMP=8 CM, IN PHASE ON OPEN BOUNDARIES) WIND FROM 70 DEG T AT 26 KT

CURRENTS

TIME= 32400SEC

LAYER 1



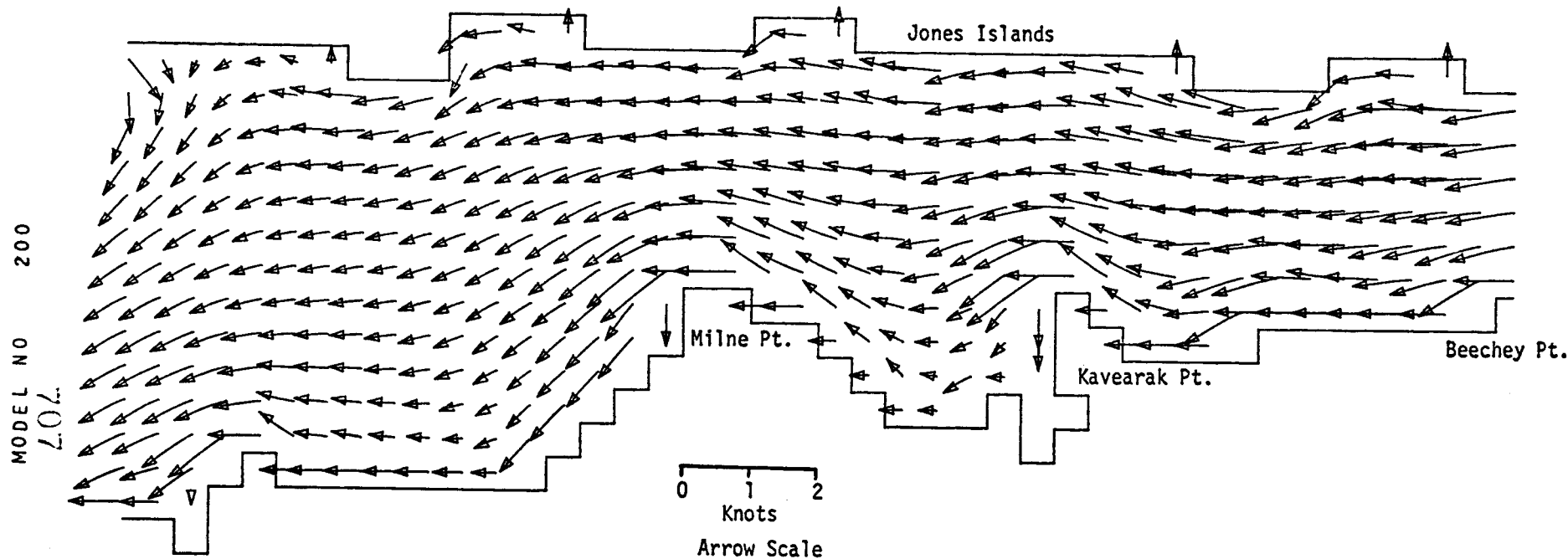
SIMPSON LAGOON  
M2 TIDE (AMP=8 CM, IN PHASE ON OPEN BOUNDARIES) WIND FROM 70 DEG T AT 26 KT



CURRENTS

TIME= 36000SEC

LAYER 1

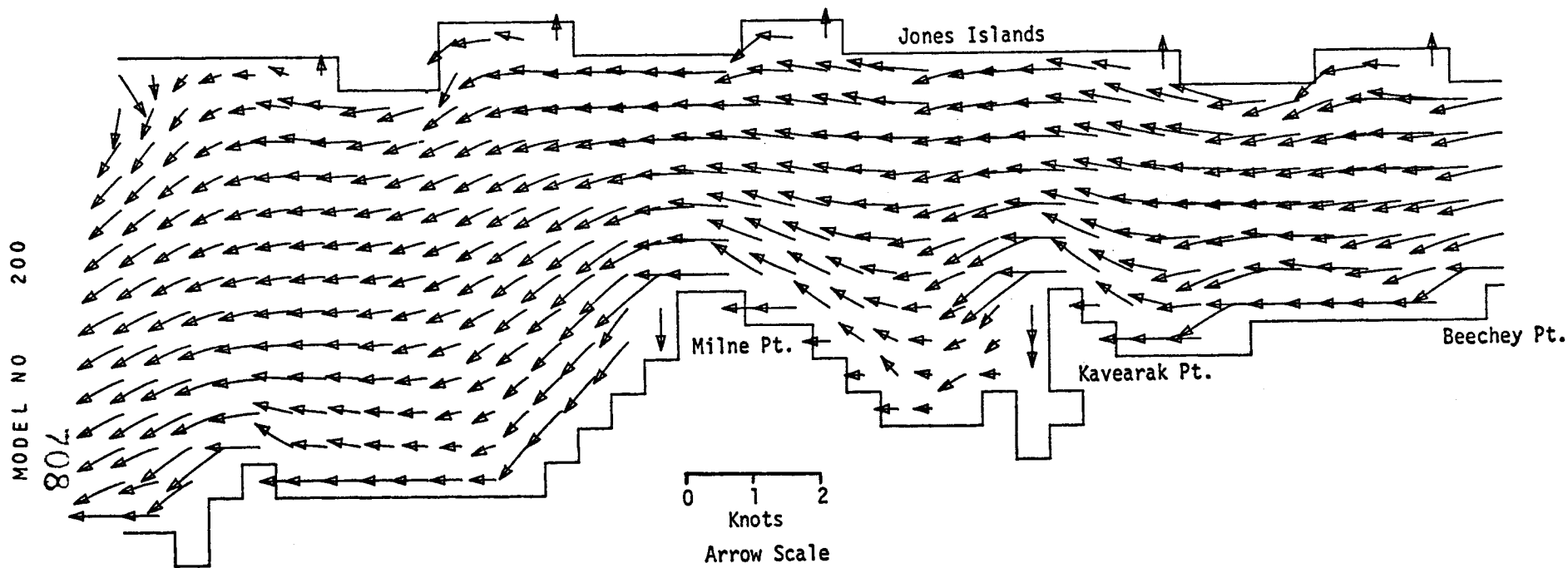


SIMPSON LAGOON  
M2 TIDE (AMP=8 CM, IN PHASE ON OPEN BOUNDARIES) WIND FROM 70 DEG T AT 26 KT

CURRENTS

TIME= 39600SEC

LAYER 1



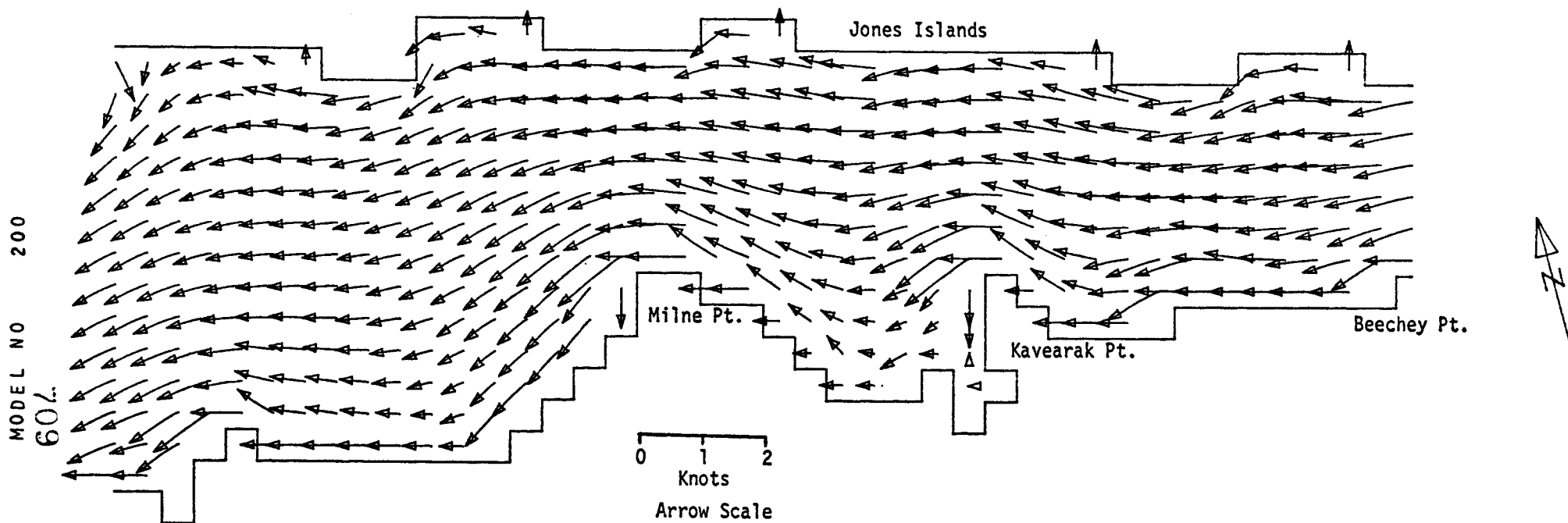
SIMPSON LAGOON

M2 TIDE (AMP=8 CM, IN PHASE ON OPEN BOUNDARIES) WIND FROM 70 DEG T AT 26 KT

CURRENTS

TIME= 43200SEC

LAYER 1

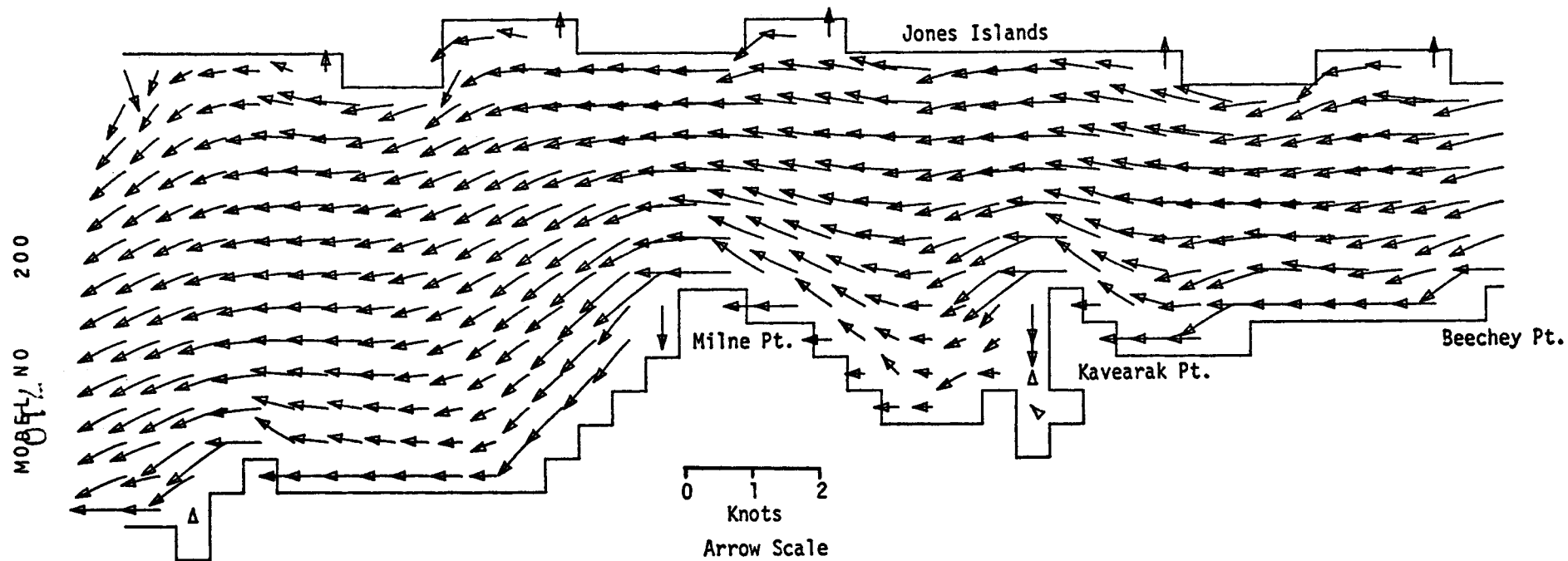


SIMPSON LAGOON  
M2 TIDE (AMP=8 CM, IN PHASE ON OPEN BOUNDARIES) WIND FROM 70 DEG T AT 26 KT

CURRENTS

TIME= 46800SEC

LAYER 1



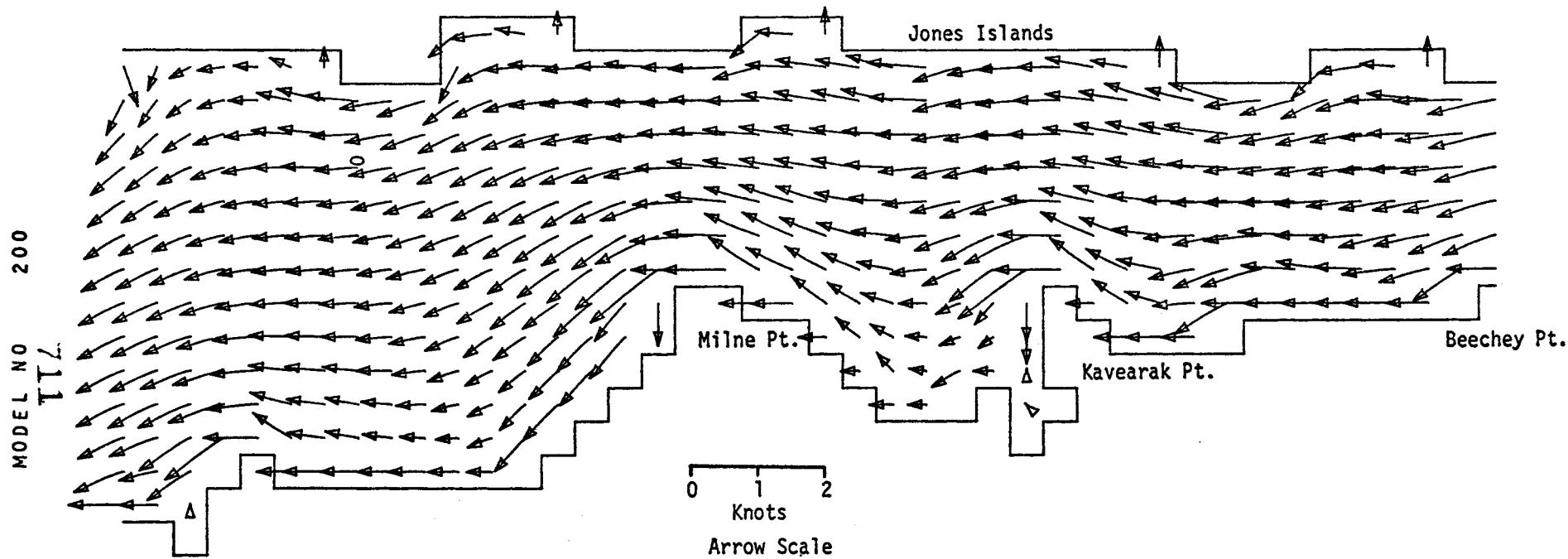
SIMPSON LAGOON

M2 TIDE (AMP=8 CM, IN PHASE ON OPEN BOUNDARIES) WIND FROM 70 DEG T AT 26 KT

CURRENTS

TIME= 50400SEC

LAYER 1



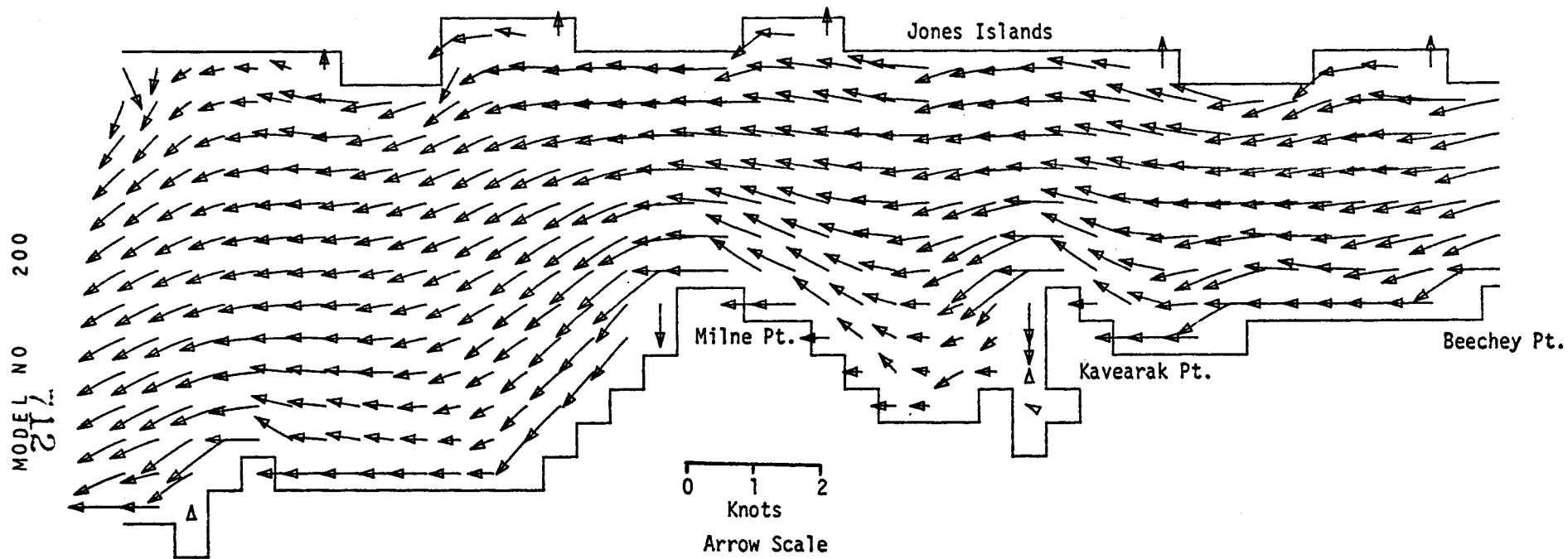
SIMPSON LAGOON

M2 TIDE (AMP=8 CM, IN PHASE ON OPEN BOUNDARIES) WIND FROM 70 DEG T AT 26 KT

CURRENTS

TIME= 54000SEC

LAYER 1



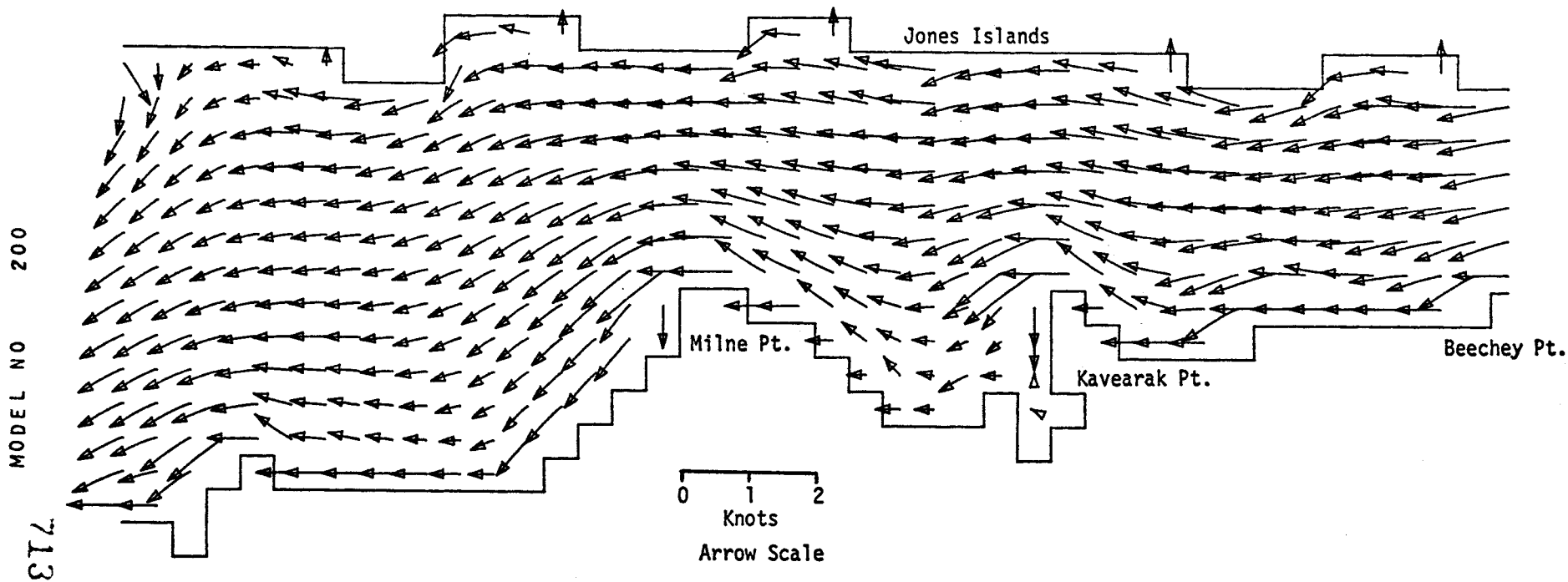
SIMPSON LAGOON

M2 TIDE (AMP=8 CM, IN PHASE ON OPEN BOUNDARIES) WIND FROM 70 DEG T AT 26 KT

CURRENTS

TIME= 57600SEC

LAYER 1

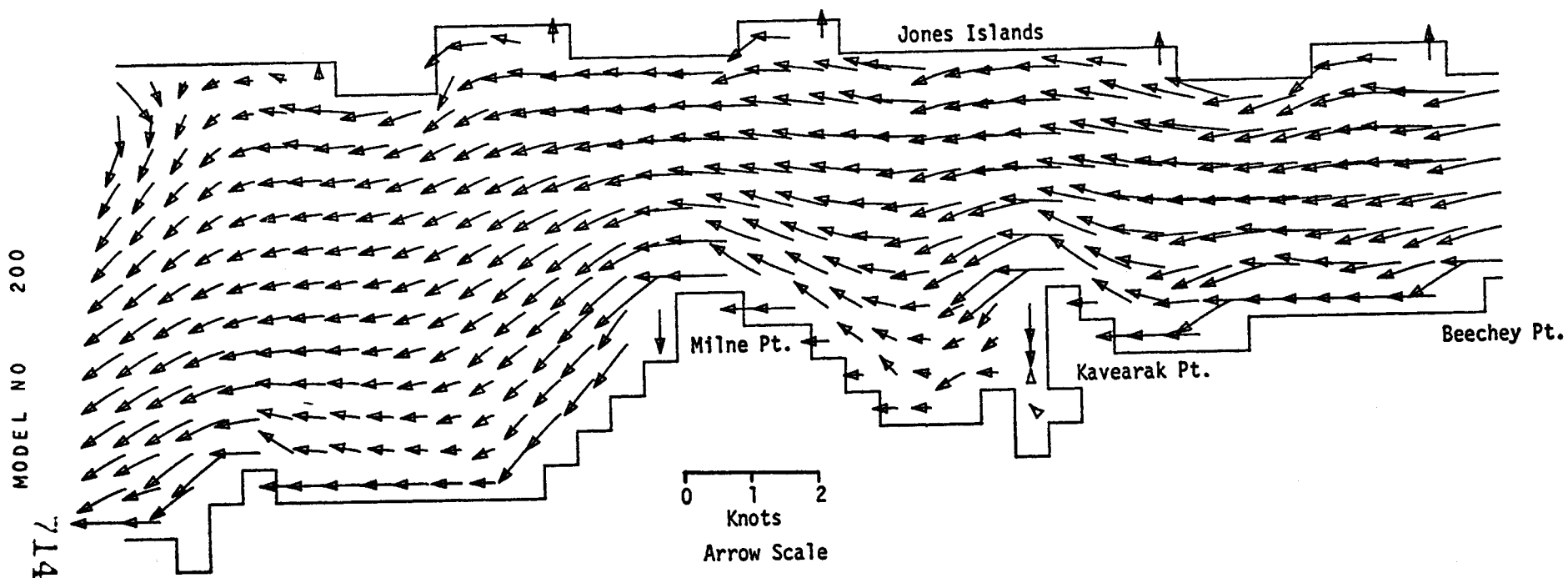


SIMPSON LAGOON  
M2 TIDE (AMP=8 CM, IN PHASE ON OPEN BOUNDARIES) WIND FROM 70 DEG T AT 26 KT

CURRENTS

TIME= 61200SEC

LAYER 1



SIMPSON LAGOON  
M2 TIDE (AMP=8 CM, IN PHASE ON OPEN BOUNDARIES) WIND FROM 70 DEG T AT 26 KT



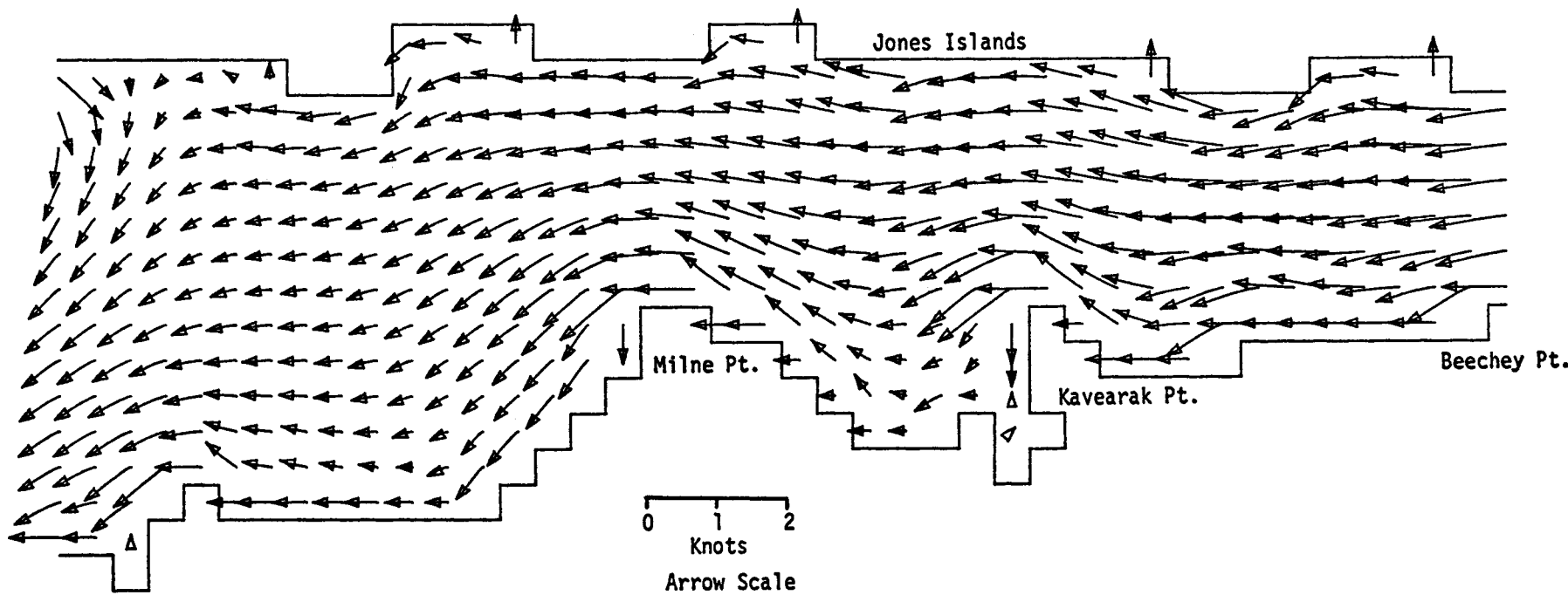
CURRENTS

TIME= 64800SEC

LAYER 1

MODEL NO 200

ST 7.



SIMPSON LAGOON

M2 TIDE (AMP=8 CM, IN PHASE ON OPEN BOUNDARIES) WIND FROM 70 DEG T AT 26 KT

APPENDIX G

SIMPSON LAGOON  
M2 TIDE WITH 8 CM AMPLITUDE INPUT IN PHASE  
ON OPEN BOUNDARIES  
26 KT WIND FROM 250°T

ENVIRONMENTAL PROTECTION AGENCY  
MARINE AND FRESHWATER ECOLOGY BRANCH  
OCEAN MASS TRANSPORT MODEL

M2 TIDE (AMP=8 CM, IN PHASE ON OPEN BOUNDARIES) WIND FROM 250 DEG T AT 26 KT  
BEAUFORT SEA SHELF STUDY  
GRID 200 SIMPSON LAGOON AT 1/2 KM GRID SPACING

|                       |      |                 |                |                 |
|-----------------------|------|-----------------|----------------|-----------------|
| GRID GEOMETRY         | ROWS | 18              | COLUMNS        | 42              |
| GRID LENGTH           |      | 50000. CM       | ROTATION ANGLE | 345.0 DEG       |
| WIND DRAG COEFFICIENT |      | .0024           | MID LATITUDE   | 70.500 DEG. (N) |
| FRICTION COEFFICIENT  |      | .0030000 CM/SEC |                |                 |

|                      |          |         |         |
|----------------------|----------|---------|---------|
|                      | LAYER 1  | LAYER 2 | LAYER 3 |
| INITIAL LAYER DEPTHS | 300.0000 | .0000   | .0000   |
| SMOOTHING FACTORS    | .9900    | .0000   | .0000   |
| DENSITY              | 1.0200   | .0000   | .0000   |

|                                 |             |                           |          |
|---------------------------------|-------------|---------------------------|----------|
| RESULTS SAVED AT MODULUS (TIME, | 3600 SEC)=0 | RESULTS SAVED STARTING AT | 3600 SEC |
| COMPUTATIONS STARTED AT         | 0 SEC       |                           |          |
| ENDED AT                        | 64800 SEC   |                           |          |
| INCREMENTED BY                  | 60 SEC      |                           |          |
| LAYER3 PRINT OUT STARTED        |             | 3600 SEC. FREQUENCY OF    | 3600 SEC |

|                               |     |           |        |          |          |       |
|-------------------------------|-----|-----------|--------|----------|----------|-------|
| TIDAL INPUT AT                | ROW | 2 THRU 17 | COLUMN | 1 THRU 1 | TIME LAG | 0 SEC |
|                               |     | M2        | S2     | 01       | K1       |       |
| PHASE ANGLES (DEG/HR)         |     | 270.00    | .00    | .00      | .00      |       |
| AMPLITUDES (CM)               |     | 8.00      | .00    | .00      | .00      |       |
| LOWER LAYER WEIGHTING FACTORS |     | LAYER 2=  | .00    | LAYER 3= | .00      |       |

|                               |     |           |        |            |          |       |
|-------------------------------|-----|-----------|--------|------------|----------|-------|
| TIDAL INPUT AT                | ROW | 3 THRU 10 | COLUMN | 42 THRU 42 | TIME LAG | 0 SEC |
|                               |     | M2        | S2     | 01         | K1       |       |
| PHASE ANGLES (DEG/HR)         |     | 270.00    | .00    | .00        | .00      |       |
| AMPLITUDES (CM)               |     | 8.00      | .00    | .00        | .00      |       |
| LOWER LAYER WEIGHTING FACTORS |     | LAYER 2=  | .00    | LAYER 3=   | .00      |       |

|                       |           |         |         |         |
|-----------------------|-----------|---------|---------|---------|
|                       | M2        | S2      | 01      | K1      |
| TIDAL SPEEDS (DEG/HR) | 26.984000 | .000000 | .000000 | .000000 |

|                         |     |           |                        |                |
|-------------------------|-----|-----------|------------------------|----------------|
| WIND INPUT AT           | ROW | 1 THRU 18 | COLUMN                 | 1 THRU 42      |
| COMPUTATIONS STARTED AT |     | 60 SEC    |                        |                |
| ENDED AT                |     | 64800 SEC | DIRECTION 250 DEG TRUE | SPEED 13 M/SEC |

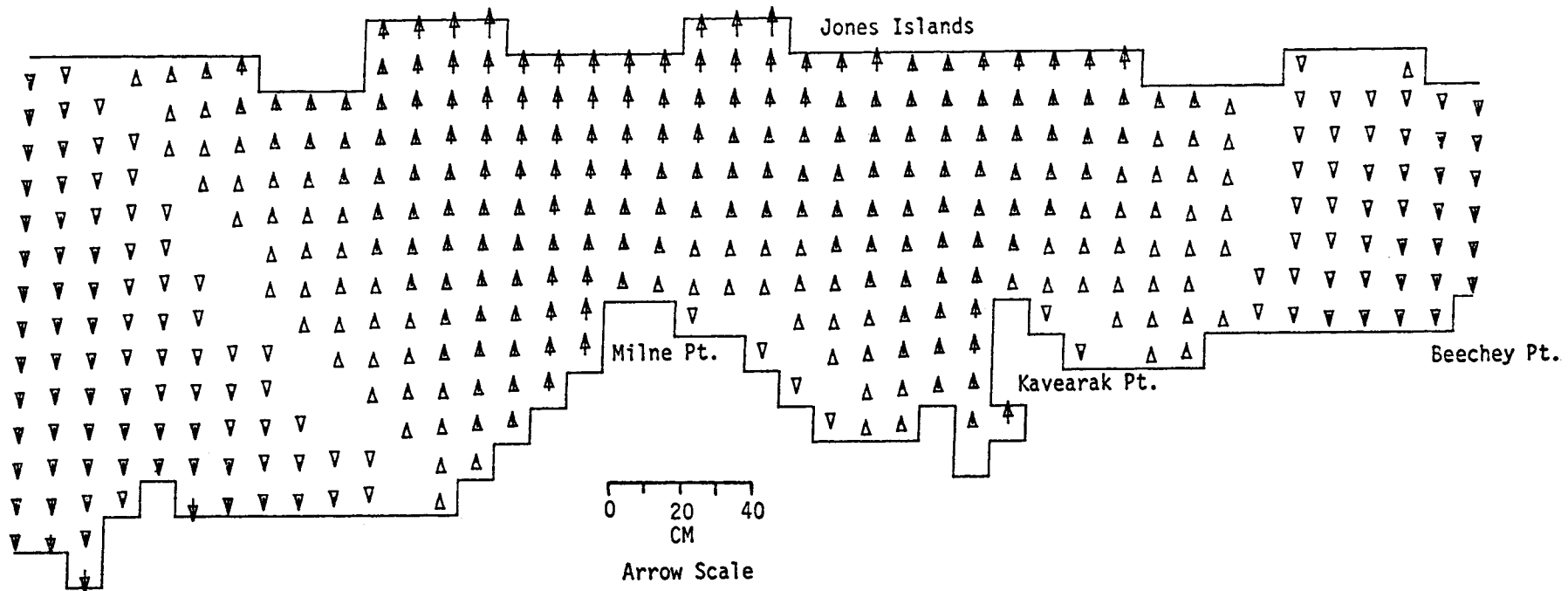
SEA LEVEL

SEA LEVEL

TIME= 3600SEC

LAYER 1

MODEL NO 200  
6T7



SIMPSON LAGOON  
M2 TIDE (AMP=8 CM, IN PHASE ON OPEN BOUNDARIES) WIND FROM 250 DEG T AT 26 KT

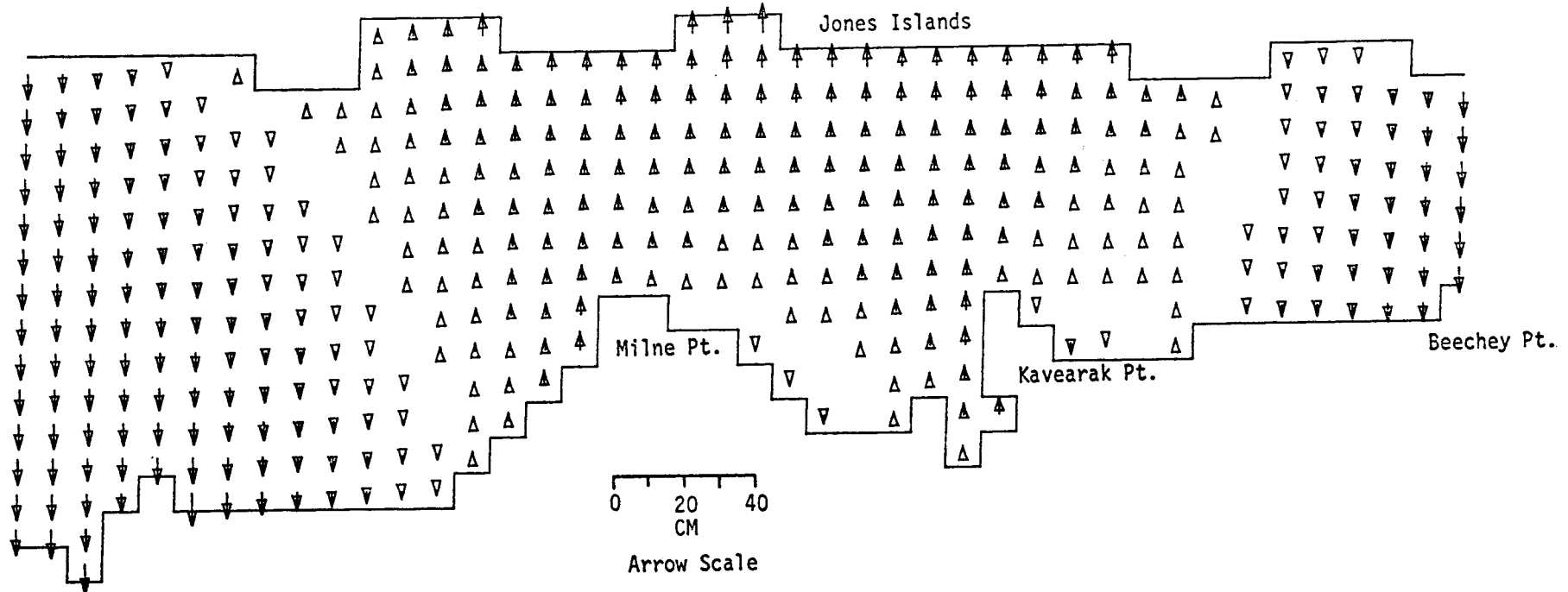
SEA LEVEL

TIME= 7200SEC

LAYER 1

MODEL NO 200

720



SIMPSON LAGOON  
M2 TIDE (AMP=8 CM, IN PHASE ON OPEN BOUNDARIES) WIND FROM 250 DEG T AT 26 KT

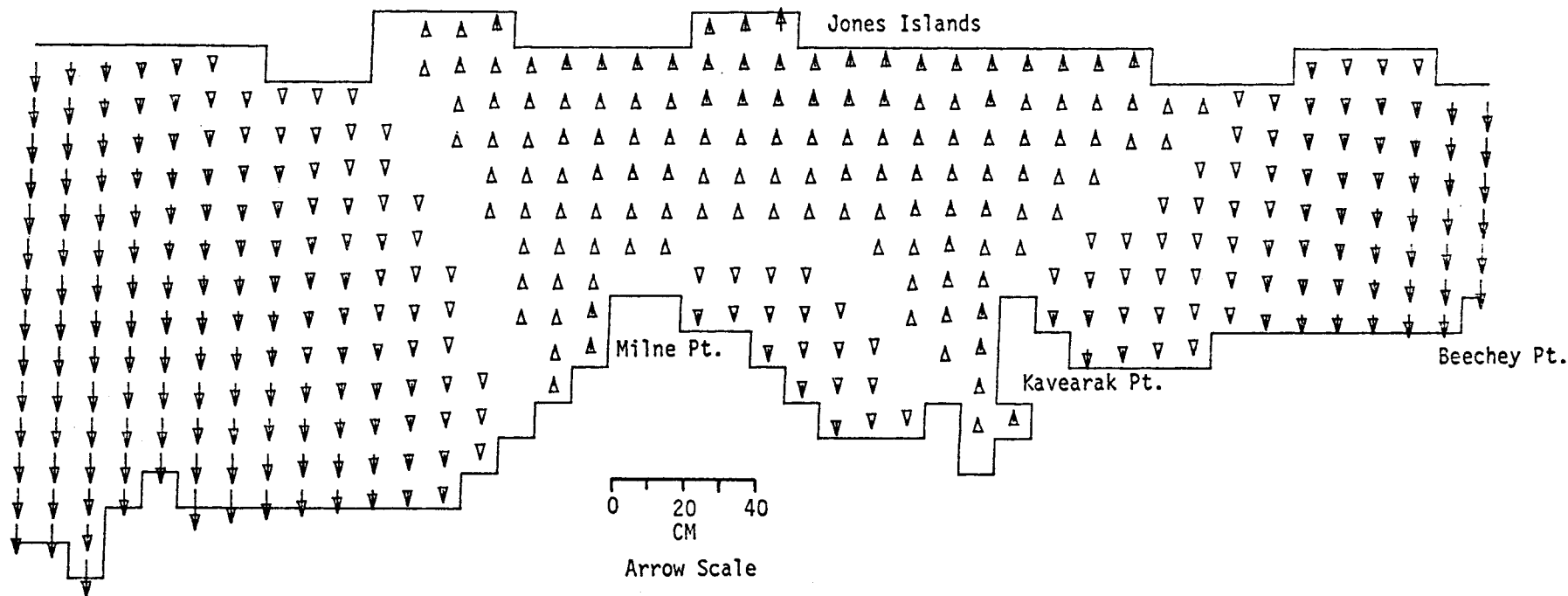
SEA LEVEL

TIME= 10800SEC

LAYER 1

MODEL NO 200

721



SIMPSON LAGOON

M2 TIDE (AMP=8 CM, IN PHASE ON OPEN BOUNDARIES) WIND FROM 250 DEG T AT 26 KT

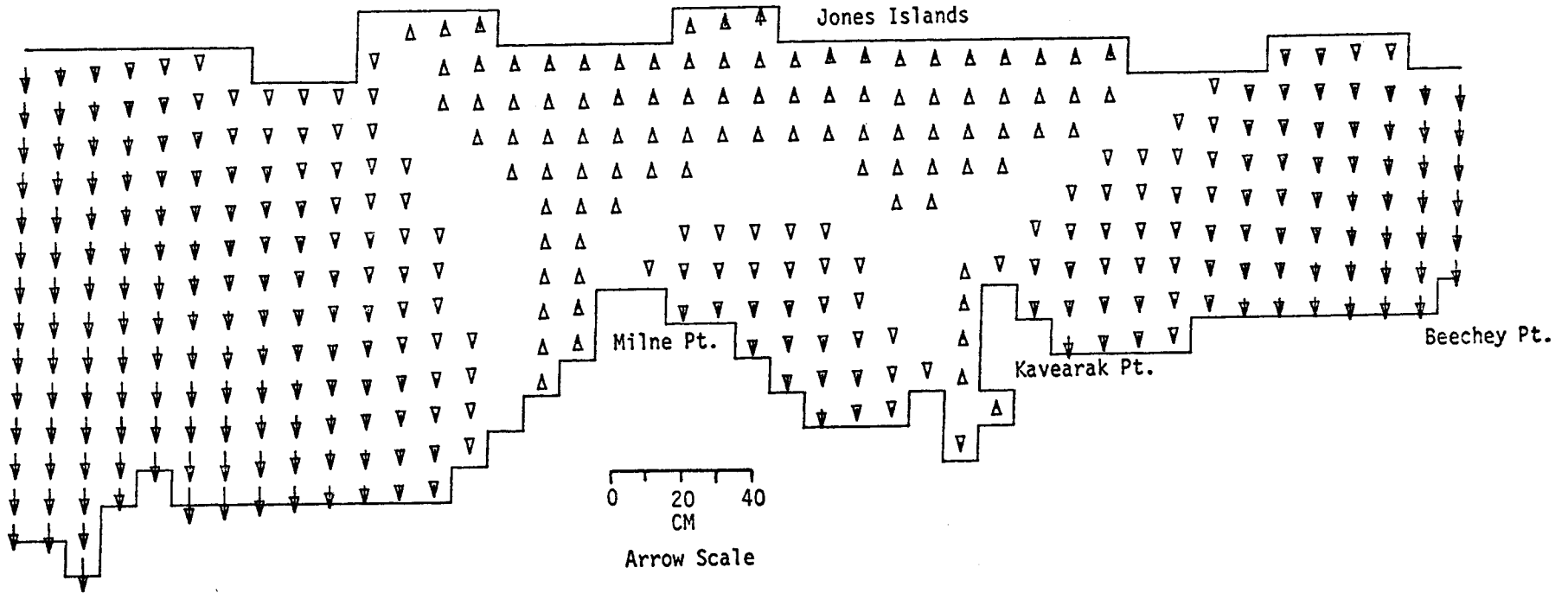
SEA LEVEL

TIME= 14400SEC

LAYER 1

MODEL NO 200

722



SIMPSON LAGOON  
M2 TIDE (AMP=8 CM, IN PHASE ON OPEN BOUNDARIES) WIND FROM 250 DEC T AT 26 KT



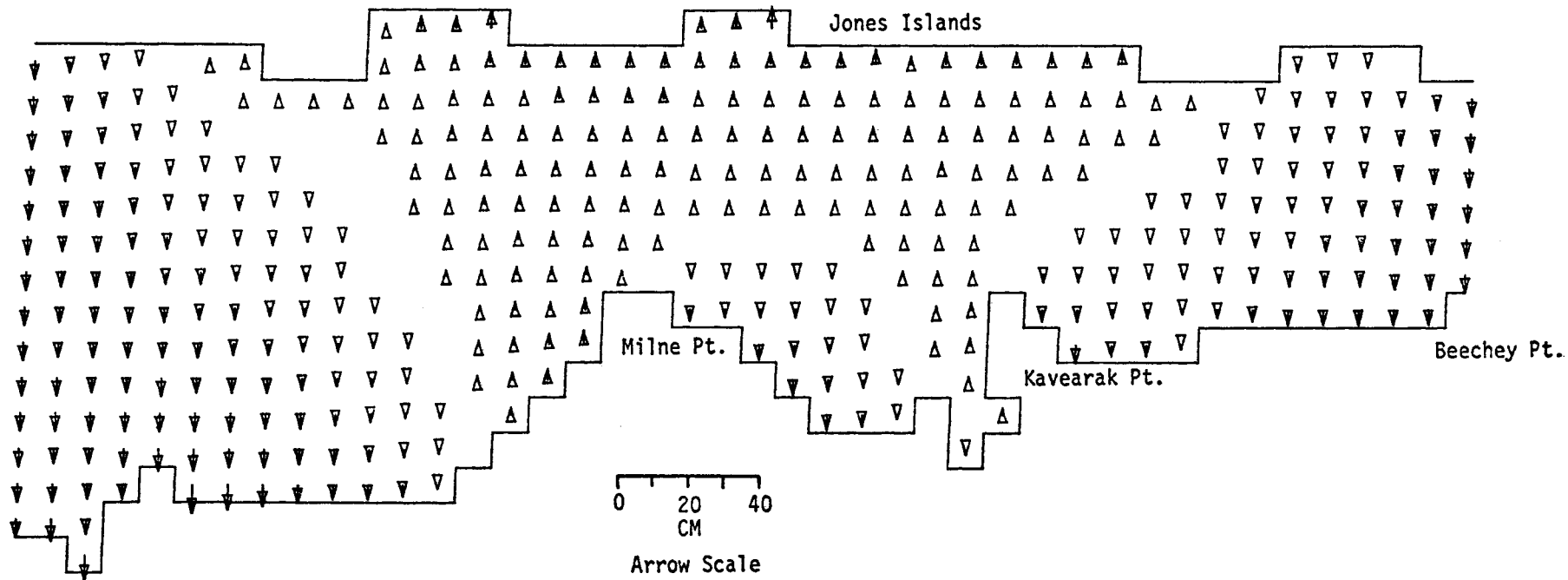
SEA LEVEL

TIME= 18000SEC

LAYER 1

MODEL NO 200

723



SIMPSON LAGOON  
M2 TIDE (AMP=8 CM, IN PHASE ON OPEN BOUNDARIES) WIND FROM 250 DEG T AT 26 KT

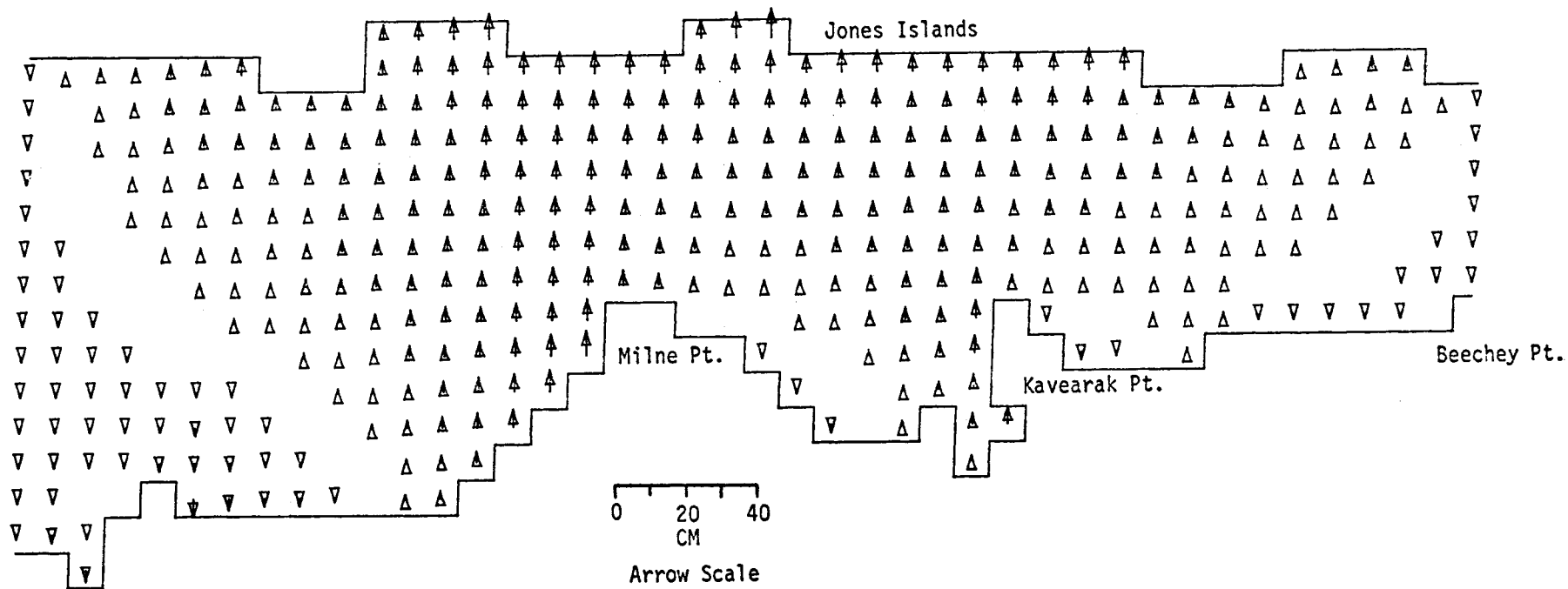
SEA LEVEL

TIME= 21600SEC

LAYER 1

MODEL NO 200

724



SIMPSON LAGOON  
M2 TIDE (AMP=8 CM, IN PHASE ON OPEN BOUNDARIES) WIND FROM 250 DEG T AT 26 KT

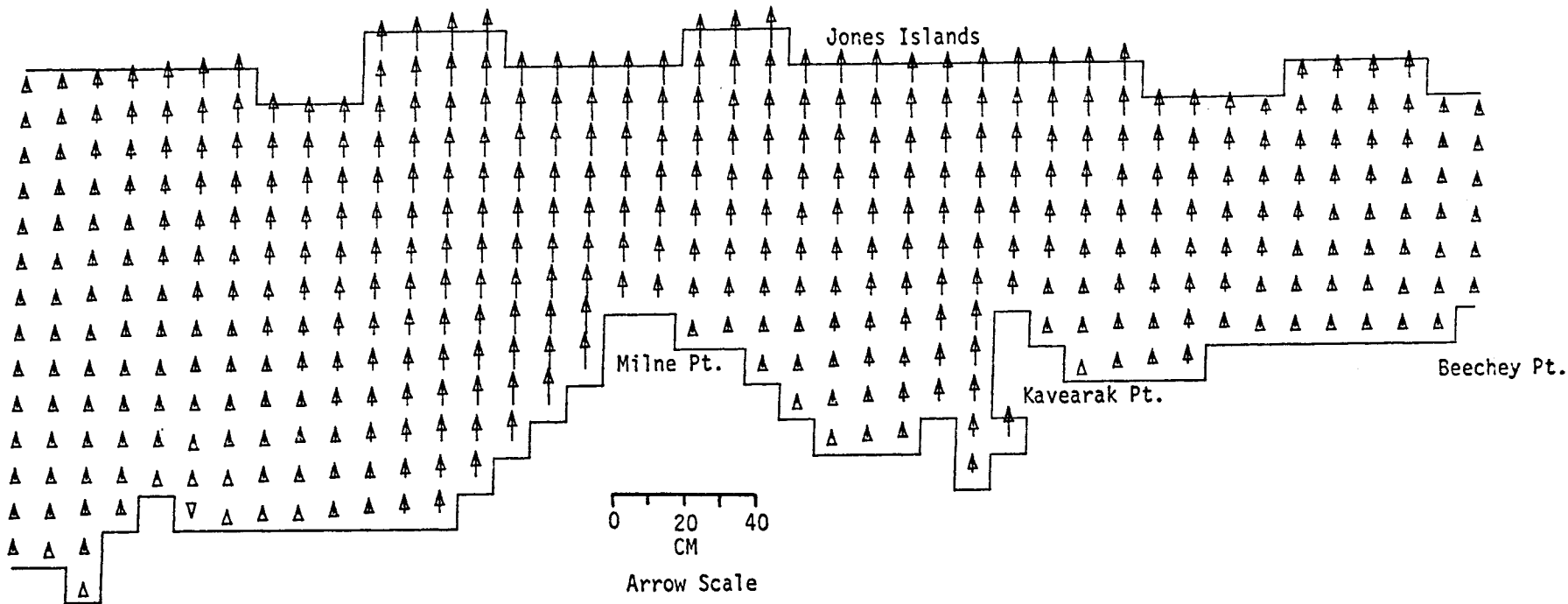
SEA LEVEL

TIME= 25200SEC

LAYER 1

MODEL NO 200

725



SIMPSON LAGOON  
M2 TIDE (AMP=8 CM, IN PHASE ON OPEN BOUNDARIES) WIND FROM 250 DEG T AT 26 KT

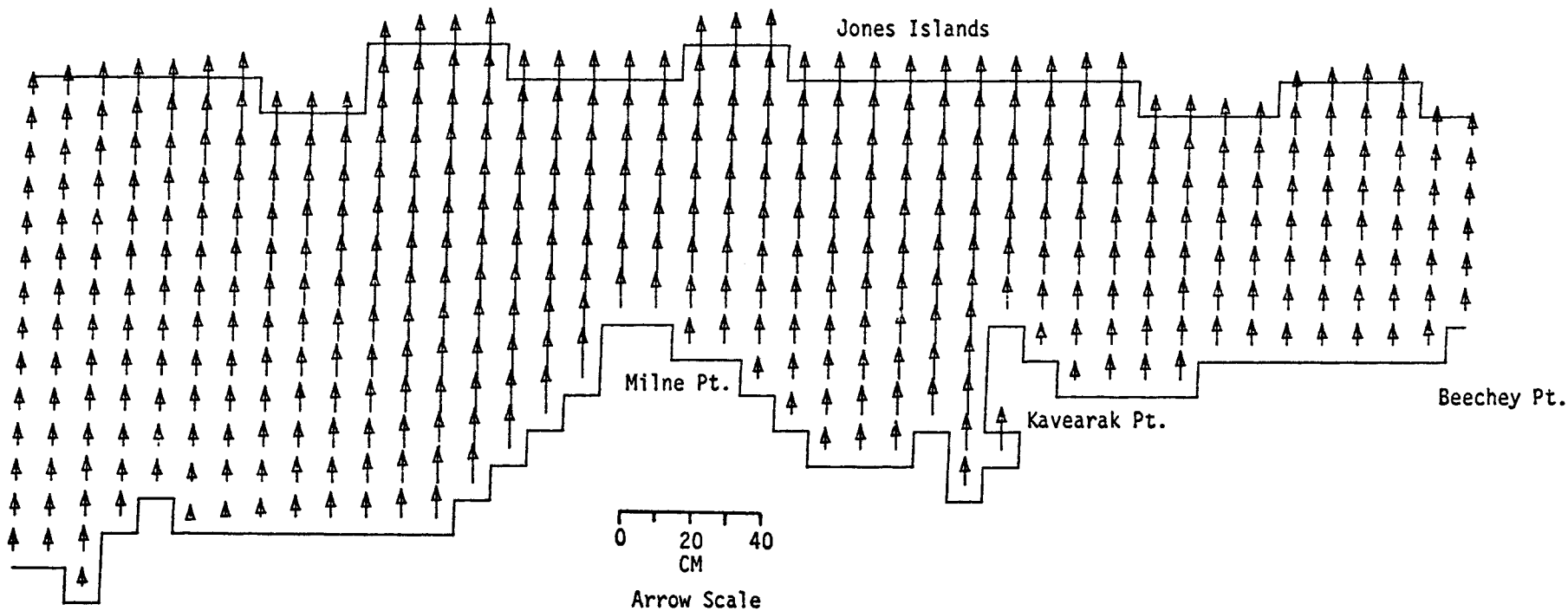
SEA LEVEL

TIME= 28800SEC

LAYER 1

MODEL NO 200

726



SIMPSON LAGOON  
M2 TIDE (AMP=8 CM, IN PHASE ON OPEN BOUNDARIES) WIND FROM 250 DEG T AT 26 KT

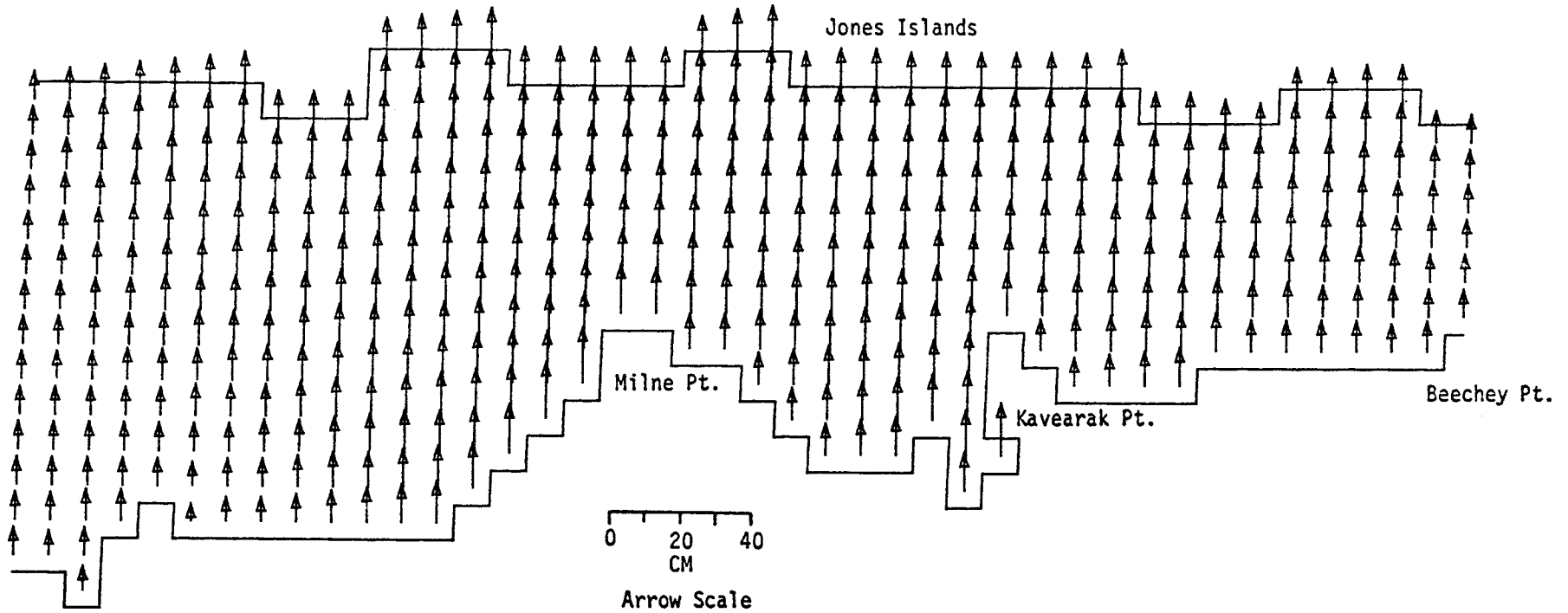
MODEL NO 200

727

S A LEVEL

TIME= 32400SEC

LAYER 1



SIMPSON LAGOON  
M2 TIDE (AMP=8 CM, IN PHASE ON OPEN BOUNDARIES) WIND FROM 250 DEG T AT 26 KT

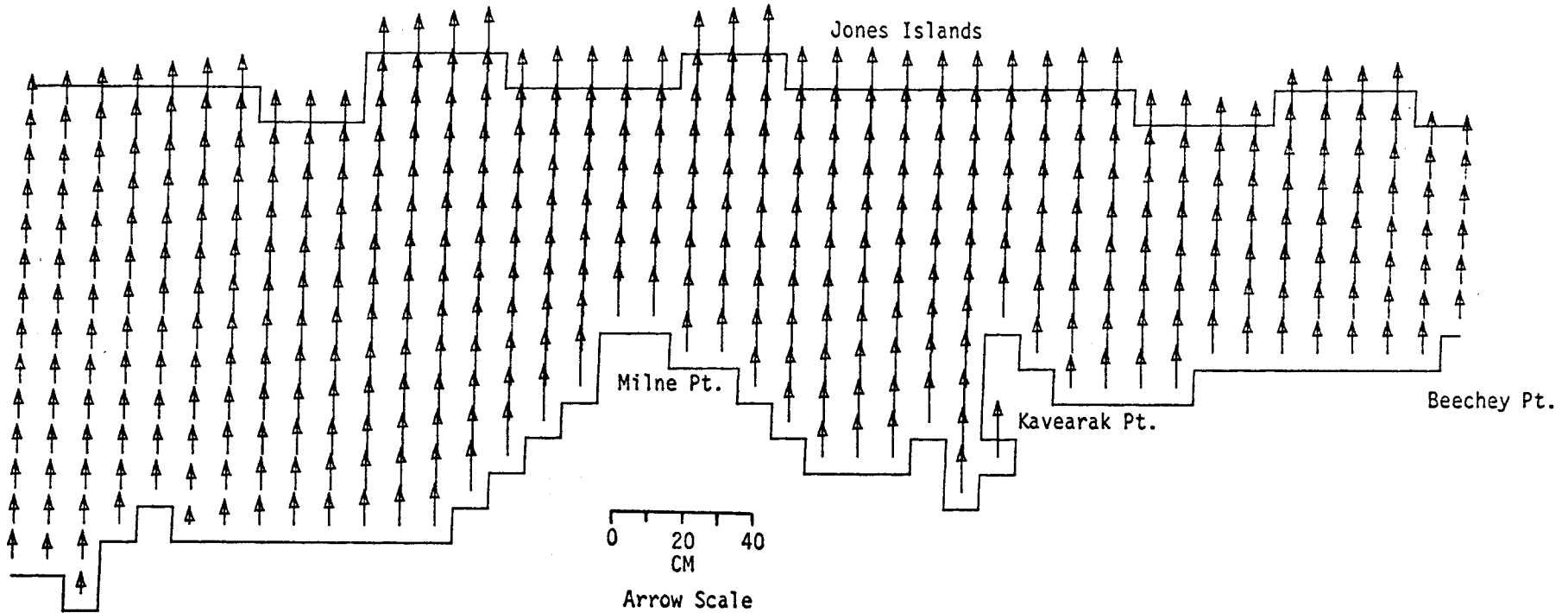
SEA LEVEL

TIME= 36000SEC

LAYER 1

MODEL NO 200

728



SIMPSON LAGOON

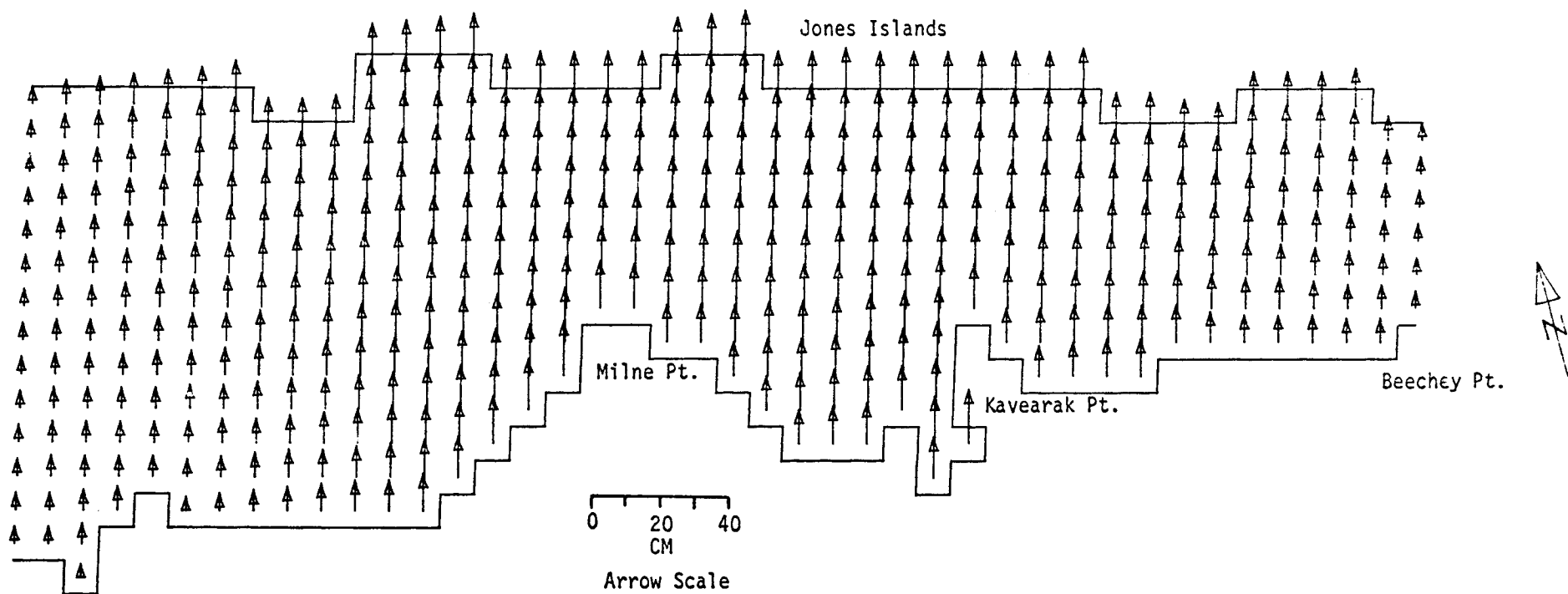
M2 TIDE (AMP=8 CM, IN PHASE ON OPEN BOUNDARIES) WIND FROM 250 DEG T AT 26 KT

MODEL NO 200  
627

SEA LEVEL

TIME= 39600SEC

LAYER 1



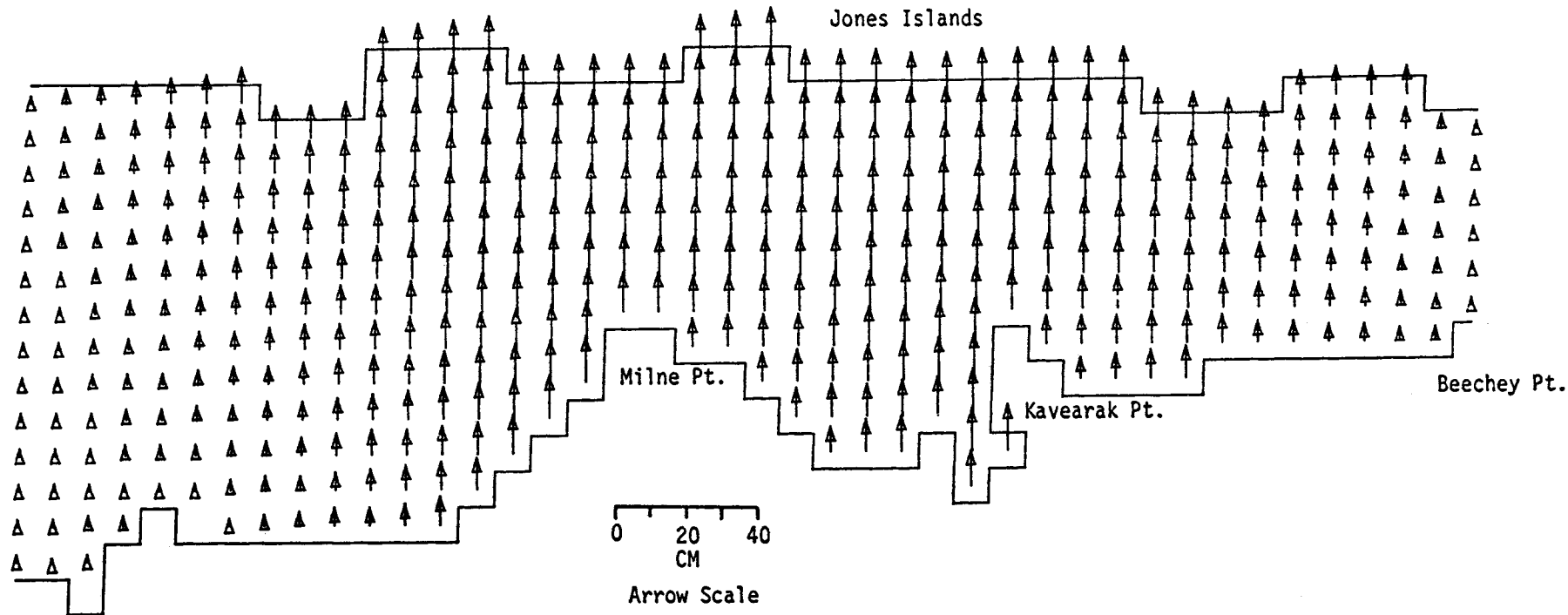
SIMPSON LAGOON  
M2 TIDE (AMP=8 CM, IN PHASE ON OPEN BOUNDARIES) WIND FROM 250 DEG T AT 26 KT

SEA LEVEL

TIME= 43200SEC

LAYER 1

MODEL NO 200  
037



SIMPSON LAGOON  
M2 TIDE (AMP=8 CM, IN PHASE ON OPEN BOUNDARIES) WIND FROM 250 DEG T AT 26 KT



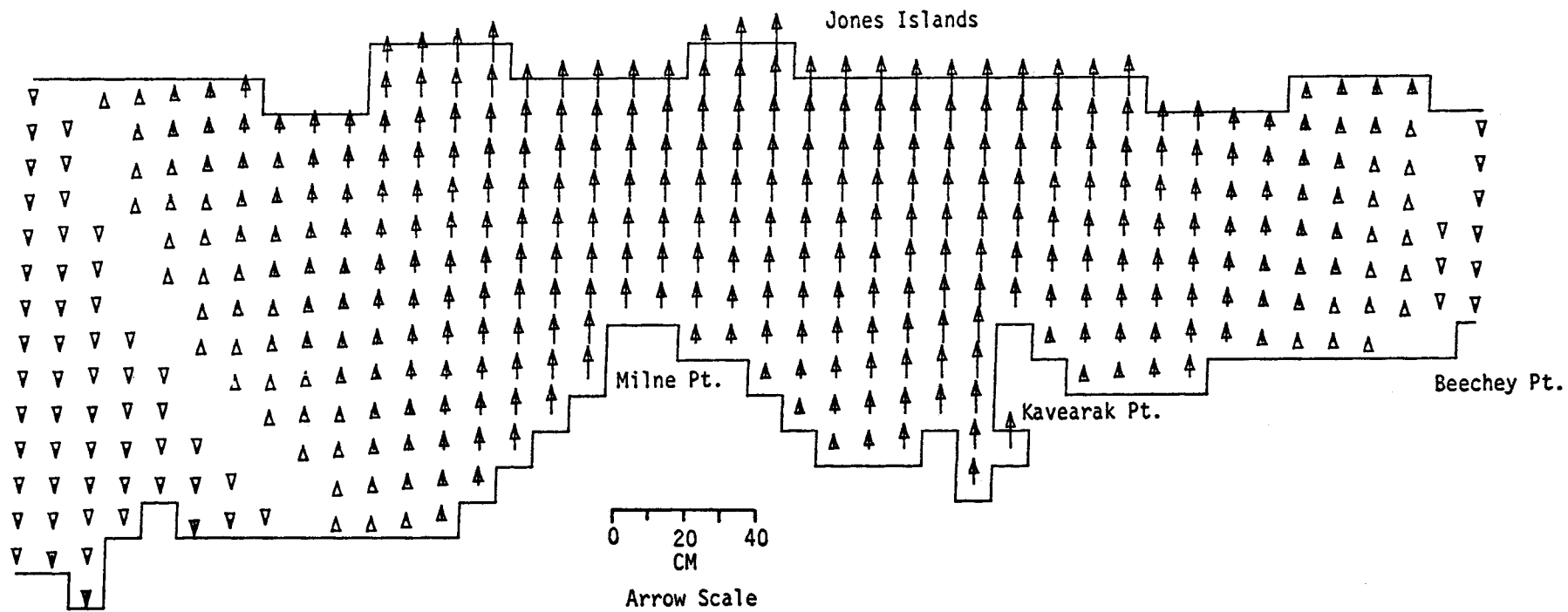
SEA LEVEL

TIME= 46800SEC

LAYER 1

MODEL NO 200

TS1



SIMPSON LAGOON

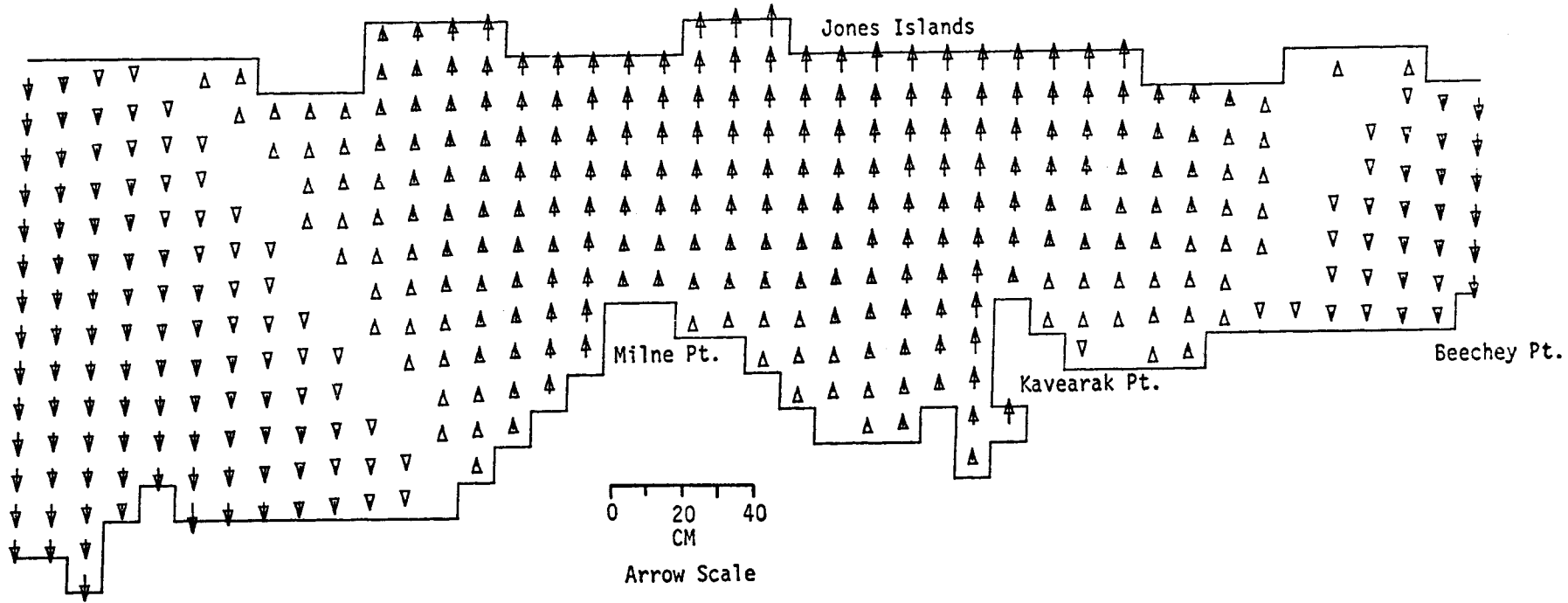
M2 TIDE (AMP=8 CM, IN PHASE ON OPEN BOUNDARIES) WIND FROM 250 DEG T AT 26 KT

SEA LEVEL

TIME= 50400SEC

LAYER 1

MODEL NO 200  
732



SIMPSON LAGOON  
M2 TIDE (AMP=8 CM, IN PHASE ON OPEN BOUNDARIES) WIND FROM 250 DEG T AT 26 KT

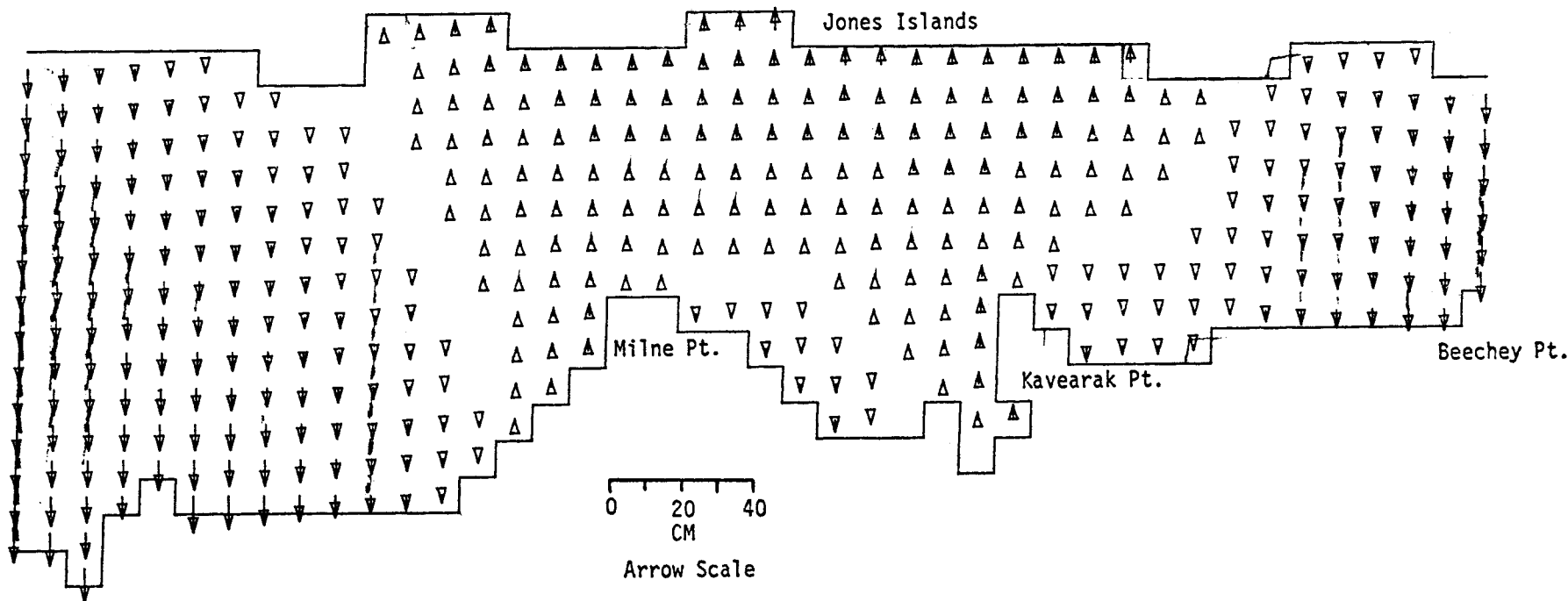
SEA LEVEL

TIME= 54000SEC

LAYER 1

MODEL NO 200

733



SIMPSON LAGOON  
M2 TIDE (AMP=8 CM, IN PHASE ON OPEN BOUNDARIES) WIND FROM 250 DEG T AT 26 KT

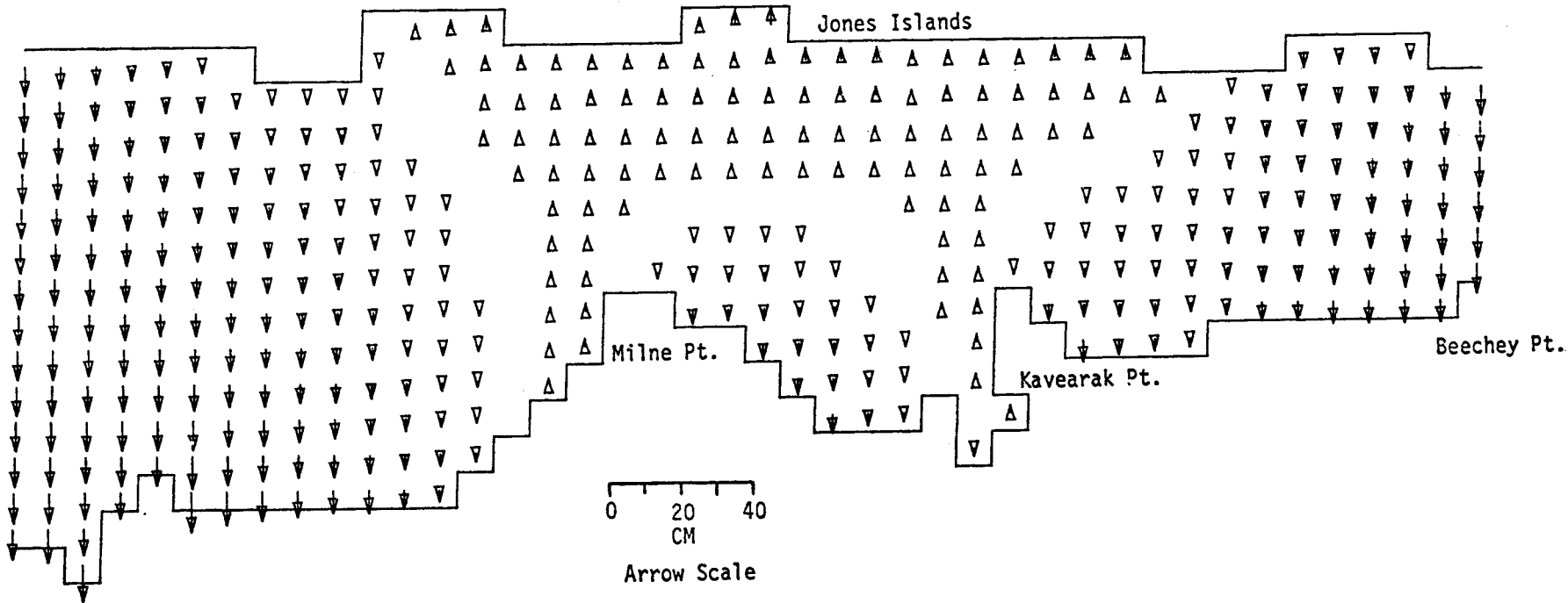
SEA LEVEL

TIME= 57600SEC

LAYER 1

MODEL NO 200

734



SIMPSON LAGOON  
M2 TIDE (AMP=8 CM, IN PHASE ON OPEN BOUNDARIES) WIND FROM 250 DEG T AT 26 KT

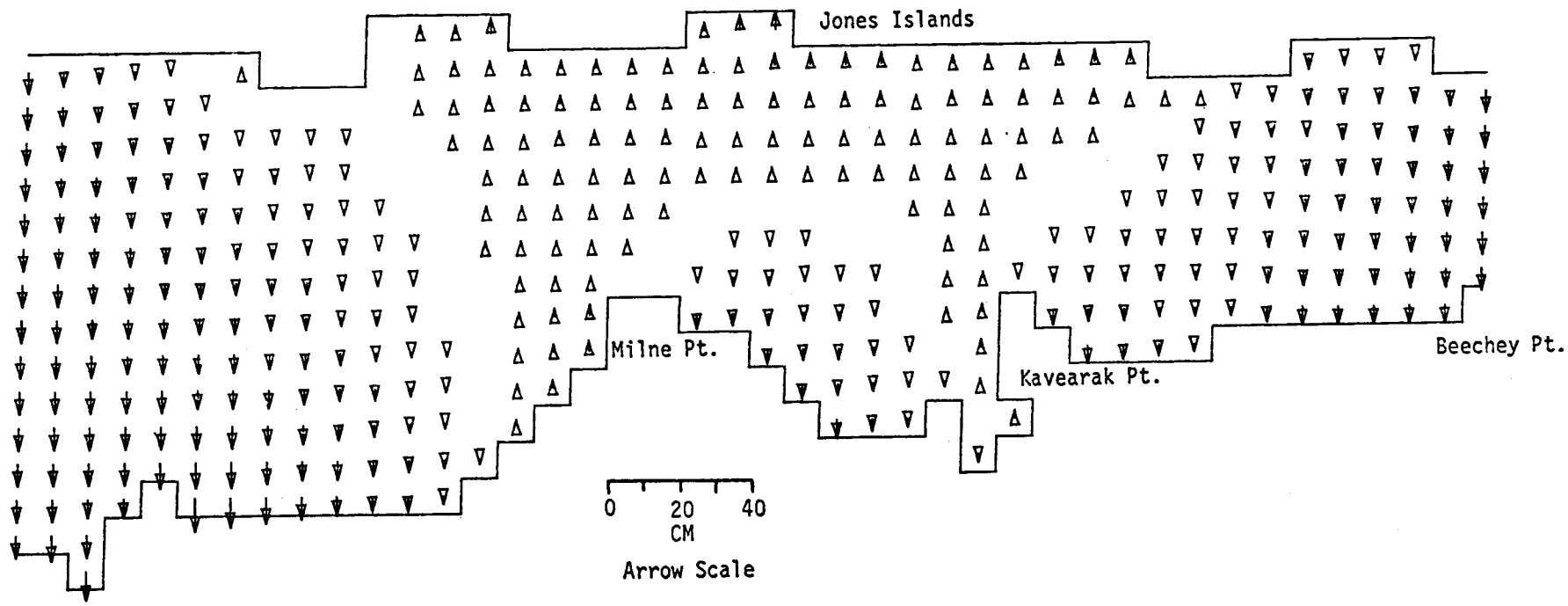
SEA LEVEL

TIME= 61200SEC

LAYER 1

MODEL NO 200

735



SIMPSON LAGOON  
M2 TIDE (AMP=8 CM, IN PHASE ON OPEN BOUNDARIES) WIND FROM 250 DEG T AT 26 KT

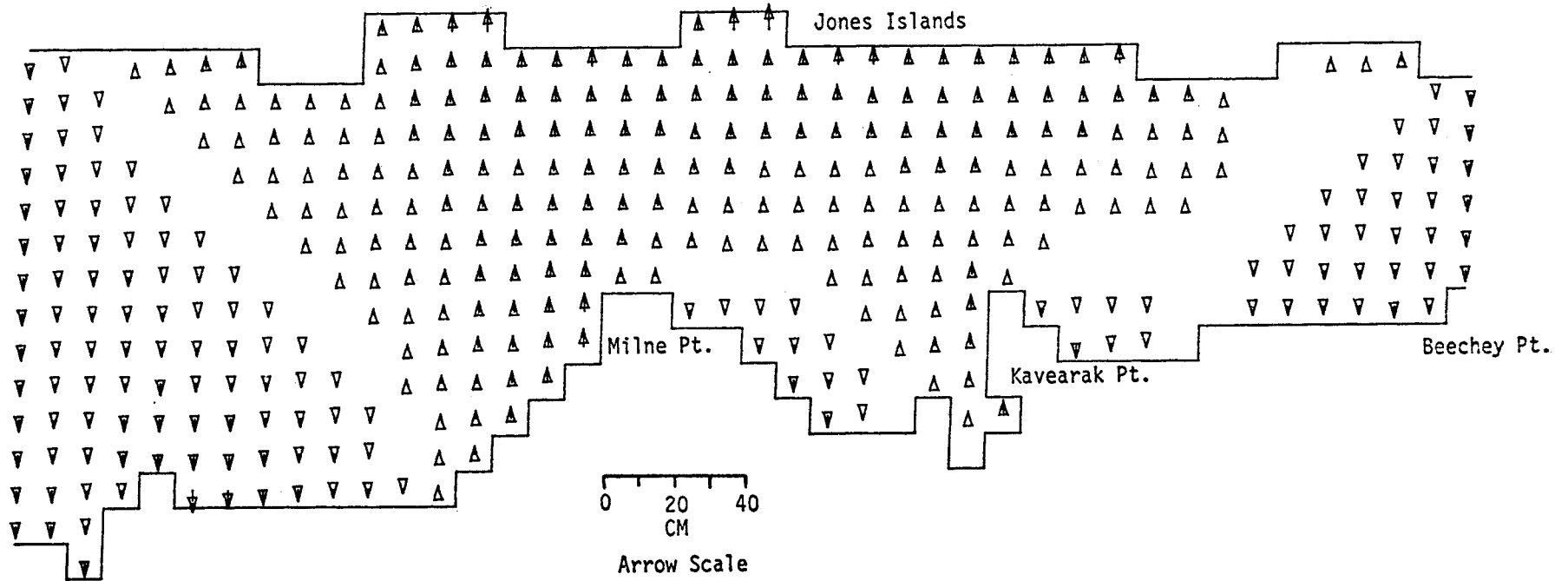
SEA LEVEL

TIME= 64800SEC

LAYER 1

MODEL NO 200

987.



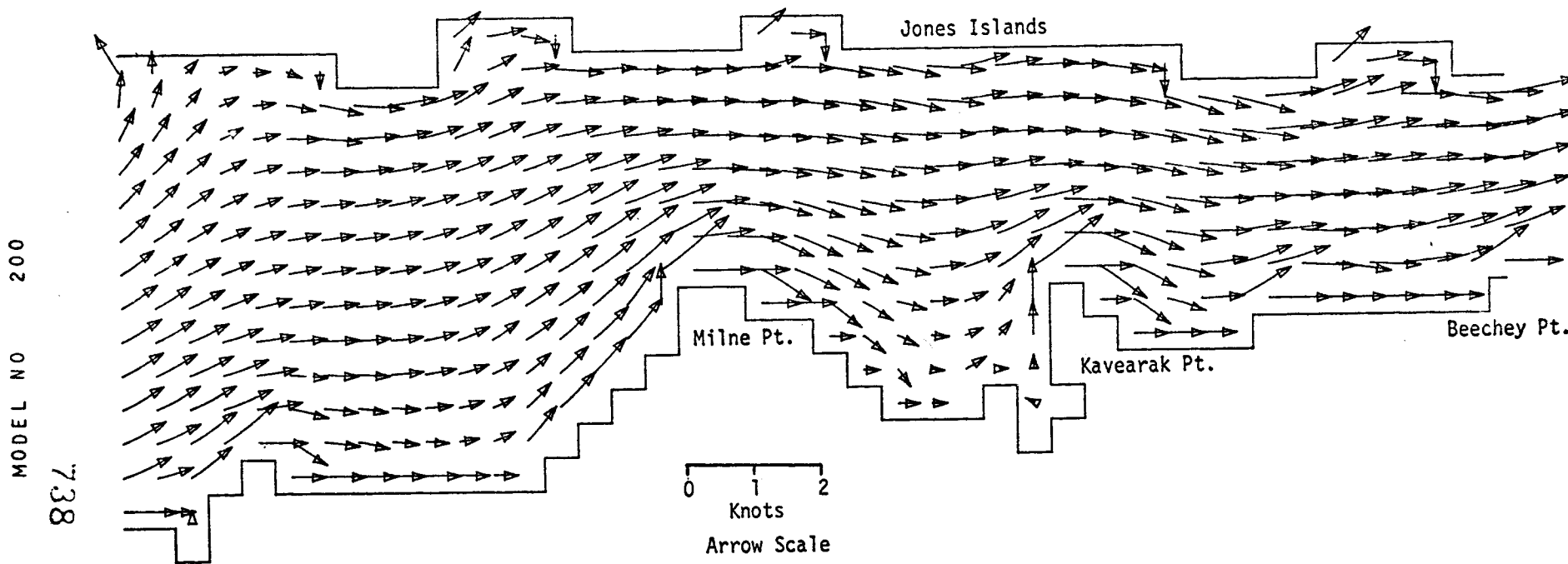
SIMPSON LAGOON  
M2 TIDE (AMP=8 CM, IN PHASE ON OPEN BOUNDARIES) WIND FROM 250 DEG T AT 26 KT

CURRENTS

CURRENTS

TIME= 3600SEC

LAYER 1



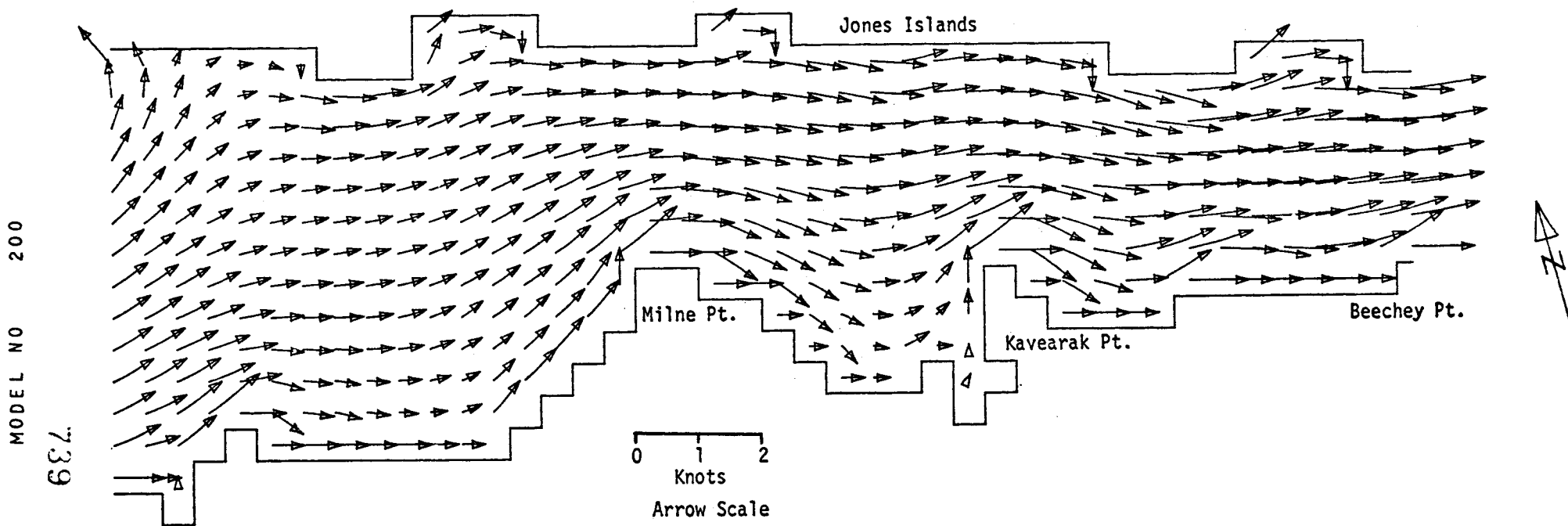
SIMPSON LAGOON  
M2 TIDE (AMP=8 CM, IN PHASE ON OPEN BOUNDARIES) WIND FROM 250 DEG T AT 26 KT



CURRENTS

TIME= 7200SEC

LAYER 1



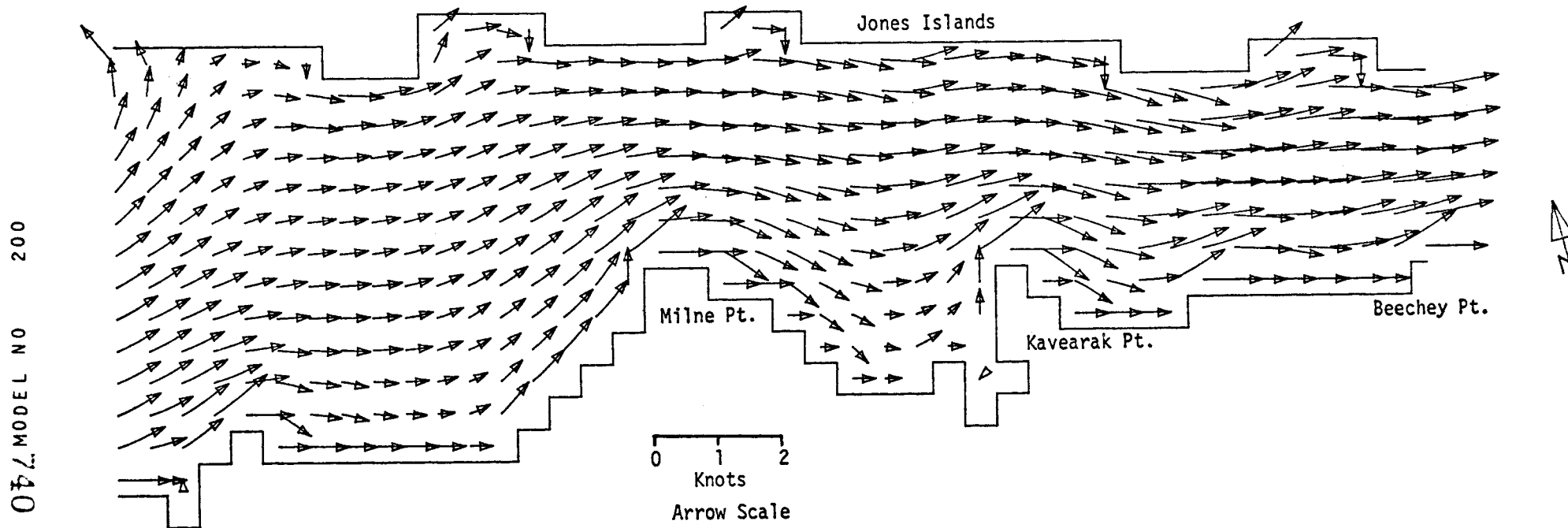
SIMPSON LAGOON

M2 TIDE (AMP=8 CM, IN PHASE ON OPEN BOUNDARIES) WIND FROM 250 DEG T AT 26 KT

CURRENTS

TIME= 10800SEC

LAYER 1

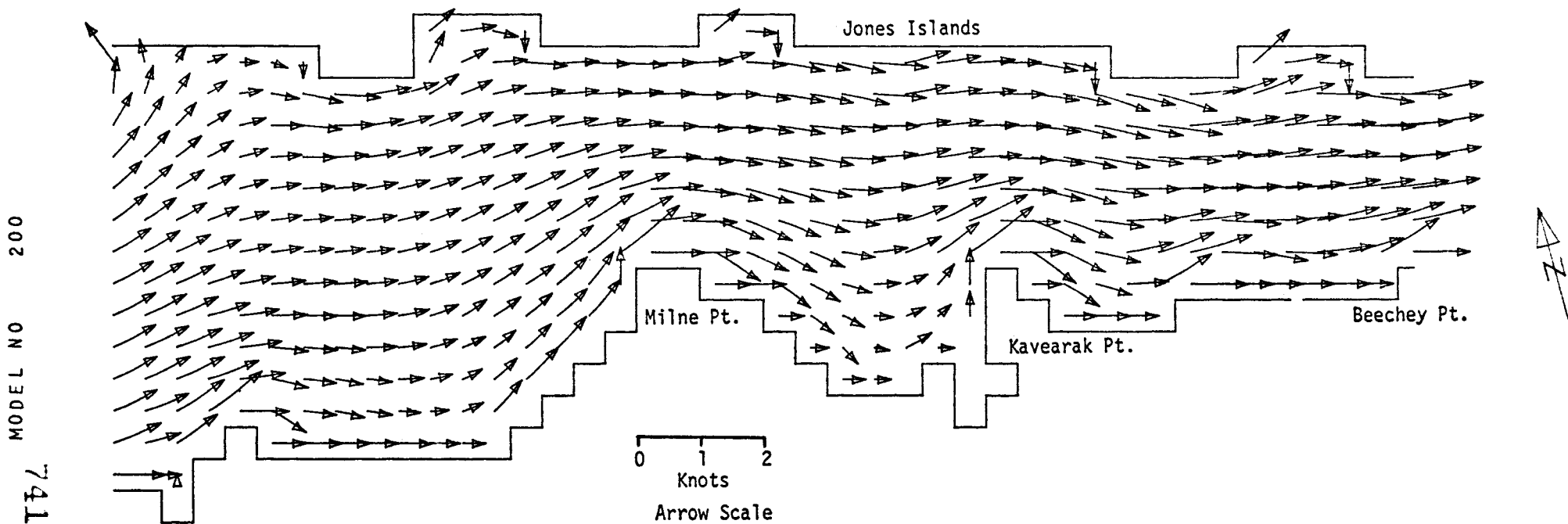


SIMPSON LAGOON  
M2 TIDE (AMP=8 CM. IN PHASE ON OPEN BOUNDARIES) WIND FROM 250 DEG T AT 26 KT

CURRENTS

TIME= 14400SEC

LAYER 1

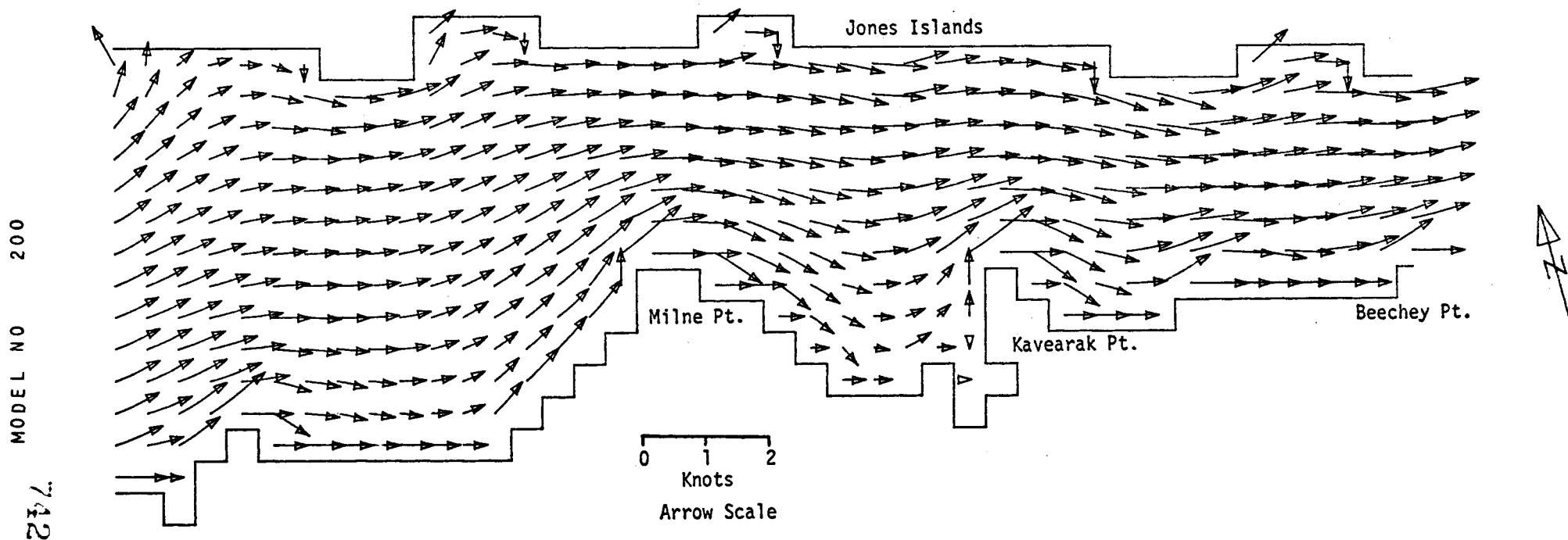


SIMPSON LAGOON  
M2 TIDE (AMP=8 CM, IN PHASE ON OPEN BOUNDARIES) WIND FROM 250 DEG T AT 26 KT

CURRENTS

TIME= 18000SEC

LAYER 1

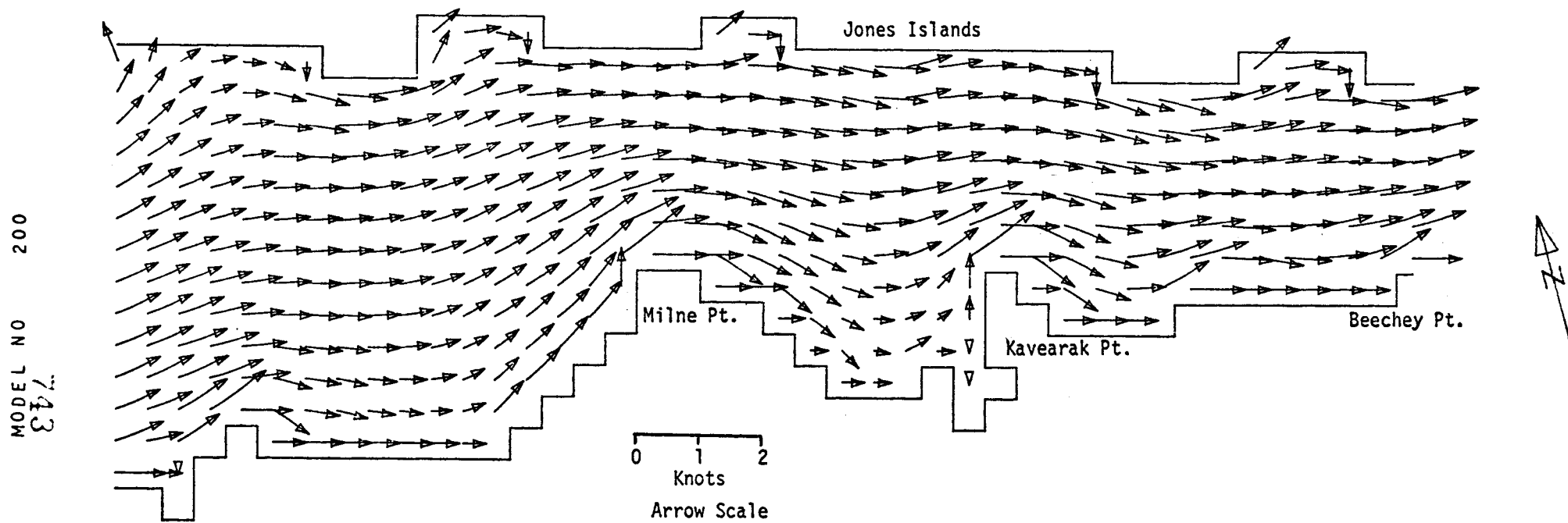


SIMPSON LAGOON  
M2 TIDE (AMP=6 CM, IN PHASE ON OPEN BOUNDARIES) WIND FROM 250 DEG T AT 26 KT

CURRENTS

TIME= 21600SEC

LAYER 1



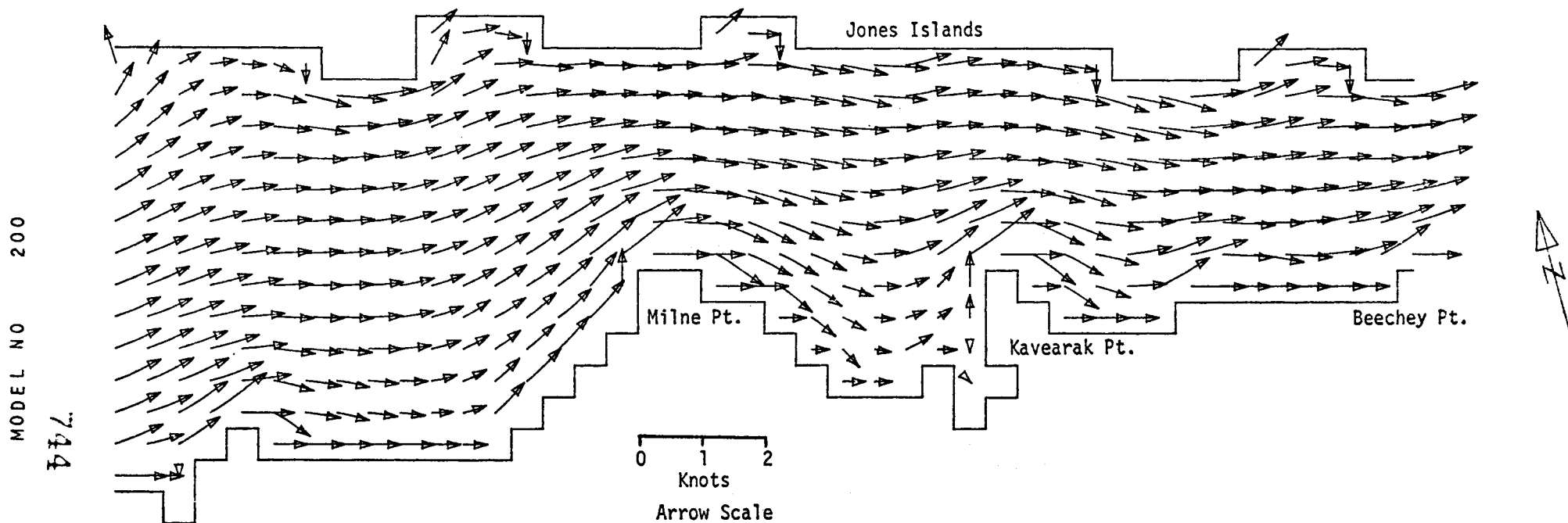
SIMPSON LAGOON

M2 TIDE (AMP=8 CM. IN PHASE ON OPEN BOUNDARIES) WIND FROM 250 DEG T AT 26 KT

CURRENTS

TIME= 25200SEC

LAYER 1

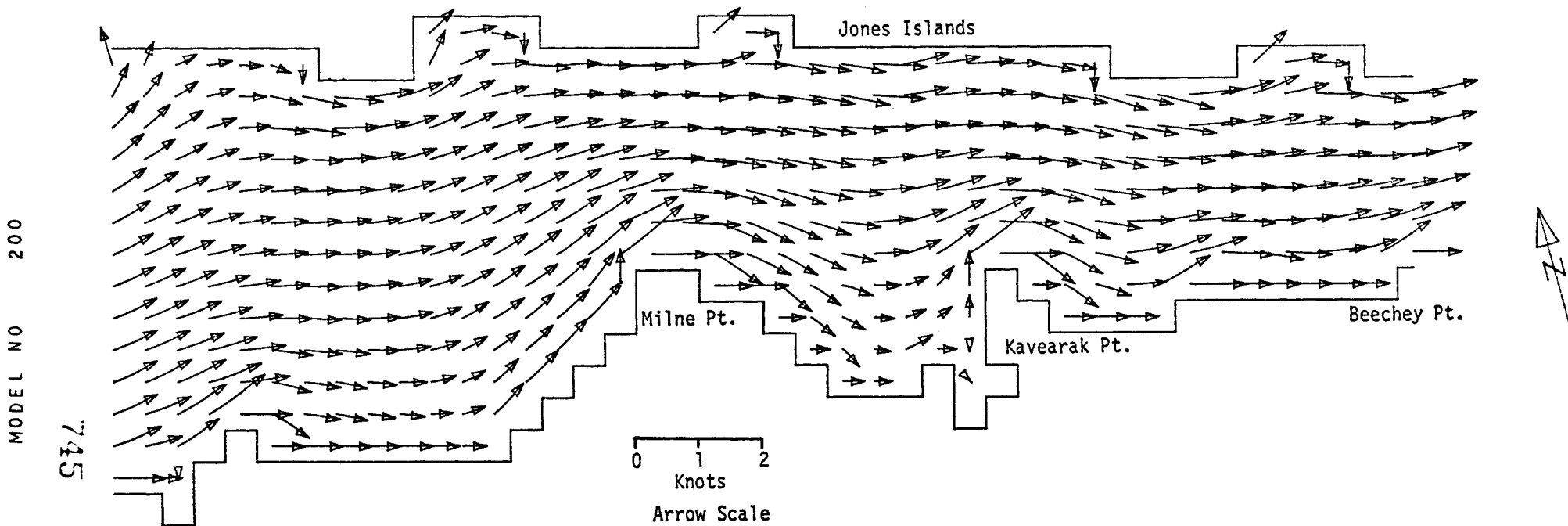


SIMPSON LAGOON  
M2 TIDE (AMP=8 CM, IN PHASE ON OPEN BOUNDARIES) WIND FROM 250 DEG T AT 26 KT

CURRENTS

TIME= 28800SEC

LAYER 1



SIMPSON LAGOON

M2 TIDE (AMP=8 CM, IN PHASE ON OPEN BOUNDARIES) WIND FROM 250 DEG T AT 26 KT

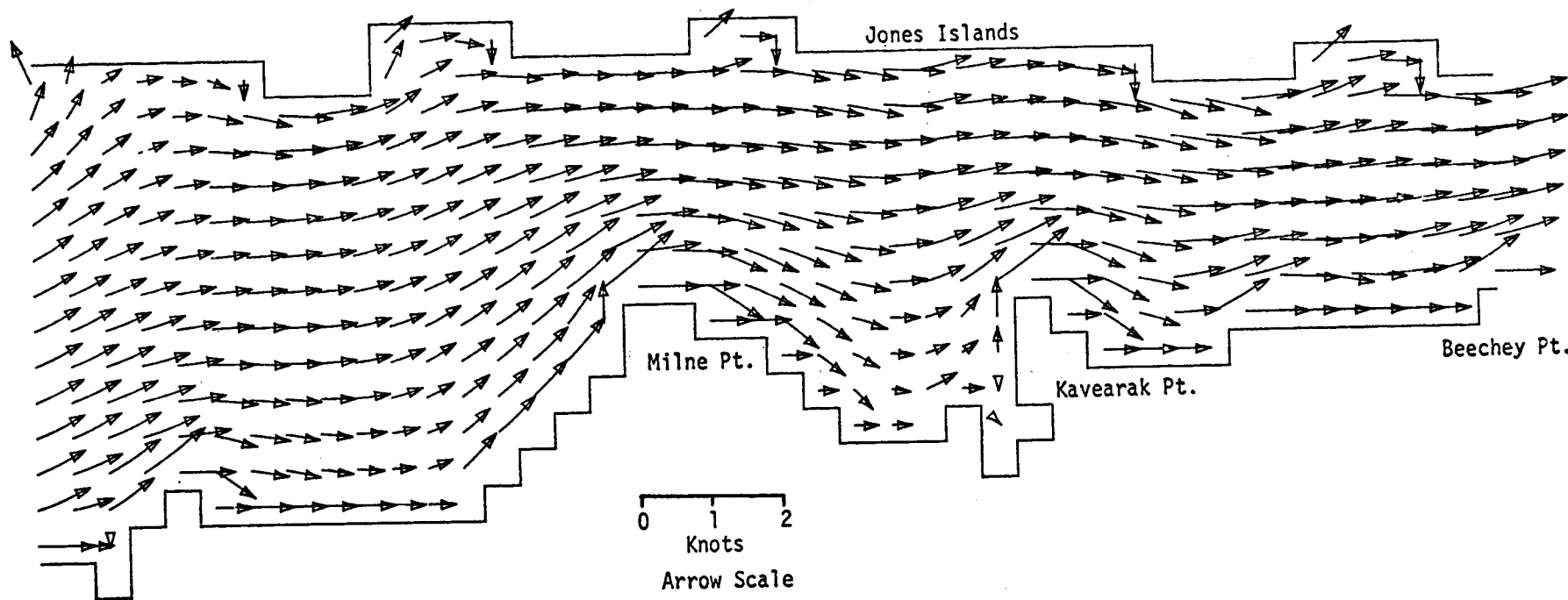
CURRENTS

TIME= 32400SEC

LAYER 1

MODEL NO. 200

746



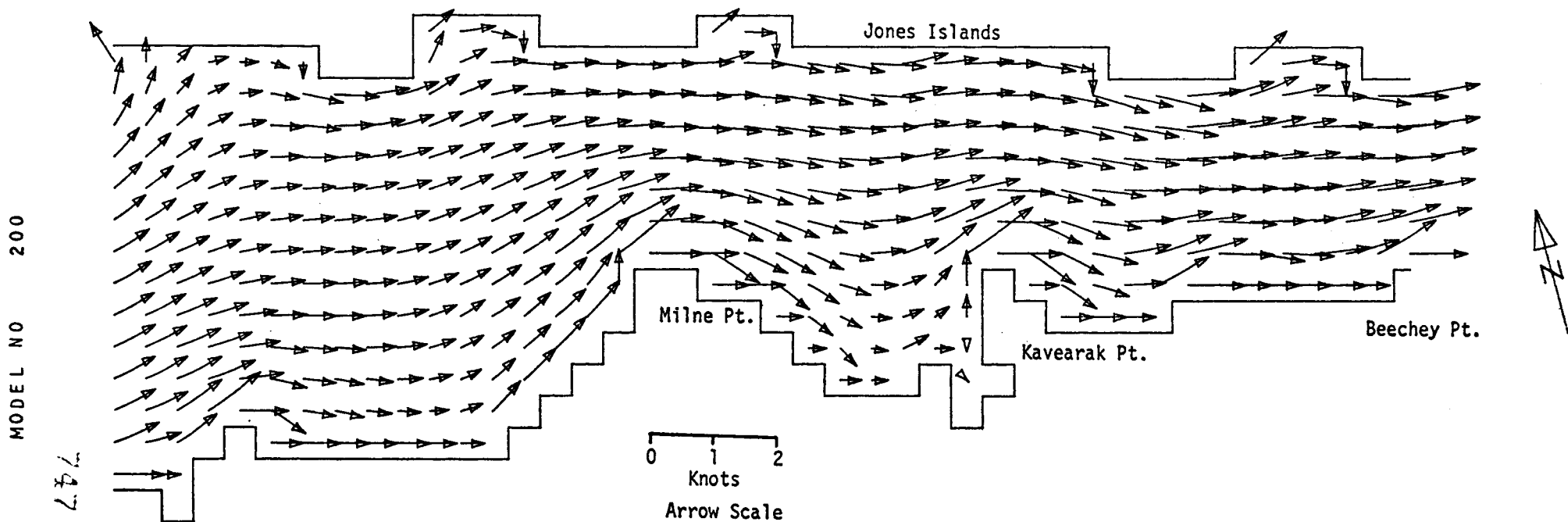
SIMPSON LAGOON  
M2 TIDE (AMP=8 CM, IN PHASE ON OPEN BOUNDARIES) WIND FROM 250 DEG T AT 26 KT



CURRENTS

TIME= 36000SEC

LAYER 1

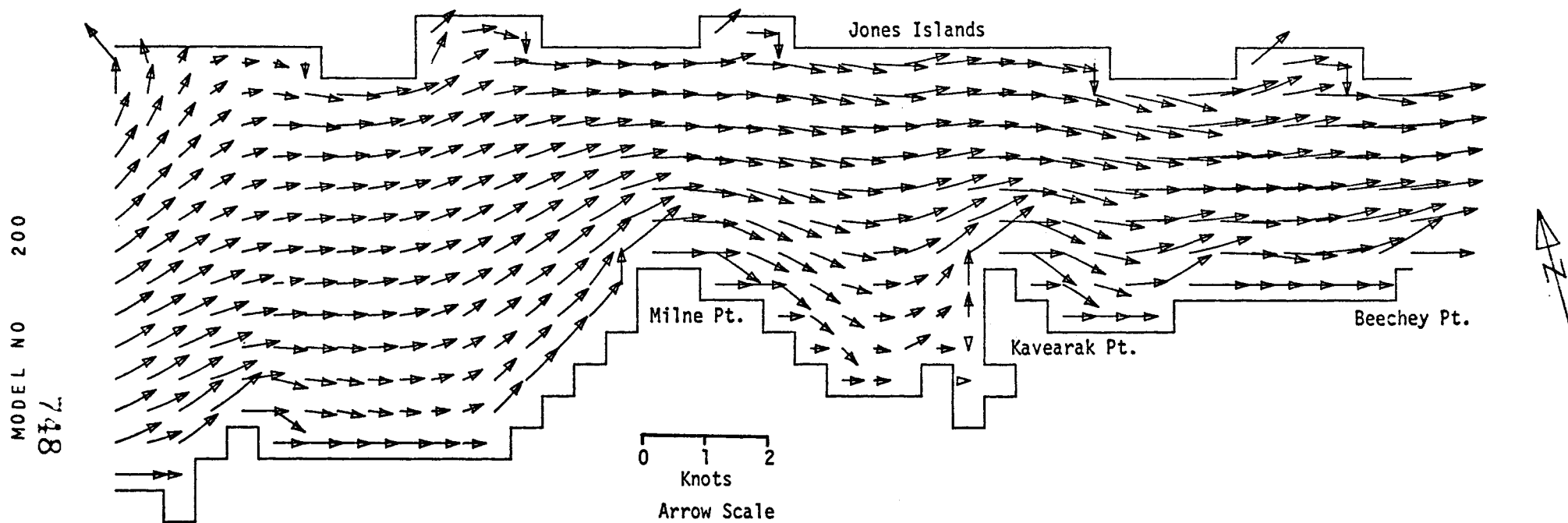


SIMPSON LAGOON  
M2 TIDE (AMP=8 CM, IN PHASE ON OPEN BOUNDARIES) WIND FROM 250 DEG T AT 26 KT

CURRENTS

TIME= 39600SEC

LAYER 1



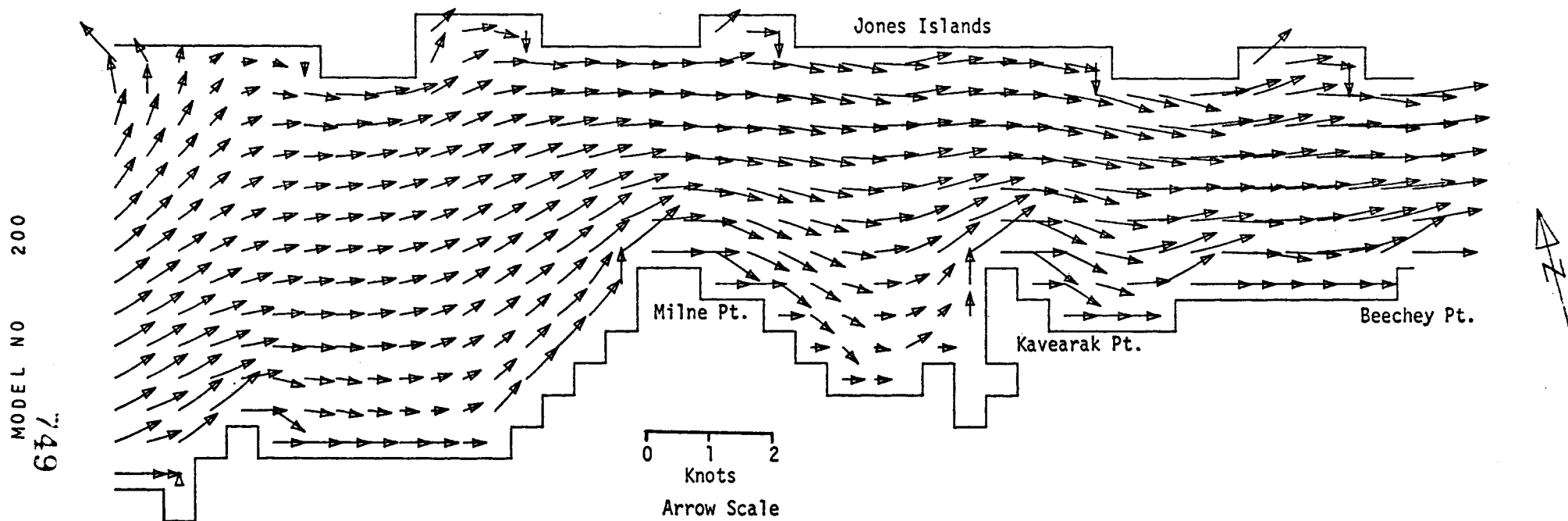
SIMPSON LAGOON

M2 TIDE (AMP=8 CM, IN PHASE ON OPEN BOUNDARIES) WIND FROM 250 DEG T AT 26 KT

CURRENTS

TIME= 43200SEC

LAYER 1



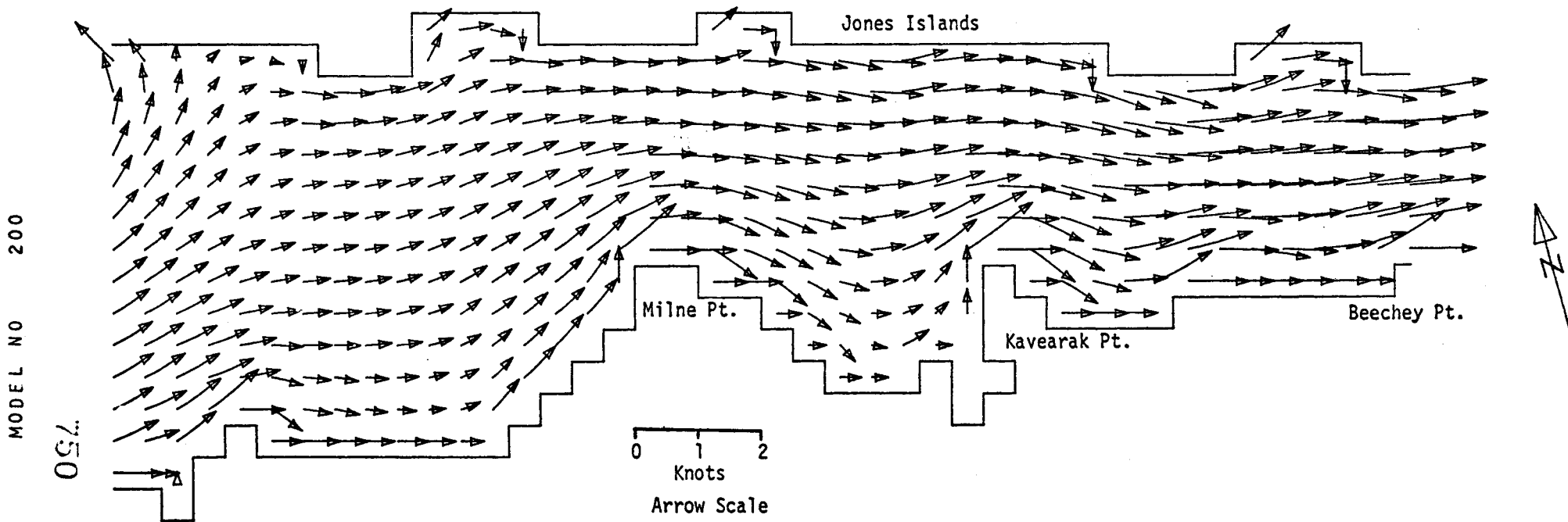
SIMPSON LAGOON

M2 TIDE (AMP=8 CM, IN PHASE ON OPEN BOUNDARIES) WIND FROM 250 DEG T AT 26 KT

CURRENTS

TIME= 46800SEC

LAYER 1



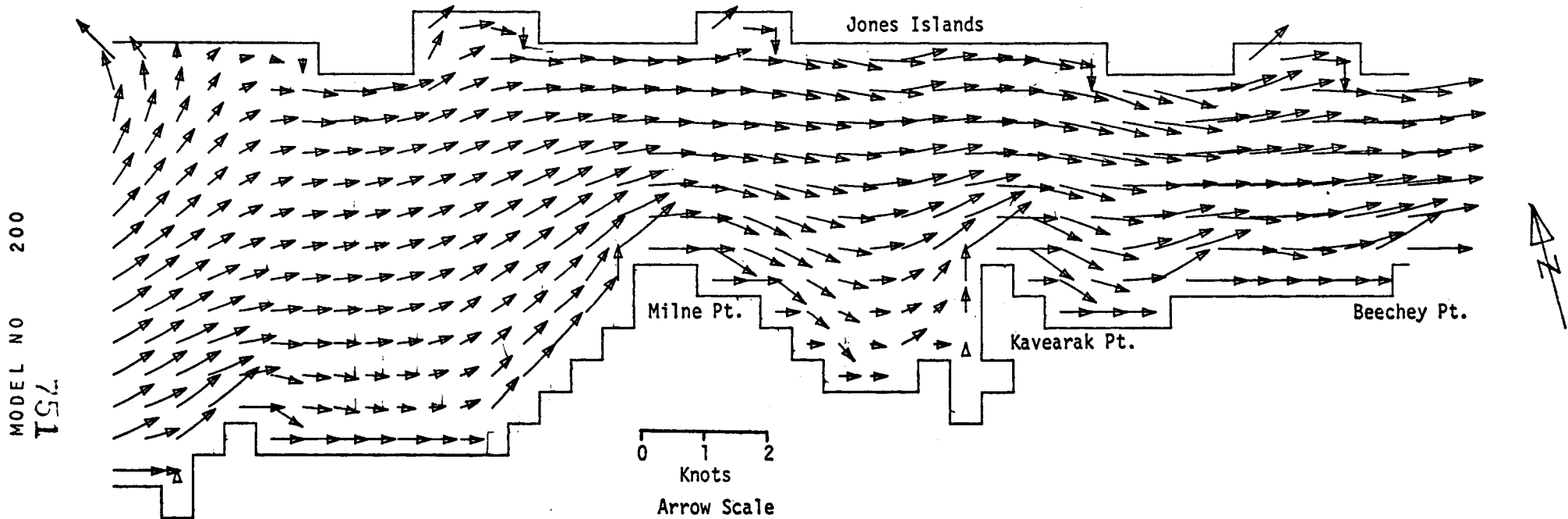
SIMPSON LAGOON

M2 TIDE (AMP=8 CM, IN PHASE ON OPEN BOUNDARIES) WIND FROM 250 DEG T AT 26 KT

CURRENTS

TIME= 50400SEC

LAYER 1

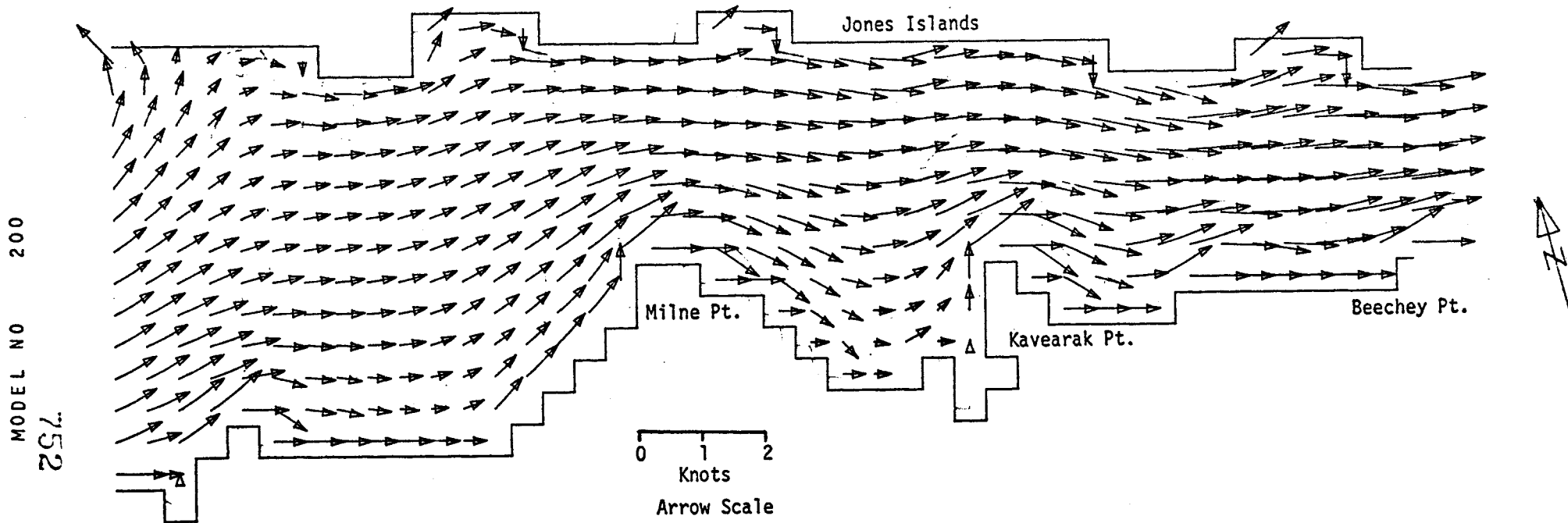


SIMPSON LAGOON  
M2 TIDE (AMP=8 CM, IN PHASE ON OPEN BOUNDARIES) WIND FROM 250 DEG T AT 26 KT

CURRENTS

TIME= 54000SEC

LAYER 1



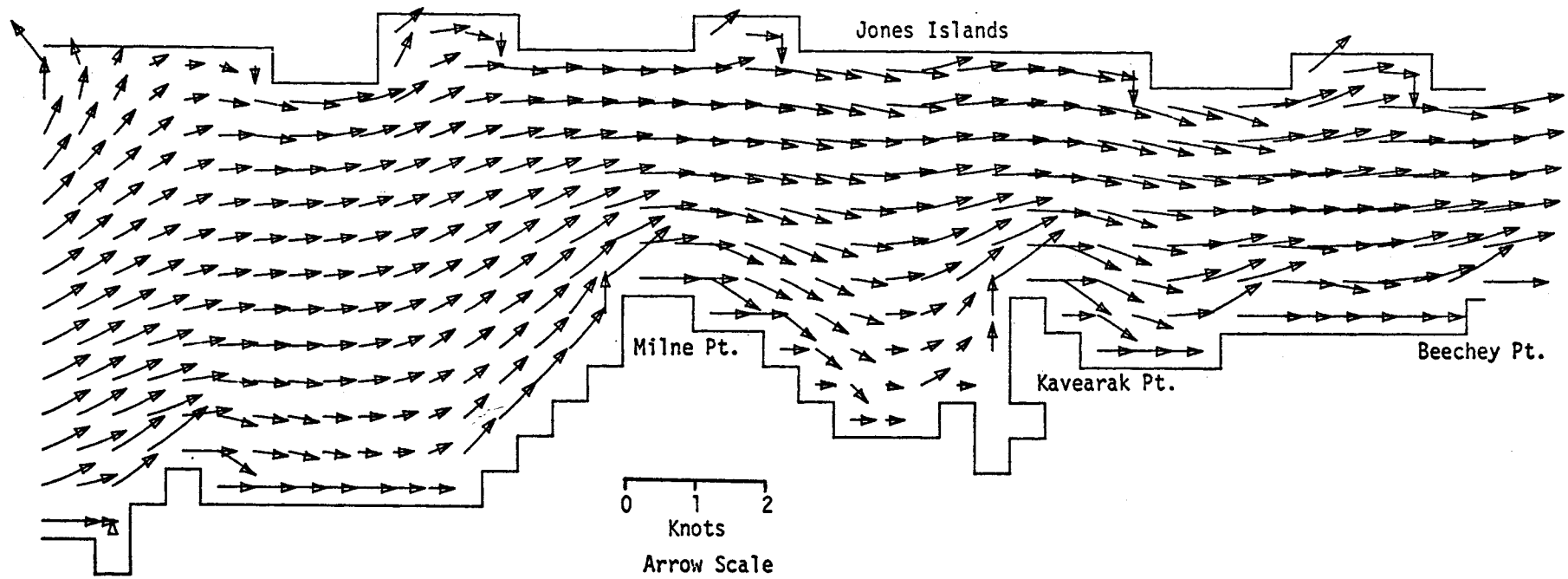
SIMPSON LAGOON  
M2 TIDE (AMP=8 CM, IN PHASE ON OPEN BOUNDARIES) WIND FROM 250 DEG T AT 26 KT

CURRENTS

TIME= 57600SEC

LAYER 1

MODEL NO  
200  
753

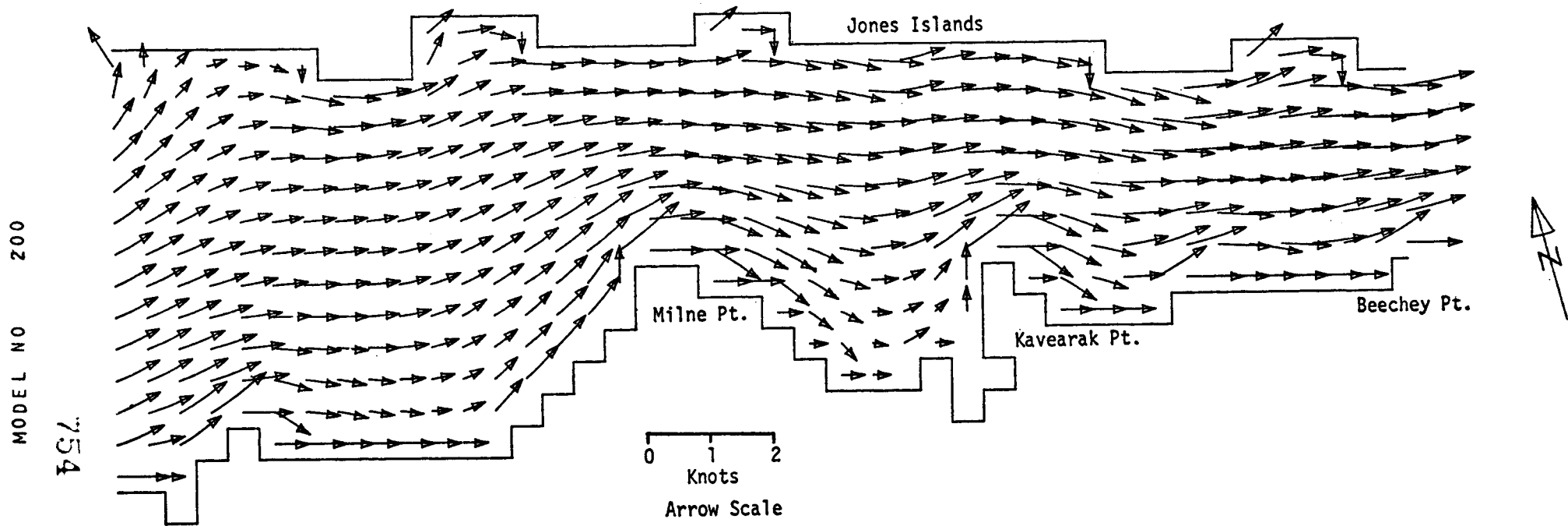


SIMPSON LAGOON  
M2 TIDE (AMP=8 CM, IN PHASE ON OPEN BOUNDARIES) WIND FROM 250 DEG T AT 26 KT

CURRENTS

TIME= 61200SEC

LAYER 1



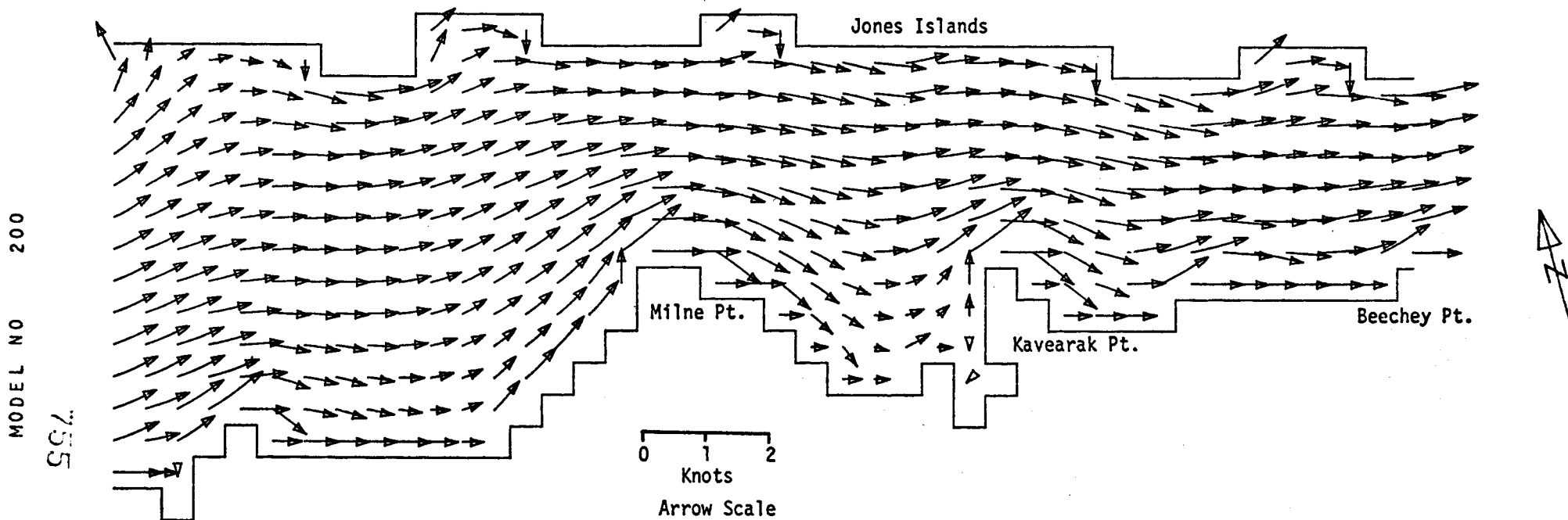
SIMPSON LAGOON  
M2 TIDE (AMP=8 CM, IN PHASE ON OPEN BOUNDARIES) WIND FROM 250 DEG T AT 26 KT



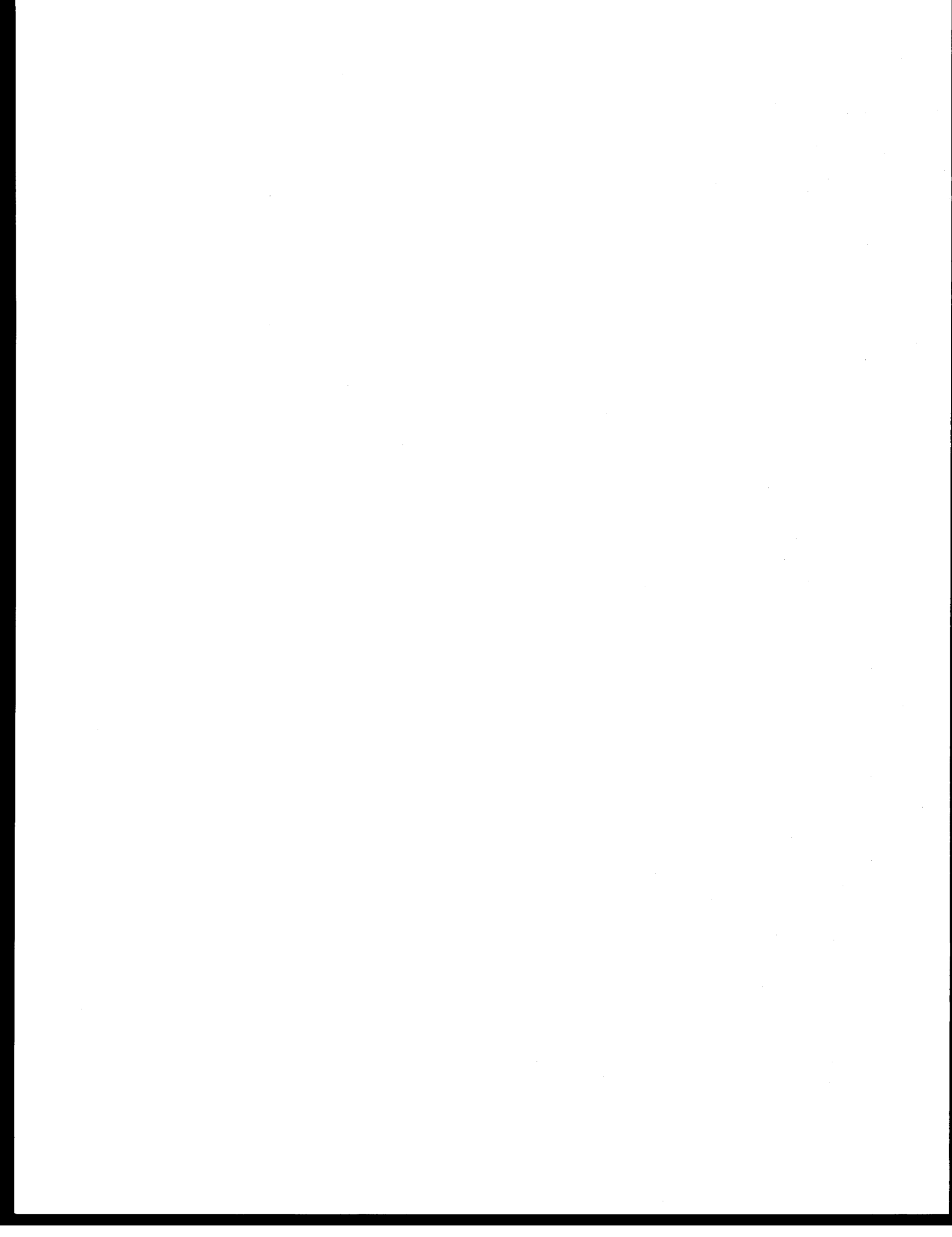
CURRENTS

TIME= 64800SEC

LAYER 1



SIMPSON LAGOON  
M2 TIDE (AMP=8 CM, IN PHASE ON OPEN BOUNDARIES) WIND FROM 250 DEG T AT 26 KT



ANNUAL REPORT

MARINE CLIMATOLOGY OF THE GULF OF ALASKA AND  
THE BERING AND BEAUFORT SEAS

Harold W. Searby  
Arctic Environmental Information and Data Center

Contract # 03-5-022-56  
Research Unit # 347  
Reporting Period 7/1/75-3/31/76  
Number of Pages 12

UNIVERSITY OF ALASKA

March 31, 1976

I. Summary of objectives, conclusions and implications with respect to OCS oil and gas development.

The objective of the project is to provide detailed marine and coastal climatology for input into the planning and operational phases of oil and gas development on the continental shelf. Conclusions normally resulting from a project will not result from this one. Decisions coming from private industry relating to their projects will use the climatological information as a partial basis for their conclusions. The same reasoning applies for implications.

II. Introduction.

- A. All available climatological data for the Gulf of Alaska, Bering and Beaufort Seas will be used in determining and publishing the present state of the knowledge in this area. To best do this an atlas will be produced and published for each of the three areas mentioned above. Summarized data for period of record for coastal stations will also be included.

\*This project is being conducted jointly with the National Climatic Center (NCC), a part of NOAA's Environmental Data Service. Principal Investigator for the NCC is William A. Brower, Jr., D5312. Much of the data summary work mentioned above will be done in Asheville, North Carolina, at the NCC.

- B. Specific objectives are to present information on temperature, precipitation, wind, and how they relate to such things as cloud cover, wave heights, and visibility (fog). Storm tracks and frequencies, storm surges and coastal flooding are being studied and will be part of the presentation. Such things as potential superstructure icing, tides, surface currents, immersion hypothermia and topography of both land and sea will also be included. More detail on content is found in the original proposal.
- C. Extremely severe weather conditions can and do occur over all of the continental shelf areas of Alaska as well as coastal and interior portions. This makes it important that the intensities and durations of storms are known and available for use in planning, design and actual operations.

### III. Current state of knowledge.

It is not necessary or practical timewise to acquire new data through field programs. It is necessary, however, and is being done, to combine large quantities of raw data that have been acquired in recent years. Knowledge of the specific parameters mentioned in II above is already in a published form, but for some areas is based on small amounts of data. It is not only possible but probable that much of the present shelf material will change substantially with the addition of more recent data.

### IV. Study area.

Included in the study area is the outer continental shelf of all of Alaska, and the entire coast. The area is to be covered by three atlases, one each for the Gulf of Alaska, the Bering Sea, and the Beaufort Sea.

### V. Sources, methods and rationale of data collection.

No new data will be collected through field programs. The data used are those already in the files of one of Environmental Data Service's numerous data centers. These data come from many sources. The marine data consist of observations made by "ships of opportunity" traversing Alaskan waters. The land data have been acquired from the National Weather Service through its various observational programs.

### VI. Results.

Results for this project will be in the form of the completed atlases. At this point efforts have been toward searching out and compiling data. Following this stage the data will be put into a format for publication. The format will be both tabular and graphic with emphasis on graphics. Samples are enclosed.

VII. Discussion.

Although increased knowledge is expected to result from this project, portions of the study area, because of their isolated nature, will have insufficient data for an accurate determination of all weather conditions. The resulting summaries will be qualified to show this.

VIII. Conclusions.

The summary work done for this project will update previous summaries and in addition add several new ones. It will also place together in one publication what has previously been spread through several publications. Both time and money will be saved by users.

IX. Needs for further study.

Considerable attention has been given to developing a history of storm surges. However, the scope of this study in terms of funds and time is such that more work needs to be done on this particular item. A fairly extensive bibliography can be put together on storm surges, but the ones surveyed by the principal investigator so far do not make a study of the storm itself. If this were done, it would be possible to more accurately predict the occurrence of storms having a potential for causing damage. A better knowledge of the stresses resulting from such storms will help in the engineering of equipment and structures used in the development of the outer continental shelf.

X. Summary of 4th quarter operations.

A. Ship Activities

None

B. Laboratory Activities

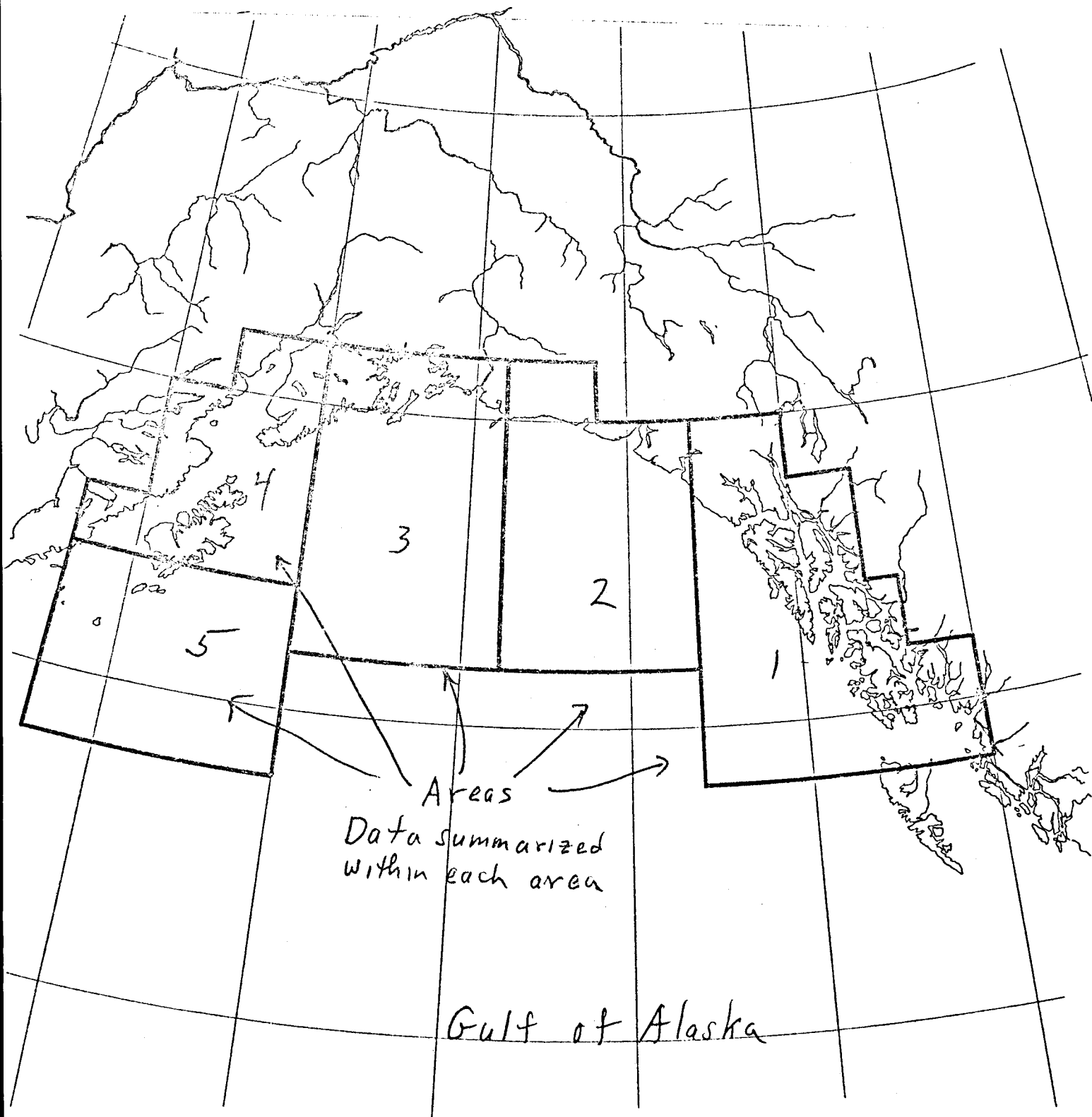
None

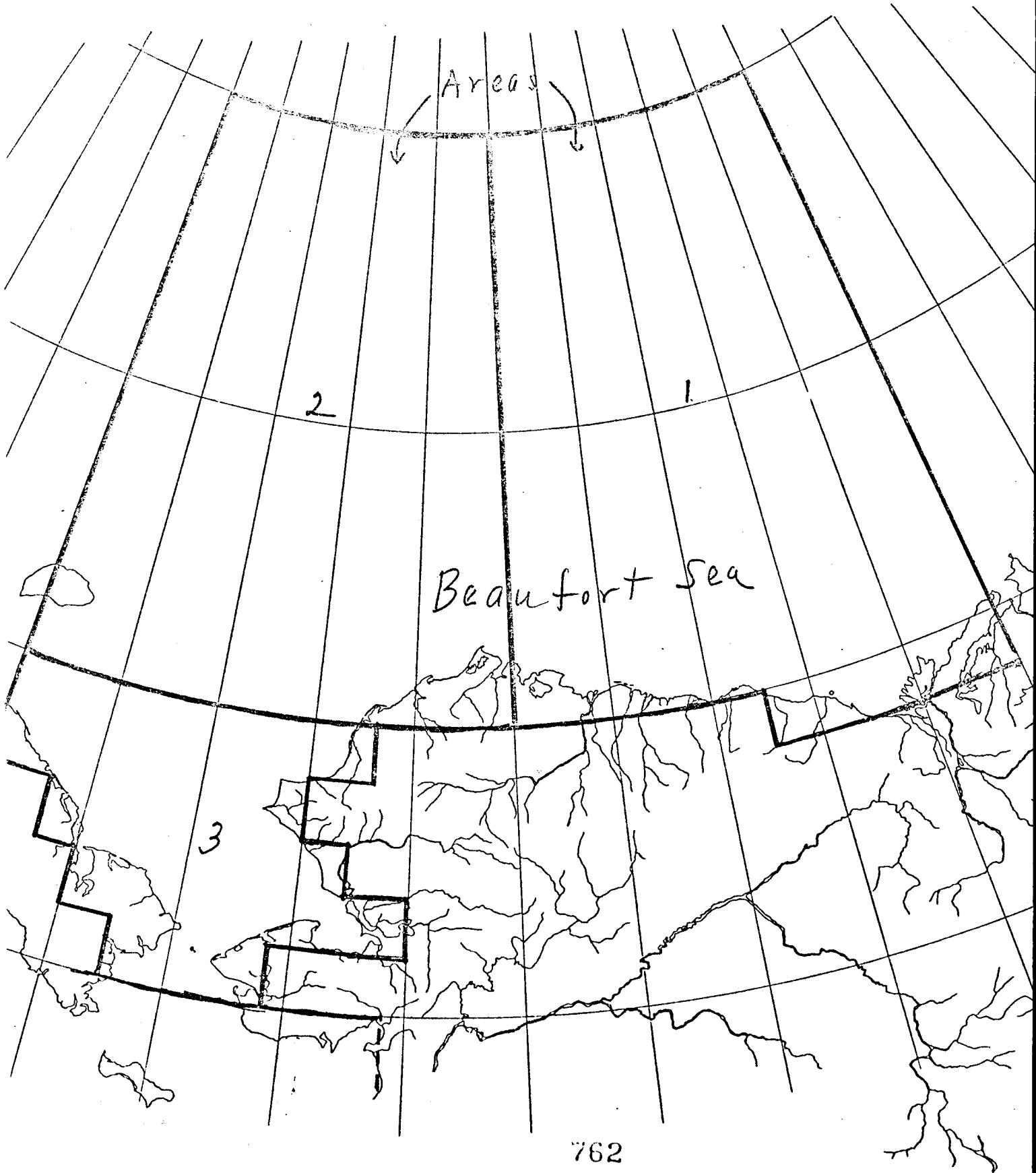
C. Results

To date, about 90 percent of the extremes data has been compiled, and additional storm damage information is being sought. No analysis work has been made available from the NCC as yet. Our graphics department has completed the base maps to be used in publication. We expect to make a coordination trip to the NCC during the next quarter. Results of this coordination will make it possible to move into another phase of the project, that of graphics work in preparation for putting together a final product.

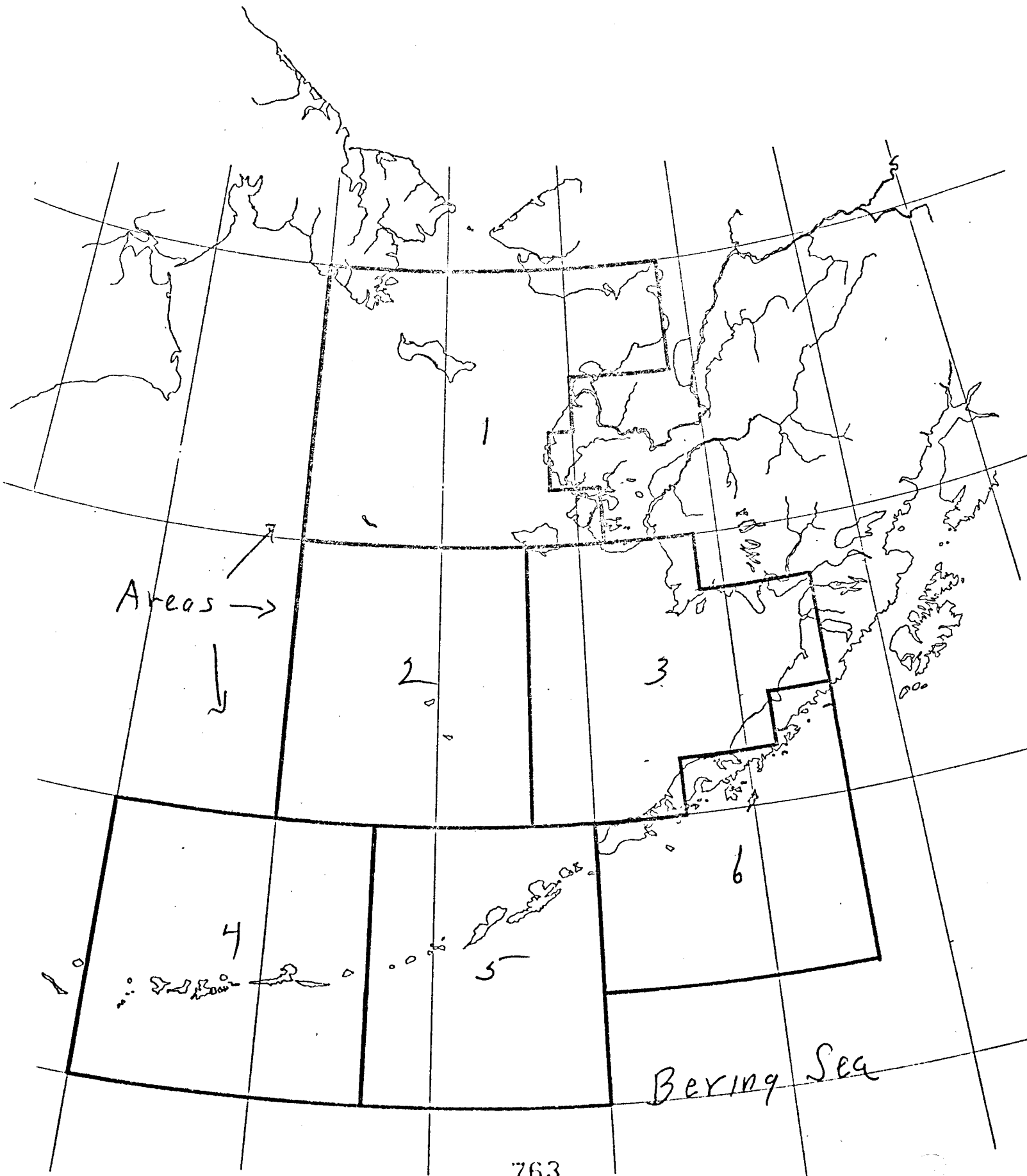
D. Problems Encountered

Difficult to acquire storm surge data.





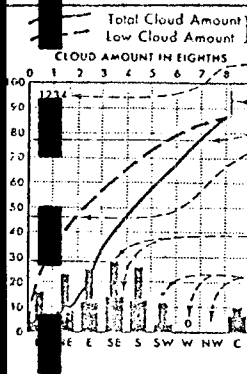




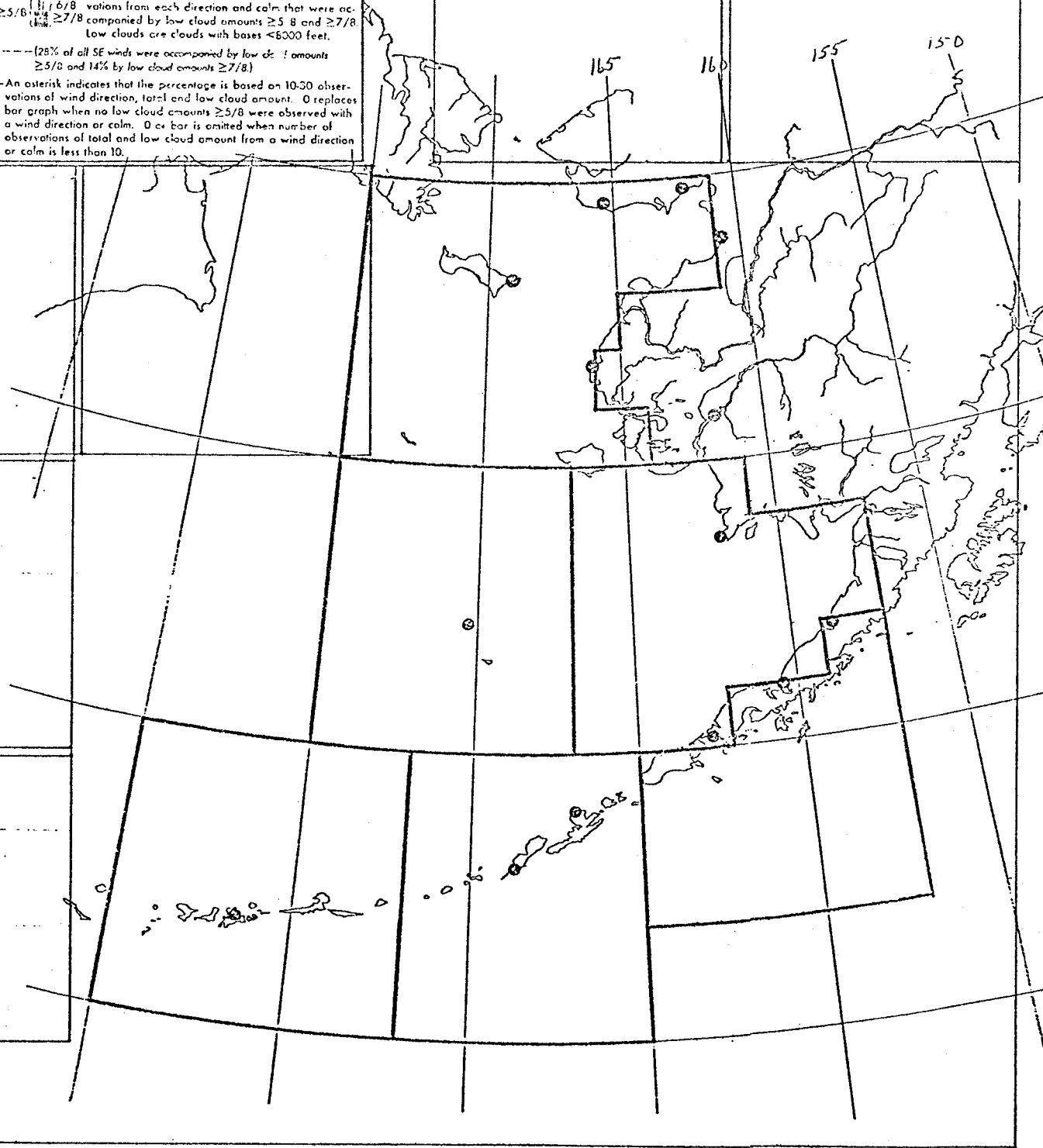
Areas →

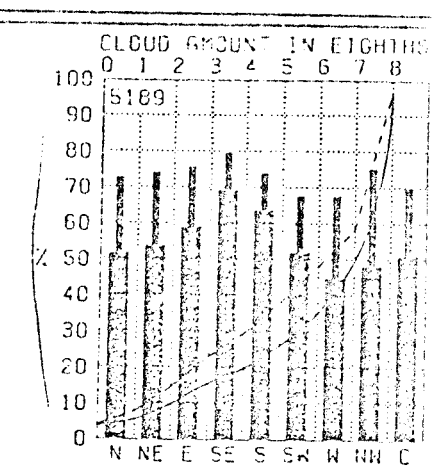
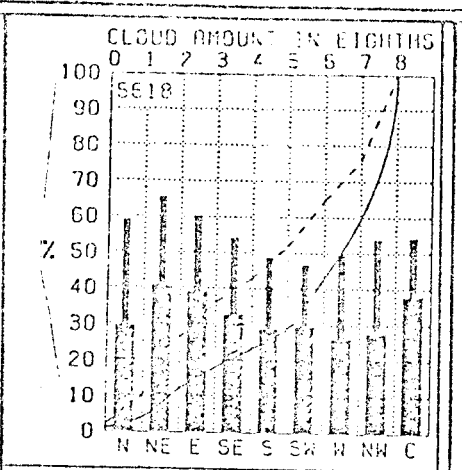
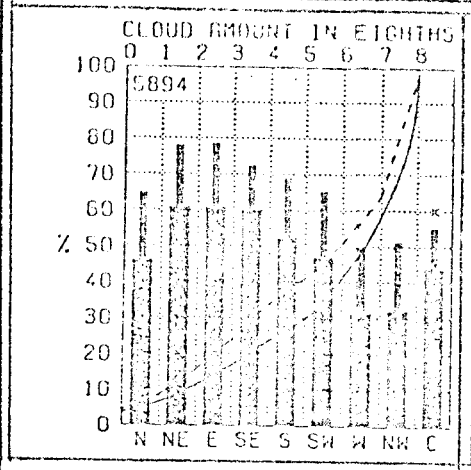


Bering Sea



Total Cloud Amount  
 Low Cloud Amount  
 CUMULATIVE PERCENT FREQUENCY OF INDICATED CLOUD AMOUNT EQUAL TO OR LESS THAN THE AMOUNT INTERSECTED BY THE CURVE.  
 Number of observations.  
 Observations.  
 (77% of all total cloud amounts were  $\leq 7/8$ )  
 (46% of all low cloud amounts were  $\leq 2/8$ )  
 5/8 & Low cloud amount: Percent frequency of observations from each direction and calm that were accompanied by low cloud amounts  $\geq 5/8$  and  $\geq 7/8$ . Low clouds are clouds with bases  $< 8000$  feet.  
 (28% of all SE winds were accompanied by low cloud amounts  $\geq 5/8$  and 14% by low cloud amounts  $\geq 7/8$ )  
 An asterisk indicates that the percentage is based on 10-30 observations of wind direction, total and low cloud amount. O replaces bar graph when no low cloud amounts  $\geq 5/8$  were observed with a wind direction or calm. O or bar is omitted when number of observations of total and low cloud amount from a wind direction or calm is less than 10.



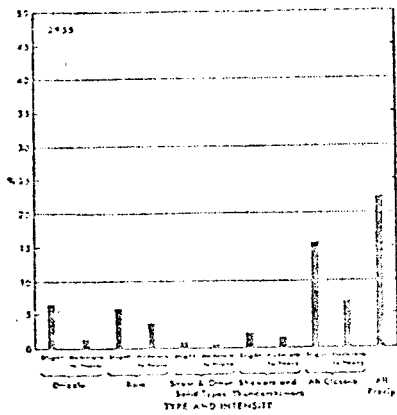


3/1

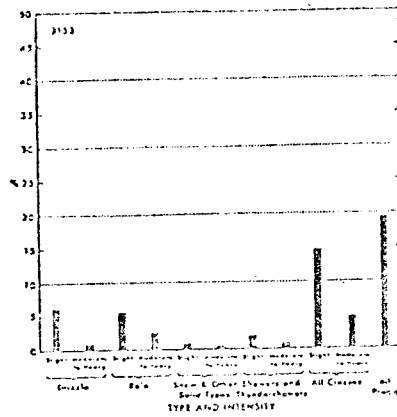
# 9. PRECIPITATION TYPES

JANU

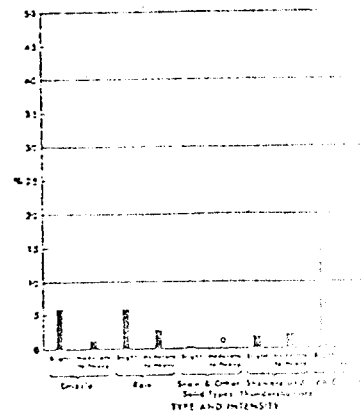
AREA 1



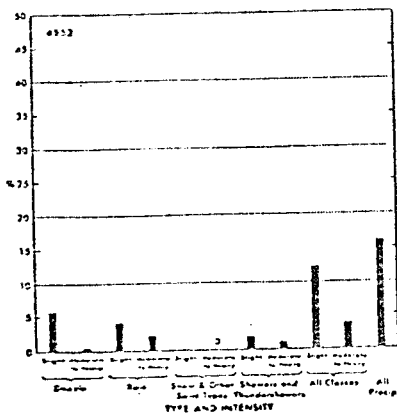
AREA 2



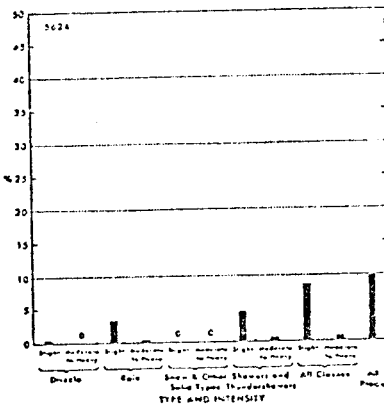
AREA 3



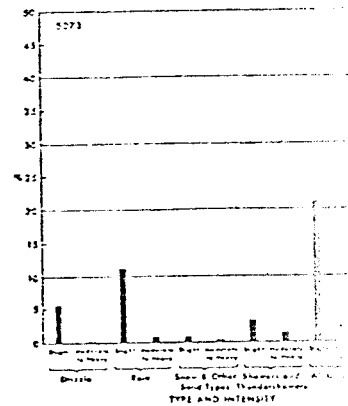
AREA 4



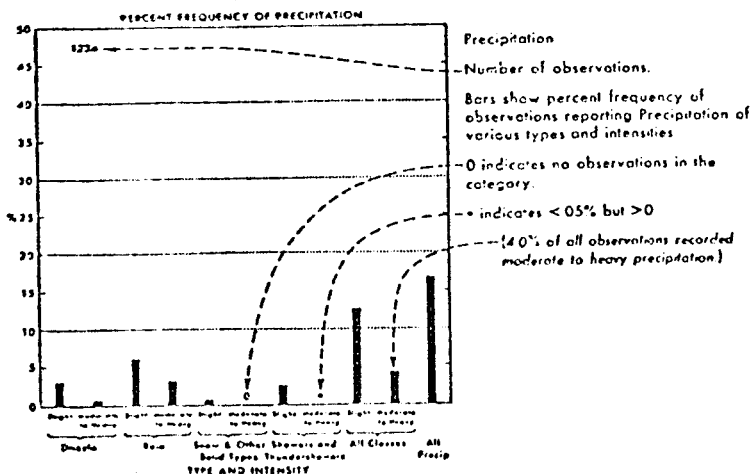
OWS N



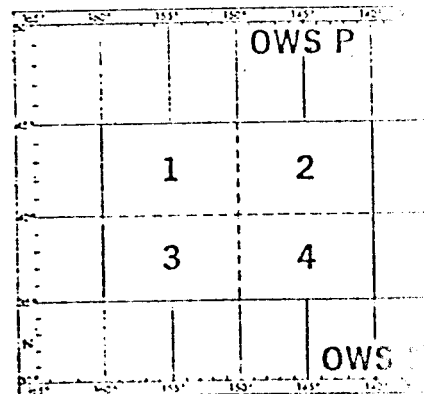
OWS P



## LEGEND



## AREA MAP



|                        |  |  |                               |
|------------------------|--|--|-------------------------------|
| 50.1   40.1<br>90   -4 | Temperature<br>←————→                            | Mean Annual Maximum<br>Highest   | Mean Annual Minimum<br>Lowest |
| 114.30<br>54.87   7.59 | Total Precipitation<br>(Rain and Snow)<br>←————→ | Average Annual<br>Greatest Month   Greatest Day                          |                               |
| 58.5<br>46.9   14.2    | Snowfall<br>←————→                               | Average Annual<br>Greatest Month   Greatest Day                          |                               |
| 40                     | Snowdepth<br>←————→                              | Annual Maximum on Ground   |                               |
| 5SE 9.3<br>15SE 52     | Surface Wind<br>←————→                           | Prevailing Direction Average Annual Speed<br>Fastest Direction and Speed |                               |
| 14.7<br>22.6   5.8     | Tides (annual)<br>←————→                         | Average Diurnal<br>Highest   Lowest                                      |                               |

OCS COORDINATION OFFICE

University of Alaska

ENVIRONMENTAL DATA SUBMISSION SCHEDULE

DATE: March 31, 1976

CONTRACT NUMBER: 03-5-022-56      T/O NUMBER: 25      R.U. NUMBER: 347

PRINCIPAL INVESTIGATOR: Mr. Harold W. Searby

No environmental data are to be taken by this task order as indicated in the Data Management Plan. A schedule of submission is therefore not applicable<sup>1</sup>.

NOTE:      <sup>1</sup> Data Management Plan has been approved and made contractual.

OCS COORDINATION OFFICE

University of Alaska

ESTIMATE OF FUNDS EXPENDED

DATE: March 31, 1976  
 CONTRACT NUMBER: 03-5-022-56  
 TASK ORDER NUMBER: 25  
 PRINCIPAL INVESTIGATOR: Mr. Harold W. Searby

Period July 1, 1975 - March 31, 1976\* (9 mos)

|                  | <u>Total Budget</u> | <u>Expended</u>  | <u>Remaining</u> |
|------------------|---------------------|------------------|------------------|
| Salaries & Wages | 19,700.00           | 6,226.00         | 13,474.00        |
| Staff Benefits   | 3,349.00            | 990.00           | 2,359.00         |
| Equipment        | -0-                 | -0-              | -0-              |
| Travel           | 1,000.00            | -0-              | 1,000.00         |
| Other            | <u>883.00</u>       | <u>61.60</u>     | <u>821.40</u>    |
| Total Direct     | <u>24,932.00</u>    | <u>7,277.60</u>  | <u>17,654.40</u> |
| Indirect         | <u>11,268.00</u>    | <u>3,561.27</u>  | <u>7,706.73</u>  |
| Task Order Total | <u>36,200.00</u>    | <u>10,838.87</u> | <u>25,361.13</u> |

\* Preliminary cost data, not yet fully processed.

PART III  
ANNUAL REPORT

Contract #: N.A.  
Research Unit #: 347  
Reporting Period: Annual  
Number of Pages: 14

"Marine Climatology of the Gulf of Alaska  
and the Bering and Beaufort Seas"  
Climatic Atlases (3)

Principal Investigators

Harold W. Searby  
Associate in Climatology  
Arctic Environmental Information  
and Data Center  
University of Alaska  
707 'A' Street  
Anchorage, AK 99501  
Comm: (907) 279-4523

William A. Brower, Jr., D5312  
Applied Climatology Branch  
National Climatic Center  
Federal Building, Room 401  
Asheville, NC 28801  
Comm: (704) 258-2850 x266  
FTS : 672-0266

March 26, 1976



## ANNUAL REPORT

### I. Summary of objectives, conclusions and implications with respect to OCS oil and gas development.

The investigation is to establish descriptive climatology and data analyses of marine and atmospheric parameters for the outer continental shelf waters of Alaska and determine if results have the necessary temporal and spatial resolution to provide an assessment of risks involved with operating energy related structures in these waters.

### II. Introduction

As weather plays a governing role in determining the nature of offshore operations, it is important to have a knowledge of average or frequently occurring weather conditions in planning for efficient and safe operations. Evaluation of extremes or rarely occurring conditions is essential before designing, constructing, and operating permanent platforms and structures within an oceanic environment. Such information is also a necessary aid in developing onshore supporting activities and for assessing the onshore impact of offshore activities.

The NCC and AEIDC are presently involved in a joint study to determine and publish a descriptive climatology for those Alaskan waters that are important to resource development of the outer continental shelf (OCS). The evaluation is to be in the form of a climatic atlas for each of three marine and coastal areas; the Gulf of Alaska, the Bering Sea, and the Chuckchi-Beaufort Seas.

### III. Current state of knowledge

The U.S. Navy Marine Climatic Atlas of the World, Vol. II, North Pacific Ocean (1959), one of eight volumes in a series of atlases of the world, has had wide acceptance as an authoritative reference for large scale operational planning and research.

The present study will provide three atlases to represent the total of the Alaskan waters and each will be based on more than 20 years of additional marine data. Also, as marine data are typically sparse in the near coastal zone, a zone of sharp gradients and complex climate, data for 49 coastal stations will be included. Such a combination should provide the best possible climatological picture for the coastal waters of Alaska.

#### IV. Study Area

The study area covers the Alaskan waters and coastal areas within 50° - 80°N and 130° - 180°W. The total area will be presented in three climatic atlases: the Gulf of Alaska, 50° - 65°N, 130° - 155°W; Bering Sea, 50° - 65°N, 155° - 180°W; and Chuckchi-Beaufort Sea, 65° - 80°N, 130° - 180°W.

#### V. Sources, methods and rationale of data collection

The climatological analyses of the Alaskan waters will be based on 600,000 surface marine observations and two million (3-hourly) observations for 49 (selected) coastal stations which are presently contained in NCC's digital data base. Environmental records and publications held by NCC and AEIDC are to provide supplemental information. (Such a data bank will be of significant importance to OCSEAP Principal Investigators and to others).

#### VI. Results

The climatic data in each atlas are to be represented monthly, by isopleths (lines connecting points of equal magnitude) on charts and by statistical graphs and tables (see attachment 1, Alaskan Coastal Zone Atlas Contents).

Each atlas will be 11" x 11" in size and contain some 480 pages, of which 228 will be 3-color charts, each page having an opposing page of graphs for selected marine areas and coastal stations. The remaining pages will consist of statistical tables and a descriptive narrative of the atlas content.

#### VII. Discussion

A special effort was undertaken to digitize surface marine observations for the Alaskan area for the period 7/73 - 12/74. However, because there were still insufficient marine data available north of 60° latitude, data for 16 additional Alaskan and for six Russian coastal stations were processed to supplement the data of the originally proposed 27 coastal stations and marine areas.

Interaction continues between NCC and AEIDC to refine atlas specifications in order to provide as comprehensive a product as time and funds permit.

### VIII. Conclusions

As of 3/15/76, NCC has expended 76% of the \$71.5K funded for FY-76 (through 6/30). Although our rate of spending per quarter differs from that estimated last July, our present rate of spending and the remaining work required will assure the spending of all monies allotted. Because of additional data requirements, we have asked for an extra \$10K for FY-76 so we can continue the Project without interruption.

The voluminous data processing is now nearing completion. About 60% of the 8,160 statistical graphs have been computer produced and plotting of parameter statistics for 360 charts in preparation for isopleth analysis is to begin this month. Although we are presently two months behind schedule, we plan to have sufficient materials ready on schedule (July 1976) to forward to AEIDC for their graphics to begin preparation for printing of the first atlas, the Climatic Atlas for the Gulf of Alaska.

### IX. Need for further study

See attachment 2, FY 77 Alaskan OCSEAP Proposals.

### X. Not applicable.

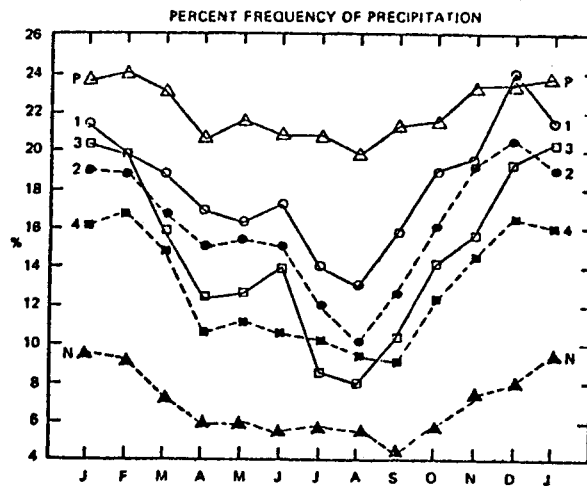
PROPOSED  
ALASKAN COASTAL ZONE ATLAS  
Provisional

## TABLE OF CONTENTS

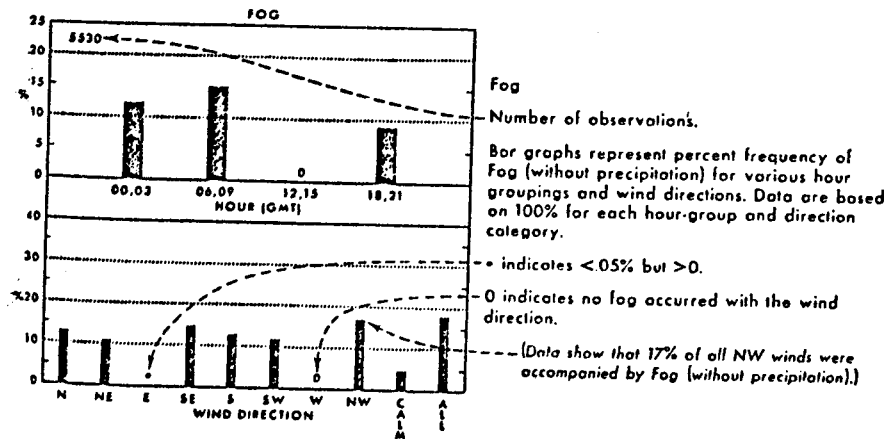
- I. Foreword, Introduction, Geographic Reference Chart.
- II. General Climatology (Special items to be covered in text and/or presented in graph, table or chart form).
  - A. "Annual March" of selected elements
  - B. Fog information
  - C. Extratropical cyclone information
  - D. Storm surges
  - E. High wind and wave recurrence intervals
  - F. Potential superstructure icing
  - G. Tides - type, range, etc.
  - H. Surface currents - speed/direction
  - I. Topography - land and sea
  - J. Coastal flooding
- III. Discussion of the Data Base, Discussion of the Charts and Graphs, Notes to Users, References.
- IV. Climatic Charts with Graphs of Marine Areas and Selected Coastal Stations - to be displayed (monthly or seasonally, as appropriate) on a base map that locates land stations and marine areas and includes isopleth analyses when appropriate.
  - A. Cloud Cover - Wind Direction
  - B. Visibility - Wind Direction
  - C. Low Cloud Ceiling - Visibility
  - D. Precipitation - Wind Direction
  - E. Precipitation Types
  - F. Air Temperature - Wind Direction
  - G. Air Temperature - Wind Speed
  - H. Wet Bulb Temperature - Relative Humidity
  - I. Sea Surface Temperature
  - J. Wave Height - Direction
  - K. Wave Height - Period
  - L. Wind Speed - Direction
  - M. Sea-Level Pressure
  - N. Hours Duration of Gales - Days Interval Between Gales

Detailed Provisional Contents of Alaskan Coastal Climatology Atlas \*

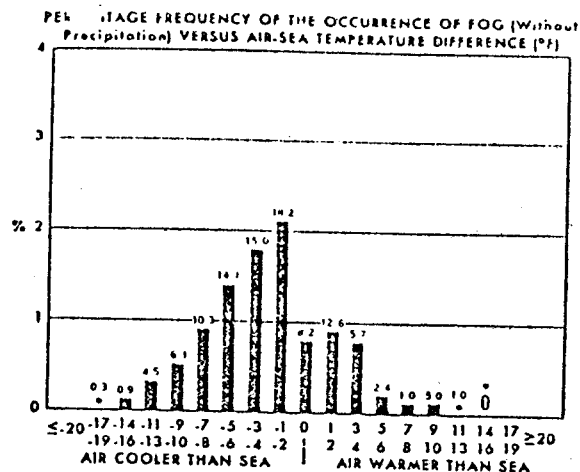
- I. Introduction Material  
Foreword, Introduction, Geographic Reference Chart
- II. General Climatology  
Items of special interest are covered here.
  - A. Annual march of selected elements include monthly graphs to show annual variations of such items as cloud cover, visibility, fog, precipitation, air temperature, sea surface temperature, waves, wind and sea level pressure. A sample graph appears below:



- B. Fog information for fog-prone areas (If fog is extremely prevalent, fog material is covered in the "Climatic Charts" section).



\*Sample graphs are based on dummy data and are not necessarily representative of U.S. Coastal Areas.

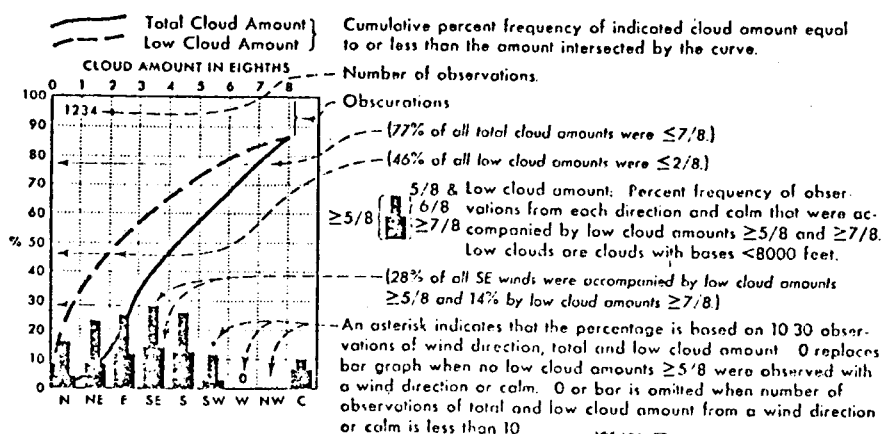


- C. Principal extratropical cyclone tracks and frequencies are presented on small-scale charts.
  - D. Storm surges are documented on a map of the area.
  - E. High wind and wave recurrence intervals give estimates of 5, 10, 25, 50 and 100 year return periods of these phenomena.
  - F. Superstructure icing potential is shown via small-scale seasonal charts.
  - G. Other pertinent topics of a local nature are covered. These may include major drainage areas, ice free shipping seasons, major coastal geographic features, extreme observed wave heights and winds, wind chill table, immersion hypothermia table (or shown on chart), etc.
- III. Discussions of the data base, charts, graphs and special notes to users are narrative descriptions. Notes will mention the use of marine data, which is not abundant in some marine areas (a chart of obs per 1<sup>o</sup> will be included). Use of "off-the-shelf" data is explained.

References will be of standard form.

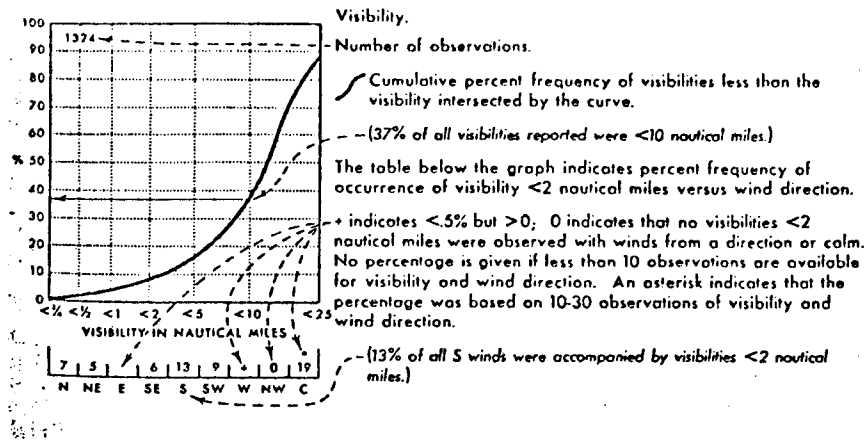
- IV. Major climatic charts. Chart types and sample legends are shown below.

A. Cloud Cover-Wind Direction



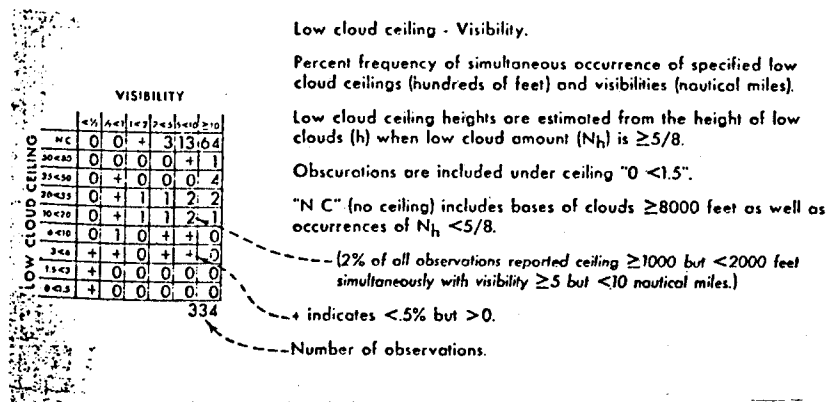
Isopleths: Percent frequency of total cloud amount  $\leq 2/8$ .  
 Percent frequency of low cloud amount  $\geq 5/8$ .

B. Visibility - Wind Direction

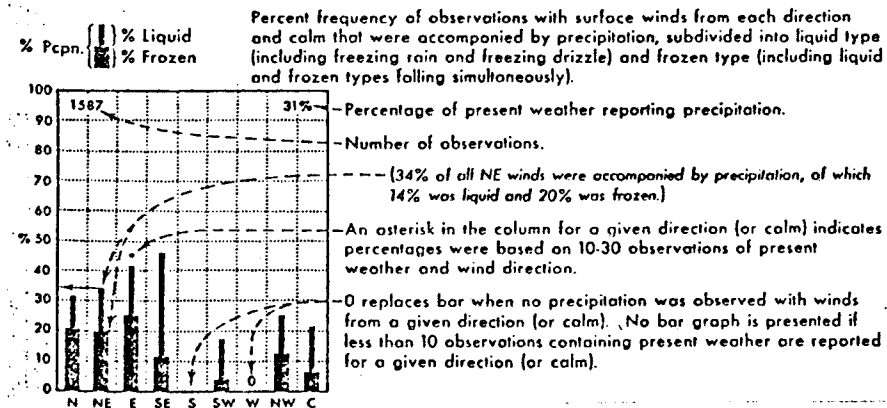


Isopleths: Percent frequency of visibility <math>< 2</math> nautical miles.  
 Percent frequency of visibility  $\geq 5$  nautical miles.

C. Low Cloud Ceiling - Visibility

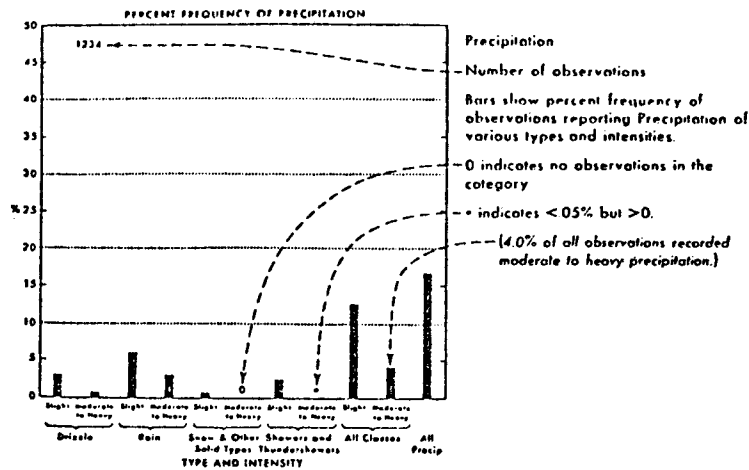


D. Precipitation - Wind Direction



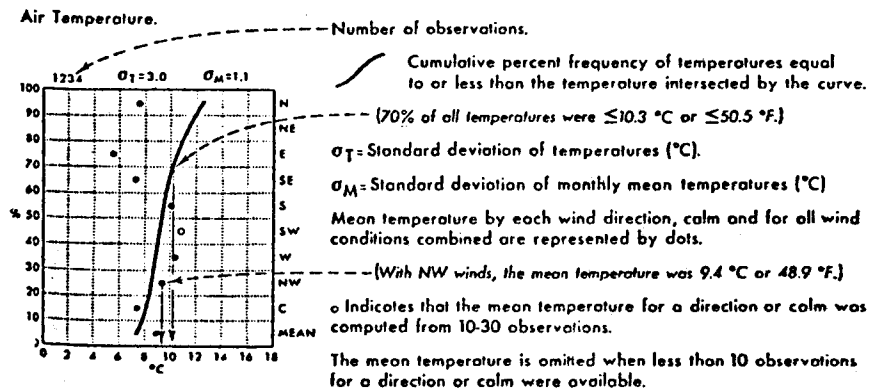
Isopleths: Percent frequency of precipitation. (Note—display monthly mean precipitation values at selected coastal stations).

## E. Precipitation Types



Isopleths: Percent frequency of frozen precipitation. (Note—display monthly mean snowfall amounts at selected coastal stations).

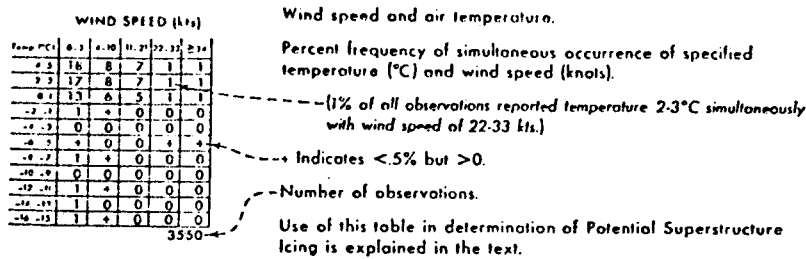
## F. Air Temperature - Wind Direction



Isopleths: Mean Air Temperature

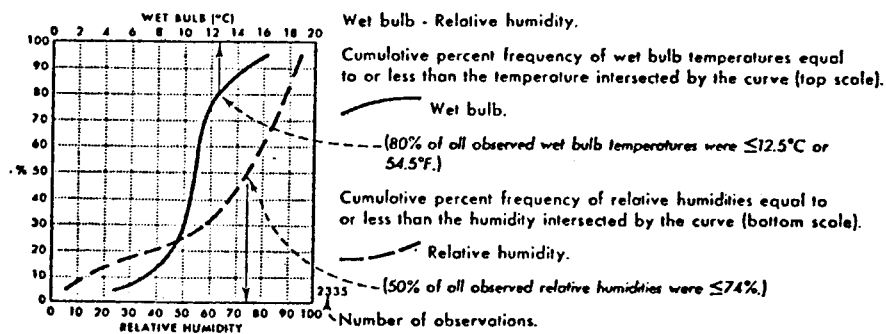


### G. Air Temperature - Wind Speed



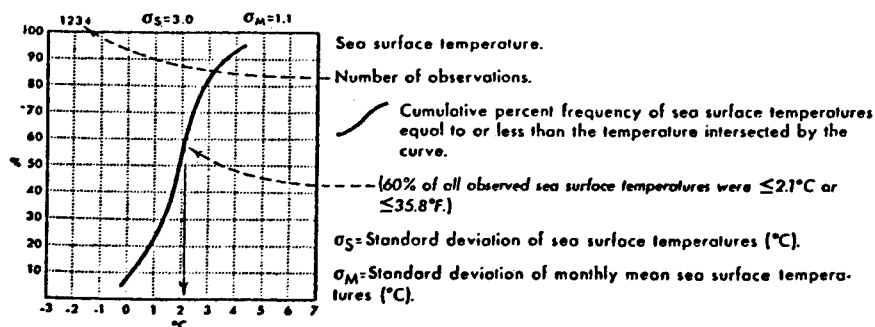
Isopleths: 1% and 99% air temperatures.

### H. Wet Bulb Temperature - Relative Humidity



Isopleths: Percent frequency of Temperature-Humidity Index (THI)  $\geq 24^\circ\text{C}$ .

### I. Sea Surface Temperature



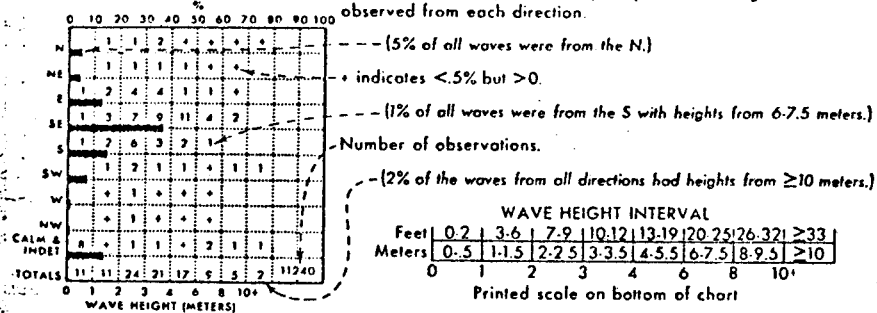
Isopleths: Mean 1% and 99% Sea Surface Temperature

## J. Wave Height - Direction

Wave direction and height.

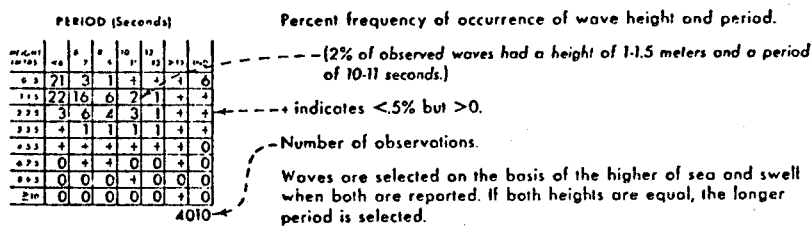
Direction frequency (top scale): Bars represent percent frequency of waves from each direction

Height frequency (bottom scale): Printed figures represent percent frequency of wave heights observed from each direction.



Isopleths: Percent frequency of waves less than 1.5 meters.  
 Percent frequency of waves less than 2.5 meters.

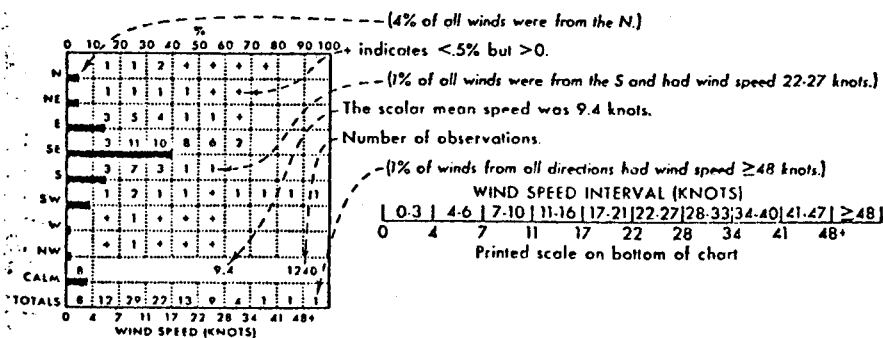
## K. Wave Height - Period



Isopleths: Percent frequency of waves  $\geq 3.5$  meters.  
 Percent frequency of waves  $\geq 6.0$  meters.  
 (Note—display observed extreme wave heights at observation points).

## L. Wind Speed - Direction

Direction frequency (top scale): Bars represent percent frequency of winds observed from each direction. Speed frequency (bottom scale): Printed figures represent percent frequency of wind speeds observed from each direction.



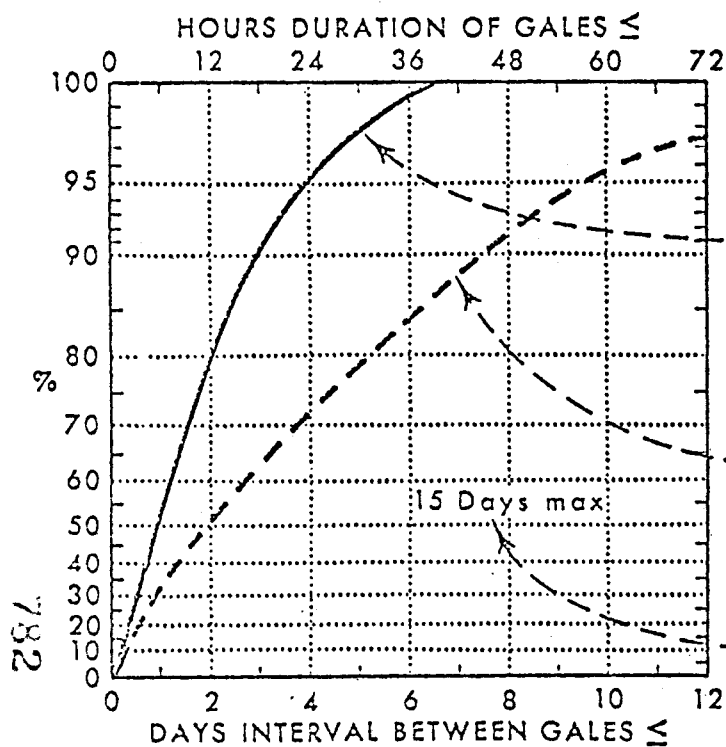
Isopleths: Scalar mean wind speed. (Note—display observed extremes at observation points).

M. Sea Level Pressure

Graphs: Percent frequency of sea level pressure similar to the sea surface temperature graphs.

Isopleths: Mean sea level pressure. (Note—display primary/secondary storm tracks).

N. Hours Duration of Gales - Days Interval Between Gales  
(see attached page)



Hours duration of gales - Days interval between gales.

Cumulative percent frequency of hours duration of gales equal to or less than the number of hours intersected by the solid curve (based on gales which began in this month).

--- (98% of gales had a duration  $\leq 30$  hours.)

Cumulative percent frequency of days interval between gales equal to or less than the number of days intersected by the broken curve (based on gales which ended in this month).

--- (88% of gales were followed by another gale in 7 days or less.)

The maximum value(s) of hours duration and/or days interval will be displayed when the graph limits are exceeded.

--- (100% of gales were followed by another gale in 15 days or less.)

Where observations of gales are few, cumulative percent frequencies of hours duration of gales and days interval between gale are provided in tables.

Percentage frequency of gale force winds ( $\geq 34$  knot

Following is part 2 of the quarterly report R.U.# 347 for the period ending December 31, 1975. This was received after the printing of the Quarterly Reports, July - September 1975, therefore is included here.

OCS COORDINATION OFFICE

University of Alaska

Quarterly Report for Quarter Ending December 31, 1975

Project Title: Marine Climatology of the Gulf of Alaska  
and the Bering and Beaufort Seas

Contract Number: 03-5-022-56

Task Order Number: 25

Principal Investigator: Mr. Harold W. Searby

I. Task Objectives

To determine and publish the knowledge of the climatological conditions of that portion of Alaska that is important to OCS development.

II. Field and Laboratory Activities

Strictly speaking, this portion of the project has no field or laboratory activities. This is a joint project with the National Climatic Center (NCC) in Ashville, North Carolina. AEIDC responsibilities are to provide extremes of all weather elements, information on coastal damage resulting from wind generated storm flooding, check analysis work done at NCC, and through our graphics department, prepare materials for publications, including contracting for and supervising the publication of the three marine atlases.

III. Results

To date, about three-fourths of the extremes data has been compiled, and additional storm damage information is being sought. No analysis work has been made available from the NCC as yet. Our graphics department has completed the base maps to be used in publication.

IV. Problems Encountered

None.

OCS COORDINATION OFFICE

University of Alaska

ENVIRONMENTAL DATA SUBMISSION SCHEDULE

DATE: December 31, 1975

CONTRACT NUMBER: 03-5-022-56

T/O NUMBER: 25

R.U. NUMBER: 347

PRINCIPAL INVESTIGATOR: Mr. Harold W. Searby

No environmental data are to be taken by this task order as indicated in the Data Management Plan. A schedule of submission is therefore not applicable<sup>(1)</sup>.

NOTE: (1) Data management plan was submitted to NOAA in draft form on October 9, 1975 and University of Alaska approval given on November 20, 1975. We await formal approval from NOAA.

OCS COORDINATION OFFICE

University of Alaska

ESTIMATE OF FUNDS EXPENDED

DATE: December 31, 1975  
 CONTRACT NUMBER: 03-5-022-56  
 TASK ORDER NUMBER: 25  
 PRINCIPAL INVESTIGATOR: Mr. Harold W. Searby

Period July 1 -- December 31, 1975 \* (6 mos)

|                  | <u>Total Budget</u> | <u>Expended</u> | <u>Remaining</u> |
|------------------|---------------------|-----------------|------------------|
| Salaries & Wages | 19,700.00           | 3,988.17        | 15,711.83        |
| Staff Benefits   | 3,349.00            | 677.97          | 2,671.03         |
| Equipment        | -0-                 | -0-             | -0-              |
| Travel           | 1,000.00            | -0-             | 1,000.00         |
| Other            | <u>883.00</u>       | <u>14.49</u>    | <u>868.51</u>    |
| Total Direct     | 24,932.00           | 4,680.63        | 20,251.37        |
| Indirect         | <u>11,268.00</u>    | <u>2,281.23</u> | <u>8,986.77</u>  |
| Task Order Total | <u>36,200.00</u>    | <u>6,961.86</u> | <u>29,238.14</u> |

\* Preliminary cost data, not yet fully processed.



DRAFT

ANNUAL REPORT

Research Unit # 357  
Reporting Period 4/1/75-3/31/76  
Number of Pages 1 + 132

PHYSICAL OCEANOGRAPHY OF THE GULF OF ALASKA

Co-Principal Investigators:

F. Favorite, NOAA, NMFS, NWFC

and

J. H. Johnson, NOAA, NMFS, PEG

April 1, 1976

## ANNUAL REPORT

### I. Summary of objectives, conclusions, and implications with respect to OCS oil and gas development

This is a concise summary of the physical oceanography of the Gulf of Alaska with emphasis on water circulation and transport. It provides background information for OCSEAP field programs and should assist in determining the location and intensity of direct current measurements required to define patterns in this highly complex flow regime thereby determining the potential movement of oil spills from offshore drill sites.

### II. Introduction

See (I) above.

### III. Current state of knowledge

See attached report.

### IV. Study area

Gulf of Alaska

### V. Sources, methods and rationale of data collection

Historical data available from literature, NODC Geofile, coastal stations, NCAR, and FNWC.

### VI. Results

See attached report.

### VII. Discussion

See attached report.

### VIII. Conclusions

See attached report.

### IX. Needs for further study

Ongoing OCSEAP Research Units are addressing needs for further study.

### X. Summary of 4th quarter operations

Attached report will be submitted in final form as NWFC Processed Report.

DRAFT

NORTHWEST FISHERIES CENTER

PROCESSED REPORT

MARCH 1976

PHYSICAL OCEANOGRAPHY OF THE GULF OF ALASKA

by

W. J. Ingraham, Jr., A. Bakun and F. Favorite

Prepared by:  
Northwest Fisheries Center  
National Marine Fisheries Service  
2725 Montlake Boulevard E.  
Seattle, Washington 98112

# PHYSICAL OCEANOGRAPHY OF THE GULF OF ALASKA

## ABSTRACT

- I. INTRODUCTION
- II. WATER PROPERTIES
  - A. Temperature
  - B. Salinity
  - C. Water Masses
- III. CURRENTS
  - A. Drift Studies
  - B. Geostrophic Flow
  - C. Volume Transport
- IV. WIND-STRESS TRANSPORTS
  - A. Pressure Fields
  - B. Transport Fields
  - C. Numerical Models
- V. COASTAL SEA LEVELS
  - A. Sea Level Pressures
  - B. Mean Sea Levels
  - C. Relation to Transport
- VI. SURFACE CONVERGENCE AND DIVERGENCE
  - A. Vicinity of the Coastal Boundary
  - B. Interior of the Gulf
  - C. Conditions - 1973, 1974 and 1975
- VII. SUMMARY AND CONCLUSIONS
- VIII. ACKNOWLEDGMENTS
- IX. LITERATURE CITED
- X. APPENDIX

# PHYSICAL OCEANOGRAPHY OF THE GULF OF ALASKA

## INTRODUCTION

Although extensive oceanographic investigations have been carried out in the Gulf of Alaska in the last two decades, our knowledge of actual conditions and processes and their cause and effect is still inadequate to permit any accurate short- or long-term forecasts of oceanic conditions. However, a fairly extensive data base exists, and the purpose of this report is to summarize the state of our knowledge concerning the physical environment of offshore areas of the Gulf of Alaska prior to the commencement of present OCSEAP<sup>1/</sup> investigations. The Gulf of Alaska is considered to extend southward from the coast to a line from Dixon Entrance to Unimak Pass, essentially 54°N.

It should be recognized at the outset that the ocean is a turbulent regime that can be characterized only by statistical techniques based on extensive time-series data on water properties and direct current measurements collected on appropriate space scales. Such data are not available for the Gulf of Alaska area. Physical oceanographic studies up to the present time have been limited to aperiodic, widely-spaced station data of an exploratory nature obtained primarily to provide background information on general flow and ranges of environmental conditions related to specific aspects of fisheries investigations (Favorite, 1975). The most recent and comprehensive are those of the International North Pacific Fisheries Commission (INPFC). General environmental conditions in the Subarctic Pacific Region for the years 1953 to 1971 have been summarized by Dodimead, Favorite and Hirano (1963), and Favorite, Dodimead and Nasu (1976); the latter provides an extensive bibliography that is not reproduced in this

<sup>1/</sup> Outer Continental Shelf Environmental Assessment Program.

report. There is also extensive but fragmentary information available in reports of results of Soviet fishing activities (e.g. Moiseev, 1963-70)<sup>2/</sup>. Although the presently available station data are extensive, they are aperiodic, non-synoptic and lack the close grid spacing, wide area coverage, repetitive observations, and direct current measurements necessary to characterize the specific nature of flow.

A general assessment of oceanographic conditions can be made from knowledge of meteorology and bathymetry. With respect to water properties, we can expect seasonal changes in both temperature and salinity. Northward flow into the gulf brings unseasonably warm water into the gulf year round. Winter cooling will gradually erode the high temperatures in surface layer, but these will quickly be restored by seasonal warming in spring and summer. The vertical extent of winter cooling or convective overturn will depend on the stability of the water column, and this is affected primarily by the distribution of salinity with depth. Because there is an excess of precipitation over evaporation and extensive dilution in spring and summer from the extensive coastal watershed, a dilute surface layer can be expected to be underlain by a halocline. The readjustment of mass as a result of the general cyclonic flow around the gulf will result in a horizontal divergence and an upward vertical transfer in the center of the gulf. This is manifested in a doming or ridging of isolines of water properties in that area resulting in high salinities and low temperatures at the surface, particularly during winter when this process is most active.

There is a general eastward surface flow across the North Pacific Ocean composed of the northern sector of the anticyclonic flow in the central North Pacific gyre driven by winds associated with the Eastern Pacific high pressure system, and the southern sector of the general cyclonic flow of

<sup>2/</sup> See also Bogdanov (1961), Plakhotnik (1962), and Filatova (1973).

the Subarctic Pacific gyre, driven by interactions of the Aleutian Low pressure system. This confluence and the subsequent eastward advection of meridional admixtures of subarctic and subtropic waters is subjected to various bathymetric conditions on reaching the eastern side of the ocean: first, a gradual shoaling, reducing the water column by half (from 6,000 - 3,000 m); second, the interference of numerous seamounts, (some extending to within 500 m of the surface); and, finally, an abrupt continental shelf. This results in marked changes in the fields of acceleration, vorticity and turbulence, as well as a predominant separation of flow into northward and southward components and associated disturbances of vertical strata. The northward branch, increasing in planetary vorticity, impinges on the head of the Gulf of Alaska where it is constrained by the land mass and is forced southwestward along the Alaska Peninsula. In order to accomplish this it must displace the northeastward flow into the gulf offshore, away from the continental slope. The vorticity balance of this southwestward flow is altered not only as a result of southward displacement, but also as a result of increasing depth ( 5,000 to 7,000 m) on encountering the eastern end of the Aleutian Trench. Further, we can anticipate that frictional and tidal effects on the shallow continental shelf will result in considerably reduced flow over the shelf compared to flow along and seaward of the continental slope, and that flow along the edge of the shelf will be complicated by internal waves and horizontal shelf waves.

The greatest fluctuations in flow conditions will be associated with the intensification of winds in winter. The center of the Aleutian Low travels in an anticyclonic pattern; present in late spring and summer in the northern Bering Sea, it occurs in the Gulf of Alaska in late fall, and in the western Aleutian area in winter. Thus, maximum cyclonic winds occur

in the Gulf of Alaska from November to January. Maximum Ekman transport will occur at this time, piling up water along the coast and resulting in a seaward flow along the bottom. Maximum total transport also occurs at this time greatly increasing northward flow into the gulf. In summer, a northward displacement of the Eastern Pacific High results in anticyclonic winds resulting in an offshore component of Ekman transport at the surface and a compensatory onshore flow over the continental shelf. Minimum overall transport also occurs at this time.

Thus there is a potential for considerable complexity and great variability in actual conditions, and it is these time-dependent phenomena that we are most interested in. All data available will be used to define physical conditions in the gulf as accurately and completely as possible.

It is difficult to assess how representative the oceanographic data being collected or analyzed are in defining conditions in a particular area unless some measure of variability over extended time periods is available. About a century ago it was recognized that oceanic conditions in the gulf were considerably warmer than corresponding latitudes at the western side of the ocean (Dall, 1882) and this was attributed to the influence of the "Kuro Siwo" because of the known analogous effects of the Gulf Stream in the Atlantic Ocean on the climate of Europe. Although data from the "China steamers" between San Francisco, Yokohama and Hong Kong in the 1870's provided extensive data on conditions in the central Pacific Ocean, even the gold rushes and subsequent commercial traffic to Alaska failed to provide a data base documenting oceanographic conditions in the gulf. There are surface temperature data for the Gulf of Alaska from the 19th century, presumably from government and commercial vessels, but these are too



fragmentary in time and space to establish climatic trends. Nevertheless, there are historical records of monthly mean air temperatures at Sitka that began when this location, called New Archangel, was controlled by the Russian-America Company (Dall, 1879) that are fairly complete to this date. Considering all years data are available since 1828 (Fig. 1), positive annual anomalies of greater than  $1.5^{\circ}$  were recorded in 1829, 1869, 1915, 1926, 1940 and 1941; whereas, only in 1955 did a negative anomaly greater than  $1.5^{\circ}$  occur. Cycles of 4-5 year duration are apparent in the data from 1850-71. The period from 1920 to 1947 was characterized by above normal conditions; however, there was a marked decline of over  $3^{\circ}$  from 1940 to 1950. Below normal conditions have occurred from 1965 to the present. Perhaps the most significant aspect of these data is that the annual mean temperature for 1828-76 is precisely the same as the present day mean compiled and used by the National Weather Service,  $6.3^{\circ}\text{C}$  ( $43.3^{\circ}\text{F}$ ). Thus, both short-term fluctuations of 1-4 years and long-term trends, such as the cooling evident from 1940-55 have occurred. Although we have acquired sea level pressure data as far back as 1900, sea level data prior to 1930 are available only at Ketchikan, and oceanographic station data are generally available only since 1950. The longer records will be utilized where applicable, but most comparisons and interactions will of necessity be based on data from the 25-year period 1950-74.

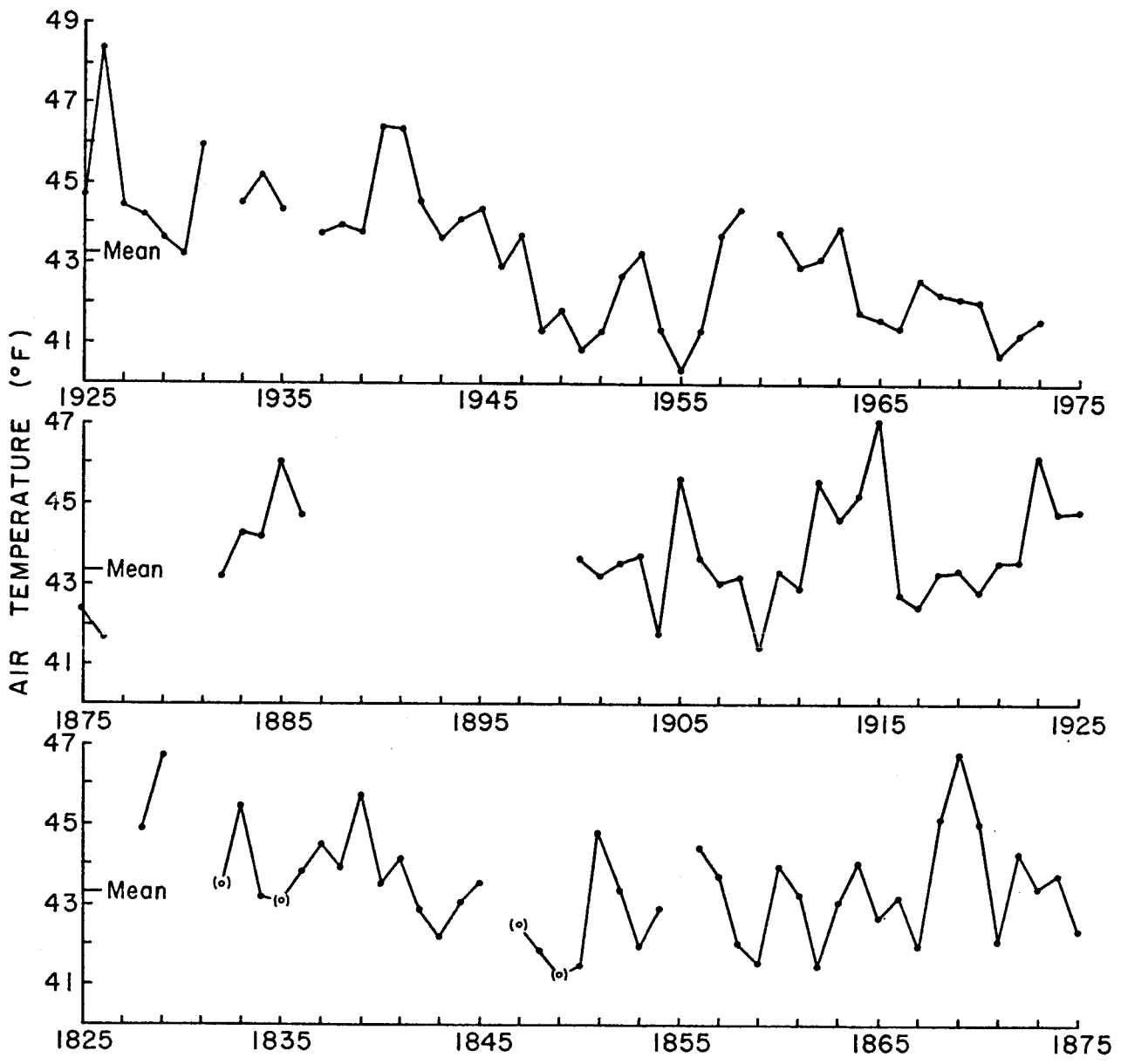


Figure 1. Air temperatures at Sitka (New Archangel) 1828-1974.

## II. WATER PROPERTIES

Abrupt changes from normal conditions are usually quickly detected, but gradual changes over long periods often pass unnoticed; nevertheless, quantification of either requires an adequate data base. Reasonably complete time-series data in the gulf are available at shore stations, but none is available at specific locations in oceanic areas of the gulf<sup>3/</sup>. In the latter case, in order to obtain any semblance of time-series data, observations over extensive areas must be averaged over large intervals; such data provide an indication of trends but, obviously, numerous spatial and temporal phenomena are masked by the averaging process.

### A. Temperature

Although observations at shore stations are the most complete source of temperature data, only surface values are obtained. Monthly mean values (referred to 1950-74 mean, where data are available) for Ketchikan, Sitka, Yakutat, Seward, Kodiak and Dutch Harbor indicate a progressively colder regime from southeastern Alaska around the gulf to the end of the Alaska Peninsula with one exception, that temperatures in winter at Dutch Harbor are about 2 or 3 C<sup>0</sup> higher than at Kodiak (Fig. 2a). In southeastern Alaska the seasonal temperature range is about 9 C<sup>0</sup> (from 5 to 14°C at Ketchikan and 3 to 12° at Seward), but the range increases to 11 C<sup>0</sup> at Kodiak (1 to 12°) and decreases to 8 C<sup>0</sup> at Dutch Harbor. Minima occur in January at Kodiak and in February at all other locations, maxima occur in July at Seward and in August at all other locations.

There are a number of oceanographic atlases of large areas of the Pacific Ocean that permit a general assessment of mean temperatures in the offshore waters of the Gulf of Alaska (e.g. LaViolette and Seim (1969)) present monthly mean, minimum and maximum sea surface temperatures based on a

<sup>3/</sup> Extensive data are available at Ocean Station "P" southward of the gulf -50°N, 145°W (e.g. Tabata 1965 and Fofonoff and Tabata 1966).

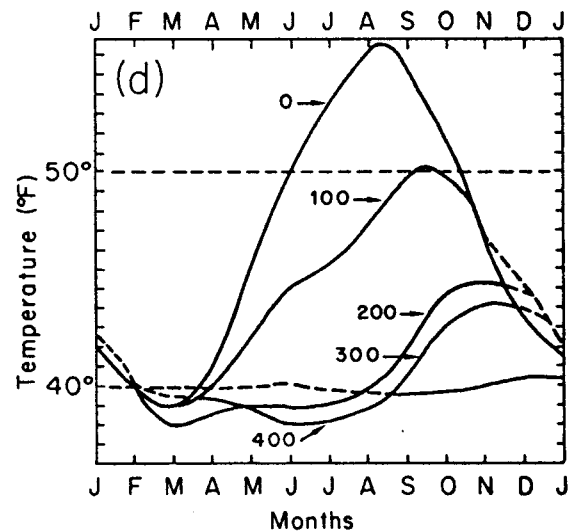
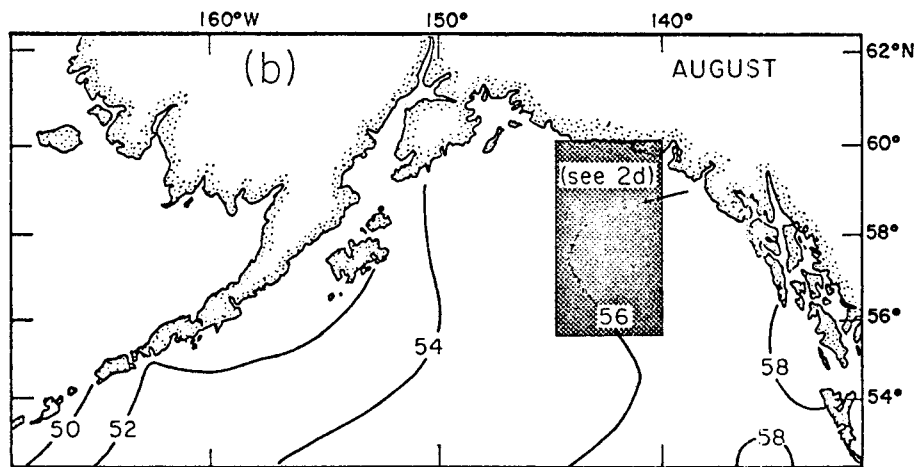
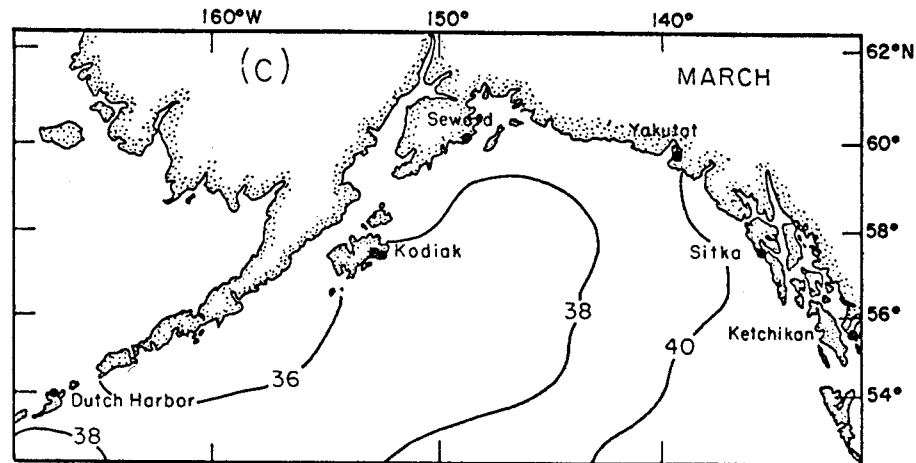
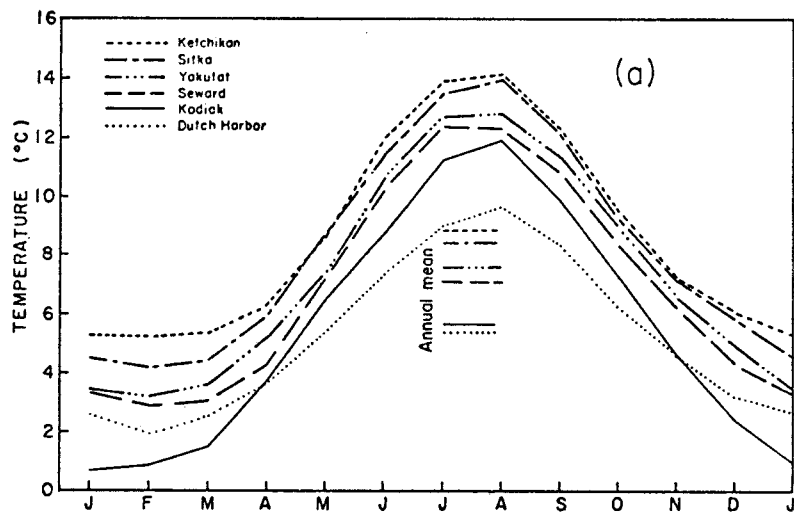


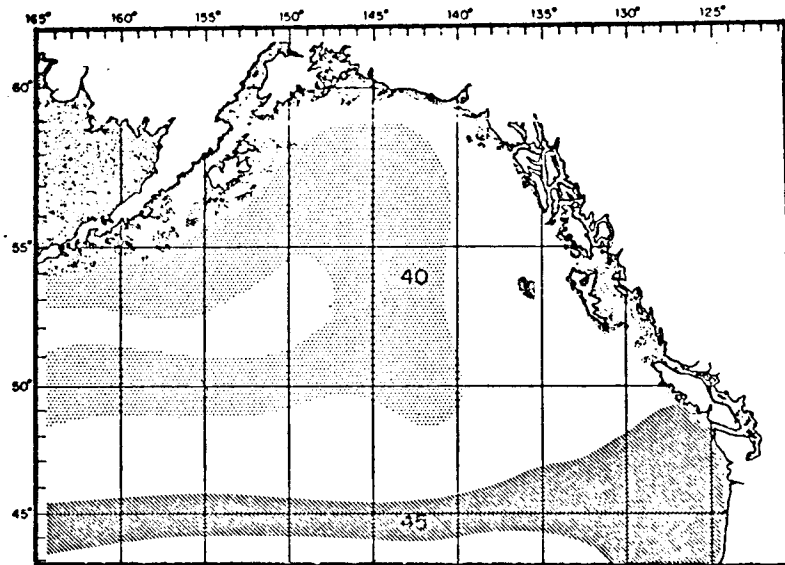
Figure 2. Sea temperature data: (a) monthly mean (1950-74) sea surface temperatures at the indicated coastal stations; (b and c) surface temperature distributions August and March (from Robinson and Bauer, 1971); and (d) monthly mean temperatures at 100 ft (30.5m) intervals to 400 ft (121.9m) in 5x5° Marsden quadrant 195-3, 55-60°N, 140-145°W (from Robinson, 1957).

1 x 1° grid), and there are also a few that are limited specifically to the gulf and adjacent area--e.g. Robinson (1957), Giovando and Robinson (1965) and Robinson and Baur (1971). These data are not only easily accessible, but adequately representative of mean conditions; thus, there is little need for an extensive summary here. It should be pointed out, however, that such atlases are representative only of offshore areas where mixing and stirring moderate the extreme conditions that occur in shallow inshore areas which are influenced by ice-melt in winter and spring, and runoff and warming over tidal shoals in spring and summer<sup>4/</sup>. Maximum surface temperature, 14°C, occurs in August, but conditions are sufficiently similar in September to consider either month as representative, and minimum surface temperature, 3.5°C, occurs in March (Fig. 2b and c) - temperatures of 0°C, or lower, can be found in Prince William Sound and Cook Inlet depending on the extent of ice cover.

A representative seasonal temperature cycle to a depth of 122 m (400 ft) is afforded by a compilation of station and bathythermograph (BT) data in the 5 x 5° quadrangle from 55-60°N, 140-145°W (Fig. 2d). Near isothermal conditions are present from the surface to approximately 100 m during January-March and represent the vertical extent of convective turnover during winter. This process not only determines the extent of the surface layer in winter, but results in the formation of a temperature-minimum stratum (~3°C) at depths of 75 to 150 m when surface waters are warmed in spring and summer. Wind mixing and stirring result in the formation of a warm surface layer in summer of 20-30 m thickness that is underlain by a sharp thermocline extending to the depth of winter overturn. Subsequent downward diffusion in spring, summer and autumn gradually erodes but

<sup>4/</sup> See Muench and Schmidt (1975) for a discussion of conditions in Prince William Sound.

(a)



(b)

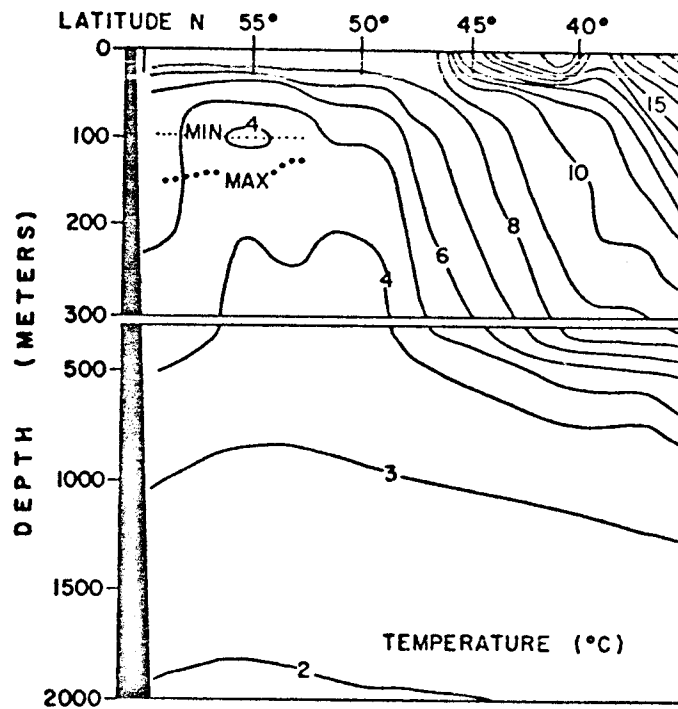


Figure 3. Geographic range of selected isotherms ( $^{\circ}\text{F}$ ) at 400 ft (121.9m) (from Robinson, 1957), and vertical section of long-term mean temperatures (based on  $2 \times 2^{\circ}$  grid) along  $145^{\circ}\text{W}$ .

seldom eliminates the temperature-minimum stratum, particularly in the central part of the gulf. The effects of this process are evident until November. However, year round temperatures of 4.5 to 5.0°C occur near 122 m around the periphery of the gulf, over the continental shelf and slope. These temperatures, 1-2°C higher than those in the temperature-minimum stratum, appear as a mesothermal, or temperature-maximum, stratum, but are merely representative of conditions in the water column below the influence of local seasonal effects.

Further information on conditions at 122 m is provided by a plot of the geographical extent of selected isotherms (Fig. 3a): the zonal trends south of 50°N suggest an eastward flow toward the coast; the abrupt northward trend of the 4.4°C isotherm boundaries west of 140°W suggests a broad variable northward flow into the gulf east of 150°W; the westward continuation of this feature south of the Alaska peninsula suggests a westward return flow in that area; and, finally, the tongue-like area westward of 147°W between 51° and 54° suggests the presence of an eastward intrusion of cold water from the west or an area of upward vertical transfer of cold water from depth, or both. A vertical temperature profile along 145°W (Fig. 3b) based on long-term mean temperatures from all station data (2 x 2° grid) clearly exhibits a ridging of the 4 and 5° isotherms in the zone between 48-57°N; and the effects of temperature on geostrophic flow dictate an eastward, onshore flow to the south of this zone and a westward return flow north of the zone.

Mean temperature distributions below the range of the shallow bathythermograph (450' or 137 m) must be obtained from station data and are not

readily accessible. Plots based on long-term mean data ( $2 \times 2^\circ$  grid) at depths of 200, 500, 1000 and 2000 m (Fig. 4) clearly indicate the northward sweep of warm water into the gulf on the eastern side and the permanence of the cold intrusion isolated offshore on the western side; the two features exist at all levels. It should be noted that data averaged in this manner ( $2 \times 2^\circ$  grid) do not adequately represent temperature fields in the narrow boundary current at the western side of the gulf, particularly south of the Alaska Peninsula, but the gradual lowering of temperature from  $5 - 4^\circ\text{C}$  in an east-west direction around the gulf at 200 m, which is considered the seaward limit of the continental shelf, is fairly representative of actual conditions as far west as Kodiak Island. A grid of less than  $1/2 \times 1/2^\circ$  would be required to show continuity of isotherms west of this area, and the paucity of data prevent this. Data obtained east of Kodiak Island in spring 1972 (Fig. 5) indicate characteristics of the distribution of  $4-5^\circ\text{C}$  water near 200 m in this area; and there are numerous examples of the continuity of this temperature-maximum stratum from the gulf westward out along the Aleutian Islands (e.g. Ingraham and Favorite, 1968) based on closely spaced station data from individual cruises.

At all levels from 200 to 2000 m the mean temperature distributions suggest a confluence of cold oceanic water entering the gulf in a northeasterly direction and warm water entering in a northwesterly direction. There is also a perturbation evident in isotherms in the eastern side of the gulf at 200, 500 and 1000 m that appears to suggest that flow related to the former has a blocking effect on flow related to the latter. These phenomena are discussed in later Sections on Water Properties and Currents.

Anomalies from monthly mean surface temperatures at shore stations around the gulf indicate that marked short-term deviations occur at indi-



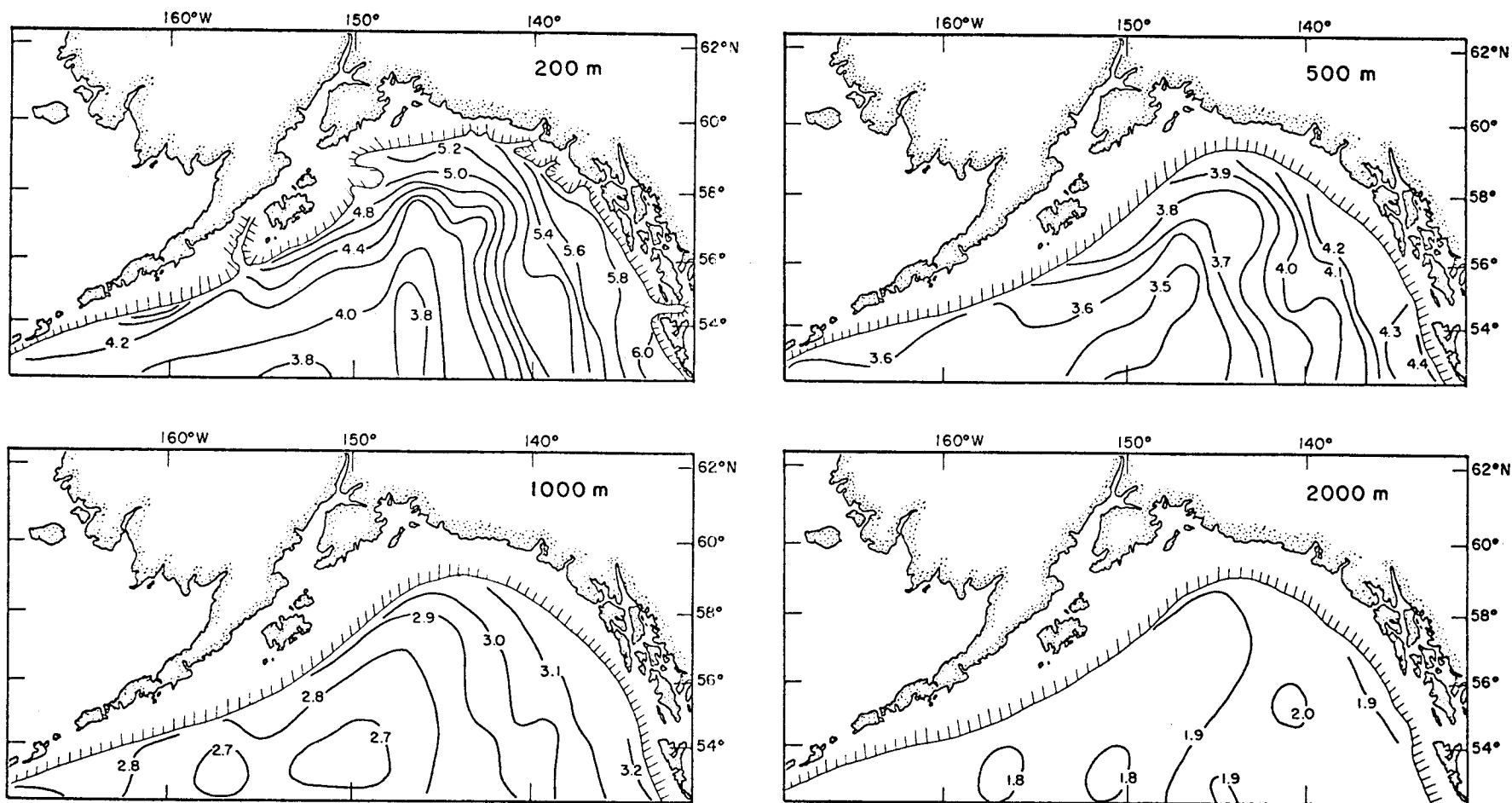


Figure 4. Long-term mean temperature distributions (based on  $2 \times 2^\circ$  grid) at 200, 500, 1000 and 2000 m.

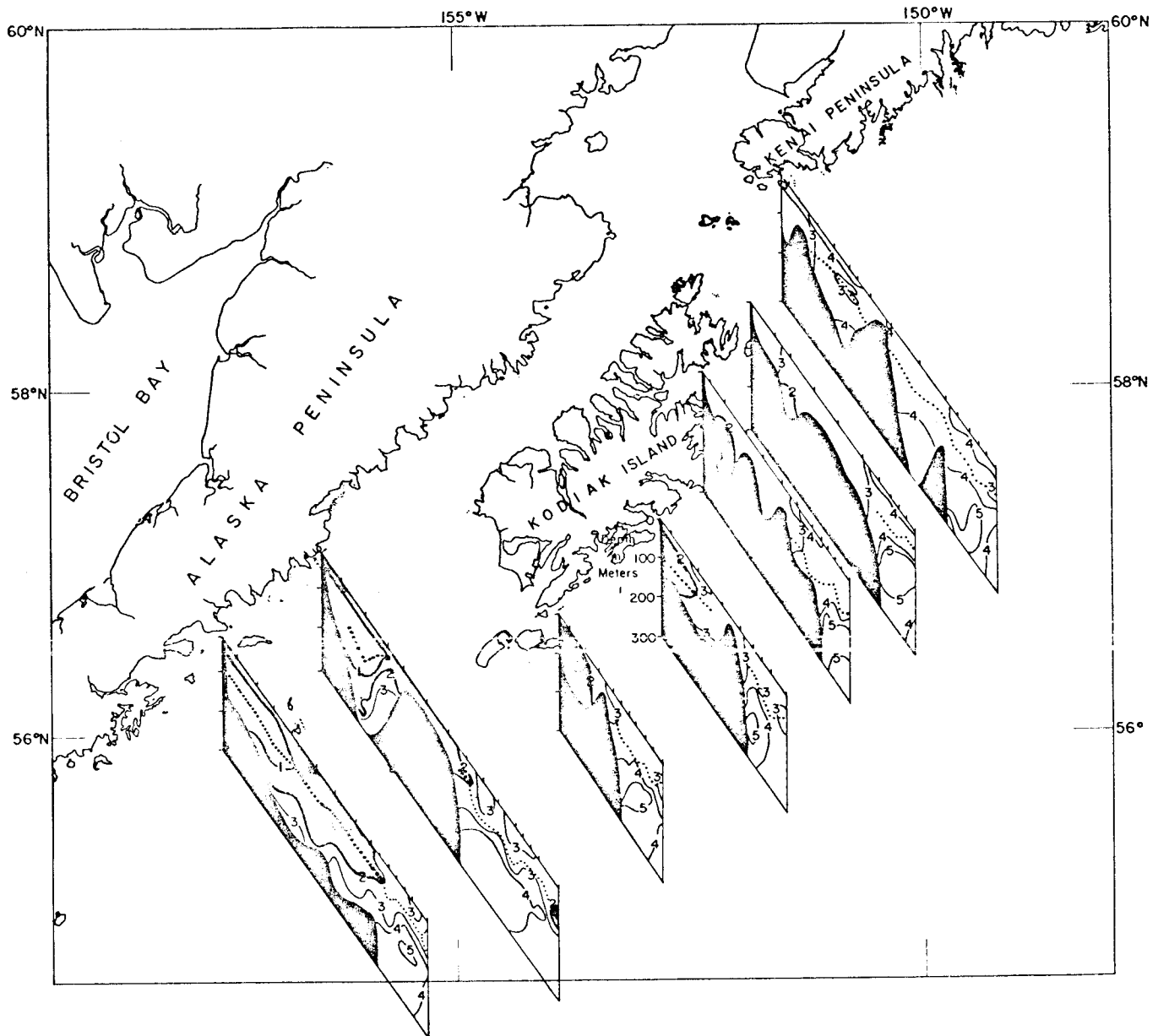


Figure 5. Vertical sections of temperature ( $^{\circ}\text{C}$ ) along lines of stations (RV George B. Kelez, April-May 1972 - Ticks indicate station locations) normal to the shelf edge indicating temperature-minimum stratum (dotted), and temperature-maximum ( $4-5^{\circ}\text{C}$ ) seaward of the shelf edge.

vidual stations that are not manifested at others. There is a similarity in the medium - term (1-3 years) trends, that is not apparent in the long-term trends (Fig. 6). For example, only at Dutch Harbor and Sitka is there evidence of a prolonged cooling period, 1958-73. The 12-month running mean clearly indicates cold periods centered around 1955 and 1972, and warm periods around 1958, 1963 and 1968. Similar trends in the oceanic area ( $5 \times 5^\circ$  Marsden quadrant 195-3;  $55-60^\circ\text{N}$ ,  $140-145^\circ\text{W}$ ) are evident (Fig. 7), and the transpacific occurrence of large areas of positive and negative anomalies at periods of 5-6 years has been pointed out by (Favorite and McLain, 1973). There are sufficient station data in offshore areas during the period 1955-1963 to indicate temperature changes that can occur at depth during cold and warm periods. Comparison of data in summer 1956 and 1958 indicates that values in the temperature-minimum stratum were over  $10^\circ$  lower in 1956 over a wide area in the gulf (Fig. 8). Assuming winter convective overturn to 100 m, this represents a difference of  $10,000 \text{ cal/cm}^2$  (of sea surface), a significant change in the heat content of the water column and the heat budget of the area.

Temperature anomalies in the water column are related also to advective processes. It is difficult to isolate the effects of winter turnover from advection in the upper 100 m or so, but at depths below seasonal influences there are secular changes that can be detected even with fragmentary data. Favorite (1975) has shown the apparent eastward intrusion of cold water from the west into the gulf indicated by the distribution of temperature on the salinity surface =  $34.0 \text{ }^\circ/\text{oo}$  (which occurs at about 250 m) from 1955 to 1962. Any consideration of flow at depth in the gulf must take into

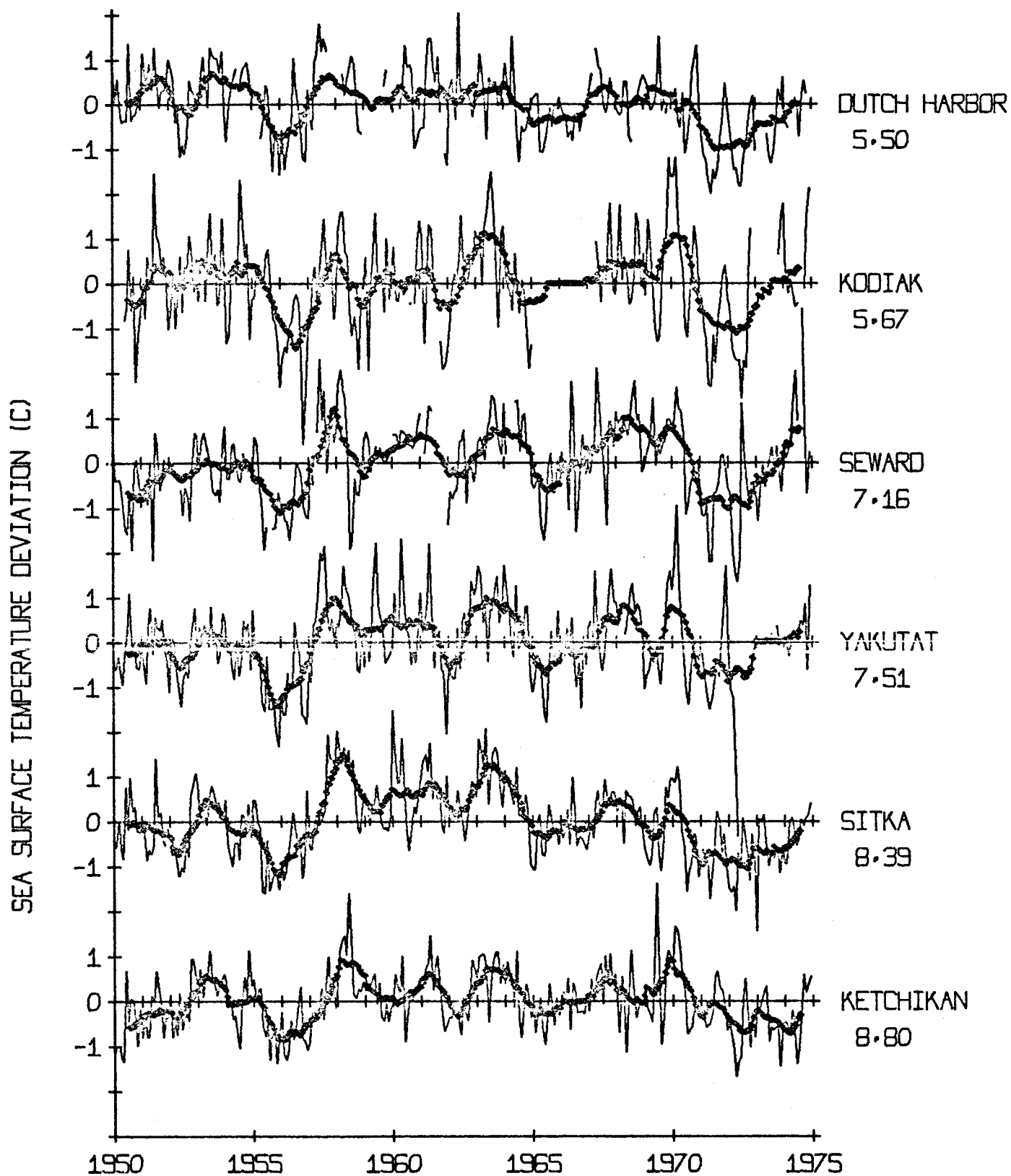


Figure 6. Deviations ( $C^{\circ}$ ) in sea surface temperature from monthly mean (1950-74) values at the indicated coastal stations; dotted segment indicates 12-month running mean.

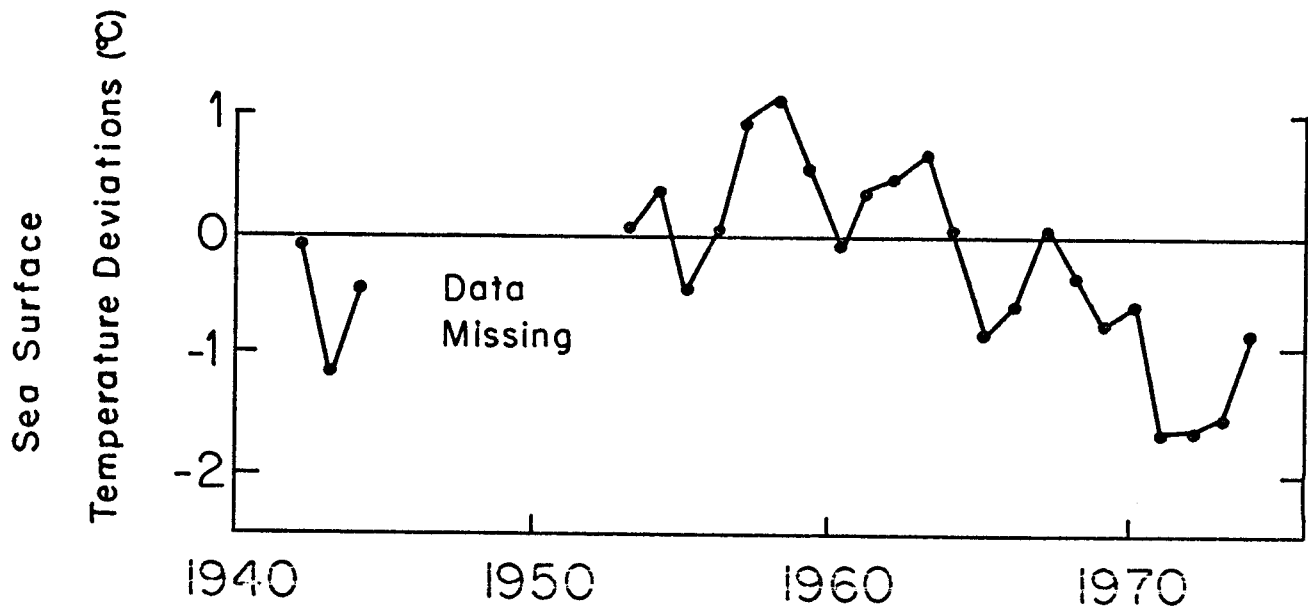


Figure 7. Deviations ( $^{\circ}\text{C}$ ) in sea surface temperature from annual mean (1948-67) values in  $5 \times 5^{\circ}$  Marsden quadrant 195-3 (see Fig. 2) reflecting a cooling trend since 1958.

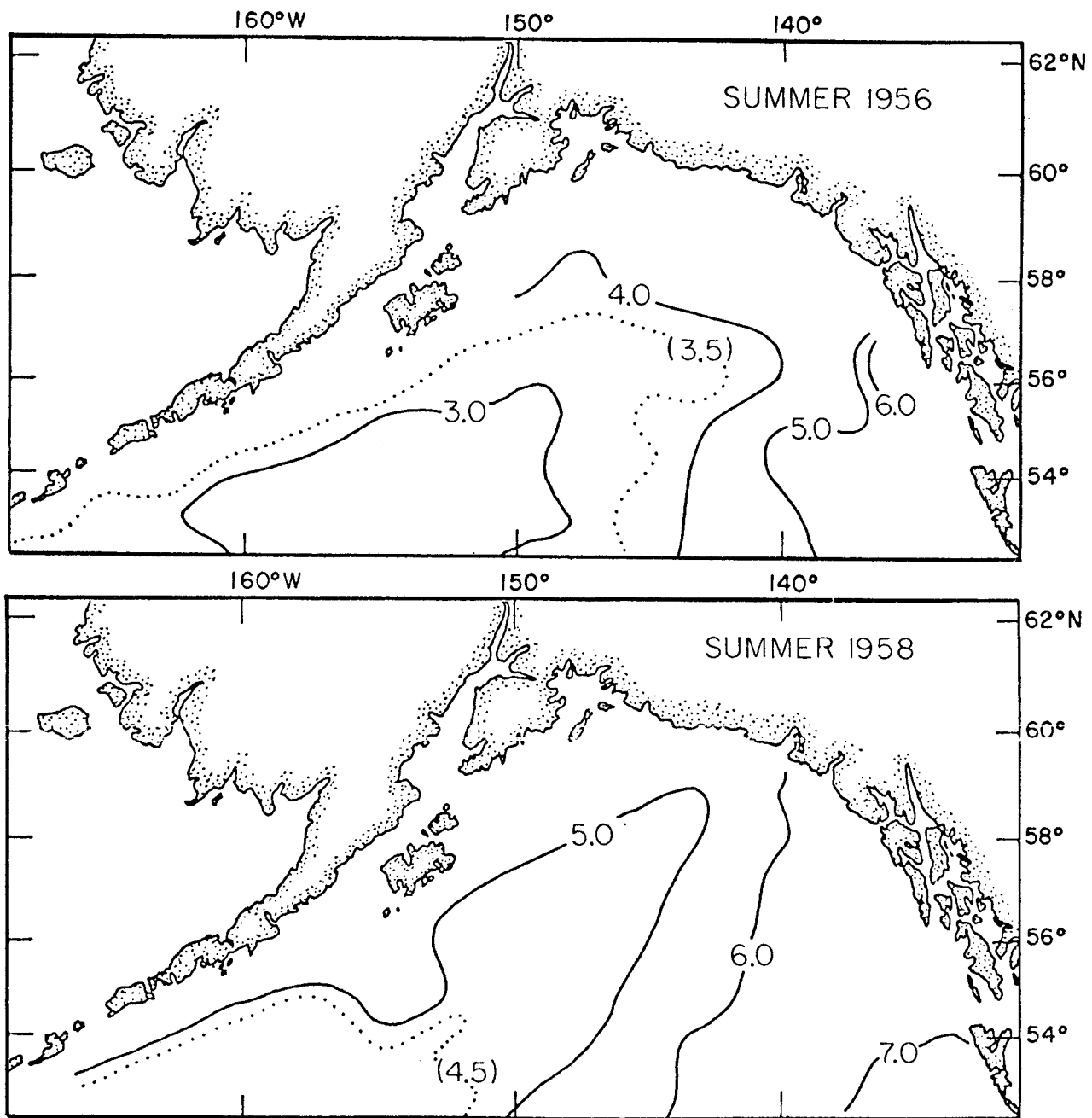


Figure 8. Temperatures ( $^{\circ}\text{C}$ ) in the subsurface temperature-minimum stratum ( $\sim 75\text{--}125\text{m}$ ) indicating much warmer conditions in summer 1958 compared to summer 1956 (from Dodimead et al, 1963).

consideration the fact that this anomalously cold water intruded nearly to the continental shelf in the eastern part of the gulf in 1961 (Fig. 9).

#### B. Salinity

Atlases depicting salinity distributions (e.g. Muromtsev, 1958; Barkley, 1968) provide limited information on actual conditions because of the paucity of these data. This is unfortunate because in many instances extensive salinity data, particularly near the surface, would provide more information concerning flow than temperature data. Because of a net excess of precipitation over evaporation (Jacobs, 1951) and extensive runoff, Tully and Barber (1960) have likened the oceanic regime to an estuarine system.

Although extensive runoff around the gulf in spring and summer dilutes coastal waters, this flow is difficult to quantify. Some clues as to the timing of this phenomenon are available from data on the monthly mean discharge from the Copper River, the dominant system in the area. Minimum discharge occurs from December to April; flow increases in May and reaches a maximum in July (Fig. 10). The effects of coastal runoff on offshore conditions is evident in station data averaged by season and  $2 \times 2^\circ$  quadrangles (Fig. 11). Spring and summer data are the most complete but, although values as low as 16-18 ‰ occur in inshore areas, the  $2 \times 2^\circ$  grid is too coarse to reflect precise inshore minima. Nevertheless, the seasonal offshore movement of coastal dilution is evident, specifically, the 32.0 ‰ isohaline, which moves offshore as much as 200 km in summer compared to its position in winter. Also evident is a region of high salinity in the southwestern part of the gulf reflecting vertical divergence.

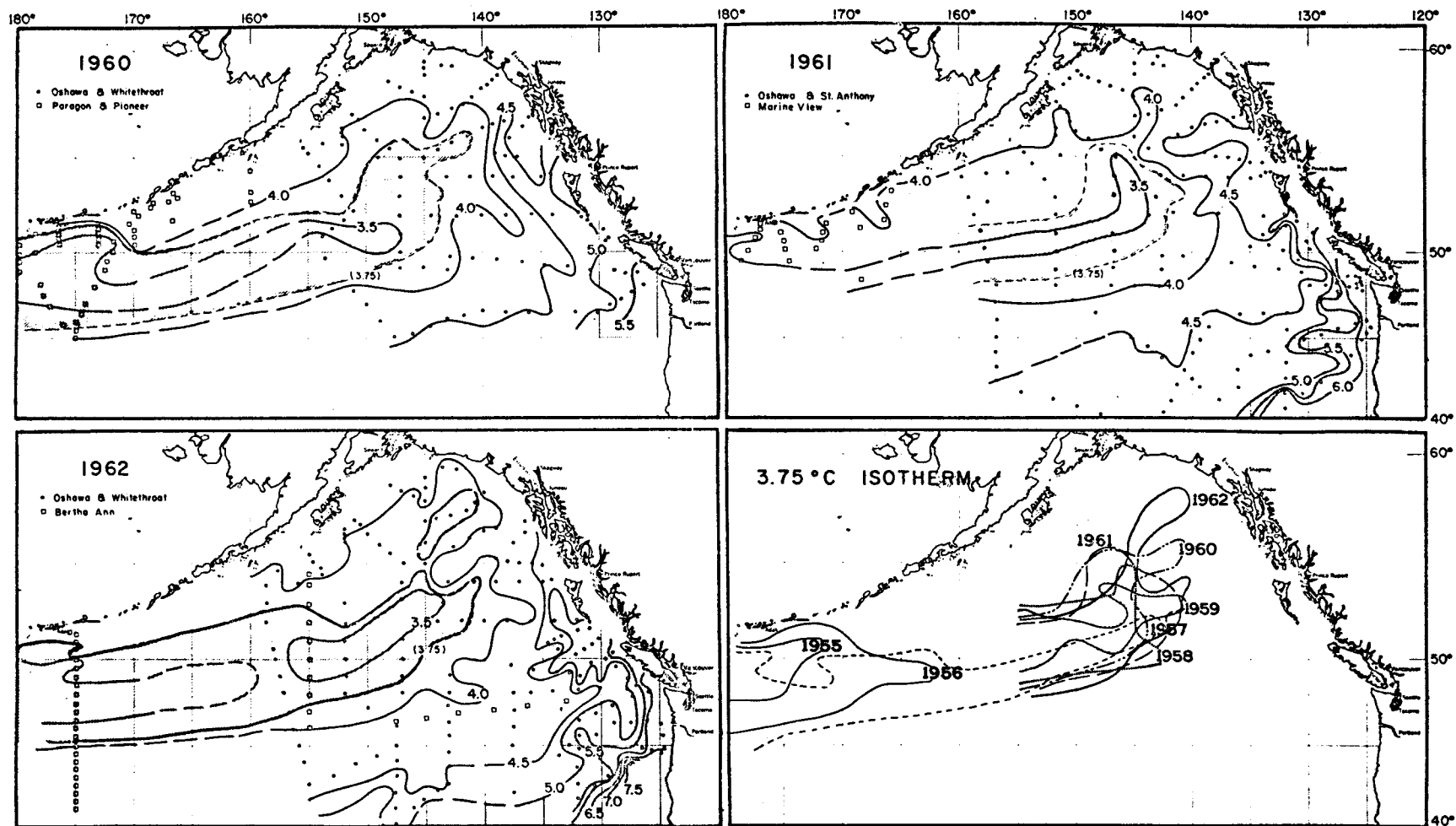


Figure 9. Temperatures ( $^{\circ}\text{C}$ ) on surface of salinity =  $34.0$  ‰ ( $\sim 300\text{m}$ ) in 1960, 61 and 62; and the configuration of the  $3.75^{\circ}\text{C}$  isotherm in 1955, 56, 57, 58, 59, 60, 61 and 1962.



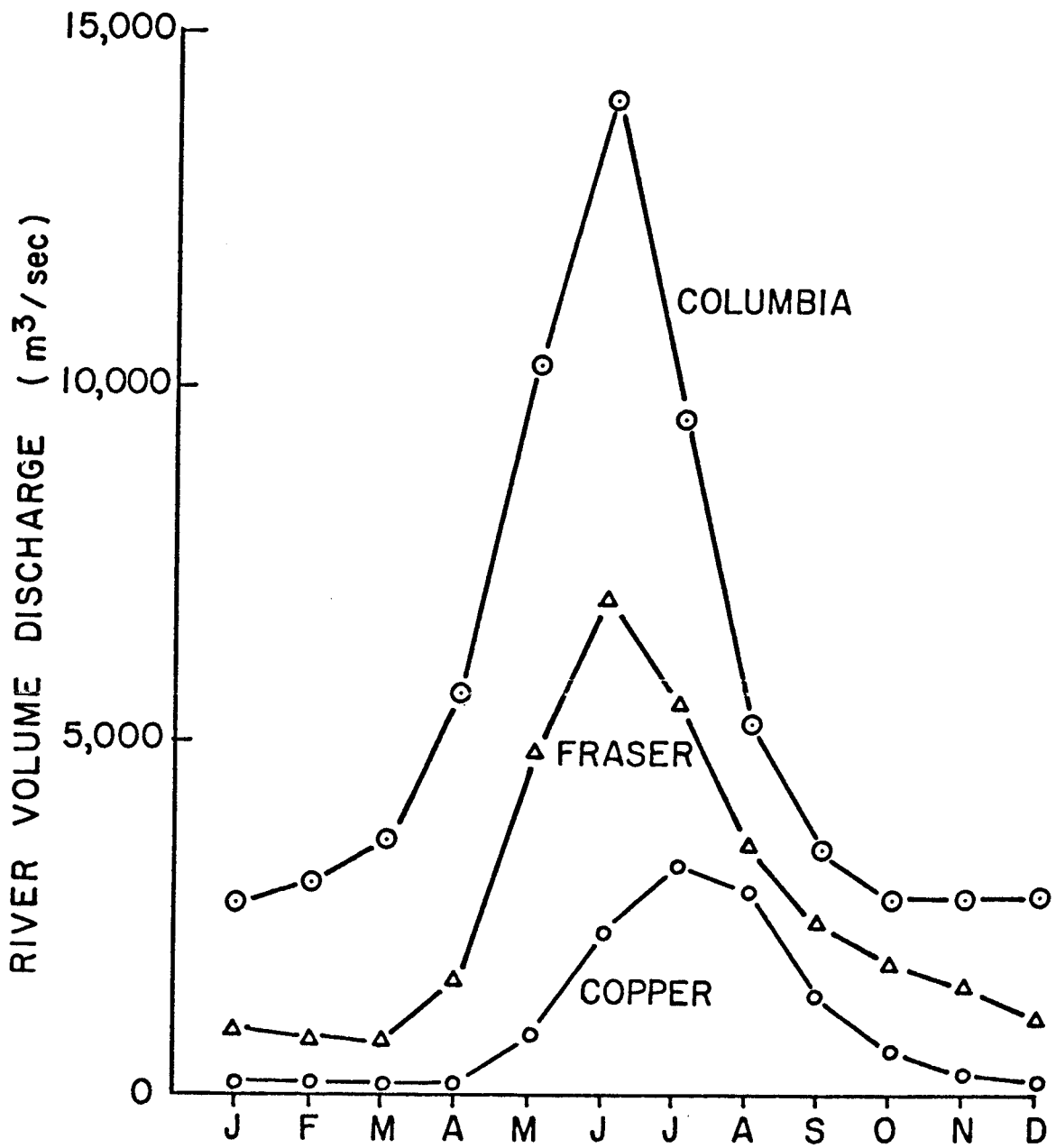


Figure 10. Monthly mean discharge (m<sup>3</sup>/sec) from the Columbia, Fraser and Copper Rivers showing relative volume and month of peak runoff.

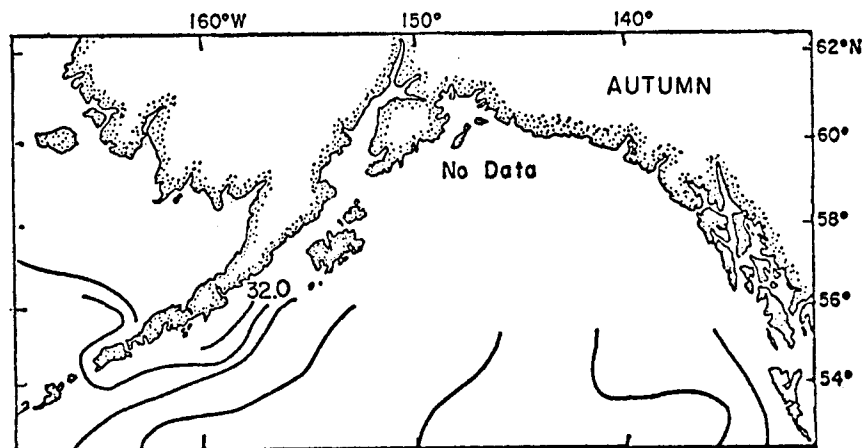
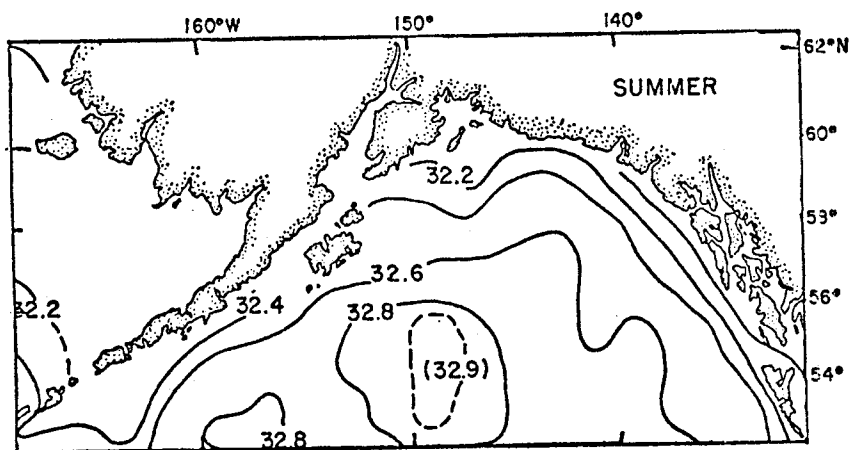
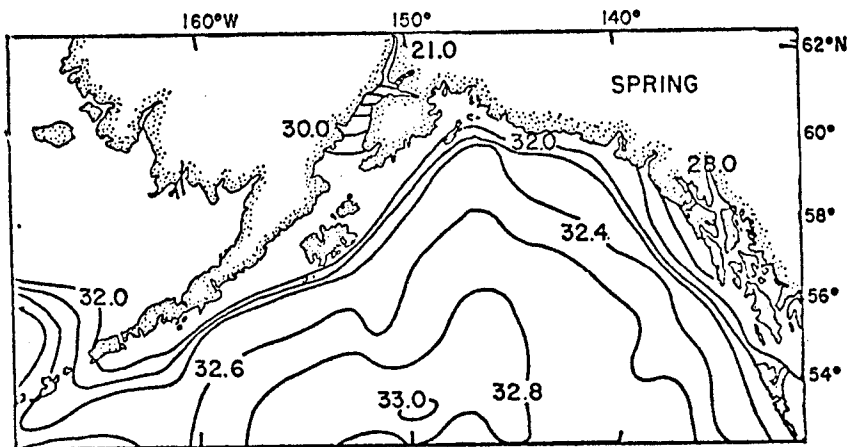
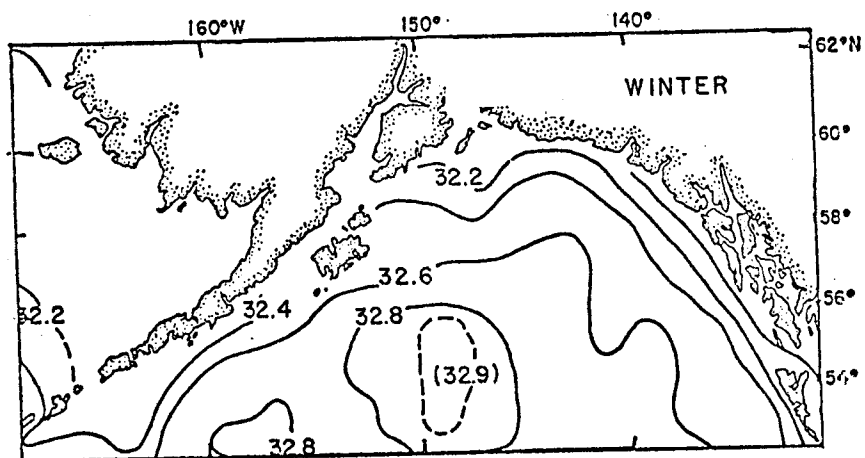


Figure 11. Long-term mean seasonal surface salinity distributions (based on a  $2 \times 2^\circ$  grid) showing marked coastal dilution in summer and maximum values in southwest part of the gulf.

Maximum values ( $>33.0$  ‰) in this area are evident in spring rather than as might be expected in winter, but this is believed due to limited data in the winter period.

Associated with the dilute surface layer is the marked halocline between 100-200 m (Fig. 12) evident in a vertical profile along  $145^{\circ}\text{W}$ . This feature gives a marked stability to the water column and greatly influences the vertical extent of winter convection and, thus, effects the vertical distribution of temperature and other water properties.

The salinity data are inadequate to show convincingly any anomalous salinity distributions in the gulf either in time or space. This does not mean that they do not occur. Considerable variability in the timing and volume discharge of coastal runoff takes place. An example of the variability possible is evident in the distributions of surface salinity off southeastern Alaska in summer 1957 and 1958 (Fig. 13). Considerable offshore dilution is evident in the 1958 distribution compared to that in 1957. However, the distributions represent mean fields over 3 month periods constructed from various data points, and it is difficult to ascertain which, if either, represents average or anomalous conditions.

There has always been speculation as to the existence of a frontal zone at the edge of the continental shelf indicating not only boundary processes such as shelf waves, but a simple separation of dilute coastal from saline oceanic water. Data from a continuously recording surface salinograph (Fig. 14) obtained during numerous transects of a short line of stations normal to the shelf edge eastward of Kodiak Island in spring 1972 (Favorite and Ingraham, 1976a) prove the existence of such a frontal

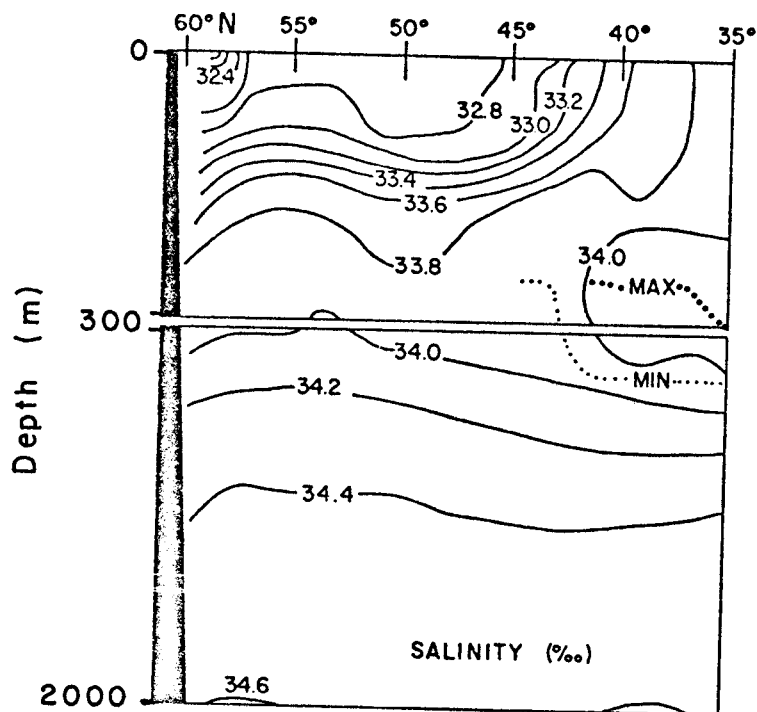


Figure 12. Vertical section of long-term mean salinities (based on  $2 \times 2^\circ$  grid) along  $145^\circ\text{W}$  showing: the dilute surface layer north of  $45^\circ\text{N}$ , particularly near  $60^\circ\text{N}$ ; the ridging or doming of isolines at  $55^\circ\text{N}$ ; and, the halocline between 100-200 m.

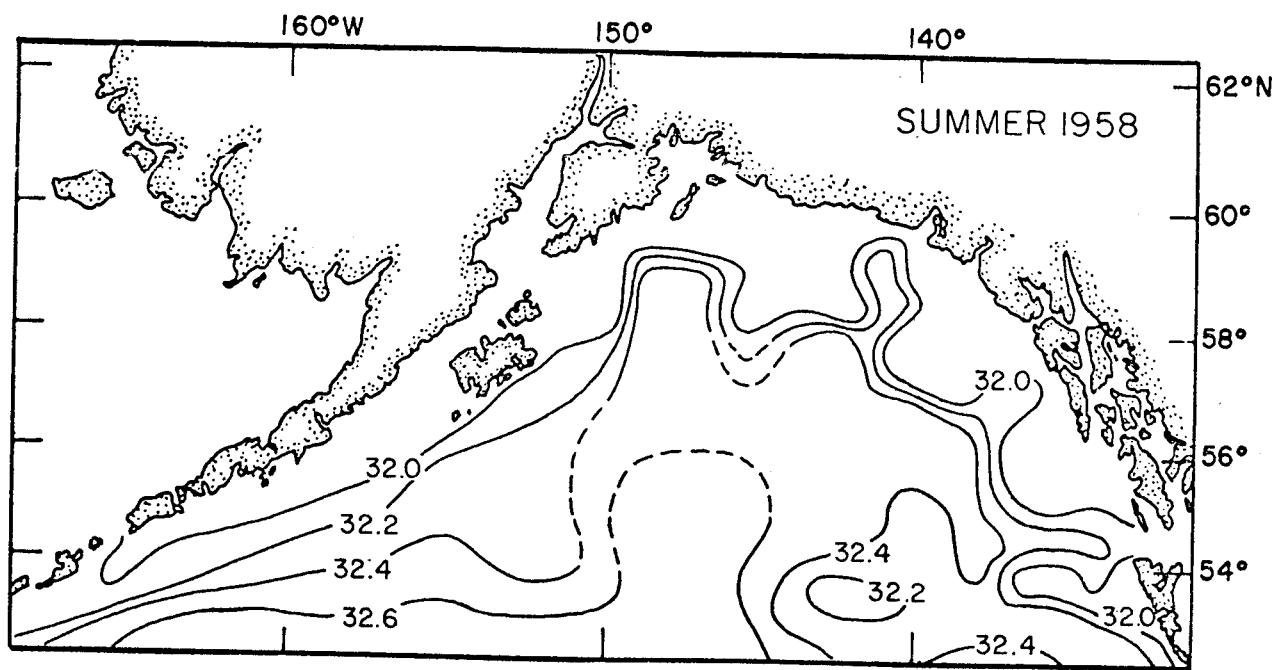
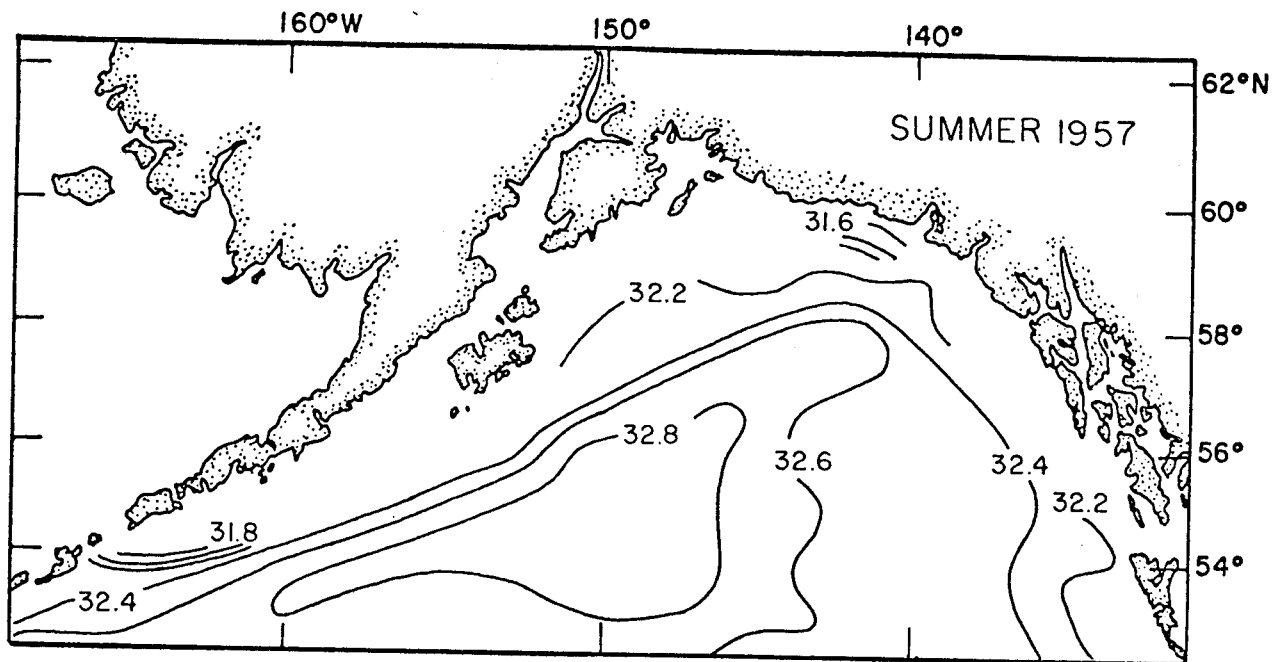


Figure 13. Surface salinity during summer 1957 and 1958 showing the extensive dilution off southeastern Alaska in the latter period reflecting the highly variable conditions that can occur in the surface layer (from Dodimead et al, 1963).

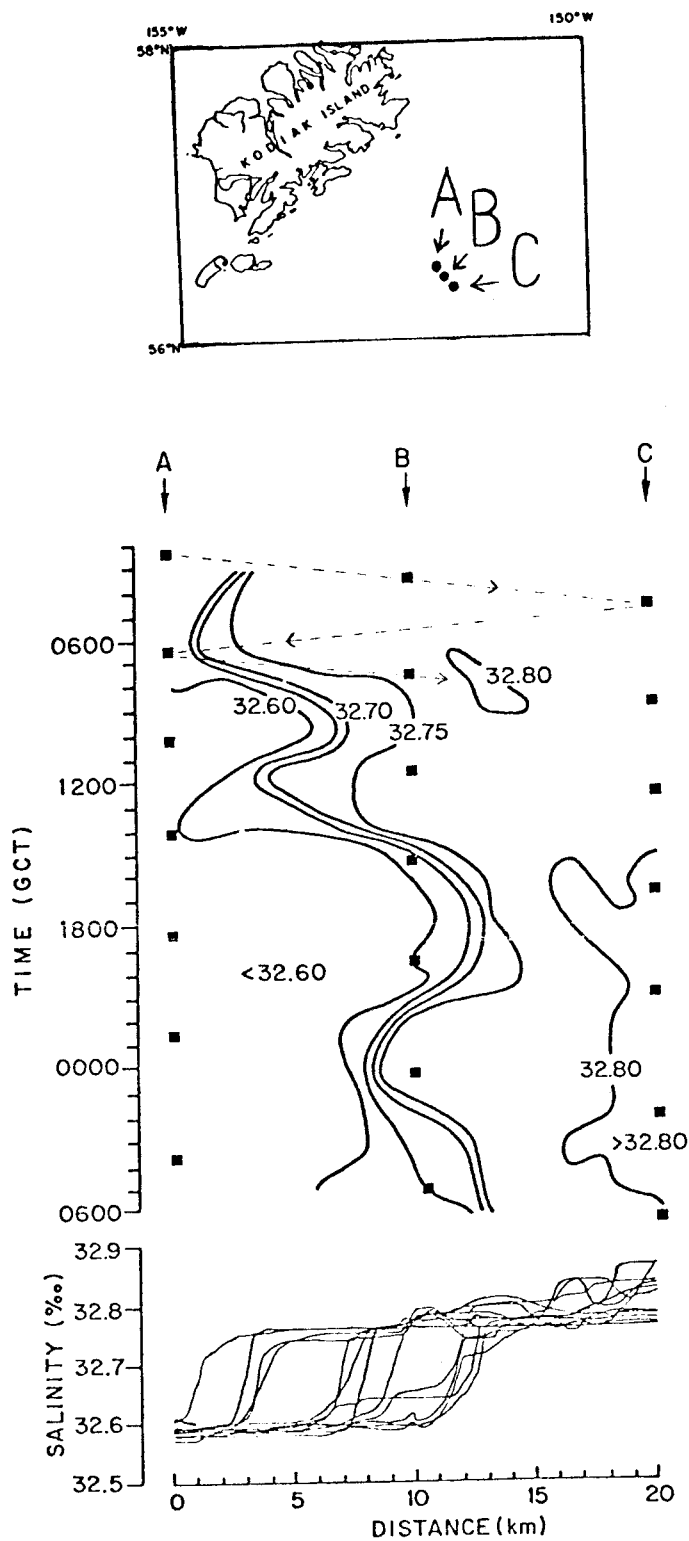


Figure 14. Surface salinity front detected seaward of Kodiak Island in the vicinity of the edge of the continental shelf (RV George B. Kelez, May 5-6, 1972) using constantly recording salinograph while occupying repetitive stations: A, B, C (dashed lines indicate vessel movement).

zone. Salinity distributions at 200, 500, 1000 and 2000 m (Fig. 15) reflect primarily the presence of the surface divergence in the offshore portion of the western gulf and the suggestion of cyclonic circulation found in the temperature distributions. There is also an obvious area of dilution off Cape Spencer in the 200 m temperature field.

### C. Water Masses

All oceanic waters attain marked characteristics when they are in contact with the atmosphere and these characteristics are subsequently altered by lateral and vertical mixing. When discrete temperature and corresponding salinity values of a water parcel below the depth of seasonal influences are plotted against each other a well-defined temperature-salinity (T-S) curve results that is characteristic of a given area and defines a water mass (Sverdrup, Johnson and Fleming, 1942). Such a curve defines the Subarctic Water Mass, characteristic of the area lying generally north of 50°N in the eastern North Pacific Ocean.

The low temperatures and salinities that distinctly define this curve are due in part to the waters moving eastward at depth from the Okhotsk Sea, a general vertical movement of intermediate water due to the Ekman divergence at the surface, and an undetermined northward transport of deep water in the Pacific basin that is deflected upward in this area by the land boundaries in the gulf and the Aleutian-Commander island arc. Modifications to this basic T-S curve are caused by a northward flow of warm water on the eastern side of the gulf that originates not only from eastward flow south of 50°N, but also from northward flow in the California Undercurrent. The latter is manifested at the surface in winter, but is overridden at the surface in summer by a southward flow stemming from the southern branch of the easterly onshore flow.

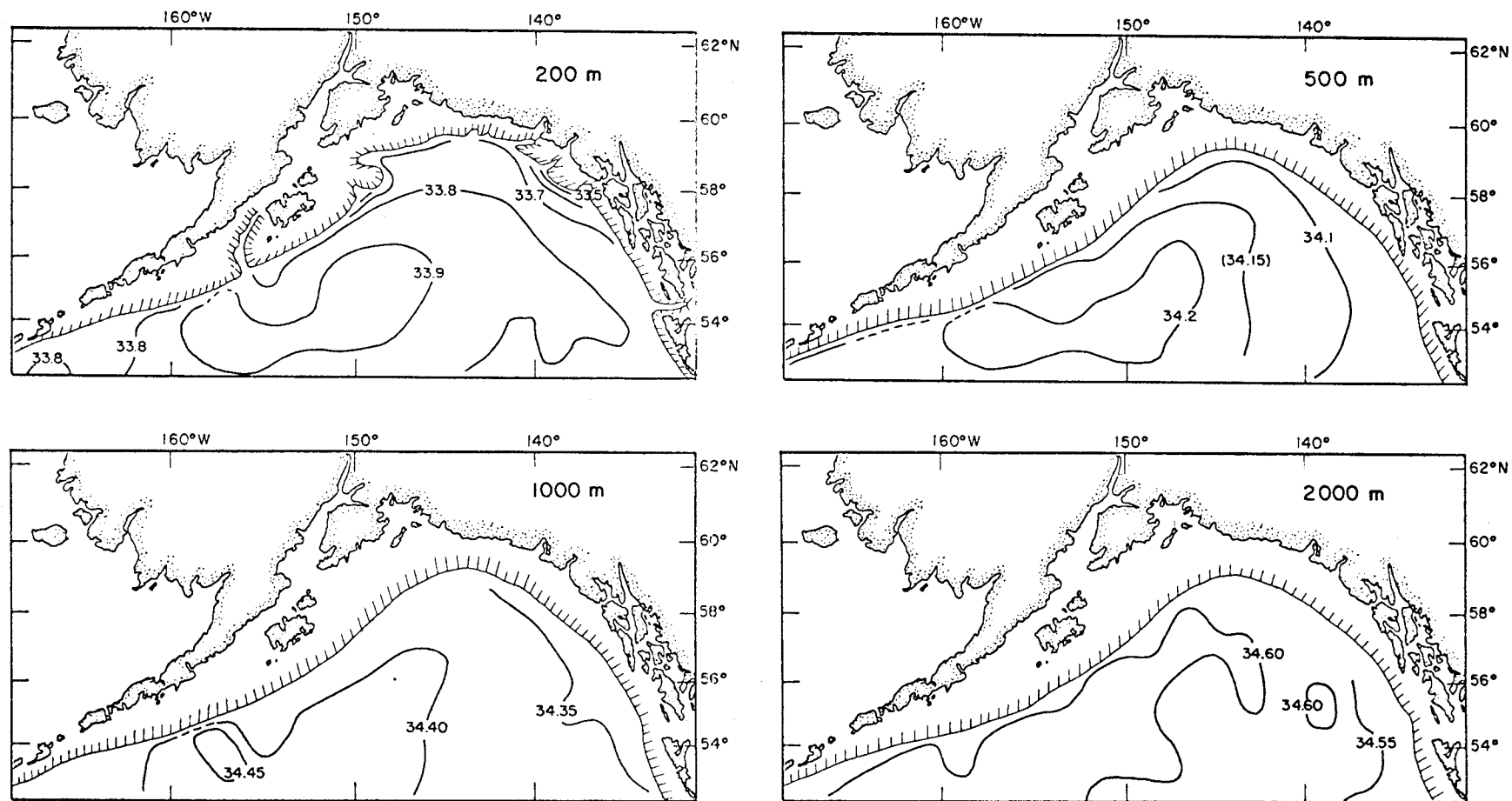


Figure 15. Long-term mean salinity distributions (based on  $2 \times 2^\circ$  grid) at 200, 500, 1000 and 2000 m.



Monthly mean, as well as maximum and minimum, values of temperature and salinity at standard depths were computed from all station data by 2 x 2° quadrangles and are presented in the form of T-S curves at 4 selected locations at which winter and summer data were available (Figs. 16 and 17). Because of the paucity of data, in some instances only 3 stations, the curves and extreme values must be considered as only indicative of conditions rather than representing precise values and ranges. The water mass at the head of the gulf (area A) is formed from the merging of three major water masses moving northward into the gulf. In general, all have equivalent surface temperatures during the periods of maximum heating (summer, 13-14°C) and cooling (winter, 4-5°C), except in area B where winter temperatures of 3°C are evident, and there is a noticeable decrease in surface salinity shoreward from areas B to D, the greatest dilution occurring in area A. The elimination in winter of the temperature gradient, or thermocline, evident in the upper 50-75 m of the water column during summer is readily apparent in all areas. There are marked differences in temperatures from 100 and 300 m, about 3°C, between areas B and D; conditions at these depths in areas C and A reflect an admixture of the water masses in areas B and D, although the temperature maximum between 150 and 250 m is maintained. There is also a suggestion of a downward diffusion of summer heating below 125 m during winter. Below 300 m the T-S curves in areas A, B and C are similar and follow the trend of the general Subarctic Water Mass curve, however, there is a significant departure from this curve in area D attributed to northward flow along the coast. As might be expected, variability in temperature and salinity conditions is largely

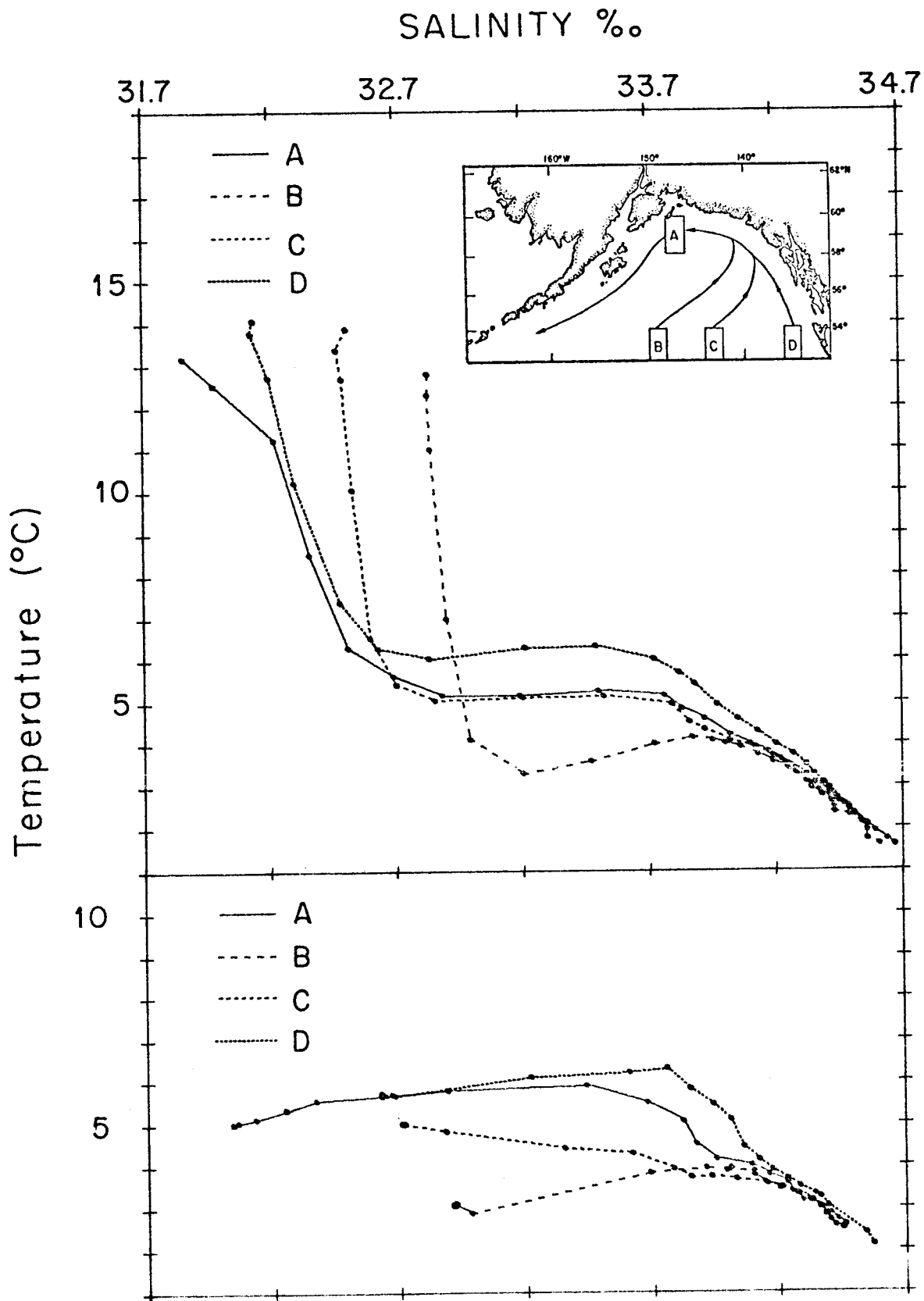


Figure 16. Long-term summer and winter mean temperature-salinity (T-S) relations at standard depths in the indicated  $2 \times 2^\circ$  quadrangles showing characteristics of the various water masses funneling into the gulf.

820

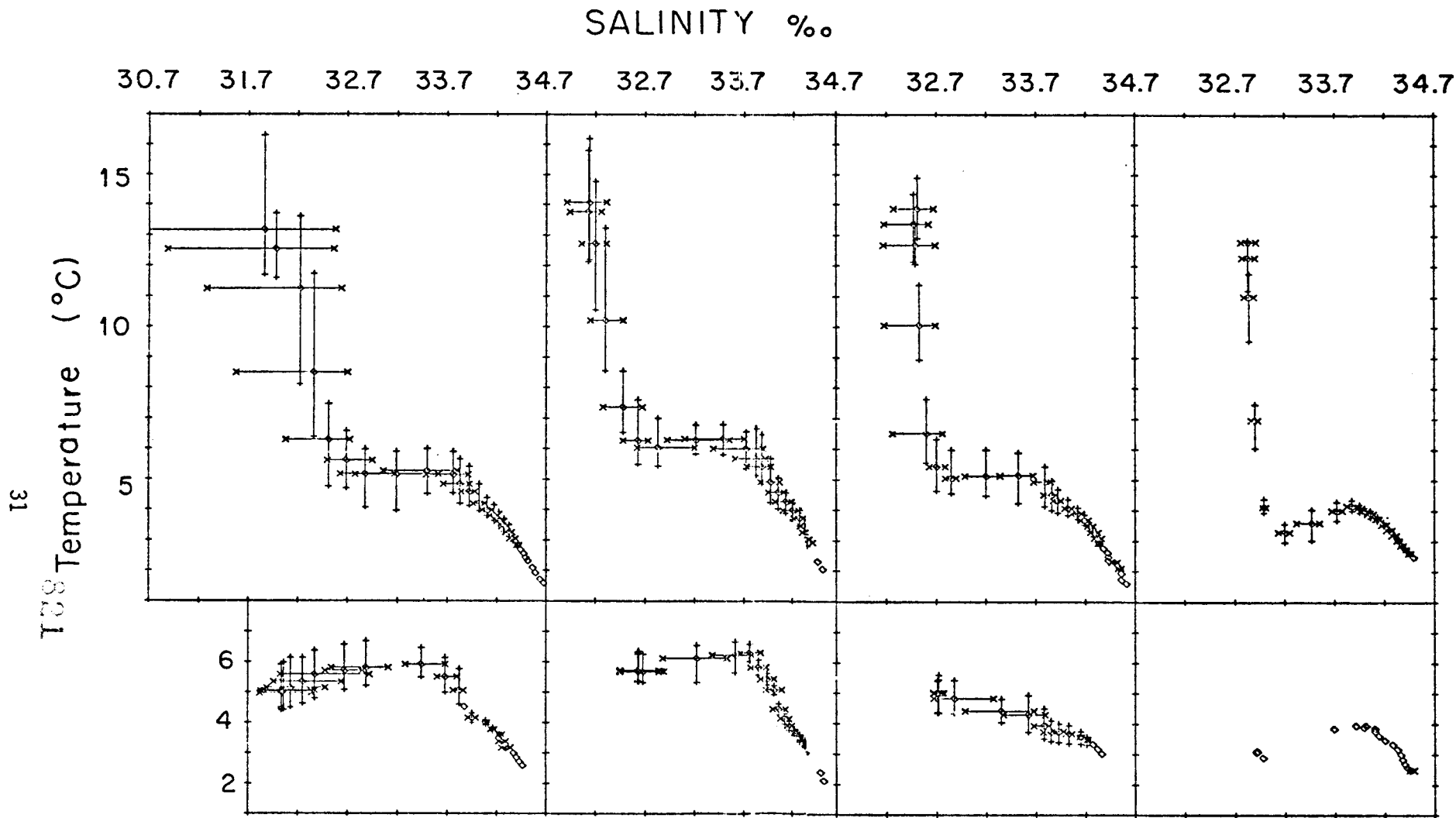


Figure 17. Maximum and minimum temperature-salinity (T-S) values at standard depths for the T-S curves shown in Figure 16.

limited to the upper 300 m of the water column and the greatest ranges occur in area A, primarily because that 2 x 2° quadrangle encompasses part of the continental shelf and is subjected to coastal runoff. Obviously conditions at the head of the gulf are dependent upon the relative components of flow in these three water masses.

### III. CURRENTS

Bering, Chirikof, Cook, Clerke, Portlock, Dixon and countless other early explorers of the coastline around the gulf encountered the treacherous winds and coastal currents that exist in the area, and such information reported by mariners is constantly updated in the Alaska Coast Pilots. There are also early papers that synthesize this information. Wild (1877) presented a Current Chart of the Ocean that showed northward flow into the gulf stemming from a bifurcation of eastward onshore flow into northward and southward trending branches that occurred well seaward of Vancouver Island. Dall (1899) reported that the zone of separation was just seaward of Vancouver Island. Schultz (1911) indicated that only in summer did the separation occur at this latitude; during winter it occurred off the California coast near  $41^{\circ}\text{N}$ . Such schemes were largely based on sporadic reports and data from ship's logs, but the absence in the gulf of extensive commercial vessel traffic, whose daily observations of set and drift have provided an extensive historical data base on circulation in other areas, has resulted in a paucity of specific information concerning flow. Drift bottle studies provide information concerning gross circulation patterns, however, only the release and recovery points are known and actual trajectories are subject to various interpretations. The computation of geostrophic currents in which the relative field of currents is derived from the observed field of mass in the ocean, provides an indirect method of estimating oceanic flow. This method has several shortcomings and requires extensive synoptic observations at sea which are not possible to obtain from present platforms. Nevertheless, this method permits the calculation of relative currents and transports

that provide considerable insight into oceanic flow throughout the area observations are made. No significant direct current measurements have been made in offshore waters of the gulf prior to OCSEAP studies. However, measurements off the west coast of Vancouver Island where a similar climate occurs reveals interesting patterns of onshore and offshore flow that are probably duplicated in gulf waters (Dodimead et al. 1963).

Long before planned drift bottle or drift float programs were instigated, the presence of debris from Japanese fishing operations and remnants of California redwood trees on the southeast Alaskan coast signaled two widely differing sources of water flowing into the gulf. Although there have been a number of recoveries of bottles or floats from a variety of experiments, there are several studies that provide most of the basic information that can be deduced by such studies.

The first extensive study was conducted by the International Fisheries Commission (Fig. 18); over 4,000 bottles were released from 1930-34 (Thompson and Van Cleve, 1936). Those released along an east-west line across the gulf from Baranof to Kodiak Island and at several locations inshore along the Alaska Peninsula in spring 1930 indicated a broad northward flow into the head of the gulf, with recoveries only at Cape St. Elias and Cook Inlet, and a southwestward drift along the Alaska peninsula and through Unimak Pass. Releases just east of Kodiak Island were recovered only along the southern coast of the island and on the Alaska peninsula to the west and north of the island; releases from three locations inshore along the Alaska Peninsula indicated a southwestward drift along the coast. Releases off the west coast of the

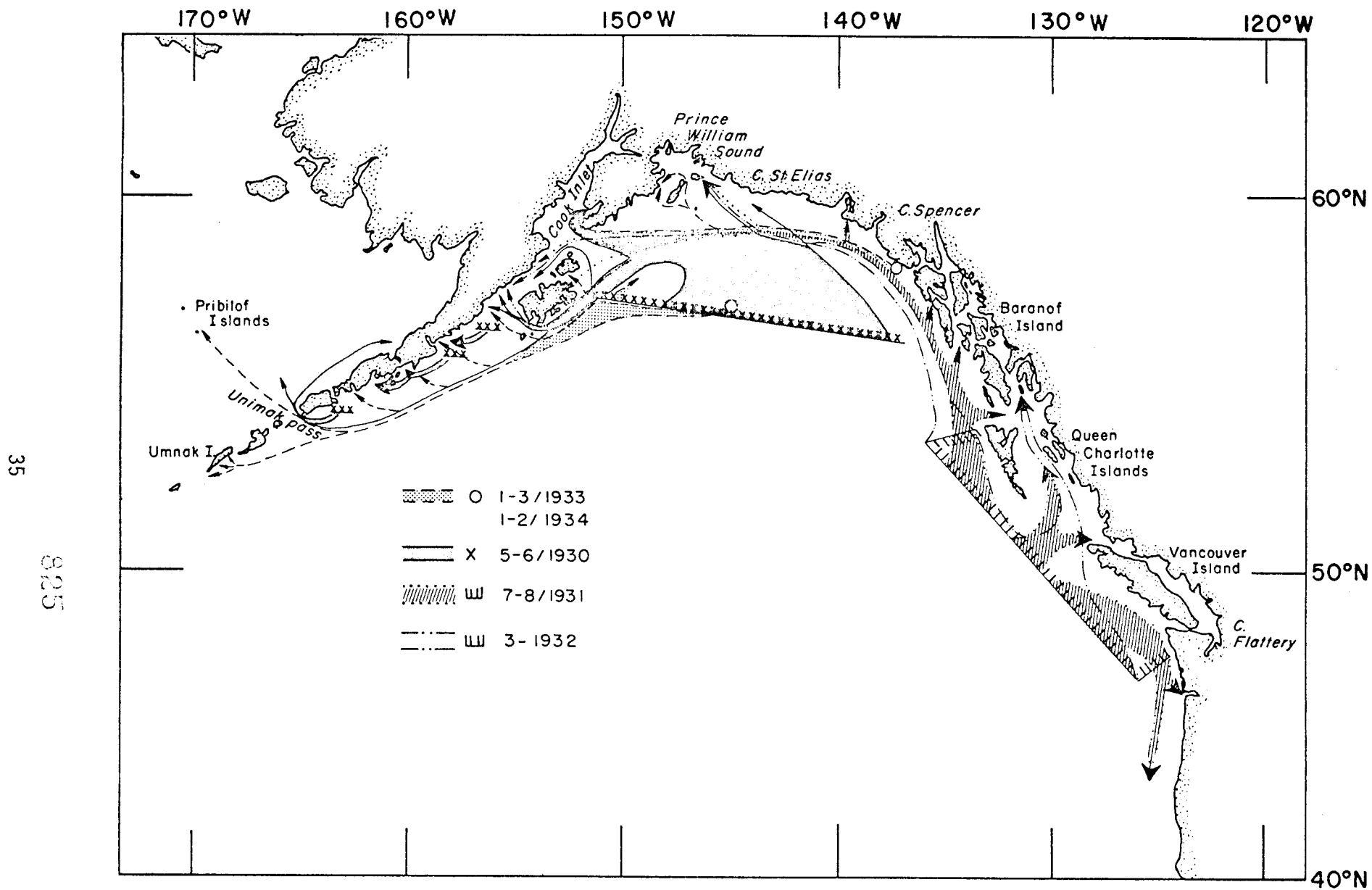


Figure 18. Schematic diagram of significant results of drift bottle studies conducted by the International Fisheries Commission (IFC) 1930-34 (adapted from Thompson and Van Cleve, 1936).

Queen Charlotte and Vancouver Islands in summer 1931 indicated a marked bifurcation of onshore flow at the northern end of Vancouver Island. Two bottles in the northern component of flow were recovered near Cape Spencer and one on Kodiak Island. In a similar experiment in spring 1932, except for one recovery at Cape Flattery (directly east of the release point), all recoveries were made northward of the release points, at various locations around the gulf. The western most recovery was made in Shelikof Strait and numerous recoveries were made in Prince William Sound where none was recovered in the 1930 and 1931 experiments. Releases north of  $50^{\circ}30'N$  and recovered north of  $57^{\circ}N$  were estimated to travel 9.4 miles per day. In winter 1933 and 1934, releases just north of Cape Spencer were recovered in Prince William Sound, along the west coast of the gulf, and on the Pribilof and Umnak Islands. These studies reflected a southward shift in winter of the zone of separation of the onshore flow off Vancouver Island that had been indicated earlier (Schutz, 1911). The northward branch, which moves cyclonically around the gulf, had a general drift of about 20 cm/sec and an inherent onshore component. Although a large cyclonic gyre encompassing the entire gulf at the latitude of Kodiak Island was inferred, there is no evidence other than delays between release and recovery to justify such a conclusion. The authors noted that, although westerly flow was predominant, at the rear of the gulf, the currents were not regular or constant.

A subsequent experiment was conducted by the Pacific Oceanographic Group (POG), Nanaimo, from August 1956 to August 1959 (Dodimead and Hollister, 1962). Forty-two releases (33,869 bottles) were made from Ocean Station "P" ( $50^{\circ}N$ ,  $145^{\circ}W$ ) and surrounding locations. Twenty-three of the releases



were made at Ocean Station "P" at approximately 6-week intervals and these indicated a fairly complicated pattern in drift currents between the station and the North American coast. For example, of 998 bottles released on August 25, 1956 only one of the 114 recoveries was made north of Ketchikan and it was made on Middleton Island; whereas of 1,008 bottles released on August 24, 1957, all of the 39 recoveries were made at or west of Middleton Island. Of particular interest to the present study are the 5 releases north of Ocean Station "P", especially the 2 that were made north of 55°N (Fig. 19). At the 3 locations south of 55°N between 155 and 160°W, an easterly set was indicated, recoveries being made throughout the head of the gulf. However, recoveries from the two releases north of 55°N (approx. 142°W) made on February 17, 1957 and August 17, 1957 were made only at the western side. Perhaps of more significance is that recoveries from the winter release were recovered as far north as the Pribilof Islands, as far west in the Aleutian area as Amchitka Island, as far east as the Washington-Oregon-California coast, and as far south as the Hawaiian Islands and Wake Islands--a tremendous dispersal that requires considerable thought when one contemplates possible oil pollution in the head of the gulf and the subsequent formation of floating tar balls.

Whereas the IFC studies were concerned with coastal drift<sup>5/</sup> and the POG studies largely with onshore drift from discrete offshore locations, the studies conducted by the National Marine Fisheries Service Northwest Fisheries Center (formerly Bureau of Commercial Fisheries Biological Laboratory) extended over a large area of the northern North Pacific Ocean.

<sup>5/</sup> See Ingraham and Hastings (1974) for results of seabed drifter study off Kodiak Island in May 1972.

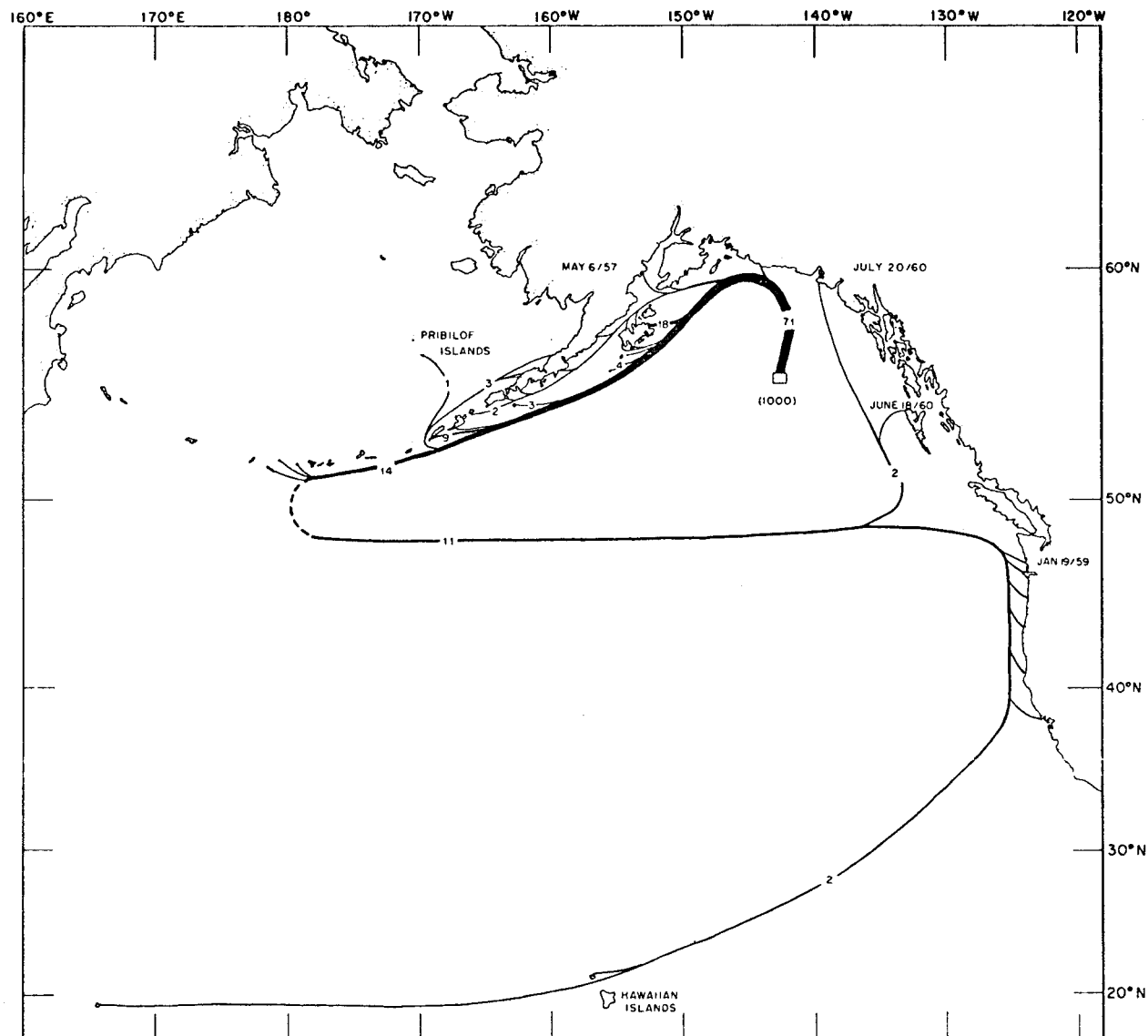


Figure 19. Release and recovery locations of drift bottles released by the Pacific Oceanographic Group (Nanaimo) in February 1957 showing the wide dispersal to the Bering Sea, the Aleutian Islands, Washington-Oregon-California coast, the Hawaiian Islands and Wake Island (from Dodimead and Hollister, 1962).

The two experiments that pertain to flow in the gulf were conducted in 1962 (Favorite, 1964) and in 1964 (Fish, 1971); releases made along extended north-south and east-west cruise tracks (Fig. 20) indicated the broad north-south oceanic boundaries of eastward surface flow that moves directly into the gulf or toward the coasts of British Columbia, Washington, and Oregon where, in winter, a northward flow surfaces along the coast (Reid, Roden and Wyllie, 1958; Burt and Wyatt, 1964; and others).

#### B. Geostrophic Flow

The geostrophic (dynamic) method has been thoroughly described and evaluated (e.g. Fomin, 1964); basically, the method, which requires a balance between Coriolis and pressure gradient forces permits the computation of current relative to that at an arbitrary and perhaps fictional depth, selected in the belief that it is deep enough for isopleths of density and pressure to be parallel and thus a depth or level at which no motion exists (a zero reference level); no accelerations or physical boundaries are permitted. Fleming (1955) has presented a chart showing the locations in the northern North Pacific Ocean where the oceanographic station data required by his method had been obtained prior to 1955, and Dodimead et al (1963) showed station locations from 1955-59, as well as winter and summer fields of geopotential topography. McEwen, Thompson and Van Cleve (1930) and Thompson, McEwen and Van Cleve (1936) were the first to use this method in the Gulf of Alaska and found a westward flow in excess of 50 cm/sec at the edge of the continental shelf. The complexity of geostrophic flow in this area was evident in the closely spaced station data obtained by Doe (1955). Roden (1969) and Thomson (1972) have contributed to present knowledge of flow around the gulf.

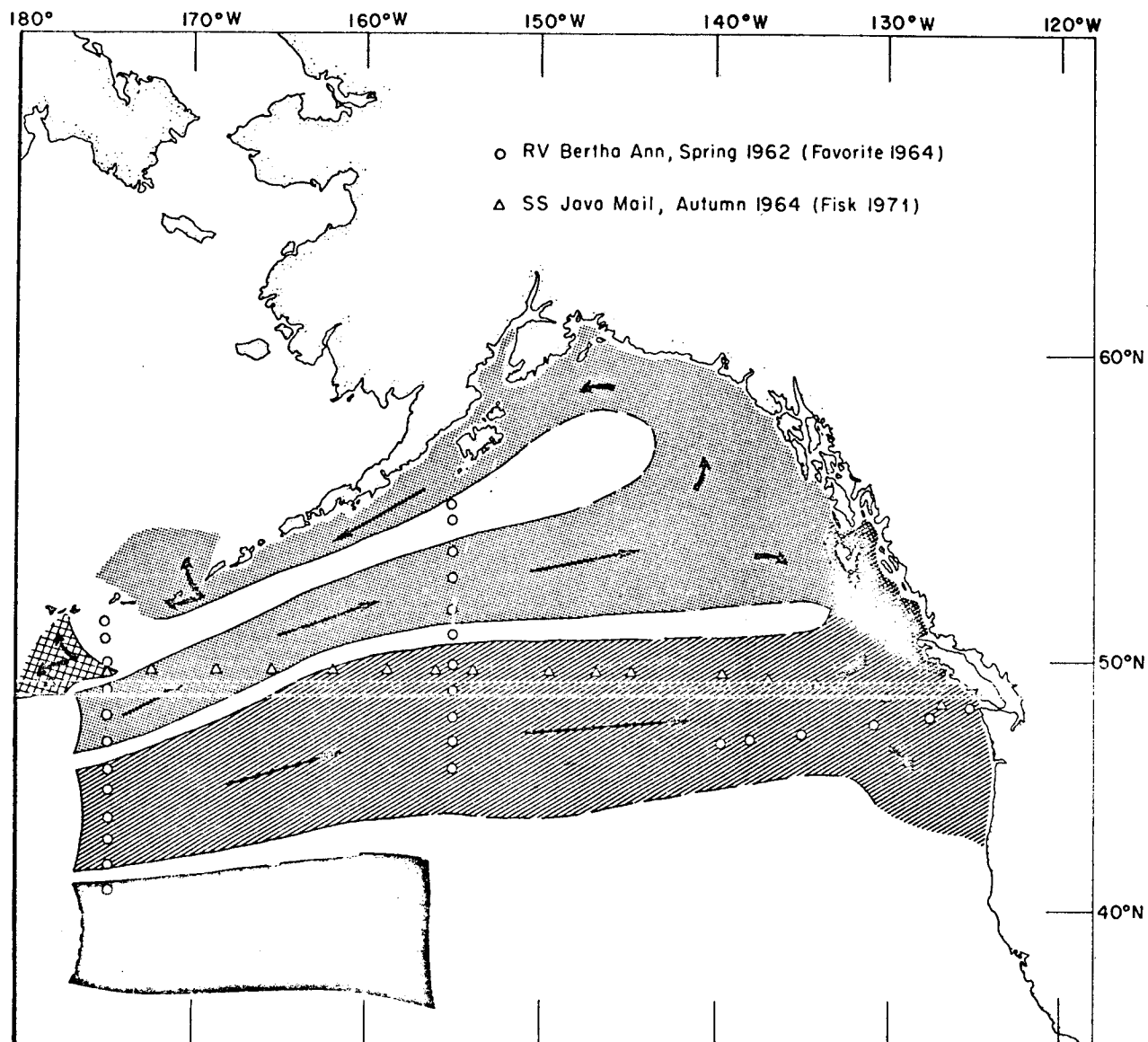


Figure 20. Schematic diagram of results of drift bottle studies by the Northwest Fisheries Center (Seattle) in 1962 and 1964 showing the general nature of easterly onshore drift.

The locations of all oceanographic station data on file at NODC (prior to OCSEAP studies) and used in this report are shown in Figure 21. Current speeds normal to a line between two oceanographic stations are obtained by the Sandstrom Helland-Hansen equation:

$$V = \frac{10}{f\Delta x} \left[ \int_0^D \delta_1 dp - \int_0^D \delta_2 dp \right] \quad (1)$$

where D is the accepted depth-of-no-motion expressed in decibars;  $\delta$ , the geopotential anomaly; x, distance between stations; f, Coriolis acceleration; and, p, pressure.

Computations of geopotential anomalies at all stations were averaged by 2 x 2° quadrangles to obtain long-term means and seasonal (winter, spring, summer and autumn) means for the depth intervals 0/300 db, considered to be the layer of seasonal influence, and 0/2000 db, where 2000 db is considered to represent a level-of-no-motion. Mean values over such large areas (over 20,000 km) cannot be expected to reflect boundary currents over the narrow continental slope but general circulation patterns are evident. Data for winter, spring and summer are sparse, from 1 to 30 or more observations per quadrangle, with an average of about 10; data for autumn are only 20% available. At Ocean Station "P", observations are more numerous and provide at least a qualitative check on surrounding data. For example, in the mean summer data there are 112 observations at the quadrangle associated with Ocean Station "P"; mean value 0.53 dyn cm; although there are only 11 observations in the quadrangle to the west, and 10 in the quadrangle to the east, the mean values are 0.52 and 0.53 dyn cm respectively.

The seasonal mean fields of geopotential topography for the depth interval 0/300 db (Fig. 22) are quite similar. The longitude of the topographic low, 149°W is the same for all seasons but the latitude shifts

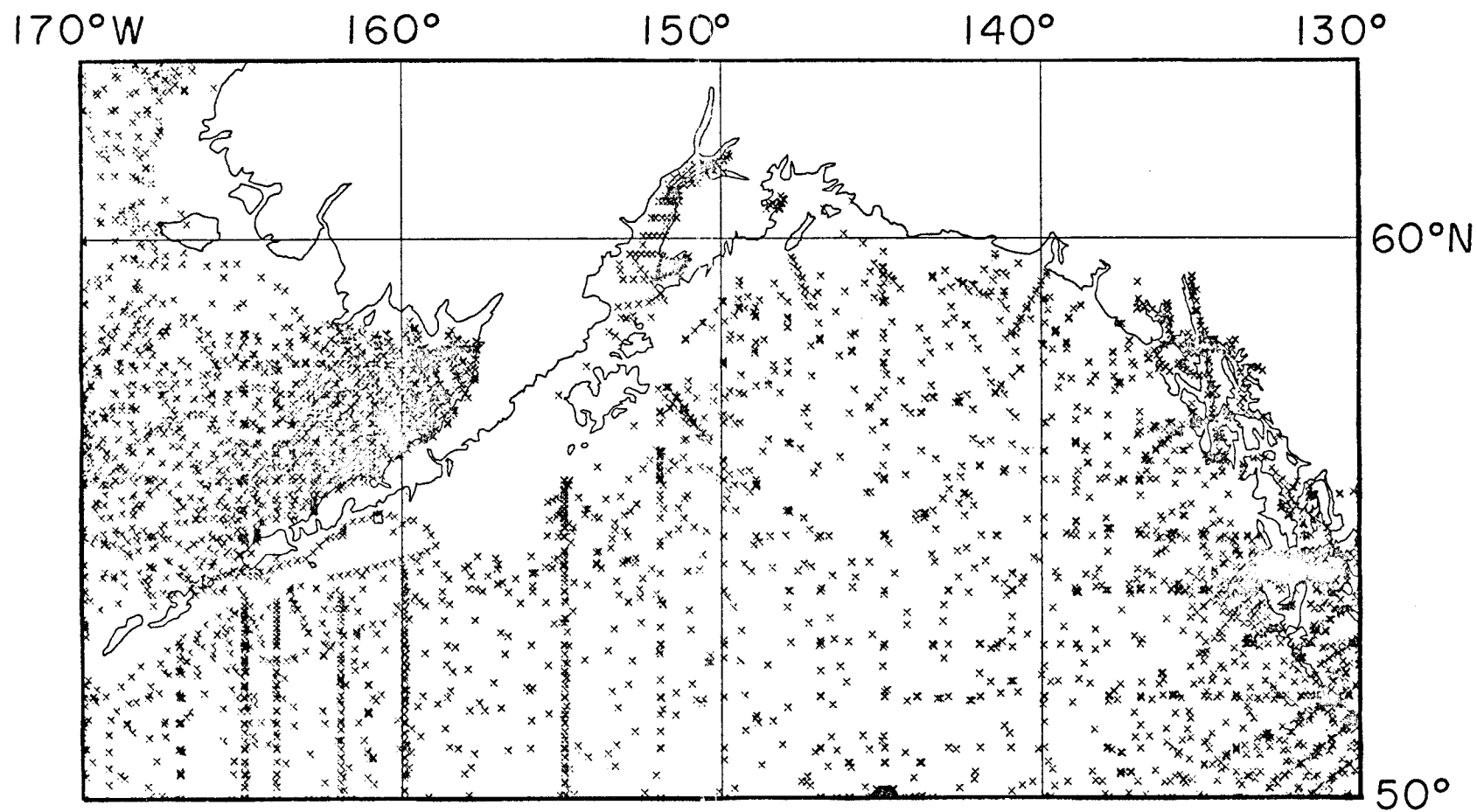


Figure 21. Locations of oceanographic stations in National Oceanographic Data Center geofile.

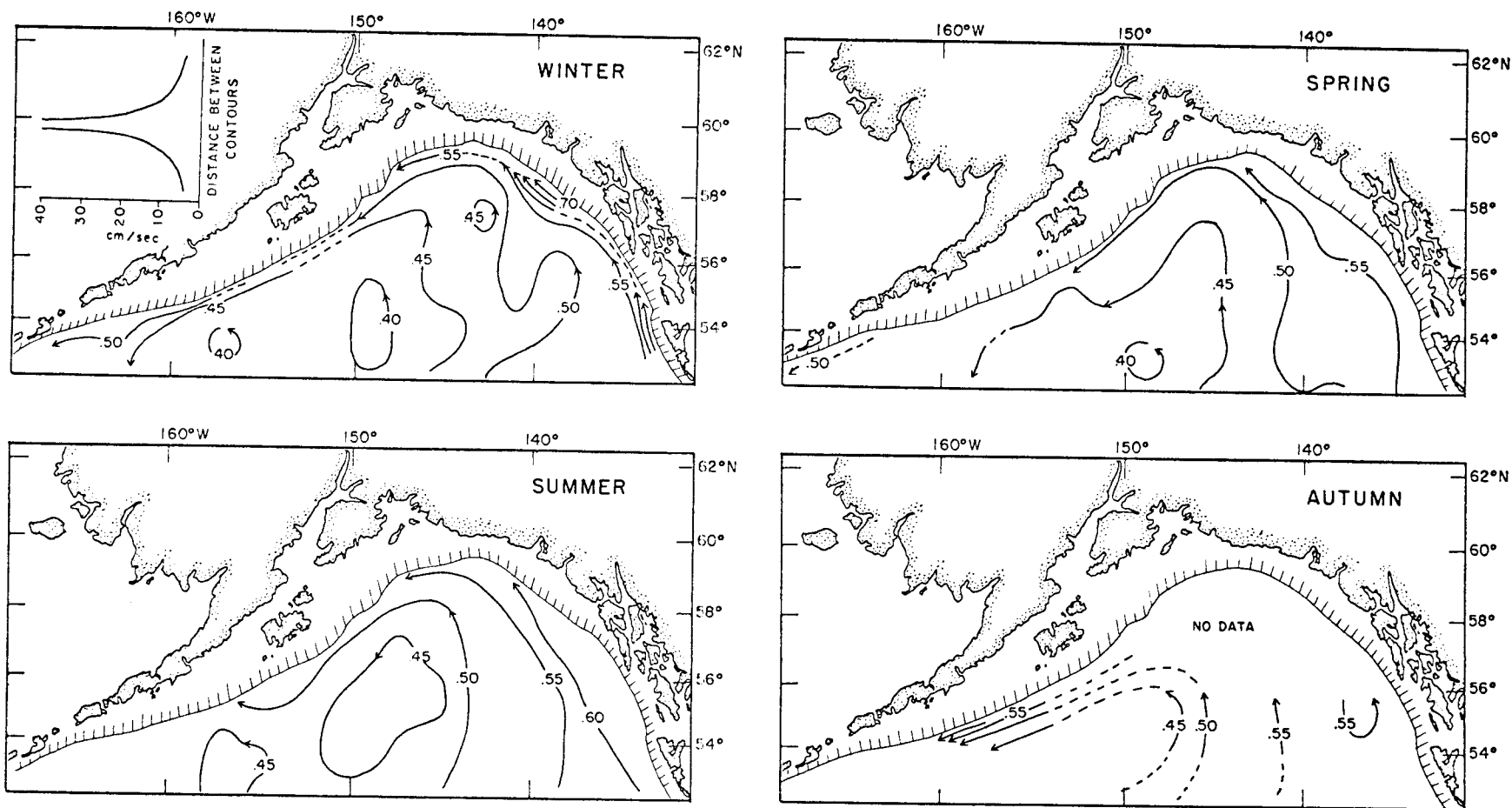


Figure 22. Long-term seasonal mean geopotential topographies, 0/300 db, (based on  $2 \times 2^\circ$  grid) showing variability in geostrophic flow particularly the high velocities at the eastern side of the gulf (the broad grid spacing prevents showing the boundary current at the western side).

from  $53^{\circ}\text{N}$  in spring to  $55^{\circ}\text{N}$  in summer while winter is intermediate at  $54^{\circ}\text{N}$  (autumn data is lacking). Although numerous variations in the configurations of the respective isopleths occur, there is a difference of 15-20 dyn cm between the topographic low in the southwestern part of the gulf and the topographic high near the coast at the eastern edge of the gulf. Further, isopleths are not continuous around the gulf but, rather than representing a discontinuity in flow, as will be shown in the next section, this is primarily due to narrow width of the boundary current in the northern and western part of the gulf. Speeds of 3 - 5 miles per day and a northward transport, east of the topographic low, of 3 Sv are indicated.

The winter and summer mean fields of geopotential topography for 0/2000 db (Fig. 23) are generally similar to those for 0/300 db. The position of the topographic low remains near  $55^{\circ}\text{N}$ ,  $149^{\circ}\text{W}$ . The difference in topography across the eastern side of the gulf changes from 35-40 dyn cm in summer to 50 dyn cm in winter indicating some winter acceleration; speeds are 20 and 25 cm/sec and transports are 12 and 15 Sv, respectively. Isopleths at northern and western sides of the gulf are discontinuous as before. As might be expected from the foregoing, the long-term mean field of geopotential topography for 0/2000 db is not much different from either of the above and the apparent conclusion one can draw is that in winter the baroclinic mode reflects an increase in flow of about 20 percent, and this increase stems largely from adjustment in the mass field below 300 m.



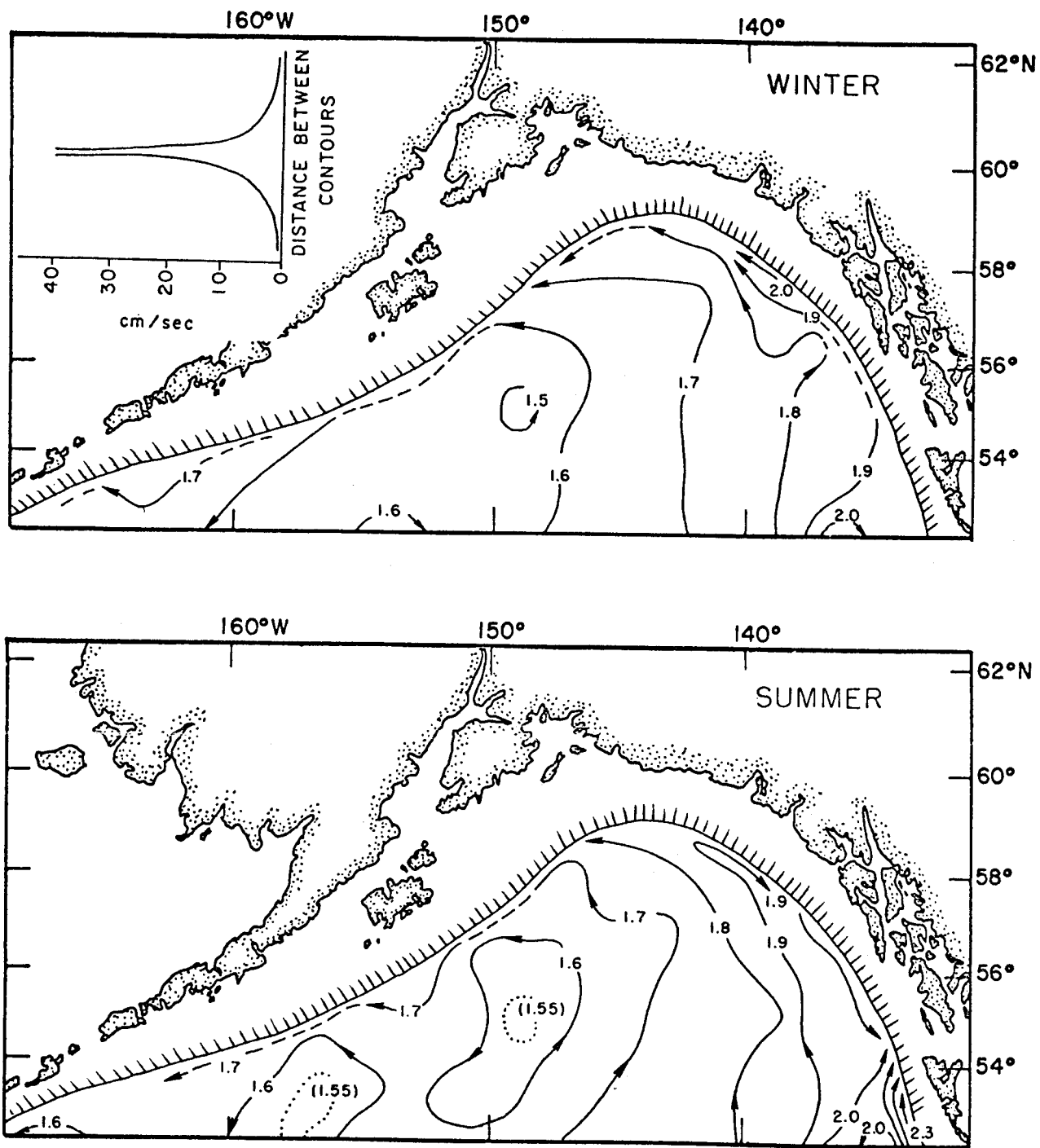


Figure 23. Long-term seasonal geopotential topographies 0/2000 db (based on  $2 \times 2^\circ$  grid) showing generally similar features of cyclonic flow.

Because of the paucity and non-synoptic nature of the station data in the gulf, it is difficult to ascertain if irregularities in geopotential topographies are real or caused by the lack of synoptic data. However, there are three aspects that can be explored: are there patterns in individual years that are not obvious in the mean flow; what are the apparent fluctuations in transport, and do accelerations in the boundary current result in discontinuities in geostrophic flow on the western side of the gulf? Because most of the data that permit answering these questions were obtained in the period 1955-63 and many of the observations were limited to 1000 m at that time (even though this was not considered a realistic level-of-no-motion), some comparisons must be made in reference to this level.

One pattern that is represented in one form or another is an extensive perturbation in the northward flow at the eastern side of the gulf. Examples of this are found in the geopotential topography (0/1000 db) for winter and summer 1957 (Fig. 24). The configuration of the isopleths suggests a possible blockage of westward flow at the head of the gulf resulting in a seaward plume that extends over 500 km in a southwesterly direction. The apparent effect of this phenomenon is a convergence of isopleths, and thus an acceleration of northward flow, at the eastern side of the gulf. Unfortunately neither closely spaced or repetitive stations have ever been made in this area so the actually physical nature or cause of this feature cannot be ascertained. This is also true of features at the western side of the gulf. At times there is an

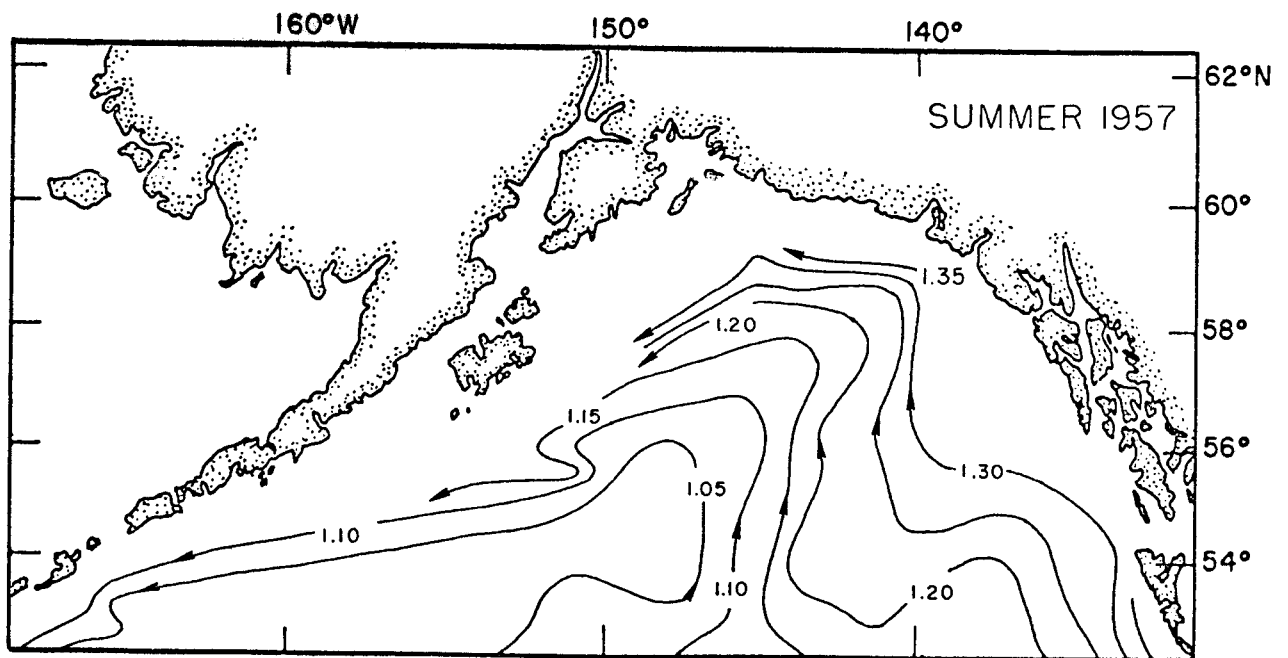
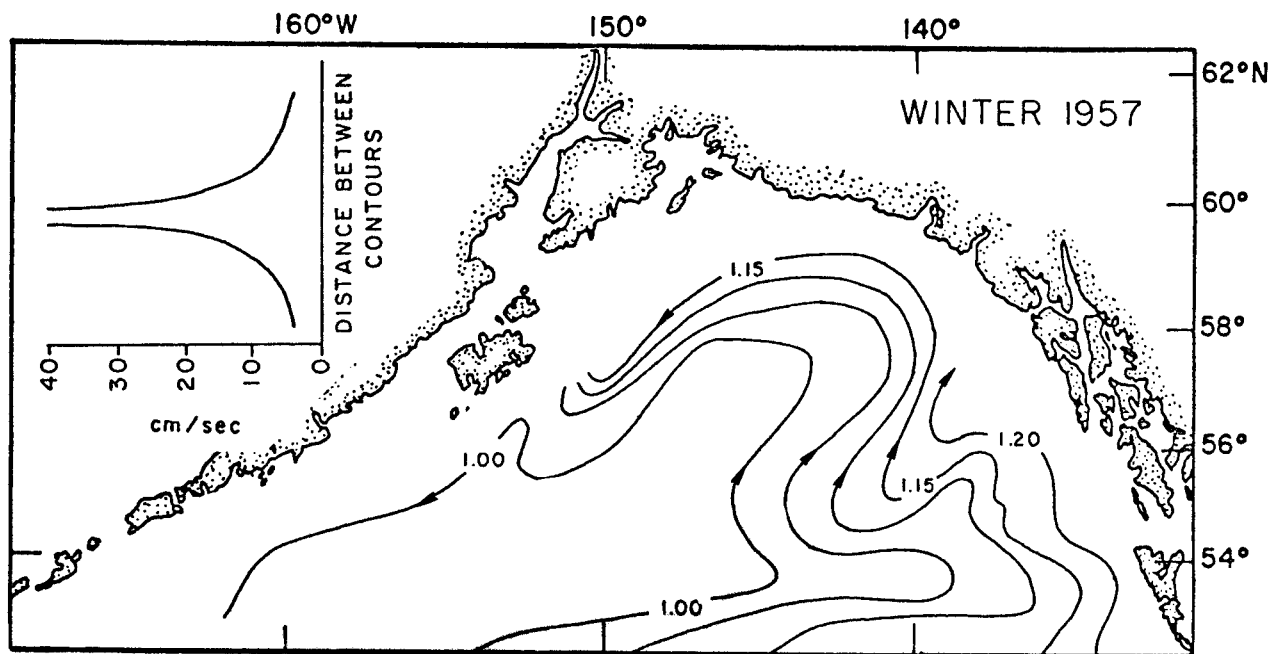


Figure 24. Geopotential topographies, 0/1000 db, winter and summer 1957 showing perturbation in flow at eastern side of the gulf.

indication of eddies breaking off to the east of the boundary current seaward of Kodiak Island (Dodimead et al, 1963), but there is also evidence that this is not a permanent feature of flow in this area.

The question as to whether or not there is continuity of geostrophic flow around the gulf would require extensive observations and extensive direct current measurements. However, some new insight into the boundary flow was obtained in 1972 when closely spaced observations were made on transects of the continental shelf and slope approximately 100 km apart east of Kodiak Island (Favorite and Ingraham, 1976a). It was discovered that approximately 70% of the westward flow out of the gulf occurred within 50 km of the shelf. Geostrophic velocities of 50 cm/sec (referred to 1000 db) occurred in a narrow band approximately 20 km wide and in one instance, velocities of 100 cm/sec (referred to 1500 db) were estimated within a 10 km band. Little evidence of any major perturbations were evident in the nearly 600 km stretch along the continental slope in this area. Thus, it would appear that when appropriate observations are made, fairly reasonable continuity may be obtained.

#### C. Volume Transports

Fluctuations in transport can be estimated by the difference in geopotential topography across the eastern part of the gulf. Data from 1954-62 (Table 1) indicates that the mean transport from 0 - 1000 m is approximately 8 Sv and individual values range from about 6 - 12 Sv, with no particular pattern to winter or summer values. Bennett (1958) reported that when observations are available to 2000 m the transport nearly doubles to approximately 15 Sv, with individual values ranging

Table 1. Northward volume transport (0 to 1000 m - to the nearest 0.5 Sv) into the gulf across 55°N, computed from geopotential topography (the lowest value in the Alaskan Gyre versus the inshore value at the location of the 1000-m isobath at the eastern side of the gulf).

| Period        | Transport (Sv) |
|---------------|----------------|
| 1954 (summer) | 9.0            |
| 1955 (summer) | 9.0            |
| 1956 (summer) | 7.5            |
| 1957 (winter) | 6.5            |
| 1957 (summer) | 7.0            |
| 1959 (winter) | 8.5            |
| 1959 (summer) | 9.0            |
| 1960 (winter) | 12.0           |
| 1960 (summer) | 8.0            |
| 1961 (spring) | 6.5            |
| 1962 (spring) | 6.5            |
| Mean          | 8.1            |

from 13.5 - 16 Sv, and again no particular pattern to winter and summer values is evident. Thus, it would appear that the year to year seasonal fluctuations may be as great or greater than the within year seasonal ones.

#### IV. WIND STRESS-TRANSPORTS

Because of the paucity of data on actual winds, the wind-stress at the sea surface is obtained from distributions of sea level pressure. It should be noted at the outset that there is an unavoidable bias in long-term sea level pressure data because of not only the varying intensity and location of reports from shipping, but because of modern devices and techniques. The establishment of Ocean Station "P" in the mid-forties, the availability of satellite imagery showing cloud patterns in the mid-sixties, and the placement of ocean data buoys in the mid-seventies, all permit an increasingly better estimate of the sea level pressure fields and associated gradients. Several grid spacings are used in this report and each will be defined as encountered.

##### A. Pressure Fields

In order to obtain an initial assessment of variability of pressure, the historical sea level pressure data at  $5 \times 5^\circ$  grid points were obtained from the National Center for Atmospheric Research (NCAR) and monthly mean fields (composed of 12 hourly and in some instances 24 hourly data) from 1899-1972 were plotted to ascertain the relative frequency at which the central pressure of the Aleutian low falls within the selected low pressure intervals (Fig. 25). In 6 instances the monthly mean pressure was less than 985 mb, these occurred in either December or January; in 32 instances it was less than 990 mb, all occurred from October to March; and in 91 instances it was less than 995 mb, all occurred from September to April. Although it appears that data from 1899-1950 are fairly representative of the period 1950-1972, we are concerned with the curl of the wind-stress and therefore details of the first and second derivative fields, and not

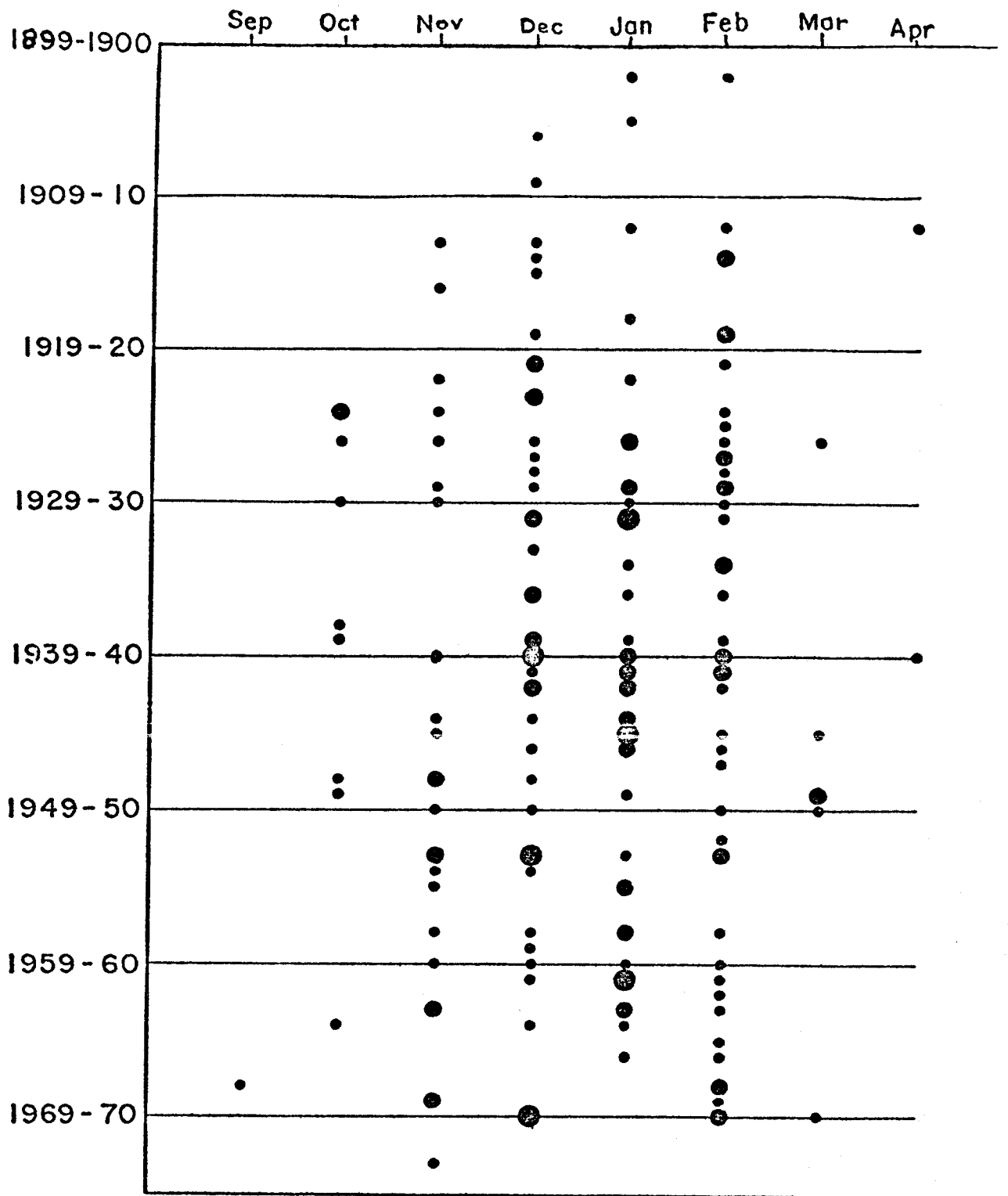


Figure 25. Frequency of monthly mean sea level pressure minima of the Aleutian low: < 995 mb (●), < 990 mb (●), and < 985 mb (●).



merely the absolute value of pressure minima. If we choose 55°N, 155°W near the approximate center of the Alaskan Gyre, data at this grid point, deviations from monthly means, 12-month running means and power spectrum provide an indication of the general variability of sea level pressures. Deviations from monthly mean pressures do not exceed  $\pm 5$  mb and, except for the extended period, roughly 12 years, of positive deviations from 1901-1912 (which may be due to limited data), departures from normal are generally of 1-4 years duration. Particularly noticeable is the extended period of below normal pressures centered around 1940. The power spectrum (cycles less than 1.5 years not shown because of the obvious annual periodicity) based on annual mean values reflect cycles of 2.7, 6.7 and 13.3 years (Fig. 26). The 6.7 years is the approximate periodicity of oceanic temperature cycles (5.6 years) found by Favorite and McLain (1973). The 13.3 years suggests an influence of the sunspot cycle of 12.3 years. Favorite and Ingraham (1976b) have shown that if mean pressures from October to March for the three years centered around the period of sunspot maxima and minima from 1899 - 1972 are calculated, with only one exception (1958), the center of the Aleutian low occurs in the central Aleutian area during periods of the sunspot maxima and in the Gulf of Alaska during periods of the sunspot minima; mean pressures are 2 mb lower during the latter period.

#### B. Transport Fields

Total integrated transports (wind-stress transports) are derived from the mean pressure fields by deriving a wind field that is transformed into a stress field. The nature of the coupling of energy between wind-stress and water transport is not precisely known and certainly varies under different conditions. When the water is warmer than the air, a

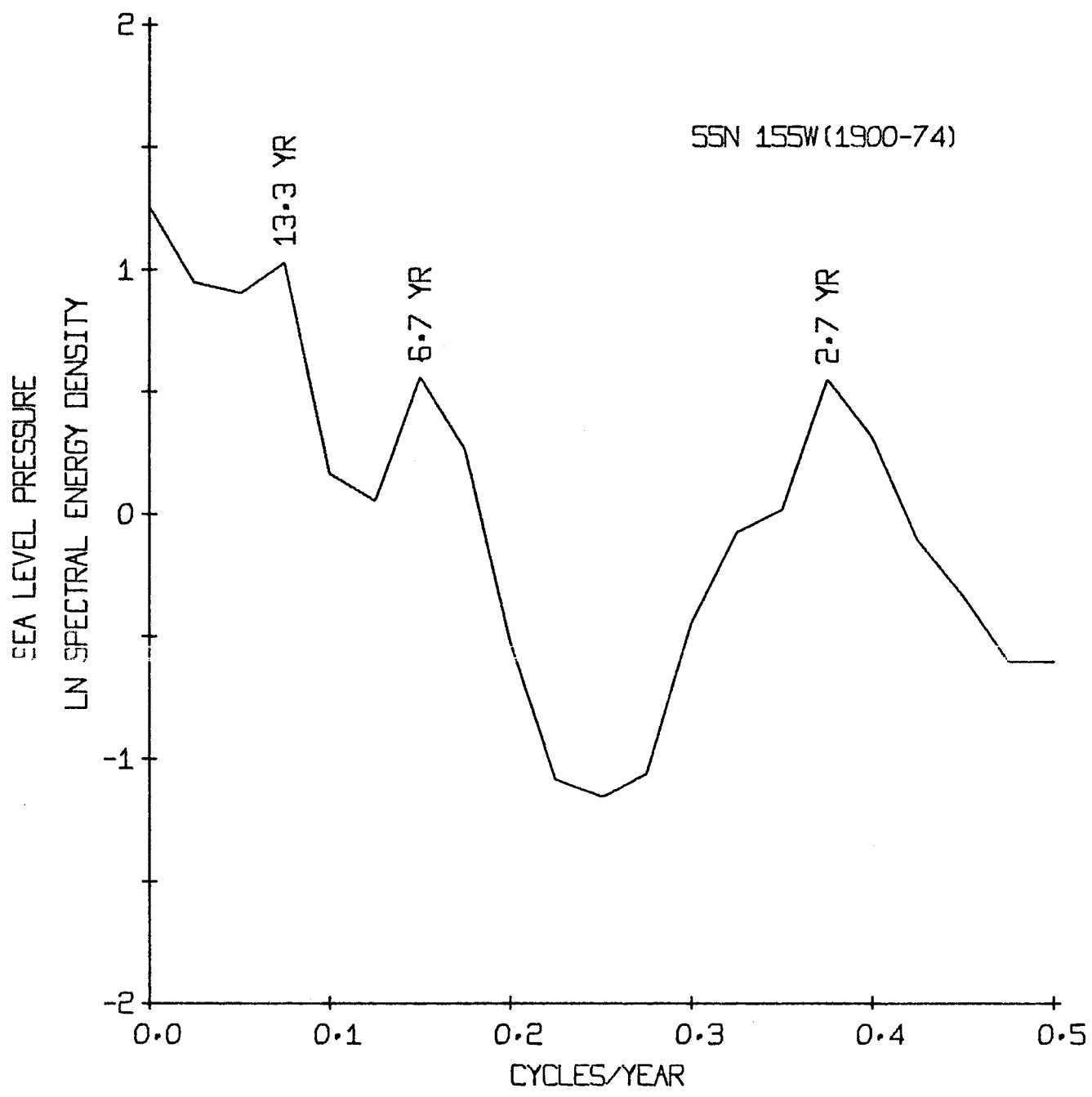


Figure 26. Spectral energy density, annual mean sea level pressure at 55°N, 155°W 1900-74 (20 lags) indicating cycles of 2.6, 6.7 and 13.3 years.

turbulent boundary layer exists and exchange of energy is more effective than when the water is colder than the air and a stable layer exists at the air-sea interface. Further, when interpolation and averaging processes are taken into account, caution must be exercised in interpreting results. However, a number of authors (e.g. Wyrтки, 1964) have indicated the usefulness of this technique in estimating flow.

Sverdrup (1947), by including the pressure gradient term in the Ekman transport equation, arrived at the following:

$$-f v = \frac{1}{\rho} \frac{\partial p}{\partial x} + \frac{\partial}{\partial z} \left( A_z \frac{\partial u}{\partial z} \right) \quad (2)$$

$$f u = -\frac{1}{\rho} \frac{\partial p}{\partial y} + \frac{\partial}{\partial z} \left( A_z \frac{\partial v}{\partial z} \right) \quad (3)$$

After cross differentiating and integrating from the surface to an unspecified depth-of-no-motion one obtains the transport equation:

$$M_y = \left( \frac{\partial \tau_x}{\partial x} - \frac{\partial \tau_y}{\partial y} \right) / \beta \quad (4)$$

where  $\tau$  is the wind stress and  $\beta$  the variation of the Coriolis parameter with latitude  $\left( \frac{\partial f}{\partial y} \right)$ . This shows for steady non-divergent flow the total meridional transport,  $M_y$ , is directly related to the curl of the wind stress and independent of the details of the mass distribution as long as the pressure gradient is baroclinically compensated at depth.

Using the technique devised by Fofonoff (1962) and the program constructed by Bakun (1973), geostrophic winds were computed from sea level pressure values (interpolated from the  $5 \times 5^\circ$  field) computed on an equilateral triangular grid, 222 km on a side, centered at  $47^\circ\text{N}$ ,  $170^\circ\text{W}$ . Pressure data archived on magnetic tape were arranged on the computation grid surrounding each selected location using Bessel's central difference formula. Finite difference first and second derivatives were formed and the geostrophic wind field was computed in spherical

coordinates:

$$u_g = -\frac{1}{\rho R_f} \frac{\partial P}{\partial \phi} \quad (5)$$

$$\frac{\partial u_g}{\partial \phi} = -\frac{1}{\rho R_f} \left( \frac{\partial^2 P}{\partial \phi^2} - \frac{\partial P}{\partial \phi} \cot \phi \right) \quad (6)$$

$$\frac{\partial u_g}{\partial \lambda} = -\frac{1}{\rho R_f} \frac{\partial^2 P}{\partial \lambda^2} \quad (7)$$

$$v_g = \frac{1}{\rho R_f \cos \phi} \frac{\partial P}{\partial \lambda} \quad (8)$$

$$\frac{\partial v_g}{\partial \phi} = \frac{1}{\rho R_f \cos \phi} \left( \frac{\partial^2 P}{\partial \phi \partial \lambda} + \frac{\partial P}{\partial \lambda} [\tan \phi - \cot \phi] \right) \quad (9)$$

$$\frac{\partial v_g}{\partial \lambda} = \frac{1}{\rho R_f \cos \phi} \frac{\partial^2 P}{\partial \lambda^2} \quad (10)$$

where  $\phi$  and  $\lambda$  are the latitude and longitude coordinates respectively,  $u_g$  and  $v_g$  are the eastward and northward components of geostrophic wind,  $\rho$  is the atmospheric pressure,  $\rho$  is the density of air (considered to be a constant equal to 0.00122 gm/cm),  $R$  is the mean radius of the earth and  $f$  is the Coriolis parameter.

These are transformed to estimates of the wind field near the sea surface by rotating the geostrophic wind 15 degrees to the left and contacting it by 30 percent to approximate, in a simplified manner, the effect of friction in the planetary boundary layer:

$$u = a_1 u_g + b_1 v_g \quad (11)$$

$$\frac{\partial u}{\partial \phi} = a_1 \frac{\partial u_g}{\partial \phi} + b_1 \frac{\partial v_g}{\partial \phi} \quad (12)$$

$$v = a_2 u_g + b_2 v_g \quad (13)$$

$$\frac{\partial v}{\partial \lambda} = a_2 \frac{\partial u_g}{\partial \lambda} + b_2 \frac{\partial v_g}{\partial \lambda} \quad (14)$$

where  $u$  and  $v$  are the eastward and northward components of surface wind,  $\vec{V}$ , and the transformation coefficients are:  $a_1 = 0.7 \cos(15^\circ)$ ,

$$b_1 = 0.7 \sin(15^\circ), a_2 = -0.7 \sin(15^\circ), b_2 = 0.7 \cos(15^\circ).$$

Derivatives of surface wind speed,  $|\vec{v}| = \sqrt{u^2 + v^2}$  are computed according to:

$$\frac{\partial |\vec{v}|}{\partial \phi} = \left( u \frac{\partial u}{\partial \phi} + v \frac{\partial v}{\partial \phi} \right) \frac{1}{|\vec{v}|} \quad (15)$$

$$\frac{\partial |\vec{v}|}{\partial \lambda} = \left( u \frac{\partial u}{\partial \lambda} + v \frac{\partial v}{\partial \lambda} \right) \frac{1}{|\vec{v}|} \quad (16)$$

The stress on the sea surface,  $\vec{\tau}$ , was computed using a relatively high value, 0.0026, of the constant drag coefficient to partially offset the effect of using mean data:

$$\vec{\tau} = \rho C_D |\vec{v}| \vec{v} \quad (17)$$

$$\frac{\partial \tau_\phi}{\partial \lambda} = \rho C_D \left( v \frac{\partial |\vec{v}|}{\partial \lambda} + |\vec{v}| \frac{\partial v}{\partial \lambda} \right) \quad (18)$$

$$\frac{\partial \tau_\lambda}{\partial \phi} = \rho C_D \left( u \frac{\partial |\vec{v}|}{\partial \phi} + |\vec{v}| \frac{\partial u}{\partial \phi} \right) \quad (19)$$

where  $\tau_\phi$  and  $\tau_\lambda$  are the northward and eastward components of  $\vec{\tau}$ . The curl of the wind stress is then determined as

$$\nabla \times \vec{\tau} = \frac{1}{R} \left( \frac{1}{\cos \phi} \frac{\partial \tau_\phi}{\partial \lambda} - \frac{\partial \tau_\lambda}{\partial \phi} + \tau_\lambda \tan \phi \right) \quad (20)$$

Integration of wind-stress curl along a parallel of latitude from an eastern boundary, in this case the west coast of North America, to successive grid points results in a total transport across that parallel of latitude; and eastward flow is obtained by satisfying continuity between grid points along two parallels of latitude. Welander (1959) has shown that wind-stress transport in a semi-enclosed basin (such as the Gulf of Alaska) must flow out in the form of a western boundary jet because

eastern boundary currents are excluded, thus, northward transports across 55°N are considered to exit the gulf along the western shore.

When one considers the nature of the variability in location and frequency of ship reports that make up the bulk of these pressure data, the averaging processes involved, and the theory employed, there are severe limitations associated with this method of obtaining flow, but it provides an indication of the continuity of events that is unattainable from the fragmentary station data obtained only aboard research vessels. Mean (1950-74) seasonal integrated total transports (Fig. 27) indicate a maximum northward transport in excess of 19 Sv into the gulf in winter and an accompanying closed circulation in the gulf area. Northward transport drops to less than 5 Sv in spring and summer and is concentrated at the western side of the gulf, whereas there is a suggestion of southward flow ( $< 1$  Sv) at the eastern side. Intense northward transport greater than 15 Sv is reestablished in autumn, but the closed circulation evident in winter east of 155°W is not developed.

There are marked departures from mean conditions and these are most readily apparent in winter. Two winter periods, in 1963 and 1969, have been selected to reflect the range in values obtained in the period 1950-74 (Fig. 28). Computed northward transport in 1963 was less than 10 Sv, whereas, in 1969 it was nearly 3 times as great, in excess of 25 Sv. Thus, considerable variability in flow is indicated not only seasonally, but annually and marked deviations from the smoothed isopleths presented must occur. One can only conclude that, although a basic cyclonic flow

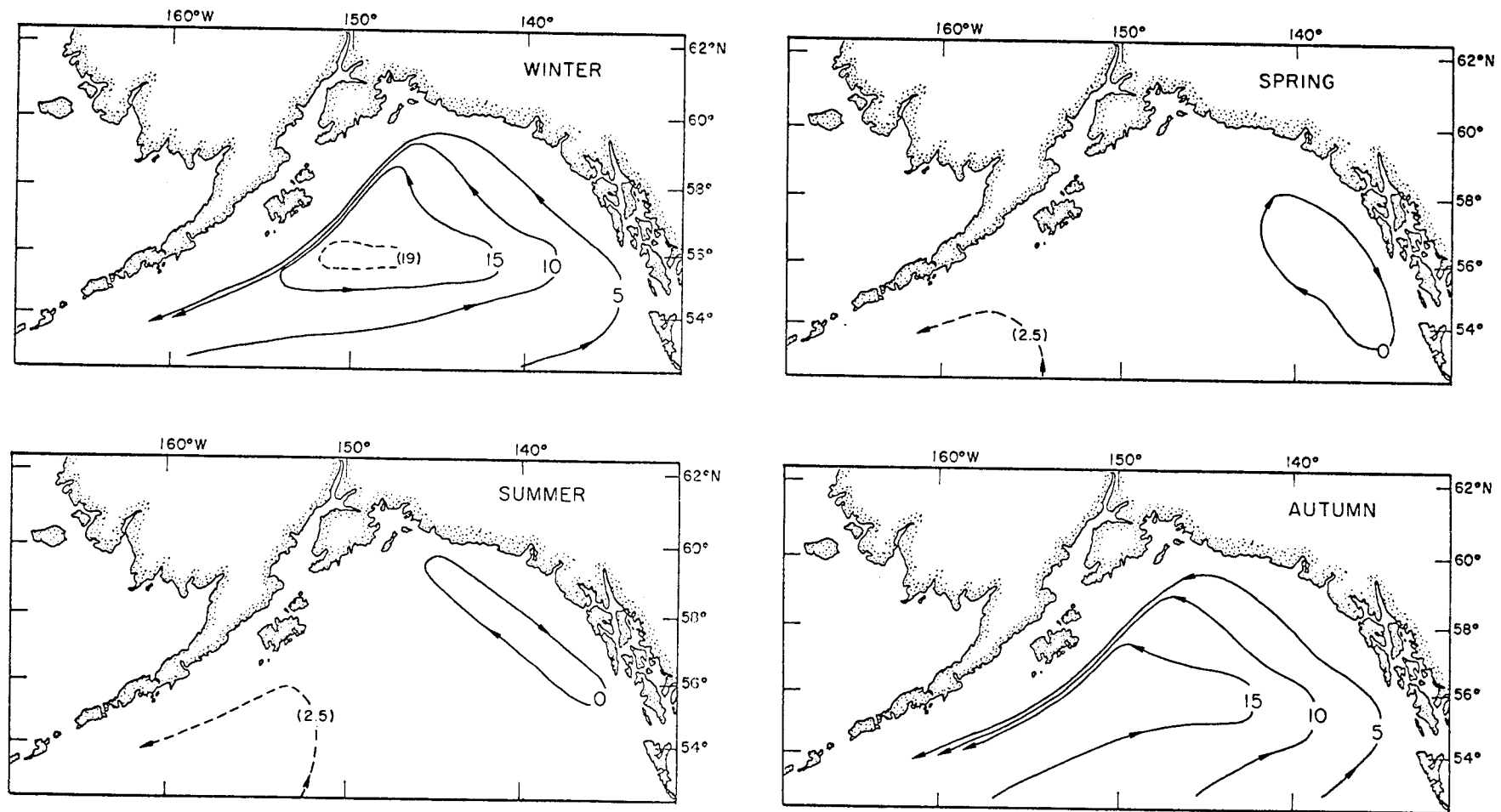


Figure 27. Seasonal mean (1950-74) integrated total transports (Sv) indicating general cyclonic flow with marked winter intensification of flow.

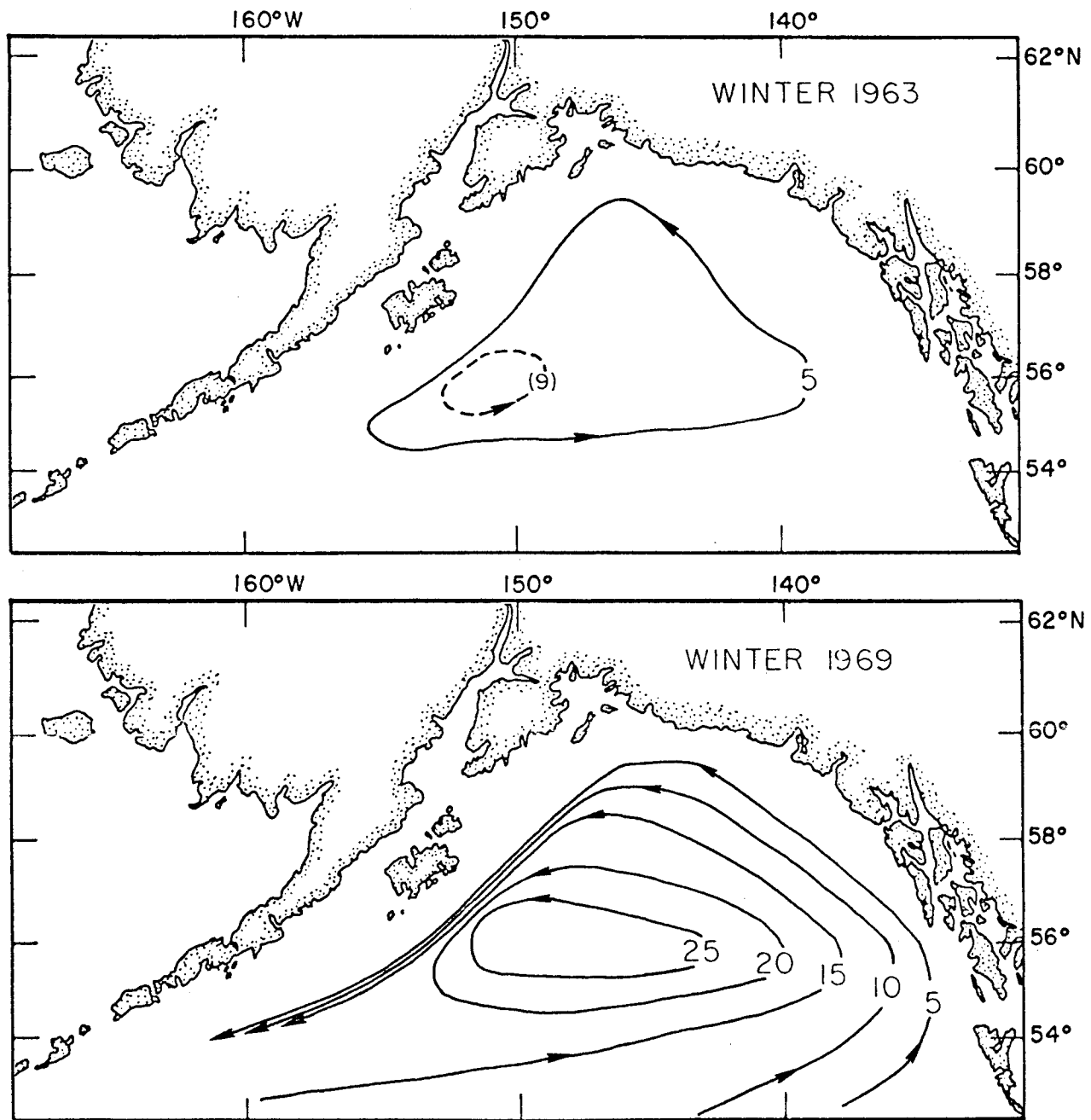


Figure 28. Total integrated transports for winter (Jan. Feb. Mar.) 1963 and 1969 indicating variability in winter flow.



exists in the gulf, the variations and perturbations in flow due to variable wind-stresses result in a highly complex flow regime.

### C. Numerical Model

Further refinements of estimates of water transport in the gulf, over those obtained by integrated total transport method, are obtained by expanding basic assumptions in the total integrated transport method to permit inclusion of variable bathymetry and to incorporate analyses in a numerical model first devised by Galt (1973) for an enclosed basin. This was configured to fit the North Pacific Ocean, Bering Sea, and Okhotsk Sea on the 222 km equilateral triangular grid mentioned in the previous section. Although limited to the barotropic flow assumption, the model provides an initial look at actual isopleths of flow considering the great increase in complexity of designing a baroclinic or multilayer model. Because of problems associated with specifying initial stream lines and vorticity on an arbitrary mid-ocean southern boundary for the Gulf of Alaska, the larger ocean area with a southern boundary far away from the area of interest was selected for the model. This exploratory version would show if a more detailed grid within the Gulf of Alaska as a subset of this large area model would be informative.

The basic model outputs are time dependent solutions of the transport stream function which, when presented in maps and contoured, give transport stream lines of flow. As before, the wind stress curl field is computed from sea level pressure; the bathymetry is scaled relative to the mean depth from flat bottom (0%) to actual bathymetry (100%) to simulate the effect of stratification; and coefficients may be selected which govern the

character of the solution by scaling the importance of nonlinear advection ( $\alpha$ ), lateral friction ( $\beta$ ), and bottom friction ( $\delta$ ). As the model spins up from zero initial stream function and vorticity, maps may be obtained at any time interval which is a multiple of the time step (6 hours or less) to show the development of flow which in most cases reaches near steady state after about 60 days or 240 time steps. Caution must be taken when interpreting the results because of the barotropic assumption which allows minor changes in deep bathymetry to affect flow. Further, short (one month or less) periods of unusually intense wind stress curl patterns give unrealistically high transports if run to a steady solution a considerable time beyond their actual duration.

The model is based on a nondimensionalized vorticity equation (1) which is obtained by cross differentiation and subtraction of the vertically integrated equations of motion:

$$\frac{\partial \xi}{\partial t} = (\nabla \times \psi \vec{k}) \cdot \left( \frac{\alpha \xi + f}{h} \right) + \beta \nabla^2 \xi - \frac{\delta}{h} \left[ \xi + \nabla \psi \cdot \nabla \left( \frac{1}{h} \right) \right] + \nabla \times \left( \frac{\tau}{h} \right), \quad (21)$$

where  $\xi$  is the vertical component of vorticity  $\left( \frac{\partial v}{\partial x} - \frac{\partial u}{\partial y} \right)$ ;  $u$  and  $v$  are the horizontal components of velocity;  $h$  is the depth,  $f$  is the Coriolis parameter;  $\alpha$ ,  $\beta$ , and  $\delta$  are constants that specify the effectiveness of the nonlinear advection, horizontal and vertical frictional forces respectively;  $\tau$  is the wind stress; and  $\psi$  is the transport stream function defined by  $-hu = \frac{\partial \psi}{\partial y}$  and  $hv = \frac{\partial \psi}{\partial x}$ . The continuity equation

$$\frac{\partial (hu)}{\partial x} + \frac{\partial (hv)}{\partial y} = 0, \quad (22)$$

and finally a relationship between stream function and vorticity

$$\nabla \left( \frac{1}{h} \nabla \psi \right) = \xi \quad , \quad (23)$$

complete the basic equations of the model. For further information on finite difference forms see Galt (1973).

A typical run of the model includes the following sequence of events throughout the 17 x 42 point array over the area from 33-61°N and 140°E-120°W. Initially the vorticity ( $\xi$ ) and stream function ( $\psi$ ) values are set to zero at each of the 714 grid points. Then the rate of change of vorticity ( $\frac{d\xi}{dt}$ ) is computed at each grid point from equation (21) and integration of the rate of change over one time step interval (6 hours) gives a new vorticity value at each grid point. Using equation (23), new values for the transport stream function are computed from the new vorticity values by an over-relaxation technique, and streamfunction values at each grid point are contoured to indicate the new magnitude and direction of flow. This sequence is repeated. The model approaches steady conditions when the gradients are such that the terms on the right hand side of equation (21) approach zero indicating a balance between vorticity dissipation (by advection of potential vorticity, lateral friction, and bottom friction) and vorticity input at each grid point (the wind stress curl field).

Using the 25 year mean annual wind stress and a 10% bathymetry factor, the model after 60 days spin up shows the generally accepted features of flow around the Gulf of Alaska (Fig. 29). The cyclonic flow, western boundary intensification, and magnitude of transport (about 20 Sv) generally agree with the geostrophic calculations from field measurements

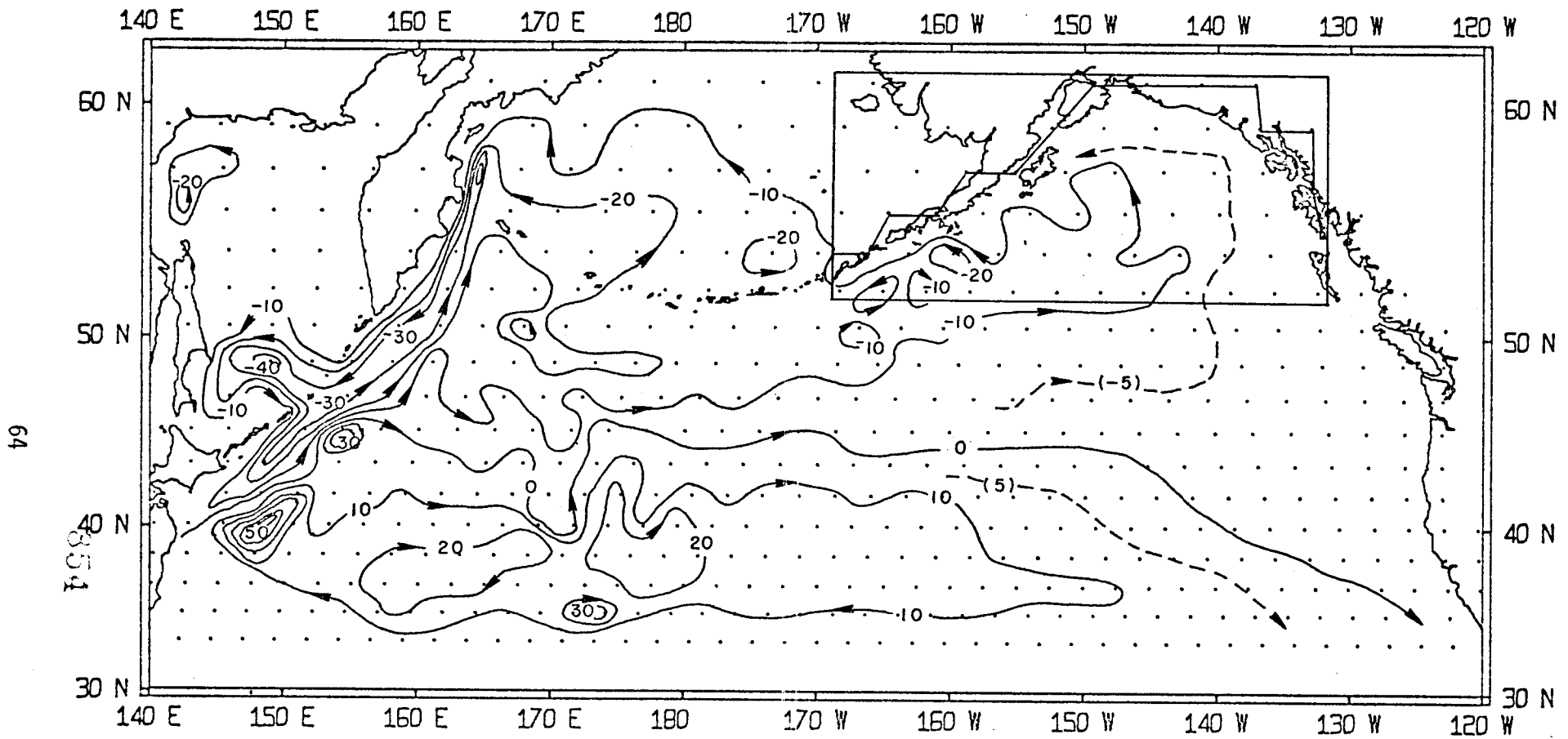


Figure 29. Numerical model of Transpacific ocean transports (Sv) using annual mean (1950-74) wind stress, 10% bathymetry factor, and  $\alpha$ ,  $\beta$ ,  $\gamma$  coefficients.

of temperature and salinity if a reference level-of-no-motion of about 2000 db is used. Next the sea level pressure data were averaged by seasons to observe the effect of variable wind-stress. All factors except wind stress input were kept the same for each of the four runs which were driven by the seasonal mean (1950-74) wind-stresses, only the gulf portion of the model is presented (Fig. 30). As expected, the autumn and winter transport patterns are much more intense than the annual mean pattern, and the maximum transport of 63 Sv across  $54^{\circ}\text{N}$  (between  $130^{\circ}$  and  $160^{\circ}\text{W}$ ) occurred for autumn conditions; the winter transport was 51 Sv followed by summer with 13 Sv and spring with 11 Sv. The general asymmetric cyclonic features of flow were quite similar during both of the high transport seasons and both of the low transport seasons, but details were considerably different.

During autumn and winter an intense boundary current develops on the western side of the gulf, about 2 grid lengths offshore, over the continental slope. Eddy-like features form south of the boundary current. The lack of synopticity and closely spaced stations in historical oceanographic data has precluded detecting the existence of these eddies, other than perhaps isolated instances, which have been generally overlooked. At the eastern side of the gulf, the streamlines of easterly flow converge indicating higher velocities near Yakutat. The flow remains about the same magnitude zonally across the head of the gulf and intensifies as it is forced southwestward by the land boundary off Kodiak Island and the Alaska Peninsula.

During the spring and summer low wind stress period, flow is considerably reduced in magnitude, and the center of cyclonic flow shifts southward.

66  
856

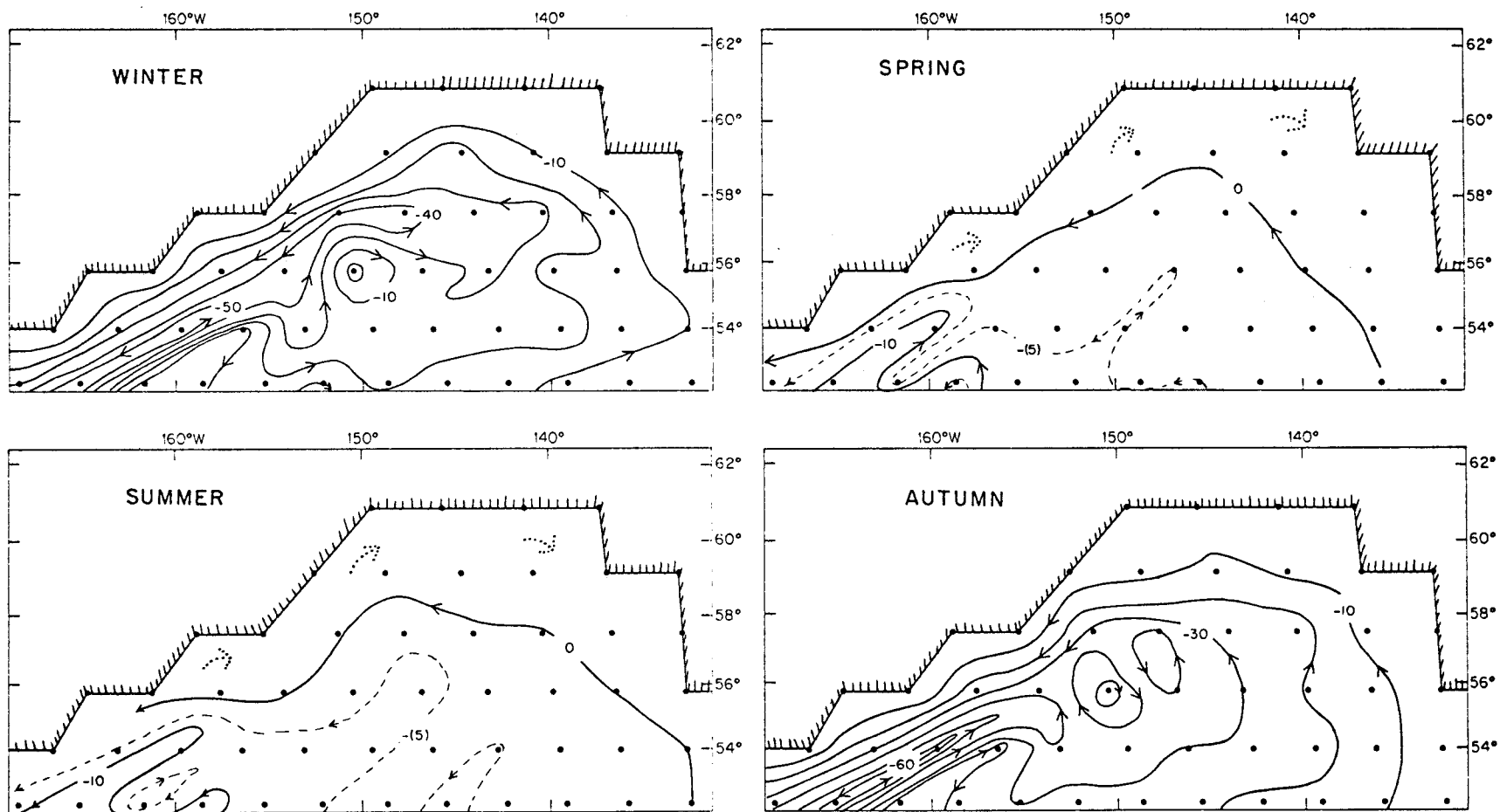


Figure 30. Seasonal mean transports (Sv) in the gulf obtained from numerical model studies suggesting a greater complexity in flow than evident in Fig. 27.

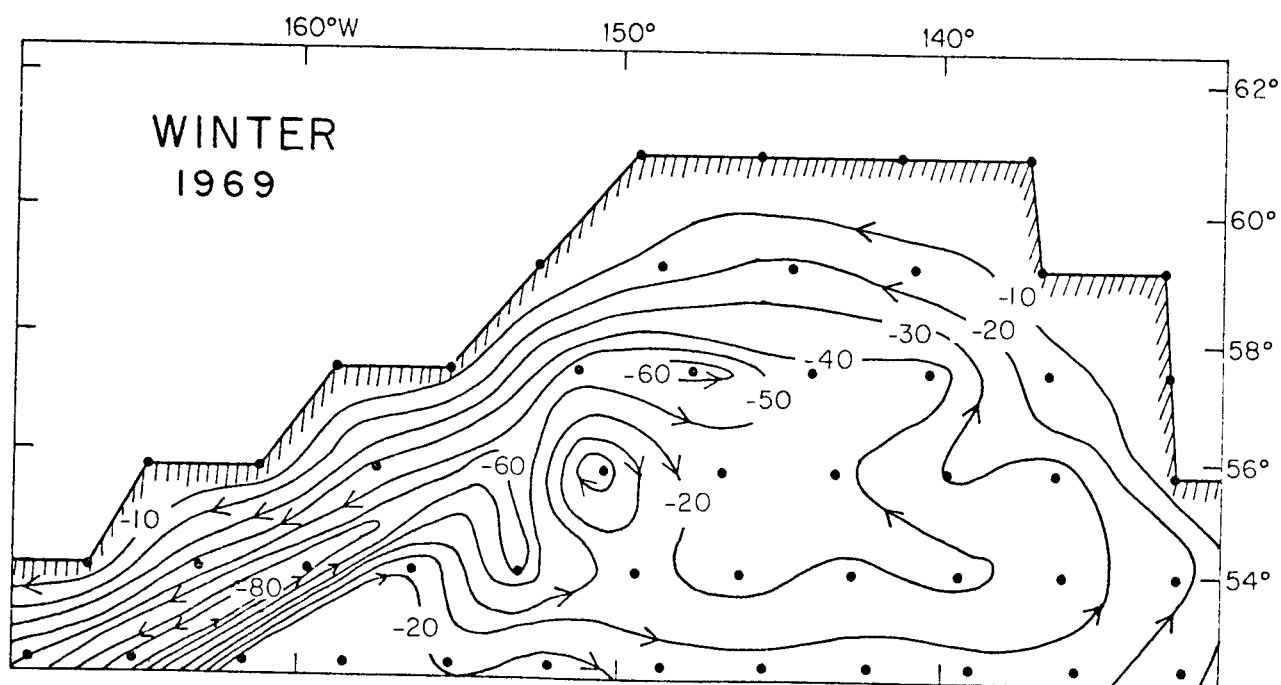
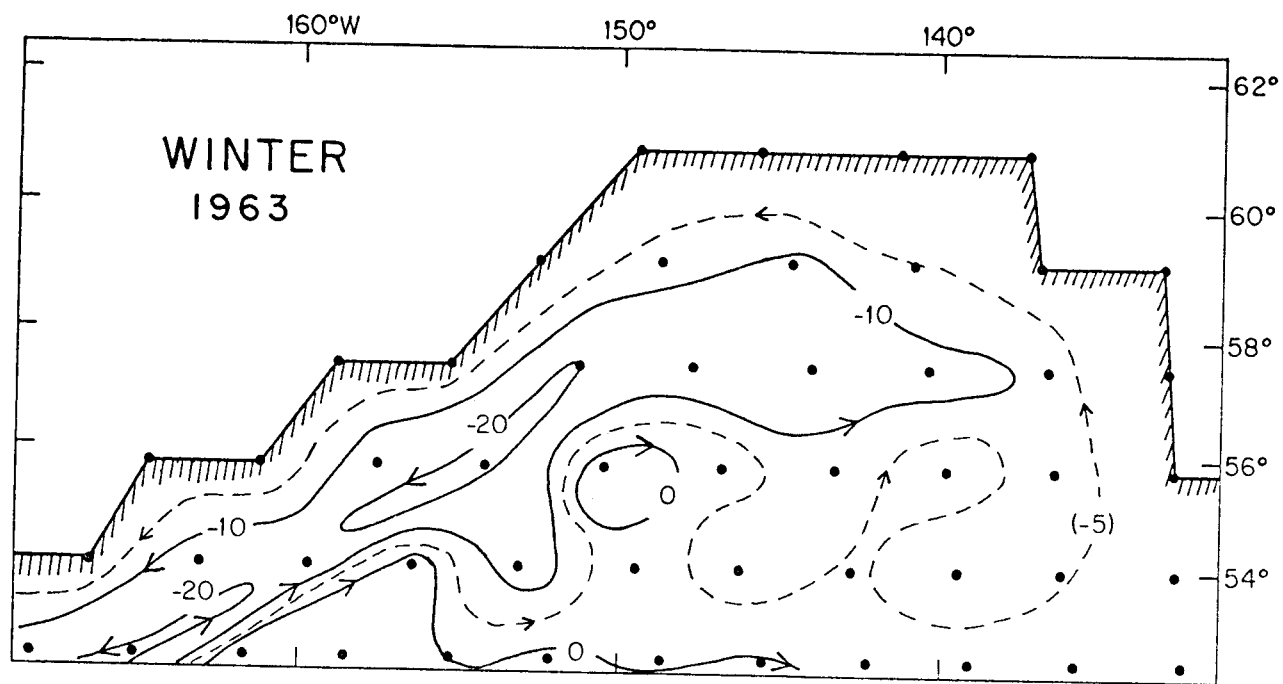


Figure 31. Numerical model transports (streamline interval 10 Sv) for winter (Jan. Feb. Mar.) 1963 and 1969 suggesting greater complexity in flow than evident in Fig. 28.

A new feature appears in the form of an inshore return flow of 1-3 Sv over the shelf that is not evident in the 10 (or 5) Sv contour interval shown. This is perhaps much more significant in terms of mean velocity considering that the transport in this area is confined to within a depth interval of 200m compared to the offshore depth interval of about 4000m. Other features of spring and summer transports include weak eddies or meanders, a broad northerly flow at the east side of the gulf, and a slight intensification of the southwesterly flow at the western side of the gulf.

Computed wind-stress fields for winter 1963 and 1969 (based upon extremes in the integrated total transport (wind-stress transport) time series) were selected to show the variability that may be expected during the high wind stress period (Fig. 31). The general features of the mean winter condition are clearly present, with 1969 having a high transport value of 83 Sv compared to only 22 Sv in 1963. The greatest departure in 1969 from mean conditions occurs in the eastern gulf where the easterly flow is contained about 400 farther south than normal, resulting in a more intense northwesterly flow along the coast. This was apparently associated with unusually strong positive wind-stress curl in the eastern gulf.

These numerical model studies suggest that flow in the gulf does not appear to be of a typically uniform cyclonic nature, but rather a funneling of northward flow into the head of the gulf that exists as a narrow boundary flow at the western side. Closure may well occur in nature (see Surface Salinity section) in the surface layer, which is generally isolated from the deeper flow by the halocline at 100-300m. Future studies should take into account the stratification or baroclinic effects.



## V. COASTAL SEA LEVELS

The geopotential topography computed from hydrographic data provides a relative indication of sea surface slopes but observations at shore stations are a direct measurement of actual sea level. Daily means of hourly heights referred to a local datum are recorded at selected coastal stations and the data are on file at NOAA Headquarters (Rockville). Although weekly and even daily departures from normal sea level have shown good correlations with coastal flow regimes in the Coastal Upwelling Experiments (CUE) off Oregon, monthly mean sea level data are appropriate for discussing the seasonal and longer-term variations which are the focus of this chapter. Distortions caused by changes in atmospheric pressure are corrected as follows:

$$\delta h = \frac{1}{\rho g} \delta p \quad (24)$$

where  $h$  is the change in sea level,  $\rho$  the density of water,  $g$  the acceleration of gravity and  $p$  the atmospheric pressure. Steric effects which may result in seasonal differences as great as 6 cm are not compensated for because usually only departures from monthly means are considered.

LaFond (1939) showed that nearly all variations in sea level on the west coast of the United States could be accounted for by changes in the geopotential topography of the ocean off the coast and thus, were directly related to ocean currents. Jacobs (1939) reported that such relations were not due to changes in the density of surface water but actual slopes caused by atmospheric interactions. Pattullo et al (1955) found that in

the northern North Pacific isostatic adjustments (steric and pressure effects) did not account for all seasonal departures from mean sea level, and Pattullo (1960) noted that in low latitudes sea level was high in summer but north of 40°N there was a distinct change of phase and sea levels around the Gulf of Alaska were highest in December. Local effects of river discharge on sea level at the mouth of the Columbia River were noted by Roden (1960) in a study of non-seasonal variations in sea level along the west coast of North America; only a moderate to poor coherence in relation to local sea surface temperatures were found. Sea level data south of Ketchikan were studied by Saur (1962) and deviations from isostasy were attributed to variability in ocean currents. Favorite (1974) showed that the anomalous increase in sea level at Yakutat during winter could be explained by an accompanying increase in northward wind-stress transports, and Reid and Mantyla (1975) have indicated that the winter increase in sea level along the entire coast of the northern North Pacific Ocean is due to increased flow in the overall subarctic cyclonic gyre.

#### A. Sea Level Pressures

A general gradual increase in monthly mean sea level pressure is evident at Ketchikan, Sitka, Yakutat, Seward, Kodiak and Dutch Harbor from February to July (Fig. 32) and this is followed by an abrupt decrease from July to October. Somewhat constant but low pressures prevail from November until January when an anomalous secondary maxima occurs that is probably caused in part by a westward shift in the center of the Aleutian low from the gulf to the central Aleutian Islands that occurs at this time.

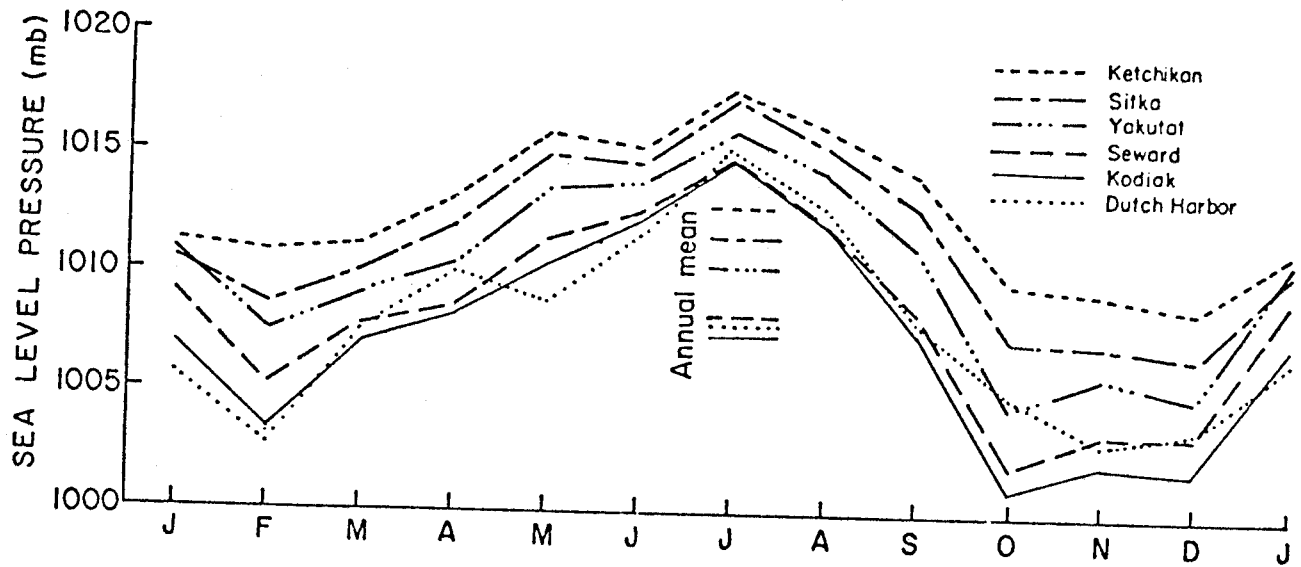


Figure 32. Monthly mean (1950-74) sea level pressure (mb) at the indicated coastal stations indicating maxima in July and minima in October.

Deviations from monthly means, and 12-month running means of sea level pressures for the 6 locations for 1950-74 (Fig. 33) indicate a marked similarity that is even reflected in abrupt anomalies of only a month or so duration. The abrupt increase in pressure in late 1950 at Dutch Harbor was evident at all stations, although decreasing in intensity to the south. In 1957 an abrupt increase and a subsequent decrease was evident at all locations and other examples are evident. Thus, there is a general response throughout the area to short or prolonged events but periods of positive or negative anomalies appear to be limited to from one month to about a year.

Spectral energy densities were computed for monthly mean values at each of the coastal stations over the period 1950-74 using a lag time of approximately 13 percent of the record length (40 lags over a continuous record of 300 data points). All locations exhibit maximum energy density at a frequency of approximately .085 cy/mo or 1 year (Fig. 34). Although the limited number of data points prohibits meaningful analysis of lower frequencies, there is an indication that the total energy distribution at these frequencies increases from Ketchikan to Dutch Harbor and a consistent indication of an energy peak at .025 cy/mo or 3.3 years. A coherency test using the coherence square technique shows a maximum coherence at a frequency of 1 year at all stations. Comparisons of data at all locations with those at Ketchikan indicates that there is also a good spatial coherence around the gulf (Fig. 35).

#### B. Mean Sea Levels

Monthly mean (1950-74) sea levels corrected for atmospheric pressure at Ketchikan, Sitka, Yakutat, Seward, Kodiak and Dutch Harbor (Fig. 36) reflect considerable coherence. Unfortunately there is no horizontal

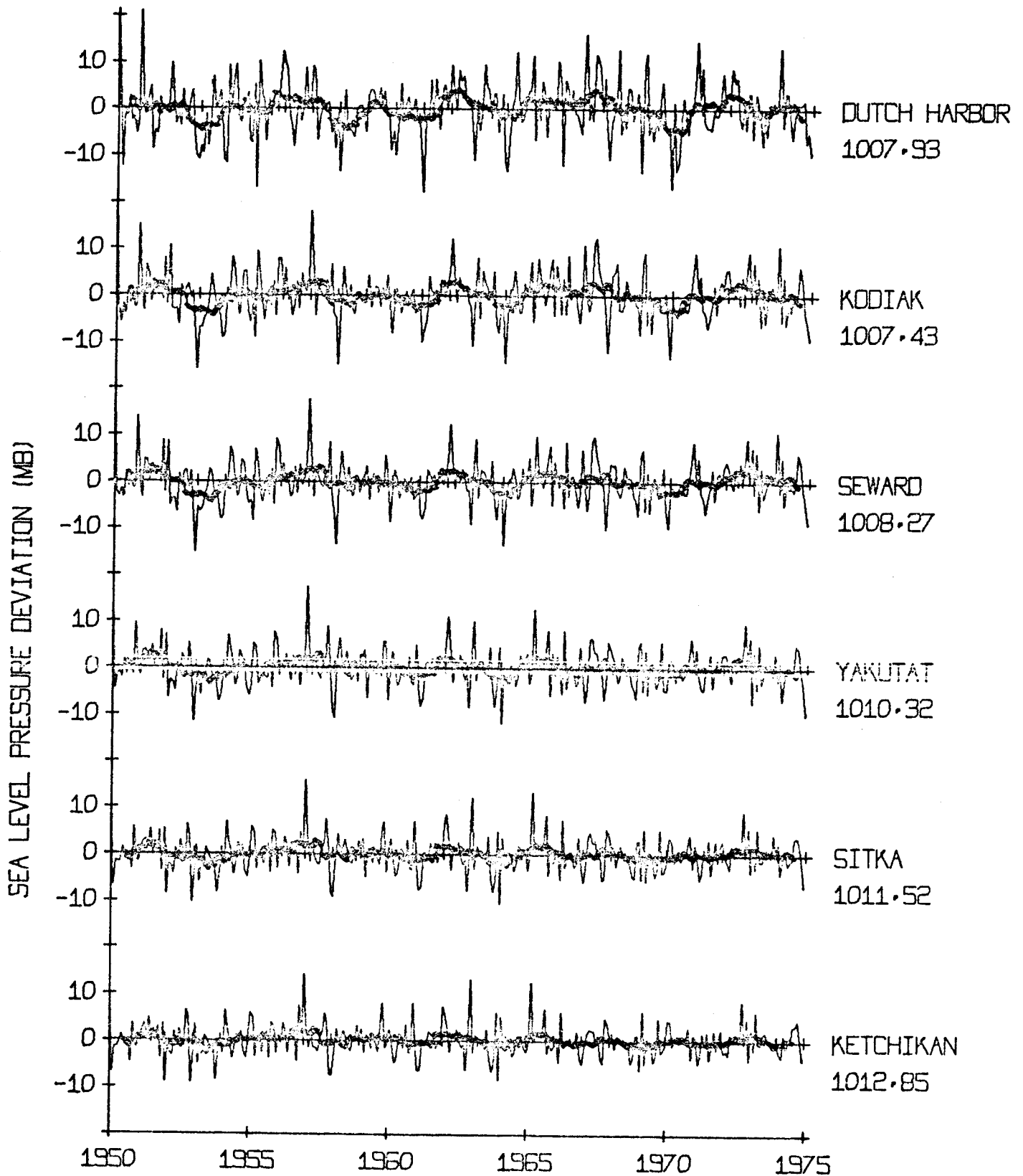


Figure 33. Deviations in sea level pressure (mb) from monthly mean (1950-74) values at the indicated coastal stations and 12-month running mean (dotted line).

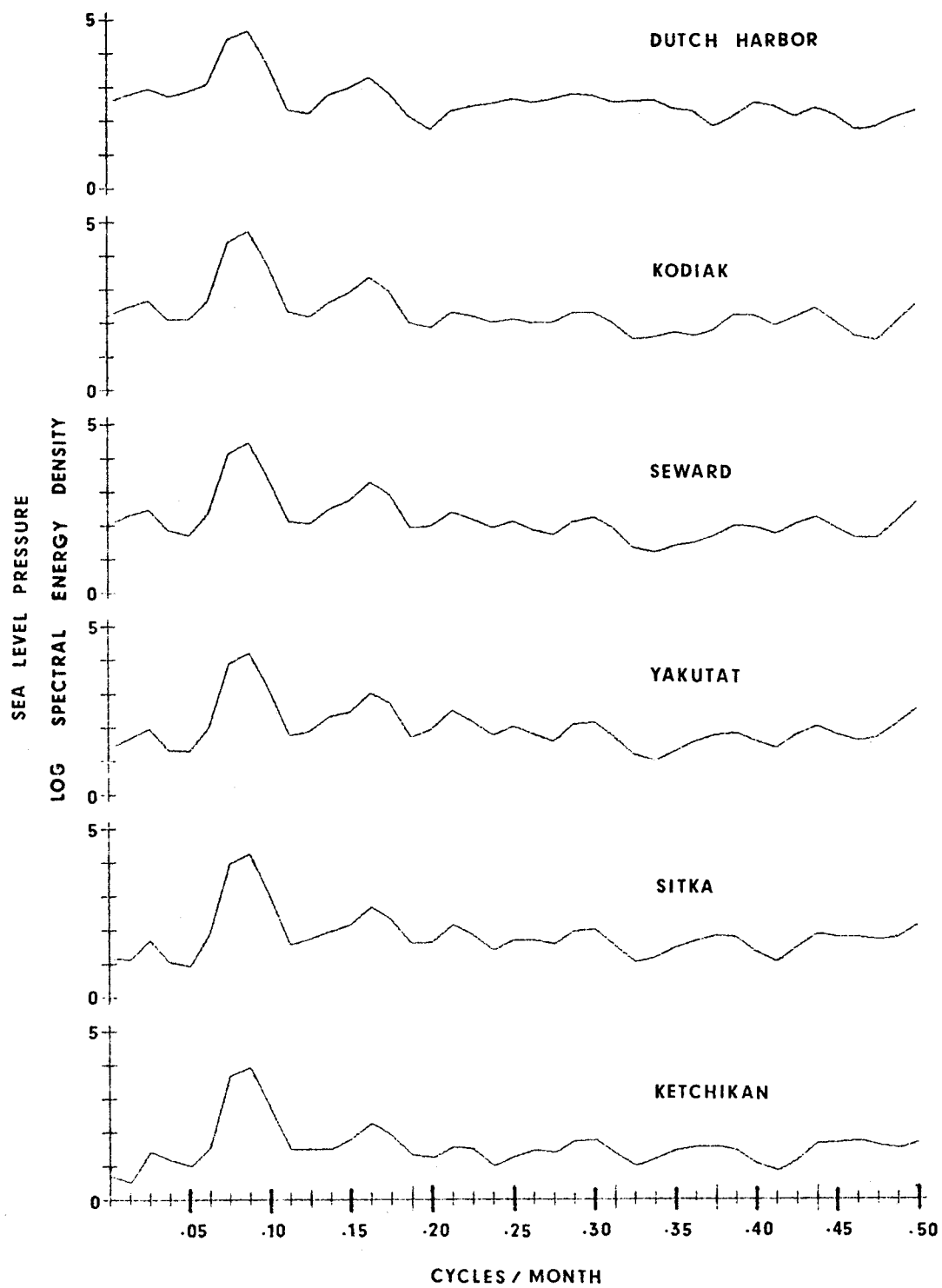


Figure 34. Spectral energy densities (40 lags) for sea level pressure at the indicated coastal stations indicating dominant annual cycle.

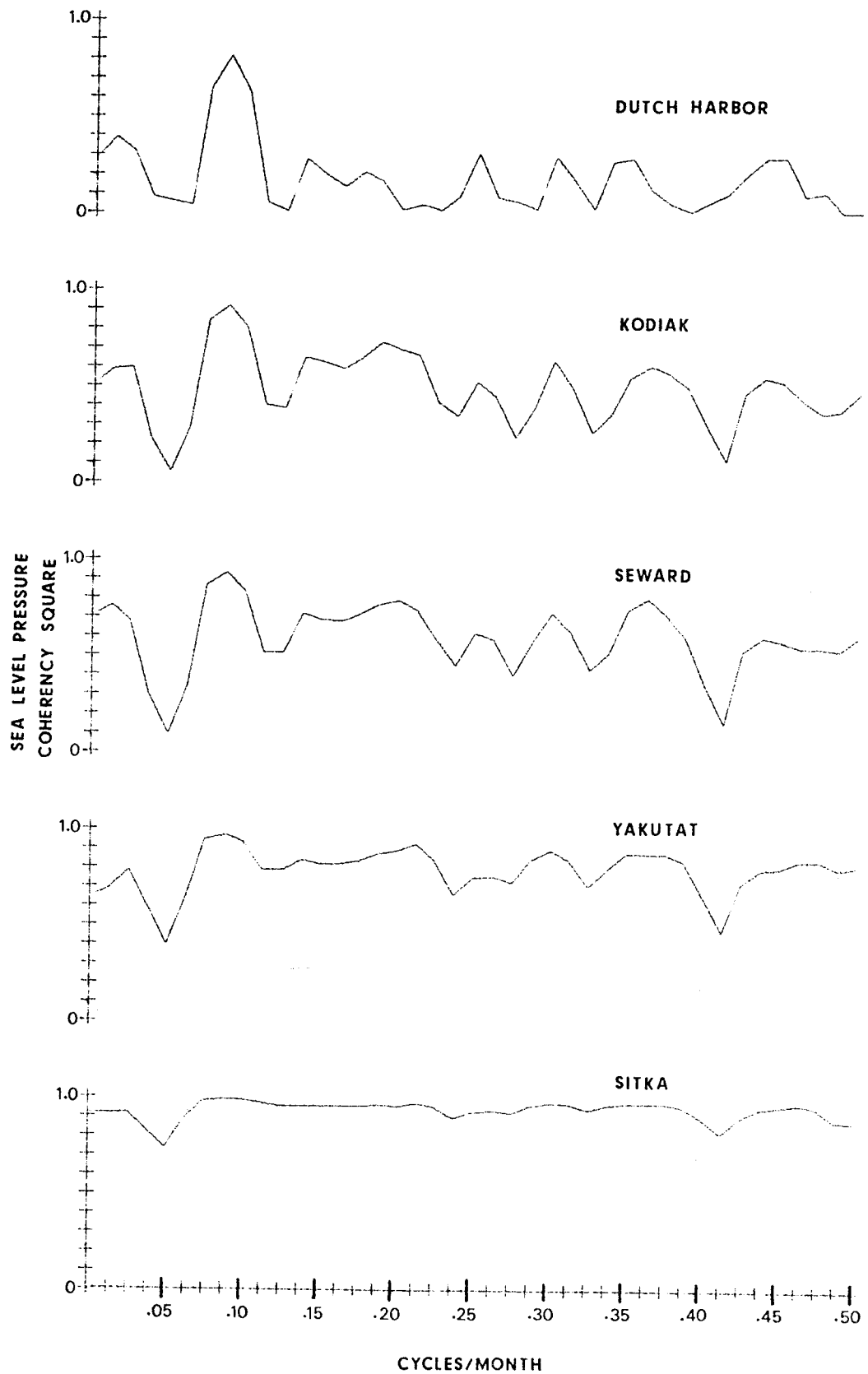


Figure 35. Coherence in sea level pressure at the indicated coastal stations, using Ketchikan as reference station, showing good coherence ( $>0.9$ ) for annual cycle (.085 cy/mo).

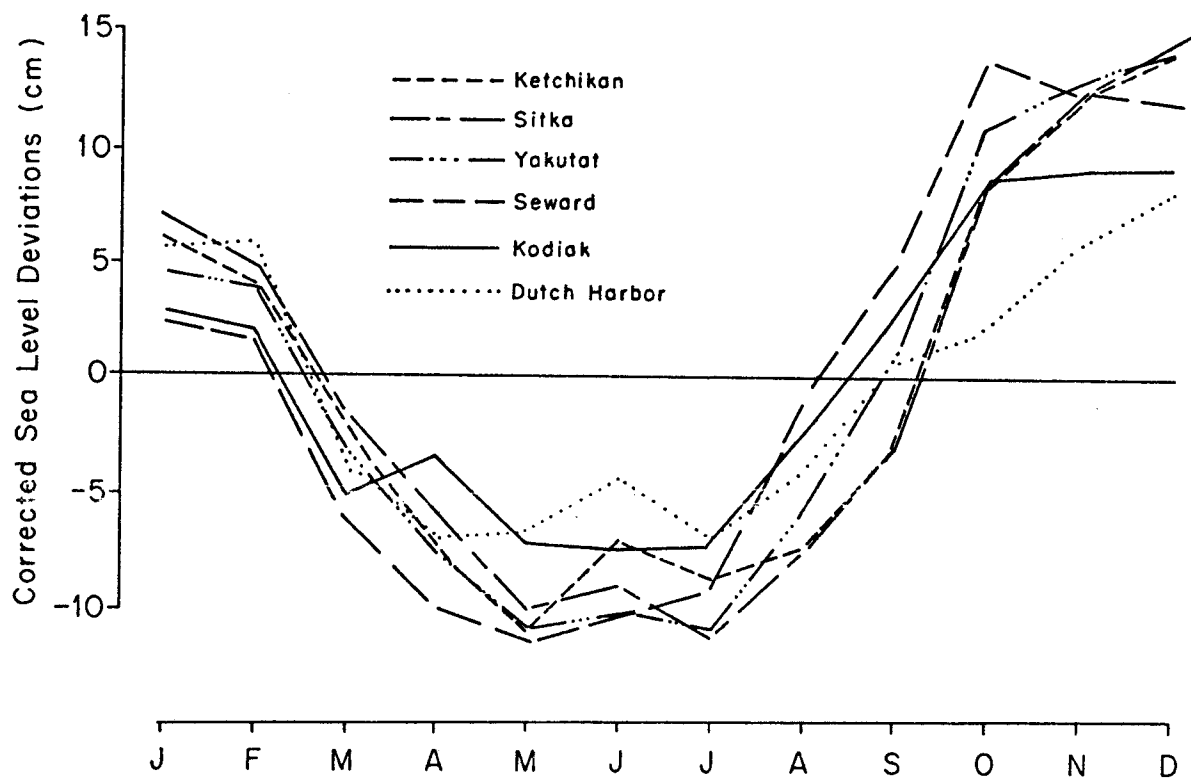


Figure 36. Deviations in corrected (for atmospheric pressure) sea level (cm) from monthly mean (1950-74) values at the indicated coastal stations showing increase in sea level in winter.



control between the various stations that would permit relating levels at the various sites to a common datum which would permit ascertaining relative levels. Deviations from monthly mean sea level for 1950-74 and 12-month running mean corrected sea level were compiled (Fig. 37). Here again there is continuity in short pulses (e.g. November 1952, January 1958, and others). However, positive and negative anomalies extend for longer periods up to 4 years. Well above normal sea level was evident at Dutch Harbor from 1957-61 and at Ketchikan from 1966-70. The apparent progressive lowering of sea level at Dutch Harbor from 1957 to 1974 is not evident at the other stations, but the below normal levels are evident from 1970 to 1974. These data can be grossly summarized for the area Sitka to Kodiak as follows: 1950-54 above normal, 1955-57 below normal, 1958-62 above normal, 1963 below normal, 1964-69 normal, 1970-74 below normal. As might be anticipated, power spectral analysis (40 lags) for corrected sea level at the coastal stations exhibits the 1 year frequency (Fig. 38). Data at Dutch Harbor, Seward, Yakutat and Ketchikan indicate significant energy densities at periods of less than one year and there is a high coherence ( $>.9$ ) at this frequency at all stations compared to Ketchikan (Fig. 39). In contrast to sea level pressure, there is a marked coherence at 0.5 cy/mo. As before, the limited data points do not permit clear definition of periods greater than 1 year.

### C. Relation to Transport

An increase in sea level normally signifies an increase in northward flow into the gulf. Such considerations can only be made when equivalent transport data are available. Obviously this cannot be obtained from

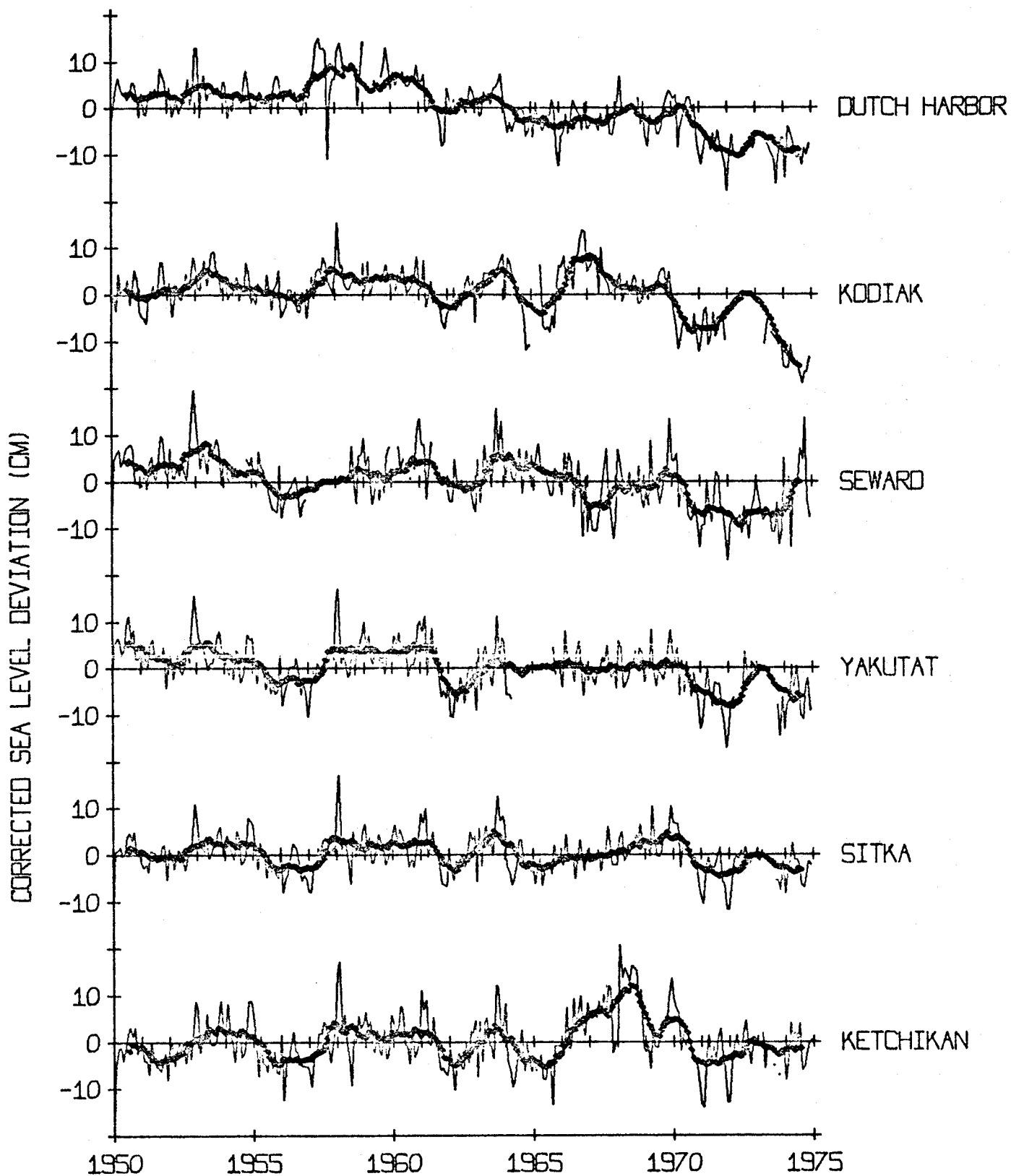


Figure 37. Deviations in corrected sea level (cm) from monthly mean (1950-74) values at the indicated coastal stations and 12-month running mean (dotted line).

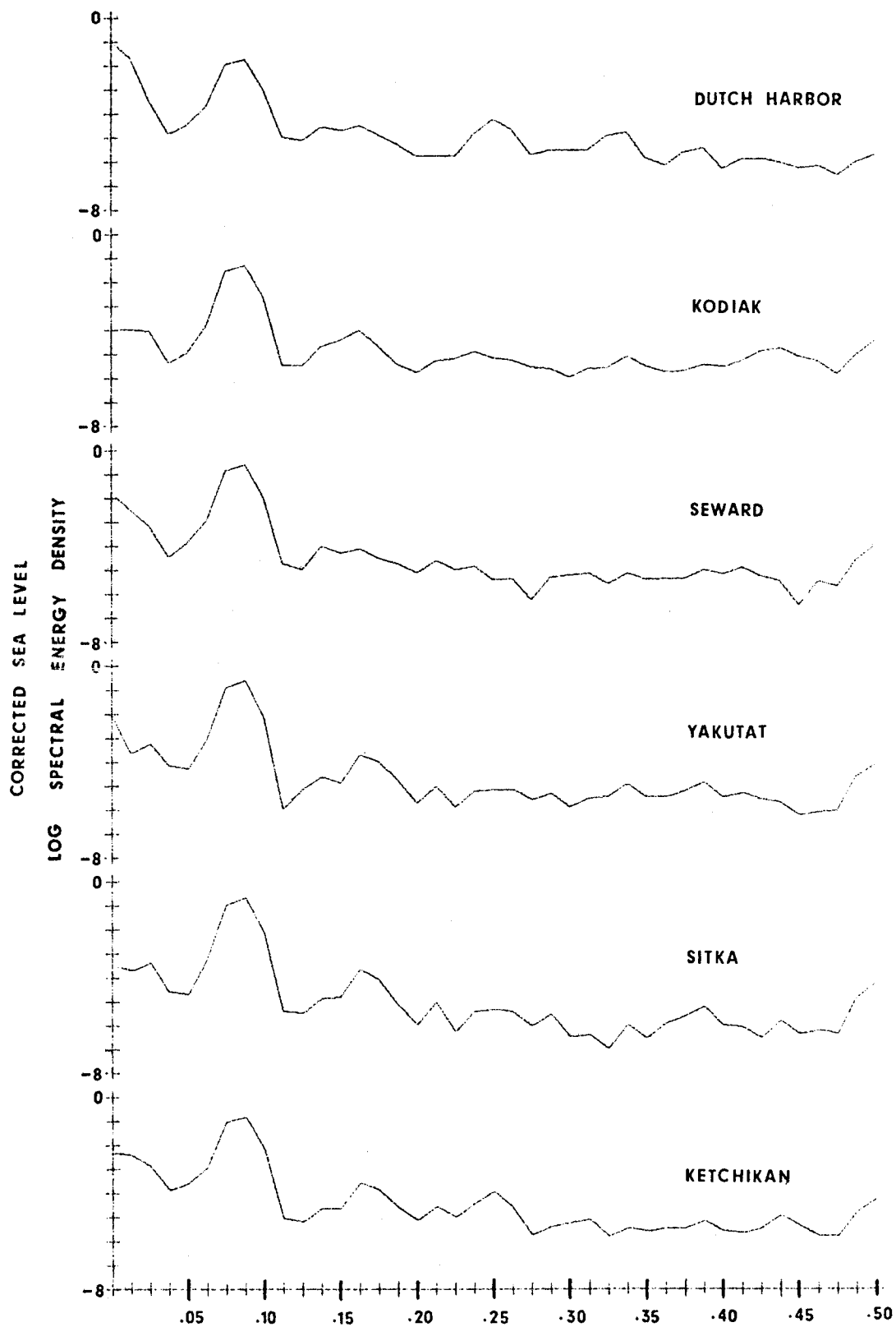


Figure 38. Spectral energy densities (40 lags) for corrected sea level at the indicated coastal stations showing the dominant 1 year cycle.

869

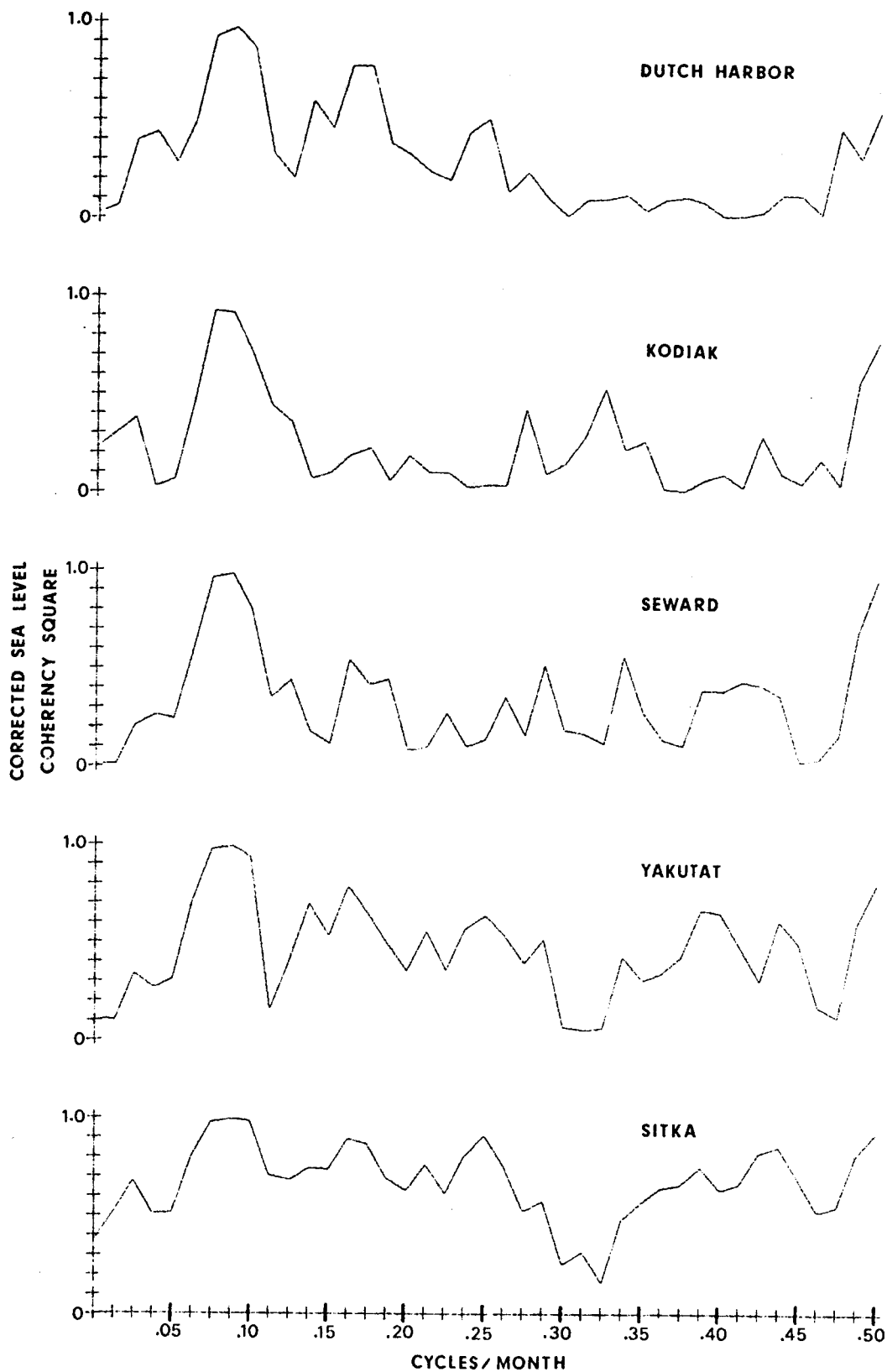


Figure 39. Coherence in corrected sea level at the indicated coastal stations, using Ketchikan as a reference station, showing good coherence (>0.9) for annual cycle.

station data which are available only for one or two months in a limited number of years. However, comparisons can be made with wind-stress transports. Monthly mean wind-stress transports across 55°N (+northward; -southward) computed for the years 1900-74 indicate a mean transport of 11.22 Sv (Fig. 40). There is a progressive increase in the 25-year mean values from 8.39 to 10.90 to 14.35 Sv that is probably primarily, if not almost entirely, due to progressively better definition of sea level pressure fields; thus, limited comparisons between past and more recent data can be made. Further, the high monthly mean wind-stresses in winter are not of sufficient duration for the calculated transports to become established, but the presence of additional energy is indicated.

The individual monthly mean transports in 1950-74 have a greater range ( $\sim 80$  Sv) than in the previous two 25-year periods ( $\sim 60$  Sv). The following winters stand out as having high northward transport: 1908-09, 1949-50, 1955-56, 1958-59 and 1965-66. Anomalous southward transports are indicated in: fall 1900, winter 1920, winter 1929, fall 1930, summer 1936, summer 1958 and fall 1965.

Transport ranges reflected in the 12-month running means are quite similar ( $\sim 12$  Sv) for the three 25-year periods. Except for the years 1950-1965 when there is evidence of an approximate 3-year cycle there is no immediately apparent suggestion of any other periodicities. The long data record (900 data points) provides the first substantial look at periods greater than one year and spectral analyses using 80 and 160 lags substantiate the peak near 3 years.

MEAN 1900 - 1974 = 11.22 SV

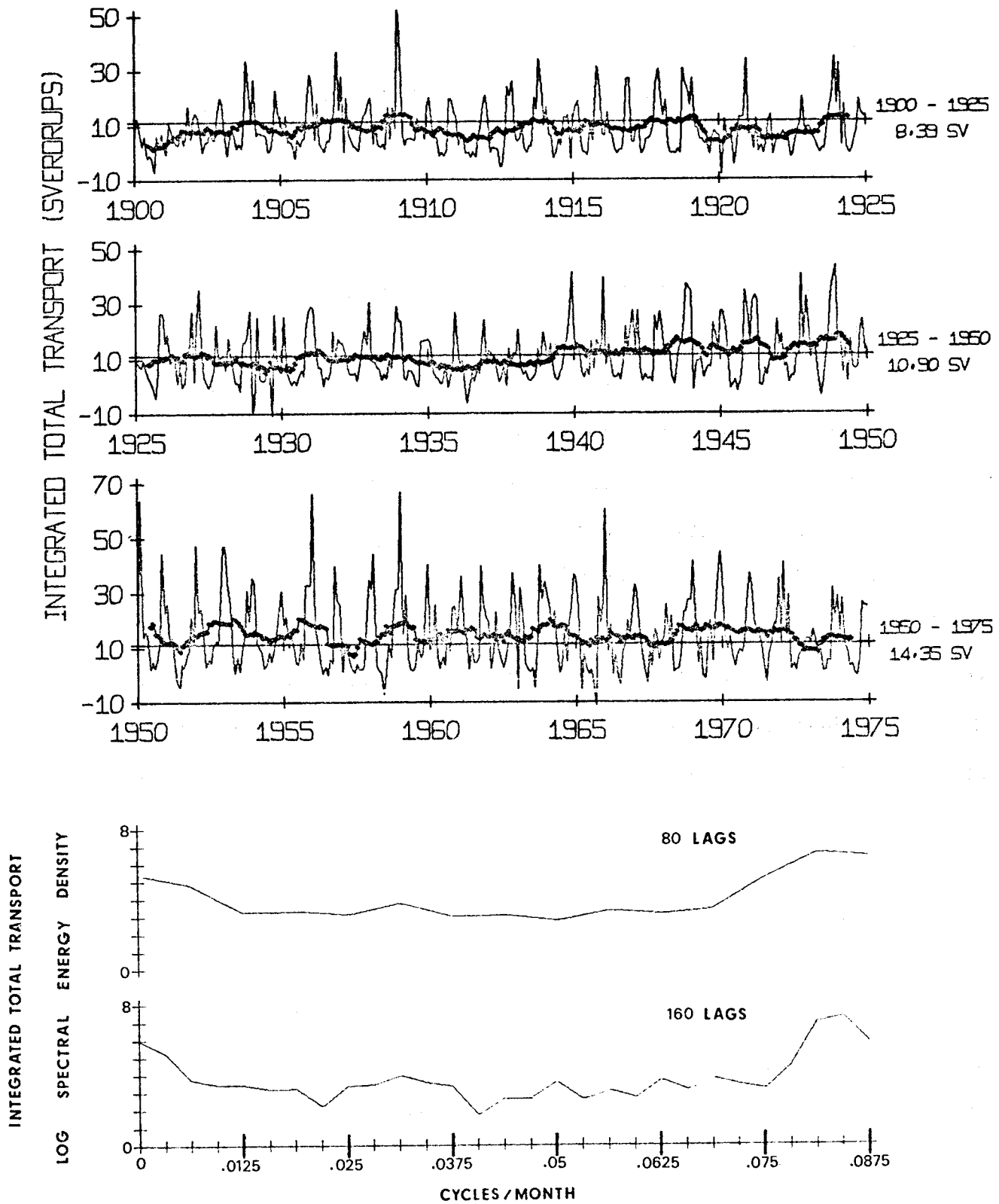


Figure 40. Monthly integrated total transports (Sv) across 55°N (+northward, -southward) 1900-74, 12-month running mean (dotted line), and spectral energy density (80 and 160 lags).

## VI. SURFACE CONVERGENCE AND DIVERGENCE

The surface wind drift, i.e. the water carried along in the very surface layer of the ocean under the direct action of the wind, usually contributes only slightly to the surface velocity field, and because of its limited vertical extent is nearly always negligible in terms of total mass transport. However, the surface drift field can contain very large convergences and divergences, which may fluctuate rapidly, both in pattern and intensity. These convergences and divergences create pressure gradients and redistributions of mass which alter the underlying geostrophic currents. Because it is likely that these alterations are highly important on the scales of interest to OCSFAP field programs, a rather detailed study of the convergence-divergence pattern in the surface waters of the Gulf of Alaska has been made.

The energetic winter season dominates the annual cycle. Typically, positive wind stress curl associated with an atmospheric low pressure system induces divergent surface drift. Where the coastal boundary of the Gulf presents a barrier to this drift, convergence and intense downwelling result (Bakun, 1975). Such a situation would act to intensify the characteristic ridging of the density structure in the interior of the Gulf and to steepen the plunge of the isopycnals toward the coast. This "pumping" between the coastal and offshore areas would tend to build up baroclinicity through the winter season, which apparently would dissipate during the more relaxed portion of the year.

In order to investigate the coupled system, indices of divergence of wind-induced surface flow at 6-hourly intervals from January, 1967 through December 1975 were generated at 15 locations indicated in Figure 41. The surface flow field is approximated as Ekman Transport and an

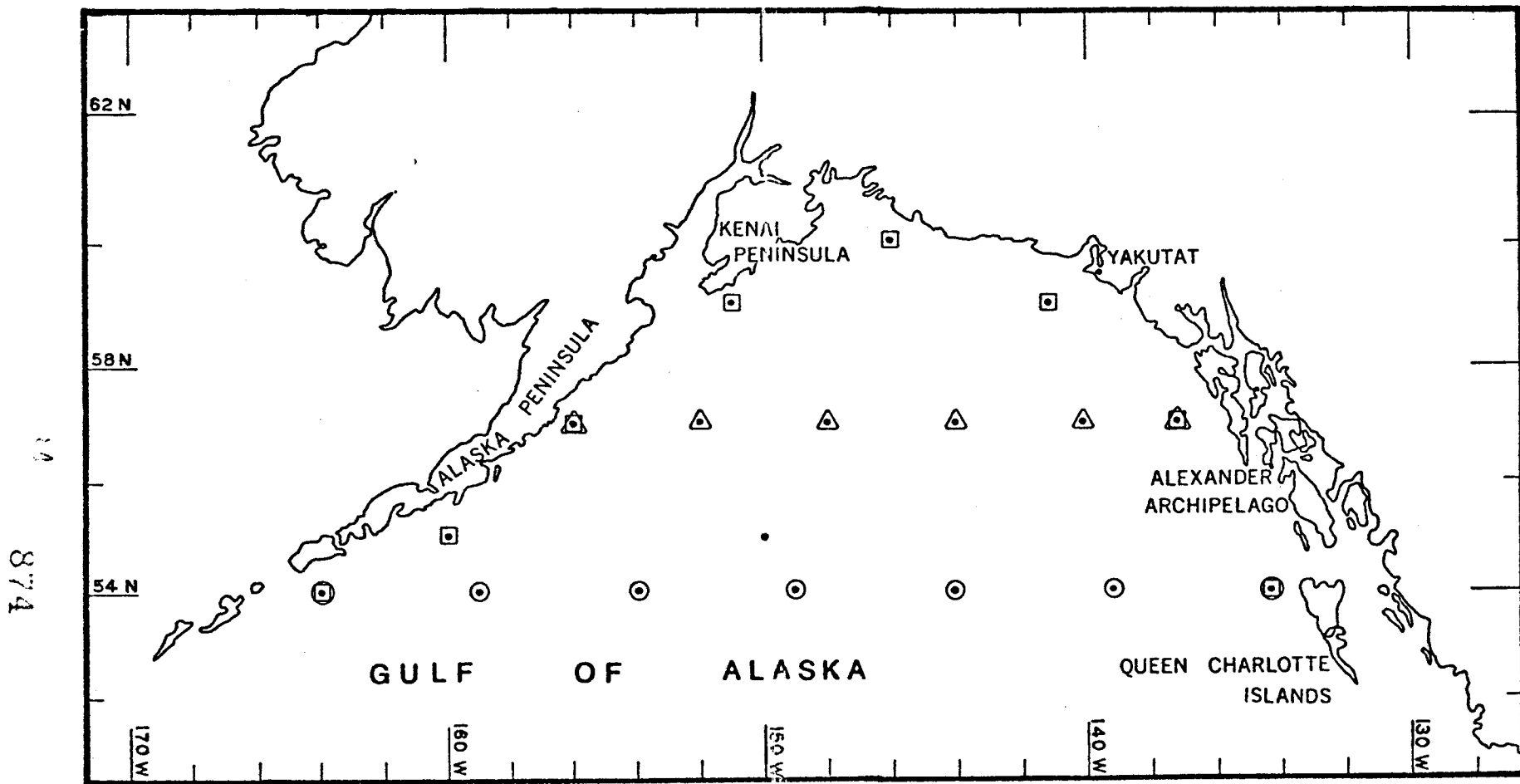


Figure 41 - Chart of the Gulf of Alaska region, showing locations at which time series of surface convergence-divergence indices were computed.



example segment of the time series at one location is shown (Fig. 42).

In the previous sections data fields averaged over a month or longer have been discussed. This is because attention has been focused on lower frequency, relatively slowly changing components of the variations. either because we are not equipped to deal with the shorter term variability or because sparsity of data requires that we collect observations over some time interval in order to get an adequate sample. Now an attempt will be made to deal with the synoptic scale. Such an approach is called for in this case because the extremely large variance of the surface divergence field on short time scales requires that proper interpretation of even the longer period variations be made within the framework of the process as it is actually occurring on the synoptic scale.

On this scale attention shifts from such mean pressure features as the Aleutian Low, or a Continental High, to individual traveling storm systems. Major winter storm tracks cut directly across the gulf from the southwest toward the northeast. Mean speeds of storm movement along these tracks are of the order of 25 knots (Klein, 1957). During the summer a larger proportion of storms turn northward through the Bering Sea and so are not felt with full intensity in the Gulf of Alaska. In addition, the summer storms are normally much less intense than the winter storms. The available reports of wind speed and direction for an area such as the gulf tend to be sparse and unevenly distributed. Example distributions of reports (Fig. 43) show that major fraction of available reports come from shore stations which, being subject to topographical influences, may not be completely representative of conditions offshore. The distribution of the observations taken at sea changes continually, and for any single observation, random errors in measurement or position may introduce

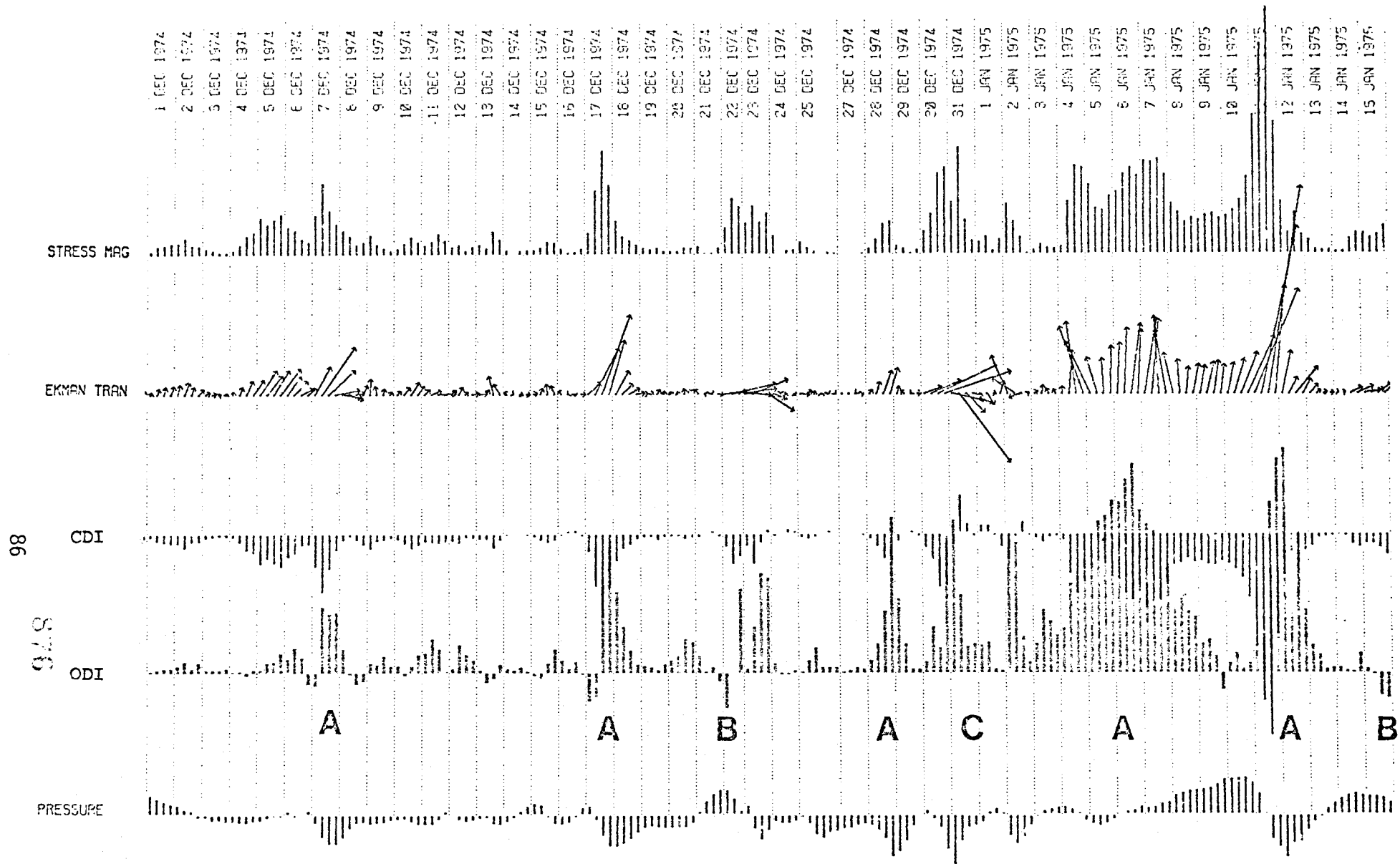


Figure 42 - Example time series segment (49N, 141W, Dec. 1, 1974 - Jan. 15, 1975). Upper graph indicates the stress magnitude at each 6-hourly synoptic sampling. Second graph indicates the magnitude and direction of Ekman transport; north is toward the top, etc. Third graph indicates the coastal divergence index (CDI). Fourth graph indicates the offshore divergence index (ODI). Large letters refer to type of event according to classification of Fig. 44.

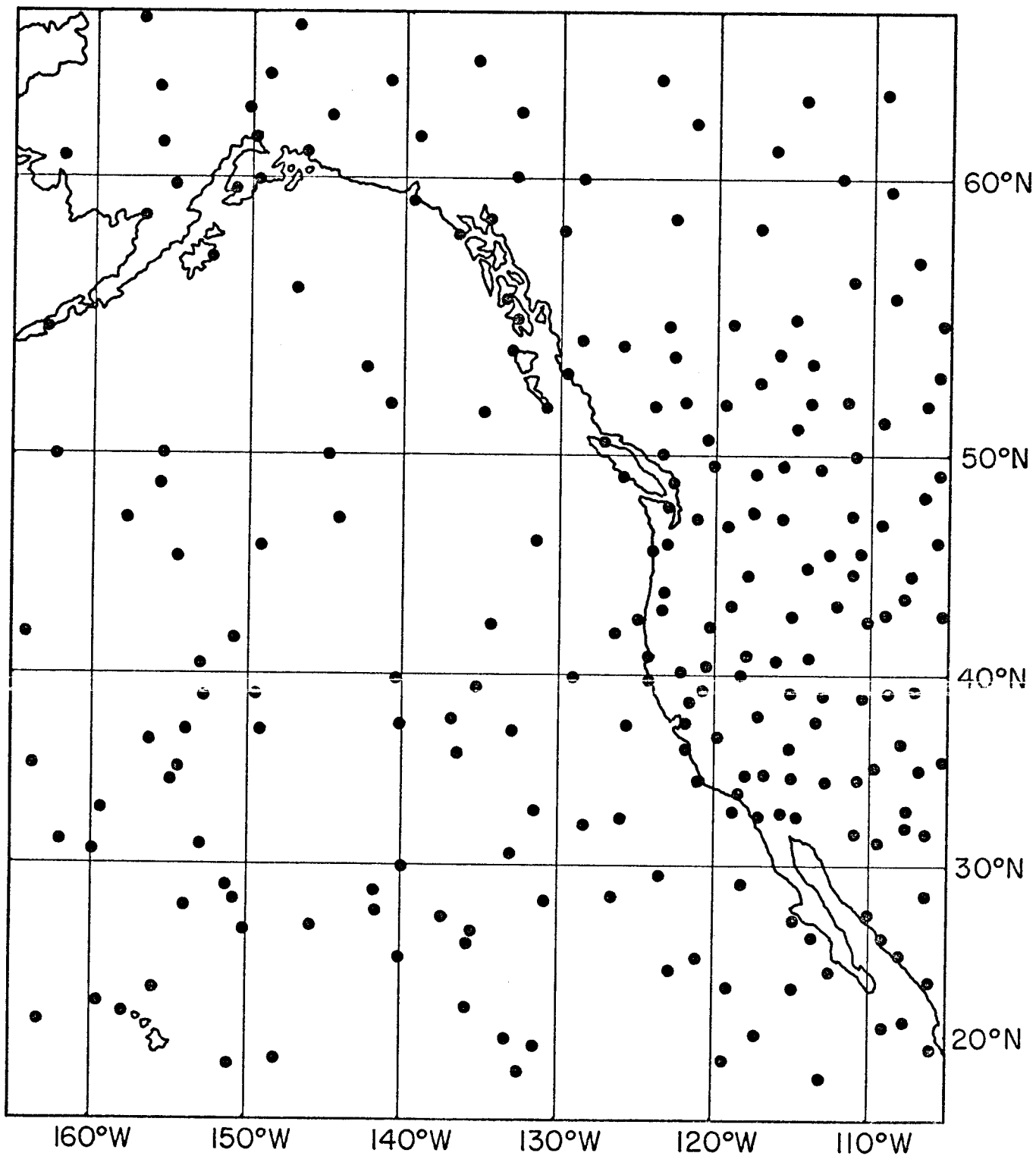


Figure 43 - Distribution of observations made at 1800 GMT, 5 January 1974, which arrived at Fleet Numerical Weather Central in time for incorporation in the operational surface pressure analysis.

variability which is greater than the variability in the process itself (Nelson, 1974).

One way to arrive at a fairly consistent time series is to make use of analysed products produced by meteorological agencies. For this portion of the study 6-hourly synoptic surface atmospheric pressure analyses produced by Fleet Numerical Weather Central (FNWC) have been used. These analyses incorporate all available wind reports in the form of equivalent pressure gradients. The use of the pressure reports, which are linked to the wind field through well-known relationships, effectively increases the data base.

The method of atmospheric pressure analysis presently in use at FNWC is described by Holl and Mendenhall (1972). The basic steps in the analysis are as follows:

- Preparation of "first guess" field: The pressure analysis for the previous synoptic sampling, 6 hours earlier, is extrapolated forward using a computation of 6-hour upper air movement and a 6-hour surface forecast using the FNWC primitive equation computer forecast model.
- Assembly of new information: new reports are compared to the first guess field, subjected to a gross error check, and assigned a reliability value; surface wind reports are assembled in a gradient field.
- Blending for pressure: a blending equation of 61 terms which take into account the pressure, gradient, second-differences, cross differences, and Laplacians, plus the reliability value of each of these, is used to assemble a "best fit" pressure field.

- . Computation of reliability field: depending on the amount and reliability of information available, each grid-point value is assigned a reliability.
- Reevaluation and lateral rejection: reports are again compared to blended pressure field and reliability field and assigned new reliability values; those failing to meet criteria are rejected.
- Recycling: a new assembly is made according to the new first guess field and assigned reliabilities. The whole process is then repeated a third time to gain further accuracy.

In order to produce the computed indices discussed in this section pressure data from FNWC fields archived on magnetic tape were arranged on a 3-degree computational grid and the curl of the wind stress,  $\nabla \times \vec{\tau}$  derived as shown in equations 5-20, except that constant drag coefficient of 0.0013, appropriate for synoptic rather than mean data, was used.

The Ekman transport,  $\vec{E}$ , is derived as

$$\vec{E} = \frac{1}{f} \vec{\tau} \times \vec{k} \quad (25)$$

where  $\vec{k}$  is a unit vector directed vertically upward.

The divergence of Ekman transport integrated over the width of the coastal upwelling-downwelling boundary zone, per unit length of coast, is given, to a high degree of approximation, by the offshore component. Bakun (1973) called this by the term upwelling index. In this report we refer to it as the coastal divergence index, abbreviated as CDI.

$$CDI = \vec{E} \cdot \vec{n} \quad (26)$$

where  $\vec{n}$  is a unit vector normal to the coast. Units used are metric tons per second per 100-meter length of coast.

Away from the boundary zone the divergence of Ekman transport is computed as

$$\text{ODI} = \nabla \cdot \vec{E} = \frac{1}{f} \nabla \times \vec{\tau} - \frac{\beta}{f} \vec{E} \cdot \vec{j} \quad (27)$$

where  $\beta$  indicates the meridional derivative of  $f$ . ODI stands for offshore divergence index. The values presented in this report are in terms of vertical velocity (millimeters per day) through the bottom of the Ekman layer required to balance the computed divergence.

#### A. Vicinity of the coastal boundary

Various combinations of coastal and offshore convergence or divergence occur near the coastal boundary (Fig. 44). Both types A and B are characterized by coastal convergence (negative CDI) in the coastal boundary zone; surface water is piled up toward the coast with a resulting depression of the isopycnals, tending to intensify counter-clockwise flow along the border of the gulf. In the case of type A, divergence immediately offshore of the boundary zone (positive ODI) would favor confinement of the intensification to a narrow zone next to the coast. In the type B situation continued convergence offshore of the boundary zone (negative ODI) would spread the effect toward the interior of the Gulf.

Under situations C and D, coastal divergence (positive CDI) would favor clockwise circulation along the boundary of the Gulf (or deceleration of counter-clockwise flow, etc.). Correspondingly, type C (positive ODI) would tend to spread the effect, while type D (negative ODI) would tend to confine it to the immediate boundary zone.

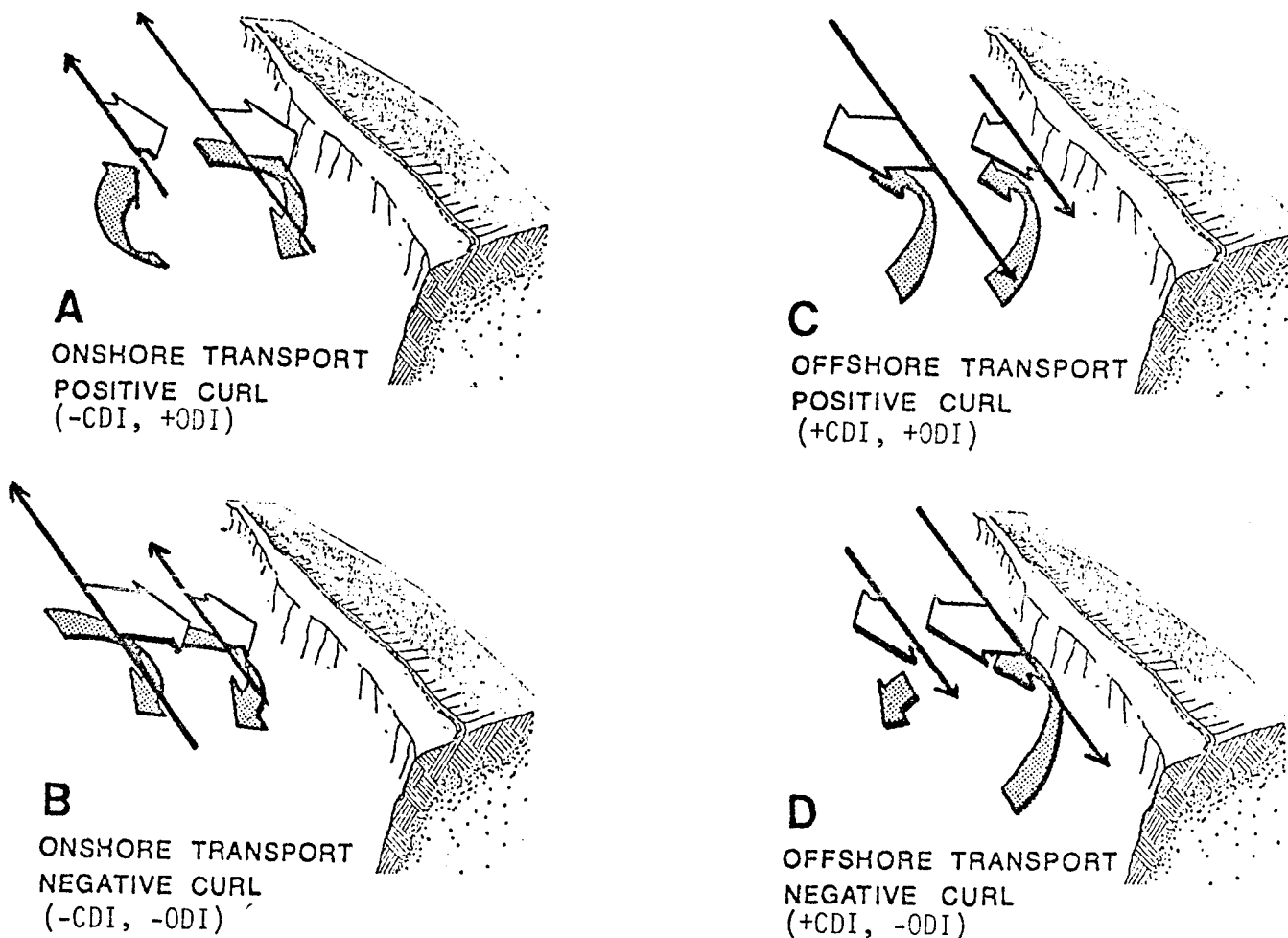
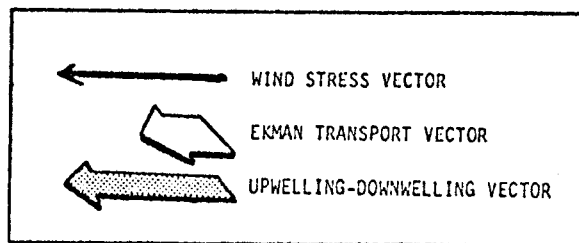


Figure 44 - Classification of indicated events according to combination of coastal and offshore convergence or divergence. A. Onshore Ekman transport and positive wind stress curl; convergence and downwelling at the coast, divergence and upwelling offshore. B. Onshore Ekman transport and negative wind stress curl; convergence and downwelling at the coast, continued convergence offshore. C. Offshore Ekman transport and positive wind stress curl; divergence and upwelling at the coast, continued divergence offshore. D. Offshore Ekman transport and negative wind stress curl; divergence and upwelling at the coast, convergence offshore.

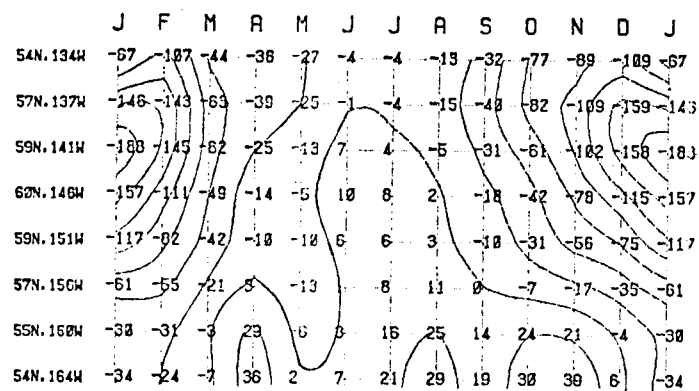
The monthly frequency distributions of coastal divergence indices (CDI), at the near coastal locations (surrounded by squares in Fig. 41) show strongly negative mean values during the winter, indicating convergence and resulting downwelling at the coast (Fig. 45). The area of greatest intensity extends from the Kenai Peninsula (59°N, 151W) to the Alexander Archipelago (57N, 137W), reaching a maximum near Yakutat (59N, 141W). This situation relaxes during the remainder of the year; coastal divergence (positive CDI) is indicated on average over much of the gulf during summer. This "summer upwelling season" is longest in the southwest portion, extending from April to December near the extremity of the Alaska Peninsula and exhibiting three separate maxima (April, August, and November). The season of mean upwelling becomes progressively shorter and less intense with distance clockwise around the gulf, lasting three months off the Kenai Peninsula and essentially vanishing off the Alexander Archipelago.

The maximum variance corresponds in season and location to maximum absolute values of the mean. Standard deviations are larger than the means. Thus the winter season is characterized by highly energetic pulsations and relaxations of coastal convergence. In other seasons, the general trend is for the variance to decrease with the mean. The most stable situation appears to be the summer season in the northern gulf (59N, 151W; 60N, 146W; 59N, 141W). The three separate maxima exhibiting fairly similar mean positive CDI values off the lower Alaska Peninsula (54N, 164W; 55N, 160W) appear quite distinct in terms of variance. The August maximum in the mean shows the lowest variance, whereas, the November maximum exhibits standard deviations nearly three times those of August. Thus, the mean



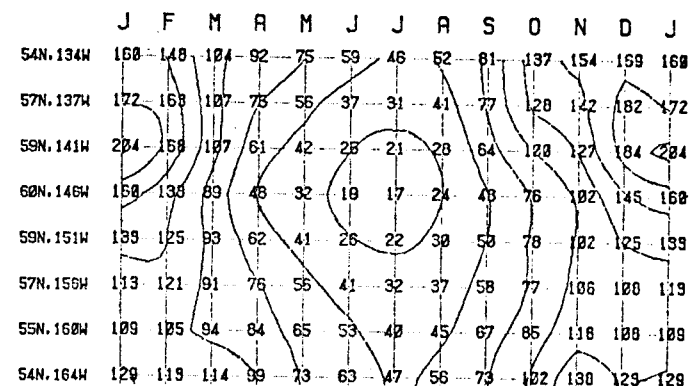
MEAN.

COI



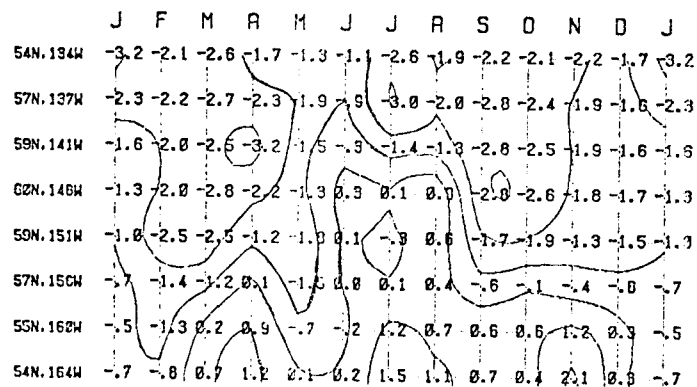
STANDARD DEVIATION

COI



SKEWNESS.

COI



KURTOSIS.

COI

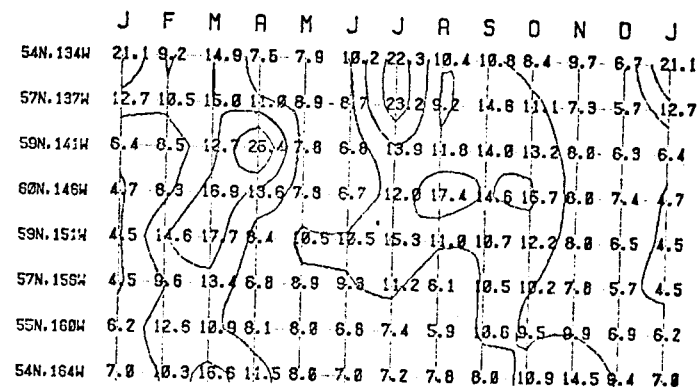


Figure 45 - Moments of the frequency distributions of coastal divergence indices (CDI) grouped by month at the near-coastal locations indicated by triangles in Fig. 41. Mean: units are cubic meters per second transported off each 100-meter width of coast; contour interval is 25. Standard Deviation: units and contour interval are the same as for the mean. Skewness: contour interval is one normalized unit. Kurtosis: contour interval is 5 normalized units.

upwelling indicated for November represents an energetic mix of upwelling and downwelling events, with the balance tipped slightly toward upwelling.

The skewness tends to have the same sign as the mean; i.e. extreme events during downwelling seasons tend to be downwelling events, and those during upwelling seasons to be upwelling events. Some modification of this general pattern appears in the northern gulf where the distribution of skewness shows a tendency to be more negative than the mean (i.e. a considerable contribution from relatively extreme downwelling events even during seasons of mean upwelling). Off the lower Alaska Peninsula an expansion of the period of positive skewness beyond that of positive mean value indicates relative importance of extreme upwelling events, most probably related to very intense storms centered north of the Alaska Peninsula.

In all months and locations the kurtosis is larger than 3.0 indicating that there appears to be a much larger contribution of extreme events than would be the case in a Gaussian process. The details of the distribution of kurtosis are controlled to some extent by the fact that the kurtosis is normalized against the variance; thus, the winter season exhibits relatively low kurtosis because the variance is high (i.e. events which would be "extreme" at other seasons are the norm during winter). When a winter-type storm appears in the spring, for example, it contributes to a higher kurtosis because the general level of activity is lower. The relatively high kurtosis during the summer season indicates that the generally stable situation is interrupted only infrequently. Large contributions to the variance from extreme events are indicated for the lower Alaska Peninsula area during the fall season.

The monthly frequency distributions of offshore divergence indices (ODI) at the near coastal locations (Fig. 46) have mean values which are positive, indicating divergence on the average offshore of the coastal upwelling-downwelling zone, except during January in the southwestern Gulf and during the summer from the Kenai Peninsula eastward. Strongest divergence on average occurs near Yakutat during winter, corresponding in season and location to the maximum negative CDI values.

The ODI variance is largest in winter, but rather than corresponding in location to the mean as was the case for the CDI values, there is a double maximum (59N, 151W; 57N, 137W) with a relative minimum in the area of the maximum mean values. In the southwestern Gulf the period of maximum variance shifts to the fall.

The skewness of the monthly ODI distributions tends to be positive; extreme events are characterized by divergent surface drift associated with cyclonic storms. Some of the monthly distributions in the northern and eastern gulf exhibit a slight negative skewness in the spring or summer. The kurtosis indicates major contributions to the variance from infrequent, extreme events.

Comparison of mean CDI and ODI values confirms that, in a mean sense, the preeminent situation along the coastal boundary of Gulf is type "A" (see Fig. 44). The extreme energy of the downwelling at the coast and divergence offshore associated with winter storm systems completely dominates the annual cycle. Table 2 lists the "types" corresponding to the monthly mean situation at the various locations. Type D is restricted to the extremely low-energy summer situation in the northern gulf. The

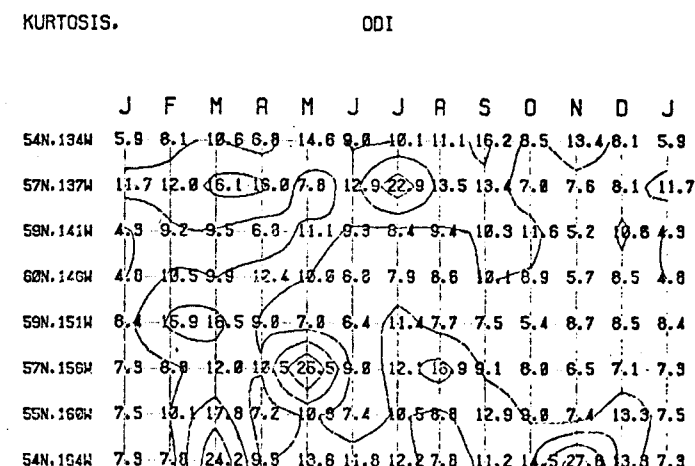
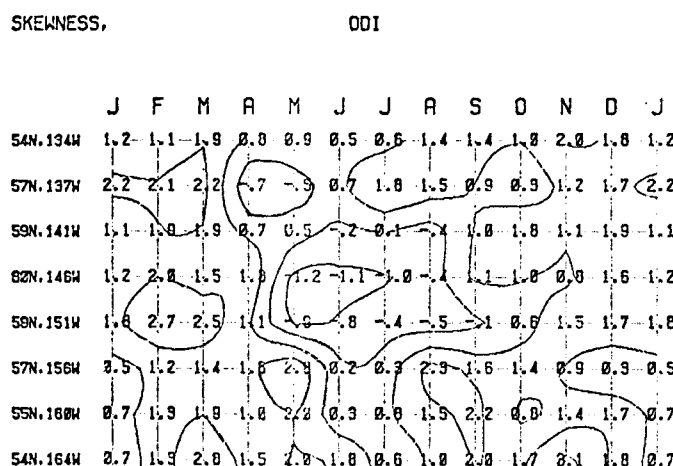
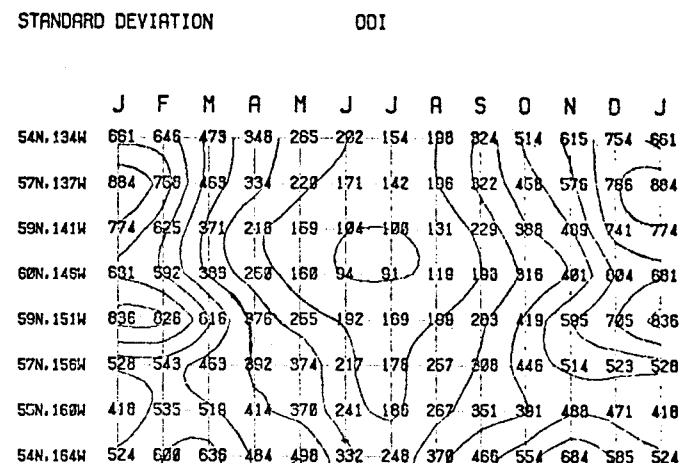
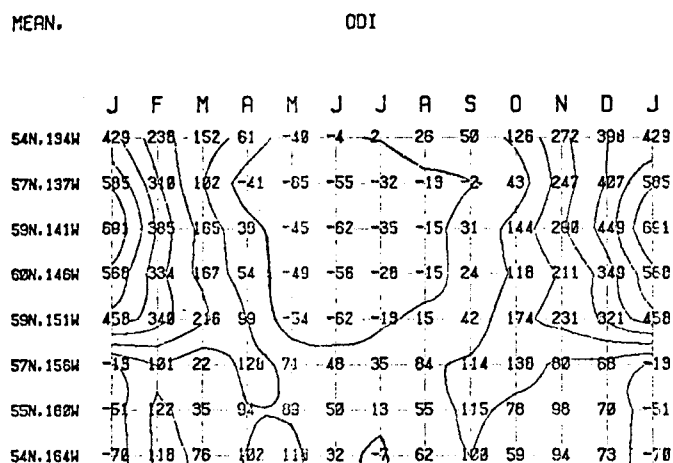


Figure 46 - Moments of the frequency distributions of offshore divergence indices (ODI) grouped by month at the near-coastal locations indicated by triangles in Fig. 41. Mean: units are millimeters per day upward velocity through the bottom of the Ekman layer required to balance the indicated divergence; contour interval is 100. Standard deviation: units and contour interval are as for the mean. Skewness: contour interval is one normalized unit. Kurtosis: contour interval is 5 normalized units.

TABLE 2 - Monthly mean "types" of convergence-divergence couple, according to the classification of Figure 44, characterizing the near-coastal locations indicated by triangles in Figure 41.

|           | Jan | Feb | Mar | Apr | May | Jun | Jul | Aug | Sep | Oct | Nov | Dec |
|-----------|-----|-----|-----|-----|-----|-----|-----|-----|-----|-----|-----|-----|
| 54N, 164W | B   | A   | A   | C   | C   | C   | C   | C   | C   | C   | C   | C   |
| 55N, 160W | B   | A   | A   | C   | A   | C   | C   | C   | C   | C   | C   | A   |
| 57N, 156W | B   | A   | A   | C   | A   | C   | C   | C   | C   | A   | A   | A   |
| 59N, 151W | A   | A   | A   | A   | B   | D   | D   | C   | A   | A   | A   | A   |
| 60N, 140W | A   | A   | A   | A   | B   | D   | D   | D   | A   | A   | A   | A   |
| 59N, 141W | A   | A   | A   | A   | B   | D   | D   | B   | A   | A   | A   | A   |
| 57N, 137W | A   | A   | A   | B   | B   | B   | B   | B   | B   | A   | A   | A   |
| 54N, 134W | A   | A   | A   | A   | B   | B   | A   | A   | A   | A   | A   | A   |

coastal area of the lower Alaska Peninsula is, on average, under a type C situation over much of the year; considering this surface drift effect alone, the net tendency would seem to be to break down some of the baroclinicity built up in the type A situation further east.

The fraction of 6-hourly samplings during each month characterized by the various event types are summarized for several locations (Fig. 47). The seasonal shift from type A to type D at 59N, 141W is well illustrated. In this presentation, all periods, even where the index values were so small as to be negligibly different from zero, were included in calculating the percentages. When the weaker events are excluded the percentage of the dominant event type increases. By progressively increasing the required intensity the percentages of the less common types would eventually approach zero.

In order to perform spectral analysis on seasonal time series of substantial length, we have constructed composite winter and summer time series of the indices at each location. For example, winter time series were formed of all values within weeks of which the first day falls within the months of December, January, or February. Thus, the first week of December, 1974 follows directly after the last week in February, 1973. Summer series were similarly formed from values within weeks which begin in June, July, or August, etc. This procedure affects only the longer period spectral estimates which tend to be lost in the unresolvable seasonal and climatic scale energy. The results effectively summarize the features observed from analysis of the various short, properly continuous, seasonal segments of the time series.

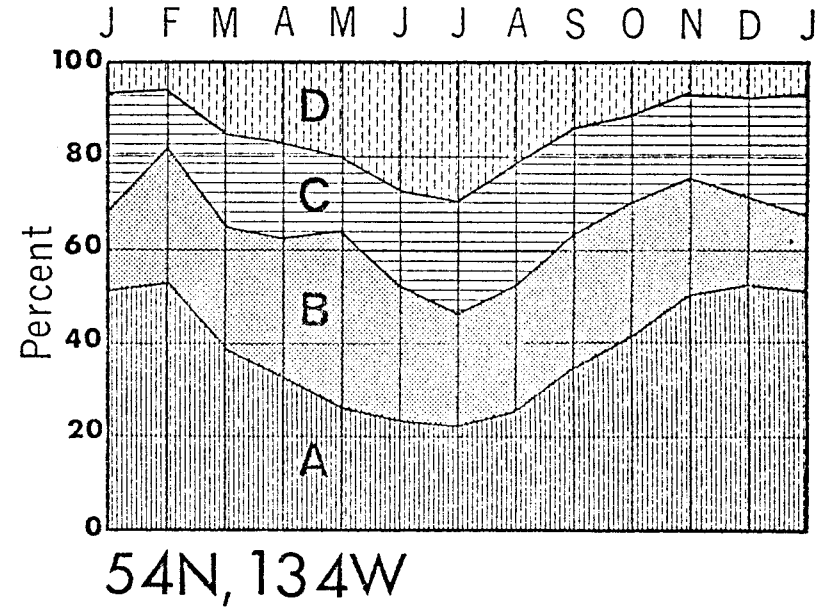
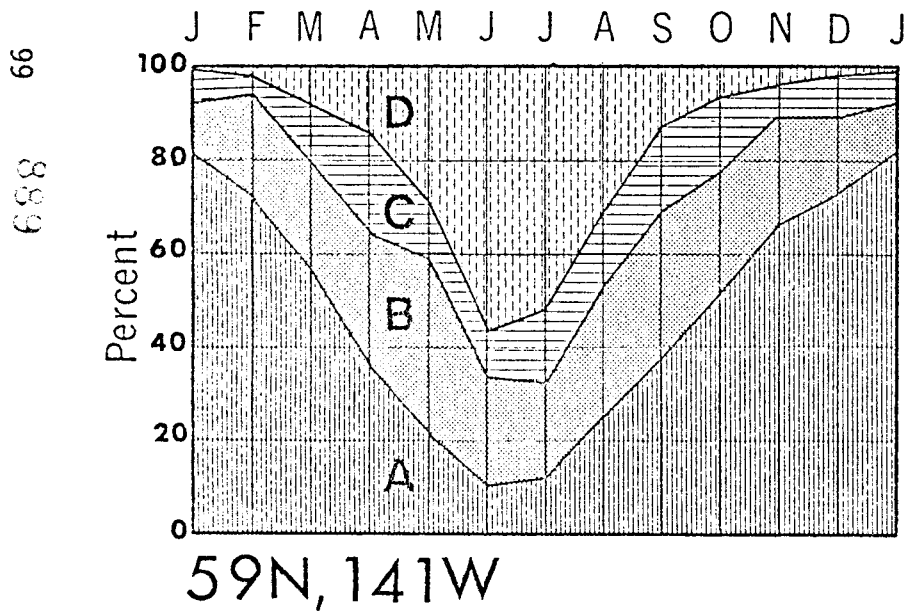
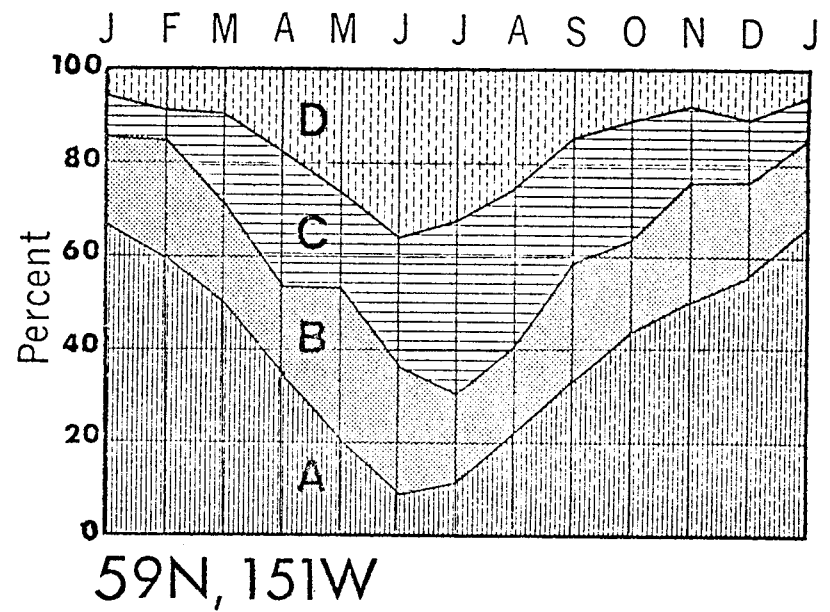
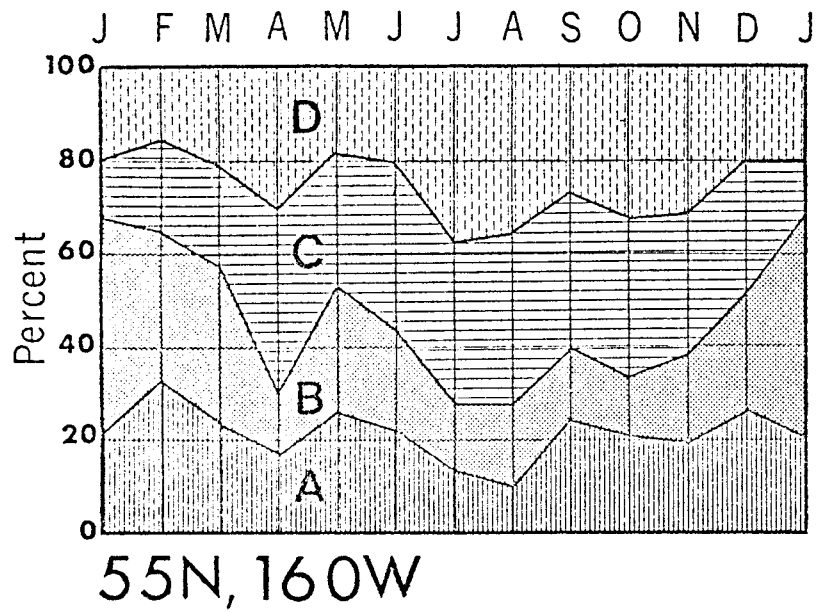


Figure 47 - Percentages, by month, of 6-hourly synoptic samplings characterized by each of the "event types" classified in Fig. 44.

Autocorrelation functions were computed from the CDI series (Fig. 48) and from the ODI series (Fig. 49). In all cases autocorrelation drops off rapidly within the first several days; time scales of individual events are characteristically short. A diurnal fluctuation, most marked in the CDI series, is apparent during summer (and less markedly in spring) at near-coastal locations in the northern and eastern Gulf. A somewhat lower frequency oscillation, indicating the "event" scale, is visible in many of the functions.

Examples of cross correlations between the CDI indices and ODI indices at the same location (Fig. 50) show that cross correlation tends to be negative for short lag periods, most markedly in the winter in the northeastern Gulf where the type A situation (negative CDI, positive ODI) predominates. Indications of negative cross correlations during summer in the same area are related to the predominance of Type D. Off the Alaska Peninsula cross correlation is low, indicating a rather complex mixture of event types and intensities.

Power spectra corresponding to the autocorrelation functions (see Figs. 48 and 49) have been constructed (Figs. 51 and 52) based on 100 lags of seasonal data series containing over 3000 data points each. This translates to about 66 degrees of freedom, representing considerable stability in the resulting spectral estimates. The spectra are similar in general form, resembling "red noise" spectra. Such spectra, which are characterized by a general decrease in energy from lower to higher frequencies, are indicative of temporal persistence within the series.



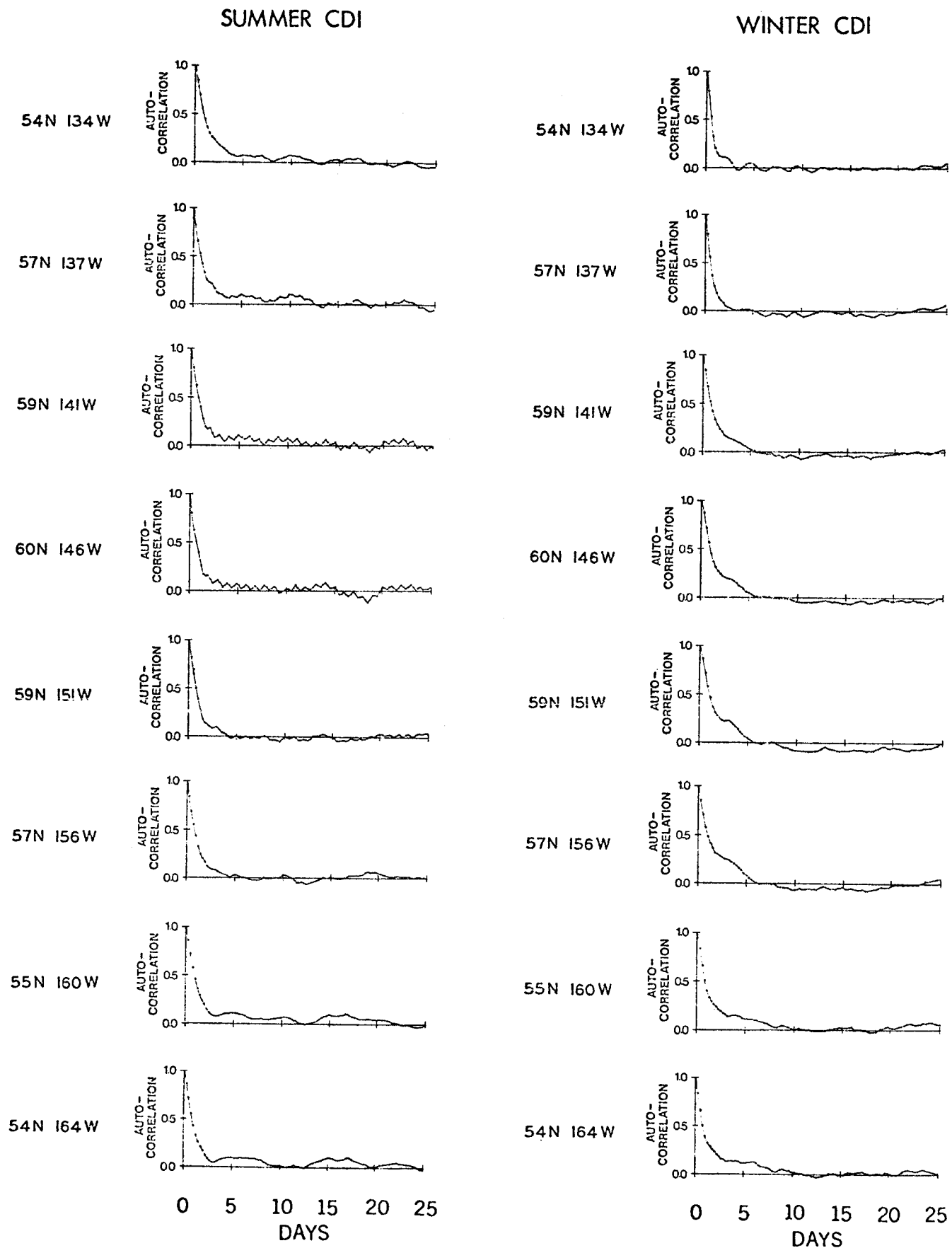


Figure 48 - Autocorrelation functions for coastal divergence indices (CDI) at the near-coastal locations.

SUMMER ODI

WINTER ODI

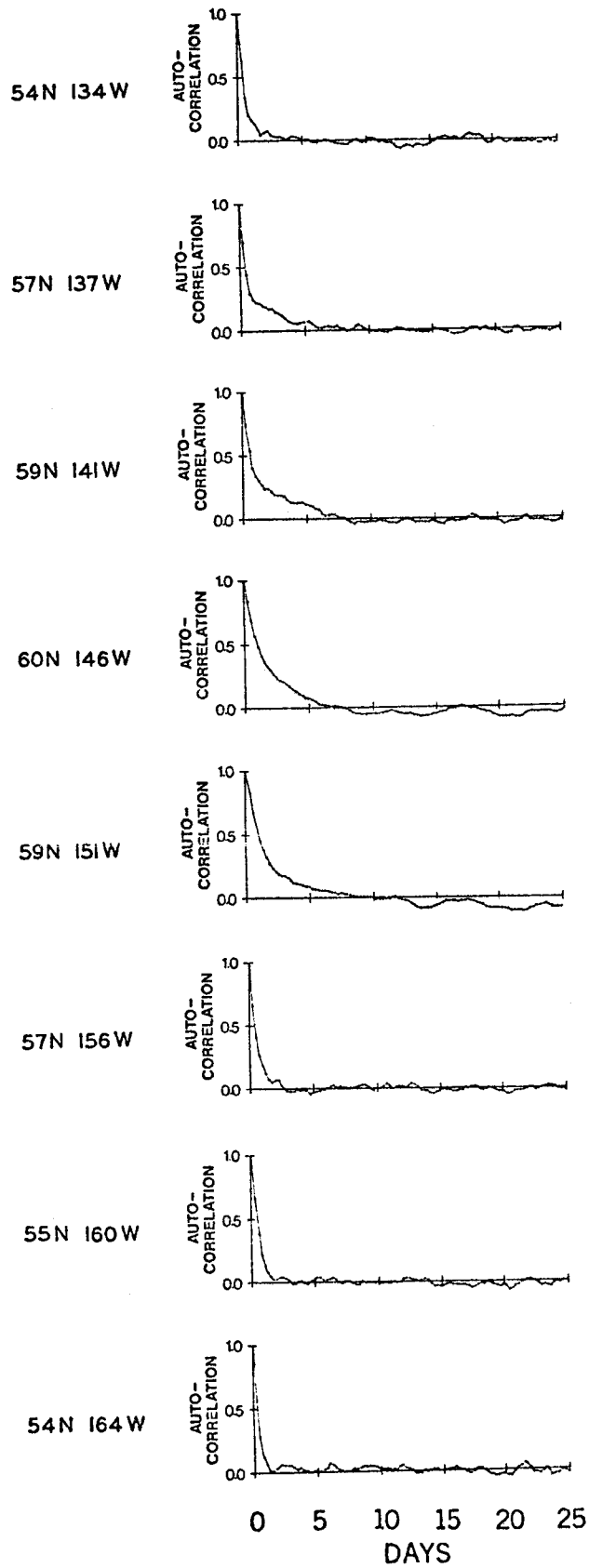
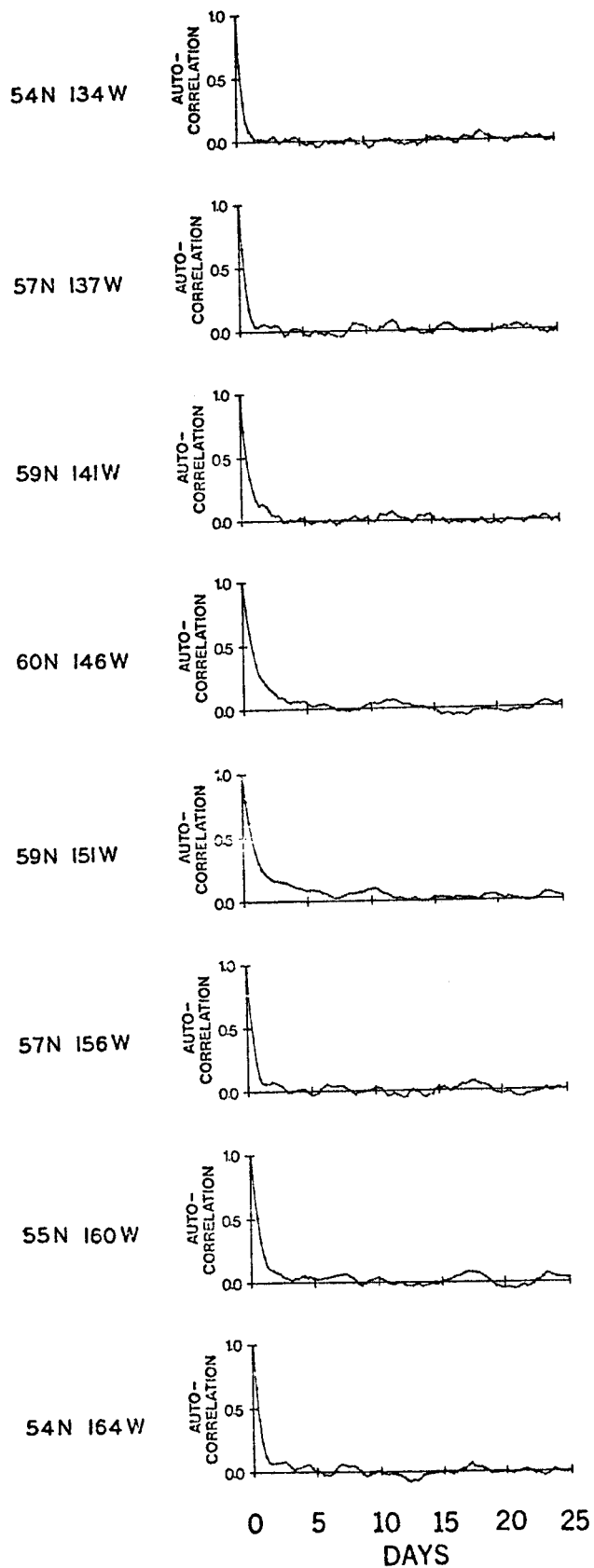


Figure 49 - Autocorrelation functions for offshore divergence indices (ODI) at the near-coastal locations.

# CDI VS. ODI

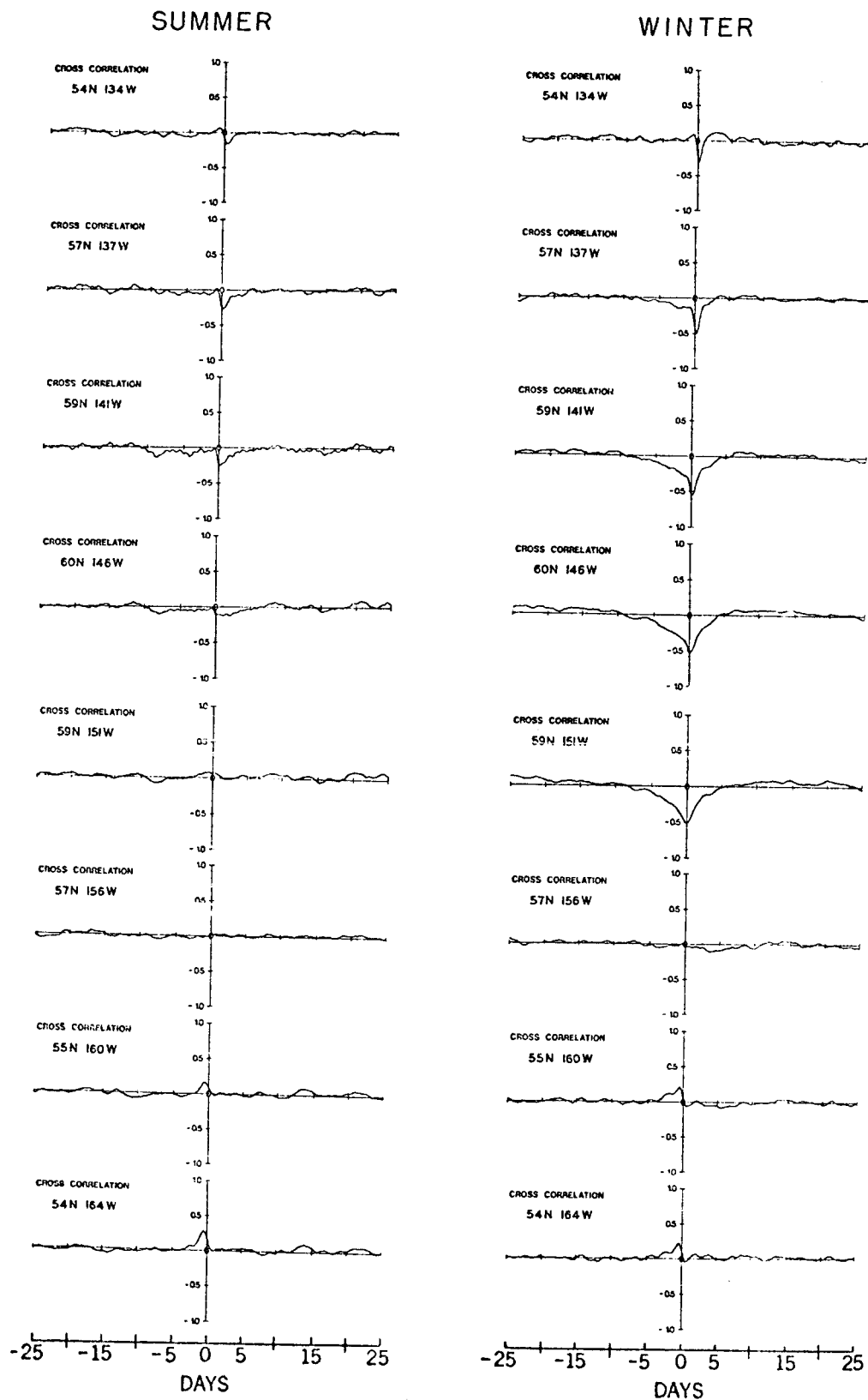


Figure 50 - Cross correlation functions for coastal divergence indices (CDI) v.s. offshore divergence indices at the near-coastal locations. Summer functions are on the left; winter functions on the right.

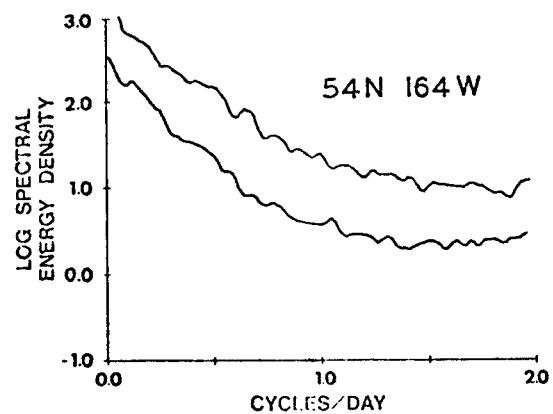
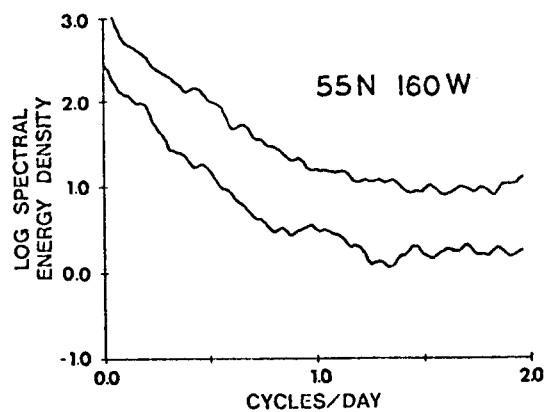
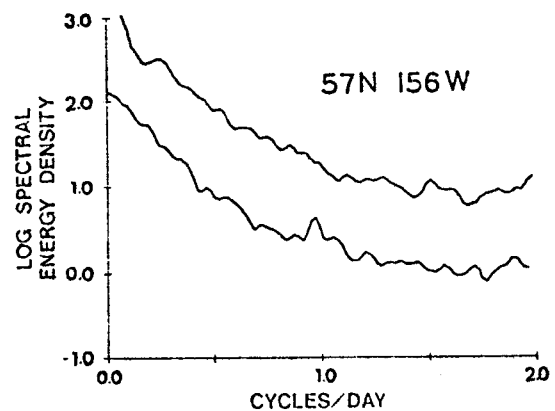
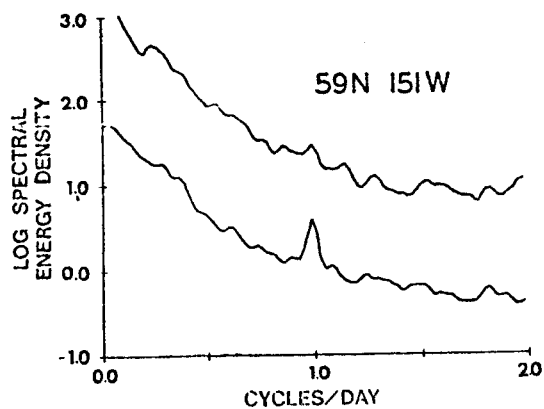
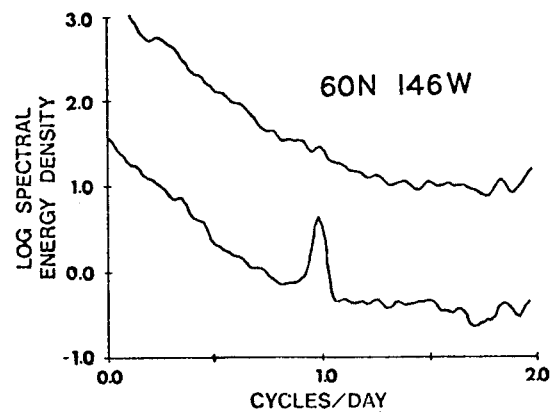
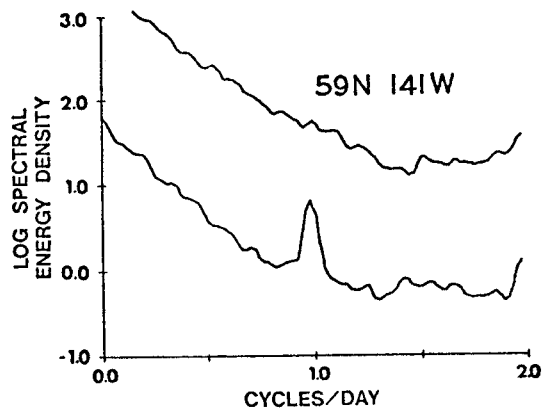
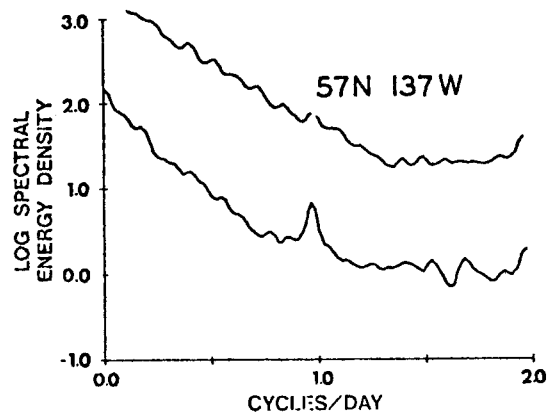
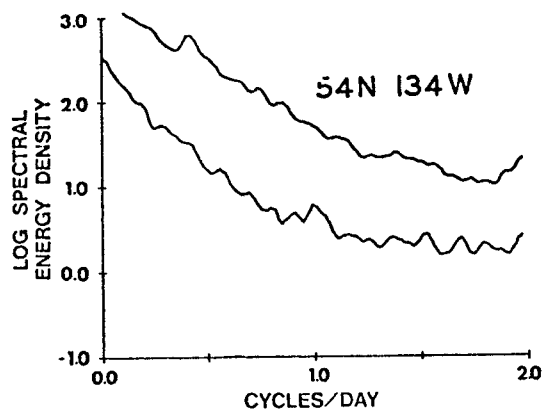


Figure 51 - Power spectra for coastal divergence indices (CDI). Winter and summer spectra at each location are superimposed. Higher energy (upper) trace plots the winter spectrum.

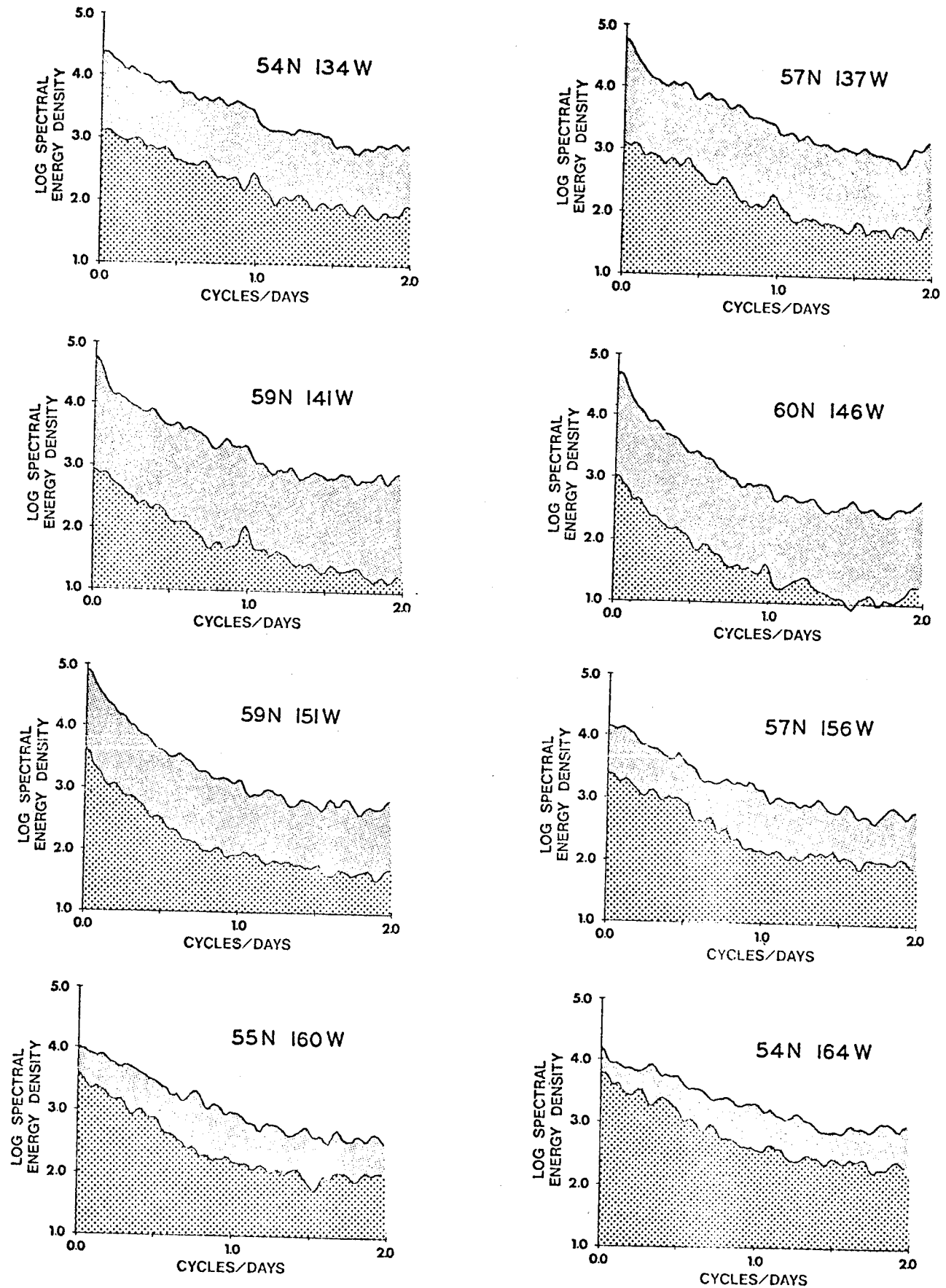


Figure 52 - Power spectra for offshore divergence indices (ODI) at near-coastal locations. Winter and summer spectra at each location are superimposed. Higher energy (upper) trace plots the winter spectrum.

Superimposed are several other features of interest. Considerable energy is spread over the "event scale" of periods of somewhat greater than a day to a week or more. In certain of the series this stands out as a broad hump representing a quasi-periodicity, that is a definite rhythm, albeit somewhat irregular. The only true periodicity is the diurnal fluctuation which stands out as a definite spike in the spring and summer spectra at locations in the northern and eastern gulf. The smaller spike at the semi-diurnal frequency appears merely because the diurnal variation is not perfectly sinusoidal, the morning to afternoon intensification being generally more rapid than the evening to morning relaxation.

Coherence functions for the CDI v.s. the ODI winter series (Fig. 53) indicate maximum coherence at the "event" and longer frequency bands in the "type A" area in the northern and eastern Gulf. Coherence is progressively less toward the southwest. During the summer coherence is minimal except at the diurnal frequency. In general, coherence between the CDI and ODI series at the same location is small compared to, for example, the coherence between series of the same type of index at adjacent locations (Fig. 54). The indication is that the CDI and ODI signals act as semi-independent variables, less so in the fairly well defined "type A" situation of cyclonic winter storms moving through the northern and eastern Gulf, and more so in the Alaska Peninsula area where the various combinations of angle of storm movement in relation to the coast, position of storm center north or south of the coastal boundary, etc., introduces a much larger degree of randomness.

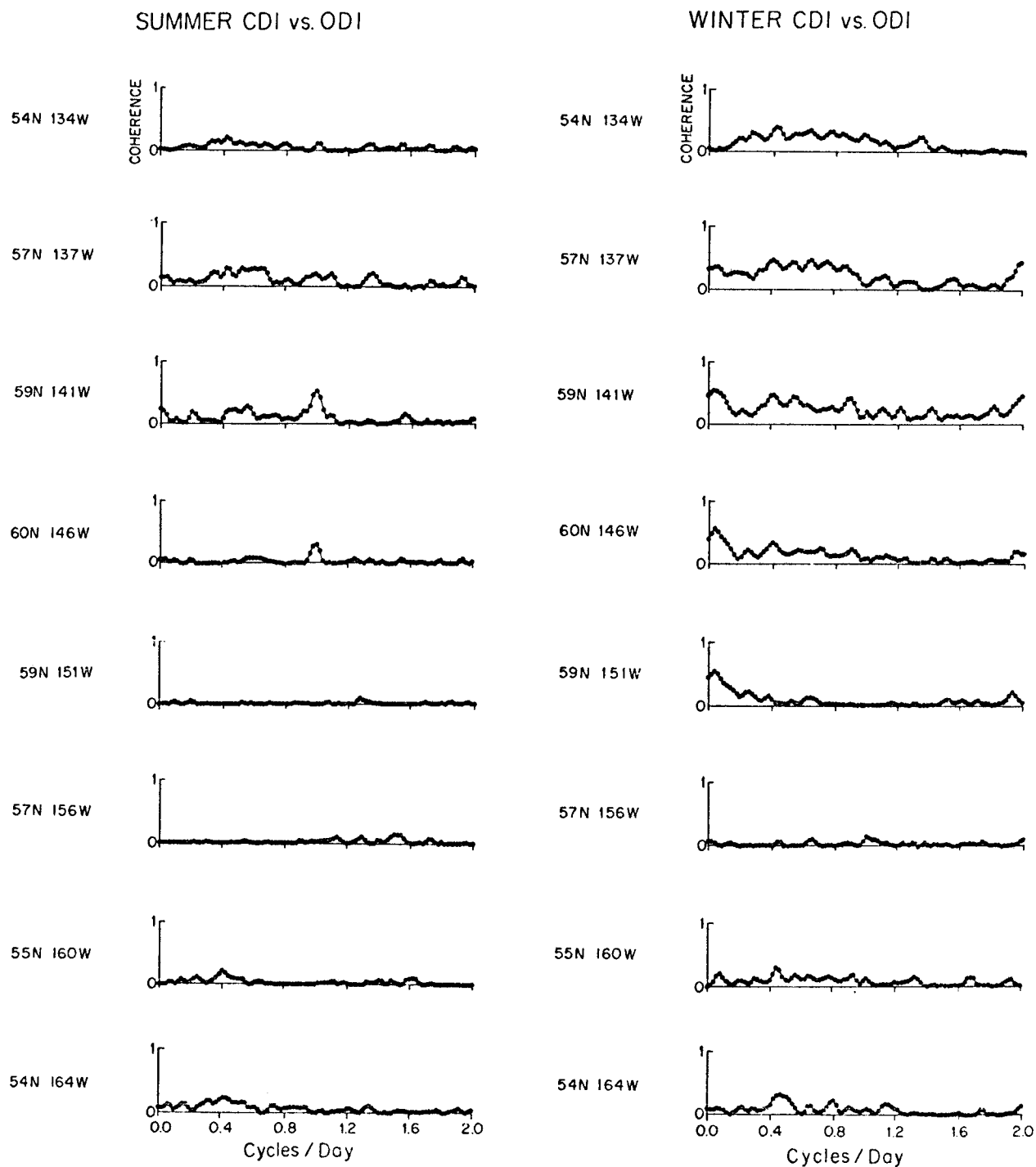


Figure 53 - Coherence functions for coastal divergence indices (CDI) v.s. offshore divergence indices (ODI).

60N 146W vs. 59N 141W

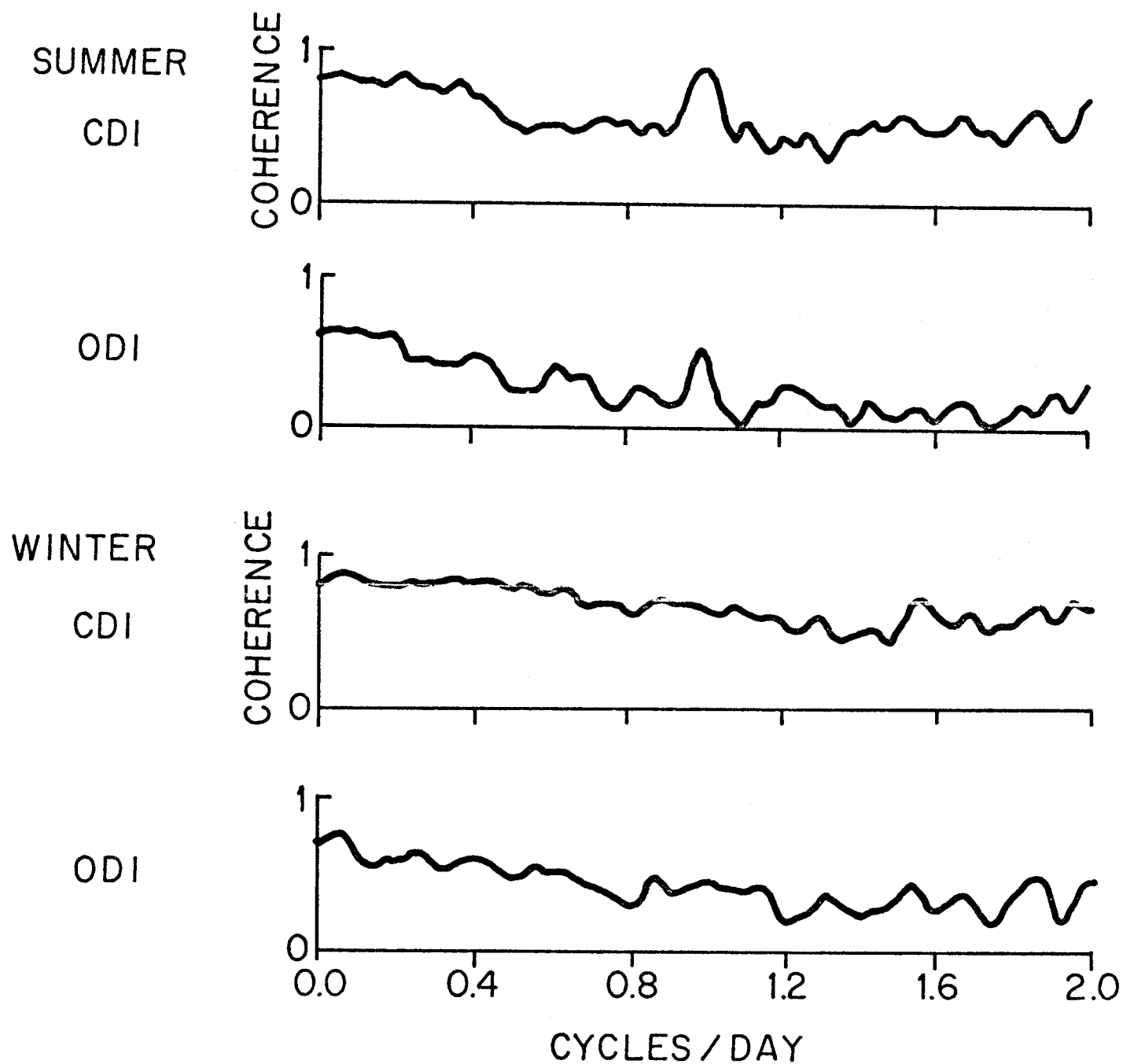


Figure 54 - Coherence functions between index series at adjacent locations: 60N, 146W v.s. 59N, 141W.



## B. Interior of the Gulf

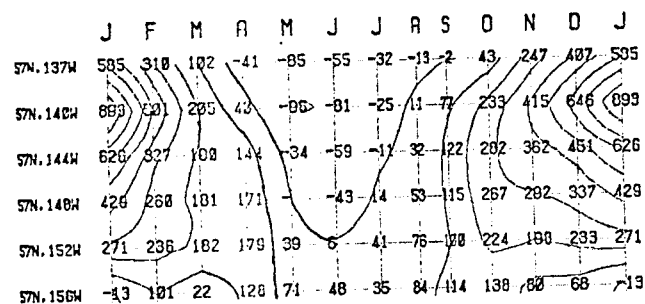
Away from the influence of the coastal boundary the CDI computations are, of course, not applicable; the distribution of surface divergence is indicated by the ODI series. The monthly frequency distributions of ODI series along 57°N (Fig. 55) and along 54°N (Fig. 56) show strongly positive mean ODI values during winter in the eastern portion of the gulf, reaching a maximum at 57N, 140W. This location thus appears as the point of maximum intensity of winter divergence. Intensity decreases from this location in all directions, but least rapidly to the north where the intersection of the lobe of intense divergence with the coast results in the maximum type A offshore divergence - coastal downwelling couple at 59N, 141W, described in the previous section. The mean intensities along 54N are much lower than at 57N.

The maximum mean negative values during the summer are likewise at 57N, 140W. The period of mean summer convergence (negative ODI values) which lasts from May through August along the coast in the northern and eastern Gulf (see Fig. 46) becomes progressively shorter westward along 57N, finally disappearing near 150W longitude. Along 57N mean convergence appears only during May and June at the near coastal location, 54N, 134W (Fig. 57).

The series at 57N, 140W also exhibits the greatest variance (see Fig. 56) during winter of any of the locations studied. Thus this location appears to mark a region of "maximum energy" in the surface divergence field of the Gulf of Alaska, both in the sense of amplitude of the seasonal mean signal and in the "spectral energy" sense of

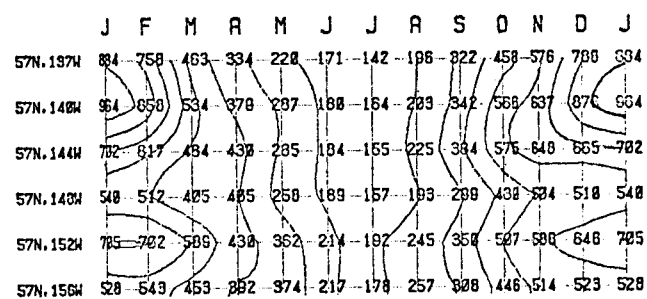
MEAN.

ODI



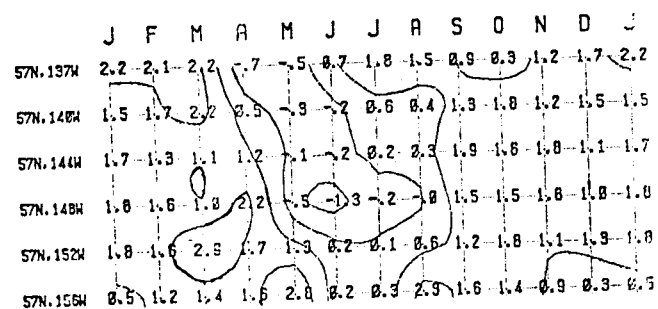
STANDARD DEVIATION

ODI



SKEWNESS.

ODI



KURTOSIS.

ODI

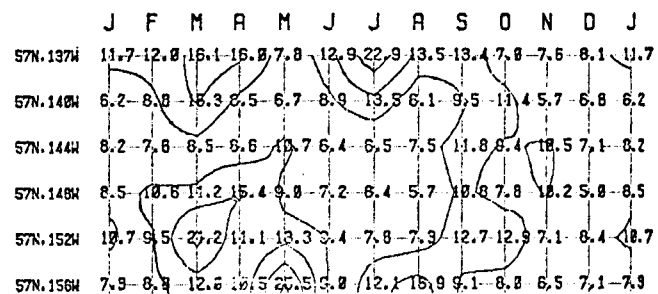


Figure 55 - Moments of the frequency distributions of offshore divergence indices (ODI) grouped by month at the locations along 57N indicated by square symbols in Fig. 41. Mean: units are millimeters per day upward velocity through the bottom of the Ekman layer required to balance the indicated divergence; contour interval is 100. Standard deviation: units and contour interval are as for the mean. Skewness: contour interval is one normalized unit. Kurtosis: contour interval is 5 normalized units.

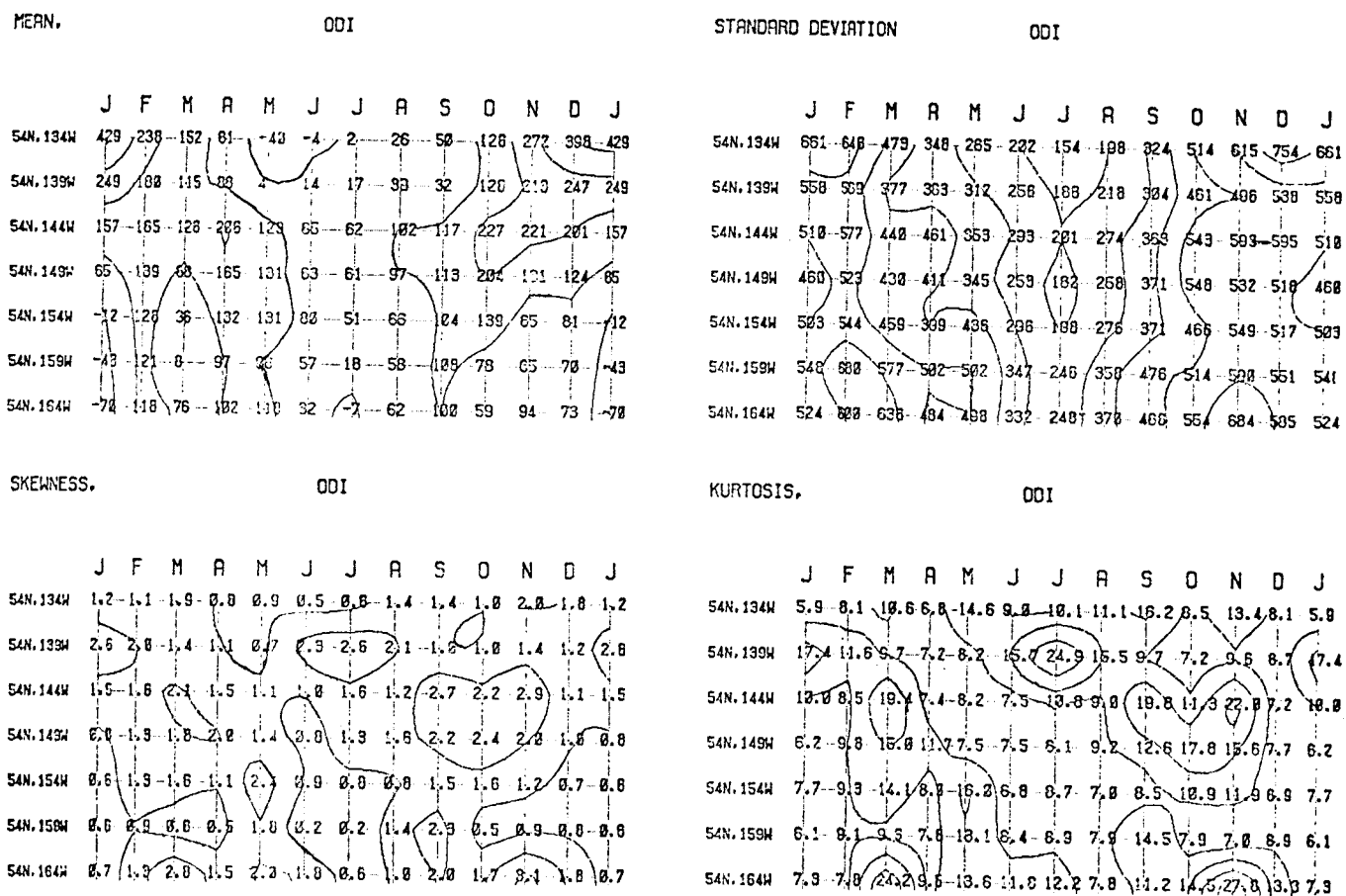


Figure 56 - Moments of the frequency distributions of offshore divergence indices (ODI) grouped by month at the locations along 54N indicated by circle symbols in Fig. 41. Mean: units are millimeters per day upward velocity through the bottom of the Ekman layer required to balance the indicated divergence; contour interval is 100. Standard deviation: units and contour interval are as for the mean. Skewness: contour interval is one normalized unit. Kurtosis: contour interval is 5 normalized units.

extremely rapid and strong pulsations. A lesser maxima in variance at 57N, 152W is apparently connected to the maxima along the coast at 59N, 151W (Fig. 46).

The skewness is negative along 54N latitude (Fig. 56) and, except for a limited period during the summer convergence season, along 57N latitude (see Fig. 55). Extreme events are usually divergent. The kurtosis as before, indicates major importance of rather infrequent, very intense events.

Power spectra for summer and winter ODI series at locations along 57N (Fig. 57) and at locations along 54N (Fig. 58) indicate that winter energy tends to be greatest to the north and east and summer energy is greatest to the south and west. The spike indicating the diurnal periodicity during summer is most prominent near the point of "maximum energy" at 57N, 140W. To the west and south the diurnal spike disappears.

Examples of cross correlations between the "maximum energy" locations at 57N, 140W and several surrounding locations (Fig. 59) indicate that correlation is highest at zero lag between 57N, 140W and the point of maximum winter "type A" coastal situation at 59N, 141W. A suggestion of higher correlation at positive lags between 57N, 140W and 57N, 137W and at negative lags between 57N, 140W and 57N, 144W illustrates the general eastward progression of the signal. Correlation with a location to the south, 54N, 139W, is considerably lower and is highest at a negative lag of one 6-hour period, even though the southern location is one degree further east. This indicates the northward progression of the signal which added to the eastward progression matches the general northeastward trend of the storm tracks. Correlation with the point at

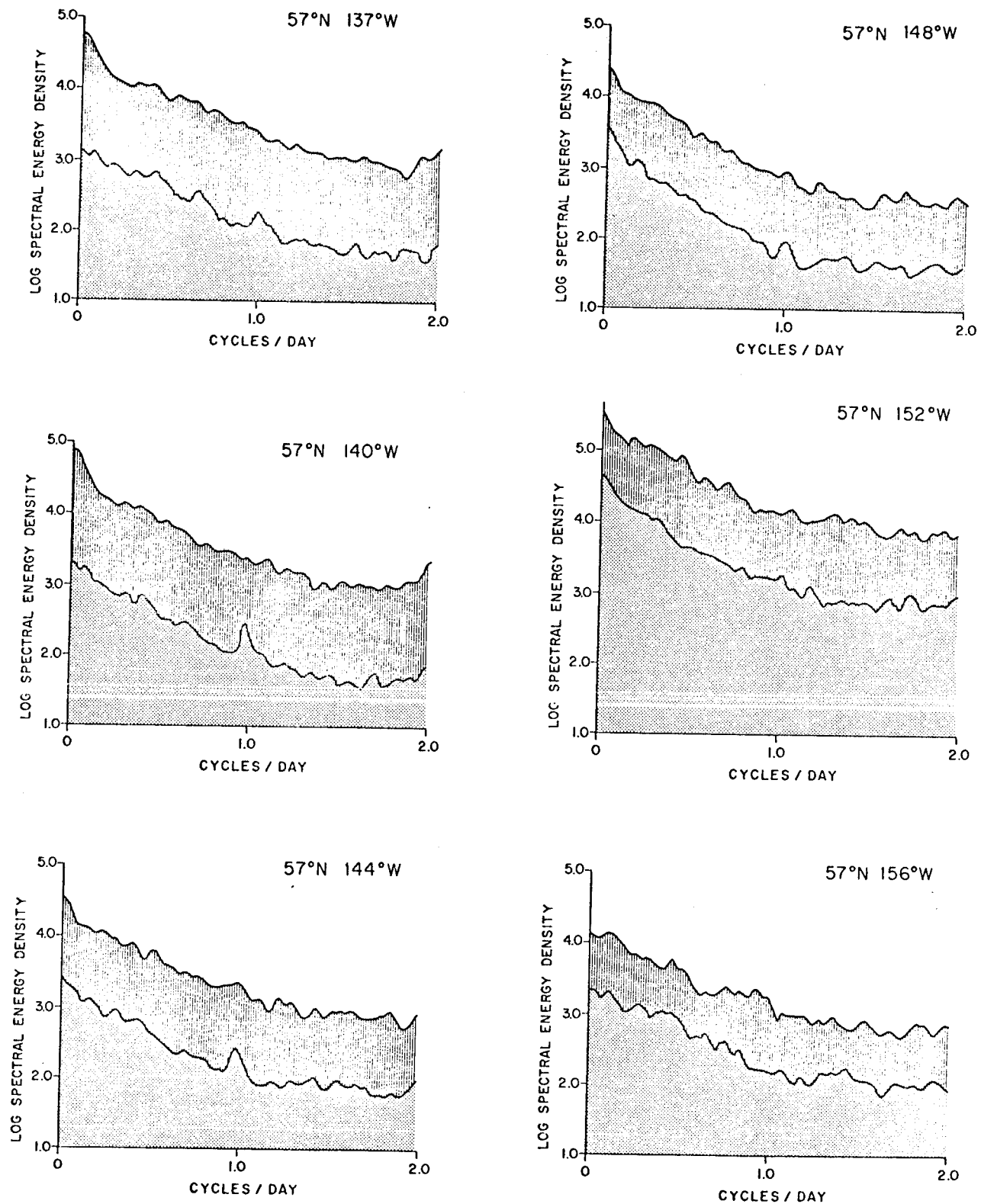


Figure 57 - Power spectra for offshore divergence indices (ODI) at locations along 57N latitude (locations indicated by squares in Fig. 41.) Winter and summer spectra at each location are superimposed. Higher energy (upper) trace plots the winter spectrum.

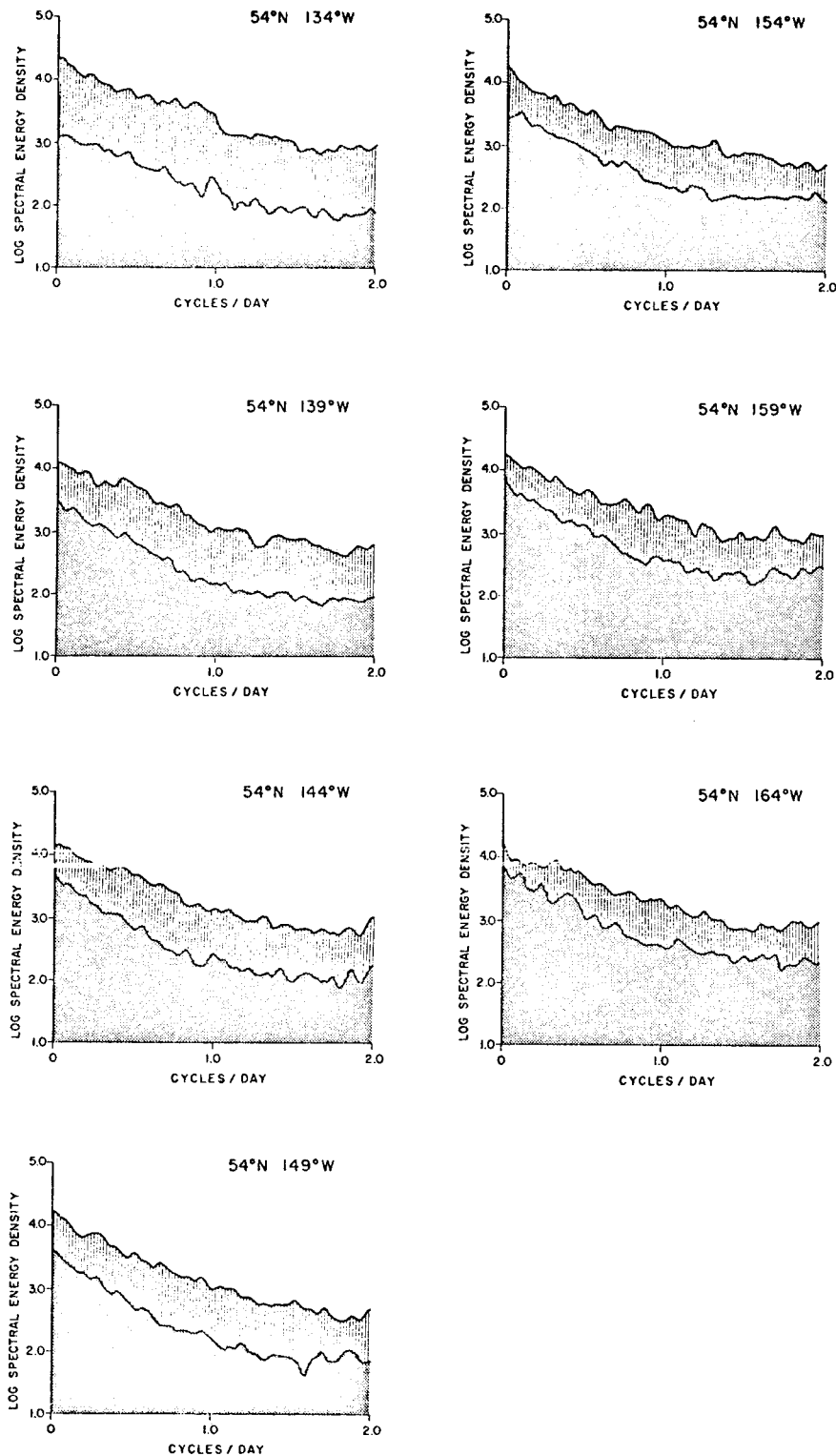


Figure 58 - Power spectra for offshore divergence indices (ODI) at locations along 54N latitude (locations indicated by circles in Fig. 41.) Winter and summer spectra at each location are superimposed. Higher energy (upper) trace plots the winter spectrum.

CROSS CORRELATION

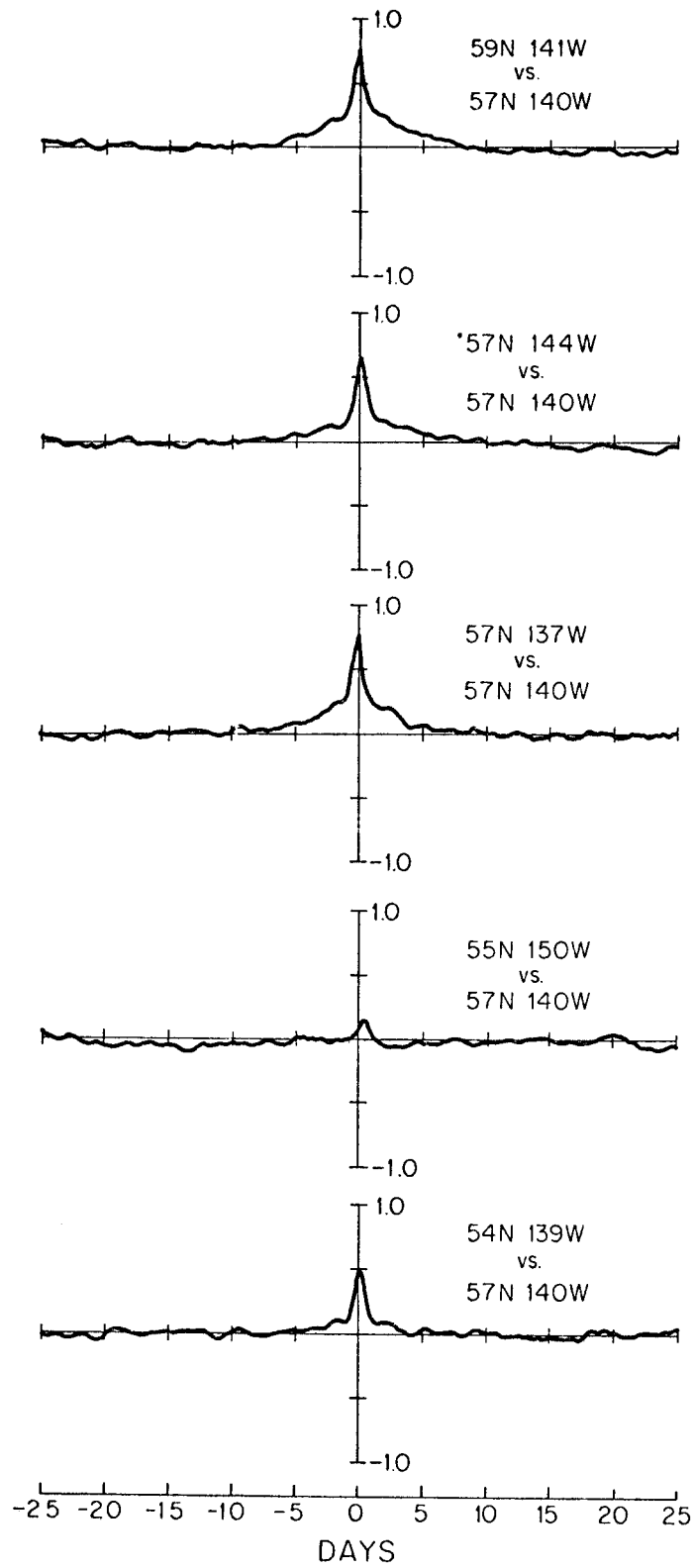


Figure 59 - Cross correlation functions for the winter ODI series at 57N, 140W v.s. winter ODI series at several surrounding locations.

55N, 150W is quite low, reaching its greatest value at negative lags of two 6-hour periods in the winter and three six hour periods in the summer; the progression is slower in the summer than in the winter.

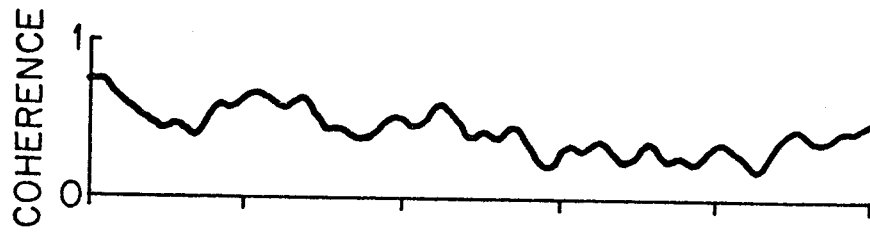
Coherence functions corresponding to the cross-correlation functions of Fig. 59 indicate that the signal at 59N, 141W appears strongly related to that at 57N, 140W (Fig. 60). The adjacent points along 57N are likewise quite strongly related, particularly in the "event" frequency range. However, the coherence with the location to the south, 54N, 139W, is considerably less. Coherence with the signal at 55N, 150W, although on the line of general storm progression, is so low that it is not possible to prove statistically the signals are even related. This indicates considerable modification of the storm systems as they move across the gulf, consistent with its description as a region of strong atmospheric cyclogenesis.

#### C. Conditions - 1973, 1974 and 1975

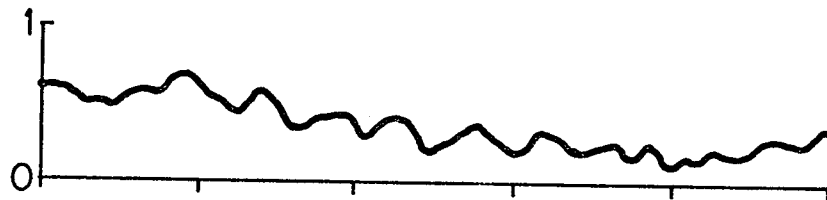
The monthly mean CDI and ODI values at the near-coastal locations and the monthly mean ODI values at locations along 57N for the individual years 1973, 1974, and 1975 (Fig. 61) show distributions which are rather complicated in detail. However, it may be useful to delineate certain major features which may have had important effects on the ocean environment during these most recent years of increased field studies. In early 1973, maximum magnitudes of both the ODI and CDI indices appeared during January at 57N, 151W; apparently, the maximum strength of the winter "type A" couple was located in the northwestern Gulf, rather than in its "usual" position in the northeastern Gulf as indicated by the



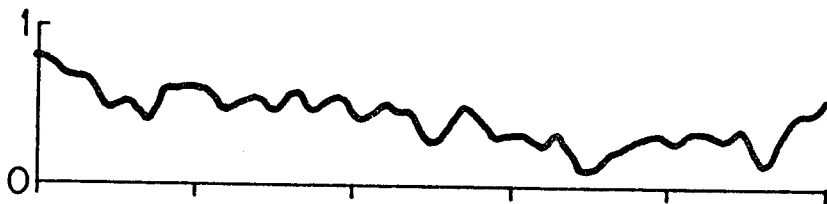
59N 141W  
vs.  
57N 140W



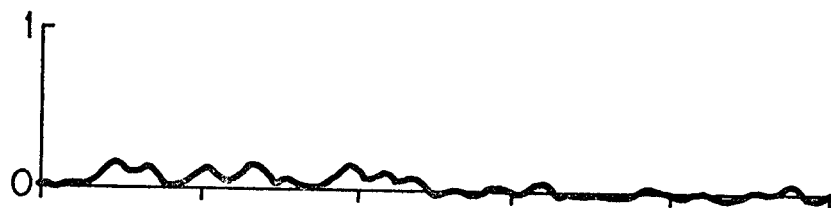
57N 144W  
vs.  
57N 140W



57N 137W  
vs.  
57N 140W



55N 150W  
vs.  
57N 140W



54N 139W  
vs.  
57N 140W

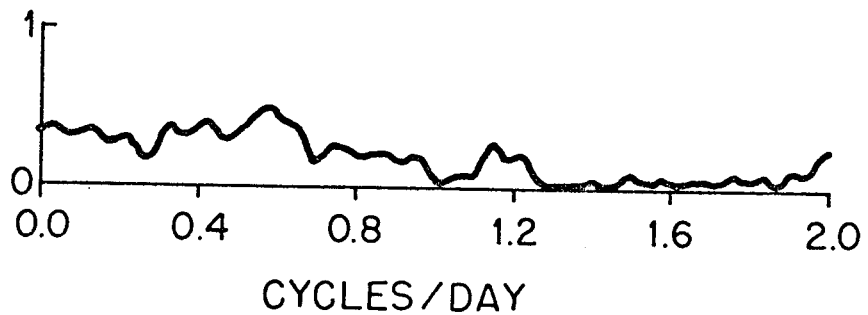


Figure 60 - Coherence functions for the winter ODI series at 57N, 140W v.s. winter ODI series at several surrounding locations.

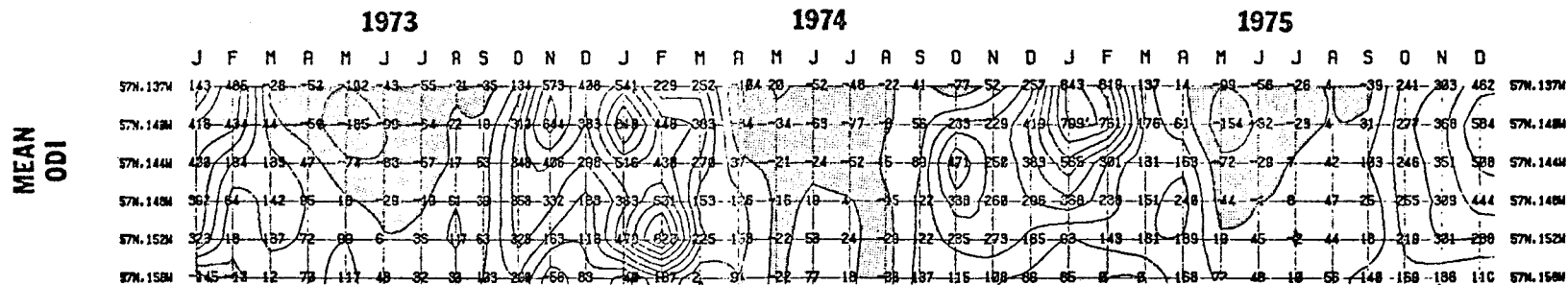
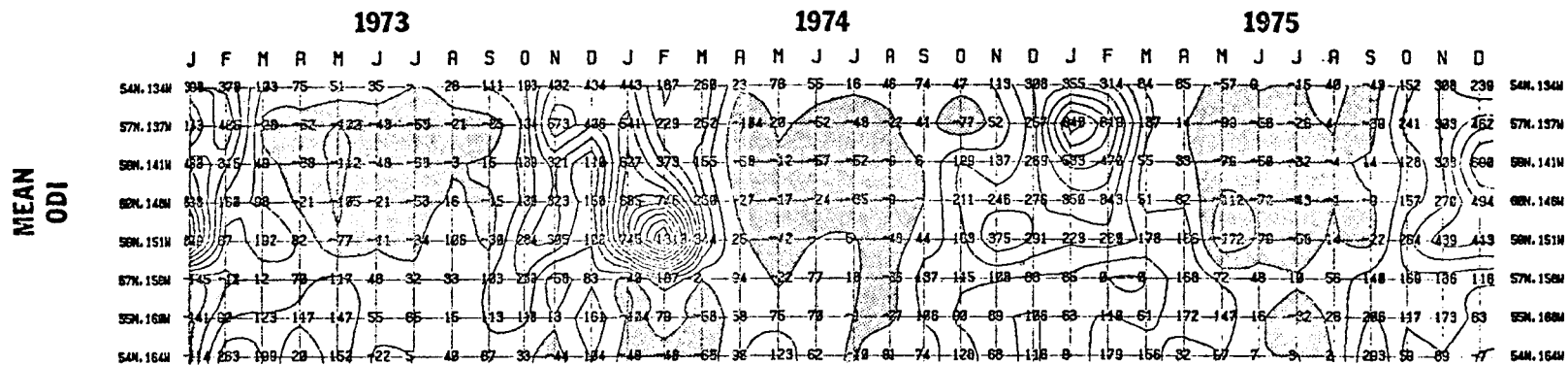
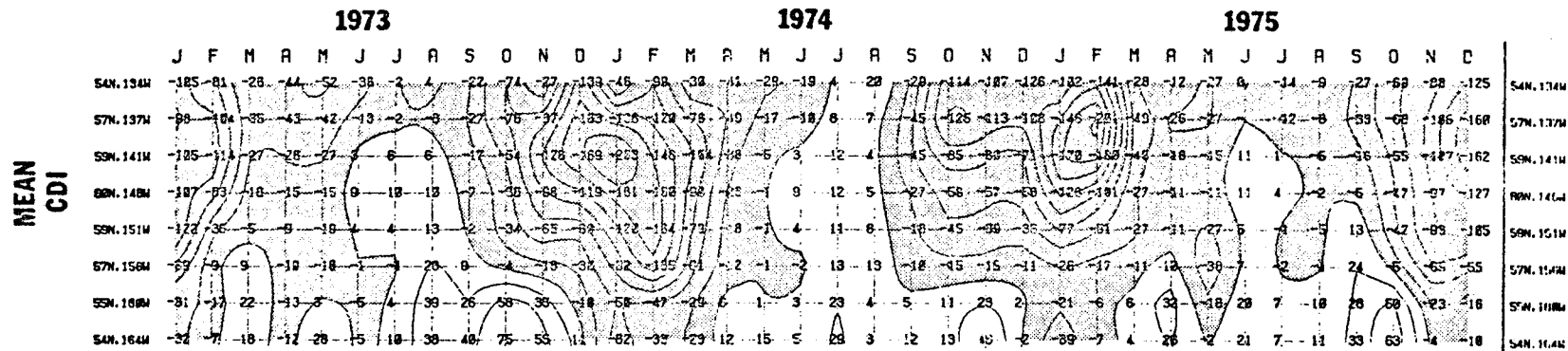


Figure 61 - Monthly means of index series for the years 1973, 1974, and 1975. Top figure: CDI series at near-coastal locations; units are cubic meters per second transported off each 100-meter width of coast. Middle figure: ODI series at near coastal locations; units are millimeters per day upward velocity through the bottom of the Ekman layer required to balance the indicated divergence. Bottom figure: ODI series at locations along 57N latitude; units, etc., are same as for middle figure.

nine-year composite mean monthly distributions (see Figs. 45 and 46). Lower than normal magnitudes of both types of indices during February and March throughout the northern Gulf point to an unusually rapid relaxation of the winter situation. For example, an early transition to a "type C" couple is indicated off the Alaskan Peninsula during March, where normally the transition occurs in April (Table 2). The trend toward less positive than normal ODI values in the northern Gulf continued through the spring to considerably stronger than normal negative values in May, representing quite energetic downward pumping in the offshore area, particularly in the northeastern Gulf. The last quarter of 1973 featured a strong predominance of coastal upwelling along the outer Alaskan Peninsula.

During the first quarter of 1974, stronger than normal convergence (negative CDI values) is indicated along the coast of the Gulf of Alaska, except in the extreme east. Maximum offshore divergence (positive ODI values) appeared, as in the previous year, in the northwestern Gulf. An extremely large mean ODI value was computed for February at 59N, 151W. Actually, anomalously large values appeared during all of the first three months of 1974 at both 59N, 151W, and 60N, 146W. The values at 59N, 141W, the normal maximum along the coast, although much smaller than those further east, were near the 9-year mean values for that location. The result is an extremely strong "type A" couple for the northern Gulf during early 1974. The implication is that dramatically increased baroclinicity in the ocean structure may have had an important effect on the dynamics of the area for some period to follow.

During the spring and summer of 1974, the indices tended to have values near the seasonal means, but by fall a situation of weaker than normal coastal convergence (smaller negative CDI values) seems to have set it. This situation generally persisted through the whole winter over much of the Gulf and was coupled with generally weaker than normal divergence offshore during December and January. An exception was the eastern Gulf where a reasonably strong "type A" couple is indicated for January and February. In total, the winter of 1974-75 appears to have been one of less energetic "type A" pumping than seems to be normal. Certainly the situation contrasts highly with the very energetic situation of the previous winter.

## VII. SUMMARY AND CONCLUSIONS

Our knowledge of the physical oceanography of the Gulf of Alaska is quite inadequate to forecast flow. This stems largely from the lack of a persistent, challenging oceanographic program that permits progressive advances based on acquired knowledge. The focus of attention has been not only limited, but intermittent, however, this has not been due to a lack of interest on the part of the oceanographer, rather because of lack of funds, equipment, and adequate theory. Thus, a normal advance from the descriptive phases of presenting observed and steady-state conditions to the analytical phases of understanding processes and forecasting various time-dependent phenomena has not taken place.

There have been several periods of rather extensive research activity: in the late 19th century by the U.S. Bureau of Fisheries, the late 1920's and early 1930's by the International<sup>6/</sup> North Pacific Fisheries Commission, and in recent years by the Institute of Marine Science of the University of Alaska<sup>6/</sup>. The interval between periods of activity has gradually decreased from about 50 years to the order of 5 years or less, and hopefully the instigation of the OCSEAP studies will result in the continuing research effort required to obtain adequate knowledge concerning flow.

The dominant physical phenomena in the Gulf of Alaska is the Aleutian low pressure system whose center moves anti-cyclonically out of the northern Bering Sea in early autumn, crosses the Alaska Peninsula and attains a mean position of about 55°N, 155°W in the gulf in late fall and early winter. During winter it moves southwestward to about

<sup>6/</sup> See Rosenberg (1972).

50°N, 175°E before returning northward into the western Bering Sea in late winter and early spring. The cyclogenesis and cold air advection in the gulf associated with the mean position of the low pressure center in fall and winter determines the extent and intensity of winter overturn and vertical divergence, as well as, the containment of precipitation, in the form of ice and snow along the coast and in the snowshed ringing the gulf which determines to a great extent the amount of dilution in coastal waters in spring and summer. Station data are marginally adequate in period 1955-62 to show considerable differences between the upper layer temperature distributions in 1956 and 1958, and between the surface salinity distributions in 1957 and 1958, but these are certainly not extreme conditions. Approximate ranges for temperatures in coastal waters are -1.8 to 18°C, and in the central part of the gulf, 1 to 14°C; approximate ranges of salinity in coastal waters are several parts per thousand to 32.6 ‰ and in the central part of the gulf, 32.2 to 33.0 ‰. At depth, below the effects of seasonal influences, conditions are somewhat in a steady-state condition, this makes it difficult to trace anomalous intrusions, or percentage of flow attributed to various sources without extensive data, but there is evidence in the temperature fields that significant changes can occur over periods of several years and certainly longer trends must also exist. Temperature data in the gulf are considered too fragmentary to show the rather consistent 2-3 year variations of  $\pm 1-2^{\circ}\text{C}$  detected in the central and western parts of the Pacific Ocean by Favorite and McLain (1973).

In regard to surface flow, drift bottle studies have shown that the source of surface flow into the gulf is not from the Kuroshio but largely from the Oyashio and its extension the Subarctic Current, and there is a well documented coastal flow northward along the west coasts of the United States and Canada that also extends into the gulf. Studies have shown that the nature of the separation of the Subarctic Current off the coast is quite variable and complex and, thus, the effect of the northern branch of this flow, which penetrates into the gulf, is equally variable and complex. There is an indisputable onshore component of surface flow around the gulf. But it is not known whether the drifting objects are transported around the gulf largely seaward of the continental shelf and only when they are carried out of the oceanic flow and over the shelf are they trapped in a coastal regime and carried directly ashore, or whether, in spite of tidal currents and increased frictional effects, there is continuity in northward flow in offshore and onshore areas that results in a gradual dispersal of floating objects on the coast as the flow sweeps around the gulf. Nevertheless, it is apparent that floating objects released over the continental shelf at the eastern part of the gulf drift into coastal embayments such as Prince William Sound and Cook Inlet, and move southwestward on either side of Kodiak Island. Further, there is evidence that floating objects in the northern part of the gulf have a potential for wide dispersal: northward into Bering Sea, westward out along the Aleutian Islands, eastward in the Subarctic Current to the coast of Southeastern Alaska, the west

coasts of British Columbia, Washington, Oregon and California, and westward again to the central Pacific Islands and the Asian coast.

Geostrophic currents are somewhat of a dilemma. First, closely spaced data suggest that the broad sweep of cyclonic flow around the gulf, generally shown in atlases or summaries of widely spaced data, is actually a highly turbulent regime composed of eddies of various dimensions. There is a frequent suggestion of a large perturbation at the eastern side of the gulf whose dimensions and configuration do not suggest a shelf wave phenomenon, but rather the possibility that at times some of the northward flow funneling into the eastern side of the gulf is unable to move westward across the head of the gulf and is found to turn back on itself. Second, although geostrophic currents clearly reflect the area of divergence, the Ridge Domain, a dominant oceanographic feature in the gulf, there are no direct measurements that permit ascertaining to what extent this feature is governed by (1) Ekman transport (2) a normal internal readjustment of mass between two opposing flows, and (3) a vertical movement of northward flowing deep water, caused by the effect of the land barrier imposed by the gulf. Third, the high velocity cyclonic flow at the edge of the continental shelf is also a dominant feature and an inshore countercurrent is usually detected in geostrophic computations. At this time it is not clear whether this is an aspirative phenomenon not uncommon under such circumstances, whether it is merely an error caused by inadequacies in this method in the presence of physical boundaries, or whether it is largely the effect of eddies or shelf waves along the edge of the



continental shelf. Finally, there is the large variability in transport computed from wind-stress estimates in one instance (1960) a 50% increase in mean flow, and a 100% increase over low flows, but there is no consistent evidence of winter intensification in flow expected as a result of increased wind-stress during that period. However, increases in sea levels at coastal stations in winter suggest that there is at least a barotropic response. Thus, it would appear that winter intensification of flow does occur but the pulses of winter wind-stress are of too short a duration for the distribution of mass to adjust to the actual flow regime; however, over decades and centuries the calculated geostrophic regime appears to have adjusted to an integrated, quasi-steady state between the effects of winter intensification and summer relaxation. Thus, there may be an inherent under-estimation of actual flow in summer when using the wind-stress transport method. The long data record of sea surface pressures provides a qualitative indication of transport variability. Spectral energy densities indicate a dominant annual period and a suggestion of an approximate 3-year period. The latter is evident primarily in the decade 1950-59 and does not appear to be a dependable forecasting index. Although monthly transports occasionally show totally unrealistic values, quarterly means and 12-month running means indicate a relatively ordered system (within limits) with no apparent indices to forecast anomalous events.

Of course, wind-stress estimates are merely that, estimates, and so are the outputs of model studies whose results are largely

dependent on wind-stress inputs. It should also be obvious that fluctuations in conditions in the gulf are also influenced by various external and internal forces throughout the Pacific Ocean. Nevertheless, considerable advances in our knowledge of the physical oceanography of the gulf will come from short-period monitoring of actual conditions and extensive direct current measurements, not only across the shelf, but also across the slope and in the Ridge Domain. OCSEAP studies are beginning to provide such data.

Studies of surface divergence indices show the extreme variability in direction and intensity of wind-stress in time and space around the gulf, as well as insight into mechanisms that essentially pump water in contact with the shelf shoreward in summer and seaward in winter. The eastern side of the gulf has been shown to be the most energetic in regard to these processes and considerable variability is apparent. An attractive feature of the ODI and CDI computations is their basis in data fields that are routinely prepared and made available in real-time by meteorological agencies; in fact the fields are forecast over periods up to 72 hours or more. Thus, there is a potential for a very inexpensive, real-time monitoring of conditions affecting the flow field in the gulf. Hopefully the OCSEAP studies now underway will help to establish the quantitative linkages required to translate such information into a practical tool for marine environmental management.

LITERATURE CITED

- Bakun, Andrew  
1973. Coastal upwelling indices, west coast of North America. U.S. Dep. Commer. Natl. Oceanic Atmos. Admin., Tech. Rep. NMFS SSRF-671. 103 p.
- Bakun, Andrew  
1975. Daily and weekly upwelling indices, west coast of North America, 1967-73. U.S. Dep. Commer., Natl. Oceanic Atmos. Admin., Tech. Rep. NMFS SSRF-693. 114 p.
- Barkley, Richard A.  
1968. Oceanographic atlas of the Pacific Ocean. Univ. Hawaii Press, Honolulu. 20 p., 156 figs.
- Bennett, E. B.  
1959. Some oceanographic features of the northeast Pacific Ocean during August 1955. J. Fish. Res. Bd. Canada 16(5):565-633.
- Bogdanov, K. T.  
1961. (Water circulation in the Gulf of Alaska and its seasonal variability). Okeanologiya 1(5):815-824. In Russian. (Transl. in Deep-Sea Res., 1963, 10(4):479-487.)
- Burt, Wayne V., and Bruce Wyatt.  
1964. Drift bottle observations of the Davidson current off Oregon, p. 156-165. In: Kozo Yoshida (ed.), Studies on oceanography. Univ. Tokyo Press.
- Dall, W. H.  
1879. Meteorology, Appendix 1. In: Pacific Coast Pilot, coasts and island of Alaska, 2nd ser. 375 p. Gov. Print. Off., Washington, D.C.
- Dall, W. H.  
1882. Report on the currents and temperatures of Bering Sea and the adjacent waters. U.S. Coast and Geodetic Survey, Report 1880, app. 16:297-340, pl. 80.
- Dall, W. H.  
1899. The mollusk fauna of the Pribilof Islands. In: U.S. Treasury Dep. Committee on Fur-seal Invest., The fur seals and sea-islands of the North Pacific Ocean, pt. 3, p. 539-545, chart. Washington, Govt. Print. Off.
- Dodimead, A. J., F. Favorite, and T. Hirano  
1963. Salmon of the North Pacific Ocean--Part II. Review of oceanography of the Subarctic Pacific Region. Int. North Pac. Fish. Comm., Bull. 13. 195 p.

- Dodimead, A. J., and H. J. Hollister.  
 1962. Canadian drift bottle releases in the North Pacific Ocean. Fish. Res. Board Can., Manuscr. Rep. Ser. (Oceanogr. Limnol.) 141. 64 p. + 44 figs. (Processed.)
- Doe, L. A. E.  
 1955. Offshore waters of the Canadian Pacific coast. J. Fish. Res. Board Can. 12(1):1-34.
- Favorite, Felix.  
 1964. Drift bottle experiments in the northern North Pacific Ocean, 1962-1964. J. Oceanogr. Soc. Japan 20(4):160-167.
- Favorite, Felix.  
 1974. On flow into Bering Sea through Aleutian Islands passes p. 3-37. In: D. W. Hood and E. J. Kelley (eds.), Oceanography of the Bering Sea. Inst. Mar. Sci. Occas. Publ. No. 2, Univ. Alaska, Fairbanks.
- Favorite, Felix.  
 1975. The physical environment of biological systems in the Gulf of Alaska. Proceedings, Arctic Institute of North America symposium on science and natural resources in the Gulf of Alaska. Oct. 16-17, 1975, Anchorage (In Press).
- Favorite, F., A. J. Dodimead, and K. Nasu.  
 1976. Oceanography of the Subarctic Pacific Region 1960-72. Int. North Pac. Fish. Comm., Bull. 33 (In press.).
- Favorite, F., and W. J. Ingraham, Jr.  
 (1976 a) On flow in the northwestern Gulf of Alaska May 1972. J. Oceanogr. Soc. Japan.
- Favorite, F., and W. J. Ingraham, Jr.  
 (1976 b). Sunspot activity and oceanic conditions in the northeastern North Pacific Ocean. NMFS Status of the Environment Report, 1975 (in preparation).
- Favorite, Felix, and Douglas R. McLain.  
 1973. Coherence in transpacific movements of positive and negative anomalies of sea surface temperature, 1953-60. Nature (London) 244(5412): 139-143.
- Filatova, Z. A. (ed.).  
 1973. Kompleksnye issledovaniya materikovogo sklona v raione zaliva Alyaska (Multidisciplinary investigations of the continental slope in the Gulf of Alaska area). IV. Inst. Okeanol. 91. 260 p. (Transl., Fish. Res. Board Can., 1974, Transl. Ser. 3204.)
- Fisk, Donald M.  
 1971. Recoveries from 1964 through 1968 of drift bottles released from a merchant vessel, S. S. Java Mail, en route Seattle to Yokohama, October 1964. Pac. Sci. 25(2):171-177.

- Fofonoff, N. P.  
1962. Machine computations of mass transport in the North Pacific Ocean. J. Fish. Res. Board Can. 19(6): 1121-1141.
- Fofonoff, N. P., and S. Tobata.  
1966. Variability of oceanographic conditions between Ocean Station "P" and Swiftsure Bank off the Pacific coast of Canada. J. Fish. Res. Board Can. 23(6): 825-868.
- Fleming, R. H.  
1955. Review of oceanography of the northern Pacific. Int. North Pac. Fish. Comm., Bull. 2. 43 p.
- Fomin, L. M.  
1964. The dynamic method in oceanography. Elsevier Publ. Co., New York. 212 p.
- Galt, J. A.  
1973. A numerical investigation of Arctic Ocean dynamics. J. Phys. Oceanog. 3(4): 379-396.
- Giovando, L. F., and Margaret K. Robinson.  
1965. Characteristics of the surface layer in the northeast Pacific Ocean. Fish. Res. Board Can., Manuscr. Rep. Ser. (Oceanogr. Limnol.) 205. 13 p., 2 tables, 28 figs.
- Holl, M. M. and B. R. Mendenhall.  
1972. Fields by information blending, sea-level pressure version. (U.S.) Fleet Numer. Weather Central, Monterey, Calif., FNWC Tech. Note 72-2. 66 p.
- Ingraham, W. James, Jr., and F. Favorite.  
1968. The Alaskan Stream south of Adak Island. Deep-Sea Res. 15(4): 493-496.
- Ingraham, W. James, Jr., and James R. Hastings.  
1974. Seabed drifters used to study bottom currents off Kodiak Island. Mar. Fish. Rev. 36(8): 39-41.
- Jacobs, Woodrow C.  
1939. Sea level departures on the California coast as related to the dynamics of the atmosphere over the North Pacific Ocean. J. Mar. Res. 2: 181-193.
- Jacobs, Woodrow C.  
1951. The energy exchange between sea and atmosphere and some of its consequences. Bull. Scripps Inst. Oceanogr. 6: 27-122.
- Klein, W. H.  
1957. Principal tracks and mean frequencies of cyclones and anti-cyclones in the northern hemisphere. U.S. Dep. Commer., Weather Bur. Res. Paper 40. 60 p.

- LaViolette, Paul E., and Sandra E. Seim.  
 1969. Monthly charts mean minimum and maximum sea surface temperature of the North Pacific Ocean. (U.S.) Naval Oceanogr. Office, Spec. Publ. 123. 58 p.
- McEwen, George F., Thomas G. Thompson, and Richard Van Cleve.  
 1930. Hydrographic sections and calculated currents in the Gulf of Alaska, 1927 to 1928. Rep. Int. Fish. Comm. 4. 36 p.
- Moiseev, P. A. (ed.)  
 1963-1970. Sovetskie rybokhozyaistvennye issledovaniya v severo-vostochnoi chasti Tikhogo okeana (Soviet fisheries investigations in the northeastern Pacific). In 5 parts. Pt. 1 - Tr. Vses. Nauchno-issled. Inst. Morsk. Rybn. Khoz. Okeanogr. (VNIRO) 48 (also Isv. Tikhookean. Nauchnoissled. Inst. Morsk. Rybn. Khoz. Okeanogr. (TINRO)50), 1963, 316 p.; Pt. 2 - Tr. VNIRO 49 (Izv. TINRO 51), 1964, 272 p; Pt. 3-Tr. VNIRO 53 (Izv. TINRO 52), 1964, 341 p.; Pt. 4- Tr. VNIRO 58 (Izv. TINRO 53), 1965, 345 p.; Pt. 5- Tr. VNIRO 70 (Izv. TINRO 72), 1970, 454 p. (Complete transl. of all 5 parts avail. Natl. Tech. Inf. Serv., Springfield, Va.--Pt. 1, 1968, 333 p., TT 67-51203; Pt. 2, 1968, 289 p., TT 67-51204; Pt. 3, 1968, 338 p., TT 67-51205; Pt. 4, 1968, 375 p., TT 67-51206; Pt. 5, 1972, 462 p., TT 71-50127.)
- Muench, Robin D. and C. Michael Schmidt.  
 1975. Variations in the hydrographic structure of Prince William Sound. Inst. Mar. Sci. Rep. R75-1. Univ. Alaska, Anchorage. 135 p.
- Muromtsev, A. M.  
 1958. Osnovnye cherty gidrologii Tikhogo okeana (Principal hydrological features of the Pacific Ocean). Gidrometeorol. Izd., Leningrad. 631 p.; App. 2, Atlas of vertical profiles and maps indicating temperature, salinity, density and oxygen content. 124 p. (Transl. 1963, Natl. Tech. Inf. Serv., Springfield, Va., TT 63-11065.)
- Nelson, C. S.  
 1974. Wind stress climatology off the west coast of North America (abst) (0-2). AGU Fall Annu. Meet. EOS, Trans. Am. Geophys. Union 56(12): 1132.
- Pattullo, June G.  
 1960. Seasonal variation in sea level in the Pacific Ocean during the International Geophysical Year, 1957-1958. J. Mar. Res. 18: 168-184.
- Pattullo, June, Walter Munk, Roger Revelle and Elizabeth Strong.  
 1955. The seasonal oscillation in sea level. J. Mar. Res. 14: 88-156.

- Plakhotnik, A. F.  
 1962. *Gidrologiya severo-vostochnoi chasti Tikhogo Okeana (obzor literaturnykh istochnikov)*. (Hydrology of the northeastern Pacific Ocean - review of literature sources). *Tr. Vses. Nauchn.-issled. Inst. Morsk. Rybn. Khoz. Okeanogr.* 46: 190-201.
- Reid, J. L., and A. W. Mantyla.  
 1975. On the seasonal variation of sea elevations along the coast of the northern North Pacific Ocean. *AGU Fall Annu. Meet., Trans. Am. Geophys. Union* 56(12): 1009.
- Reid, Joseph L., Jr., Gunnar I. Roden, and John G. Wyllie.  
 1958. Studies of the California Current system. *Prog. Rep. Calif. Coop. Oceanic Fish. Invest.*, 1 July 1956 - 1 Jan. 1958: 28-56.
- Robinson, Margaret K.  
 1957. Sea temperature in the Gulf of Alaska and in the northeast Pacific Ocean, 1941-1952. *Bull. Scripps Inst. Oceanogr.* 7(1): 1-98, 61 figs.
- Robinson, Margaret K., and Roger A. Bauer.  
 1971. Atlas of monthly mean surface and subsurface temperature and depth of the top of the thermocline, North Pacific Ocean. (U.S.) *Fleet Numer. Weather Central, Monterey, Calif.* 24 p. + 72 figs. (Processed.)
- Roden, Gunnar I.  
 1960. On the nonseasonal variations in sea level along west coast of North America. *J. Geophys. Res.* 65: 2809-2826.
- Roden, Gunnar I.  
 1969. Winter circulation in the Gulf of Alaska. *J. Geophys. Res.* 74(18): 4523-4534.
- Rosenberg, Donald H. (ed.)  
 1972. A review of the oceanography and renewable resources of the northern Gulf of Alaska. *Univ. Alaska, Fairbanks, Inst. Mar. Sci., IMS Rep. R72-23.* 690 p.
- Saur, J. F. T.  
 1962. The variability of monthly mean sea level at six stations in the eastern North Pacific Ocean. *J. Geophys. Res.* 67: 2781-2790.
- Schulz, Bruno.  
 1911. Die stromungen und die temperaturverhaltnisse des Stillen Ozeans nordlich von 40° N-Br. einschliesslich des Bering-meeres. *Ahn. Hydrogr. Marit. Meteorol.* 39: 177-190, 242-264.
- Sverdrup, H. U.  
 1947. Wind-driven currents in a baroclinic ocean; with applications to the equatorial currents of the Eastern Pacific. *Proc. Natl. Acad. Sci.* 33: 318-326.

- Sverdrup, H. U., M. S. Johnson, and R. H. Fleming.  
1942. The oceans: their physics, chemistry and general biology. Prentice-Hall, Inc., New York. 1087 p.
- Tabata, Sueumu.  
1965. Variability of oceanographic conditions at Ocean Station "P" in the northeast Pacific Ocean. Trans. Royal Soc. Can. 3, Ser. 4, Sect. 3: 367-418.
- Thompson, Thomas G., George F. McEwen, and Richard Van Cleve.  
1936. Hydrographic sections and calculated currents in the Gulf of Alaska 1929. Rep. Int. Fish. Comm. 10. 32 p.
- Thompson, William F., and Richard Van Cleve.  
1936. Life history of the Pacific halibut. (2) Distribution and early life history. Rep. Int. Fish. Comm. 9. 184 p.
- Thomson, Richard E.  
1972. On the Alaskan Stream. J. Phys. Oceanogr. 2(4): 363-371.
- Tully, J. P., and F. G. Barber.  
1960. An estuarine analogy in the subarctic Pacific Ocean. J. Fish. Res. Board Can. 17(1): 91-112.
- Welander, Pierre.  
1959. On the vertically integrated mass transport in the oceans. P. 95-101. In: B. Bolin (ed.), The atmosphere and the sea in motion. Rockefeller Inst. Press in association with Oxford Univ. Press, New York.
- Wild, John James.  
1877. Thalassa, an essay on the depth, temperature, and currents of the ocean. Marcus Ward & Co., London. 140 p.
- Wyrтки, Klaus.  
1964. Total integrated mass transports and actual circulation in the eastern South Pacific Ocean, p. 47-52. In: K. Yoshida (ed.), Studies on oceanography. Univ. Wash., Seattle.



Annual Report

Contract #R7120848

Research Unit #367

Reporting Period: 1 July 1975  
1 March 1976

Number of Pages: 69

Near-Shore Atmospheric Modification

R. Michael Reynolds

and

Bernard Walter

Pacific Marine Environmental Laboratory-NOAA

1 April 1976

## I. Summary of Objectives

Many near surface meteorological processes act to modify the surface winds in the coastal regions of Alaska. The modification is generally extensive enough to seriously effect any attempts at relating synoptic weather maps to surface conditions. A typical example is the case of a predicted mild Easterly wind which in actuality is a strong Northerly near the coast, principally due to drainage from the interior. Further from shore, the lower continental air becomes modified by both the warmer seas and upper-level entrainment of the air above, thus altering its speed and direction.

The oceanic water near the surface is strongly influenced by the surface stress. As the wind makes a change in speed or direction, the water near the surface is strongly affected almost immediately. Then with time, the momentum change diffuses downward modifying the interior flow on a much larger time scale. The flow at depth in the oceanic mixed layer is thus related to a weighted average of past winds; in effect its response is analogous to a low pass filter whose cut-off frequency increases as the surface is approached.

The above comments indicate that a thorough knowledge of coastal wind conditions are an important consideration in offshore industrial development through its effects both on mean flow and the trajectory of surface contaminants.

The work under R.U.367 is designed to define which processes are acting to modify coastal winds, how prevalent they are, and how far off shore they act. Shipboard measurements coupled with all available meteorological data have been utilized in this goal. In addition, a study of computer simulation of coastal meteorological conditions has been undertaken to assess the applicability of a numerical model in making predictions of coastal winds.

The work is a necessary compromise between describing larger scale flows and detailing the energetics of the planetary boundary layer. Both ends of this spectrum are important contributions to the study, due to the juxtaposition of different processes.

## II. Introduction

### A. General nature and scope of study

As outlined in the summary, the study is aimed at defining those processes on the Alaskan coastline which control the magnitude and direction of surface winds. Also, the reduction in coastal effects offshore and the longshore variation are considered.

"Taku winds" is a local term referring to valley winds which pour out of the Taku glacier valley in the Juneau area. Glacial valleys such as this dominate the entire southern Alaskan coastline, and act as funnels. Periodically, during favorable meteorological conditions, and especially during the winter, cold air from the continent flows down the terrain slope, orographically channelled by these estuaries, resulting in outpouring of cold, dry air over the warmer oceanic waters. Winds such as these are well known in estuaries such as Valdez, Copper River Delta, Icy Bay, Yakutat and Juneau. In all these areas winds have been reported in excess of 100 mph. Offshore, the winds blow counter to the prevailing wave direction producing steep, rough seas. Fishermen are wary of estuary entrances such as these because of the possibility of high seas, winds, and icebergs (Searby, 1969).

Field data will shed light on dominant processes thus aiding in development of an accurate predictive model. A part of this study was to consider numerical models for meso-scale meteorology; to assess their applicability to the Alaskan coastline situation. There exist many boundary layer models of varying degrees of complexity. Since numerical prediction of surface winds is the desired output, a simple one-level model, if accurate, is superior to a complex multi-level model requiring much more computer time. Available models have been considered and future plans are to compare simple and complex models to actual field data.

### B. Specific Objectives

Our meteorological program in the Gulf of Alaska is presently concentrating on developing the capability to predict surface winds over the ocean based on synoptic maps, especially near the coast. We are developing field instrumentation and computer modelling techniques toward understanding the complicated processes active near the shore.

The field program has been geared toward examining the structure of the atmospheric boundary layer in the vicinity of Malaspina Glacier. Mean measurements of winds, temperature, moisture, and ocean bulk temperature are taken at the surface and up to an altitude above the continental air. Stations are made by ship on a line perpendicular to the coast. By examining upper-air data, the influence of thermal wind, surface latent and sensible heat flux, and upper-level entrainment on the rotation of the wind direction in the boundary layer will be examined.

Three cruises have been made to the Icy Bay-Yakutat area where radiosondes and surface observations have been made. The last study, made in March 1976 aboard the ship DISCOVERER, produced what appears to be an excellent data set. Weather conditions were ideal. The addition of meteorological sensors on a bow mounted boom and a tethered balloon profiler allowed increased accuracy and detail. However, even though all three cruises took place in different weather conditions, noticeable coastal effects were observed. Notably, as the coast is approached, the wind direction becomes predominantly offshore. Tethered balloon measurements indicate this is a low level effect as the wind changes direction and reduces speed suddenly at altitudes of approximately 200 meters. These results will be discussed in detail in section VI.

### C. Relevance to problems of petroleum development

Knowledge of surface winds is an important consideration in predicting wave development, surface currents (thus oil spill trajectory), and aircraft safety. The presence of strong valley winds will affect shipping, local surface currents, and possibly eject icebergs into the coastal waters.

Persistent coastal winds will have a longer term effect on the general shelf circulation possibly altering midwater and bottom currents. As circulation models develop with our understanding of the meteorology, better wind fields can be used to improve the model.

### III. Current State of Knowledge

This section will outline the fundamental processes which generate, maintain, and modify continental effects on the oceanic boundary layer along the Alaskan coast. Radiative cooling, large scale pressure patterns, and orography combine to generate coastal wind anomalies. As these winds move over the water they exchange energy across the sea surface both by momentum transfer and more importantly by heat and moisture transfer. During most, if not all the year, the continental air is colder than the water and often very dry. Thus, the upward heat flux creates an unstable boundary layer. The upward heat flux warms the mixed boundary layer and thereby reduces the convective intensity (see Fig. 3.1.).

Discussion below covers orographic effects, the unstable boundary layer, air-modification, and thermal wind effects with special emphasis on variations in surface and geostrophic winds. Finally, a review of existing models of boundary layer flow will be given.

This section is not intended to be a definitive review of atmospheric boundary layer dynamics. It is a descriptive coverage of the principal mechanisms active in determining the wind structure in a coastal planetary boundary layer.

928  
5

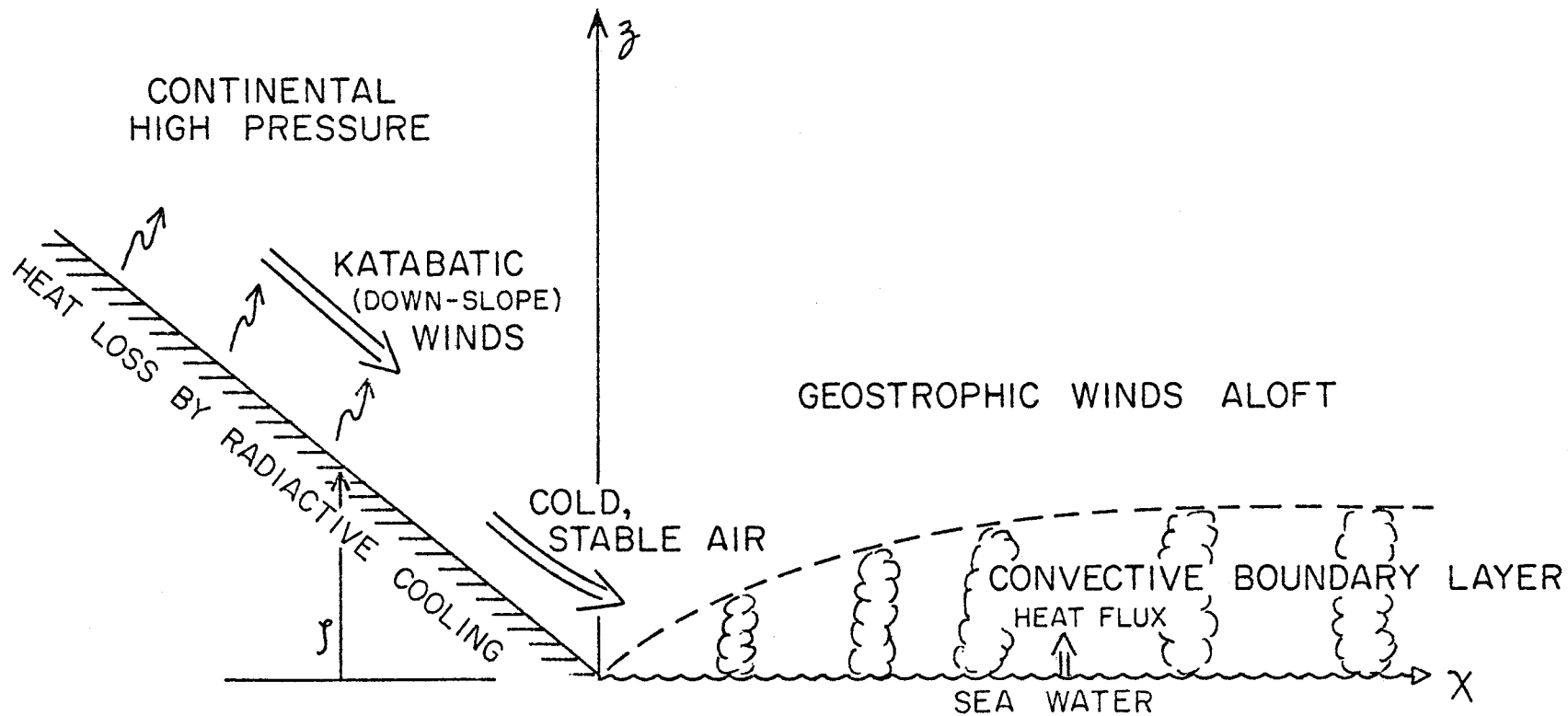


Figure 3.1. Two-dimensional cross section of the Alaskan Coast during Winter.

## A. Katabatic Flow

The first adequate theory of large-scale katabatic flow was developed by Ball (1956,1960). His theory covers situations including zero pressure gradient in the free atmosphere to pressure gradient flow with or without friction. Ball's analysis considers a neutrally stratified layer below an inversion and surface friction in the form  $\rho k v^2$  where  $v$  is the wind velocity. Some implications of Ball's theory will be considered below. Comparison of measured winds by Weller (1969) at MacRobertson Land in Antarctica with the results from Ball's theory using a constant inversion strength of  $5^\circ\text{C}$  and a gradual inland increase in the inversion height shows remarkably good agreement. Ball's simple theory was extended by Gutman and Malbakhov (1965) for a polytropic atmosphere without a horizontal pressure gradient but with turbulent transfer of momentum and heat. Radock (1972) gives a comparison of Ball's theory with that of Gutman and Malbakhov and makes an evaluation of the energy transfers taking place along an air trajectory from the interior to the edge of Antarctica. Kilday (1970) has done a thorough analysis of the synoptic conditions which are favorable for cold katabatic-type winds in Southeast Alaska. These winds which occur at Juneau, Alaska are called Taku winds, and it is possible to extend the situations conducive to the formation of these winds to other areas along the Gulf of Alaska coast.

Katabatic winds are observed where there are large sloping ice-covered areas (such as are found along the Alaska Gulf coast, in Greenland and Antarctica). Here, net radiation at the snow-air interface is dominated by energy loss to space, and thus inversional thermal stratification prevails in the lower atmospheric layer. At the edges of these ice fields the denser air near the surface will show a tendency to down-slope motion due to gravitational acceleration and katabatic winds of large magnitude can be frequently observed (Lettau, 1967). As mentioned above, Ball's theory is quite simplified, but is able to explain many of the observed phenomena associated with katabatic flow. It is assumed that steady state prevails, the upwind supply of cold air is taken as given and the potential temperature of the katabatic flow is constant. The steady state continuity eq. is given by

$$d(hu)/dx = 0$$

where  $h$  is the inversion height,  $u$  is the velocity, and  $x$  is the horizontal distance measured downstream from an arbitrary fixed reference point. If vertical accelerations are neglected the equation of motion is then

$$d/dx(hu^2) = h\theta'g\alpha/\theta - (h\theta'g/\theta)dh/dx - (h/\rho)dp/dx - ku^2$$

where  $\theta$  = potential temperature  
 $\theta'$  = potential temperature deficit of the cold air  
 $\alpha$  = angle of inclination of the ice slope  
 $dp/dx$  = pressure gradient in the air above the inversion  
 $k$  = a dimensionless constant

These strong katabatic winds can lead to a hydraulic jump effect which can result in a sharp boundary between strong coastal winds and comparatively calm conditions at sea. When a jump occurs, the inversion changes abruptly from a low level with strong winds to a higher level with reduced surface wind speeds. A critical height  $h_c$  can be defined,  $h_c = \theta Q^2 / \theta' g$ , where  $Q = hu = \text{constant}$  depending on the rate of supply of cold air. The flow is called tranquil if  $h > h_c$  and shooting if  $h < h_c$ . If the flow is tranquil then no jump can occur and light winds are observed at the coast. On the other hand if the flow is shooting a jump will occur near the coast. If the jump is situated inland then only light winds will be observed at the coast, but if it is situated out to sea then strong winds will be observed at a coastal station. The factors that determine the location of the jump are the supply of cold air  $Q$ , the boundary layer height out over the sea and the angle of the slope down which the air is flowing. The occurrence of jump conditions has been observed by Weller (1969) in Antarctica at Mawson. Observations over extended periods of time show that the maximum mean wind speed occurs some 20-30km inland from the coast. Frequent situations where the katabatic wind abruptly decouples from the coastal ice slope surface at a critical flow number (the hydraulic jump described by Ball (1956) ) or overrides the coast at some height explains the occurrence of low coastal wind speeds. This situation is shown in Fig. 3.2. Once the katabatic winds reach the flat sea off the coast, Fig. 3.3. shows that this dissipation occurs within 15km from the coast. Tauber (1959) reports that katabatic winds at Mirny station extends to 12-14km offshore. Wind vectors outside this narrow coastal belt are controlled by the pressure gradient.

Kilday (1970) has performed a study to determine the conditions favorable for the occurrence of cold katabatic type winds in Southeast Alaska. The following discussion will be based primarily on Kilday's results. Well developed katabatic type winds occur where the terrain drops sharply, and where there are mountain ranges near and parallel to the coast, producing a sharp climatic difference between the interior and the coast. This is the situation that is present along the Gulf of Alaska coast. If a very cold air mass passes over a mountain barrier, or if under the right pressure conditions, deeply chilled continental air is forced across the mountain ranges, the cold air cascades down the steep slopes to the warm coast. Katabatic winds observed at Juneau, Alaska are called Taku winds. Observations indicate that the time of onset of the winds is independent of a diurnal effect and that the maximum velocities can occur at any time of the day or night. The duration of the meteorological conditions favorable to the onset of these winds may vary from 1-2 days to 2-3 weeks. This does not mean that these winds will blow continuously during this period, but it remains a constant threat.

On the average, these conditions last 3-4 days. The duration is greatest when lows stagnate in the Southeastern Gulf or when a series of weak frontal cyclones move from the West to reinforce the Gulf low. Lows that move rapidly through the Southeastern Gulf produce the short periods.



Taku winds are classified into two types - cyclonic and anticyclonic - according to the general synoptic situation. If the winds are due primarily to a well developed ridge of high pressure over the Yukon Territory and Western British Columbia, they are classified as anticyclonic. If the winds are due to a deepening low approaching the coast of Southeast Alaska, they are classified as cyclonic. In the latter case there is often a transition between the two depending on the path of the low when it reaches the Gulf of Alaska. In either type, isobars along the coast are tightly packed and winds blow predominantly across isobars and offshore.

The anticyclonic type produces very strong, gusty winds, and there are often calm periods between the violent gusts. The weather remains clear, dry and generally quite cold. The cyclonic type is characterized by cloudy skies, snow and only moderately cold temperatures. The cyclonic is the less violent of the two and the winds are more constant and do not exhibit the extreme gustiness found in the anticyclonic type.

The synoptic patterns conducive to the development of the Takus can be classified into three general categories. The most common category features a blocking ridge aloft which develops over the Bering Sea and the Western half of Alaska and is associated with a surface high-pressure area that covers most of the mainland of Alaska North of the Alaska Range. A weak frontal cyclone moves from the West into the northern Gulf and deepens rapidly as it swings southeastward along the coast to the Queen Charlotte Islands where it stagnates and begins to fill. A cold low aloft is associated with the surface low in the vicinity of the Charlottes, while another cold low aloft exists over Northwestern Canada. At times there has been indications that the flow associated with these upper-level lows contributes to other factors responsible for cascading the cold air Southwestward down the slopes of the Alaska Coast Range.

In the second category, the winds are dependent on a strong high pressure center over Northwestern Canada with the extension of the high pressure Southward over Western Canada. It is opposed by a weak trough of low pressure along the Southeast Alaska Coast. The surface high is associated with a large, closed, warm high aloft over the northern Gulf and the mainland of Alaska. The flow associated with this high aloft is responsible for bringing the cold air Southward over the Coastal Range. This is revealed by the large drop in temperature aloft at Whitehorse, Yakutat, and Annette Island.

The third category produces the most prolonged periods of Taku and the most severe ones. The dominant features of this type is a stagnant low over the southeastern Gulf with the closed surface high over the Yukon Basin and the blocking high aloft over the Bering Sea with a ridge Northeastward through Alaska. The Arctic Front lies between Petersburg and Annette Is. Cold arctic air flows down Lynn Canal and Taku Inlet and out through Icy Strait and Cross Sound into the rear of the low in the Southeastern Gulf while warm, moist maritime air flows Northward along the coastal waters from Washington and Vancouver

Is. these two factors not only help to maintain the depth of the low, but also provide the sharp contrast in air masses between Southeast Alaska and the Yukon Territory which appears to be one of the main prerequisites of a strong Taku.

It must be remembered that the above descriptive analysis applies to Taku winds observed at Juneau but it only takes a minor extrapolation to determine the conditions necessary to cause severe downslope winds along other areas of the Gulf of Alaska coast.

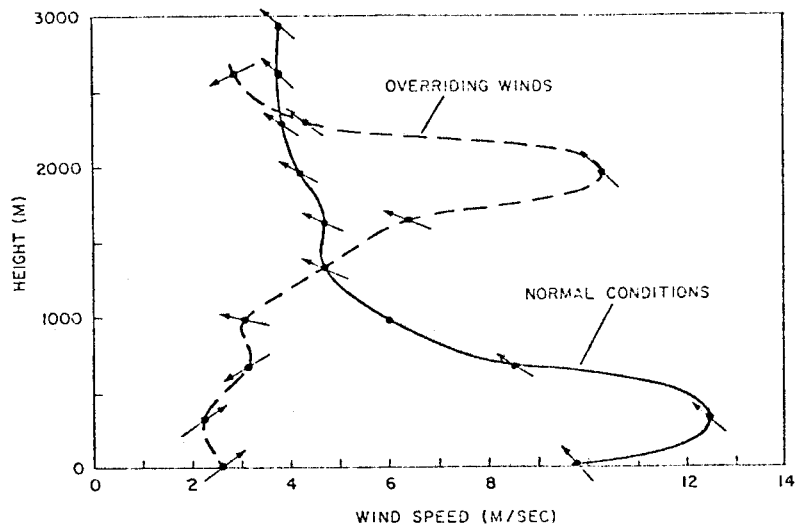


**Fig. 3.2**  
 Vertical wind profile during July at Mawson from daily balloon flights at 06, 12 and 18 GMT. Arrows indicate compass wind directions. ----- Normal conditions, ——— Overriding winds

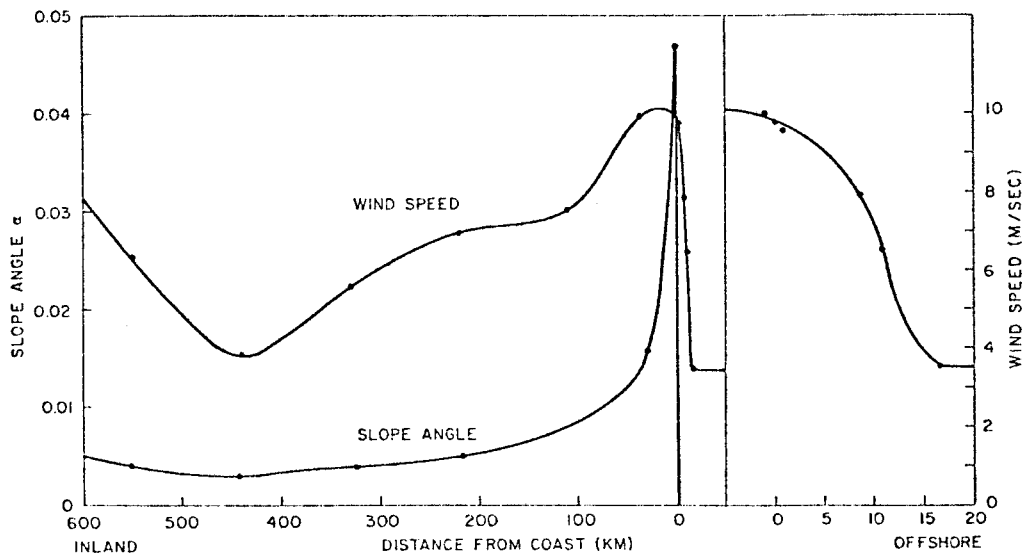


**Fig. 3.3**  
 Wind speed and slope angle observations in MacRobertson Land along the 62°E meridian. The insert shows the wind speeds offshore in greater detail

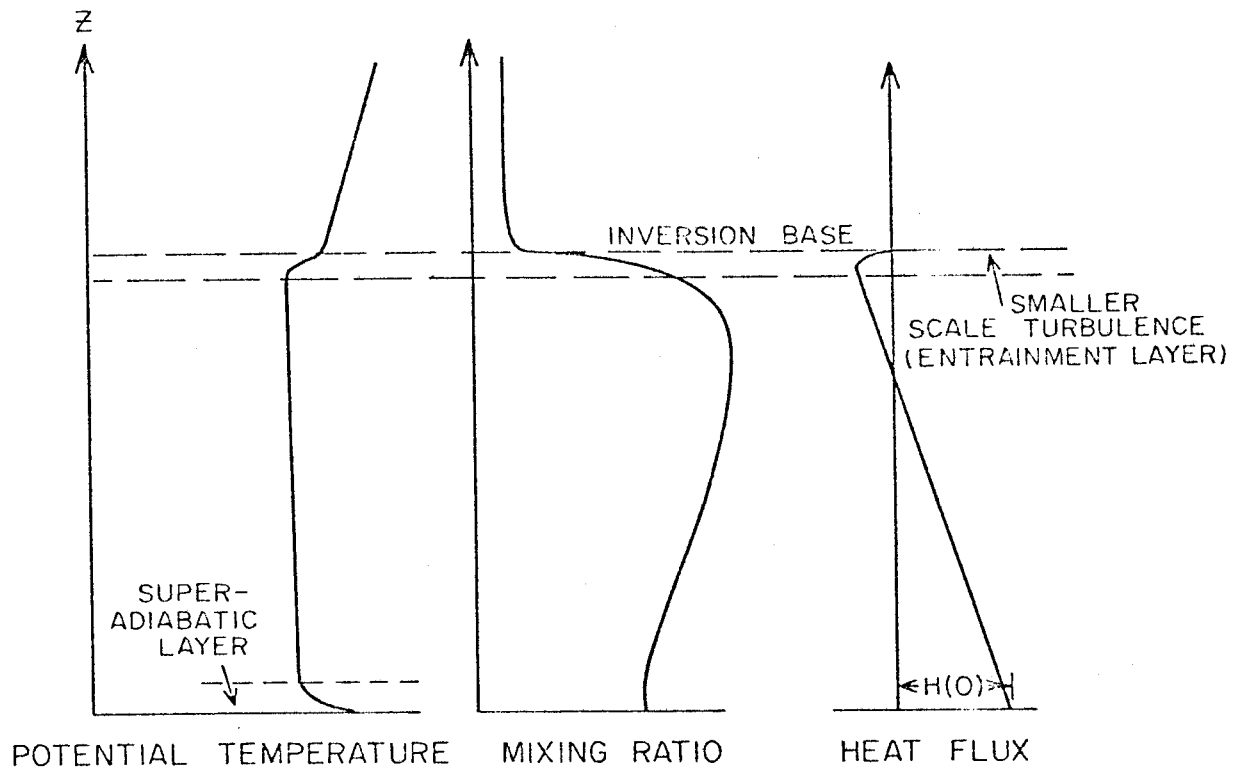


Fig. 3.4 Schematic representation of the unstable boundary layer

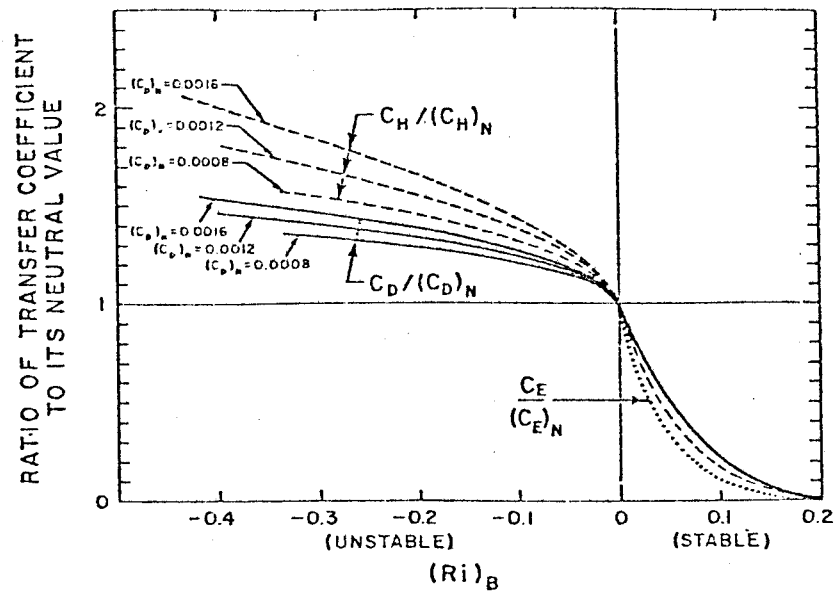


Fig. 3.5 Ratios of transfer coefficient to its neutral value from diabatic profile theory, over a wide range of bulk Richardson number. (after Deardorff, 1968)

## B. The unstable boundary

Boundary layer dynamics over land has been studied extensively for various conditions of stability Businger (1972). Since the diabatic boundary layer over the sea surface is generally observed to be either unstable or neutral, especially off the Alaskan coast, the unstable boundary layer will be discussed here.

Observations of the unstable boundary layer approximately agree with the following model, schematically drawn in Fig.3.4.

(i) The surface layer is usually defined as the lowest part of the boundary layer, where fluxes of momentum, heat and moisture can be considered constant. This requirement is fulfilled in about the lowest 10-20 meters. The interaction with the surface is strong, and adjustment with the surface conditions is rapid. Hence a quasi-steady state may often be assumed. Careful measurements of the surface layer, reviewed in detail by Businger (1973), indicate that turbulent fluxes can be related to mean profiles (or over the ocean, to air-sea differences) with a reasonable accuracy.

Within the surface layer winds are unidirectional, and have a profile which is a function of stability. The temperature gradient is super-adiabatic. The height of the unstable surface layer is scaled by the Obukhov Length given by

$$L_0 = - \frac{T_s u_*^3}{g (\omega' T_s') k}, \text{ and } \mathcal{J} = z/L_0.$$

Inside the unstable surface layer, well known empirical relationships are expected to hold:

$$\phi_m = \frac{kz}{u_*} \frac{\partial u}{\partial z} = (1 - \alpha_m \mathcal{J})^{-1/4}; \quad \alpha_m \approx 15$$

$$\phi_h = \frac{kz}{\theta_*} \frac{\partial \theta}{\partial z} = .74 (1 - \alpha_h \mathcal{J})^{-1/2}; \quad \alpha_h \approx 4.7$$

$$\phi_q = \frac{kz}{q_*} \frac{\partial q}{\partial z} = .74 (1 - \alpha_h \mathcal{J})^{-1/2}$$

$$\mathcal{J} \approx R_i$$

Therefore, the fluxes of momentum, heat and vapor are

$$F_m(z) = \rho u_*^2 = \rho k^2 z^2 (\partial u / \partial z)^2 (1 - \alpha_m R_i)^{1/2}$$

$$F_h(z) = \rho c_p k^2 z^2 (\partial u / \partial z) (\partial \theta / \partial z) (1 - \alpha_h R_i)^{1/2}$$

$$\overline{F}_q(z) = \rho L k^2 z^2 (\partial u / \partial z) (\partial q / \partial z) (1 - \alpha_h Ri)^{1/2}$$

where

$$Ri \equiv \frac{g(\partial \theta / \partial z)}{\theta (\partial u / \partial z)^2}, \text{ the Richardson Number}$$

$$j \equiv - \frac{k \beta \overline{w' T_r'}}{T_r u_*^3}$$

$$\theta_* \equiv - \frac{\overline{w' T_r'}}{u_*}$$

$$q_* \equiv - \frac{\overline{q' w'}}{u_*}$$

These equations can be rewritten in finite difference form as simply,

$$F_m = -\rho C_D (u_i - u_s)^2$$

$$F_h = -\rho C_H u_i (\theta - \theta_s)$$

$$\overline{F}_q = -\rho L C_H u_i (q_i - q_s)$$

The parameters  $C_D$ ,  $C_H$  are termed the bulk transfer coefficients. At present there is no indication that humidity needs its own transfer coefficient, thus moisture and heat transfer coefficients are assumed equal. The bulk transfer coefficients are therefore given by

$$C_D = \frac{(1 - \alpha_m Ri)^{1/2} k^2}{(\ln z_1/z_0)^2}$$

and

$$C_H = \frac{(1 - \alpha_h Ri)^{1/2} k^2}{(\ln z_1/z_0)^2}$$

Fleagle and Businger treat the coefficients as constant,  $C_H \approx 2 \times 10^{-3}$ . However, they are obviously functions of stability and their variation. Deardorff (1968) related the bulk coefficients to the neutral case. Fig. 3.5. is a plot of  $C_D/C_{DN}$  and  $C_H/C_{HN}$  as a function of bulk Richardson Number, represented by

$$J = z/L_o = \frac{k C_H/C_{DN}}{C_{DN}^{1/2} (C_D/C_{DN})^{3/2}} \left\{ \frac{g z}{T_v (\bar{u} - U_s)^2} \left[ \bar{\theta} - \theta_o + 0.61 \frac{C_E}{C_H} (\bar{q} - q_o) \right] \right\}$$

where  $T_v$  = virtual temperature at height  $z$   
 $C_H, C_{HN}$  = heat flux bulk coefficient for unstable and neutral case,  
 $C_E, C_{EN}$  = vapor flux bulk coefficient for unstable and neutral case,  
 $C_D, C_{DN}$  = drag coefficient for unstable and neutral case,  
 $\bar{u}$  = wind velocity at height  $z$ ,  
 $U_s$  = sea surface velocity in direction of  $\bar{u}$ ,  
 $q$  = mixing ration at height  $z$ ,  
 $q_o$  = sat mixing ration at temperature  $\theta_o$   
 $\theta_o$  = ocean bulk temperature,  
 $\bar{\theta}$  = air potential temperature at height  $z$ ,  
 $k$  = von Karmans constant,  $\approx 0.35$

The quantity within braces  $\{ \}$  is the bulk Richardson number,  $R_{iB}$ , which may serve as a dimensionless stability parameter. It contains quantities which can be measured easily by a good set of surface observations. The stability is an important parameter in determining the characteristics of the mixed layer.

Typical examples of stability in Alaskan waters based on Deardorff's formulation  $[(\bar{u} - U_s) = 5 \text{ m/s}, (\bar{\theta} - \theta_o) = -5^\circ \text{C}, (\bar{q} - q_o) = 2 \times 10^{-3}, z = 10 \text{ m}]$

$$R_{iB} = -0.14$$

$$J = -0.72$$

$$L_o = -14 \text{ meters}$$

Thus in the above example, the surface layer height is of the order of the ship, about 14 meters high. It will be shown later that a measurement of meteorological conditions from this height is important in describing the variation of wind in the mixed layer. Beneath the measurement,  $z < -L_o$ , the wind, temperature, and humidity follow a roughly logarithmic profile which is a function of the heat and vapor fluxes, i.e., the stability.

(ii) Above the surface layer, for  $z \gg -L_o$ , the gradient of potential temperature vanishes. This layer is called the mixed layer and is typically 300-1000 meters high. Convective cells act to uniformly mix the atmosphere to the height where buoyancy effects are overcome by the stable atmosphere above.

(iii) The top of the mixed layer is usually capped by an inversion where warmer air from above is entrained into the mixed layer below. This

entrainment layer is discussed by Ball (1960), Stull (1975), and Tennekes (1973). The entrainment process implies mass transfer downward, which acts to increase inversion height (Reynolds, et. al, 1970) and increases the gravitational potential energy. Humidity has little effect on the mixed layer height, and consequently a discontinuity in humidity is expected at the top of the convection layer (Fig. 3.4). Because turbulence must be destroyed by small eddies, the entrainment layer is expected to be both stable and dominated by smaller scale turbulence than that created below.

(iv) As mentioned above, the humidity profile is expected to be constant in the mixed layer with a sharp transition in the entrainment layer to the upper air humidity, and a sharp transition to saturation at the sea surface. Measurements of the Alaskan offshore situation fit this model with one exception. Near shore, the humidity profile appears to have a maximum in the upper portion of the mixed layer, below the inversion base. An understanding of this humidity profile should yield new insight into the dynamics of the developing mixed layer in coastal, air-modification situations.

(v) The heat flux is the dominant factor in the formation of the unstable boundary. Because of the low temperatures, latent heat transfer from evaporation and net radiative heating are small. In this case, heat flux is approximately linear in the mixed layer (constant in the surface layer). The heat flux, given by  $\rho C_p \overline{w'T}$  is a dominant term in the generation of kinetic energy through the buoyancy force. Thus the heat flux is given by

$$F_H(z) = F_H(0) \left[ 1 - \frac{z}{h_0} \right]$$

where  $h_0$  = level of zero heat flux,  
and  $F_H(0)$  = heat flux at the surface.

The value of  $h_0$  and  $F_H(h)$  are difficult terms to assess; measurements show a fair degree of scatter, and theoretical development is not satisfactory either. Typically, the downward heat flux,  $F_H(h) \approx .1F_H(0)$  and  $h_0 \approx .8h$ . The entrained heat and mass influence boundary layer development and must be accounted for in making accurate predictions of wind structure.

(vi) A prediction of the mean winds in the unstable boundary layer based on synoptic scale parameters is one of the principal aims in boundary layer research. The Alaskan study is no different. A knowledge of the geostrophic wind vector,  $\bar{G}$ , from the surface maps together with surface observations over a meso-scale area should be sufficient information to predict surface stress, based on existing quasi-stationary models. However, the measurements need to be accurate. Also, several complicating factors such as non-stationarity, and thermal winds must be considered.

General reviews of the models for predicting winds in the boundary layers are given by Brown (1974) and Tennekes (1973). At present there



are several theoretical models based on different parameterization schemes. Unfortunately, there is little good field data suitable to verify these models, especially over the ocean (recent GARP experiments may correct this situation).

The angle between geostrophic wind vector  $\vec{G}$  and the surface layer wind vector  $\vec{U}_1$  is given by  $\alpha = \alpha(\mu)$ , a function of the stability factor  $\mu$  (see Fig. 3.6.). Simple numerical solutions of the boundary layer are given by Estoque (1973) which demonstrate some of the expected structure in an unstable boundary layer, especially the effects of instability on surface stress,  $U_*$ , and veering angle  $\alpha$ . The effect of instability is to increase the surface stress, decrease  $\alpha$ , increase low-level wind speeds, and increase the boundary layer height.

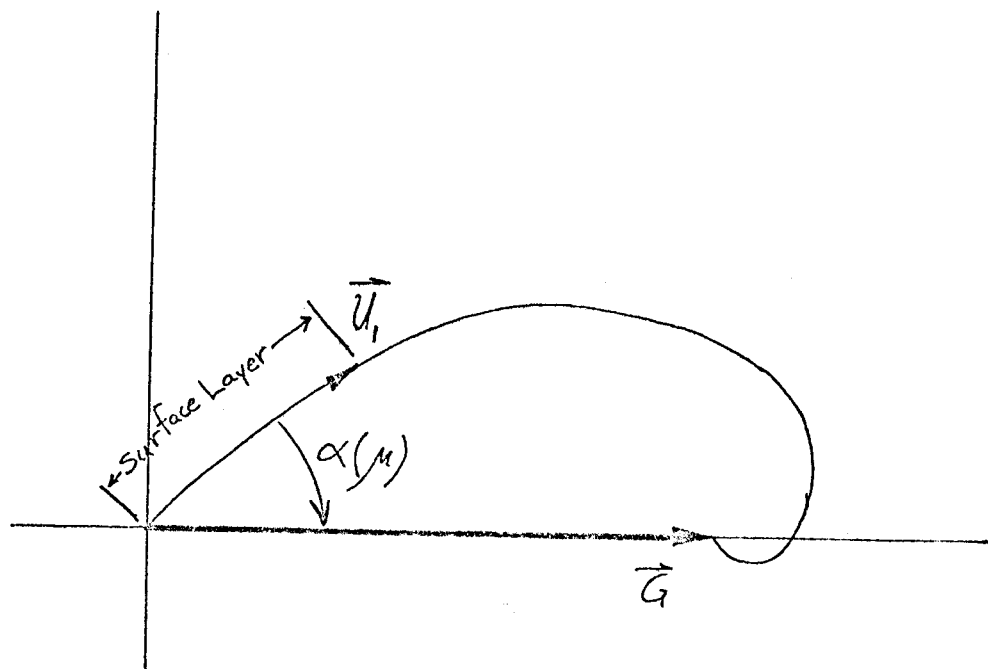


Fig. 3.6 Hodography of boundary layer winds.

### C. Air Modification

The term "air modification" generally applies to an air mass which is advected over a region where heat is exchanged with the Earth's surface by vertical fluxes of energy. A typical example of such modification is when large scale weather patterns drive air of arctic origin over warmer seas as occurs off the coast of Alaska, China and the Eastern U.S.A. The unstable situation produces high positive flux of both latent and sensible heat, with the development of a sharp inversion. Alternatively, if warm air is advected over a cold surface as when summer continental air or chinook winds move over cold water such as Puget Sound, the boundary layer is stabilized and heat flux reduced considerably. In either of these situations, the advective terms in the equation of heat or moisture transfer dominate the time dependent terms.

Arctic air modification has been studied recently in the Great Lakes (Lenshow, 1973; Bean, et.al., 1975). When air of arctic continental origin flows over the warmer lakes, a large amount of moisture is transferred to the atmosphere and released as rain or snow on the lee side. Studies of air modification over the Western North Atlantic have been conducted by Craddock (1951), and the Western Pacific analogy was studied by Manabe (1957, 1958), Ninomiya (1972) and in two detailed GARP experiments called the Air Mass Transformation Experiment (AMTEX). (Lenshow, 1974).

An example of a cold air outbreak on the Alaskan coast is seen in Fig. 5.1., as secondary rolls, ubiquitous elements of boundary layers, pick up moisture over the water and produce roll clouds.

A simple yet elegant model of air modification is presented by Fleagle and Businger (1963). Beginning with the Thermodynamic Equation, and assuming molecular, radiation, and liquid water terms are negligible,

$$\left(\frac{T}{\theta}\right) \frac{d\theta}{dt} = \frac{\partial}{\partial z} (-\overline{w'T'})$$

The model is steady state, the x axis is aligned with the mean wind U which is assumed unidirectional in the boundary layer. After integrating over the vertical axis,

$$F_H(0) - F_H(h) = c_p \int_0^h \rho U \frac{T}{\theta} \frac{d\theta}{dz} dz$$

where  $F_H(0)$  is the heat flux at the lower surface,  
 $F_H(h)$  is the heat flux at the inversion base,  
h is the height of the inversion base - the bottom of the entrainment region.

The air modification profile is not expected to be significantly different than the horizontally homogeneous, quasi-stationary, convective boundary layer with the exception that time is transposed to distance via the mean

wind. That is, where in the capped inversion model  $d/dt \nu a / \partial t$ , the important term in air modification is advection,  $d/dt \nu a / \partial t$ . Within the boundary layer humidity,  $q$  and potential temperature,  $\theta$  are approximately constant and  $F_H$  varies linearly (Fig. 3.3.). The Businger model ignores the entrainment region thus assuming a simple geometric relation,

$$dh = \frac{d\theta}{(\Gamma - \gamma)_u} \frac{T}{\theta}$$

where

$$\Gamma = g/c_p, \quad \text{the adiabatic lapse rate,}$$

$$\gamma = -\partial T / \partial z, \quad \text{the actual lapse rate.}$$

It has been shown (Stull, 1975) that the downward heat flux from above is not necessarily a negligible term and can be a significant fraction, say 20%, of  $F_H(0)$ . However, inclusion of the entrainment region to the model complicates analysis considerably, and is not done in this simple model.

In bulk parameterization form,

$$-C_H \rho_i (u_i - u_s) (\theta_i - \theta_s) = \int_{z_i}^h \rho u \frac{T}{\theta} \frac{\partial \theta}{\partial x} dz$$

the height  $z_i$  is selected near the top of the surface layer, so that  $\theta$  is approximately constant with  $z$  ( $z_i, h$ ). Hence the integration above is straightforward,

$$-C_H \rho_i (u_i - u_s) (\theta_i - \theta_s) = \langle \rho u \frac{T}{\theta} \rangle \frac{\partial \theta_i}{\partial x} h$$

where  $\langle \cdot \rangle$  indicates an average over the boundary layer. By simple geometry, (see Fig. 3.7) a straight line can be drawn at constant  $\theta = \theta_i$ , to the intersection of the upper-air temperature profile. The inversion base height in this simple model is simply

$$h = \frac{\theta_i(x) - \theta_i(0)}{(\partial \theta / \partial z)_u} = \frac{\theta_i(x) - \theta_i(0)}{(\Gamma - \gamma)_u} \left( \frac{T}{\theta} \right),$$

and

$$\frac{dh}{dx} = \frac{1}{(\partial \theta / \partial z)_u} \frac{\partial \theta_i}{\partial x}.$$

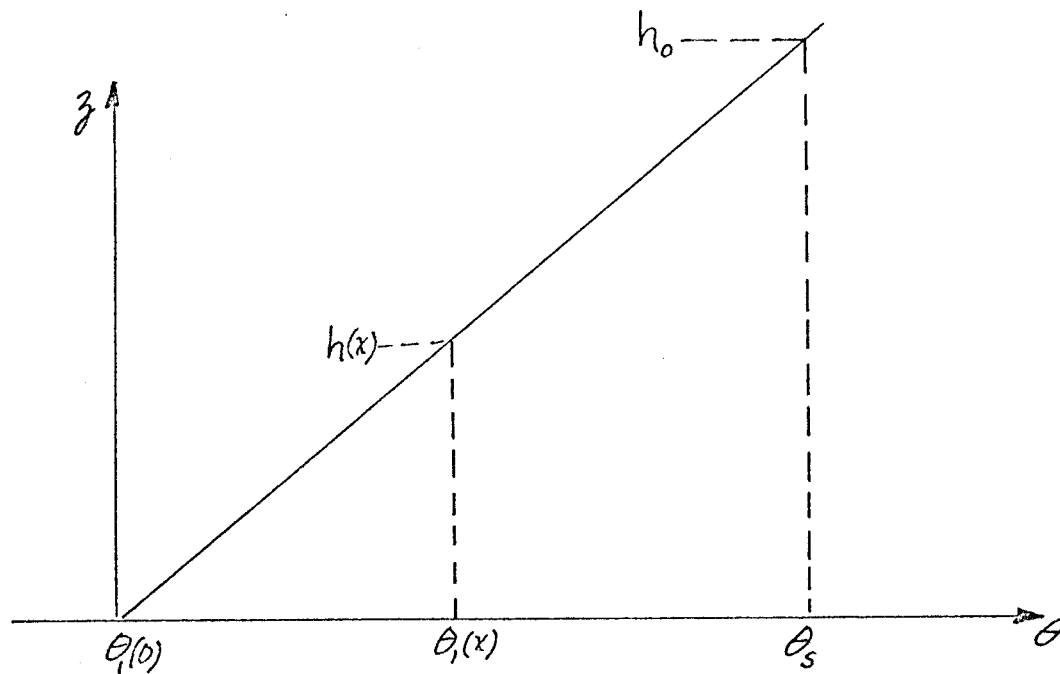


Fig. 3.7 Sketch of simple geometric solution to inversion height.

Only  $\theta_1$  is considered a variable of offshore distance  $x$ . In terms of the non-dimensional variables

$$\theta^* \equiv - \frac{\theta_1 - \theta_1(0)}{\theta_1(0) - \theta_s}$$

$$\xi \equiv x \left[ - \frac{C_H \rho_1 (u_1 - u_s) (\partial \theta / \partial z)_u}{\langle \rho u T / \theta \rangle (\theta_1(0) - \theta_s)} \right] = C_H x / h_0$$

Thus

$$\frac{\theta^*}{1 - \theta^*} d\theta^* = d\xi$$

which integrates to

$$\ln(1 - \theta^*) + \theta^* = -\xi$$

which is shown in Fig. 3.8.

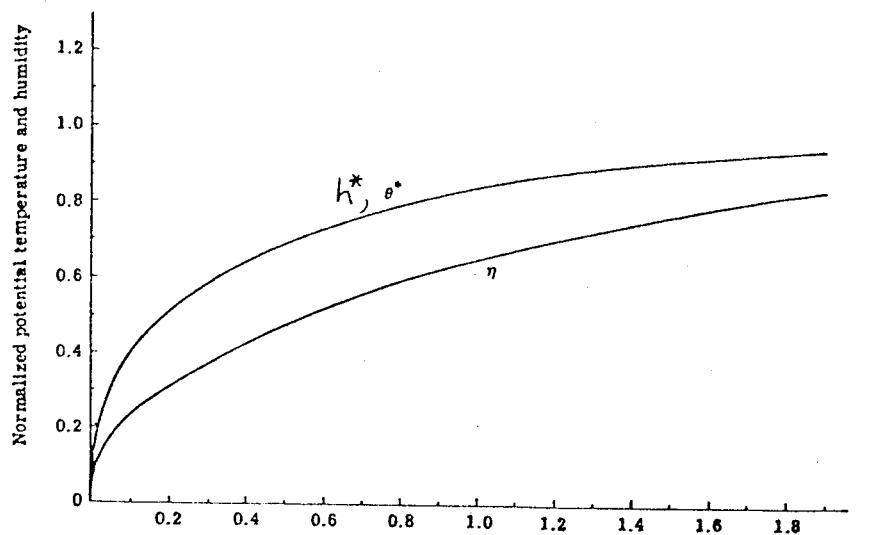


Fig. 3.8 Normalized potential temperature ( $\theta^*$ ) and humidity ( $\zeta$ ) plotted as a function of distance ( $\xi$ ) over a warm ocean (after Fleagle and Businger, 1963).

The relationship for inversion height is derived as

$$d\xi = dh^* \left( \frac{h^*}{1-h^*} \right)$$

where

$$h^* \equiv - \frac{h (\theta_1(0) - \theta_s)}{(\partial\theta_1/\partial z)_u} = \frac{h}{h_0}$$

or

$$\ln(1-h^*) + h^* = -\xi,$$

which is the same curve as  $\theta^*$  on the Figure.

The relationship for mixing ratio,  $q$ , is derived by assuming the humidity has no appreciable affect on inversion height which is geometrically dependent on the temperature distribution only. A discontinuity in humidity is expected when  $z = h$ . Let  $q_1(x)$  be the mixing ratio in the mixed layer, and  $q_2$  be the humidity of the air above.

$$\rho u \frac{dq}{dx} = - \frac{\partial}{\partial z} \rho \overline{w'q'}$$

which upon integration becomes

$$\langle \rho u \rangle \frac{dq}{dx} h = - C_H \rho_1 (u_1 - u_s)(q_1 - q_s) - (\rho u)_h (q_1 - q_2) \frac{dh}{dx}.$$

The last term represents the entrainment of upper air into the mixed layer as a result of boundary layer growth. The mixed layer height  $h$  is a function of the temperature structure hence  $q_1$  can be solved as a function of  $\theta_1$ . For simplification assume  $\langle \rho u \rangle \approx \rho_1(u_1 - u_s) \approx (\rho u)_h$ , and cancel these terms from the above equation. Then approximately

$$\theta^* \frac{d\theta^*}{d\xi} = (1 - \theta^*) - \theta^* \frac{d\theta^*}{d\xi}$$

where

$$\theta^* = \frac{\theta_1(x) - \theta_2}{(\theta_s - \theta_2)}$$

Rewriting this equation in terms of  $\theta^*$ ,

$$d\theta^*/d\theta^* = (\theta^* - \theta^*) / \theta^*(1 - \theta^*)$$

A formulation in terms of  $\xi$ , is not easy as there is no straightforward inversion. The solution was solved by Businger as a power series solution yielding

$$\theta^* \approx 1 + \frac{1 - \theta^*}{\theta^*} \ln(1 - \theta^*)$$

which is plotted in Fig. 3.8.

The formulation presented above is a very simplified model. It does not include vertical variations in  $u$ , and assumes total mixing. The interface at  $z = h$  is assumed to be a step function with no downward heat flux. Hence boundary layer growth is a function of the surface heat flux only which can be related to simple bulk parameter formulations. Also, large scale convergence or divergence can affect the mixed layer growth significantly. These considerations have been treated by some authors cited in the introduction for similar cases of horizontally homogeneous unstable boundary layers.

The above simple model has been adapted to weather prediction schemes in Great Britain where air from Northern Europe blows across the North Sea before arriving at the Great Britain coast (Blackall, 1973 and Grant, 1975). A study of 23 cases of air modification resulted in mean dew point error of  $-0.4^\circ\text{C}$  with a standard deviation of errors of  $0.95^\circ\text{C}$ .

Thus, even though this model is simplistic, it can be easily extended to cover more complex dynamics. Further, it can be used to predict stability and inversion growth with some degree of accuracy - important terms in estimating actual thermal effects on wind distribution.

#### D. Thermal Winds

In estimating the distribution of winds in the planetary boundary layer two important terms must be considered. One important term is the heat flux, expressed as a stability factor, Obukhov Length, or bulk Richardson number as discussed in section III.B. A second consideration is the baroclinic effect, a vertical variation of the large-scale pressure gradient - usually termed the thermal wind. Numerical computations of the effect of thermal wind on a hodograph such as Fig. 3.6., were made by Blackadar (1965) for a pressure gradient which varies linearly with height. In terms of the geostrophic wind, this variation is represented by

$$\vec{V}_g = \vec{V}_{g_0} + \vec{A}z,$$

where  $\vec{V}_{g_0}$  is the surface geostrophic wind as defined by the surface pressure gradient,

$\vec{V}_g$  is the geostrophic wind at height  $z$ ,

$\vec{A}$  is the vectorial rate of increase of  $\vec{V}_g$ .

The results of Blackadar's calculations for four different cases of  $\vec{A}$  are shown in Fig. 3.9., with  $G/f=84 \times 10^5$ ,  $|\vec{A}|/f=42$ , and  $z_0=1\text{cm}$ . It should be noted, that even though there is a large distortion in the wind spiral, the surface stress is largely determined by the surface geostrophic wind, and is only slightly influenced by the baroclinicity.

Hence, a good (emphasis on good) set of surface pressure observations are adequate to determine reasonably accurate estimates of surface winds even though the winds 1000 meters aloft show marked baroclinic adjustment. It remains to determine how an air modification event such as that discussed in section III-C acts to distort the surface pressure field.

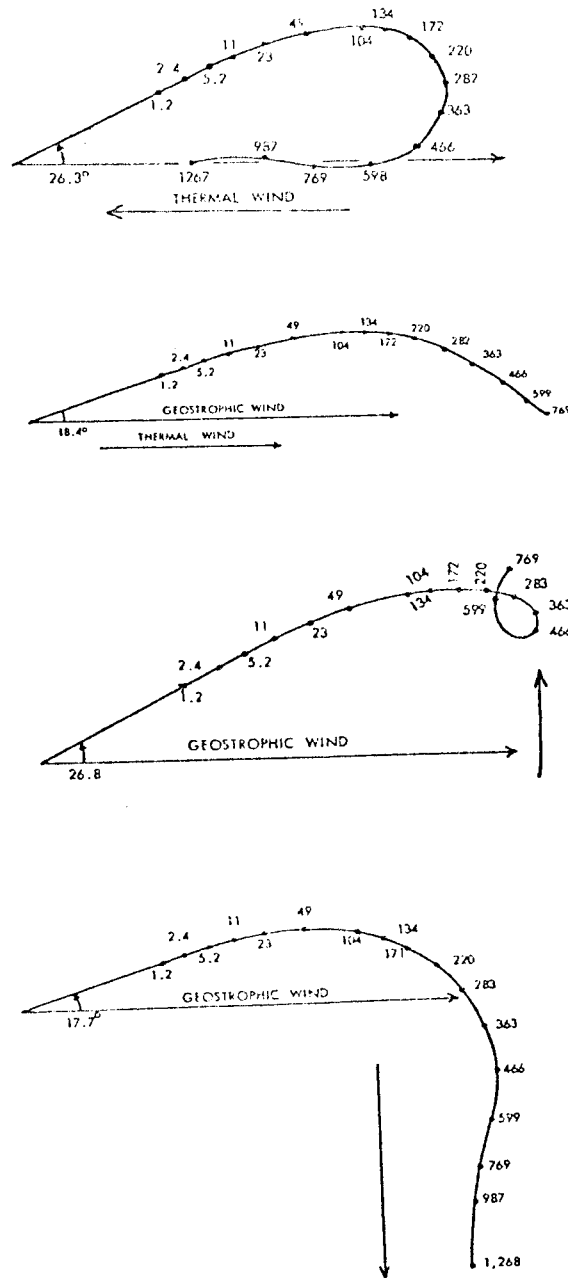


Fig. 3.9 Effect of baroclinicity (thermal wind) in modifying the boundary layer hodography (from Blackadar, 1965).



## E. Mesoscale Models

The term mesoscale refers to atmospheric phenomena which occur on scales of 10-500 km. Routine synoptic analysis is not able to resolve mesoscale motions so that in order to study these phenomena effectively one approach might be to use a mesoscale data collecting network in all of the areas one is interested in evaluating. An alternative choice is to employ a mesoscale numerical model in which a certain level of confidence has been developed. This model can then be used to calculate mesoscale atmospheric parameters in regions of interest. In studying the behavior of coastal winds along the Gulf of Alaska we are faced with the problem of being able to define what the wind pattern looks like within the first 50 km or so out from the coast given a certain prevailing synoptic situation. The approach that has been adopted here is the use of some type of mesoscale numerical model to evaluate the wind field behavior.

A number of existing mesoscale models have been investigated and an attempt will be made here to briefly describe some of them and to comment on their usefulness and limitations.

Fosberg, et.al. (1975) have developed a numerical model for estimating airflow patterns over complex terrain. This is a simple one layer model of atmospheric boundary layer flow. It is developed from the divergence and vorticity equations where the advection terms are neglected. The first step in the solution is to transfer the large scale background wind into a terrain induced modification of the throughflow. This provides a local throughflow wind. Next, a thermal and frictional modification of the vorticity and divergence is introduced, and these changes are superimposed on the terrain induced flow. Finally, stream functions and velocity potentials are calculated so that the wind speed and direction can be defined at all interior points. There are a number of limitations which are imposed by the simplifications. Moving flow systems and flows which are characterized by intermittency or by separation are explicitly excluded because advection was eliminated and because the model was intended to depict quasi-steady state processes. Coefficients describing static stability and overall wind throughflow place spatial limits on the model because constant static stability prohibits larger scale baroclinicity and the single valued wind vector prohibits large scale flow discontinuity. Also, the neglect of advective processes excludes strong interaction of the mesoscale with larger scales and does not allow for modification of the downwind environment.

Atmospheric processes that are simulated reasonably well are local thermally driven flows such as mountain and valley winds. Interactions of these local flows with each other and influence of the larger scale potential flow on these local winds are also included in the resultant flow. The basic reason these thermally driven flows are determined properly is that the thermal forcing processes are stationary and locked to the terrain features. Thus neglect of the advective process is permissible.

Lavoie (1972) has developed a three-layer model which was original-

ly used to study outbreaks of arctic air over the Great Lakes. There is a constant flux layer in contact with the ground, a well-mixed planetary boundary layer topped by an inversion, and a deep stratum of overlying stable air. Lavoie makes the hypothesis that the atmospheric response on the mesoscale is dictated primarily by the behavior of the mixed layer as a whole with only secondary dependence upon the detailed vertical structure of the surface layer or upon the vertical structure of the overlying stable layer. The model is applied to mesoscale phenomena whose characteristic wavelength is of the order of tens of kilometers in the horizontal and less than 5 km in the vertical. The time dependent equations are solved for velocity, potential temperature, boundary layer height, and specific humidity with steady state boundary conditions. Wind, layer depth, moisture and potential temperature are prescribed to be initially uniform over the whole grid. There are a number of weaknesses in the model which must be considered. The most important among these is the parameterization of the effect of the overlying atmosphere. No provision is made for heat or mass flux downward through the inversion, and this could be a serious omission. Also, the utility of the present model in forecasting is severely limited unless the requirement for horizontal homogeneity of initial conditions can be relaxed. Also the present model is limited for forecasting purposes by its finite-difference scheme which is more suitable to generating steady-state solutions than to simulating transient features. This limitation can be removed by selecting a more appropriate numerical scheme.

A very sophisticated air-sea or air-land boundary-layer model has been developed by Jacobs et.al. (1974). The model solutions are subject to terrain effects in the atmospheric layer and physical (lateral and bottom) boundaries in the water layer. The model is mathematically and physically based on the Eulerian conservation equations for momentum, heat, water vapor, salinity, and air and water pollutants, and is subject to a set of complicated boundary conditions necessary for physical and mathematical consistencies. The model is capable of examining the transport and diffusion processes in the air and/or water planetary boundary layer. The principal processes parameterized are boundary-layer turbulence in stratified (humidity, salinity, and temperature dependent) conditions, cloud-dependent radiative heating, and, for a set of vertical grid points which contain an air-water interface, mixing due to wind-generated waves on the interface. Horizontal diffusion is incorporated through a strongly and implicitly diffusive finite-difference scheme for the horizontal advection terms. However, terms representing other transport and diffusion processes were explicitly included in the differential equations. The vertical transfer processes are simulated on a relatively fine grid (i.e., of the order of meters and tens of meters) whereas the horizontal grid spacing is of the order of kilometers.

Two versions of the general three-dimensional model have been developed. The models differ in their treatment of the dynamics of the water. One version allows a water surface to vary in height from a mean elevation as a function of time. This is the FREE SURFACE version, and it allows gravity waves on the air-water interface to be explicitly defined in the solutions. This version has a limitation in that it requires a substantial amount of computer time to simulate several days, and therefore, its application is very costly. A second version, called the RIGID

LID version, was developed, in which the mean height of the water surface height is not predicted as a function of time by prescribed. It requires far less computer time for an equivalent simulation than does the FREE SURFACE version. The model has built in options enabling it to be run in a one-, two- or three-dimensional mode. (The above description of the model was taken basically from Jacobs, et.al. (1974) ).

There are several limitations with this model that must be considered. The model is quite complex and includes many processes. Thus it is difficult to sort out the role that various processes play. The cost involved in running the model is another serious consideration. The FREE SURFACE version is 4.5 times more expensive as the RIGID LID version (this is based on CDC-7600 charges). Reprogramming of the model would result in some cost reductions. The model requires the detailed specification of a large number of parameters as initial conditions and this could place some restrictions on any attempt to use it in a semi-operational mode.

Mahrer and Pielke (1974) have reported on the use of a two dimensional mesoscale model in studying the flow over mountains. The model uses a boundary-layer formulation where both the surface layer and the planetary boundary layer may vary with time. The model used is a two dimensional version of the University of Virginia three dimensional mesoscale model. The basic equations in the Cartesian coordinate system are transformed into a terrain-following coordinate system  $(x, y, z^*, t)$  by the transformation  $z^* = \bar{s}(z - z_G) / (s - z_G)$  where  $\bar{s}$  is the initial height of the top of the model,  $s$  is the material surface top of the model and  $z_G$  is the ground elevation. The equations of motion, potential temperature and continuity for hydrostatic flow are solved in this model.

Nickerson and Magaziner (1976) have developed a three-dimensional primitive equation mesoscale model using 15 levels, a modified sigma coordinate system and including moisture. It assumes a constant flux layer between the surface and the first vertical grid point (at 18 meters above the ground). The eddy exchange coefficients in this layer are obtained from the Bussinger-Dyer surface layer formulation. It assumes a boundary layer above the constant flux layer extending upward to one kilometer. Staggered grids are used where  $u$  and  $v$  are defined on one grid system while the thermodynamic variables are defined on another. Their vertical motion is defined at distances between these levels. A centered difference scheme is used to represent the time derivative, except that every fifth time step a time and space uncentered Matsuno procedure is used. At present the thermodynamic variables are specified at all boundaries, while winds are specified on inflow boundaries. This model has a very versatile display package available which allows the results to be interpreted quite easily. It includes a cold cloud microphysics package and a radiation balance calculation is planned for the future. Taken together the above features make this model extremely powerful. The only drawback to the model is that it consumes a large amount of computer time and hence is very expensive to run. This fact alone may be enough to rule out its use in certain applications.

A one-level mesoscale numerical model has been developed by Jensen and Danard (1975) for calculating surface winds in the Juan de Fuca, Haro,

and Georgia Straits. It is possible to apply this model to other areas by inputting the appropriate terrain. The three basic equations constituting the model are (a) the pressure tendency equation, (b) the first law of thermodynamics, and (c) the equation of motion. Differences in surface friction and temperature due to land-water contrast are included in addition to terrain effects. The numerical model computes the initial surface wind by assuming a balance between pressure gradient, Coriolis and frictional forces. The model then calculates the temperature changes in the boundary layer due to flow over orographic obstacles and due to heating or cooling by the underlying surface. From the hydrostatic equation, the surface pressure field is modified. This in turn affects the horizontal pressure gradient forces which change the surface wind. Initial values of surface temperature pressure and potential temperature are obtained as follows. Using the thermal wind equation, the mean isobaric temperature gradient is obtained for the area of concern from the observed variation in the horizontal pressure gradient force between sea-level and 850 mb. The 850 mb height gradient and mean isobaric temperature gradient computed as described above. The 850 mb and 700 mb temperature at the reference station give a lapse rate which initially is assumed to apply everywhere in the region. This lapse rate permits one to compute the surface temperature at any location from the 850 mb level to the surface to give the surface pressure. Finally, the surface potential temperature is calculated from the surface temperature and pressure. Thus the model can be initialized by taking data from a surface chart, an 850 mb chart and a radiosonde sounding in the area of interest. Although the temperature gradient could be measured directly from an 850 mb chart, the procedure used in the model ensures that the horizontal pressure gradient force at the earth's surface is equal to the value obtained by assuming a linear variation between sea-level and 850 mb. The model is highly parameterized as one would expect with a simplified one layer model that calculates winds just at the surface, but important items such as surface frictional forces, diabatic heating, frictionally-induced vertical motion, and terrain are considered.

Comparison of model results with observations in the Straits of Juan de Fuca, Haro, and Georgia indicate quite good agreement. This model bears serious consideration because of its simplicity, and ease of initialization. Although agreement has been obtained between model results and observations in one area some caution must be used in applying the model in another area such as the Gulf of Alaska where terrain variations and air-sea temperature differences are much more severe. Extensive testing and verification must be done before the model results can be accepted with confidence.

#### IV. Study Area

The study area being considered exists on several scales. The accompanying maps of the Gulf of Alaska indicates these different scales. Data from the Summary of Synoptic Meteorological Observations (SSMO's) published by the U.S. Naval Weather Service Command is being analyzed for the three areas shown enclosed by the dashed lines (Fig. 4.1.). This will give an overall view of wind behavior along the Gulf of Alaska. Next, wind data from the stations Middleton Is., Cordova, Yakatoga, and Yakutat will be analyzed and an attempt will be made to define the alongshore wind behavior from Cordova to Yakutat. This then defines a smaller study area than that being considered above (dotted lines). Finally, the field program of meteorological measurements made from the NOAA ships has as its study area the section of coast from Icy Bay to Yakutat Bay and extending to about 50 km offshore.

9529

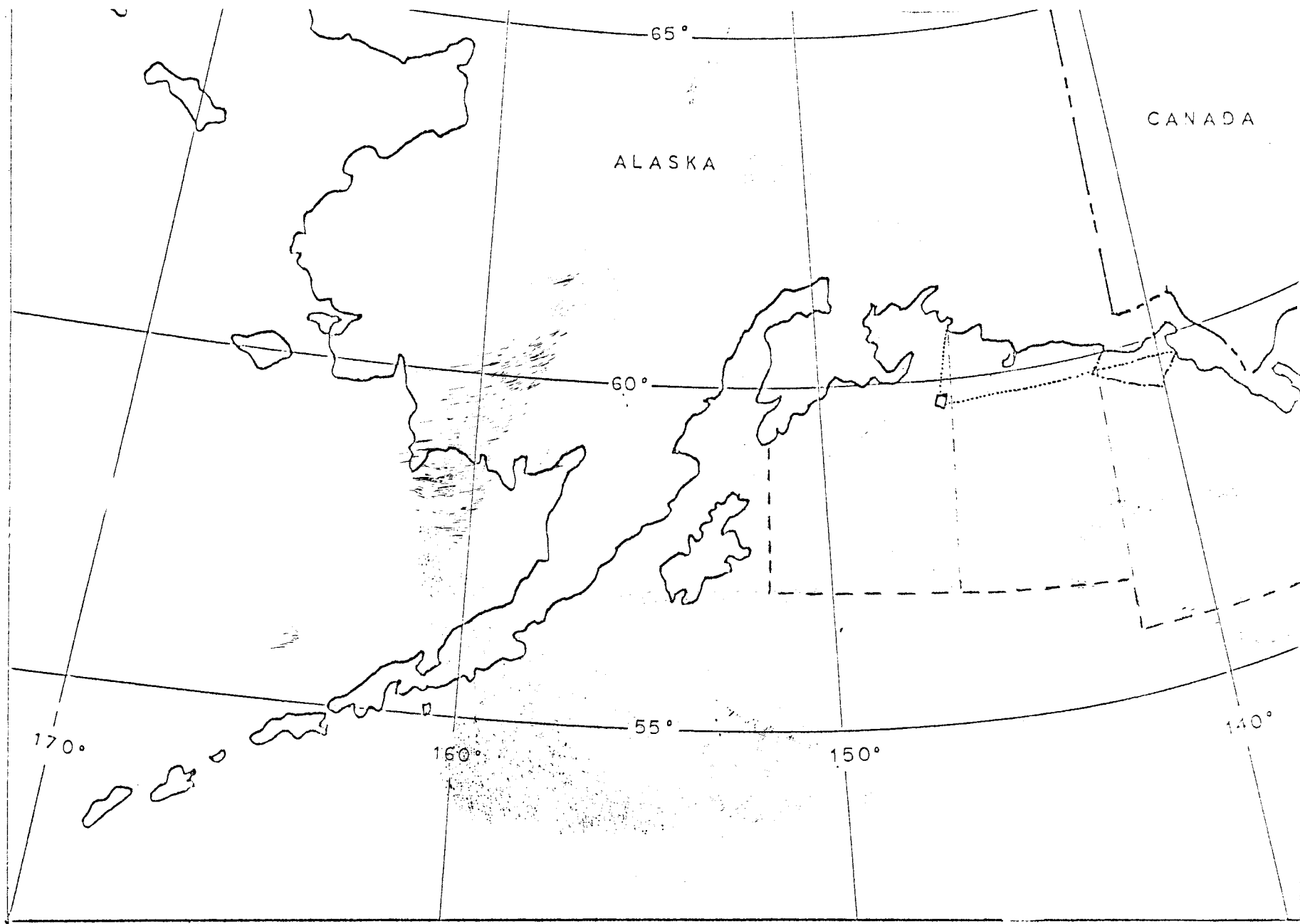


Fig. 4.1. Study Area.

## V. Sources, Methods, and Rationale of Data Collection

There are a number of sources of data that are being used in analyzing the larger scale and longer term wind variations. First is the Summary of Synoptic Meteorological observations (SSMO's) published by the U.S. Naval Weather Service Command for the areas of Sitka, Cordova, and Seward. The location of these areas are shown in Fig. 4.1., which was discussed earlier. The SSMO's contain tables of percentage frequency of wind direction by speed and by hour and also percentage frequency of wind speed by hour for each month of the year. From this data one is able to plot wind roses for each area and compare how the wind direction probability for one area relates to that of another area.

Another attempt at looking at longer term wind variations along the coast, but on a smaller scale than that given by SSMO data, involves considering a long period of synoptic surface observations at a number of stations along the coast. Data has been obtained for Cordova, Middleton Island, Yakatoga, and Yakutat for about a twenty year time period (ten years at Middleton Is.). Again, monthly statistical analyses are being performed on the data from each station. Inter-station relationships will be established in addition to relating the wind direction statistics at these stations to the results obtained from the SSMO data analysis.

Meteorological data from buoy EB-33 located at 58.5°N, 141°W has been obtained for approximately a one year time period. Also, synoptic surface charts for the Gulf of Alaska are received routinely. By picking a series of pressure values off of the synoptic charts and using a computer program that is available, the geostrophic wind speed and direction is calculated for each six-hourly synoptic chart. Thus statistics can be developed for the wind speed reduction factor and the veering angle between the geostrophic wind calculated as shown above and the surface wind measured by EB-33. Since EB-33 also measures the air-sea temperature difference it may be possible to relate variations in the wind speed reduction factor and veering angle to boundary layer stability.

Finally, both visual and infrared very high resolution satellite pictures are available from the NOAA-4 Satellite. The drainage of cold continental air from the land over the warmer waters off the coast leads to the formation of horizontal roll clouds which are oriented in the direction of the boundary layer winds (see Fig. 5.1.). By inspecting these satellite photographs it is at times possible to follow the trajectory of the surface winds flowing offshore from the interior as they veer while traversing the near-shore region and merge into the basically geostrophic flow further out over the water. Fig. 5.1. is a case of drainage winds in the Juneau area. The roll clouds in this infrared photo stream directly offshore. There are two distinct flow patterns seen. The northern group (A) rotate clockwise as the coastal wind merges

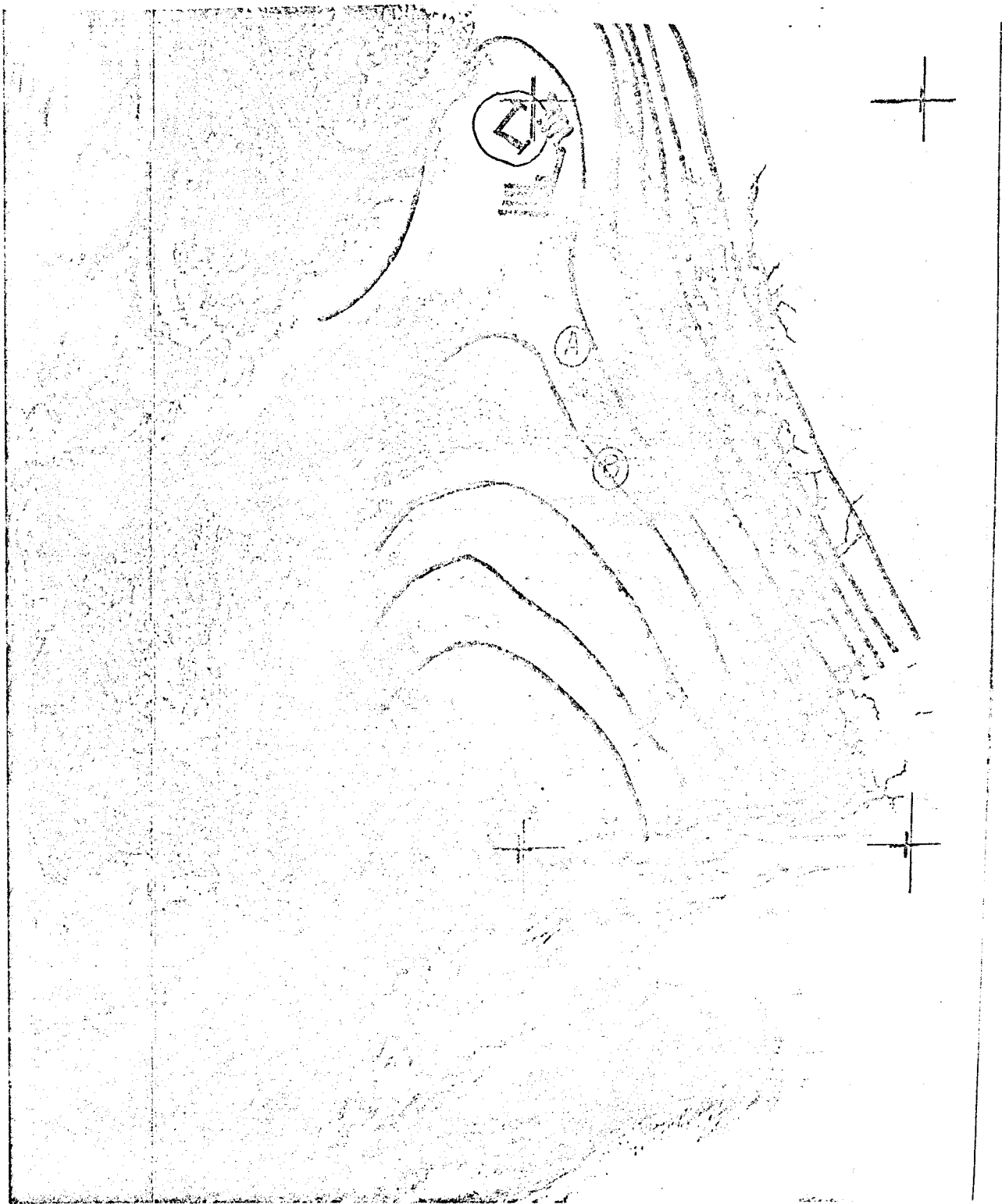


Fig. 5.1. Satellite photo of the Gulf of Alaska showing offshore winds and modification into synoptic scale pattern.



into the larger scale flow. However, the Southern group (B) tends to rotate very slightly in a counter-clockwise pattern. The pattern of the two cloud groups is explained by overlaying the synoptic weather analysis. The photo indicates it takes about 70-75 km for the roll coming out of Cross Sound to curve into the basic flow direction.

The nearshore structure of the boundary layer, especially vertical variations is examined by several types of instruments. A bow-mounted boom of simple concept was constructed. This instrument will be used to make as good a set of surface observations as possible. The instrument measures temperature, humidity, and winds at about 10 meters above the water. As discussed in detail above, a good set of surface observations are necessary to appropriately parameterize the fluxes of heat, momentum, and moisture across the air-sea interface. The bow sensor telemeters its data to a receiving recorder aft. Telemetry allows easy operation without long signal lines.

Standard radiosondes provide a rough profile of temperature and humidity to altitudes well above the mixed layer. Mixed layer height is easily ascertained. The height of the mixed layer,  $h$ , an important term in theoretical models of boundary layers is easily estimated by the radiosondes.

Finally, the same package used on the bow boom is adapted for a tethered balloon system, boundary layer profiler (BLP). The BLP is a proven design (developed and tested at NCAR). It was given a trial in March 1976 and should prove to be a most useful tool. The details of the lower mixed layer - surface layer region as well as the entrainment region can be detailed. The unit measures winds directly, a measurement not possible with the radiosonde.

## VI. Results

### A. Field investigation - 3 February 1975

A brief exploratory set of radiosondes were released in early February 1975 from the Ship OCEANOGRAPHER. This meteorological work was part of a physical oceanographic cruise, thus, by necessity, had to acquiesce to its schedule. Twenty radiosondes were released at various stations from Resurrection Bay to Yakutat, but only ascent numbers 6 - 11 will be considered here (see Fig. 6.1.).

Examination of data from data buoy EB-33, approximately 150 km offshore from Yakutat, show typical winter data (Fig. 6.2.). Twice during the month outbreaks of cold air occur when air-sea temperature difference drops sharply. Only on one brief period was the air warmer than the water. During the cold air periods, which lasted 3 - 4 days, the winds shifted to Northerly or Northeasterly indicating flow directly offshore.

Radiosondes 6 - 11 were released from 0428-1838 GMT, 3 February 1975. Fig. 6.3. summarizes the surface meteorological observations made by the ship during this track line. The offshore modification of winds and temperature are obvious, however, while the winds measured by EB-33 during this period were approximately constant, the temperature was observed to increase, a result of the sudden decrease in wind speed the day before. Off-shore increase of temperature is expected, but in this case, separation of ocean heating from radiation is difficult. Spatial separation between EB-33 and the radiosonde section makes quantitative comparison difficult.

The weather during this period was clear and calm as a high pressure system successfully blocked the normal progression of storms generated in the vicinity of the Aleutian Low. Clear weather coupled with weak synoptic scale winds result in an ideal period for examining the modification of continental polar air offshore (c.f. Section 3.A). In particular, during ascents 6 - 11 this process is well represented. Based on the simple model of an unstable mixed layer presented in Section III B, C, an interpretation of the radiosonde ascents can be made. Fig. 6.4. is a comparison of radiosonde data from Yakutat and an ascent 33 km offshore (#8). This example shows the strong ground based inversion at Yakutat. The mixed layer at station 8 has an altitude of about 600 meters, above which it agrees well with the Yakutat sounding. The temperature profile shows an expected constant value of  $-2^{\circ}\text{C}$  and the entrainment region is evident both in the temperature and mixing ratio plots. As mentioned above, humidity is an excellent indicator of the inversion height. Figure 6.5. is a section of the mixing ratio profile. Profile 6 and 7 are closer into shore where convection is strong. This is evident in Fig. 6.5. where the entrainment layer is thick apparently extending from about 430 - 700 meters. Profile 8 - 11 show a much sharper transition from mixed layer to upper stable air. In all pro-

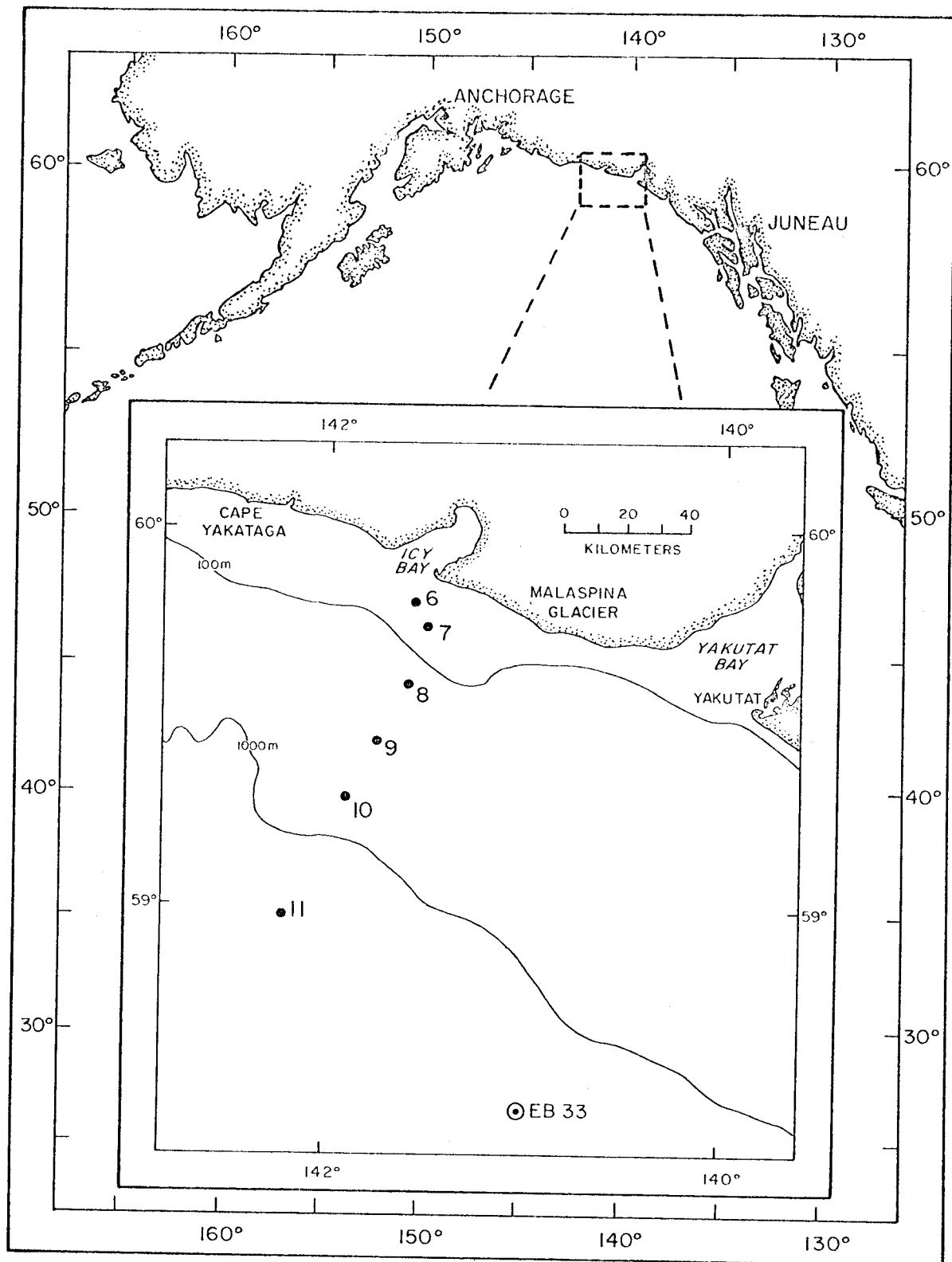


Fig. 6.1. Map showing Feb. 1975 experiment location, radiosonde ascent positions, and EB-33.

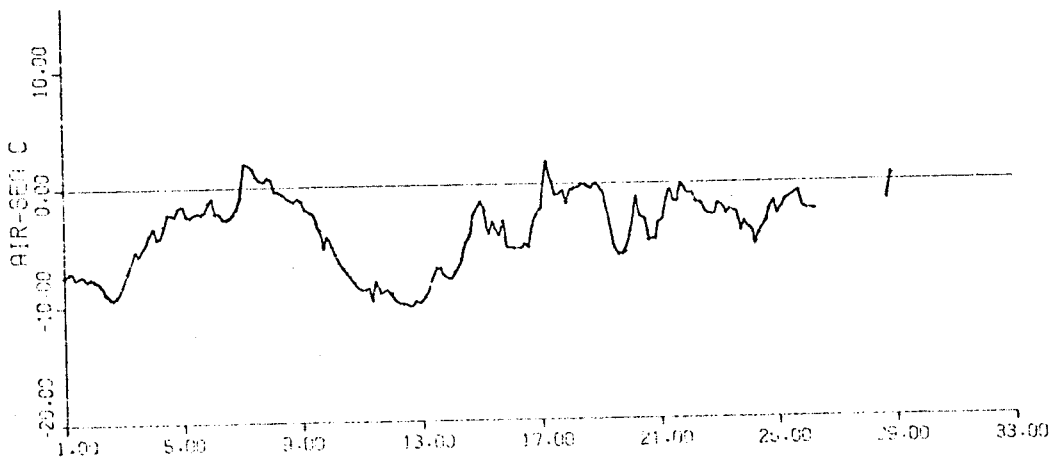
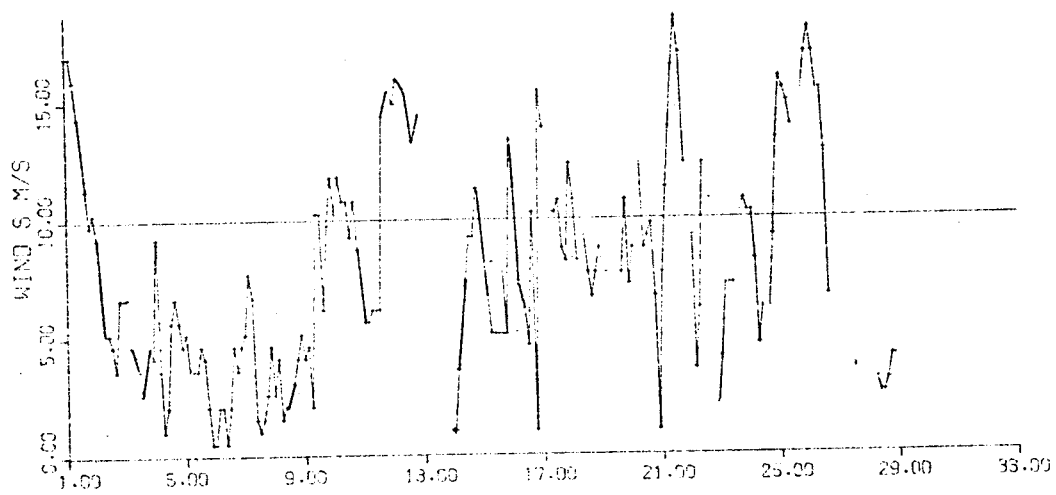
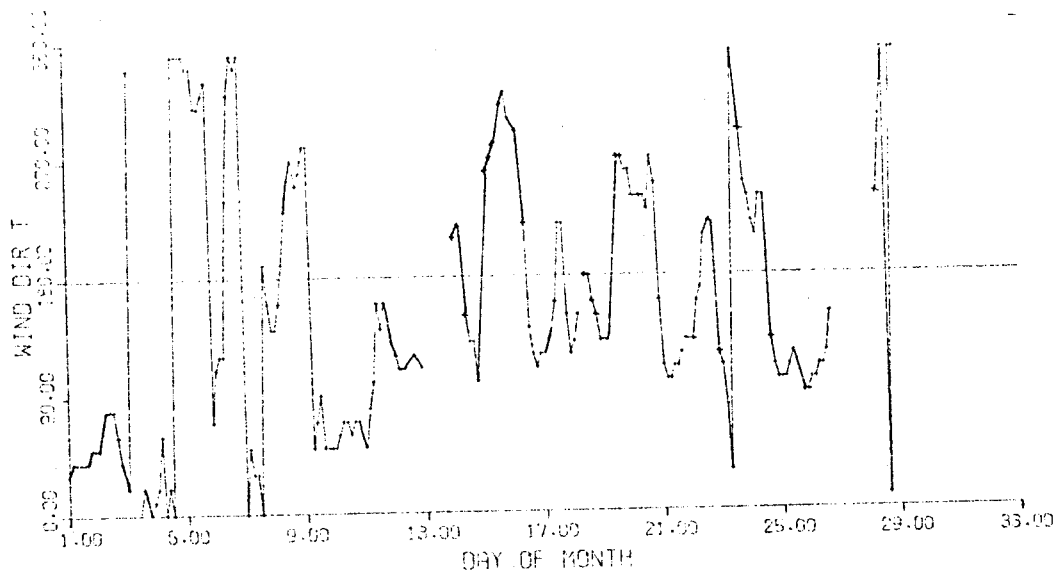


Fig. 6.2. Data from EB-33 for Feb. 1975.

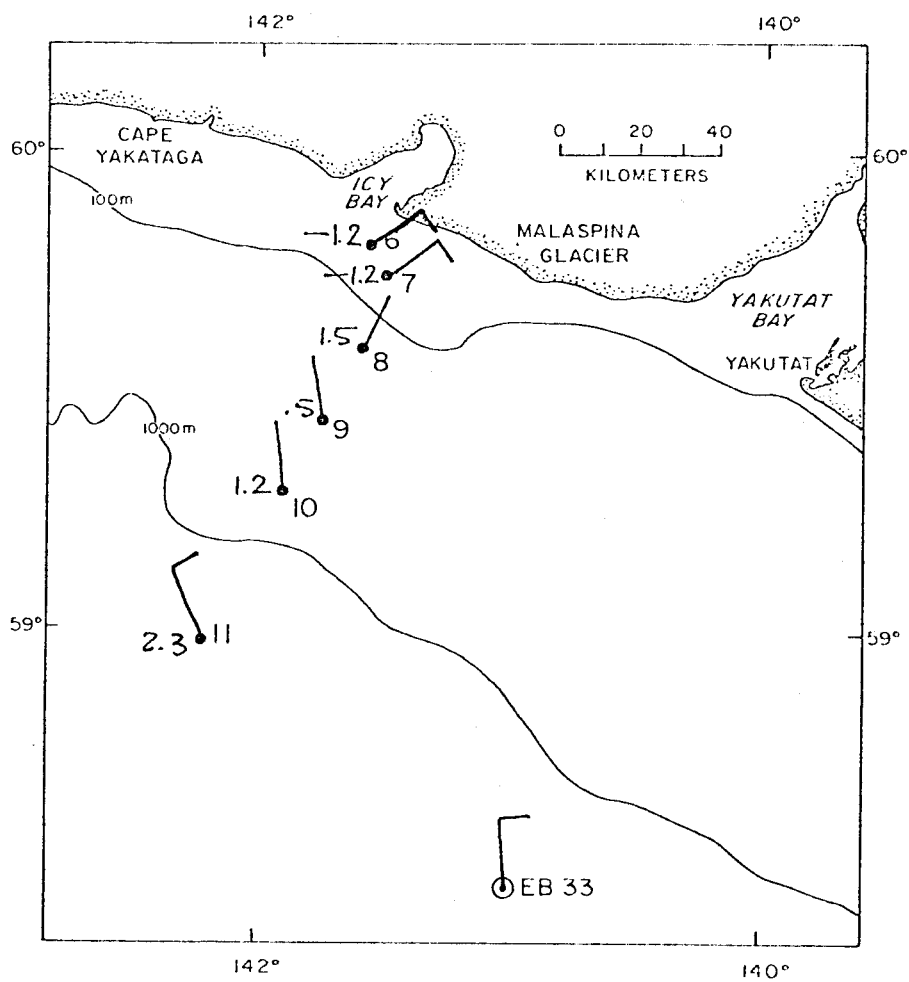


Fig. 6.3. Surface observations of wind and temperature for 3 Feb. 1975. Wind barb = 5 knots, no barb = 0-2 knots

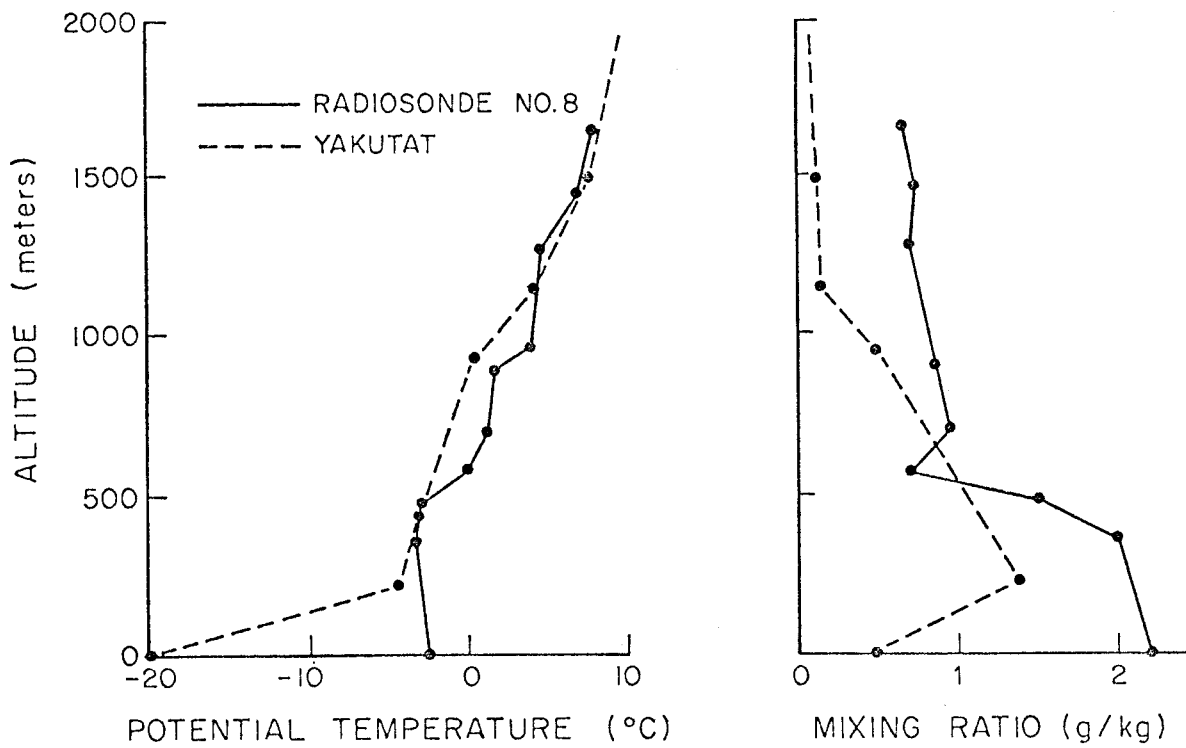


Fig. 6.4. Comparison of Profile #8 with Yakutat - potential temperature and mixing ratio

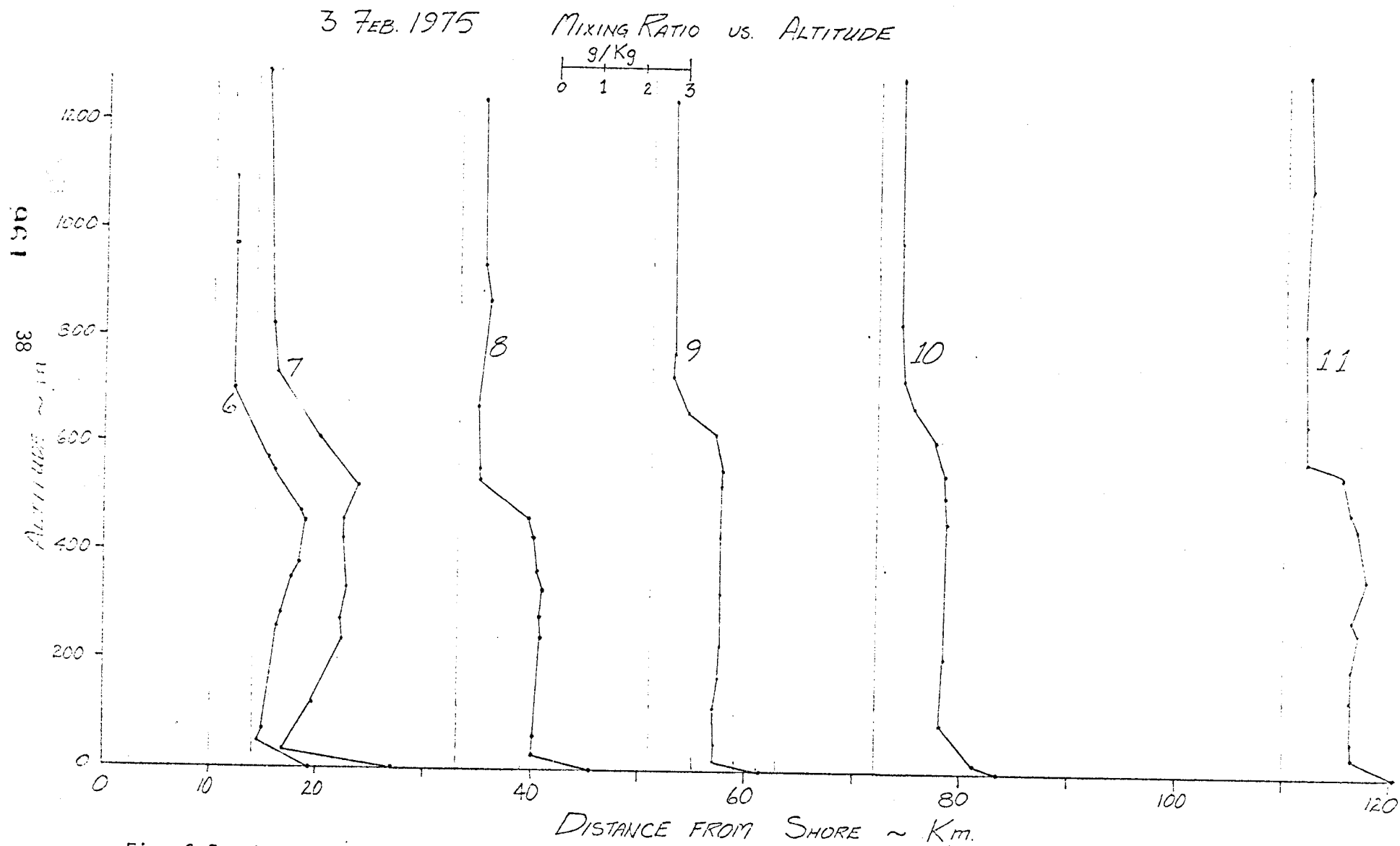


Fig. 6.5. Modification of humidity profiles offshore. Feb. 1975

files, the mixing ratio shows a slight maximum near the top of the mixed layer. The maximum becomes less pronounced as distance offshore is increased. Deardorff and Willis (197 ) have detected a similar phenomenon in a laboratory model of point and line sources of passive contaminants in a convective boundary layer. The maximum and its modification offshore are related to a vertical scaling velocity,  $w^*$ . Future experiments should examine this relationship in more detail, especially the effect of  $w_*$  on the wind profile.

In all cases, at low levels a sharp increase in water content is observed. It is expected that humidity should increase to saturation at the sea surface, but the warm ship must have affected these measurements also (surface measurements were taken from the ships bridge log). In future experiments, care will be taken in surface measurements to avoid future problems.

There is a vague tendency for the mixed layer to grow offshore. However, overall synoptic scale subsidence, occurring concurrently, was superimposed on the growth. Inclusion of subsidence effects in resolving boundary layer growth is a difficult problem requiring good synoptic coverage to reasonably calculate convergence.



## B. Field Investigation - November 1975

Meteorological data were collected for the period 20-21 November, 1976, from radiosonde launches off of the NOAA Ship DISCOVERER. The launch sites (Fig. 6.6) comprise a four station track perpendicular to the coastal area near Icy Bay and two isolated stations, one about five miles west of the outermost track station, the other in Yakutat Bay. Hourly ships weather observations were taken to be compared with shore data provided by the Yakutat office of the National Weather Service in the form of twice daily rawinsonde and hourly surface data. Synoptic weather information was categorized from surface and upper air prognoses broadcast from Pearl Harbor and received aboard the DISCOVERER, and from 6 hourly surface pressure analyses and satellite photographs furnished by the Anchorage branch of the National Weather Service.

The November, 1975 observation period was typical of wintertime conditions in the Alaskan Region (Figs. 6.7.a & b). The upper level flow was characterized by a large amplitude wave oriented NW-SE with trough line passing from Siberia across the Aleutians to central Alaska. The ridge line closely paralleled the North American West coast mountain structure. Cyclonic disturbances generated in the Western Pacific were thus swept through the trough and up past the western boundary of the operations area.

At 00Z, 20 November, a strong (1044 mb) high pressure zone centered at 74°N, 131°W, overlay Northwestern Canada and Alaska. A complex low system extended Southeast across the Aleutians with a 976 mb low centered in the Bering Sea at 59°N, 178°E and a 984 mb low at 53°N, 160°W. The resulting pressure gradient for the operating area is portrayed in Fig. 6.7.a. Notable here is the tongue of high pressure just North of the Icy Bay, Yakutat Bay areas; and the approach of the storm from the SW. Geostrophic wind velocity for the area computes to 110° at about 20 kts. For comparison purposes Yakutat measured surface winds of 208°/3 kts while environmental buoy 33 (58.5°N, 141°W) measured 080°/25 kts for 00Z.

As the day progressed the ridge north of Yakutat became less pronounced as the surface low moved its way into the Gulf from the SW. Yakutat experienced some light wet snow at about 12Z. By 00Z, 21 November, the high pressure center had strengthened to 1052 mb and moved NE to 76°N, 122°W. The Gulf of Alaska low had moved slightly NE to 52°N, 157°W. A strong low pressure system (960 mb) developed at the tip of the Aleutians (151°N, 172°E), incorporating the Bering Sea low of the previous day in its circulation. Yakutat surface pressure dropped to about 1018 mb; the resulting geostrophic flow in the operations area was from about 120° at 20 knots. By 12Z, 21 November, the advancing low had collapsed the high pressure ridge and pressures on the coast began falling rapidly. The 18Z surface pressure analysis shows one cell of the surface low in the operating area.

On November 20, 1975 the DISCOVERER took shelter in Yakutat Bay

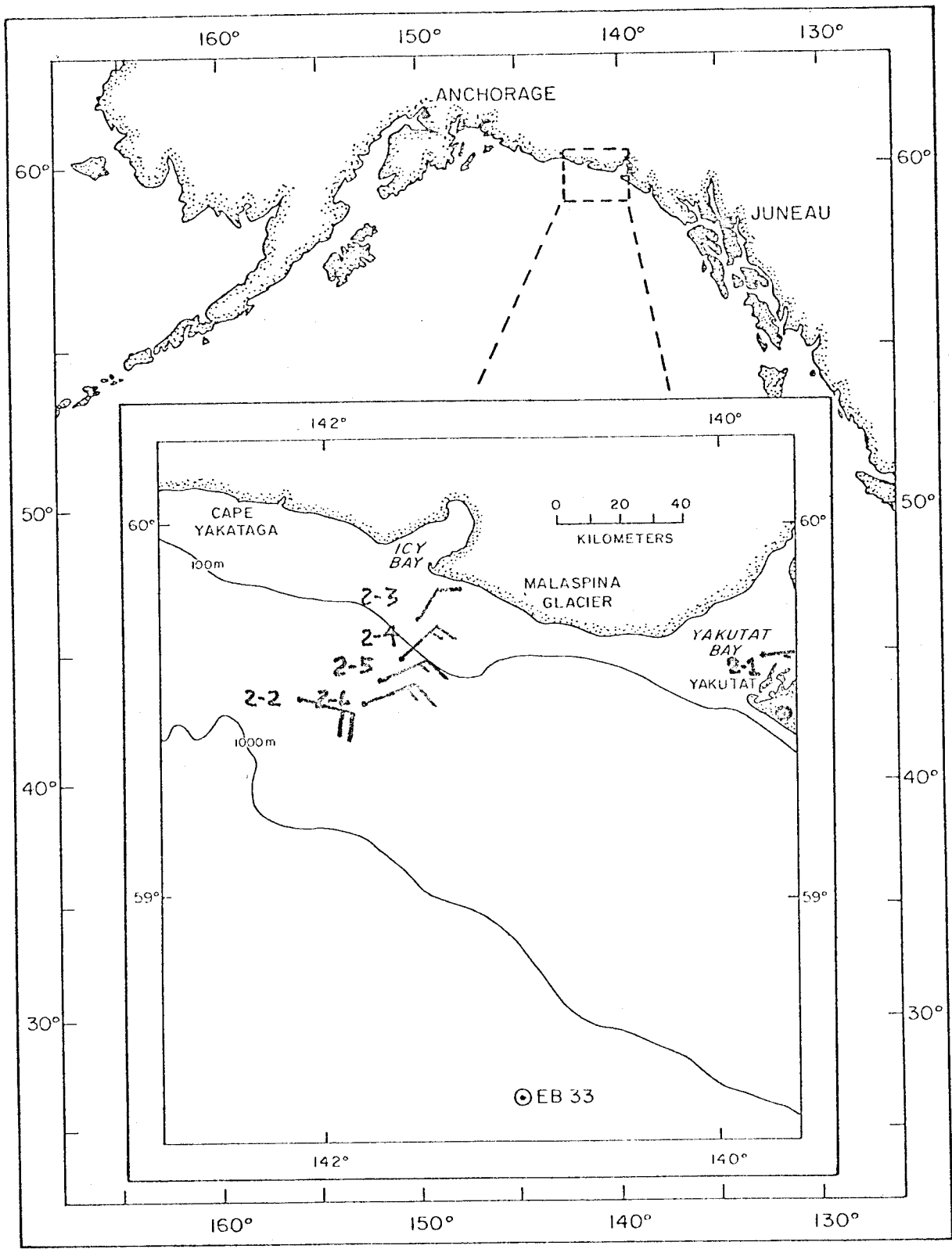


Fig. 6.6. Radiosonde observation stations, November 1975.

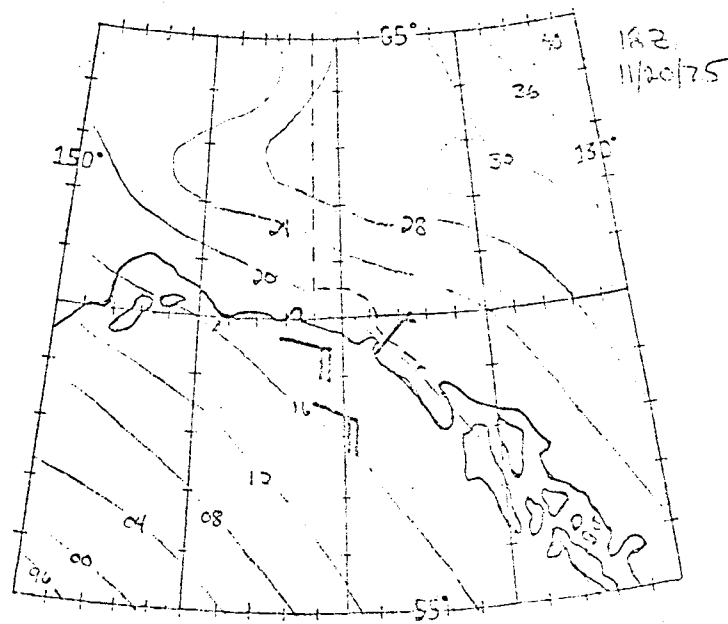
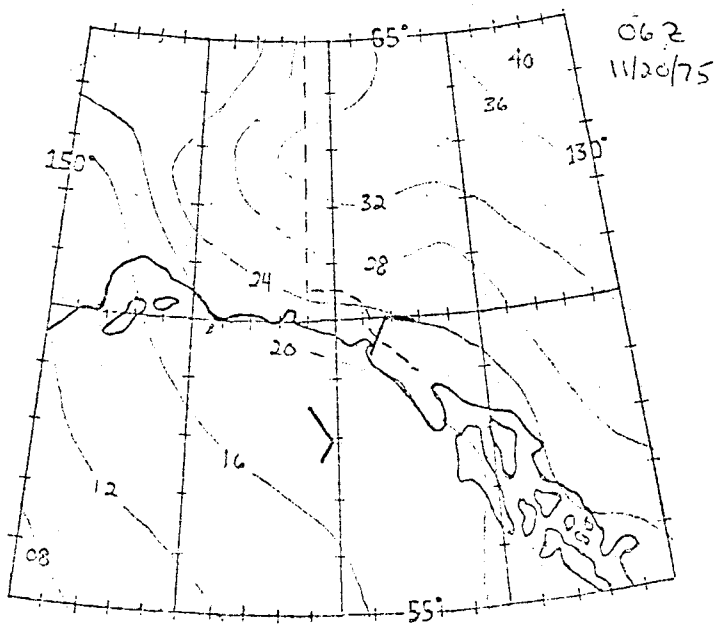
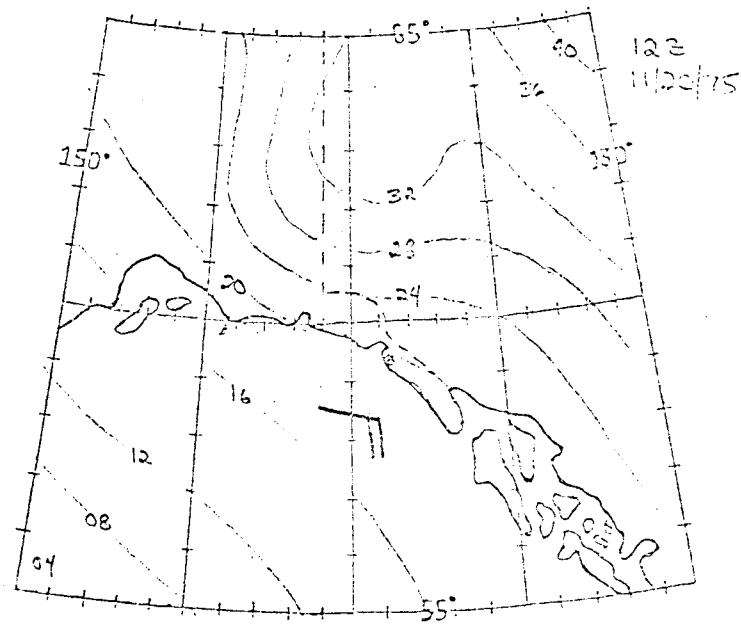
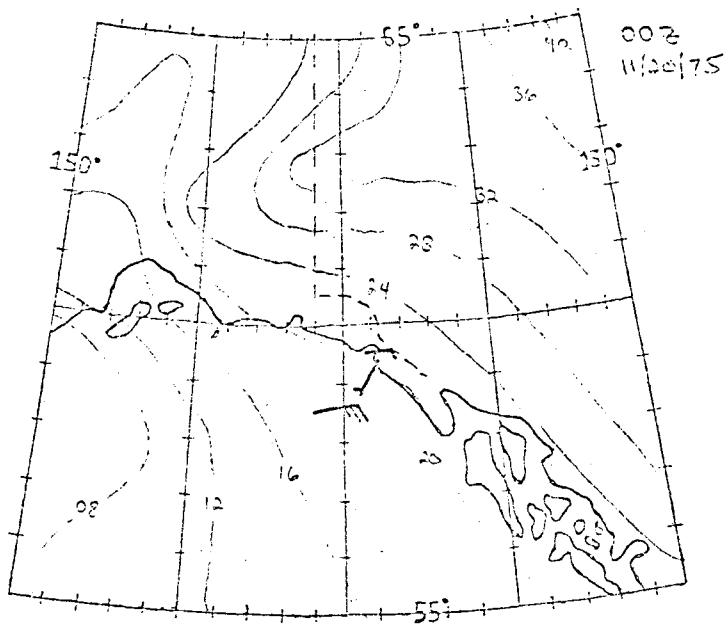


Fig 6.7a. Surface Pressure Analysis 11/20/75.

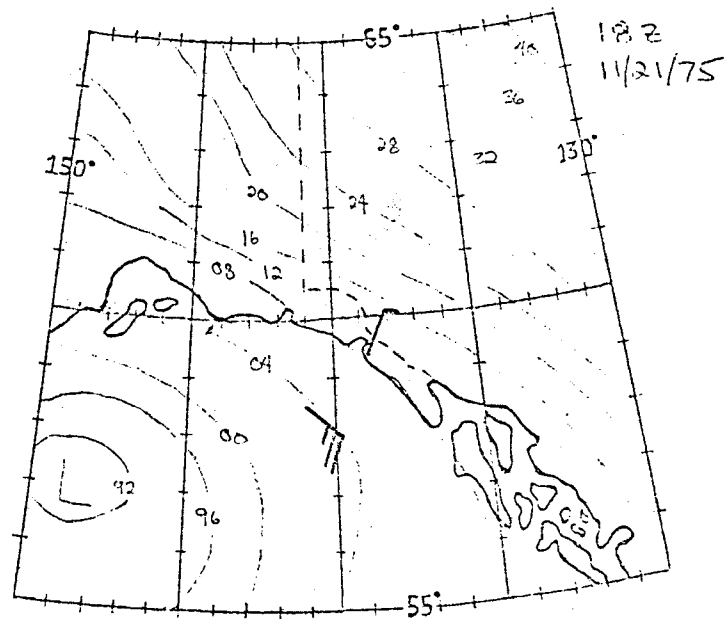
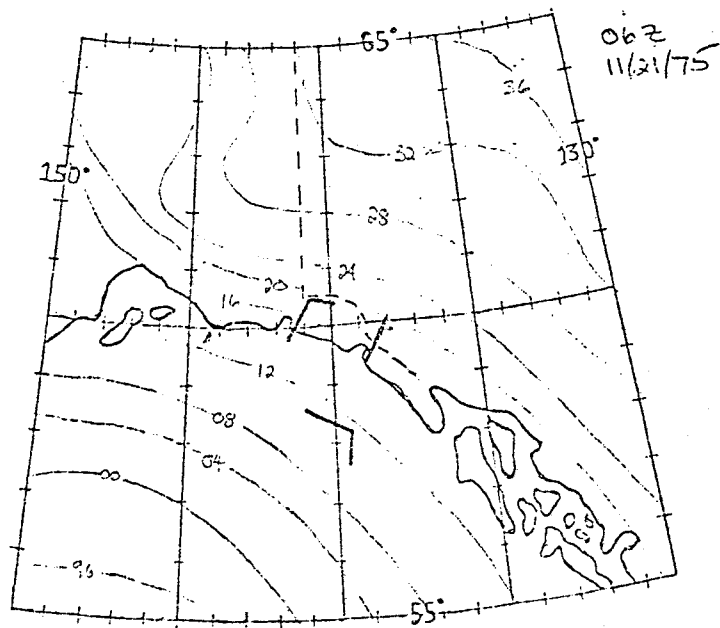
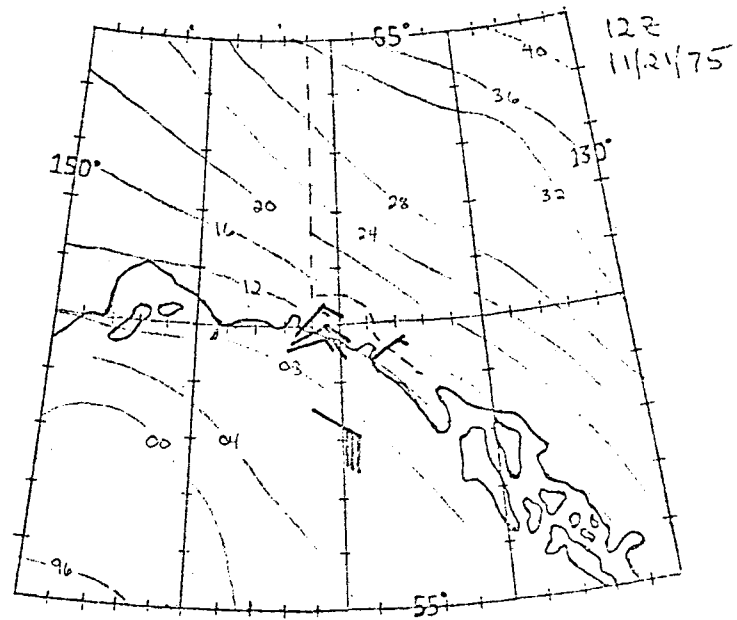
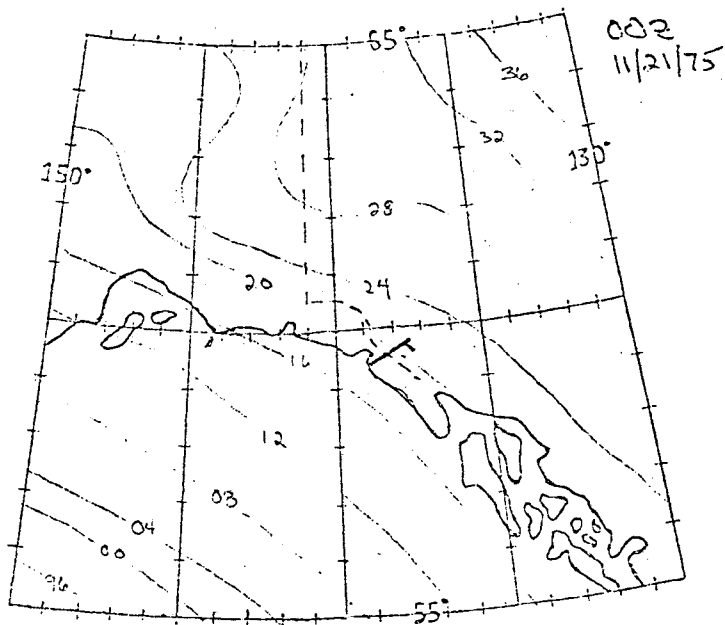


Fig 6.7 b. Surface Pressure Analysis 11/21/75

about 20 km NW of the Yakutat NWS office. Radiosonde 2-1, launched at 0121Z from location 59°37.8'N, 139°48-0'W, and the 00Z Yakutat rawinsonde ascent afford an optimum comparison of marine and terrestrial low-level atmospheric structure.

The wind profile (assumed common to both soundings) is shown in Fig. 6.8. Katabatic surface winds were light from about 060°; at an altitude of about 750m the wind had veered parallel to the coast and achieved 10m/sec magnitude, near geostrophic conditions. At about 1750m a wind speed minimum of 5 m/sec occurred.

Figure 6.9. shows the plotted potential temperature and mixing ratio profiles for both stations. The 00Z 20 November Yakutat sounding begins with a strong temperature inversion to about 200m indicating the presence of cold, dry, dense continental air. This is capped by a thin near-adiabatic layer to 500m accompanied by increasing moisture content. A more stable layer extends to 1500m and a relative humidity maximum. The sounding remains stable above this point.

The marine sounding, 2-1, differs radically in the lowest layers, the strong stable surface layer being modified by passage over the sea-surface. Strong air-sea temperature and moisture differences have developed a shallow (80m) well-mixed convective layer capped by a stable, but warmer, layer extending to about 200 m. As in the land sounding, a mixed adiabatic layer follows; however, it is much thicker extending to a lower, well-defined cloud base at 1000 m. The soundings finally match at about 1900 m.

Perusal of plotted wind vectors on the surface pressure analyses (Figs. 6.7.a and 6.7.b) indicates that on all but two occasions (00Z, November 20 and 12Z November 20) Yakutat surface winds were offshore and cross-isobaric, on the other hand, winds at EB-33, about 120 km off the coast, agree well with the surface isobars (except for slight frictional departure) and are a good indicator of geostrophically-balanced wind velocities.

Furthermore, hourly wind entries from the ship's deck log show the wind varying from 345° to 070° while the ship was within 20 km of the coast (except for a three hour period beginning at 10Z, November 20, in Yakutat Bay when winds were from the South). Outward ship excursions to about 55 km resulted in an Easterly wind direction, 080°-115°.

The radiosonde series 2 - 3 through 2 - 6 provides an excellent picture of the seaward extent of katabatic flow (Fig. 6.6.). These surface wind observations were made during the period 08-12Z, November 21 when surface winds at EB-33 were from 120° at 30 kts. At station 2 - 3, 14 km from the coast, winds were directly off the coast (030°/10 kts). By station 2- 6, 42 km out, surface winds were from 070° at 15 kts. At a distance of 60 km from the coast the ship's deck log shows the wind to be from 115° at 20 kts.

At the coast, katabatic forcing obviously dominates the pressure

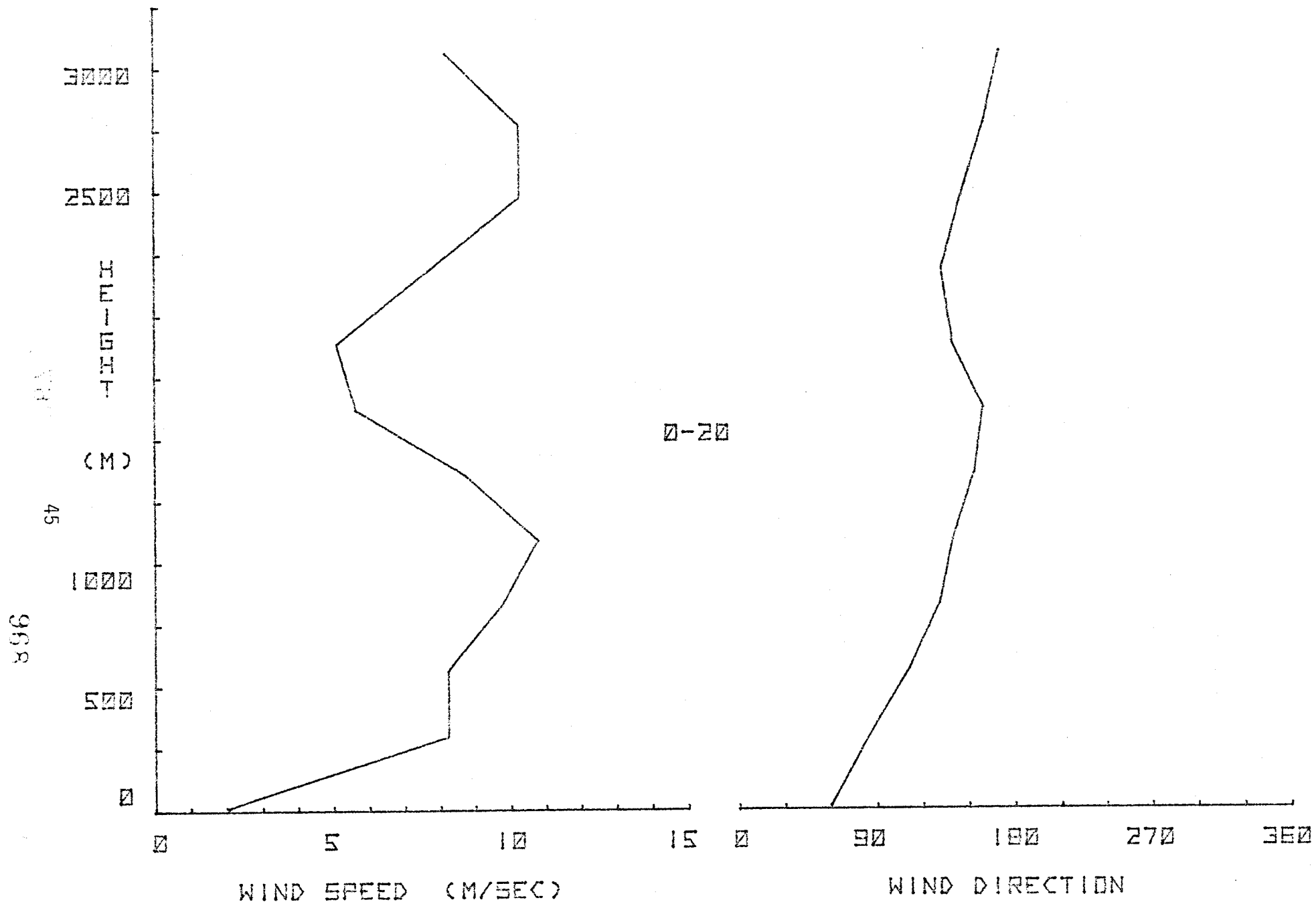


Fig. 6.8. Vertical profiles of wind speed and direction, Yakutat 00Z, 20 November 1975.

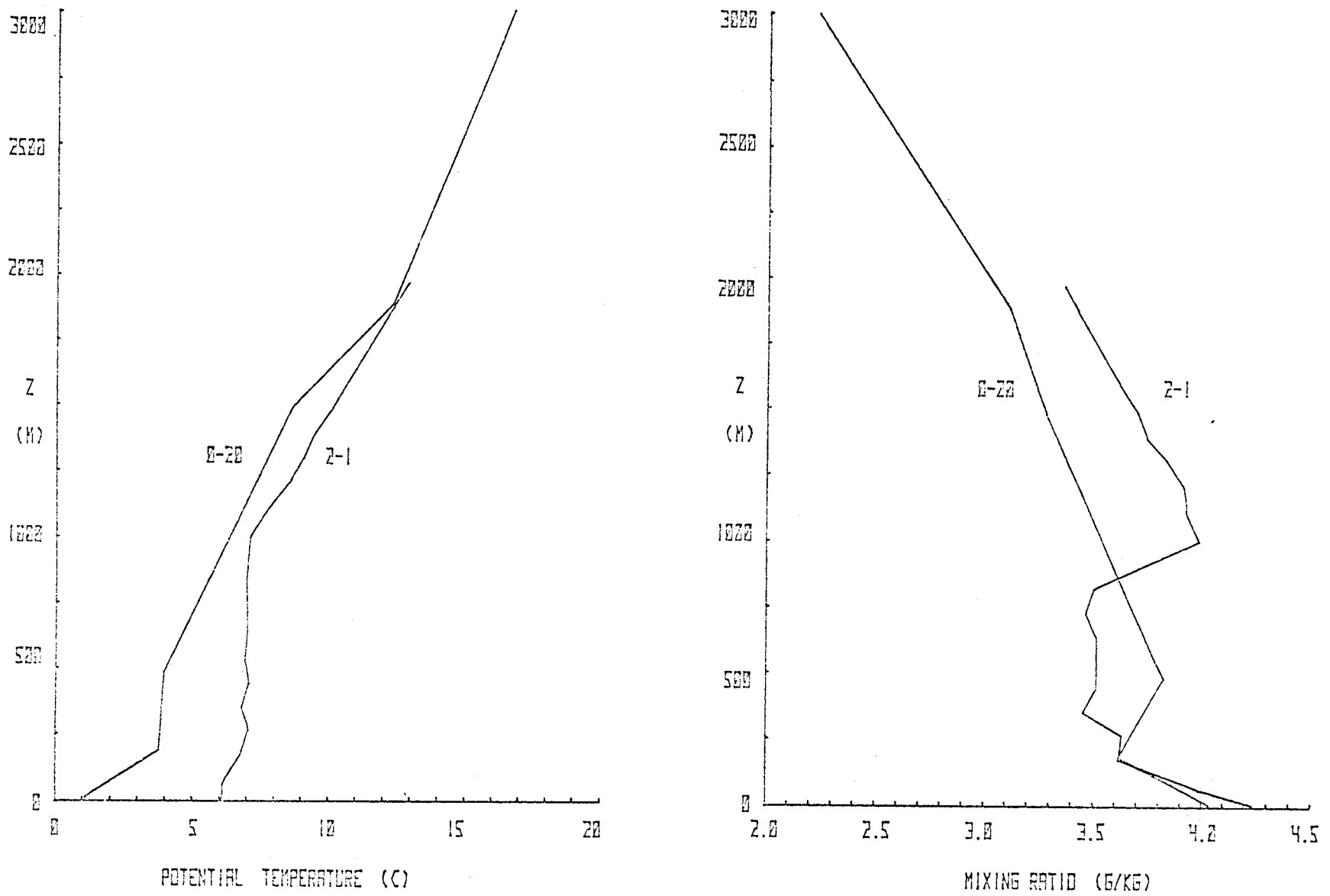


Fig. 6.9. Comparison of Yakutat 00Z 20 November and marine station 2-1 profiles.

gradient - coriolis force - katabatic force wind balance. However, as downslope gravitational acceleration obviously ceases at the coast, katabatic flow must be inertial from that point. Surface friction then acts to delay the katabatic term until the geostrophic balance between pressure gradient and coriolis forces is acquired. Under the above-described weather conditions, geostrophic balance is achieved at about 50 - 75 km from the coast.

The radiosonde series 2 - 3 through 2 - 6 (Fig. 6.6.) was analyzed with respect to the modification process discussed in Section III C. Figure 6.10. compares the potential temperature and mixing ratio profiles for the four stations (due to instrument failure, data from flights 2 - 3 and 2 - 4 were limited to about 500 m altitude). From the surface to about 150 m, the innermost station, 2 - 3, exhibited the coldest temperatures and lowest mixing ratio. As the flow moved seaward it became progressively warmer and more moist. Above this height a general reversal in the temperature trend took place as deeper surface convection at the outermost stations mixed cool surface air aloft.

A close examination of the individual profiles indicates that the surface convective layer grew in thickness from about 75 m at station 2 - 3 (where the profile still shows slight stability) to about 230 m at the outermost station, 2 - 6. This bottom layer was capped by a strong stable layer of decreasing humidity rising from about 75 m to 150 m altitude at the nearshore stations to about 230 m to 450 m away from the coast. Above this a moderately stable, dry air layer of about 500 m thickness underlay a thick dry adiabatic layer finally giving way to a permanent inversion at cloud base (1500 m).

The 12Z, 21 November, Yakutat rawinsonde and the radiosonde from station 2 - 6 were launched simultaneously allowing comparison of the above described profiles with a coastal station. The Yakutat wind profile is given by Fig. 6.11. It is similar to the 00Z 20 November profile previously discussed. Low level katabatic winds gave way to on-shore geostrophic values after about 300 m. A mid-level (1500 m) wind speed minimum again manifested itself. The potential temperature and mixing ratio profiles for Yakutat's 12Z 21 November launch are compared to those of station 2 - 6 in figure 6.12. The strong nighttime surface inversion is classically contrasted by the deep modified surface convection layer of the maritime station. Thereafter the profiles are similar, consisting of a moderately stable layer to about 750 m capped by a deep near-adiabatic layer and permanent inversion. The marine profile is cooler and more moist up to cloud base because of the low-level convection.



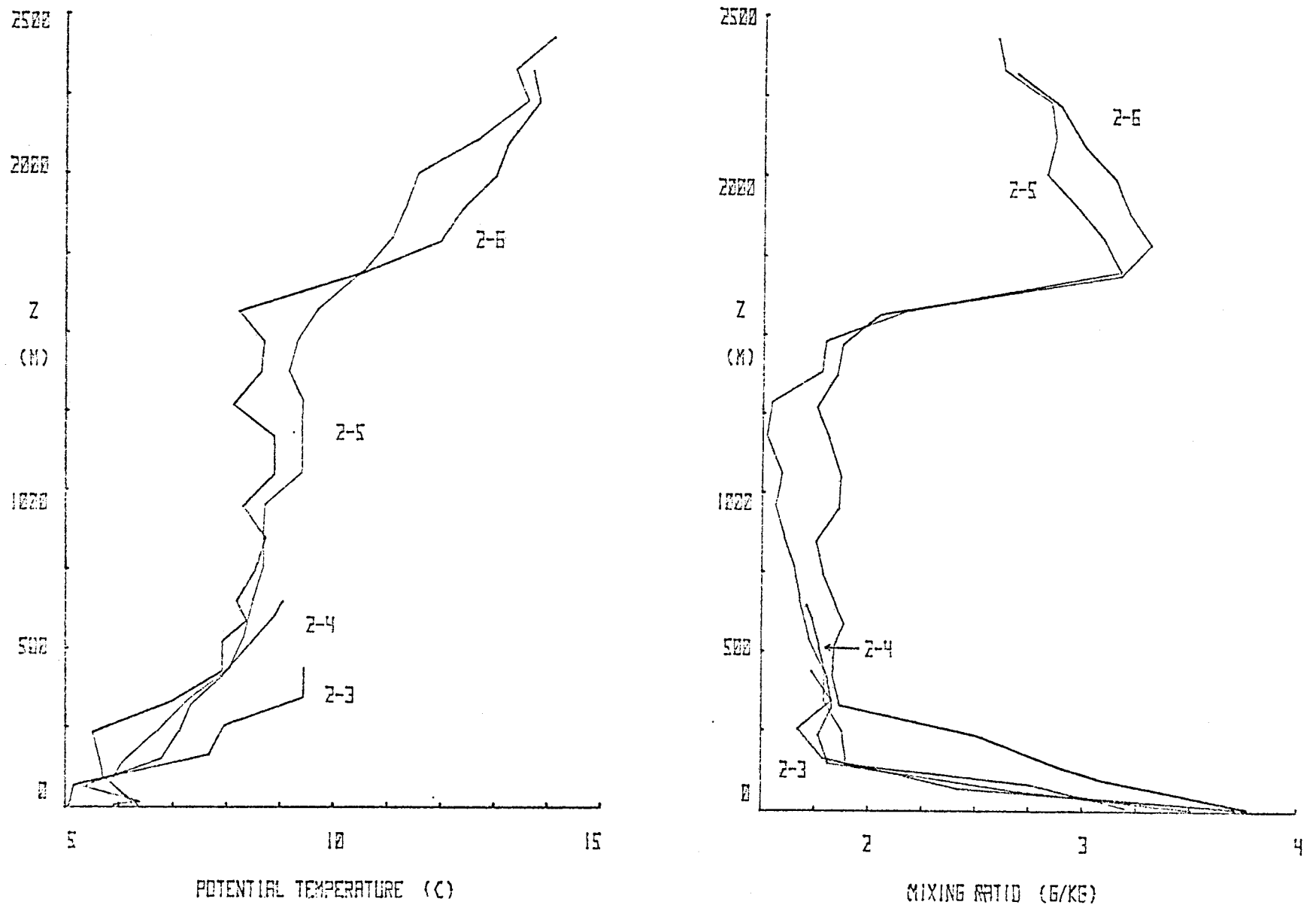


Fig. 6.10. Comparison of marine stations 2-3, 2-4, 2-5, 2-6.

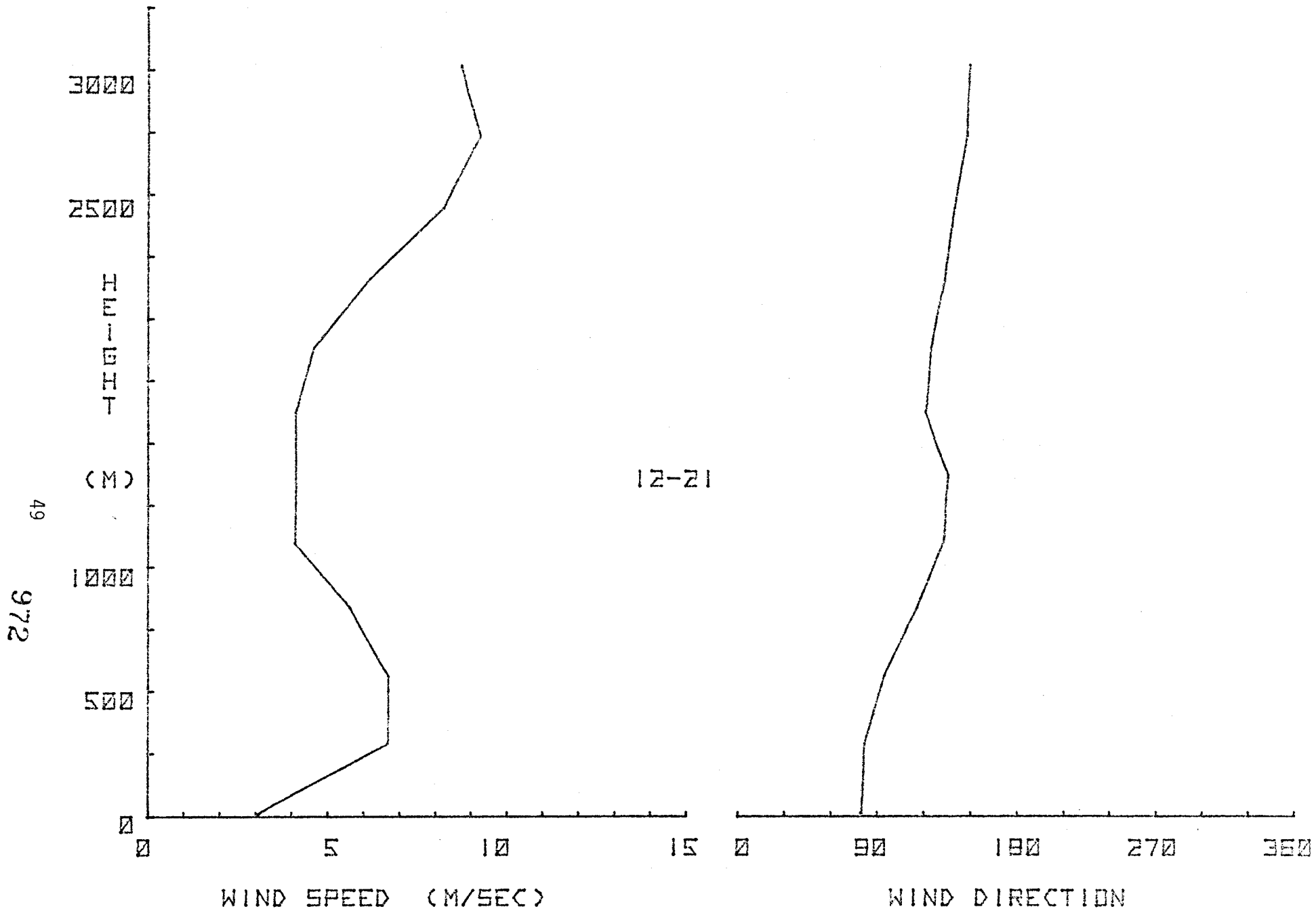


Fig. 6.11. Vertical profile of wind speed and direction for Yakutat 12Z 21 Nov. 1975.

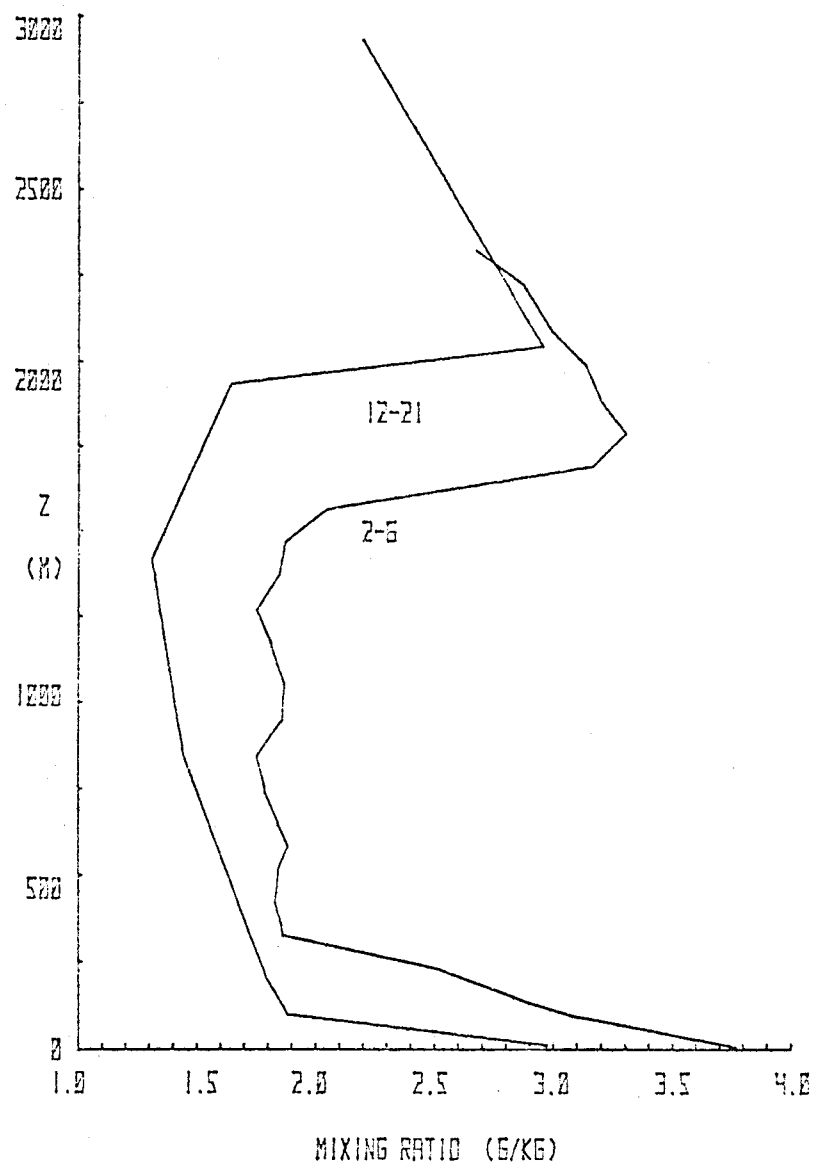
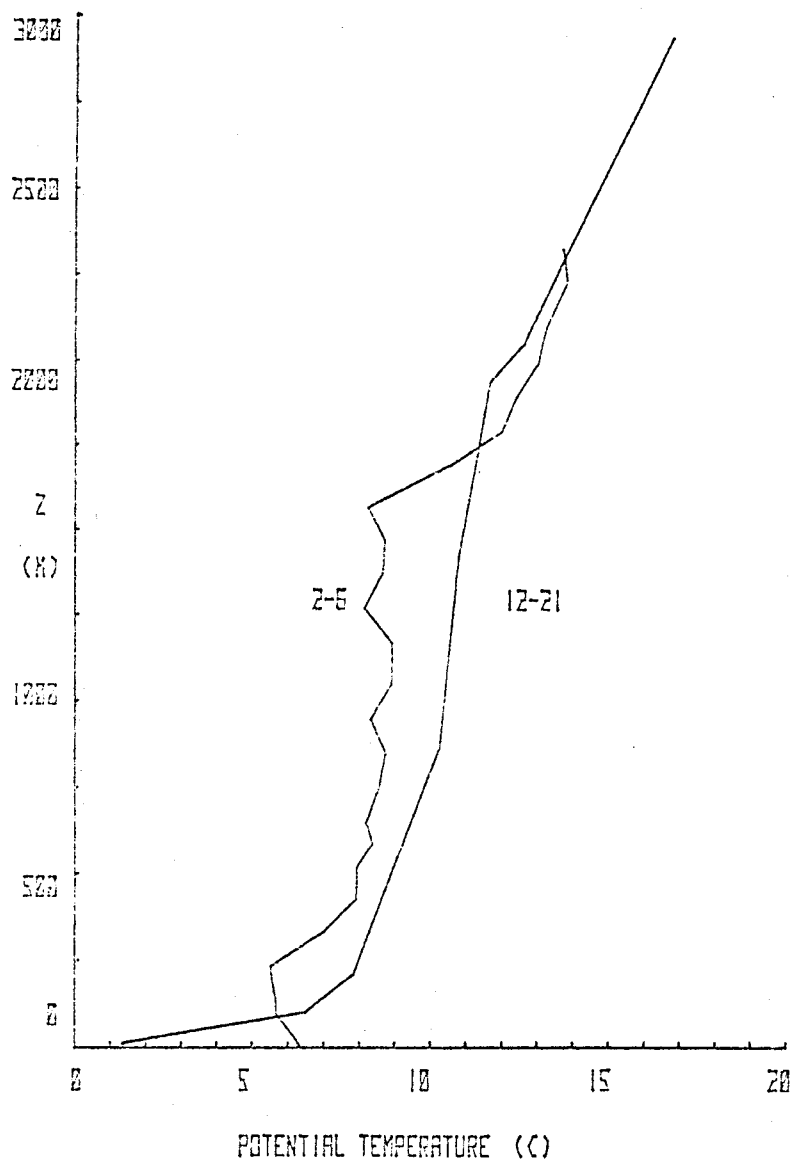


Fig. 6.12. Comparison of Yakutat 12Z, 21 November and marine station 2-6.

### C. Field investigation - March 1976

In order to better understand the mechanisms of katabatic flow and nearshore air mass modification an extensive field effort was executed in March, 1976 in the Icy Bay-Yakutat Bay coastal region of the Gulf of Alaska. Data were collected at 36 stations (Fig. 6.13.) employing radiosonde ascents for low-level temperature and humidity structure, tethered boundary layer sounding balloon and instrument package for detailed boundary layer temperature, humidity and wind profiles, and instrumented bow boom for accurate meteorological surface information. Track lines were constructed to observe air modification and seaward katabatic flow extent normal to the coast of Icy Bay and Malaspina Glacier. Saw-tooth station arrays along the Sitkagi Bluffs were patterned to define the horizontal and vertical katabatic flow influences.

The large-scale weather situation varied significantly from that experienced during November, 1975. The 500 mb flow for the first several days showed a large amplitude wave over the northern Pacific with the trough over Siberia and the ridge line along the Western coast of the United States. Geostrophic flow in the operating area was generally from the South. A slight retrogression carried surface cyclones Northward along the Western Alaska coasts, up into the interior, and down into central Alaska. Observations conducted on March 7 were somewhat influenced by a closed low pressure system just North of the Aleutian chain. On about 8 March the upper level wave disintegrated bringing the region under a nearly zonal flow regime with a slight ridge in the Gulf of Alaska area. A surface level high pressure pocket developed over the operating area on March 9 resulting in excellent mesoscale meteorological activity as evidenced by marine cumulus generation and cloud streets normal to the coast.

As of this date, the radiosonde sounding from station M-1 and the corresponding Yakutat rawinsonde (Fig. 6.15 and Fig. 6.16.) from 00Z, 10 March, have been analyzed. Yakutat surface winds, in contradiction to the katabatic flow observed at M1, were southerly (perhaps due to local orographic effects). At about 500 m a rapid directional change is noted as the winds decrease and move through North to a Westerly geostrophic flow at about 2 km. As might be expected, with southerly surface flow, the Yakutat sounding shows no surface layer inversion although a permanent upper level inversion and cloud base are present at about 1500 m. The M1 sounding is quite similar except for a 100 m thick surface unstable layer and a lower (500 m) cloud base.

As of the time of this report, a great deal of data remain to be processed. A more complete description of the data will be given in future reports.

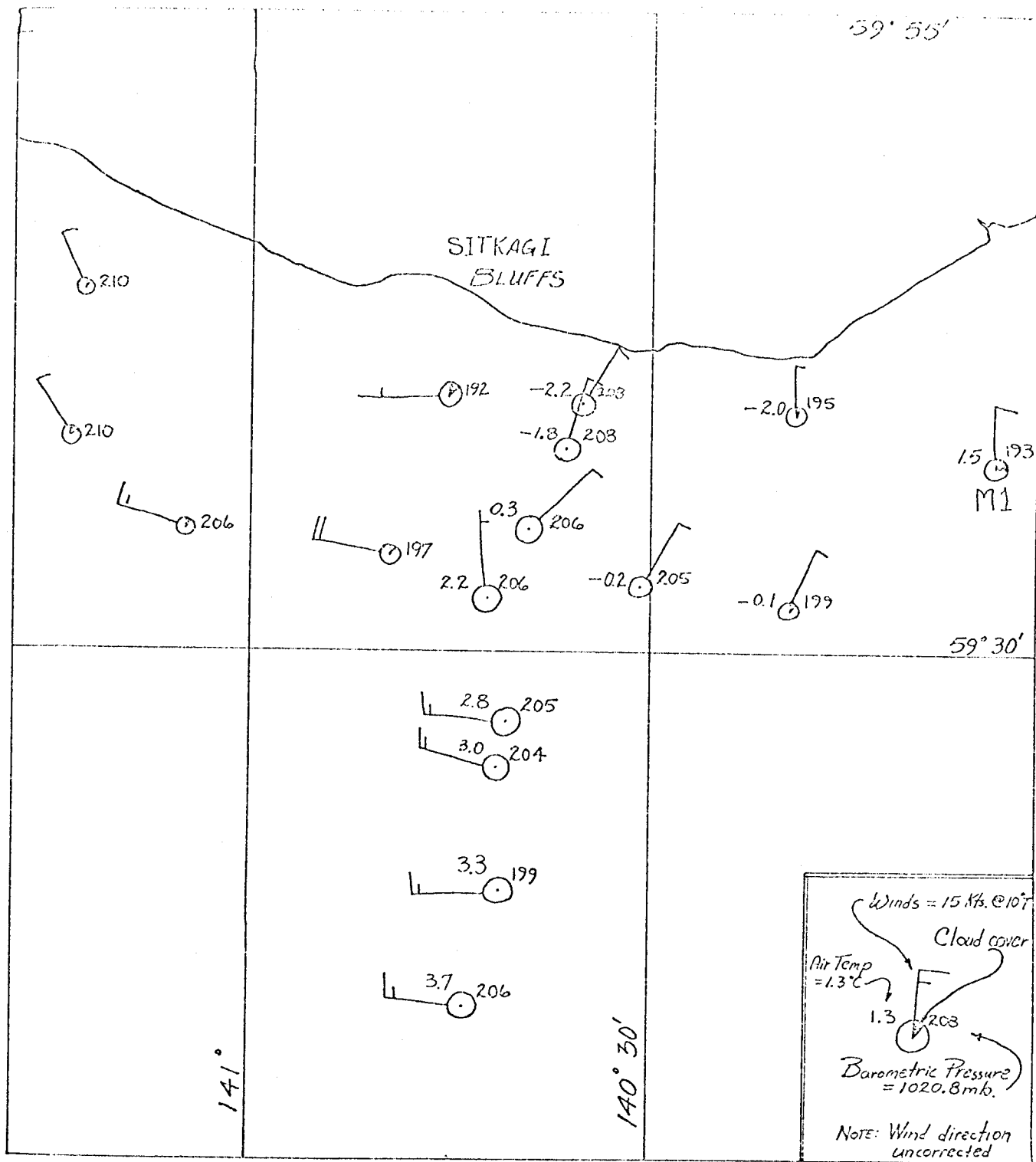


Fig. 6.13. Surface observations taken during March, 1976.

53

976

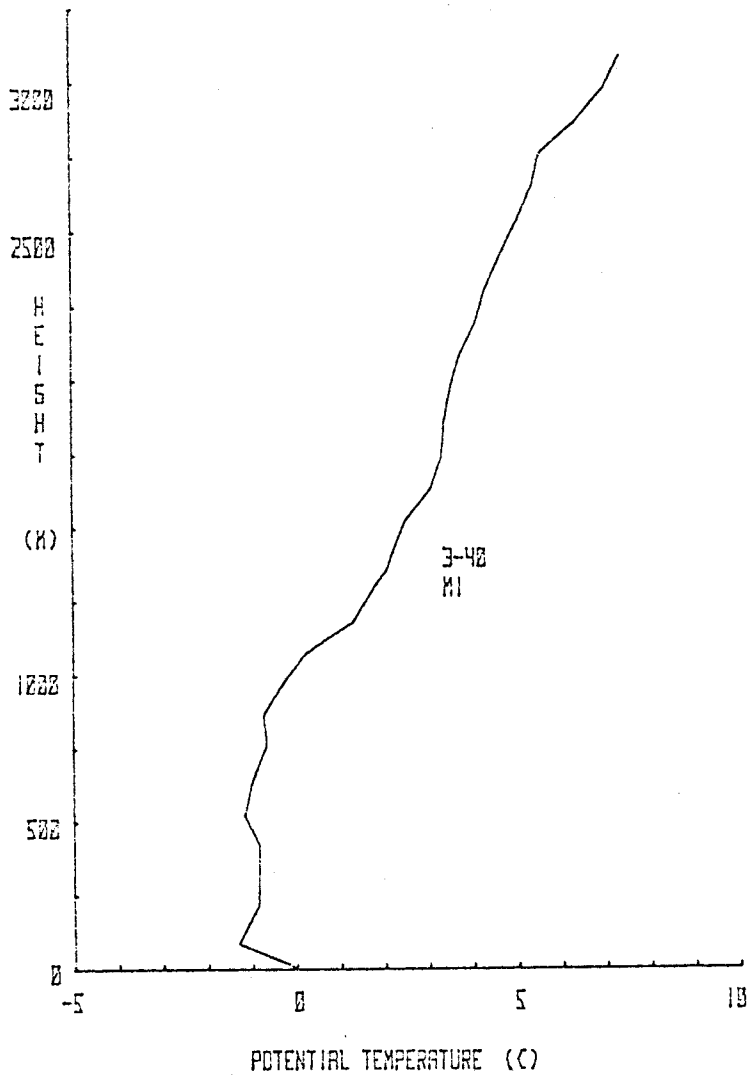


Fig. 6.14. Vertical profile for marine station M1.

977

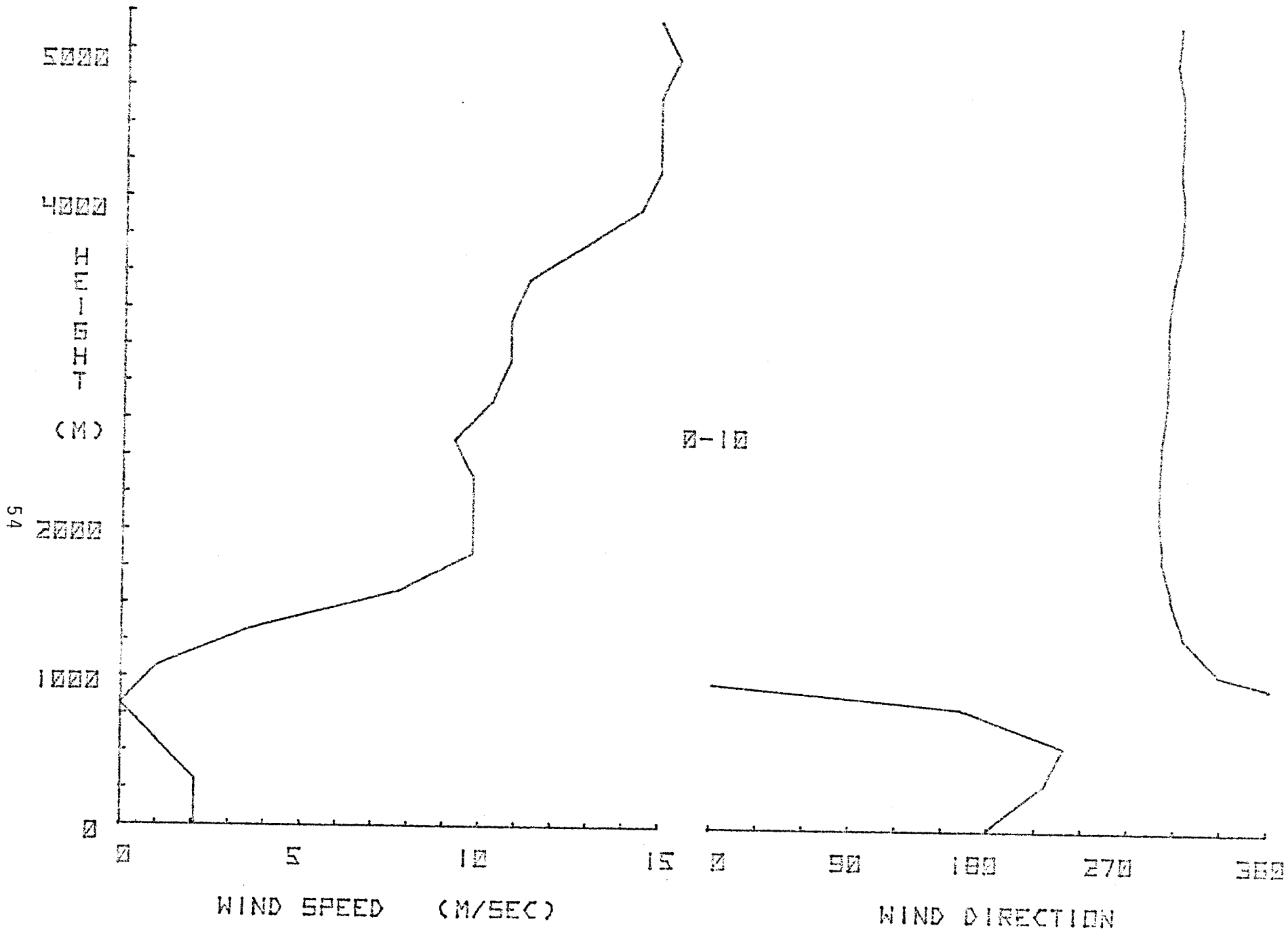


Fig. 6.15. Vertical profile of wind and speed direction for Yakutat 00Z, 10 March 1975.

55  
978

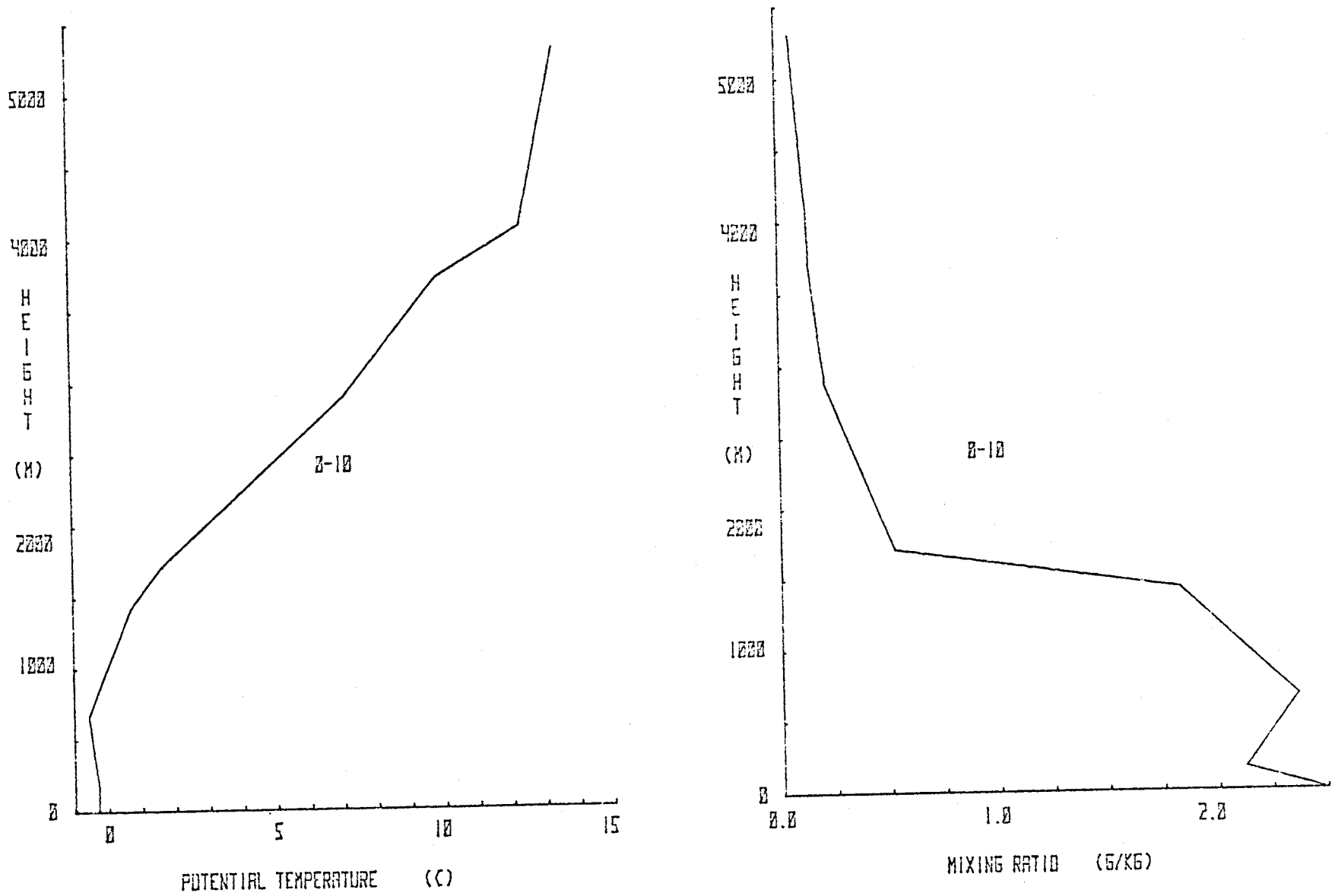


Fig. 6.16. Yakutat radiosonde profiles for 00Z, 10 March 1976.



#### D. Climatology and Modelling

Initial analysis of the SSMO data has begun. Figures 6.17 shows monthly wind roses which have been plotted for the Cordova sector (the left, center, and right sectors respectively, indicated on Fig. 4.1.). The concentric circles that are drawn on the plots note each 10% probability interval, and the wind directions are broken down into 8 different directions. The synoptic data tapes for Cordova, Middleton Is., Yakatoga, and Yakutat have been received and a computer program for decoding the tapes and processing the data is being written. As yet, no analysis is available from this source. Figure 6.18 shows a plot of wind speed measured by EB-33 vs geostrophic wind speed computed from synoptic charts for January, 1975. Calculation of geostrophic winds for additional months is proceeding. The data shown in Figure 4 are daily mean values. Notable is the apparent mean offset of about 10 kts.

Some results have been obtained in an attempt to better understand the general synoptic situations existing in the Gulf of Alaska. Appendix A is a copy of a preliminary descriptive analysis of the weather in the Gulf of Alaska by season. This analysis indicates some of the basic features of the weather situations and includes Gordon Kilday's description of Taku winds observed at Juneau, Alaska along with the synoptic situations favorable to the formation of these winds (referenced earlier in Section III). A very extensive study of the meteorological conditions prevailing in Alaska has been performed by Putnins (1966). In this study, the generalized weather situations over Alaska were determined for every day of the period January 1, 1945 to March 31, 1963 in such a way that for every day of this period a specific surface pressure pattern could be assigned. The flow at 500 mb over Alaska was also taken into account. Twenty-two specific surface patterns were selected. The statistical evaluation of these particular generalized weather situations involves: The frequencies of these weather stations by month and year, the mean and maximum duration of every weather situation, and the probabilities of the weather situations following a selected weather situation. Also, the annual course of every weather situation is discussed.

Finally, progress is being made toward the adaptation of an existing mesoscale numerical model to the Gulf of Alaska coast region. The model developed by M. Danard (discussed in Section III) originally for use in the Straits of Juan de Fuca, Haro and Georgia is in the process of being modified so that it can be run on the University of Washington's CDC-6400 computer. Also, copies of Jensen and Pandolfo's model and Fosberg's model (both discussed in Section III) have been obtained and are available for use. The present effort though is in obtaining a running version of Danard's model.

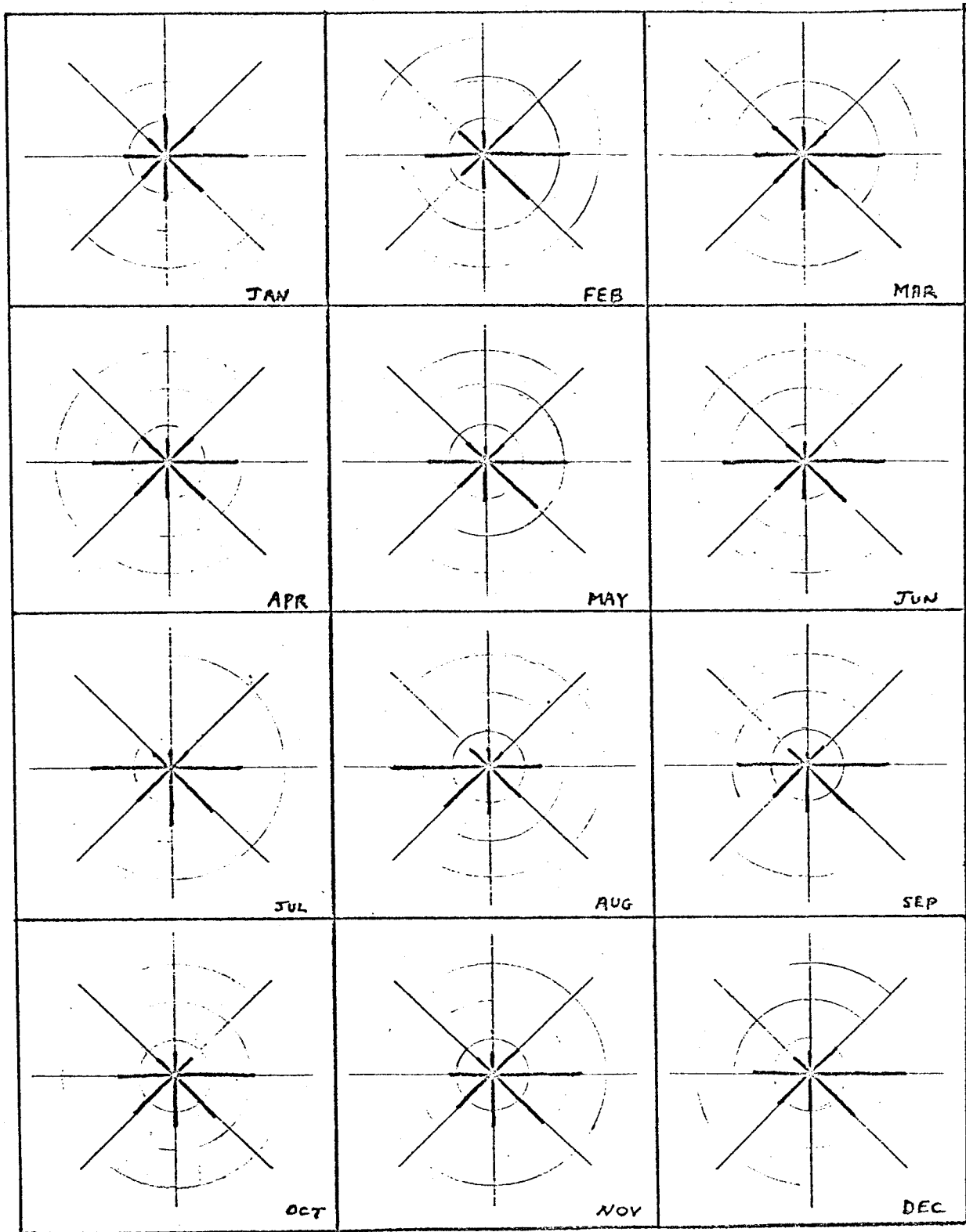


Fig 6.17. Average monthly wind roses for Cordova.

T86

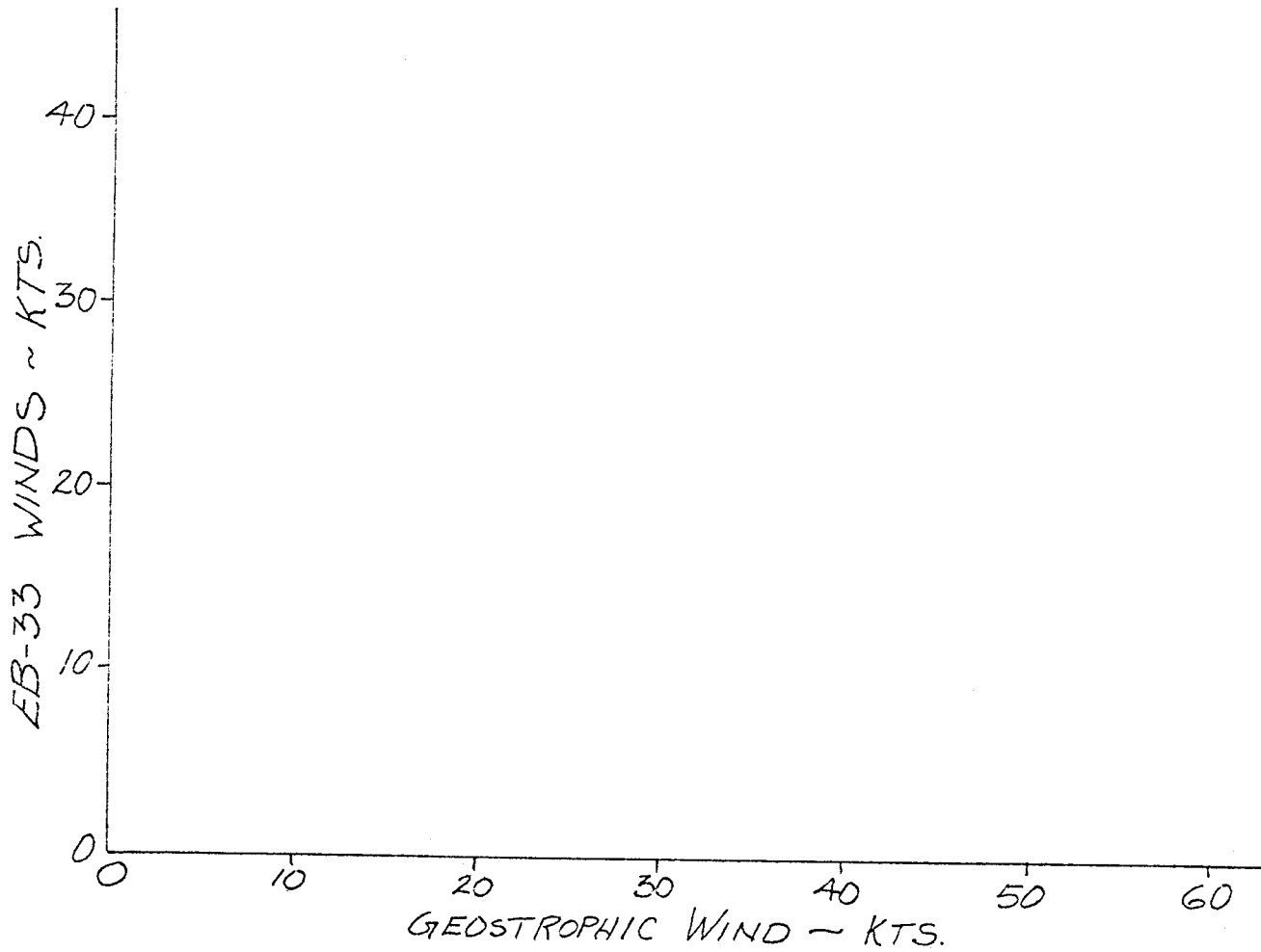


Fig. 6.18. Comparison of EB-33 measured wind with catastrophic wind calculated from surface analysis maps.

APPENDIX A  
Gulf of Alaska Weather Summary

Summer

The summer regime is in effect during the latter part of May, June, July and the first part of August. During this period, a deep thermal low develops over interior Alaska extending into the Yukon Territories. The central pressure is typically 1004 mb. At this same time a high pressure area is located near 40°N, 150°W in the Pacific Ocean. This synoptic situation creates a significant pressure gradient across the Alaska Gulf coast directed toward interior Alaska and causes the generation at times of strong winds (>50 kts) across mountain passes and along valleys inland from the coast and also in the waterways along the Alaskan panhandle. This situation may cause periods of significant Southerly flow in the area of the Copper River Delta. Also during these months sea-breeze effects along the coast become a factor to consider and may be quite strong at times. This sea-breeze effect can be considered as a wind which is superposed on the general synoptic flow. The pressure gradients are quite weak over the gulf and the passage of fronts brings generally low-level clouds and associated rain and drizzle. Strong frontal activity with high wind conditions are generally absent at this time.

Fall

During the latter part of August and the first part of September, storms from the Bering Sea begin to make their way into interior Alaska bringing associated low level clouds. The strong thermal low that was present in the summer months begins to dissipate and its center shifts Eastward to South central Yukon Territories. The latter part of September, October, November, and the beginning of December are transition months. This is the time period of deepening of the Aleutian low and the passage of strong frontal systems through the Gulf area. Storms that curve Northward and remain in Area I shown on Fig.A1 tend to be relatively weak and not of much concern. Those that end up in the sector shown as Area II (the "pocket") tend to deepen rapidly and have high wind conditions associated with them. The Fall season is a particularly bad time of the year when considering the effects of weather on an oil spill. During this time of the year storms move rapidly through the area of concern each with a different track. This leads to gusty, high wind conditions with wind directions changing rapidly. This is a situation that is very conducive to spreading an oil spill very quickly. Thus, conditions are present which could lead to the spreading of an oil spill over large distances and thereby impacting a larger land area than it would if the wind were just blowing from one general direction.

Winter

The winter conditions (January, February and March) are basically

opposite to those present during the summer. In the winter a very strong, cold high pressure area (central pressure reaching 1050 mb) develops over interior Alaska. This in combination with the Aleutian low out over the Gulf leads to a strong pressure gradient across the coast and pointing outward. This leads to the occurrence of very strong (>100 kts) winds flowing out of such passes as the Copper River, Icy Bay and Yakutat Bay. These winds extend out over the water for 20 - 25 miles, and extremely turbulent conditions are present. The flow of this very cold, dry continental air over the relatively warm ocean causes extremely unstable conditions to occur thus contributing to the violent nature of these downslope winds. From a study done of Taku winds (down-slope winds observed at Juneau) by Gordon Kilday, observations indicate that the time of onset of the winds is independent of a diurnal effect and that the winds exhibit some diurnal variation but maximum velocities can occur at any time of the day or night. The duration of the meteorological conditions favorable to the onset of Taku winds may vary from 1 - 2 days to 2 - 3 weeks. This does not mean that these winds will blow continuously during this period, but it remains a constant threat. On the average, these conditions last 3 - 4 days. The duration is greatest when lows stagnate in the Southeastern Gulf or when a series of weak frontal cyclones move from the west to reinforce the Gulf low. Lows that move rapidly through the Southeastern Gulf produce the short periods.

Taku winds are classified into two types - cyclonic and anticyclonic according to the general synoptic situation. If the winds are due primarily to a well developed ridge of high pressure over the Yukon Territory and western British Columbia, they are classified anticyclonic. If the winds are due to a deepening low approaching the coast of Southeast Alaska, they are classified cyclonic. In the latter there is often a transition between the two depending on the path of the low when it reaches the Gulf of Alaska. In either type, isobars along the coast are tightly packed and winds blow predominantly across isobars and offshore.

The anticyclonic type produces very strong, gusty winds, and there are often periods between the violent gusts. The weather remains clear, dry and generally quite cold. The cyclonic type is characterized by cloudy skies, snow, and only moderately cold temperatures. The cyclonic type is the less violent of the two and the winds are more constant and do not exhibit the extreme gustiness found in the anticyclonic type.

The synoptic patterns conducive to the development of Takus can be classified into three general categories. The most common category features a blocking ridge aloft which develops over the Bering Sea and the Western half of Alaska and is associated with a surface high-pressure area that covers most of the mainland of Alaska north of the Alaska Range. A weak frontal cyclone moves from the West into the Northern Gulf and deepens rapidly as it swings southeastward along the coast to the Queen Charlotte Islands where it stagnates and begins to fall. A cold low aloft is associated with the surface low in the vicinity of the Charlottes, while another cold low aloft exists over Northwestern Canada. At times there have been indications that the flow associated with these

upper-level lows contributes to other factors responsible for cascading the cold air Southwestward down the slopes of the Alaska Coast Range.

In the second category, the winds are dependent on a strong high pressure center over Northwestern Canada with the extension of the high pressure Southward over Western Canada. It is opposed by a weak trough of low pressure along the Southeast Alaska Coast. The surface high is associated with a large, closed, warm high aloft over the Northern Gulf and the mainland of Alaska. The flow associated with this high aloft is responsible for bringing the cold air southward over the Coastal Range. This is revealed by the large drop in temperature aloft at Whitehorse, Yakutat, and Annette Is.

The third category produces the most prolonged periods of Taku and the most severe ones. The dominant features of this type is a stagnant low over the Southeastern Gulf with the closed surface high over the Yukon Basin and the blocking high aloft over the Bering Sea with a ridge Northeastward through Alaska. The Arctic Front lies between Petersburg and Annette Is. Cold arctic air flows down Lynn Canal and Taku Inlet and out through Icy Strait and Cross Sound into the near of the low in the Southeastern Gulf while warm, moist maritime air flows Northward along the coastal waters from Washington and Vancouver Is. These two factors not only help to maintain the depth of the low, but also provide the sharp contrast in air masses between Southeast Alaska and the Yukon Territory which appears to be one of the main prerequisites of a strong Taku.

It must be remembered that the above descriptive analysis applies to Taku winds observed at Juneau but it only takes a minor extrapolation to determine the conditions necessary to cause severe downslope winds along other areas of the Gulf of Alaska coast.

### Spring

The months of April and May are again transition months where the lows moving through the Gulf gradually become less severe and their tracks shift more toward the western Gulf than the eastern Gulf. Also at the time the cold continental high over the interior of Alaska begins to weaken and dissipate.

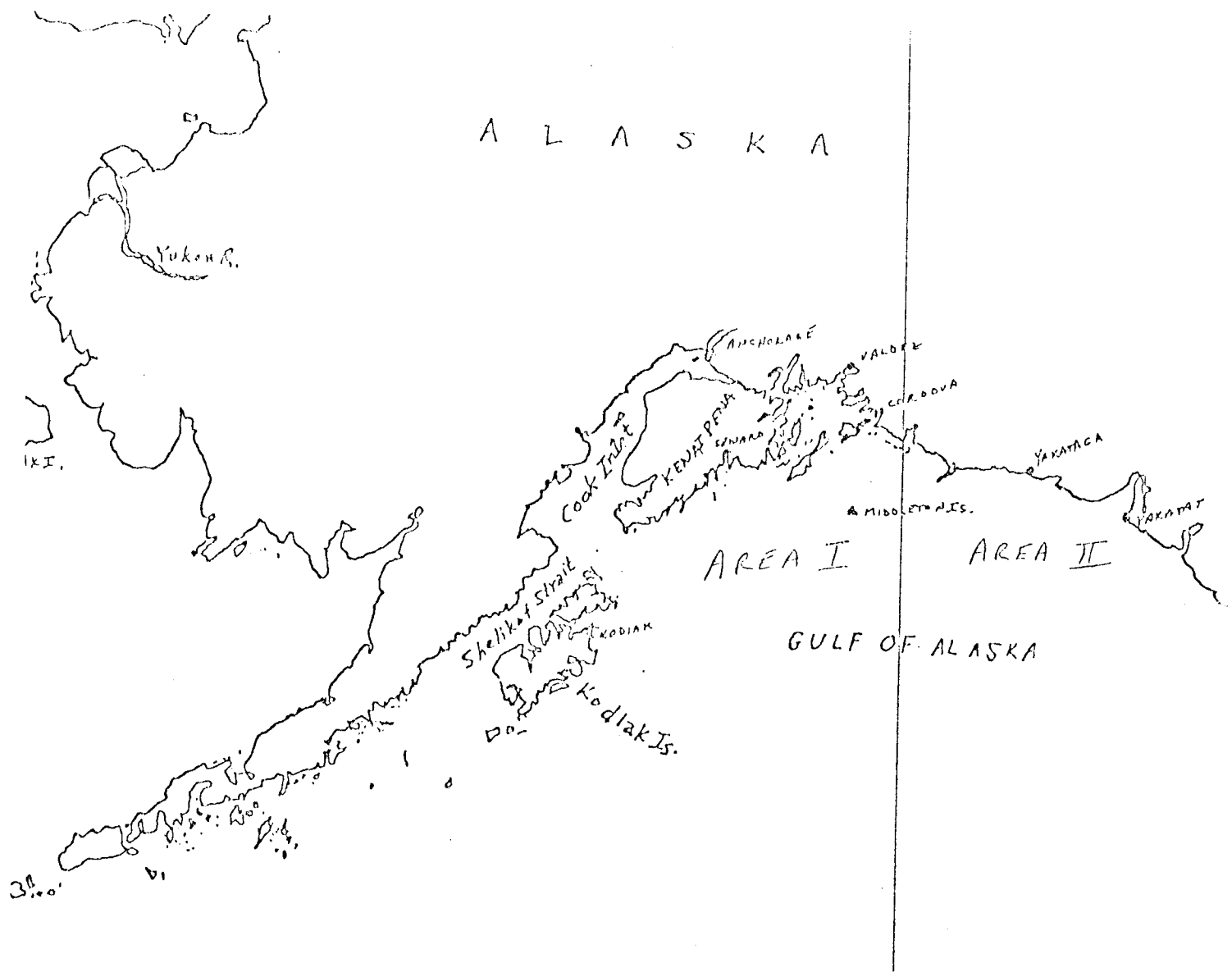


Figure A.1.

## VII. Discussion

## VIII. Conclusions

Figure 6.14. shows a plot of surface winds measured by EB-33 vs geostrophic winds. The usual relationship assumed when calculating surface winds from geostrophic winds is that  $V_{SFC} = 0.75 V_G$ . The slope in Fig. 6.14. shows a much lower slope. This is a result from only one month's data and the inclusion of a larger amount of data may modify this conclusion. An attempt to relate the air-sea temperature difference to both the reduction factor and the geostrophic to surface veering angle show that there is no clear-cut correlation between these parameters. A preliminary plot of individual six hourly speed values showed a large amount of scatter. Little or no relationship between EB-33 speeds and geostrophic wind speeds could be deduced from these individual values. If this result continues to hold after analysis of further data then the validity of using geostrophic winds in order to define a surface wind field must be questioned.

Field studies made to date both verify the spatial variation in surface winds, and document their offshore gradient. In three different yet typical weather situations, definite offshore winds were observed, even with no cloud signature. Katabatic flows responsible for these lower level winds show strong modification as they are absorbed into the main flow. In all field cases and several satellite photos, a typical turning radius (i.e., adjustment scale length) is 70 - 80 km.

The boundary layer is comprised of a katabatic flow of varying depth (200 - 1000 meters has been observed) under the larger scale air mass. In instances when the air mass is also offshore, air-modification effects will erode the katabatic layer and the height  $h$  will continue growing at a higher rate (due to the lower lapse rate above).

It has been decided, for reasons such as ease of initialization, and of running, that the mesoscale numerical model studies will initially employ M. Danards model. This model includes most of the physical processes that are considered important in modifying the nearshore atmospheric flow along the Alaskan coast. More sophisticated models can be considered later if unsatisfactory results are obtained in these initial runs.



## IX. The Need for Further Study

Work to date has verified the persistence and magnitude of coastal process. A review of available routine data has demonstrated several techniques of assessing quantitatively the long-term statistical characteristics of these processes, as well as various ways of recognizing them in near-real time. A continuing and closer analysis of VHRR satellite photos taken over the Gulf of Alaska along with the concurrent synoptic weather situation is necessary. Newly proposed sites for Data Buoys should lead to more definitive statistics. Several promising models, especially one designed for predicting surface stress, have been reviewed and are being prepared for trial runs in a Gulf of Alaska situation.

Future work should now be aimed at (i) extending our definition of the active processes occurring, including their initiation and modification, (ii) defining the quality which synoptic measurements must have to accurately forecast mesoscale flow patterns, and (iii) providing a set of trial runs for predictive numerical models. The trials should cover locales and times when a high quality set of field data is available to compare with computed stress.

Thus a mesoscale meteorological network must be established in a key area. The measurements taken by this network will provide a long term data useful for detailing coastal vs offshore gradients. In addition to this network, a field experiment where vertical and horizontal variations are detailed carefully is required. Ideally, an instrumented airplane could vastly reduce confusion in sorting spatial from temporal effects. These sited needs for study will soon be presented in a more detailed proposal.

## References

- Ball, F.K. (1956) The Theory of Strong Katabatic Winds. Australian Journal of Physics, 9, 373-386.
- Ball, F.K. (1960a) Winds on the Ice Slopes of Antarctica. Proceedings of the Symposium on Antarctic Meteorology, J.W. Arrowsmith Ltd., Bristol Great Britain, p. 9-16.
- Ball, F.K. (1960b) Control of Inversion Height by Surface Heating. Quart. J. Roy. Met. Soc., 86, 483-494.
- Bean, B.R., C.B. Emmanuel, R.O. Gilmer, and R.E. McGavin (1975) Spatial and Temporal Variations of the Turbulent Fluxes of Heat, Momentum, and Water Vapor Over Lake Ontario During IFYGL. NOAA Technical Report ERL 313-WMPO 5, 57 pp.
- Blackadar, A.K. (1965) A single layer theory of the vertical distribution of wind in a baroclinic neutral atmospheric boundary layer. Final Rept., Contract AF (604)-6641, Dept. of Meteorology, Pennsylvania State University, 1-22.
- Blackall, R.M. (1973) Warming of the Troposphere by the Sea. The Meteorological Magazine, 102, pp. 65-73.
- Brown, R.A. (1974) Analytical Methods in Planetary Boundary-Layer Modeling. John Wiley and Sons, Inc., 148 pp.
- Busch, N.E. (1973) On the Mechanics of Atmospheric Turbulence. In Workshop on Micrometeorology, ed. Duane A. Haugen, American Met. Society, 1-65.
- Businger, J.A. (1972) The Atmospheric Boundary Layer. Remote Sensing of the Troposphere, Chap. 6, U.S. Dept. of Commerce, NOAA.
- Businger, J.A. (1973) Turbulent Transfer in the Atmospheric Surface Layer. In Workshop on Micrometeorology, ed. Duane A. Haugen, AMS, pp. 67-98.
- Climatological and Oceanographic Atlas for Mariners, Volume II, North Pacific Ocean (1961) Prepared by Office of Climatology and Oceanographic Analysis Division, Dept. of Commerce.
- Craddock, J.M. (1951) The warming of arctic air masses over the eastern North Atlantic. Quart. J. Roy. Meteor. Soc., 77, 355-364.
- Deardorff, J.W. and G.E. Willis (1975) A Parameterization of Diffusion into the Mixed Layer. J. of App. Met., 14, 1451-1458.
- Estoque, M.A. (1973) Numerical Modelling of the Planetary Boundary Layer. In Workshop on Micrometeorology, ed. Duane A. Haugen, A. Met. Soc., pp. 217-268.

- Fleagle, R.G. and J.A. Businger (1963) An Introduction to Atmospheric Physics. Academic Press, 346 pp.
- Fosberg, M.A., W.E. Marlatt, L. Krupnak, (1975) Estimation of Airflow Patterns Over Complex Terrain.
- Grant, K. (1975) The Warming and Moistening of Cold Air Masses by the Sea. The Meteorological Magazine, 104, pp. 1-9.
- Gutman, L.N., and V.M. Malbakhov, (1965) To the theory of katabatic winds of Antarctica, Meteorologicheskii Issledovaniya, 9, p. 150-155.
- Jacobs, C.A., J.P. Pandolfo, and M.A. Atwater (1974) A Description of a General Three-Dimensional Numerical Simulation Model of a Coupled Air-Water and/or Air-Land Boundary Layer, vol I. The Center for the Environment and Man, Inc, Rept. No. 4131-509a, 111 pp.
- Jensen, J.V. and M.B. Danard, (1975) A Numerical Model for Surface Winds in Juan de Fuca, Haro and Georgia Straits. Technical Report, Atmospheric Dynamics Corporation, R.R. a, Elmira, Ontario, 73 pp.
- Kilday, G.D., 1970, Taku Winds at Juneau, Alaska, National Weather Service Office Memo.
- Lavoie, R.L. 1972, A Mesoscale Numerical Model of Lake-Effect Storms, J. Atm. Sci., V 29, p. 1025-1040.
- Lenshow, D.H. (1973) Two Examples of Planetary Boundary Layer Modification Over the Great Lakes. J. Atm. Sci., 30, 568-581.
- Lenshow, D.H. (1974) The Air Mass Transformation Experiment (AMTEX): Preliminary Results from 1974 and Plans for 1975. Bull. Am. Meteor. Society, 55, 1228-1235.
- Lettan, H. (1967), Small to Large-scale Features of Boundary Layer Structure over Mountain Slopes, in Proc. of the Symposium on Mountain Meteorology, ed. E.R. Reiter and J.L. Rasmussen, Dept. of Atm. Sci., Colo. State Univ., Ft. Collins, Colo. pp. 1-73.
- Mahrer, Y., and R.A. Pielke (1974) A Numerical Study of the Air Flow Over Mountains Using the Two-Dimensional Version of the University of Virginia Mesoscale Model, J. Atm. Sci., V. 32, p. 2144-2155.
- Manabe, S. (1957) On the modification of air-mass over the Japan Sea when the outburst of cold air predominates. J. Meteor. Soc. Japan, 35, 311-326.
- Manabe, S. (1958) On the estimation of energy exchange between the Japan Sea and the atmosphere during the winter based upon the energy budget of both the atmosphere and the sea. J. Meteor. Soc. Japan, 36, 123-134.

- Nickerson, E.C. and E.L. Magaziner (1976) The Numerical Simulation of Orographically Induced Non-Precipitating Clouds, unpublished manuscript.
- Ninomiya (1972) Heat and water-vapor budget over the East China Sea in the winter season. J. Meteor. Soc. Japan, 50, 1-16.
- Radock, U. (1972) On the Energetics of Surface Winds over the Antarctic Ice Cap, unpubl.
- Reynolds, R.M. and J.T. Gething (1970) Acoustic Sounding at Benalla, Victoria and Julia Creek. Queensland. Project EAR, Report VII, University of Melbourne, Meteorology Department, Parksville Victoria.
- Putnins, P. (1966) Studies on the Meteorology of Alaska, Environmental Data Services, Silver Springs, Md., 90 pp.
- Searby, H.W. (1969) Coastal Weather and Marine Data Summary for the Gulf of Alaska, Cape Spencer Westward to Kodiak Island. ESSA Tech. Memo EDSTM8, 30 pp.
- Stull, R.B. (1973) Inversion Rise Model Based on Penetrative Convection. J. Atm. Sci. 30, 1092-1099.
- Stull, R.B. (1975) Temperature Inversions Capping Atmospheric Boundary Layers. PgD. Thesis, University of Washington, 218, pp.
- Tauber, G.M. (1960) Characteristics of Antarctic Katabatic Winds, *In Proc. of the Symposium on Antarctic Meteorology*, p. 3 - 8.
- Tennekes, H. and J.L. Lumley (1972) A First Course in Turbulence. The MIT Press, 300 pp.
- Tennekes, H. (1973) A Model for the Dynamics of the Inversion Above a Convective Boundary Layer. J. Atmos. Sci., 30, 558-567.
- U.S. Navy Hydrographic Office (1944) Weather Summary-Alaska Area. Pub. No. 526, 279 pp.
- Weller, G.E. (1969) A Meridional Surface Wind Speed Profile in MacRobertson Land, Antarctica, PAGEOPH, V77, p. 193-200.
- Winston, Jay S. (1955) Physical aspects of rapid cyclogenesis in the Gulf of Alaska. Tellus, 12:4, 481-500.

## X. Summary of Activities

During the period 17 - 22 November, 1975, Bernie Walter (PMEL) and Al Macklin (Private Meteorologist) took part in the NEGOA Leg III cruise aboard the NOAA Ship DISCOVERER in order to make nearshore meteorological observations. Six radiosonde soundings of the lower atmosphere were completed at the following times and locations

|     |          |       |                        |
|-----|----------|-------|------------------------|
| 2-1 | 11/20/75 | 0121Z | 59°37.8'N 139°48.0'W   |
| 2-2 | 11/20/75 | 2032Z | 59°34.04'N 142°10.25'W |
| 2-3 | 11/21/75 | 0836Z | 59°45.8'N 141°37.6'W   |
| 2-4 | 11/21/75 | 0931Z | 59°40.7'N 141°37.6'W   |
| 2-5 | 11/21/75 | 1019Z | 59°37.0'N 141°44.2'W   |
| 2-6 | 11/21/75 | 1115Z | 59°33.5'N 141°47.0'W   |

On 5 - 6 February, 1976, Bernie Walter visited ERL, Boulder, Colorado, to discuss (1) Everett Nickerson's 3-dimensional mesoscale model and its application to the Gulf of Alaska coast, (2) preliminary planning for NASA Convair 990 research flight scheduled for April 9, 1976, and (3) possible use of NOAA instrumented aircraft in future meteorological data collecting programs in OCSEAP.

On February 29 and March 1, 1976, Bernie Walter again visited ERL to discuss planning of the OCSEAP Meteorology Program.

During the period 1 - 11 March, 1976, Mike Reynolds (PMEL) and Al Macklin made low-level meteorological observations in the Gulf of Alaska. Surface observations, radiosonde ascents, and tethered balloon boundary layer flights were made at the following times and locations.

| STN  | DATE  | TIME  | LOCATION |           | BOW | MSM'T | RSONDE | TETHERED<br>BALLOON |
|------|-------|-------|----------|-----------|-----|-------|--------|---------------------|
|      |       |       | N        | W         |     |       |        |                     |
| M1   | 03/09 | 2010Z | 59°37.3' | 140°03.7' | ✓   | ✓     | ✓      |                     |
| M2   |       | 1457Z | 59°31.8' | 140°19.6' | ✓   | ✓     |        |                     |
| M3   |       | 1625Z | 59°39.5' | 140°19.0' | ✓   | ✓     |        |                     |
| M4   |       | 1347Z | 59°32.7' | 140°31.0' | ✓   | ✓     |        |                     |
| M6   | 03/08 | 1545Z | 59°40.1' | 140°36.0' | ✓   | ✓     |        |                     |
| M7   |       | 1640Z | 59°38.0' | 140°37.3' | ✓   | ✓     |        |                     |
| M8   |       | 1716Z | 59°35.3' | 140°40.4' | ✓   | ✓     |        |                     |
| M9   |       | 1838Z | 59°31.4' | 140°40.1' |     |       |        |                     |
| M10  |       | 1931Z | 59°30.0' | 140°40.9' | ✓   | ✓     |        |                     |
| M11  |       | 2048Z | 59°24.6' | 140°43.6' | ✓   | ✓     |        |                     |
| M12  |       | 2224Z | 59°20.5' | 140°38.8' | ✓   | ✓     |        |                     |
| M13  |       | 2332Z | 59°15.8' | 140°48.2' | ✓   | ✓     |        |                     |
| M6B  | 03/09 | 1230Z | 59°39.8' | 140°35.1' | ✓   | ✓     | ✓      |                     |
| M7B  |       | 0834Z | 59°38.0' | 140°36.7' | ✓   | ✓     |        |                     |
| M8B  | 03/09 | 0734Z | 59°34.8' | 140°39.5' | ✓   | ✓     |        |                     |
| M9B  |       | 0644Z | 59°32.1' | 140°42.7' | ✓   | ✓     |        |                     |
| M10B |       | 0543Z | 59°27.2' | 140°40.9' | ✓   | ✓     |        |                     |
| M11B |       | 0426Z | 59°25.6' | 140°41.9' | ✓   | ✓     |        |                     |
| M12B |       | 0335Z | 59°20.6' | 140°41.5' | ✓   | ✓     |        |                     |
| M13B |       | 0150Z | 59°16.1' | 140°44.1' | ✓   | ✓     |        |                     |
| M14  |       | 0031Z | 59°10.9' | 140°48.4' | ✓   | ✓     |        |                     |
| M15  | 03/08 | 1448Z | 59°40.1' | 140°45.9' | ✓   | ✓     |        |                     |
| M16  |       | 1215Z | 59°33.8' | 140°49.8' | ✓   | ✓     |        |                     |
| M17  |       | 1038Z | 59°42.6' | 140°57.6' | ✓   | ✓     | ✓      |                     |
| M18  |       | 0830Z | 59°34.8' | 141°04.6' | ✓   | ✓     |        |                     |
| M19  |       | 0618Z | 59°44.0' | 141°12.5' | ✓   | ✓     | ✓      |                     |
| M20  |       | 0356Z | 59°38.3' | 141°17.8' | ✓   | ✓     | ✓      |                     |
| M21  | 03/07 | 1456Z | 59°46.5' | 141°25.0' |     | ✓     |        |                     |
| M22  |       | 1246Z | 59°48.9' | 141°38.0' |     | ✓     |        |                     |
| M23  |       | 0729Z | 59°49.8' | 141°47.7' |     | ✓     |        |                     |
| M24  |       | 0818Z | 59°46.0' | 141°52.0' |     | ✓     |        |                     |
| M23B |       | 1130Z | 59°50.2' | 141°46.8' |     | ✓     |        |                     |
| M24B |       | 1020Z | 59°46.9' | 141°52.8' |     | ✓     |        |                     |
| M25  |       | 0917Z | 59°41.5' | 141°57.1' |     | ✓     |        |                     |
| M26  |       | 0621Z | 59°56.0' | 141°55.0' |     | ✓     |        |                     |

